:orge I. Bell
ımuel Glasstone

NUCLEAR REACTOR THEORY

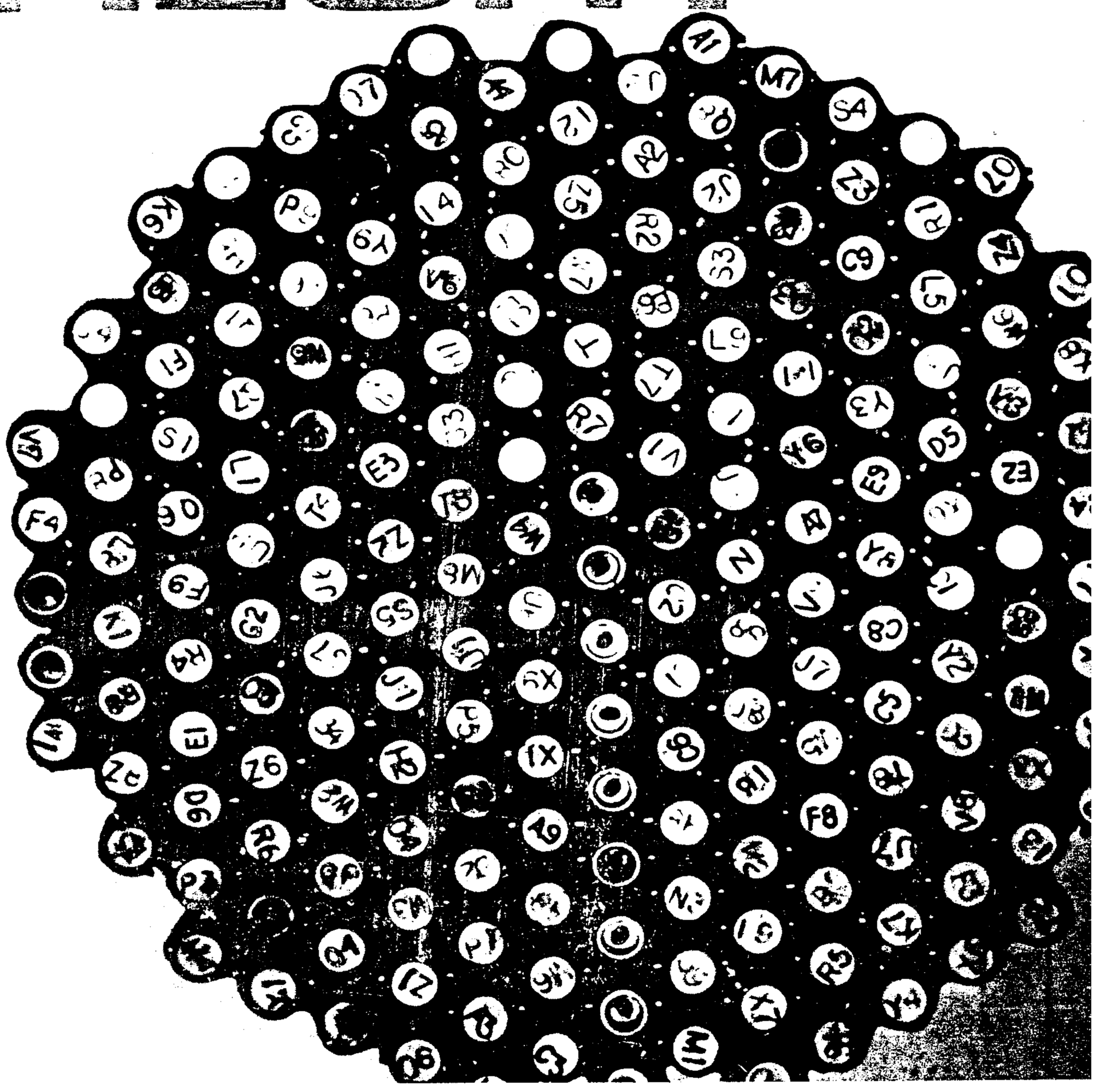

Nuclear Reactor Theory

George I. Bell
University of California
Los Alamos Scientific Laboratory

Samuel Glasstone
University of California
Los Alamos Scientific Laboratory

Published Under Auspices of The
Division of Technical Information
United States Atomic Energy Commission

Van Nostrand Reinhold Company
New York / Cincinnati / Toronto / London / Melbourne

Van Nostrand Reinhold Company Regional Offices:
New York Cincinnati Chicago Millbrae Dallas

Van Nostrand Reinhold Company Foreign Offices:
London Toronto Melbourne

Library of Congress Catalog Card Number: 73-122674

Manufactured in the United States of America

Published by Van Nostrand Reinhold Company
450 West 33rd Street, New York, N.Y. 10001

Published simultaneously in Canada by Van Nostrand Reinhold Ltd.

15 14 13 12 11 10 9 8 7 6 5 4 3 2 1

PREFACE

The purpose of this book is to explain the most important physical concepts and mathematical methods commonly used in predicting the behavior of neutrons in nuclear reactors. An effort has been made to avoid mathematical complexity that does not lead to a significant increase in physical understanding or is not used in actual reactor design studies. In a few instances, therefore, where it appears justified, lengthy derivations have been omitted and only the conclusion given, with references to the relevant literature.

The book is more or less self-contained and could serve as an introduction to reactor theory for physicists, mathematicians, and engineers. We have assumed, however, that the reader is familiar with such topics as the fission process, neutron cross sections, and the moderation and diffusion of neutrons. Thus, one of the more elementary texts on nuclear reactor theory would provide the necessary background. An adequate knowledge of mathematics is, of course, a requirement. Previous experience with vector analysis, partial differential equations, eigenvalue problems, and Laplace and Fourier transforms is desirable, although not necessary for an understanding of the basic principles. Some of the special mathematical procedures used in the text are explained in an Appendix and, in other cases, references are given to standard works.

Many people have helped us in one way or another in the preparation of this book, and we take this opportunity to express our indebtedness to them. We offer our thanks to Milton Edlund for his participation in the planning phase and to Robert Pigeon, AEC Division of Technical Information, for obtaining reviews of the draft manuscript. In this connection, we are grateful to Noel Corngold, Kent Hansen, William Hendry, Kaye Lathrop, Norman McCormick, Lothar Nordheim, and Paul Zweifel for their helpful comments. John Lamarsh

also assisted us by a careful reading of the draft, and we have profited greatly from suggestions based on his extensive experience in teaching nuclear reactor theory. Finally, we are happy to acknowledge the competence of Ruth Beaty and Margo Lang in typing a difficult manuscript.

GEORGE I. BELL
SAMUEL GLASSTONE

October 1970

CONTENTS

1. THE NEUTRON TRANSPORT EQUATION

1.1 DERIVATION OF THE TRANSPORT EQUATION

1.1a Introduction

The behavior of a nuclear reactor is governed by the distribution in space, energy, and time of the neutrons in the system, and one of the central problems of reactor theory is to predict this distribution. In principle, this can be done by solving the neutron transport equation, often called the Boltzmann equation because of its similarity to the expression obtained by L. Boltzmann in connection with the kinetic theory of gases. In this chapter, various versions of the neutron transport equation are derived, and some general properties of its solution are discussed.

The neutron distribution problem could be solved by inserting into the transport equation a complete set of the appropriate cross sections, which represent the neutron interaction probabilities, together with the geometrical arrangement of the materials in the system. Numerical solutions could then be obtained by suitable computation procedures, e.g., by Monte Carlo methods. In practice, however, this proves not to be possible. First, the cross sections and their variation with neutron energy are very complicated and not completely known, and second, the geometrical arrangement of the materials in a reactor is so complex that the transport equation cannot be solved in a reasonable time even with a computer. In any event, solution of the neutron transport equation is so difficult that, except in the simplest cases, approximate forms of the equation must be used. These approximations are outlined at the end of this chapter and they are treated in detail in the book.

Before proceeding to the derivation of the transport equation, certain quantities required to describe the neutron transport problem will be defined, and a consistent notation will be presented. It will be seen that this notation differs in some respects from that employed in elementary reactor theory, but this is often a consequence of the introduction of extra variables in neutron transport theory. No great difficulty should be experienced, however, in adjustment to the notation used here.

1.1b Definitions and Notation

Neutron as a Point Particle

In transport theory, a neutron is considered to be a point particle in the sense that it can be described completely by its position and velocity. The point description would appear to be reasonable because the reduced wavelength of a neutron is small in comparison with macroscopic dimensions and neutron mean free paths.

According to the de Broglie equation, the reduced wavelength, λ of a particle is given by

$$\lambda = \frac{\hbar}{p},$$

where $\hbar$ is Planck's constant divided by 2π and p is the momentum of the particle. For a neutron this takes the form

$$\lambda = \frac{4.55 \times 10^{-10}}{\sqrt{E}} \text{ cm},$$

where E is the neutron energy in electron volts. Even for a neutron with 0.01 eV energy, λ is 4.55×10^{-9} cm, which is almost an order of magnitude less than the distances between atoms in a solid and several orders of magnitude less than macroscopic dimensions and mean free paths. Thus, it is reasonable to regard the position of a neutron as a quantity which can be specified accurately.

It is possible, in fact, to choose the position and velocity (or momentum) of a neutron with sufficient precision and not violate the Heisenberg uncertainty relationship $\Delta x\, \Delta p \simeq \hbar$. If an uncertainty Δx in position of 10^{-4} cm can be tolerated, the momentum uncertainty corresponds to a negligible uncertainty in the energy, i.e.,

$$\Delta E \simeq 10^{-5}\sqrt{E},$$

where ΔE and E are in electron volts.[1]

For neutrons of very low energy, the wavelength becomes very large and the neutron cannot, of course, be localized. The treatment of neutron transport developed in this book is then not valid and a quantum-mechanical formulation would be required.[2] The problem is of no practical significance in reactor physics,

however, since a negligible number of neutrons have energies which are so low that the conventional point-particle description is seriously in error. Furthermore, the transport equation is generally taken to hold even at arbitrarily low neutron energies, although in these circumstances the relationship of the solutions to physical reality becomes uncertain.

The neutron has a spin and a magnetic moment, which can lead to polarization that has an effect on neutron transport. But, as will be seen in §1.4b, this effect is small in most practical situations. If necessary, an approximate allowance can be made by minor modifications of the scattering cross sections.

For the present, the neutron will consequently be regarded as a point particle, with a position described by the vector $\mathbf{r}$ and a velocity by the vector $\mathbf{v}$. The velocity vector is often represented by

$$\mathbf{v} = v\boldsymbol{\Omega},$$

where v ($= |\mathbf{v}|$) is the neutron speed, i.e., the (scalar) magnitude of the velocity, and $\boldsymbol{\Omega}$ is a unit vector in the direction of motion, i.e., in the same direction as $\mathbf{v}$.

It is often convenient to specify the unit vector, $\boldsymbol{\Omega}$, in a polar coordinate system, i.e., by the polar angle θ and the azimuthal angle φ, as shown in Fig. 1.1. Cartesian coordinates of $\boldsymbol{\Omega}$ are then

$$\Omega_x = \sin\theta\cos\varphi \qquad \Omega_y = \sin\theta\sin\varphi \qquad \Omega_z = \cos\theta.$$

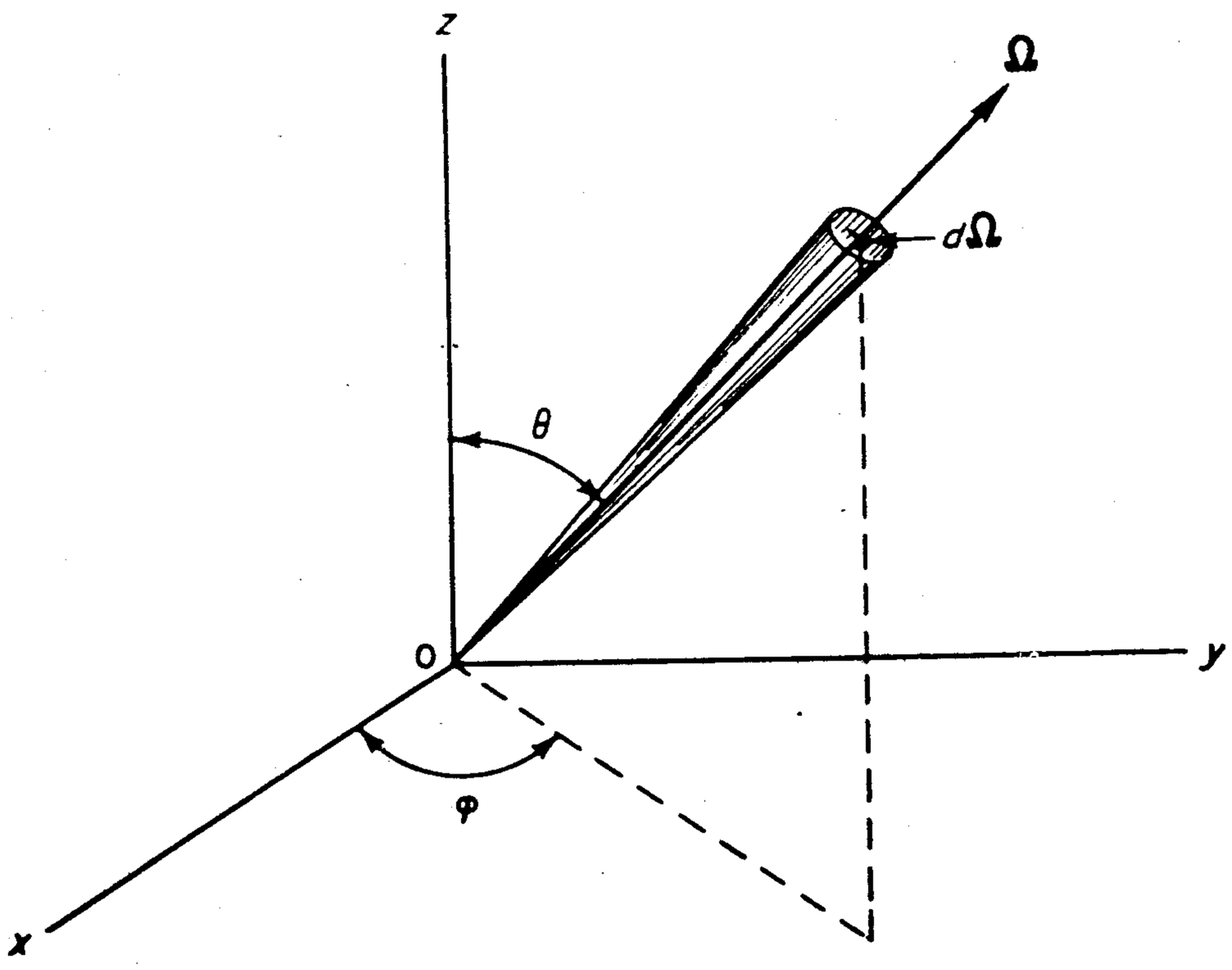

FIG. 1.1 POLAR COORDINATES.

Neutron Density and Flux

To describe a population of neutrons a quantity, called the *neutron angular density* in this book, is introduced. It is represented by

$$\text{Angular density} = N(\mathbf{r}, \boldsymbol{\Omega}, E, t) \tag{1.1}$$

and is defined as the probable (or expected) number of neutrons at the position $\mathbf{r}$ with direction $\boldsymbol{\Omega}$ and energy E at time t, per unit volume per unit solid angle per unit energy, e.g., per cm^3 per steradian per MeV. Consequently,

$$N(\mathbf{r}, \boldsymbol{\Omega}, E, t)\, dV\, d\boldsymbol{\Omega}\, dE$$

is the expected number of neutrons in the volume element dV about $\mathbf{r}$, having directions within $d\boldsymbol{\Omega}$ about $\boldsymbol{\Omega}$ (Fig. 1.2) and energies in dE about E at time t.*

If $\boldsymbol{\Omega}$ is expressed in polar coordinates, then $d\boldsymbol{\Omega} = \sin\theta\, d\theta\, d\varphi$, where the element of solid angle $d\boldsymbol{\Omega}$ is defined by the ranges θ, $\theta + d\theta$ and φ, $\varphi + d\varphi$. In later sections of this book, e.g., §1.3a, $\cos\theta$ is often represented by μ, so that

$$d\boldsymbol{\Omega} = d\mu\, d\varphi.$$

In the definition of the neutron angular density given above, the expression "probable (or expected) number of neutrons" is meant to imply that fluctuations

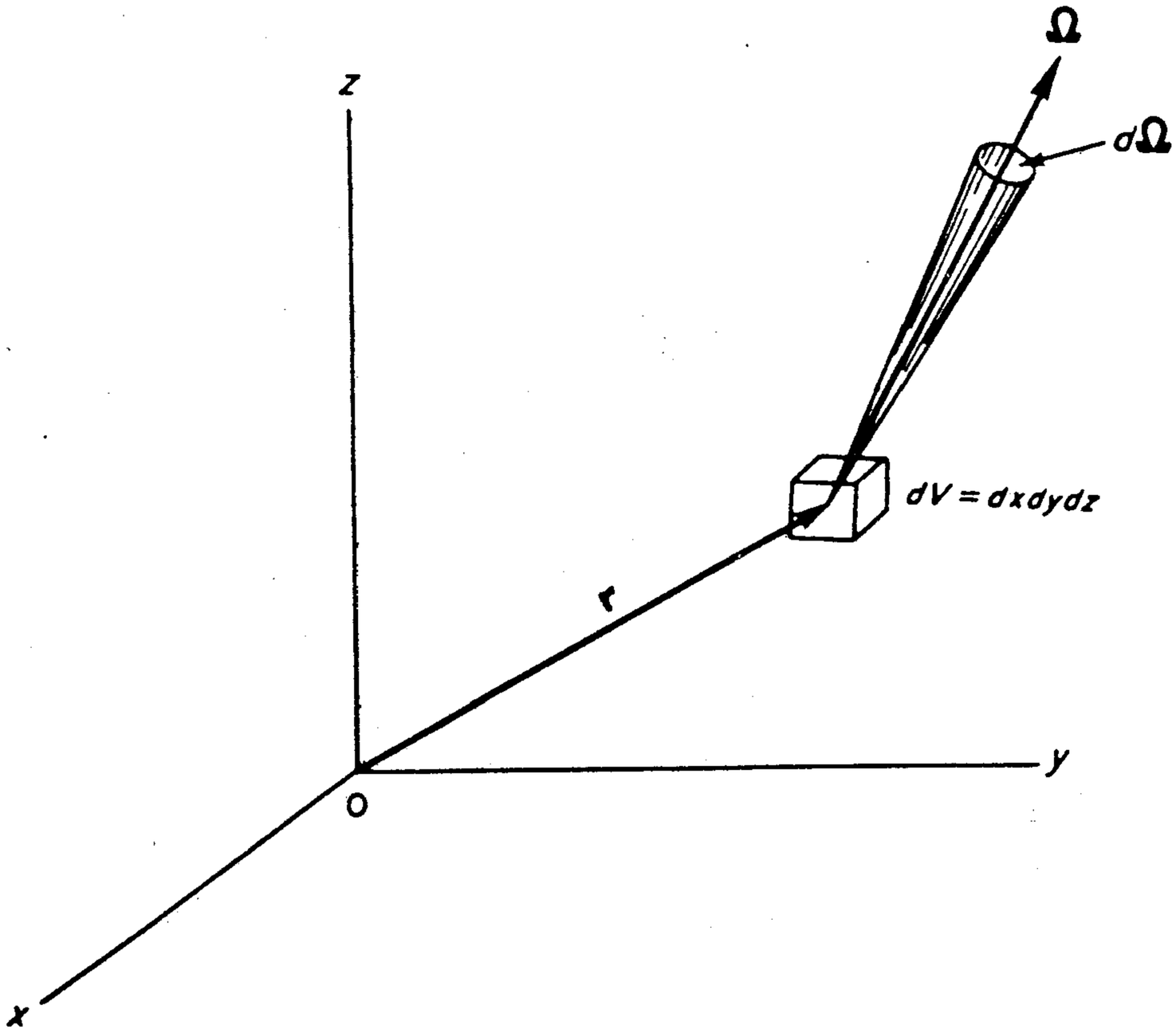

FIG. 1.2 THE VOLUME ELEMENT dV AND THE DIRECTIONAL ELEMENT $d\Omega$.

* The volume element about $\mathbf{r}$ is sometimes represented by $d\mathbf{r}$ or by d^3r, but dV is more explicit.

from the mean neutron population are not taken into account. If the neutron population under consideration is large, then the actual population will be close to the expected (or average) value and the fluctuations will be relatively small. If, on the other hand, the neutron population is small, it is still important to be able to describe the average behavior, even though the actual population at any instant in time is unlikely to resemble the average value. These points are discussed further in §1.4c.

The integral of the neutron angular density over all directions (or all solid angles) is the energy-dependent *neutron density*, $n(\mathbf{r}, E, t)$; thus,

$$\text{Neutron density} = \int_{4\pi} N(\mathbf{r}, \boldsymbol{\Omega}, E, t)\, d\boldsymbol{\Omega} \equiv n(\mathbf{r}, E, t), \tag{1.2}$$

where the symbol 4π implies integration over all directions. Hence, $n(\mathbf{r}, E, t)$ is the expected number of neutrons at $\mathbf{r}$, with energy E at time t, per unit volume per unit energy. If polar coordinates are used to specify $\boldsymbol{\Omega}$, then the neutron density is defined by

$$n(\mathbf{r}, E, t) \equiv \int_{-1}^{1} \int_{0}^{2\pi} N(\mathbf{r}, \boldsymbol{\Omega}, E, t)\, d\varphi\, d\mu,$$

where, as above, $\mu = \cos\theta$.

The product of $\mathbf{v}$ and the neutron angular density is called the *neutron angular current* or the *vector flux*; that is,

$$\text{Vector flux} = \mathbf{v}N(\mathbf{r}, \boldsymbol{\Omega}, E, t). \tag{1.3}$$

It is a vector function of the four variables $\mathbf{r}$, $\boldsymbol{\Omega}$, E, and t with direction $\boldsymbol{\Omega}$. Its magnitude, i.e., $vN(\mathbf{r}, \boldsymbol{\Omega}, E, t)$, is sometimes called the *scalar flux*. In this book, however, it is referred to as the neutron *angular flux*, because of the dependence on angle; it is represented by $\Phi(\mathbf{r}, \boldsymbol{\Omega}, E, t)$, so that

$$\text{Angular flux} = vN(\mathbf{r}, \boldsymbol{\Omega}, E, t) \equiv \Phi(\mathbf{r}, \boldsymbol{\Omega}, E, t). \tag{1.4}$$

The integral of the angular flux over all directions, which is also equal to $vn(\mathbf{r}, E, t)$, is called the *total flux*, $\phi(\mathbf{r}, E, t)$, i.e.,

$$\text{Total flux} = vn(\mathbf{r}, E, t) = \int_{4\pi} \Phi(\mathbf{r}, \boldsymbol{\Omega}, E, t)\, d\boldsymbol{\Omega} \equiv \phi(\mathbf{r}, E, t). \tag{1.5}$$

The total flux is thus the same as the ordinary flux of neutrons of energy E at the position $\mathbf{r}$ and time t per unit energy. Both the angular flux and the total flux are sometimes referred to as the "flux," but the context, symbol, and arguments of the function indicate which type of flux is intended.*

* Some writers employ the same symbol for the vector flux and the total flux; the distinction is then indicated by the argument $(\mathbf{r}, \boldsymbol{\Omega}, E, t)$ or $(\mathbf{r}, E, t)$. By using the separate symbols Φ and ϕ, the distinction is clear even when the argument is omitted for simplicity of representation. The symbols N and n, for angular and (total) neutron density, respectively, are used in this book for the same reason.

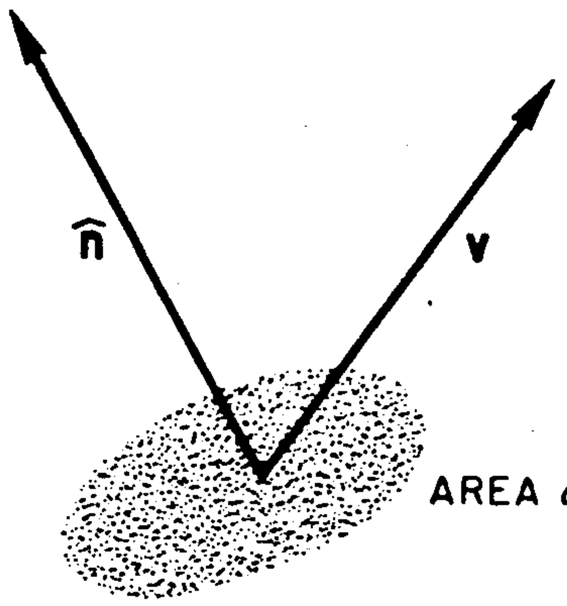

FIG. 1.3 UNIT VECTOR NORMAL TO SURFACE ELEMENT dA.

Neutron Current

If $\hat{\mathbf{n}}$ represents a unit vector normal to a surface, so that $\hat{\mathbf{n}}\,dA$ is the vector normal to a surface element of area dA (Fig. 1.3), then $\hat{\mathbf{n}}\,dA\cdot\mathbf{v}N(\mathbf{r}, \boldsymbol{\Omega}, E, t)$ is the number of neutrons crossing the surface element per unit solid angle per unit energy in unit time. (A crossing is counted as negative if $\hat{\mathbf{n}}\,dA\cdot\mathbf{v} < 0$.) Integration over all directions gives the net number of neutrons per unit energy and time crossing dA; thus,

$$\text{Net number of neutrons crossing } dA = \hat{\mathbf{n}}\,dA\cdot\int_{4\pi}\mathbf{v}N(\mathbf{r}, \boldsymbol{\Omega}, E, t)\,d\boldsymbol{\Omega}.$$

The integral in this expression is called the *neutron current* and is represented by $\mathbf{J}(\mathbf{r}, E, t)$, so that

$$\int_{4\pi}\mathbf{v}N(\mathbf{r}, \boldsymbol{\Omega}, E, t)\,d\boldsymbol{\Omega} = v\int_{4\pi}\boldsymbol{\Omega}N(\mathbf{r}, \boldsymbol{\Omega}, E, t)\,d\boldsymbol{\Omega} \equiv \mathbf{J}(\mathbf{r}, E, t). \qquad (1.6)$$

TABLE 1.1. COMPARISON OF SYMBOLS

	This Book	*W. & W.*[1]	*D.*[2]	*C. & Z.*[3]	*G. & E.*[4]	*L.*[5]
Angular Density	N	—	N	Ψ	—	—
Density	n	n	n	ρ	n	n
Angular flux	Φ	f	ψ	—	F	—
Total flux	ϕ	Φ	ρ	—	ϕ	ϕ
Current	$\mathbf{J}$	$\mathbf{J}$	$\mathbf{j}$	$\mathbf{J}$	$\mathbf{J}$	$\mathbf{J}$

[1] Weinberg, W., and E. P. Wigner, "The Physical Theory of Neutron Chain Reactors," University of Chicago Press, 1958.
[2] Davison, B., "Neutron Transport Theory," Oxford University Press, 1957.
[3] Case, K. M., and P. F. Zweifel, "Linear Transport Theory," Addison-Wesley Publishing Co., Inc., 1967.
[4] Glasstone, S., and M. C. Edlund, "The Elements of Nuclear Reactor Theory, D. Van Nostrand Co., Inc., 1952.
[5] Lamarsh, J. R., "Introduction to Nuclear Reactor Theory," Addison-Wesley Publishing Co., Inc., 1966.

It is the net number of neutrons of energy E at $\mathbf{r}$ and time t crossing unit area per unit energy and time. The current is thus a vector having as a component in any direction the net number of neutrons crossing a unit area perpendicular to that direction per unit energy and time, for given values of energy, time, and position.

A comparison of the symbols used in this book with those employed in other familiar texts is given in Table 1.1.

Independent Sources

The independent (or extraneous) neutron sources, usually abbreviated to *sources*, are neutron sources which are not dependent on the neutron density of the system. They arise from events other than neutron collisions, i.e., not from fission, $(n, 2n)$, and similar neutron reactions. The sources under consideration thus involve neutrons produced in (α, n) and spontaneous fission processes and also by the action of cosmic-ray particles. The independent sources are represented by $Q(\mathbf{r}, \mathbf{\Omega}, E, t)$, which is the probability per unit time that a neutron of energy E will appear at $\mathbf{r}$ per unit volume per unit solid angle per unit energy, i.e., $Q\, dV\, d\mathbf{\Omega}\, dE$ is the expected rate at which neutrons appear in volume dV with direction in $d\mathbf{\Omega}$ and energy in dE.

Cross Sections and Transfer Probabilities

Since microscopic cross sections are used only in some special cases in this text, it is convenient to employ a lower case sigma (σ) to represent *macroscopic cross sections*, reserving capital sigma (Σ) to indicate summation. The quantity $\sigma(\mathbf{r}, E)$ is defined as the total collision (or interaction) cross section of a neutron at position $\mathbf{r}$ having energy E (in the laboratory system). It is the probability of neutron interaction per unit distance of neutron travel and has the dimensions of a reciprocal length. The reciprocal of σ is, of course, the neutron mean free path.

The cross section has been taken to be a function of $\mathbf{r}$ and E only, but there are a few situations in which it may depend upon $\mathbf{\Omega}$ or t. If there is a physically preferred direction in a medium, which can be used to define directions, then σ may be a function of $\mathbf{\Omega}$. For example, a direction of fluid flow or of crystal orientation could determine a dependence of σ on $\mathbf{\Omega}$. In most cases, this will influence only thermal neutrons and the effects may usually be neglected. A variation of σ with t may arise in fuel depletion (or burnup) calculations; it is then so slow, however, that it is easily separable from the neutron transport problem. More general variations of cross sections with time will be treated in Chapters 9 and 10.

The total cross section $\sigma(\mathbf{r}, E)$ is the sum of the partial cross sections for all possible types of neutron-nucleus collisions. The partial cross sections are

indicated, in general, by the nature of the particle emerging from a collision; thus $\sigma_n(\mathbf{r}, E)$ and $\sigma_{n'}(\mathbf{r}, E)$ represent elastic and inelastic scattering cross sections, respectively, and $\sigma_\gamma(\mathbf{r}, E)$ is the cross section for radiative capture. A special case arises in connection with the fission cross section which is indicated by $\sigma_f(\mathbf{r}, E)$.

In neutron transport theory, it is required to describe the probability that the neutrons emerging from a collision have various directions and energies. A form of differential cross section is defined for collisions, such as scattering, fission, and $(n, 2n)$ reactions, from which neutrons emerge, as the cross section for neutrons of initial direction $\mathbf{\Omega}'$ and energy E' emerging from a collision in the interval $d\mathbf{\Omega}$ about $\mathbf{\Omega}$ and energy dE about E. This quantity may be expressed, in general for the reaction (n, x), by

$$\text{Differential cross section} = \sigma_x(\mathbf{r}, E')f_x(\mathbf{r}; \mathbf{\Omega}', E' \to \mathbf{\Omega}, E),$$

where σ_x is the cross section for a reaction of type x for neutrons of energy E' and $f_x(\mathbf{r}; \mathbf{\Omega}', E' \to \mathbf{\Omega}, E)\, d\mathbf{\Omega}\, dE$ is the probability that if a neutron of direction $\mathbf{\Omega}'$ and energy E' has a collision of type x, there will emerge from the collision a neutron in the direction interval $d\mathbf{\Omega}$ about $\mathbf{\Omega}$ with energy in dE about E. For scattering (elastic or inelastic) collisions one neutron emerges for each neutron colliding with a nucleus; the transfer probabilities may consequently be normalized to unity. Thus, for elastic scattering, integration over all directions and energies gives

$$\iint f_n(\mathbf{r}; \mathbf{\Omega}', E' \to \mathbf{\Omega}, E)\, d\mathbf{\Omega}\, dE = 1,$$

and a similar expression applies to inelastic scattering. For fission, however, the normalization is different, as will be seen shortly. For (n, γ), (n, α), and other reactions from which neutrons do not emerge, f is, of course, zero.

For *elastic scattering* of neutrons from initially stationary nuclei, f_n is a function only of $\mathbf{\Omega}' \cdot \mathbf{\Omega} = \mu_0$, where μ_0 is the cosine of the (scattering) angle (θ) between the directions of motion of the neutron before and after the collision in the laboratory system (Fig. 1.4). For scattering nuclei of mass A times the mass of a neutron, the value of μ_0 is determined uniquely by E/E';[3] thus,

$$\mu_0 = \frac{1}{2}\left[(A + 1)\sqrt{\frac{E}{E'}} - (A - 1)\sqrt{\frac{E'}{E}}\right] \equiv S.$$

In this case, f_n may be represented by

$$f_n(\mathbf{r}; \mathbf{\Omega}', E' \to \mathbf{\Omega}, E) = f_n(\mathbf{r}; E' \to E)\, \delta(\mu_0 - S), \tag{1.7}$$

where δ is the Dirac delta function (see Appendix); that is, $\delta(\mu_0 - S)$ is zero except when $\mu_0 = S$ and $\int \delta(\mu_0 - S)f(\mu_0)\, d\mu_0 = f(S)$ if the range of integration includes the value $\mu_0 = S$.

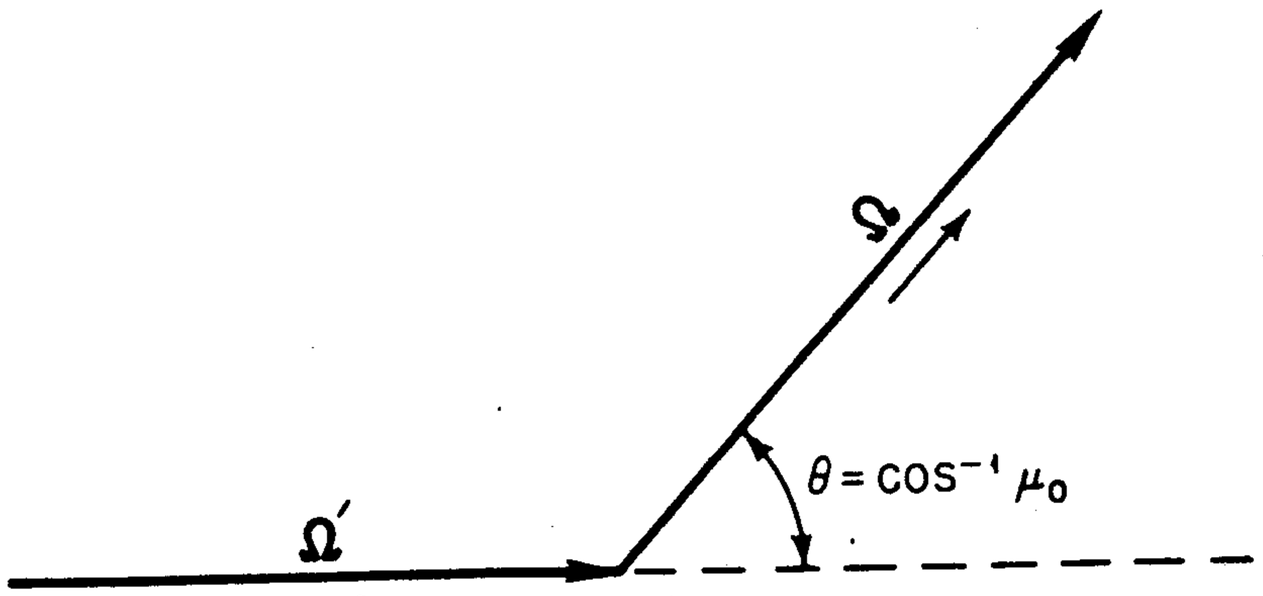

FIG. 1.4 DIRECTIONS OF MOTION OF NEUTRON BEFORE AND AFTER ELASTIC SCATTERING.

If the elastic scattering is spherically symmetric (isotropic) in the center-of-mass system, it is known[4] that

$$f_n(\mathbf{r}; E' \to E) = \frac{1}{2\pi(1-\alpha)E'} \quad \text{if} \quad \alpha E' \leqslant E \leqslant E'$$
$$= 0 \quad \text{if} \quad E > E' \quad \text{or} \quad E < \alpha E'$$

where

$$\alpha \equiv [(A-1)/(A+1)]^2.$$

For more general angular distributions, however, this simple representation is not possible (see Chapter 4). Consideration will be given in Chapter 7 to the effects of nuclear motion and chemical binding.

In the foregoing, it has been assumed that the transport medium consists of a single nuclear species. If the medium is a mixture of different nuclei, however, the f values are obtained in a manner similar to that used in deriving the overall macroscopic cross section from the individual microscopic cross sections.[5]

For *fission*, it is a good approximation to assume that the neutrons are emitted isotropically in the laboratory system; hence, it is possible to write

$$f_f(\mathbf{r}; \boldsymbol{\Omega}', E' \to \boldsymbol{\Omega}, E)\, d\boldsymbol{\Omega}\, dE = \frac{1}{4\pi}\, \nu(\mathbf{r}; E' \to E)\, d\boldsymbol{\Omega}\, dE,$$

where $\nu(\mathbf{r}; E' \to E)\, dE$, referred to as the *spectrum of the fission neutrons*, is the probability that a fission caused by a neutron at $\mathbf{r}$ with energy E' will lead to a neutron within dE about E. Furthermore, $\nu(\mathbf{r}; E' \to E)$ is normalized so that

$$\frac{1}{4\pi}\iint \nu(\mathbf{r}; E' \to E)\, d\boldsymbol{\Omega}\, dE = \int \nu(\mathbf{r}; E' \to E)\, dE = \bar{\nu}(\mathbf{r}, E'),$$

where $\bar{\nu}(\mathbf{r}, E')$ is the average number of neutrons produced by a fission at $\mathbf{r}$ caused by a neutron of energy E'. It will be noted that the spectrum of fission neutrons is allowed to depend on the energy (E') and the material in the medium, through $\mathbf{r}$.

For the present, no distinction is made between prompt and delayed neutrons. All neutrons are assumed to emerge promptly from fission, thus ignoring the delayed neutrons; alternatively, the delayed neutrons are assumed to be included with the prompt neutrons. In Chapter 9, however, when reactor dynamics is discussed, allowance is made for the delayed neutrons by introducing a time delay between the neutron-nucleus collision and neutron emission in fission.

If $\sigma(\mathbf{r}, E')$ is the *total* cross section for all interactions, including those from which neutrons do not emerge, then the total probability per unit distance at $\mathbf{r}$ for the transfer of a neutron from $\mathbf{\Omega}'$, E' to $\mathbf{\Omega}$, E, as a result of all interactions can be written as

$$\begin{matrix}\text{Total probability of neutron} \\ \text{transfer from } \mathbf{\Omega}', E' \text{ to } \mathbf{\Omega}, E\end{matrix} = \sigma(\mathbf{r}, E')f(\mathbf{r}; \mathbf{\Omega}', E' \to \mathbf{\Omega}, E),$$

which defines the function f. This result may be expressed in an alternative manner by considering the separate interactions x in which neutrons are produced; thus,

$$\sigma(\mathbf{r}, E')f(\mathbf{r}; \mathbf{\Omega}', E' \to \mathbf{\Omega}, E) = \sum_x \sigma_x(\mathbf{r}, E')f_x(\mathbf{r}; \mathbf{\Omega}', E' \to \mathbf{\Omega}, E),$$

where the sum over x includes elastic and inelastic scattering (with the f's normalized to unity), fission (with f normalized to $\bar{\nu}(\mathbf{r}, E')$), the $(n, 2n)$ reaction (with f normalized to 2), and so on. Upon integration over all directions $\mathbf{\Omega}$ and over all final energies E, it is found upon rearrangement that

$$\begin{aligned}\iint f(\mathbf{r}; \mathbf{\Omega}', E' \to \mathbf{\Omega}, E)\, d\mathbf{\Omega}\, dE &= \frac{\sigma_n(\mathbf{r}, E') + \sigma_{n'}(\mathbf{r}, E') + \sigma_f(\mathbf{r}, E')\bar{\nu}(\mathbf{r}, E') + \cdots}{\sigma(\mathbf{r}, E')} \\ &\equiv c(\mathbf{r}, E), \qquad (1.8)\end{aligned}$$

where the subscripts n, n', f, etc., refer to elastic scattering, inelastic scattering, fission, etc., respectively.

The right side of equation (1.8), and hence also the integral on the left, is clearly the mean number of neutrons emerging per collision at $\mathbf{r}$ of neutrons of energy E'. This quantity has been represented by the symbol $c(\mathbf{r}, E)$. For pure capture collisions, e.g., (n, γ) and (n, α), in which no neutrons are produced, $c = 0$, for scattering collisions $c = 1$, and for fission $c = \bar{\nu}$. The quantity c can be introduced as a factor in the neutron transport equation, as will be seen in Chapter 2.

The fission part of the total probability of neutron transfer from $\mathbf{\Omega}'$, E' to $\mathbf{\Omega}$, E may be separated from that due to other collisions by writing

$$\begin{aligned}\sigma(\mathbf{r}, E')f(\mathbf{r}; \mathbf{\Omega}', E' \to \mathbf{\Omega}, E) = &\frac{1}{4\pi}\sigma_f(\mathbf{r}, E')\nu(\mathbf{r}; E' \to E) \\ &+ \sum_{x \neq f} \sigma_x(\mathbf{r}, E')f_x(\mathbf{r}; \mathbf{\Omega}', E' \to \mathbf{\Omega}, E),\end{aligned}$$

where the summation over $x \neq f$ is for all nonfission interactions from which neutrons emerge.

Interaction Rates

The macroscopic cross section, σ_x, is the probability that a neutron will undergo a particular reaction, indicated by x, in unit distance. If v is the speed of the neutron, then $v\sigma_x$ is the corresponding probability per unit time. Hence, if N is the angular density of neutrons under consideration, the interaction rate, in appropriate units, is given by $v\sigma_x N$. For unit volume and energy, the interaction rate is obtained by integrating over all neutron directions to obtain $v\sigma_x n$. Thus $v\sigma_x(\mathbf{r}, E)n(\mathbf{r}, E, t)$ gives the number of interactions of type x made with nuclei by neutrons of speed v, and corresponding energy E, at position $\mathbf{r}$ and time t per unit volume per unit energy per unit time. The total number of interactions (or collisions) is obtained by using σ, the total macroscopic cross section, which is the sum of all the σ_x values.

To determine the rate at which neutrons emerge from an interaction of type x, the appropriate f_x must be included for the interaction and the neutron parameters before and after interaction must be identified. The number of neutrons per unit volume having directions within $d\Omega'$ about Ω' and energies within dE' about E' is $N(\mathbf{r}, \Omega', E', t)\, d\Omega'\, dE'$. The rate, in neutrons per unit volume and time at $\mathbf{r}$ and t, at which such neutrons are transferred by interactions of type x into final directions within $d\Omega$ about Ω and final energies within dE about E is then

$$v'\sigma_x(\mathbf{r}, E')f_x(\mathbf{r}; \Omega', E' \rightarrow \Omega, E)N(\mathbf{r}, \Omega', E', t)\, d\Omega'\, dE'\, d\Omega\, dE.$$

The total rate at which neutrons are transferred is obtained by integrating over all initial neutron directions and energies, i.e., over $d\Omega'$ and dE', and summing over all reactions, i.e., summing over x.

The foregoing results are used in various forms in the development of the neutron transport equation.

1.1c Derivation of the Neutron Transport Equation

According to the definition given earlier, $N(\mathbf{r}, \Omega, E, t)\, dV\, d\Omega\, dE$ is the probable number of neutrons at time t in a volume element dV having energies in dE about E and directions within a narrow beam $d\Omega$ about Ω. Consider now what happens to this group (or packet) of neutrons as they are followed for a time interval Δt. It is assumed in the following that the cross sections are continuous functions of position in the vicinity of position $\mathbf{r}$. The special case of an interface at which cross sections change discontinuously will be considered shortly.

Those neutrons of energy E which suffer a collision may be regarded as being lost from the packet, whereas those which do not collide remain. The distance

traveled by a neutron in time Δt is $v\,\Delta t$; hence, the probability that a neutron makes a collision in this time is $\sigma(\mathbf{r}, E)v\,\Delta t$ to first order in Δt. The probability that a neutron does not undergo a collision in time Δt and remains in the packet is consequently $1 - \sigma(\mathbf{r}, E)v\,\Delta t$. It follows, therefore, that

$$\begin{pmatrix}\text{Number of neutrons}\\ \text{remaining in packet}\end{pmatrix} = N(\mathbf{r}, \boldsymbol{\Omega}, E, t)[1 - \sigma(\mathbf{r}, E)v\,\Delta t]\,dV\,d\boldsymbol{\Omega}\,dE.$$

These neutrons will arrive at the position $\mathbf{r} + \boldsymbol{\Omega}v\,\Delta t$ at time $t + \Delta t$.

In addition to neutrons lost from the packet by collisions, some may enter it as a result of collisions by neutrons outside the packet and from independent sources. The latter two quantities are given by

$$\begin{pmatrix}\text{Number of neutrons entering}\\ \text{packet as a result of collisions}\end{pmatrix} = \left[\iiint \sigma(\mathbf{r}, E')f(\mathbf{r}; \boldsymbol{\Omega}', E' \to \boldsymbol{\Omega}, E)v'N(\mathbf{r}, \boldsymbol{\Omega}', E', t)\,d\boldsymbol{\Omega}'\,dE'\right] dV\,d\boldsymbol{\Omega}\,dE\,\Delta t$$

and

$$\begin{pmatrix}\text{Number of neutrons entering}\\ \text{packet from sources}\end{pmatrix} = Q(\mathbf{r}, \boldsymbol{\Omega}, E, t)\,dV\,d\boldsymbol{\Omega}\,dE\,\Delta t.$$

By adding the three terms given above and eliminating $dV\,d\boldsymbol{\Omega}\,dE$, the neutron angular density at the position $\mathbf{r} + \boldsymbol{\Omega}v\,\Delta t$ at time $t + \Delta t$ is found to be

$$N(\mathbf{r} + \boldsymbol{\Omega}v\,\Delta t, \boldsymbol{\Omega}, E, t + \Delta t) = N(\mathbf{r}, \boldsymbol{\Omega}, E, t)(1 - \sigma v\,\Delta t) + \left[\iiint \sigma' f v' N(\mathbf{r}, \boldsymbol{\Omega}', E', t)\,d\boldsymbol{\Omega}'\,dE'\right]\Delta t + Q\,\Delta t \tag{1.9}$$

where, to simplify the representation,

$$\sigma \equiv \sigma(\mathbf{r}, E),$$
$$\sigma' f \equiv \sigma(\mathbf{r}, E')f(\mathbf{r}; \boldsymbol{\Omega}', E' \to \boldsymbol{\Omega}, E), \quad \text{frequently written as } \sigma f(\mathbf{r}; \boldsymbol{\Omega}', E' \to \boldsymbol{\Omega}, E),$$
$$Q \equiv Q(\mathbf{r}, \boldsymbol{\Omega}, E, t).$$

Upon dividing both sides of this expression by Δt and letting $\Delta t \to 0$, the result, after rearrangement, is

$$\lim_{\Delta t \to 0}\left[\frac{N(\mathbf{r} + \boldsymbol{\Omega}v\,\Delta t, \boldsymbol{\Omega}, E, t + \Delta t) - N(\mathbf{r}, \boldsymbol{\Omega}, E, t)}{\Delta t}\right] + \sigma v N(\mathbf{r}, \boldsymbol{\Omega}, E, t) = \iint \sigma' f v' N(\mathbf{r}, \boldsymbol{\Omega}', E', t)\,d\boldsymbol{\Omega}'\,dE' + Q. \tag{1.10}$$

The first term on the left of equation (1.10) is the total time derivative of the neutron angular density; that is to say, it is the derivative with respect to time as it would appear to an observer moving with the packet of neutrons. It will be denoted by dN/dt, where N represents $N(\mathbf{r}, \boldsymbol{\Omega}, E, t)$.

If the term $N(\mathbf{r}, \mathbf{\Omega}, E, t + \Delta t)$ is added and subtracted from the numerator in the square brackets in equation (1.10), two expressions are obtained which can be readily evaluated. Thus,

$$\lim_{\Delta t \to 0} \left[\frac{N(\mathbf{r}, \mathbf{\Omega}, E, t + \Delta t) - N(\mathbf{r}, \mathbf{\Omega}, E, t)}{\Delta t} \right] = \frac{\partial N}{\partial t} \tag{1.11}$$

and

$$\lim_{\Delta t \to 0} \left[\frac{N(\mathbf{r} + \mathbf{\Omega} v\, \Delta t, \mathbf{\Omega}, E, t + \Delta t) - N(\mathbf{r}, \mathbf{\Omega}, E, t + \Delta t)}{\Delta t} \right] = v\mathbf{\Omega} \cdot \nabla N(\mathbf{r}, \mathbf{\Omega}, E, t). \tag{1.12}$$

The last result can be readily derived in Cartesian coordinates in which $\mathbf{r}$ has components x, y, z, and $\mathbf{\Omega}$ has components Ω_x, Ω_y, Ω_z. The left side of equation (1.12) can then be written as

$$\lim_{\Delta t \to 0} \left[\frac{N(x + \Omega_x v\, \Delta t, y + \Omega_y v\, \Delta t, z + \Omega_z v\, \Delta t, \ldots) - N(x, y, z, \ldots)}{\Delta t} \right]$$

$$= v\Omega_x \frac{\partial N}{\partial x} + v\Omega_y \frac{\partial N}{\partial y} + v\Omega_z \frac{\partial N}{\partial z},$$

where N is written for $N(x, y, z, \ldots)$. This expression is v times the directional derivative of N in the direction $\mathbf{\Omega}$; it can consequently be represented by $v\mathbf{\Omega} \cdot \nabla N$, as in equation (1.12).

Upon inserting equations (1.10), (1.11), and (1.12) into equation (1.1), the result is

$$\frac{\partial N}{\partial t} + v\mathbf{\Omega} \cdot \nabla N + \sigma v N = \iint \sigma' f v' N'\, d\mathbf{\Omega}'\, dE' + Q, \tag{1.13}$$

where

$$N \equiv N(\mathbf{r}, \mathbf{\Omega}, E, t)$$
$$N' \equiv N(\mathbf{r}, \mathbf{\Omega}', E', t),$$

and σ, $\sigma' f$, and Q are as defined above, in order to avoid unnecessary complexity. Equation (1.13) is the basic form of the *neutron transport equation*. In spite of certain minor limitations, which have been indicated earlier and which will be considered more fully in §1.4, the transport equation has been found to be satisfactory for treating most problems in reactor physics.

Before proceeding further, it is of interest to consider the physical significance of the first two terms on the left side of equation (1.13) which together are equal to the first term on the left of equation (1.10). The quantity $\partial N/\partial t$ is the time rate of change of the neutron angular density at the fixed position $\mathbf{r}$; this differs from dN/dt, the rate of change within the packet which is moving with the neutron velocity $\mathbf{v} = v\mathbf{\Omega}$. The difference, $-v\mathbf{\Omega} \cdot \nabla N$, represents the rate of change of the neutron angular density at the position $\mathbf{r}$ due to streaming of the

neutrons, i.e., motion of the neutrons in a straight line without any collisions. The rate of change computed by an observer moving with the neutron packet is dN/dt, with no contribution from streaming, whereas if it is determined by a stationary observer at $\mathbf{r}$ the result is $\partial N/\partial t$ which includes the change due to neutron streaming. The term $v\boldsymbol{\Omega}\cdot\nabla N$ is consequently sometimes referred to as the *streaming term* in the neutron transport equation.

That this term does indeed represent the effect of streaming may be seen by deriving the rate at which neutrons stream through a small volume element. Let this element be bounded by planes having the coordinates x, $x + \Delta x$; y, $y + \Delta y$; and z, $z + \Delta z$, so that the volume $dV = \Delta x\,\Delta y\,\Delta z$ (Fig. 1.5). The number of neutrons in the volume element that are moving in the direction $\boldsymbol{\Omega}$ is then $N(x, y, z, \boldsymbol{\Omega}, E, t)\,dV$. The rate at which neutrons enter the volume element as a result of motion across the two faces perpendicular to the x direction, i.e., the faces with coordinates x and $x + \Delta x$, is then

$$\begin{aligned}&\text{Number of neutrons entering}\\&\text{volume element per unit time} = v_x N(x, y, z)\,\Delta y\,\Delta z,\\&\text{(across face at } x)\end{aligned}$$

$$\begin{aligned}&\text{Number of neutrons leaving}\\&\text{volume element per unit time} = v_x N(x + \Delta x, y, z)\,\Delta y\,\Delta z,\\&\text{(across face at } x + \Delta x)\end{aligned}$$

where v_x is the x component of the velocity; the arguments $(\boldsymbol{\Omega}, E, t)$ have been omitted for simplicity. The difference between these two numbers gives the x component of the streaming rate of the neutrons, i.e., the rate of change of the neutron angular flux in dV due to neutrons crossing the two faces of the volume element for which x is constant. It follows, therefore, that

$$\text{Streaming rate } (x \text{ coordinate}) = -v_x \frac{\partial N}{\partial x}\,dV = -(\mathbf{v}\cdot\nabla N)_x\,dV,$$

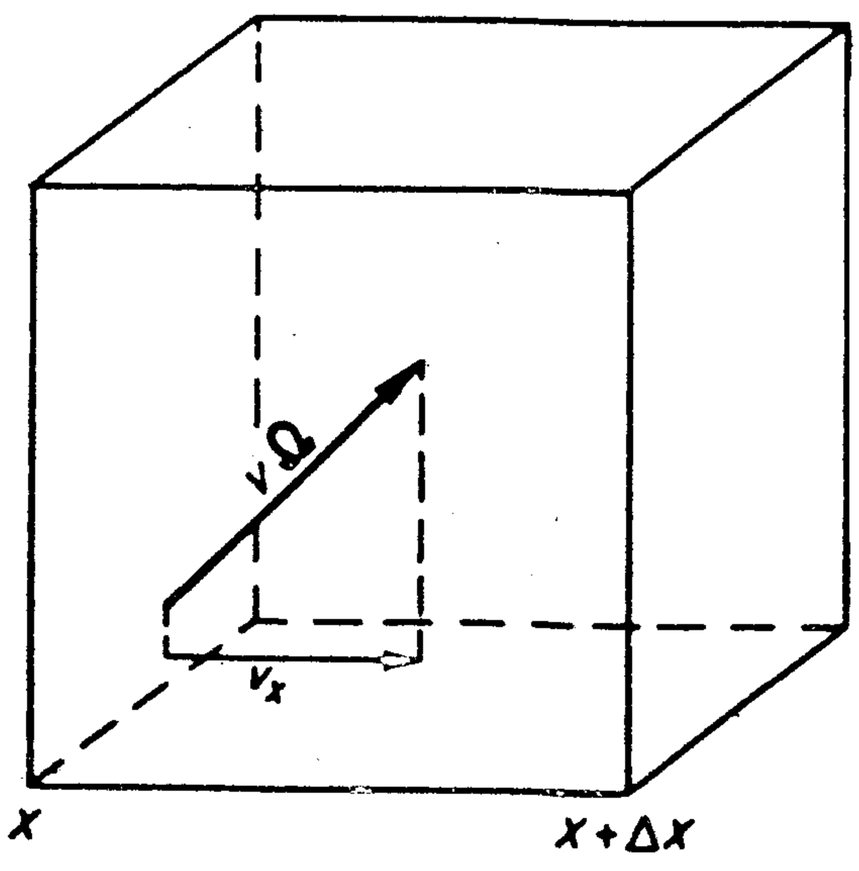

FIG. 1.5 CALCULATION OF STREAMING TERM.

and hence the net rate at which neutrons enter the small volume element due to streaming is then $-\mathbf{v}\cdot\nabla N$ per unit volume. This quantity is equal to $-v\boldsymbol{\Omega}\cdot\nabla N$; consequently,

$$\frac{\partial N}{\partial t} = \frac{dN}{dt} - v\boldsymbol{\Omega}\cdot\nabla N.$$

The foregoing discussion of the streaming term could be elaborated somewhat to provide an alternative method of deriving the neutron transport equation.[6] In such a derivation, attention is fixed on a small stationary volume element at the position $\mathbf{r}$. The rate of change of the neutron angular density in the volume element then results from both collisions and streaming. The transport equation is obtained by adding these contributions.

The neutron transport equation (1.13) may also be expressed in terms of the angular flux Φ, which is equal to vN; thus, writing

$$\Phi = vN \equiv \Phi(\mathbf{r}, \boldsymbol{\Omega}, E, t),$$
$$\Phi' = v'N' \equiv \Phi(\mathbf{r}, \boldsymbol{\Omega}', E', t),$$

the result is

$$\frac{1}{v}\cdot\frac{\partial\Phi}{\partial t} + \boldsymbol{\Omega}\cdot\nabla\Phi + \sigma\Phi = \iint \sigma' f \Phi'\, d\boldsymbol{\Omega}'\, dE' + Q. \tag{1.14}$$

This is the form of the transport equation that will be used most frequently in later chapters.

1.1d Interface and Boundary Conditions

Some Interface Conditions

It was postulated in the derivation of the neutron transport equation that the cross sections are continuous functions of position in the vicinity of $\mathbf{r}$. However, solutions to the transport equation are frequently sought in spatial regions where there are interfaces between different materials. At such interfaces, the cross sections are discontinuous and it is necessary to consider how the transport equation is to be used in these circumstances.

The important point to bear in mind is that the number of neutrons in a packet is not changed merely by crossing a physical interface. This means that the neutron angular density must be continuous in $\mathbf{r}$ as the interface is crossed or, more formally, $N(\mathbf{r} + s\boldsymbol{\Omega}, \boldsymbol{\Omega}, E, t + s/v)$ must be a continuous function of s, where s is a distance along $\boldsymbol{\Omega}$. Hence, the neutron transport equation is to be regarded as applying on either side of the interface and the continuity condition is to be used at the interface.[7]*

* Although the discussion of interface and boundary conditions in this section refers in particular to the neutron angular density, it is equally applicable to the angular flux. The conclusions are used in the latter sense in several subsequent chapters.

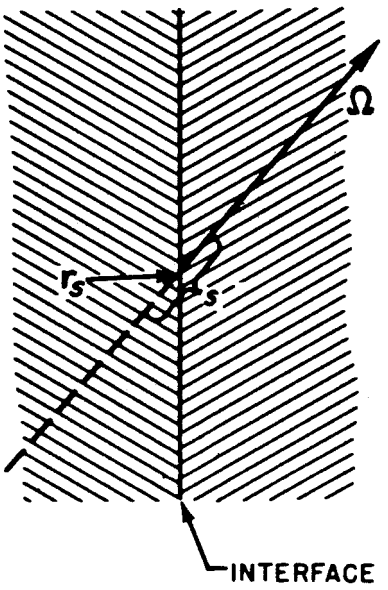

FIG. 1.6 DERIVATION OF CONTINUITY CONDITION.

The continuity condition given above could also have been deduced in the course of deriving the transport equation. It would only be necessary to consider equation (1.10) in the situation where $\mathbf{r}$ and $\mathbf{r} + \Omega v\,\Delta t$ lie on opposite sides of an interface at $\mathbf{r}_s$. Suppose

$$\mathbf{r} = \mathbf{r}_s - \tfrac{1}{2}s\Omega \quad \text{and} \quad \mathbf{r} + \Omega v\,\Delta t = \mathbf{r}_s + \tfrac{1}{2}s\Omega,$$

where s is a distance along Ω between the points on either side of the interface, as represented in Fig. 1.6. It would be found that

$$\lim_{s\to 0}\left[N\left(\mathbf{r}_s + \tfrac{1}{2}s\Omega, \Omega, E, t + \frac{s}{2v}\right) - N\left(\mathbf{r}_s - \tfrac{1}{2}s\Omega, \Omega, E, t - \frac{s}{2v}\right)\right] = 0,$$

which is the same as the continuity condition.

Although in physical systems the neutron angular density is always continuous in the sense described here, it is sometimes convenient to consider a neutron source as being concentrated on a surface (§1.1f). At such a surface source, the neutron angular density is not continuous, but the discontinuity can be determined, as will be seen in the next chapter. Similarly, it is sometimes desirable to represent a thin strongly absorbing region as a surface of discontinuity in the neutron angular density. The required discontinuity can then be derived in an analogous manner.

Boundary Conditions

The neutron transport equation is usually regarded as describing the transport of neutrons in a finite region of space, in which cross sections are known functions of position and energy. Such an equation has an infinite number of possible solutions within any spatial region and in order to determine which of

these corresponds to the physical problem it is necessary to specify the appropriate conditions on the neutron angular density at the boundary of the region.*

In general, the region of interest is surrounded by a convex (or non-reentrant) surface; that is to say, a straight line segment connecting any two points in the region lies entirely within the region. A neutron leaving the surface of such a region cannot intersect the surface again. If the physical surface is a reentrant one, it can be assumed to be surrounded by a convex surface at which the boundary conditions are imposed. If neutrons enter the region from external sources, then the incoming neutron flux must be specified.

If no neutrons enter from external sources and if a neutron, once it leaves the surface, cannot return, then the surface is called a *free surface*. The boundary conditions on the neutron angular density at a free surface are as follows. Let $\hat{\mathbf{n}}$ be a unit vector in the direction of the outward normal at a position $\mathbf{r}$ on the surface. Then any neutron at $\mathbf{r}$ having $\hat{\mathbf{n}}\cdot\boldsymbol{\Omega} > 0$ will be crossing the surface in an outward direction whereas a neutron for which $\hat{\mathbf{n}}\cdot\boldsymbol{\Omega} < 0$ will be crossing in the inward direction. Hence, the requirement that there be no incoming neutrons is that for all positions $\mathbf{r}$ on the boundary surface

$$N(\mathbf{r}, \boldsymbol{\Omega}, E, t) = 0 \quad \text{if} \quad \hat{\mathbf{n}}\cdot\boldsymbol{\Omega} < 0. \tag{1.15}$$

In a practical situation it is, of course, not possible to isolate a system completely from its environment. A neutron leaving the system will have a finite probability of returning; hence, the free-surface boundary conditions are an idealization. Nevertheless, they are very useful because (*a*) for many systems the probability of neutron return is negligible, and (*b*) it is always possible to choose the bounding surface far enough from the volume of interest that approximate boundary conditions suffice. For example, small deviations from free-surface boundary conditions imposed at the outside of a reactor shield, or even of the reflector, have a negligible effect on the criticality.

1.1e Conservation Relations

The neutron transport equation is simply a statement of neutron conservation as applied to an infinitesimal element of volume, direction, and energy. If it is integrated over all directions, the result will be a statement of neutron conservation for a small element of volume and energy. Before performing the integration, however, it should be noted that since the gradient operator involves derivatives

* In addition to conditions at the boundary of the spatial region, some conditions on the neutron density, or alternatively on the source and cross sections, may be required at high energies.[8] Normally, the energy variable is restricted to a finite range $0 \leqslant E \leqslant E_{max}$; neutrons of higher energy than E_{max} are not considered except insofar as they may produce some neutrons with $E < E_{max}$ which would be included in the source, Q. Furthermore, initial conditions on the neutron angular density are required in order to determine the solution to the transport equation, as will be seen in §1.5a.

with respect to position coordinates only, it follows that

$$\boldsymbol{\Omega}\cdot\nabla N = \nabla\cdot\boldsymbol{\Omega}N \tag{1.16}$$

and hence

$$v\int_{4\pi}\boldsymbol{\Omega}\cdot\nabla N\,d\boldsymbol{\Omega} = v\nabla\cdot\int_{4\pi}\boldsymbol{\Omega}N\,d\boldsymbol{\Omega} = \nabla\cdot\mathbf{J},$$

in accordance with the definition of the neutron current, $\mathbf{J}$, in equation (1.6).

Integration of equation (1.13) over all values of $\boldsymbol{\Omega}$ consequently gives

$$\frac{\partial n}{\partial t} + \nabla\cdot\mathbf{J} + \sigma v n = \int \sigma(\mathbf{r}; E' \to E)v'n'\,dE' + Q, \tag{1.17}$$

where

$$n \equiv n(\mathbf{r}, E, t) \quad \text{and} \quad n' \equiv n(\mathbf{r}, E', t)$$

are the neutron densities. In this expression, also

$$Q \equiv Q(\mathbf{r}, E, t) = \int Q(\mathbf{r}, \boldsymbol{\Omega}, E, t)\,d\boldsymbol{\Omega}$$

and

$$\sigma(\mathbf{r}; E' \to E) \equiv \int \sigma(\mathbf{r}, E')f(\mathbf{r}; \boldsymbol{\Omega}', E' \to \boldsymbol{\Omega}, E)\,d\boldsymbol{\Omega}. \tag{1.18}$$

That is, the integral of $\sigma' f$ over all final directions gives $\sigma(\mathbf{r}; E' \to E)$, which is defined to be the cross section at $\mathbf{r}$ for collisions which result in a neutron of energy E' being replaced by one of energy E.

Integration of equation (1.17) over a finite region of volume and energy now yields a conservation equation for the whole population of neutrons in the region. Thus, the result of integrating equation (1.17) over a finite volume and over energy is

$$\underbrace{\frac{\partial \iiint n\,dV\,dE}{\partial t}}_{\text{I}} + \underbrace{\iint\int \nabla\cdot\mathbf{J}\,dV\,dE}_{\text{II}} + \underbrace{\iint v\sigma n\,dV\,dE}_{\text{III}} = \underbrace{\iiint\int \sigma(\mathbf{r}; E' \to E)v'n'\,dE'\,dV\,dE}_{\text{IV}} + \underbrace{\iint Q\,dV\,dE}_{\text{V}}. \tag{1.19}$$

Each of the five terms in equation (1.19) has a clear physical significance, as will now be shown.

The quantity $\iiint n\,dV\,dE$ is the total number of neutrons in the space–energy region under consideration; hence, term I is the time rate of change of the total number of neutrons in this region.

In connection with term II, the divergence theorem may be used to write

$$\iint_V \nabla \cdot \mathbf{J}\, dV\, dE = \iint_A \mathbf{J} \cdot \hat{\mathbf{n}}\, dA\, dE,$$

where dA refers to an element of area, A, on the bounding surface of the region, V, under consideration and $\hat{\mathbf{n}}$ is a unit vector normal to the surface element and directed outward from the region. By definition, $\mathbf{J} \cdot \hat{\mathbf{n}}$ is the net number of neutrons crossing unit area of the surface in unit time. Hence, term II is the net number of neutrons flowing out of the space-energy region per unit time.

Term III is the rate at which neutrons are entering into collisions in the given region, i.e., the total collision rate, and IV is the rate at which they emerge from these collisions. Hence, IV − III is the net rate at which neutrons are generated in collisions. Finally, term V gives the rate at which neutrons from independent sources are introduced into the region. If equation (1.19) is rearranged in the form

$$\text{I} = (\text{IV} - \text{III}) + \text{V} - \text{II},$$

it does indeed represent neutron conservation in the space-energy region under consideration, for this expression states that

$$\begin{pmatrix}\text{Rate of change}\\ \text{of neutrons}\end{pmatrix} = \begin{pmatrix}\text{Net rate of generation}\\ \text{of neutrons in collisions}\end{pmatrix} + \begin{pmatrix}\text{Rate of introduction}\\ \text{of source neutrons}\end{pmatrix} - \begin{pmatrix}\text{Net rate of outflow}\\ \text{of neutrons.}\end{pmatrix}$$

1.1f Linearity of the Transport Equation: Green's Function

It may be noted that the homogeneous (source-free) neutron transport equation

$$\frac{1}{v}\frac{\partial \Phi}{\partial t} + \boldsymbol{\Omega} \cdot \nabla \Phi + \sigma \Phi = \iint \sigma' f \Phi'\, d\boldsymbol{\Omega}'\, dE'$$

is linear, where the term "linear" implies that if Φ_1 and Φ_2 (or N_1 and N_2 in the corresponding expression for $\partial N/\partial t$) are solutions then $\Phi_1 + \Phi_2$ (or $N_1 + N_2$) is also a solution. Certain (homogeneous) boundary conditions must be satisfied, as will be seen shortly.

For the inhomogeneous transport equation, i.e., for a system with a source, the linearity has a related consequence. If a solution Φ_1 corresponds to a source Q_1 and a solution Φ_2 to a source Q_2, then, subject to certain boundary conditions, the flux $\Phi_1 + \Phi_2$ is a solution for the source $Q_1 + Q_2$. In general, if a complex source Q can be divided into a number of simpler sources, Q_i, so that

$$Q = \sum_i Q_i,$$

then the angular flux Φ corresponding to the source Q will be

$$\Phi = \sum_i \Phi_i,$$

where each Φ_i is a solution of the transport equation for the source Q_i, provided the boundary conditions mentioned below are satisfied.

The result given above depends on the existence of boundary conditions for the problem so that all solutions Φ_i and also their sum, Φ, satisfy these conditions. Such boundary conditions are often called homogeneous. For a volume source with free-surface boundary conditions, i.e., no incoming neutrons, as defined earlier, this is certainly the case. If the boundary conditions correspond to an incident flux, the latter can be treated as a surface source with free-surface boundary conditions, as will be seen below.

The additivity of the individual values of Φ_i suggests that the solution of the transport equation for any arbitrary complex source could be obtained by the superposition (or integral) of the solutions for simple point (or other) sources. The solution for the simple source is known as *Green's function* for the problem, and various special forms can be found for different geometries. The (one-speed) Green's function for plane geometry will be derived in Chapter 2.

As an example of the use of Green's function, consider, first, the time-independent neutron transport equation (1.14) for the flux, i.e., with $\partial\Phi/\partial t = 0$. The results will be generalized later to the time-dependent situation. Let the Green's function $G(\mathbf{r}_0, \boldsymbol{\Omega}_0, E_0 \to \mathbf{r}, \boldsymbol{\Omega}, E)$ be the neutron angular flux at $\mathbf{r}, \boldsymbol{\Omega}, E$ due to a unit point source, i.e., a source emitting 1 neutron/sec, located at $\mathbf{r}_0, \boldsymbol{\Omega}_0, E_0$. By definition, this satisfies the transport equation (1.14); thus, for free-surface boundary conditions,

$$\boldsymbol{\Omega}\cdot\nabla G + \sigma G = \int\int \sigma' f G' \, d\boldsymbol{\Omega}' \, dE' + \delta(\mathbf{r} - \mathbf{r}_0)\,\delta(\boldsymbol{\Omega} - \boldsymbol{\Omega}_0)\,\delta(E - E_0), \quad (1.20)$$

where

$$G \equiv G(\mathbf{r}_0, \boldsymbol{\Omega}_0, E_0 \to \mathbf{r}, \boldsymbol{\Omega}, E)$$

and

$$G' \equiv G(\mathbf{r}_0, \boldsymbol{\Omega}_0, E_0 \to \mathbf{r}, \boldsymbol{\Omega}', E').$$

The other symbols have the same significance as before.

If $\Phi(\mathbf{r}, \boldsymbol{\Omega}, E)$ is the solution of the transport equation for the arbitrary source $Q(\mathbf{r}, \boldsymbol{\Omega}, E)$, then because of the linearity of this equation

$$\Phi(\mathbf{r}, \boldsymbol{\Omega}, E) = \int\int\int Q(\mathbf{r}_0, \boldsymbol{\Omega}_0, E_0) G(\mathbf{r}_0, \boldsymbol{\Omega}_0, E_0 \to \mathbf{r}, \boldsymbol{\Omega}, E) \, dV_0 \, d\boldsymbol{\Omega}_0 \, dE_0. \quad (1.21)$$

As already mentioned, Q can be either a volume source with free-surface conditions or a surface source chosen to reproduce the incident flux condition, or

some combination of the two. The magnitude of the equivalent surface source, represented by $Q_s(\mathbf{r}, \mathbf{\Omega}, E)$, can be determined by supposing the incident flux at a point $\mathbf{r}$ on the surface is $\Phi_{inc}(\mathbf{r}, \mathbf{\Omega}, E)$ per unit direction and energy. Then the number of neutrons crossing an element of area dA with outward normal $\hat{\mathbf{n}}$ will be given by

$$\text{Number of neutrons crossing} = -\hat{\mathbf{n}}\cdot\mathbf{\Omega}\Phi_{inc}(\mathbf{r}, \mathbf{\Omega}, E)\, dA$$

per unit direction and energy. The minus sign is introduced because $\hat{\mathbf{n}}$ is an outward normal and $\mathbf{\Omega}$ is an inward direction, so that $\hat{\mathbf{n}}\cdot\mathbf{\Omega} < 0$. Hence, this incident flux may be replaced by an equivalent surface source such that

$$Q_s(\mathbf{r}, \mathbf{\Omega}, E) = -\hat{\mathbf{n}}\cdot\mathbf{\Omega}\Phi_{inc}(\mathbf{r}, \mathbf{\Omega}, E). \tag{1.22}$$

The fact that Green's function has been written for a time-independent problem is of no particular significance. A time-dependent function

$$G(\mathbf{r}_0, \mathbf{\Omega}_0, E_0, t_0 \rightarrow \mathbf{r}, \mathbf{\Omega}, E, t)$$

can be obtained simply by adding the time derivative on the left of equation (1.20) and including the factor $\delta(t - t_0)$ in the delta function representing the point source.

Some special forms of Green's function will be derived in later sections of this book, and relationships between various Green's functions will be indicated.

1.2 INTEGRAL EQUATION FOR NEUTRON TRANSPORT

1.2a Introduction

The neutron transport equation is an integro-differential equation for the neutron angular density (or flux). In this section an equivalent integral equation will be derived. This raises the question of whether there is or is not also an equivalent purely differential expression for the neutron transport problem. The answer is that there is not, for the following reason. In deriving the transport equation it was necessary to consider the neutron angular density in the immediate (space-time) vicinity only of the point under consideration, whereas the whole range of energies and angles had to be included in the transport equation for the angular density at a particular energy and angle. Hence, the formulation is local, involving derivatives, in space and time, but it is extended, involving integrals, in energy and angle.

The physical basis of the foregoing situation is that, in a collision, the position and time associated with a neutron change continuously whereas the energy and angle will change in a discontinuous manner. As a consequence, a mathematical formulation of the neutron transport problem must contain integrals over energy and angle. In the multigroup treatments of the transport equation, described in Chapters 4 and 5, these integrals are approximated by sums.

1.2b Derivation of the Integral Equation

Since the neutron transport equation is a linear first order partial differential–integral equation, it can be converted into an integral equation by a standard procedure known as the method of characteristics,[9] as will be shown below. Two special cases of the integral equation will then be derived: one for isotropic scattering and the other for general anisotropic scattering. The integral equation for neutron transport can also be obtained directly from neutron conservation considerations, as will be indicated.

For the application of the method of characteristics to the neutron transport equation, the latter, in the form of equation (1.14), may be written as

$$\frac{1}{v}\frac{\partial}{\partial t}\Phi(\mathbf{r}, \mathbf{\Omega}, E, t) + \mathbf{\Omega}\cdot\nabla\Phi + \sigma\Phi = q(\mathbf{r}, \mathbf{\Omega}, E, t), \tag{1.23}$$

where $q(\mathbf{r}, \mathbf{\Omega}, E, t)$ is given by

$$q(\mathbf{r}, \mathbf{\Omega}, E, t) \equiv \iint \sigma(\mathbf{r}, E')f(\mathbf{r}; \mathbf{\Omega}', E' \to \mathbf{\Omega}, E)\Phi(\mathbf{r}, \mathbf{\Omega}', E', t)\, d\mathbf{\Omega}'\, dE' + Q(\mathbf{r}, \mathbf{\Omega}, E, t). \tag{1.24}$$

Thus, q is the total rate at which neutrons appear at $\mathbf{r}$, $\mathbf{\Omega}$, E, and t as a result of both collisions and the independent source, Q.

The first two (derivative) terms on the left side of equation (1.23) may be written, in a cartesian coordinate system, as

$$\left(\frac{1}{v}\frac{\partial}{\partial t} + \Omega_x\frac{\partial}{\partial x} + \Omega_y\frac{\partial}{\partial y} + \Omega_z\frac{\partial}{\partial z}\right)\Phi$$

and, in the method of characteristics, a corresponding total derivative can be represented by

$$\frac{d\Phi}{ds} = \frac{\partial\Phi}{\partial t}\frac{dt}{ds} + \frac{\partial\Phi}{\partial x}\frac{dx}{ds} + \frac{\partial\Phi}{\partial y}\frac{dy}{ds} + \frac{\partial\Phi}{\partial z}\frac{dz}{ds}.$$

Upon identifying terms in these two expressions, it is found that

$$\frac{dt}{ds} = \frac{1}{v} \quad \text{with solutions} \quad t = t_0 + \frac{s}{v}$$

$$\left.\begin{aligned} \frac{dx}{ds} &= \Omega_x & x &= x_0 + s\Omega_x \\ \frac{dy}{ds} &= \Omega_y & y &= y_0 + s\Omega_y \\ \frac{dz}{ds} &= \Omega_z & z &= z_0 + s\Omega_z \end{aligned}\right\} \mathbf{r} = \mathbf{r}_0 + s\mathbf{\Omega}$$

where t_0, x_0, y_0, and z_0 are arbitrary constants. Hence, the transport equation (1.23) can be written as

$$\frac{d}{ds}\Phi\left(\mathbf{r}_0 + s\boldsymbol{\Omega}, \boldsymbol{\Omega}, E, t_0 + \frac{s}{v}\right) + \sigma\Phi = q\left(\mathbf{r}_0 + s\boldsymbol{\Omega}, \boldsymbol{\Omega}, E, t_0 + \frac{s}{v}\right). \quad (1.25)$$

The $\mathbf{r}(s)$ and $t(s)$ curves are called the characteristic curves of the differential equation, and for every $\mathbf{r}_0$ and t_0, at fixed values of $\boldsymbol{\Omega}$ and E, there is one curve passing through that point. The derivative in equation (1.25) is a derivative along a characteristic curve and it is evidently $1/v$ times the total time derivative (dN/dt) in the original derivation of the neutron transport equation; s, as before, is a distance along the direction $\boldsymbol{\Omega}$ of neutron travel. Indeed equation (1.25) is, except for notation, just the same as equation (1.10).

Equation (1.25) is seen to be a linear first-order ordinary differential equation which may be integrated. This can be done by introducing an integrating factor, so that equation (1.25) becomes

$$\frac{d}{ds}\left[\Phi\left(\mathbf{r}_0 + s\boldsymbol{\Omega}, \boldsymbol{\Omega}, E, t_0 + \frac{s}{v}\right)\exp\int^s \sigma(\mathbf{r}_0 + s'\boldsymbol{\Omega}, E)\,ds'\right]$$

$$= \exp\left[\int^s \sigma(\mathbf{r}_0 + s'\boldsymbol{\Omega}, E)\,ds'\right] q\left(\mathbf{r}_0 + s\boldsymbol{\Omega}, \boldsymbol{\Omega}, E, t_0 + \frac{s}{v}\right). \quad (1.26)$$

This expression is now integrated from $s = -\infty$, and as a result the integral terms will include earlier times, to some upper limit s.

If it is assumed that

$$\Phi\left(\mathbf{r}_0 + s\boldsymbol{\Omega}, \boldsymbol{\Omega}, E, t_0 + \frac{s}{v}\right) \to 0 \quad \text{as} \quad s \to -\infty,$$

as would be true, for example, if there were no neutrons in the system at times long past, then the left side of equation (1.26) becomes

$$\Phi\left(\mathbf{r}_0 + s\boldsymbol{\Omega}, \boldsymbol{\Omega}, E, t_0 + \frac{s}{v}\right)\exp\int^s \sigma(\mathbf{r}_0 + s'\boldsymbol{\Omega}, E)\,ds'.$$

Upon multiplying both sides of the equation by $\exp\left(-\int^s \sigma\,ds'\right)$, the result is

$$\Phi\left(\mathbf{r}_0 + s\boldsymbol{\Omega}, \boldsymbol{\Omega}, E, t_0 + \frac{s}{v}\right)$$

$$= \int_{-\infty}^{s} \exp\left[\int_{s'}^{s} -\,\sigma(\mathbf{r}_0 + s''\boldsymbol{\Omega}, E)\,ds''\right]\left[q\left(\mathbf{r}_0 + s'\boldsymbol{\Omega}, \boldsymbol{\Omega}, E, t_0 + \frac{s'}{v}\right)\right] ds'.$$

This expression can be simplified to some extent by setting

$$\mathbf{r}_0 + s\boldsymbol{\Omega} = \mathbf{r} \quad \text{and} \quad t_0 + \frac{s}{v} = t$$

and changing the signs of the variables so that the integration runs from 0 to ∞ and 0 to s' in the two integrals. It is thus found that

$$\Phi(\mathbf{r}, \mathbf{\Omega}, E, t) = \int_0^\infty \exp\left[-\int_0^{s'} \sigma(\mathbf{r} - s''\mathbf{\Omega}, E)\, ds''\right] q\left(\mathbf{r} - s'\mathbf{\Omega}, \mathbf{\Omega}, E, t - \frac{s'}{v}\right) ds', \tag{1.27}$$

which is the required form of the integral transport equation for the neutron angular flux.

Equation (1.27) implies that the flux at $\mathbf{r}$ is made up of neutrons which appeared in the direction $\mathbf{\Omega}$ and energy E at all other possible positions $\mathbf{r} - s'\mathbf{\Omega}$, with all positive values of s', multiplied by the attenuation factor

$$\exp\left[-\int_0^{s'} \sigma(\mathbf{r} - s''\mathbf{\Omega}, E)\, ds''\right]$$

by which the flux is reduced in going to $s = 0$. The integration over s' to ∞ can be terminated at the boundary if there is no incoming flux. Similarly, in the treatment above, it would not be necessary to let $s \to -\infty$ but only to let $\mathbf{r} + s\mathbf{\Omega}$ proceed to the boundary. If there is incoming flux, this can be replaced by a surface source as in §1.1f, together with free-surface boundary conditions.

Attention may be called to two points of interest. Since $1/\sigma$ is equal to the mean free path, the exponent in the attenuation factor is equal to the number of collision mean free paths along the straight line between $\mathbf{r}$ and $\mathbf{r} - s'\mathbf{\Omega}$. It is frequently called the *optical path length* between the two points and is denoted by $\tau(E; \mathbf{r} - s'\mathbf{\Omega} \to \mathbf{r})$. If σ is constant, it is simply $\sigma s'$.

Further, if the explicit form of q, as given by equation (1.24), is introduced into equation (1.27), the result may be written as

$$\Phi = \mathbf{K}\Phi + Q', \tag{1.28}$$

where $\mathbf{K}$ is the required integral operator and Q' is a known function, assuming Q to be known. Consider the solutions of equation (1.28) obtained by iteration; thus,

$$\begin{aligned} \Phi_0 &= Q', \\ \Phi_1 &= \mathbf{K}\Phi_0, \\ &\vdots \quad \vdots \\ \Phi_{n+1} &= \mathbf{K}\Phi_n. \end{aligned}$$

Clearly Φ_0 is the angular flux of neutrons which have made no collisions after being introduced from the independent source: this will be called the flux of uncollided neutrons. Similarly, Φ_1 is the flux of first-collision neutrons, i.e., those which have made only one collision, and so on. If the series $\sum_{n=0}^{\infty} \Phi_n$ converges, it represents a solution to equation (1.28). This approach, in which neutrons are enumerated by collisions, is often useful and will be utilized in subsequent chapters.

1.2c Isotropic Scattering and Source

The integral transport equation (1.27) can be integrated over all directions to yield equations that are useful in some instances. Consider, for example, the simple case of isotropic scattering and an isotropic source, where f and Q are not dependent on Ω or Ω'. It is then possible to write

$$\sigma f(\mathbf{r}; \Omega', E' \to \Omega, E) = \frac{1}{4\pi}\sigma(\mathbf{r}; E' \to E),$$

in accordance with the definition of $\sigma(\mathbf{r}; E' \to E)$ in equation (1.18), and

$$Q(\mathbf{r}, \Omega, E, t) = \frac{1}{4\pi} Q(\mathbf{r}, E, t).$$

Hence, from the definition in equation (1.24),

$$q(\mathbf{r}, \Omega, E, t) = \frac{1}{4\pi}\int \sigma(\mathbf{r}; E' \to E)\phi(\mathbf{r}, E', t)\, dE' + \frac{1}{4\pi} Q(\mathbf{r}, E, t),$$

where the integral of the angular flux on the right side has been replaced by the corresponding $\phi(\mathbf{r}, E', t)$.

The expression for q obtained in this manner may be inserted into equation (1.27) and integration carried out over all directions, Ω, to give the total neutron flux, $\phi(\mathbf{r}, E, t)$. The quantity $ds'\, d\Omega$ on the right side is just a volume element, dV'', divided by $(s')^2$. The integration goes over the volume of the system; hence, replacing $\mathbf{r} - s'\Omega$ by $\mathbf{r}'$ and $ds'\, d\Omega$ by $dV''/(s')^2 = dV''/|\mathbf{r} - \mathbf{r}'|^2$, it is found that

$$\phi(\mathbf{r}, E, t) = \int \frac{\exp\left[-\tau(E; \mathbf{r}' \to \mathbf{r})\right]}{4\pi|\mathbf{r}-\mathbf{r}'|^2}\, dV'' \times \left[\int \sigma(\mathbf{r}'; E' \to E)\phi\left(\mathbf{r}', E', t - \frac{|\mathbf{r} - \mathbf{r}'|}{v}\right) dE' + Q\left(\mathbf{r}', E, t - \frac{|\mathbf{r} - \mathbf{r}'|}{v}\right)\right]. \quad (1.29)$$

Equation (1.29) for isotropic scattering and an isotropic source has been frequently used in one-speed problems where the energy variable is absent. It should be observed that it is an expression for the total flux alone; the angular distribution of the neutrons does not enter because both scattering and source are assumed to be isotropic.

If R is written for $|\mathbf{r} - \mathbf{r}'|$, then in the simple case of *total* cross section independent of position and no dependence of ϕ on time, equation (1.29) becomes

$$\phi(\mathbf{r}, E) = \int \frac{e^{-\sigma(E)R}}{4\pi R^2}\, dV''\left[\int \sigma(\mathbf{r}'; E' \to E)\phi(\mathbf{r}', E')\, dE' + Q(\mathbf{r}', E)\right]. \quad (1.30)$$

In this form, it can be seen that the quantity in the square brackets in equation (1.30), and hence also in equation (1.29), is the rate at which neutrons of energy

E appear (isotropically) at $\mathbf{r}'$ due both to collisions and to the independent source at $\mathbf{r}'$. The factor $e^{-\sigma R}/4\pi R^2$ is the probability that a neutron appearing at $\mathbf{r}'$ will reach $\mathbf{r}$ without suffering a collision. The integration over all values of $\mathbf{r}'$ is equivalent to adding neutrons from all possible sources. It is of interest to note that $e^{-\sigma R}/4\pi R^2$ is Green's function (§1.1f) for a unit isotropic source at $\mathbf{r}'$ in an absorbing medium. Similar expressions in other forms of the integral transport equation are also Green's functions.

The foregoing interpretation may be reversed to provide an alternative method for obtaining the integral transport equation on the basis of neutron conservation, analogous to that used in deriving the integro-differential form of the equation. For simplicity, the time-independent case of isotropic scattering and an isotropic source will be treated. Consider the neutrons which at time t are present in a volume element dV about $\mathbf{r}$; the expected flux is then $\phi(\mathbf{r}, E)\, dV$ per unit energy. Each of these neutrons must have either reached $\mathbf{r}$ directly from the source, without intervening collisions, or it must have had a last collision before proceeding to $\mathbf{r}$. All the neutrons at $\mathbf{r}$ may thus be divided into two categories, according to whether the neutrons have or have not come directly from the source.

Consider a volume element dV' at $\mathbf{r}'$ (Fig. 1.7). The expected rate at which neutrons emerge from collisions and from the source is then

$$\text{Rate at which neutrons emerge from } dV' = [\sigma(\mathbf{r}'; E' \to E)\phi(\mathbf{r}', E') + Q(\mathbf{r}', E)]\, dV'.$$

These neutrons emerge isotropically from dV' and so if there were no attenuation between $\mathbf{r}'$ and $\mathbf{r}$, they would contribute an amount

$$\frac{[\sigma(\mathbf{r}'; E' \to E)\phi(\mathbf{r}', E') + Q(\mathbf{r}', E)]\, dV'}{4\pi|\mathbf{r} - \mathbf{r}'|^2}$$

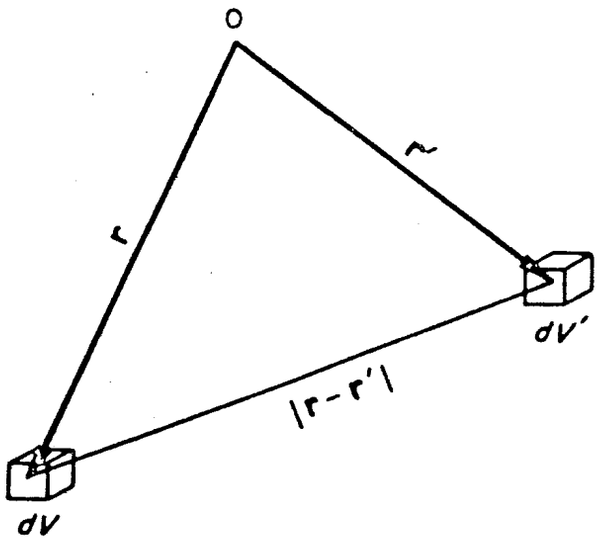

FIG. 1.7 VOLUME ELEMENTS FOR INTEGRAL EQUATION.

toward the flux of the neutrons at $\mathbf{r}$. The attentuation by the medium, however, reduces this flux by the factor $e^{-\sigma|\mathbf{r}-\mathbf{r}'|}$. The flux $\phi(\mathbf{r}, E)$ of neutrons of energy E at $\mathbf{r}$ may now be found by summing the contributions from all possible volume elements dV'. The result is then equivalent to equation (1.30). The foregoing derivation of the integral equation has referred to an especially simple case, but the same general procedure can be used to obtain equation (1.27).

1.2d Anisotropic Scattering

When neutron scattering is anisotropic, an integral equation for ϕ alone cannot be obtained because the angular dependence of the neutron distribution must be included. Nevertheless, it is possible to derive an integral equation where the kernel is similar to that in equation (1.29). To do this, it should first be noted again that q is the sum of source neutrons plus those that appear as the result of collisions. Let $\Psi(\mathbf{r}, \Omega_0, E_0, t)$ represent the collision source, i.e., the number of neutrons per unit time and unit volume that, due to collisions, appear per steradian about Ω_0 and per unit energy about E_0; thus,

$$\Psi(\mathbf{r}, \Omega_0, E_0, t) \equiv \iint \Phi(\mathbf{r}, \Omega, E, t)\sigma f(\mathbf{r}; \Omega, E \to \Omega_0, E_0)\, d\Omega\, dE$$

and

$$q(\mathbf{r}, \Omega, E, t) \equiv \Psi(\mathbf{r}, \Omega, E, t) + Q(\mathbf{r}, \Omega, E, t).$$

Equation (1.27) is now multiplied by $\sigma f(\mathbf{r}; \Omega, E \to \Omega_0, E_0)$ and integrated over $d\Omega$ and dE; the result is found to be

$$\begin{aligned}\Psi(\mathbf{r}, \Omega_0, E_0, t) = \int dE \int d\Omega \int_0^\infty \exp\left[-\int_0^{s'} \sigma(\mathbf{r} - s''\Omega, E)\, ds''\right] \\ \times \sigma f(\mathbf{r}; \Omega, E \to \Omega_0, E_0) \\ \times \left[\Psi\left(\mathbf{r} - s'\Omega, \Omega, E, t - \frac{s'}{v}\right) + Q\left(\mathbf{r} - s'\Omega, \Omega, E, t - \frac{s'}{v}\right)\right] ds'.\end{aligned}$$

By writing $\mathbf{r}'$ for $\mathbf{r} - s'\Omega$, as in §1.2c, and changing to volume integration, so that

$$\int d\Omega \int_0^\infty ds' = \int \frac{dV'}{|\mathbf{r} - \mathbf{r}'|^2},$$

and noting that

$$\Omega = \frac{\mathbf{r} - \mathbf{r}'}{|\mathbf{r} - \mathbf{r}'|},$$

this expression takes the form

$$\Psi(\mathbf{r}, \mathbf{\Omega}_0, E_0, t) = \int dE \int \frac{dV'}{|\mathbf{r} - \mathbf{r}'|^2} \exp\left[-\tau(E; \mathbf{r}' \to \mathbf{r})\right]$$
$$\times \sigma f\left(\mathbf{r}; \frac{\mathbf{r} - \mathbf{r}'}{|\mathbf{r} - \mathbf{r}'|}, E \to \mathbf{\Omega}_0, E_0\right)$$
$$\times \left[\Psi\left(\mathbf{r}', \frac{\mathbf{r} - \mathbf{r}'}{|\mathbf{r} - \mathbf{r}'|}, E, t - \frac{|\mathbf{r} - \mathbf{r}'|}{v}\right)\right.$$
$$\left. + Q\left(\mathbf{r}', \frac{\mathbf{r} - \mathbf{r}'}{|\mathbf{r} - \mathbf{r}'|}, E, t - \frac{|\mathbf{r} - \mathbf{r}'|}{v}\right)\right]. \quad (1.31)$$

Except for the factor σf in the integrand of equation (1.31), the integral kernel is similar to that in equation (1.29). Integral equations of the form of equation (1.31) have been used in the study of one-speed problems and of simple forms of anisotropy.[10]

Solutions of the energy-dependent integral transport equation have not been widely employed in general reactor problems. Nevertheless, the integral equation approach, in which the flux at $\mathbf{r}$ is represented as made up of contributions from all $\mathbf{r}'$, has been found useful for many special cases. Examples will be given in the determination of collision probabilities in Chapters 2 and 8, and in a widely used method of computing thermal neutron spectra in Chapter 7. In one-speed problems, the integral method has often been utilized in the derivation of the mathematical properties of the solutions.[11]

1.3 THE TRANSPORT EQUATION FOR SPECIAL GEOMETRIES

1.3a Plane and Spherical Geometries

In solving the neutron transport equation, it is necessary to have expressions for the quantity $\mathbf{\Omega} \cdot \nabla N$ which appears in the streaming term of the equation. Such expressions can be derived quite simply for coordinate systems where the position vector $\mathbf{r}$ is given in terms of rectangular, spherical, or cylindrical coordinates. Two angular coordinates are required to specify the neutron direction and these are chosen to be a polar angle and an azimuthal angle (see §1.7a). Computation of $\mathbf{\Omega} \cdot \nabla N$ is facilitated by noting that it is the directional derivative of N in the direction $\mathbf{\Omega}$. Some examples are given below; the energy and time variables are suppressed to simplify the notation.

For plane geometry, in which the neutron angular density (for a specific energy) is a function only of z and θ (Fig. 1.8),

$$\mathbf{\Omega} \cdot \nabla N = \frac{dN}{ds} = \frac{\partial N}{\partial z}\frac{dz}{ds} = \frac{\partial N}{\partial z}\cos\theta = \mu\frac{\partial N}{\partial z},$$

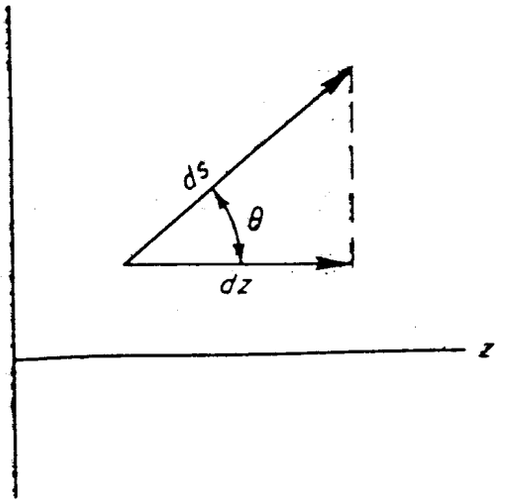

FIG. 1.8 NEUTRON MOTION IN PLANE GEOMETRY

where $\mu = \cos\theta$. For this geometry, it is convenient to set $N(\mathbf{r}, \mathbf{\Omega})$ equal to $N(z, \mu)$, and when integrating over all directions, $d\mathbf{\Omega}$ may be replaced by $d\mu\, d\varphi$ in polar coordinates (§1.1b). Since the neutron distribution in plane geometry has azimuthal symmetry, integration over φ gives 2π, and hence for integration over $\mathbf{\Omega}$, $d\mathbf{\Omega} = 2\pi\, d\mu$. Thus, for plane geometry,

$$\int N(\mathbf{r}, \mathbf{\Omega})\, d\mathbf{\Omega} = 2\pi \int_{-1}^{1} N(z, \mu)\, d\mu.$$

For *spherical geometry*, i.e., spherically symmetrical about a point, it is convenient to give the neutron direction $\mathbf{\Omega}$ relative to the radius vector $\mathbf{r}$. If, in particular,

$$\mathbf{\Omega} \cdot \hat{\mathbf{r}} = \mu,$$

where $\hat{\mathbf{r}}$ is a unit vector, then N is a function of r and μ only. But as the neutron

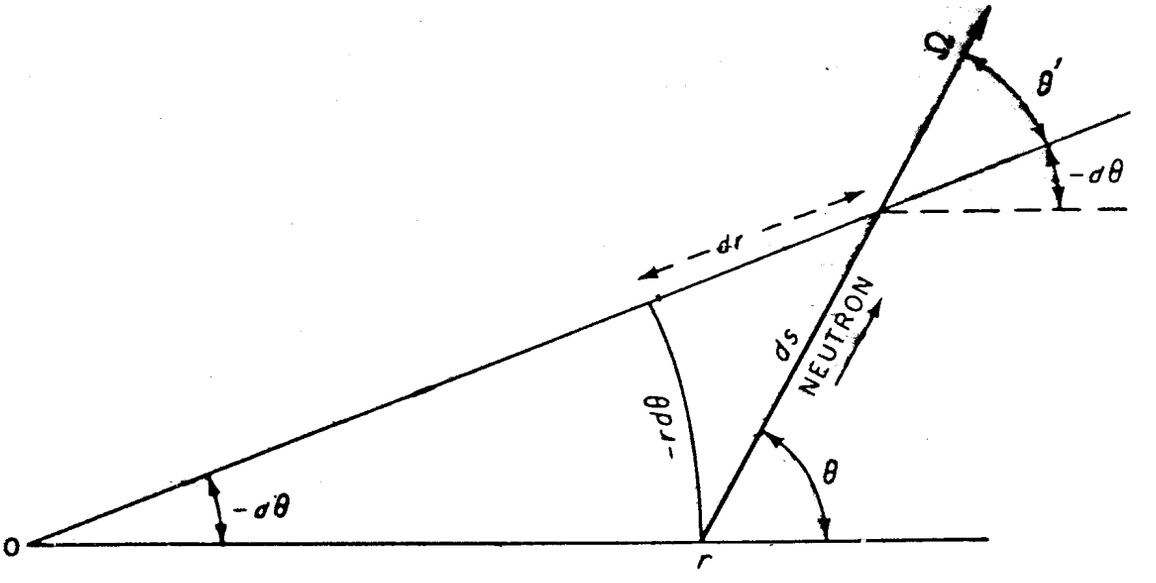

FIG. 1.9 NEUTRON MOTION IN SPHERICAL GEOMETRY.

moves with constant $\mathbf{\Omega}$, the value of μ changes from $\cos\theta$ to $\cos\theta'$ (Fig. 1.9). Hence

$$\mathbf{\Omega}\cdot\nabla N(r,\mu) = \frac{dN(r,\mu)}{ds} = \frac{\partial N}{\partial r}\frac{dr}{ds} + \frac{\partial N}{\partial \mu}\frac{d\mu}{ds}.$$

But

$$\frac{dr}{ds} = \mu = \cos\theta$$

and

$$\frac{d\mu}{ds} = \frac{d\cos\theta}{d\theta}\frac{d\theta}{ds} = -(\sin\theta)\left(-\frac{\sin\theta}{r}\right) = \frac{1-\mu^2}{r}.$$

Consequently,

$$\mathbf{\Omega}\cdot\nabla N(r,\mu) = \mu\frac{\partial N}{\partial r} + \frac{1-\mu^2}{r}\frac{\partial N}{\partial \mu}. \tag{1.32}$$

More general expressions for $\mathbf{\Omega}\cdot\nabla N$ (or $\mathbf{\Omega}\cdot\nabla\Phi$) and for $\int d\mathbf{\Omega}$ in various rectangular, spherical, and cylindrical geometries are given in §1.7a. It should be noted that the expressions involving N and Φ have exactly the same dependence on all the variables.

1.3b Conservation Form for Curved Geometries

It was noted earlier that the neutron transport equation is simply a statement of neutron conservation in an infinitesimal element of direction, volume, and energy ($d\mathbf{\Omega}$, dV, and dE). When integrated over all directions and over a finite volume, the result is a relation for the conservation of neutrons in that volume. For performing these integrations in curved geometries, it is convenient to express $\mathbf{\Omega}\cdot\nabla N$ in a particular form which facilitates the integration procedure. The term $\mathbf{\Omega}\cdot\nabla N$ is then said to be expressed in *conservation form*.

Consider the simple case of a system with spherical symmetry. The integral of $\mathbf{\Omega}\cdot\nabla N\,dV\,d\mathbf{\Omega}$ over a finite volume and all directions is obtained by writing $4\pi r^2\,dr$ for dV and integrating over r from r_1 to r_2 (Fig. 1.10) and replacing $d\mathbf{\Omega}$ by $2\pi\,d\mu$ and integrating over μ from -1 to 1. The latter substitution is permissible because the neutron distribution in spherical geometry is azimuthally symmetrical, as it is for plane geometry (§1.3a). Thus, the integral under consideration can be written

$$\iint \mathbf{\Omega}\cdot\nabla N\,dV\,d\mathbf{\Omega} = \int_{r_1}^{r_2} 4\pi r^2 \int_{-1}^{1} 2\pi(\mathbf{\Omega}\cdot\nabla N)\,d\mu\,dr \tag{1.33}$$

$$= \frac{4\pi}{v}\int_{r_1}^{r_2} r^2[\nabla\cdot\mathbf{J}(\mathbf{r})]\,dr$$

$$= \frac{4\pi}{v}\,[r_2^2 J(r_2) - r_1^2 J(r_1)], \tag{1.34}$$

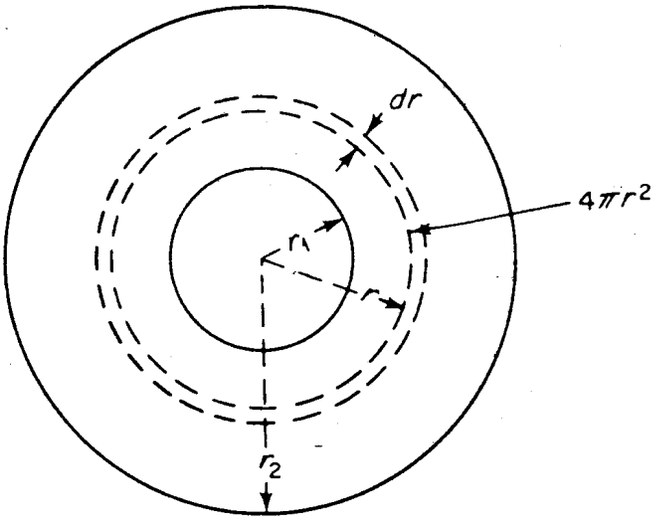

FIG. 1.10 CALCULATION OF STREAMING TERM IN CONSERVATION FORM IN SPHERICAL GEOMETRY.

recalling the definition of the neutron current in equation (1.6). This result should, of course, be obtainable by substituting the right side of equation (1.32) in the second integrand on the right of equation (1.33) and performing the integration directly. The two terms obtained in this manner combine mathematically to yield equation (1.34), as required, but the individual terms have no physical significance.

A preferable approach is to express the right side of equation (1.32) in an alternative form, i.e.,

$$\mu \frac{\partial N}{\partial r} + \frac{1-\mu^2}{r}\frac{\partial N}{\partial \mu} = \frac{\mu}{r^2}\frac{\partial (r^2 N)}{\partial r} + \frac{1}{r}\frac{\partial [(1-\mu^2)N]}{\partial \mu}. \tag{1.35}$$

When this expression is multiplied by the volume element $4\pi r^2\, dr$, it is seen that the first term on the right is a function of μ, namely μ, multiplied by a derivative with respect to r, whereas the second term is a function of r, namely r, multiplied by a derivative with respect to μ. When the right side of equation (1.35) is integrated over r and μ, as above, the first term gives the right side of equation (1.34) directly, and the integral of the second term goes to zero. Thus,

$$\int_{r_1}^{r_2} 4\pi r^2 \int_{-1}^{1} \frac{2\pi}{r^2}\,\mu \frac{\partial (r^2 N)}{\partial r}\, d\mu\, dr = \frac{4\pi}{v}\int_{r_1}^{r_2} \frac{\partial [r^2 J(r)]}{\partial r}\, dr$$

$$= \frac{4\pi}{v}\,[r_2^2 J(r_2) - r_1^2 J(r_1)],$$

which is the net rate at which neutrons leave the volume divided by the neutron speed, v,* and

$$\int_{r_1}^{r_2} 4\pi r^2 \int_{-1}^{1} \frac{2\pi}{r}\frac{\partial [(1-\mu^2)N]}{\partial \mu}\, d\mu\, dr = \int_{r_1}^{r_2} 8\pi^2 r\, dr [(1-\mu^2)N]_{\mu=-1}^{\mu=1} = 0.$$

* When the angular flux, Φ, is used in place of the angular density, N, as in §§1.7a, 5.3b, the integral gives the actual rate at which neutrons leave the volume.

The two terms on the right side of equation (1.35) thus have physical significance when integrated over a finite volume and all directions, and they express $\mathbf{\Omega}\cdot\nabla N$ for spherical geometry in conservation form.

In general, when $\mathbf{\Omega}\cdot\nabla N$ is written in conservation form, the coefficient of each derivative term multiplied by the volume element does not involve the variable of differentiation. When integrated over all directions and a volume bounded by surfaces along which one space variable is constant, the terms can be readily interpreted as currents across such surfaces (see last paragraph in §1.7a). This property of the conservation forms makes them useful in deriving difference approximations to the transport equation (see Chapter 5) or in considering boundary conditions. Expressions for $\mathbf{\Omega}\cdot\nabla\Phi$, which also apply to $\mathbf{\Omega}\cdot\nabla N$, in conservation form for spherical and cylindrical geometries are included in the appendix to this chapter (§1.7a).

1.3c Special Forms of the Integral Equation

It was seen in §1.2c that when the source and scattering are isotropic and the cross sections are independent of position within the region being considered, the integral equation takes the particularly simple form of equation (1.30); the latter, in which ϕ is independent of time, may be written as

$$\phi(\mathbf{r}, E) = \int \frac{e^{-\sigma(E)R}}{4\pi R^2} q(\mathbf{r}', E)\, dV', \tag{1.36}$$

where

$$R = |\mathbf{r} - \mathbf{r}'|$$

and

$$q(\mathbf{r}', E) = \int \sigma(E' \to E)\phi(\mathbf{r}', E')\, dE' + Q(\mathbf{r}', E).$$

Furthermore, when the geometrical region is simple, the spatial integral may be simplified.

In *plane geometry*, with q a function of x and E only, Fig. 1.11 shows that the volume element

$$dV' = 2\pi r'\, dx'\, dr'.$$

Moreover,

$$R^2 = |x - x'|^2 + (r')^2,$$

so that, if $x - x'$ is constant,

$$R\, dR = r'\, dr'.$$

Equation (1.36) then takes the form

$$\phi(x, E) = \frac{1}{2}\int dx' \int_{|x-x'|}^{\infty} q(x', E)\frac{e^{-\sigma(E)R}}{R}\, dR$$

$$= \frac{1}{2}\int q(x', E)E_1[\sigma(E)|x - x'|]\, dx' \tag{1.37}$$

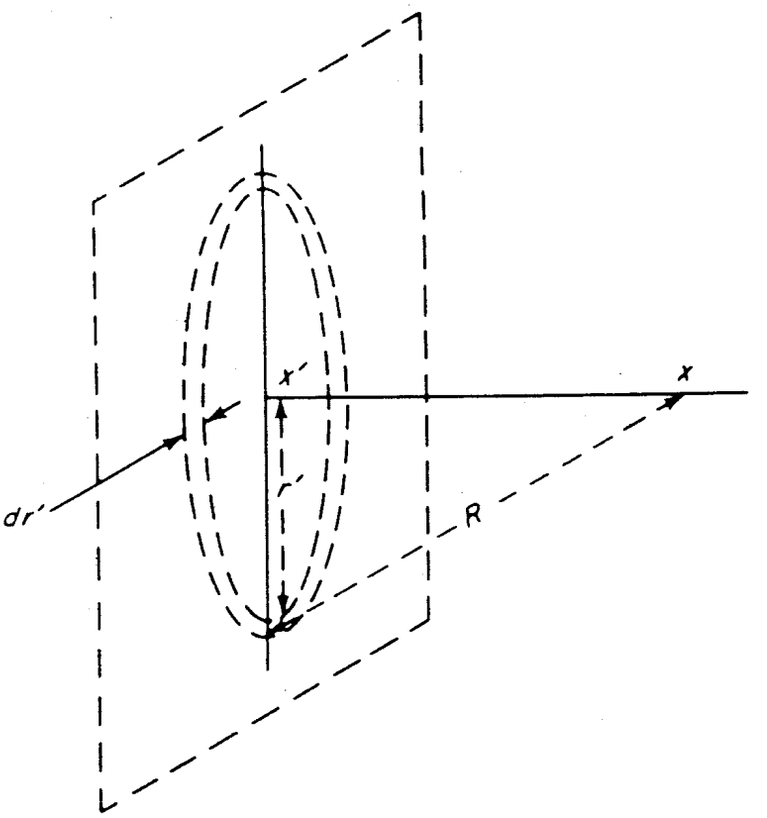

FIG. 1.11 CALCULATION OF INTEGRAL TRANSPORT EQUATION IN PLANE GEOMETRY.

where the symbol E_1 stands for the first order exponential integral function (see Appendix). For an infinite slab of thickness $2a$, this becomes

$$\phi(x, E) = \frac{1}{2}\int_{-a}^{a} q(x', E)E_1[\sigma(E)|x - x'|]\,dx'. \tag{1.38}$$

Similarly, for *spherical geometry*, with q a function of r and E only, then from Fig. 1.12,

$$dV' = 2\pi(r')^2\,dr'\,d(\cos\theta)$$

and

$$R^2 = r^2 + (r')^2 - 2rr'\cos\theta,$$

so that for fixed r and r',

$$-d(\cos\theta) = \frac{R\,dR}{rr'}.$$

Hence, equation (1.36) can be written as

$$\phi(r, E) = \frac{1}{2}\int_0^{\infty} (r')^2 q(r', E)\,dr' \int_{|r-r'|}^{r+r'} \frac{e^{-\sigma(E)R}}{rr'R}\,dR$$

and

$$r\phi(r, E) = \frac{1}{2}\int_0^{\infty} r'q(r', E)\{E_1[\sigma(E)|r - r'|] - E_1[\sigma(E)(r + r')]\}\,dr'. \tag{1.39}$$

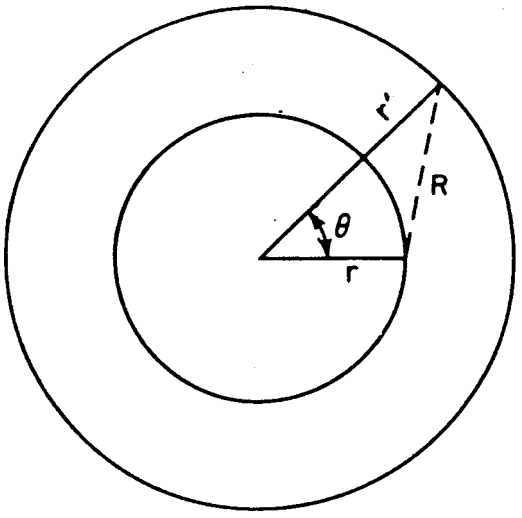

FIG. 1.12 CALCULATION OF INTEGRAL TRANSPORT EQUATION IN SPHERICAL GEOMETRY.

For a homogeneous sphere of radius a, equation (1.39) becomes

$$r\phi(r, E) = \frac{1}{2}\int_0^a r'q(r', E)\{E_1[\sigma(E)|r - r'|] - E_1[\sigma(E)(r + r')]\}\, dr'. \qquad (1.40)$$

If $q(-r, E)$ is taken to be equal to $q(r, E)$, then the second term in the integral can be written as

$$\frac{1}{2}\int_{-a}^0 r'q(r', E)E_1[\sigma(E)|r - r'|]\, dr'$$

and then equation (1.40) reduces to

$$r\phi(r, E) = \frac{1}{2}\int_{-a}^a r'q(r', E)E_1[\sigma(E)|r - r'|]\, dr'. \qquad (1.41)$$

This equation may be considered to apply for $-a \leqslant r \leqslant a$, with $\phi(-r, E) = \phi(r, E)$.

Comparison of equation (1.41) with equation (1.38) shows that for a homogeneous sphere of radius a the quantities $r\phi(r, E)$ and $rq(r, E)$ are related to the planar quantities $\phi(x, E)$ and $q(x, E)$, respectively, for an infinite slab of thickness $2a$. By using this fact, it is sometimes possible to relate solutions of the transport equation for slabs to those of spheres (§2.5f). It should be noted that since, by definition, $\phi(r, E) = \phi(-r, E)$ and $q(r, E) = q(-r, E)$, the functions $r\phi(r, E)$ and $rq(r, E)$ of r must be odd, i.e., $r\phi(r, E) = -[-r\phi(-r, E)]$ and $rq(r, E) = -[-rq(-r, E)]$. For the symmetric slab, however, the corresponding functions of x are even, since $\phi(x, E) = \phi(-x, E)$ and $q(x, E) = q(-x, E)$.

1.4 LIMITATIONS OF THE NEUTRON TRANSPORT EQUATION

1.4a Introduction

In deriving the neutron transport equation, some assumptions were made which may not always be justified in practice. In order of their appearance in the preceding text, the most important are: (1) that the neutron is a point particle characterized completely by its position and velocity; (2) that the medium contains a large enough number of neutrons so that deviations from the expected (or probable) number can be ignored but not so large that they change the medium in times of interest; and (3) the neglect of delayed neutrons. These assumptions will be discussed in turn.

1.4b Neutron as a Point Particle

In considering the neutron as a point particle, i.e., a particle which can be described completely by its position and velocity, the effect of polarization, which could influence neutron transport, has been neglected. Polarization effects can arise because the neutron has a spin and a magnetic moment. In particular, when a beam of neutrons with energy large enough for $l > 0$ interactions to be significant, in practice when $E \gtrsim 100$ keV (cf. §1.6c), is scattered by an unpolarized target, the neutrons become polarized due to neutron-nucleus (spin–orbit) interaction. This polarization affects the subsequent scattering of the neutron, and a transport theory with appropriate allowance for polarization has been developed.[12] Although in principle there are situations where the effects on neutron transport could be large, e.g., fast neutrons diffusing in helium, it does not appear that this is so in practical situations. In any event, allowance for polarization can be made in the P_1 approximation to the transport equation (see §1.6d) by a suitable small modification of the cross sections.

Neutron polarization can also arise from the scattering of neutrons by nuclei with oriented spins, e.g., oriented protons, from scattering by magnetic materials, due to the interaction between the magnetic moment of the neutron and the atomic magnetic field, and from small-angle scattering arising from the interaction of the magnetic moment of the neutron (for $l > 0$) with the electric field of the nucleus. None of these effects, however, is important for neutron transport in a reactor.

At very low neutron energies, the neutron wavelength becomes comparable with the internuclear spacing. Interference effects could then arise between the neutron waves scattered from various nuclei. These coherent scattering effects will depend on both the scattering nuclei and their positions in space, i.e., in the crystal structure. The scattering is then affected by the orientation of the crystal axes relative to the direction of the neutrons. The phenomenon is important in the physics of low-energy neutrons, but it is usually not significant for reactor

theory. Further reference to the subject will be made in Chapter 7 on neutron thermalization.

1.4c The Expected (or Probable) Value

In deriving the transport equation for the expected (or probable) value of the neutron density, fluctuations from the mean were not taken into account. As a general rule, in a power reactor the fluctuations are small in comparison with the average neutron density and then the transport equation can be used to express the "expected" behavior. In addition, fluctuations have no effect on the *average* neutron density and hence the transport equation is valid for the *average* neutron angular density no matter how large the fluctuations may be.

There are some practical situations, however, in which the departure from the average behavior is relatively large and cannot be overlooked. In particular, deviations from the mean commonly occur in the startup of a reactor in which the system is brought up to (or through) critical with a weak source. There is then, for example, a certain probability that the reactor may go beyond prompt critical before any neutron signal is detected. For dealing with such behavior, stochastic theories of neutron transport and multiplication have been developed in which the probabilities of various exceptional events are considered along with more normal situations.[13] The procedures will not be discussed in detail in this book, but it is of interest to note that in one approach an equation is derived for a probability function which is closely related to the Boltzmann equation; it includes nonlinear fission terms where the probability of two neutrons from fission leads to a square term, and so on.[14]

Fluctuations during startup are important in reactors which depend on such weak sources as spontaneous fission, (α, n) and (γ, n) reactions, and cosmic-ray neutrons. In pulsed reactors, it is desirable to use a strong source for startup, so that departure from the average behavior is small, or a very weak source; there is then a high probability that assembly to the desired state of supercriticality will be attained before the first persistent (divergent) fission chain is initiated.

Even when a reactor is operating in the steady state, there are minor fluctuations in the neutron flux, usually referred to as reactor noise. This noise is a direct consequence of the fission process itself. It will be shown in Chapter 9 that information about the lifetimes of delayed neutrons and other matters of interest can be obtained from a study of reactor noise. The fluctuations in the steady state do not, however, represent large deviations from the neutron angular density (or flux) predicted by the transport equation.

The limitation was indicated earlier that the neutron density must not be so large that the medium changes appreciably in times of importance for neutron transport. Clearly, in a reactor operating at high power, the composition and temperature, and hence the macroscopic cross sections, will change gradually with time. The time scale for these changes, however, is very long compared with

neutron transport times. The problem is therefore treated by a series of static calculations in which compositions, etc., are changed from one calculation to the next. The same procedure is generally used for shutdown and startup problems where the changes are so relatively slow that a series of static calculations is usually adequate; this question will be examined further in Chapter 9, where it will be seen that in treating rapid transients, e.g., in power excursions, the changes of cross section are taken into account in various ways.

The neglect of neutron-neutron collisions in the transport theory can be readily justified. Even in a thermal reactor operating at the high (thermal) neutron flux of 10^{16} neutrons per cm^2 per sec, the neutron density is less than 10^{11} neutrons per cm^3. This is small compared to nuclear densities which are of the order of 10^{22} nuclei per cm^3 in solids. Hence, neutron-neutron collisions will be very much less frequent than neutron-nuclei collisions. As a result of the neglect of neutron-neutron scattering, the neutron transport equation is linear. In the kinetic theory of gases, where collisions among the particles are important, the transport (Boltzmann) equation includes nonlinear collision terms.

1.4d Delayed Neutrons

When necessary, there is no difficulty in allowing for delayed neutrons, provided that the precursors decay where they are formed, i.e., there is no transport of the precursors. This is done by introducing into the scattering kernel the possibility of a time delay between neutron absorption and emission. The subject will be treated in Chapter 9, but in the meantime it may be regarded as only a formal complication. It is necessary, however, to keep in mind the distinction between prompt critical, i.e., criticality without delayed neutrons, and delayed critical, in which the delayed neutrons are included. In the former case, of course, the delayed neutrons can be neglected completely.

If the delayed neutron precursors can move appreciably while they are decaying, the motion must be analyzed and taken into account in both static and dynamic reactor problems. Transport of delayed neutron precursors occurs in reactors with circulating fuels and in systems with unclad fuel elements when the precursors can diffuse into the coolant.

1.5 GENERAL PROPERTIES OF SOLUTIONS OF THE TIME-DEPENDENT TRANSPORT EQUATION

1.5a The Criticality Condition: General Considerations

From physical considerations, it is to be expected that systems containing fissile nuclides can be regarded as being either subcritical, critical, or supercritical, based on the behavior of the neutron population as a function of time. Thus, the following intuitive definitions may be adopted to describe the physical

concept of criticality. A system is said to be subcritical if, for any nonzero initial neutron population, the expected population at late times, i.e., as $t \to \infty$, will die out unless it is sustained by a neutron source, internal or external. Similarly, a system is described as supercritical when the expected neutron population diverges at late times, starting from any nonzero population or with a source. Finally, a critical system is defined as one in which a steady, time-independent expected neutron population can be maintained in the absence of a source.

The foregoing definitions can be related closely to the properties of the asymptotic (as $t \to \infty$) solutions of the neutron transport equation. However, a formal mathematical analysis of the asymptotic solutions covering all situations of physical interest has not yet been made. In this section, therefore, a heuristic approach to the problem will be presented and it will be followed by a brief review of some results obtained by a formal analysis in certain special cases.

The neutron transport equation with boundary conditions defines an initial value problem. Thus, if the neutron angular density at $t = 0$, i.e., $N(\mathbf{r}, \boldsymbol{\Omega}, E, 0)$, is given, the expected density at any later time can be found, in principle, by solving the transport equation. It has been shown that such a solution exists and is unique, provided certain mathematical conditions are satisfied by cross sections and sources.[15] In practice, these conditions are satisfied for actual physical situations. The criticality of a system will now be discussed by considering the asymptotic (as $t \to \infty$) behavior of the solution to the initial value problem.

The homogeneous (source-free) neutron transport equation, i.e., equation (1.13) without Q, may be written in the form

$$\frac{\partial N}{\partial t} = -v\boldsymbol{\Omega} \cdot \nabla N - \sigma v N + \iint \sigma' f v' N' \, d\boldsymbol{\Omega}' \, dE' = \mathbf{L}N,$$

where $\mathbf{L}$ is an operator, together with the boundary condition of no incoming neutrons. Some important features of the criticality problem can be appreciated by considering solutions to the equation

$$\frac{\partial N}{\partial t} = \mathbf{L}N \tag{1.42}$$

of the form

$$N = N(\mathbf{r}, \boldsymbol{\Omega}, E)e^{\alpha t},$$

from which

$$\alpha N(\mathbf{r}, \boldsymbol{\Omega}, E) = \mathbf{L}N(\mathbf{r}, \boldsymbol{\Omega}, E).$$

There may exist many values (eigenvalues) of α, represented by α_j, with corresponding solutions (eigenfunctions) N_j, i.e.,

$$\alpha_j N_j = \mathbf{L}N_j.$$

Suppose that it is possible to expand the solution in the eigenfunctions N_j. If α_0 is the value of α_j having the largest real part, then at late times, when t is large, it is expected that the solution to the initial value problem would be proportional to $N_0(\mathbf{r}, \mathbf{\Omega}, E)e^{\alpha_0 t}$. The distinction between subcritical and supercritical systems could then be based on the sign of the eigenvalue α_0. Physically, the expectation is that α_0 would be real, i.e., no oscillations in the neutron density since they would lead to negative or imaginary density values; furthermore, N_0 would be everywhere nonnegative, i.e., no negative values of the neutron density are allowed. Then, for a subcritical system $\alpha_0 < 0$, for a critical system $\alpha = 0$, and for a supercritical system $\alpha_0 > 0$. Thus, the criticality problem becomes that of determining the sign of α_0.

It will be seen in later chapters that the eigenvalues α_j, and especially α_0, are of basic importance in reactor theory. They will be referred to, according to circumstances, by such names as "α eigenvalues," "multiplication rate eigenvalues," "decay eigenvalues," and, in dynamics problems (§10.1d), as "period eigenvalues," because they are inversely related to the reactor periods.

1.5b Spectrum of the Transport Operator and Criticality

The foregoing considerations can be expressed somewhat more precisely, although still far from rigorously, by taking the Laplace transform of equation (1.42) with respect to time. Let

$$N_\alpha \equiv \int_0^\infty e^{-\alpha t} N(\mathbf{r}, \mathbf{\Omega}, E, t)\, dt$$

and

$$F(\mathbf{r}, \mathbf{\Omega}, E) \equiv N(\mathbf{r}, \mathbf{\Omega}, E, 0),$$

where F represents the initial condition on N. The quantity N_α is a function of the complex variable α and exists if the real part of α, i.e., Re α is sufficiently large.[16] Hence, for Re α large enough,

$$\int_0^\infty \frac{\partial N}{\partial t} e^{-\alpha t}\, dt = -F + \alpha N_\alpha.$$

Since the operator $\mathbf{L}$ is independent of t, the Laplace transformation of equation (1.42) yields the result

$$(\alpha - \mathbf{L})N_\alpha = F. \tag{1.43}$$

If $\alpha - \mathbf{L}$ were merely a complex valued function, it would be possible to solve equation (1.43) for

$$N_\alpha = \frac{1}{\alpha - \mathbf{L}} F$$

and then attempt to invert the Laplace transform. Since $\alpha - \mathbf{L}$ is an operator,

however, it is necessary to consider the inverse operator $(\alpha - \mathbf{L})^{-1}$, known as the *resolvent operator*, and write

$$N_\alpha = (\alpha - \mathbf{L})^{-1}F. \tag{1.44}$$

Many of the difficulties in the mathematical analysis arise in identifying the properties of this resolvent operator.[17] Nevertheless, by formal application of the inverse Laplace transform[18] to equation (1.43), the result is

$$N(\mathbf{r}, \mathbf{\Omega}, E, t) = \frac{1}{2\pi i}\int_{b-i\infty}^{b+i\infty} (\alpha - \mathbf{L})^{-1}Fe^{\alpha t}\, d\alpha, \tag{1.45}$$

where b is any real constant lying in the complex α plane to the right of all singularities in the integrand; in other words, b is greater than the real part of α at any singularity in the integrand.

In attempting to invert the transform in equation (1.45), the singularities of the integrand, or of the resolvent operator, are very important. Suppose that the integrand has only a series of poles, indicated by crosses in Fig. 1.13, for $\alpha = \alpha_j$, where $j = 0, 1, 2, \ldots$. Then the contour could be closed by the extended path, shown by the dashed lines in the figure, picking up a residue contribution proportional to $e^{\alpha_j t}$ from each of the poles. In this event,

$$\int_{b-i\infty}^{b+i\infty} [\quad]\, d\alpha = \int_C [\quad]\, d\alpha = 2\pi i \times \text{sum of residues at poles},$$

where C represents the extended path; the assumption is made that the

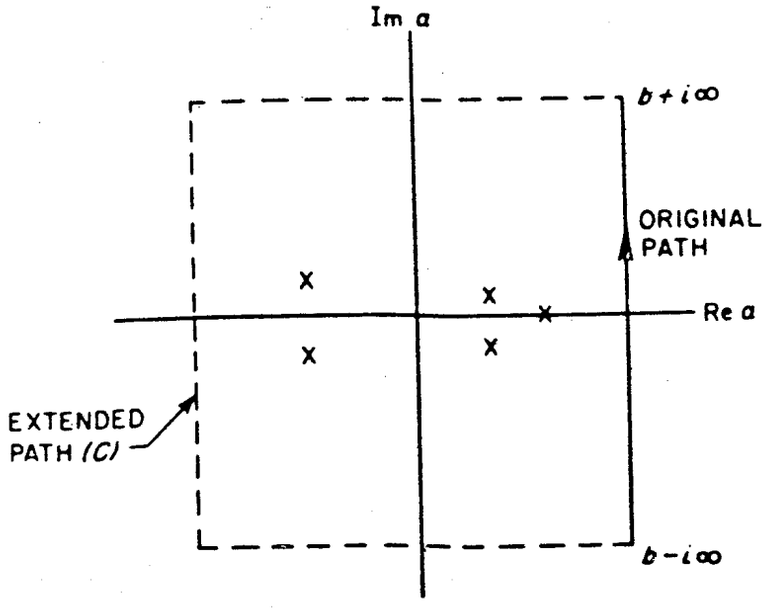

FIG. 1.13 INVERSION OF LAPLACE TRANSFORM.

contribution to the integral of the dashed part of the path is zero. A solution to equation (1.45) of the form

$$N(\mathbf{r}, \mathbf{\Omega}, E, t) = \sum_{j=0} e^{\alpha_j t} g_j(\mathbf{r}, \mathbf{\Omega}, E) \tag{1.46}$$

is then to be expected,[19] so that at late times the solution will be dominated by the term which has α_j with the largest real part; this particular eigenvalue α_j may be called α_0, assuming that the values of α_j have been ordered such that $\text{Re}\,\alpha_j \geqslant \text{Re}\,\alpha_{j+1}$.

Consequently, in order to study the asymptotic behavior with time of the time-dependent neutron transport equation, it is necessary to examine the singularities of the operator $(\alpha - \mathbf{L})^{-1}$. Such singularities will be values of α_j for which

$$(\alpha_j - \mathbf{L})N_{\alpha_j} = 0.$$

Hence,

$$\mathbf{L}N_{\alpha_j} = \alpha_j N_{\alpha_j}, \tag{1.47}$$

so that α_j is the eigenvalue corresponding to the eigenfunction N_{α_j}. The particular eigenfunction N_{α_0} corresponding to the eigenvalue α_0 would be expected to determine the solution at late times; thus,

$$N(\mathbf{r}, \mathbf{\Omega}, E, t) = Ae^{\alpha_0 t} N_{\alpha_0}(\mathbf{r}, \mathbf{\Omega}, E) \quad \text{as} \quad t \to \infty, \tag{1.48}$$

where A is a constant determined by the initial conditions $F(\mathbf{r}, \mathbf{\Omega}, E)$. The distinction between subcritical and supercritical systems could then be based on the sign of α_0, assuming α_0 to be real. In this event, the criticality problem is that of finding the conditions, i.e., radius, composition, etc., for which $\alpha_0 = 0$.

The foregoing expectations have been largely confirmed by rigorous mathematical analysis.[20] But apart from the mathematical difficulties, there are a number of circumstances which may prove to be troublesome. These arise in considering the possible eigenvalues α_j in equation (1.47), called the *spectrum of the transport operator* $\mathbf{L}$. The following situations may arise: (*a*) there exist no discrete eigenvalues α, and hence there is no value of α_0; or (*b*) the number of discrete eigenvalues may be infinite so that there are questions concerning the convergence of the series in equation (1.46); or (*c*) there may be a continuous range of α, in the left half-plane in Fig. 1.13 where $\text{Re}\,\alpha < 0$, called the continuous spectrum of $\mathbf{L}$, for which equation (1.47) can be satisfied in a limiting sense.

Actually a value of α in the continuous spectrum is not a proper eigenvalue of equation (1.47). Rather it is associated with a highly singular eigenfunction which is defined as the limit of a series of nonsingular functions that are not quite eigenfunctions. It is not possible, however, to extend the integration path in Fig. 1.13 into the region of the continuous spectrum (see Exercise 16).

In case (*c*), therefore, the contour of integration does not extend indefinitely to the left, but is stopped when the continuous spectrum is reached. The solution

to equation (1.45) will then be the series in equation (1.46) plus an additional term from the left-hand contour representing the contribution of the continuous spectrum. The three possibilities described above have all been encountered in investigations of special cases of the neutron transport equation.

1.5c Results of Rigorous Analysis of the Criticality Condition

In the first rigorous examination of the transport operator, the case considered was the one-speed problem with isotropic scattering for a bare homogeneous infinite slab, i.e., of infinite extent in two dimensions.[21] Previously, it had been assumed, by analogy with other problems in mathematical physics, that there would be an *infinite* number of discrete eigenvalues for equation (1.47) and that the corresponding eigenfunctions would form a complete set. The rigorous solution to equation (1.45), however, gave a *finite* (nonzero) set of real eigenvalues for which $\alpha_j > -\sigma v$, and in addition a continuous spectrum for all $\alpha_j < -\sigma v$, as in case (*c*) of the preceding section. The contribution from the continuous spectrum, however, decays at least as rapidly as $e^{-\sigma v t}$. Since there are always one or more discrete eigenvalues, the asymptotic solution at late times will be dominated by the discrete terms and criticality can still be rigorously determined by $\alpha_0 = 0$. Similar conclusions have been obtained in a multigroup (see §1.6d) study of a slab.[22]

A possible physical explanation for the continuous spectrum of the transport operator in a slab is the following.[23] Neutrons traveling parallel to the slab faces can proceed indefinitely without ever either colliding with nuclei or leaving the slab. Hence, even at very late times there will remain a contribution which precisely reflects the original conditions in directions nearly parallel to the slab surfaces. The neutrons traveling exactly parallel will decay as $e^{-\sigma v t}$, i.e., just like the contribution from the continuous spectrum. Support for this interpretation is found in the result that for the one-speed problem in a bare sphere, there is no continuous spectrum but only an infinite number of real discrete eigenvalues.[24]

An analysis has also been made of the energy-dependent transport equation for finite (bounded) geometry.[25] By assuming neutron speeds to be bounded away from zero and the scattering kernel to be integrable and bounded, it was found that at late times the solution of the transport equation is dominated by the contribution from a discrete eigenvalue. Asymptotically, the solution to the transport equation varies as $e^{\alpha_0 t}$, and so, for this quite general case, a critical system can be defined as one for which $\alpha_0 = 0$. For certain conditions on the scattering kernel, which are satisfied in practice for all systems containing fissile nuclei, there will always be at least one discrete eigenvalue and hence an α_0. Although this result has not been proved in general, it seems reasonable to suppose that there will always be a real α_0 and that N_{α_0} will be nonnegative.

In the foregoing, it was assumed that the neutron speeds are bounded away from zero. If zero speed is allowed then, for some simplified energy-dependent

versions of the scattering kernel that arise in neutron thermalization theory, it has been found that there is only a finite number of discrete real eigenvalues plus a continuous spectrum for all α with sufficiently negative real parts.[26] In addition, for sufficiently small systems, there are no discrete eigenvalues.[27] But these conclusions regarding the case for neutrons of zero speed do not appear to have any great relevance for the criticality problem. As noted in §1.1b, the transport equation is not meaningful for neutrons of arbitrarily small velocity (and long λ). Furthermore, a system that is so small as to have no discrete eigenvalue is clearly subcritical; for larger systems, however, an α_0 will still exist.

Another assumption made above is that the scattering kernel is bounded. It was seen earlier, in equation (1.7), however, that for elastic scattering the kernel is usually written containing a Dirac delta function and is consequently unbounded. If the thermal motion of the scattering nuclei is taken into account (Chapter 7), then this unbounded kernel is not strictly correct. When the nuclei are in a gas or liquid, they will have a continuous range of possible velocities and the scattering kernel will not have any singularities. For scattering from nuclei in crystals, on the other hand, there will be complicated singularities. Hence, scattering kernels are sometimes bounded and sometimes not. Although details of the eigenvalue spectrum are affected by a singular kernel,[28] it nevertheless appears that the concept of criticality based on the sign of α_0 may be accepted as having general applicability.

The spectrum of the transport operator and the criticality condition have been discussed in some detail because the neutron transport equation is the basis of the analysis of neutron behavior in a reactor and criticality is, of course, essential in determining the size of a reactor. For the solution of practical problems some approximation to the transport equation must be used, and then the eigenvalue of the approximate equation can be considered. In some cases, particularly for multigroup diffusion theory, much more can be said regarding the eigenvalues and eigenfunctions. This subject will be discussed in Chapter 4.

As a consequence of the linearity of the homogeneous (source-free) neutron transport equation (§1.1f), it appears that if there are many solutions of the α eigenvalue problem, then an arbitrary solution of the equation might be expanded in terms of the eigenfunctions N_i (or Φ_i) corresponding to the eigenvalue α_i. Although no such generality, i.e., completeness of eigenfunctions, has been demonstrated, the expansions are used in some approximations to the neutron transport equation, e.g., in one-speed theory in Chapter 2 and in multigroup theory, as will be seen in Chapter 4.

1.5d Existence of Time-Independent Solutions

It is of interest to consider the circumstances under which a time-independent (steady-state) solution of the transport equation may be expected to exist and,

if it does, whether or not it is unique. The homogeneous (source-free) transport equation (1.42) will have a time-independent solution, given by equation (1.47), when

$$\mathbf{L}N_{\alpha_0} = 0$$

with $\alpha_0 = 0$ for a critical system. If, as will be assumed, the persisting distribution or the critical eigenfunction, N_{α_0}, is unique, except for a multiplicative constant, then the time-independent solution is unique.

More generally, consider the inhomogeneous transport equation with a source, namely,

$$\frac{\partial N}{\partial t} = \mathbf{L}N + Q.$$

It is desired to determine the circumstances under which solutions will exist for

$$\frac{\partial N}{\partial t} = 0 \quad \text{and} \quad \mathbf{L}N + Q = 0,$$

and if these solutions will be approached from some initial conditions on N. The stipulation is made that $\mathbf{L}$ and Q are time-independent; that is, the cross sections and source are taken to be independent of time.

For a supercritical system, there can be no physical solutions for which $\partial N/\partial t = 0$; any population which is established will, in due time, be increasing as $e^{\alpha_0 t}$ with $\alpha_0 > 0$. For a subcritical system, the population at late times will be independent of the initial conditions, since the effect of these conditions will ultimately decay as $e^{\alpha_0 t}$ with $\alpha_0 < 0$. It is to be expected that, for any given source, Q, a time-independent solution will be obtained at late times. Although this expectation is reasonable, it seems to have been proved rigorously for a few special cases only[29] and for a medium which is nonmultiplying. Nevertheless, it will be assumed in this book, partly on physical grounds, that unique time-independent solutions to the transport equation exist for a critical system without a source or for a subcritical system with a steady source, regardless of whether the latter system is a multiplying one or not.

1.5e The Effective Multiplication Factor (or k) Eigenvalue

The criticality problem can often be best approached by introducing auxiliary eigenvalues. In particular $\nu(\mathbf{r}; E' \to E)$ may be replaced by $\nu(\mathbf{r}; E; \to E)/k$, and k can then be varied to obtain the criticality condition $\alpha_0 = 0$, with $k = k_{\text{eff}}$, the effective multiplication factor. This amounts to varying the number of neutrons emitted per fission by the factor $1/k_{\text{eff}}$. In the following, the subscript will be dropped from k_{eff} for brevity and hence k will denote the eigenvalue.

From a physical understanding of criticality (§1.5a), it appears that any system containing fissile material could be made critical by arbitrarily varying the number of neutrons emitted in fission. It will be assumed, therefore, that, for

any such system, there will always exist a unique positive eigenvalue, $k > 0$. By definition, k is an eigenvalue of the equation

$$v\boldsymbol{\Omega}\cdot\nabla N_k + \sigma v N_k = \iint \sum_{x \neq f} \sigma_x' f_x v' N_k' \, d\boldsymbol{\Omega}' \, dE' + \frac{1}{k}\iint \frac{1}{4\pi} \nu(\mathbf{r}; E' \to E)\sigma_f' v' N_k' \, d\boldsymbol{\Omega}' \, dE', \quad (1.49)$$

where, as in §1.1b, the summation over $x \neq f$ refers to collisions other than fission in which neutrons are produced, and N_k, N_k' are the eigenfunctions

$$N_k \equiv N_k(\mathbf{r}, \boldsymbol{\Omega}, E),$$
$$N_k' \equiv N_k(\mathbf{r}, \boldsymbol{\Omega}', E'),$$

which, it is explicitly noted, are not functions of time.

The existence of the eigenvalue k was assumed above on physical grounds and the existence of an associated nonnegative eigenfunction was also assumed. For various simple problems, the k eigenvalue spectrum has been investigated in detail. For example, in one-speed theory (see Chapter 2) with isotropic scattering, for a slab or a sphere, it has been proved[30] that there exists an infinite number of discrete real k eigenvalues and that, in particular, there will be a smallest one which is of physical interest as the effective multiplication factor. For multigroup theory there is also considerable information on the k eigenvalues and eigenfunctions as will be seen in Chapter 4.

It should be noted that the k eigenfunctions are not a complete set of functions for expansion of solutions of the transport equation.[31] In some cases of one-speed problems, however, it has been found[32] that when the k eigenfunctions are integrated over $\boldsymbol{\Omega}$, they do form a complete set for expanding functions of $\mathbf{r}$ only.

In elementary reactor theory, k is thought of as the ratio between the numbers of neutrons in successive generations, with the fission process being regarded as the birth event which separates generations of neutrons. To see what can be derived from transport theory, suppose that a pulsed source of neutrons, $Q_1(\mathbf{r}, \boldsymbol{\Omega}, E, t)$, is introduced into the system starting at $t = 0$. This is regarded as the source of first-generation neutrons, and these neutrons are lost by absorption, including fission, and by leakage (streaming). Those neutrons which are born in fission induced by the first-generation neutrons form the source for second-generation neutrons, and so on. Hence, the angular density of first-generation neutrons, N_1, is to be computed by solving the transport equation with source Q_1 and fission treated as an absorption; it is, therefore, a solution of the transport equation

$$\frac{\partial N_1}{\partial t} + v\boldsymbol{\Omega}\cdot\nabla N_1 + \sigma v N_1 = \iint \sum_{x \neq f} \sigma' f v' N_1' \, d\boldsymbol{\Omega}' \, dE' + Q_1(\mathbf{r}, \boldsymbol{\Omega}, E, t), \quad (1.50)$$

where the subscript x on σ' and f is understood.

Upon integration over time ($0 \leqslant t \leqslant \infty$), the first term on the left side of equation (1.50) gives

$$\int_0^\infty \frac{\partial N_1(\mathbf{r}, \mathbf{\Omega}, E, t)}{\partial t}\, dt = N_1(\mathbf{r}, \mathbf{\Omega}, E, \infty) - N_1(\mathbf{r}, \mathbf{\Omega}, E, 0) = 0.$$

The first term on the right of this expression is zero because the system with fission regarded as absorption must be subcritical, and since the (pulsed) source is of finite duration, the neutron density must ultimately decline to zero. The second term on the right side is zero by the postulate that the source produces the first generation of neutrons. If the quantities $\tilde{N}_1(\mathbf{r}, \mathbf{\Omega}, E)$ and $\tilde{Q}_1(\mathbf{r}, \mathbf{\Omega}, E)$ are defined by

$$\int_0^\infty N_1(\mathbf{r}, \mathbf{\Omega}, E, t)\, dt \equiv \tilde{N}_1(\mathbf{r}, \mathbf{\Omega}, E)$$

$$\int_0^\infty Q_1(\mathbf{r}, \mathbf{\Omega}, E, t)\, dt \equiv \tilde{Q}_1(\mathbf{r}, \mathbf{\Omega}, E),$$

then the integration of equation (1.50) gives

$$v\mathbf{\Omega}\cdot\nabla\tilde{N}_1 + \sigma v\tilde{N}_1 = \iint \sum_{x \neq f} \sigma' f v' \tilde{N}_1'\, d\mathbf{\Omega}'\, dE' + \tilde{Q}_1(\mathbf{r}, \mathbf{\Omega}, E). \tag{1.51}$$

Thus, $\tilde{Q}_1$ serves as the source for $\tilde{N}_1$, and since equation (1.51) refers to a subcritical system, i.e., no neutrons produced in fission, it follows from the results of the preceding section that the solution $\tilde{N}_1$ exists and is unique.[33]

From the angular density, $\tilde{N}_1$, of first-generation neutrons, the source, $\tilde{Q}_2$, of second-generation neutrons can be found by computing the fission neutrons produced by $\tilde{N}_1$; thus,

Second generation source

$$= \tilde{Q}_2(\mathbf{r}, \mathbf{\Omega}, E) = \iint \frac{1}{4\pi} \nu(\mathbf{r}; E' \to E)\sigma_f(\mathbf{r}, E')v'\tilde{N}_1'\, d\mathbf{\Omega}'\, dE'. \tag{1.52}$$

This source may now be used to determine the angular density, $\tilde{N}_2$, of second-generation neutrons and the source of third-generation neutrons, as in equations (1.51) and (1.52).

In this manner, a general iterative procedure may be defined for finding the neutron angular density in one generation after another by the recursion relation

$$v\mathbf{\Omega}\cdot\nabla\tilde{N}_i + \sigma v\tilde{N}_i = \iint \sum_{x \neq f} \sigma' f v' \tilde{N}_i'\, d\mathbf{\Omega}'\, dE' + \iint \frac{1}{4\pi} \nu'\sigma_f v'\tilde{N}_{i-1}'\, d\mathbf{\Omega}'\, dE', \tag{1.53}$$

where it is important to note that $\tilde{N}_{i-1}$ appears in the fission term and $\tilde{N}_i$ elsewhere in this equation.

As the foregoing procedure is iterated, it is to be expected that the angular density of neutrons in successive generations will increase for a supercritical system, decrease for a subcritical system, and become constant for a critical system. In any event, it is to be expected that the ratio of the densities in successive generations will approach a constant, independent of $\mathbf{r}$, $\mathbf{\Omega}$, and E. If this is so, then a comparison of equations (1.49) and (1.53) shows that the constant will be equal to k; thus,

$$\lim_{i\to\infty} \frac{\tilde{N}_i}{\tilde{N}_{i-1}} = \text{constant} = k. \tag{1.54}$$

This behavior has been confirmed rigorously for certain approximations to the transport equation,[34] and it is probably true in general. In fact, some approximation to the iterative procedure given in equation (1.53) is used in most numerical calculations of criticality, and the k is computed from equation (1.54). The procedure will be examined in detail in Chapter 4 for the multigroup diffusion approximation to transport theory.

1.5f Comparison of k and α Eigenvalues

For a critical system, i.e., when $\alpha_0 = 0$, and $k = 1$, the corresponding eigenfunctions satisfy the same equation; for any other system, however, the two eigenfunctions are different. This may be seen by writing the homogeneous eigenvalue equation (1.47) as (cf. §1.5a)

$$v\mathbf{\Omega}\cdot\nabla N_{\alpha_0} + \left(\sigma + \frac{\alpha_0}{v}\right) v N_{\alpha_0} = \int\int \sigma' f v' N'_{\alpha_0}\, d\mathbf{\Omega}'\, dE'. \tag{1.55}$$

In the critical condition, with $\alpha_0 = 0$, this becomes identical in form with equation (1.49) with $k = 1$. For other conditions, the two equations are clearly not equivalent.

It will be seen that in equation (1.55) the term α_0/v appears as an additional absorption cross section, and so it is sometimes referred to as "time absorption." In particular, it should be noted that for a subcritical system $\alpha_0/v < 0$; hence the term $\sigma + \alpha_0/v$ may be zero or negative. Such behavior may be difficult to handle in numerical computations. For this and other reasons, it is usually easier to treat criticality be evaluating k rather than α_0.

Another advantage of using k arises in calculating the neutron spectrum in a system which is actually critical, but as computed departs somewhat from criticality. In a k eigenvalue calculation, the number of neutrons per fission is varied (by $1/k$) to achieve criticality. This procedure has little effect on the neutron spectrum, and the resulting spectrum would be useful for determining power distributions, breeding ratios, etc., at least if $|1 - k| \ll 1$, i.e., if the computed system is not far from critical.

The calculation of α_0, on the other hand, is equivalent to varying the concentration of a $1/v$-absorber so as to achieve criticality, and this must affect the

neutron spectrum. For $\alpha_0 > 0$, higher energies are favored, i.e., the spectrum is hardened, whereas for $\alpha_0 < 0$, the spectrum is softened. Thus, the spectrum from an α_0 calculation should not be used in computations of neutron economy, except when actually considering the persisting time-dependent modes. The use of such modes will be described in Chapter 10 on reactor dynamics.

1.6 INTRODUCTION TO METHODS OF SOLVING THE NEUTRON TRANSPORT EQUATION

1.6a Need for Approximations

There is no possibility of obtaining exact solutions to the energy-dependent neutron transport equation for general reactor problems. A consideration of the immense amount of detail in the dependence of cross sections on neutron energy for the fissile, e.g., uranium-235 and plutonium-239, and fertile, e.g., thorium-232 and uranium-238, nuclei shows immediately that such solutions are impossible. It is necessary, therefore, to adopt approximate methods for solving the transport equation.

The most important of these are the multigroup methods in which the neutron energy interval of interest, usually from roughly 0.01 eV to 10 MeV, is divided into a finite number of intervals (or groups). It is then assumed that the cross section in each group is constant, e.g., an average over energy, independent of energy, although arbitrarily dependent on position (or composition). The other generally useful technique is the Monte Carlo method. For some problems, the multigroup and Monte Carlo procedures are combined.

Methods for solving the neutron transport problem have also been based on solution of the integral equation using either numerical or approximate kernels;[35] one of these will be described in Chapter 7. Some other formulations of the transport problem have also been proposed, e.g., the method of invariant imbedding,[36] but they have had little application in the study of nuclear reactors.

The two main techniques referred to above for solving the neutron transport equation are outlined in §§1.6d, 1.6e. Certain properties of nuclear cross sections that influence the mode of solution will, however, be considered first.

1.6b Variations of Cross Sections with Energy

Many cross sections vary so rapidly and widely with energy that it is hopeless to try to represent the energy dependence with a reasonable number, e.g., about 20, of neutron groups. This situation is most pronounced for heavy nuclei of interest in the so-called resonance energy region, lying roughly between 10^5 eV and 1 eV (see Fig. 8.1). The fertile nuclei, for example, have resonance peaks spaced some 20 eV apart, and the cross sections in the resonance region vary by several orders of magnitude. The fissile nuclei have similar resonance peaks

with a spacing of about 2 eV. In order to obtain useful group cross sections in the energy regions where the cross section versus energy curves have much fine structure, it is necessary to perform a careful analysis of the neutron energy spectrum through these regions. Such an analytical procedure is described in Chapter 8.

In addition to the resonances exhibited by heavy elements, some light elements show much detail in their cross sections at higher neutron energies that cannot be explicitly included in the group cross sections. Examples are provided by oxygen for neutron energies above 300 keV and by iron at energies in excess of about 10 keV. Here again detailed calculations of neutron spectra may be required before reasonably good group cross sections can be defined. It is now becoming the common practice to store much of the cross section fine structure data on magnetic tapes for processing by digital computers in order to generate approximate neutron spectra and group cross sections.[37]

In the thermal-neutron energy region, below approximately 1 eV, neutron cross sections may become complicated because they reflect the dynamics of energy transfer between the neutrons and nuclei which are bound in molecules or crystals. This problem will be taken up in Chapter 7. Frequently, detailed calculations must be made before adequate neutron energy spectra and group cross sections are obtained. It is, of course, not necessary to represent all thermal neutrons in one energy group, but the number of groups which include these neutrons is usually kept small, e.g., generally less than about 20 or so.

As will be seen in later chapters, the basic requirement for obtaining satisfactory group cross sections is a knowledge (or good estimate) of the neutron energy spectrum within each group. If there is much detail in the cross sections, lengthy calculations may be needed to obtain these spectra.

1.6c Anisotropy of Neutron Emission

Some comments may be made on the degree of anisotropy of neutron emission especially in elastic scattering. When a beam of monoenergetic neutrons is scattered elastically, the angular distribution of the scattered neutrons may be expanded in the form

$$\sigma(\mu_0) = \sum_{l=0}^{\infty} \sigma_l P_l(\mu_0),$$

where μ_0 is the cosine of the scattering angle in the center-of-mass system and the P_l's are the Legendre polynomials (see Appendix). For $l = 0$, i.e., s-wave scattering, $P_0(\mu)$ is unity, and the scattering is isotropic in the center-of-mass system, but for $l = 1$ (p-wave) or more, the scattering is anisotropic. It can be shown by the use of quantum mechanics that for $l > 0$, the value of σ_l is small for neutrons of low energy; hence, for such neutrons the elastic scattering is essentially isotropic in the center-of-mass system. A simple classical argument, given below, leads to results of the correct order of magnitude.

Suppose a neutron with velocity v approaches a nucleus with the impact parameter b (Fig. 1.14). Then unless b is approximately equal to or less than the sum of the nuclear radius and the range of nuclear forces, i.e.,

$$b \lesssim (1.2A^{1/3} + 1.0) \times 10^{-13} \text{ cm},$$

where A is the mass number of the nucleus, there will be no appreciable elastic scattering. If M is the mass of the nucleus and m is the mass of the neutron, the angular momentum is given by

$$\text{Angular momentum} = \frac{Mm}{M + m} vb \approx mvb,$$

if M is large compared to m. Upon equating the angular momentum to $\hbar l$, it follows that the quantum number l is given by $mvb/\hbar$. Hence, σ_l will be appreciable only for

$$l \lesssim \frac{mv(1.2A^{1/3} + 1.0) \times 10^{-13}}{\hbar} = (0.26A^{1/3} + 0.22) \times 10^{-3}\sqrt{E},$$

where E is the neutron energy in eV.

For uranium-238, for example, $A^{1/3}$ is 6.2, and the condition for σ_l to be not negligible is that $l \lesssim 1.8 \times 10^{-3}\sqrt{E}$. This would imply that $l = 1$ will begin to make a significant (anisotropic) contribution to the angular distribution in elastic scattering when E exceeds about 300 keV. For lighter nuclei, the $l = 1$ contribution will commence at higher energies. These conclusions are in qualitative agreement with experiment. Roughly speaking, the angular distribution of elastically scattered neutrons is isotropic in the center-of-mass system for neutron energies below about 100 keV; at energies above 1 MeV, the scattering is markedly anisotropic.

It should be noted, however, that scattering which is isotropic in the center-of-mass system will become anisotropic in the laboratory system; in particular, it will be peaked in the forward direction. The effect is not significant for heavy nuclei, but for light nuclei it is very important. It may be concluded, therefore,

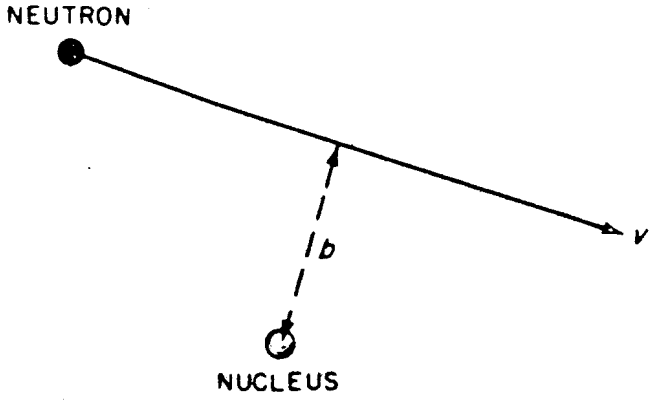

FIG. 1.14 IMPACT PARAMETER OF NEUTRON-NUCLEUS SYSTEM.

that in the laboratory system, anisotropy will be most pronounced in the scattering of fast neutrons from nuclei of all mass numbers and of neutrons of all energies from light nuclei. Thus, anisotropic elastic scattering is important in fast reactors and in thermal water-moderated systems.

When thermal neutrons are scattered from nuclei bound in crystals, there may be pronounced anisotropic scattering. An extreme example is provided by coherent scattering at sharply defined Bragg angles. Some discussion of this matter is given in Chapter 7.

Neutrons emitted in fission are usually assumed, to a good approximation, to be isotropic in the laboratory system. In inelastic scattering and $(n, 2n)$ reactions, the neutrons are often fairly isotropic, but angular distributions are becoming available from laboratory studies for use in calculations.

1.6d Multigroup Methods

It might appear, at first thought, that a systematic multigroup solution to the neutron transport equation could be obtained by integrating this equation over a finite energy range, say $E_g \leqslant E \leqslant E_{g-1}$, in each group. But this leads to an immediate complication. Suppose that for a steady-state problem, i.e., $\partial\Phi/\partial t = 0$, the neutron angular flux in the group g may be defined by

$$\Phi_g(\mathbf{r}, \Omega) = \int_{E_g}^{E_{g-1}} \Phi(\mathbf{r}, \Omega, E)\, dE.$$

Then the $\sigma\Phi$ term on the left side of the transport equation (1.14) becomes $\sigma_g(\mathbf{r}, \Omega)\Phi_g(\mathbf{r}, \Omega)$, where

$$\sigma_g(\mathbf{r}, \Omega) = \frac{\int \sigma(\mathbf{r}, E)\Phi(\mathbf{r}, \Omega, E)\, dE}{\Phi_g(\mathbf{r}, \Omega)}.$$

The group cross section, $\sigma_g(\mathbf{r}, \Omega)$ has thus acquired a dependence on Ω. In general, this is a substantial complication but it can be avoided by first assuming a form for the angular dependence of the neutron flux and then integrating over energy.

The usual first step in a multigroup approximation, therefore, is to represent the angular dependence of the neutron flux by an expansion, most commonly in spherical harmonics. (This expansion is similar to that used in §1.6c to express the angular distribution of scattered neutrons.) If there is an axis of symmetry for the angular distribution of the flux, as may occur in plane or spherical geometry, the expansion reduces to a sum of Legendre polynomials, $P_n(\mu)$, where μ is the direction cosine. Since the spherical harmonics (or Legendre polynomials) form a complete set (see Appendix), the expansion involves no approximation. In practice, however, to make calculations possible, it is necessary to terminate the series after a finite number of terms. It is in this manner that an approximation is introduced. In general, if the series is truncated after $N + 1$ terms, the result is referred to as a P_N approximation.

The next step in the solution of the neutron transport equation is to integrate over a finite energy range, i.e., an energy group, thereby defining the group cross sections and arriving at the multigroup P_N equations. When the angular distribution of the neutron flux is represented adequately by the first two Legendre polynomials, $P_0(\mu)$ and $P_1(\mu)$, the multigroup P_1 equations are obtained. It will be seen in Chapter 4 that when certain assumptions are made about the energy dependence of the neutron flux, these are equivalent to multigroup diffusion theory or to multigroup age-diffusion theory. An alternative (variational) method for deriving multigroup P_1 equations will be discussed in Chapter 6.

The multigroup P_1 equations and the related diffusion equations are the most widely used in reactor problems. In some cases, P_3 approximations and those of higher order have proved valuable. The P_N approximations with N even have usually been thought to be less accurate than those with N odd and so they have been seldom employed (see, however, Ref. 38). Other angular expansions are preferable in certain instances; for plane geometry, in particular, separate Legendre expansions for $0 \leqslant \mu \leqslant 1$ and $-1 \leqslant \mu \leqslant 0$ are superior to a single expansion. These matters are treated in Chapters 3 and 5.

In another class of multigroup methods, known as the discrete ordinates or discrete S_N (or simply S_N) methods, the neutron transport equation is solved in a discrete set of directions only. Angular integrals are then approximated by sums over discrete directions and angular derivatives by differences. These methods are described in detail in Chapter 5 where it will be seen that for plane geometry some of the S_N approximations are equivalent to P_N methods. The virtue of the S_N method is that accuracy can be increased simply by increasing the number of directions without otherwise changing the method of solution. It has been frequently used for problems where the P_1 approximation is not adequate.

The multigroup equations, both P_N and S_N, are differential equations and they are converted into a system of algebraic equations for machine computation by introducing a discrete space mesh, approximating derivatives by differences, and so on. In this form the multigroup methods are the most useful for determining overall neutron transport, e.g., criticality, power distribution, reaction rate, etc., for energy-dependent problems in fairly simple geometry. Both in principle and in practice, with fast digital computers, the multigroup equations are capable of yielding results of a higher degree of precision than is really justified by the uncertainties in the cross sections. The accuracy is improved by normalizing the calculations so as to obtain agreement with accurate critical experiments in simple geometries (see Chapter 5).

For simple geometries the main uncertainties are concerned with the values of the group constants (group cross sections) and with the degree of detail (or accuracy) required in the neutron angular expansion, in the energy spacing, i.e., number of groups, and in the space mesh. The group constants are weighted averages of the energy-dependent cross sections which appear in the complete

form of the neutron transport equation. The choice of appropriate weighting functions is a central problem. The important energy region where resonances are most pronounced is treated in Chapter 8, and the problem of determining the spectra of neutrons as they are coming into thermal equilibrium with the moderator is discussed in Chapter 7.

When the geometry of the system is more complicated, as a result of (*a*) fine structure as in a heterogeneous lattice, or (*b*) gross departure from a geometry which can be given in terms of one or two coordinates, the general multigroup equations cannot be used directly.

In treating fine structure, the customary procedure is first to make a calculation on a heterogeneous cell, i.e., a fundamental repeating unit of the lattice. The results are then used to homogenize the cell, so as to give the same neutron economy as in the heterogeneous system, for use in calculating the over-all neutron transport and economy by a multigroup (P_1 or other) method.

For the cell calculation, the neutron transport equation in a P_N or S_N approximation, with appropriate boundary conditions, may be used. Alternatively, because of the small sizes of most cells, in terms of the neutron mean free path, together with strong absorption in them, collision probabilities are frequently used in cell calculations. These probabilities are considered in Chapters 2 and 8. Integral experiments, especially on lattice multiplication are, of course, useful for normalizing and guiding calculations.

For the over-all reactor, machine calculations are now easily made for one-dimensional geometries, such as the sphere, infinite (in two dimensions) slab, and infinite cylinder. For two space dimensions, multigroup P_1 or low-order S_N calculations are performed as a matter of routine. The available space and angle mesh may, however, not be fine enough to give an adequate description of the situation. Consequently, for complicated two-dimensional or three-dimensional systems, other treatments must be used. The variational method provides one way of approaching the problem in which an attempt may be made to synthesize a two-dimensional flux, for example, by a product of two one-dimensional fluxes (see Chapter 6). If all other methods fail, a Monte Carlo calculation may be attempted.

1.6e The Monte Carlo Method

The Monte Carlo method, which has proved to be useful in some areas of reactor physics, is a numerical procedure based on statistical (or probability) theory. In neutron transport calculations, the applicability of the Monte Carlo techniques arises from the fact that, as seen earlier, the (macroscopic) cross section may be interpreted as a probability of interaction per unit distance traveled by a neutron. Thus, in the Monte Carlo method, a set of neutron histories is generated by following individual neutrons through successive collisions. The locations of actual collisions and the results of such collisions,

e.g., direction and energy of the emerging neutron (or neutrons), are determined from the range of possibilities by sets of random numbers. The Monte Carlo technique has proved useful in special cases, such as complex geometries where other methods encounter difficulties and in some cell calculations. Moreover, when there is considerable detail in the variation of the neutron cross section with energy, the Monte Carlo method eliminates the necessity for making subsidiary calculations, e.g., of resonance flux. In fact, the method is useful for determining the group constants needed in the multigroup approximations.

The random numbers required for a Monte Carlo calculation are usually generated by the computer. Thus, the computer selects numbers $\xi_1, \xi_2, \xi_3, \ldots$, at random for the interval $0 \leqslant \xi_i \leqslant 1$. This means that the probability $p(\xi_i)\, d\xi_i$ for ξ_i to lie between ξ_i and $\xi_i + d\xi_i$ is $d\xi_i$ if $0 \leqslant \xi_i \leqslant 1$, i.e., $p(\xi_i) = 1$. To see how the random numbers are employed to develop neutron histories, a simple example will be considered in which neutrons are started from a monoenergetic, isotropic, point source.

The first step is to select a neutron direction and for this the first two random numbers, ξ_1 and ξ_2, are used. An azimuthal angle may be chosen as $\varphi_1 = 2\pi\xi_1$ and the cosine of a polar angle as $\mu = 2\xi_2 - 1$; the reason is that the source is isotropic and all initial values of φ and μ are equally probable in the intervals $0 \leqslant \varphi \leqslant 2\pi$ and $-1 \leqslant \mu \leqslant 1$, respectively.

With the neutron direction chosen, the next step is to find where the first collision occurs. Let the cross section in this direction and at a distance s from the source be denoted by $\sigma(s)$. Then the probability $p(s)\, ds$ that a neutron will undergo a collision between s and $s + ds$ is

$$p(s)\, ds = \sigma(s) \exp\left[-\int_0^s \sigma(s')\, ds'\right] ds.$$

If a third random variable, ξ_3, is now taken, s can be determined by setting

$$\ln \xi_3 = -\int_0^s \sigma(s')\, ds'.$$

From this relation it follows that

$$d\xi_3 = -\sigma(s)\, ds \exp\left[-\int_0^s \sigma(s')\, ds'\right], \tag{1.56}$$

and since

$$p(s)\, ds = p(\xi_3)\, d\xi_3 = d\xi_3,$$

the quantity s is thereby selected from the correct distribution $p(s)$. The minus sign in equation (1.56) is required because s decreases as ξ_3 increases and it does not affect the probability of s lying in any particular range.

Once the location of the first collision has been determined, further random numbers are used to find the outcome of the first collision, location of the second

collision, and so on. The procedure is continued until the neutron history is terminated, for example, by leakage from the system or by absorption.

In solving the neutron transport equation by Monte Carlo methods, there are uncertainties which are not due to explicit approximations to the flux, such as arise in multigroup methods, but to the limitation in the (finite) number of neutrons examined. Such errors are more or less random and procedures have been developed for reducing the uncertainty associated with a given amount of numerical work. These are variance reducing techniques; they modify the random walk problem so as to leave the desired expectation value unchanged but reduce the variance.

Some of the techniques are indicated by common sense whereas others require further mathematical analysis. Two examples in the former category will be indicated. First, it may happen by chance that, in following a certain neutron history during moderation, the neutron is absorbed in its first collision. Instead of terminating the history, it is usually fruitful to continue but to give the neutron less weight, proportional to the probability of scattering (and no absorption) at the collision point. As a result, the history of the neutron is not terminated at the first collision, but the generation of information can be continued until the neutron history is terminated, usually when the weighting becomes negligible or the neutron escapes from the system.

Another example based on common sense is that arising in connection with two similar but not identical problems. Since the errors in Monte Carlo techniques are random in character, the solutions to these problems may be quite different. In comparing such solutions, the difference between them may be made more accurate by using the same neutron histories in the two problems; the random errors are then approximately the same in both cases.

Suppose, for example, it is required to compute the resonance escape probability of neutrons moderated in a lattice in order to find the variation with temperature arising from Doppler broadening. If two independent Monte Carlo calculations were made at two temperatures, the random errors might be so large as to mask any real difference in the solutions. If, however, the same neutron histories are used in both calculations, the difference might have significance.

More refined techniques for variance reduction could be used in a situation such as the following. Suppose it is desired to determine the contribution of source neutrons to a detector reading. It is apparent that some of these neutrons, e.g., those emitted in directions toward the detector and those of high energy, would be more likely than others to actuate the detector. If so, it would seem to be most efficient in the Monte Carlo calculation to concentrate the computation on these important neutrons. In Chapter 6, this "importance" is given a mathematical significance in terms of the solution to an adjoint transport problem. In the technique of importance sampling, neutron histories are started from the source distribution in proportion to their importance. Furthermore, at each

collision the most important neutrons can be followed preferentially with due precautions being taken not to bias the results.

Most of what can be said about Monte Carlo methods is concerned with a detailed discussion of techniques that lies outside the scope of this book. A number of references on the subject are available to the interested reader.[39] There is no doubt that Monte Carlo methods are capable of solving a variety of problems for which multigroup methods are inaccurate, and some of the results obtained will be mentioned in due course. Nevertheless, the Monte Carlo technique has not been widely used for the solution of general criticality problems because the multigroup methods are simpler to apply and are sufficiently accurate except in the special situations referred to earlier. Monte Carlo methods have been utilized extensively in reactor shielding calculations, however, to determine the leakage of neutrons (and photons) through a shield.

1.7 APPENDIX TO CHAPTER 1

1.7a General Coordinate Systems

General coordinate systems and the corresponding expressions for $\Omega \cdot \nabla \Phi$ (or $\Omega \cdot \nabla N$) and for $\int d\Omega$ are given here.

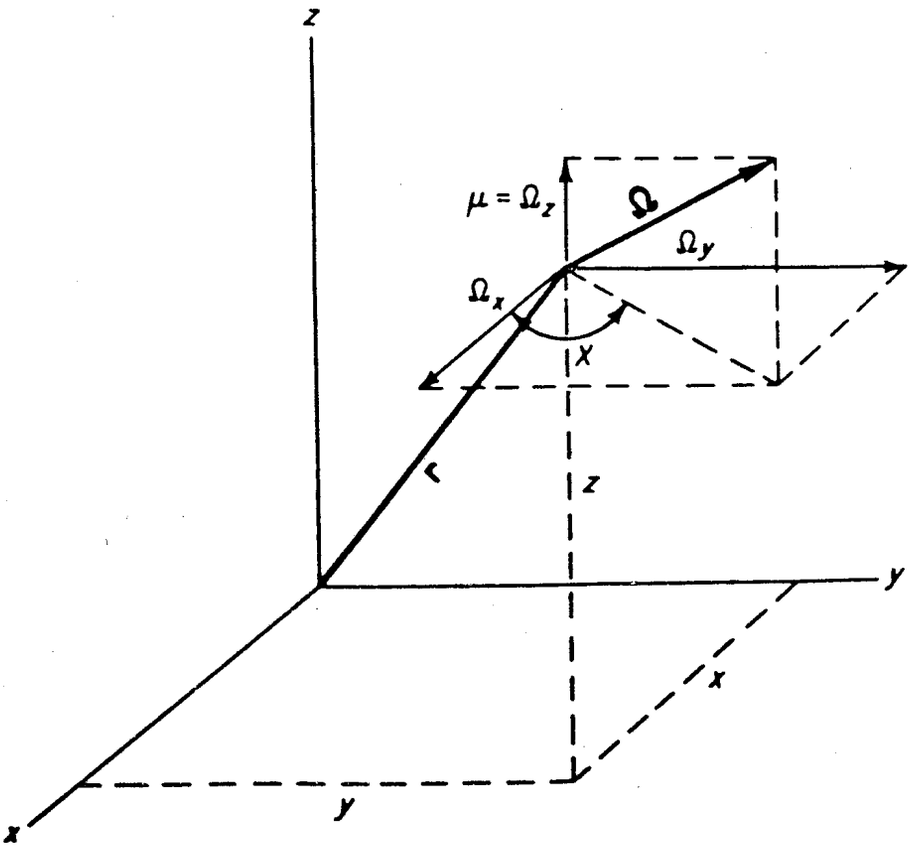

FIG. 1.15 RECTANGULAR COORDINATE SYSTEM.

Rectangular Coordinates

Position vector $\mathbf{r}$: $x, y, z,$
Neutron direction $\mathbf{\Omega}$: $\mu, \chi,$

where $\mu = \mathbf{\Omega} \cdot \hat{\mathbf{z}}$ and χ is the angle between the planes formed by the $\mathbf{\Omega}$ and $\hat{\mathbf{z}}$ vectors and by the $\hat{\mathbf{z}}$ and $\hat{\mathbf{x}}$ vectors; $\hat{\mathbf{z}}$ and $\hat{\mathbf{x}}$ are unit vectors in the z and x directions, respectively (Fig. 1.15).

Cylindrical Coordinates

Position vector $\mathbf{r}$: $r, \varphi, z,$
Neutron direction $\mathbf{\Omega}$: $\mu, \chi,$

where φ is the polar angle; $\mu = \mathbf{\Omega} \cdot \hat{\mathbf{z}}$ and χ is the angle between the planes formed by the $\mathbf{\Omega}$ and $\hat{\mathbf{z}}$ vectors and by the $\hat{\mathbf{z}}$ and $\hat{\mathbf{r}}$ vectors (Fig. 1.16).

Spherical Coordinates

Position vector $\mathbf{r}$: $r, \theta, \varphi,$
Neutron direction $\mathbf{\Omega}$: $\mu, \omega,$

where θ is the polar angle and φ the azimuthal angle; $\mu = \mathbf{\Omega} \cdot \hat{\mathbf{r}}$ and ω is the angle between the planes formed by the $\mathbf{\Omega}$ and $\hat{\mathbf{r}}$ vectors and by the $\hat{\mathbf{r}}$ and $\hat{\mathbf{z}}$ vectors (Fig. 1.17).

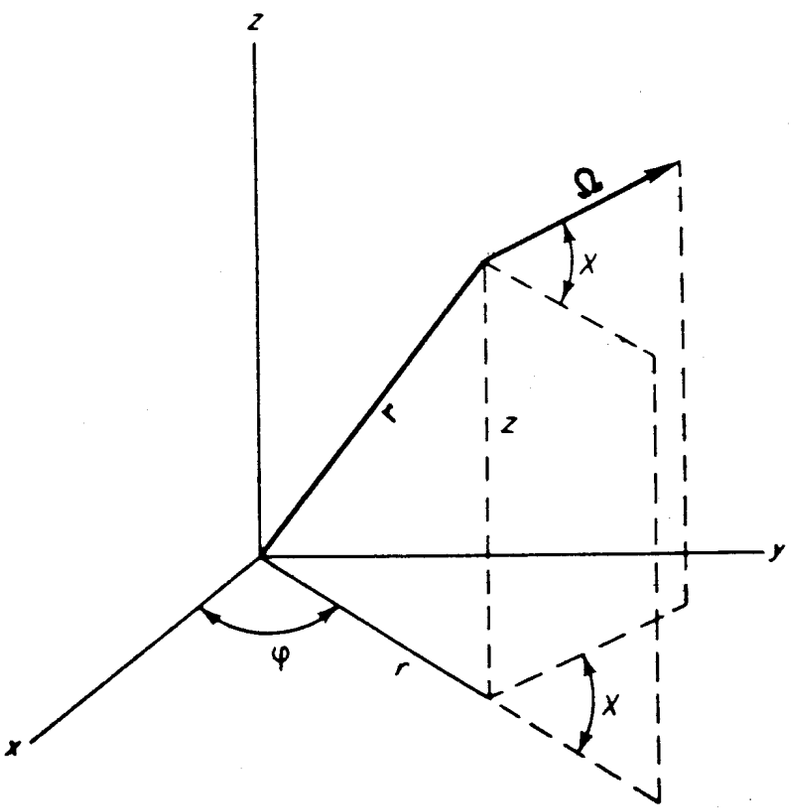

FIG. 1.16 CYLINDRICAL COORDINATE SYSTEM.

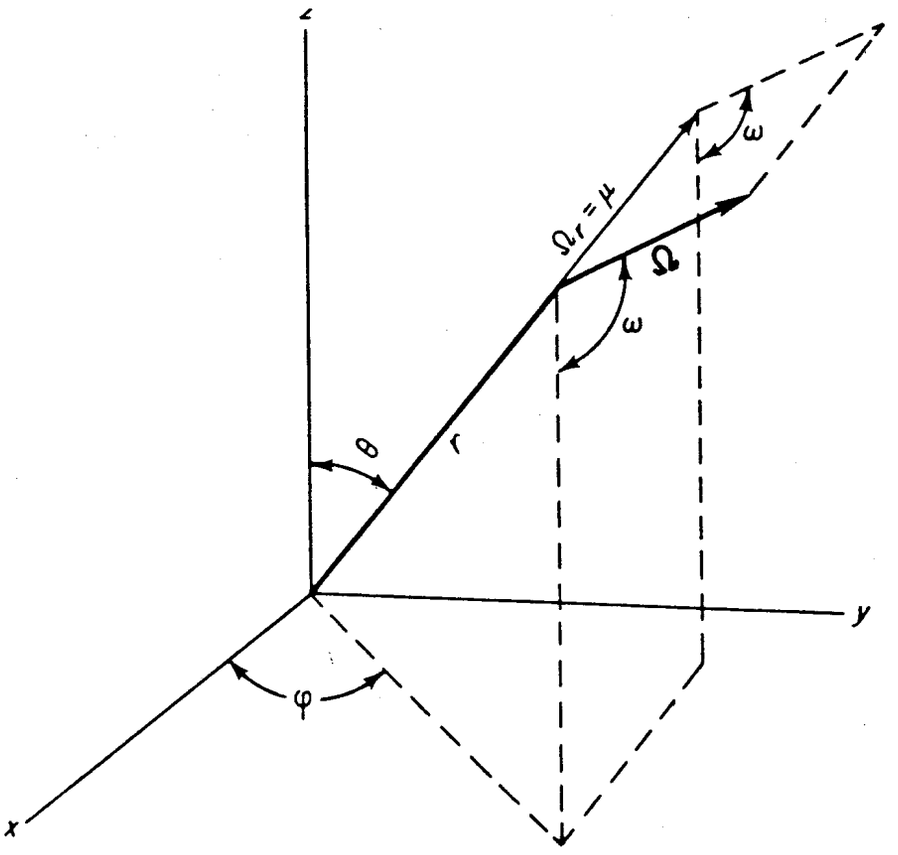

FIG. 1.17 SPHERICAL COORDINATE SYSTEM.

The values of $\boldsymbol{\Omega}\cdot\nabla\Phi$ and of $\int d\boldsymbol{\Omega}$ for various geometries are collected in Table 1.2. As mentioned in §1.3a, expressions for $\boldsymbol{\Omega}\cdot\nabla N$ can be obtained simply by replacing Φ by N.

Other representations are sometimes used for the direction coordinates and care must be taken to identify each author's particular choice; see, for example, Ref. 40 for an alternative choice of directions in cylindrical coordinates.

The following expressions give $\boldsymbol{\Omega}\cdot\nabla\Phi$ in *conservation form* for general cylindrical and spherical coordinates:

Cylindrical coordinates

$$\frac{\sqrt{1-\mu^2}\cos\chi}{r}\frac{\partial(r\Phi)}{\partial r}+\frac{\sqrt{1-\mu^2}\sin\chi}{r}\frac{\partial\Phi}{\partial\varphi}-\frac{1}{r}\frac{\partial(\Phi\sqrt{1-\mu^2}\sin\chi)}{\partial\chi}+\mu\frac{\partial\Phi}{\partial z}.$$

Spherical coordinates

$$\frac{\mu}{r^2}\frac{\partial(r^2\Phi)}{\partial r}+\frac{\sqrt{1-\mu^2}\sin\omega}{r\sin\theta}\frac{\partial\Phi}{\partial\varphi}+\frac{\sqrt{1-\mu^2}\cos\omega}{r\sin\theta}\frac{\partial(\Phi\sin\theta)}{\partial\theta}$$

$$+\frac{1}{r}\frac{\partial[(1-\mu^2)\Phi]}{\partial\mu}-\frac{\cot\theta}{r}\frac{\partial(\Phi\sqrt{1-\mu^2}\sin\omega)}{\partial\omega}.$$

TABLE 1.2. TERMS IN THE TRANSPORT EQUATION FOR SPECIAL GEOMETRIES

$\boldsymbol{\Omega}\cdot\nabla\Phi$	$\int d\Omega$
Plane: $\Phi(x;\mu)$	
$\mu\dfrac{\partial\Phi}{\partial x}$	$2\pi\int_{-1}^{1} d\mu$
Rectangular: $\Phi(x, y, z;\mu,\chi)$	
$\sqrt{1-\mu^2}\left(\cos\chi\dfrac{\partial\Phi}{\partial x}+\sin\chi\dfrac{\partial\Phi}{\partial y}\right)+\mu\dfrac{\partial\Phi}{\partial z}$	$\int_{-1}^{1} d\mu\int_{0}^{2\pi} d\chi$
Spherical (spherical symmetry): $\Phi(r;\mu)$	
$\mu\dfrac{\partial\Phi}{\partial r}+\dfrac{1-\mu^2}{r}\dfrac{\partial\Phi}{\partial\mu}$	$2\pi\int_{-1}^{1} d\mu$
Spherical (general): $\Phi(r,\theta,\varphi;\mu,\omega)$	
$\mu\dfrac{\partial\Phi}{\partial r}+\dfrac{\sqrt{1-\mu^2}}{r}\dfrac{\sin\omega}{\sin\theta}\dfrac{\partial\Phi}{\partial\varphi}+\dfrac{\sqrt{1-\mu^2}}{r}\cos\omega\dfrac{\partial\Phi}{\partial\theta}$ $+\dfrac{1-\mu^2}{r}\dfrac{\partial\Phi}{\partial\mu}-\dfrac{\sqrt{1-\mu^2}}{r}\sin\omega\cot\theta\dfrac{\partial\Phi}{\partial\omega}$	$\int_{-1}^{1} d\mu\int_{0}^{2\pi} d\omega$
Cylindrical (infinite cylinder, axial symmetry): $\Phi(r;\mu,\chi)$	
$\sqrt{1-\mu^2}\cos\chi\dfrac{\partial\Phi}{\partial r}-\dfrac{\sqrt{1-\mu^2}}{r}\sin\chi\dfrac{\partial\Phi}{\partial\chi}$	$\int_{-1}^{1} d\mu\int_{0}^{2\pi} d\chi$
Cylindrical (general): $\Phi(r,\varphi,z;\mu,\chi)$	
$\sqrt{1-\mu^2}\cos\chi\dfrac{\partial\Phi}{\partial r}+\dfrac{\sqrt{1-\mu^2}}{r}\sin\chi\left(\dfrac{\partial\Phi}{\partial\varphi}-\dfrac{\partial\Phi}{\partial\chi}\right)+\mu\dfrac{\partial\Phi}{\partial z}$	$\int_{-1}^{1} d\mu\int_{0}^{2\pi} d\chi$

The advantage of the conservation form can be seen by considering the expression for $\boldsymbol{\Omega}\cdot\nabla\Phi$ in spherical coordinates. Integration over all directions $\boldsymbol{\Omega}$, i.e., $\int_{-1}^{1} d\mu\int_{0}^{2\pi} d\omega$, removes the last two terms, whereas the first three terms represent the components of $\nabla\cdot\mathbf{J}$. If these three terms are now integrated over volume ($dV = r^2\sin\theta\, d\theta\, d\varphi$), bounded by surfaces of constant r, φ, and θ, the first term is seen to be the outward current across the two surfaces of constant r. Similarly, the second and third terms are the currents across surfaces of constant φ and θ, respectively.

EXERCISES

1. Consider a collimated beam of neutrons of intensity 1 neutron/cm^2-sec in the z direction; suppose a sphere of 1 cm radius is placed in this neutron beam. Determine the radial and other components of the incident current, as functions of position on the spherical surface, in a polar coordinate system with its origin

at the center of the sphere. What is the angular distribution of the incident neutrons, averaged over the surface of the sphere?

2. A very thin plane source (thickness Δx) of monoenergetic neutrons emits $1/\Delta x$ neutrons/cm^2-sec isotropically per unit volume. What is the angular distribution of the current (and flux) at the surface? Absorption in the source may be ignored.
3. A purely absorbing half-plane medium in which $\sigma = 1$, contains a source emitting 1 neutron/cm^3-sec. Determine the intensity and angular distribution of the flux and the current at the surface.
4. Consider a combination of two point sources present either (*a*) in a vacuum, or (*b*) in a purely absorbing medium. Compute the magnitude of the current and flux throughout space and sketch the contours of equal flux and equal current.
5. Make a detailed derivation of the transport equation by considering the rate of change of the neutron population in a volume element fixed in space, i.e., along the lines indicated on page 15.
6. Consider a bare slab of thickness d and apply one-speed diffusion theory to find α and k eigenvalues as given by this model of neutron transport. Use the diffusion equation in the form

$$\frac{1}{v}\frac{\partial \phi}{\partial t} = D\frac{\partial^2 \phi}{\partial x^2} + [(\nu - 1)\sigma_f - \sigma_a]\phi$$

and boundary conditions of zero flux on the slab surfaces. (Hint: each mode $\cos n\pi x/d$ corresponds to one eigenvalue of each kind.) Draw a sketch showing how the eigenvalues are related to each other. For comparison of the results with those of transport theory, see Ref. 41.

7. It is required to describe the transport of neutrons in a reactor in one region of which coolant is moving with high velocity, v, in the z direction. How will the transport equation be changed in this region? If, in the region under consideration, the cross sections for collisions with nuclei at rest are independent of the neutron energy, what would be the angular dependence of σ in the transport equation for the moving nuclei? (It may be found helpful in this connection to read §7.3c.) Consider qualitatively how the angular distribution of the scattered neutrons would be affected if the scattering from nuclei at rest is isotropic in the laboratory system. (After reviewing this problem, the interested reader may wish to consult Ref. 42)
8. Derive the integral equation (1.37) for plane geometry and isotropic scattering by starting from the transport equation in plane geometry with free-surface boundary conditions. (Hint: start by multiplying the transport equation by $e^{\Sigma x}$ and then integrate from a boundary to x.) Show also how an incident flux on one surface can be handled in this derivation.
9. Consider a surface source at $\mathbf{r}_s$ of intensity $Q_s(\mathbf{r}_s, \Omega, E, t)$. By regarding this source as the limit of a thin volume source and using equation (1.22), derive the discontinuity in the neutron angular density. All cross sections are to be regarded as finite. Give an alternative derivation by considering neutron conservation in a small pillbox, centered at $\mathbf{r}_s$ and having faces parallel to the surface.
10. Suppose there is a purely absorbing region of finite thickness. It is desired to represent this region as an absorbing surface across which the neutron angular

density is discontinuous. Derive the discontinuity which is required in the angular density.

11. Start with the transport equation for spherical geometry not in conservation form, i.e., with $\Omega \cdot \nabla N$ as in equation (1.32), and verify equation (1.34). Then find the particular form of the conservation relation, equation (1.19), for that geometry.
12. Derive the integral equation (1.27) using neutron conservation arguments along the lines suggested on page 26.
13. Derive the form of $\Omega \cdot \nabla N$ in cylindrical geometry as it appears in Table 1.2, assuming that N is independent of φ.
14. An instantaneous point source in an infinite medium of density ρ_0 gives a known neutron angular flux, $\Phi_0(\mathbf{r}, \mu, E, t)$. Show how the angular flux from the same source in a medium of different density ρ could be found by scaling Φ_0. (This problem arises in considering the explosion of nuclear weapons at various altitudes in the atmosphere.) Indicate some circumstances in which the scaling might be invalidated for this application.
15. For students having a knowledge of computer programming: Write a Monte Carlo program to compute the escape probability for neutrons born uniformly and isotropically in a medium with simple geometry, e.g., a slab or a sphere. The cross section may be taken to be independent of energy and the scattering to be isotropic. (Some results are given in Table 2.8.)
16. Consider the space-independent neutron transport equation in a source-free, infinite medium, i.e.,

$$\frac{\partial N}{\partial t} + \sigma v N = \iint \sigma' f v' N' \, d\Omega' \, dE',$$

and eigenvalues α for $\partial N/\partial t = \alpha N$ are sought. It is to be shown that all real negative values of α with magnitude greater than the smallest value of σv belong to the continuous spectrum. Consider a value of α for which $-|\alpha| + (\sigma v)_{E=E_0} = 0$. Construct a strongly peaked function, N_Δ, of width Δ in energy about E_0 and in angle, μ, such that the integral on the right side of the eigenvalue equation is proportional to Δ but $\iint N^2 \, d\Omega \, dE$ is independent of Δ. By taking the limit as $\Delta \to 0$ it is seen that N_Δ plays the role of a highly singular eigenfunction and hence the corresponding value of α belongs to the continuous spectrum. For further examples and discussion of such functions, see Ref. 43.

REFERENCES

1. Schiff, L. I., "Quantum Mechanics," McGraw-Hill Book Co., Inc., 1949, pp. 13, 54.
2. Osborn, R. K., and S. Yip, "The Foundations of Neutron Transport Theory," Gordon and Breach, 1966.
3. Weinberg, A. M., and E. P. Wigner, "The Physical Theory of Neutron Chain Reactors," University of Chicago Press, 1958, p. 281.
4. Lamarsh, J. R., "Introduction to Nuclear Reactor Theory," Addison-Wesley Publishing Co., Inc., 1966, Section 6-1.
5. Lamarsh, J. R., Ref. 4, Section 2-3.
6. Glasstone, S., and M. C. Edlund, "Elements of Nuclear Reactor Theory," D. Van Nostrand Co., Inc., 1952, §14.6.

7. Davison, B., "Neutron Transport Theory," Oxford University Press, 1957, Section 2.3.
8. Case, K. M., and P. F. Zweifel, "Linear Transport Theory," Addison-Wesley Publishing Co., Inc., 1967, Appendix D.
9. Courant, R., and D. Hilbert, "Methods of Mathematical Physics," Interscience Publishers, Inc., 1953, Vol. II, p. 69.
10. Davison, B., Ref. 7, Chap. XVII; Benoist, P., *Nucl. Sci. Eng.*, **30**, 85 (1967).
11. Case, K. M., and P. F. Zweifel, Ref. 8, Appendix D; G. M. Wing, "Introduction to Transport Theory," Wiley and Sons, Inc., 1962, Chap. 8.
12. Bell, G. I., and W. B. Goad, *Nucl. Sci. Eng.*, **23**, 380 (1965); Yu. N. Kazachenkov, and V. V. Orlov, *Atomn. Energiia*, (transl.), **18**, 222 (1965).
13. Bell, G. I., *Nucl. Sci. Eng.*, **21**, 390 (1965); D. R. Harris, in "Naval Reactor Physics Handbook," Vol. I, A. Radkowsky, ed., U.S. AEC, 1964, Section 5.5.
14. Bell, G. I., Ref. 13; *Proc. Symp. Appl. Math.*, "Transport Theory," Am. Math. Soc., 1969. Vol. I, p. 181.
15. Case, K. M., and P. F. Zweifel, Ref. 8, Appendix D; J. T. Marti, *Nukleonik*, **8**, 159 (1966).
16. Churchill, R. V., "Operational Mathematics," McGraw-Hill Book Co., Inc., 2nd ed., 1958, Section 3.
17. Wing, G. M., Ref. 11, Chap. 8. A thorough treatment of the mathematical background is given in E. Hille and K. S. Phillips, "Functional Analysis and Semi-Groups," Am. Math. Soc. Colloq. Publ., 1957.
18. Churchill, R. V., Ref. 16, Sections 62–64.
19. Churchill, R. V., Ref. 16, Section 67.
20. Wing, G. M., Ref. 11, Chaps. 8 and 11.
21. Lehner, J., and G. M. Wing, *Comm. Pure. Appl. Math.*, VIII, 217 (1955); *Duke Math. J.*, **23**, 125 (1956).
22. Pimbley, G. H., *J. Math. Mech.*, **8**, 837 (1959).
23. Davison, B., Ref. 7, Appendix A.
24. Van Norton, R., *Comm. Pure Appl. Math.*, XV, 149 (1962). The same conclusion was reached for arbitrary bounded geometry by S. Ukai, *J. Nucl. Sci. Tech.*, **3**, 263 (1966).
25. Jörgens, K., *Comm. Pure Appl. Math.*, XI, 219 (1958); I. Vidav, *J. Math. Anal. Appl.*, **22**, 144 (1968).
26. Kuščer, I., in "Neutron Thermalization and Reactor Spectra," IAEA, 1968, Vol. I, p. 3; M. Borysiewicz, and J. Mika, *ibid.*, Vol. I, p. 451; S. Albertoni, and B. Montagnini, *J. Math. Anal. Applic.*, **13**, 19 (1966).
27. Nelkin, M., *Physica*, **29**, 261 (1963); see also citations in Ref. 26.
28. Corngold, N., *Proc. Symp. Appl. Math.*, "Transport Theory," Am. Math. Soc., 1969, Vol. I, p. 79.
29. Case, K. M., and P. F. Zweifel, Ref. 8, Appendix D; G. M. Wing, Ref. 11, Chap. 8. Convergence has been proved for a multiplying subcritical medium in slab geometry by P. Nelson, "An Investigation of Criticality for Energy Dependent Transport in Slab Geometry," Ph.D. Dissertation, Univ. of New Mexico, 1969.
30. G. M. Wing, Ref. 11, Chap. 8; R. Van Norton, Ref. 24.
31. Davison, B., Ref. 7, Appendix A.
32. Vladimirov, V. S., *Trans. V. A. Steklov Math. Inst.*, **61** (1961), translated in Atomic Energy of Canada Report AECL-1661 (1963).
33. Case, K. M., and P. F. Zweifel, Ref. 8, Appendix D.
34. The problem is discussed in §§4.4c, 4.4d. A basic reference is R. S. Varga, *Proc. Symp. Appl. Math.*, XI, Am. Math. Soc., 1961, p. 164.
35. Honeck, H. C., *Nucl. Sci. Eng.*, **8**, 193 (1960).
36. Wing, G. M., Ref. 11, Chap. 5.
37. Parker, K., D. T. Goldman, and L. Wallin in "Nuclear Data for Nuclear Reactors," IAEA, 1967, Vol. II, p. 293.
38. Rumyantsev, G. Ya., and V. S. Shulepin, *Atomn. Energiia* (transl.), **22**, 395 (1967); J. D. Callen and J. O. Mingle, *J. Nucl. Energy*, **22**, 173 (1968).
39. Goertzel, G., and M. H. Kalos, "Monte Carlo Methods in Transport Problems," in Prog. Nucl. Energy, Series I, Vol. II, Pergamon Press, 1958, p. 315; E. D. Cashwell and

C. J. Everett, "The Monte Carlo Method for Random Walk Problems," Pergamon Press, 1959; M. H. Kalos, F. R. Nakache, and J. Celnik, Chap. 5 in "Computing Methods in Reactor Physics," H. Greenspan, C. N. Kelber, and D. Okrent, eds., Gordon and Breach, 1968. The best reference is J. Spanier and E. M. Gelbard, "Monte Carlo Principles and Neutron Transport Problems," Addison-Wesley Publishing Co., Inc., 1969.

40. Carlson, B. G., and K. D. Lathrop, Section 3.1.1 in "Computing Methods in Reactor Physics," Ref. 39.
41. Wing, G. M., Ref. 11, Chap. 8; *Proc. Symp. Appl. Math.*, XI, Am. Math. Soc., 1961, p. 140, see figure on p. 146.
42. Perkins, S. T., *Nucl. Sci. Eng.*, **39**, 25 (1970).
43. Wing, G. M., Ref. 11, Chap. 8; I. Kuščer, Ref. 26.

2. ONE-SPEED TRANSPORT THEORY

2.1 THE ONE-SPEED TRANSPORT EQUATION

2.1a Introduction

Although the primary concern in this book is with the energy-dependent neutron transport equation, there are several different situations in which solutions of the simpler one-speed problems are very useful. Consider, first, the energy-dependent transport equation (1.14) for some particular neutron energy, E. If the integral on the right side is regarded merely as a known source of neutrons, as was done in connection with the development of the integral equation in §1.2b, then the transport problem for neutrons of energy E is simply a one-speed problem in a purely absorbing medium; this is so because in every collision neutrons of energy E are removed. From this point of view, therefore, it is useful to have accurate solutions of the transport equation in purely absorbing media, and some are developed at the end of this chapter (§2.8).

Of greater importance is the fact that in this text emphasis is placed on the solution of the energy-dependent transport equation by multigroup methods. It will be seen in Chapters 4 and 5 that in these methods the energy-dependent equation is replaced by a set of coupled one-speed equations which are then solved by approximate methods. In assessing the accuracy of these approximate techniques it is desirable to have available for comparison accurate solutions of the one-speed transport problem. Moreover, from a knowledge of the general features of such solutions, it is possible to develop insight and intuition concerning the solutions of energy-dependent equations.

Finally, there are situations in which the energy-dependent cross sections may be treated as being approximately independent of energy; this is often possible,

for example, with thermal neutrons. In these circumstances, an equivalent one-speed problem may be defined by integrating over neutron energies; the solution may then give information about a problem of physical interest. It is this approach which will be taken in deriving a one-speed transport equation from the energy-dependent equation. It will be shown in the succeeding chapters, however, that the resulting equation is identical with those arising in multigroup theory.

Even in one-speed theory, only a few simple problems have been solved in closed form. The simplest situation which reveals the essential features of the general solutions is that of isotropic scattering in a uniform infinite medium containing a plane neutron source. Three methods of solving the corresponding one-speed transport equation are described in this chapter. The changes resulting from the presence of plane boundaries and from anisotropic scattering will then be examined. Finally, some reciprocity relations and collision probabilities which are useful in various reactor problems are developed.

It should be noted that the time-independent (steady-state) form of the neutron transport equation is emphasized here and in the next few chapters. Time-dependent problems are taken up in Chapters 9 and 10.

2.1b Derivation of the One-Speed Transport Equation

The general neutron transport equation for the neutron angular flux in the time-independent case, i.e., when $\partial\Phi/\partial t$ is zero, is given by equation (1.14) as

$$\Omega \cdot \nabla\Phi(\mathbf{r}, \Omega, E) + \sigma(\mathbf{r}, E)\Phi(\mathbf{r}, \Omega, E)$$

$$= \int\int \sigma(\mathbf{r}, E')f(\mathbf{r}; \Omega', E' \to \Omega, E)\Phi(\mathbf{r}, \Omega', E')\, d\Omega'\, dE' + Q(\mathbf{r}, \Omega, E). \quad (2.1)$$

It is now postulated that all neutron cross sections are independent of energy. As will be seen shortly, this leads to a form of the transport equation in which neutron energies do not appear, and the postulate is in a sense equivalent to saying that the neutrons all have the same energies (or speeds). The term one-speed theory is thus commonly employed, although it is also referred to as the constant cross-section approximation.[1]

If σ is taken to be a function of $\mathbf{r}$ only and not of E, it follows that

$$\sigma(\mathbf{r}, E) = \sigma(\mathbf{r}, E') = \sigma(\mathbf{r}).$$

Furthermore, the angular distribution of neutrons emerging from a collision, i.e.,

$$\int f(\mathbf{r}; \Omega', E' \to \Omega, E)\, dE,$$

must be independent of energy, E'; hence, this quantity may be written as

$$\int f(\mathbf{r}; \Omega', E' \to \Omega, E)\, dE = c(\mathbf{r})f(\mathbf{r}; \Omega' \to \Omega)$$

where the function $f(\mathbf{r}; \mathbf{\Omega}' \to \mathbf{\Omega})$ is normalized to unity, i.e.,

$$\int f(\mathbf{r}; \mathbf{\Omega}' \to \mathbf{\Omega})\, d\mathbf{\Omega} = 1, \tag{2.2}$$

and then $c(\mathbf{r})$ is the mean number of neutrons emerging from a collision at $\mathbf{r}$, as given by equation (1.8).

If the foregoing expressions, based on the constant cross-section postulate, are inserted into equation (2.1), it is found upon integration over energy that

$$\mathbf{\Omega}\cdot\nabla\Phi(\mathbf{r}, \mathbf{\Omega}) + \sigma(\mathbf{r})\Phi(\mathbf{r}, \mathbf{\Omega}) = \sigma(\mathbf{r})c(\mathbf{r}) \int f(\mathbf{r}; \mathbf{\Omega}' \to \mathbf{\Omega})\Phi(\mathbf{r}, \mathbf{\Omega}')\, d\mathbf{\Omega}' + Q(\mathbf{r}, \mathbf{\Omega}), \tag{2.3}$$

where the quantities $\Phi(\mathbf{r}, \mathbf{\Omega})$, $\Phi(\mathbf{r}, \mathbf{\Omega}')$, and $Q(\mathbf{r}, \mathbf{\Omega})$ are defined by

$$\int \Phi(\mathbf{r}, \mathbf{\Omega}, E)\, dE \equiv \Phi(\mathbf{r}, \mathbf{\Omega}),$$

$$\int \Phi(\mathbf{r}, \mathbf{\Omega}', E')\, dE' \equiv \Phi(\mathbf{r}, \mathbf{\Omega}'),$$

and

$$\int Q(\mathbf{r}, \mathbf{\Omega}, E)\, dE \equiv Q(\mathbf{r}, \mathbf{\Omega}).$$

Equation (2.3), in which neutron energy and velocity do not appear, is the general form of the one-speed, time-independent transport equation. It will be seen in subsequent chapters that multigroup theory involves essentially a coupled set of such equations.

It should be noted that equivalence between the one-speed transport equation and the constant cross-section formulation, integrated over energy, does not hold for general time-dependent problems. The reason is that the neutron speed appears in the term $(1/v)\, \partial\Phi/\partial t$ in equation (1.14), the time-dependent transport equation for the angular flux.

2.1c Infinite Plane Geometry

In infinite plane geometry, the quantities Φ, σ, f, and Q depend on one coordinate only. For this geometry, it was shown in §1.3a that

$$\mathbf{\Omega}\cdot\nabla N = \mu \frac{\partial N}{\partial z} \quad \text{or} \quad \mathbf{\Omega}\cdot\nabla\Phi = \mu \frac{\partial\Phi}{\partial z},$$

Furthermore, μ and μ' may be expressed by

$$\mu = \mathbf{\Omega}\cdot\hat{\mathbf{z}} \quad \text{and} \quad \mu' = \mathbf{\Omega}'\cdot\hat{\mathbf{z}},$$

where $\hat{\mathbf{z}}$ is a unit vector in the z direction. Hence, equation (2.3) may be written as

$$\mu \frac{\partial \Phi(z, \mu)}{\partial z} + \sigma(z)\Phi(z, \mu) = \sigma(z)c \int f(\mathbf{\Omega}' \to \mathbf{\Omega})\Phi(z, \mu')\, d\mathbf{\Omega}' + Q(z, \mu), \quad (2.4)$$

where c and f have been taken to be independent of position.

It will be seen in the course of this chapter that some important properties of a system are functions only of the neutron mean free path; hence, it is convenient to express distances in terms of the collision mean free path, i.e., let

$$x = \int_0^z \sigma(z')\, dz'$$

and then

$$\frac{\partial}{\partial z} = \sigma(z) \frac{\partial}{\partial x}.$$

Furthermore, suppose that neutrons emerging from collisions have an *isotropic distribution*; then, in view of the normalization condition in equation (2.2), it follows that

$$f(\mathbf{\Omega}' \to \mathbf{\Omega}) = \frac{1}{4\pi}.$$

Hence, if $d\mathbf{\Omega}'$ is replaced by $2\pi\, d\mu'$ (§1.3a) and equation (2.4) is divided through by $\sigma(z)$, the result may be written as

$$\mu \frac{\partial \Phi(x, \mu)}{\partial x} + \Phi(x, \mu) = \frac{c}{2} \int_{-1}^{1} \Phi(x, \mu')\, d\mu' + Q(x, \mu), \quad (2.5)$$

where

$$\Phi(x, \mu) \equiv \Phi[z(x), \mu]$$

and

$$Q(x, \mu) \equiv \frac{1}{\sigma(z)} Q[z(x), \mu].$$

This is a common form of the time-independent one-speed neutron transport equation in planar geometry.

For an *anisotropic* unit plane source located at $x = x_0$ emitting one neutron per second per unit area in a cone having $\mu = \mu_0$, the source term in equation (2.5) may be represented, using Dirac delta functions (see Appendix), by

$$Q(x, \mu) = \frac{\delta(x - x_0)\delta(\mu - \mu_0)}{2\pi}. \quad (2.6)$$

For an *isotropic* unit plane source at x_0,

$$Q(x, \mu) = \frac{\delta(x - x_0)}{4\pi}. \quad (2.7)$$

Solutions will be sought for equation (2.5) first in an infinite medium subject to the condition that the neutron flux vanish as $x \to +\infty$ and $-\infty$. This problem has physical significance only if $c < 1$, i.e., in a medium in which less than one neutron emerges, on the average, in each collision. If $c > 1$, the source neutrons would multiply without limit and no real and positive (physical) solutions of equation (2.5) can exist. For a finite medium, real solutions are possible for $c > 1$, although they are difficult to obtain. Nevertheless, it will be seen that solutions of the transport equation in an infinite medium can be used to derive conditions for criticality in a finite medium, when $c > 1$.

2.1d Use of Green's Function

In the present context, Green's function (§1.1f) is a solution of equation (2.5) with a simple, i.e., plane, source. For the one-speed problem, it may be represented by $G(x_0, \mu_0 \to x, \mu)$ and it is the neutron angular flux at x, μ arising from a unit source at x_0 emitting one neutron per second (per unit area for a plane source) in the direction μ_0. For an infinite medium, the Green's function so defined, abbreviated to G, is a solution of the equation

$$\mu \frac{\partial G}{\partial x} + G = \frac{c}{2}\int_{-1}^{1} G(x_0, \mu_0 \to x, \mu')\, d\mu' + \frac{\delta(x - x_0)\delta(\mu - \mu_0)}{2\pi}. \tag{2.8}$$

Thus, except when $x = x_0$ and $\mu = \mu_0$, the function G is a solution of the homogeneous equation

$$\mu \frac{\partial G}{\partial x} + G = \frac{c}{2}\int_{-1}^{1} G(x_0, \mu_0 \to x, \mu')\, d\mu', \tag{2.9}$$

with the condition

$$G \to 0 \quad \text{as} \quad x \to \pm\infty.$$

At $x = x_0$ and $\mu = \mu_0$, which corresponds to the source, a discontinuity (or jump) condition on G may be derived by integrating equation (2.8) over a small interval 2ϵ in x about x_0, namely, $x_0 - \epsilon \leqslant x \leqslant x_0 + \epsilon$. The result, for an anisotropic planar source, represented by equation (2.6), is

$$G(x_0, \mu_0 \to x_0 + \epsilon, \mu) - G(x_0, \mu_0 \to x_0 - \epsilon, \mu) = \frac{\delta(\mu - \mu_0)}{2\pi\mu}. \tag{2.10}$$

There is thus a discontinuity (or jump) in G as a function of x at $x = x_0$ when $\mu = \mu_0$. By combining this discontinuity condition with solutions of the homogeneous equation (2.9), it is possible to evaluate the infinite medium Green's function for the planar source, as will be shown later. Once this Green's function is known then, in accordance with equation (1.21), the solution to any infinite medium problem with a general source of the form $Q(x, \mu)/2\pi$ can be expressed as

$$\Phi(x, \mu) = \iint Q(x_0, \mu_0) G(x_0, \mu_0 \to x, \mu)\, dx_0\, d\mu_0. \tag{2.11}$$

Furthermore, the infinite medium Green's function can be used to describe solutions to problems involving slabs of finite thickness, i.e., where boundary conditions are imposed at finite values of x. The reason, as will be seen in §2.5a, is that the solution to the transport equation within any finite homogeneous region is the same as it would be if this region were extended to infinity and a suitable source (or sources) were placed at the boundary of the finite region.

2.2 SOLUTION OF THE ONE-SPEED TRANSPORT EQUATION BY THE SEPARATION OF VARIABLES

2.2a Introduction

The method of solution to be described in this section, although recognized by others,[2] was developed most fully by K. M. Case;[3] it is consequently frequently known as Case's method. It is analogous in some respects to the method of the separation of variables commonly used for the solution of partial differential equations. In both instances a complete set of elementary solutions is sought, and then a suitable combination of solutions is found that will satisfy the boundary conditions or the conditions at the source. The only difference is that most of the elementary solutions of the transport equation are singular. Nevertheless, they have meaning when they appear in integrals.

The approach to be used here is to find elementary solutions of the one-speed transport equation in a *source-free* infinite medium. An attempt will then be made to find a combination of elementary solutions that satisfies the source (or jump) condition for the plane Green's function. It will prove relatively straightforward to obtain such a combination of solutions for the infinite medium, but for more complicated problems, involving bounded regions, the task is too lengthy for inclusion in this book.[4]

2.2b Source-Free Infinite Medium: Asymptotic Solutions

For a source-free infinite medium with isotropic scattering, equation (2.5) becomes

$$\mu \frac{\partial \Phi(x, \mu)}{\partial x} + \Phi(x, \mu) = \frac{c}{2} \int_{-1}^{1} \Phi(x, \mu')\, d\mu' \tag{2.12}$$

in plane geometry. Since the medium contains no source, there is a possibility that $c > 1$, and this will be allowed for the present. To solve equation (2.12) by the method of separation of variables, solutions are sought of the form

$$\Phi(x, \mu) = \chi(x)\psi(\mu), \tag{2.13}$$

where $\chi(x)$ is a function of x only and $\psi(\mu)$ is a function of μ only. If equation

(2.12) is divided through by $\mu\Phi(x, \mu)$ and equation (2.13) is substituted for $\Phi(x, \mu)$ and $\Phi(x, \mu')$, it is found upon rearrangement that

$$\frac{d\chi(x)}{dx}\frac{1}{\chi(x)} = \frac{c}{2\mu\psi(\mu)}\int_{-1}^{1}\psi(\mu')\,d\mu' - \frac{1}{\mu}. \tag{2.14}$$

The left side of equation (2.14) is a function of x only, whereas the right side is a function of μ only; hence, both sides are equal to a constant. If this constant is represented by $-1/\nu$, then

$$\frac{d\chi(x)}{dx}\frac{1}{\chi(x)} = -\frac{1}{\nu},$$

so that

$$\chi(x) = \text{constant} \times e^{-x/\nu}.$$

Thus solutions to equation (2.12) are to be sought of the form

$$\Phi_\nu(x, \mu) = e^{-x/\nu}\psi_\nu(\mu), \tag{2.15}$$

where the ν is an eigenvalue corresponding to the eigenfunction $\psi_\nu(\mu)$. Special care will now be taken to examine the acceptable values of ν and the functions $\psi_\nu(\mu)$.

If equation (2.15) is substituted into (2.12), the result is

$$\left(1 - \frac{\mu}{\nu}\right)\psi_\nu(\mu) = \frac{c}{2}\int_{-1}^{1}\psi_\nu(\mu')\,d\mu'. \tag{2.16}$$

It is convenient to normalize ψ_ν so that

$$\int_{-1}^{1}\psi_\nu\,d\mu' = 1 \tag{2.17}$$

and then, upon multiplication by ν, equation (2.16) becomes (for $\nu \neq 0$)

$$(\nu - \mu)\psi_\nu(\mu) = \frac{c}{2}\nu. \tag{2.18}$$

If, for the moment, it is assumed that $\nu \neq \mu$ for all values of μ between -1 and 1, i.e., ν is not both real and in the interval $-1 \leqslant \nu \leqslant 1$, then

$$\psi_\nu(\mu) = \frac{c}{2}\frac{\nu}{\nu - \mu}. \tag{2.19}$$

This may be substituted into the normalization equation (2.17) to obtain the conditions on ν, namely $\nu = \pm\nu_0$, where $\pm\nu_0$ are the roots of

$$1 = c\nu_0 \tanh^{-1}\frac{1}{\nu_0} = \frac{c\nu_0}{2}\ln\frac{\nu_0 + 1}{\nu_0 - 1}. \tag{2.20}$$

When $c < 1$, the roots of equation (2.20) are real, but when $c > 1$ they are imaginary. These roots have also been obtained in another manner.[5]

It is seen, therefore, that there are two discrete eigenvalues $+\nu_0$ and $-\nu_0$ which satisfy equation (2.16) when $\nu \neq \mu$. The associated eigenfunctions are given by equation (2.19) as

$$\psi_0^{\pm}(\mu) = \frac{c}{2}\frac{\nu_0}{\nu_0 \mp \mu} \tag{2.21}$$

and the two solutions of equation (2.12) are then

$$\Phi_0^{\pm}(x, \mu) = e^{\mp x/\nu_0}\psi_0^{\pm}(\mu) = e^{\mp x/\nu_0}\frac{c\nu_0}{2(\nu_0 \mp \mu)}. \tag{2.22}$$

It will be seen later that, in general, there are other solutions to equation (2.12), but those in equation (2.22) dominate far from sources and boundaries; they are called the *asymptotic solutions* and Φ_0 is the *asymptotic flux*. Before returning to equation (2.16), some consideration will be given to the asymptotic (discrete) eigenvalue ν_0.

Upon expansion of the $\tanh^{-1}$ term, equation (2.20) becomes

$$1 = c\nu_0\left[\frac{1}{\nu_0} + \frac{1}{3\nu_0^3} + \frac{1}{5\nu_0^5} + \cdots\right],$$

which may be rearranged to give

$$\frac{1}{\nu_0^2} = \frac{3(1-c)}{c} - \frac{3}{5\nu_0^4} - \cdots.$$

As a first approximation, $1/\nu_0^2 \approx 3(1-c)/c$, and this may be substituted in the second term on the right to yield

$$\frac{1}{\nu_0^2} = \frac{3(1-c)}{c}\left[1 - \frac{9}{5}\frac{1-c}{c} - \cdots\right].$$

By writing $1 - (1 - c)$ for c in the denominator of the factor on the right and replacing c by unity in the denominator in the second term in the brackets, then inverting and taking the square root, the result, when c is near unity, is

$$\nu_0 = \frac{1}{\sqrt{3(1-c)}}[1 + \tfrac{2}{5}(1-c) + \cdots]. \tag{2.23}$$

It is evident, as stated above, that ν_0 is real only when $c < 1$.

Since ν_0 determines the rate of decrease of the asymptotic flux with distance, as is apparent from equation (2.22), it is here called the *asymptotic relaxation length*.* It is related to the diffusion length, L, of simple diffusion theory; the latter is given by

$$L = \frac{1}{\sqrt{3\sigma\sigma_a}},$$

* The quantity ν_0 is often referred to as the asymptotic diffusion length, but in this book the term "diffusion length" is reserved for diffusion theory. In general, a relaxation length is the distance in which the flux decreases by the factor e.

where σ is the total (macroscopic) cross section and σ_a is the absorption cross section. In the present notation, $\sigma_a = \sigma(1 - c)$; hence, with the collision mean free path as the unit of distance,

$$L = \frac{1}{\sqrt{3(1 - c)}}. \tag{2.24}$$

It is seen, therefore, that the asymptotic relaxation length of transport theory approaches the value for simple diffusion theory only when c is very close to unity (or $|1 - c| \ll 1$), i.e., in a weakly absorbing medium.

A comparison of the exact asymptotic relaxation length from transport theory, as obtained from equation (2.20), the value from equation (2.23), and the ordinary diffusion length, from equation (2.24), is given in Table 2.1.[6] For media with $c < 1$, the data are for $|\nu_0|$, whereas for media in which $c > 1$, the values are those of $|i\nu_0|$. Although the simple diffusion length, L, is a good approximation to transport theory only when $|1 - c| < 0.01$, the one additional term in the expansion in equation (2.23) gives results that agree with the exact solutions of equation (2.20) up to about $|1 - c| = 0.2$ (or more).

It is important to note that for $0 < c < 1$, the values of $|\nu_0|$ are > 1, whereas for $c > 1$, ν_0 is purely imaginary. Therefore, in neither case does ν_0 lie in the real interval $-1 \leqslant \nu_0 \leqslant 1$. It is consequently permissible to divide equation (2.18) by $\nu_0 - \mu$ in order to obtain the solution for $\psi_{\nu_0}(\mu)$ given by equation (2.19).

TABLE 2.1. COMPARISON OF RELAXATION LENGTHS FOR ISOTROPIC SCATTERING[6] (IN MEAN FREE PATHS)

c	$\|\nu_0\|$ *Exact* [*Eq.* (2.20)]	$\|\nu_0\|$ *Second Approx.* [*Eq.* (2.23)]	*Diffusion Theory* [*Eq.* (2.24)]
$c < 1$			
0.99	5.797	5.797	5.774
0.98	4.116	4.115	4.083
0.95	2.635	2.633	2.582
0.90	1.903	1.899	1.826
0.80	1.408	1.394	1.291
0.50	1.044	0.979	0.816
0	1.000	0.808	0.577
$c > 1$			
		$\|i\nu_0\|$	
1.01	5.750	5.751	5.774
1.02	4.050	4.052	4.083
1.05	2.532	2.531	2.582
1.10	1.757	1.756	1.826
1.20	1.198	1.195	1.291
1.50	0.689	0.680	0.816

2.2c Infinite Medium Continuum (Singular) Solutions

Two elementary (asymptotic) solutions, namely, $\Phi_0^+(x, \mu)$ and $\Phi_0^-(x, \mu)$, have been found to equation (2.12) for the case in which $\nu \neq \mu$. Additional solutions will now be developed for the situation in which $\nu = \mu$ and both of these quantities lie within the range -1 to 1. It was seen above that equation (2.19) is a solution of equation (2.18) for all μ in the interval $-1 \leqslant \mu \leqslant 1$ with ν not in the interval $-1 \leqslant \nu \leqslant 1$. Equation (2.19) is also an acceptable solution of equation (2.18) when ν is real and lies in the interval $-1 \leqslant \nu \leqslant 1$ provided $\nu \neq \mu$. But when $\nu = \mu$ the solution is divergent (singular) and this feature requires further examination. Moreover, it would appear that such a solution cannot satisfy the normalization condition of equation (2.17), since that condition was used previously to derive acceptable values of ν, namely $\pm\nu_0$, which have been found not to lie in the interval $-1 \leqslant \nu \leqslant 1$.

In order to determine the normalization integral for the singular ($\nu = \mu$) solution, however, it is necessary to specify how the integral of such a divergent function is to be evaluated. Moreover, as long as a solution is being considered that is divergent at $\nu = \mu$, greater generality may be allowed by trying the solution

$$\psi_\nu(\mu) = \frac{c}{2}\frac{\nu}{\nu - \mu} + \lambda(\nu)\delta(\mu - \nu), \tag{2.25}$$

where $\lambda(\nu)$ is an arbitrary function. This will still be a solution of equation (2.18) for all $\nu \neq \mu$ and it can also be interpreted as a solution for $\nu = \mu$ since it is possible to define the Dirac delta function such that

$$x\,\delta(x) \equiv 0.$$

With this more general solution, the function $\lambda(\nu)$ may be chosen so as to satisfy the normalization condition of equation (2.17). In performing the integration over μ', however, it is necessary to specify how the singular first term in equation (2.25) should be integrated. The various possible choices differ only in delta functions, and the Cauchy principal value prescription[7] is chosen in evaluating the integral; thus

$$\mathrm{P}\int_{-1}^{1} \frac{\nu}{\nu - \mu'}\,d\mu' = \lim_{\delta \to 0}\left[\int_{-1}^{\nu-\delta} \frac{\nu}{\nu - \mu'}\,d\mu' + \int_{\nu+\delta}^{1} \frac{\nu}{\nu - \mu'}\,d\mu'\right],$$

where the symbol P implies the principal value. In order to bear in mind that this requirement must be met whenever $\psi_\nu(\mu)$ is integrated, the symbol P is attached to the singular term; equation (2.25) is then written as

$$\psi_\nu(\mu) = \frac{c}{2}\,\mathrm{P}\frac{\nu}{\nu - \mu} + \lambda(\nu)\delta(\mu - \nu). \tag{2.26}$$

The arbitrary function $\lambda(\nu)$ can now be chosen so that the normalization condition is satisfied; in particular, upon evaluating the principal value integral,

$$\lambda(\nu) = 1 - c\nu \tanh^{-1} \nu. \tag{2.27}$$

It is seen that, in addition to the two discrete eigenvalues which satisfy equation (2.20), there is a continuum of eigenvalues (and eigenfunctions) corresponding to all ν between -1 and 1. The solution to equation (2.12) for $-1 \leqslant \nu \leqslant 1$, may then be represented by

$$\Phi_\nu(x, \mu) = e^{-x/\nu}\left[\frac{c}{2} \mathrm{P}\frac{\nu}{\nu - \mu} + \lambda(\nu)\delta(\mu - \nu)\right], \tag{2.28}$$

where $\lambda(\nu)$ is given by equation (2.27). Such a solution, which contains a delta function, $\delta(\mu - \nu)$, and the singular term $1/(\nu - \mu)$, is not defined at $\nu = \mu$. It can, nevertheless, be used in integrals because the manner of integrating the singular terms has been specified. Moreover, the solution may be interpreted as a "generalized function" in a formal mathematical sense[8] and constitutes an acceptable solution to equation (2.12).

It should be noted that since $-1 \leqslant \nu \leqslant 1$, the continuous solutions vary faster with x than do the asymptotic solutions. As will be seen in §2.2e, this implies that at a large distance from the source the asymptotic solutions will dominate. Near the source, however, the continuous solutions are also important and, in particular, they are necessary for fitting the jump conditions at the source position.

2.2d Completeness and Orthogonality of the Elementary Solutions

The usefulness of the functions $\Phi_\nu(x, \mu)$ lies in the fact that they, together with $\Phi_0^{\pm}(x, \mu)$, are complete and that they satisfy an orthogonality relation. The completeness means that a general solution of equation (2.12) can be written as[9]

$$\Phi(x, \mu) = a_+ \Phi_0^+(x, \mu) + a_- \Phi_0^-(x, \mu) + \int_{-1}^{1} A(\nu)\Phi_\nu(x, \mu)\, d\nu, \tag{2.29}$$

where the first two terms on the right are the asymptotic solutions and the third represents the continuous solutions; the expansion coefficients a_+ and a_- are constants and $A(\nu)$ is a function of ν. Equation (2.29) may also be written in the form

$$\Phi(x, \mu) = a_+ \psi_0^+(\mu)e^{-x/\nu_0} + a_- \psi_0^-(\mu)e^{x/\nu_0} + \int_{-1}^{1} A(\nu)\psi_\nu(\mu)e^{-x/\nu}\, d\nu. \tag{2.30}$$

The orthogonality condition is used for determining the expansion coefficients in particular problems and it can be derived by considering equation (2.16) for

$\psi_\nu(\mu)$ and multiplying by $\psi_{\nu'}(\mu)$, to obtain

$$\left(1 - \frac{\mu}{\nu}\right)\psi_\nu(\mu)\psi_{\nu'}(\mu) = \frac{c}{2}\psi_{\nu'}(\mu)\int_{-1}^{1}\psi_\nu(\mu')\,d\mu'.$$

Similarly, equation (2.16) for $\psi_{\nu'}(\mu)$ is multiplied by $\psi_\nu(\mu)$, i.e.,

$$\left(1 - \frac{\mu}{\nu'}\right)\psi_\nu(\mu)\psi_{\nu'}(\mu) = \frac{c}{2}\psi_\nu(\mu)\int_{-1}^{1}\psi_{\nu'}(\mu')\,d\mu'.$$

Upon subtracting these two equations and integrating over μ, it is evident that

$$\left(\frac{1}{\nu'} - \frac{1}{\nu}\right)\int_{-1}^{1}\mu\psi_\nu(\mu)\psi_{\nu'}(\mu)\,d\mu = 0. \tag{2.31}$$

Consequently, if $\nu' \neq \nu$, the required orthogonality relation

$$\int_{-1}^{1}\mu\psi_\nu(\mu)\psi_{\nu'}(\mu)\,d\mu = 0 \tag{2.32}$$

is obtained. The values of ν, ν' may be chosen from $\pm\nu_0$ or from the continuum.

In order to evaluate the expansion coefficients a_+, a_-, and $A(\nu)$ in equation (2.29), it is first necessary to determine the normalization integrals. For the asymptotic terms these are represented by N_0^+ and N_0^-; they are obtained by setting $\nu = \nu'$ $(= \nu_0)$ in the integral in equation (2.31), i.e.,

$$N_0^\pm = \int_{-1}^{1}\mu\psi_0^\pm(\mu)\psi_0^\pm(\mu)\,d\mu.$$

By using the values of $\psi_0^\pm(\mu)$ given in equation (2.21), it can be shown[10] that

$$N_0^\pm = \pm\frac{c}{2}\nu_0^3\left[\frac{c}{\nu_0^2 - 1} - \frac{1}{\nu_0^2}\right]. \tag{2.33}$$

The normalization integral N_ν for the continuum is more difficult to determine, but it is found[10] that

$$\int\mu\psi_{\nu'}(\mu)\psi_\nu(\mu)\,d\mu = N_\nu\delta(\nu - \nu'),$$

where

$$N_\nu = \nu\left[\lambda^2(\nu) + \frac{\pi^2c^2}{4}\nu^2\right]. \tag{2.34}$$

These orthogonality conditions will be used in the next section to derive the plane Green's function.

2.2e Infinite Medium with Plane Source

In the foregoing, the homogeneous equation (2.12), which is analogous to (2.9), has been solved and the solutions for an infinite medium were found to be

represented by equation (2.29). It is now possible to add the discontinuity (or jump) condition for a planar source at x_0, and by including the provision that the solution of the inhomogeneous equation must vanish as $|x| \to \infty$, the Green's function for the problem can be evaluated.

For $x \neq 0$, the Green's function $G(x_0, \mu_0 \to x, \mu)$, i.e., the angular flux at x, μ due to a unit source at x_0, μ_0, can be derived from equation (2.29) as having the form

$$G = a_+\psi_0^+(\mu)e^{-(x-x_0)/\nu_0} + \int_0^1 A(\nu)e^{-(x-x_0)/\nu}\psi_\nu(\mu)\,d\nu \quad \text{for} \quad x > x_0 \tag{2.35}$$

and

$$G = -a_-\psi_0^-(\mu)e^{(x-x_0)/\nu_0} - \int_{-1}^0 A(\nu)e^{-(x-x_0)/\nu}\psi_\nu(\mu)\,d\nu \quad \text{for} \quad x < x_0, \tag{2.36}$$

where, in each half-space, only those exponentials have been retained which approach zero as $|x| \to \infty$. The expansion coefficients a_+, a_-, and $A(\nu)$ for a planar source can now be determined by introducing the discontinuity condition of equation (2.10). Upon substituting the appropriate values of G from equations (2.35) and (2.36), respectively, into equation (2.10), with $x = x_0 + \epsilon$ for the first term and $x = x_0 - \epsilon$ for the second term, and letting $\epsilon \to 0$, the result is

$$a_+\psi_0^+(\mu) + a_-\psi_0^-(\mu) + \int_{-1}^1 A(\nu)\psi_\nu(\mu)\,d\nu = \frac{\delta(\mu - \mu_0)}{2\pi\mu}. \tag{2.37}$$

The next stage in the procedure is to use the orthogonality conditions to determine the expansion coefficients; equation (2.37) is multiplied by $\mu\psi_{\nu'}(\mu)$ and integrated over μ. Then, by using the normalization and orthogonality conditions, it is found that

$$a_\pm = \frac{1}{N_0^\pm}\int_{-1}^1 \frac{\mu\psi_0^\pm(\mu)\delta(\mu - \mu_0)}{2\pi\mu} = \frac{1}{2\pi N_0^\pm}\psi_0^\pm(\mu_0)$$

and

$$A(\nu) = \frac{1}{2\pi N_\nu}\psi_\nu(\mu_0),$$

where $N_0^\pm$ and N_ν are the same as before. The values of $\psi_0^\pm(\mu_0)$ and $\psi_\nu(\mu_0)$ are given by equations (2.21) and (2.26), respectively, with $\mu = \mu_0$.

By substituting these expressions into equations (2.35) and (2.36), the Green's function for the infinite medium with an anisotropic planar source can be obtained. Since G represents the angular flux at x, μ, the result can then be written as

$$\Phi(x, \mu) = \frac{1}{2\pi}\left[\pm\frac{\psi_0^\pm(\mu_0)\psi_0^\pm(\mu)e^{-|x-x_0|/\nu_0}}{N_0^\pm} + \int_0^1 \frac{\psi_{\pm\nu}(\mu_0)\psi_{\pm\nu}(\mu)e^{-|x-x_0|/\nu}}{N_\nu}\,d\nu\right]. \tag{2.38}$$

where the plus signs apply to $x > x_0$ and the minus signs to $x < x_0$. The functions $\psi_{\pm\nu}(\mu_0)$ and $\psi_{\pm\nu}(\mu)$ are as defined by equation (2.26), for $+\nu$ or $-\nu$. It may be noted that equation (2.38) contains the products of singular functions and some care must be exercised in interpreting them properly.[11]

For a unit *planar isotropic source* at x_0, the angular flux is obtained by averaging $\Phi(x, \mu)$ with respect to μ_0, i.e., by integrating equation (2.38) over μ_0 and evaluating $\frac{1}{2}\int_{-1}^{1}[\ ]\,d\mu_0$. Then by using the normalizing condition

$$\int_{-1}^{1} \psi_\nu(\mu_0)\, d\mu_0 = 1,$$

the result for $x > x_0$ is found to be

$$\Phi(x, \mu) = \frac{1}{4\pi}\left[\frac{\psi_0^+(\mu)e^{-(x-x_0)/\nu_0}}{N_0^+} + \int_0^1 \frac{\psi_\nu(\mu)e^{-(x-x_0)/\nu}}{N_\nu}\, d\nu\right] \tag{2.39}$$

and for $x < x_0$, the condition

$$\Phi[(x - x_0), \mu] = \Phi[-(x - x_0), -\mu]$$

is used. The total flux $\phi(x)$ for an isotropic unit plane source is obtained by integrating equation (2.39) over all directions, i.e., by multiplying by 2π and integrating over μ; thus,

$$\phi(x) = \frac{1}{2}\left[\frac{e^{-|x-x_0|/\nu_0}}{N_0^+} + \int_0^1 \frac{e^{-|x-x_0|/\nu}}{N_\nu}\, d\nu\right]. \tag{2.40}$$

This is the form of the Green's function for the total flux from an isotropic plane source in an infinite medium.

Provided $c < 1$, ν_0 is real and greater than unity (see Table 2.1). It is then found that as $x - x_0$ increases the integral term in equation (2.40) decreases more rapidly than does the first (asymptotic) term. An exception arises when $c = 0$, i.e., for a purely absorbing medium with no scattering; in this case the asymptotic solutions vanish since $N_0^+ \to \infty$ as $c \to 0$. Consequently, provided $c \neq 0$, when $x - x_0$ is large, that is, at points far from the source, the asymptotic solution to the neutron transport equation is dominant. As noted in §2.2b, when $c - 1 \ll 1$, simple diffusion theory provides a good approximation to the asymptotic solution.

For certain problems the orthogonality condition of equation (2.32) does not suffice to determine the expansion coefficients. This occurs when the boundary condition is applicable only over half of the μ range. It is then required to have orthogonality conditions over half the range, i.e., $\int_0^1[\ ]\,d\mu$ or $\int_{-1}^0[\ ]\,d\mu$. These can be found but they involve the theory of singular equations.[12]

The method of separation of variables has also been applied to time-dependent problems, in particular to the α eigenvalue problem of §1.5.[13]

2.2f Point and Distributed Sources

The flux from an isotropic point source in an infinite medium can be readily obtained from that for an isotropic plane source, since the latter may be regarded as a superposition of point sources. Thus, if a unit plane source is treated as if made up of point sources of unit intensity per unit area, the flux $\phi_{pl}(x)$ at a distance x from the unit infinite plane source (at $x = 0$) is related to the flux $\phi_{pt}(r)$ at a distance r from a unit point source (Fig. 2.1) by

$$\phi_{pl}(x) = 2\pi \int_0^\infty \phi_{pt}(r) y \, dy = 2\pi \int_{|x|}^\infty \phi_{pt}(r) r \, dr,$$

where, in obtaining the final form, the relation $r^2 = y^2 + x^2$ has been used. Upon differentiation with respect to x, the result is

$$\phi_{pt}(r) = -\frac{1}{2\pi r} \frac{d\phi_{pl}(x)}{dx}\bigg|_{x=r}$$

By considering the plane source solution in an infinite medium in equation (2.40), it is seen that the flux from an isotropic point source is given by

$$\phi_{pt}(r) = \frac{1}{4\pi r}\left[\frac{e^{-r/\nu_0}}{\nu_0 N_0^+} + \int_0^1 \frac{e^{-r/\nu}}{\nu N_\nu} d\nu\right],$$

so that it too contains an asymptotic part, decaying as $e^{-r/\nu_0}/r$, and a transient part decaying at least as rapidly as e^{-r}/r. Thus, for an isotropic point source the

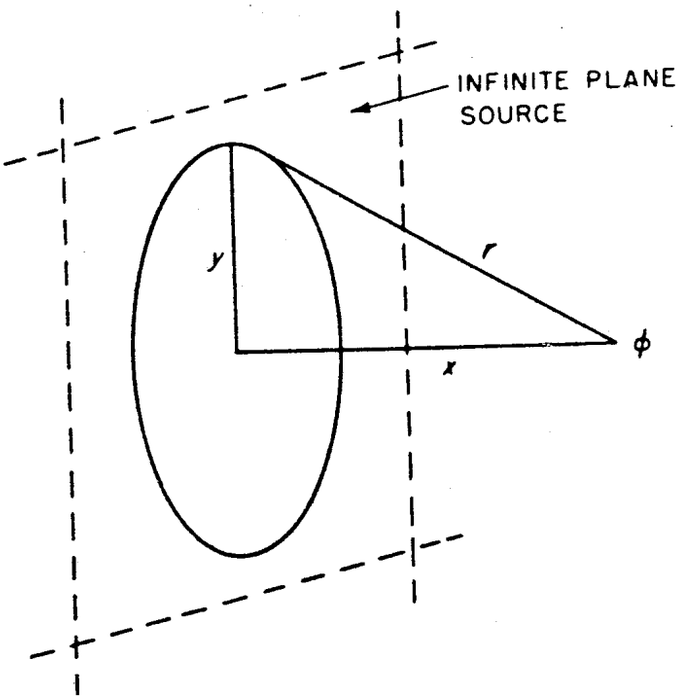

FIG. 2.1 RELATION OF POINT AND PLANE SOURCES.

asymptotic solution dominates at a distance from the source; the same conclusion holds, as will be shown later, for an anisotropic source.

Since any distributed (surface or volume) source can be treated as a superposition of point sources, it can be concluded that both asymptotic and transient terms will contribute to the flux. At points far from the source in an infinite medium, the asymptotic solution may be expected to dominate in all cases.

2.3 SOLUTION OF THE ONE-SPEED TRANSPORT EQUATION BY THE FOURIER TRANSFORM METHOD

2.3a Introduction

The second method for deriving the infinite medium Green's function is by means of Fourier transform techniques. The method of separation of variables was actually developed later than the Fourier transform method, but it was treated first because it exhibits more clearly the general nature of the solutions. Nevertheless, the solution of the one-speed neutron transport equation by using the Fourier transform is of interest not only because it is another approach, but also because it has applications in certain multigroup problems. In the discussion presented here, the case of a unit isotropic plane source is first considered, and the Green's function solution will then be used for an anisotropic source. For simplicity of representation, the source will be located at $x = 0$, instead of at $x = x_0$ as in the preceding treatment.

2.3b Infinite Medium Isotropic Source

For a unit isotropic plane source at $x = 0$, in an infinite medium, the source term $Q(x, \mu)$ is given by equation (2.7) as $\delta(x)/4\pi$; upon insertion into equation (2.5), the one-speed neutron transport equation becomes

$$\mu \frac{\partial \Phi(x, \mu)}{\partial x} + \Phi(x, \mu) = \frac{c}{2} \int_{-1}^{1} \Phi(x, \mu')\, d\mu' + \frac{\delta(x)}{4\pi}. \tag{2.41}$$

The Fourier transform $F(k, \mu)$ of $\Phi(x, \mu)$ is defined[14] by

$$F(k, \mu) = \int_{-\infty}^{\infty} e^{-ikx} \Phi(x, \mu)\, dx. \tag{2.42}$$

Equation (2.41) is multiplied by e^{-ikx} and integrated, making use of the fact that

$$\mu \int_{-\infty}^{\infty} \frac{\partial \Phi(x, \mu)}{\partial x} e^{-ikx}\, dx = \mu \Phi(x, \mu) e^{-ikx} \Big|_{-\infty}^{\infty} + ik\mu\, F(k, \mu)$$

and the requirement that

$$\Phi(x, \mu) = 0 \quad \text{at} \quad x = \pm\infty.$$

The result is

$$(1 + ik\mu)F(k, \mu) = cF(k) + \frac{1}{4\pi}. \tag{2.43}$$

where

$$F(k) = \frac{1}{2}\int_{-1}^{1} F(k, \mu)\, d\mu. \tag{2.44}$$

By assuming that $1 + ik\mu \neq 0$, equation (2.43) can be solved to give

$$F(k, \mu) = \frac{cF(k) + 1/4\pi}{1 + ik\mu}. \tag{2.45}$$

This can be integrated over μ and solved for $F(k)$; the result can then be substituted into equation (2.45) to obtain $F(k, \mu)$. Since

$$\frac{1}{2}\int_{-1}^{1} \frac{d\mu}{1 + ik\mu} = \frac{1}{2ik} \ln \frac{1 + ik}{1 - ik} = \frac{1}{k} \tan^{-1} k$$

is a real quantity, it is found in this way that

$$F(k, \mu) = \frac{1}{4\pi}(1 + ik\mu)^{-1}\left[1 - \frac{c}{2ik} \ln \frac{1 + ik}{1 - ik}\right]^{-1} \tag{2.46}$$

The angular flux may now be derived from equation (2.46) by Fourier inversion; thus,

$$\Phi(x, \mu) = \frac{1}{8\pi^2}\int_{-\infty}^{\infty} e^{ikx}(1 + ik\mu)^{-1}\left[1 - \frac{c}{2ik} \ln \frac{1 + ik}{1 - ik}\right]^{-1} dk. \tag{2.47}$$

The total flux at x is obtained by integrating over all directions, i.e., by multiplying by 2π and integrating over μ from -1 to 1. It is then found that

$$\phi(x) = \frac{1}{4\pi}\int_{-\infty}^{\infty} \left[\frac{e^{ikx}}{ik} \ln \frac{1 + ik}{1 - ik}\right]\left[1 - \frac{c}{2ik} \ln \frac{1 + ik}{1 - ik}\right]^{-1} dk. \tag{2.48}$$

2.3c Asymptotic and Transient Solutions

The solution for $\phi(x)$ given by equation (2.48) can be put in a form similar to that in equation (2.40), as the sum of an asymptotic and a transient solution, by use of contour integration. The original integration path in the complex plane is deformed, as indicated in Fig. 2.2. The integrand in equation (2.48) has a branch point at $k = i$, and so the complex plane is cut along the imaginary axis from i to $i\infty$. Moreover, the integrand has a simple pole where the denominator vanishes, when

$$1 = \frac{c}{2ik} \ln \frac{1 + ik}{1 - ik}.$$

Upon comparison with equation (2.20), it is seen that the simple pole occurs where

$$k = k_0 = \frac{i}{\nu_0}.$$

The integral along the original path is equal to that along the deformed path in Fig. 2.2 plus $2\pi i$ times the residue at k_0. The asymptotic part of the solution to equation (2.48) arises from this residue, whereas the transient part comes from integration along the cut made by the imaginary axis. The contribution of the residue to the total flux is given by

$$\phi_{as}(x) = \tfrac{1}{2} i \lim_{k \to i/\nu_0} \left(k - \frac{i}{\nu_0}\right) F(k, x),$$

where $F(k, x)$ is the integrand in equation (2.48). It is then found that

$$\phi_{as}(x) = \frac{\dfrac{1}{\nu_0}\left(1 - \dfrac{1}{\nu_0^2}\right) e^{-|x|/\nu_0}}{c\left[\dfrac{1}{\nu_0^2} - (1 - c)\right]}. \tag{2.49}$$

By recalling the value of N_0^+ given in equation (2.33), it is readily seen that this quantity is identical with the asymptotic contribution to the total flux from an isotropic plane source, located at $x_0 = 0$, as expressed by equation (2.40).

The contour shown in Fig. 2.2 is applicable only for $x > 0$. But for $x < 0$, a similar contour may be taken in the lower half-plane, the choice being made to ensure that $e^{ikx} = 0$ far from the real axis. The contribution from the residue is found to be expressed by equation (2.49) regardless of the sign of x.

The transient part of the solution to equation (2.48) is equal to the sum of the

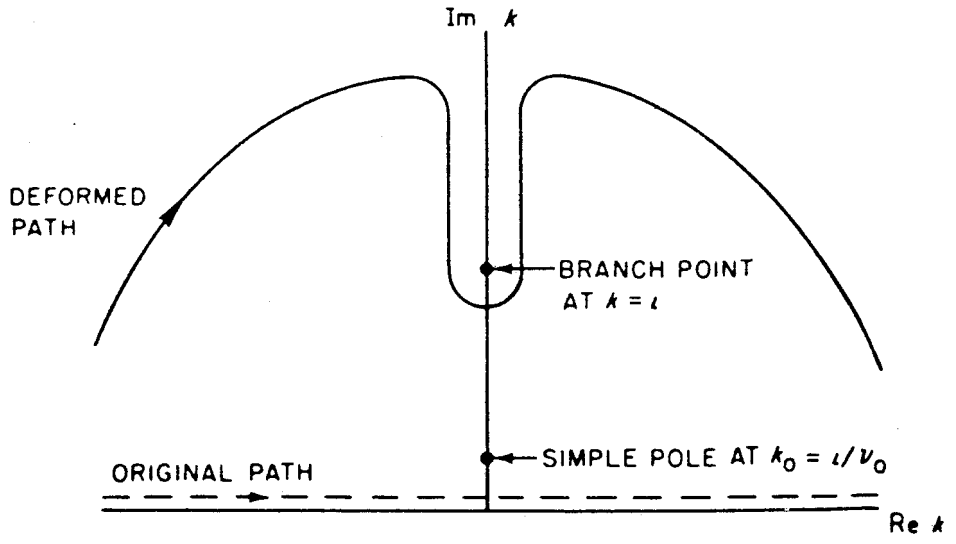

FIG. 2.2 CONTOUR INTEGRATION.

contributions from each side of the cut made by the imaginary axis. Thus, the integral on the left side, represented by I_1, is

$$I_1 = \frac{1}{4\pi}\int_{i\infty}^{i} \left[\frac{e^{ikx}}{ik}\ln\frac{1+ik}{1-ik}\right]\left[1 - \frac{c}{2ik}\ln\frac{1+ik}{1-ik}\right]^{-1} dk$$

and on the right side it is I_2, where

$$I_2 = \frac{1}{4\pi}\int_{i}^{i\infty} \left[\frac{e^{ikx}}{ik}\ln\frac{1+ik}{1-ik}\right]\left[1 - \frac{c}{2ik}\ln\frac{1+ik}{1-ik}\right]^{-1} dk.$$

The logarithmic terms $\ln(1 + ik)/(1 - ik)$ on the two sides of the cut will differ by $2\pi i$, and if the quantity Z is defined by

$$-Z \equiv 1 + ik,$$

it follows that

$$\ln\frac{1+ik}{1-ik} = -i\pi + \ln\frac{Z}{2+Z} \quad \text{in } I_1$$

and

$$\ln\frac{1+ik}{1-ik} = i\pi + \ln\frac{Z}{2+Z} \quad \text{in } I_2.$$

The integrals I_1 and I_2 may now be combined to yield

$$\phi_{\text{trans}}(x) = \int_0^\infty \frac{2(Z+1)\exp[-(Z+1)|x|]}{[2(Z+1) - c\ln(1+2/Z)]^2 + (c\pi)^2}\, dZ. \tag{2.50}$$

By converting this to the variable $\nu = 1/(1 + Z)$, the result is the same as that given by the integral term in equation (2.40). The results of the Fourier transform method are thus identical with those obtained by the separation of variables.

Some properties of the transient solution can be derived from equation (2.50). When x *is small*, i.e., near the source, the main contribution to the integral comes from large values of Z; then

$$\phi_{\text{trans}}(x) \xrightarrow[x\to 0]{} \int_0^\infty \frac{\exp[-(Z+1)|x|]}{2(Z+1)}\, dZ = \tfrac{1}{2}E_1(|x|), \tag{2.51}$$

where E_1 is the exponential integral function (see Appendix). It will now be shown that equation (2.51) represents the uncollided flux from the neutron source.

The integral form of the transport equation (1.37) for an isotropic plane source in an infinite medium may be written, for constant energy and with distance expressed in terms of the mean free path (§2.1c), as

$$\phi(x) = \frac{1}{2}\int_{-\infty}^{\infty} q(x')E_1(|x - x'|)\, dx'.$$

If $\phi(x)$ is to represent the uncollided flux, the source term, $q(x')$, will not include neutrons emerging from collisions; then,

$$q(x') = \delta(x')$$

and so

$$\phi(x) = \tfrac{1}{2}E_1(|x|).$$

This result, which is identical with equation (2.51), is the (uncollided) flux produced directly at x by a source at $x = 0$. Since E_1 diverges for $x = 0$, it is evident that the uncollided flux present in the transient part of equation (2.48) is dominant near the source. It may be noted, too, that for $c = 0$, equation (2.50) gives

$$\phi_{\text{trans}}(x) = \tfrac{1}{2}E_1(x)$$

for all x. Since the asymptotic flux is zero in this case (§2.2e), the flux is made up solely of uncollided neutrons, as is to be expected.

When x is *large*, the main contribution to equation (2.50) is from small values of Z, and the transient part of the total flux decreases as $e^{-|x|}$ as $x \to \infty$. This part therefore decreases more rapidly than does the asymptotic part at large distances from the source; the latter is then dominant. This is the same conclusion as was reached in §2.2e.

The results obtained above suggest a physical interpretation of the asymptotic and transient parts of the solution of equation (2.48). The asymptotic flux is a distribution of neutrons governed by the collisions taking place in the medium; its dependence on space and angle is determined by the properties of the medium, i.e., by c, and is independent, except for normalization, of the source. Thus, the asymptotic solution represents a situation in which collisional equilibrium exists.

The transient part, on the other hand, gives the departure of the flux from the state of collisional equilibrium caused by the neutron source. Hence, both the source and the properties of the medium affect the transient flux. Thus, for

TABLE 2.2. VALUES OF ϕ_{as}/ϕ FOR AN ISOTROPIC PLANE SOURCE.[15] (DISTANCES IN MEAN FREE PATHS)

x \ c	0	0.2	0.4	0.6	0.8	1.0
0	0	0	0	0	0	1.0
1	0	0.011	0.309	0.667	0.879	1.000
2	0	0.016	0.403	0.780	0.944	1.000
5	0	0.028	0.563	0.908	0.990	1.000
10	0	0.044	0.698	0.968	0.999	1.000
20	0	0.068	0.825	0.994	1.000	1.000

$c = 0$, i.e., in a purely absorbing medium, the source determines the neutron flux at all distances; there is never collisional equilibrium and there is no asymptotic part to the solution of equation (2.48).

For small values of c, the transient flux is larger than the asymptotic flux, i.e., $\phi_{as}/\phi \ll 1$, even at many mean free paths from the source, as may be seen from the data in Table 2.2 for an isotropic plane source.[15] On the other hand, for c near unity, collisional equilibrium can be established near the source; in fact as $c \to 1$, the transient part becomes negligible, i.e., $\phi_{as}/\phi \to 1$.

2.3d Infinite Medium Anisotropic Plane Source

With an anisotropic plane source, as in equation (2.6), but with the source at $x = 0$, the procedure described above may be followed; instead of equation (2.48), the expression now obtained for the total flux is

$$\phi(x) = \frac{1}{2\pi}\int_{-\infty}^{\infty}\left[e^{ikx}(1 + ik\mu_0)^{-1}\frac{c}{ik}\ln\frac{1 + ik}{1 - ik}\right]\left[1 - \frac{c}{2ik}\ln\frac{1 + ik}{1 - ik}\right]^{-1} dk + \frac{1}{2\pi}\int_{-\infty}^{\infty} e^{ikx}(1 + ik\mu_0)^{-1}\,dk. \quad (2.52)$$

As before, the contour in the first integral may be deformed; again, it has a pole at $k = i/\nu_0$ and a branch point at $k = i$. There is, however, an additional pole at $k = i/\mu_0$. In the second integral in equation (2.52), assuming $x > 0$ and $\mu_0 > 0$, this pole gives a contribution to $\phi(x)$ which is equal to

$$\frac{1}{\mu_0}e^{-x/\mu_0}.$$

This is the flux due to uncollided neutrons, as may be seen in the following manner.

The uncollided angular flux $\Phi_0(x, \mu)$ from a plane source should satisfy equation (2.5) with the scattering term, i.e., the integral, set equal to zero, and the source term (for a source at $x = 0$) represented by $\delta(x)\,\delta(\mu - \mu_0)\,2\pi$; thus,

$$\mu\frac{\partial\Phi_0(x, \mu)}{\partial x} + \Phi_0(x, \mu) = \frac{\delta(x)\,\delta(\mu - \mu_0)}{2\pi}. \quad (2.53)$$

For the case in which $x > 0$ and $\mu > 0$, the right side of this expression is zero, and hence the solution is

$$\Phi_0(x, \mu) = \psi_0(\mu)e^{-x/\mu}.$$

At $x = 0$ and $\mu = \mu_0$, it must satisfy the discontinuity condition, namely

$$\Phi_0(+\epsilon, \mu) - \Phi_0(-\epsilon, \mu) = \frac{\delta(\mu - \mu_0)}{2\pi\mu}.$$

Hence the solution to equation (2.53), for $x > 0$ and $\mu_0 > 0$, is

$$\Phi_0(x, \mu) = \frac{1}{2\pi\mu_0} e^{-x/\mu_0} \delta(\mu - \mu_0).$$

Upon integration over all angles, the total flux is then found to be

$$\phi_0(x) = 2\pi \int_{-1}^{1} \Phi_0(x, \mu)\, d\mu = \frac{1}{\mu_0} e^{-x/\mu_0},$$

which is identical with the expression given above for the contribution to the flux made by the pole at $k = i/\mu_0$.

By separating the uncollided flux, the solution $\Phi(x, \mu)$ to equation (2.5) is divided into two parts, i.e.,

$$\Phi(x, \mu) = \Phi_0(x, \mu) + \Phi_1(x, \mu) \tag{2.54}$$

where $\Phi_0(x, \mu)$ satisfies equation (2.53). By substituting this form into equation (2.5) and subtracting equation (2.53) it is found that the angular flux Φ_1, due to collided neutrons, must satisfy the equation

$$\mu \frac{\partial \Phi_1}{\partial x} + \Phi_1 = \frac{c}{2} \int_{-1}^{1} \Phi_1(x, \mu')\, d\mu' + \frac{c}{2} \int_{-1}^{1} \Phi_0(x, \mu')\, d\mu'. \tag{2.55}$$

It is seen, therefore, that the collided angular flux Φ_1 satisfies the inhomogeneous transport equation with an isotropic distributed source equal to the second integral in equation (2.55). This source is the distribution of neutrons emerging from their first collision and is given by

$$\frac{c}{2} \int_{-1}^{1} \Phi_0(x, \mu')\, d\mu' = \frac{c}{4\pi\mu_0} e^{-x/\mu_0},$$

since c is the average number of neutrons emerging from a collision. The corresponding total flux of collided neutrons may therefore be represented by

$$\phi_1(x) = c \int G(x' \to x) \frac{e^{-x'/\mu_0}}{4\pi\mu_0}\, dx', \tag{2.56}$$

where $G(x' \to x)$ is Green's function as given by equation (2.40) with $|x - x'|$ replacing $|x - x_0|$. When the first integral in equation (2.52) is now evaluated it is found to be equivalent to equation (2.56) and is consequently equal to $\phi_1(x)$, the total flux of collided neutrons.

Thus it is seen that the solution to a problem with an anisotropic source in a medium with isotropic scattering can be obtained from the solution for an isotropic source. The general technique of treating the uncollided neutrons and the collided ones separately has been found to be useful in solving many neutron transport problems.

2.4 SOLUTION OF THE ONE-SPEED TRANSPORT EQUATION BY THE SPHERICAL HARMONICS METHOD

2.4a Introduction

In this section, the problem of a plane isotropic source in an infinite medium will be formulated using the spherical harmonics method. The general principle of this method for solving the one-speed transport equation is that the angular (or directional) dependence of the flux is expanded in a complete set of elementary functions, such as a series of polynomials. In general geometry, spherical harmonics are a logical choice, but for plane or spherical geometry these reduce to the Legendre polynomials.

For *plane geometry*, in which Φ is a function of x and μ only, the angular dependence of Φ may be expanded in a series of Legendre polynomials with coefficients that are functions of x; thus

$$\Phi(x, \mu) = \sum_{m=0}^{\infty} \frac{2m + 1}{4\pi} \phi_m(x) P_m(\mu), \tag{2.57}$$

where the $P_m(\mu)$ are the Legendre polynomials (see Appendix) and the $\phi_m(x)$ are the expansion coefficients. Because of their orthogonality, the latter are given by

$$\phi_m(x) = \int \Phi(x, \mu) P_m(\mu)\, d\Omega = 2\pi \int_{-1}^{1} \Phi(x, \mu) P_m(\mu)\, d\mu. \tag{2.58}$$

One advantage of the Legendre expansion for the angular flux is that the first two terms, at least, have a simple physical meaning. For $m = 0$, for example, the value of $P_m(\mu)$, i.e., $P_0(\mu)$ is 1; hence, it follows from equation (2.58) that $\phi_0(x)$ is simply the total flux at x. Furthermore, for $m = 1$, $P_1(\mu)$ is μ; hence, equation (2.58) gives

$$\phi_1(x) = 2\pi \int_{-1}^{1} \mu \Phi(x, \mu)\, d\mu,$$

which is the current $J(x)$ at x in the x direction. Although most other orthogonal polynomial expansions do not have such an obvious physical significance as do the Legendre set, they have advantages in some circumstances, particularly in fitting boundary conditions, as will be seen in Chapter 3.

2.4b Infinite Medium Plane Isotropic Source

The expansion in equation (2.57) is now substituted into the one-speed transport equation (2.41) for a plane isotropic source at $x = 0$; upon multiplication by 4π, the result is

$$\mu \sum_{m=0}^{\infty} (2m + 1) \frac{d\phi_m(x)}{dx} P_m(\mu) + \sum_{m=0}^{\infty} (2m + 1) \phi_m(x) P_m(\mu) = c\phi_0(x) + \delta(x).$$

The recurrence relation (see Appendix)

$$(2m + 1)\mu P_m(\mu) = (m + 1)P_{m+1}(\mu) + mP_{m-1}(\mu)$$

is then used in the first term on the left, and the resulting expression is multiplied by $\frac{1}{2}(2n + 1)P_n(\mu)$ and integrated over μ from -1 to 1. Upon using the orthogonality of the Legendre polynomials, it is found that

$$(n + 1)\frac{d\phi_{n+1}(x)}{dx} + n\frac{d\phi_{n-1}(x)}{dx} + (2n + 1)(1 - c\,\delta_{0n})\phi_n(x) = \delta_{0n}\,\delta(x), \qquad n = 0, 1, 2, \ldots \tag{2.59}$$

where $\phi_{-1}(x) \equiv 0$ and δ_{0n} is the Kronecker delta, i.e.,

$$\delta_{0n} = 1 \quad \text{if} \quad n = 0 \qquad \text{and} \qquad \delta_{0n} = 0 \quad \text{if} \quad n \neq 0.$$

Equation (2.59) represents an infinite set of equations for the unknown functions $\phi_n(x)$. For practical purposes, this set of equations is truncated in the following manner (see, however, Ref. 16). Consider the first $N + 1$ equations of the set, i.e., those for which $n = 0, 1, \ldots, N$; these involve $N + 2$ unknowns, i.e., ϕ_n for $n = 0, 1, \ldots, N + 1$. The number of unknowns may be made equal to the number of equations by assuming

$$\frac{d\phi_{N+1}(x)}{dx} = 0,$$

thereby obtaining the so called P_N *approximation*. Since

$$\phi_{N+1}(x) = 2\pi \int_{-1}^{1} \Phi(x, \mu)P_{N+1}(\mu)\,d\mu$$

and $P_{N+1}(\mu)$ oscillates rapidly for large N, changing sign $N + 1$ times in the interval $-1 \leqslant \mu \leqslant 1$, it is reasonable to suppose that ϕ_{N+1} will be very small for large N; hence, the P_N approximation is expected to be quite accurate if N is large.

Some indication of the error involved in the P_N approximation may be obtained by noting that the P_N equations would be exact for a problem in which the source in equation (2.41) is modified by addition of the term

$$\frac{N + 1}{4\pi}\frac{d\phi_{N+1}(x)}{dx}P_N(\mu).$$

For $n = N$, this would just cancel the first term on the left of equation (2.59), which is set equal to zero in the P_N approximation. The error in the scalar flux, ϕ_0, for example, could thus be estimated as arising from a source of the form given above.[17] In practice, however, it is preferable to determine the accuracy of the P_N solutions by comparison with exact results, such as those obtained by the methods described earlier in this chapter or by accurate numerical procedures discussed in later chapters. In addition, by examining the dependence of

the results on N, it is possible to obtain an estimate of the accuracy of a particular P_N approximation. The data in Tables 2.6 and 2.7 will serve to illustrate this point.

The P_N equations could be obtained in an alternative manner, namely, by truncating the angular flux expansion of equation (2.57) after $N + 1$ terms, i.e., by setting $\phi_N = 0$ for $n > N$. The P_N approximation is often simply defined in this manner, but the method used here provides a better insight concerning what is involved in the approximation.

When $x \neq 0$, a set of homogeneous first-order differential equations with constant coefficients is obtained from the equations (2.59), and the general solution is a sum of exponentials, i.e.,

$$\phi_n(x) = \sum_{i=0}^{N} A_i g_n(\nu_i) e^{-x/\nu_i},$$

where the values of ν_i are given by the vanishing of the determinant of the coefficients in equation (2.59).[18] These coefficients of the exponentials may be found by integrating equations (2.59) over a small region including $x = 0$, as in the derivation of equation (2.37).

An alternative method is to take the Fourier transform of equations (2.59), by first defining

$$F_n(k) = \int_{-\infty}^{\infty} e^{-ikx} \phi_n(x)\, dx. \tag{2.60}$$

The equations (2.59) are then multiplied by e^{-ikx} and integrated over x between $-\infty$ and ∞; the result is

$$(n + 1)ikF_{n+1}(k) + nikF_{n-1}(k) + (2n + 1)(1 - c\,\delta_{0n})F_n(k) = \delta_{0n} \qquad n = 0, 1, \ldots, N \tag{2.61}$$

$$F_{N+1} = 0.$$

This set of $N + 1$ algebraic equations can be solved for $F_n(k)$, where $n = 0, 1, \ldots, N$.

In the P_1 approximation, for example, only $F_0(k)$ and $F_1(k)$ are nonzero, and the applicable forms of equation (2.61) are for $n = 0, 1$, i.e.,

$$ikF_1(k) + (1 - c)F_0(k) = 1$$

and

$$ikF_0(k) + 3F_1(k) = 0.$$

From these algebraic equations it is seen that

$$F_0(k) = \frac{1}{(1 - c) + \frac{1}{3}k^2}$$

and, hence, by Fourier inversion

$$\phi_0(x) \equiv \phi(x) = \frac{1}{2\pi}\int_{-\infty}^{\infty} \frac{e^{ikx}}{(1-c) + \frac{1}{3}k^2}\, dk. \tag{2.62}$$

The integral may be evaluated by contour integration or by elementary methods to give

$$\phi(x) = \frac{1}{2}\sqrt{\frac{3}{1-c}}\, e^{-\sqrt{3(1-c)}|x|}. \tag{2.63}$$

This result, in the P_1 approximation, is a good approximation to the asymptotic solution for $1 - c \ll 1$ obtained by the methods given earlier in this chapter. It takes no account, however, of the contribution of the transients which are important near the source.

2.4c Diffusion Theory and Diffusion Length

It will now be shown that the P_1 approximation in the present case, for a plane isotropic source in an infinite medium, is identical with diffusion theory. The two forms of equation (2.59) which are applicable are, for $n = 0$ and $n = 1$, respectively; that is,

$$\frac{d\phi_1(x)}{dx} + (1-c)\phi_0(x) = \delta(x) \tag{2.64}$$

and

$$\frac{d\phi_0(x)}{dx} + 3\phi_1(x) = 0. \tag{2.65}$$

Since $\phi_1(x)$ is the current $J(x)$ in the x direction and ϕ_0 is the total flux, ϕ, equation (2.65) is simply a form of Fick's law, i.e.,

$$\phi_1(x) = J(x) = -D\frac{d\phi(x)}{dx}, \tag{2.66}$$

and the diffusion coefficient $D = \frac{1}{3}$, with lengths expressed in terms of the mean free path. Upon inserting this value of $\phi_1(x)$ into equation (2.64), the result is

$$-\frac{d}{dx}\left[D\frac{d\phi(x)}{dx}\right] + (1-c)\phi(x) = \delta(x).$$

Since $1 - c$ is the equivalent of the macroscopic absorption cross section (§2.2b), this equation may be expressed in the general form

$$D\nabla^2\phi - \sigma_a\phi + Q = 0,$$

where ∇^2 is the Laplacian operator. It is then recognized as the familiar equation of diffusion theory.[19]

Furthermore $1/\sqrt{3(1-c)}$ in equation (2.63) may be identified with the diffusion length, L, as in §2.2b, and, as just seen, the diffusion coefficient is equal to $\frac{1}{3}$. Hence, equation (2.63) may be written as

$$\phi(x) = \frac{Le^{-|x|/L}}{2D},$$

which is identical with the expression derived from diffusion theory for the flux from an isotropic plane source in an infinite medium. It will be shown in §2.6b that the equivalence of the P_1 approximation to diffusion theory also extends to the case of anisotropic scattering. For energy-dependent problems, diffusion theory and the P_1 approximation are generally nonequivalent and the differences will be examined in Chapter 4.

In the odd approximations of higher order, e.g., P_3, P_5, etc., more terms appear in the solution of the transport equation. For example, in the P_3 approximation, the denominator in the integrand of equation (2.62) includes a fourth-order polynomial in k. The solution for $\phi_0(x)$ then contains two exponentials, if the solution is written in terms of $|x|$ as in equation (2.63), or four exponentials if separate solutions are written for $x > 0$ and $x < 0$. In general for a P_{2N-1} approximation, the solution contains N exponentials. As N is increased, one of these becomes a better and better approximation to the asymptotic solution whereas the others approximate transient solutions.[20] It may be mentioned that an even-order (P_{2N}) approximation has only N roots, i.e., the same number as the next lower odd-order (P_{2N-1}) approximation. For this and other reasons,[21] the even-order approximations are not commonly used. There are, however, some cases in which even-order approximations have been employed.[22] The relaxation lengths ($1/\nu_0$) corresponding to the asymptotic solutions of the one-speed neutron transport equation for several approximations are given in Table 2.3.[23] The exact values are those derived from equation (2.20), as in Table 2.1. It will be recalled that the values for the P_1 approximation are identical with those obtained for diffusion theory.

Some values of the transient exponents, ν_1, for several P_N approximations are recorded in Table 2.4.[23] It is seen that, as expected for transients, the values lie

TABLE 2.3. ASYMPTOTIC RELAXATION LENGTHS FOR P_N APPROXIMATIONS.[23] (IN MEAN FREE PATHS)

c	P_1	P_3	P_5	P_7	Exact
0.9	1.826	1.903	1.903	1.903	1.903
0.8	1.291	1.405	1.408	1.408	1.408
0.5	0.816	1.011	1.037	1.042	1.044
0	0.577	0.861	0.932	0.960	1.000

TABLE 2.4. VALUES OF EXPONENTS (ν_i) IN THE TRANSIENT TERMS FOR P_N APPROXIMATIONS[23]

		P_3	P_5		P_7		
c	P_1	ν_1	ν_1	ν_2	ν_1	ν_2	ν_3
0.9	None	0.487	0.806	0.303	0.902	0.619	0.220
0.8	None	0.466	0.793	0.295	0.895	0.609	0.215
0.5	None	0.409	0.740	0.271	0.861	0.575	0.202
0	None	0.340	0.661	0.239	0.797	0.526	0.183

in the interval $0 \leqslant \nu_i \leqslant 1$; furthermore, they are more-or-less uniformly spaced in this interval.

2.5 THE ONE-SPEED TRANSPORT EQUATION IN A FINITE MEDIUM

2.5a Introduction

The treatment in the preceding sections of this chapter has been concerned with an infinite medium. Suppose, now, that the medium does not fill all of space but has one or two plane boundaries, i.e., the medium is a half-space or an infinitely long slab of finite thickness. Exact solutions, in closed form, may still be obtained to the transport equation either by the separation of variables or by the Fourier transform method. Because the solution must be determined to match the boundary conditions over half the angular range, namely, $\Phi(x, \mu) = 0$ for either $\mu > 0$ or $\mu < 0$, whichever range represents incoming neutron directions, the mathematical problems are more difficult than for an infinite medium. The required mathematics, such as singular integral equations for the separation of variables[24] and the Wiener-Hopf method for the Fourier transform,[25] will not be given here.* Nevertheless, the general nature of the solutions can be understood by reference to the infinite-medium Green's function.

It might be thought that the results derived earlier for neutron transport in an infinite medium are of very limited applicability. This, however, is not the case, at least insofar as the general features of the solution of the neutron transport equation, such as the division of the solution into asymptotic and transient parts, are concerned. The reason is that the solution to any transport problem in a uniform finite medium bounded by a convex surface is equivalent to the solution for an infinite medium in which a suitable distribution of neutron

* These methods are not described because they are not used for the solution of practical reactor problems and because their development would be lengthy and require considerable knowledge of complex-variable theory. Moreover, the interested reader will find adequate treatments in the references given.

sources is located at the position of the boundary of the finite medium. This can be seen in the following manner.

Consider a finite uniform medium bounded by the convex surface S. A solution is being sought for the flux, within S, for some distribution of sources, also within S, subject to free-surface boundary conditions (§1.1d) on S. The solution Φ_1 to this Problem 1 is, within S, equivalent to the solution Φ_2 of Problem 2 for an infinite medium with an additional (negative) source (Fig. 2.3) as described below. Suppose the medium within S is extended to infinity while retaining the sources in this region; in addition, however, a negative surface source, directed outward, is imposed on S. The intensity, $-\hat{\mathbf{n}}\cdot\boldsymbol{\Omega}\Phi_1$, of this source is of such magnitude as to cancel exactly the outward angular neutron current in Problem 1. The asymptotic solution to Problem 2 must be chosen to vanish outside S.

Although a more formal proof of this theorem has been given,[26] a simple treatment is adequate. In Problem 1, the outward angular neutron current through any surface element dA is

$$\text{Outward angular current} = \hat{\mathbf{n}}\cdot\boldsymbol{\Omega}\Phi_1(\mathbf{r}, \boldsymbol{\Omega})\, dA \quad \text{for} \quad \hat{\mathbf{n}}\cdot\boldsymbol{\Omega} > 0.$$

This is the number of neutrons crossing dA per unit time and unit direction about $\boldsymbol{\Omega}$. Now suppose an outward surface source is imposed on S so that the outward angular current is exactly cancelled. Since it is an outward source, it cannot affect the angular flux Φ_1 within S. The intensity of this imposed source must then be $-\hat{\mathbf{n}}\cdot\boldsymbol{\Omega}\Phi_1(\mathbf{r}, \boldsymbol{\Omega})$; it is a negative source, i.e., it represents a negative number of neutrons, in an outward direction. In this new situation, therefore, there are no neutrons at all leaving S. Hence, the medium may be extended outside S, to make it an infinite medium, without affecting the solution inside S. Thus, the solution Φ_2 to Problem 2 is seen to be equivalent, within S, to the required solution Φ_1 to Problem 1.

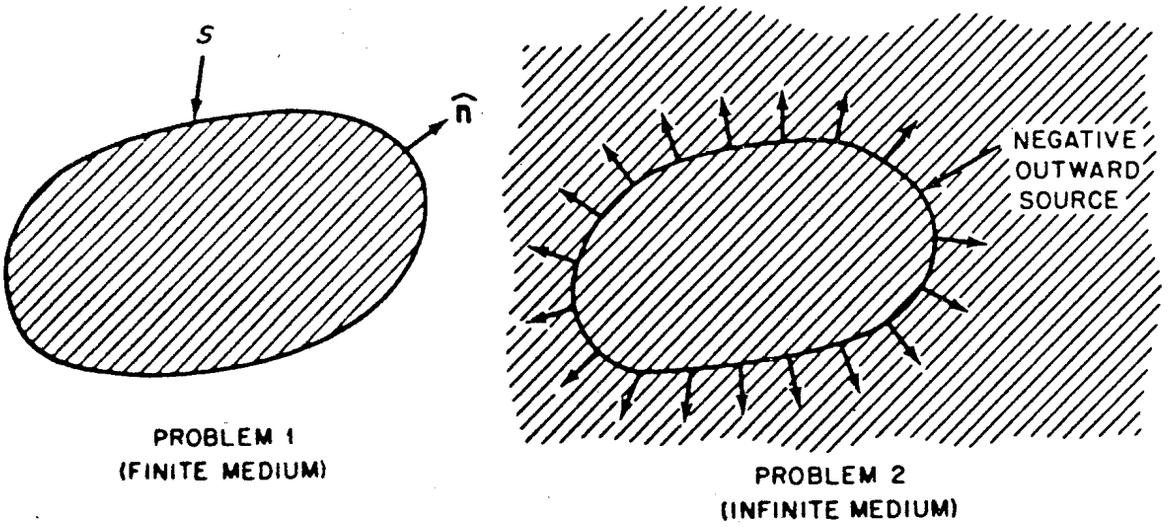

FIG. 2.3 FINITE AND INFINITE MEDIUM PROBLEMS.

For a bounded medium in infinite plane geometry, the information relating to the infinite medium plane Green's function can be used to examine the effects of the boundary, as will be shown in §2.5b. Since the boundary acts as a source in an infinite medium, it is to be expected that it will contribute both asymptotic and transient parts to the solution for the finite medium. Moreover, this will be so in any geometry, not just in infinite plane geometry. It was seen earlier that for any point or distributed source, isotropic or anisotropic, the solution consists of asymptotic and transient parts, and the former dominates at points distant from the source. The general conclusion to be drawn from the foregoing arguments is that for a finite medium with a free-surface boundary regardless of its geometry, the asymptotic solutions will dominate at a distance from the boundary as well as from the source.

Some of the results derived above will now be applied to problems involving finite media in infinite plane geometry.

2.5b The Milne Problem

The Milne problem is a classical problem in astrophysics concerned with the diffusion of radiation through a stellar atmosphere.[27] The general principles are, however, also applicable to the distribution of neutrons in a (right) half-space ($x > 0$) through which they are diffusing from a source at $x = +\infty$. For $x < 0$ (left half-space) there is a vacuum (Fig. 2.4) and a vacuum (or free-surface) boundary condition, $\Phi(0, \mu) = 0$ for $\mu > 0$, is imposed. The objective of the problem is to determine the angular dependence of the emergent neutrons at the boundary, i.e., $\Phi(0, \mu)$ for $\mu < 0$.

In accordance with the general procedure explained above, the vacuum in the left half-space may be replaced by the material medium, i.e., the medium is extended to $x = -\infty$, and a negative source is imposed at $x = 0$ directed toward negative x. If $\Phi(0, \mu)$, which is nonzero only for $\mu < 0$, represents the angular flux in the Milne problem, then the required negative source at $x = 0$ is $\mu\Phi(0, \mu)$; it is negative because it is applied for $\mu \leqslant 0$ only.

The Milne problem, i.e., the problem of a half-space with a source at infinity, is thus, for $x > 0$, equivalent to an infinite medium with a source at $x = \infty$ and

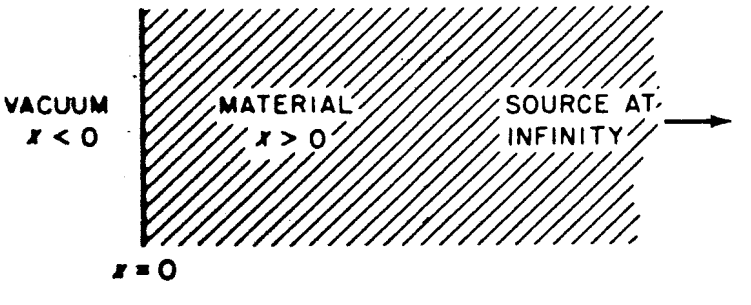

FIG. 2.4 SOURCE AT INFINITY IN A MEDIUM WITH VACUUM BOUNDARY.

a negative source at $x = 0$. Although this does not actually solve the problem, since $\Phi(0, \mu)$ for $\mu < 0$ is not yet known, it does show the character of the solution.

At some distance away, the source at infinity contributes only an asymptotic term, which may be normalized, so that

$$\text{Contribution from source at infinity} = e^{x/\nu_0}\psi_0^-(\mu).$$

The contribution of the source at the surface, i.e., at $x = 0$, can be written in terms of the infinite medium Green's function as expressed by equation (2.38). The net angular flux is then given by

$$\Phi(x, \mu) = e^{x/\nu_0}\psi_0^-(\mu) + \int_{-1}^{0} G(0, \mu_0 \to x, \mu)\mu_0\Phi(0, \mu_0)\, d\mu_0.$$

By introducing the explicit value for the Green's function, it is seen that the surface source contributes an asymptotic term containing e^{-x/ν_0} plus transients which decay more rapidly than e^{-x} with increasing distance from the surface. As far as the asymptotic solution is concerned, it is necessary only to determine the normalization of the surface term.

Analysis[28] shows that the two asymptotic exponential terms, from the source at infinity and the surface source, lead to the expression

$$\phi_{\text{asym}}(x) = f(c, \nu_0) \sinh \frac{x + x_0}{\nu_0}, \tag{2.67}$$

where $f(c, \nu_0)$ is a function of c and ν_0. It follows from this result that the extrapolated asymptotic flux, i.e., the flux extended by its natural curvature with

TABLE 2.5. EXTRAPOLATION DISTANCES AT A PLANE SURFACE FROM MILNE PROBLEM.[29] (IN MEAN FREE PATHS)

c	cx_0	x_0
0.5	0.7207	1.441
0.6	0.7155	1.192
0.7	0.7127	1.018
0.8	0.7113	0.8891
0.9	0.7106	0.7896
1.0	0.7104	0.7104
1.1	0.7106	0.6460
1.2	0.7109	0.5924
1.3	0.7113	0.5472
1.4	0.7118	0.5084
1.5	0.7123	0.4748

distance, will vanish when $x = -x_0$; the distance x_0 is called the *extrapolation distance*. For $|c - 1| \ll 1$, it is found that

$$cx_0 = 0.71044[1 + 0.0199(1 - c)^2 + O(1 - c)^3],$$

where $O(1 - c)^3$ implies a quantity of the order of $(1 - c)^3$ which is small when $|c - 1| \ll 1$. Some exact values for cx_0 as a function of c are quoted in Table 2.5[29]; the first two terms of the expression given above are a good approximation for $|c - 1| \ll 1$.

It should be pointed out that the extrapolation distances given here hold only at a *plane surface*. Different values are applicable to the asymptotic flux near a curved surface.[30]

2.5c The Critical Slab Problem

For a slab of finite thickness, having $c < 1$ and containing a neutron source, the foregoing considerations may be readily generalized to indicate the asymptotic and transient parts of the solution. Moreover, in this geometry it is possible to obtain physically significant solutions for $c > 1$, and these will now be considered.

It will be recalled (§1.5d) that meaningful solutions of the time-independent transport equation are to be expected only for a subcritical system with a source or for a critical system. An infinite medium with $c > 1$ is evidently supercritical and the asymptotic solutions found in §2.2b had ν_0 imaginary; they were thus complex or oscillatory and had no physical meaning. A slab of finite thickness with $c > 1$, however, may be subcritical or critical, in which case there will be physical solutions to the time-independent transport equation. In this section the critical slab will be examined and it will be seen that a good estimate of the critical thickness is obtained by requiring that the asymptotic flux go to zero at the extrapolated boundary.

Consider a slab extending from $0 \leqslant x \leqslant a$ in thickness. Outside the slab there is a vacuum and so the boundary conditions imposed at 0 and a are

$$\Phi(0, \mu) = \Phi(a, -\mu) = 0 \qquad \mu \geqslant 0. \tag{2.68}$$

Just as in the Milne problem, an equivalent problem may be obtained by extending the medium to infinity and adding negative outgoing sources at $x = 0$ and $x = a$. Again the solution will have an asymptotic part plus transients near $x = 0$ and $x = a$. If the critical slab is fairly thick, i.e., $a \gg 1$, which implies $c - 1 \ll 1$, then near each boundary the solution will resemble that of the Milne problem. The asymptotic flux is in general (cf. §2.2b) given by

$$\phi_{as}(x) = A \sin \frac{x}{|\nu_0|} + B \cos \frac{x}{|\nu_0|}.$$

If the flux is to be symmetric about $x = a/2$, then the asymptotic solution will be

$$\phi_{as}(x) \propto \cos \frac{x - (a/2)}{|\nu_0|}. \tag{2.69}$$

In order for the bare slab to be critical, the asymptotic flux should go to zero at the two extrapolated surfaces at $x = -x_0$ and $x = a + x_0$ (Fig. 2.5). From the boundary condition $\phi_{as}(-x_0) = 0$ and equation (2.69), it is seen that

$$\frac{-x_0 - (a/2)}{|\nu_0|} = -\frac{\pi}{2},$$

from which it follows that, for criticality,

$$\frac{a}{2} = \frac{\pi}{2} |\nu_0(c)| - x_0. \tag{2.70}$$

The argument (c) is introduced here to emphasize, as seen earlier, that $|\nu_0|$ is a function of c.

Equation (2.70) gives an estimate of the critical half-thickness of a slab as a function of c. Since this estimate is based on setting the asymptotic flux equal to zero at the extrapolated boundaries (or end points), the procedure is often referred to as the *end-point method* (or *end-point theory*),[31] although it has also been called diffusion theory.[32] In this book, however, the term diffusion theory is applied to the theory based on Fick's law with the diffusion coefficient represented by a simple expression (see, e.g., §2.4c).

It transpires that equation (2.70) is remarkably accurate, even when $c - 1$ is fairly large; this may be seen from the comparison in Table 2.6.[33] (The critical

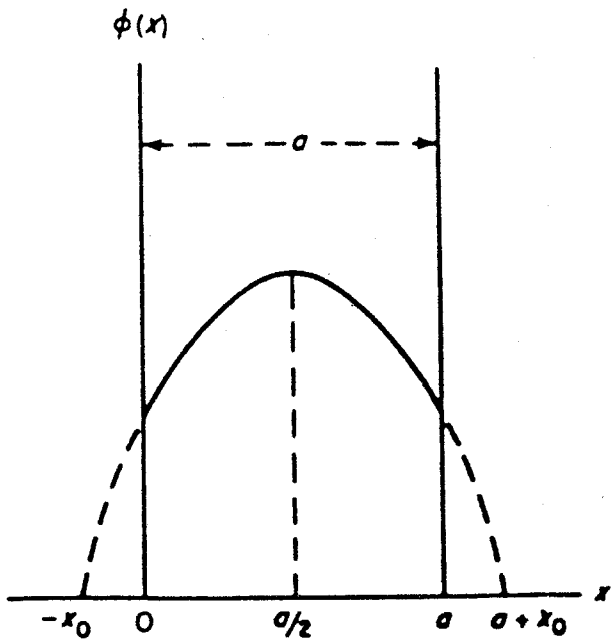

FIG. 2.5 CRITICAL SLAB PROBLEM.

TABLE 2.6. CRITICAL HALF-THICKNESSES OF AN INFINITE SLAB.[33] (IN MEAN FREE PATHS)

c	*End-point Method*	*Exact*	P_1	P_3	P_5
1.02	5.665	5.6655	5.839	5.663	5.672
1.05	3.300	3.3002	3.488	3.319	3.307
1.10	2.113	2.1134	2.309	2.135	2.121
1.20	1.290	1.2893	1.485	1.318	1.298
1.40	0.738	0.7366	0.919	0.779	0.750
1.60	0.515	0.5120	0.680	0.559	0.530

half-thickness for various P_N approximations, to which reference will be made later, are also included in the table.) The "exact" values were obtained by complete solution of the transport equation by numerical methods and variational theory (§6.4d). The error in the end-point results is only 0.25 percent for $c = 1.4$. Accurate results may also be obtained by the method of separation of variables.[34]

2.5d Spherical Harmonics Method with Boundary Conditions

The critical slab problem provides an interesting test of the accuracy of approximate solutions of the one-speed transport theory; it will consequently be utilized in connection with the spherical harmonics method as applied to a finite medium. The P_N equations for a finite medium in plane geometry, such as the critical slab, are the same as in equation (2.59) except that the right-hand side is zero. The only new feature is that the boundary conditions must be imposed.[35]

It is not possible to satisfy the exact boundary conditions, i.e., equation (2.68), in a P_N approximation having finite N. The difficulty is, once again, that the boundary conditions are imposed over half the angular range whereas the expansion coefficients apply over the whole range of μ, i.e., $-1 \leqslant \mu \leqslant 1$. There is consequently no unique way of choosing boundary conditions to represent a free surface in a P_N approximation. In the following treatment, consideration will be given to two reasonable choices; one is based on setting the odd half-range moments of the flux equal to zero, whereas the other is equivalent to replacing the vacuum outside the slab by a purely absorbing medium, i.e., a medium from which no neutrons return.

For a P_N approximation of odd order, i.e., N is odd, $N + 1$ boundary conditions are required on the $N + 1$ expansion coefficients ϕ_n, there being $(N + 1)/2$ from each boundary. A natural choice is to set

$$\int_0^1 P_i(\mu)\Phi(0, \mu)\, d\mu = \int_0^1 P_i(-\mu)\Phi(a, -\mu)\, d\mu = 0$$

$$i = 1, 3, 5, \ldots, N, \text{ with } N \text{ odd.} \qquad (2.71)$$

These are known as the Marshak boundary conditions,[36] which may also be derived from a variational principle.[37] They have the virtue of including (for $i = 1$) the condition of zero incoming current, familiar in diffusion theory. Thus for $i = 1$, $P_i(\mu) = P_1(\mu) = \mu$, and the appropriate boundary condition is

$$\int_0^1 \mu\Phi(0, \mu)\, d\mu = \int_0^1 \mu\Phi(a, -\mu)\, d\mu = 0. \tag{2.72}$$

In accordance with the results given earlier, this implies that the inward currents at $x = 0$ and $x = a$ are zero. The net current at $x = 0$

$$J_x = \int_{-1}^1 \mu\Phi(0, \mu)\, d\mu$$

is, of course, not zero. In the P_1 approximation the boundary conditions of equation (2.71) lead to an extrapolation distance, as in equation (2.67), which for $c - 1 \ll 1$ is given by[38]

$$x_0 = \tfrac{2}{3}[1 - \tfrac{4}{9}(c - 1) + \tfrac{16}{45}(c - 1)^2 + \cdots]. \quad \text{(Marshak } P_1\text{)} \tag{2.73}$$

It should be noted that the extrapolation length derived in this manner from the P_1 approximation represents the distance beyond the boundary at which the asymptotic solution to the flux, with its *natural curvature*, extrapolates to zero (Fig. 2.6). The linear extrapolation distance of diffusion theory is different in the respect that it is the distance at which the flux becomes zero when it is extrapolated in a *linear* manner beyond the boundary, and is equal to $\phi(0)/|\phi'(0)|$, where

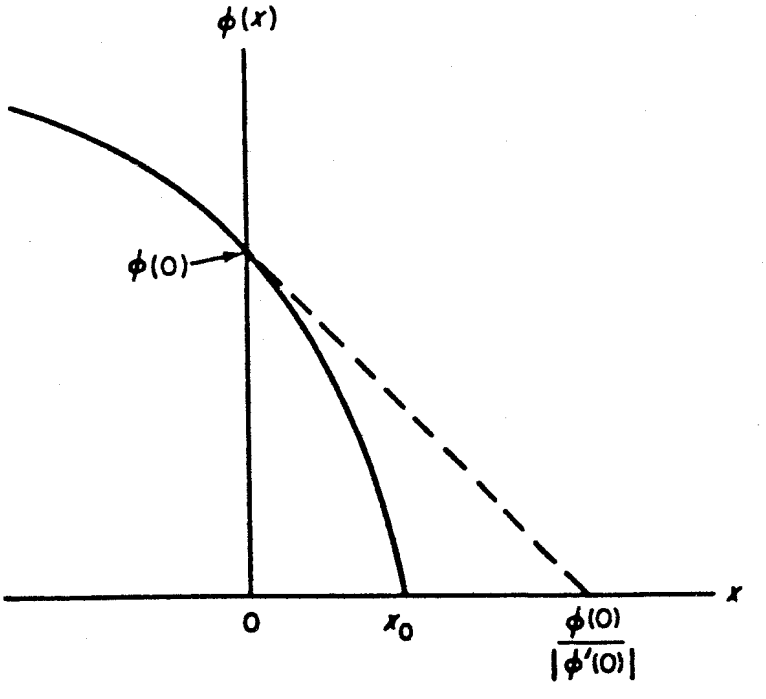

FIG. 2.6 EXTRAPOLATION OF NEUTRON FLUX AT BOUNDARY.

$\phi'(0)$ is the derivative of $\phi(x)$ with respect to x at $x = 0$. For the P_1 approximation, equation (2.57) gives

$$\Phi(x, \mu) = \frac{1}{4\pi} [\phi_0(x) + 3\mu\phi_1(x)]$$

and, hence, by equation (2.65),

$$\Phi(x, \mu) = \frac{1}{4\pi} [\phi_0(x) - \mu\phi_0'(x)].$$

By applying the Marshak boundary condition of equation (2.71), it is readily found that the linear extrapolation distance, $\phi_0(0)/|\phi_0'(0)|$, is $\frac{2}{3}$ (in mean free paths), as in ordinary diffusion theory.

Another possibility for the boundary condition is to set

$$\phi(0, \mu_i) = 0 \qquad i = 1, 2, 3, \ldots, (N + 1)/2, \text{ with } N \text{ odd},$$

for a finite number of points μ_i. When the chosen points are the positive roots of

$$P_{N+1}(\mu_0) = 0,$$

the Mark boundary conditions[39] are obtained. A derivation of these conditions for a particular form of the P_N method will be given in §5.2c. It has been shown[40] that the Mark conditions are equivalent to replacing the vacuum by a purely absorbing medium. In the P_1 approximation, the extrapolation length, x_0, based on these boundary conditions is

$$x_0 = \frac{1}{\sqrt{3}} [1 - \tfrac{1}{3}(c - 1) + \tfrac{1}{5}(c - 1)^2 + \cdots]. \quad \text{(Mark } P_1\text{)} \qquad (2.74)$$

The values for the critical half-thickness of a slab, as derived from the P_N approximation, using the Mark boundary conditions, were included in Table 2.6.

Experience indicates that the Marshak boundary conditions are somewhat more accurate than the Mark conditions,[41] at least for small N. In particular, equation (2.73) is a better approximation than equation (2.74) to the exact extrapolation distance given in §2.5b. The superiority of the Marshak boundary conditions is probably connected with their being derivable from a variational principle.[42] However, both forms of the boundary conditions have been used widely.

2.5e Adjacent Half-Spaces

The case of two adjacent, source-free media with a source at infinity (Fig. 2.7) has been solved exactly.[43] Just as a boundary with a vacuum can be treated in terms of an equivalent surface source in an infinite medium, so also the effect of one medium on an adjacent one can be described in terms of an equivalent surface source at the position of the boundary in an infinite medium. This source

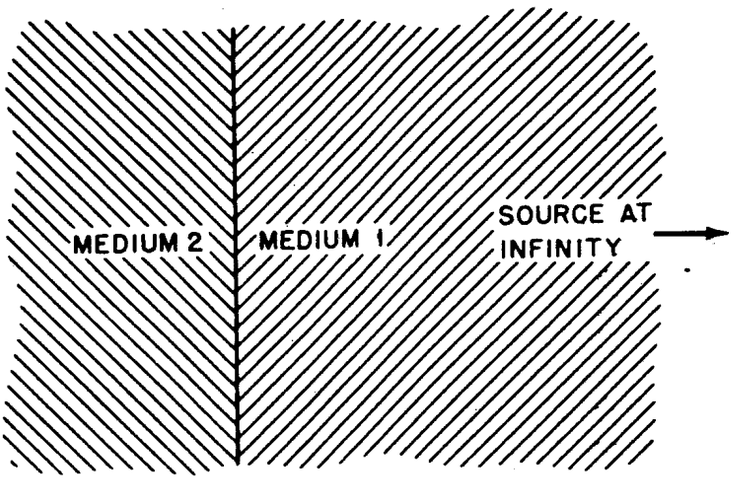

FIG. 2.7 ADJACENT HALF-SPACES WITH SOURCE AT INFINITY.

will introduce asymptotic and transient solutions to the transport equation in the adjacent media. An essential feature of the analysis is to show how the asymptotic solutions in the two media are to be connected at the boundary.

A systematic treatment of source-free, one-speed problems can be developed by considering only the asymptotic solutions in each region. These are joined across the interface by using the results mentioned above.

According to equation (2.22), the asymptotic solution of the transport equation can be written as

$$\Phi_{as}(x, \mu) = e^{\mp x/\nu_0}\psi_0^{\pm}(\mu),$$

so that by integrating over μ, and using the normalization condition of equation (2.17), it is found that

$$\phi_{as}(x) = e^{\mp x/\nu_0}.$$

It is evident, therefore, that $\phi_{as}(x)$ is a solution of the simple diffusion equation

$$\frac{d^2\phi_{as}(x)}{dx^2} - \frac{1}{\nu_0^2}\phi_{as}(x) = 0.$$

In an infinite medium, there is no special reason for choosing the x direction, and so the asymptotic flux will satisfy the general equation

$$\nabla^2\phi_{as}(\mathbf{r}) - \frac{1}{\nu_0^2}\phi_{as}(\mathbf{r}) = 0.$$

By systematically using the known solutions to this equation with exact values of ν_0, together with the interface conditions derived in the manner referred to above, a form of diffusion theory has been developed.[44] Although accurate, the theory cannot be generalized readily to multigroup solutions, and so it will find limited application in this book.

2.5f Spherical Geometry

Many of the problems of slab geometry have their counterparts in spherical geometry where exact solutions have also been found. It was seen in §1.3c, for example, that the solution of the transport equation for $r\phi$ in a sphere of radius a is related to that for ϕ in a slab of half-thickness a. Since $r\phi$ for a sphere must be an odd function of r (§1.3c), the asymptotic flux in a source-free sphere is given by

$$r\phi_{as}(r) = A \sin \frac{r}{|\nu_0|}.$$

According to the arguments for the critical slab in §2.5c, the sphere will be approximately critical when its radius a is such that ϕ_{as} is zero at the extrapolated radius, i.e., $\phi(a + x_0) = 0$; thus,

$$a = \pi|\nu_0(c)| - x_0. \tag{2.75}$$

It will be observed that the same extrapolation length appears here as in plane geometry; the linear extrapolation distance, however, is different in the two cases.

Values of critical radii determined from equation (2.75) are quoted in Table 2.7, together with the "exact" results and those given by the P_1, P_3, and P_5 approximations with Mark boundary conditions.[45] The agreement between the end-point and exact values is again seen to be very good. The development of the P_N method for spherical geometry is given in §3.3a.

The method of separation of variables has also been applied to spherical geometry.[46] As in the case of a slab of finite thickness, the procedure involves the solution of singular integral equations. In this manner, systematic improvements to equation (2.75) have been obtained.[47]

In conclusion, it should be remembered that the equivalence between a slab and a sphere holds only for constant cross sections independent of position (see §1.3c).

TABLE 2.7. CRITICAL RADII OF A SPHERE.[45] (IN MEAN FREE PATHS)

c	*End Point*	*Exact*	P_1	P_3	P_5
1.02	12.027	12.0270	12.252	12.045	12.034
1.05	7.277	7.2772	7.543	7.296	7.284
1.10	4.873	4.8727	5.177	4.895	4.880
1.20	3.172	3.1720	3.513	3.204	3.181
1.40	1.985	1.9854	2.353	2.039	1.999
1.60	1.476	1.4761	1.850	1.550	1.497

2.6 ANISOTROPIC SCATTERING

2.6a Plane Geometry: Spherical Harmonics

In realistic multigroup problems the scattering is invariably anisotropic and the effect of such scattering on solutions of the transport equation must be examined. Plane geometry will be considered, as before, although in many respects spherical geometry is just as simple.

In plane geometry with anisotropic scattering, the one-speed neutron transport equation (2.5) takes the form

$$\mu \frac{\partial \Phi(x, \mu)}{\partial x} + \Phi(x, \mu) = c \int_0^{2\pi} d\varphi' \int_{-1}^{1} f(\Omega' \to \Omega) \Phi(x, \mu')\, d\mu' + Q(x, \mu), \tag{2.76}$$

where the angular flux $\Phi(x, \mu)$ and the source $Q(x, \mu)$ are assumed to be independent of the azimuthal angle φ. Except for special cases, such as when the medium is moving or consists of a single crystal, $f(\Omega' \to \Omega)$ is a function of $\Omega \cdot \Omega' = \mu_0$ only (§1.1b), where Ω' and Ω are the neutron directions before and after scattering, respectively. Consequently, $f(\Omega' \to \Omega)$ may be expanded as the sum of a series of Legendre polynomials, i.e.,

$$f(\Omega' \to \Omega) = f(\mu_0) = \sum_{l=0}^{\infty} \frac{2l + 1}{4\pi} f_l P_l(\mu_0). \tag{2.77}$$

By the orthogonality of these polynomials,

$$f_l = 2\pi \int_{-1}^{1} f(\mu_0) P_l(\mu_0)\, d\mu_0 \tag{2.78}$$

with the normalization condition

$$f_0 = 2\pi \int_{-1}^{1} f(\mu_0)\, d\mu_0 = 1.$$

As seen in §1.6c, the P_0 term (isotropic scattering) is dominant except for scattering by light elements and for neutrons of high energy.

According to the addition theorem of Legendre polynomials (see Appendix)

$$P_l(\mu_0) = P_l(\mu) P_l(\mu') + 2 \sum_{m=1}^{l} \frac{(l - m)!}{(l + m)!} P_l^m(\mu) P_l^m(\mu') \cos m(\varphi - \varphi'),$$

where μ and μ' are the direction cosines and φ and φ' are the azimuthal angles specifying the directions Ω and Ω', respectively, and the $P_l^m(\mu)$ are associated Legendre polynomials (see Appendix). Upon insertion of this into equation

(2.77) and the result into equation (2.76), the terms containing $\cos m(\varphi - \varphi')$ vanish upon integration over φ'; then

$$\mu \frac{\partial \Phi(x, \mu)}{\partial x} + \Phi(x, \mu) = \frac{c}{2} \sum_{l=0}^{\infty} (2l + 1) f_l P_l(\mu) \int_{-1}^{1} \Phi(x, \mu') P_l(\mu')\, d\mu' + Q(x, \mu). \tag{2.79}$$

The angular flux, Φ, and the source, Q, are also expanded in Legendre polynomials; thus,

$$\Phi(x, \mu) = \sum_{m=0}^{\infty} \frac{2m + 1}{4\pi} \phi_m(x) P_m(\mu) \tag{2.80}$$

as in equation (2.57), and correspondingly

$$Q(x, \mu) = \sum_{m=0}^{\infty} \frac{2m + 1}{4\pi} Q_m(x) P_m(\mu), \tag{2.81}$$

where, by the orthogonality of the polynomials,

$$\phi_m(x) = \int \Phi(x, \mu) P_m(\mu)\, d\Omega = 2\pi \int_{-1}^{1} \Phi(x, \mu) P_m(\mu)\, d\mu$$

and similarly,

$$Q_m(x) = 2\pi \int_{-1}^{1} Q(x, \mu) P_m(\mu)\, d\mu.$$

If $Q(x, \mu)$ is an isotropic source, then for $m = 1$, it is seen that $Q_1(x)$ is zero.

When the expansions of equations (2.80) and (2.81) are inserted into equation (2.79) and the recurrence relation for Legendre polynomials is used, it is found that

$$\sum_{m=0}^{\infty} \left[\frac{d\phi_m(x)}{dx} \{(m + 1) P_{m+1}(\mu) + m P_{m-1}(\mu)\} + (2m + 1) \phi_m(x) P_m(\mu) \right]$$
$$= c \sum_{l=0}^{\infty} (2l + 1) f_l \phi_l(x) P_l(\mu) + \sum_{m=0}^{\infty} (2m + 1) Q_m(x) P_m(\mu).$$

Upon multiplying both sides by $\frac{1}{2}(2n + 1)P_n(\mu)$, integrating over μ from -1 to 1, and making use of the orthogonality of the Legendre polynomials, the result is

$$(n + 1) \frac{d\phi_{n+1}(x)}{dx} + n \frac{d\phi_{n-1}(x)}{dx} + (2n + 1)(1 - c f_n) \phi_n(x) = (2n + 1) Q_n(x),$$
$$n = 0, 1, 2, \ldots \tag{2.82}$$

with the requirement that $\phi_{-1}(x)$ is zero. As in §2.4b, a P_N approximation may be defined by considering the first $N + 1$ of these equations and setting $d\phi_{N+1}/dx = 0$.

A result corresponding to equation (2.82) in spherical geometry will be derived in §3.3a.

2.6b Diffusion Theory and the Transport Cross Section

In the P_1 approximation, i.e., with $n = 0$ and 1, equation (2.82) gives

$$\frac{d\phi_1(x)}{dx} + (1 - c)\phi_0(x) = Q_0(x) \tag{2.83}$$

and

$$\frac{d\phi_0(x)}{dx} + 3(1 - cf_1)\phi_1(x) = 3Q_1(x). \tag{2.84}$$

Furthermore, if $Q_1(x)$ is zero, i.e., for an *isotropic or zero source*, equations (2.83) and (2.84) are identical with equations (2.64) and (2.65), respectively, except that $3\phi_1(x)$ in equation (2.65) is replaced by $3(1 - cf_1)\phi_1(x)$ in equation (2.84). As before, therefore, equations (2.83) and (2.84), for isotropic or zero source, are equivalent to simple (Fick's law) diffusion theory, except that

$$D = \frac{1}{3(1 - cf_1)}.$$

It is seen that $1 - cf_1$ is what is usually called the *transport cross section* and $1/(1 - cf_1)$ is the *transport mean free path*, with distances in units of the collision mean free path.

The physical significance of f_1 may be seen by writing out the expression for the average cosine of the scattering angle, $\bar{\mu}_0$; thus,

$$\bar{\mu}_0 = \frac{2\pi \int_{-1}^{1} \mu_0 f(\mu_0)\, d\mu_0}{2\pi \int_{-1}^{1} f(\mu_0)\, d\mu_0} = \frac{f_1}{f_0} = f_1,$$

since f_0 is normalized to unity. Thus, f_1 is equal to the mean cosine of the scattering angle in a collision. In a medium containing no fissile material, with $c < 1$, the mean cosine of the scattering angle may be designated $\bar{\mu}_{0s}$. Furthermore, in such a medium, $c = \sigma_s/\sigma$, where σ_s is the scattering cross section and σ is the collision (total) cross section; it follows, therefore, that

$$\sigma(1 - cf_1) = \sigma - \sigma_s\bar{\mu}_{0s} \equiv \sigma_{tr},$$

where σ_{tr} is the *transport cross section*. Hence, with distances in units of the collision mean free path, the diffusion coefficient derived above can be represented by

$$D = \frac{1}{3(\sigma - \sigma_s\bar{\mu}_{0s})} = \frac{1}{3\sigma_{tr}},$$

as commonly used in a modification of simple diffusion theory.

For a source-free medium, both Q_0 and Q_1 are zero; it follows then from equations (2.83) and (2.84) that

$$\frac{d^2\phi_0}{dx^2} - 3(1 - c)(1 - cf_1)\phi_0 = 0$$

or, since $1 - c$ is equivalent to σ_a,

$$\frac{d^2\phi_0}{dx^2} - 3\sigma_a\sigma_{tr}\phi_0 = 0.$$

The solution to this (diffusion) equation is of the form $e^{\pm x/L}$, where the relaxation (diffusion) length L is given by

$$L = \frac{1}{\sqrt{3\sigma_a\sigma_{tr}}}$$

or, in the original notation,

$$L = \frac{1}{\sqrt{3(1 - c)(1 - cf_1)}}. \tag{2.85}$$

For isotropic scattering, f_1 is zero, and this reduces to the diffusion theory result given earlier. A more exact calculation of the relaxation length will be developed shortly.

It has thus been shown that the P_1 approximation to the one-speed transport theory is equivalent to ordinary diffusion theory in a source free medium, regardless of whether the scattering is anisotropic, as considered here, or isotropic, as mentioned earlier. In multigroup theory, however, scattering from higher groups constitutes an anisotropic source and then diffusion theory and the P_1 approximation are not equivalent.

It should be noted that in P_1 theory, with an isotropic source, the anisotropic scattering enters only in determining f_1 and thus the transport cross section. Consequently, in the P_1 approximation, anisotropic scattering could be treated as being isotropic but with a cross section reduced by the factor $1 - \bar{\mu}_0$. This result suggests that in more general transport problems, even when P_1 theory is not used, it may be a reasonable approximation to replace anisotropic scattering by isotropic scattering with a cross section reduced by $1 - \bar{\mu}_0$. In one-speed theory this procedure is known as the *transport approximation* and it has been found to be quite accurate in many applications.[48] (See also §5.4b.)

2.6c The Asymptotic Relaxation Length

Exact values of the asymptotic relaxation length can be obtained from equation (2.79) by trying solutions of the form

$$\Phi(x, \mu) = e^{-x/\nu}\psi(\nu, \mu), \tag{2.86}$$

so that for $\nu \neq 0$ and $Q = 0$, equation (2.79) becomes

$$(\nu - \mu)\psi(\nu, \mu) = \frac{c\nu}{2} \sum_{l=0}^{L} (2l + 1) f_l P_l(\mu) \psi_l(\nu) \tag{2.87}$$

with

$$\psi_l(\nu) = \int_{-1}^{1} \psi(\nu, \mu) P_l(\mu)\, d\mu.$$

It is assumed here that the scattering expansion may be terminated after $L + 1$ terms.*

Since asymptotic solutions are being sought, it will be postulated, as in the method of separation of variables for isotropic scattering (§2.2b), that ν is not in the interval $-1 \leqslant \nu \leqslant 1$. If equation (2.87) is now divided by $\nu - \mu$ and multiplied by $\int_{-1}^{1} P_m(\mu)\, d\mu$, a series of equations connecting the $\psi_m(\nu)$ values is found to be

$$\psi_m(\nu) = \frac{c}{2} \sum_{l=0}^{L} (2l + 1) f_l \psi_l(\nu) \int_{-1}^{1} \frac{P_l(\mu') P_m(\mu')}{1 - \mu'/\nu}\, d\mu' \qquad m = 0, 1, 2, \ldots. \tag{2.88}$$

The first $L + 1$ of these equations give $L + 1$ equations in $L + 1$ unknowns; hence, the determinants of the coefficients must be zero, i.e.,

$$\left| \delta_{lm} - \frac{c}{2} (2l + 1) f_l \int_{-1}^{1} \frac{P_l(\mu') P_m(\mu')}{1 - \mu'/\nu}\, d\mu' \right| = 0, \tag{2.89}$$

where δ_{lm} is the Kronecker data, i.e., 1 when $l = m$, otherwise zero. For $c = 1$, the determinant in equation (2.89) is satisfied by $\nu = \pm\infty$, and for c near to unity, ν will be large. The quantity $1/(1 - \mu'/\nu)$ may then be expanded in a power series and the determinant can be written as

$$\begin{vmatrix} 1 - c\left(1 + \frac{1}{3\nu^2} + \cdots\right) & f_1 \frac{c}{\nu}\left(1 + \frac{3}{5\nu^2} + \cdots\right) & -\frac{2}{3} f_2 \frac{c}{\nu^2}\left(1 + \frac{6}{7\nu^2} + \cdots\right) & \cdots \\ \frac{1}{3}\frac{c}{\nu}\left(1 + \frac{3}{5\nu^2} + \cdots\right) & 1 - f_1 c\left(1 + \frac{3}{5\nu^2} + \cdots\right) & \frac{2}{3} f_2 \frac{c}{\nu}\left(1 + \frac{6}{7\nu^2} + \cdots\right) & \cdots \\ -\frac{2}{15}\frac{c}{\nu^2}\left(1 + \frac{6}{7\nu^2} + \cdots\right) & \frac{2}{5} f_1 \frac{c}{\nu}\left(1 + \frac{6}{7\nu^2} + \cdots\right) & 1 - f_2 c\left(1 + \frac{11}{21\nu^2} + \cdots\right) & \cdots \\ \cdots & \cdots & \cdots & \cdots \end{vmatrix} = 0$$

Since solutions are being sought for large values of ν, the terms far from the main diagonal may be ignored. Furthermore, the term in the expansion of the

* Note that L in equation (2.87) is the limiting value of l, and not the diffusion length of the preceding section.

determinant that arises from the product of the diagonal elements is given approximately by

$$\text{Product of diagonal elements} \approx (1 - c)\prod_{i=1}(1 - f_i c).$$

All other terms in the expansion are of the order of $1/\nu^2$ or smaller, and therefore the diagonal term must also be of the order of $1/\nu^2$ or smaller if the determinant is to vanish. In fact for $1 - c \ll 1$, the first factor, namely $1 - c$, is small, and it will be smaller than any other factor, since $f_i < 1$. Hence, the first element of the determinant must be of order $1/\nu^2$ and the largest terms in the determinant, i.e., $O(1/\nu^2)$, are found by multiplying the diagonal elements, except for the first two, by the subdeterminant

$$\begin{vmatrix} 1 - c - \dfrac{c}{3\nu_0^2} & f_1\dfrac{c}{\nu_0} \\ \dfrac{c}{3\nu_0} & 1 - f_1 c \end{vmatrix} = 0,$$

which must be zero if the full determinant is zero. It follows, therefore, that

$$\nu_0 = \frac{1}{\sqrt{3(1 - c)(1 - cf_1)}}[1 + O(1 - c)]. \tag{2.90}$$

When $1 - c \ll 1$ the quantity in the brackets is close to unity, and the result is equal to the relaxation length, given by equation (2.85), derived from the P_1 approximation.

Better approximations to the asymptotic relaxation length can be obtained by the use of the full determinant. This treatment also leads to additional roots of the determinant and thus to additional discrete eigenvalues ν.[49] Further discussion of the asymptotic relaxation length is given in Ref. 50.

2.6d General Solution by Separation of Variables

The general nature of the solution of the one-speed transport equation with anisotropic scattering may be found by multiplying equation (2.87) by $\int_{-1}^{1} P_m(\mu)\,d\mu$, as before, but not dividing by $\nu - \mu$. In this way a recursion relation between the various values of ψ_m is obtained,[51] namely,

$$(2m + 1)\nu(1 - cf_m)\psi_m(\nu) - (m + 1)\psi_{m+1}(\nu) - m\psi_{m-1}(\nu) = 0. \tag{2.91}$$

If $\psi_0(\nu)$ is normalized so that

$$\psi_0(\nu) = 1,$$

forms of equation (2.91) are

$$\psi_1(\nu) = \nu(1 - c)$$
$$\psi_2(\nu) = \tfrac{3}{2}\nu^2(1 - cf_1)(1 - c) - \tfrac{1}{2}$$

and so on. Since the $\psi_m(\nu)$ have been found in this manner, equation (2.87) may be used to write

$$\psi(\nu, \mu) = \frac{c}{2} \mathrm{P} \frac{\nu}{\nu - \mu} \sum_{l=1}^{L} (2l + 1) f_l P_l(\mu) \psi_l(\nu) + \lambda(\nu)\delta(\mu - \nu) \qquad (2.92)$$

by analogy with equation (2.26) for isotropic scattering.

The discrete eigenvalues ν of equation (2.92) may be found by integrating over μ and setting the result equal to unity. Solutions have been obtained for some special cases. The singular eigenfunctions have been examined and the completeness of the discrete plus singular eigenfunctions has been established.[52]

In general, it is seen that by expanding the scattering cross sections in Legendre polynomials, the solution to the one-speed transport equation for anisotropic scattering can be obtained by the separation of variables in much the same way as it is for isotropic scattering.

2.7 RECIPROCITY RELATIONS

2.7a Derivation of the General Relation

The flux of neutrons at a point $\mathbf{r}_2$ due to a source at $\mathbf{r}_1$ can be related to the flux at $\mathbf{r}_1$ due to a source at $\mathbf{r}_2$ by means of the one-speed transport equation. Such *reciprocity relations*, as they are called, are frequently useful in relating the solution of a particular problem to that of a simpler problem or to one for which the solution is known. The only assumption made is the same as that in §2.6a, namely, that the scattering function $f(\mathbf{r}; \boldsymbol{\Omega}' \to \boldsymbol{\Omega})$ depends only on the scattering angle, and so is a function of $\boldsymbol{\Omega} \cdot \boldsymbol{\Omega}' = \mu_0$. Actually, a slightly less stringent assumption, that $f(\mathbf{r}; \boldsymbol{\Omega}' \to \boldsymbol{\Omega}) = f(\mathbf{r}; -\boldsymbol{\Omega} \to -\boldsymbol{\Omega}')$, would be adequate here. In energy-dependent or multigroup problems similar reciprocity relations exist but, except for neutron thermalization (Chapter 7), they involve solutions of adjoint equations (see Chapter 6).

Consider neutron transport in a region bounded by a convex surface. In this section, it will be convenient to allow a boundary condition of a *specified* incoming flux, rather than zero incoming flux, i.e., free-surface conditions, thereby departing from the usual procedure of replacing an incoming flux by a surface source plus a free surface. In Case A, let the source be $Q_1(\mathbf{r}, \boldsymbol{\Omega})$ and the angular flux $\Phi_1(\mathbf{r}, \boldsymbol{\Omega})$; the boundary conditions are represented by $\Phi_{\mathrm{inc},1}(\mathbf{r}, \boldsymbol{\Omega})$, where $\mathbf{r}$ represents a position on the boundary, and $\hat{\mathbf{n}} \cdot \boldsymbol{\Omega} < 0$, where $\hat{\mathbf{n}}$ is a unit vector in the direction outward normal to the surface (§1.1d). Similarly, in Case B, the source, flux, and boundary conditions, for the same surface, are $Q_2(\mathbf{r}, \boldsymbol{\Omega})$, $\Phi_2(\mathbf{r}, \boldsymbol{\Omega})$, and $\Phi_{\mathrm{inc},2}$ for $\hat{\mathbf{n}} \cdot \boldsymbol{\Omega} < 0$, respectively. The functions Φ_{inc} are assumed to be known.

Since the scattering function is assumed to depend only on the scattering

angle, $f(\mathbf{r}; \Omega' \to \Omega)$ may be replaced by $f(\mathbf{r}, \Omega \cdot \Omega')$. Hence, for $\Phi_1(\mathbf{r}, \Omega)$, the one-speed, time-independent transport equation (2.3) can be written as

$$\Omega \cdot \nabla \Phi_1(\mathbf{r}, \Omega) + \sigma(\mathbf{r})\Phi_1(\mathbf{r}, \Omega) = \sigma(\mathbf{r})c(\mathbf{r}) \int f(\mathbf{r}, \Omega \cdot \Omega')\Phi_1(\mathbf{r}, \Omega')\, d\Omega' + Q_1(\mathbf{r}, \Omega) \tag{2.93}$$

with $\Phi_1(\mathbf{r}, \Omega) = \Phi_{\text{inc},1}(\mathbf{r}, \Omega)$ if $\mathbf{r}$ is on the bounding surface and $\hat{\mathbf{n}} \cdot \Omega < 0$. Although σ, c, and f are functions of $\mathbf{r}$, this dependence will not be included specifically in the subsequent discussion. The corresponding equation for $\Phi_2(\mathbf{r}, \Omega)$ is

$$\Omega \cdot \nabla \Phi_2(\mathbf{r}, \Omega) + \sigma\Phi_2(\mathbf{r}, \Omega) = \sigma c \int f(\Omega \cdot \Omega')\Phi_2(\mathbf{r}, \Omega')\, d\Omega' + Q_2(\mathbf{r}, \Omega), \tag{2.94}$$

with $\Phi_2(\mathbf{r}, \Omega) = \Phi_{\text{inc},2}(\mathbf{r}, \Omega)$ for $\mathbf{r}$ on the boundary and $\hat{\mathbf{n}} \cdot \Omega < 0$. It has been shown that the source and boundary conditions in equation (2.93) and (2.94) uniquely determine the solutions[53] when $c(\mathbf{r}) < 1$, and this is assumed to be true for any subcritical system.

Suppose that in equation (2.94) and its boundary condition, the signs of Ω and Ω' are changed. This will leave the f term unaffected and integration over all directions Ω' will still be over all directions. Consequently, equation (2.94) may be written

$$-\Omega \cdot \nabla \Phi_2(\mathbf{r}, -\Omega) + \sigma\Phi_2(\mathbf{r}, -\Omega) = \sigma c \int f(\Omega \cdot \Omega')\Phi_2(\mathbf{r}, -\Omega')\, d\Omega' + Q_2(\mathbf{r}, -\Omega). \tag{2.95}$$

Equation (2.93) is now multiplied by $\Phi_2(\mathbf{r}, -\Omega)$ and equation (2.95) by $\Phi_1(\mathbf{r}, \Omega)$, and the expressions obtained are subtracted. The result is next integrated over all angles and over the whole volume under consideration; the terms involving σ and σc then cancel.

The two gradient terms in the integral, namely,

$$\iint [\Phi_2(\mathbf{r}, -\Omega)\Omega \cdot \nabla \Phi_1(\mathbf{r}, \Omega) + \Phi_1(\mathbf{r}, \Omega)\Omega \cdot \nabla \Phi_2(\mathbf{r}, -\Omega)]\, dV\, d\Omega$$

may be combined, by noting that $\Omega \cdot \nabla \Phi = \nabla \cdot \Omega\Phi$, to yield

$$\iint \nabla \cdot \Omega\Phi_1(\mathbf{r}, \Omega)\Phi_2(\mathbf{r}, -\Omega)\, dV\, d\Omega.$$

Then by using the divergence theorem, this volume integral may be converted to a surface integral and the result obtained is

$$\int d\Omega \int dV \nabla \cdot \Omega\Phi_1(\mathbf{r}, \Omega)\Phi_2(\mathbf{r}, -\Omega) = \int d\Omega \int_A dA\, \hat{\mathbf{n}} \cdot \Omega\Phi_1(\mathbf{r}, \Omega)\Phi_2(\mathbf{r}, -\Omega),$$

where dV is a volume element and dA is an element of surface on the boundary represented by A.

If this relationship is used, the integration referred to in the last paragraph but one can be expressed as

$$\iint \hat{\mathbf{n}}\cdot\boldsymbol{\Omega}\Phi_1(\mathbf{r},\boldsymbol{\Omega})\Phi_2(\mathbf{r},-\boldsymbol{\Omega})\,d\boldsymbol{\Omega}\,dA$$

$$= \iint [Q_1(\mathbf{r},\boldsymbol{\Omega})\Phi_2(\mathbf{r},-\boldsymbol{\Omega}) - Q_2(\mathbf{r},-\boldsymbol{\Omega})\Phi_1(\mathbf{r},\boldsymbol{\Omega})]\,d\boldsymbol{\Omega}\,dV. \quad (2.96)$$

On the left-hand side, the angular integration may be divided into two parts, one for which $\hat{\mathbf{n}}\cdot\boldsymbol{\Omega} < 0$ and the other for $\hat{\mathbf{n}}\cdot\boldsymbol{\Omega} > 0$. Thus,

$$\text{Left side of equation (2.96)} = \iint_{\hat{\mathbf{n}}\cdot\boldsymbol{\Omega}<0} \hat{\mathbf{n}}\cdot\boldsymbol{\Omega}\Phi_1(\mathbf{r},\boldsymbol{\Omega})\Phi_2(\mathbf{r},-\boldsymbol{\Omega})\,d\boldsymbol{\Omega}\,dA$$

$$+ \iint_{\hat{\mathbf{n}}\cdot\boldsymbol{\Omega}>0} \hat{\mathbf{n}}\cdot\boldsymbol{\Omega}\Phi_1(\mathbf{r},\boldsymbol{\Omega})\Phi_2(\mathbf{r},-\boldsymbol{\Omega})\,d\boldsymbol{\Omega}\,dA.$$

In the first of these integrals, represented by I_1, it is seen that $\hat{\mathbf{n}}\cdot\boldsymbol{\Omega} < 0$ and Φ_1 is the boundary value $\Phi_{\text{inc},1}$; hence,

$$I_1 = -\iint_{\hat{\mathbf{n}}\cdot\boldsymbol{\Omega}<0} |\hat{\mathbf{n}}\cdot\boldsymbol{\Omega}|\Phi_{\text{inc},1}(\mathbf{r},\boldsymbol{\Omega})\Phi_2(\mathbf{r},-\boldsymbol{\Omega})\,d\boldsymbol{\Omega}\,dA.$$

In the second integral, I_2, the variable may be changed from $\boldsymbol{\Omega}$ to $-\boldsymbol{\Omega}$, so that the integral is now over $\hat{\mathbf{n}}\cdot\boldsymbol{\Omega} < 0$, and Φ_2 is the boundary value $\Phi_{\text{inc},2}$; thus,

$$I_2 = \iint_{\hat{\mathbf{n}}\cdot\boldsymbol{\Omega}<0} |\hat{\mathbf{n}}\cdot\boldsymbol{\Omega}|\Phi_1(\mathbf{r},-\boldsymbol{\Omega})\Phi_{\text{inc},2}(\mathbf{r},\boldsymbol{\Omega})\,d\boldsymbol{\Omega}\,dA.$$

The left side of equation (2.96) is then obtained by summing I_1 and I_2; consequently, this equation may be written as

$$\iint_{\hat{\mathbf{n}}\cdot\boldsymbol{\Omega}<0} |\hat{\mathbf{n}}\cdot\boldsymbol{\Omega}|[\Phi_1(\mathbf{r},-\boldsymbol{\Omega})\Phi_{\text{inc},2}(\mathbf{r},\boldsymbol{\Omega}) - \Phi_{\text{inc},1}(\mathbf{r},\boldsymbol{\Omega})\Phi_2(\mathbf{r},-\boldsymbol{\Omega})]\,d\boldsymbol{\Omega}\,dA$$

$$= \iint [Q_1(\mathbf{r},\boldsymbol{\Omega})\Phi_2(\mathbf{r},-\boldsymbol{\Omega}) - Q_2(\mathbf{r},-\boldsymbol{\Omega})\Phi_1(\mathbf{r},\boldsymbol{\Omega})]\,d\boldsymbol{\Omega}\,dV, \quad (2.97)$$

which is the desired reciprocity relation in a general form. A number of special forms of this equation are of interest.

2.7b Applications of the Reciprocity Relation

(i) Suppose there are no incoming neutrons in either Case A or Case B; then $\Phi_{\text{inc},1} = \Phi_{\text{inc},2} = 0$. Consequently, it follows from equation (2.97) that

$$\iint Q_1(\mathbf{r},\boldsymbol{\Omega})\Phi_2(\mathbf{r},-\boldsymbol{\Omega})\,d\boldsymbol{\Omega}\,dV = \iint Q_2(\mathbf{r}_2,-\boldsymbol{\Omega})\Phi_1(\mathbf{r},\boldsymbol{\Omega})\,d\boldsymbol{\Omega}\,dV. \quad (2.98)$$

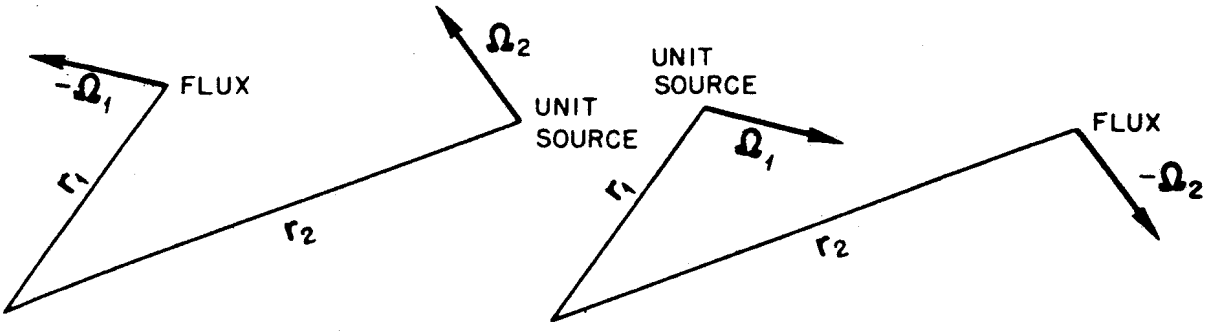

FIG. 2.8 REPRESENTATION OF OPTICAL RECIPROCITY THEOREM; THE TWO FLUXES ARE EQUAL.

Furthermore, if in Case A the source is a point source at $\mathbf{r}_1$ with direction $\boldsymbol{\Omega}_1$, then

$$Q_1(\mathbf{r}, \boldsymbol{\Omega}) = \delta(\mathbf{r} - \mathbf{r}_1)\delta(\boldsymbol{\Omega} - \boldsymbol{\Omega}_1),$$

and if in Case B the point source is at $\mathbf{r}_2$ with direction $\boldsymbol{\Omega}_2$,

$$Q_2(\mathbf{r}, \boldsymbol{\Omega}) = \delta(\mathbf{r} - \mathbf{r}_2)\delta(\boldsymbol{\Omega} - \boldsymbol{\Omega}_2).$$

If the flux at $\mathbf{r}$, $\boldsymbol{\Omega}$ due to the point source in Case A is represented by the Green's function $G(\mathbf{r}_1, \boldsymbol{\Omega}_1 \rightarrow \mathbf{r}, \boldsymbol{\Omega})$, with analogous symbols for other cases, it follows from equation (2.98) that

$$G(\mathbf{r}_2, \boldsymbol{\Omega}_2 \rightarrow \mathbf{r}_1, -\boldsymbol{\Omega}_1) = G(\mathbf{r}_1, \boldsymbol{\Omega}_1 \rightarrow \mathbf{r}_2, -\boldsymbol{\Omega}_2). \tag{2.99}$$

This equation states that the angular flux at $\mathbf{r}_1$ in the direction $-\boldsymbol{\Omega}_1$, due to a unit source at $\mathbf{r}_2$ in direction $\boldsymbol{\Omega}_2$ is equal to the flux at $\mathbf{r}_2$ in direction $-\boldsymbol{\Omega}_2$, due to a unit source at $\mathbf{r}_1$ in direction $\boldsymbol{\Omega}_1$. Thus, according to equation (2.99), in one-speed theory the angular flux is the same in the two situations depicted in Fig. 2.8. The relation in the form of equation (2.99) is frequently referred to as the *optical reciprocity theorem*, because of its similarity to a theorem in optics.

If the point sources are isotropic, a similar relation applies to the total flux. Thus, for isotropic sources

$$Q_1 = \frac{1}{4\pi}\delta(\mathbf{r} - \mathbf{r}_1) \quad \text{and} \quad Q_2 = \frac{1}{4\pi}\delta(\mathbf{r} - \mathbf{r}_2),$$

and if $G(\mathbf{r}_1 \rightarrow \mathbf{r}_2)$ represents the total flux at $\mathbf{r}_2$ due to an isotropic unit source at $\mathbf{r}_1$, it follows from equation (2.98) that

$$G(\mathbf{r}_1 \rightarrow \mathbf{r}_2) = G(\mathbf{r}_2 \rightarrow \mathbf{r}_1).$$

(ii) Suppose, again, that there are no incoming neutrons, and that the volume under consideration is divided into two separate regions (Fig. 2.9) with volumes V_1 and V_2. A practical situation of this type might be a fuel element and the moderator of a heterogeneous reactor. For the present, however, a completely general case will be considered. Let Q_1 be an isotropic source of intensity

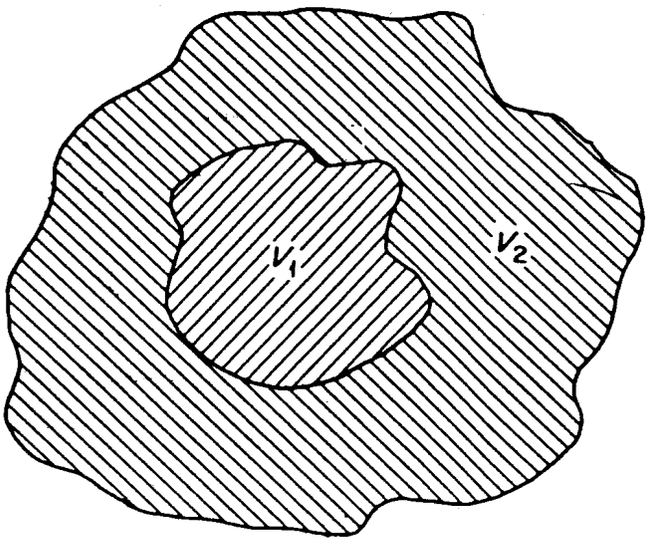

FIG. 2.9 VOLUME DIVIDED INTO TWO SEPARATE REGIONS.

$1/4\pi V_1$ in V_1 and zero in V_2, and let Q_2 be an isotropic source of intensity $1/4\pi V_2$ in V_2 and zero in V_1. Thus, Q_1 is a uniform source emitting 1 neutron/sec in the volume V_1 and Q_2 is a uniform source emitting 1 neutron/sec in V_2. Equation (2.98) then reduces to

$$\frac{1}{V_1}\int_{V_1}\phi_2(\mathbf{r})\,dV = \frac{1}{V_2}\int_{V_2}\phi_1(\mathbf{r})\,dV. \tag{2.100}$$

Let the neutron absorption cross section in V_1 have the constant value σ_1, whereas that in V_2 has the constant value σ_2. Then the rate of neutron absorption in V_1 due to a uniform unit source in V_2 is also the probability that a neutron produced uniformly in V_2 will be absorbed in V_1. This is represented by $P_{2\to1}$ and is given by

Rate of neutron absorption in V_1 due to unit source in V_2

$$= \sigma_1\int_{V_1}\phi_2(\mathbf{r})\,dV \equiv P_{2\to1}.$$

The quantity $P_{1\to2}$ may be defined in a similar manner and hence it follows from equation (2.100) that

$$\sigma_2 V_2 P_{2\to1} = \sigma_1 V_1 P_{1\to2}. \tag{2.101}$$

In the next section, and also in Chapter 8, it will be seen that this relationship is useful in treating heterogeneous media. It is important to note that there is no restriction on the geometrical forms of the regions V_1 and V_2; some possibilities are indicated in Fig. 2.10. The regions need not be convex, since they can always be surrounded by a convex free surface so that equation (2.97) can be applied.

The reciprocity relation between region 1, e.g., a fuel lump, and region 2, e.g., surrounding moderator, may be understood by the following heuristic argument. Suppose that all space is filled with a uniform and isotropic flux. Then no

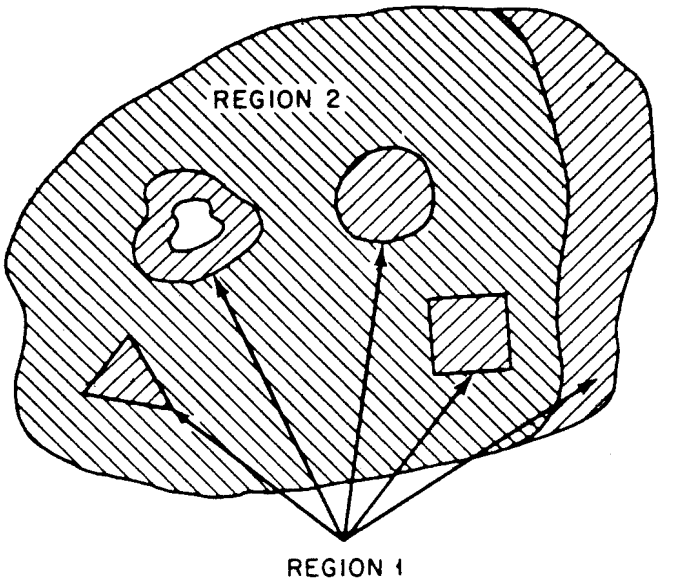

FIG. 2.10 POSSIBLE SHAPES OF TWO REGIONS.

net current will flow between the two regions. Such a situation would be realized by a source which will precisely balance the absorption in each region, i.e., $\sigma_1/4\pi$ in region 1 and $\sigma_2/4\pi$ in region 2. Then $\sigma_2 V_2 P_{2\to 1}$ is the flow of neutrons from 2 to 1 which must be exactly balanced by the flow $\sigma_1 V_1 P_{1\to 2}$ in the opposite direction from 1 to 2. The general derivation given above is, of course, more precise and shows that the result is independent of the geometry of the system. In practice, V_1 is usually a more-or-less periodic array of fuel elements in the moderator V_2, and the general reciprocity relation is still applicable (§2.8c).

(iii) A third example of interest is that in which in Case A there is an incoming boundary flux $\Phi_{\text{inc},1}$ but no source and in Case B there is a uniform source $Q_2(\mathbf{r}, \Omega) = 1$ throughout the volume but $\Phi_{\text{inc},2} = 0$. Equation (2.97) then becomes

$$\iint_{\hat{\mathbf{n}}\cdot\hat{\Omega}<0} |\hat{\mathbf{n}}\cdot\Omega|\,\Phi_{\text{inc},1}(\mathbf{r}, \Omega)\Phi_2(\mathbf{r}, -\Omega)\,d\Omega\,dA = \int \phi_1(\mathbf{r})\,dV. \tag{2.102}$$

Case A is here related to an albedo problem and Case B to a problem in escape probability. For example, suppose that in Case A there is incident on a planar surface at $x = 0$ a unit flux in the direction μ_0 (Fig. 2.11A); then

$$\Phi_{\text{inc},1}(\mathbf{r}, \Omega) = \frac{1}{2\pi}\,\delta(\mu - \mu_0).$$

In the albedo problem, it is required to determine the probability of neutron reflection from the surface. Equation (2.102) then becomes

$$\mu_0\Phi_2(0, -\mu_0) = \int_0^\infty \phi_1(x)\,dx. \tag{2.103}$$

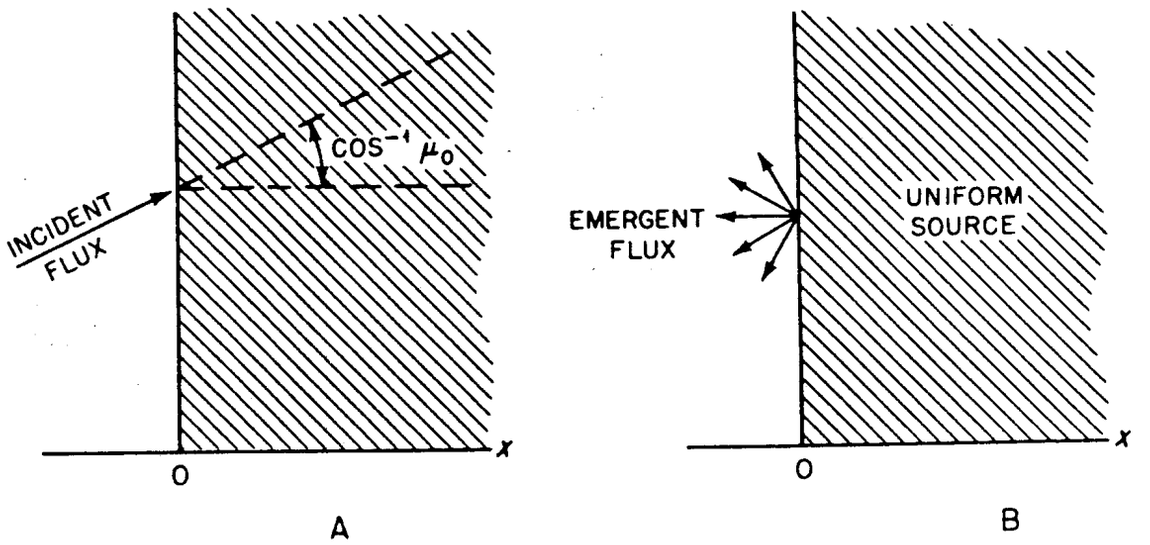

FIG. 2.11 ALBEDO AND ESCAPE PROBABILITY PROBLEMS.

The right side of equation (2.103) multiplied by the absorption cross section is clearly the rate at which the neutrons are absorbed. Case B (Fig. 2.11B) is equivalent to the half-space problem with a uniform source. If the angular dependence of the emergent angular distribution from this source, i.e., $\Phi_2(\mathbf{r}, -\mathbf{\Omega}) = \Phi(0, \mu)$ at the boundary, is known, then the solution of the albedo problem is obtained from equation (2.103).

If $\Phi_{\text{inc},1}$ in the situation described by equation (2.102) is isotropic and equal in magnitude to $1/\pi A$, where A is the total area of the surface under consideration, then 1 neutron/sec is incident on the surface in Case A. Further, suppose Q_2 is $1/4\pi V$, where V is the volume, so that 1 neutron sec is produced uniformly and isotropically in Case B. Then, from equation (2.102)

$$\frac{1}{A}\iint_{\hat{\mathbf{n}}\cdot\hat{\mathbf{\Omega}}>0} \hat{\mathbf{n}}\cdot\mathbf{\Omega}\Phi_2(\mathbf{r}, \mathbf{\Omega})\, d\mathbf{\Omega}\, dA = \frac{1}{4V}\int \phi_1(\mathbf{r})\, dA. \tag{2.104}$$

The integral on the left side represents the number of neutrons per second crossing the surface and is, therefore, the escape probability, P_{esc}, i.e., the probability that neutrons born uniformly and isotropically in a volume will escape without making a collision. For constant absorption cross section, the integral on the right side of equation (2.102) is the neutron absorption rate in Case A divided by the cross section; this quantity is denoted by P_{abs}/σ, where P_{abs} is the probability that a random incident neutron will be absorbed and σ is the constant absorption cross section. Consequently, equation (2.104) leads to

$$P_{\text{abs}} = \frac{4V\sigma}{A} P_{\text{esc}}, \tag{2.105}$$

which will be used later.

The foregoing treatment has been concerned with the one-speed transport equation. It will be seen in Chapter 6 how the relations obtained here can be

generalized to energy-dependent problems by the use of adjoint functions. It may be noted, however, that if neutrons of a single energy are considered in an energy-dependent problem, any process which removes neutrons from that energy group can be treated as an absorption. The relations derived above then hold with the energy present as a parameter which determines the cross section and sources. In this sense, the results obtained will be found useful in connection with resonance absorption problems (see Chapter 8).

2.8 COLLISION PROBABILITIES

2.8a Introduction

Diffusion theory (or other P_N approximation of low order) fails whenever the angular dependence of the flux is complicated or varies rapidly over angle (μ) or distance (x): this is especially the case, as has been seen, near localized sources and boundaries or in strongly absorbing media ($c \ll 1$). Instead of utilizing approximations of higher order in such situations, some special methods based on the use of collision probabilities in purely absorbing media are frequently useful.[54]

Consider a common situation in which reactor fuel, localized in the form of lumps, e.g., rods, is surrounded by moderator. It is then sometimes useful to formulate the problem in terms of the probability that a neutron which appears in some region makes its next collision in that region. In a lattice structure, for example, fission neutrons may be born more-or-less uniformly in a fuel rod; then, for the computation of the fast multiplication, it is required to determine the probability that these neutrons will undergo collisions in the rod before escaping. The neutrons which escape will be slowed down in the moderator, and for calculating resonance absorption the probability may be determined that the moderated neutrons will make their next collision in the fuel (see Chapter 8). Collision probabilities have also been incorporated in a widely used diffusion theory calculation involving thermal neutrons.[55]

In the typical one-speed collision probability calculation, the space is considered to be divided into a finite number of regions and it is assumed that neutrons are produced uniformly and isotropically in one of these regions. The problem is then to determine the probability that neutrons make their next collision in the source region or in one of the other regions. Frequently, there are only two regions, namely, fuel and moderator. Some general methods are presented below for calculating collision probabilities which are often used in conjunction with the reciprocity relations derived above in the treatment of heterogeneous media.

2.8b Escape Probabilities: The Chord Method

Suppose neutrons are generated isotropically and uniformly in a convex region of volume V containing material of constant (total) cross section σ. Now, consider a neutron which is produced at position $\mathbf{r}$ with direction Ω. If $R(\mathbf{r}, \Omega)$ is the

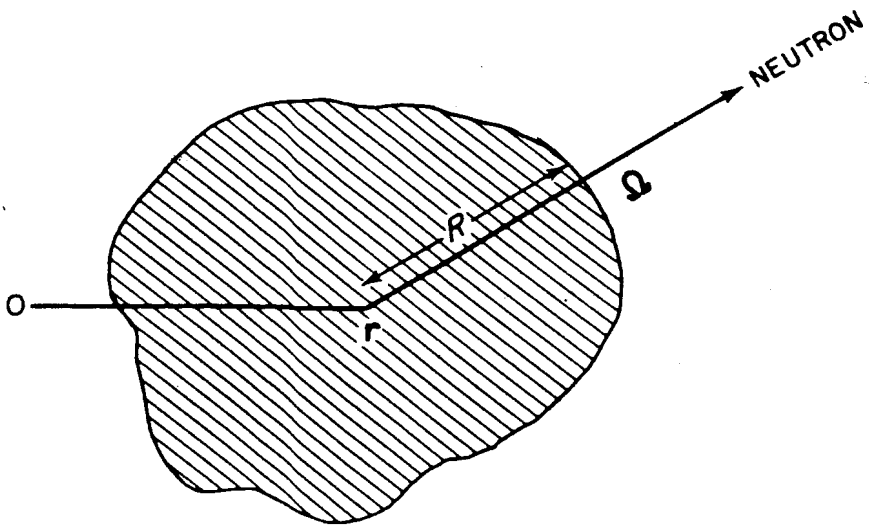

FIG. 2.12 CALCULATION OF ESCAPE PROBABILITY.

distance from this point to the boundary of the region (Fig. 2.12) in the direction Ω, the probability that the neutron will escape from the region without making a collision is

$$\text{Probability of escape} = e^{-\sigma R(\mathbf{r},\Omega)}.$$

But with a uniform and isotropic source, the probability that a neutron will be generated in the direction $d\Omega$ about Ω and position in the volume element dV about $\mathbf{r}$ is

$$\text{Probability of generation} = \frac{d\Omega}{4\pi}\frac{dV}{V}.$$

The escape probability P_{esc} for neutrons born in the whole volume V is obtained by integrating the product of the two probabilities derived above over all directions and volume; thus,

$$P_{esc} = \frac{1}{4\pi V}\int\int e^{-\sigma R(\mathbf{r},\Omega)}\, d\Omega\, dV. \tag{2.106}$$

For the evaluation of this expression, the volume V is divided into tubes parallel to a fixed direction Ω (Fig. 2.13); a typical tube then has a length R_s and a cross-sectional area $(\hat{\mathbf{n}}\cdot\Omega)\, dA$, so that

$$dV = (\hat{\mathbf{n}}\cdot\Omega)\, dA\, dR,$$

with $\hat{\mathbf{n}}\cdot\Omega > 0$. Consequently, equation (2.106) may be integrated over R to yield

$$P_{esc} = \frac{1}{4\pi\sigma V}\int\int_{\hat{\mathbf{n}}\cdot\Omega>0} \hat{\mathbf{n}}\cdot\Omega(1 - e^{-\sigma R_s})\, d\Omega\, dA. \tag{2.107}$$

If the dimensions of the body are large compared with the neutron mean free

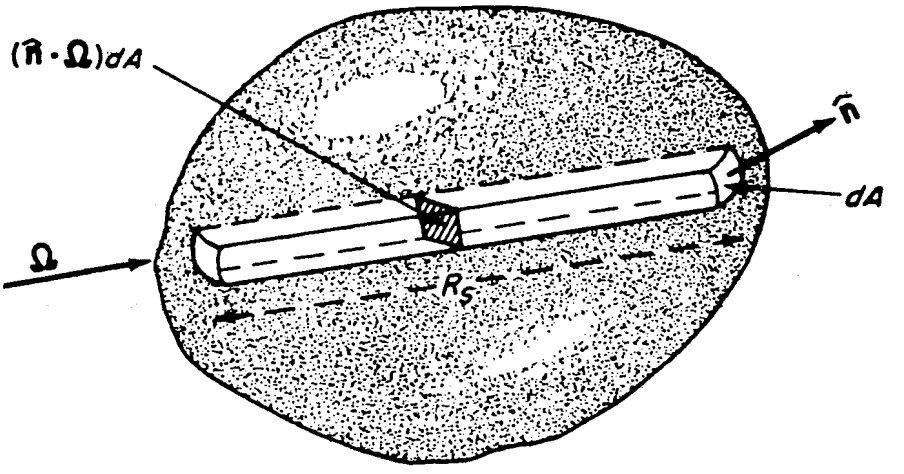

FIG. 2.13 VOLUME DIVIDED INTO PARALLEL TUBES.

path, $1/\sigma$, the exponential term can be set equal to zero, and the integral is simply

$$\iint_{\hat{\mathbf{n}}\cdot\Omega>0} \hat{\mathbf{n}}\cdot\Omega\, d\Omega\, dA = \pi A,$$

where A is the total surface area. Consequently, equation (2.107) becomes

$$P_{\text{esc}} = \frac{A}{4\sigma V} \tag{2.108}$$

for bodies with dimensions that are large relative to a mean free path. Numerically, $A/4\sigma V$ is equal to the fraction of neutrons generated within a quarter of a mean free path, i.e., $1/4\sigma$, of the surface. It is, therefore, as if all neutrons born within a quarter mean free path of the surface escape.

Equation (2.108) can be derived in a simple manner by assuming that, on the scale of a mean free path, the surface of a "large" body can be treated as a plane. Consider, therefore, an infinite half-space and a plane boundary (Fig. 2.14). The half-space contains a uniform source Q_0 per unit volume, i.e., $Q_0/4\pi$ per unit solid angle per unit volume. A neutron born at O at a distance x from the surface and directed at an angle θ to the x coordinate, where $\mu = \cos\theta$, will have a probability $e^{-\sigma x/\mu}$ of escaping without making a collision. The total number of neutrons escaping per unit area can be found by integrating over μ for $0 \leqslant \mu \leqslant 1$ and over x from $0 \leqslant x \leqslant \infty$; hence

$$\begin{aligned}\text{Number of neutrons escaping per unit area} &= \frac{Q_0}{4\pi}\left[2\pi\int_0^1\int_0^\infty e^{-\sigma x/\mu}\,dx\,d\mu\right] \\ &= \frac{Q_0}{4\sigma}.\end{aligned}$$

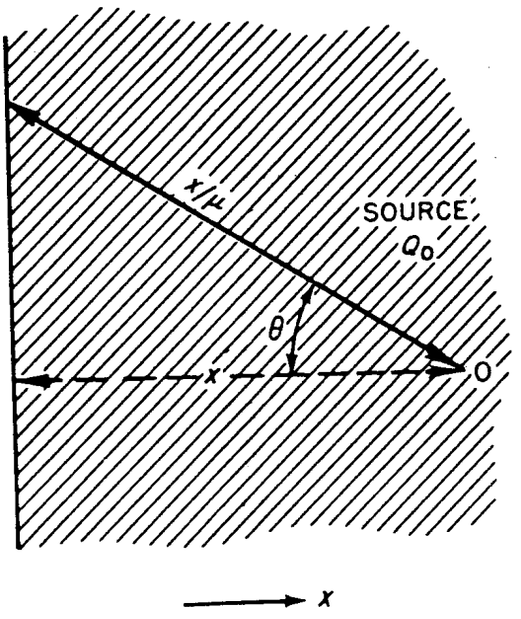

FIG. 2.14 INFINITE HALF-SPACE WITH UNIFORM SOURCE AND PLANE BOUNDARY.

The total number of neutrons escaping from the area A is then $Q_0 A/4\sigma$; the probability that a neutron will escape is thus $A/4\sigma V$, as in equation (2.108).

Since P_{esc} given by equation (2.108) applies to large bodies, whereas for small bodies P_{esc} must approach unity, a rational approximation proposed by E. P. Wigner[56] for bodies of all sizes is

$$P_{esc} \simeq \frac{1}{1 + 4\sigma V/A} \quad \text{(Wigner rational approximation).} \tag{2.109}$$

In Table 2.8,[57] this approximation is compared with the results of exact calculations for spheres and slabs and infinitely long cylinders; $\bar{R}$, which is defined below, is the average chord length, so that $\sigma\bar{R}$ is the average chord length expressed in mean free paths. It is seen that the Wigner rational approximation is in general too small, but it is frequently accurate enough to be useful. For example, it facilitates the treatment of resonance escape in heterogeneous systems (see Chapter 8).

The evaluation of P_{esc} from equation (2.107) has been carried out along the following lines.[58] Let chords be drawn from a surface element dA (Fig. 2.15) such that their number in direction Ω is proportional to $|\hat{\mathbf{n}}\cdot\Omega|$. Let $p(R)\,dR$ be the probability that the chord is of length between R and $R + dR$; then

$$p(R)\,dR = \frac{\iint_{R_s} |\hat{\mathbf{n}}\cdot\Omega|\,d\Omega\,dA}{\iint |\hat{\mathbf{n}}\cdot\Omega|\,d\Omega\,dA} \tag{2.110}$$

where R_s is between R and $R + dR$ and integration is restricted to $\hat{\mathbf{n}}\cdot\Omega > 0$.

TABLE 2.8. ESCAPE PROBABILITIES[57]

$\sigma\bar{R}$	*Sphere*	*Cylinder*	*Slab*	*Rational approximation*
0.04	0.978	0.974	0.952	0.962
0.1	0.946	0.939	0.902	0.909
0.2	0.896	0.885	0.837	0.823
0.3	0.850	0.819	0.785	0.769
0.5	0.767	0.753	0.701	0.667
1	0.607	0.596	0.557	0.500
2	0.411	0.407	0.390	0.333
3	0.302	0.302	0.295	0.250
5	0.193	0.193	0.193	0.167
10	0.099	0.099	0.100	0.091

The denominator, as before, is equal to πA. Furthermore, the average chord length, $\bar{R}$, is defined by

$$\bar{R} = \frac{\iint R|\hat{\mathbf{n}}\cdot\boldsymbol{\Omega}|\, d\boldsymbol{\Omega}\, dA}{\iint |\hat{\mathbf{n}}\cdot\boldsymbol{\Omega}|\, d\boldsymbol{\Omega}\, dA}. \tag{2.111}$$

The volume of each tube of length R (in Fig. 2.13) is equal to $R|\hat{\mathbf{n}}\cdot\boldsymbol{\Omega}|\, dA$; hence the total volume V is given by

$$\int R|\hat{\mathbf{n}}\cdot\boldsymbol{\Omega}|\, dA = V.$$

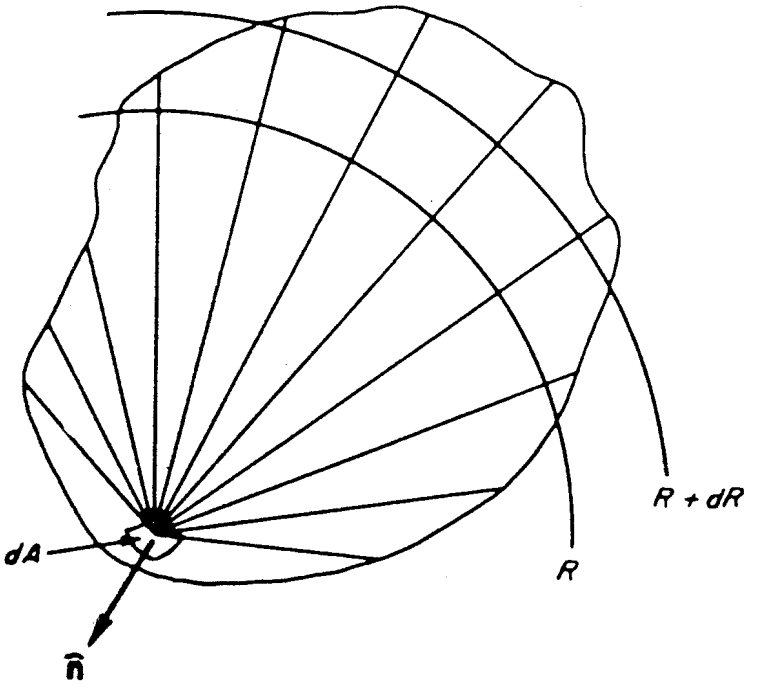

FIG. 2.15 CHORDS FROM SURFACE ELEMENT dA.

Consequently, equation (2.111) becomes

$$\bar{R} = \frac{4V}{A}. \tag{2.112}$$

Upon insertion of equations (2.110) and (2.112) into equation (2.107) the result is

$$P_{\text{esc}} = \frac{1}{\sigma \bar{R}} \int p(R)(1 - e^{-\sigma R})\, dR, \tag{2.113}$$

and the rational approximation equation (2.109) may be written

$$P_{\text{esc}} \simeq \frac{1}{1 + \sigma \bar{R}} \quad \text{(rational approximation)}. \tag{2.114}$$

For simple geometries, the probability $p(R)$ can be found and then P_{esc} can be derived exactly from equation (2.113).[59]

Consider, for example, an infinite slab of thickness a; the chords are chosen so that the number in $d\mu$ is proportional to μ, where $\mu = \cos\theta = a/R$ (Fig. 2.16). From equation (2.110),

$$-p(R)\, dR = 2\mu\, d\mu,$$

and hence,

$$p(R) = \frac{2a^2}{R^3}.$$

Consequently, equation (2.113) can be written as

$$P_{\text{esc}} = \frac{1}{\sigma \bar{R}} \int_a^\infty \frac{2a^2}{R^3} (1 - e^{-\sigma R})\, dR. \tag{2.115}$$

In this case, it follows from equation (2.112) that

$$\bar{R} = 2a.$$

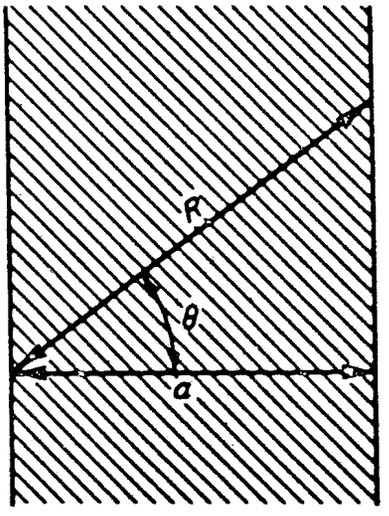

FIG. 2.16 CHORDS IN INFINITE SLAB.

Evaluation of the integral then gives

$$P_{esc} = \frac{1}{a\sigma}\left[\tfrac{1}{2} - E_3(a\sigma)\right], \tag{2.116}$$

where E_3 is the exponential integral function of the third order (see Appendix).

For a sphere of radius a, equation (2.113) takes the form[60]

$$P_{esc} = \frac{3}{8(a\sigma)^3}\left[2(a\sigma)^2 - 1 + (1 + 2a\sigma)e^{-2a\sigma}\right]. \tag{2.117}$$

Corresponding expressions have been evaluated for infinite cylinders, spheroids, and hemispheres,[61] and also for finite cylinders and cuboids.[62]

The region from which the probability of neutron escape has been derived above may be regarded as a lump of fuel, volume V_F, surrounded by a moderator, volume V_M (Fig. 2.17). The escape probability is thus equivalent to $P_{1\to 2}$ for purely absorbing media* in §2.7b, which is represented here by the symbol $P_{F\to M}$; thus,

$$P_{esc} = P_{F\to M}.$$

It is now possible to find $P_{M\to F}$ in terms of P_{esc} from equation (2.101), where $P_{M\to F}$ is the probability that a neutron produced uniformly in the moderator region M makes its first collision in the fuel lump, F.

For this simple geometry, i.e., a single lump of fuel in an extensive moderator, the reciprocity relation may be developed from the following argument. Suppose there is a uniform and isotropic source of intensity $1/4\pi V_M$ in a large volume V_M

* Since P_{esc} is the probability of escape without collision from medium 1 and, in addition, the neutron must not return from medium 2, P_{esc} is equivalent to $P_{1\to 2}$ provided that, in computing the latter, all collisions are regarded as absorptions or, in other words, the media are treated as being purely absorbing.

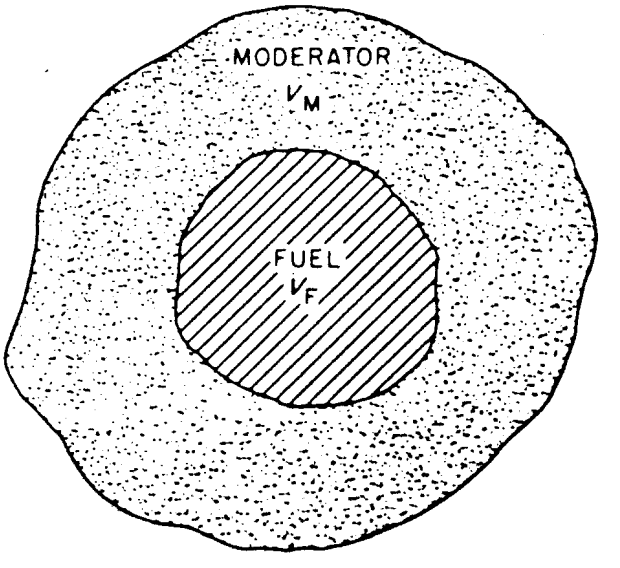

FIG. 2.17 FUEL AND MODERATOR REGIONS.

of the moderator. The flux incident on V_M will appear to be like that from an infinite medium; thus, writing σ_M for the moderator cross section,

$$\frac{1}{4\pi V_M \sigma_M} = \Phi_{inc}(\mathbf{r}, \Omega).$$

The collision rate in the fuel region F due to this source, i.e., $P_{M\to F}$, is then

$$P_{M\to F} = \frac{1}{4\pi\sigma_M V_M} \iint_{\hat{\mathbf{n}}\cdot\Omega<0} |\hat{\mathbf{n}}\cdot\Omega|(1 - e^{-\sigma_F R_s})\, d\Omega\, dA.$$

Upon comparison with $P_{F\to M}$, given by equation (2.107), with V_F and σ_F, and noting that the integrals have the same value for $\hat{\mathbf{n}}\cdot\Omega > 0$ and for $\hat{\mathbf{n}}\cdot\Omega < 0$, it follows that

$$\sigma_M V_M P_{M\to F} = \sigma_F V_F P_{F\to M},$$

which is exactly equivalent to the reciprocity relation of equation (2.101). Equation (2.105) may be derived directly in a similar manner.

2.8c The Dancoff Correction

In the practical case in which a number of fuel rods in a periodic array are separated by moderator which is not very thick, in mean free paths, the foregoing calculations can still give the probability for a neutron to escape from a fuel rod. To compute the probability, $P_{F\to M}$, that a neutron born in the fuel will make its next collision in the moderator, the escape probability for a single rod must be multiplied by the probability that the escaped neutron will make its next collision in the moderator.

For this purpose, by using equations (2.111) and (2.112), equation (2.107) may be written as

$$P_{esc} = \frac{\iint \hat{\mathbf{n}}\cdot\Omega(1 - e^{-R_s\sigma})\, d\Omega\, dA}{\sigma\bar{R}\iint \hat{\mathbf{n}}\cdot\Omega\, d\Omega\, dA}, \tag{2.118}$$

where P_{esc} is represented as an average over direction ($d\Omega$) and surface (dA) and the integrals are to be evaluated over $\hat{\mathbf{n}}\cdot\Omega > 0$. For any surface element dA and direction Ω, the chord under consideration may be extended and further fuel elements may be intercepted, as indicated in Fig. 2.18. Hence, in computing $P_{F\to M}$, the contribution of this chord should be reduced by

$$(1 - e^{-\sigma_M R_{M1}}) + e^{-\sigma_M R_{M1}} e^{-\sigma_F R_{F2}}(1 - e^{-\sigma_M R_{M2}}) + \cdots,$$

where $e^{-\sigma R}$ is the transmission probability and $1 - e^{-\sigma R}$ the collision probability in the indicated regions. Consequently, this factor must be included in the integrand of equation (2.118) to give $P_{F\to M}$. Because of the resulting complexity, Monte Carlo methods are often used for computing $P_{F\to M}$. The integrand is sampled at random $d\Omega\, dA$ points and in this manner the integral is approximated.

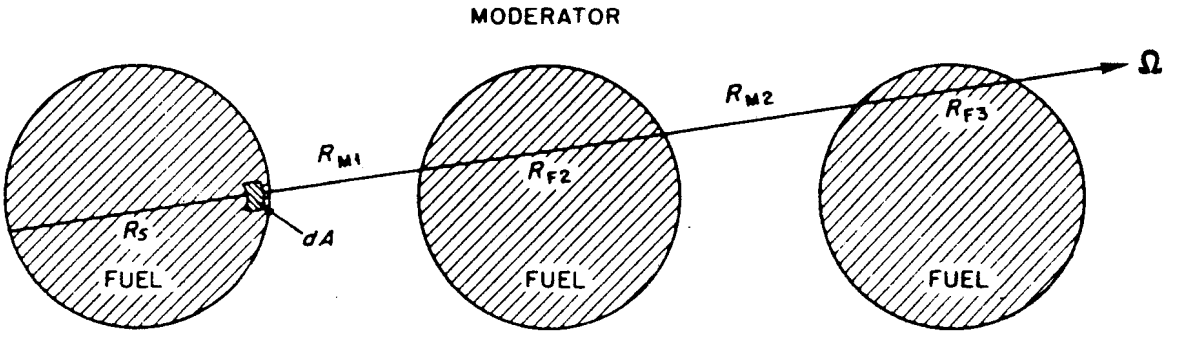

FIG. 2.18 PERIODIC ARRAY OF FUEL RODS.

In spite of the complexity of the integrand, useful approximations to $P_{F\to M}$ can be found by simple methods. For this purpose, the following probabilities are defined for the case in which neutrons are produced uniformly in the fuel:

P_M^i = probability that a neutron incident on the moderator after i previous traversals of fuel will collide in the moderator.

P_F^i = probability that a neutron incident on fuel after i previous traversals of fuel will collide in fuel.

Then,

$$P_{F\to M} = P_{esc}[P_M^0 + (1 - P_M^0)(1 - P_F^0)P_M^1 + (1 - P_M^0) \times (1 - P_F^0)(1 - P_M^1)(1 - P_F^1)P_M^2 + \cdots]. \quad (2.119)$$

In the majority of cases, the first few terms of this expression are the most important and a good approximation can be obtained by replacing all the P_M^i by P_M^0 and all the P_F^i by P_F^0. After summation of the series, it is found that

$$P_{F\to M} \approx P_{esc} \frac{P_M^0}{1 - (1 - P_M^0)(1 - P_F^0)}. \quad (2.120)$$

It is customary to set $P_M^0 = 1 - C$, where C is called the *Dancoff correction*.[63] Extensive tabulations of this correction factor are available and a selection of values is given in Table 2.9.[64] Furthermore, from equations (2.105) and (2.112), it is possible to write

$$P_F^0 \approx \sigma_F \bar{R}_F P_{esc},$$

and then equation (2.120) becomes

$$P_{F\to M} \approx P_{esc} \frac{1 - C}{1 - C(1 - \sigma_F \bar{R}_F P_{esc})}. \quad (2.121)$$

The Dancoff correction is often calculated for "black," i.e., perfectly absorbing, cylinders, and considerable work has been done on this subject.[65]

TABLE 2.9. DANCOFF CORRECTIONS[64]

d/r \ $r\sigma$	0	0.25	0.50	1.0	1.5	2.0
2.0	0.182	0.170	0.160	0.144	0.132	0.123
2.5	0.136	0.107	0.0849	0.0550	0.0364	0.0245
4.0	0.081	0.040	0.0205	0.0057	0.0016	0.0005
7.0	0.046	0.0094	0.0021	0.0001	–	–
10.0	0.032	0.0028	0.0003	–	–	–

r = radius of fuel cylinder
d = spacing between cylinder centers
σ = macroscopic cross section of moderator
Correction in table is for one adjacent fuel cylinder. For lattices, a sum is taken over all adjacent cylinders, i.e., $C = \sum_j C_j$, with C_j taken from the table.

For preliminary survey calculations, it is adequate to use the rational approximation of equation (2.114) for P_{esc}, and then equation (2.121) takes the form

$$P_{F\to M} \approx \frac{(1 - C)\bar{R}_F}{\sigma_F + (1 - C)\bar{R}_F}. \tag{2.122}$$

By comparison with equation (2.114) it is seen that, in the rational approximation, the Dancoff correction is equivalent to increasing the mean chord length, $\bar{R}_F$, by the factor $1/(1 - C)$ or, what is the same thing, decreasing the surface area of fuel by $1 - C$.

Fair accuracy is also obtained by using the rational approximation for $P_M^0 = 1 - C$: thus, from equations (2.105), (2.112), and (2.114),

$$P_M^0 = \sigma_M \bar{R}_M P_{esc,M} \approx \frac{\sigma_M \bar{R}_M}{1 + \sigma_M \bar{R}_M}.$$

Substitution of this expression for $1 - C$ in equation (2.122) then gives the so-called fully rational approximation to $P_{F\to M}$,

$$P_{F\to M} \approx \frac{1}{1 + \sigma_F \tilde{R}_F} \quad \text{(fully rational)}, \tag{2.123}$$

where $\tilde{R}_F$ is the effective chord length defined by

$$\tilde{R}_F = \bar{R}_F \frac{1 + \sigma_M \bar{R}_M}{\sigma_M \bar{R}_M}. \tag{2.124}$$

The accuracy of this fully rational approximation is similar to that for P_{esc} obtained by using the Wigner rational approximation, as given in Table 2.8. A detailed comparison of the results obtained by various methods of computation is to be found in the literature.[66]

The fully rational approximation to $P_{F\to M}$ has desirable limiting properties. **First,** if the moderator is thick in mean free paths, so that $\sigma_M \bar{R}_M$ is large, it follows from equation (2.124) that $\tilde{R}_F \approx \bar{R}_F$. Then $P_{F\to M}$, as given by equation

(2.123), approximates P_{esc} as expressed by equation (2.114). Second, if both fuel and moderator regions are thin in mean free paths, i.e., $\sigma_F \bar{R}_F \ll 1$ and $\sigma_M \bar{R}_M \ll 1$, a neutron will, on the average, cross both regions several times before making a collision; as far as a neutron is concerned, therefore, the system is essentially homogeneous. For $\sigma_M \bar{R}_M \ll 1$, equation (2.124) becomes

$$\tilde{R}_F \approx \frac{\bar{R}_F}{\sigma_M \bar{R}_M}.$$

If $\bar{R}_F$ and $\bar{R}_M$ are expressed in terms of equation (2.112) and this result for $\tilde{R}_F$ is substituted into equation (2.123), it is found that

$$P_{F \to M} \approx \frac{\sigma_M V_M}{\sigma_F V_F + \sigma_M V_M}, \tag{2.125}$$

as would be expected in the homogeneous limit. It will be noted that in deriving equation (2.125), the only assumption made is that $\sigma_M \bar{R}_M \ll 1$, i.e., that the moderator is thin; the result is thus independent of the fuel thickness. The reason is that the neutron flux is nearly uniform in both fuel and moderator provided the moderator is thin and the source is in the fuel. In order that both $P_{F \to M}$ and $P_{M \to F}$ have the form for a homogeneous system, however, it is necessary that both fuel and moderator be thin, i.e., $\sigma_F \bar{R}_F \ll 1$ and $\sigma_M \bar{R}_M \ll 1$.

Finally, in connection with the fully rational approximation, it can be shown that the fully rational forms of $P_{M \to F}$ and $P_{F \to M}$ satisfy the exact reciprocity relation of equation (2.101).

It may be mentioned in conclusion that, as will be seen in Chapter 8, collision probabilities are useful for computing resonance absorption of neutrons in reactor lattices, i.e., periodic arrays of fuel elements. For "tight" lattices, in which the fuel elements are closely spaced, such as are common in water-moderated reactors, the collision probabilities are determined by using the Dancoff corrections to the escape probability or equivalent methods, as described above.

EXERCISES

1. Use the integral equation (1.37) of plane geometry to find the discrete eigenvalues of §2.2b. Suggest other possible ways of finding them (see Ref. 67).
2. Show that equation (2.50) is the same as the transient part of equation (2.40).
3. Verify equation (2.52). Students familiar with complex variable theory should also attempt to evaluate the solution.
4. Derive equation (2.82) in detail.
5. Obtain an expression for the values of ν_l (§2.4b) in the P_3 approximation.
6. Derive the flux from a plane isotropic source in an infinite medium in the four ways indicated below, and compare and discuss the results for $c = 0.5$ and 0.9.
   (*a*) Exact transport theory; use Tables 8 and 21 in Ref. 68.
   (*b*) Diffusion theory; use L given by equation (2.24).

(*c*) Asymptotic diffusion theory; use exact values of ν_0 in Table 2.1.
(*d*) An approach in which the uncollided flux is treated separately and used as the source for a diffusion theory calculation of the collided flux (cf. Ref. 69).

7. Derive equation (2.116) from the integral equation (1.37) for the neutron flux in plane geometry. Take the source as constant, compute the absorption, and hence the escape probability for a purely absorbing medium. Determine the angular distribution of the emerging flux and current, and also obtain the escape probability from the total emerging current.
8. Show that the fully rational forms of $P_{F\to M}$ and $P_{M\to F}$, as defined in §2.8c, satisfy equation (2.101).
9. Derive $P_{F\to M}$ and the Dancoff correction for a periodic array of fuel and moderator slabs having thicknesses d_F and d_M mean free paths, respectively. Consider the limits of large and small spacings and examine the validity of equation (2.116) and of the rational approximation for $P_{F\to M}$. The interested student may review the corresponding problem for a periodic array of fuel cylinders (cf. Ref. 70).
10. Suppose that a right half-space ($x > 0$) is a uniform medium, with $\sigma = 1$ and $c < 1$, containing an isotropic uniform source, Q_0. The left half-space ($x < 0$) is a vacuum and free-surface boundary conditions apply at $x = 0$. Discuss the exact solution of the one-speed, time-independent transport equation near the boundary, far from the boundary, etc. Obtain the exact solution for $c = 0$ and relate it to the general discussion.[71]
11. In a medium consisting of uranium-235, the neutrons are essentially all fast ($E \gtrsim 100$ keV) and, as a first approximation, all the neutrons may be considered to have the same energy. Calculate the critical radius and mass of a sphere of uranium-235 (density 18.8 g/cm^3) by (*a*) end-point theory and (*b*) diffusion theory, assuming isotropic scattering. The following data are to be used: $\sigma_f = 1.3$ barns, $\sigma_s = 4.0$ barns, $\sigma_\gamma = 0$, and $\bar{\nu} = 2.5$. (The results may be compared with the critical radius of the Godiva assembly in Table 5.6.)
12. Consider a reactor lattice consisting of three regions, namely, fuel, cladding, and a thick moderator with volumes V_F, V_C, and V_M, respectively. Define a consistent set of collision probabilities $P_{F\to C}$, etc., and derive the reciprocity relations between them.
13. Derive equation (2.117).

REFERENCES

1. Davison, B., "Neutron Transport Theory," Oxford University Press, 1957, Chap. IV.
2. Davison, B., Ref. 1, p. 268; N. G. Van Kampen, *Physica*, **21**, 949 (1955); E. P. Wigner, *Proc. Symp. Appl. Math.*, XI, Am. Math. Soc., 1961, p. 89.
3. Case, K. M., *Ann. Phys.*, 9, 1 (1960); see also K. M. Case and P. F. Zweifel, "Linear Transport Theory," Addison-Wesley Publishing Co., Inc., 1967, Chap. 4.
4. Case, K. M., and P. F. Zweifel, Ref. 3, Chaps. 4–6.
5. Davison, B., Ref. 1, Section 5.1.
6. Exact values from K. M. Case, F. de Hoffmann, and G. Placzek, "Introduction to the Theory of Neutron Diffusion," Vol. I, U.S. AEC Report, 1953, Table 9.
7. Whittaker, E. T., and G. N. Watson, "A Course of Modern Analysis," Cambridge University Press, 1946, p. 75.
8. A good introduction is M. J. Lighthill, "Introduction to Fourier Analysis and Generalized Functions," Cambridge University Press, 1958. The definitive work is L. Schwartz, "Théorie des Distributions," I and II, Hermann et Cie., Paris, 1950, 1951.
9. Case, K. M., and P. F. Zweifel, Ref. 3, Section 4.6.

10. Case, K. M., and P. F. Zweifel, Ref. 3, Section 4.5.
11. Josephs, A. M., and J. J. McInerney, *Nucl. Sci. Eng.*, **22**, 119 (1965); H. G. Kaper, *ibid.*, **24**, 423 (1966).
12. Case, K. M., and P. F. Zweifel, Ref. 3, Chap. 4; N. I. Muskhelishvili, "Singular Integral Equations," Noordhoff, Groningen, 1953.
13. Case, K. M., and P. F. Zweifel, Ref. 3, Chap. 7; R. L. Bowden and C. D. Williams, *J. Math. Phys.*, **5**, 1527 (1964).
14. Sneddon, J. M., "Fourier Transforms," McGraw-Hill Book Co., Inc., 1951, Chap. 1.
15. Case, K. M., *et al.*, Ref. 6, Table 21.
16. Abu-Shumays, I. K., and E. H. Bareis, *J. Math. Phys.*, **9**, 1722 (1968). The relation between P_N theory and the method of separation of variables is explored by T. Nonnenmacher, *Atomkernenergie*, **12**, 183 (1967).
17. Hendry, W., *Nucl. Sci. Eng.*, **30**, 307 (1967); W. Kofink, in "Developments in Transport Theory," E. Inönü and P. F. Zweifel, eds., Academic Press, 1967, p. 149.
18. Davison, B., Ref. 1, p. 116.
19. Glasstone, S., and M. C. Edlund, "The Elements of Nuclear Reactor Theory," D. Van Nostrand Co., Inc., 1952, Chap. V; J. R. Lamarsh, "Introduction to Nuclear Reactor Theory," Addison-Wesley Publishing Co., Inc., 1966, Chap. 5.
20. Davison, B., Ref. 1, p. 119.
21. Davison, B., Ref. 1, Chap. X.
22. Rumyantsev, G. Ya., and V. S. Shulepin, *Atomn. Energiia* (transl.), **22**, 395 (1967); J. D. Callen and J. O. Mingle, *J. Nucl. Energy*, **22**, 173 (1968).
23. Davison, B., Ref. 1, p. 119.
24. See citations in Ref. 12.
25. Davison, B., Ref. 1, Section 6.1.
26. Case, K. M., *et al.*, Ref. 6, p. 129.
27. Davison, B., Ref. 1, Section 6.1.
28. Davison, B., Ref. 1, Section 6.2.
29. Case, K. M., *et al.*, Ref. 6, Table 23.
30. Davison, B., Ref. 1, Sections 8.2, 8.3.
31. Frankel, S., and E. Nelson, "Methods of Treatment of Displacement Integral Equations," U.S. AEC Report AECD-3497 (1953).
32. Davison, B., Ref. 1, Chap. VIII.
33. Carlson, B. G., and G. I. Bell, *Proc. Second U.N. Conf. on Peaceful Uses of At. Energy*, **16**, 535 (1958).
34. Case, K. M., and P. F. Zweifel, Ref. 3, Section 6.6; G. J. Mitsis, *Nucl. Sci. Eng.*, **17**, 55 (1963).
35. Davison, B., Ref. 1, Section 10.3.
36. Davison, B., Ref. 1, Section 10.3.6.
37. Vladimirov, V. S., Trans. V. A. Steklov Math. Inst., **61** (1961), translated in Atomic Energy of Canada Report AECL-1661 (1963); J. A. Davis, *Nucl. Sci. Eng.*, **25**, 189 (1966).
38. Davison, B., Ref. 1, Section 10.5.
39. Davison, B., Ref. 1, Section 10.3.4.
40. Mark, J. C., "The Spherical Harmonics Method," I and II, Natl. Res. Council Canada, At. Energy Reports MT 92 (1944), MT 97 (1945).
41. Gelbard, E. M., Chap. 4 in "Computing Methods in Reactor Physics," H. Greenspan, C. N. Kelber, and D. Okrent, eds., Gordon and Breach, 1968.
42. See citations in Ref. 37.
43. Davison, B., Ref. 1, Chap. VII.
44. Davison, B., Ref. 1, Chap. VIII.
45. Carlson, B. G., and G. I. Bell, Ref. 33.
46. Mitsis, G. J., "Transport Solutions to the Monoenergetic Critical Problems," Argonne National Laboratory Report ANL-6787 (1963).
47. Mitsis, G. J., Ref. 46, Section 4.6.
48. Carlson, B. G., "Neutron Diffusion Theory—The Transport Approximation," U.S. AEC Report AECU-725 (originally LA-1061 (1950)); G. I. Bell, G. E. Hansen, and H. A. Sandmeier, *Nucl. Sci. Eng.*, **28**, 376 (1967).

49. Mika, J. R., *Nucl. Sci. Eng.*, **11**, 415 (1961); K. M. Case and P. F. Zweifel, Ref. 3, Section 4.10. The determinant was given by B. Davison, Ref. 1, Section 17.3.
50. Inönü, E., and A. I. Usseli, *Nucl. Sci. Eng.*, **23**, 251 (1965).
51. See citations in Ref. 49.
52. See citations in Ref. 49; also J. R. Mika, *J. Math. Phys.*, **7**, 833 (1966).
53. Case, K. M., and P. F. Zweifel, Ref. 3, Appendix D.
54. Case, K. M., *et al.*, Ref. 6, Chap. II.
55. Amouyal, A., P. Benoist, and J. Horowitz, *J. Nucl. Energy*, **6**, 79 (1957).
56. Wigner, E. P., *et al.*, *J. Appl. Phys.*, **2**, 257, 260, 271 (1955).
57. Nordheim, L. W., *Proc. Symp. Appl. Math.*, XI, Am. Math. Soc., 1961, p. 58; exact values from K. M. Case, *et al.*, Ref. 6, Tables 2, 3, 4.
58. Case, K. M., *et al.*, Ref. 6, Section 10.
59. Case, K. M., *et al.*, Ref. 6, Section 10.
60. Case, K. M., *et al.*, Ref. 6, Section 10.2.
61. Case, K. M., *et al.*, Ref. 6, Sections 10.2, 10.4, 10.5.
62. Carlvik, I., *Nucl. Sci. Eng.*, **30**, 150 (1967).
63. Dancoff, S. M., and M. Ginsburg, "Surface Resonance Absorption in Close Packed Lattices," Manhattan Project Report CP-2157 (1944).
64. "Reactor Physics Constants," Argonne National Laboratory Report ANL-5800 (1963), Table 4-25.
65. Ref. 64, Section 4.2.
66. Nordheim, L. W., Ref. 57, Section 7.
67. Davison, B., Ref. 1, Chap. V.
68. Case, K. M., *et al.*, Ref. 6.
69. Harris, D. R., "Collided Flux Diffusion Theory," Westinghouse Report WAPD-TM-801 (1968).
70. Fukai, Y., *Nucl. Sci. Eng.*, **9**, 370 (1961); A. Sauer, *ibid.*, **16**, 329 (1963).
71. Davison, B., Ref. 1, Section 6.5.

3. NUMERICAL METHODS FOR ONE-SPEED PROBLEMS: SIMPLE P_N APPROXIMATIONS

3.1 EXPANSION OF FLUX IN LEGENDRE POLYNOMIALS FOR PLANE GEOMETRY

3.1a Introduction

In the preceding chapter, several methods were described for solving the one-speed transport equation. The emphasis was on procedures for obtaining accurate solutions for very simple situations and on the general properties of these solutions. In the present chapter, consideration will be given to some methods for arriving at approximate numerical solutions of problems with more complicated geometries and source distributions. The one-speed transport equation will be treated here, but it will be seen in Chapter 4 that the techniques developed are directly applicable in the multigroup methods used for the solution of realistic (energy-dependent) physical problems.

The procedures to be discussed in this chapter are based on the expansion of the angular distribution of the neutron flux, i.e., the dependence of Φ on the direction Ω, in a complete set of orthogonal functions, namely, the Legendre

polynomials in simple geometries and the spherical harmonics in general. The expansions are truncated after a few terms in order to develop practical methods for solving the resulting form of the neutron transport equation. The spatial dependence of the angular flux is obtained by imposing a discrete space mesh and evaluating the flux at discrete space points, rather than as a continuous function of position. In an alternative general procedure, which will be developed in Chapter 5, the direction variable, $\mathbf{\Omega}$, is also treated as discrete.

In Chapter 2, a general form of the time-independent, one-speed neutron transport equation was derived as equation (2.3). This expression will be presented here with a slightly different notation which is desirable in order to establish the connection between the results obtained in this chapter and those in Chapter 4.

As before, it will be assumed that scattering is a function only of the cosine of the scattering angle, i.e., $\mu_0 = \mathbf{\Omega}\cdot\mathbf{\Omega}'$, where $\mathbf{\Omega}'$ and $\mathbf{\Omega}$ are the neutron directions before and after scattering, respectively. A quantity $\sigma_s(\mathbf{r}, \mathbf{\Omega}\cdot\mathbf{\Omega}')$ is then defined by

$$\sigma_s(\mathbf{r}, \mathbf{\Omega}\cdot\mathbf{\Omega}') \equiv \sigma(\mathbf{r})c(\mathbf{r})f(\mathbf{r}; \mathbf{\Omega}' \to \mathbf{\Omega}), \tag{3.1}$$

where the notation σ_s is intended to suggest, although not to be limited to, a scattering cross section.

It will be assumed in the present chapter that

$$\int \sigma_s(\mathbf{r}, \mathbf{\Omega}\cdot\mathbf{\Omega}')\, d\mathbf{\Omega}' < \sigma(\mathbf{r}),$$

implying that $c(\mathbf{r})$, the mean number of neutrons emerging from a collision, is less than unity. There will then exist a unique, time-independent solution to the transport problem with a given source (§1.5d).

With this change in notation, the one-speed transport equation (2.3) becomes

$$\mathbf{\Omega}\cdot\nabla\Phi(\mathbf{r}, \mathbf{\Omega}) + \sigma(\mathbf{r})\Phi(\mathbf{r}, \mathbf{\Omega}) = \int \sigma_s(\mathbf{r}, \mathbf{\Omega}\cdot\mathbf{\Omega}')\Phi(\mathbf{r}, \mathbf{\Omega}')\, d\mathbf{\Omega}' + Q(\mathbf{r}, \mathbf{\Omega}). \tag{3.2}$$

Methods will first be examined for solving this equation in plane geometry. Then more general geometries will be considered, with particular emphasis on the P_1 and diffusion approximations. Finally, some more specialized treatments for plane and cylindrical geometries will be described.

3.1b Plane Geometry: Spherical Harmonics Expansion

From the arguments in §2.1c, it follows that, in infinite plane geometry, Φ can be expressed as a function of the spatial coordinate, x, and of the direction

cosine, μ, relative to the x axis, i.e., $\mu = \mathbf{\Omega}\cdot\hat{\mathbf{x}}$, where $\hat{\mathbf{x}}$ is a unit vector in the x direction. Hence, with $\mu_0 = \mathbf{\Omega}\cdot\mathbf{\Omega}'$, equation (3.2) becomes

$$\mu\frac{\partial\Phi(x,\mu)}{\partial x} + \sigma(x)\Phi(x,\mu) = \int \sigma_s(x,\mu_0)\Phi(x,\mu')\,d\mathbf{\Omega}' + Q(x,\mu)$$

$$= \int_0^{2\pi} d\varphi' \int_{-1}^{1} \sigma_s(x,\mu_0)\Phi(x,\mu')\,d\mu' + Q(x,\mu), \qquad (3.3)$$

where φ' is the azimuthal angle corresponding to the direction $\mathbf{\Omega}'$.

These results are equivalent to equations (2.4) and (2.5), except that the total cross section, σ, and the scattering function, σ_s, are here arbitrary functions of position x, whereas in Chapter 2 it was usually assumed that σ_s/σ is independent of position.

The procedure for solving equation (3.3) is similar to that used for anisotropic scattering in plane geometry in Chapter 2. First, the scattering function is expanded in Legendre polynomials, by writing

$$\sigma_s(x,\mu_0) = \sum_{l=0}^{\infty} \frac{2l+1}{4\pi}\sigma_{sl}(x)P_l(\mu_0)$$

and then $P_l(\mu_0)$ is expressed in terms of the Legendre polynomials and associated Legendre functions of the direction cosines μ and μ' by using the addition theorem. Upon carrying out the integration over φ' as described in §2.6a, equation (3.3) then leads to the result, analogous to equation (2.79),

$$\mu\frac{\partial\Phi}{\partial x} + \sigma(x)\,\Phi$$

$$= \sum_{l=0}^{\infty} \frac{2l+1}{2}\sigma_{sl}(x)P_l(\mu)\int_{-1}^{1}\Phi(x,\mu')P_l(\mu')\,d\mu' + Q(x,\mu). \qquad (3.4)$$

The angular flux, Φ, and source, Q, are now also expanded in Legendre polynomials, and by following the steps described in §2.6a it is found that

$$(n+1)\frac{d\phi_{n+1}(x)}{dx} + n\frac{d\phi_{n-1}(x)}{dx} + (2n+1)\sigma_n(x)\phi_n(x)$$

$$= (2n+1)Q_n(x), \qquad n = 0, 1, 2, \ldots \qquad (3.5)$$

where the quantity $\sigma_n(x)$ is defined by

$$\sigma_n(x) \equiv \sigma(x) - \sigma_{sn}(x). \qquad (3.6)$$

The expansion coefficients ϕ_n and Q_n (cf. §2.6a) are given by the orthogonality conditions as

$$\phi_n(x) = 2\pi \int_{-1}^{1} \Phi(x, \mu) P_n(\mu)\, d\mu \tag{3.6a}$$

and

$$Q_n(x) = 2\pi \int_{-1}^{1} Q(x, \mu) P_n(\mu)\, d\mu. \tag{3.6b}$$

Apart from the treatment here of σ and σ_s as space dependent, equation (3.5) is the same as equation (2.82), in which σ was unity.

Since the Legendre polynomials are complete for functions in the range of $-1 \leqslant \mu \leqslant 1$, the set of equations (3.5) is equivalent to the original one-speed transport equation in infinite plane geometry. The only assumption made is that σ_s is a function of $\boldsymbol{\Omega} \cdot \boldsymbol{\Omega}'$ and, as noted in Chapter 1, this is a good approximation in most physical situations.

Although Legendre polynomials were used above to represent the angular dependence of the neutron flux, the set of equations (3.5) is said to result from the use of the method of spherical harmonics. In plane geometry, however, it was not necessary to expand the angular dependence of the flux in spherical harmonics; because of the symmetry of the angular flux about the x axis, the expansion could be made in those spherical harmonics which are symmetrical about the rotation axis, namely, the Legendre polynomials (see Appendix). More general situations, where this is not possible, will be encountered later in this chapter.

3.1c The P_N Approximation

In order to solve the infinite set of equations (3.5) it is necessary to place a limit on the number in the set. As explained in §2.4b, this is done by setting

$$\frac{d\phi_{N+1}(x)}{dx} = 0,$$

thereby reducing the number of unknowns to $N + 1$. The resulting set of $N + 1$ equations in $N + 1$ unknowns then represents the P_N approximation for the one-speed neutron transport problem.

3.1d The P_1 Approximation

From the considerations in Chapter 2, it would appear that reasonably accurate solutions might be obtained for small N if the systems under consideration were large and neutron absorption small. Most reactors are, in fact, large systems and for computing the gross spatial dependence of the flux the P_1 approximation ($N = 1$) has been found to be very useful.

In this case, the only equations that need to be considered are those for which $n = 0$ and $n = 1$ in the set of equation (3.5). Moreover, as seen in §2.4a, the quantities $\phi_0(x)$ and $\phi_1(x)$ which appear in these equations are equal to the total flux, $\phi(x)$, and the current in the x direction, J_x, respectively; thus, from equation (3.6a),

$$\phi_0(x) = 2\pi \int_{-1}^{1} \Phi(x, \mu)\, d\mu = \phi(x)$$

and

$$\phi_1(x) = 2\pi \int_{-1}^{1} \mu\Phi(x, \mu)\, d\mu = J(x).$$

The two equations from the set in equation (3.5) can thus be written as

$$\frac{dJ(x)}{dx} + \sigma_0(x)\phi(x) = Q_0(x) \tag{3.7}$$

and

$$\frac{d\phi(x)}{dx} + 3\sigma_1(x)J(x) = 3Q_1(x), \tag{3.8}$$

where, from equation (3.6b),

$$Q_0(x) = 2\pi \int_{-1}^{1} Q(x, \mu)\, d\mu$$

and

$$Q_1(x) = 2\pi \int_{-1}^{1} \mu Q(x, \mu)\, d\mu.$$

If $Q(x, \mu)$ is an isotropic source, then $Q_1(x) = 0$. It is of interest to note that, in the terminology of §2.6b, σ_0 is the absorption cross section and σ_1 is the transport cross section.

If the source is isotropic, so that Q_1 is zero, equation (3.8) becomes a form of Fick's law, namely,

$$J(x) = -D(x)\frac{d\phi(x)}{dx}$$

with $D = 1/3\sigma_1$. This result may be combined with equation (3.7) to give a diffusion equation

$$-\frac{d}{dx}\left[D(x)\frac{d\phi(x)}{dx}\right] + \sigma_0(x)\phi(x) = Q_0(x). \tag{3.9}$$

The procedures for solving these P_1 and diffusion equations for the spatial distribution of the neutron flux will be described later in this chapter.

It will be seen in Chapter 4 that, in multigroup theory, the source, equivalent to Q_1, in a group is rarely isotropic. The transition from P_1 theory to diffusion theory will then involve some physical assumptions (§4.3b).

3.1e Boundary and Interface Conditions

To obtain solutions to the P_N equations, or to spherical harmonics equations in general, boundary conditions are required. Thus, for a set of $N + 1$ ordinary, first-order differential equations for the $N + 1$ scalar expansion coefficients, it is necessary to have $N + 1$ conditions. Furthermore, the set of equations (3.5) are not defined at interfaces, where $\sigma_n(x)$ is discontinuous; consequently, interface conditions are also required.

Free-Surface Conditions

Suppose that a solution for the P_N equations is sought for a region $0 \leqslant x \leqslant a$ and that free-surface boundary conditions (§1.1d) are to be imposed at the two surfaces for which $x = 0$ and $x = a$. It was seen in §2.5d that the exact boundary conditions cannot be satisfied in a P_N approximation and there is some freedom in the choice of approximate boundary conditions. For example, either Marshak or Mark boundary conditions can be used.

For the P_1 approximation, the Marshak conditions of zero incoming current (§2.5d) would be [cf. equation (2.72)]

$$\int_0^1 \frac{\mu}{4\pi} [\phi(0) + 3\mu J(0)]\, d\mu = 0$$

and

$$\int_{-1}^0 \frac{\mu}{4\pi} [\phi(a) + 3\mu J(a)]\, d\mu = 0,$$

which lead to the conditions

$$J(0) = -\tfrac{1}{2}\phi(0) \quad \text{and} \quad J(a) = \tfrac{1}{2}\phi(a).$$

More generally, the requirement of zero incoming current could be represented by

$$\hat{\mathbf{n}} \cdot \mathbf{J} = \tfrac{1}{2}\phi, \tag{3.10}$$

where $\hat{\mathbf{n}}$ is an outward unit normal vector.

For diffusion theory, Fick's law in plane geometry is

$$\mathbf{J} = -D \frac{d\phi}{dx} \hat{\mathbf{x}},$$

and then equation (3.10) can be written as

$$\phi + 2D \frac{d\phi}{dx} \hat{\mathbf{n}} \cdot \hat{\mathbf{x}} = 0.$$

In general, since

$$\mathbf{J} = -D \nabla \phi,$$

the Marshak boundary condition in equation (3.10) for diffusion theory becomes

$$\phi + 2D\nabla\phi\cdot\hat{\mathbf{n}} = 0. \tag{3.11}$$

Boundary conditions such as those in equations (3.10) and (3.11) are frequently used to represent a free surface in plane geometry. In diffusion theory, the flux is often simply set equal to zero on some extrapolated boundary, as described in §2.5d.

Reflecting and Periodic Boundary Conditions

It is often required to perform a calculation of the neutron flux for a unit cell of a periodic lattice. As an example, consider a regular array of fuel sheets separated by moderator in a critical assembly. In these circumstances, a calculation can be made for a cell composed of half a single fuel sheet plus half the moderator and then periodic boundary conditions can be imposed (see Fig. 3.1). The neutron flux is an even function of μ at $x = 0$ and $x = x_a$, so that odd-order expansion coefficients would have to vanish at these two points. For example, in P_1 theory, J would be zero at $x = 0$ and $x = x_a$. Conditions of this type are sometimes referred to as *reflecting boundary conditions*, since they would be obtained if specular reflecting surfaces were placed at the boundaries. An alternative approach is to make the cell run from $x = 0'$ to $x = x_b$ in Fig. 3.1; the requirement is then that $\phi_n(0') = \phi_n(x_b)$ for all values of n considered. These are called *periodic boundary conditions*. Either reflecting or periodic boundary conditions will give the required $N + 1$ conditions in plane geometry.

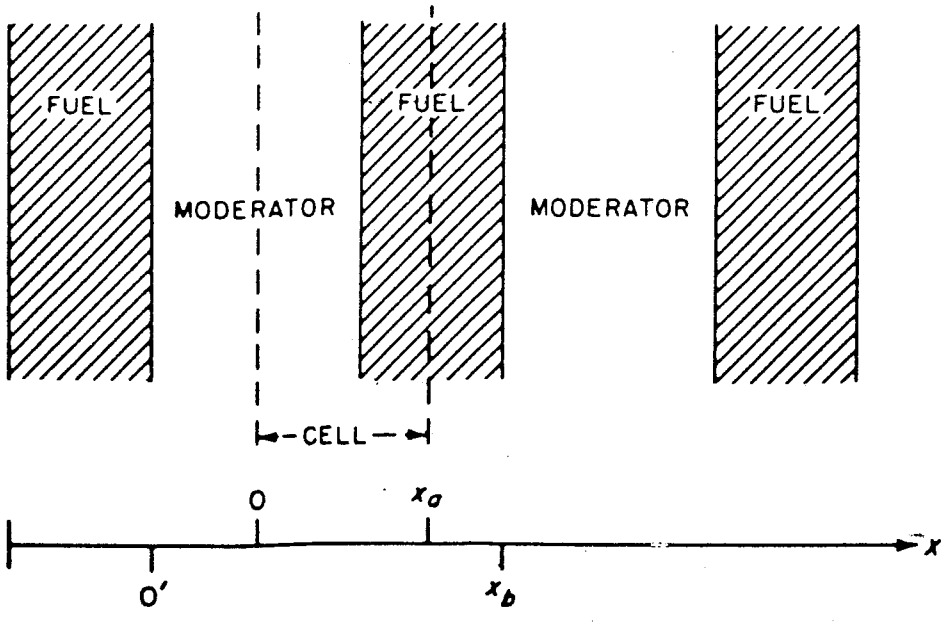

FIG. 3.1 BOUNDARY CONDITIONS IN PERIODIC LATTICE.

General Boundary Condition in Diffusion Theory

In diffusion theory, a variety of situations can be included in the general boundary condition

$$\phi + b\hat{\mathbf{n}}\cdot\nabla\phi = 0, \tag{3.12}$$

where b is a nonnegative function on the boundary. Thus, if $b = 2D$, the free-surface Marshak condition of equation (3.11) is obtained. On the other hand, if b is very large, the condition becomes essentially one of zero current (or reflection) on the boundary. As indicated, the function b must be nonnegative, otherwise, since ϕ is positive, the neutron flux would exhibit the unphysical behavior of increasing outward beyond the boundary. The general boundary condition in equation (3.12) will be used from time to time in this chapter and the next.

Interface Conditions

At various interfaces between different regions in a reactor system, the cross sections change discontinuously. The expansion coefficients, however, are continuous across interfaces. It was seen in §1.1d that $\Phi(\mathbf{r} + s\boldsymbol{\Omega}, \boldsymbol{\Omega}, E, t + s/v)$ is a continuous function of s. In the present context of a time-independent, one-speed problem in plane geometry, this means that $\Phi(x + s\mu, \mu)$ must be a continuous function of s. It follows, therefore, except possibly for $\mu = 0$, that $\Phi(x, \mu)$ is a continuous function of x. (The special case of $\mu = 0$ is treated in §3.5a.) Since for any $\mu \neq 0$, the angular flux Φ is a continuous function of x, so also will be the integrals of Φ over μ, i.e., $\phi_n(x)$. Thus, the expansion coefficients are continuous functions of x.*

When localized strong absorbers of neutrons are to be treated in a P_1 calculation, or by any other low-order approximation to the angular dependence of the flux, then the interface conditions are often adjusted to give results which are in better agreement with "exact" solutions. The treatment of such adjustments is usually called blackness theory.[2]

3.2 DIFFERENCE EQUATIONS IN PLANE GEOMETRY

3.2a Difference Equations in the P_1 Approximation

A practical method for solving the P_1 equations (3.7) and (3.8) is based on superimposing a discrete mesh of space points on the region of interest. Consider a system composed of a finite number of space regions; it is supposed that

* For P_N approximations of even order, the foregoing continuity conditions are not self-consistent and must be modified[1]; they are correct, however, for the odd-order approximations. In reactor calculations, the latter are used much more frequently than approximations of even order.

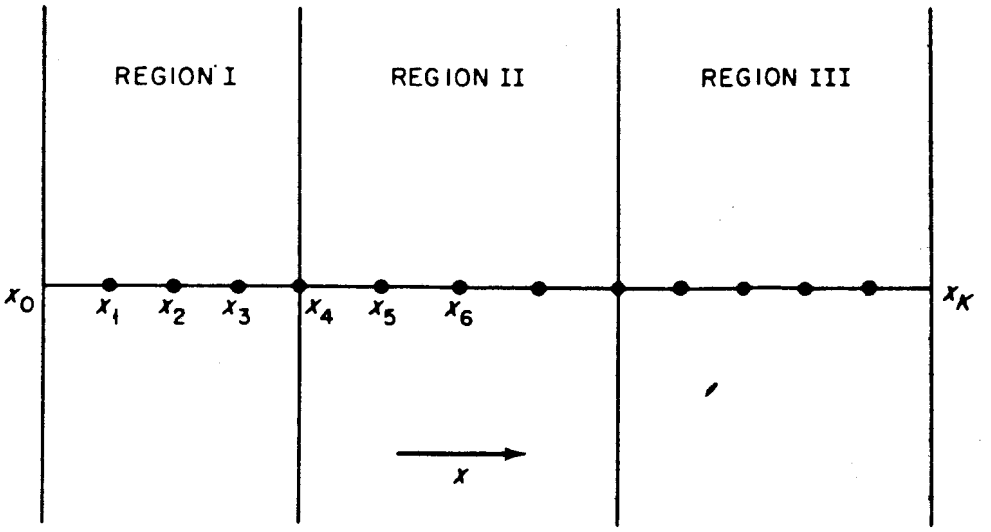

FIG. 3.2 MESH POINTS IN ONE DIMENSION.

within each region the cross sections σ_0 and σ_1 exhibit no spatial variation. Most physical systems can be closely approximated by such a set of discrete regions and usually each physical region with a uniform chemical composition will be represented by one of these regions.

In plane (one-dimensional) geometry, a set of points x_k, where $k = 0, 1, \ldots, K$ is chosen such that the boundaries of the problem are at x_0 and x_K and there is a point at each interface between two regions (Fig. 3.2). The distances between successive points should ordinarily be small compared with a neutron mean free path; for a typical practical one-dimensional problem, K might be of the order of 50. Consider the mesh in the vicinity of x_k, as indicated in Fig. 3.3. It is possible to derive difference equations which approximate equations (3.7) and

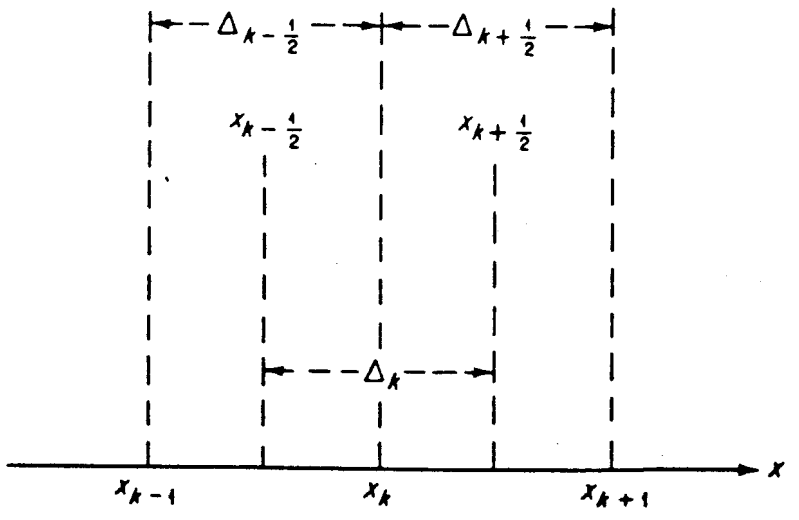

FIG. 3.3 MESH IN VICINITY OF x_k.

(3.8) by integrating over a region of x in this figure. If equation (3.7) is integrated from $x_{k-(1/2)}$ to $x_{k+(1/2)}$, where

$$x_{k-(1/2)} = \tfrac{1}{2}(x_{k-1} + x_k) \quad \text{and} \quad x_{k+(1/2)} = \tfrac{1}{2}(x_k + x_{k+1}),$$

it is found that

$$J_{k+(1/2)} - J_{k-(1/2)} + \int_{x_{k-(1/2)}}^{x_{k+(1/2)}} \sigma_0(x)\phi(x)\,dx = \int_{x_{k-(1/2)}}^{x_{k+(1/2)}} Q_0(x)\,dx, \quad (3.13)$$

where $J_{k+(1/2)}$ is the value of J at $x = x_{k+(1/2)}$, etc. Since σ_0 is constant between any two mesh points, the integrals may be approximated by

$$\int_{x_{k-(1/2)}}^{x_{k+(1/2)}} \sigma_0(x)\phi(x)\,dx \simeq \frac{\sigma_{0,k+(1/2)}\Delta_{k+(1/2)} + \sigma_{0,k-(1/2)}\Delta_{k-(1/2)}}{2}\phi_k \equiv b_{0k}\phi_k \quad (3.14)$$

$$\int_{x_{k-(1/2)}}^{x_{k+(1/2)}} Q_0(x)\,dx \simeq \frac{\Delta_{k+(1/2)} + \Delta_{k-(1/2)}}{2} Q_{0k} = \Delta_k Q_{0k} \quad (3.15)$$

and then, from equation (3.13),

$$J_{k+(1/2)} - J_{k-(1/2)} + b_{0k}\phi_k = \Delta_k Q_{0k}, \quad (3.16)$$

where ϕ_k and Q_{0k} are the values of ϕ and Q_0 at $x = x_k$.

Similarly, equation (3.8) can be integrated over the interval $x_k \leqslant x \leqslant x_{k+1}$ or $x_{k-1} \leqslant x \leqslant x_k$ to obtain equations for $J_{k+(1/2)}$ and $J_{k-(1/2)}$ in terms of ϕ_{k-1}, ϕ_k, and ϕ_{k+1}. By using the same approximation for the integrals as before, it is found that

$$\phi_{k+1} - \phi_k + 3\sigma_{k+(1/2)}\Delta_{k+(1/2)}J_{k+(1/2)} = \Delta_{k+(1/2)}Q_{1,k+(1/2)} \quad (3.17)$$

$$\phi_k - \phi_{k-1} + 3\sigma_{k-(1/2)}\Delta_{k-(1/2)}J_{k-(1/2)} = \Delta_{k-(1/2)}Q_{1,k-(1/2)}. \quad (3.18)$$

3.2b Approximation Errors in the Difference Equations

In deriving equations (3.16), (3.17), and (3.18), the integrals, such as those in equations (3.14) and (3.15), were approximated in a very simple manner. Better approximations to these integrals could have been used, but the resulting difference equations would have been more complicated than equation (3.16). Experience has shown, however, that in reactor calculations such complications are not worth the extra effort required for their treatment.[3] Nevertheless, it is of interest to consider the magnitude of the error involved in the approximation used above.

Suppose, for simplicity, that the point x_k does not lie on an interface, so that $\sigma_0(x)$ is a constant in the integral in equation (3.14). The approximation in this equation consequently is equivalent to setting

$$\int_{x_{k-(1/2)}}^{x_{k+(1/2)}} \phi(x)\,dx \simeq \Delta_k\phi_k.$$

If $\phi(x)$ is assumed to be continuous and differentiable as many times as required, it may be expanded in a Taylor series; thus,

$$\phi(x) = \phi(x_k) + (x - x_k)\phi'(x_k) + \frac{(x - x_k)^2}{2!}\phi''(x_k) + \cdots,$$

where the primes indicate derivatives with respect to x. When this expression for $\phi(x)$ is used in the integral for $\phi(x)$, it is found that

$$\int_{x_{k-(1/2)}}^{x_{k+(1/2)}} \phi(x)\,dx = \Delta_k\phi_k + [(\tfrac{1}{2}\Delta_{k+(1/2)})^2 - (-\tfrac{1}{2}\Delta_{k-(1/2)})^2]\frac{\phi'}{2}(x_k)$$

$$+ [(\tfrac{1}{2}\Delta_{k+(1/2)})^3 - (-\tfrac{1}{2}\Delta_{k-(1/2)})^3]\frac{\phi''(x_k)}{3!} + \cdots. \quad (3.19)$$

Hence, equation (3.14) is obtained by truncating equation (3.19) after the first term.

The resulting truncation error can be estimated from the magnitude of the first neglected term in equation (3.19). In general, for a nonuniform spacing of the mesh points, this will be the second term on the right of the equation. For a uniform mesh, however, $\Delta_{k+(1/2)} = \Delta_{k-(1/2)} = \Delta$ and then the coefficient of $\phi'(k)$ is zero; the first neglected term is now the third in equation (3.19) and it is equal to $(\frac{1}{3!}\Delta^3)\phi''(x_k)$. In either case, it is evident that the neglected term can be made small compared to $\Delta_k\phi_k$ by selection of a sufficiently fine space mesh, i.e., small values of Δ_k. The mesh can be relatively coarse, however, where the flux does not change very rapidly, for then ϕ' and ϕ'' are small in comparison with ϕ. Some discussion of the effects of the truncation errors in certain reactor calculations will be found in Ref. 4.

As a practical matter, the truncation effects can be examined by varying, e.g., halving, the mesh spacing in a problem of interest and determining the magnitude of the resulting change in the flux or other calculated quantity. In this manner it is found that, as a rule of thumb, the choice of one mesh point per mean free path is reasonable. Where the flux is changing rapidly in space, a somewhat finer mesh is desirable, but where it is varying slowly a coarser mesh will suffice.

3.2c Solving the P_1 Difference Equations

The system of equations (3.16), (3.17), and (3.18), plus boundary conditions, could be solved directly. For application in multigroup diffusion theory in Chapter 4, however, it is convenient to solve equations (3.17) and (3.18) for $J_{k-(1/2)}$ and $J_{k-(1/2)}$ and substitute in equation (3.16); the result is

$$a_{k,k-1}\phi_{k-1} + a_{k,k}\phi_k + a_{k,k+1}\phi_{k+1} = s_k, \quad (3.20)$$

where the coefficients $a_{k,k-1}$, $a_{k,k}$, and $a_{k,k+1}$ are given by

$$a_{k,k+1} = -\frac{1}{3\sigma_{k+(1/2)}\,\Delta_{k+(1/2)}} = a_{k+1,k} \tag{3.21}$$

$$a_{k,k-1} = -\frac{1}{3\sigma_{k-(1/2)}\,\Delta_{k-(1/2)}} = a_{k-1,k} \tag{3.22}$$

$$a_{kk} = b_{0k} - a_{k,k-1} - a_{k,k+1} \tag{3.23}$$

and s_k represents the source term

$$s_k = \Delta_k Q_{0k} - \frac{Q_{1,k+(1/2)}}{3\sigma_{k+(1/2)}} + \frac{Q_{1,k-(1/2)}}{3\sigma_{k-(1/2)}}. \tag{3.24}$$

Equation (3.20) can be derived for $k = 1, 2, \ldots, K-1$, so that there are $K-1$ equations for the $K+1$ unknowns, $\phi_0, \phi_1, \phi_2, \ldots, \phi_K$, the neutron fluxes at the mesh points. The remaining two equations must be obtained from boundary conditions. For a vacuum (free-surface) boundary, it is convenient and sufficiently accurate for most P_1 calculations simply to set $\phi_0 = \phi_K = 0$ and let x_0 and x_K be at some extrapolated boundaries. With these boundary conditions, ϕ_0 and ϕ_K can be eliminated from the set of equations (3.20), thereby making the number of unknowns equal to the number of equations.

If the vectors $\boldsymbol{\phi}$ and $\mathbf{s}$, having $\{\phi_k\}$ and $\{s_k\}$ as their components, are defined by

$$\boldsymbol{\phi} = \begin{pmatrix} \phi_0 \\ \phi_1 \\ \phi_2 \\ \vdots \\ \phi_K \end{pmatrix} \qquad \mathbf{s} = \begin{pmatrix} s_0 \\ s_1 \\ s_2 \\ \vdots \\ s_K \end{pmatrix}$$

and the matrix $\mathbf{A}$, with components $a_{n,m}$ by

$$\mathbf{A} = \begin{pmatrix} a_{00} & a_{01} & 0 & 0 & & \\ a_{10} & a_{11} & a_{12} & 0 & & \\ 0 & a_{21} & a_{22} & a_{23} & & \\ 0 & 0 & a_{32} & a_{33} & \ddots & \\ & & & & \ddots & a_{K,K} \end{pmatrix}$$

then equation (3.20) may be written in matrix form; thus,

$$\mathbf{A}\boldsymbol{\phi} = \mathbf{s}. \tag{3.25}$$

It will be recalled that in this equation $\mathbf{A}$ and $\mathbf{s}$ are known, and $\boldsymbol{\phi}$ is to be found. Formally, if an inverse exists of the matrix $\mathbf{A}$, i.e., $\mathbf{A}^{-1}$, such that $\mathbf{A}^{-1}\mathbf{A} = \mathbf{I}$, the unit matrix, then equation (3.25) could be multiplied by $\mathbf{A}^{-1}$ and solved for $\boldsymbol{\phi}$; that is,

$$\boldsymbol{\phi} = \mathbf{A}^{-1}\mathbf{s}. \tag{3.26}$$

The problem of solving for the spatial distribution of the neutron flux is consequently reduced to that of inverting the matrix **A**.

For the case under consideration, all values of $a_{n,m}$ are zero except those for which $m = n - 1, n, n + 1$; the inversion of the matrix can then be readily effected. More direct methods for finding $\boldsymbol{\phi}$ can, however, be used in the present case. As an example, the *Gauss elimination method* will be described. By starting with equation (3.20) with $k = 1$ and using the boundary condition $\phi_0 = 0$ (or some other boundary conditions that eliminates ϕ_0), this equation becomes

$$a_{11}\phi_1 + a_{12}\phi_2 = s_1, \tag{3.27}$$

and hence

$$\phi_1 = \frac{-a_{12}\phi_2 + s_1}{a_{11}}.$$

Next consider equation (3.20) with $k = 2$; it is found that

$$a_{21}\phi_1 + a_{22}\phi_2 + a_{23}\phi_3 = s_2. \tag{3.28}$$

Upon substituting the value for ϕ_1 given in equation (3.27), it is possible to solve for ϕ_2 in terms of ϕ_3.

By repeating this process, the equation (3.20) for $k = K - 1$ is finally reached and since $\phi_K = 0$, this is

$$a_{K-1,K-2}\phi_{K-2} + a_{K-1,K-1}\phi_{K-1} = s_{K-1}. \tag{3.29}$$

But an expression for ϕ_{K-2} in terms of ϕ_{K-1} has been obtained from the preceding $(k = K - 2)$ equation, and so equation (3.29) can be solved to obtain an explicit value for ϕ_{K-1}. The chain of equations can now be reversed to find the other values of ϕ_k. It can be shown that, because the diagonal elements of the matrix **A** are larger than the off-diagonal elements, this scheme is stable for numerical work.[5] The procedure just described is often called the *method of sweeps*[6]; the name derives from the fact that two sweeps through the mesh, one in the direction of increasing x and the other in the direction of decreasing x, are required to determine the solutions.

The essential point about the method of sweeps is that, in each step, an equation like (3.27) is solved for the particular component ϕ_k which has the largest coefficient and then that ϕ_k is eliminated from the following equation. If the reverse procedure had been adopted, namely, if equation (3.27) had been solved for ϕ_2 in terms of ϕ_1, and ϕ_1 had been carried through the chain of equations, the coefficient of ϕ_1 would increase exponentially. It would then become so large that the method would be unstable against numerical round-off errors.

The solution in the case given above was simple because the matrix **A** is tridiagonal; that is to say, only the elements on the main diagonal and the two adjacent diagonals are nonzero. When the geometry is not one-dimensional, however, the matrix is more complex, as will be seen shortly, and other methods, iterative rather than direct, of matrix inversion are used. These methods take

advantage of some general properties of the matrix **A**, which are evident in the simple case already considered. In particular it is apparent from their definitions in equations (3.21), (3.22), and (3.23), and (3.14) where b_{0k} is defined, that the elements of **A** have the following properties:

(i) $a_{n,n} > 0; a_{n,m} < 0$ if $m \neq n; a_{n,m} = a_{m,n}$

(ii) $a_{n,n+1} \neq 0$

(iii) $|a_{n,n}| > \sum_{m \neq n} |a_{n,m}|$.

In technical terms, the property (ii) makes sure that the matrix is irreducible; physically, this means that a neutron can get from any one point to any other point in the mesh. Property (iii) implies strict diagonal dominance, i.e., that the cross section σ_0, defined by equation (3.6) and in accordance with the assumption stated after equation (3.1), is positive. The matrix **A** is then said to be *irreducibly diagonally dominant*. This property guarantees that the matrix is nonsingular and has an inverse; a solution for $\boldsymbol{\phi}$ given by equation (3.26) then surely exists.[7]

No mention has been made thus far about conditions at the interfaces between the regions in Fig. 3.2. They are, in fact, automatically satisfied by the difference equations. Consider a very fine mesh such that all the Δ values approach zero in the vicinity of an interface at x_k; then it follows from equations (3.16), (3.17), and (3.18) that both ϕ and J are continuous across the interface.

The difference equations for the P_1 method have been derived by making particular approximations to the integrals in equations (3.14) and (3.15). Other simple approximations would lead to difference equations like equation (3.20), except that the coefficients $a_{n,m}$ would be slightly different, but they would still have the properties (i), (ii), and (iii) enumerated above. Diffusion theory also gives rise to the same difference equations although with different coefficients. Since diffusion theory is used extensively, it is of interest to develop the appropriate difference equations.

3.2d Difference Equations in Diffusion Theory

Diffusion theory can be regarded as being equivalent to the first P_1 equation, i.e., equation (3.7),

$$\frac{dJ(x)}{dx} + \sigma_0(x)\phi(x) = Q_0(x) \tag{3.30}$$

together with Fick's law

$$J(x) = -D(x)\frac{d\phi(x)}{dx}. \tag{3.31}$$

The difference equation corresponding to equation (3.30) is the same as for

equation (3.7), namely, equation (3.16). For currents at $x_{k+(1/2)}$ and $x_{k-(1/2)}$, equation (3.31) may be approximated by

$$J_{k+(1/2)} \simeq -D_{k+(1/2)} \frac{\phi_{k+1} - \phi_k}{\Delta_{k+(1/2)}} \tag{3.32}$$

$$J_{k-(1/2)} \simeq -D_{k-(1/2)} \frac{\phi_k - \phi_{k-1}}{\Delta_{k-(1/2)}}. \tag{3.33}$$

Upon substituting equations (3.32) and (3.33) in equation (3.16), a difference equation of the form of equation (3.20) is obtained with the coefficients

$$a_{k,k+1} = -\frac{D_{k+(1/2)}}{\Delta_{k+(1/2)}} = a_{k+1,k}$$

$$a_{k,k} = b_{0k} - a_{k,k-1} - a_{k,k+1}$$

$$a_{k,k-1} = -\frac{D_{k-(1/2)}}{\Delta_{k-(1/2)}} = a_{k-1,k}$$

and

$$s_k = \Delta_k Q_{0k}.$$

Once more it can be shown that the elements of the matrix **A** have the properties referred to earlier.

In deriving the difference equations, a space region extending from $x_{k-(1/2)}$ to $x_{k+(1/2)}$ was considered, and the various terms in the equation correspond to accountings of the neutron economy. This will be seen more clearly below in connection with spherical geometry. Thus, the difference equation may be regarded as a neutron balance (or conservation) equation for a small region in the system. It is important to have this conservation property in the difference equations, so that track can be kept of the fate of all fission neutrons in a numerical solution. In a criticality calculation, the balance between the production and loss of neutrons is, of course, decisive; it is essential, therefore, that neutrons are not created or destroyed in an artificial or uncertain manner.

3.2e Solution of the P_N Equations

In the preceding sections a numerical method was described for solving the P_1 and diffusion theory equations in plane geometry. The P_N equations for higher values of N can be converted into a system of difference equations in a similar manner. Several methods are available for solving these equations,[8] and one versatile technique will be described in Chapter 5. Moreover, it will be seen in §3.5b that the "double P_N" method is superior to the P_N method in plane geometry. Some results obtained by both of these two procedures will be given in Chapter 5.

3.3 FLUX EXPANSION IN SPHERICAL AND GENERAL GEOMETRIES

3.3a Expansions in Spherical Geometry

The discussion so far has been concerned with plane geometry and consideration will now be given to the application of the spherical harmonics method to other geometries. For a system which is symmetrical about a point, spherical coordinates may be used, and it will be shown that the spherical harmonics equations are then very similar to those for plane geometry. Such systems will be treated in the present section, and more general geometries, for which expansion of the neutron flux distribution in terms of Legendre polynomials is not adequate, will be described in §3.3c for the P_1 approximation. The use of spherical harmonics in cylindrical geometry will be taken up in §3.6b.

For a system which is symmetric about a point, the neutron angular flux is a function only of the distance, r, from the point and of $\mu = \boldsymbol{\Omega}\cdot\hat{\mathbf{r}}$ (§1.3a); the expression for $\boldsymbol{\Omega}\cdot\nabla\Phi$ is then given by equation (1.32) with Φ replacing N. Hence, the time-independent, one-speed transport equation in spherical coordinates takes the form

$$\mu\frac{\partial\Phi(r,\mu)}{\partial r} + \frac{1-\mu^2}{r}\frac{\partial\Phi}{\partial\mu} + \sigma\Phi = \sum_{l=0}^{\infty}\frac{2l+1}{2}\sigma_{sl}(r)P_l(\mu)\int_{-1}^{1}\Phi(r,\mu')P_l(\mu')\,d\mu' + Q(r,\mu), \quad (3.34)$$

where, as in the derivation of equation (3.4), the scattering function, σ_s, has been expanded in Legendre polynomials, and the addition theorem for these polynomials and the azimuthal symmetry of the flux have been used.

If, now, Φ and Q are expanded in Legendre polynomials, as in equations (2.80) and (2.81), and the same procedure followed as in §3.1b for plane geometry, it is found that all the terms in equation (3.34) except $[(1-\mu^2)/r]\,\partial\Phi/\partial\mu$ give terms corresponding to those in equation (3.5). To evaluate this exceptional term, the relation

$$(1-\mu^2)\frac{dP_m(\mu)}{d\mu} = \frac{m(m+1)}{2m+1}[P_{m-1}(\mu) - P_{m+1}(\mu)]$$

may be used. The expression satisfied by the expansion coefficients $\phi_n(r)$ in spherical geometry, equivalent to equation (3.5), is then

$$(n+1)\left(\frac{d}{dr}+\frac{n+2}{r}\right)\phi_{n+1}(r) + n\left(\frac{d}{dr}-\frac{n-1}{r}\right)\phi_{n-1}(r) + (2n+1)\sigma_n(r)\phi_n(r) = (2n+1)Q_n(r) \qquad n = 0, 1, 2, 3\ldots. \quad (3.35)$$

This infinite set of equations is similar to that for plane geometry, and P_1 approximations and the same numerical techniques can be used here, just as for

plane geometry. The boundary conditions, however, are somewhat different, as will be seen below.

The two equations for the P_1 approximation in spherical geometry are

$$\left(\frac{d}{dr} + \frac{2}{r}\right) J(r) + \sigma_0(r)\phi(r) = Q_0(r) \tag{3.36}$$

and

$$\frac{d\phi(r)}{dr} + 3\sigma_1(r)J(r) = 3Q_1(r), \tag{3.37}$$

where, as before, ϕ and $J(r)$ are written for ϕ_0 and ϕ_1, respectively. These equations differ from the corresponding equations (3.7) and (3.8) in plane geometry by the presence of the term $2J(r)/r$ in equation (3.36). The reason for this will be apparent in due course.

It is sometimes convenient to write equation (3.36) in the form

$$\frac{1}{r^2}\frac{d}{dr}[r^2 J(r)] + \sigma_0(r)\phi(r) = Q_0(r). \tag{3.38}$$

If the source is isotropic, so that $Q_1(r) = 0$, equation (3.37) may be used to eliminate $J(r)$ from equation (3.38); by writing D for $1/3\sigma_1$, as in §3.1d, the result is

$$-\frac{1}{r^2}\frac{d}{dr}\left[r^2 D \frac{d\phi(r)}{dr}\right] + \sigma_0(r)\phi(r) = Q_0(r). \tag{3.39}$$

This equation is in conservation form in the sense defined in §1.3b, since upon multiplying by a volume element $4\pi r^2\, dr$, the derivative term in equation (3.39) contains no functions of r outside. Use will be made of this fact shortly.

3.3b Boundary Conditions in Spherical Geometry

For a spherical region, free-surface boundary conditions can be imposed, as in plane geometry, giving $\frac{1}{2}(N + 1)$ conditions for a P_N approximation. The remaining conditions must be determined at the origin, i.e., at the center of the sphere. It is required that the angular flux, Φ, be finite at the origin; hence, the coefficients $\phi_n(0)$ must be finite for $n = 0, 1, 2, \ldots, N$ in a P_N approximation. It can be shown that for analytical work this provides the additional $\frac{1}{2}(N + 1)$ conditions.[9]

An alternative condition that is useful for numerical calculations is to require that Φ be an even function of μ at the origin, i.e., $\phi_n(0) = 0$ for n odd. This will be used in Chapter 5. In fact, the neutron flux should be isotropic at the origin in spherical geometry and this condition can also be imposed.[10] In the P_1 approximation, the current would be set to zero at the origin, i.e., $J(0) = 0$.

3.3c Difference Equations in Spherical Geometry

Difference equations may be derived for spherical geometry, in much the same way as for plane geometry. Consider, for example, equation (3.39) for diffusion theory; the fact that this equation is in conservation form is more important than in plane geometry, as indicated at the end of §3.2d. If equation (3.39) is multiplied by $4\pi r^2$ and integrated from $r_{k-(1/2)}$ to $r_{k+(1/2)}$, the result is

$$-4\pi r^2 D \frac{d\phi}{dr}\Big|_{r_{k-(1/2)}}^{r_{k+(1/2)}} + 4\pi \int_{r_{k-(1/2)}}^{r_{k+(1/2)}} r^2 \sigma_0 \phi \, dr = 4\pi \int_{r_{k-(1/2)}}^{r_{k+(1/2)}} r^2 Q_0 \, dr. \qquad (3.40)$$

By assuming, for simplicity, that the cross sections are the same on both sides of r_k, equation (3.40) may be approximated to

$$-4\pi r_{k+(1/2)}^2 D \frac{(\phi_{k+1} - \phi_k)}{\Delta_{k+(1/2)}} + 4\pi r_{k-(1/2)}^2 D \frac{(\phi_k - \phi_{k-1})}{\Delta_{k-(1/2)}}$$

$$+ \frac{4\pi\sigma_0}{3}(r_{k+(1/2)}^3 - r_{k-(1/2)}^3)\phi_k = \frac{4\pi}{3}(r_{k+(1/2)}^3 - r_{k-(1/2)}^3)Q_{0k}, \qquad (3.41)$$

where $\Delta_{k+(1/2)} = r_{k+1} - r_k$, etc. In order, from left to right, the terms represent the following quantities: net flow of neutrons across the outer surface of the region, net flow across the inner surface, absorption, and source. The difference equations (3.41) are again of the form of equation (3.20), and the same methods of solution may be used.

In spherical geometry, the conditions at the origin must be imposed in place of one of the boundary conditions of plane geometry. For spherical geometry, the required conditions can be derived from equation (3.40) by integrating from $r = 0$ to $r = r_{1/2}$. In this way a two-term relation is obtained involving only ϕ_0 and ϕ_1. It could be written in the form of equation (3.41) by setting $\phi_{k-1} = 0$ and $r_{k-(1/2)} = 0$.

3.3d Expansions in General Geometry

The plane and spherical geometries considered so far are unique in the respect that there is everywhere a preferred direction in space, i.e., $\hat{\mathbf{x}}$ or $\hat{\mathbf{r}}$, and the neutron flux is independent of rotations about this direction. In other words, the flux distribution is azimuthally symmetrical. Thus, for these two geometries, the directional (Ω) dependence of the neutron flux can be specified with only one variable, μ. In any other geometry, the angular distribution of the flux will not have azimuthal symmetry and so an additional variable is necessary to represent direction. Examples of the choice of variables for different geometries were given in the appendix to Chapter 1. It is always possible, however, to expand the angular dependence of the neutron flux in a set of spherical harmonics.

If the unit vector Ω is specified by two angular coordinates, i.e., a polar angle θ and an azimuthal angle φ, then the expansion for the angular flux in one-speed theory may be written as

$$\Phi(\mathbf{r}, \Omega) = \sum_{l=0}^{\infty} \sum_{m=-l}^{l} \phi_{lm}(\mathbf{r})\, Y_{lm}(\theta, \varphi),$$

where the functions Y_{lm} are the spherical harmonics (see Appendix). The latter are expressed in terms of associated Legendre functions P_l^m of $\mu(= \cos\theta)$ and trigonometric functions as

$$Y_{lm}(\theta, \varphi) = \sqrt{\frac{2l+1}{4\pi}\frac{(l-m)!}{(l+m)!}}\, P_l^m(\mu) e^{im\varphi}.$$

The usefulness of the spherical harmonics depends on the following properties: (*a*) they are a complete set of functions in the sense that any continuous function of θ and φ may be expanded in spherical harmonics, (*b*) they are orthonormal, and (*c*) when the scattering function, σ_s, is expanded in Legendre polynomials, as before, the orthogonality of the spherical harmonics leads to simplifications, as will be seen in §3.3e.

When the angular dependence of the neutron flux is expanded in a set of spherical harmonics, the resulting equations are relatively complicated, because of the streaming term $(\Omega \cdot \nabla\Phi)$ in the transport equation, and they will not be given here.[11] The special case of cylindrical geometry will, however, be examined in §3.6b.

3.3e The P_1 Approximation in General Geometry

For the present purpose, it is sufficient to consider the P_1 approximation only in general geometry. This can be derived by systematically truncating the spherical harmonics expansion, but an alternative derivation may provide better physical insight into the situation.

It follows from equation (2.57) that, in both plane and spherical geometries, the P_1 approximation is equivalent to assuming that

$$\Phi(x, \mu) = \frac{1}{4\pi}[\phi_0(x) + 3\mu\phi_1(x)], \tag{3.42}$$

where r will replace x in spherical geometry. As seen in §3.1d, $\phi_0(x)$ is the total flux and $\phi_1(x)$ is the neutron current in the x direction; hence, in the P_1 approximation,

$$\Phi(x, \mu) = \frac{1}{4\pi}[\phi(x) + 3\mu J(x)]. \tag{3.43}$$

This relation cannot apply in general since J is usually a vector instead of the scalar appearing in equation (3.43), but the latter can be extended to general

geometry. In particular, $\mu J(x)$ is equal to $\mathbf{\Omega}\cdot\mathbf{J}(x)$, so that equation (3.43) may be written as

$$\Phi(\mathbf{r}, \mathbf{\Omega}) = \frac{1}{4\pi}[\phi(\mathbf{r}) + 3\mathbf{\Omega}\cdot\mathbf{J}(\mathbf{r})]. \tag{3.44}$$

This result is correct for plane and spherical geometries and it can be proved to be the P_1 approximation to the angular flux, independent of geometry, by carrying out the expansion in spherical harmonics.

It will now be shown that the P_1 approximation to Φ, as given by equation (3.44), is consistent with the definitions of ϕ and J. For this purpose, certain mathematical identities are required and these are collected for convenience in Table 3.1; the coordinate system used in the derivation is given in the appendix to this chapter.

If equation (3.44) is integrated over $\mathbf{\Omega}$, the result is

$$\int \Phi(\mathbf{r}, \mathbf{\Omega})\, d\mathbf{\Omega} = \frac{1}{4\pi}\left[\phi(\mathbf{r})\int d\mathbf{\Omega} + 3\mathbf{J}(\mathbf{r})\cdot\int \mathbf{\Omega}\, d\mathbf{\Omega}\right], \tag{3.45}$$

where $\phi(\mathbf{r})$ and $\mathbf{J}(\mathbf{r})$ have been placed outside the integrals because they do not depend on $\mathbf{\Omega}$. The left side of this equation is simply the total flux $\phi(\mathbf{r})$ and the values of the integrals on the right side are obtained from Table 3.1. It is then seen that equation (3.45) reduces to the identity

$$\phi(\mathbf{r}) \equiv \phi(\mathbf{r}).$$

Upon multiplying equation (3.45) by $\mathbf{\Omega}$ and integrating over $\mathbf{\Omega}$, it is found that

$$\int \mathbf{\Omega}\Phi(\mathbf{r}, \mathbf{\Omega})\, d\mathbf{\Omega} = \frac{1}{4\pi}\left[\phi(\mathbf{r})\int \mathbf{\Omega}\, d\mathbf{\Omega} + 3\left\{\mathbf{J}(\mathbf{r})\cdot\int \mathbf{\Omega}\right\}\mathbf{\Omega}\, d\mathbf{\Omega}\right]. \tag{3.46}$$

The left side is, by definition, $\mathbf{J}(\mathbf{r})$; by using the second and third identities in Table 3.1, the first term on the right side of equation (3.46) is found to be zero

TABLE 3.1. MATHEMATICAL IDENTITIES

$\int d\mathbf{\Omega} = 4\pi$
$\int \mathbf{\Omega}\, d\mathbf{\Omega} = 0$
$\int \mathbf{\Omega}(\mathbf{\Omega}\cdot\mathbf{A})\, d\mathbf{\Omega} = \frac{4\pi}{3}\mathbf{A}$
$\int (\mathbf{\Omega}\cdot\mathbf{A})(\mathbf{\Omega}\cdot\mathbf{B})\, d\mathbf{\Omega} = \frac{4\pi}{3}\mathbf{A}\cdot\mathbf{B}$
A and B are any two vectors that are not dependent on $\mathbf{\Omega}$.

whereas the second term is $\mathbf{J}(\mathbf{r})$. Hence, both sides of the equation are equal to $\mathbf{J}(\mathbf{r})$, again indicating consistency of equation (3.44). This equation will consequently be taken to represent the P_1 approximation for the neutron angular flux distribution in general geometry.

The time-independent form of the one-speed transport equation was given in equation (3.2), and it will be repeated here for convenience; thus,

$$\boldsymbol{\Omega}\cdot\nabla\Phi(\mathbf{r},\boldsymbol{\Omega}) + \sigma(\mathbf{r})\Phi(\mathbf{r},\boldsymbol{\Omega}) = \int \sigma_s(\mathbf{r},\boldsymbol{\Omega}\cdot\boldsymbol{\Omega}')\Phi(\mathbf{r},\boldsymbol{\Omega}')\,d\boldsymbol{\Omega}' + Q(\mathbf{r},\boldsymbol{\Omega}). \tag{3.47}$$

It will be recalled that in obtaining this equation the reasonable assumption was made that the scattering function, σ_s, depends only on $\boldsymbol{\Omega}\cdot\boldsymbol{\Omega}'$. Hence, σ_s can be expanded in Legendre polynomials, $P_l(\mu_0)$. By use of the addition theorem of spherical harmonics (see Appendix), equation (3.47) then becomes

$$\begin{aligned}\boldsymbol{\Omega}\cdot\nabla\Phi(\mathbf{r},\boldsymbol{\Omega}) + \sigma(\mathbf{r})\Phi(\mathbf{r},\boldsymbol{\Omega}) = \int \sum_{l=0}^{\infty} \frac{2l+1}{4\pi}\,\sigma_{sl}(\mathbf{r}) \\ \times \left[P_l(\mu)P_l(\mu') + 2\sum_{m=1}^{l}\frac{(l-m)!}{(l+m)!}P_l^m(\mu)P_l^m(\mu')\cos m(\varphi-\varphi')\right] \\ \times \Phi(\mathbf{r},\boldsymbol{\Omega}')\,d\boldsymbol{\Omega}' + Q(\mathbf{r},\boldsymbol{\Omega}).\end{aligned} \tag{3.48}$$

As before, μ' and φ' are the coordinates specifying $\boldsymbol{\Omega}'$, whereas μ and φ specify $\boldsymbol{\Omega}$. (The coordinates might be given in any of the systems in §1.7a, where, however, the azimuthal direction coordinate has the symbol χ or ω, rather than φ.)

If the P_1 approximation for $\Phi(\mathbf{r},\boldsymbol{\Omega})$, i.e., equation (3.44), is introduced into equation (3.48), all the integrals over $\boldsymbol{\Omega}'$ on the right side are zero, except those for which $l = 0$ or $l = 1$ (see Appendix). For $l = 0$, the quantity in the square bracket in equation (3.48) reduces to unity and the integral over $\boldsymbol{\Omega}'$ gives $\sigma_{s0}(\mathbf{r})\phi(\mathbf{r})$; for $l = 1$, the square bracket is $\cos\theta\cos\theta' + \sin\theta\sin\theta'\cos(\varphi-\varphi')$, where $\theta = \cos^{-1}\mu$ and $\theta' = \cos^{-1}\mu'$, and the integral over $\boldsymbol{\Omega}'$ is equal to $3\sigma_{s1}\boldsymbol{\Omega}\cdot\mathbf{J}$. Hence equation (3.48) becomes

$$\begin{aligned}\boldsymbol{\Omega}\cdot\nabla[\phi(\mathbf{r}) + 3\boldsymbol{\Omega}\cdot\mathbf{J}(\mathbf{r})] + \sigma[\phi(\mathbf{r}) + 3\boldsymbol{\Omega}\cdot\mathbf{J}(\mathbf{r})] \\ = \sigma_{s0}(\mathbf{r})\phi(\mathbf{r}) + 3\sigma_{s1}(\mathbf{r})\boldsymbol{\Omega}\cdot\mathbf{J}(\mathbf{r}) + 4\pi Q(\mathbf{r},\boldsymbol{\Omega}).\end{aligned} \tag{3.49}$$

Integration of equation (3.49) and use of the last identity in Table 3.1, with $\mathbf{A}$ equivalent to ∇ and $\mathbf{B}$ to $\mathbf{J}$, gives

$$\nabla\cdot\mathbf{J}(\mathbf{r}) + \sigma_0(\mathbf{r})\phi(\mathbf{r}) = Q_0(\mathbf{r}), \tag{3.50}$$

where σ_0 and Q_0 are defined by

$$\sigma_0(\mathbf{r}) \equiv \sigma(\mathbf{r}) - \sigma_{s0}(\mathbf{r}) \quad \text{and} \quad Q_0(\mathbf{r}) \equiv \int Q(\mathbf{r},\boldsymbol{\Omega})\,d\boldsymbol{\Omega}.$$

Next, equation (3.49) is multiplied by Ω and integrated over Ω; the result, based on the identities in Table 3.1, is found to be

$$\nabla\phi(\mathbf{r}) + 3\sigma_1(\mathbf{r})\mathbf{J}(\mathbf{r}) = 3\mathbf{Q}_1(\mathbf{r}), \tag{3.51}$$

where

$$\sigma_1(\mathbf{r}) \equiv \sigma(\mathbf{r}) - \sigma_{s1}(\mathbf{r}) \quad \text{and} \quad \mathbf{Q}_1(\mathbf{r}) \equiv \int \Omega Q(\mathbf{r}, \Omega)\, d\Omega.$$

Equations (3.50) and (3.51) are the P_1 approximations to the neutron transport equation in general geometry. It should be observed that equation (3.50) is exact, since it is precisely equivalent to the time-independent conservation equation (1.17). On the other hand, equation (3.51) represents a P_1 approximation; in an exact spherical harmonics equation additional terms, arising from the streaming term in the transport equation, would be included on the left side of equation (3.51).

If the source is isotropic, $Q_1(\mathbf{r})$ is zero and then equation (3.51) may be written in the form of Fick's law of diffusion, i.e.,

$$\mathbf{J}(\mathbf{r}) = -D\nabla\phi(\mathbf{r}),$$

where $D = 1/3\sigma_1$. As in §3.1d, this may be used to eliminate $\mathbf{J}(\mathbf{r})$ from equation (3.50) to yield the familiar diffusion equation

$$-\nabla \cdot D\nabla\phi(\mathbf{r}) + \sigma_0(\mathbf{r})\phi(\mathbf{r}) = Q_0(\mathbf{r}). \tag{3.52}$$

The preceding development has shown the kind of assumptions involved in a systematic derivation of Fick's law from the one-speed neutron transport equation. Their significance in multigroup theory will be examined in the next chapter.

3.3f The P_1 Approximation in One-Dimensional Geometries

The P_1 equations for general geometry involve exactly the same cross sections, i.e., $\sigma_0(\mathbf{r})$ and $\sigma_1(\mathbf{r})$, as do the P_1 equations in plane geometry. The geometry enters only through the explicit forms of the gradient and divergence operators, apart from the boundary conditions.

In spherical coordinates, the radial component of the divergence is

$$\frac{1}{r^2}\frac{d(r^2 J_r)}{dr} = \left(\frac{d}{dr} + \frac{2}{r}\right) J_r,$$

and this is just the form in the P_1 equation (3.36). For an infinitely long cylinder, the current is also radial, so that

$$\nabla \cdot \mathbf{J} = \frac{1}{r}\frac{d(rJ_r)}{dr} = \left(\frac{d}{dr} + \frac{1}{r}\right) J_r.$$

Thus, in three geometries, namely, plane, sphere, and infinite cylinder, where the

spatial distribution of the flux depends on only one coordinate, the first P_1 equation can be written in the general form

$$\left(\frac{d}{dr} + \frac{n}{r}\right) J(r) + \sigma_0 \phi(r) = Q_0(r), \tag{3.53}$$

where

$n = 0$ for plane
$n = 1$ for cylinder
$n = 2$ for sphere.

An alternative form of the first term is

$$\left(\frac{d}{dr} + \frac{n}{r}\right) J(r) = \frac{1}{r^n} \frac{d}{dr} [r^n J(r)].$$

It may be noted, too, that in equation (3.51) the current has a component in only one direction and that for spherical or cylindrical geometry $\nabla\phi = d\phi/dr$. Hence, equation (3.51) for these geometries in the P_1 approximation may be written

$$\frac{d\phi(r)}{dr} + 3\sigma_1(r) J(r) = 3Q_1(r). \tag{3.54}$$

Furthermore, a similar equation would apply in plane geometry with x replacing r.

The diffusion equation (3.52) for the three one-dimensional geometries may similarly be written as

$$-\frac{1}{r^n} \frac{d}{dr} \left[r^n D \frac{d\phi(r)}{dr} \right] + \sigma_0(r)\phi(r) = Q_0(r), \tag{3.55}$$

where n has the significance given above.

It is seen that equations of the same form, namely, equations (3.53) and (3.54) for the P_1 approximation and equation (3.55) for diffusion theory, are applicable to plane, infinite cylindrical, and spherical geometries. Similarly, difference equations may be developed for these three one-dimensional geometries and, except for minor variations in the boundary conditions, they can all be solved in the manner outlined in §3.2c. Problems in two-dimensional geometry are more complex and these will be considered for diffusion theory in the next section.

3.4 THE DIFFUSION EQUATION IN TWO DIMENSIONS

3.4a Difference Equations in Two Dimensions

Difference equations that approximate the P_1 and diffusion equations can be derived for systems requiring geometrical representation in two (or three) dimensions. As in §3.2c, a set of difference equations can be written as a matrix

equation which must be inverted to obtain the neutron flux at points in a two-dimensional space mesh. The matrix is, however, more complicated than that for a one-dimensional geometry, so that it is not practical to invert it directly; instead iterative methods must be used. Furthermore, the matrix is usually of much higher order since many more space points (typically of the order of 10^3) are required to approximate a two-dimensional system. For three-dimensional geometry, the number is, of course, even larger.

For simplicity, the difference equations will be examined for diffusion theory for a system in rectangular geometry in two dimensions. If the space coordinates are x and y, the diffusion equation (3.52) for $\phi(x, y)$ becomes

$$-\frac{\partial}{\partial x}\left(D\frac{\partial \phi}{\partial x}\right) - \frac{\partial}{\partial y}\left(D\frac{\partial \phi}{\partial y}\right) + \sigma_0 \phi = Q_0. \tag{3.56}$$

A rectangular mesh is constructed consisting of points whose coordinates are, in general,

$$x_k \quad \text{with} \quad k = 0, 1, 2, \ldots, K$$

and

$$y_m \quad \text{with} \quad m = 0, 1, 2, \ldots, M.$$

Let $\phi(x_k, y_m)$ be represented by $\phi_{k,m}$. As before, it is convenient to have space points located on the interfaces between regions. For simplicity, however, in the following treatment a single region will be considered in which D, σ_0, and mesh spacing are constant. A portion of the mesh is shown in Fig. 3.4.

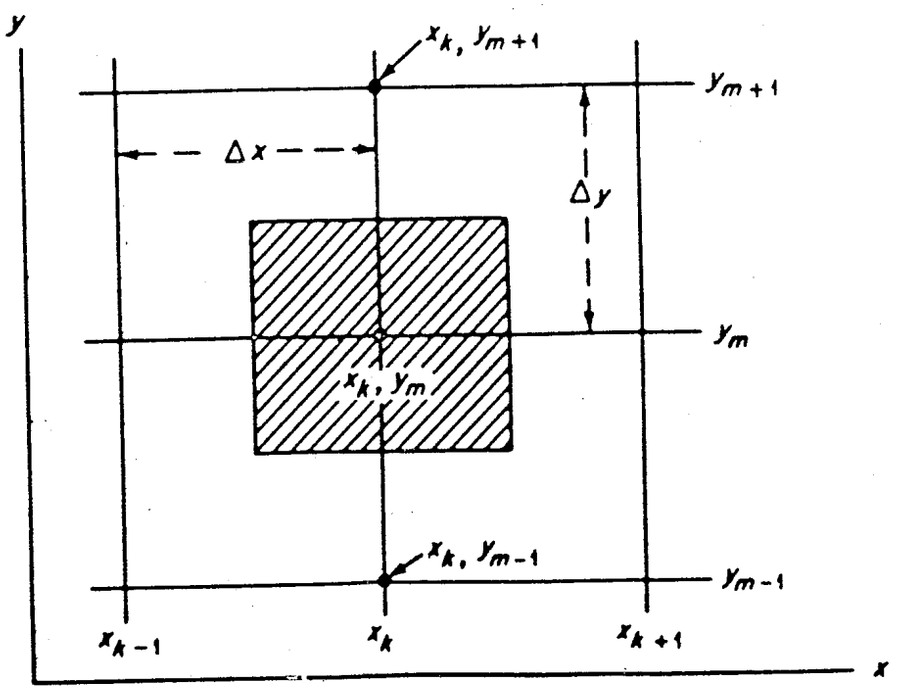

FIG. 3.4 MESH POINTS IN TWO DIMENSIONS.

Equation (3.56) is now integrated over the small shaded rectangle which is bounded by the lines $x = x_k \pm \frac{1}{2}\Delta x$ and $y = y_m \pm \frac{1}{2}\Delta y$; the result is

$$-D\int_{y_m-(1/2)\Delta y}^{y_m+(1/2)\Delta y} dy\left(\frac{\partial\phi}{\partial x}\right)_{x_k-(1/2)\Delta x}^{x_k+(1/2)\Delta x} - D\int_{x_k-(1/2)\Delta x}^{x_k+(1/2)\Delta x} dx\left(\frac{\partial\phi}{\partial y}\right)_{y_m-(1/2)\Delta y}^{y_m+(1/2)\Delta y}$$

$$+\sigma_0\int_{x_k-(1/2)\Delta x}^{x_k+(1/2)\Delta x} dx\int_{y_m-(1/2)\Delta y}^{y_m+(1/2)\Delta y}\phi\,dy = \int dx\int dy Q_0. \quad (3.57)$$

The derivatives are approximated by

$$\frac{\partial\phi}{\partial x}\Bigg|_{x_k-(1/2)\Delta x}^{x_k+(1/2)\Delta x} \simeq \frac{\phi_{k+1,m}-\phi_{k,m}}{\Delta x} - \frac{\phi_{k,m}-\phi_{k-1,m}}{\Delta x}$$

$$= \frac{\phi_{k+1,m}-2\phi_{k,m}+\phi_{k-1,m}}{\Delta x}$$

and similarly for y, and each integral is approximated by the value of the integrand at the midpoint multiplied by the range of integration; equation (3.57) then becomes

$$-D\frac{\Delta y}{\Delta x}[\phi_{k+1,m}-2\phi_{k,m}+\phi_{k-1,m}] - D\frac{\Delta x}{\Delta y}[\phi_{k,m+1}-2\phi_{k,m}+\phi_{k,m-1}]$$

$$+\sigma_0\,\Delta x\Delta y\phi_{k,m} = \Delta x\Delta y Q_{k,m} \quad (3.58)$$

or, after collecting coefficients of $\phi_{k,m}$,

$$-D\frac{\Delta y}{\Delta x}[\phi_{k+1,m}+\phi_{k-1,m}] - D\frac{\Delta x}{\Delta y}[\phi_{k,m+1}+\phi_{k,m-1}]$$

$$+\phi_{k,m}\left[\sigma_0\Delta x\Delta y + 2D\left\{\frac{\Delta x}{\Delta y}+\frac{\Delta y}{\Delta x}\right\}\right] = \Delta x\Delta y Q_{k,m}. \quad (3.59)$$

Although more complicated and somewhat more accurate approximations could be written for the integrals in equation (3.57), the simple approximations given above are usually adequate for diffusion theory calculations.[12] To some extent, it is possible to choose between a fine mesh with simple coefficients in the difference equations, and a coarser mesh with more complicated coefficients.

3.4b Two-Dimensional Difference Equations in Matrix Form

The set of equations (3.59) can be written in matrix form. To do this, it is necessary only to introduce a consistent ordering of the ϕ terms, so that a rectangular array of $\{\phi_{k,m}\}$ can be represented by a vector, $\boldsymbol{\phi}$. An obvious choice is to start in the lower left corner and number a row at a time. All boundary points are eliminated by the use of boundary conditions, e.g., for free surfaces, by setting

$$\phi_{k,m} = 0 \quad \text{if} \quad k = 0 \text{ or } K$$

and

$$\phi_{k,m} = 0 \quad \text{if} \quad m = 0 \text{ or } M.$$

A single index

$$j = 1, 2, \ldots, (K-1)(M-1),$$

where

$$j = k + (m-1)(K-1),$$

is used to identify the vector components, ϕ_j.

With this ordering to define the components of a vector $\boldsymbol{\phi}$, the set of difference equations (3.59) can be written in matrix form [cf. equation (3.25)] as

$$\mathbf{A}\boldsymbol{\phi} = \mathbf{s}. \tag{3.60}$$

The diagonal components of the matrix $\mathbf{A}$, represented by $\sigma_0 \Delta x \Delta y + 2D[(\Delta x/\Delta y) + (\Delta y/\Delta x)]$, are once more positive, whereas those off the diagonal, e.g., $-D(\Delta y/\Delta x)$, are negative or zero; the sum of the off-diagonal elements in any one row is less than the diagonal element. Thus, the matrix $\mathbf{A}$ has diagonal dominance and satisfies properties (i) and (iii) of §3.2c. It is, however, no longer tridiagonal, for in every row there are four nonzero off-diagonal elements, except for the rows corresponding to points adjacent to the boundaries, which have only three such elements. The matrix is still irreducible, but now $a_{j,j+1} = 0$ for points adjacent to the right and left boundaries, i.e., when the point j is next to the right boundary, point $j+1$ is next to the left boundary and hence there is no term coupling these two points. In any event, the matrix $\mathbf{A}$ is again irreducibly diagonally dominant; therefore, it has an inverse[13] and equation (3.60) can be solved for $\boldsymbol{\phi}$ in terms of $\mathbf{s}$, by writing $\boldsymbol{\phi} = \mathbf{A}^{-1}\mathbf{s}$, as before.

3.4c Solving the Matrix Equations by Iteration

Since it is now not practical to invert the whole matrix $\mathbf{A}$ directly, iterative methods are used. To understand the principle involved, let the matrix $\mathbf{A}$ be written as the sum of three matrices, i.e.,

$$\mathbf{A} = \mathbf{D} - \mathbf{U} - \mathbf{L}, \tag{3.61}$$

where $\mathbf{D}$ is a diagonal (nonzero entries only on main diagonal), $\mathbf{U}$ is an upper triangular (nonzero entries only above main diagonal), and $\mathbf{L}$ is a lower triangular (nonzero entries only below main diagonal) matrix.

Because of the diagonal dominance of $\mathbf{A}$, the elements of $\mathbf{D}$ are, generally speaking, larger than those of $\mathbf{U}$ and $\mathbf{L}$. This suggests the possibility of moving the smaller, off-diagonal terms to the right side of equation (3.60) to give

$$\mathbf{D}\boldsymbol{\phi} = [\mathbf{U} + \mathbf{L}]\boldsymbol{\phi} + \mathbf{s}, \tag{3.62}$$

for which a solution may be sought by iteration. First, it is convenient to multiply both sides of equation (3.62) by $\mathbf{D}^{-1}$, the inverse of $\mathbf{D}$, such that $\mathbf{D}^{-1}\mathbf{D} = \mathbf{I}$, the unit matrix. Since $\mathbf{D}$ is a diagonal matrix, every element in $\mathbf{D}^{-1}$ is the reciprocal of the corresponding element in $\mathbf{D}$, i.e., $(\mathbf{D}^{-1})_{jj} = 1/(\mathbf{D})_{jj}$; hence, $\mathbf{D}^{-1}$ is

readily derived from $\mathbf{D}$. As a result of the multiplication by $\mathbf{D}^{-1}$ it is found that equation (3.62) becomes

$$\boldsymbol{\phi} = \mathbf{D}^{-1}[\mathbf{U} + \mathbf{L}]\boldsymbol{\phi} + \mathbf{D}^{-1}\mathbf{s}. \tag{3.63}$$

A guess is now made for $\boldsymbol{\phi}$, namely $\boldsymbol{\phi}^{(0)}$, on the right side of this equation, which is then solved for $\boldsymbol{\phi}$, indicated by $\boldsymbol{\phi}^{(1)}$ on the left. An iterative process can then be defined by

$$\boldsymbol{\phi}^{(i+1)} = \mathbf{D}^{-1}[\mathbf{U} + \mathbf{L}]\boldsymbol{\phi}^{(i)} + \mathbf{D}^{-1}\mathbf{s}, \tag{3.64}$$

where $\boldsymbol{\phi}^{(i)}$ is the vector which has been found after i iterations. This procedure converges to a correct solution, as may be seen from the following considerations. Let the error vector $\boldsymbol{\epsilon}^{(i)}$ represent the difference between $\boldsymbol{\phi}^{(i)}$ and the true solution $\boldsymbol{\phi}$, i.e.,

$$\boldsymbol{\epsilon}^{(i)} = \boldsymbol{\phi}^{(i)} - \boldsymbol{\phi}.$$

Then $\boldsymbol{\epsilon}^{(i)}$ satisfies the homogeneous equation

$$\boldsymbol{\epsilon}^{(i+1)} = \mathbf{D}^{-1}[\mathbf{U} + \mathbf{L}]\boldsymbol{\epsilon}^{(i)}.$$

If the error vector $\boldsymbol{\epsilon}^{(0)}$ is expanded as a sum of the eigenvectors of $\mathbf{D}^{-1}[\mathbf{U} + \mathbf{L}]$ times arbitrary coefficients,* each iteration multiplies an eigenvector by its corresponding eigenvalue. It will be shown below that all eigenvalues of the matrix $\mathbf{D}^{-1}[\mathbf{U} + \mathbf{L}]$ have absolute values less than unity; hence, it follows that

$$\boldsymbol{\epsilon}^{(i)} \to 0 \quad \text{as} \quad i \to \infty.$$

To show that the eigenvalues of $\mathbf{C} = \mathbf{D}^{-1}[\mathbf{U} + \mathbf{L}]$ are less than unity, it should be noted that the matrix $\mathbf{C}$ has positive or zero elements and that the sum of the elements in any row is less than unity, i.e.,

$$\sum_j C_{ij} < 1.$$

Suppose $\mathbf{x}$ is the eigenvector with the largest eigenvalue, λ, then

$$C\mathbf{x} = \lambda\mathbf{x}.$$

If the element x_i is as large in magnitude as any element of x, then

$$\sum_j C_{ij}x_j = \lambda x_i$$

or

$$\lambda = \sum_j C_{ij}(x_j/x_i).$$

* Such an expansion is always possible since the eigenvectors of a real symmetric matrix form an acceptable basis for this expansion and $\mathbf{D}^{-1}[\mathbf{U} + \mathbf{L}]$ is a real symmetric matrix.[14]

By taking absolute values and noting that $|C_{ij}| = C_{ij}$, it follows that

$$|\lambda| \leqslant \sum_j C_{ij}(|x_j/x_i|).$$

But since $(|x_j/x_i|) \leqslant 1$, by choice of i,

$$|\lambda| \leqslant \sum C_{ij} < 1.$$

Thus it has been shown that the largest eigenvalue is less than unity; consequently, all the eigenvalues of the matrix $\mathbf{D}^{-1}[\mathbf{U} + \mathbf{L}]$ must be less than unity. The eigenvalue having the largest absolute magnitude is called the *spectral radius* of the matrix. Hence, the foregoing result is that the spectral radius of $\mathbf{D}^{-1}[\mathbf{U} + \mathbf{L}]$ is less than unity.

The iteration procedure described above is sometimes known as the *point Jacobi* or *Richardson method.*[15] Although it is workable, it is not nearly as rapidly convergent as several other iterative techniques. Basically, the reason is that the spectral radius of $\mathbf{D}^{-1}[\mathbf{U} + \mathbf{L}]$ is usually quite close to unity, and so the error dies away slowly.

3.4d Improved Iteration Procedures

More powerful iterative methods are available,[16] but their detailed treatment lies outside the scope of this text. Brief mention may be made, however, of some iterative procedures of interest. The first is motivated by the following physical consideration. Suppose that equation (3.64) is being used to obtain the flux vector $\boldsymbol{\phi}^{(l+1)}$. In computing any component of $\boldsymbol{\phi}^{(l+1)}$, for example $\phi_j^{(l+1)}$, only values of the flux from the last iteration, i.e., $\boldsymbol{\phi}^{(l)}$, will be used on the right-hand side of the equation. It would seem, therefore, that once a new component, $\phi_j^{(l+1)}$, has been computed, it would be advantageous to use it, instead of $\phi_j^{(l)}$, for determining the subsequent components of $\boldsymbol{\phi}^{(l+1)}$, i.e., the components $\phi_k^{(l+1)}$ with $k > j$. Thus, a new flux component would affect the flux calculation before the iteration is completed.

The iterative scheme

$$[\mathbf{D} - \mathbf{L}]\boldsymbol{\phi}^{(l+1)} = \mathbf{U}\boldsymbol{\phi}^{(l)} + \mathbf{s} \tag{3.65}$$

is just such a procedure; it is referred to as the *Liebmann* or *Gauss-Seidel method.* Since the matrix $[\mathbf{D} - \mathbf{L}]$ is triangular, including the main diagonal, its inverse can be found readily or, what amounts to the same thing, equation (3.65) can be solved for $\boldsymbol{\phi}^{(l+1)}$. Thus, consider equation (3.65) as a set of equations for the components of $\boldsymbol{\phi}^{(l+1)}$. The first contains only one component, i.e., $\phi_1^{(l+1)}$, which can be solved for directly; the second contains two components, i.e., $\phi_1^{(l+1)}$ and $\phi_2^{(l+1)}$, one being known and the other can be solved for, etc. In this way all of the $\phi_j^{(l+1)}$ can be evaluated successively for $j = 1, 2, \ldots$. Hence, in determining $\phi_j^{(l+1)}$ each of the components of $\boldsymbol{\phi}^{(l+1)}$ is used as it is computed.

A further generalization of the foregoing method is suggested by the following considerations. If $\phi_j^{(i+1)}$ differs significantly from $\phi_j^{(i)}$, it is reasonable to suppose that a better estimate could be obtained by extrapolating somewhat beyond $\phi_j^{(i+1)}$ given by equation (3.65). In order to do this, equation (3.65) is rearranged in the form

$$\boldsymbol{\phi}_L^{(i+1)} = \mathbf{D}^{-1}[\mathbf{U}\boldsymbol{\phi}_L^{(i)} + \mathbf{L}\boldsymbol{\phi}_L^{(i+1)} + \mathbf{s}], \tag{3.66}$$

where the flux vector has been given the subscript L to indicate that the Liebmann iterative procedure is being considered. To obtain an extrapolated estimate of $\boldsymbol{\phi}^{(i+1)}$ no longer equal to $\boldsymbol{\phi}_L^{(i+1)}$, the quantity $(\omega - 1)(\boldsymbol{\phi}^{(i+1)} - \boldsymbol{\phi}^{(i)})$, where ω is a constant larger than unity, could be added to the right side of equation (3.66). If in this added term $\boldsymbol{\phi}^{(i+1)}$ is replaced by $\mathbf{D}^{-1}(\mathbf{U}\boldsymbol{\phi}^{(i)} + \mathbf{L}\boldsymbol{\phi}^{(i+1)} + \mathbf{s})$, the iterative scheme

$$\boldsymbol{\phi}^{(i+1)} = \omega\mathbf{D}^{-1}[\mathbf{U}\boldsymbol{\phi}^{(i)} + \mathbf{L}\boldsymbol{\phi}^{(i+1)} + \mathbf{s}] + (1 - \omega)\boldsymbol{\phi}^{(i)} \tag{3.67}$$

is obtained. If equation (3.67) is now multiplied through by $\mathbf{D}$ and rearranged, the result is

$$(\mathbf{D} - \omega\mathbf{L})\boldsymbol{\phi}^{(i+1)} = [(1 - \omega)\mathbf{D} + \omega\mathbf{U}]\boldsymbol{\phi}^{(i)} + \omega\mathbf{s}. \tag{3.68}$$

This is known as the *accelerated Liebmann method* or the *point successive overrelaxation method.* The quantity ω is the acceleration parameter and if properly chosen gives a very effective iteration scheme. It is readily verified that for any ω this equation is satisfied by $\boldsymbol{\phi}^{(i)} = \boldsymbol{\phi}^{(i+1)} = \boldsymbol{\phi}$, the exact solution.

The optimum value of ω may be estimated by recalling (§3.4c) that the rate of decay of an error in the initial estimate of $\boldsymbol{\phi}$, i.e., $\boldsymbol{\phi}^{(0)}$, is dependent upon the spectral radius of a matrix. This spectral radius thus determines the rate of convergence of the iterative scheme. If, in the present case, the ith flux iterate is again written as

$$\boldsymbol{\phi}^{(i)} = \boldsymbol{\phi} + \boldsymbol{\epsilon}^{(i)},$$

where $\boldsymbol{\phi}$ is the true solution and $\boldsymbol{\epsilon}^{(i)}$ is the error vector, then it is found from equation (3.68) that $\boldsymbol{\epsilon}^{(i+1)}$ satisfies

$$\boldsymbol{\epsilon}^{(i+1)} = [\mathbf{D} - \omega\mathbf{L}]^{-1}[(1 - \omega)\mathbf{D} + \omega\mathbf{U}]\boldsymbol{\epsilon}^{(i)} = \mathbf{C}^*(\omega)\boldsymbol{\epsilon}^{(i)}. \tag{3.69}$$

where this equation defines the matrix $\mathbf{C}^*(\omega)$. From the arguments in §3.4c, it follows that the optimum value of ω will be that which leads to the smallest (absolute) value of the spectral radius of $\mathbf{C}^*(\omega)$. Methods for estimating the eigenvalues of matrices may thus be used for finding the optimum acceleration parameter.[17]

By using the iterative procedures described above, or even better ones,[18] a satisfactory solution for the vector $\boldsymbol{\phi}$ can readily be obtained with a fast computer even when the space mesh contains thousands of points. It will be seen in the next chapter that, in multigroup theory, the iterations for determining the spatial distribution of the neutron flux (within a single energy group) are called

"inner" iterations. This distinguishes them from the "outer" iterations used in criticality and related calculations (§4.4d).

3.4e Difference Equations for More General Cases

The results in the preceding sections have referred in particular to difference equations derived for rectangular geometry. Similar equations may also be developed for other two-dimensional geometries,[19] although the geometrical factors in the coefficients are more complicated. The same methods of solving difference equations can be used in both cases.

For three-dimensional geometry, the difference equations at a point would involve coupling with six other points, rather than with four points as in equation (3.59). Nevertheless, the same kinds of iterative methods can be employed to solve the equations. In three dimensions, however, the number of mesh points required to represent a reactor is often so large that the computations become impractical. Other approaches will be referred to in Chapters 6 and 10.

Although the difference equations have been derived here for diffusion theory, analogous equations may be readily obtained for the P_1 approximation. When the P_1 or diffusion theories do not represent the angular flux adequately, more general expansions in spherical harmonics may be used. Their application to plane and spherical geometries has already been considered and will be described for cylindrical geometry in §3.6b. For more complex geometries, the spherical harmonics methods are so complicated that alternative procedures, especially the method of discrete ordinates (Chapter 5) and Monte Carlo techniques, have generally been used.

3.5 THE DOUBLE-P_N APPROXIMATION

3.5a Discontinuity of Angular Flux at an Interface

The Legendre expansion of the flux has an important deficiency in plane geometry. At a plane interface, the neutron angular flux distribution, as a function of μ, will generally be discontinuous at $\mu = 0$. But any finite sum of Legendre polynomials over the range $-1 \leqslant \mu \leqslant 1$ will be continuous at $\mu = 0$, and so will be a poor representation of the angular flux near interfaces. This difficulty is also responsible for the uncertainty in the free-surface boundary conditions; as stated in §2.5d, the boundary conditions cannot be satisfied exactly and various approximations have been proposed. These considerations have led to the suggestion that separate expansions be used for the angular ranges $-1 \leqslant \mu \leqslant 0$ and $0 \leqslant \mu \leqslant 1$.

Before proceeding further, it is necessary to clarify the situation concerning the behavior of the neutron angular flux across an interface. The angular flux, $\Phi(x, \mu)$, is a function of both x and μ. It has been seen (cf. §3.1e) that, if μ is

fixed (and $\neq 0$), i.e., for a given direction, the angular density (or flux) must be continuous as a function of x across an interface. But, when considered as a function of μ, with x fixed at an interface, the angular flux is discontinuous at $\mu = 0$. That such is the case may be shown in the following manner.

Suppose there is a plane interface between two media at $x = x_0$ and consider the neutrons at x_0 having direction cosines $+\epsilon$ and $-\epsilon$, as represented in Fig. 3.5. All the neutrons at the interface having $\mu = +\epsilon$ will have come from the medium at the left of the interface, whereas those with $\mu = -\epsilon$ will have come from the medium at the right. Since the two media are different,

$$\Phi(x_0, +\epsilon) \neq \Phi(x_0, -\epsilon)$$

for any finite value of ϵ. Hence, the angular flux must be discontinuous at $\mu = 0$.

The magnitude of the discontinuity can be found from the integral form of the transport equation for plane geometry or by starting with the transport equation (3.3) in plane geometry and deriving the required integral equation from it. The latter procedure will be used here, with equation (3.3) written as

$$\mu \frac{\partial \Phi(x, \mu)}{\partial x} + \sigma(x)\Phi(x, \mu) = q(x, \mu) \tag{3.70}$$

where q stands for the whole right-hand side of equation (3.3) and is, therefore, discontinuous at the interface between two media. The values of σ and q in the medium at the left of the interface are represented by σ^- and q^-, respectively, and by σ^+ and q^+ for the medium at the right. If equation (3.70) is divided by μ

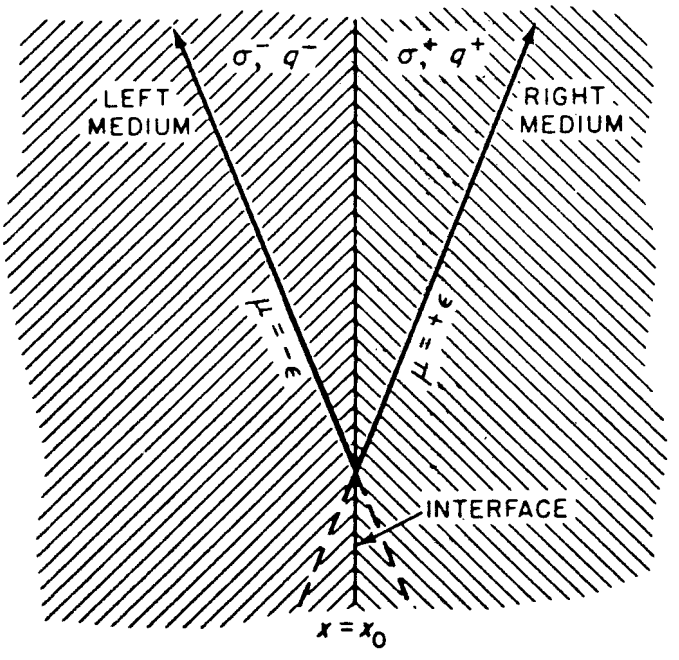

FIG. 3.5 ANGULAR FLUX AT A PLANE INTERFACE.

and multiplied throughout by the integrating factor $\exp\left[\int^x (\sigma/\mu)\,dx'\right]$, it is seen that

$$\frac{\partial}{\partial x}\left\{\Phi(x,\mu)\exp\left[\frac{1}{\mu}\int^x \sigma(x')\,dx'\right]\right\} = \frac{q(x,\mu)}{\mu}\exp\left[\frac{1}{\mu}\int^x \sigma(x')\,dx'\right]. \tag{3.71}$$

For $\mu = +\epsilon$, equation (3.71) is integrated from $x = -\infty$ to $x = x_0$; the result is

$$\Phi(x_0, +\epsilon) = \frac{1}{\epsilon}\int_{-\infty}^{x_0} \left\{q^-(x', +\epsilon)\exp\left[-\frac{1}{\epsilon}\int_{x'}^{x_0}\sigma^-(x'')\,dx''\right]\right\} dx',$$

noting that the neutrons to the right of the interface originate from the medium on the left.

When $+\epsilon$ is small, the only contribution to the integral comes from x' very close to x_0; hence q^- and σ^- may be set equal to their values at $x = x_0$; the integral can then be evaluated to yield

$$\Phi(x_0, +\epsilon) = \frac{q^-(x_0, +\epsilon)}{\sigma^-(x_0)}.$$

On the other hand, when $\mu = -\epsilon$, equation (3.71) is integrated from $x = \infty$ to $x = x_0$, and when $-\epsilon$ is numerically small, it is found in the manner described above that

$$\Phi(x_0, -\epsilon) = \frac{q^+(x_0, -\epsilon)}{\sigma^+(x_0)}.$$

Thus, the discontinuity in Φ at $\mu = 0$ is given by

$$\text{Discontinuity in } \Phi \text{ at } \mu = 0 = \lim_{\epsilon \to 0}\left[\Phi(x, +\epsilon) - \Phi(x_0, -\epsilon)\right]$$

$$= \frac{q^-(x_0, 0)}{\sigma^-(x_0)} - \frac{q^+(x_0, 0)}{\sigma^+(x_0)}.$$

The quantities $q^{\pm}(x_0, 0)$ can be calculated from the right-hand side of equation (3.3).

A simple and obvious example of discontinuity in the angular flux for $\mu = 0$ at an interface arises for the case of a free (planar) surface. If, in Fig. 3.5, there is a medium at the left of the boundary at x_0, from which neutrons can emerge, but there are no incoming neutrons, it follows that $\Phi(x_0, \mu)$ is finite for all values of $\mu > 0$, but is zero for all $\mu < 0$. Clearly, therefore, there must be a discontinuity in the angular flux for $\mu = 0$ at a free surface.

By applying the arguments developed above it can be shown that at a *curved* interface, the angular flux will *not* be discontinuous as a function of direction, μ. Consider a curved interface with a local radius of curvature R, as indicated in Fig. 3.6. In this case, neutrons moving with the direction cosine $\mu = \cos\theta$, as shown, can come from the source q^- over a distance $s = 2R\mu$ in the left medium, and from the source q^+ over the remainder of the reversed extrapolated path.

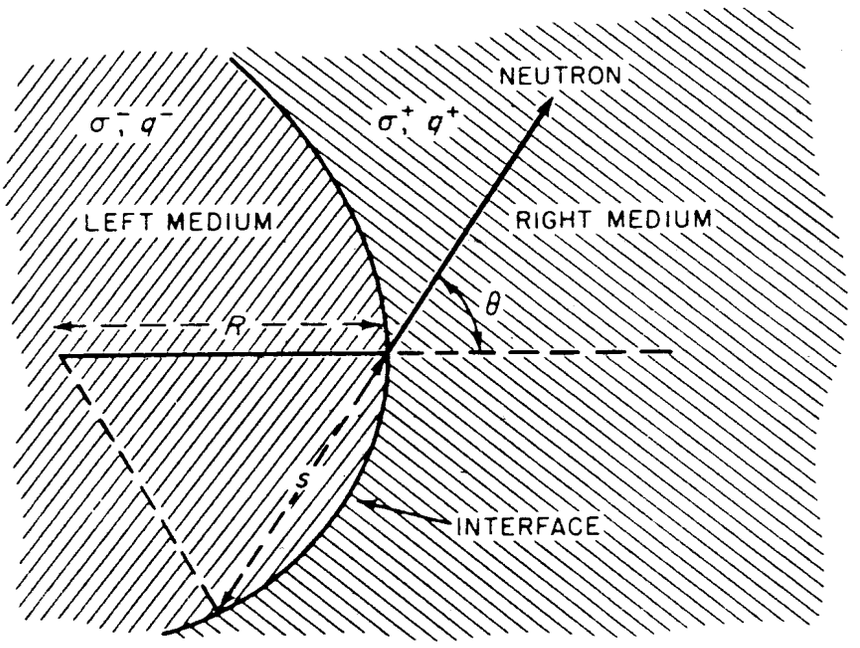

FIG. 3.6 ANGULAR FLUX AT A CURVED INTERFACE.

Thus, as $\mu \to 0$, so $s \to 0$, and the contribution to the angular flux from the neutron source q^- (and cross section σ^-) in the left medium approaches zero continuously. Hence, the angular flux will be continuous as a function of the direction μ, and there is no discontinuity for $\mu = 0$.*

3.5b Yvon's Method

When separate Legendre expansions are used for the two half-ranges in μ at a plane interface, the treatment is known as the double-P_N approximation or J. J. Yvon's method.[21] In this approximation it is possible to satisfy the free-surface boundary conditions exactly and also to allow for discontinuities at interfaces. As a result, the method is remarkably accurate in plane geometry (§5.2g).

In order to examine the double-P_N equations, a time-independent, one-speed transport problem will be considered in plane geometry with no source, i.e. equation (3.4) with $Q = 0$; thus,

$$\mu \frac{\partial \Phi(x, \mu)}{\partial x} + \sigma(x)\Phi(x, \mu) = \sum_{l=0}^{\infty} \frac{2l + 1}{2} \sigma_l(x) P_l(\mu) \int_{-1}^{1} \Phi(x, \mu') P_l(\mu')\, d\mu'. \qquad (3.72)$$

* Although the angular flux is not discontinuous at $\mu = 0$, its derivative with respect to μ will be discontinuous and the flux may change rapidly with μ near $\mu = 0$. Moreover, such discontinuities in the angular derivative are present at points outside the interface of Fig. 3.6 and for directions having $\mu > 0$.[20]

In the double P_N approximation, it is assumed that

$$\Phi(x, \mu) = \sum_{n=0}^{N} (2n + 1)[\phi_n^+(x)P_n^+(2\mu - 1) + \phi_n^-(x)P_n^-(2\mu + 1)] \tag{3.73}$$

with the following definitions:

$$\begin{aligned} P_n^+(2\mu - 1) &= P_n(2\mu - 1) \quad \mu \geqslant 0 \\ &= 0 \qquad\qquad\quad \mu < 0 \\ P_n^-(2\mu + 1) &= P_n(2\mu + 1) \quad \mu < 0 \\ &= 0 \qquad\qquad\quad \mu \geqslant 0. \end{aligned}$$

It will be noted that over a half-range the argument $(2\mu \mp 1)$ of the appropriate $P_n^{\pm}$ varies between -1 and $+1$.

Equation (3.73) may now be substituted into equation (3.72) and the result multiplied by $P_m^+(2\mu - 1)$ or $P_m^-(2\mu + 1)$; integration over μ from -1 to 1 then gives equations satisfied by $\phi_m^{\pm}(x)$. The left side can be treated in essentially the same way as the full P_N expansion and is no more complicated. The right-hand side, however, contains terms involving products of the full-range and half-range polynomials. If the constants p_{lm}^+ and p_{lm}^- are defined by

$$p_{lm}^+ = \int_{-1}^{1} P_l(\mu)P_m^+(2\mu - 1)\, d\mu$$

$$p_{lm}^- = \int_{-1}^{1} P_l(\mu)P_m^-(2\mu + 1)\, d\mu,$$

equation (3.72) becomes

$$\frac{m}{2m + 1}\frac{d\phi_{m-1}^{\pm}(x)}{dx} + \frac{m + 1}{2m + 1}\frac{d\phi_{m+1}^{\pm}(x)}{dx} \pm \frac{d\phi_m^{\pm}(x)}{dx} + 2\sigma(x)\phi_m^{\pm}(x)$$

$$= \sum_{l=0}^{\infty} (2l + 1)\, p_{lm}^{\pm}\sigma_l(x) \sum_{n=0}^{N} (2n + 1)[p_{ln}^+\phi_n^+(x) + p_{ln}^-\phi_n^-(x)]. \tag{3.74}$$

In the particular case of isotropic scattering, the sum over l has but one term, for $l = 0$; it then follows that $p_{0n}^{\pm}$ is equal to the Kronecker delta δ_{0n} (§2.4b) and the right-hand side of equation (3.74) is simply

$$\sigma_0(x)[\phi_0^+(x) + \phi_0^-(x)].$$

More generally, if the cross-section expansion is terminated at $l = L$, then the sum over n contains only terms with $n \leqslant L$. It is seen, however, that, as noted in §3.3d, the anisotropic scattering terms are more complicated than in P_N theory.[22]

With the double-P_N approximation, free-surface boundary conditions can be satisfied exactly. If the problem is over the domain $0 \leqslant x \leqslant a$, the free-surface conditions are simply

$$\phi_n^+(0) = 0 \quad \text{and} \quad \phi_n^-(a) = 0.$$

In the one-speed problem, and assuming $\sigma_l = 0$ for $l > 2$, the double-P_N equations can be cast into the same form as the few-group diffusion equations (cf. §4.3b) and may be solved in the same way.[23] Another method for solving very similar equations is given in §5.2d. In some examples in Chapter 5 it will be seen that for plane geometry the double-P_1 approximation is remarkably good; it is consistently better than the P_3 approximation and much better than P_1 theory. Double-P_N methods have been found to be useful for treating lattice problems which are often well approximated by plane geometry. The double-P_N approximation has also been applied in spherical geometry,[24] but here it seems to have no particular advantages (§5.3b).

3.6 REACTOR CELL CALCULATIONS

3.6a The Wigner-Seitz Approximation

In many reactors the fuel elements are arranged in a periodic manner, so that the system, at least in the central part of the core, can be regarded as being made up of a number of identical unit cells (Fig. 3.7). In these circumstances, spatial distribution of the neutron flux in the reactor will have a periodic fine structure which can be found by computing the flux within a unit cell. Such cell calculations have often been made by the method of spherical harmonics, particularly when the fuel element has a simple geometry, e.g., a cylinder as in Fig. 3.7. When the fuel elements have a more complicated shape, however, Monte Carlo calculations must be used.

Even when the fuel elements are cylindrical, geometrical problems arise because the cell boundary is not cylindrical, but more commonly has a square or hexagonal cross section. The flux in such a cell will actually be a function of three space variables. To simplify the problem, it is first assumed that the cell is

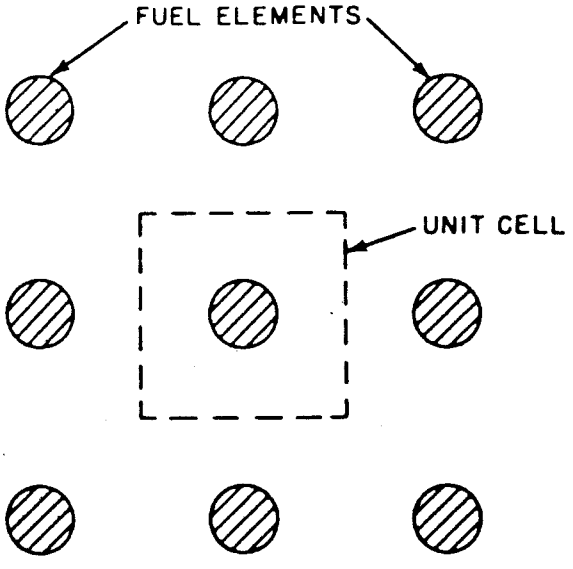

FIG. 3.7 PERIODIC ARRANGEMENT OF IDENTICAL UNIT CELLS.

infinitely long; this is usually a good approximation since the ratio of the length to the diameter of a unit cell in a reactor is invariably large. The flux thus becomes a function of two space coordinates. Next, it is usually assumed that the actual cell boundary can be replaced by a cylindrical boundary such that the volume of the cell remains unchanged (Fig. 3.8). This assumption is often called the *Wigner-Seitz approximation*, because of its similarity to that approximation in solid-state theory.

The validity of the Wigner-Seitz cell approximation has been examined, with particular reference to the transport of thermal neutrons according to diffusion theory.[25] Of considerable importance is the choice of boundary conditions to be imposed on the cylindrical cell. In the actual cell, either periodic or reflecting boundary conditions (§3.1e) could be used, but with the equivalent cylindrical cell the situation is less clear. At first thought, reflecting boundary conditions on the cylindrical surface might seem to be reasonable. If the angular flux is given in the system of cylindrical coordinates described in §1.7a, then the reflecting boundary conditions would require that

$$\Phi(\mathbf{r}, \mu, \chi) = \Phi(\mathbf{r}, \mu, \pi - \chi).$$

Such boundary conditions have been found to be satisfactory when the moderator region is several neutron mean free paths in thickness. But when the moderator is thin, the results can be misleading. A possible reason for this can be seen from Fig. 3.9.[26] In the cylindrical cell with reflecting boundary conditions, a neutron incident on the boundary would generally be reflected in such a manner that its path could not intersect the fuel element (Fig. 3.9A) unless the neutron were scattered in the moderator. In the actual cell, on the other hand, as indicated in Fig. 3.9B, neutrons "reflected" at the boundary could enter the fuel even without scattering. The use of reflection boundary conditions would thus be

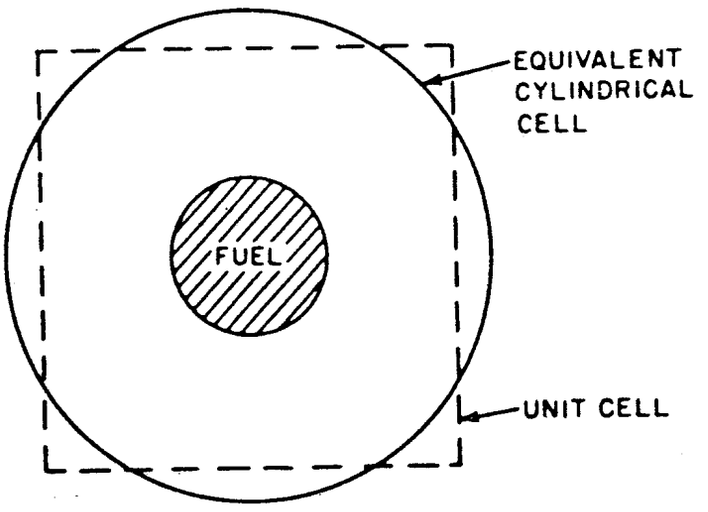

FIG. 3.8 CYLINDRICAL CELL EQUIVALENT TO UNIT CELL

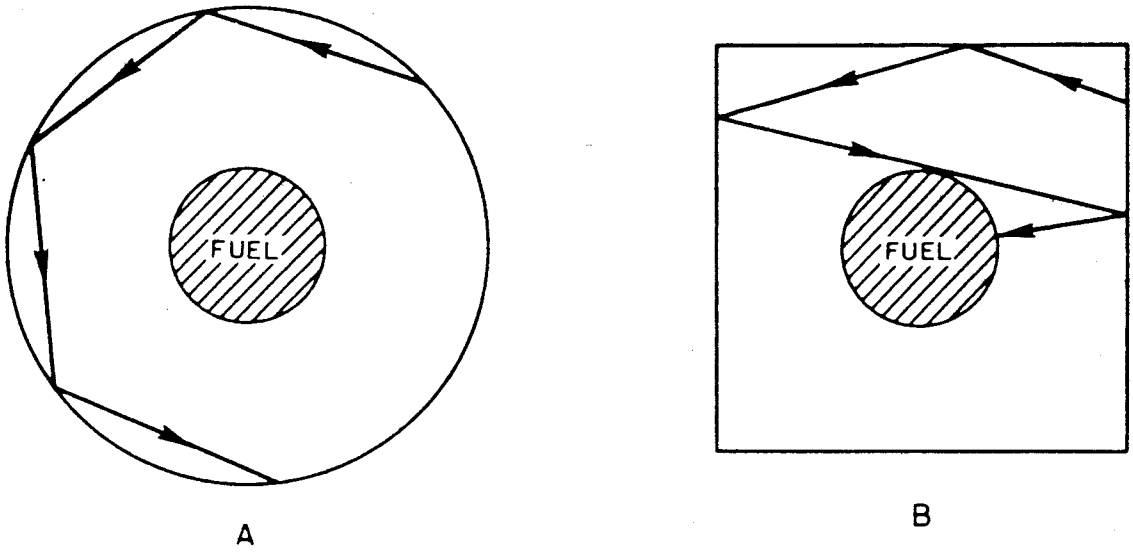

FIG. 3.9 TYPICAL PATHS FOR UNSCATTERED NEUTRON IN (A) EQUIVALENT CYLINDRICAL CELL, (B) ACTUAL UNIT CELL.

expected to make the flux too high in the moderator and calculations show that such is the case.

For thin moderator regions, the Wigner-Seitz approximation gives better agreement with accurate (Monte Carlo) calculations when other boundary conditions are imposed. The general sense of these conditions is to give a more diffuse reflection of the neutrons from the boundary of a cylindrical cell, as opposed to the specular reflection in Fig. 3.9. They are often referred to as "white" boundary conditions and the precise method by which they are imposed depends on the method being used to solve the transport problem under consideration. Some examples are given in the next paragraph.

The cell may be regarded as being surrounded by a purely scattering region at the outside of which reflecting boundary conditions are imposed.[27] A condition of zero flux gradient can be used at the boundary.[28] In the discrete ordinates method (Chapter 5), an isotropic incident current can be imposed to balance the outgoing current.[29] These procedures have all been used successfully in cell calculations. Nevertheless, in novel situations it is advisable to check the results for the cylindrical cell approximation and given boundary conditions with those obtained by Monte Carlo calculations for the actual geometry.

3.6b The Spherical Harmonics Method for Cylindrical Cells

The method of spherical harmonics is often used to compute the neutron flux distribution in cylindrical geometry. For the whole reactor, the P_1 approximation or diffusion theory, as described in preceding sections of this chapter, is usually adequate. In an individual cell, however, there are often thin or strongly-absorbing regions for which P_1 theory is not satisfactory. Expansions of the

angular flux in spherical harmonics are then sometimes used to obtain better solutions of the transport equation. The resulting system of equations is more complicated than for plane or spherical geometry (§§3.1b, 3.3c) because of the dependence of the angular flux on two neutron direction coordinates.

The angular flux (in one-speed theory) may be expanded in spherical harmonics by writing

$$\Phi(r,\mu,\chi) = \sum_{l=0}^{\infty} \frac{2l+1}{4\pi} \left[P_l(\mu)\phi_l^0 + 2\sum_{m=1}^{l} \frac{(l-m)!}{(l+m)!} P_l^m(\mu) \cos m\chi \, \phi_l^m(r) \right], \tag{3.75}$$

where, because of the orthogonality of the associated Legendre functions P_l^m (see Appendix), the expansion coefficients are given by

$$\phi_l^m(r) = \int_{-1}^{1} \int_{0}^{2\pi} \Phi(r, \mu, \chi) P_l^m(\mu) \cos m\chi \, d\chi \, d\mu. \tag{3.76}$$

It will be noted that equation (3.75) contains no terms in sin $m\chi$, as would the more general expression in §3.3d, since by symmetry Φ must here be an even function of χ.

The transport equation may be written in the form of equation (3.48), with $\Omega \cdot \nabla\Phi$ as given for an infinite cylinder in Table 1.2 (§1.7a); thus,

$$\begin{aligned} &\sqrt{1-\mu^2} \left[\cos\chi \frac{\partial\Phi}{\partial r} - \frac{\sin\chi}{r} \frac{\partial\Phi}{\partial\chi} \right] + \sigma\Phi \\ &\quad = \int_{-1}^{1} \int_{0}^{2\pi} \sum_{l'=0}^{\infty} \frac{2l'+1}{4\pi} \sigma_{sl'}(r) \left[P_{l'}(\mu) P_{l'}(\mu') + 2 \sum_{m'=1}^{l'} \frac{(l'-m')!}{(l'+m')!} \right. \\ &\qquad \left. \times P_{l'}^{m'}(\mu) P_{l'}^{m'}(\mu') \cos m'(\chi - \chi') \Phi(r, \mu', \chi') \right] d\chi' \, d\mu' + Q(r, \mu, \chi). \end{aligned} \tag{3.77}$$

Upon inserting equation (3.75) into equation (3.77), the integrals can be evaluated and the result can be written as

$$\begin{aligned} &\sqrt{1-\mu^2} \left[\cos\chi \frac{\partial\Phi}{\partial r} - \frac{\sin\chi}{r} \frac{\partial\Phi}{\partial\chi} \right] + \sigma\Phi \\ &\quad = Q(r, \mu, \chi) + \sum_{l'=0}^{\infty} \frac{2l'+1}{4\pi} \sigma_{sl'}(r) \\ &\qquad \times \left[P_{l'}(\mu)\phi_{l'}^0(r) + 2 \sum_{m'=1}^{l'} \frac{(l'-m')!}{(l'+m')!} P_{l'}^{m'}(\mu) \cos m'\chi \, \phi_{l'}^{m'}(r) \right]. \end{aligned} \tag{3.78}$$

To arrive at the set of equations satisfied by the expansion coefficients ϕ_l^m, equation (3.78) is multiplied by $P_l^m(\mu) \cos m\chi$ and integrated over all neutron directions. When the term $\partial\Phi/\partial\chi$ is integrated by parts and use is made of the

recursion equations satisfied by the associated Legendre functions, the derivative terms on the left side can be expressed in terms of $\phi_{l\pm1}^{m\pm1}$ and their radial derivatives. The resulting equations can be represented by

$$F_l^{m+1}(r) + F_l^{m-1}(r) + [\sigma(r) - \sigma_{sl}(r)]\phi_l^m = Q_{lm}(r),$$

where F_l^{m+1}, F_l^{m-1}, and Q_{lm} are defined by

$$F_l^{m+1} \equiv \frac{1 + \delta_{m0}}{2(2l+1)}\left\{\left[\frac{d\phi_{l+1}^{m+1}}{dr} + (m+1)\frac{\phi_{l+1}^{m+1}}{r}\right] - \left[\frac{d\phi_{l-1}^{m+1}}{dr} + (m+1)\frac{\phi_{l-1}^{m+1}}{r}\right]\right.$$

$$F_l^{m-1} \equiv \frac{1 - \delta_{m0}}{2(2l+1)}\left\{(l+m-1)(l+m)\left[\frac{d\phi_{l-1}^{m-1}}{dr} - (m-1)\frac{\phi_{l-1}^{m-1}}{r}\right]\right.$$

$$\left.-(l-m+1)(l-m+2)\left[\frac{d\phi_{l+1}^{m-1}}{dr} - (m-1)\frac{\phi_{l+1}^{m-1}}{r}\right]\right.$$

and

$$Q_{lm} \equiv \int_{-1}^{1}\int_{0}^{2\pi} Q(r, \mu, \chi)P_l^m(\mu)\cos m\chi \, d\chi \, d\mu.$$

These equations which are satisfied by the expansion coefficients ϕ_l^m are evidently quite complicated; for a detailed discussion of their use the literature should be consulted.[30] An alternative way of treating the problem of cylindrical geometry, by the method of discrete ordinates, is mentioned in Chapter 5.

3.6c Use of Cell Calculations

Once the neutron flux has been computed within a cell, the results may be incorporated into the gross neutron diffusion calculation for the whole reactor. The usual procedure is to homogenize the cells, giving the materials "effective" cross sections in the following manner. The cell calculations would yield the reaction and scattering rates for all the materials in the cell for neutrons of a given energy (or speed). When the cells are homogenized, the effective cross sections are defined in such a way that the reaction rates are preserved when integrated over a cell.

Suppose, for example, that $\sigma_x(\mathbf{r})$ represents the cross section for a given reaction, x, for neutrons of a given energy at position $\mathbf{r}$ within the cell. If $\phi(\mathbf{r})$ is the computed flux in the cell calculation, then the effective cross section, $\bar{\sigma}_x$, may be defined as

$$\bar{\sigma}_x = \frac{\int_{\text{cell}} \sigma_x(\mathbf{r})\phi(\mathbf{r})\, dV}{\int_{\text{cell}} \phi(\mathbf{r})\, dV},$$

so that the over-all reaction rate for the homogenized system will be equal to that within the cell. Other definitions of an effective cross section are possible, but the one given here is both simple and convenient.

Shielding (or disadvantage) factors can also be defined for any kind of neutron reaction as the ratio between the actual reaction rate and that which would be found for the same material exposed to the volume averaged flux. Thus, the shielding factor, S_x, for a reaction of type x can be represented by

$$S_x \equiv \frac{\int_{\text{cell}} \sigma_x \phi \, dV}{\frac{\int_{\text{cell}} \phi \, dV}{V_{\text{cell}}} \int_{\text{cell}} \sigma_x \, dV}$$

where the numerator is the actual reaction rate, i.e., reactions of type x per sec per cell of volume V_{cell}, and the denominator is the reaction rate which would exist if all the material were exposed to the average flux given by $\int \phi \, dV / V_{\text{cell}}$.

In terms of S_x, therefore, $\tilde{\sigma}_x$ may be written as

$$\tilde{\sigma}_x = S_x \frac{\int_{\text{cell}} \sigma_x \, dV}{V_{\text{cell}}}.$$

If the reactions were taking place in a fuel element of uniform composition having a volume V_{fuel}, then $\int \sigma_x \, dV$ would be equal to $\sigma_x V_{\text{fuel}}$. Under these conditions,

$$\tilde{\sigma}_x V_{\text{cell}} = S_x \sigma_x V_{\text{fuel}},$$

where both sides represent the reaction rate per cell and per unit flux.

By using such effective cross sections or shielding factors, all reaction rates in the homogenized cell will be equal to those in the actual heterogeneous cell. The treatment of leakage (or streaming) effects in homogenized lattices is more difficult. In some systems, neutrons can diffuse more freely parallel to the fuel rods, e.g., in coolant channels, than perpendicular to them. Hence, in a homogenized core the diffusion coefficient will depend to some extent on the direction of the flux gradient. This complicated problem will not be treated here, but the interested reader may be referred to the literature.[31]

3.7 CONCLUSION

3.7a Other Methods for Solving the Transport Equation

All the methods for solving the neutron transport equation in this chapter have been based on the expansion of the directional dependence of the neutron angular flux in spherical harmonics (or Legendre polynomials) and then deriving equations for the expansion coefficients by using the orthogonality of the polynomials.

Expansions in other sets of orthogonal polynomials are possible and for the one-speed problem in plane geometry the Chebeyshev, Gegenbauer, and Jacobi polynomials have been tried, among others.[32] But there has been relatively little use of such expansions, partly because the Legendre polynomials have certain

advantages. For example, it has been seen that, in plane geometry, the first two terms of the expansion represent the total flux and the current, respectively, and so have clear physical significance; more generally, the first four terms of the spherical harmonics expansion will be the flux and three components of the current vector. Furthermore, it is easy to treat anisotropic scattering and, as seen in §3.1b and §3.3e, this does not introduce any coupling between the equations for the various Legendre components.

Another general method, in which $\mathbf{\Omega}$ is treated as a discrete rather than as a continuous variable, will be developed in Chapter 5. In addition, numerical methods based on the solution of the integral form of the transport equation are sometimes useful and one will be described in Chapter 7 in connection with the problem of neutron thermalization.

When the geometry is too complicated for explicit treatment by any of the procedures mentioned above, various combinations of solutions in simple geometry are often employed. An example was just given, in §3.6c, where the neutron flux was first computed in a cell and the cell was then homogenized for representation of the gross flux throughout the reactor in a P_1 (or similar) calculation. An approach of a quite different type is the synthesis of two-dimensional fluxes from the solutions to one-dimensional problems (§6.4j). Finally, Monte Carlo methods are useful for treating complex geometries.

Other numerical techniques have been used for the solution of certain neutron transport problems. Among these, mention may be made of the method of moments[33] which has been applied to compute neutron penetration through homogeneous media, e.g., in shielding calculations. Studies have also been made of the method of invariant imbedding,[34] a technique whereby a linear transport problem with boundary conditions at two ends of an interval is replaced by a nonlinear problem with conditions at a single boundary. It is not yet clear, however, if this method will prove useful in practical reactor problems.

3.8 APPENDIX TO CHAPTER 3

In order to derive the identities given in Table 3.1, the direction $\mathbf{\Omega}$ is first expressed in cartesian coordinates, i.e.,

$$\mathbf{\Omega} = \Omega_x \hat{\mathbf{x}} + \Omega_y \hat{\mathbf{y}} + \Omega_z \hat{\mathbf{z}}. \tag{3.79}$$

In polar coordinates (see Fig. 1.1)

$$\begin{aligned} \Omega_x &= \sin\theta \cos\varphi \\ \Omega_y &= \sin\theta \sin\varphi \\ \Omega_z &= \cos\theta, \end{aligned}$$

and hence

$$\int d\mathbf{\Omega} = \int_0^{2\pi} \int_{-1}^{1} \sin\theta \, d\theta \, d\varphi.$$

By using these coordinates, it is seen that

$$\int \Omega_x \, d\Omega = \int \Omega_y \, d\Omega = \int \Omega_z \, d\Omega = 0$$

$$\int \Omega_x^2 \, d\Omega = \int \Omega_y^2 \, d\Omega = \int \Omega_z^2 \, d\Omega = \frac{4\pi}{3}$$

$$\int \Omega_x \Omega_y \, d\Omega = \int \Omega_y \Omega_z \, d\Omega = \int \Omega_x \Omega_z \, d\Omega = 0$$

and thus the results in Table 3.1 can be obtained.

EXERCISES

1. Develop a detailed derivation of equation (3.5).
2. Make the expansion in spherical harmonics as given in §3.3d and show that this can be reduced to equation (3.44) for the P_1 approximation.
3. Carry out in detail the derivation of equation (3.49) from equation (3.48).
4. Derive difference equations for P_1 (or diffusion) theory in two-dimensional (r, z) geometry.[35] Express them in matrix form and verify that the matrix has the desired properties.
5. Consider a hypothetical problem in which ϕ and s are vectors with two components and the matrix A in equation (3.60) is given by

$$\mathbf{A} = \begin{pmatrix} a & -1 \\ -1 & a \end{pmatrix}$$

where $a > 1$. It is desired to solve equation (3.60) by the point successive over-relaxation method, i.e., by using equation (3.68). Determine the optimum acceleration parameter, ω, for $a = \frac{5}{3}$.[36] For what range of ω will this method be superior to the Liebmann method, i.e., $\omega = 1$?
6. In solving a system of diffusion theory difference equations in two dimensions, e.g., equation (3.60), it is possible to regard the flux components in a given line of the two-dimensional array as the unknowns at any instant and to use one-dimensional methods to obtain them. This is known as the "line relaxation" method. Suggest an iterative scheme for solving the two-dimensional equation using this method. The merit of the procedure may be evaluated by reference to the literature.[37]
7. Consider a spherical region of radius R in which there is a uniform and isotropic source of neutrons; the neutron cross section in the region is assumed to be negligible. Compute the angular flux (in vacuum) at a point r outside the sphere. Discuss the relevance of the result to the considerations at the end of §3.5a (especially the footnote).
8. Consider a reactor lattice in which a cell has a hexagonal cross section. It is desired to make a two-dimensional diffusion-theory calculation of the flux in such a cell. By symmetry, only one-sixth of the hexagon, i.e., an equilateral triangle, needs to be considered and suppose that an equilateral space mesh is imposed. Start from the diffusion equation in (x, y) geometry and devise an

approximating 7-point difference equation to apply at any interior point, i.e., not on an interface. Does the difference equation derived depend on the choice of the x direction? Devise a consistent ordering to write the difference equations in a matrix form and suggest some boundary conditions to eliminate the boundary points. Discuss the properties of the matrix.[38]

9. Derive equation (3.74).

REFERENCES

1. Davison, B., "Neutron Transport Theory," Oxford University Press, 1957, Section 10.3; E. M. Gelbard, Chap. 4 in "Computing Methods in Reactor Physics," H. Greenspan, C. N. Kelber, and D. Okrent, eds., Gordon and Breach, 1968.
2. Maynard, C. W., in "Naval Reactors Physics Handbook," Vol. I, A. Radkowsky, ed., U.S. AEC, 1964, Section 3.6; S. P. Congdon and M. P. Mendelson, *Nucl. Sci. Eng.*, 33, 151 (1968).
3. Butler, M. K., and J. M. Cook, in "Computing Methods in Reactor Physics," Ref. 1, p. 43.
4. Butler, M. K., and J. M. Cook, Ref. 3, Section 1.4.2.
5. Varga, R. S., "Matrix Iterative Analysis," Prentice-Hall, Inc., 1962, Chaps. 1, 2.
6. Ehrlich, R., and H. Hurwitz, Jr., *Nucleonics*, **12**, No. 2, 23 (1954); Butler M. K., and J. M. Cook, Ref. 3, p. 46.
7. Varga, R. S., Ref. 5, p. 23.
8. Gelbard, E. M., Ref. 1, Chap. 4.
9. Davison, B., Ref. 1, Section 11.3.1.
10. Gelbard, E. M., Ref. 1, Section 4.4.
11. Davison, B., Ref. 1, Chap. XII; A. M. Weinberg and E. P. Wigner, "The Physical Theory of Neutron Chain Reactors," University of Chicago Press, 1958, p. 226.
12. Hassit, A., Chap. 2 in "Computing Methods in Reactor Physics," Ref. 1.
13. Varga, R. S., Ref. 5, p. 23.
14. Dennery, P., and A. Krzywicki, "Mathematics for Physicists," Harper and Row, Publishers, 1967, Chap. 2.
15. Varga, R. S., Ref. 5, p. 57.
16. Varga, R. S., Ref. 5, Chaps. 3, 4, 5, 7; E. L. Wachspress, "Iterative Solutions of Elliptic Systems and Applications to the Neutron Diffusion Equations of Reactor Physics," Prentice-Hall, Inc., 1966, Chapters 4, 5, 6; A. Hassit, Ref. 12.
17. Young, D. M., *Trans. Am. Math. Soc.*, 76, 92 (1954); R. S. Varga, Ref. 5, Chap. 9; E. L. Wachspress, Ref. 16, Section 4.6; A. Hassit, Ref. 12.
18. See citations in Ref. 16.
19. Hassit, A., Ref. 12.
20. Gelbard, E. M., Ref. 1, p. 317.
21. Mertens, R., *Simon Stevin Supplement*, 30 (1954); J. J. Yvon, *J. Nucl. Energy*, Part I, 4, 305 (1957).
22. Gerstl, S. A. W., and W. Kofink, *Nucl. Sci. Eng.*, 33, 249 (1968).
23. Gelbard, E. M., J. Davis, and P. Pearson, *Nucl. Sci. Eng.*, 5, 36 (1959).
24. Gelbard, E. M., Ref. 1.
25. Dudley, T. E., and P. B. Daitch, *Nucl. Sci. Eng.*, 25, 75 (1966); J. Adir and J. R. Lamarsh, *ibid.*, 35, 14 (1969).
26. Newmarch, D., "Errors due to the Cylindrical Cell Approximation in Lattice Calculations," U.K. AEA Report AEEW-R-34 (1960); E. M. Gelbard, Ref. 1, pp. 329 *et seq.*
27. Honeck, H. C., *Nucl. Sci. Eng.*, 18, 49 (1964).
28. Gelbard, E. M., Ref. 1.
29. Carlson, B. G., and K. D. Lathrop, p. 230 in "Computing Methods in Reactor Physics," Ref. 1.
30. Gelbard, E. M., Ref. 1.

31. Benoist, P., *Nucl. Sci. Eng.*, **34**, 285 (1968), where further references will be found. See also P. F. Palmedo and J. F. Conant, *ibid.*, **36**, 326 (1969); D. R. Harris and J. A. Mitchell, *Trans. Am. Nucl. Soc.*, **12**, 636 (1969).
32. Bell, G. I., B. G. Carlson, and K. D. Lathrop, *Proc. Third U.N. Conf. on Peaceful Uses of At. Energy*, **2**, 25 (1965).
33. Goldstein, H., "Fundamental Aspects of Reactor Shielding," Addison-Wesley Publishing Co., Inc., 1959, Section 6.5.
34. Kaplan S., and E. M. Gelbard, *J. Math. Anal. Applic.*, **11**, 538 (1965); K. M. Case and P. F. Zweifel, "Linear Transport Theory," Addison-Wesley Publishing Co., Inc., 1968, Chap. 9; G. M. Wing, "Introduction to Transport Theory," Wiley and Sons, Inc., 1962, Chap. 5.
35. Hassit, A., Ref. 12, pp. 98 *et seq.*
36. Hassit, A., Ref. 12, pp. 127 *et seq.*
37. Hassit, A., Ref. 12, p. 133; E. L. Wachspress, Ref. 16, Chap. 4.
38. Wagner, M. R., "GAUGE, A Two-Dimensional Few Group Neutron Diffusion Depletion Program for a Uniform Triangular Mesh," Gulf General Atomic Report GA-8307 (1968); see also *Nucl. Sci. Eng.*, **35**, 299 (1969).

4. SOLUTION OF THE TRANSPORT EQUATION BY MULTIGROUP METHODS

4.1 INTRODUCTION

4.1a Outline of the Multigroup Method

In this chapter, the energy-dependent neutron transport equation will be considered and some practical and widely used methods for its solution will be developed. These methods are based on the expansion of the directional dependence of the neutron angular flux in spherical harmonics (or Legendre polynomials), as in Chapter 3. Furthermore, the energy variable is not treated as being continuous, but the range of interest is divided into a finite number of discrete energy groups. Division of the neutron energy into a number of groups has led to the use of the term *multigroup method* or *multigroup theory*.

It will be seen that for each energy group there is a one-speed problem which may be solved by the methods of the preceding chapter. For simplicity and because they are commonly used in reactor calculations, emphasis will be placed on the P_1 and diffusion approximations.

4.1b Comments on Other Methods of Solution

It is of interest to consider, first, some other approaches which have been taken, in particular the extension to energy-dependent problems of some of the methods

used for one-speed theory in Chapter 2. In §2.2, the method of separation of variables was developed to obtain exact (or very accurate) solutions in simple cases. This method has been extended to treat energy-dependent problems in plane geometry,[1] the energy dependence being included either by allowing discrete energy groups or by expanding the energy dependence in modes. Such procedures could be used to obtain accurate solutions to a few test problems. Since a computer is usually required for the calculations, however, it has proved more convenient in practice to obtain the desired accurate solutions to test problems in other ways, e.g., by the discrete ordinates method (Chapter 5) or by Monte Carlo techniques.

Fourier transform methods have been applied to energy-dependent problems both for infinite media[2] and the so-called bare homogeneous reactor. In the latter case, this somewhat heuristic approach has led to "asymptotic reactor theory."[3] These methods will be discussed only briefly here and primarily as a means for finding group cross sections in §4.5.

4.1c Treatment of Variables

The time-independent neutron transport equation involves three independent variables, namely, neutron direction Ω, energy E, and position $\mathbf{r}$. There are several possible ways for treating these variables. In the approach to be adopted here, the dependence of the neutron angular flux on Ω is expanded as a series of orthogonal polynomials, whereas the other two variables appear in discrete form. It is of interest to consider if other approaches, in which, for example, energy or space dependence is expanded in a few modes, might be equally fruitful. In practice, however, this has been found not to be so, and the treatment described in this chapter has proved to be more versatile than these alternatives.

In the first place, the range of angular variables is clearly fixed, and the kinds of angular dependence the neutron flux will have within that range are much the same in different problems. On the other hand, the dependence of the flux on energy and position will be completely different in, for example, a small fast reactor and a large thermal reactor. Nevertheless, for a limited number of reactor types, it may be possible to approximate the energy dependence of the flux by a few, perhaps one or two, terms (modes) of an expansion.[4] In addition, for systems with large (in mean paths) simple regions, such as the bare homogeneous reactor, the spatial distribution of neutrons can also be approximated by one or two modes. It is for such systems that asymptotic reactor theory is useful. Although expansions of the neutron flux in simple energy or space modes may be useful in special cases, they are not capable of treating the great variety of systems for which solutions can be obtained by the multigroup spherical harmonics method.

Another approach is to abandon the use of modes altogether and to take all variables, including Ω, to be discrete rather than continuous. This procedure

will be described in Chapter 5 in which the method of discrete ordinates and the discrete S_N method are developed. These "altogether discrete" methods can also be used to treat a variety of problems of practical significance.

4.2 SPHERICAL HARMONICS EQUATIONS IN PLANE GEOMETRY

4.2a Introduction

Consideration will now be given to the development of the multigroup spherical harmonics method for energy-dependent-problems. Since all the geometrical considerations are the same as for one-speed theory, as described in Chapter 3, most of the discussion in the present chapter will be concerned with plane geometry. Occasionally, however, results from Chapter 3 will be used to obtain equations in more general geometry.

4.2b Expansion of the Scattering Function

The time-independent neutron transport equation in plane geometry may be written

$$\mu \frac{\partial \Phi(x, \mu, E)}{\partial x} + \sigma(x, E)\Phi(x, \mu, E)$$

$$= \int\int \sigma(x, E')f(x; \Omega', E' \to \Omega, E)\Phi(x, \mu', E')\, d\Omega'\, dE' + Q(x, \mu, E). \quad (4.1)$$

It will be assumed, as in §3.1b, that the angular variation of the scattering function, f, depends only on the scattering angle, $\mu_0 = \Omega \cdot \Omega'$. Then σf may be expanded in a set of Legendre polynomials of μ_0; thus,

$$\sigma(x, E')f(x; \Omega', E' \to \Omega, E) = \sigma(x, E')f(x; E' \to E, \mu_0)$$

$$= \sum_{l=0}^{\infty} \frac{2l + 1}{4\pi} \sigma_l(x; E' \to E)P_l(\mu_0), \quad (4.2)$$

where the expansion coefficients, $\sigma_l(x; E' \to E)$, are given by

$$\sigma_l(x; E' \to E) = 2\pi \int_{-1}^{1} \sigma(x, E')f(x; E' \to E, \mu_0)P_l(\mu_0)\, d\mu_0. \quad (4.3)$$

If the expansion of equation (4.3) is inserted into equation (4.1), use of the addition theorem for Legendre polynomials and integration over azimuthal angles (§2.6a) gives

$$\mu \frac{\partial \Phi}{\partial x} + \sigma\Phi = \sum_{l=0}^{\infty} \frac{2l + 1}{2} P_l(\mu) \int \sigma_l(x; E' \to E) \int_{-1}^{1} \Phi(x, \mu', E')$$

$$\times P_l(\mu')\, d\mu'\, dE' + Q(x, \mu, E). \quad (4.4)$$

Before proceeding, it is of interest to examine the expansion coefficients for some special cases. If the neutron scattering is isotropic in the laboratory system, as it is approximately for fission and for inelastic scattering from heavy nuclei, then only σ_0 is nonzero. For the more interesting case of elastic scattering (cross section σ_s), from a stationary nucleus of atomic number A, that is isotropic in the center-of-mass coordinate system then (§1.1b)

$$\begin{aligned}\sigma(x, E')f(x; E' \to E, \mu_0) &= \frac{\sigma_s(x, E')}{2\pi(1-\alpha)E'}\,\delta(\mu_0 - S) \quad \text{if} \quad \alpha E' \leqslant E \leqslant E' \\ &= 0 \quad \text{if} \quad E > E' \quad \text{or} \quad E < \alpha E'\end{aligned} \tag{4.5}$$

where, as in §1.1b, S is defined by

$$S \equiv \frac{1}{2}\left[(A+1)\sqrt{\frac{E}{E'}} - (A-1)\sqrt{\frac{E'}{E}}\right]$$

and α is given by

$$\alpha \equiv [(A-1)/(A+1)]^2.$$

Upon insertion of this result into equation (4.3), the expansion coefficients can be written as

$$\begin{aligned}\sigma_l(x; E' \to E) &= \frac{\sigma_s(x, E')}{(1-\alpha)E'}\,P_l(S) \quad \text{if} \quad \alpha E' \leqslant E \leqslant E' \\ &= 0 \quad \text{if} \quad E > E' \quad \text{or} \quad E < \alpha E'.\end{aligned} \tag{4.6}$$

It follows, therefore, that within the energy range which can be reached by elastic scattering from energy E' there are an infinite number of σ_l values.

More generally, an elastic scattering cross section, isotropic or anisotropic, may be expressed as a Legendre polynomial series in the center-of-mass scattering angle ω. Instead of equation (4.5), the cross section may now be represented by

$$\sigma(x, E')f(x; E' \to E, \mu_0)\,dE = \sum_{n=0}^{\infty} \frac{2n+1}{4\pi}\,\sigma_{sn}(x, E')P_n(\cos\omega)\,d\cos\omega\,\delta(\mu_0 - S). \tag{4.7}$$

Since, for elastic scattering[5]

$$\cos\omega = 1 - \frac{(A+1)^2}{2A}\left(1 - \frac{E}{E'}\right),$$

it is possible to eliminate $\cos\omega$ from equation (4.7) to give

$$\sigma(x, E')f(x; E' \to E, \mu_0)\,dE = \frac{1}{(1-\alpha)E'}\sum_{n=0}^{\infty}\frac{2n+1}{2\pi}\,\sigma_{sn}(x, E')P_n\left[1 - \frac{(A+1)^2}{2A}\left(1 - \frac{E}{E'}\right)\right] \times \delta(\mu_0 - S)\,dE. \tag{4.8}$$

The expansion coefficient is then found from equation (4.3) to be

$$\sigma_l(x; E' \to E) = \frac{1}{(1-\alpha)E'} \sum_{n=0}^{\infty} (2n+1)\sigma_{sn}(x, E')P_n\left[1 - \frac{(A+1)^2}{2A}\left(1 - \frac{E}{E'}\right)\right] \times P_l\left(\frac{A+1}{2}\sqrt{\frac{E}{E'}} - \frac{A-1}{2}\sqrt{\frac{E'}{E}}\right), \quad (4.9)$$

with the expression for S being written out in full.

Equation (4.9), or even equation (4.6), is complicated enough to be formidable for hand calculation. With the availability of digital computers, however, the task is relatively simple. Microscopic scattering cross section data are usually stored on tape and are processed before any multigroup cross sections are derived for use in a transport calculation (see §4.5a).

4.2c The Spherical Harmonics Equations

The angular distributions of the neutron flux and the source may now be expanded in a set of Legendre polynomials (§2.6a); thus,

$$\Phi(x, \mu, E) = \sum_{m=0}^{\infty} \frac{2m+1}{4\pi} \phi_m(x, E)P_m(\mu) \quad (4.10)$$

$$Q(x, \mu, E) = \sum_{m=0}^{\infty} \frac{2m+1}{4\pi} Q_m(x, E)P_m(\mu), \quad (4.11)$$

where

$$\phi_m(x, E) = \int \Phi(x, \mu, E)P_m(\mu)\, d\Omega = 2\pi \int_{-1}^{1} \Phi(x, \mu, E)P_m(\mu)\, d\mu \quad (4.12)$$

and

$$Q_m(x, E) = 2\pi \int_{-1}^{1} Q(x, \mu, E)P_m(\mu)\, d\mu. \quad (4.13)$$

These expansions are now inserted into equation (4.4) and the result is multiplied by $P_n(\mu)$; upon integration over μ from -1 to 1, and using the orthogonality of the Legendre polynomials, the energy-dependent spherical harmonics equations are obtained as

$$(n+1)\frac{\partial \phi_{n+1}(x, E)}{\partial x} + n\frac{\partial \phi_{n-1}}{\partial x} + (2n+1)\sigma(x, E)\phi_n = (2n+1)\int \sigma_n(x; E' \to E)\phi_n(x, E')\, dE' + (2n+1)Q_n(x, E).$$

$$n = 0, 1, 2, 3, \ldots. \quad (4.14)$$

This infinite set of differential equations, for $n = 0, 1, 2, 3, \ldots$, is equivalent to the original neutron transport equation (4.1). As in §3.1c, the P_N approximation is obtained by considering the first $N + 1$ of this set and letting $\partial\phi_{N+1}/\partial x = 0$; this is equivalent to truncating the expansion in equation (4.10) after $N + 1$ terms.

So far, the procedure has been the same as in Chapter 3, except that energy appears here as a variable. Similarly, the usual boundary conditions given in Chapter 3 may be imposed, again with energy included as a parameter. It should be noted, however, that the scattering integrals in equation (4.14) contain contributions from energy E'. These terms act as an anisotropic source as far as the neutrons of energy E are concerned.

4.2d The P_1 Approximation and Diffusion Theory

As in Chapter 3, ϕ_0 is identical with the total flux, ϕ, and ϕ_1 with the neutron current, J, in the x direction; from equation (4.14), the P_1 equations ($n = 0$ and $n = 1$) can consequently be written as

$$\frac{\partial J(x, E)}{\partial x} + \sigma(x, E)\phi(x, E) = \int \sigma_0(x; E' \to E)\phi(x, E')\, dE' + Q_0(x, E) \quad (4.15)$$

and

$$\frac{\partial \phi(x, E)}{\partial x} + 3\sigma(x, E)J(x, E) = 3\int \sigma_1(x; E' \to E)J(x, E')\, dE' + 3Q_1(x, E). \quad (4.16)$$

For a wide variety of reactor problems, the P_1 approximation has been found to be very useful. Briefly, these problems may be described as either involving survey calculations, for which high accuracy is not required, or calculations on large systems, in which the important regions are several neutron mean free paths in thickness. For such large systems, the angular flux can, for the most part, be represented by the first two Legendre polynomials.

Furthermore, an experienced reactor analyst can frequently obtain accurate results from the P_1 approximation even in situations where it is not strictly applicable. In particular, cross sections can be adjusted to give agreement with experimental data, e.g., by the use of synthetic kernels,[6] or accurate transport theory results can be incorporated into the weaker portions of the P_1 analysis.[7] With the development of faster digital computers and the availability of better cross section data, many of these techniques are now lapsing into disuse, whereas others are too specialized for discussion in this book. Nevertheless, the P_1 approximation (and the related diffusion theory) are used extensively in reactor analysis and so they will be considered in detail here.

Before casting the P_1 equations into multigroup form, the relationship between the P_1 approximation and diffusion theory will be examined. It will be

observed that, in the P_1 equations (4.15) and (4.16), coupling between the various neutron energies is present through the integrals over energy on the right-hand sides. Such integrals can be incorporated into the multigroup formulations (§§4.3a, 4.3b), but the scattering integral in equation (4.16) has often been approximated in a form leading to an energy-dependent diffusion theory. The reasons for this are, to some extent, historical, since the first multigroup methods[8] were developed starting from age-diffusion theory, rather than from transport theory. Furthermore, the methods for solving diffusion theory equations have a particularly firm mathematical basis (§4.4f).

In any event, the essential postulate of diffusion theory is that the neutron current, which is $J(x, E)$ in the present case, is given by a diffusion coefficient multiplied by the gradient of the flux; thus,

$$J(x, E) = -D(x, E)\frac{\partial \phi(x, E)}{\partial x}. \tag{4.17}$$

Equation (4.17), which is a form of Fick's law, is now used, instead of equation (4.16), to eliminate J from equation (4.15) to give the diffusion equation

$$-\frac{\partial}{\partial x}\left[D(x, E)\frac{\partial \phi(x, E)}{\partial x}\right] + \sigma(x, E)\phi(x, E)$$

$$= \int \sigma_0(x; E' \to E)\phi(x, E')\,dE' + Q_0(x, E). \tag{4.18}$$

This equation has been used extensively as the basis for multigroup calculations. It is of interest, therefore, to examine the diffusion theory equation (4.18), and to consider in what sense it is an approximation to the P_1 equations (4.15) and (4.16), and what might be a reasonable choice for $D(x, E)$.

It will be recalled (§§2.6b, 3.1d) that, for the one-speed problem, diffusion theory is equivalent to the P_1 approximation provided the source is isotropic. In the energy-dependent situation, however, as in equation (4.16), both Q_1 and the integral (scattering) term act as anisotropic sources of neutrons at energy E; the equivalence between P_1 and diffusion theories is consequently destroyed. If the source and scattering were isotropic, σ_1 and Q_1 would both be zero and then equation (4.16) would be equivalent to Fick's law with the diffusion coefficient being equal to $1/3\sigma(x, E)$. Although it is frequently a good approximation to regard the source as isotropic, so that $Q_1 = 0$, it is seldom possible, however, to take the scattering to be isotropic. Hence, it is necessary to approximate the integral in equation (4.16) in order to arrive at a simple and reasonable expression for the diffusion coefficient.

Suppose that the source is isotropic, i.e., $Q_1 = 0$; then equations (4.16) and (4.17) would be the same provided the diffusion coefficient

$$D(x, E) = \frac{1}{3}\left[\sigma(x, E) - \frac{\int \sigma_1(x; E' \to E)J(x, E')\,dE'}{J(x, E)}\right]^{-1}. \tag{4.19}$$

A simple approximation to the integral can be obtained by expanding it in a Taylor series in the lethargy (see §4.7d) and retaining only the first term. An equivalent result follows from the heuristic argument that the integral represents a contribution from the slowing down of neutrons having energies $E' > E$; this is almost the same as the slowing down from E to lower energies, i.e.,

$$\int \sigma_1(x; E' \to E)J(x, E')\,dE' \approx \int \sigma_1(x; E \to E')J(x, E)\,dE'.$$

This result may be written in the form

$$\int \sigma_1(x; E' \to E)J(x, E')\,dE' \approx \sigma_0(x, E)\bar{\mu}_0(x, E)J(x, E), \tag{4.20}$$

where

$$\sigma_0(x, E) \equiv \int \sigma_0(x; E \to E')\,dE' \tag{4.21}$$

and

$$\bar{\mu}_0(x, E) \equiv \frac{\int \sigma_1(x; E \to E')\,dE'}{\int \sigma_0(x; E \to E')\,dE'}. \tag{4.22}$$

That $\bar{\mu}_0(x, E)$ represents an average scattering angle, as the symbol implies, follows from the definitions of σ_0 and σ_1 given by equation (4.3). When the values are inserted into equation (4.22), it is found that

$$\bar{\mu}_0(x, E) = \frac{\iint \mu_0 f(x; E \to E', \mu_0)\,d\mu_0\,dE'}{\iint f(x; E \to E', \mu_0)\,d\mu_0\,dE'}$$

and so $\bar{\mu}_0$ is the average of the scattering angle μ_0.

If the integral in equation (4.19) is approximated by equation (4.20), the result is

$$D(x, E) = \tfrac{1}{3}[\sigma(x, E) - \bar{\mu}_0(x, E)\sigma_0(x, E)]^{-1}. \tag{4.23}$$

This expression for the diffusion coefficient is commonly used; it is, in fact, a natural generalization of the equation for $D(x)$ in one-speed theory (§2.6b).

It is thus seen that diffusion theory represents a form of the P_1 approximation in which the contribution of the anisotropic scattering to the energy transfer has been approximated. In many instances this approximation is a good one, as will be seen in §4.7, where the relationship of P_1 theory to age-diffusion and other theories will be examined. For situations involving large energy transfer and anisotropic scattering of neutrons, e.g., with hydrogen, the approximation leading to diffusion theory would not be expected to be satisfactory.

4.3 THE P_N MULTIGROUP EQUATIONS

4.3a Energy Groups and Group Constants

The energy-dependent P_N equations (4.14) will now be put into multigroup form. Multigroup theory does not imply any restrictions on the energy-dependent cross sections; hence, these cross sections may be very complicated functions of energy, as they often are in reality.

The first step in the development of multigroup theory is to divide the neutron energy range of interest, i.e., $E_{\min} \leqslant E \leqslant E_{\max}$, into a finite number, G, of intervals separated by the energies E_g, where $g = 1, 2, 3, \ldots, G$, as shown in Fig. 4.1. Each energy interval is called a group and the number of the group is the g value for the lower energy limit. The order of numbering is such that as g increases, the energy decreases, i.e., $E_g > E_{g+1}$. Consequently, if a neutron is generated in fission in group 1, it may then pass during moderation from group 1 to 2, from 2 to 3, and so on; or, in general, from g' to g with $g > g'$. The usual strategy adopted in solving the multigroup equations proceeds by first solving the equations for group 1, then for group 2, and so on.

For an accurate multigroup calculation, the neutron energy interval would be divided, typically, into 20 (or more) groups. Whenever possible, the energy range for a group is chosen so that the variation of important cross sections within the group is kept reasonably small. That is to say, the group boundaries are selected, if possible, to correspond to neutron energies where cross sections undergo a marked change. Apart from such special circumstances, however, the groups are often chosen so that $E_g - E_{g+1}$ is roughly constant, i.e., at equal lethargy intervals (§4.7a).

The next step is to integrate the energy-dependent P_N equations (4.14) over the group energy interval, i.e., $E_g \leqslant E \leqslant E_{g-1}$. If the integral over E' is expressed as the sum of integrals over all the energy groups, i.e.,

$$\int dE' = \sum_{g'} \int_{E_{g'}}^{E_{g'-1}} dE',$$

the result is found to be

$$(n+1)\frac{d\phi_{n+1,g}(x)}{dx} + n\frac{d\phi_{n-1,g}(x)}{dx} + (2n+1)\sigma_{n,g}(x)\phi_{n,g}(x)$$

$$= (2n+1)\sum_{g'=1}^{G} \sigma_{n,g\to g'}(x)\phi_{n,g'}(x) + (2n+1)Q_{n,g}(x).$$

$$n = 0, 1, 2, \ldots \quad g = 1, 2, \ldots, G \qquad (4.24)$$

The group flux expansion coefficients, $\phi_{n,g}$, are defined by

$$\phi_{n,g}(x) = \int_{E_g}^{E_{g-1}} \phi_n(x, E')\,dE' \equiv \int_g \phi_n(x, E')\,dE' \qquad (4.25)$$

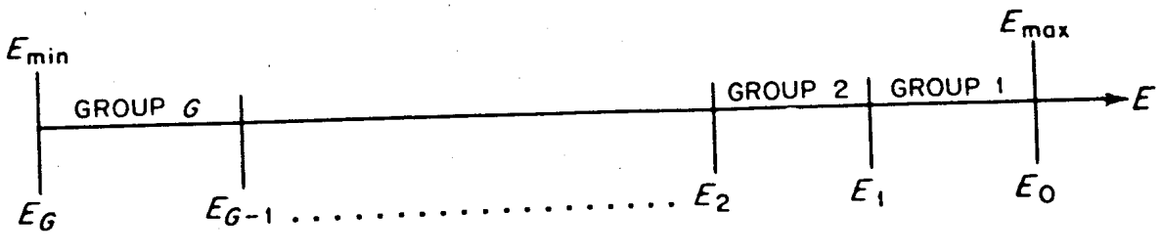

FIG. 4.1 DIVISION OF NEUTRON ENERGY RANGE INTO G GROUPS.

and the group cross sections, or *group constants*, as they are commonly called, are defined by

$$\sigma_{n,g}(x) \equiv \frac{\int_g \sigma(x, E)\phi_n(x, E)\, dE}{\phi_{n,g}(x)} \tag{4.26}$$

and

$$\sigma_{n,g'\to g}(x) \equiv \frac{\int_{g'} \phi_n(x, E') \int_g \sigma_n(x; E' \to E)\, dE\, dE'}{\phi_{n,g'}(x)}. \tag{4.27}$$

The quantities defined by equation (4.27) are sometimes known as the *transfer cross sections*, since they refer to the transfer of neutrons from group g' to group g, including $g = g'$. It should be noted that if the total cross section were independent of E, i.e., $\sigma(x, E) = \sigma(x)$, then $\sigma_{n,g}(x)$ would be equal to $\sigma(x)$ for all values of n. Thus, $\sigma_{n,g}$ is found to be largely independent of n. On the other hand, $\sigma_{n,g'\to g}$ usually depends strongly on n, because it is defined in equation (4.27) in terms of the cross section, σ_n.

It is important to observe that the set of multigroup equations (4.24) are still exact and equivalent to the transport equation. But they involve the group constants and hence, according to equations (4.26) and (4.27), the functions $\phi_n(x, E)$ within the various groups, and these functions are not known. This point may be understood better by supposing that a group structure be set up with only a single group to span the whole energy range of interest. The result would then be simply a one-group (or one-speed) problem, which could be used for the exact determination of eigenvalues (§4.4), reaction rates, etc. Such a representation is, of course, not likely to be useful because the appropriate one-group cross sections would not be known. These require a knowledge of the weighting functions, $\phi_n(x, E)$, as stated above. For a satisfactory one-group calculation, the energy dependence of the neutron flux, i.e., of the weighting functions, over the whole range of interest would have to be known accurately. Consequently, the one-group method is not useful for solving the transport equation.

In a simple system or one in which the energy dependence is well understood, acceptable accuracy may be achieved by the use of a few groups. In most cases, however, a considerable number, e.g., about 20, of energy groups is used. The energy variation of the flux must then be known reasonably accurately in the

groups where there is fine structure, caused by resonances or thermalization, for example; for the other groups, a less accurate estimate of the energy dependence is usually adequate.

The purpose of the foregoing discussion is to emphasize the importance in multigroup theory of an accurate knowledge of the group constants, and this depends on the evaluation of the energy dependence of the flux within each group, i.e., on the values of $\phi_n(x, E)$. Some ways of estimating their dependences will be described in §4.5, and a variational method for deriving them in a self-consistent manner will be discussed in Chapter 6.

Examination of equations (4.26) and (4.27) shows that the group cross sections are functions of position; in fact, if the quantities $\phi_n(x, E)$ depend on position and energy in a nonseparable way, the group cross sections will be space-dependent even if σ and σ_n are not. In practice, a reactor is usually divided into a number of regions of uniform chemical composition, for calculational purposes, and within each region the group cross sections are taken to be independent of position. It is possible, however, to divide up a region of uniform composition into several parts with different ϕ_n and, hence, different group cross sections. In some situations, e.g., in burnup problems (Chapter 10), the group cross sections may be different at each spatial mesh point in the reactor.

If the variation of neutron flux and cross sections with energy were known accurately within each group, then the set of multigroup equations (4.24) would be just as exact as the transport equation. In practice, however, this is not so, particularly because estimated values of the energy dependence of the flux are used in determining the group constants. In order to proceed with the development of the multigroup treatment, it will be assumed that the group constants are known.

4.3b The P_1 Multigroup Equations

The P_N multigroup approximation is obtained by a procedure similar to that used in §4.2c for the P_N approximation, by setting

$$\frac{d}{dx}(\phi_{N+1,g}) = 0, \qquad g = 1, 2, \ldots, G.$$

As a result, equation (4.24) yields a set of coupled one-speed equations, one for each group, where the coupling arises through the $\sigma_{n,g'\to g}$ terms. For a fixed g, the corresponding equation is exactly equivalent to that for a one-speed problem, as in §3.1b, for example, with the terms involving $\sigma_{n,g'\to g}$ for $g \neq g'$ representing an anisotropic source of neutrons into group g. The methods used for solving the one-speed equations are then similar to those described in Chapter 3. In this section, the P_1 multigroup equations will be considered.

In general geometry, the multigroup P_1 approximation may be derived by

starting from the energy-dependent P_1 equations analogous to the one-speed equations (3.50) and (3.51), namely,

$$\nabla \cdot \mathbf{J}(\mathbf{r}, E) + \sigma(\mathbf{r}, E)\phi(\mathbf{r}, E) = \int \sigma_0(\mathbf{r}; E' \to E)\phi(\mathbf{r}, E')\, dE' + Q_0(\mathbf{r}, E) \quad (4.28)$$

and

$$\nabla\phi(\mathbf{r}, E) + 3\sigma(\mathbf{r}, E)\mathbf{J}(\mathbf{r}, E) = 3\int \sigma_1(\mathbf{r}, E' \to E)\mathbf{J}(\mathbf{r}, E')\, dE' + 3\mathbf{Q}_1(\mathbf{r}, E). \quad (4.29)$$

When these equations are integrated over an energy group $E_g \leqslant E \leqslant E_{g-1}$, the result is

$$\nabla \cdot \mathbf{J}_g(\mathbf{r}) + \sigma_{0,g}(\mathbf{r})\phi_g(\mathbf{r}) = \sum_{g'=1}^{G} \sigma_{0,g' \to g}(\mathbf{r})\phi_{g'}(\mathbf{r}) + Q_{0,g}(\mathbf{r}) \quad (4.30)$$

$$\nabla\phi_g(\mathbf{r}) + 3\sigma_{1,g}(\mathbf{r})\mathbf{J}_g(\mathbf{r}) = 3\sum_{g'=1}^{G} \sigma_{1,g' \to g}(\mathbf{r})\mathbf{J}_{g'}(\mathbf{r}) + 3\mathbf{Q}_{1,g}(\mathbf{r}), \quad (4.31)$$

$$g = 1, 2, \ldots, G$$

where the following definitions have been used:

$$\phi_g \equiv \int_g \phi(\mathbf{r}, E)\, dE = \int_g\int \Phi(\mathbf{r}, \boldsymbol{\Omega}, E)\, d\boldsymbol{\Omega}\, dE$$

$$\mathbf{J}_g \equiv \int_g \mathbf{J}(\mathbf{r}, E)\, dE = \int_g\int \boldsymbol{\Omega}\Phi(\mathbf{r}, \boldsymbol{\Omega}, E)\, d\boldsymbol{\Omega}\, dE$$

$$Q_{0,g} \equiv \int_g Q_0(\mathbf{r}, E)\, dE = \int_g\int Q(\mathbf{r}, \boldsymbol{\Omega}, E)\, d\boldsymbol{\Omega}\, dE$$

$$\mathbf{Q}_{1,g} \equiv \int_g \mathbf{Q}_1(\mathbf{r}, E)\, dE = \int_g\int \boldsymbol{\Omega}Q(\mathbf{r}, \boldsymbol{\Omega}, E)\, d\boldsymbol{\Omega}\, dE.$$

The group constants are defined in the same way as in equations (4.26) and (4.27) but with ϕ replacing ϕ_0, $\mathbf{J}$ replacing ϕ_1, and $\mathbf{r}$ replacing x. It is assumed that all the components of $\mathbf{J}$ have the same energy dependence within a group. If, more generally, these components had different energy dependences, then the terms $\sigma_{1,g}\mathbf{J}_g$ and $\sigma_{1,g' \to g}\mathbf{J}_{g'}$ would not necessarily have the same directions as $\mathbf{J}_g$ and $\mathbf{J}_{g'}$. In these circumstances, the quantities σ_1 would be interpreted as tensors. Such complexity does not seem warranted, however, in view of the approximate nature of P_1 theory and the uncertainty concerning the neutron energy dependences within the groups.

If an energy-dependent form of Fick's law in general geometry is postulated, i.e.,

$$\mathbf{J}(\mathbf{r}, E) = -D(\mathbf{r}, E)\nabla\phi(\mathbf{r}, E). \quad (4.32)$$

then the group current can be expressed by integrating this equation over group g; the result is

$$\mathbf{J}_g(\mathbf{r}) = -D_g(\mathbf{r})\nabla\phi_g(\mathbf{r}), \tag{4.33}$$

where the group diffusion coefficient, D_g, is defined by

$$D_g(\mathbf{r}) = \frac{\int_g D(\mathbf{r}, E)\nabla\phi(\mathbf{r}, E)\,dE}{\nabla\phi_g(\mathbf{r})}. \tag{4.34}$$

With this definition, the multigroup diffusion equation is obtained by inserting equation (4.33) into (4.30); thus,

$$-\nabla\cdot D_g(\mathbf{r})\nabla\phi_g(\mathbf{r}) + \sigma_{0,g}(\mathbf{r})\phi_g(\mathbf{r}) = \sum_{g'=1}^{G} \sigma_{0,g'\to g}(\mathbf{r})\phi_{g'}(\mathbf{r}) + Q_{0,g}(\mathbf{r}). \tag{4.35}$$

A number of potentially uncertain approximations have been introduced in deriving the multigroup diffusion theory equation (4.35) from P_1 theory. Usually, therefore, a multigroup P_1 solution to the transport equation would be preferable to one obtained from multigroup diffusion theory.

4.3c A Simple Source Problem

The multigroup P_1 equations (4.30) and (4.31) and the multigroup diffusion theory equation (4.35) are approximations to a time-independent neutron transport equation; hence they might be used in an effort to solve any time-independent transport problem. Two cases are of special interest: one is that of a subcritical system with an independent source, and the other is that of a critical system.

For a subcritical system with a source, the equations mentioned above, together with boundary conditions for each group as described in Chapter 3, are sufficient to define the problem.* They should, therefore, determine a solution uniquely. This has been proved rigorously for multigroup diffusion theory and for a bare homogeneous reactor (see §1.5d).[9]

In order to understand what is involved in obtaining such a solution, a particularly simple problem will be considered in which an isotropic source, Q_0, is given and in which the neutrons cannot gain (but only lose) energy in collisions, i.e., $\sigma_{g'\to g} = 0$ if $g' > g$. Physically, the latter postulate would be applicable if there were no fissile material in the system and all thermal neutrons were

* In practice, the boundary conditions are, for simplicity, often taken to be independent of the group; for example, for a free surface, the flux may be set to zero at the same extrapolated boundary for each group.

in a single energy group. Suppose that a solution of the P_1 equations were sought for such a problem. Equations (4.30) and (4.31) would take the form

$$\nabla \cdot \mathbf{J}_g(\mathbf{r}) + \sigma_{0,g}(\mathbf{r})\phi_g(\mathbf{r}) = \sum_{g' \le g} \sigma_{0,g' \to g}(\mathbf{r})\phi_{g'}(\mathbf{r}) + Q_{0,g}(\mathbf{r}) \tag{4.36}$$

$$\nabla \phi_g(\mathbf{r}) + 3\sigma_{1,g}(\mathbf{r})\mathbf{J}_g(\mathbf{r}) = 3 \sum_{g' \le g} \sigma_{1,g' \to g}(\mathbf{r})\mathbf{J}_{g'}(\mathbf{r}) \tag{4.37}$$

$$g = 1, 2, \ldots, G.$$

This system of G equations can be solved two equations at a time, starting with the lowest value of g. Thus, consider the equations for $g = 1$. The source $Q_{0,g}'$ is known and the equations contain only the unknowns ϕ_1 and $\mathbf{J}_1$; to obtain the latter, it is necessary to solve a one-speed problem. Once ϕ_1 and $\mathbf{J}_1$ have been determined, the equations for $g = 2$ can be considered; now the only unknowns are ϕ_2 and $\mathbf{J}_2$ and these may, once again, be found by solving a one-speed problem. Hence, in this simple case, the solution of the multigroup problem may be found by solving in succession a set of G one-speed problems, with $g = 1, 2, \ldots, G$, using the methods of Chapter 3.

The foregoing procedure is not restricted to P_1 theory and multigroup P_N equations could be solved in the same manner for this simple source problem. In fact, any of the methods used for the solution of one-speed problems could be applied in multigroup form.

4.4 EIGENVALUE PROBLEMS IN MULTIGROUP THEORY

4.4a The Reactivity Eigenvalue

The consideration of criticality is generally referred to as an eigenvalue problem because such problems are concerned with the determination of the reactivity eigenvalue, i.e., the effective multiplication factor, k, in the time-independent equation (1.49), and of other eigenvalues of interest. It will be recalled from §1.5e that k is defined in such a manner that criticality is achieved by dividing the number of neutrons per fission by k.

If fission neutrons are emitted isotropically in the laboratory coordinate system, then the energy spectrum of these neutrons can be described as part of the term $\sigma_{0,g' \to g}$. In particular, it is possible to write

$$\sigma_{0,g' \to g}(\mathbf{r}) = \sigma_{s0,g' \to g}(\mathbf{r}) + \nu\sigma_{f,g' \to g}(\mathbf{r}), \tag{4.38}$$

where $\nu\sigma_{f,g' \to g}\phi_{g'}$ is the rate at which fission neutrons appear in group g as a result of fissions brought about by neutrons in group g'. The cross section $\sigma_{s0,g' \to g}$ accounts for all other transfers from group g' to group g; the subscript s suggests scattering, as before, but it now includes contributions from $(n, 2n)$ reactions. Thus, s is equivalent to the symbol $x \neq f$ used in §1.1b; the latter is

not employed here, however, because it makes the subscripts too cumbersome.

With the notation of equation (4.38), the multigroup P_1 equations for the reactivity eigenvalue k, related to equations (4.30) and (4.31) are*

$$\nabla \cdot \mathbf{J}_g(\mathbf{r}) + \sigma_{0,g}(\mathbf{r})\phi_g(\mathbf{r}) = \sum_{g'} \sigma_{s0,g'\to g}(\mathbf{r})\phi_{g'}(\mathbf{r}) + \frac{1}{k}\sum_{g'} \nu\sigma_{f,g'\to g}(\mathbf{r})\phi_{g'}(\mathbf{r}) \tag{4.39}$$

$$\nabla\phi_g(\mathbf{r}) + 3\sigma_{1,g}(\mathbf{r})\mathbf{J}_g(\mathbf{r}) = 3\sum_{g'} \sigma_{1,g'\to g}(\mathbf{r})\mathbf{J}_{g'}(\mathbf{r}). \tag{4.40}$$

These differ from the general P_1 equations (4.30) and (4.31) in the respect that the extraneous source terms are set equal to zero, and the fission neutrons have been separated from the others. In addition, the eigenvalue k has been introduced so that exact criticality can be achieved.

For multigroup diffusion theory, the expression for the eigenvalue k corresponding to equation (4.35) is

$$-\nabla \cdot D_g(\mathbf{r})\nabla\phi_g(\mathbf{r}) + \sigma_{0,g}(\mathbf{r})\phi_g(\mathbf{r}) = \sum_{g'} \sigma_{s0,g'\to g}(\mathbf{r})\phi_{g'}(\mathbf{r}) + \frac{1}{k}\sum_{g'} \nu\sigma_{f,g'\to g}(\mathbf{r})\phi_{g'}(\mathbf{r}). \tag{4.41}$$

It will be seen in §4.4c that the existence of the eigenvalue k has been proved rigorously for multigroup diffusion theory, and that much is known, in general, about the corresponding eigenfunction $\phi_g(\mathbf{r})$.

4.4b The Multiplication Rate Eigenvalue

The eigenvalue (or criticality) problem can also be considered in terms of the multiplication rate (or period) eigenvalues α. It will be recalled from §1.5c that the eigenfunctions (or modes) corresponding to the values of α are defined as solutions of the source-free, time-dependent transport equation for which

$$\frac{1}{v}\frac{\partial}{\partial t}\Phi(\mathbf{r}, \Omega, E, t) = \frac{\alpha}{v}\Phi(\mathbf{r}, \Omega, E, t).$$

Thus, in P_1 multigroup theory, the α eigenvalue problem is expressed by

$$\frac{\alpha}{v_{0,g}}\phi_g(\mathbf{r}) + \nabla \cdot \mathbf{J}_g(\mathbf{r}) + \sigma_{0,g}(\mathbf{r})\phi_g(\mathbf{r}) = \sum_{g'} \sigma_{0,g'\to g}(\mathbf{r})\phi_{g'}(\mathbf{r}) \tag{4.42}$$

$$3\frac{\alpha}{v_{1,g}}\mathbf{J}_g(\mathbf{r}) + \nabla\phi_g(\mathbf{r}) + 3\sigma_{1,g}(\mathbf{r})\mathbf{J}_g(\mathbf{r}) = 3\sum_{g'} \sigma_{1,g'\to g}(\mathbf{r})\mathbf{J}_{g'}(\mathbf{r}), \tag{4.43}$$

* A slightly different method for representing the summation over g' is used here for simplicity.

where the group velocities, which now enter explicitly for the first time, are defined by

$$\frac{1}{v_{0,g}} = \frac{\int_g \frac{1}{v}\phi(\mathbf{r}, E)\,dE}{\phi_g(\mathbf{r})}$$

$$\frac{1}{v_{1,g}} = \frac{\int_g \frac{1}{v}\mathbf{J}(\mathbf{r}, E)\,dE}{\mathbf{J}_g(\mathbf{r})}.$$

In practice, it is generally assumed that $v_{0,g} = v_{1,g}$ and that both are independent of position.

For multigroup diffusion theory, a Fick's law relationship between $\mathbf{J}_g$ and $\nabla\phi_g$ may be postulated to obtain the α eigenvalue equation

$$\frac{\alpha}{v_{0,g}}\phi_g(\mathbf{r}) - \nabla\cdot D_g(\mathbf{r})\nabla\phi_g(\mathbf{r}) + \sigma_{0,g}(\mathbf{r})\phi_g(\mathbf{r}) = \sum_{g'}\sigma_{0,g'\to g}(\mathbf{r})\phi_{g'}(\mathbf{r}). \tag{4.44}$$

It should be observed that, in trying to derive Fick's law from equation (4.43), it would be necessary to neglect the term $3(\alpha/v_{1,g})\mathbf{J}_g$ in order to obtain a diffusion coefficient, D_g, independent of α. This neglect is quite conventional in time-dependent diffusion theory.[10]

As in the general criticality equation (1.55), the term $(\alpha/v_{0,g})\phi_g$ appears in the multigroup P_1 equation (4.42) for α and in the multigroup diffusion theory equation (4.44). It is thus equivalent to a "1/v" absorber and, for positive α, it is often said to represent "time absorption" as stated in §1.5f.

4.4c Eigenvalues and Eigenfunctions for Multigroup Diffusion Theory

The equations given in the preceding section for the k and α eigenvalues in multigroup P_1 and diffusion theories are applicable to eigenfunctions which satisfy appropriate boundary conditions. It was seen in §§1.5c, 1.5e in what sense these eigenvalues exist for the complete transport equation, and consideration must now be given to their properties in multigroup equations. It is in connection with multigroup diffusion theory, in particular, that information has been obtained concerning the existence of the eigenvalues and the nature of the corresponding eigenfunctions.

In one approach,[11] the k and α eigenvalue equations (4.41) and (4.44), respectively, are considered to apply to some finite region in space. For boundary conditions, a linear relationship, similar to the one in equation (3.12), is assumed to hold between the group flux and its normal derivative of the form $\phi_g + h_g\hat{\mathbf{n}}\cdot\nabla\phi_g = 0$, where $\hat{\mathbf{n}}$ is an outward normal and h_g is any nonnegative piecewise continuous function defined on the boundary. This condition is general enough

to include any of the diffusion theory boundary conditions mentioned in §3.1e. In addition, the assumptions are made that there is continuity of the flux and of the current at interfaces, and that the flux has bounded and continuous second derivatives. Some very minor conditions are also imposed on the group constants, but they are satisfied by any potentially critical system.

On the basis of the foregoing postulates, it has been shown[12] that there will always exist a reactivity eigenvalue, k_0, for equation (4.41) such that k_0 is real, positive, and larger in magnitude than any other eigenvalue. The k_0 is called a *positive dominant eigenvalue* and it is clearly of physical interest since the situation with the largest $k = k_0$ will be that which is critical with the least number of neutrons per fission. Moreover, corresponding to k_0, there is an eigenfunction (and also an adjoint eigenfunction) which is unique, except for normalization, and is nonnegative everywhere within the bounded region of space. Of course, a physical total flux must be everywhere positive or zero, and so this nonnegativity of the eigenfunction is a satisfactory feature.

There are presumably other eigenvalues, smaller in magnitude than k_0, for which the corresponding eigenfunctions are sometimes negative or even complex, but no single one of these higher modes can be realized physically. Although these higher modes can be found explicitly for simple cases, such as the one-group approximation in simple geometry, little is known about such modes in general.

The existence and properties of the positive dominant reactivity eigenvalue, k_0, and its associated eigenfunction provide a firm mathematical basis to the k eigenvalue problem. Consider, now, the α eigenvalue problem, defined by equation (4.44), with the same boundary conditions. It has been shown[13] that in this case there will exist a dominant eigenvalue, α_0, which is real and larger (more positive) than the real part of any other eigenvalue, and that the associated eigenfunction (and its adjoint) is everywhere nonnegative. Thus, the α eigenvalue problem is also on a firm basis.

In addition, for either a homogeneous system, which means here that all the group constants are independent of position within the system, or for one-dimensional geometry, i.e., plane, infinite cylinder, or sphere, the set of α eigenfunctions is complete in the sense that a solution to the time-dependent initial value problem can be written as a sum of the eigenfunctions, each multiplied by $e^{\alpha_i t}$ with α_i the corresponding α eigenvalue. The expansion coefficients can be found by using α modes for the adjoint solution (see Chapter 6). Expansions in the α modes, as a means for solving time- and space-dependent problems in reactor dynamics, will be employed in Chapter 10.

The mathematical methods used to derive the properties of the eigenvalues and eigenfunctions of the multigroup diffusion theory given above are beyond the scope of this text. The interested reader can refer to the original report of the work.[14] It is worth making some generalizations, however, concerning the approaches used. In particular, it should be noted that the operators involved in

transport theory are *positive operators* in the sense that, if the neutron distribution is initially positive, it will remain positive, or at least nonnegative, at all subsequent times. This positivity of operators is an essential aspect of the derivations of the dominant eigenvalues and nonnegative eigenfunctions described above. The importance of positivity in the operators has been emphasized in various connections[15] and reference to it will be made in §4.4g.

4.4d Solving the Eigenvalue Problem

The multigroup eigenvalue problem involves a set of coupled one-speed equations, such as equations (4.39) and (4.40), one for each group. In this section a systematic way of solving such equations will be described. It will be assumed throughout that any one-speed problem with a known source and a nonmultiplying medium can be solved by the methods of Chapter 3, as indicated in §4.3c.

Suppose it is required to solve the set of multigroup P_1 equations (4.39) and (4.40) for the eigenvalue k and the associated eigenfunction. The procedure adopted is based on that described in §1.5e of treating the neutrons one generation at a time, with fission being regarded as the birth event which separates successive generations. To start the calculations a guess is made concerning the spatial distribution of fissions, and this forms the source for the first generation of neutrons. Although the guess can be completely arbitrary, the closer it is, on the basis of previous experience, to the actual distribution of fissions the faster does the calculation converge.

By treating fission as absorption (cf. §1.5e), the flux, ϕ_1, of the first generation of neutrons is computed with the arbitrary fission distribution. The procedure used is similar to that described in §4.3c for a known source. The fission distribution corresponding to this flux, ϕ_1, is next computed and this forms the source for a new flux, ϕ_2, of neutrons of the second generation, and so on for subsequent generations. In this manner a convergent iterative procedure is defined; the ratio of the fluxes in successive generations approaches a constant, and this is k; thus, in accordance with equation (1.54)

$$\lim_{i\to\infty}\frac{\phi_i}{\phi_{i-1}} = \text{constant} = k.$$

In practice, this iterative scheme can be used to solve the P_1 equations (4.39) and (4.40) in the following manner. Let $\phi_g^{(n)}(\mathbf{r})$ be a flux obtained from an n-fold application of the iterative scheme represented by

$$\nabla\cdot\mathbf{J}_g^{(n)}(\mathbf{r}) + \sigma_{0,g}(\mathbf{r})\phi_g^{(n)}(\mathbf{r}) = \sum_{g'}\sigma_{s0,g'\to g}(\mathbf{r})\phi_{g'}^{(n)}(\mathbf{r}) + \frac{1}{k^{(n-1)}}\sum_{g'}\nu\sigma_{f,g'\to g}(\mathbf{r})\phi_{g'}^{(n-1)}(\mathbf{r}) \quad (4.45)$$

$$\nabla\phi_g^{(n)}(\mathbf{r}) + 3\sigma_{1,g}(\mathbf{r})\mathbf{J}_g^{(n)}(\mathbf{r}) = 3\sum_{g'}\sigma_{s1,g'\to g}(\mathbf{r})\mathbf{J}_{g'}^{(n)}(\mathbf{r}). \quad (4.46)$$

These equations are identical with equations (4.39) and (4.40), respectively, with each $\mathbf{J}_g$ and ϕ_g bearing the superscript (n), *except* that the fission terms have the superscript $(n-1)$. The iterative scheme is thus similar to that in equation (1.53) except that the fission term explicitly contains the factor $1/k^{(n-1)}$. The quantity $k^{(n-1)}$ is the estimate of k obtained after $n-1$ iterations and may be defined by the ratio

$$k^{(n)} \equiv \frac{\nu F^{(n)}}{\nu F^{(n-1)}/k^{(n-1)}}, \tag{4.47}$$

where

$$\nu F^{(n)} \equiv \int \sum_{g=1}^{G} \sum_{g'=1}^{G} \nu\sigma_{f,g'\to g}(\mathbf{r})\phi_{g'}^{(n)}(\mathbf{r})\, dV. \tag{4.48}$$

Thus, $k^{(n)}$ is the ratio of the total number of fission neutrons produced by $\phi^{(n)}$, i.e., $\nu F^{(n)}$, to the total number of fission neutrons that form the source for $\phi^{(n)}$, i.e., $\nu F^{(n-1)}/k^{(n-1)}$.

This iterative scheme is essentially equivalent to that described above and in §1.5e. The only difference is that now the fission term is, each time, divided by a current estimate of k. As a consequence of equation (4.47), the integral of the fission source, i.e., $\nu F^{(n)}/k^{(n)}$, is independent of n. Since the fission source is thus normalized to be independent of n, the flux $\phi^{(n)}$ will converge to a value also independent of n. Hence, assuming that the iteration converges, it follows that

$$\lim_{n\to\infty} k^{(n)} = k$$

and

$$\lim_{n\to\infty} \phi^{(n)} = \phi,$$

where ϕ is a solution of equations (4.39) and (4.40).

The convergence of this procedure has been established for the difference form of the multigroup diffusion theory (§4.4f) and experience has shown that the convergence is actually much more general (§4.4g). The fact that $\phi^{(n)}$ becomes independent of n is a great convenience in some numerical work. For example, it is advantageous to use $\phi^{(n-1)}$ as a first guess for $\phi^{(n)}$ when performing iterations for the space distribution of the neutron flux (cf. §§3.4c, 3.4d).

In order to put the iterative scheme described above into operation, a guess is made of the fission source, i.e.,

$$\text{Guessed fission source} = \frac{1}{k^{(0)}} \sum_{g'} \nu\sigma_{f,g'\to g}(\mathbf{r})\phi_{g'}^{(0)}(\mathbf{r}).$$

This quantity is then regarded as a known source in equations (4.45) and (4.46) for $n = 1$, and the equations are solved for $\phi_g^{(1)}$ and $\mathbf{J}_g^{(1)}$. If there is no scattering of neutrons to higher energies, i.e., $\sigma_{s0,g'\to g} = \sigma_{s1,g'\to g} = 0$ if $g' > g$, then the solutions may be found by solving successively a series of one-speed problems

for each of the G groups, as in §4.3c. Thus, the equations for $g = 1$ involve only $\phi_1^{(1)}$ and $\mathbf{J}_1^{(1)}$ as unknowns and these can be found by solving a one-speed problem with a known source. With these quantities known, the equations for $g = 2$ are considered; they involve the unknowns $\phi_2^{(1)}$ and $\mathbf{J}_2^{(1)}$ which may again be obtained by solving a one-speed problem.

Once the flux $\phi_g^{(1)}$ has been found for all the G groups, a new estimate of k is made from equation (4.47). As desired, this equation gives $k^{(1)}$ as the ratio between the number of fission neutrons emitted in successive iterations; thus, $\nu F^{(0)}/k^{(0)}$ is the (guessed) source of fission neutrons for the computation of $\phi^{(1)}$, and $\nu F^{(1)}$ is the number of fission neutrons obtained from the flux $\phi^{(1)}$. Hence, equation (4.47) may be written for $n = 1$ as

$$k^{(1)} = \frac{\text{Fission neutrons produced by } \phi^{(1)}}{\text{Fission neutron source for } \phi^{(1)}}.$$

A new source of fission neutrons, namely,

$$\frac{1}{k^{(1)}} \sum_{g'} \nu\sigma_{f,g' \to g}(\mathbf{r})\phi_{g'}^{(1)}(\mathbf{r})$$

may now be derived and equations (4.45) and (4.46) solved for $\phi_g^{(2)}$ and $\mathbf{J}_g^{(2)}$, and the iterative procedure may be carried on for successive values of n. The calculation will be assumed to have converged when $k^{(n)}$ is sufficiently close to $k^{(n-1)}$, that is, when

$$\left| \frac{k^{(n)}}{k^{(n-1)}} - 1 \right| < \epsilon,$$

where ϵ is some predetermined small number, which might be of the order of 10^{-4} or so.

In practice, since $k^{(n)}$ as computed in this manner often converges more rapidly than the spatial flux distribution, a separate criterion is sometimes imposed on the flux. For example, it might be required that

$$\max \left| \frac{\phi^{(n)}}{\phi^{(n-1)}} - 1 \right| < \epsilon_1,$$

where ϵ_1 is another small number and the maximum is to be determined over a selected set of space points and energy groups.[16]

It is seen that the general strategy used in solving the reactivity eigenvalue equations involves two different kinds of computational problems. One is that of solving for the spatial distribution of one-group fluxes in problems with known sources; for two- and three-dimensional problems this is done by the so-called inner iteration procedure described in §§3.4c, 3.4d. The other problem involves iteration of the fission source until convergence is attained; such iterations are usually called *outer* (or *source* or *power*) *iterations* to distinguish them from the inner iterations for the within-group fluxes.

There are two main reasons for adopting this calculational approach. First, as already noted, it can be shown, rigorously in some cases and by experience in others, that $k^{(n)}$ does indeed converge to a constant which is the desired eigenvalue. The convergence is often rapid, and even when it is normally not, the underlying mathematical theory can be used to speed up the convergence. Second, when neutrons gain energy only as a result of fission, and the fission is treated accordingly, the group equations can be solved successively, as seen above, rather than simultaneously. This results in a considerable simplification in the computations.

When the thermal neutrons are divided into several energy groups, because of variations in cross section, neutrons can pass from a lower to a higher energy group as a result of scattering; this is known as *up-scattering*. Then successive solution of the group equations is not possible. But if the number of thermal groups is small, it is convenient to solve most of the group equations in succession. Additional iterations of the thermal groups may be necessary to obtain their convergence. The up-scattering may slow down the convergence quite significantly, and special procedures have been proposed for overcoming this drawback. For one-dimensional problems, it has been suggested that all the group equations should be solved simultaneously by a "stabilized march" method.[17] This is a direct procedure somewhat analogous to the method of sweeps described in §3.2c. Other methods have also been applied to this problem.[18]

If some eigenvalue other than k, such as α or a critical size or composition, is being sought, it is frequently found in the following manner. Suppose that it is desired to find the composition for which a reactor of a given size will be critical. For the required composition, the equations (4.39) and (4.40) will have a solution for $k = 1$, i.e., the system is critical, whereas for any other composition the equations would have a solution for $k \neq 1$, i.e., the system is subcritical or supercritical.

The composition that will make $k = 1$ is determined by first guessing a composition, represented by $c^{(0)}$ and then finding $k^{(0)}$ for this composition, as described above. In general, the guess will be wrong, so that $k^{(0)}$ will not be unity. A second guess, $c^{(1)}$, is then made and the corresponding value of $k^{(1)}$ is computed. With $k^{(0)}$ and $k^{(1)}$ known for two compositions, $c^{(0)}$ and $c^{(1)}$, it is possible to make a better guess, $c^{(2)}$, for the critical composition, e.g., by assuming a linear relationship between k and c. By proceeding in this manner, the required critical composition can be readily determined. Other eigenvalues, such as α and critical dimensions, are also frequently found by the same general procedure.

4.4e Difference Equations for the Multigroup Eigenvalue Problem

The equations for any one group in multigroup theory can be written in exactly the same form as for a one-speed problem. Consider, for example, the P_1

equations (4.39) and (4.40) for the group g and for the eigenvalue k. If the group index is deleted, i.e., $\mathbf{J}$ is used for $\mathbf{J}_g$ and ϕ for ϕ_g, these equations can be written in the form

$$\nabla \cdot \mathbf{J}(\mathbf{r}) + \sigma_0(\mathbf{r})\phi(\mathbf{r}) = Q_0(\mathbf{r}) \tag{4.49}$$

$$\nabla\phi(\mathbf{r}) + 3\sigma_1(\mathbf{r})\mathbf{J}(\mathbf{r}) = 3\mathbf{Q}_1(\mathbf{r}), \tag{4.50}$$

where the quantities σ_0, σ_1, Q_0, and $\mathbf{Q}_1$ are here defined by

$$\sigma_n(\mathbf{r}) \equiv \sigma_{n,g}(\mathbf{r}) - \sigma_{sn,g\to g}(\mathbf{r}) \quad \text{with} \quad n = 0, 1 \tag{4.51}$$

$$Q_0(\mathbf{r}) \equiv \sum_{g' \neq g} \sigma_{s0,g'\to g}(\mathbf{r})\phi_{g'}(\mathbf{r}) + \frac{1}{k}\sum_{g'} \nu\sigma_{f,g'\to g}(\mathbf{r})\phi_{g'}(\mathbf{r}) \tag{4.52}$$

$$\mathbf{Q}_1(\mathbf{r}) \equiv \sum_{g' \neq g} \sigma_{s1,g'\to g}(\mathbf{r})\mathbf{J}_{g'}(\mathbf{r}). \tag{4.53}$$

It should be noted that the scattering terms for which $g' = g$ have been moved to the left sides of equations (4.49) and (4.50), by using equation (4.51) to define $\sigma_n(\mathbf{r})$. The fission term with $g' = g$ has been retained, however, on the right-hand side of equation (4.49) since, as described in §4.4d, the fissions are treated as a known source when ϕ and $\mathbf{J}$ are being computed. Hence, the quantities Q_0 and $\mathbf{Q}_1$ can be considered as known in the one-speed problem defined by equations (4.49) and (4.50). These equations are seen to be identical with equations (3.50) and (3.51), respectively. Moreover, σ_0 will be positive, so that the one-speed problem corresponds to that in a nonmultiplying medium and consequently has a unique solution.

The equations (4.49) and (4.50) can be reduced to difference-equation form by introduction of a suitable space mesh and they can be solved by the methods described in Chapter 3. In general, the same space mesh would be used for all of the energy groups.

Although the P_1 equations have been treated here, as an example, similar considerations apply to the more general spherical harmonics expansions. The special case of diffusion theory will be examined in more detail in the next section.

4.4f Analysis of the Multigroup Eigenvalue Problem in Diffusion Theory: Outer Iterations

The system of difference equations for multigroup diffusion theory has been subjected to thorough analysis.[19] Particular emphasis has been placed upon the reactivity eigenvalue problem and some results of the analysis will be considered here.

The multigroup diffusion equation (4.41) for the k eigenvalue problem may be written

$$-\nabla \cdot D_g(\mathbf{r})\nabla\phi_g(\mathbf{r}) + [\sigma_{0,g}(\mathbf{r}) - \sigma_{s0,g\to g}(\mathbf{r})]\phi_g(\mathbf{r}) = \sum_{g' \neq g} \sigma_{s0,g'\to g}(\mathbf{r})\phi_{g'}(\mathbf{r}) + \frac{\nu F_g(\mathbf{r})}{k}, \quad (4.54)$$

where νF_g represents the source of fission neutrons in group g and is given by

$$\nu F_g(\mathbf{r}) \equiv \sum_{g'} \nu\sigma_{f,g'\to g}(\mathbf{r})\phi_{g'}(\mathbf{r}). \quad (4.55)$$

It is assumed, as usual, that ϕ_g and $D\nabla\phi_g$ are continuous across interfaces and that boundary conditions are of the form

$$\phi_g(\mathbf{r}) + b(\mathbf{r})\hat{\mathbf{n}} \cdot \nabla\phi_g(\mathbf{r}) = 0,$$

with $b(\mathbf{r})$ nonnegative and $\mathbf{r}$ on the boundary (§4.4c).

For each neutron group, difference equations may be derived as in Chapter 3. In plane geometry, for example, equation (4.54) may be represented by

$$-\frac{d}{dx}\left[D_g(x)\frac{d\phi_g(x)}{dx}\right] + \sigma_{0g}(x)\phi_g(x) = Q_{0g}(x), \quad (4.56)$$

which has the same form as equation (3.9) with

$$\sigma_{0g}(x) \equiv \sigma_{0,g}(x) - \sigma_{s0,g\to g}(x)$$

$$Q_{0g}(x) \equiv \sum_{g' \neq g} \sigma_{s0,g'\to g}(x)\phi_{g'}(x) + \frac{\nu F_g(x)}{k}.$$

When the differential equation (4.56) is reduced to a difference equation, the system of difference equations may be expressed, as in equations (3.25) and (3.60), by

$$\mathbf{A}_g\boldsymbol{\phi}_g = \mathbf{s}_g, \quad (4.57)$$

where $\boldsymbol{\phi}_g$ is the vector having as components the values of ϕ_g at the mesh points x_m.* $\mathbf{A}_g$ is a known matrix, as given in §3.2c, and $\mathbf{s}_g$ is a vector (§3.2d) for which the m component is

$$(s_g)_m = \Delta_m\left[\sum_{g' \neq g} \sigma_{s0,g'\to g}(x_m)\phi_{g'}(x_m) + \frac{\nu F_g(x_m)}{k}\right].$$

In addition, from equation (4.55),

$$\nu F_g(x_m) = \sum_{g'} \nu\sigma_{f,g'\to g}(x_m)\phi_{g'}(x_m).$$

* In order to avoid confusion with the reactivity eigenvalue, the mesh points are represented by x_m rather than as x_s in §3.2a, etc.

More generally, for example in two-dimensional geometry, the source vector $\mathbf{s}_g$ for group g may be written as

$$\mathbf{s}_g = \sum_{g' \neq g} \mathbf{B}_{g' \to g} \boldsymbol{\phi}_{g'} + \frac{\nu \mathbf{F}_g}{k}, \tag{4.58}$$

where $\mathbf{B}_{g' \to g}$ is a diagonal matrix with nonnegative components and $\nu \mathbf{F}_g$ is a vector. In plane geometry, the m, m component of $\mathbf{B}_{g' \to g}$ is

$$(B_{g' \to g})_{m,m} = \Delta_m \sigma_{s0,g' \to g}(x_m),$$

and the mth component of $\nu \mathbf{F}_g$ is $\Delta_m \nu F_g(x_m)$. In general, $\nu \mathbf{F}_g$ may be written

$$\nu \mathbf{F}_g = \sum_{g'} \mathbf{C}_{g' \to g} \boldsymbol{\phi}_{g'} \tag{4.59}$$

where $\mathbf{C}_{g' \to g}$ is a diagonal matrix with nonnegative components, which are given for plane geometry by

$$(C_{g' \to g})_{m,m} = \Delta_m \nu \sigma_{f,g' \to g}(x_m).$$

When equation (4.58) is inserted into equation (4.57), it is found that

$$\mathbf{A}_g \boldsymbol{\phi}_g = \sum_{g' \neq g} \mathbf{B}_{g' \to g} \boldsymbol{\phi}_{g'} + \frac{\nu \mathbf{F}_g}{k}. \tag{4.60}$$

The set of difference equations (4.59) and (4.60) constitutes the multigroup eigenvalue problem which is to be solved by outer iterations as described in §4.4d. The solution gives the effective multiplication factor, k, together with the associated eigenfunction, $\boldsymbol{\phi}_g$, for each group, i.e., $g = 1, 2, \ldots, G$. In the present notation, the scheme of outer iterations, which was represented in the P_1 approximation by equations (4.45) through (4.48), is expressed by

$$\mathbf{A}_g \boldsymbol{\phi}_g^{(n)} = \sum_{g' \neq g} \mathbf{B}_{g' \to g} \boldsymbol{\phi}_{g'}^{(n)} + \frac{\nu \mathbf{F}_g^{(n-1)}}{k^{(n-1)}} \tag{4.61}$$

corresponding to equations (4.45) and (4.46), where

$$\nu \mathbf{F}_g^{(n-1)} = \sum_{g'} \mathbf{C}_{g' \to g} \boldsymbol{\phi}_{g'}^{(n-1)}. \tag{4.62}$$

In addition, the estimate for k, i.e., $k^{(n)}$, may be computed from equation (4.47), i.e.,

$$k^{(n)} = \frac{\nu F^{(n)}}{\nu F^{(n-1)}/k^{(n-1)}}, \tag{4.63}$$

where, in the present notation, $\nu F^{(n)}$, the total source of fission neutrons, may be represented as

$$\nu F^{(n)} = \sum_{g} \nu \mathbf{F}_g^{(n)} \cdot \mathbf{I}, \tag{4.64}$$

where $\mathbf{I}$ is a vector having unit components, such that $\nu\mathbf{F}_g \cdot \mathbf{I}$ is a sum over volume elements or the volume integral of νF_g.

As explained in §4.4d, the procedure for solving the equations (4.61) through (4.64) is to guess $\nu F_g^{(0)}/k^{(0)}$, compute $\phi_g^{(1)}$ from equation (4.61), and then derive $\nu F_g^{(1)}/k^{(1)}$ from equations (4.62), (4.63), and (4.64). The iteration procedure is continued until convergence is obtained.

The system of equations (4.59) and (4.60) has been analyzed and it has been shown[20] that the largest eigenvalue, k, is positive and simple, and that its corresponding unique eigenvector, $\boldsymbol{\phi}$, can be chosen to have nonnegative components. Moreover, the procedure of iterating on the fission density was proved to converge to this eigenvector. These conclusions are analogous to those described in §4.4c for the multigroup equations with continuous space dependence of the neutron flux. In addition, they provide a sound basis for the outer iterations. As in the case of the inner iterations, various methods are available for accelerating the convergence of the outer iterations.[21]

The discrete time-dependent multigroup equations, obtained by adding $(\alpha/v_g)\,\partial\phi_g/\partial t$ to the left side of equation (4.54) and setting $k = 1$, have also been considered.[22] For the initial value problem, the solution has an exponential time behavior, proportional to $e^{\alpha t}$, as $t \to \infty$. Hence, the criticality state of the system can be based on the sign of α. The results given in §1.5 for general transport theory and in §4.4c for multigroup diffusion theory with continuous space dependence of the flux are carried over to multigroup diffusion theory with discrete spatial variation of the neutron flux. In addition, the coefficient of the exponential solution is given by the product of the initial flux vector and the normalized positive eigenvector of the adjoint equations (see Chapter 6). When a source is present, a finite time-dependent solution as $t \to \infty$ can be obtained only for a subcritical system, in agreement with physical expectations, as discussed in §1.5d.

4.4g Outer Iterations in the Multigroup P_1 Approximation

The analysis in the preceding section was based on multigroup diffusion theory. For most other approximations, including P_1 theory, the corresponding mathematical analysis has not been carried out. In many instances the conclusions will presumably not apply, since the system of difference equations will not correspond to a positive operator.[23] Nevertheless, the general strategy of outer iterations has been used successfully in most multigroup problems, including, for example, those based on spherical harmonics or the method of discrete ordinates (§5.4c) in which this procedure has no firm mathematical basis. Under such conditions the outer iteration procedure may not always yield a stable numerical solution; nevertheless, it has been found to be extremely fruitful in practice.

In view of the relationship between the P_1 approximation and diffusion theory, it is of interest to consider why the results of the diffusion theory analysis

in §4.4f are not applicable to P_1 theory. The explanation may be found in equation (3.24), which represents a component of the source vector for a one-speed problem in the P_1 approximation. The appropriate multigroup forms for Q_0 and $\mathbf{Q}_1$ are given by equations (4.52) and (4.53), respectively. Upon combining these results, it is found that the source vector in a P_1 calculation cannot be expressed in the simple form of equation (4.58) which applies to diffusion theory.

It appears possible that, in some circumstances, a source component term, $(s_m)_g$, might be negative and, furthermore, a flux component might also be negative. The difference equations could then not correspond to a positive operator and even the existence of an eigenvalue, k, might be in doubt. In any case, it is evident that the mathematical analysis for diffusion theory cannot be applied without modification to the P_1 approximation.

4.4h General Comments on the Eigenvalue Problem

In general, the solution of the eigenvalue problem in multigroup P_1 or diffusion theory can be based on the system of inner and outer iterations. For one-dimensional geometries, the inner iteration is not necessary, as seen in Chapter 3. If up-scattering occurs, then iteration for the groups involved in up-scattering is also required, unless a direct method such as the stabilized march technique is used. In all cases, procedures for accelerating convergence of the iterations are adopted. In practice, too, it is advisable to allow some interdependence between inner and outer iterations; for example, it is unnecessary to spend time obtaining accurately converged group fluxes when working with a rough estimate of the fission source.

Multigroup P_1 and diffusion theory codes form the basis of much reactor design. In these codes a system of equations, such as equations (4.61) through (4.64), is solved on a fast digital computer; the essential features of such codes will be discussed at the end of this chapter. When the geometry of the system can be approximated by one or two space coordinates, and when conditions for the validity of P_1 theory are fulfilled, the results obtained are accurate. Even when the P_1 approximation is not strictly valid, the experienced designer can use various devices, such as renormalization of group constants to agree with the data from integral experiments and incorporation of results from the unapproximated transport theory, as noted in §4.2d, in order to obtain accurate solutions to certain problems.

When P_1 theory is not valid, but the geometry is simple, multigroup equations involving spherical harmonics of higher order can be used, as indicated for plane geometry in §4.3a. Multigroup methods can be developed similarly on the basis of any of the procedures mentioned in Chapter 3 for approximating the directional dependence of the neutron angular flux. Highly accurate alternative methods are described in the next chapter.

4.5 DETERMINATION OF MULTIGROUP CROSS SECTIONS

4.5a Microscopic Cross Sections

Two separate stages are involved in obtaining the individual group cross sections. First, the microscopic cross sections and their variations with energy for all the isotopes and neutron reactions of interest must be available. And second, an estimate must be made of the dependence on energy, within each group, of the neutron flux and of as many of the Legendre components of the angular flux as are required for the expansion being used. These two ingredients are then combined in expressions of the form of equations (4.26) and (4.27) to determine the group constants.

When reliable experimental data for the microscopic cross sections are available, they should be used. If the required cross sections have not been measured or if the experimental results are of doubtful accuracy, then theoretical cross sections must be employed. The evaluation of measured and theoretical data, in order to arrive at a "best" or most reliable set of cross sections, is an important aspect of the effort to place nuclear reactor theory on a sound basis.

For many years, experimental neutron cross sections were not accurate enough for direct use in reactor criticality calculations. The values were therefore adjusted, usually in multigroup form, in order to obtain agreement between the calculations and the results of some integral experimental quantities, e.g., neutron age to thermal and the critical masses derived from critical (or exponential) experiments. At present, however, the situation is greatly improved. Several evaluated compilations of neutron cross sections are available[24] and, in conjunction with reliable methods of computation, they can be counted upon to give reasonably good results.

Nevertheless, for criticality calculations, the delicate balance between neutron creation and loss may be easily upset by even small discrepancies in the cross sections. Consequently, some adjustment in the data may still be required to fit the results of critical (and other) experiments (§§5.4c, 6.3f). Such adjustments, however, are now usually of a minor character and are frequently not required at all. Moreover, it is possible to adjust the cross sections in a systematic manner so as to keep the changes small and often within the range of the experimental uncertainties.[25]

The aim of the cross section evaluation is to obtain a complete set of microscopic cross section data in a form which can be readily processed by a digital computer. The set should be complete in the sense that it includes all nuclides and neutron reactions that are significant for the problems under consideration. In practice, the data are generally stored on magnetic tape in the form of microscopic cross sections and angular distributions, especially for elastic scattering, at discrete neutron energies. For performing integrations over energy and angle,

which are required for determining group constants, the computer can interpolate between the available data points. Alternatively, the interpolations can be done beforehand in order to obtain microscopic cross sections at a standard set of finely spaced energies; the results are then stored on magnetic tape for use by the computer.

Special procedures are required for the treatment of resonances and of thermalization effects. In the resonance region there is so much fine structure in the neutron cross sections of the heavy nuclides of interest in reactor problems that many thousands of data points would be required for an accurate representation of the dependence of the cross sections on energy. Moreover, the cross sections vary with the temperature of the medium, because of the Doppler broadening of the resonances as the temperature increases. It is more convenient, therefore, to store the data in the form of resonance parameters for those resonances which have been resolved experimentally, and as statistical distributions of parameters for the unresolved resonances.

More will be said about resonance absorption in Chapter 8, but it may be mentioned here that the treatment of resonances, especially in the unresolved region, is on a less firm basis than most other aspects of nuclear reactor physics. Closer association is required, therefore, with integral experiments. In the unresolved resonance region, the average fission and capture cross sections and the statistical distribution of resonance parameters may be known. But there is no guarantee that the actual values do not deviate from the average values in a moderate energy range. Such uncertainties are important for calculations involving large fast reactors which may have a significant proportion of neutrons in the unresolved resonance region.

In the thermal energy range, a scattering model is often specified for computing cross sections, which are a function of the temperature, as well as of the chemical composition of the medium. The problems of thermalization are discussed in Chapter 7.

4.5b Estimation of Within-Group Fluxes

The next step in the evaluation of the group constants, for example, as given by equations (4.26) and (4.27), is to estimate for each group the energy dependence of the total neutron flux, ϕ_0, and the current, ϕ_1, i.e., the first two terms of the Legendre expansion of the angular flux, and such other components (ϕ_n) as may be required. In many cases, simple prescriptions based on qualitative features of the infinite medium solutions are adequate. For example, it is often assumed that the energy dependence of the total flux and of the components of the angular flux are proportional to the fission spectrum at energies $\gtrsim$ 1MeV and to $1/E$ at lower energies. This approach has been reasonably successful when a fairly large number, e.g., about 20, of energy groups are employed. It is very convenient in the respect that group constants can be computed for each

nuclide, independent of all the others which are actually affecting the within-group fluxes. Since the group cross sections obtained in this manner are independent of the composition and geometry, the same set may be used for many problems; such sets of group constants have been tabulated for ready reference.[26]

When the number of groups is small, it is essential, if reasonably accurate calculations are to be made, to allow for variations in composition, and also of geometry. By using the assumption that the collision (or slowing down) density is proportional to $1/E$,[27] the within-group fluxes will depend on all the nuclides present. Another scheme is to postulate that the over-all angular flux is a separable function of angle and energy within a group, i.e., $\Phi(x, \mu, E) = \psi(x, \mu)\phi(E)$, and then to try to estimate only the energy dependence of the total flux.[28]

A systematic approach to the problem of within-group fluxes, which can be used for both moderately large and small numbers of groups, is based on what is known as the B_N approximation to the neutron transport equation. This is discussed in the next section. A variational procedure for determining the group constants in a self-consistent manner, which makes use of the adjoint to the neutron flux, is described in Chapter 6.

4.5c The B_N Method

The basis of the B_N method, as a means of estimating within-group neutron fluxes, is that the spatial dependence of the over-all angular flux can often be approximated by a cosine or exponential term. Thus, by assuming the spatial distribution to be independent of neutron energy, it is possible to write, in plane geometry,

$$\Phi(x, \mu, E) = e^{-iBx}\psi(B, \mu, E), \tag{4.65}$$

where B^2 is the familiar buckling.[29] For a bare homogeneous reactor, it is known from asymptotic reactor theory that B^2 is the lowest eigenvalue of the Helmholtz (or wave) equation, i.e., $\nabla^2\phi = -B^2\phi$, with the boundary condition of zero flux at the extrapolated boundary of the system. Thus, for example, for a bare sphere

$$B^2 = \left(\frac{\pi}{R}\right)^2$$

and for a cylinder

$$B^2 = \left(\frac{2.405}{R}\right)^2 + \left(\frac{\pi}{H}\right)^2,$$

where R and H are the extrapolated radius and height respectively. For a reflected reactor, B is expected to be a real number in the core and an imaginary number in the reflector.

In general, it is usually not difficult to estimate values of B which will provide an approximation to the spatial form of the flux in various regions of a reactor. After the multigroup calculations have been completed, the spatial distribution of the neutron flux in the solution can be compared with that based on the assumed value of B. If the difference is significant, the solution may be iterated until good agreement is obtained. It has been found in practice, however, that the results are not very sensitive to the values of B assumed in deriving the spatial distribution of the flux.[30]

Of course, if the neutron flux really varied as e^{-iBx} for all energies, the simple asymptotic reactor theory could be used to determine the conditions for criticality. In these circumstances, the multigroup approach to the problem, as described in this chapter, would be unnecessary. The fact is, however, that although the assumed spatial dependence of the flux is good enough for evaluating within-group fluxes, it is usually inadequate for the over-all criticality problem.

If equation (4.65) is inserted into the neutron transport equation (4.4) with $Q(x, \mu, E)$ replaced by an isotropic fission source, $\frac{1}{2}F(E)e^{-iBx}$, and an additional subscript, s, for scattering is added to σ_l, the result is

$$\sigma\left(1 - \frac{iB\mu}{\sigma}\right)\psi(B, \mu, E)$$

$$= \sum_{l=0}^{\infty} \frac{2l+1}{2} P_l(\mu) \int \sigma_{sl}(E' \to E) \int_{-1}^{1} \psi(B, \mu', E') P_l(\mu')\, d\mu'\, dE' + \tfrac{1}{2}F(E). \quad (4.66)$$

As in P_N theory, this could be multiplied by $P_n(\mu)$ and integrated over μ from -1 to 1 to obtain equations satisfied by the Legendre components of $\psi(B, \mu, E)$. More rapid convergence of the expansion is achieved, however, by using the procedure employed in §2.6d in connection with anisotropic scattering.[31] Equation (4.66) is divided by $1 - (iB\mu/\sigma)$, multiplied by $P_n(\mu)$, and then integrated to obtain, for $n = 0, 1, 2, \ldots$,

$$\sigma(E)\phi_n(B, E)$$

$$= \sum_{l=0}^{L'} (2l+1) A_{ln}(B, E) \int \sigma_{sl}(E' \to E)\phi_l(B, E')\, dE' + A_{0n}(B, E)F(E). \quad (4.67)$$

The coefficients A_{ln} are defined by

$$A_{ln}(B, E) \equiv \frac{1}{2}\int_{-1}^{1} \frac{P_l(\mu)P_n(\mu)}{1 - \dfrac{iB\mu}{\sigma(E)}}\, d\mu \quad (4.68)$$

and $\phi_n(B, E)$ is given by

$$\phi_n(B, E) \equiv \int_{-1}^{1} \psi(B, \mu, E)P_n(\mu)\, d\mu.$$

The coefficients A_{ln} can be found by utilizing the fact that they satisfy the recurrence relation

$$\frac{1}{y}(2l+1)A_{jl}(y) - (l+1)A_{j,l+1} - lA_{j,l-1} = \frac{\delta_{jl}}{y},$$

where

$$y \equiv \frac{iB}{\sigma(E)}$$

and δ_{jl} is the Kronecker delta, as can be verified from equation (4.68) and the general recurrence relation, given in the Appendix, for Legendre polynomials. Furthermore,

$$A_{jl} = A_{lj} \quad \text{and} \quad A_{00} = \frac{\tanh^{-1} y}{y}.$$

The set of coupled integral equations (4.67) can be solved numerically for $\phi_n(B, E)$ provided the sum on the right-hand side is truncated. For example, when the series is terminated by assuming $\phi_l = 0$ for $l > N$, the result is the B_N approximation. This approximation converges much more rapidly, as a function of N, than would the corresponding P_N approximation. To illustrate this point, it may be noted that, for isotropic scattering, the right-hand side of equation (4.67) would contain only the ϕ_0 (i.e., $l = 0$) component. From the equation for $n = 0$, it is possible to solve for ϕ_0 *exactly*, and the successive components could then also be obtained exactly from the equations with $n = 1, 2, 3, \ldots$. The B_N approximation would then give the first $N + 1$ components exactly. When the scattering is not isotropic but there are only a few important terms in the sum over l, it is reasonable to suppose that convergence will occur rapidly.

For use in deriving within-group fluxes, a value of B is estimated, the series in equation (4.67) is truncated, and the resulting set of equations is solved for $\phi_n(B, E)$ by numerical methods, i.e., by replacing the integral by a sum, and so forth. The energy dependence of $\phi_n(E)$, which is required for deriving the group constants, is then assumed to be the same as that of $\phi_n(B, E)$. Either this or very similar procedures are used for generating group constants in a variety of codes.[32] Accurate results can be obtained with as few as four groups if the buckling is known fairly well. The method has been applied in the study of water-moderated[33] and most other types of reactors.

4.5d Overlapping Energy Groups

In the foregoing treatment, it has been assumed that the group structure is such as to permit subdivision of the energy range into a set of nonoverlapping groups. It is possible, however, to use groups which overlap in energy. Such a situation could arise, for example, in a medium with a temperature discontinuity; it might then be reasonable to represent the thermal flux by two groups, with

different group cross sections, each characteristic of one of the two temperatures. In cases of this kind, calculation of the group constants requires a physical model for the within-group spectra and for the mechanisms which transfer neutrons from one group to the other.[34]

4.6 OUTLINE OF A MULTIGROUP CALCULATION

4.6a Reactor Codes

The various stages of a multigroup calculation are illustrated by the block diagram in Fig. 4.2. At the present time, all of the calculations are carried out more-or-less automatically by an electronic digital computer, starting from the input data and problem specification, in accordance with the instructions provided by a suitable "code" or program. Many codes have been developed for performing reactor calculations,[35] and new ones are introduced from time to time. The manner in which these codes function will be indicated shortly, and some specific examples will be given in §10.3c.

Although the evaluation of the group cross sections is included in the scheme in Fig. 4.2, this stage of the calculation is often carried out in a separate computer program which furnishes the group constants for the multigroup program; this is, however, only an operational detail.

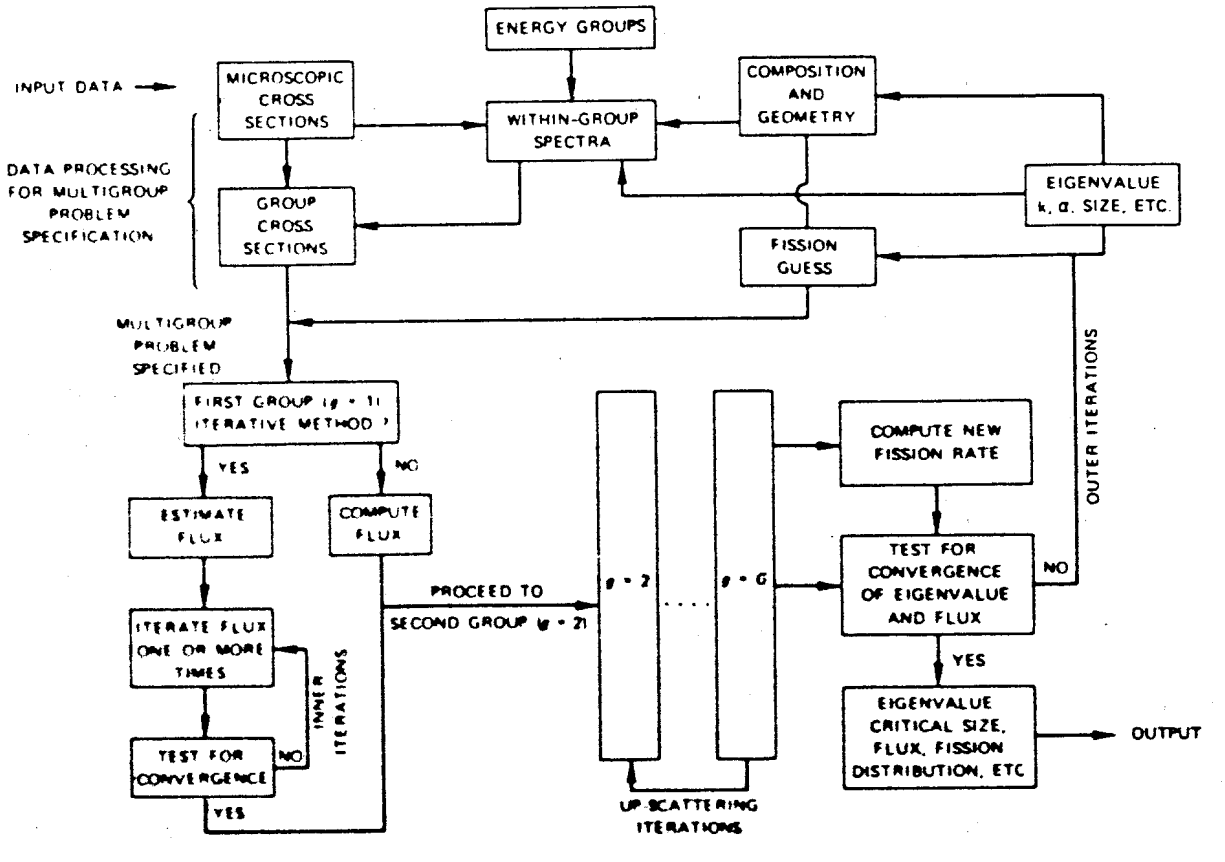

FIG. 4.2 STAGES OF A MULTIGROUP CALCULATION.

In general the input to a computer code includes three main aspects, which are described below. They are: (1) the data required to generate the group constants; (2) certain quantities which serve both as input and as factors determining the choice of code; and (3) the specifications of the problem for which a solution is being sought.

Generation of the group constants requires the microscopic cross sections as a function of energy, together with specifications of the energy groups, i.e., number and individual energy ranges, and the geometry and composition of the system under consideration. From this information, the group constants are evaluated, e.g., by the B_N method. If the whole energy range is divided into a moderately large number of groups, tabulated group cross sections for individual nuclides, independent of geometry and composition, may sometimes be used directly.

The quantities which represent input data and which also determine the code to be used are the geometry of the system and the approximation to the angular flux distribution. The geometry may be one-dimensional, e.g., slab, sphere, or infinite cylinder, or it may be two- or three-dimensional. Different computer programs are generally used according to the number of space dimensions of the system. Typically, the number of points in the space mesh might be $(50)^d$, where d is the number of space dimensions. The nature of the approximation to the angular flux distribution, e.g., P_1, P_3, double-P_1, etc., is part of the code; in multigroup calculations for whole reactors, P_1, diffusion, and age-diffusion approximations are commonly used. In addition, the value of l may be specified at which cut off is to take place in the Legendre expansion of the scattering function in equation (4.2).

Finally, among the specifications which define the problem for which a solution is being sought are (*a*) the boundary conditions, e.g., free surface, periodic, or reflecting, and (*b*) whether the system includes an independent (or extraneous) neutron source or if an eigenvalue is being sought. For a subcritical system with an independent source, the magnitude of this source must be specified. In an eigenvalue problem, the required solution may have as an eigenvalue either the effective multiplication factor, i.e., k, the time rate of multiplication, represented by α, the concentration of fissile material required for criticality in a region, or reflector thickness, etc. Hence, the nature of the eigenvalue must be specified. If it is k, it is automatically included in the guessed fission source described in §4.4d. On the other hand, if another equivalue is required a guess must be made as to its magnitude.

4.6b Computation of an Eigenvalue Problem

In the following, it will be assumed that an eigenvalue problem is to be solved, for example, for the purpose of determining the effective multiplication factor or the conditions for criticality in a given system. Once the group constants have

been defined, together with the geometry and composition of the system and the nature of the problem to be solved, a fission source is guessed. The spatial distribution of the total flux in the first group ($g = 1$) may then be computed either directly, for a one-dimensional system, or by using inner iterations. If approximations of higher order than P_1 are involved, then components of the angular flux are required in addition to the total flux and current. When the flux is known for the first group, the calculation can proceed to the next ($g = 2$) group, with the guessed fission source, and so on through all the G groups. If some of the groups involve up-scattering then separate iterations will be required unless special methods, such as the stabilized march technique, are employed.

When all the group fluxes are known, the solution is tested for convergence as described in §4.4d. If it has not converged, then outer iterations are continued until $k^{(n)}$ is sufficiently close to $k^{(n-1)}$. If the eigenvalue k is being sought, together with the associated eigenfunction, i.e., the neutron flux distribution, the calculation is now complete. However, it is still worth checking to determine if the computed group fluxes are more-or-less consistent with the within-group fluxes postulated in generating the group constants. If there is a significant inconsistency, then it may be necessary to redetermine the group constants and to reiterate the procedure until convergence is attained.

Suppose it is desired to determine the conditions for criticality; the value of k derived in the manner described above should then be unity. If it is not, the dimensions or composition (or both) of the system are changed, as described at the end of §4.4d. The whole computation, including recalculation of group constants, if necessary, is then repeated until k is found to be unity.

Various methods are commonly used for accelerating the convergence of both inner and outer iterations. According to the arguments in §4.4f, k calculations are guaranteed to converge, at least in multigroup diffusion theory. For more complicated, but physically reasonable eigenvalues, such as material concentrations or region thicknesses, convergence generally occurs in practice, although difficulties can arise from the use of overambitious accelerating procedures.

Since the calculations described above yield the neutron flux distribution in both space and energy, the code can include instructions to the computer to determine various quantities that are related to the flux distribution and cross sections. Thus, in addition to the required eigenvalue and corresponding eigenfunction, the computer printout may include such information as fission (or power) density as a function of position, total power generation, conversion (or breeding) ratios, fuel burnup, and so on (Chapter 10).

Finally, the code may be constructed so as to compute the adjoint to the neutron flux. As mentioned earlier, this information can be employed to determine the group constants in a self-consistent manner. Several uses of the adjoint in reactor calculations will be discussed in Chapter 6.

4.7 APPENDIX: RELATIONSHIP BETWEEN P_1, AGE-DIFFUSION, AND OTHER THEORIES

4.7a The Lethargy Variable

In elementary slowing-down theory,[36] it is convenient to use the *lethargy* variable, u ($= \ln E_0/E$), in treating neutron moderation. The reason is, of course, that in elastic scattering a neutron tends to lose a *fraction*, rather than a given amount, of its energy. Hence, a logarithmic energy scale is appropriate where moderation by elastic scattering is predominant. For example, the neutron flux per unit lethargy is approximately constant in many slowing-down problems. In multigroup calculations a logarithmic energy scale is often adopted in setting up the group boundaries for the energy range, e.g., 1 eV $\leqslant E \leqslant$ 0.1 MeV, where slowing down of neutrons by elastic scattering is important. At higher and lower energies, however, other choices are more appropriate.

Lethargy is not used in the main text of this book, primarily because it is an awkward energy variable for use in describing cross sections. The application of the lethargy variable to multigroup problems will be treated in this appendix, however, because it provides a convenient way of obtaining the relationship between P_1 and age-diffusion theories. Some of the early multigroup methods were first applied to age-diffusion theory[37] and they are quite capable of treating a limited class of reactors with good accuracy.

In the following, plane geometry will be considered for simplicity, but the formulation could be readily generalized to any geometry, as in Chapter 3. The lethargy, u, of a neutron of energy E is defined by

$$u = \ln \frac{E_0}{E},$$

where E_0 is some maximum energy, commonly taken as 10 MeV.

4.7b Elastic Scattering in Terms of Lethargy

Let the angular flux of neutrons per unit lethargy be represented by $\Psi(x, \mu, u)$; it is related to the angular flux, Φ, per unit energy by

$$\Phi(x, \mu, E)\,|dE| = \Psi(x, \mu, u)\,|du|,$$

and since

$$|du| = \frac{1}{E}\,|dE|,$$

it follows that

$$\Psi(x, \mu, u) = E\Phi(x, \mu, E)$$

and

$$\Phi(x, \mu, E) = \frac{e^u}{E_0}\,\Psi(x, \mu, u).$$

Similarly, let the source per unit lethargy be $Q(x, \mu, u)$ and let $f(x; u' \to u, \mu_0)$ be the probability of scattering from lethargy u' into a unit lethargy range about u for the scattering angle $\cos^{-1}\mu_0$.

For elastic scattering that is isotropic in the center-of-mass system, equation (4.5) may then be expressed in terms of the lethargy variable by

$$\sigma(x, u')f(x; u' \to u, \mu_0) = \frac{\sigma_s(x, u')}{2\pi(1 - \alpha)} \frac{E}{E'} \delta(\mu_0 - S)$$

$$= \frac{\sigma_s(x, u')}{2\pi(1 - \alpha)} e^{u' - u} \delta(\mu_0 - S) \quad \text{if} \quad u' \leqslant u \leqslant u' - \ln \alpha$$

$$= 0 \quad \text{if} \quad u < u' \quad \text{or} \quad u > u' - \ln \alpha, \tag{4.69}$$

where S is given in terms of lethargy by

$$S \equiv \tfrac{1}{2}[(A + 1)e^{(1/2)(u' - u)} - (A - 1)e^{(1/2)(u - u')}].$$

In the foregoing,

$$\sigma(x, u') = \sigma(x, E')$$

and

$$u' = \ln \frac{E_0}{E'}.$$

4.7c The P_1 Approximation in Terms of Lethargy

The transport equation (4.1) in plane geometry for the lethargy variable is

$$\mu \frac{\partial \Psi(x, \mu, u)}{\partial x} + \sigma(x, u)\Psi(x, \mu, u) = 2\pi \int\int_{-1}^{1} \sigma(x, u')f(x; u' \to u, \mu_0)$$

$$\times \Psi(x, \mu', u')\, d\mu'\, du' + Q(x, \mu, u). \tag{4.70}$$

Hence, upon expanding in Legendre polynomials,

$$\Psi(x, \mu, u) = \sum_{m=0}^{\infty} \frac{2m + 1}{4\pi} \psi_m(x, u)P_m(\mu)$$

$$Q(x, \mu, u) = \sum_{m=0}^{\infty} \frac{2m + 1}{4\pi} Q_m(x, u)P_m(\mu)$$

$$\sigma(x, u')f(x; u' \to u, \mu_0) = \sum_{l=0}^{\infty} \frac{2l + 1}{4\pi} \sigma_l(x; u' \to u)P_l(\mu_0).$$

These expansions are inserted into equation (4.70) and upon truncation after two terms, i.e., by making the P_1 approximation, it is found that

$$\frac{\partial \psi_1(x, u)}{\partial x} + \sigma(x, u)\psi_0(x, u) = \int \sigma_0(x; u' \to u)\psi_0(x, u')\, du' + Q_0(x, u) \tag{4.71}$$

$$\frac{\partial \psi_0(x, u)}{\partial x} + 3\sigma(x, u)\psi_1(x, u) = 3\int \sigma_1(x; u' \to u)\psi_1(x, u')\, du' + 3Q_1(x, u). \tag{4.72}$$

Equations (4.71) and (4.72) are equivalent to the P_1 equations (4.15) and (4.16), except that all functions of energy have been replaced by the corresponding functions of lethargy. As before, ψ_0 and ψ_1 are equivalent to the total neutron flux and the current, respectively. A set of multigroup equations could now be obtained by integrating equations (4.71) and (4.72) over the lethargy range representing each energy (lethargy) group, and so on, in the manner described in §4.3a.

4.7d Age-Diffusion Theory

In order to derive age-diffusion theory, the integrals over u' in equations (4.71) and (4.72) are evaluated approximately by expanding the integrands in a Taylor series about lethargy u. From elementary slowing-down theory, it is known that the flux ψ_0, or the collision density $\sigma_0\psi_0$, will be nearly constant in many situations, e.g., in the moderation of neutrons in the energy range of, say, 1 eV $\lesssim E \lesssim$ 0.1 MeV (or $4 \lesssim u \lesssim 16$), by graphite or beryllium. Hence, for such cases, the Taylor expansion should be quite good.

In expanding the integrands in a Taylor series, two terms are retained for equation (4.71) and one for equation (4.72). The situation is somewhat clearer when the cross sections in the integrals are written as functions of u' and $u - u'$; thus,

$$\sigma_l(x; u' \to u) = \sigma_l(x, u', u - u').$$

Then the expansions of the integrands are

$$\sigma_0(x, u', u - u')\psi_0(x, u') \approx \sigma_0(x, u, u - u')\psi_0(x, u) - (u - u')\frac{\partial \sigma_0\psi_0}{\partial u}$$

$$\sigma_1(x, u', u - u')\psi_1(x, u') \approx \sigma_1(x, u, u - u')\psi_1(x, u).$$

Upon inserting these expressions into equations (4.71) and (4.72) and using the notation

$$\int \sigma_0(x, u, u - u')\, du' \equiv \sigma_0(x, u) \tag{4.73}$$

$$\int (u - u')\sigma_0(x, u, u - u')\, du' \equiv \xi(u)\sigma_0(x, u) \tag{4.74}$$

$$\int \sigma_1(x, u, u - u')\, du' \equiv \bar{\mu}_0(u)\sigma_0(x, u), \tag{4.75}$$

it is found from equation (4.71) that

$$\frac{\partial \psi_1}{\partial x} + (\sigma - \sigma_0)\psi = \frac{\partial}{\partial u}(\xi \sigma_0 \psi_0) + Q_0 \tag{4.76}$$

and from equation (4.72) that

$$\frac{\partial \psi_0}{\partial x} + 3(\sigma - \bar{\mu}_0 \sigma_0)\psi_1 = 3Q_1. \tag{4.77}$$

For isotropic scattering in the center-of-mass system, for a single element, so that σf is given by equation (4.69), it follows from equations (4.73), (4.74), and (4.75) that

$$\sigma_0 = \sigma_s(x, u)$$

$$\xi = 1 + \frac{\alpha \ln \alpha}{1 - \alpha}$$

$$\bar{\mu}_0 = \frac{2}{3A}.$$

These quantities have their elementary interpretations, respectively, as the scattering cross section, the mean logarithmic energy loss for neutron-nucleus collision, and the mean cosine of the scattering angle.[38]

For an isotropic source, $Q_1 = 0$, and equation (4.77) represents a form of Fick's law with the diffusion coefficient the same as in equation (4.23); thus,

$$\psi_1 = -D \frac{\partial \psi_0}{\partial x} \quad \text{and} \quad D = \tfrac{1}{3}(\sigma - \bar{\mu}_0 \sigma_0)^{-1}.$$

As before, the Fick's law expression may be used to eliminate ψ_1 from equation (4.76); the resulting age-diffusion equation is

$$-\frac{\partial}{\partial x}\left(D \frac{\partial \psi_0}{\partial x}\right) + (\sigma - \sigma_0)\psi_0 = \frac{\partial}{\partial u}(\xi \sigma_0 \psi_0) + Q_0. \tag{4.78}$$

The quantity $\xi \sigma_0 \psi_0$ is commonly called the slowing-down density and is denoted by the symbol $q(x, u)$.

For some situations, equation (4.78) may be simplified further. For example, if $Q_0 = 0$ and there is no neutron absorption, so that $\sigma = \sigma_0$, and the quantities D, ξ, and σ are independent of energy (or lethargy), equation (4.78) may be written

$$\frac{\partial^2 q(x, u)}{\partial x^2} = \frac{\xi \sigma_0}{D} \frac{\partial q}{\partial u} = \frac{\partial q}{\partial \tau}, \tag{4.79}$$

where τ, called the Fermi age, is defined by

$$\tau(u) \equiv \int_0^u \frac{D}{\xi \sigma_0} du' = \int_0^u \frac{du'}{3\xi \sigma_0^2 (1 - \bar{\mu}_0)}.$$

Equation (4.79) is frequently referred to as the Fermi age equation, here given in plane geometry. Solutions for simple cases will be found in the standard reactor theory texts.

From the present point of view, it is seen that age-diffusion theory may be regarded as resulting from the approximation of the slowing-down integrals of the energy-dependent P_1 theory. The approximation to the integral in equation (4.71) represents the age aspect, whereas the diffusion aspect arises from the approximation to the integral in equation (4.72). Both approximations should be good for problems in which the collision density varies gradually and smoothly with energy. Such is usually the case when the moderating system consists of elements with fairly large or large mass numbers. When hydrogen is present, however, a neutron can lose a considerable proportion of its energy in a scattering collision and the age-diffusion approximations are not valid. A thorough discussion of the conditions of validity of age-diffusion theory will be found in the literature.[39]

Other related approximations to the slowing-down integrals are of historical interest and some practical importance. For example, in treating neutron moderation in a medium containing hydrogen as well as heavier elements, the age-diffusion approximation can sometimes be made for the contributions to the slowing down integrals due to collisions with the heavier nuclei, whereas the full integrals are retained for collisions with hydrogen. This treatment is known as the Selengut-Goertzel method.[40] Among other methods of deriving the integrals mention may be made of that of Greuling and Goertzel.[41] Since these approximations to P_1 theory are becoming less important in reactor analysis, they will not be described here.[42]

4.7e Multigroup Age-Diffusion Theory

In order to develop a multigroup form of age-diffusion theory, the lethargy range $0 \leq u \leq u_{max}$ is subdivided into a number of groups with lethargy boundaries $u_0 (=0), u_1, u_2, \ldots, u_G (=u_{max})$. Equation (4.78) is then integrated over one such group, from u_{g-1} to u_g, and the group diffusion constant, absorption cross section, and source are defined as in §§4.3a, 4.3b, at least if D is piecewise constant. The only new feature arises from the slowing down term which gives

$$\int_{u_{g-1}}^{u_g} \frac{\partial}{\partial u}(\xi\sigma_0\psi_0)\,du = \xi\sigma_0\psi_0(x, u_g) - \xi\sigma_0\psi_0(x, u_{g-1}).$$

Thus the group equation involves the fluxes, or slowing down densities, at both end-points of the group, as well as the group flux $\int_g \psi\,du$. To eliminate one or the other, it is necessary to postulate some relation between the group flux and the fluxes at the group end-points. A number of choices are possible to complete the specification of the multigroup problem[43]; for example, ψ_0 is assumed to vary linearly with u within a group.

EXERCISES

1. Suppose that neutrons are being moderated in water, and consider an energy region in which the cross sections of both hydrogen and oxygen are constant. In a multigroup problem, the energy groups are such that $E_{g-1} = 3E_g$. Derive the P_1 (or P_N) group constants for hydrogen and oxygen, i.e., $\sigma_{n,g}$ and $\sigma_{n,g'\to g}$, for isotropic scattering in the center-of-mass system, assuming (*a*) $\phi_n(E)$ = constant and (*b*) $\phi_n(E) \propto 1/E$ within a group. Discuss the results.
2. Make the P_3 approximation to the one-speed equation (3.5) in plane geometry, and consider new independent variables $F_0 = \phi_0 + 2\phi_2$ and $F_1 = \phi_2$. Use these variables in the P_3 equations and combine them to eliminate ϕ_1 and ϕ_3, thus obtaining two second-order equations resembling those of a two-group diffusion theory. Show how the result can be used to solve the P_3 equations. This method can be extended to P_N and double-P_N equations in slab geometry.[44]
3. Definitions of an energy-dependent diffusion coefficient, other than that given by equation (4.23), are potentially more accurate. Consider the following two alternatives for use in developing multigroup diffusion theory: (*a*) by using equation (4.19) and (*b*) by deriving a form of Fick's law from equation (4.31) with $\mathbf{Q}_1 = 0$. Discuss the difficulties and advantages of these possibilities.[45]
4. In connection with the preceding exercise, suppose that neutrons from a 2-MeV source are being moderated in a hydrogenous medium, such that the energy dependence of the flux and current, for computing the group constants, can be approximated by that in an infinite medium of hydrogen.[46] Suppose that a group structure with boundaries at 2.1, 1.4, 0.9, 0.4, . . . MeV is used. Determine the group diffusion coefficients for these first few groups according to equations (4.19) and (4.23). The hydrogen cross section may be taken to be proportional to $1/\sqrt{E}$ in the given energy range.
5. Verify that, for isotropic scattering in the center-of-mass system, σ_0, ξ, and $\bar{\mu}_0$ have the values given in §4.7d.

REFERENCES

1. Leonard, A., and J. H. Ferziger, *Nucl. Sci. Eng.*, **26**, 170, 181 (1966); T. Yoshimura and S. Katsuragi, *ibid.*, **33**, 297 (1968); D. R. Metcalf and P. F. Zweifel, *ibid.*, **33**, 307, 318 (1968).
2. Davison, B., "Neutron Transport Theory," Oxford University Press, 1957, Chaps. XXIV, XXVI.
3. Weinberg, A. M., and E. P. Wigner, "The Physical Theory of Neutron Chain Reactors," University of Chicago Press, 1958, Chap. XII; J. H. Ferziger and P. F. Zweifel, "The Theory of Neutron Slowing Down in Nuclear Reactors," The M.I.T. Press, 1966, Section I.C.
4. Driscoll, M. J., and J. Kaplan, *Trans. Am. Nucl. Soc.*, **9**, 137 (1966); W. M. Stacey, Jr., *Nucl. Sci. Eng.*, **28**, 443 (1967); "Modal Approximations," The M.I.T. Press, 1967.
5. Weinberg, A. M., and E. P. Wigner, Ref. 3, p. 280.
6. Weinberg, A. M., and E. P. Wigner, Ref. 3, p. 373.
7. "Naval Reactor Physics Handbook," Vol. I, A. Radkowsky, ed., U.S. AEC, 1964, Sections 4.2, 4.3.
8. Ehrlich, R., and H. Hurwitz, Jr., *Nucleonics*, **12**, No. 2, 23 (1954).
9. Habetler, G. J., and M. A. Martino, *Proc. Symp. Appl. Math.*, **XI**, Am. Math. Soc., 1961, p. 127.
10. Weinberg, A. M., and E. P. Wigner, Ref. 3, p. 235.
11. Habetler, G. J., and M. A. Martino, Ref. 9.

12. Habetler, G. J., and M. A. Martino, Ref. 9.
13. Habetler, G. J., and M. A. Martino, Ref. 9.
14. Habetler, G. J., and M. A. Martino, Ref. 9.
15. Birkhoff, G., *Proc. Symp. Appl. Math.*, XI, Am. Math. Soc., 1961, p. 116; *Rend. Matematica*, **22**, 102 (1963).
16. Butler, M. K., and J. M. Cook, in "Computing Methods in Reactor Physics," H. Greenspan, C. N. Kelber, and D. Okrent, eds., Gordon and Breach, 1968, p. 52.
17. Edwards, D. R., and K. F. Hansen, *Nucl. Sci. Eng.*, **25**, 58 (1966).
18. Hassit, A., in "Computing Methods in Reactor Physics," Ref. 16, Section 2.15.
19. Birkhoff, G., and R. S. Varga, *J. Soc. Indust. Appl. Math.*, **6**, 354, (1958); R. S. Varga, *Proc. Symp. Appl. Math.*, XI, Am. Math. Soc., 1961, p. 164; R. Froehlich, *Nucl. Sci. Eng.*, **34**, 57 (1968); *Nukleonik*, **11**, 255 (1968).
20. See citations in Ref. 19.
21. Varga, R. S., Ref. 19; A. Hassit, Ref. 18, Section 2.16.
22. Varga, R. S., Ref. 19.
23. Birkhoff, G., Ref. 15.
24. Parker, K., D. T. Goldman, and L. Wallin, in "Nuclear Data for Nuclear Reactors," IAEA, 1967, Vol. II, p. 293.
25. Hemment, P. C. E., and E. D. Pendlebury, Proc. Int. Conf. on Fast Critical Experiments and their Analysis, Argonne National Laboratory Report ANL-8320 (1966), p. 88.
26. "Reactor Physics Constants," Argonne National Laboratory Report ANL-5800 (1962), Section 7.1.2; S. Yiftah, D. Okrent, and P. Moldauer, "Fast Reactor Cross Sections—A Study Leading to a Sixteen Group Cross Section Set," Pergamon Press, 1960; W. H. Roach, *Nucl. Sci. Eng.*, **8**, 621 (1960).
27. Glasstone, S., and M. C. Edlund, "Elements of Nuclear Reactor Theory," D. Van Nostrand Co., Inc., 1952, Chap. VI; J. R. Lamarsh, "Introduction to Nuclear Reactor Theory," Addison-Wesley Publishing Co., Inc., 1966, Chap. 6.
28. Pomraning, G. C., *J. Nucl. Energy*, **18**, 497 (1964); *Nucl. Sci. Eng.*, **19**, 250 (1964).
29. Glasstone, S., and M. C. Edlund, Ref. 27, §7.23; A. M. Weinberg, and E. P. Wigner, Ref. 3, p. 383; J. R. Lamarsh, Ref. 27, p. 291.
30. Ref. 7, pp. 207 *et seq.*
31. Hurwitz, H., Jr., and P. F. Zweifel, *J. Appl. Phys.*, **26**, 923 (1955); J. E. Wilkins, R. L. Hellens, and P. F. Zewifel, *Proc. First U.N. Conf. on Peaceful Uses of Atomic Energy*, **5**, 62 (1955).
32. Ref. 7, pp. 218 *et seq.*; G. D. Joanou, E. J. Leshan, and J. S. Dudek, "GAM-1, A Consistent P_1 Multigroup Code for the Calculation of the Fast Neutron Spectra and Multigroup Constants," General Atomic Report GA-1850 (1961).
33. Ref. 7, Section 2.8.
34. Calame, G. P., and F. D. Federighi, *Nucl. Sci. Eng.*, **10**, 190 (1961).
35. Butler, M. K., *et al.*, "Argonne Code Center: Compilation of Program Abstracts," Argonne National Laboratory Report ANL-7411 (1968) and supplements issued subsequently.
36. See citations in Ref. 27.
37. Ehrlich, R., and H. Hurwitz, Jr., Ref. 8.
38. Glasstone, S., and M. C. Edlund, Ref. 27, §§5.22, 6.21; J. R. Lamarsh, Ref. 27, Sections 2-9, 6-4; A. M. Weinberg and E. P. Wigner, Ref. 3, p. 282.
39. Davison, B., Ref. 2, Chap. XXIII; R. E. Marshak, *Rev. Mod. Phys.*, **19**, 185 (1947).
40. Weinberg, A. M., and E. P. Wigner, Ref. 3, p. 362; Ref. 7, pp. 203, 226; J. H. Ferziger and P. F. Zweifel, Ref. 3, pp. 153 *et seq.*
41. Greuling, E., and G. Goertzel, *Nucl. Sci. Eng.*, **7**, 69 (1960).
42. Ferziger, J. H., and P. F. Zweifel, Ref. 3, Section III C.
43. Ehrlich, R., and H. Hurwitz, Jr., Ref. 8.
44. Gelbard, E. M., J. Davis, and J. Pearson, *Nucl. Sci. Eng.*, **5**, 36 (1959); E. M. Gelbard in "Computing Methods in Reactor Physics," Ref. 16, pp. 301 *et seq.*
45. Joanou, G. D., and A. H. Kazi, *Trans. Am. Nucl. Soc.*, **6**, 173 (1963); G. Rakavy and Y. Yeivin, *Nucl. Sci. Eng.*, **15**, 158 (1963).
46. Glasstone, S., and M. C. Edlund, Ref. 27, pp. 148 *et seq*; J. R. Lamarsh, Ref. 27; Section 6-3.

5. DISCRETE ORDINATES AND DISCRETE S_N METHODS

5.1 INTRODUCTION

5.1a Special Features of the Discrete Ordinates Methods

The discrete ordinates and related methods of obtaining numerical solutions of the energy-dependent neutron transport equation have been used extensively in reactor calculations. The essential basis of these methods is that the angular distribution of the neutron flux is evaluated in a number of discrete directions, instead of using spherical harmonics, as in Chapters 3 and 4. By considering enough directions, it is possible, in principle, to obtain a solution of the transport equation to any desired degree of accuracy, subject only to the limitations of the available computing machine. It will be seen that some versions of these discrete methods are related to the method of spherical harmonics.

In the solution of practical problems by discrete ordinates techniques, a discrete energy variable is introduced, by means of a multigroup approximation, and a discrete space mesh is used for the spatial coordinates as in the preceding chapter. Consequently, all the independent variables of the time-independent neutron transport equation, namely, space, $\mathbf{r}$, direction, $\mathbf{\Omega}$, and energy, E, are treated as discrete. As compared with the method of spherical harmonics, the distinguishing feature of the method of discrete ordinates is the discrete treatment of the angular (or direction) variable.

A number of new and important problems arise in the development of the method. They are: (1) the choice of the particular discrete directions; (2) the

approximation of the integrals over the direction variable; and (3) the approximation of the derivatives of the neutron angular flux with respect to the components of Ω appearing in the transport equation in curved geometries (§§5.3a, 5.3b). These problems will be treated in the present chapter, but it may be stated at the outset that there are no unique solutions to them. This lack of uniqueness, is, however, not unexpected. In the P_N approximation, the choices of energy groups and a space mesh are not unique, but must be based on physical insight and experience. The same factors determine the choice of direction and other parameters in the method of discrete ordinates.

In order to minimize the formidable notational complexity, it will be convenient to consider first the one-speed transport equation. Subsequently, the solution of the energy-dependent problem by multigroup methods will be examined: as in Chapter 4, this involves a set of coupled one-speed differential equations. The determination of reliable group constants is once again an essential requirement for obtaining a satisfactory solution.

5.1b Plane and Curved Geometries

The discrete ordinates method of solving the one-speed transport equation will be treated initially in plane geometry. This is not only a simple case of interest, but it is also an idealization of some lattices. It is for the one-speed problem in plane geometry that a relationship is particularly clear between the use of discrete directions and of spherical harmonics to represent the angular distribution of the neutron flux.

A special aspect of plane geometry (or of rectangular cartesian coordinates in general) is that the direction of a neutron, as specified by direction cosines relative to local coordinates, does not change as the neutron streams, that is, moves through the medium without making any collisions. In plane geometry, therefore, the only concern is with problems (1) and (2) mentioned above, i.e., choice of direction and the evaluation of integrals.

In curved geometry, i.e., in systems of spherical or cylindrical coordinates, however, the situation is different and the angular derivatives in the transport equation must be approximated in addition. These derivatives arise because, in streaming, the direction variable of a neutron changes continuously in curved geometry. Hence, the streaming term, $\Omega \cdot \nabla \Phi$, in the transport equation will introduce derivatives with respect to the components of Ω. Suppose, for example, that the neutron direction in spherical coordinates is described by μ, i.e., the direction cosine relative to the radius vector; then it is evident that μ increases continuously as the neutron streams through the medium (Fig. 5.1). In a later section it will be shown how this situation is treated by discrete S_N techniques.

An alternative approach would be to describe the neutron motion relative to a fixed direction in space, rather than to local coordinates. This would be

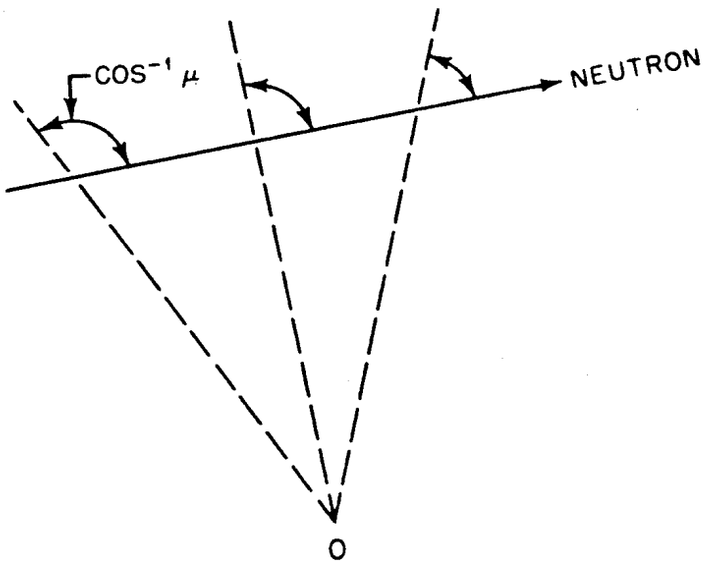

FIG. 5.1 CHANGE IN DIRECTION COSINE OF STREAMING NEUTRON.

equivalent to considering characteristic directions in the integral form of the neutron transport equation (§1.2b). Numerical solutions of the integral equation or, what is the same thing, solutions of the transport equation by the method of characteristics have been obtained[1]; they will, however, not be described in this book.

5.2 DISCRETE ORDINATES FOR ONE SPEED IN PLANE GEOMETRY

5.2a Isotropic Scattering

The method of discrete ordinates (or discrete directions) in plane geometry was first proposed[2] and developed in detail[3] for the study of radiation transfer problems in stellar atmospheres. This treatment utilized a special choice of directions and a particular method of numerical integration, using the Gauss quadrature formula (cf. §5.2c). In the development given here, a more general procedure will first be described.

The one-speed transport equation in plane geometry for isotropic scattering and a generalized source may be written (see §2.1c) as

$$\mu \frac{\partial \Phi(x, \mu)}{\partial x} + \sigma(x)\Phi(x, \mu) = \frac{c(x)\sigma(x)}{2} \int_{-1}^{1} \Phi(x, \mu')\, d\mu' + Q(x, \mu). \qquad (5.1)$$

Consider this equation for a set of discrete directions $\{\mu_i\}$; if the integral were evaluated by a numerical quadrature formula involving $\Phi(x, \mu_i)$, there would be

obtained a set of coupled first-order differential equations for $\Phi(x, \mu_i)$ that would be equivalent to equation (5.1). Thus, if the integral is represented by

$$\int_{-1}^{1} \Phi(x, \mu')\, d\mu' \simeq \sum_{i=1}^{N} w_i \Phi(x, \mu_i), \tag{5.2}$$

where the w_i are the quadrature weights (or weighting factors), equation (5.1) becomes

$$\mu_j \frac{\partial \Phi(x, \mu_j)}{\partial x} + \sigma(x)\Phi(x, \mu_j) = \frac{c(x)\sigma(x)}{2} \sum_{i=1}^{N} w_i \Phi(x, \mu_i) + Q(x, \mu_j)$$
$$j = 1, 2, \ldots, N. \tag{5.3}$$

This set of N coupled differential equations can be solved readily by finite difference techniques once the boundary conditions and the character of the problem are specified.

So far nothing has been said about the choice of the set of direction cosines, $\{\mu_i\}$, nor of the associated quadrature weights, $\{w_i\}$. The accuracy which can be achieved in solving the equations (5.3) for a given N will depend, however, to a large extent on making a good choice. The following properties of the w_i and μ_i seem to be reasonable requirements:

(1) Since the integral in equation (5.1) is always positive (or nonnegative), it is required that $w_i > 0$ for all i.

(2) A symmetric choice of directions and weights about $\mu = 0$, i.e.,

$$\mu_i = -\mu_{N+1-i} \quad \text{and} \quad w_i = w_{N+1-i},$$

is suggested so that the formulation will be symmetric upon reflection. In other words, the solution will not depend on which side of a slab is designated as the right side and which as the left side.*

(3) It is required that if $\Phi(x, \mu)$ is a polynomial of low order in μ, then the quadrature formula of equation (5.2) should give the exact value of the integral. This implies that

$$\sum_{i=1}^{N} w_i \mu_i^n = \frac{2}{n+1} \quad \text{for } n \text{ even}$$

and

$$\sum_{i=1}^{N} w_i \mu_i^n = 0 \quad \text{for } n \text{ odd.}$$

Actually, the condition for n odd is guaranteed by property (2).

The values of n for which these relations should be satisfied must now be considered. Suppose that N is even; then there are N values of μ_i and N values

* If, in a particular situation, the flux is known to be highly asymmetric, it may be advantageous to use unsymmetrical quadrature sets; for example, if the flux is peaked near $\mu = +1$, it may be useful to have the discrete directions closer together in this vicinity.[4]

of w_i, or $2N$ parameters in all to be determined. Condition (2) implies that only N of these are independent. If there were N independent parameters for fitting condition (3) with n even, then it might be possible to satisfy this condition for $n = 0, 2, 4, \ldots, 2N - 2$, but not beyond. If such a choice is made, it will determine μ_i and w_i uniquely as the Gauss quadrature[5] set of directions and weights; the weights are all positive and satisfy condition (1). It is not necessary, however, to satisfy condition (3) for so many values of n (with n even); in this event, there is some freedom to impose other conditions. More will be said about this presently.

5.2b Discrete Ordinates and Spherical Harmonics

Before proceeding to consider some special choices of μ_i, w_i, the relationship between the methods of discrete ordinates and spherical harmonics will be examined. In the spherical harmonics (P_N) procedure the integrals involved are [cf. equation (2.58)]

$$\phi_n(x) = \int \Phi(x, \mu)P_n(\mu)\, d\Omega = 2\pi \int_{-1}^{1} \Phi(x, \mu)P_n(\mu)\, d\mu.$$

The equivalent quantities for the discrete ordinates treatment are defined by using the quadrature formula as in equation (5.2); thus,

$$\tilde{\phi}_n(x) = 2\pi \sum_{i=1}^{N} w_i \Phi(x, \mu_i)P_n(\mu_i), \tag{5.4}$$

where the symbol $\tilde{\phi}_n(x)$ is used to indicate an approximation to $\phi_n(x)$ that is obtained from the quadrature formula.

To find equations satisfied by the $\tilde{\phi}_n(x)$, equation (5.3) is multiplied by $2\pi(2n + 1)w_jP_n(\mu_j)$ and summed over j; with the recurrence relation for Legendre polynomials and the requirement (3) given above for all $n \leqslant N - 1$, the result is

$$(n + 1)\frac{d\tilde{\phi}_{n+1}}{dx} + n\frac{d\tilde{\phi}_{n-1}}{dx} + (2n + 1)\sigma(x)[1 - c(x)\,\delta_{0n}]\tilde{\phi}_n = (2n + 1)\tilde{Q}_n(x)$$

$$n = 0, 1, 2, \ldots, N - 1, \tag{5.5}$$

where

$$\tilde{Q}_n(x) = 2\pi \sum_{i=1}^{N} w_i Q(x, \mu_i)P_n(\mu_i)$$

and δ_{0n} is the Kronecker delta.

It should be noted that equation (5.5) represents a set of N equations, selected since there are only N independent quantities $\Phi(x, \mu_i)$ available. That is, for $n \geqslant N$, the value of $\tilde{\phi}_n$ can be expressed in terms of $\{\tilde{\phi}_n\}$ with $n \leqslant N - 1$ in the following way. If $\tilde{\phi}_n$ were known for $n \leqslant N - 1$, equation (5.4) could be solved

for $\Phi(x, \mu_i)$ with $i = 1, 2, \ldots, N$, and then $\tilde{\phi}_n$ could be found from equation (5.4) for any $n \geqslant N$.

Comparison of equation (5.5) with the equation of the spherical harmonics method, such as equation (2.59), shows that $\tilde{\phi}_n(x)$ satisfies the same set of equations as does $\phi_n(x)$ in the spherical harmonics treatment.

In the spherical harmonics expansion of the angular flux, the series of terms in the summation of polynomials is truncated by assuming that $d\phi_N(x)/dx = 0$ for a P_{N-1} approximation and boundary conditions are used. It will be recalled that this truncation or an equivalent (§2.4b) is required in order to have the same number of unknown functions, ϕ_n, as equations relating them, e.g., equations (2.59). But for the system of equations (5.5) it is not possible simply to set $d\tilde{\phi}_N(x)/dx = 0$, because $\tilde{\phi}_N$ may be derived from the fundamental quantities $\Phi(x, \mu_i)$ by means of equation (5.4), and therefore $d\tilde{\phi}_N/dx$ is determined. By a special choice of μ_i, however, namely, $\{\mu_i\}$ is the set of N zeros of the polynomial $P_N(\mu)$, i.e.,

$$P_N(\mu_i) = 0, \tag{5.6}$$

$d\tilde{\phi}_N(x)/dx$ is automatically zero. The set of equations (5.5) for isotropic scattering is then identical with the truncated set of spherical harmonics.

From the properties of the Legendre polynomials, it is known that $P_N(\mu)$ will have exactly N zeros in the range $-1 \leqslant \mu \leqslant 1$, and so these values form an acceptable set for the present requirement. For N even, there are an even number of directions and an even number of equations (5.5) corresponding to the odd-order spherical harmonics equations. Thus, $N = 2$ in the discrete ordinates procedure corresponds to a P_1 approximation.

5.2c Gauss Quadrature Parameters

If the $\{\mu_i\}$ are chosen, as indicated above, to satisfy equation (5.6), then the $\{w_i\}$ will be determined from requirement (3) for $n \leqslant N - 1$. These quadrature parameters are, in fact, the Gauss quadrature set which is widely used in numerical integration.[7] Such a set of order N, i.e., N values of μ_i and N values of w_i, is the only set having the property that the integration formula of equation

TABLE 5.1. CONSTANTS FOR THE GAUSS QUADRATURE FORMULA[7]

$N = 2$:	$w_1 = w_2 = 1.000$	$\mu_1 = -\mu_2 = 0.57735$
$N = 4$:	$w_1 = w_4 = 0.65215$	$\mu_1 = -\mu_4 = 0.33998$
	$w_2 = w_3 = 0.34785$	$\mu_2 = -\mu_3 = 0.86114$
$N = 6$:	$w_1 = w_6 = 0.46791$	$\mu_1 = -\mu_6 = 0.23862$
	$w_2 = w_5 = 0.36076$	$\mu_2 = -\mu_5 = 0.66121$
	$w_3 = w_4 = 0.17132$	$\mu_3 = -\mu_4 = 0.93247$

(5.2) is exact for a polynomial in μ of order $2N - 1$. From the discussion in §5.2a, it is known that this is the polynomial of highest order that can be integrated exactly by an expression with N directions and N weights. The values of μ_i and w_i in the Gauss quadrature set for $N = 2$, 4, and 6 are presented in Table 5.1.[7]

Some consideration must now be given to boundary conditions. For a vacuum (free-surface) boundary, with no incoming neutrons, it is natural to assume that $\Phi(x, \mu_j) = 0$ for all incoming directions. If the domain of interest is a slab of thickness a, i.e., $0 \leqslant x \leqslant a$, then

$$\Phi(0, \mu_j) = 0 \quad \text{for } \mu_j > 0$$

and

$$\Phi(a, \mu_j) = 0 \quad \text{for } \mu_j < 0.$$

These boundary conditions are then identical with the Mark boundary conditions of the spherical harmonics method (§2.5d).

The method of discrete ordinates with constants from the Gauss quadrature set is thus seen to be equivalent to the method of spherical harmonics with Mark boundary conditions. In particular, the approximate integrals, $\tilde{\phi}_n$, as given by the summation of equation (5.4), satisfy the same equations and boundary conditions as do the ϕ_n of the spherical harmonics method. The same neutron flux and the same eigenvalues are obtained by both methods. Furthermore, if the angular dependence of the flux $\Phi(x, \mu)$ for $\mu \neq \mu_i$ is given by the usual spherical harmonics expansion

$$\Phi(x, \mu) = \sum_{n=0}^{N-1} \frac{2n + 1}{4\pi} P_n(\mu)\tilde{\phi}_n(x), \tag{5.7}$$

both discrete and spherical harmonics methods lead to the same results for the angular distribution. In addition it can be shown that equation (5.7) gives the same values for $\Phi(x, \mu_i)$ as were used to derive the $\{\tilde{\phi}_n\}$. Consider, for example, the one and only polynomial of order $N - 1$ which can be passed through the points $\Phi(x, \mu_i)$: the quantities $\tilde{\phi}_n(x)$ defined in equation (5.4) are exact for such a polynomial. This polynomial is uniquely determined by $\{\tilde{\phi}_n\}$ and is given by equation (5.7).

It is of interest to recall that in Chapter 2 no particular justification was given for the Mark boundary conditions. It now appears, however, that they are natural free-surface boundary conditions for the discrete ordinates method with Gauss quadrature constants, and hence for the equivalent spherical harmonics method.

5.2d The Double-P_N Method in Discrete Ordinates

It was seen in §3.5a that there is, in general, a discontinuity in the angular neutron flux for $\mu = 0$ at an interface (or boundary) in plane geometry. It was then

found useful to treat each side of the discontinuity separately in solving the transport equation by expansion of the angular flux distribution in terms of Legendre polynomials. A similar double-P_N approach has been used in the discrete ordinates method by making separate expansion in the ranges $-1 \leqslant \mu \leqslant 0$ and $0 \leqslant \mu \leqslant 1$.[8]

If the Gauss quadrature is utilized with N points in each of these two ranges, the discrete directions $\{\mu_i\}$ are now given in terms of the directions used earlier (see Table 5.1) by

$$\mu_i' = \frac{\mu_i}{2} + \frac{1}{2} = -\mu_{2N+1-i}' \quad \text{with} \quad i = 1, 2, \ldots, N,$$

and the weighting factors are

$$w_i' = \frac{w_i}{2} = w_{2N+1-i}'.$$

Consequently, there are now $2N$ directions and $2N$ weighting factors. For either positive or negative μ, there are N directions corresponding to the N roots of P_N fitted to the range $0 \leqslant \mu \leqslant 1$. Such a choice with $2N$ directions would be called a double-P_{N-1} approximation; thus, for example, the double-P_1 approximation has four discrete directions. The double-P_N approach has proved to be very useful in applying the method of discrete ordinates to slab problems because of the ability to treat interfaces in a simple manner. For curved geometries, however, there are no discontinuities in the flux and then the double-P_N method has no particular merit, as will be seen later.

5.2e Anisotropic Scattering

For anisotropic scattering, the foregoing treatment must be modified. If the scattering depends only on μ_0, the cosine of the scattering angle in the laboratory system, the right side of equation (5.1), which will be represented by $q(x, \mu)$, can be written as

$$q(x, \mu) = c(x) \int \sigma f(x, \mu_0)\Phi(x, \mu')\, d\Omega' + Q(x, \mu).$$

Expansion of the σf in Legendre polynomials, in the usual way (§4.2b), and multiplication by 2π for integration over all azimuthal angles, gives

$$q(x, \mu) = \frac{c(x)}{2} \sum_{l=0}^{\infty} (2l + 1)\sigma_l P_l(\mu) \int_{-1}^{1} P_l(\mu')\Phi(x, \mu')\, d\mu' + Q(x, \mu). \quad (5.9)$$

Upon introduction of the quadrature formula of equation (5.2), the right side of equation (5.9) becomes

$$q(x, \mu_j) = \frac{c(x)}{2} \sum_{l=0}^{\infty} (2l + 1)\sigma_l P_l(\mu_j) \sum_{i=1}^{N} w_i P_l(\mu_i)\Phi(x, \mu_i) + Q(x, \mu_j). \quad (5.10)$$

In practice, the sum over l will be cut off at L; it is then necessary to specify L cross sections, σ_l, in order to perform the summation. Otherwise, the procedure is the same as that described for isotropic scattering.

For comparison with the equations of spherical harmonics, equation (5.3), with the right-hand side given by equation (5.10), is again multiplied by $w_j P_n(\mu_j)$ and summed over j. If the full-range Gauss quadrature set with N directions is used, then, since the scheme is exact for polynomials of order $2N - 1$, it is found that

$$\sum_{j=1}^{N} w_j P_n(\mu_j) \frac{2l+1}{2} P_l(\mu_j) = \delta_{ln} \quad \text{for} \quad l + n \leqslant 2N - 1,$$

where δ_{ln} is the Kronecker delta. Hence, provided $l + n \leqslant 2N - 1$, there will be just the same terms on the right-hand side as occur in the spherical harmonics expansion. If $L \geqslant N$, however, additional terms will be present, although they are seldom of any significance. Thus, with one minor exception, the Gauss discrete ordinates methods and that of spherical harmonics are equivalent for anisotropic scattering.

5.2f Solution of the Discrete Ordinates Equations

In describing a method for solving the system of equations (5.3), it will be assumed that the problem is too complicated for a solution in closed form to be practical, so that a numerical solution is being sought. The first step, as in Chapter 3, is to introduce a space mesh, i.e., a set of discrete values of x, namely x_k, where $k = 0, 1, 2, \ldots, K$, such that the left boundary of the system is at x_0 and the right boundary at x_K; as a rule, points are also chosen to lie on any interfaces that may be present. The derivative terms are then approximated by finite differences, such as

$$\left.\frac{\partial \Phi(x, \mu_j)}{\partial x}\right|_{x = x_{k+(1/2)}} \simeq \frac{\Phi(x_{k+1}, \mu_j) - \Phi(x_k, \mu_j)}{x_{k+1} - x_k},$$

where $x_{k+(1/2)}$ is midway between x_k and x_{k+1}, i.e.,

$$x_{k+(1/2)} = \tfrac{1}{2}(x_k + x_{k+1}).$$

If, as before, the right-hand side of equation (5.3) is represented by the symbol $q(x, \mu_j)$, to allow for the possibility of anisotropic scattering, this equation at the point $x_{k+(1/2)}$ becomes

$$\mu_j \frac{\Phi(x_{k+1}, \mu_j) - \Phi(x_k, \mu_j)}{x_{k+1} - x_k} + \sigma(x_{k+(1/2)}) \Phi(x_{k+(1/2)}, \mu_j) = q(x_{k+(1/2)}, \mu_j). \quad (5.11)$$

According to equation (5.3), or (5.10) in general, $q(x_{k+(1/2)}, \mu_j)$ depends on $\Phi(x_{k+(1/2)}, \mu_i)$, and for small N, at least, the dependence is simple enough for a rapid solution of equation (5.11) for the $\Phi(x, \mu_j)$ to be possible.[9] A more general

method of solution by iteration will be described here, however, because it is also applicable to more complicated situations such as curved geometries in two dimensions. Exactly the same procedure can be used for any number, N, of directions; this represents a great advantage of the discrete ordinates method.

To start with, it is assumed that $q(x, \mu_j)$ is known; a value is guessed the first time and thereafter it is available as a result of each preceding iteration. The term $\Phi(x_{k+(1/2)}, \mu_j)$ is usually eliminated by expressing it as an average of the Φ values on either side; thus,

$$\Phi(x_{k+(1/2)}, \mu_j) \simeq \frac{\Phi(x_k, \mu_j) + \Phi(x_{k+1}, \mu_j)}{2}.$$

Upon inserting this into equation (5.11), the resulting expression can be solved for $\Phi(x_{k+1}, \mu_j)$ in terms of $\Phi(x_k, \mu_j)$, or vice versa. If $\Delta_{k+(1/2)}$ is defined by

$$\Delta_{k+(1/2)} \equiv x_{k+1} - x_k,$$

and the arguments of quantities at $x_{k+(1/2)}$ are dropped, it is found from equation (5.11) that

$$\Phi(x_{k+1}, \mu_j) = \frac{1 - \sigma\Delta/2\mu_j}{1 + \sigma\Delta/2\mu_j} \Phi(x_k, \mu_j) + q \frac{\Delta}{\mu_j(1 + \sigma\Delta/2\mu_j)}$$

(use for $\mu_j > 0$) (5.12)

and

$$\Phi(x_k, \mu_j) = \frac{1 + \sigma\Delta/2\mu_j}{1 - \sigma\Delta/2\mu_j} \Phi(x_{k+1}, \mu_j) - q \frac{\Delta}{\mu_j(1 - \sigma\Delta/2\mu_j)}$$

(use for $\mu_j < 0$). (5.13)

With vacuum boundary conditions, $\Phi(x_0, \mu_j)$ is zero for all positive μ_j; hence, $\Phi(x_k, \mu_j)$ for positive μ_j can then be found by repeated application of equation (5.12). Similarly, $\Phi(x_K, \mu_j)$ is zero for all negative μ_j and equation (5.13) can be applied to determine $\Phi(x_k, \mu_j)$ for negative values of μ_j. The value of q, i.e., $q(x_{k+(1/2)}, \mu_j)$, can then be recalculated and the problem can be solved by iteration. Various methods for accelerating the procedure have been suggested.[10]

If there are reflecting boundary conditions at $x = x_K$, then $\Phi(x_K, \mu_j)$ may be found for negative μ_j by setting

$$\Phi(x_K, \mu_j) = \Phi(x_K, -\mu_j).$$

If there are reflecting boundary conditions at both interfaces, i.e., at x_0 and x_K, a somewhat more general procedure may be adopted. For example, it is possible to run a series of $\frac{1}{2}N$ problems, where for the nth problem the boundary condition at x_0 is

$$\Phi(x_0, \mu_j) = \delta_{jn},$$

where δ_{jn} is the Kronecker delta. By taking an appropriate linear combination of these $\frac{1}{2}N$ conditions, the reflecting boundary condition

$$\Phi(x_0, \mu_j) = \Phi(x_0, -\mu_j)$$

can be satisfied.

Reference may be made to some important features of equations (5.12) and (5.13). First, it will be recalled that equation (5.12) was to be used for positive μ_j and equation (5.13) for negative μ_j. In both cases, the coefficient of Φ on the right-hand side is then less than unity. As a consequence, errors in Φ, which may be introduced in the numerical approximation, e.g., by round off, are attenuated rather than amplified as a result of repeated application of the equations. More generally, the rule is that in integrating along a neutron direction, the procedure should be in the direction of neutron travel in order to minimize the accumulation of numerical errors. For $\mu > 0$, this would be from x_k to x_{k+1}, as in equation (5.12), whereas for $\mu < 0$ the direction would be from x_{k+1} to x_k, as in equation (5.13).

A second point to be noted is that if Δ is large in comparison with $|2\mu_j|/\sigma$, the coefficients of Φ on the right side of equations (5.12) and (5.13) become negative. If q is small, negative values of Φ, which are physically and numerically undesirable, are then obtained. Actually, the coefficient in equation (5.12) is simply an approximation to $\exp(-\sigma\Delta/\mu_j)$, and so Δ cannot be taken too large without loss of accuracy.

In order to show this, consider equation (5.12) in the absence of a source, that is,

$$\Phi(x_{k+1}, \mu_j) = \frac{1 - \sigma\Delta/2\mu_j}{1 + \sigma\Delta/2\mu_j} \Phi(x_k, \mu_j). \tag{5.14}$$

The source-free transport equation for $\mu = \mu_j$ is

$$\mu_j \frac{\partial\Phi(x, \mu_j)}{\partial x} + \sigma\Phi(x, \mu_j) = 0,$$

so that upon dividing by μ_j and introducing the integrating factor $\exp \int \frac{\sigma}{\mu_j} dx'$, the result is

$$\frac{\partial}{\partial x}\left[\Phi(x, \mu_j) \exp \int^x \frac{\sigma}{\mu_j} dx'\right] = 0.$$

Upon integration from x_k to x_{k+1}, it is found that

$$\Phi(x_{k+1}, \mu_j) = e^{-\sigma\Delta/\mu_j}\Phi(x_k, \mu_j).$$

Comparison with equation (5.14) shows that the coefficient of $\Phi(x_k, \mu_j)$ in this equation, and hence also in equation (5.12), is an approximation for $e^{-\sigma\Delta/\mu_j}$. Although this approximation is poor when Δ is too large, it is in error by only 1 percent when $\sigma\Delta/\mu_j = 0.5$.

As the number of angular directions, N, is increased, some of the values of μ_j, in particular $\mu_{(1/2)N}$, will become increasingly closer to zero. It is necessary, therefore, simultaneously to increase the number of space points, i.e., to decrease Δ, in order to avoid large values of $\sigma\Delta/\mu_{(1/2)N}$.

The foregoing system of difference equations may lead to negative values of the neutron flux; hence, it does not correspond to a positive operator (§4.4c). Thus, it is not possible to use the theory of such operators to establish, as for multigroup diffusion theory in §4.4f, the existence of eigenvalues and to accelerate convergence. Alternative difference schemes have been used to preserve positive values of the flux,[11] but they have been found to be generally less accurate than the scheme given here.

5.2g Results of Discrete Ordinates Calculations

By using the procedure described above, the one-speed transport equation can be solved by the method of discrete ordinates. Such a one-speed problem would normally arise in the treatment of one group in a multigroup calculation, as seen in §4.3b and as will be considered in §5.3e. The method may also be used to solve simple one-speed test problems; the accuracy of the procedure for various choices of quadrature coefficients can thereby be assessed. As an example, the computed critical thicknesses of bare slabs are given in Table 5.2. In making the calculations, the iterative method of §5.2f was applied with the following refinement: since there is no external source, the thickness is varied until the iterations converge. The procedure is analogous to that described in §4.4d with q now playing the role of νF.

The values recorded in Table 5.2 are the critical half-thicknesses, in terms of neutron mean free paths, as functions of c, for the simple P_{N-1} and double-$P_{(1/2)N-1}$ Gauss quadrature schemes with various numbers of directions, N. In the numerical computations the space mesh consisted of $4N$ equally spaced intervals in each case.[12] The results of exact calculations[13] are given for comparison. The accuracy attainable by the double-P_N method is seen to be very striking.

TABLE 5.2 CALCULATED CRITICAL HALF-THICKNESSES OF SLABS USING GAUSS QUADRATURE.[12,13] (IN MEAN FREE PATHS)

	P_{N-1}			*Double-*$P_{(1/2)N-1}$		
c \ N	2	4	6	4	6	*Exact*
1.02	5.856	5.687	5.675	5.670	5.668	5.665
1.05	3.496	3.321	3.308	3.299	3.301	3.300
1.10	2.315	2.136	2.121	2.107	2.114	2.113
1.20	1.487	1.319	1.299	1.278	1.290	1.289
1.40	0.920	0.778	0.750	0.723	0.736	0.737
1.60	0.680	0.559	0.530	0.503	0.510	0.512

A comparison has also been made of the critical half-thicknesses of slabs obtained by the method of discrete ordinates with those given by the "exact" method of the separation of variables (see Chapter 2) for anisotropic scattering.[14] For this purpose the angular distribution of the scattered neutrons was taken to be that for hydrogen, and either two or three terms in its expansion were retained in both treatments. Various ratios of anisotropic to isotropic scattering were considered. By using a large number of space points, namely 75, and the double-P_7, i.e., $N = 16$, quadrature scheme, the results obtained from the discrete ordinate method generally agreed with the "exact" values to within one part in 10^4; in most cases the agreement was even better. Thus, a considerable degree of accuracy can be attained in plane geometry by using a high-order discrete ordinates method. It is of interest to mention that, even for the most complicated scattering, the time taken to solve a problem of this type on a modern digital computer is only a minute or less.

The Gauss quadrature formula for approximating the integral in the transport equation has the advantage of giving fairly accurate results with a relatively small number of terms. It does not constitute, however, the only practical choice of directions and weighting factors for representing the angular distribution of the neutron flux. Other schemes have been proposed and mention may be made of one which involves directions equally spaced in μ^2; this has some useful symmetry properties when generalized to geometries of more than one dimension (§5.3c).

5.3 DISCRETE ORDINATES FOR ONE SPEED IN CURVED GEOMETRIES

5.3a Introduction

It was mentioned earlier that in curved geometry a problem arises because the angular coordinate of the neutron, in a local coordinate system, changes due to streaming, i.e., to collision-free motion. Consequently, a further coupling is introduced between equations describing neutron flows in discrete directions. Spherical geometry will be treated here, although the techniques to be described are also applicable to other curved geometries.

In spherical geometry the one-speed transport equation may be written as (§1.3a).

$$\mu \frac{\partial \Phi(r, \mu)}{\partial r} + \frac{1}{r}(1 - \mu^2) \frac{\partial \Phi(r, \mu)}{\partial \mu} + \sigma(r)\Phi(r, \mu) = q(r, \mu), \qquad (5.15)$$

where the source term $q(r, \mu)$ may include anisotropic scattering and anisotropic sources, as discussed in the preceding section. The treatment of the source term is the same as in plane geometry and so it will not be considered here in any detail. In more general geometries, the only difference is that the scattering

source is not simply a sum of Legendre polynomials but involves spherical harmonics; the latter are present, as pointed out in §3.3e because there is no azimuthal symmetry to eliminate terms from the addition theorem of Legendre polynomials.

The new problem in spherical geometry is how to approximate the second term on the left-hand side of equation (5.15) and especially the derivative factor $\partial\Phi/\partial\mu$. Various possibilities have been proposed,[15] most of which introduce a complicated coupling between the angular fluxes, $\Phi(r, \mu_i)$, for various values of μ_i. For example,[16] equations (5.4) and (5.7) could be used, with r replacing x, to write

$$\Phi(r, \mu) \approx \sum_{n=0}^{N-1} \frac{2n+1}{2} P_n(\mu) \sum_{i=1}^{N} w_i \Phi(r, \mu_i) P_n(\mu_i)$$

so that

$$\left.\frac{\partial\Phi}{\partial\mu}\right|_{\mu=\mu_j} \approx \sum_{n=0}^{N-1} \frac{2n+1}{2} \left.\frac{\partial P_n(\mu)}{\partial\mu}\right|_{\mu=\mu_j} \sum_{i=1}^{N} w_i \Phi(r, \mu_i) P_n(\mu_i)$$

$$= \sum_{i=1}^{N} \left[\sum_{n=0}^{N-1} \frac{2n+1}{2} \left.\frac{\partial P_n(\mu)}{\partial\mu}\right|_{\mu=\mu_j} w_i P_n(\mu_i) \right] \Phi(r, \mu_i). \tag{5.16}$$

Such a choice can be shown to give a discrete ordinates method which is equivalent to the spherical harmonics method in spherical geometry as described in §3.3a.

A simple procedure was proposed by B. Carlson in his original S_N method.[17] The dependence of $\Phi(r, \mu)$ on μ was approximated by a series of connected straight line segments between $\mu = -1$ and $\mu = 1$; thus, the letter S stands for segments. In one-dimensional geometries, N indicates the number of segments chosen to

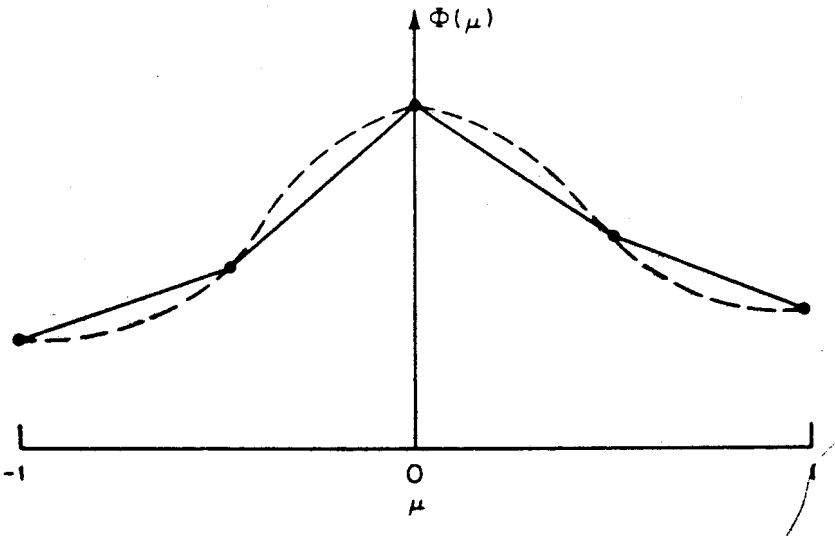

FIG. 5.2 LINEAR SEGMENTS APPROXIMATING ACTUAL ANGULAR FLUX DISTRIBUTION.

represent the angular distribution of the neutron flux. With N segments, there will be $N + 1$ discrete directions, including $\mu = -1$ and 1. In Fig. 5.2, the actual distribution between $\mu = -1$ and 1 is indicated by the broken line, and it is approximated by four linear segments, so that in this one-dimensional system N is 4. Obviously, the larger the number of directions used to express the angular flux distribution, the better the approximation.

By introducing this representation into equation (5.15), and integrating over a μ interval, explicit expressions were found to be satisfied by the values of Φ at the junction points. In this approximation the only free parameters were the values of μ separating the various segments. Subsequently, it was recognized that the resulting equations were only a special case of a more general formulation using discrete ordinates. This led to the development of the discrete S_N method which will now be described.[18]

5.3b The Conservation Principle

It should be noted at the outset that in curved geometries there are special angles along which the neutron direction variables do not change as a result of streaming. For spheres, these directions are for $\mu = -1$ and $\mu = +1$, corresponding to motion straight in toward the center or straight out, respectively. For these values of μ, the coefficient $(1 - \mu^2)/r$ of $\partial\Phi/\partial\mu$ in equation (5.15) is zero, and with known q, the equation can be solved exactly as in plane geometry. (At the origin a neutron can change from $\mu = -1$ to $\mu = +1$ discontinuously, but this can be imposed as a symmetry condition (§5.3d).) In curved geometry, the solutions in special directions can be utilized for boundary conditions on the angular dependence of the neutron flux, but they are not usually used in evaluating the integrals for determining the source term. The general practice in spherical geometry is to compute $\Phi(r, -1)$ from the boundary conditions at the outer radius by integrating equation (5.15) numerically assuming $q(r, \mu)$ to be known.

In deriving the numerical approximation to the transport equation, one principle is very helpful. It is that a difference equation for a fundamental r, μ cell should obey an explicit conservation law for the neutron economy in that cell; each term in the equation should clearly represent a physical component in the neutron conservation, such as absorption in the cell or flow across a face. When the conservation principle is included in the difference equations, the latter are always more readily interpreted and are usually more accurate than when the derivatives are simply replaced by differences without attention being paid to conservation. Moreover, in the absence of such a principle, the possible difference equations are so numerous that a good choice is difficult to make except by a process of trial and error. This is the reason why the neutron transport equation was expressed in conservation form in §1.3b.

To apply the conservation principle, equation (5.15) may be written, according to equation (1.35), as

$$\frac{\mu}{r^2}\frac{\partial}{\partial r}(r^2\Phi) + \frac{1}{r}\frac{\partial}{\partial \mu}[(1-\mu^2)\Phi] + \sigma\Phi = q, \tag{5.17}$$

where the argument (r, μ) has been omitted for simplicity. As seen in §1.3b, integration of the first term on the left side of equation (5.17) over all directions and over a bounded volume gives the net outward neutron current, whereas the second term is zero.

The same result, and the conservation relation, may be derived by integrating equation (5.17) over a region in r, μ space. Thus upon integration over a volume from r_i to r_{i+1}, i.e., multiplication by $4\pi r^2$ and integration over r from r_i to r_{i+1}, and over all directions, i.e., multiplication by 2π and integration over μ from -1 to 1, the first term in equation (5.17) becomes

$$4\pi(r_{i+1})^2 2\pi \int_{-1}^{1} \mu\Phi(r_{i+1}, \mu)\, d\mu - 4\pi(r_i^2)2\pi \int_{-1}^{1} \mu\Phi(r_i, \mu)\, d\mu = A_{i+1}J_{i+1} - A_iJ_i, \tag{5.18}$$

where $A_i = 4\pi r_i^2$ is the area of the surface of radius r_i, and

$$J_i = 2\pi \int_{-1}^{1} \mu\Phi(r_i, \mu)\, d\mu$$

is the outward radial current at $r = r_i$; A_{i+1} and J_{i+1} have the same respective significances at $r = r_{i+1}$. The second term on the left of equation (5.17), after the integration over the specified volume and all directions, is zero. Hence, the net result of the integration may be written as

$$A_{i+1}J_{i+1} - A_iJ_i = 8\pi^2 \int_{r_i}^{r_{i+1}} r^2\, dr \int_{-1}^{1} (q - \sigma\Phi)\, d\mu \tag{5.19}$$

$$= \text{source} - \text{sink}$$

since the q term represents the neutron source and $\sigma\Phi$ the neutrons lost in various collisions. Equation (5.19) is thus an obvious conservation relationship: the net rate at which neutrons flow out of the specified volume is equal to that supplied by the source minus the loss due to interactions (collisions) with nuclei.

5.3c Derivation of the Difference Equations

The foregoing procedure will now be followed except that the integration will be over a limited range (or segment) of μ. Consider a μ, r mesh, as in Fig. 5.3, where the $\{r_i\}$ are chosen so that points occur on boundaries between regions and the cross sections are assumed to be constant within an interval r_i, r_{i+1}; the points μ_n, etc. are selected to coincide with the μ values in the quadrature formula

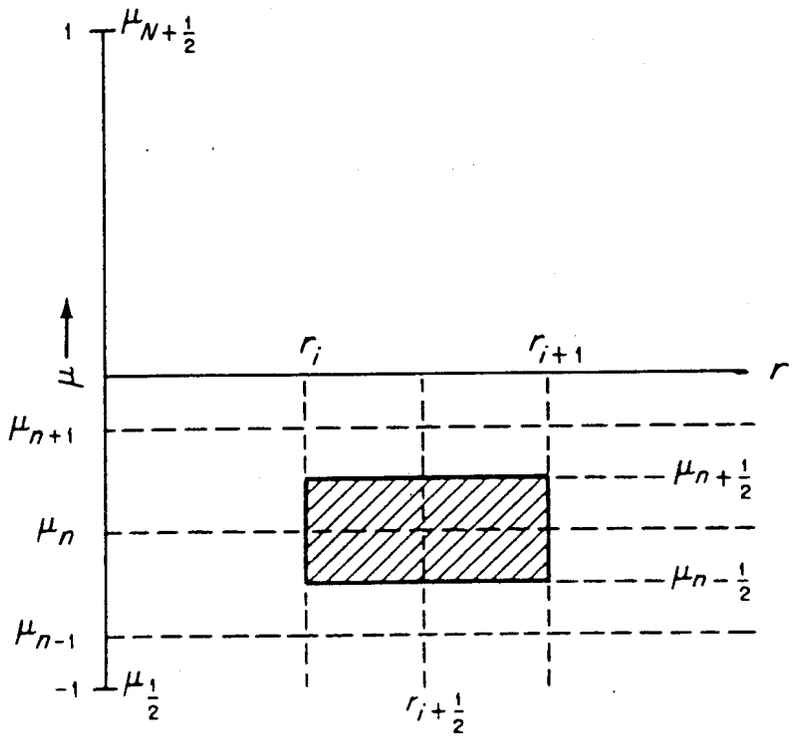

FIG. 5.3 PORTION OF A r, μ MESH.

of equation (5.2). Consider a typical cell, bounded by r_i, r_{i+1} and by $\mu_{n-(1/2)}$, $\mu_{n+(1/2)}$, as shown in Fig. 5.3. The direction $\mu_{1/2}$ is chosen to be -1, so that along this special direction the transport equation can be solved by the methods of plane geometry. Moreover, for an N-point quadrature, $\mu_{N+(1/2)}$ must then be equal to 1.

Suppose equation (5.17) is integrated over the volume of the cell and over a segment of μ between $\mu_{n-(1/2)}$ and $\mu_{n+(1/2)}$. The source (q) minus collision ($\sigma\Phi$) terms then become

$$8\pi^2 \int_{r_i}^{r_{i+1}} r^2\, dr \int_{\mu_{n-(1/2)}}^{\mu_{n+(1/2)}} [q(r,\mu) - \sigma\Phi(r,\mu)]\, d\mu$$

$$\approx 8\pi^2 w_n \int_{r_i}^{r_{i+1}} r^2 [q(r,\mu_n) - \sigma\Phi(r,\mu_n)]\, dr$$

$$= 2\pi w_n V[\bar{q}(r_{i+(1/2)},\mu_n) - \sigma\bar{\Phi}(r_{i+(1/2)},\mu_n)],$$

where V is the volume given by

$$V = \tfrac{4}{3}\pi(r_{i+1}^3 - r_i^3).$$

In evaluating the integral over μ, one term of the quadrature formula, i.e.,

$$\int_{\mu_{n-(1/2)}}^{\mu_{n+(1/2)}} f(\mu)\, d\mu \approx w_n f(\mu_n),$$

has been used, and $\bar{q}$ and $\bar{\Phi}$ are volume averages over the cell, e.g.,

$$\bar{q}(r_{i+(1/2)}, \mu_n) \approx \frac{4\pi}{V} \int_{r_i}^{r_{i+1}} r^2 q(r, \mu_n)\, dr.$$

Turning now to the first term on the left of equation (5.17), this can be integrated by using the same approximation for the partial μ integral to give

$$2\pi w_n \mu_n [A_{i+1}\Phi(r_{i+1}, \mu_n) - A_i \Phi(r_i, \mu_n)].$$

The second term can be integrated first over the limited range of μ and then over the volume of the cell; the result is

$$8\pi^2 \int_{r_i}^{r_{i+1}} r[(1 - \mu_{n+(1/2)}^2)\Phi(r, \mu_{n+(1/2)}) - (1 - \mu_{n-(1/2)}^2)\Phi(r, \mu_{n-(1/2)})]\, dr.$$

This can be approximated in various ways but it can be represented simply by

$$2\pi[a_{n+(1/2)}\Phi(r_{i+(1/2)}, \mu_{n+(1/2)}) - a_{n-(1/2)}\Phi(r_{i+(1/2)}, \mu_{n-(1/2)})],$$

where the coefficients $a_{n\pm(1/2)}$ remain to be determined. The complete difference equation, resulting from the integration of the one-speed transport equation (5.17), is then

$$\mu_n[A_{i+1}\Phi(r_{i+1}, \mu_n) - A_i\Phi(r_i, \mu_n)] + \frac{a_{n+(1/2)}\Phi(r_{i+(1/2)}, \mu_{n+(1/2)}) - a_{n-(1/2)}\Phi(r_{i+(1/2)}, \mu_{n-(1/2)})}{w_n} = V(\bar{q} - \sigma\bar{\Phi}). \quad (5.20)$$

To determine the values of $a_{n+(1/2)}$, consider an infinite medium in which the flux is constant and isotropic. Such a situation will arise, approximately at least, near the center of a large sphere. In this case, there is no net current, and the conservation principle requires that

$$\bar{q} = \sigma\bar{\Phi}.$$

For equation (5.20) to be consistent with this limiting situation, it is necessary, since all the Φ values are assumed to be the same, that

$$\mu_n w_n (A_{i+1} - A_i) = -a_{n+(1/2)} + a_{n-(1/2)}. \quad (5.21)$$

This is a recursion relation from which the value of $a_{n+(1/2)}$ can be determined if $a_{n-(1/2)}$ is known.

It will now be shown that $a_{1/2}$ should be zero and, hence, once this choice is made all subsequent values of a can be determined by means of equation (5.21). Suppose equation (5.20) is multiplied by w_n and summed over all values of n, where $n = 1, 2, \ldots, N$, for an N-point quadrature formula. Agreement with equation (5.19) can be obtained only if the sum of the a terms is zero; thus,

$$\sum_{n=1}^{N} a_{n+(1/2)}[\Phi(r_{i+(1/2)}, \mu_{n+(1/2)}) - a_{n-(1/2)}\Phi(r_{i+(1/2)}, \mu_{n-(1/2)})] = -a_{1/2}\Phi(r, \mu_{1/2}) + a_{N+(1/2)}\Phi(r, \mu_{N+(1/2)}) = 0. \quad (5.22)$$

This result should be true regardless of the dependence of Φ on r and μ; hence, it is necessary that

$$a_{1/2} = a_{N+(1/2)} = 0.$$

Incidentally, for a symmetric quadrature scheme, as is nearly always used, $a_{1/2}$ and $a_{N+(1/2)}$ must be identical, in any event.

With $a_{1/2} = 0$, equation (5.21) for $n = 1$ yields

$$a_{3/2} = -\mu_1 w_1 [A_{i+1} - A_i],$$

and so on for $n = 2$, etc. It should be observed that $a_{n+(1/2)}$ depends not merely on n, but also on i. Since $A_{i+1} - A_i$ is always positive, and $\mu_1 < 0$, it follows that $a_{3/2}$ is positive. By repeated application of equation (5.21), it is then seen that $a_{n+(1\,2)}$ will always be positive provided $\mu_n < 0$. When $\mu_n > 0$, however, n in equation (5.21) is set equal to N, and since $a_{N+(1/2)} = 0$, it follows that $a_{N-(1/2)}$ is positive; the same will be true for $a_{N-(3/2)}$, etc. It is thus found that all values of a are positive.

If equation (5.21) were not used to determine $a_{n+(1/2)}$ and the integral of the second term in equation (5.17) had been approximated in another manner, it would be found that the numerical solution could not yield an isotropic flux at the center of the sphere. Apart from this, the resulting difference equations might be almost as accurate as obtained above. It seems to be generally advisable, however, to build as many features as possible of the exact solutions into the difference equations. Actually, even for the approximation given here the central flux is not exactly isotropic.[19]

The terms in equation (5.20) can be interpreted in the following manner. When multiplied by w_n, the first two terms on the left side are the neutron flows across the areas of radii r_{i+1} and r_i in the nth μ interval. The a terms represent streaming flows which transfer neutrons from the $n - \frac{1}{2}$ direction into the n interval and from the n interval into the $n + \frac{1}{2}$ direction, respectively; the terms on the right-hand side are, of course, the source and the sink.

5.3d Solution of the Difference Equation

As it stands, the one-speed equation (5.20) cannot be solved because there are too many $\Phi(r, \mu)$ values. Consequently, some further relations between them must be postulated. Suppose the problem being solved is one with a boundary condition at the outer radius, r_I. As was the case for plane geometry, the calculation of Φ is initiated with some postulated value of the source term $q(r, \mu)$, so that $\bar{q}$ is known. Starting at the outer boundary with the boundary condition given as the incoming angular flux $\Phi(r, \mu)$ for $\mu < 0$, the special direction $\mu = -1$ is considered. From equation (5.15) it is seen that for $\mu = -1$, the transport equation is just as for plane geometry, e.g., equation (5.1) with the right side written as q. Hence, in this direction integration is performed inward to the

center, in a manner similar to that used in plane geometry, so that $\Phi(r_{i+(1/2)}, \mu_{1/2})$ can be determined for all values of i, with $\mu_{1/2} = -1$.

Next, the inward integration is started for μ_1; at any step in this process $\Phi(r_{i+(1/2)}, \mu_{1/2})$ is known and $\Phi(r_{i+1}, \mu_1)$ is obtained from the preceding step, or initially from the boundary conditions. Thus, in equation (5.20), for $n = 1$, the quantities $\Phi(r_{i+(1/2)}, \mu_{1/2})$ and $\Phi(r_{i+1}, \mu_1)$ are known and the unknown quantities are $\Phi(r_i, \mu_1)$, $\Phi(r_{i+(1/2)}, \mu_{3/2})$, and $\bar{\Phi}(r_{i+(1/2)}, \mu_1)$. Methods for eliminating two of the three unknowns are developed below.

In general, for any $\mu_n < 0$, the unknown quantities in equation (5.20) are $\Phi(r_i, \mu_n)$, $\Phi(r_{i+(1/2)}, \mu_{n+(1/2)})$, and $\bar{\Phi}(r_{i+(1/2)}, \mu_n)$; hence, two additional relations are required between these three quantities in order to solve the equation. The simplest of such relations is the so-called "diamond" difference scheme wherein Φ is assumed to be linear between adjacent r, μ mesh points (Fig. 5.4); thus

$$2\bar{\Phi}(r_{i+(1/2)}, \mu_n) \simeq \Phi(r_{i+1}, \mu_n) + \Phi(r_i, \mu_n) \tag{5.23}$$

$$\simeq \Phi(r_{i+(1/2)}, \mu_{n+(1/2)}) + \Phi(r_{i+(1/2)}, \mu_{n-(1/2)}). \tag{5.24}$$

Equations (5.23) and (5.24) may now be used in equation (5.20) to eliminate $\Phi(r_i, \mu_n)$ and $\Phi(r_{i+(1/2)}, \mu_{n+(1/2)})$; upon solving for $\bar{\Phi}(r_{i+(1/2)}, \mu_n)$, it is found that

$$\bar{\Phi}(r_{i+(1/2)}, \mu_n) = \frac{-\mu_n(A_i + A_{i+1})\Phi(r_{i+1}, \mu_n) + (1/w_n)(a_{n+(1/2)} + a_{n-(1/2)}) \times \Phi(r_{i+(1/2)}, \mu_{n-(1/2)}) + V\bar{q}}{-\mu_n(A_i + A_{i+1}) + (1/w_n)(a_{n+(1/2)} + a_{n-(1/2)}) + \sigma V}, \tag{5.25}$$

where equation (5.21) has been used to write the denominator in a symmetrical form. Once $\bar{\Phi}$ has been found in this way, by using the $\Phi(r_{i+1}, \mu_n)$ and $\Phi(r_{i+(1/2)}, \mu_{n-(1/2)})$ obtained above, equation (5.23) and (5.24) may be applied to determine $\Phi(r_i, \mu_n)$ and $\Phi(r_{i+(1/2)}, \mu_{n+(1/2)})$ which will be required for subsequent steps.

By repeating this procedure, the values of $\bar{\Phi}$ may be found for all space points and all ingoing direction, i.e., for $\mu_n < 0$. For outgoing directions, i.e., for $\mu_n > 0$, integration is performed outward in accordance with the principle stated earlier that numerical errors are minimized if the integration is in the direction of neutron motion. To get started on the integration some condition on isotropy of the neutron flux at the center may be used. Thus, it is assumed that

$$\Phi(0, \mu_n) = \Phi(0, -\mu_n), \tag{5.26}$$

where, for positive μ_n, the right-hand side is known from the inward integration; thus, $\Phi(0, \mu_n)$ is available for starting the outward integration. In this direction, $\Phi(r_i, \mu_n)$ is known and $\Phi(r_{i+1}, \mu_n)$ is unknown; hence equation (5.25) is replaced by

$$\bar{\Phi}(r_{i+(1/2)}, \mu_n) = \frac{\mu_n(A_i + A_{i+1})\Phi(r_i, \mu_n) + (1/w_n)(a_{n+(1/2)} + a_{n-(1/2)}) \times \Phi(r_{i+(1/2)}, \mu_{n-1/2}) + V\bar{q}}{\mu_n(A_i + A_{i+1}) + (1/w_n)(a_{n+(1/2)} + a_{n-(1/2)}) + \sigma V}. \tag{5.27}$$

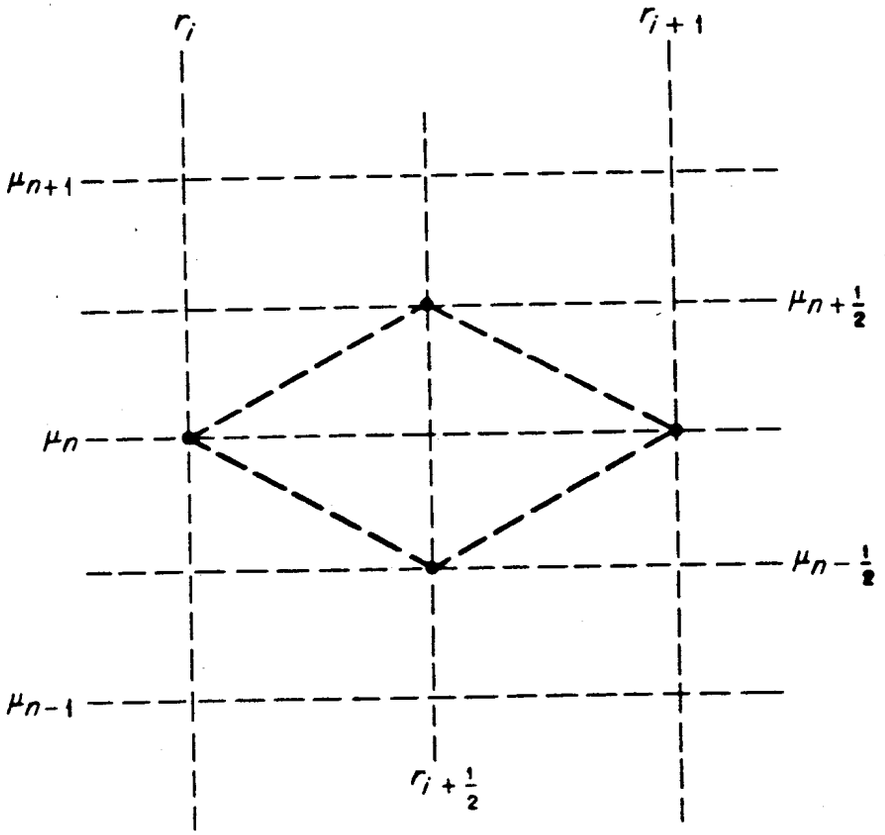

FIG. 5.4 THE r, μ MESH FOR A "DIAMOND" DIFFERENCE SCHEME.

In this manner, $\bar{\Phi}$ may be found for all angles μ_n and all space points $r_{i+(1/2)}$. By using these values, $\bar{q}$ can be recomputed and the process repeated until convergence is obtained. These repetitions are inner iterations analogous to those described in Chapter 3 for determining the within-group (or one-speed) spatial distribution of the flux based on P_1 or diffusion approximations. In practice the convergence may be accelerated by using the method of scaling or other techniques.[20]

Because of the complex structure of the difference equations, the matrices involved in the iteration are quite involved. Consequently, the procedures which have been used are not as well understood mathematically, nor as highly developed, as are those employed in P_1 or diffusion theory. The iteration techniques have been found empirically to accelerate convergence, but they have not yet been analyzed formally. One reason is that, as noted in §5.2f, when Δ is large the solutions to the equations may not be positive for all values of r_i, μ_n. This means that the positivity property of the transport operator (§4.4c) is being violated by the approximation and the analysis then becomes more complicated.

It was mentioned earlier that the difference equations derived above are not the only ones which could be used to approximate the original differential equation (5.17). Those given here have been preferred for the following reasons: (*a*) several general principles are embodied in their derivation; (*b*) the treatment is readily extended to other geometries for which the transport equation was

expressed in conservation form in Chapter 1; and (*c*) the results obtained have been found to be more accurate than those given by other difference equations. It should be pointed out, however, that the possible difference schemes have not been studied exhaustively; for example, variational derivations, along the lines indicated at the end of Chapter 6, were not reported until 1968.[21]

In applying the method of discrete ordinates to spherical geometry use may be made of any of the quadrature points and weights, mentioned in connection with plane geometry, e.g., the Gauss quadrature set. Some indication of the accuracy which can be achieved in such calculations, using Gauss quadrature and Mark boundary conditions, is obtained from the results given in Table 5.3[22] for the critical radii, expressed in units of mean free path, of bare spheres. As in Table 5.2, the space mesh was made up of $4N$ equal intervals, where N is the number of discrete directions. In the original S_N method, N represented the number of segments (§5.3*a*), but in the modified form described here, N is the number of directions.

It is seen that a high degree of accuracy can be attained when N is large. Surprisingly accurate critical radii, within about 1 percent of the exact results, are possible, however, with $N = 4$, i.e., in the S_4 approximation, for all values of c in the table. With the available fissile materials, the highest c, effectively about 1.6, arises in a one-group treatment of an assembly of plutonium-239. It is evident, therefore, that for a wide range of criticality problems the S_4 calculations should give acceptable accuracy. For $c - 1 \ll 1$, even the S_2 approximation is quite accurate: in these circumstances, the critical system is large and then any low-order approximation to the angular flux distribution, including diffusion theory, as seen in Chapter 2, gives acceptable accuracy.

The critical radii of bare spheres have also been calculated by the discrete ordinates method with directions and weights given by separate Gauss quadrature sets for the range $-1 \leqslant \mu < 0$ and $0 \leqslant \mu \leqslant 1$.[22] The procedure, which is equivalent to the double-P_N method that proved so satisfactory in plane geometry (Table 5.2), gives little, if any, improvement over the results obtained by the

TABLE 5.3 CALCULATED CRITICAL RADII OF SPHERES BY S_N METHOD USING GAUSS QUADRATURE.[22] (IN MEAN FREE PATHS)

c \ N	2	4	8	16	*Exact*
1.02	11.917	12.028	12.031	12.032	12.027
1.05	7.153	7.261	7.273	7.276	7.277
1.10	4.750	4.850	4.866	4.871	4.873
1.20	3.062	3.146	3.165	3.170	3.172
1.40	1.894	1.961	1.978	1.983	1.985
1.60	1.400	1.454	1.470	1.474	1.476

use of a single quadrature set over the whole range $-1 \leqslant \mu \leqslant 1$. This is probably because in spherical geometry the flux is continuous at $\mu = 0$, as noted in §3.5a.

5.3e The Discrete Ordinates Method in General Geometry

The procedures described above for plane and spherical geometries may be extended to more general geometry. The approach will be discussed briefly here and further details will be found in Ref. 23.

The method of discrete ordinates in two- and three-dimensional rectangular geometries is much the same as for plane geometry. In particular, the direction variables of a neutron do not change during streaming, and derivatives with respect to angular variables are not present in the transport equation (§1.7a). Two angular coordinates are now required in order to specify neutron direction, and integrals over $\mathbf{\Omega}$ will involve sums over both direction coordinates. For example, if the direction is represented by a direction cosine μ and an azimuthal angle χ, as in Table 1.2, it would be possible to write

$$\int \Phi(\mathbf{r}, \mathbf{\Omega})\, d\mathbf{\Omega} = \int_0^{2\pi} d\chi \int_{-1}^{1} d\mu \Phi(\mathbf{r}, \mu, \chi)$$

$$\approx \sum_{m=1}^{M} \frac{2\pi}{M} \sum_{n=1}^{N} w_n \Phi(\mathbf{r}, \mu_n, \chi_m),$$

where the directions μ_n and weights w_n might be chosen from a Gauss quadrature set and the χ_m directions are, in this example, equally spaced in the interval $0 \leqslant \chi \leqslant 2\pi$, i.e.,

$$\chi_m = \frac{m - \frac{1}{2}}{M} 2\pi, \qquad m = 1, 2, \ldots, M.$$

Such a choice would provide the basis for a reasonable discrete ordinates method, but it has a disadvantage which is especially apparent in three dimensions. The directions and weights depend on which physical direction is chosen as the z axis, i.e., the polar axis. Thus, the solution will depend on the alignment of the coordinates. This undesirable feature may be avoided by a special choice of direction coordinates that is invariant under rotation through 90° about any of the coordinate axes. It has been shown[24] that this rotation invariance condition constrains the values of μ_n to be equally spaced in μ^2, i.e.,

$$\mu_n^2 = \mu_1^2 + \frac{2(n-1)}{N-2}(1 - 3\mu_1^2), \qquad n = 1, 2, \ldots, N/2$$

and such direction sets have frequently been used in S_N calculations (§5.4d). The first direction cosine, μ_1, is found by imposing condition (3) of §5.2a for $n = 2$.

For curved geometries, other than spherical, it is also necessary to specify two direction coordinates. This is true even for an infinitely long cylinder in

which the angular flux depends only on one position coordinate, r (see Table 1.2). The integrations over neutron directions may be treated as in rectangular geometry. In addition, the derivatives with respect to angular coordinates must be approximated. As for spherical geometry, the difference equations may be based on conservation principles. Moreover, the transport equation may first be solved in special directions along which the neutron direction coordinates do not change with streaming; the results may then be used as boundary conditions for the main system of equations.

For cylindrical geometry, for example, these special directions are those for which $\mu = \pm 1$, i.e., neutron motion parallel to the cylinder axis, or $\sin \chi = 0$, i.e., motion toward or away from the cylinder axis (see Fig. 1.16). Diamond difference approximations, such as in equations (5.23) and (5.24), can be used to reduce the number of unknowns to the number of difference equations. The latter should be evaluated, as explained in §§5.2e, 5.3d, in the direction of neutron motion.

When the angular dependence of the neutron flux does not have an axis of symmetry, the treatment of anisotropic scattering given in §5.2e can be generalized. As before, the cross section is expanded in Legendre polynomials, the addition theorem of these polynomials is used (§2.6a), and the resulting integrals in the transport equation are approximated by sums.

Furthermore, when the angular flux depends on two direction (angle) coordinates, other methods for solving the transport equation can be developed by assuming that the dependence on one coordinate is continuous, but the other is represented in discrete form. For example, with the two angular variables μ and χ, the μ might be treated as a discrete variable, whereas the dependence of the flux on χ might be given by a sum of trigonometric functions.[25]

From what has been stated here, it is apparent that many possible discrete ordinates approximations to the transport equation can be considered. Of course, the desirable approximations are those which are both accurate and rapid for numerical computation. The methods referred to in this section have been proved useful for solution of practical problems; in addition, a number of modifications have been proposed,[26] some of which may be found to be advantageous.

5.4 MULTIGROUP (ENERGY-DEPENDENT) PROBLEMS

5.4a Expansion of Scattering Cross Sections in Spherical Harmonics

The development of the discrete ordinates methods given above has been concerned with the angular distribution of neutrons in a one-speed problem. It is necessary now to consider the treatment of realistic, energy-dependent situations

by means of multigroup methods. The main problem here, as will be seen shortly, is the consistent determination of the group cross sections.

Just as in the multigroup spherical harmonics approach, in Chapter 4, the energy-dependent multigroup equations are derived by integration over a number of energy intervals (or groups). In the discrete ordinates methods, these equations are evaluated in certain discrete directions. As stated in §1.6d, however, such a procedure would generally lead to group cross sections depending on direction; in addition there would be uncertainty in the evaluation of the transfer cross sections.

To facilitate the determination and handling of group cross sections, it has become the practice to adopt the procedure from the spherical harmonics method and introduce expansion of the scattering cross sections in Legendre polynomials. Once this has been done, the group constants are similar to those used in the spherical harmonics multigroup treatment. Nevertheless, there remain some differences and, in particular, some free parameters are available in the group constants for the discrete ordinates methods described here; possible choices are considered later in this chapter.

In order to focus attention on the new features, the energy-dependent transport equation will be considered, for simplicity, in plane geometry; thus,

$$\mu \frac{\partial \Phi(x, \mu, E)}{\partial x} + \sigma(x, E)\Phi(x, \mu, E) = 2\pi \iint \sigma f(x; E', \mu' \to E, \mu)\Phi(x, \mu', E')\, d\mu'\, dE' + Q(x, \mu, E). \quad (5.28)$$

The group constants which will be derived for plane geometry can be used for any geometry. The scattering cross section is expanded in Legendre polynomials in the usual way (§4.2b) to give

$$\mu \frac{\partial \Phi}{\partial x} + \sigma\Phi = \sum_{l=0}^{\infty} \frac{2l+1}{4\pi} P_l(\mu) \int \phi_l(x, E')\sigma_l(x; E' \to E)\, dE' + Q, \quad (5.29)$$

where the arguments have been dropped on the left-hand side and, as in §4.2b,

$$\sigma f(x; E', \mu' \to E, \mu) = \sum_{l=0}^{\infty} \frac{2l+1}{4\pi} \sigma_l(x; E' \to E) P_l(\mu_0)$$

$$\phi_l(x, E) = 2\pi \int_{-1}^{1} P_l(\mu)\Phi(x, \mu, E)\, d\mu.$$

As before, μ_0 is the cosine of the scattering angle.

It should be evident that the foregoing expansion of the scattering term in the transport equation as a sum of Legendre polynomials is not a necessary feature of the discrete ordinates methods. Other polynomials, polynomials plus delta

functions, or explicit integrations of the differential cross sections could be employed. The expansion in terms of Legendre polynomials (or spherical harmonics), however, has been commonly used. It appears to be the natural approach because spherical harmonics are a representation of the three-dimensional rotation group.[27]

In general, multigroup discrete ordinates codes solve a system of coupled one-speed equations of the form

$$\mu \frac{\partial \psi_g(x, \mu)}{\partial x} + \sigma_g(x)\psi_g(x, \mu) = \sum_{l=0}^{\infty} \frac{2l+1}{4\pi} P_l(\mu) \sum_{g'=1}^{G} \psi_{l,g'}(x)\sigma_{g'\to g}^{(l)}(x) + Q_g(x, \mu), \quad g = 1, 2, \ldots, G \quad (5.30)$$

where

$$\psi_{l,g'}(x) = 2\pi \sum_{i=1}^{N} w_i P_l(\mu_i)\psi_{g'}(x, \mu_i) \simeq 2\pi \int_{-1}^{1} P_l(\mu)\psi_{g'}(x, \mu)\, d\mu$$

and g is the group index, with $E_g \leqslant E \leqslant E_{g-1}$, as in Chapter 4. In practice the sum over l will, of course, be terminated at some value $l = L$. If this equation is considered for a fixed group it is seen to correspond to a one-speed problem having a right-hand side with anisotropic scattering and an anisotropic source as in equation (5.9). As in §4.3b, in equation (5.30) the terms on the right side with $g' = g$ act as the anisotropic scattering, whereas those with $g' \neq g$ would be considered part of the independent source for a one-group calculation. Thus, the source for the one-speed problem in group g would be, in the notation of equation (5.9),

$$q(x, \mu) = \sum_{l=0}^{L} \frac{2l+1}{4\pi} P_l(\mu) \sum_{g' \neq g} \psi_{l,g'}(x)\sigma_{g'\to g}^{(l)}(x) + Q_g(x, \mu).$$

It is now required to make a suitable choice of the group cross sections, so that the solution $\psi_g(x, \mu)$ of equation (5.30) will correspond closely to the integral of $\Phi(x, \mu, E)$ over the energy interval of each group g.

5.4b Determination of Group Constants

If equation (5.29) is simply integrated over the energy interval from E_g to E_{g-1}, and the definitions

$$\Phi_g(x, \mu) \equiv \int_{E_g}^{E_{g-1}} \Phi(x, \mu, E)\, dE = \int_g \Phi(x, \mu, E)\, dE$$

are used, it is apparent that equation (5.30) is not obtained by replacing Φ_g with

ψ_g. As noted in §5.4a, the reason is that the second term on the left side of equation (5.29) becomes $\sigma_g(x, \mu)\Phi_g(x, \mu)$, where

$$\sigma_g(x, \mu) \equiv \frac{\int_g \sigma(x)\Phi(x, \mu, E)\, dE}{\int_g \Phi(x, \mu, E)\, dE},$$

so that σ_g is dependent upon μ. This difficulty can be overcome in a number of ways.

One possibility is to postulate that within an energy group the dependence of Φ on E is separable from its dependence on x and μ; thus,

$$\Phi(x, \mu, E) = f_1(x, \mu)f_2(E).$$

This would make σ_g independent of μ, and then an equivalence could be established between equation (5.29) and (5.30). Although the approximation of separability can be used in some practical cases, it is not generally good and should not be employed indiscriminately. An alternative approach, which is satisfactory in all situations, is presented below.[28]

First, the angular flux in the second term on the left-hand side of equation (5.29) is expanded as a sum of polynomials, i.e.,

$$\Phi(x, \mu, E) = \sum_{l=0}^{\infty} \frac{2l + 1}{4\pi} P_l(\mu)\phi_l(x, E),$$

and then the equation is integrated over E; the result is

$$\mu \frac{\partial \Phi_g(x, \mu)}{\partial x} = \sum_{l=0}^{N} \frac{2l + 1}{4\pi} P_l(\mu) \sum_{g'=1}^{G} \phi_{l,g'}(x)[\sigma_{l,g'\to g}(x) - \sigma_{l,g}(x)\,\delta_{g',g}] + Q_g(x, \mu), \quad (5.31)$$

where $\delta_{g',g}$ is the Kronecker delta and

$$\sigma_{l,g}(x) \equiv \frac{\int_g \sigma(x, E)\phi_l(x, E)\, dE}{\phi_{l,g}(x)} \quad (5.32)$$

and

$$\sigma_{l,g'\to g}(x) \equiv \frac{\int_{g'} \phi_l(x, E') \int_g \sigma_s(x; E' \to E)\, dE\, dE'}{\phi_{l,g'}(x)} \quad (5.33)$$

are the flux-averaged group cross sections, precisely as in equations (4.26) and (4.27), respectively. If now the product $\sigma_g(x)\Phi_g(x, \mu)$ is added to both sides of equation (5.31), with $\Phi_g(x, \mu)$ expanded as a sum of polynomials on the right side but not on the left, it is found that

$$\mu \frac{\partial \Phi_g(x, \mu)}{\partial x} + \sigma_g(x)\Phi_g(x, \mu) = \sum_{l=0}^{N} \frac{2l + 1}{4\pi} P_l(\mu) \sum_{g'=1}^{G} \phi_{l,g'}(x) \times \{\sigma_{l,g'\to g}(x) + [\sigma_g(x) - \sigma_{l,g}(x)]\,\delta_{g',g}\} + Q_g(x, \mu). \quad (5.34)$$

Provided estimates of ϕ_l are available, as in Chapter 4, for use in equations (5.32) and (5.33), all the cross sections are known in equation (5.34), except for the σ_g which are still undetermined.

It is now seen that equation (5.34) is identical in form with equation (5.30); the group constants in the latter can then be chosen so that the corresponding terms in equations (5.30) and (5.34) are equal. For $g' \neq g$, the transfer cross sections $\sigma^{(l)}_{g'\to g}$ in equation (5.30) must satisfy the requirement that

$$\sigma^{(l)}_{g'\to g} = \sigma_{l,g'\to g} \quad (\text{for } g' \neq g) \tag{5.35}$$

and the transfer cross sections $\sigma_{l,g'\to g}$ are the same as in P_N theory [equation (4.27)]. For $g' = g$, the only necessary constraint is

$$\sigma_{l,g\to g} + \sigma_g - \sigma_{l,g} = \sigma^{(l)}_{g\to g}. \tag{5.36}$$

Here, $\sigma_{l,g\to g}$ and $\sigma_{l,g}$ are known, in principle, from equations (5.32) and (5.33), but σ_g and $\sigma^{(l)}_{g\to g}$ are unknown; an exact result can be obtained, however, provided the latter are chosen to satisfy equation (5.36).

In practice, the sum over l in equation (5.30) or (5.34) will be terminated after some finite number, e.g., $L + 1$, of terms. Thus, in the summation over l from $l = 0$ to $l = L$, there will be $L + 1$ terms. Consequently, there are only $G(L + 1)$ equations for determining the $G(L + 1)$ values of the transfer cross section $\sigma^{(l)}_{g\to g}$ and the G values of the collision cross section σ_g; thus, G extra conditions must be imposed. One possibility is to chose $\sigma_g = \sigma_{0,g}$, so that the collision cross section σ_g in equation (5.34) is simply the flux-averaged collision cross section from equation (5.32), i.e.,

$$\sigma_g = \sigma_{0,g} \quad (\text{consistent } P \text{ approximation}). \tag{5.37}$$

The name "consistent P" approximation is given to equation (5.37) because if, with this choice of σ_g, equation (5.34) is integrated over all angles, the result is identical with the first of the multigroup P_N equations, as in equation (4.24). It will be recalled that this equation, which is derived from (4.14), is exact, except for the uncertainties in evaluating the group constants. Since the choice of σ_g in equation (5.37) is consistent with the P_N equation (4.24), it is called the consistent P approximation.

A more refined procedure would be based on choosing σ_g so that the first neglected term in the summation in equation (5.34), i.e., for $l = L + 1$, is small. The neglected term is

$$\frac{1}{4\pi}(2L + 3)P_{L+1}(\mu) \sum_{g'=1}^{G} \phi_{L+1,g'}\{\sigma_{L+1,g'\to g} + [\sigma_g - \sigma_{L+1,g}]\,\delta_{g'g}\} \tag{5.38}$$

and in order to minimize it, information is required concerning the dependence of $\phi_{L+1,g'}$ on g'. For most energy groups in reactor problems, the scattering into

a group of neutrons from higher energy groups is roughly balanced by the scattering out to lower energy groups. If this is the case, then

$$\sum_{g'=1}^{G} \phi_{L+1,g'}\sigma_{L+1,g'\to g} \simeq \sum_{g'=1}^{G} \phi_{L+1,g}\sigma_{L+1,g\to g'}, \tag{5.39}$$

where the left side is the scattering into group g from all other groups and the right side is the corresponding scattering out. If equation (5.39) is substituted into the expression (5.38) and the result set equal to zero and solved for σ_g, it is found that

$$\sigma_g = \sigma_{L+1,g} - \sum_{g'=1}^{G} \sigma_{L+1,g\to g'} \quad \text{(extended transport approximation).} \tag{5.40}$$

The choice of σ_g just described is called the "extended transport" approximation for the following reason. In one-speed theory, the transport approximation consisted in replacing anisotropic scattering by isotropic scattering and using the transport cross section (§2.6b). In the present energy-dependent situation, the use of equation (5.40) with $L = 0$, i.e., assumed isotropic scattering, has much the same effect and leads to a multigroup transport approximation. Consequently, when σ_g is derived from equation (5.40) with $L \neq 0$, it is referred to as an extended transport approximation.[29]

In order to determine the group constants for application in equation (5.30), the values of $\sigma_{l,g}$ and $\sigma_{l,g'\to g}$ must be obtained from equations (5.32) and (5.33). To do this, estimates are required of the within-group flux, i.e., ϕ_0, for each group, and of the other ϕ_l terms in the Legendre expansion of the flux, as well as a knowledge of the variation of the microscopic cross sections with energy. The problem is similar to that discussed in Chapter 4 in connection with the multigroup constants for the P_N (and related) approximations. The choice of the number of groups is essentially the same as described in the preceding chapter.

5.4c Multigroup Discrete Ordinates Calculations

The methods for solving multigroup problems in the discrete ordinates approximation, based on the use of an appropriate digital computer code, are the same in principle as those for the P_N and related approximations. A four-point Gauss (or other) quadrature set (μ_i, w_i), which is incorporated in the code, is good for most one-dimensional criticality calculations, as indicated earlier. The scattering terms in equation (5.30) can be approximated to any desired value of L. Few problems have been encountered for which $L = 3$ is not adequate and usually the $L = 0$ transport approximation or the $L = 1$ consistent P approximation suffices.

The discrete ordinates codes can be used to solve eigenvalue problems or they can be applied to subcritical systems which include an extraneous source. In general, all the procedures, including inner and outer iterations, evaluation of

the effective multiplication factor or of α, and determination of criticality conditions are the same as described at the end of Chapter 4. An example of the application of such a code is given below.

5.4d An Application to Fast-Neutron Systems

The method of discrete ordinates is a versatile tool for the solution of neutron transport problems in relatively simple geometry. In this section, an example will be given of the application of the method to some fast-neutron systems. The considerations which determine the procedure, especially the anisotropic approximation and the choice of the number of energy groups, will be explained, and the results of the calculations, particularly of the effective multiplication factor (or k eigenvalue) and of the critical radii of spherical assemblies, will be compared with experimental data on fast-neutron critical assemblies.

Good agreement between computed and observed values depends, not only on the use of accurate methods for solving the transport equation, but also on the availability of reliable neutron cross sections. Consequently, some of the problems involved in determining the adequacy of nuclear data for reactor calculations will be examined. Several "libraries" of cross sections in a form suitable for computer processing are available[30] and one which provides suitable input data for a multigroup, discrete ordinates calculation is used.

The present discussion will refer, primarily, to relatively simple, metal systems containing fissile material and operating with a fast-neutron spectrum. In fast reactors containing appreciable amounts of elements of low mass number, such as sodium as coolant and oxygen or carbon as the oxide or carbide, respectively, of uranium or plutonium, the neutron spectrum will be shifted to lower energies. In these circumstances, neutron absorption in the resonance region becomes important; this subject will be treated in Chapter 8, but for the assemblies described here, resonance absorption is not significant.

To permit a meaningful comparison between calculation and experiment, the computations will be made for fast critical assemblies, having simple geometry and composition, which have been the subject of careful experimental studies. These include the (approximately) spherical* assemblies Godiva, of unreflected uranium metal enriched to 93.9 atomic percent in uranium-235,[31] Jezebel, of unreflected metallic (95%) plutonium-239,[32] and Topsy, of 94.0% uranium-235 metal with a thick reflector of natural uranium.[33]

Few, if any, of the cross sections in the library referred to earlier are known to $\pm 1\%$; typically, even the most important fast-neutron cross sections will have experimental uncertainties of plus or minus a few percent. Consequently, it is not to be expected that agreement between experimental values of k or critical radius and those calculated from the library data will be better than a few

* The assemblies mentioned here are not exactly spherical and minor corrections are made to arrive at the dimensions of a critical sphere.

percent. Nevertheless, for establishing accurate computing methods and in particular for evaluation of the accuracy of the cross sections, it is desirable that all approximations in the transport computations should be such that the resulting uncertainties are small in comparison with a few percent.

Discrete Ordinates Calculations

The reference fast critical assemblies mentioned above consist of highly enriched fissile material, and they are consequently quite small. It is evident, therefore, that P_1 or diffusion theory is inadequate and a more accurate solution of the neutron transport must be used. To determine what this might be, consider, for simplicity, a one-speed treatment. Since the mean number of neutrons, c, emerging from a collision is approximately 1.3 for uranium-235 and 1.5 for plutonium-239, it is apparent from Table 2.7 that even a P_5 approximation will give errors in the critical radius of about 1%. For the cases considered here, a multigroup discrete ordinates calculation was used with the S_8 approximation. According to the results in Table 5.3, for a one-speed problem, this should give critical radii within about 0.3% of the values obtained by the exact solution of the neutron transport equation. The corresponding error in k is roughly 0.15%. Similar conclusions concerning the accuracy to be expected from the S_8 approximation are applicable to multigroup theory.[34]

In making the calculations the first point to consider is how accurately the angular distribution of scattered neutrons must be taken into account, i.e., how many terms are required in a Legendre expansion such as that in equation (5.34). From the shapes of the curves of the differential elastic cross sections versus scattering angle for neutrons in the energy range of interest,[35] it might be imagined that several terms in the Legendre expansion would have to be included. Typical curves for the elastic scattering of neutrons of higher energy (2.5 MeV) and lower energy (0.65 MeV) by uranium are given in Fig. 5.5.

It will now be shown, however, by examining the sensitivity of the results to the number of terms, that quite accurate results can be obtained by means of a P_2 or P_3 representation of the anisotropic scattering. In fact, even the $L = 0$ extended transport approximation (§5.4b) is reasonably adequate for many fast critical assemblies. That such is the case is apparent from the values in Table 5.4 of the critical radius of the Godiva assembly computed by the S_8 method for various approximations to the anisotropic scattering.[36] The number of terms in the Legendre expansion of the scattering cross section is equal to $L + 1$ in each case. These calculations were performed using six energy groups, which will be described below, and the DTF IV discrete ordinates code.

The reason why the extended transport approximation represents the scattering moderately well even when $L = 0$ is that the pronounced forward peaks, which occur in the differential elastic cross-section curves at energies above about 1 MeV (see the upper curve in Fig. 5.5), are not important for the neutron

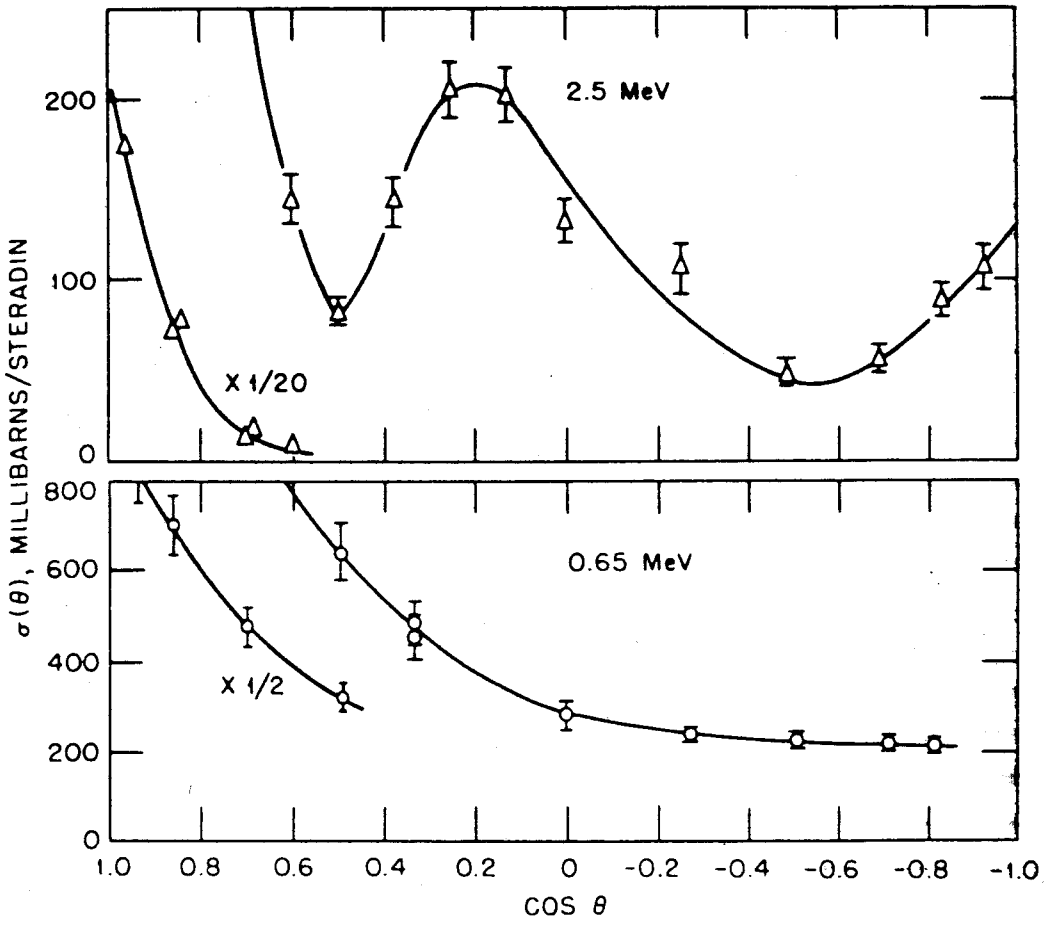

FIG. 5.5 DIFFERENTIAL ELASTIC SCATTERING CROSS SECTIONS OF URANIUM VS SCATTERING ANGLE IN THE CENTER-OF-MASS SYSTEM (AFTER M. D. GOLDBERG, *ET AL.*, REF. 35).

transport and are largely ignored in the extended transport approximations. Forward scattering is like no scattering at all, since the neutrons continue to travel in the same direction, and so it can be neglected. For the calculations described below, a consistent P_2, i.e., $L = 2$, approximation was made to the anisotropic scattering. The results in Table 5.4 indicate that this should introduce no significant error.

Next, there is the question of the number of energy groups to use for these computations and how to obtain estimates of the within-group neutron fluxes. An effort was made to minimize the sensitivity of the results to these fluxes by using many energy groups, up to 24 in number, to span the energy range 17 keV $\leqslant E_n \leqslant$ 14 MeV. The within-group fluxes were generated from a B_0 calculation (§4.5c) of the detailed energy dependence of the neutron flux in the Godiva assembly using the library cross sections. The value of the buckling, B^2, was taken to be $\pi^2 (R + x_0)^2$, where x_0, the extrapolation distance (§2.5b), was estimated from the average values of the transport cross section and c. The neutron spectrum obtained in this manner was taken to be the same for all the

TABLE 5.4. CRITICAL RADIUS OF THE GODIVA ASSEMBLY FOR DIFFERENT APPROXIMATIONS TO THE SCATTERING[36]

	Critical Radius (cm)	
L	*Consistent P* [*Equation* (5.37)]	*Extended Transport* [*Equation* (5.40)]
0	7.865	8.779
1	8.863	8.808
2	8.810	8.809
3	8.810	8.809

assemblies studied; all the Legendre components of the flux were also assumed to have the same energy dependence in each case.

To show that the calculations are indeed insensitive to the within-group fluxes, provided the number of groups is fairly large, the spectrum referred to above was employed to compute k for the Godiva, Jezebel, and Topsy critical assemblies and for a bare sphere of uranium-233. The number of energy groups was either 6, 12, or 24. The ranges of the six groups were 14 to 3 MeV, 3 to 1.4 MeV, 1.4 to 0.9 MeV, 0.9 to 0.4 MeV, 0.4 to 0.1 MeV, and 0.1 MeV to 17 keV.* For the 12- and 24-group calculations, these ranges were divided into two or four groups, respectively, of equal lethargy width. The results of the computations, based on the known critical radii, are given in Table 5.5.[37] It is evident that the calculated values of k are not sensitive to the number of energy groups and, hence, to the within-group neutron fluxes when the number of groups is sufficiently large.

TABLE 5.5. DEPENDENCE OF CALCULATED k ON NUMBER OF ENERGY GROUPS[37]

	Number of Groups		
Assembly	6	12	24
Godiva	0.9960	0.9911	0.9912
Jezebel	1.0045	1.0035	1.0039
Topsy	0.9965	0.9925	0.9907
Uranium-233 sphere	1.0106	1.0110	1.0115

* This six-group structure evolved from an original three-group representation in which the boundaries between the groups were set at 1.4 and 0.4 MeV, since these energies represent the (approximate) fission thresholds of uranium-238 and neptunium-237, respectively. Thus, a uranium-238 fission counter would give the neutron flux in the first (highest energy) group, and a neptunium-237 counter that in the first two groups.

The multigroup calculations used to obtain the data in the table, as well as those for the fast-neutron systems described below, were performed with the DTF IV code, a versatile discrete-ordinates program for solving the transport equation in one dimension with anisotropic scattering.[38] The particular S_8 quadrature set employed had equally spaced values of μ^2 (§5.3e). The spatial distribution of the flux was determined by using 20 radial mesh points.

From the arguments presented above, it may be concluded that the 24-group, S_8 calculations, with a P_2 approximation to the scattering anisotropy, should be sufficient to provide an accurate treatment of neutron transport in fast (metal) assemblies. Hence, when this procedure is used, together with the data from a particular cross-section library, for computing the k of experimental critical systems, it will provide a good test of the accuracy of the library for fast-neutron systems. The results of such computations of k for a variety of fast critical assemblies are summarized in Table 5.6.[39]

All the systems, except ZPR-III 48, were small and were simple in both composition, as indicated in the table, and geometry (approximately spherical). ZPR-III 48 simulated a fast reactor with a core consisting mainly of carbides of uranium-238 and plutonium-239, with sodium as coolant and iron as the structural material; the reflector was largely uranium. For the reason given earlier, the neutron spectrum in such a system extends to lower energies than for the other (heavy metal) assemblies. The cross-section treatment used here, especially the choice of energy groups and the neglect of resonance absorption, would thus not be expected to be suitable for treatment of the ZPR-III 48 assembly. It has been included here, however, as a matter of general interest.

TABLE 5.6. COMPUTED VALUES OF THE EFFECTIVE MULTIPLICATION FACTOR FOR FAST CRITICAL ASSEMBLIES[39]

*Assembly**		*Core Radius*	*Calculated*
Core	*Reflector*	*(cm)*	*k*
Uranium-233	None	5.965	1.0115
Uranium-235 (Godiva)	None	8.710	0.9912
Plutonium-239 (Jezebel)	None	6.285	1.0039
Uranium-235 (37.5%)	None	14.57	0.9855
Uranium-235 (16.7%)	7.6 cm uranium	20.32	0.9893
Uranium-235	1.8 cm uranium	7.725	0.9907
Uranium-235	8.9 cm uranium	6.391	0.9939
Uranium-235 (Topsy)	Thick uranium	6.045	0.9907
Uranium-235	5.1 cm iron	7.39	0.9756
Uranium-235	4.6 cm thorium	7.80	0.9905
ZPR-III 48 (see text)	30 cm uranium	47.42	1.016

* For descriptions of the assemblies, see Ref. 40.

Adequacy of Cross-Section Data

From the results in Table 5.6, it is apparent that the computed values of k are, at worst, within a percent or two of unity for essentially all the critical assemblies. It may be concluded, therefore, that the cross-section library is as accurate as can be expected for predicting criticality in fast (metal) reactor systems. In view of the assemblies considered, however, the cross sections of only a few nuclides, in particular uranium-233, -235, and -238 and plutonium-239, and to a lesser extent thorium, iron, carbon, and sodium, are actually tested by the data in Table 5.6.

A closer examination of the results in the table suggests some possibilities for improvement in the cross-section library. For example, it is seen that, for all the assemblies containing uranium-235, k is less than unity; this would imply that the values of ν or σ_f used in the computations are too small. Furthermore, the very low value of k for the system with the iron reflector indicates that the cross section of iron would merit reexamination. Information concerning the reliability of a cross-section library can also be obtained from calculations and observations of the effect on k (or on the reactivity) of introducing various materials into a critical assembly. This approach will be described in §6.3f.

Another way of determining the accuracy of cross-section data is to compare the computed group fluxes with actual measurements. Without going into details, some general features of such measurements may be mentioned. A common experimental technique is to make use of activation detectors. Threshold detection, such as by the $^{31}P(n, p)^{31}Si$ reaction with a threshold at about 2.7 MeV, and by the $^{238}U(n, f)$ reaction with a threshold around 1.4 MeV, are useful for characterizing the high-energy portion of the neutron spectrum. For neutrons of lower energy, (n, γ) detectors, such as gold in the $^{197}Au(n, \gamma)^{198}Au$ reaction, are employed. Relative (fission) activation of the fissile nuclides can be used to characterize the neutron spectrum, because the fission cross sections vary somewhat differently with neutron energy.

In activation measurements, in general, the common practice is to determine the ratios of the activities of several detectors; such ratios have been called spectral indices.[41] The advantage of this technique is that it minimizes the effects of uncertainties in the irradiation history of the detector.

The neutron spectrum can sometimes be measured directly. For example, time-of-flight experiments have been used for subcritical systems.[42] For either subcritical or critical assemblies, nuclear emulsions or proton-recoil proportional counters can be employed.[43] Comparison of the results of measurements with the computed flux provides a good test for inelastic scattering cross sections; these are the most important quantities for neutron energy loss with heavy nuclei.

It is evident that procedures are available for characterizing the neutron spectra in fast reactors. By comparison with the results of multigroup calculations, confidence may be gained both in the reliability of the method of computation and in the library of cross sections. If discrepancies are observed between

calculations and observations, the source of such discrepancies can often be determined and methods can be suggested for eliminating them.

EXERCISES

1. Consider the discrete ordinates equation (5.3) for a source-free homogeneous slab with $N = 2$ and with $\mu_1 = -\mu_2$. Derive equations satisfied by the sum and difference of the two angular flux components, $\Phi(x, \mu_1)$ and $\Phi(x, \mu_2)$, and show that, with an appropriate choice of μ_1, the flux will have the exact asymptotic diffusion length.[44] The scattering should be assumed to be isotropic.
2. By using off-center difference approximations for the derivatives in equation (5.3), such as

$$\left.\frac{\partial \Phi}{\partial x}\right|_{x=x_k} \simeq \frac{\Phi(x_{k+1}, \mu_j) - \Phi(x_k, \mu_j)}{\Delta x},$$

   show that difference equations can be obtained from which Φ will always be positive, no matter what the spacing. (Such difference equations are, however, generally less accurate than the central difference equations which may lead to negative values of the angular flux.[45])
3. In the Liebmann iterative procedure (§3.4d), it was found efficient to use all the latest flux values as they become available. Suggest a way in which this might be done in solving the discrete ordinates equation (5.3). Indicate some possible advantages and disadvantages as compared with the method in §5.2f.[46]
4. Show that the discrete ordinates equations for spherical geometry with Gauss quadrature, and the angular derivative approximated by equation (5.16), are equivalent to the spherical harmonics equations (3.35).
5. Suppose the angular dependence of the neutron flux is represented by straight line segments, as in Fig. 5.2. By integrating over an angular interval, derive equations satisfied by the neutron flux at the junction points in plane (or spherical) geometry. (These are the original S_N equations.[47]) Describe a method for solving the equations along the lines indicated in the text.
6. Show that in the limit, when $r_i/\Delta\sigma$ is very large, the difference equations (5.25) and (5.27) reduce to those for plane geometry; Δ is the distance between adjacent radial mesh points.
7. For those who have computed the group constants in Exercise 1 of Chapter 4: evaluate the multigroup constants according to the consistent P and extended transport approximations for $L = 1$.
8. Develop discrete ordinates difference equations for cylindrical geometry by selecting a set of discrete directions and a quadrature formula and working through the steps outlined in §5.3e. In case of difficulty, Ref. 48 may be consulted.

REFERENCES

1. Yetman, D., *et al.*, "9-NIOBE," United Nuclear Corp. Report NDA 2413-18 (1961); V. S. Vladimirov, Dissertation, referred to in G. Marchuk, *Atomn. Energiia* (transl.), **11**, 1000 (1962).
2. Wick, G. C., *Z. Physik*, **121**, 702 (1943).

3. Chandrasekhar, S., "Radiative Tranfer," Oxford University Press, 1950, Chap. II.
4. Carbone, R. J., and K. D. Lathrop, *Nucl. Sci. Eng.*, **35**, 139 (1969).
5. Chandrasekhar, S., Ref. 3.
6. Chandrasekhar, S., Ref. 3.
7. Abramowitz, M., and I. E. Stegun, eds., "Handbook of Mathematical Functions," Dover Publications, Inc., 1965, pp. 916–919.
8. Sykes, J. B., *Monthly Not. Roy. Astron. Soc.*, **111**, 377 (1951).
9. Carlson, B. G., and K. D. Lathrop in "Computing Methods in Reactor Physics," H. Greenspan, C. N. Kelber, and D. Okrent, eds., Gordon and Breach, 1968, p. 216; E. M. Gelbard *ibid.*, Section 4.2.
10. Carlson, B. G., and K. D. Lathrop, Ref. 9, p. 224; E. M. Gelbard, Ref. 9, Section 4.2.
11. Carlson, B. G., "Numerical Solution of Transient and Steady State Transport Problems," Los Alamos Scientific Laboratory Report LA-2260 (1959); E. M. Gelbard, Ref. 9, Section 4.2; K. D. Lathrop, "Spatial Differencing of the Transport Equation: Positivity vs. Accuracy," in Neutron Transport Theory Conference, AEC Report ORO 3858-1 (1969).
12. Lee, C. E., "The Discrete S_N Approximation to Transport Theory," Los Alamos Scientific Laboratory Report LA-2595 (1962), Table 8.1.
13. Carlson, B. G., and G. I. Bell, *Proc. Second U.N. Conf. on Peaceful Uses of At. Energy*, **16**, 535 (1958).
14. Lathrop, K. D., and A. Leonard, *Nucl. Sci. Eng.*, **22**, 115 (1965).
15. Chandrasekhar, S., Ref. 3, §91; E. M. Gelbard, Ref. 9, Section 4.4.
16. Gelbard, E. M., Ref. 9, Section 4.4.
17. Carlson, B. G., "Solutions of the Transport Equation by S_N Approximations," Los Alamos Scientific Laboratory Report LA-1599 (1953).
18. Carlson, B. G., and G. I. Bell, Ref. 13; B. G. Carlson and K. D. Lathrop, Ref. 9, Section 3.3.
19. Carlson, B. G., and K. D. Lathrop, Ref. 9, Section 3.1.4.
20. Carlson, B. G., and K. D. Lathrop, Ref. 9, p. 224; E. M. Gelbard and L. A. Hageman, *Nucl. Sci. Eng.*, **37**, 288 (1969); B. E. Clancy and I. J. Donnelly, *ibid.*, **39**, 398 (1970).
21. Kaplan, S., *Nucl. Sci. Eng.*, **34**, 76 (1968); E. M. Gelbard and M. Natelson, *Trans. Am. Nucl. Soc.*, **11**, 530 (1968).
22. Lee, C. E., Ref. 12; Table 8.3; B. G. Carlson and G. I. Bell, Ref. 13.
23. Carlson, B. G., and K. D. Lathrop, Ref. 9, Chap. 3.
24. Lee, C. E., Ref. 12; B. G. Carlson and K. D. Lathrop, Ref. 9, Section 3.3.
25. Hendry, W. L., *Nucl. Sci. Eng.*, **34**, 76 (1968).
26. Lathrop, K. D., *Nucl. Sci. Eng.*, **32**, 357 (1968); E. M. Gelbard and M. Natelson, Ref. 21; E. M. Gelbard, Ref. 9, Chap. 4.
27. Wigner, E. P., "Group Theory and its Application to the Quantum Mechanics of Atomic Spectra," Academic Press, 1959, Chap. 15.
28. Bell, G. I., G. E. Hansen, and H. A. Sandmeier, *Nucl. Sci. Eng.*, **28**, 376 (1967); G. C. Pomraning, *Trans. Am. Nucl. Soc.*, **8**, 488 (1965).
29. Bell, G. I., *et al.*, Ref. 28.
30. Parker, K., D. T. Goldman, and L. Wallin, in "Nuclear Data for Nuclear Reactors," IAEA, 1967, Vol. II, p. 293.
31. Peterson, R. E., and G. A. Newby, *Nucl. Sci. Eng.*, **1**, 112 (1956).
32. Jarvis, G. A., *et al.*, *Nucl. Sci. Eng.*, **8**, 525 (1960).
33. White, R. H., *Nucl. Sci. Eng.*, **1**, 53 (1956).
34. Kiehn, R. M., *Nucl. Sci. Eng.*, **4**, 166 (1958).
35. Goldberg, M. D., V. M. May, and J. R. Stehn, "Angular Distributions in Neutron Induced Reactions," Vol. II ($Z = 23$-94), Brookhaven National Laboratory Report BNL-400 (1962).
36. Bell, G. I., *et al.*, Ref. 28.
37. Mills, C. B., *Nucl. Applic.*, **5**, 211 (1968).
38. Lathrop, K. D., "DTF-IV, a Fortran-IV Program for Solving the Multigroup Transport Equation with Anisotropic Scattering," Los Alamos Scientific Laboratory Report LA-3373 (1965).

39. Mills, C. B., Ref. 37. For extensive discussions of similar analyses, see "Fast Reactor Physics," IAEA, Vols. I and II (1968).
40. See citations in Refs. 31, 32, 33, 37.
41. Grundl, J., and A. Unser, *Nucl. Sci. Eng.*, **8**, 598 (1960); C. C. Byers, *ibid.*, **8**, 608 (1960); W. G. Davey, *ibid.*, **26**, 149 (1966); F. Pistella, *ibid.*, **34**, 329 (1968).
42. Stevens, C. A., in Proc. Conf. on Neutron Cross Sections and Technology, National Bureau of Standards Special Publication, No. 299 (1968), Vol. II, p. 1143; J. M. Neill, *et al.*, *ibid.*, Vol. II, p. 1183.
43. Stewart, L., *Nucl. Sci. Eng.*, **8**, 595 (1960); C. A. Stevens, Ref. 42.
44. Jauho, P., and H. Kalli, *Nucl. Sci. Eng.*, **33**, 251 (1968).
45. Gelbard, E. M., Ref. 9, p. 301.
46. Gelbard, E. M., Ref. 9, p. 299.
47. Carlson, B. G., Ref. 17; B. G. Carlson and G. I. Bell, Ref. 13.
48. Carlson, B. G., and K. D. Lathrop, Ref. 9.

6. THE ADJOINT EQUATION, PERTURBATION THEORY, AND VARIATIONAL METHODS

6.1 THE ADJOINT FUNCTION AND ITS APPLICATIONS

6.1a Introduction

In this chapter, consideration will be given to the equation which is adjoint to the neutron transport equation. The solutions to an adjoint equation will be seen to be, in a sense, orthogonal to the solutions of the transport equation. Moreover, the former have a clear physical significance as the "importance" of neutrons within a particular system. For these and other reasons, the solutions to the adjoint to the transport equation are widely used in perturbation theory and variational calculations relating to the behavior of nuclear reactors.

Among the more important applications which will be described in this chapter are the following: determination of the changes in the multiplication rate constant, α, and the effective multiplication factor, k, resulting from small changes in cross sections; the calculation of critical dimensions; the evaluation of group constants for multigroup calculations; and the use of solutions of one-dimensional problems to derive solutions for more complex geometries.

The first step in the development is to define certain quantities which will be used here. Let $\psi(\xi)$ and $\phi(\xi)$ both be functions of the same variables, represented by the general symbol ξ; the *inner product* of these two functions is then expressed and defined by

$$(\psi, \phi) \equiv \int \psi(\xi)\phi(\xi)\, d\xi, \tag{6.1}$$

where the integration is carried over the whole accessible range of the variables. If ψ and ϕ are any "acceptable" or "well-behaved" functions, in the sense that they satisfy certain boundary and smoothness (continuity) conditions, then a *Hermitian* or *self-adjoint* operator $\mathbf{M}$ is one for which the inner products $(\psi, \mathbf{M}\phi)$ and $(\phi, \mathbf{M}\psi)$ are equal, i.e.,

$$(\psi, \mathbf{M}\phi) = (\phi, \mathbf{M}\psi). \tag{6.2}$$

The eigenfunctions of Hermitian operators are orthogonal and the eigenvalues are always real.

In quantum mechanics, operators representing physical quantities are Hermitian and they operate on wave functions. Both the operators and the wave functions in quantum mechanics are complex, and so complex conjugates are used in defining the inner products.

In the treatment of neutron transport theory, the operators and the functions on which they operate, e.g., the neutron angular flux, are real and complex conjugates are not required. However, the operator associated with the transport equation is not self-adjoint.

If an operator $\mathbf{L}$ is not self-adjoint, it is possible in the following way to define an operator $\mathbf{L}^\dagger$ that is adjoint to $\mathbf{L}$. The operator, $\mathbf{L}^\dagger$, will operate on functions $\psi^\dagger$, often called *adjoint functions*, which may satisfy boundary conditions different from those satisfied by the functions ϕ on which $\mathbf{L}$ operates. The adjoint operator, $\mathbf{L}^\dagger$, is then defined by the requirement that

$$(\psi^\dagger, \mathbf{L}\phi) = (\phi, \mathbf{L}^\dagger\psi^\dagger) \tag{6.3}$$

for any "acceptable" functions ϕ and $\psi^\dagger$. The eigenfunctions of the adjoint operator, $\mathbf{L}^\dagger$, are then orthogonal to those of the operator $\mathbf{L}$. Thus, if ϕ is an eigenfunction of $\mathbf{L}$, such that

$$\mathbf{L}\phi = \lambda\phi,$$

and $\psi^\dagger$ is an eigenfunction of $\mathbf{L}^\dagger$ such that

$$\mathbf{L}^\dagger\psi^\dagger = \eta\psi^\dagger,$$

equation (6.3) gives

$$(\lambda - \eta)(\psi^\dagger, \phi) = 0.$$

Hence, if $\lambda \neq \eta$, then $(\psi^\dagger, \phi) = 0$, i.e., eigenfunctions of $\mathbf{L}$ and $\mathbf{L}^\dagger$ corresponding to different eigenvalues (λ and η) are orthogonal. If, on the other hand,

$(\psi^\dagger, \phi) \neq 0$, then $\lambda = \eta$. These considerations will now be applied to the transport equation.

6.1b The Transport Operator

A neutron transport operator $\mathbf{L}$ may be defined by writing the time-independent form of the transport equation (1.14) as

$$\mathbf{L}\Phi(\mathbf{r}, \Omega, E) + Q(\mathbf{r}, \Omega, E) = 0, \tag{6.4}$$

where

$$\mathbf{L}\Phi(\mathbf{r}, \Omega, E) = -\Omega \cdot \nabla\Phi(\mathbf{r}, \Omega, E) - \sigma\Phi + \iint \sigma f(\mathbf{r}; \Omega', E' \to \Omega, E)\Phi(\mathbf{r}, \Omega', E')\, d\Omega'\, dE'. \tag{6.5}$$

The operator $\mathbf{L}$, as will be shown below, is not self-adjoint. In other words, if $\psi(\mathbf{r}, \Omega, E)$ and $\phi(\mathbf{r}, \Omega, E)$ are functions of $\mathbf{r}, \Omega, E$ satisfying the required continuity and boundary conditions, then

$$(\psi, \mathbf{L}\phi) \neq (\phi, \mathbf{L}\psi),$$

where in determining the inner products the integration in equation (6.1) is over all directions Ω, all neutron energies, and the finite volume on the surface of which the boundary conditions are imposed.

To demonstrate that the inner products are not equal, consider, first, the gradient (or streaming) term; in $(\psi, \mathbf{L}\phi)$ this term is

$$\iiint -\psi[\Omega \cdot \nabla\phi]\, dV\, d\Omega\, dE,$$

whereas in $(\phi, \mathbf{L}\psi)$ it is

$$\iiint -\phi[\Omega \cdot \nabla\psi]\, dV\, d\Omega\, dE.$$

In general, these two quantities are different. Similarly, the integral term in $(\psi, \mathbf{L}\phi)$ will be

$$\int \cdots \int \psi(\mathbf{r}, \Omega, E)\sigma f(\mathbf{r}; \Omega', E' \to \Omega, E)\phi(\mathbf{r}, \Omega', E')\, dV\, d\Omega\, dE\, d\Omega'\, dE'$$

and in $(\phi, \mathbf{L}\psi)$, with the terms in ψ and ϕ interchanged, the value will clearly be different. Hence, it follows that $(\psi, \mathbf{L}\phi)$ and $(\phi, \mathbf{L}\psi)$ are not equal and the transport operator is not self-adjoint.

6.1c The Adjoint to the Transport Operator

As indicated earlier, however, it is possible to define an operator $\mathbf{L}^*$, adjoint to $\mathbf{L}$, so that any function ψ^* fulfilling continuity and boundary conditions, which may be different from those on ϕ, will satisfy the relationship

$$(\psi^*, \mathbf{L}\phi) = (\phi, \mathbf{L}^*\psi^*).$$

Since, in this chapter, $\mathbf{L}$ will operate on the neutron angular flux, the adjoint operator, $\mathbf{L}^\dagger$, will be defined by the requirement that

$$(\Phi^\dagger, \mathbf{L}\Phi) = (\Phi, \mathbf{L}^\dagger\Phi^\dagger), \tag{6.6}$$

where $\Phi^\dagger$ is sometimes referred to as the adjoint (angular) flux or, more commonly, as the *adjoint function* (or, in brief, as the *adjoint*); Φ and $\Phi^\dagger$ are any two functions satisfying the appropriate boundary and continuity conditions for the angular flux and adjoint, respectively. By considering the left side of equation (6.6), it is possible to derive the necessary form for $\mathbf{L}^\dagger$ and the boundary conditions on $\Phi^\dagger$. For simplicity, however, the procedure adopted here will be to write down the expression for the adjoint operator and show that it indeed obeys equation (6.6).

The function Φ may be taken to satisfy the free-surface boundary conditions in §1.1d; thus, $\Phi(\mathbf{r}, \boldsymbol{\Omega}, E) = 0$ for all $\mathbf{r}$ on the convex boundary and all incoming neutron directions, i.e., for $\hat{\mathbf{n}}\cdot\boldsymbol{\Omega} < 0$. Then the adjoint function will satisfy the boundary conditions that $\Phi^\dagger(\mathbf{r}, \boldsymbol{\Omega}, E) = 0$ for all $\mathbf{r}$ on the boundary and for all outgoing directions, i.e., $\hat{\mathbf{n}}\cdot\boldsymbol{\Omega} > 0$. Moreover, it is assumed that both Φ and $\Phi^\dagger$ are continuous functions of space, as described in §1.1d, so that no difficulties arise when their gradients are computed. Then, in accordance with the definition of the adjoint transport operator, $\mathbf{L}^\dagger$, in equation (6.6),

$$\mathbf{L}^\dagger\Phi^\dagger(\mathbf{r}, \boldsymbol{\Omega}, E) = \boldsymbol{\Omega}\cdot\nabla\Phi^\dagger(\mathbf{r}, \boldsymbol{\Omega}, E) - \sigma\Phi^\dagger + \iint \sigma f(\mathbf{r}; \boldsymbol{\Omega}, E \to \boldsymbol{\Omega}', E')\Phi^\dagger(\mathbf{r}, \boldsymbol{\Omega}', E')\, d\boldsymbol{\Omega}'\, dE'. \tag{6.7}*$$

The following differences should be noted between $\mathbf{L}^\dagger$ as given by equation (6.7) and $\mathbf{L}$ as defined by equation (6.5): (*a*) the gradient terms have opposite signs and (*b*) the before and after parts of the scattering function σf have been interchanged, i.e., $\boldsymbol{\Omega}', E' \to \boldsymbol{\Omega}, E$ in $\mathbf{L}$ becomes $\boldsymbol{\Omega}, E \to \boldsymbol{\Omega}', E'$ in $\mathbf{L}^\dagger$.

It will now be shown that $\mathbf{L}^\dagger$ is indeed the adjoint operator in the respect that equation (6.6) is satisfied, i.e.,

$$\int\int\int \Phi^\dagger\mathbf{L}\Phi\, dV\, d\boldsymbol{\Omega}\, dE = \int\int\int \Phi\mathbf{L}^\dagger\Phi^\dagger\, dV\, d\boldsymbol{\Omega}\, dE,$$

for any functions Φ and $\Phi^\dagger$ satisfying the boundary and continuity conditions. In view of the expressions for $\mathbf{L}\Phi$ and $\mathbf{L}^\dagger\Phi^\dagger$ in equations (6.5) and (6.7), it is evident that each side of equation (6.6) consists of three analogous terms, one involving the gradient, the second containing σ, and the third σf. The terms with σ alone are clearly identical, and so also are those with σf as may be seen by interchanging the integration variables $\boldsymbol{\Omega}'$, E' and $\boldsymbol{\Omega}$, E on one side. It remains,

* The σ in the integrand of equation (6.7) is $\sigma(\mathbf{r}, E)$, whereas in the integrand in equation (6.5) it is $\sigma(\mathbf{r}, E')$, as is apparent from the respective arguments of f. The reader should become accustomed to considering the combination σf as a whole.

therefore, to show that the gradient terms are equal. The difference, Δ, between the two gradient terms in equation (6.6) is

$$\Delta = \iiint [\Phi^\dagger(\mathbf{\Omega}\cdot\nabla\Phi) + \Phi(\mathbf{\Omega}\cdot\nabla\Phi^\dagger)]\, dV\, d\mathbf{\Omega}\, dE, \tag{6.8}$$

and it is required to prove that $\Delta = 0$. The procedure is similar to that given in §2.7a in the derivation of the optical reciprocity theorem.

Since ∇ does not operate on directions, it is permissible to write

$$\mathbf{\Omega}\cdot\nabla\Phi = \nabla\cdot\mathbf{\Omega}\Phi \quad \text{and} \quad \mathbf{\Omega}\cdot\nabla\Phi^\dagger = \nabla\cdot\mathbf{\Omega}\Phi^\dagger.$$

The two terms in equation (6.8) may now be combined to give

$$\Delta = \iiint \nabla\cdot\mathbf{\Omega}\Phi^\dagger\Phi\, dV\, d\mathbf{\Omega}\, dE.$$

The volume integral can be converted to a surface integral by use of the divergence theorem, with the result

$$\Delta = \iiint_{A_B} \hat{\mathbf{n}}\cdot\mathbf{\Omega}\Phi^\dagger(\mathbf{r}, \mathbf{\Omega}, E)\Phi(\mathbf{r}, \mathbf{\Omega}, E)\, dA\, d\mathbf{\Omega}\, dE,$$

where the surface integration is over the bounding surface, A_B, on which the boundary conditions are imposed. On this surface, however, $\Phi^\dagger\Phi$ is zero, since according to the boundary conditions given above $\Phi^\dagger$ is zero for $\hat{\mathbf{n}}\cdot\mathbf{\Omega} > 0$ and Φ is zero for $\hat{\mathbf{n}}\cdot\mathbf{\Omega} < 0$. Consequently, $\Delta = 0$, and hence equation (6.6) is satisfied.

6.1d The Adjoint Function and Neutron Importance

It will be recalled from §1.5d that the time-independent transport equation has a physically meaningful solution for a subcritical system containing a steady (time-independent) source. Similarly, for a subcritical system, the time-independent adjoint equation will have a solution (the adjoint function) for a steady source. The significance of this solution will be examined here; the time-dependent problem will be treated in later sections.

The physical significance of the energy-dependent adjoint function can be understood by considering a steady-state subcritical system containing an arbitrary, steady source, $Q(\mathbf{r}, \mathbf{\Omega}, E)$. Suppose there is present a neutron detector, such as one based on the $^{10}\mathrm{B}(n, \alpha)$ or the $^{235}\mathrm{U}(n, f)$ reaction, with a response proportional to the macroscopic cross section, $\sigma_d(\mathbf{r}, E)$, of the detector nuclide, e.g., σ_d is the probability of a count in the detector per unit distance of neutron

travel. The neutron angular flux in the system satisfies the time-independent transport equation (6.4), i.e.,

$$\mathbf{L}\Phi = -Q$$

or

$$\boldsymbol{\Omega}\cdot\nabla\Phi + \sigma\Phi = \iint \sigma f(\mathbf{r}; \boldsymbol{\Omega}', E' \to \boldsymbol{\Omega}, E)\Phi(\mathbf{r}, \boldsymbol{\Omega}', E')\, d\boldsymbol{\Omega}'\, dE' + Q(\mathbf{r}, \boldsymbol{\Omega}, E), \quad (6.9)$$

with the usual free-surface boundary condition of no incoming neutrons. In addition, consider the inhomogeneous adjoint equation with the source $\sigma_d(\mathbf{r}, E)$, that is,

$$\mathbf{L}^\dagger\Phi^\dagger = -\sigma_d$$

or

$$-\boldsymbol{\Omega}\cdot\nabla\Phi^\dagger + \sigma\Phi^\dagger = \int \sigma f(\mathbf{r}; \boldsymbol{\Omega}, E \to \boldsymbol{\Omega}', E')\Phi^\dagger(\mathbf{r}, \boldsymbol{\Omega}', E')\, d\boldsymbol{\Omega}'\, dE' + \sigma_d(\mathbf{r}, E) \quad (6.10)$$

with the boundary condition of no outgoing adjoint flux $\Phi^\dagger$.

Equation (6.9) is now multiplied by $\Phi^\dagger$ and equation (6.10) by Φ; the resulting expressions are subtracted and the difference is integrated over all variables. By using the definition of the adjoint operator in equation (6.6), it is then found that

$$\int Q(\mathbf{r}, \boldsymbol{\Omega}, E)\Phi^\dagger(\mathbf{r}, \boldsymbol{\Omega}, E)\, dV\, d\boldsymbol{\Omega}\, dE = \int \sigma_d(\mathbf{r}, E)\Phi(\mathbf{r}, \boldsymbol{\Omega}, E)\, dV\, d\boldsymbol{\Omega}\, dE. \quad (6.11)$$

The right-hand side of this expression is simply proportional to the response of the detector to the source Q.

The source is, however, quite arbitrary and could be a unit source with particular values of $\mathbf{r}_0$, $\boldsymbol{\Omega}_0$, E_0, i.e., a product of delta functions, in which case it is seen that

$$\Phi^\dagger(\mathbf{r}_0, \boldsymbol{\Omega}_0, E_0) = \int \sigma_d\Phi\, dV\, d\boldsymbol{\Omega}\, dE.$$

Hence, $\Phi^\dagger(\mathbf{r}_0, \boldsymbol{\Omega}_0, E_0)$ is proportional to the detector response to such a unit source. In other words, the adjoint function, $\Phi^\dagger$, is a measure of the "importance" of a neutron in contributing to the response of the detector. This physical significance of the adjoint is in harmony with the condition of zero outgoing adjoint flux at the free-surface boundary; clearly, a neutron at the free-surface boundary of a system and about to leave it has no "importance" since it cannot return.

It is seen from equation (6.10) that $\Phi^\dagger$ does not have any units. If σ_d is the probability of a count per unit distance of neutron travel, then from equation (6.11), $\int Q\Phi^\dagger\, dV\, d\boldsymbol{\Omega}\, dE$ is the expected counting rate due to the source Q, and

$\Phi^\dagger(\mathbf{r}_0, \Omega_0, E_0)$ is the expected counts per neutron with position $\mathbf{r}_0$, direction Ω_0, and energy E_0.*

One use of the adjoint function is apparent from equation (6.11). If it is desired to determine the response of a given detector to neutrons of many energies, it is not necessary to perform calculations of the neutron flux for each neutron source (or energy). A single calculation of the adjoint, together with the application of equation (6.11), will suffice to compute the detector response for any source.

The results derived above depend on the postulated boundary conditions of no incoming neutrons and no outgoing adjoint. By permitting incoming neutrons, equation (6.11) will contain an additional term for such neutrons and the result could be used to determine the response of a detector to the incoming neutrons.

Let the boundary conditions on the incoming flux be

$$\Phi(\mathbf{r}, \Omega, E) = \Phi_{\text{inc}}(\mathbf{r}, \Omega, E) \quad \text{for} \quad \hat{\mathbf{n}} \cdot \Omega < 0$$

and $\mathbf{r}$ on the boundary, and on the outgoing adjoint

$$\Phi^\dagger(\mathbf{r}, \Omega, E) = \Phi^\dagger_{\text{out}}(\mathbf{r}, \Omega, E) \quad \text{for} \quad \hat{\mathbf{n}} \cdot \Omega > 0$$

and $\mathbf{r}$ on the boundary. These conditions must, of course, be known in order to obtain a solution to the problem. Then, proceeding in the same manner as used above to verify equation (6.6) the result is

$$\int_{\hat{\mathbf{n}}\cdot\hat{\Omega}<0}\int\int\int |\hat{\mathbf{n}} \cdot \Omega|[\Phi(\mathbf{r}, -\Omega, E)\Phi^\dagger_{\text{out}}(\mathbf{r}, -\Omega, E) - \Phi_{\text{inc}}(\mathbf{r}, \Omega, E)\Phi^\dagger(\mathbf{r}, \Omega, E)]\, dA\, d\Omega\, dE$$

$$= \int\int\int [Q(\mathbf{r}, \Omega, E)\Phi^\dagger(\mathbf{r}, \Omega, E) - \sigma_a(\mathbf{r}, E)\Phi(\mathbf{r}, \Omega, E)]\, dV\, d\Omega\, dE. \quad (6.12)$$

This equation is the energy-dependent generalization of the one-speed reciprocity relation of equation (2.97). From this more general form, special cases can be obtained as for the one-speed relation.

6.1e Adjoint of Green's Functions

From equation (6.11) a relationship which will be used later can be derived between a Green's function and its adjoint. Suppose the source $Q(\mathbf{r}, \Omega, E)$ and

* It would be possible to normalize the "source" in equation (6.10) differently and thereby give $\Phi^\dagger$ some units. If, for example, σ_a in this equation were replaced by $q\sigma_a$, where q is the number of coulombs of charge collected in a count, $\Phi^\dagger$ would be the expected number of coulombs collected per neutron, and equation (6.11) would relate electrical currents in amperes. In general, the units of $\Phi^\dagger$ are determined by the units of the source term or an "initial" condition (§6.1k) and may be selected in a variety of ways for different problems.

the analogous source, here denoted by $Q^\dagger$ instead of σ_d, for the adjoint problem can be represented by products of delta functions; thus,

$$Q(\mathbf{r}, \boldsymbol{\Omega}, E) = \delta(\mathbf{r} - \mathbf{r}_0)\,\delta(\boldsymbol{\Omega} - \boldsymbol{\Omega}_0)\,\delta(E - E_0)$$

and

$$Q^\dagger(\mathbf{r}, \boldsymbol{\Omega}, E) = \delta(\mathbf{r} - \mathbf{r}_1)\,\delta(\boldsymbol{\Omega} - \boldsymbol{\Omega}_1)\,\delta(E - E_1).$$

Let

$$\Phi(\mathbf{r}, \boldsymbol{\Omega}, E) = G(\mathbf{r}_0, \boldsymbol{\Omega}_0, E_0 \to \mathbf{r}, \boldsymbol{\Omega}, E)$$

and

$$\Phi^\dagger(\mathbf{r}, \boldsymbol{\Omega}, E) = G^\dagger(\mathbf{r}_1, \boldsymbol{\Omega}_1, E_1 \to \mathbf{r}, \boldsymbol{\Omega}, E).$$

Then, if $Q^\dagger$ is substituted for σ_d in equation (6.11), it follows that

$$G^\dagger(\mathbf{r}_1, \boldsymbol{\Omega}_1, E_1 \to \mathbf{r}_0, \boldsymbol{\Omega}_0, E_0) = G(\mathbf{r}_0, \boldsymbol{\Omega}_0, E_0 \to \mathbf{r}_1, \boldsymbol{\Omega}_1, E_1), \tag{6.13}$$

which relates the Green's function and its adjoint.

6.1f The One-Speed Adjoint Equation

In *one-speed theory*, the operator in the time-independent transport equation, equivalent to equation (6.5), is defined by [cf. equation (2.3)]

$$\mathbf{L}\Phi(\mathbf{r}, \boldsymbol{\Omega}) = -\boldsymbol{\Omega}\cdot\nabla\Phi(\mathbf{r}, \boldsymbol{\Omega}) - \sigma\Phi + \sigma c\int f(\mathbf{r}; \boldsymbol{\Omega}' \to \boldsymbol{\Omega})\Phi(\mathbf{r}, \boldsymbol{\Omega}')\,d\boldsymbol{\Omega}', \tag{6.14}$$

and the adjoint operator [cf. equation (6.7)] by

$$\mathbf{L}^\dagger\Phi^\dagger(\mathbf{r}, \boldsymbol{\Omega}) = \boldsymbol{\Omega}\cdot\nabla\Phi^\dagger(\mathbf{r}, \boldsymbol{\Omega}) - \sigma\Phi^\dagger + \sigma c\int f(\mathbf{r}; \boldsymbol{\Omega} \to \boldsymbol{\Omega}')\Phi^\dagger(\mathbf{r}, \boldsymbol{\Omega}')\,d\boldsymbol{\Omega}'. \tag{6.15}$$

If it is assumed that $f(\mathbf{r}; \boldsymbol{\Omega}' \to \boldsymbol{\Omega}) = f(\mathbf{r}; \boldsymbol{\Omega} \to \boldsymbol{\Omega}')$, which is the case if f is a function only of the scattering angle, $\boldsymbol{\Omega}\cdot\boldsymbol{\Omega}'$, as has been assumed in previous chapters, then the adjoint operator $\mathbf{L}^\dagger$ differs from $\mathbf{L}$ only in the sign of the first (gradient or streaming) term on the right of the equations given above. Furthermore, $\mathbf{L}$ will usually operate on functions, Φ, which satisfy the free-surface boundary condition of zero incoming flux, whereas $\mathbf{L}^\dagger$ will operate on functions, $\Phi^\dagger$, which satisfy the free-surface boundary condition of zero outgoing adjoint flux. It would seem, therefore, that, for a one-speed problem, Φ and $\Phi^\dagger$ might differ only in the sign of $\boldsymbol{\Omega}$.

The situation may be made more precise by considering the inhomogeneous adjoint transport equation

$$\mathbf{L}^\dagger\Phi^\dagger = -Q^\dagger(\mathbf{r}, \boldsymbol{\Omega}),$$

where $\Phi^\dagger$ satisfies the free-surface adjoint boundary conditions. If a function ψ is defined such that

$$\psi(\mathbf{r}, -\boldsymbol{\Omega}) = \Phi^\dagger(\mathbf{r}, \boldsymbol{\Omega}), \tag{6.16}$$

then ψ evidently satisfies the relation

$$Q^\dagger(\mathbf{r}, \Omega) = -\Omega \cdot \nabla\psi(\mathbf{r}, -\Omega) + \sigma\psi(\mathbf{r}, -\Omega) - \sigma c \int f(\mathbf{r}; \Omega \to \Omega')\psi(\mathbf{r}, -\Omega')\, d\Omega'. \tag{6.17}$$

Upon changing the variable from Ω to $-\tilde{\Omega}$, equation (6.17) becomes

$$Q^\dagger(\mathbf{r}, -\tilde{\Omega}) = \tilde{\Omega} \cdot \nabla\psi(\mathbf{r}, \tilde{\Omega}) + \sigma\psi(\mathbf{r}, \tilde{\Omega}) - \sigma c \int f(\mathbf{r}; -\tilde{\Omega} \to \Omega')\psi(\mathbf{r}, -\Omega')\, d\Omega'. \tag{6.18}$$

In the last term, Ω' is now changed to $\Omega'' = -\Omega'$ as the variable of integration, and then the integral in equation (6.18) becomes

$$I = \int f(\mathbf{r}; -\tilde{\Omega} \to -\Omega'')\psi(\mathbf{r}, \Omega'')\, d\Omega''.$$

Next, it is assumed that

$$f(\mathbf{r}; -\tilde{\Omega} \to -\Omega'') = f(\mathbf{r}; \Omega'' \to \tilde{\Omega})$$

which, again, is true for a function of $\Omega \cdot \Omega'$ only, but is more generally a condition of time-reversal invariance[1]; consequently,

$$I = \int f(\mathbf{r}; \Omega'' \to \tilde{\Omega})\psi(\mathbf{r}, \Omega'')\, d\Omega''.$$

This is the same form as the integral in equation (6.14), with allowance for the different variables. Consequently, equation (6.18) may be written as

$$-Q^\dagger(r, -\tilde{\Omega}) = \mathbf{L}\psi(\mathbf{r}, \tilde{\Omega}), \tag{6.19}$$

and ψ satisfies the flux free-surface boundary condition that it is zero if $\hat{\mathbf{n}} \cdot \tilde{\Omega} < 0$ on the boundary. It follows that ψ is the flux due to a source $Q^\dagger(\mathbf{r}, -\Omega)$, a result which will be used in §6.1g.

In a *critical system*, with no extraneous source, $Q = 0$, so that

$$\mathbf{L}\Phi(\mathbf{r}, \Omega) = 0.$$

Moreover, the adjoint problem has a solution for $Q^\dagger = 0$ (§6.1j), so that, from equation (6.19),

$$\mathbf{L}\psi(\mathbf{r}, \Omega) = 0.$$

Thus, $\Phi(\mathbf{r}, \Omega)$ and $\psi(\mathbf{r}, \Omega)$ satisfy the same equation and, in addition, they satisfy the same free-surface boundary conditions. Hence, if the functions are appropriately normalized so that $\Phi(\mathbf{r}, \Omega) = \psi(\mathbf{r}, \Omega)$, then, by the definition of ψ in equation (6.16),

$$\Phi(\mathbf{r}, \Omega) = \Phi^\dagger(\mathbf{r}, -\Omega). \tag{6.20}$$

It is seen, therefore, that for the one-speed transport problem, the angular flux and its adjoint are very similar, differing for a critical system only in the sign of the neutron direction vectors for a time-independent situation, i.e., the flux at $\mathbf{r}$ in the direction $\mathbf{\Omega}$ is equal to the adjoint at $\mathbf{r}$ in direction $-\mathbf{\Omega}$. If time were included as a variable, there would also be a difference in the time (§6.1k). The reason for this similarity of the flux and adjoint is that the one-speed transport operator is "almost" self-adjoint; for a true self-adjoint operator $\mathbf{L}^\dagger = \mathbf{L}$, but in the present case this is not completely true because of the difference in sign of the streaming term.

6.1g One-Speed Reciprocity Relation

Some of the equations given above may be used to derive a one-speed reciprocity relation. Suppose that $Q^\dagger$ is a delta function source, namely

$$Q^\dagger(\mathbf{r}, \mathbf{\Omega}) = \delta(\mathbf{r} - \mathbf{r}_1)\,\delta(\mathbf{\Omega} - \mathbf{\Omega}_1),$$

and hence $\Phi^\dagger$ is the adjoint Green's function (§6.1e)

$$\Phi^\dagger(\mathbf{r}, \mathbf{\Omega}) = G^\dagger(\mathbf{r}_1, \mathbf{\Omega}_1 \rightarrow \mathbf{r}, \mathbf{\Omega}).$$

But according to equation (6.19), ψ is the Green's function

$$\psi(\mathbf{r}, \mathbf{\Omega}) = G(\mathbf{r}_1, -\mathbf{\Omega}_1 \rightarrow \mathbf{r}, \mathbf{\Omega}),$$

and since $\Phi^\dagger(\mathbf{r}, \mathbf{\Omega}) = \psi(\mathbf{r}, -\mathbf{\Omega})$ by definition, it follows that

$$G^\dagger(\mathbf{r}_1, \mathbf{\Omega}_1 \rightarrow \mathbf{r}, \mathbf{\Omega}) = G(\mathbf{r}_1, -\mathbf{\Omega}_1 \rightarrow \mathbf{r}, -\mathbf{\Omega}).$$

When this result is introduced into the general equation (6.13), with $\mathbf{r}_0$ replaced by $\mathbf{r}_2$, and so on, i.e.,

$$G^\dagger(\mathbf{r}_1, \mathbf{\Omega}_1, E_1 \rightarrow \mathbf{r}_2, \mathbf{\Omega}_2, E_2) = G(\mathbf{r}_2, \mathbf{\Omega}_2, E_2 \rightarrow \mathbf{r}_1, \mathbf{\Omega}_1, E_1),$$

it is seen that

$$G(\mathbf{r}_1, \mathbf{\Omega}_1 \rightarrow \mathbf{r}_2, \mathbf{\Omega}_2) = G(\mathbf{r}_2, -\mathbf{\Omega}_2 \rightarrow \mathbf{r}_1, -\mathbf{\Omega}_1), \tag{6.21}$$

which is the required one-speed reciprocity relationship. This is the same as the optical reciprocity relation given in equation (2.99), except that the sign of $\mathbf{\Omega}_2$ has been reversed.

6.1h The Adjoint Integral Transport Equation

It has been shown that in the one-speed critical problem, the neutron angular flux differs from its adjoint only in the sign of the direction vector. It is evident, therefore, that the total flux, ϕ, obtained by integrating Φ over all directions $\mathbf{\Omega}$, i.e.,

$$\phi(\mathbf{r}) = \int \Phi(\mathbf{r}, \mathbf{\Omega})\, d\mathbf{\Omega}$$

must be equal to its adjoint; thus,

$$\phi(\mathbf{r}) = \phi^\dagger(\mathbf{r}).$$

This indicates that the transport operator for the one-speed integral equation for the total flux must be self-adjoint. The reason is that in the one-speed problem the kernel of the integral is symmetric in $\mathbf{r}$ and $\mathbf{r}'$; a theory of such kernels and their eigenvalues and eigenfunctions has been developed.[2]

It was seen in §§1.2c, 1.2d that only for isotropic scattering is it possible to write an integral equation for the total flux, namely equation (1.29). In the one-speed problem, the kernel of this equation is symmetric. With anisotropic scattering there is no integral equation for the total flux or density [cf. §1.2d and equation (1.31)]; nevertheless, relations such as those in equations (6.20) and (6.21) are valid in one-speed problems with anisotropic scattering.

For the general energy-dependent situation, the integral kernel is asymmetric even for isotropic scattering, and the operator, as already seen, is not self-adjoint. There is then no relation between the flux and its adjoint, except as may be given by such expressions as equation (6.12). It will be shown in §7.2c, however, that for thermal neutrons the flux and its adjoint are related in a simple manner because the transport operator for thermal neutrons can be made "almost" self-adjoint in an elementary way.

6.1i Direct Derivation of an Equation for the Neutron Importance

By using the physical interpretation of the adjoint function as a neutron importance, it is possible to derive directly from first principles an equation satisfied by the neutron importance, equivalent to the adjoint transport equation. The opportunity will be taken to make the treatment quite general by including time dependence.[3]

The first step in the derivation is to develop an operational definition of "importance." Consider a system containing a neutron detector which is characterized by the macroscopic cross section $\sigma_d(\mathbf{r}, E, t)$, such that for a neutron at $\mathbf{r}$ there is a probability $v\sigma_d(\mathbf{r}, E, t)$ per unit time of the detector being activated, i.e., of registering a count. As before, v is the speed of the neutron. By including the time dependence in σ_d, allowance can be made for the possibility that the detector is not turned on all the time; thus, σ_d would be zero if the detector were not operating. Suppose a neutron at position $\mathbf{r}$ and direction $\mathbf{\Omega}$ has energy E at time t; then its importance, $\Phi^\dagger(\mathbf{r}, \mathbf{\Omega}, E, t)$, may be defined as the expected detector activity, e.g., expected number of counts, that will be produced at all subsequent times by the neutron itself or by the secondary neutrons generated, as a result of scattering, fission, etc., by the neutron in question.

An equation satisfied by the neutron importance will now be obtained by a method similar to that used in Chapter 1 to derive the transport equation. Consider a neutron at position $\mathbf{r}$ having direction $\mathbf{\Omega}$ and energy E at time t. It will be assumed, for the moment, that the neutron is not at the detector position, so that it cannot activate the detector during a short time interval Δt. Thus, in

time Δt, the neutron will either move to the position $\mathbf{r} + \Omega v \Delta t$ or it will suffer a collision. The probability that it does not make a collision is $1 - \sigma v \Delta t$ and the probability that it will make a collision is $\sigma v \Delta t$, where σ represents $\sigma(\mathbf{r}, E)$. The number of detector counts to be expected from the neutron at time t is equal to the number of counts expected from the neutron plus its progeny at time $t + \Delta t$. In other words, the importance of the neutron at time t can be represented by

$$\begin{pmatrix}\text{Importance}\\ \text{of neutron}\\ \text{at time } t\end{pmatrix} = \begin{pmatrix}\text{Probability}\\ \text{of no}\\ \text{collision}\\ \text{in time } \Delta t\end{pmatrix}\begin{pmatrix}\text{Importance}\\ \text{of neutron}\\ \text{at time}\\ t + \Delta t\end{pmatrix} + \begin{pmatrix}\text{Probability}\\ \text{of collision}\\ \text{in time}\\ \Delta t\end{pmatrix}\begin{pmatrix}\text{Importance}\\ \text{of neutrons}\\ \text{expected}\\ \text{to emerge}\\ \text{from}\\ \text{collisions}\end{pmatrix}$$

I II III IV

that is,

$$\Phi^\dagger(\mathbf{r}, \Omega, E, t) = \underset{\text{I}}{[(1 - \sigma v \Delta t)]}\underset{\text{II}}{[\Phi^\dagger(\mathbf{r} + \Omega v \Delta t, \Omega, E, t + \Delta t)]} + \underset{\text{III}}{[\sigma v \Delta t]}\underset{\text{IV}}{\left[\iint \sigma f(\mathbf{r}; \Omega, E \to \Omega', E')\Phi^\dagger(\mathbf{r}, \Omega', E', t)\, d\Omega'\, dE'\right]}, \tag{6.22}$$

where the quantities I, II, III, IV in the square brackets represent those indicated correspondingly above. Equation (6.22) is a mathematical statement of the conservation of neutron importance. If the neutron is in the detector at the time t, there will be an additional probability $v\sigma_d \Delta t$ that the detector will be activated during the interval Δt, and this quantity must be included in the neutron importance at time t. Hence, for completeness, the quantity $v\sigma_d \Delta t$ must be added to the right side of equation (6.22).

Equation (6.22) is now divided by $v\Delta t$, and the limit is taken as $\Delta t \to 0$. By using the relationship

$$\lim_{\Delta t \to 0}\left[\frac{\Phi^\dagger(\mathbf{r} + \Omega v \Delta t, \Omega, E, t + \Delta t) - \Phi^\dagger(\mathbf{r}, \Omega, E, t)}{v\Delta t}\right] = \Omega \cdot \nabla\Phi^\dagger + \frac{\partial \Phi^\dagger}{v\partial t},$$

analogous to the one derived in §1.1c, and defining

$$Q^\dagger(\mathbf{r}, E, t) \equiv \sigma_d(\mathbf{r}, E, t),$$

it is thus found that

$$-\frac{1}{v}\frac{\partial \Phi^\dagger}{\partial t} - \Omega \cdot \nabla\Phi^\dagger + \sigma\Phi^\dagger = \iint \sigma f(\mathbf{r}; \Omega, E \to \Omega', E')\Phi^\dagger(\mathbf{r}, \Omega', E', t)\, d\Omega'\, dE' + Q^\dagger(\mathbf{r}, E, t). \tag{6.23}$$

This is the fundamental (adjoint) equation to be satisfied by any time-dependent importance function. In the time-independent case, the first term on the left side of equation (6.23), and the time variable, t, may be removed. The result is then seen to be identical with equation (6.10), with $Q^\dagger(\mathbf{r}, E)$ in place of $\sigma_d(\mathbf{r}, E)$.

The boundary condition in equation (6.23) is obtained by noting that a neutron which is just about to leave a free surface must have zero importance, since by definition of a free surface it cannot return. Consequently, the appropriate free-surface boundary condition is

$$\Phi^\dagger(\mathbf{r}, \boldsymbol{\Omega}, E, t) = 0 \quad \text{for} \quad \hat{\mathbf{n}}\cdot\boldsymbol{\Omega} > 0$$

and all $\mathbf{r}$ on the boundary.

It is of interest to compare equation (6.23) with the time-dependent neutron transport equation. As seen in Chapter 1, the latter may be regarded as defining an initial value problem; given $\Phi(\mathbf{r}, \boldsymbol{\Omega}, E, 0)$, the transport equation can be used, in principle, to determine Φ at all subsequent times. The situation is quite different for equation (6.23), which, by contrast, may be regarded as defining a final value problem. That is to say, if $\Phi^\dagger$ is given at some final time, $t = t_f$, the values of $\Phi^\dagger$ may be found at earlier times by integrating equation (6.23) backward in time. Mathematically, the reason for the difference is that the time derivative in equation (6.23) is opposite in sign to that in the transport equation (1.14).

In physical terms, this means that the activity of a detector (or adjoint source) at some particular time affects the importance for activating the detector of neutrons at all earlier times, but it can have no effect on the importance of neutrons at later times. For the flux, however, the situation is just the opposite; the source at any given time will have no effect on the flux at earlier times but it affects the flux at later times.

6.1j Spectrum of the Adjoint Operator and Criticality

The adjoint transport equation (6.23) may be written in the form

$$-\frac{1}{v}\frac{\partial \Phi^\dagger}{\partial t} = \mathbf{L}^\dagger\Phi^\dagger + Q^\dagger. \tag{6.24}$$

where $\mathbf{L}^\dagger$ is the time-independent adjoint operator given in equation (6.7). As in the case of the neutron transport equation treated in §1.5a, solutions may be sought for the homogeneous equation

$$-\frac{1}{v}\frac{\partial \Phi^\dagger}{\partial t} = \mathbf{L}^\dagger\Phi^\dagger. \tag{6.25}$$

In particular, solutions for which

$$\frac{\partial \Phi_i^\dagger}{\partial t} = -\alpha_i^\dagger \Phi_i^\dagger \tag{6.26}$$

or

$$\frac{\alpha_i^\dagger}{v} \Phi_i^\dagger = \mathbf{L}^\dagger \Phi_i^\dagger \tag{6.27}$$

are of interest. It is then found[4] that the spectrum of the adjoint operator $v\mathbf{L}^\dagger$, i.e., the values of $\alpha_i^\dagger$ for which equation (6.27) has a solution, will be similar to that for the neutron transport equation considered in §1.5b. There will then be a real value of $\alpha_i^\dagger$, designated $\alpha_0^\dagger$, which is larger, i.e., more positive, than the real part of any other value of $\alpha_i^\dagger$, and the associated eigenfunction $\Phi_0^\dagger$ will be assumed to be everywhere nonnegative. As in Chapter 1, the criticality of the system can then be based on the sign of $\alpha_0^\dagger$; for $\alpha_0^\dagger > 0$, the system is supercritical, for $\alpha_0^\dagger = 0$ it is critical, and for $\alpha_0^\dagger < 0$ it is subcritical.

It should be noted, however, in view of equation (6.26), that in the supercritical system, when $\alpha_0^\dagger$ is positive, the importance, $\Phi^\dagger$, decreases with time. This is in accord with the physical interpretation of the importance function. A neutron at an early time in a supercritical system will be relatively more important than one at a later time because the early neutron will have additional time to multiply and will thus lead to greater detector activity.

Relationships between α_0 and $\alpha_0^\dagger$ and the corresponding flux and its adjoint, respectively, can be derived in the following manner. Consider the equation satisfied by the angular flux eigenfunction, Φ_j, that is,

$$\frac{\alpha_j}{v} \Phi_j = \mathbf{L}\Phi_j, \tag{6.28}$$

and the adjoint eigenvalue $\alpha_i^\dagger$ and the corresponding eigenfunction $\Phi_i^\dagger$ which are related by equation (6.27). The quantities Φ_j and $\Phi_i^\dagger$ are assumed to satisfy the usual continuity and free-surface conditions. Equation (6.27) is now multiplied by Φ_j and equation (6.28) by $\Phi_i^\dagger$, and the results are integrated over the complete range of the variables $\mathbf{r}$, Ω, E. Upon subtraction, it is found that

$$(\alpha_j - \alpha_i^\dagger)\left(\frac{1}{v} \Phi_i^\dagger, \Phi_j\right) = (\Phi_i^\dagger, \mathbf{L}\Phi_j) - (\Phi_j, \mathbf{L}^\dagger \Phi_i^\dagger).$$

By definition of the adjoint operator, $\mathbf{L}^\dagger$, the two inner products on the right side are equal; hence,

$$(\alpha_j - \alpha_i^\dagger)\left(\frac{1}{v} \Phi_i^\dagger, \Phi_j\right) = 0. \tag{6.29}$$

If $i = j = 0$, so that the fundamental eigenvalues are being considered, then

both $\Phi_0^\dagger$ and Φ_0 will be nonnegative, and the inner product in equation (6.29) will be positive. It follows, therefore, that

$$\alpha_0 = \alpha_0^\dagger.$$

On the other hand, if $\alpha_j \neq \alpha_i^\dagger$, then according to equation (6.29)

$$\left(\frac{1}{v}\,\Phi_i^\dagger, \Phi_j\right) = 0$$

or, in other words, $\Phi_i^\dagger$ and Φ_j are orthogonal, with a weight factor of $1/v$. Use will be made of this orthogonality relationship in due course.

6.1k Interpretations of the Time-Dependent Adjoint Function

In Chapter 1, the various kinds of solutions to be expected for the flux in subcritical, critical, and supercritical systems were discussed at some length. Analogous conclusions are applicable to the adjoint function.[5] Thus, for any system there will be a solution of the time-dependent final value adjoint problem. If it is assumed that the detector is shut off permanently at the final time $t = t_f$, so that $\Phi^\dagger(\mathbf{r}, \mathbf{\Omega}, E, t_f) = 0$, then the physical interpretation of the solution as an importance for detector activation is the same as in §6.1i. If, on the other hand, $\Phi^\dagger$ is finite at $t = t_f$, the solution can still be chosen so as to have physical significance. It will now be shown, as an example, that if $\Phi^\dagger(\mathbf{r}, \mathbf{\Omega}, E, t_f)$ is chosen to be unity for all values of $\mathbf{r}$, $\mathbf{\Omega}$, E in the system, then the solution to the source-free adjoint equation, i.e., equation (6.23) with $Q^\dagger = 0$, at earlier times may be interpreted as the expected number of neutrons in the system at $t = t_f$ arising from a neutron at $\mathbf{r}$, $\mathbf{\Omega}$, E, t.

To prove that this is the case, consider the time-dependent transport equation without an independent source, i.e.,

$$\frac{1}{v}\frac{\partial \Phi}{\partial t} = \mathbf{L}\Phi, \tag{6.30}$$

and the corresponding adjoint equation

$$-\frac{1}{v}\frac{\partial \Phi^\dagger}{\partial t} = \mathbf{L}^\dagger\Phi^\dagger. \tag{6.31}$$

Suppose a solution is being sought to equation (6.30) for the initial condition, at $t = 0$, of one neutron present at $\mathbf{r}_0$, $\mathbf{\Omega}_0$, E_0; this condition may be represented by

$$\Phi(\mathbf{r}_0, \mathbf{\Omega}_0, E_0, 0) = v_0\,\delta(\mathbf{r} - \mathbf{r}_0)\,\delta(\mathbf{\Omega} - \mathbf{\Omega}_0)\,\delta(E - E_0). \tag{6.32}$$

The solution for equation (6.31) is being sought for the postulated final condition at $t = t_f$, namely,

$$\Phi^\dagger(\mathbf{r}, \mathbf{\Omega}, E, t_f) = 1. \tag{6.33}$$

Equation (6.30) is now multiplied by $\Phi^\dagger$ and equation (6.31) by Φ; integration is carried over the whole range of the variables $\mathbf{r}$, $\mathbf{\Omega}$, E and the results are subtracted. It is then found that

$$\left(\frac{1}{v}\Phi^\dagger, \frac{\partial\Phi}{\partial t}\right) + \left(\frac{1}{v}\Phi, \frac{\partial\Phi^\dagger}{\partial t}\right) = \frac{\partial}{\partial t}\left(\frac{1}{v}\Phi^\dagger, \Phi\right) = (\Phi^\dagger, \mathbf{L}\Phi) - (\Phi, \mathbf{L}^\dagger\Phi^\dagger) = 0, \quad (6.34)$$

since the difference of the inner products on the right is zero, by the definition of $\mathbf{L}^\dagger$. Upon integration of the second expression over t from $t = 0$ to $t = t_f$, the result is

$$\left(\frac{1}{v}\Phi^\dagger, \Phi\right)_{t=0} = \left(\frac{1}{v}\Phi^\dagger, \Phi\right)_{t=t_f}. \quad (6.35)$$

Because of the initial condition on Φ, given by equation (6.32), the left side of equation (6.35) is simply $\Phi^\dagger(\mathbf{r}_0, \mathbf{\Omega}_0, E_0, 0)$; furthermore, by the final condition on $\Phi^\dagger$, given by equation (6.33), the right side of equation (6.35) is the integral of Φ/v $(= N)$ over all $\mathbf{r}$, $\mathbf{\Omega}$, E; hence,

$$\Phi^\dagger(\mathbf{r}_0, \mathbf{\Omega}_0, E_0, 0) = \iiint N(\mathbf{r}, \mathbf{\Omega}, E, t_f)\, dV\, d\mathbf{\Omega}\, dE.$$

The quantity on the right is the expected number of neutrons at the time t_f; hence the interpretation of $\Phi^\dagger$ given above has been established.

If $\Phi^\dagger$ were chosen to be unity at t_f in some subregion of $\mathbf{r}$, $\mathbf{\Omega}$, E, the solution $\Phi^\dagger$ at earlier times would correspond to the expected neutron population in the subregion. By taking the subregion to be very small, a relation between the time-dependent flux and adjoint Green's functions, analogous to equation (6.13), i.e.,

$$G^\dagger(\mathbf{r}_1, \mathbf{\Omega}_1, E_1, t_1 \rightarrow \mathbf{r}_0, \mathbf{\Omega}_0, E_0, t_0) \underset{t_1 > t_0}{=} G(\mathbf{r}_0, \mathbf{\Omega}_0, E_0, t_0 \rightarrow \mathbf{r}_1, \mathbf{\Omega}_1, E_1, t_1) \quad (6.36)$$

can be derived.

Conclusions similar to those reached above are applicable to the time-independent situations, i.e., with $\partial\Phi^\dagger/\partial t = 0$, such as exist for a subcritical system with a constant source or an exactly critical system with no independent source. In the former case, the adjoint function is a neutron importance, as derived in §6.1d. For the exactly critical system, $\alpha_0^\dagger = 0$, and the corresponding fundamental eigenvalue, $\Phi_0^\dagger(\mathbf{r}, \mathbf{\Omega}, E)$, may be interpreted as the importance of a neutron at $\mathbf{r}$, $\mathbf{\Omega}$, E for establishing the fundamental flux mode. This follows from equation (6.35) provided t_f is large and certain consequences of exact criticality are assumed, as will now be demonstrated.

It is known, from Chapter 1, that in an exactly critical source-free system the flux at late times will be independent of time and proportional to the fundamental flux mode $\Phi_0(\mathbf{r}, \mathbf{\Omega}, E)$, where the amplitude, A, is a function of the initial neutron parameters, $\mathbf{r}_0$, $\mathbf{\Omega}_0$, E_0. Thus, if t_f is large, it is possible to write

$$\Phi(\mathbf{r}, \mathbf{\Omega}, E, t_f) = A(\mathbf{r}_0, \mathbf{\Omega}_0, E_0)\Phi_0(\mathbf{r}, \mathbf{\Omega}, E) \quad \text{for } t_f \text{ large.} \quad (6.37)$$

The mode Φ_0 may be normalized arbitrarily, and a convenient choice is to set

$$\iiint \frac{1}{v} \Phi_0(\mathbf{r}, \mathbf{\Omega}, E)\, dV\, d\mathbf{\Omega}\, dE = 1.$$

Similarly, the solution to the adjoint problem at times much earlier than t_f will approach a constant, C, multiplied by the normalized fundamental adjoint mode, that is,

$$\Phi^\dagger(\mathbf{r}, \mathbf{\Omega}, E, 0) = C\Phi_0^\dagger(\mathbf{r}, \mathbf{\Omega}, E). \tag{6.38}$$

By substituting equations (6.37) and (6.38) into equation (6.35), it is found that

$$\Phi_0^\dagger(\mathbf{r}_0, \mathbf{\Omega}_0, E_0) = \frac{1}{C} A(\mathbf{r}_0, \mathbf{\Omega}_0, E_0). \tag{6.39}$$

This means that the time-independent adjoint function $\Phi_0^\dagger(\mathbf{r}_0, \mathbf{\Omega}_0, E_0)$ for a critical system is proportional to the amplitude of the fundamental (or persisting) mode established by a neutron at $\mathbf{r}_0, \mathbf{\Omega}_0, E_0$.

6.1m Expansion of Time-Dependent Solutions

It is known that, for certain discrete values of the α_j, solutions are possible for the equation

$$\frac{\alpha_j}{v} \Phi_j = \mathbf{L}\Phi_j \quad \text{with} \quad j = 0, 1, 2, \ldots \tag{6.40}$$

In general, as seen in Chapter 1, there is no reason to believe that the set of eigenfunctions $\{\Phi_j\}$ is complete in the sense that a solution to the initial value problem could be expanded in these eigenfunctions. For some simple approximations to transport theory, however, e.g., multigroup diffusion theory in one dimension with continuous space variable (§4.4c),[6] and for systems of difference equations (§4.4f), the eigenfunctions are complete and an expansion may be utilized for time-dependent solutions. Since such expansions are employed in kinetic studies, they will be outlined here. Although the general transport operator notation will be used, it must be understood that the procedure is valid only for special cases such as those just indicated.

Consider the homogeneous initial value problem in which the solution is sought of

$$\frac{1}{v} \frac{\partial \Phi}{\partial t} = \mathbf{L}\Phi, \tag{6.41}$$

where $\Phi(\mathbf{r}, \mathbf{\Omega}, E, 0)$ is known. The fundamental assumption is now made that at any time, t, the solution may be expanded in terms of the flux eigenfunctions corresponding to the α_j eigenvalues; thus,

$$\Phi(\mathbf{r}, \mathbf{\Omega}, E, t) = \sum_{j=0}^{\infty} a_j(t)\Phi_j(\mathbf{r}, \mathbf{\Omega}, E). \tag{6.42}$$

If this is substituted into equation (6.41), it is found that

$$\frac{1}{v}\sum_j \frac{da_j}{dt}\,\Phi_j = \sum_j a_j \mathbf{L}\Phi_j = \sum_j a_j \frac{\alpha_j}{v}\,\Phi_j, \tag{6.43}$$

using the definition of Φ_j in equation (6.40).

Equation (6.43) is now multiplied by $\Phi_i^\dagger$ and integrated over all variables. By introducing the orthogonality relationship derived from equation (6.29), i.e.,

$$\left(\frac{1}{v}\,\Phi_i^\dagger, \Phi_j\right) = 0 \quad \text{for} \quad i \neq j,$$

it is found that

$$\frac{da_i}{dt} = \alpha_i a_i$$

or

$$a_i(t) = a_i(0)e^{\alpha_i t}. \tag{6.44}$$

The initial value, $a_i(0)$, is found by multiplying equation (6.42) at $t = 0$ by $(1/v)\Phi_i^\dagger$ and integrating; the result is

$$a_i(0) = \frac{((1/v)\Phi_i^\dagger, \Phi(t=0))}{((1/v)\Phi_i^\dagger, \Phi_i)}.$$

The solution to equation (6.42) is consequently

$$\Phi(\mathbf{r}, \Omega, E, t) = \sum_{j=0}^{\infty} \frac{((1/v)\Phi_j^\dagger, \Phi(t=0))}{((1/v)\Phi_j^\dagger, \Phi_j)}\, e^{\alpha_j t}\Phi_j(\mathbf{r}, \Omega, E). \tag{6.45}$$

In this expression, it is seen that $\Phi_j^\dagger$ is a measure of the importance of a neutron in establishing the flux mode Φ_j. It was shown earlier, without using an expansion such as equation (6.42), that this is true for the particular case of $j = 0$.

The expansion in equation (6.45) will be most useful in practice if only a few terms suffice to give a good representation of the solution. Further reference to the subject will be made in Chapter 10. Expansions of this type can be used to solve the inhomogeneous time-dependent neutron transport equation

$$\frac{1}{v}\frac{\partial \Phi}{\partial t} = \mathbf{L}\Phi + Q.$$

The procedure is the same as that described above except that the differential equation for $a_i(t)$ contains $(\Phi_i^\dagger, Q)$; however, it can be readily integrated even if Q is a function of time.

6.2 THE ADJOINT OPERATORS IN APPROXIMATE METHODS

6.2a Introduction

In Chapters 3, 4, and 5, various methods were described for obtaining approximate numerical solutions to the time-independent transport equation. In this

section, consideration will be given to some of the equations which are adjoint to those arising in the approximate methods, particularly in P_1 and diffusion theories.[7] As in the preceding chapters, the one-speed problem will be examined first and then the results will be extended to multigroup situations.

6.2b One-Speed P_1, Diffusion, and S_N Theories

In one-speed P_1 theory, the angular flux is assumed to be given by equation (3.44), i.e.,

$$\Phi(\mathbf{r}, \Omega) = \frac{1}{4\pi}[\phi(\mathbf{r}) + 3\Omega \cdot \mathbf{J}(\mathbf{r})]. \tag{6.46}$$

If a similar form is assumed for the adjoint, namely,

$$\Phi^\dagger(\mathbf{r}, \Omega) = \frac{1}{4\pi}[\phi^\dagger(\mathbf{r}) + 3\Omega \cdot \mathbf{J}^\dagger(\mathbf{r})], \tag{6.47}$$

it is seen that the inner product, with integration over all Ω and $\mathbf{r}$ (volume), gives

$$\iint \Phi^\dagger \Phi \, d\Omega \, dV = \frac{1}{4\pi}\int [\phi^\dagger(\mathbf{r})\phi(\mathbf{r}) + 3\mathbf{J}^\dagger(\mathbf{r}) \cdot \mathbf{J}(\mathbf{r})] \, dV, \tag{6.48}$$

where the identities in Table 3.1 have been used to evaluate the integrals over Ω.

In §3.3e, when the neutron angular flux given by equation (6.46) was inserted into the one-speed, time-independent transport equation, $\mathbf{L}\Phi = -Q$, equation (3.49) was obtained. From this the two P_1 equations (3.50) and (3.51) were derived; they are, omitting the argument $(\mathbf{r})$,

$$\nabla \cdot \mathbf{J} + \sigma_0 \phi = Q_0 \tag{6.49}$$

$$\nabla \phi + 3\sigma_1 \mathbf{J} = 3\mathbf{Q}_1. \tag{6.50}$$

The inner product of $\Phi^\dagger$ and $\mathbf{L}\Phi$ could be obtained by multiplying equation (3.49) by $\Phi^\dagger$, as given by equation (6.47), and integrating over all Ω and $\mathbf{r}$. It is then found that the result is the same as if the inner product were formed by multiplying equation (6.49) by $\phi^\dagger$ and equation (6.50) by $\mathbf{J}^\dagger$, adding and integrating over volume. With the inner product formed in this way, it can be seen that, in the one-speed P_1 approximation, the adjoint equations corresponding to $\mathbf{L}\Phi^\dagger = -Q^\dagger$, are

$$-\nabla \cdot \mathbf{J}^\dagger + \sigma_0 \phi^\dagger = Q_0^\dagger \tag{6.51}$$

$$-\nabla \phi^\dagger + 3\sigma_1 \mathbf{J}^\dagger = 3\mathbf{Q}_1^\dagger. \tag{6.52}$$

Moreover, if the flux satisfies the boundary conditions $\hat{\mathbf{n}} \cdot \mathbf{J} = a\phi$ (cf. §3.1e, where $a = \frac{1}{2}$), the adjoint must satisfy $\hat{\mathbf{n}} \cdot \mathbf{J}^\dagger = -a\phi^\dagger$.

To verify that equations (6.51) and (6.52) are adjoint to equations (6.49) and (6.50), respectively, multiply equation (6.49) by $\phi^\dagger$ and equation (6.50) by $\mathbf{J}^\dagger$.

and subtract equation (6.51) multiplied by ϕ and equation (6.52) multiplied by $\mathbf{J}\cdot$. The left sides become

$$I = \int [\phi^\dagger \nabla\cdot\mathbf{J} + \mathbf{J}^\dagger\cdot\nabla\phi + \phi\nabla\cdot\mathbf{J}^\dagger + \mathbf{J}\cdot\nabla\phi^\dagger]\, dV$$

$$= \int \nabla\cdot[(\phi^\dagger\mathbf{J}) + (\phi\mathbf{J}^\dagger)]\, dV$$

$$= \int [(\hat{\mathbf{n}}\cdot\mathbf{J})\phi^\dagger + (\hat{\mathbf{n}}\cdot\mathbf{J}^\dagger)\phi] dA,$$

and upon using the boundary conditions, this gives

$$I = \int (a\phi\phi^\dagger - a\phi^\dagger\phi)\, dA = 0.$$

The one-speed diffusion equation (3.52), i.e.,

$$-\nabla\cdot D\nabla\phi + \sigma_0\phi = Q_0, \tag{6.53}$$

is self-adjoint. This means that the adjoint flux, $\phi^\dagger$, satisfies an equation of the same form, namely,

$$-\nabla\cdot D\nabla\phi^\dagger + \sigma_0\phi^\dagger = Q_0^\dagger.$$

The boundary conditions are also the same for both flux and adjoint; for example, if

$$\hat{\mathbf{n}}\cdot\nabla\phi + b\phi = 0,$$

then so also

$$\hat{\mathbf{n}}\cdot\nabla\phi^\dagger + b\phi^\dagger = 0.$$

In this case, an inner product would be formed by multiplying equation (6.53) by $\phi^\dagger$ and integrating over volume.

In the one-speed discrete ordinates methods, the adjoint equations are obtained by reversing all neutron directions. For example, in the equations (5.3) for plane geometry, $\mu_j \partial\Phi/\partial x$ would be changed to $-\mu_j \partial\Phi^\dagger/\partial x$.

In the foregoing discussion the operators which are adjoint to certain differential operators were considered. When the differential equations are reduced to difference equations, care must be taken to ensure that the "adjoint difference equations" are really adjoint to the difference equations for the flux. For example, in two-dimensional diffusion theory (§3.4b), the flux was represented by a vector $\boldsymbol{\phi}$ with as many components as mesh points and the difference equations were written as

$$\mathbf{A}\boldsymbol{\phi} = \mathbf{s},$$

with $\mathbf{A}$ a matrix. The operator adjoint to $\mathbf{A}$ is the transposed matrix, denoted here by $\mathbf{A}^\dagger$, formed by interchanging rows and columns, i.e., $[\mathbf{A}^\dagger]_{ij} = [\mathbf{A}]_{ji}$.* For

* There is, unfortunately, an entirely different matrix which is usually called the matrix adjoint to A.*

the special case of diffusion theory, it was seen that $\mathbf{A}$ was symmetric; hence, $\mathbf{A}^\dagger = \mathbf{A}$ and the difference equations are self-adjoint.

For more complicated approximations to the angular flux, the analysis of the difference equations is more difficult. It has been found, for example, that the "adjoint difference equations" used in certain S_N codes are not quite adjoint to the difference equations for the neutron flux in curved geometry.[9]

6.2c Multigroup P_1 and Diffusion Theories

The time-independent multigroup P_1 equations for a source Q in a subcritical system were given by equations (4.30) and (4.31) as

$$\nabla \cdot \mathbf{J}_g + \sigma_{0,g}\phi_g = \sum_{g'} \sigma_{0,g'\to g}\phi_{g'} + Q_{0,g} \tag{6.54}$$

$$\nabla \phi_g + 3\sigma_{1,g}\mathbf{J}_g = 3\sum_{g'} \sigma_{1,g'\to g}\mathbf{J}_{g'} + 3\mathbf{Q}_{1,g}, \tag{6.55}$$

$$g = 1, 2, \ldots, G$$

where the summation over g' is from $g' = 1$ to $g' = G$. The corresponding adjoint equations for a source $Q^\dagger$ are

$$-\nabla \cdot \mathbf{J}_g^\dagger + \sigma_{0,g}\phi_g^\dagger = \sum_{g'} \sigma_{0,g\to g'}\phi_{g'}^\dagger + Q_{0,g}^\dagger \tag{6.56}$$

$$-\nabla \phi_g^\dagger + 3\sigma_{1,g}\mathbf{J}_g^\dagger = 3\sum_{g'} \sigma_{1,g\to g'}\mathbf{J}_{g'}^\dagger + 3\mathbf{Q}_{1,g}^\dagger, \tag{6.57}$$

$$g = 1, 2, \ldots, G.$$

The latter differ from the flux equations (6.54) and (6.55) in two respects: first, the signs of the derivative terms are reversed, as in one-speed theory, and second, g and g' are interchanged in the transfer cross sections, in accord with the general feature of the scattering kernel noted in §6.1c. If the boundary condition for the flux is $\hat{\mathbf{n}} \cdot \mathbf{J}_g = a_g\phi_g$, then for the adjoint the boundary condition is $\hat{\mathbf{n}} \cdot \mathbf{J}_g^\dagger = -a_g\phi_g^\dagger$. An inner product is formed, for example, by multiplying equation (6.54) by $\phi_g^\dagger$, equation (6.55) by $\mathbf{J}_g^\dagger$, and adding; the result is summed over g and integrated over volume.

It should be pointed out that the adjoint equations (6.56) and (6.57) could not have been derived by integrating an energy-dependent adjoint equation over an energy interval corresponding to the group g. In particular, the required cross sections, which are flux-weighted averages, would not be obtained. This problem is examined in §6.4h, where it will be seen how multigroup flux and adjoint equations can be derived from the energy-dependent P_1 equation; the group cross sections are then weighted by both flux and adjoint.

In multigroup diffusion theory, the time-independent equation is

$$-\nabla \cdot D_g \nabla \phi_g + \sigma_{0,g}\phi_g = \sum_{g'} \sigma_{0,g' \to g}\phi_{g'} + Q_{0,g} \tag{6.58}$$

and the corresponding adjoint equation will then be

$$-\nabla \cdot D_g \nabla \phi_g^\dagger + \sigma_{0,g}\phi_g^\dagger = \sum_{g'} \sigma_{0,g \to g'}\phi_{g'}^\dagger + Q_{0,g}^\dagger, \tag{6.59}$$

which differs from equation (6.58) in the respect that g and g' have been interchanged in the group transfer cross sections. Thus, if these cross sections are regarded as elements of a $G \times G$ matrix, then in the adjoint multigroup equations the matrix of transfer cross sections is transposed from that for the flux equations. This is a general feature of multigroup equations and not only those of diffusion theory; it arises from the general form of the adjoint transfer operator.

6.3 PERTURBATION THEORY

6.3a Applications of Perturbation Theory

Suppose a multiplying system is near critical and a small change (or perturbation) is made in the system; it is then required to determine how the system responds to this perturbation, e.g., the change may be sought in α, the multiplication rate eigenvalue, or in k, the effective multiplication factor. If the perturbation is small enough, it is not necessary to perform a complete, new calculation for the perturbed system or for each perturbation of interest. Instead, by means of perturbation theory, the adjoint function can be used to obtain the response to the small perturbation. Some of the more important applications of perturbation theory are indicated below.

In experiments with critical assemblies, it is a common practice to introduce a small amount of a material of interest and to observe the accompanying change in the criticality (or reactivity). The worth or effectiveness of the given material determined in this manner is often interpreted in terms of effective absorption or transport cross sections. From the measured effectiveness, deductions can be made concerning the cross sections, or if the cross sections are known the experimental results can provide information concerning the neutron flux and importance. An example of the use of the reactivity effectiveness to evaluate cross-section data is given in §6.3f.

Moreover, in the performance of criticality calculations, it is useful to know how sensitive the computed eigenvalues are to uncertainties in the input cross sections. This sensitivity can be determined by considering the cross section uncertainties as perturbations. From such studies, the cross sections can be

adjusted, within experimental uncertainty, so as to obtain better agreement with a variety of clean critical experiments.

Small changes in reactor geometry, e.g., thermal expansion, in composition, e.g., as a result of burnup, and in neutron spectrum, e.g., due to the Doppler effect, occur during reactor operation. The effect of these changes on the reactivity of the system can be found by means of perturbation theory.

Finally, in reactor calculations the actual geometry or cross sections may be simplified in order to obtain a problem which can be solved by means of a particular code. The effects of such simplifications on criticality can often be estimated by perturbation theory.

6.3b Perturbation of the Multiplication Rate Constant, α

As a first example of the application of perturbation theory, the change in α resulting from a change in cross sections will be determined. In the present treatment, delayed neutrons will be neglected, although they should be included in deriving the effect of a small perturbation on the multiplication rate constant. The procedures used, however, are much the same as those described here, as will be seen when the problem with delayed neutrons is considered in §9.2b.

In a multiplying system with no extraneous source, the transport equation, obtained by substituting $\alpha\Phi$ for $\partial\Phi/\partial t$, can be written as

$$\frac{\alpha}{v}\Phi + \Omega\cdot\nabla\Phi + \sigma\Phi = \int \sigma f(\mathbf{r};\Omega',E'\to\Omega,E)\Phi(\mathbf{r},\Omega',E')\,d\Omega'\,dE' \quad (6.60)$$

and the corresponding adjoint function for the unperturbed system satisfies the relationship

$$\frac{\alpha^\dagger}{v}\Phi^\dagger - \Omega\cdot\nabla\Phi^\dagger + \sigma\Phi^\dagger = \int \sigma f(\mathbf{r};\Omega,E\to\Omega',E')\Phi^\dagger(\mathbf{r},\Omega',E')\,d\Omega'\,dE', \quad (6.61)$$

both with the usual free-surface boundary conditions. The fundamental modes of these equations are being treated here: hence α and $\alpha^\dagger$ are the quantities formerly denoted by α_0 and $\alpha_0^\dagger$. Consider now a perturbed system with a new macroscopic cross section σ^*, so that

$$\sigma^* = \sigma + \Delta\sigma \quad \text{and} \quad \sigma^* f^* = \sigma f + \Delta(\sigma f).$$

Such a perturbation could arise from changes in density or in the microscopic cross sections, or from the movement of an interface. For the perturbed cross section, the equation for the perturbed eigenvalue, α^*, is

$$\frac{\alpha^*}{v}\Phi^* + \Omega\cdot\nabla\Phi^* + \sigma^*\Phi^*$$

$$= \int \sigma^* f^*(\mathbf{r};\Omega',E'\to\Omega,E)\Phi^*(\mathbf{r},\Omega',E')\,d\Omega'\,dE', \quad (6.62)$$

where Φ^* is the perturbed flux.

Equation (6.62) is multiplied by $\Phi^\dagger$ and equation (6.61) by Φ^*; the latter is subtracted from the former and the result is integrated over all $\mathbf{r}$, $\mathbf{\Omega}$, E to give

$$(\alpha^* - \alpha^\dagger) \iiint \frac{1}{v} \Phi^* \Phi^\dagger \, dV \, d\mathbf{\Omega} \, dE$$

$$= - \iiint (\Delta\sigma) \Phi^* \Phi^\dagger \, dV \, d\mathbf{\Omega} \, dE + \int \cdots \int \Delta[\sigma f(\mathbf{r}; \mathbf{\Omega}', E' \to \mathbf{\Omega}, E)]$$

$$\times \Phi^*(\mathbf{r}, \mathbf{\Omega}', E') \Phi^\dagger(\mathbf{r}, \mathbf{\Omega}, E) \, dV \, d\mathbf{\Omega}' \, dE' \, d\mathbf{\Omega} \, dE. \quad (6.63)$$

It will be noted that this equation is exact and holds for any $\Delta\sigma$ and $\Delta(\sigma f)$, large or small.

For small perturbations, it is assumed that

$$\Phi^* = \Phi + \Delta\Phi,$$

where Φ is the solution to equation (6.60). This expression for Φ^* may be substituted into equation (6.63) and all terms containing $\Delta\Phi$ may be ignored since they are always multiplied by another Δ term, and hence are of second order in small quantities. Furthermore, $\alpha^* - \alpha^\dagger$ may be replaced by $\Delta\alpha$, since $\alpha = \alpha^\dagger$ for the fundamental eigenvalues. The result is

$$\Delta\alpha \iiint \frac{1}{v} \Phi^\dagger \Phi \, dV \, d\mathbf{\Omega} \, dE$$

$$\simeq - \iiint (\Delta\sigma) \Phi^\dagger \Phi \, dV \, d\mathbf{\Omega} \, dE + \int \cdots \int \Delta[\sigma f(\mathbf{r}; \mathbf{\Omega}', E' \to \mathbf{\Omega}, E)]$$

$$\times \Phi(\mathbf{r}, \mathbf{\Omega}', E') \Phi^\dagger(\mathbf{r}, \mathbf{\Omega}, E) \, dV \, d\mathbf{\Omega}' \, dE' \, d\mathbf{\Omega} \, dE, \quad (6.64)$$

where $\Delta\alpha$ is the change in α due to the perturbations $\Delta\sigma$ in σ and $\Delta(\sigma f)$ in σf. This equation for $\Delta\alpha$ involves only the unperturbed flux and its adjoint, together with the changes in the cross sections. These changes are weighted by both the neutron flux and its adjoint (or importance) to determine the effect on the multiplication rate constant.

An insight into the sensitivity of α to changes in σ can be obtained by considering the one-speed case. According to equation (6.20),

$$\Phi^\dagger(\mathbf{r}, \mathbf{\Omega}) = \Phi(\mathbf{r}, -\mathbf{\Omega})$$

for a critical system, but it can be shown, by the method of §6.1f, that this is also true for the fundamental α (or k) mode in a subcritical or supercritical system. Equation (6.64) then takes the form

$$\frac{\Delta\alpha}{v} \iint \Phi(\mathbf{r}, -\mathbf{\Omega}) \Phi(\mathbf{r}, \mathbf{\Omega}) \, dV \, d\mathbf{\Omega}$$

$$= - \iint (\Delta\sigma) \Phi(\mathbf{r}, -\mathbf{\Omega}) \Phi(\mathbf{r}, \mathbf{\Omega}) \, dV \, d\mathbf{\Omega} + \iiint \Delta[\sigma f(\mathbf{r}; \mathbf{\Omega}' \to \mathbf{\Omega})]$$

$$\times \Phi(\mathbf{r}, \mathbf{\Omega}') \Phi(\mathbf{r}, -\mathbf{\Omega}) \, dV \, d\mathbf{\Omega}' \, d\mathbf{\Omega}. \quad (6.65)$$

Some physical aspects of this equation can be understood by considering a bare sphere.

Suppose, in the first place, there is a change $\Delta\sigma = \Delta\sigma_a$ in the absorption cross section, but no change in the scattering (including fission) cross section, so that $\Delta(\sigma f) = 0$. For such a perturbation, in one-speed theory, equation (6.65) reduces to

$$\Delta\alpha = \text{Constant}\left[-\iint \Delta\sigma_a(\mathbf{r})\Phi(\mathbf{r}, -\mathbf{\Omega})\Phi(\mathbf{r}, \mathbf{\Omega})\, dV\, d\mathbf{\Omega}\right]. \tag{6.66}$$

As seen in §3.3b, at the center of the sphere Φ will be isotropic and usually a maximum; hence a positive $\Delta\sigma_a$ at $\mathbf{r} = 0$ will give a relatively large and negative $\Delta\alpha$. That is to say, an increase in the absorption cross section at the center of a spherical multiplying medium will cause a relatively large decrease in the multiplication rate constant, α. At a free surface, e.g., on the boundary of the sphere, however, $\Phi(\mathbf{r}, \mathbf{\Omega}) = 0$ if $\hat{\mathbf{n}}\cdot\mathbf{\Omega} < 0$, and the product $\Phi(\mathbf{r}, -\mathbf{\Omega})\Phi(\mathbf{r}, \mathbf{\Omega})$ is zero for all values of $\mathbf{\Omega}$. Thus, the value of α is unaffected by a small change in the absorption cross section at the surface of the sphere. These conclusions are in agreement with expectation on physical grounds.

Consider, next, a perturbation of the scattering cross section, with the absorption cross section remaining unchanged. Suppose a small isotropic increment is added to the scattering, so that $\Delta\sigma = \Delta\sigma_s(\mathbf{r})$ and $\Delta(\sigma f) = \Delta\sigma_s(\mathbf{r})/4\pi$. For this case, the integration over $\mathbf{\Omega}'$ and $\mathbf{\Omega}$ in the last term of equation (6.65) may be carried out; the result is

$$\Delta\alpha = \text{Constant}\left[-\iint \Delta\sigma_s(\mathbf{r})\Phi(\mathbf{r}, -\mathbf{\Omega})\Phi(\mathbf{r}, \mathbf{\Omega})\, dV\, d\mathbf{\Omega} + \int \frac{\Delta\sigma_s(\mathbf{r})}{4\pi}\phi^2(\mathbf{r})\, dV\right]. \tag{6.67}$$

At the center of a sphere,

$$\Phi(\mathbf{r}, \mathbf{\Omega}) = \frac{1}{4\pi}\phi(\mathbf{r}),$$

since the flux is isotropic; hence, the two terms on the right side of equation (6.67) are identical and $\Delta\alpha$ is zero. Thus, changes only in scattering at the center of a sphere of multiplying material will not affect α. For a scattering perturbation at the surface, however, the first term on the right side of equation (6.67) is zero, since $\Phi(\mathbf{r}, -\mathbf{\Omega})\Phi(\mathbf{r}, \mathbf{\Omega})$ is zero, as seen above, but the second term is positive; hence, $\Delta\alpha$ will be positive, and there will be an increase in α.

The respective effects on α of changing the absorption and scattering cross sections are thus quite different, as indicated qualitatively in Fig. 6.1. The curves show the general nature of the changes in α resulting from an increase in absorption or scattering cross sections as a function of radial distance in a bare sphere of radius r_{max}.

Before leaving this topic, it is necessary to sound a note of caution. If a strongly absorbing material is introduced into a multiplying system, the value

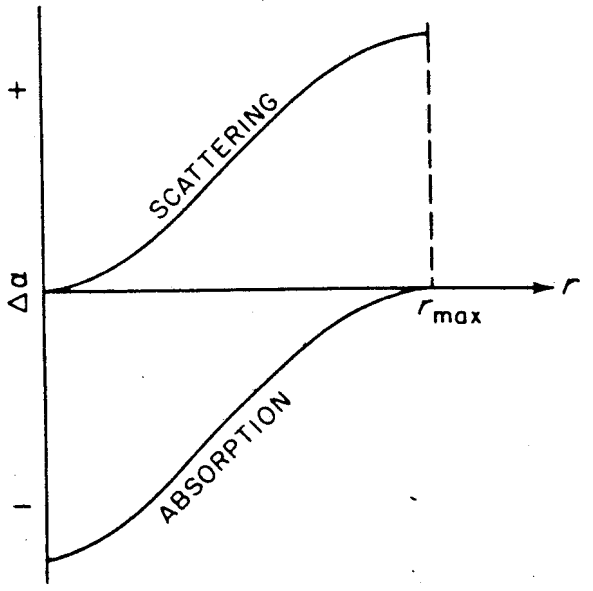

FIG. 6.1 QUALITATIVE EFFECTS ON α OF LOCAL INCREASE IN ABSORPTION AND SCATTERING CROSS SECTIONS IN A BARE SPHERE.

of $\Delta\sigma$ will be large and then perturbation theory may fail. The reason is that in going from equation (6.63), which is exact, to equation (6.64), the assumption is made that $\Delta\Phi$ is small in comparison with Φ in the region where the change in the cross section occurs. Consequently, the essential requirement for equation (6.64) to be applicable is that the local perturbation of the flux must be small.

When this $\Delta\Phi$ is not small, as in the case of strong local absorption, it may sometimes be possible to estimate $\Delta\Phi$ and Φ^* and use the exact equation (6.63) instead of equation (6.64). For example, a gold foil would cause a serious perturbation of the flux in its vicinity only for neutrons with energies close to the 5-eV resonance. This perturbation might then be calculated by the methods given in Chapter 8. Some authors apply the term perturbation theory when referring to the use of equation (6.63) with a known value of the perturbed flux, Φ^*; the use of equation (6.64) is then called first-order perturbation theory.[10]

6.3c Perturbation of the Effective Multiplication Factor

A treatment similar to that used in the preceding section for the eigenvalue α can be applied to derive the effect of a perturbation on the eigenvalue k, the effective multiplication factor. The transport equation for this eigenvalue is equation (1.49) and, in terms of the neutron angular flux instead of the angular density, it is

$$\boldsymbol{\Omega}\cdot\nabla\Phi + \sigma\Phi = \iint \sum_{x\neq f} \sigma_x f_x(\mathbf{r}; \boldsymbol{\Omega}', E' \to \boldsymbol{\Omega}, E)\Phi(\mathbf{r}, \boldsymbol{\Omega}', E')\, d\boldsymbol{\Omega}'\, dE' + \frac{1}{k}\iint \frac{1}{4\pi}\nu\sigma_f(\mathbf{r}; E' \to E)\Phi(\mathbf{r}, \boldsymbol{\Omega}', E')\, d\boldsymbol{\Omega}'\, dE'. \tag{6.68}$$

The corresponding adjoint equation for the eigenvalue $k^\dagger$ is

$$-\boldsymbol{\Omega}\cdot\nabla\Phi^\dagger + \sigma\Phi^\dagger = \iint \sum_{x\neq f} \sigma_x f_x(\mathbf{r};\, \boldsymbol{\Omega}, E \to \boldsymbol{\Omega}', E')\Phi^\dagger(\mathbf{r}, \boldsymbol{\Omega}', E')\, d\boldsymbol{\Omega}'\, dE'$$

$$+ \frac{1}{k^\dagger}\iint \frac{1}{4\pi}\nu\sigma_f(\mathbf{r};\, E \to E')\Phi^\dagger(\mathbf{r}, \boldsymbol{\Omega}', E')\, d\boldsymbol{\Omega}'\, dE'. \qquad (6.69)$$

Of particular interest are the fundamental (largest) eigenvalues k and $k^\dagger$, for which, according to considerations of §§1.5e, 6.1j, Φ and $\Phi^\dagger$ are nonnegative. It can then be shown, by using the same procedure as in §6.1j, that $k = k^\dagger$. This is done by multiplying equation (6.68) by $\Phi^\dagger$ and equation (6.69) by Φ, subtracting and integrating the result over all $\mathbf{r}$, $\boldsymbol{\Omega}$, and E. The gradient terms are eliminated, as before, by assuming free-surface boundary conditions on Φ and $\Phi^\dagger$.

Suppose that equations (6.68) and (6.69) apply to an unperturbed reference system. The most important of such systems, in practice, is an exactly critical system, for which $k = k^\dagger = 1$. In the general case, however, for a perturbed system having cross sections σ^*, $\sigma_x^* f_x^*$, and $\nu^*\sigma_f^*$ and eigenvalue k^*, the angular flux Φ^* satisfies equation (6.68) with all appropriate quantities being perturbed, and hence marked with an asterisk; thus,

$$\boldsymbol{\Omega}\cdot\nabla\Phi^* + \sigma^*\Phi^* = \iint \sum_{x\neq f} \sigma_x^* f_x^*(\mathbf{r};\, \boldsymbol{\Omega}', E' \to \boldsymbol{\Omega}, E)\Phi^*(\mathbf{r}, \boldsymbol{\Omega}', E')\, d\boldsymbol{\Omega}'\, dE'$$

$$+ \frac{1}{k^*}\int \frac{1}{4\pi}\nu^*\sigma_f^*(\mathbf{r};\, E' \to E)\Phi^*(\mathbf{r}, \boldsymbol{\Omega}', E')\, d\boldsymbol{\Omega}'\, dE'. \qquad (6.70)$$

If equation (6.70) is now multiplied by $\Phi^\dagger(\mathbf{r}, \boldsymbol{\Omega}, E)$ and equation (6.69) by $\Phi^*(\mathbf{r}, \boldsymbol{\Omega}, E)$, and the resulting expressions are subtracted and integrated over all $\mathbf{r}$, $\boldsymbol{\Omega}$, and E, an exact equation is obtained, analogous to equation (6.63).

In general,

$$\frac{1}{k^*} = \frac{1}{k^*} - \frac{1}{k} + \frac{1}{k} = -\frac{\Delta k}{kk^*} + \frac{1}{k},$$

where $\Delta k = k^* - k$ is the perturbation in the effective multiplication factor. For the special case of a critical reference system, $k = 1$; hence,

$$\frac{1}{k^*} = 1 - \frac{\Delta k}{k^*},$$

where Δk is now the departure from criticality.

In applying perturbation theory, it is assumed that, to first order, Φ^* may be replaced by Φ. It is thus found that, as a result of the perturbations $\Delta\sigma$ and

$\Delta(\sigma f)$ in cross sections, the change Δk in the effective multiplication factor of a critical system is given by

$$\frac{\Delta k}{k^*}\int\cdots\int\frac{1}{4\pi}\,\nu\sigma_f(\mathbf{r};E'\to E)\Phi^\dagger(\mathbf{r},\boldsymbol{\Omega},E)\Phi(\mathbf{r},\boldsymbol{\Omega}',E')\,dV\,d\boldsymbol{\Omega}'\,dE'\,d\boldsymbol{\Omega}\,dE$$

$$\approx -\iiint\Delta\sigma(\mathbf{r},E)\Phi^\dagger(\mathbf{r},\boldsymbol{\Omega},E)\Phi(\mathbf{r},\boldsymbol{\Omega},E)\,dV\,d\boldsymbol{\Omega}\,dE$$

$$+\int\cdots\int\Delta[\sigma f(\mathbf{r};\boldsymbol{\Omega}',E'\to\boldsymbol{\Omega},E)]\Phi^\dagger(\mathbf{r},\boldsymbol{\Omega},E)$$

$$\times\,\Phi(\mathbf{r},\boldsymbol{\Omega}',E')\,dV\,d\boldsymbol{\Omega}'\,dE'\,d\boldsymbol{\Omega}\,dE. \quad (6.71)$$

The perturbations $\Delta\sigma$ and $\Delta(\sigma f)$ are just as defined in §6.2b, and the warning expressed above, that $\Delta\sigma$ must not be large, is equally applicable here. Since $k^*\approx 1$, equation (6.71) provides, upon setting $k^*=1$, a first-order expression for Δk. The complete equation for $\Delta k/k^*$ is useful, however, as will be seen in Chapter 9.

It will be observed that equation (6.71) for the change in k, resulting from changes in cross sections, is analogous to equation (6.64) for the change in α. In fact the right-hand sides of the two equations have the same form; the only difference is that in equation (6.71) the flux and adjoint are the eigenfunctions for the k and k^* eigenvalues, whereas in equation (6.64) they are the eigenfunctions for the α and α^* eigenvalues, respectively. In one-speed theory, the effects on k of simple cross-section perturbations are similar to those given by equations (6.66) and (6.67) for changes in α, which are illustrated qualitatively in Fig. 6.1.

6.3d Perturbation of a Critical System

Further understanding of the adjoint function and of perturbation theory can be gained by considering an unperturbed reference system at critical, i.e., one with $\alpha=0$, and comparing it with a perturbed, slightly subcritical, system which is maintained in a steady state by a source. For the reference system, the equations for the flux and its adjoint may then be written as

$$\boldsymbol{\Omega}\cdot\nabla\Phi+\sigma\Phi=\iint\sigma f(\mathbf{r};\boldsymbol{\Omega}',E'\to\boldsymbol{\Omega},E)\Phi\,d\boldsymbol{\Omega}'\,dE' \quad (6.72)$$

and

$$-\boldsymbol{\Omega}\cdot\nabla\Phi'+\sigma\Phi'=\iint\sigma f(\mathbf{r};\boldsymbol{\Omega},E\to\boldsymbol{\Omega}'E')\Phi'\,d\boldsymbol{\Omega}'\,dE'. \quad (6.73)$$

For a subcritical perturbed system which is maintained in a steady state by a source, the transport equation is

$$\boldsymbol{\Omega}\cdot\nabla\Phi^*+\sigma^*\Phi^*=\iint\sigma^*f^*(\mathbf{r};\boldsymbol{\Omega}',E'\to\boldsymbol{\Omega},E)\Phi^*\,d\boldsymbol{\Omega}'\,dE'+Q(\mathbf{r},\boldsymbol{\Omega},E), \quad (6.74)$$

where, as before,

$$\sigma^* = \sigma + \Delta\sigma \quad \text{and} \quad \sigma^* f^* = \sigma f + \Delta(\sigma f).$$

The quantities $\Delta\sigma$ and $\Delta(\sigma f)$ represent differences between the perturbed (subcritical) system and the reference (critical) system. Equation (6.73) is multiplied by Φ^* and equation (6.74) by $\Phi^\dagger$, and the results are subtracted and integrated over the range of variables; it is then found that

$$\iiint Q\Phi^\dagger \, dV \, d\Omega \, dE$$

$$= \iiint \Delta\sigma\Phi^*\Phi^\dagger \, dV \, d\Omega \, dE - \int \cdots \int \Delta[\sigma f(\mathbf{r}; \Omega', E' \to \Omega, E)]$$

$$\times \Phi^*(\mathbf{r}, \Omega', E')\Phi^\dagger(\mathbf{r}, \Omega, E) \, dV \, d\Omega' \, dE' \, d\Omega \, dE. \quad (6.75)$$

If the perturbed system is close to critical, it may be anticipated that

$$\Phi^* \simeq C\Phi,$$

where Φ is the solution of the critical equation (6.72) that has been normalized in some definite, but arbitrary, manner, and C is a constant for a given normalization of the flux. Then equation (6.75) reduces to

$$\iiint Q\Phi^\dagger \, dV \, d\Omega \, dE$$

$$= C\left[\iiint \Delta\sigma\Phi\Phi^\dagger \, dV \, d\Omega \, dE - \int \cdots \int \Delta(\sigma f)\Phi\Phi^\dagger \, dV \ldots dE\right]. \quad (6.76)$$

It should be noted that, unlike the eigenfunctions corresponding to the α eigenvalues, the quantities Φ, Φ^*, and $\Phi^\dagger$ in equations (6.72), etc., have measurable steady-state values representing the existing experimental situation. Some interesting conclusions can thus be drawn from equation (6.76), of which two will be mentioned here.

Consider a subcritical system having some definite perturbation, i.e., $\Delta\sigma$ and $\Delta(\sigma f)$ are fixed. Then, according to equation (6.76), C, which is proportional to the perturbed angular flux, Φ^*, produced by the source Q, is proportional to the integral of $Q\Phi^\dagger$. In other words, Φ^* is proportional to the integral of $Q\Phi^\dagger$. Thus, $\Phi^\dagger$ is again seen to be the importance of neutrons in populating the persisting mode (for a subcritical system).

Another situation of interest is that of the same source in a sequence of subcritical multiplying systems of the same type. Suppose that the ith of these systems has perturbations from critical given by $a_i(\Delta\sigma)$ and $a_i[\Delta(\sigma f)]$, where a_i is proportional to the deviation from critical, whereas $\Delta\sigma$ and $\Delta(\sigma f)$ are the same for all the systems. Then, it follows from equation (6.76) that $1/C$ is proportional to a_i. Furthermore, C is proportional to the detector response, and hence to the multiplication of the system; consequently, the multiplication is

inversely proportional to the perturbation from the critical. This relation is the basis of a familiar experimental method for determining the conditions of criticality; the reciprocal of the multiplication, i.e., $1/M$, is plotted against some parameter, usually the mass, for a number of subcritical assemblies and extrapolated to $1/M = 0$ in an almost linear manner.

6.3e Perturbations in Multigroup Diffusion Theory

In the preceding sections some general results were derived for changes in the eigenvalues α or k as given by perturbation theory, based on the transport equation. Analogous expressions can be obtained for various approximations to the transport equation. As an example, consideration will be given here to the change in k based on the differential equations of multigroup diffusion theory.

Equation (4.41) for the eigenvalue k in multigroup diffusion theory can be written as

$$-\nabla \cdot D_g \nabla \phi_g + \sigma_{0,g}\phi_g = \sum_{g'} \left(\sigma_{s0,g'\to g}\phi_{g'} + \frac{\nu\sigma_{f,g'\to g}}{k}\phi_{g'}\right). \tag{6.77}$$

This expression applies to the unperturbed system. The corresponding adjoint equation for the eigenvalue $k^\dagger$, which is equal to k, as seen above, is

$$-\nabla \cdot D_g \nabla \phi_g^\dagger + \sigma_{0,g}\phi_g^\dagger = \sum_{g'} \left(\sigma_{s0,g\to g'}\phi_{g'}^\dagger + \frac{\nu\sigma_{f,g\to g'}}{k^\dagger}\phi_{g'}^\dagger\right). \tag{6.78}$$

The equation for the flux in the perturbed system with eigenvalue k^* is

$$-\nabla \cdot D_g^* \nabla \phi_g^* + \sigma_{0,g}^*\phi_g^* = \sum_{g'} \left(\sigma_{s0,g'\to g}^*\phi_{g'}^* + \frac{\nu\sigma_{f,g'\to g}^*}{k^*}\phi_{g'}^*\right), \tag{6.79}$$

where the perturbed quantities are again marked by an asterisk. The perturbations, which are assumed to be small, are then given by

$$\begin{aligned}
\Delta D_g &= D_g^* - D_g \\
\Delta\sigma_{0,g} &= \sigma_{0,g}^* - \sigma_{0,g} \\
\Delta\sigma_{s0,g'\to g} &= \sigma_{s0,g'\to g}^* - \sigma_{s0,g'\to g} \\
\Delta(\nu\sigma_{f,g'\to g}) &= \nu\sigma_{f,g'\to g}^* - \nu\sigma_{f,g'\to g} \\
\Delta k &= k^* - k.
\end{aligned}$$

Equation (6.78) is now multiplied by ϕ_g^* and equation (6.79) by ϕ_g and the results are subtracted. Upon summing over g and integrating over volume, it is found that

$$\sum_g \int \left[-\phi_g^\dagger \nabla\cdot(D_g^*\nabla\phi_g^*) + \phi_g^*\nabla\cdot(D_g\nabla\phi_g^\dagger) + \Delta\sigma_{0,g}\phi_g^\dagger\phi_g^*\right] dV$$

$$= \sum_g \int \left[\sum_{g'} \Delta\sigma_{s0,g'\to g}\phi_g^\dagger\phi_{g'}^* + \sum_{g'}\left(\frac{\nu\sigma_{f,g'\to g}^*}{k^*} - \frac{\nu\sigma_{f,g'\to g}}{k}\right)\phi_g^\dagger\phi_{g'}^*\right] dV. \tag{6.80}$$

The first two terms on the left side of equation (6.80) reduce to

$$\sum_g \int [-\phi_g^\dagger \nabla \cdot (\Delta D_g \nabla \phi_g^*)]\, dV,$$

since, as in the one-speed problem (§6.2b), the remaining contributions cancel upon integration by parts and use of the boundary conditions. The last two terms on the right side of the equation may be simplified by using the relationship

$$\begin{aligned}\frac{\nu\sigma_f^*}{k^*} - \frac{\nu\sigma_f}{k} &= \frac{\nu\sigma_f + \Delta(\nu\sigma_f)}{k + \Delta k} - \frac{\nu\sigma_f}{k} \\ &\approx \frac{\nu\sigma_f + \Delta(\nu\sigma_f)}{k}\left(1 - \frac{\Delta k}{k}\right) - \frac{\nu\sigma_f}{k} \\ &\approx \frac{\Delta(\nu\sigma_f)}{k} - \frac{\nu\sigma_f}{k^2}\,\Delta k.\end{aligned}$$

Upon substitution into equation (6.80) and solving for Δk, the result is

$$\frac{\Delta k}{k^2} \approx \frac{\displaystyle\sum_g \int \left[\phi_g^\dagger \nabla \cdot (\Delta D_g \nabla \phi_g) - \Delta\sigma_{0,g}\phi_g^\dagger \phi_g + \sum_{g'} \Delta\sigma_{s0,g'\to g}\phi_g^\dagger \phi_{g'} + \sum_{g'} \frac{\Delta(\nu\sigma_{f,g'\to g})}{k}\phi_g^\dagger \phi_{g'}\right] dV}{\displaystyle\sum_g \int \sum_{g'} \nu\sigma_{f,g'\to g}\phi_g^\dagger \phi_{g'}\, dV} \tag{6.81}$$

The asterisks have been removed from ϕ^* on the assumption that the perturbations are small and $\phi \approx \phi^*$, so that first-order perturbation theory is applicable. Of course, if the reference system is critical, $k = 1$.

In the special case of one-speed diffusion theory, the sums over g and g' may be deleted. Moreover, $\phi^\dagger$ is now equal to ϕ, and equation (6.81) reduces to

$$\frac{\Delta k}{k^2} = \frac{\displaystyle\int \left[\phi \nabla \cdot (\Delta D \nabla \phi) - \Delta\sigma_a \phi^2 + \frac{\Delta(\nu\sigma_f)}{k}\phi^2\right] dV}{\displaystyle\int \nu\sigma_f \phi^2\, dV}.$$

where $\Delta\sigma_a = \Delta\sigma_0 - \Delta\sigma_{s0}$ is the perturbation of the absorption cross section (§3.1d). This equation may be simplified further by using the identity

$$\begin{aligned}\int [\phi \nabla \cdot (\Delta D \nabla \phi)]\, dV &\equiv \int [\nabla \cdot (\phi \Delta D \nabla \phi) - \Delta D (\nabla \phi)^2]\, dV \\ &= \int \hat{\mathbf{n}} \cdot \phi \Delta D \nabla \phi\, dA - \int \Delta D (\nabla \phi)^2\, dV. \end{aligned} \tag{6.82}$$

In many problems, e.g., if $\Delta D = 0$ at the surface or if ϕ is assumed to be zero at the surface, the first term on the right of equation (6.82) is zero. In these cases,

$$\frac{\Delta k}{k^2} = \frac{\int \left[-\Delta D(\nabla\phi)^2 + \left\{ \frac{\Delta(\nu\sigma_f)}{k} - \Delta\sigma_a \right\} \phi^2 \right] dV}{\int \nu\sigma_f \phi^2 \, dV}. \tag{6.83}$$

The denominator of equation (6.83) is a constant. Hence, according to one-speed diffusion theory, the effect on k of a small change in cross section, either $\Delta\sigma_a$ or $\Delta(\nu\sigma_f)$, is proportional to the square of the flux at the position of the change. The effect of a change, ΔD, in the diffusion coefficient is seen to be proportional to the square of the gradient of the flux. An expression analogous to equation (6.83) is often derived directly from one-speed diffusion theory.[11]

6.3f An Application of Perturbation Theory

It was mentioned in §5.4d that, in addition to the method given there for assessing the adequacy of nuclear data for making neutron transport calculations, there is another procedure based on reactivity effects. The latter approach, which is described here, involves measuring the changes in reactivity accompanying the insertion of small samples of materials at various positions in a critical assembly and comparing the results with those obtained by using perturbation theory and discrete ordinates multigroup calculations. The reactivity observations made in this connection have been mainly with the Godiva, Jezebel, and Topsy fast (metal) assemblies and, to a lesser extent, with a bare sphere of uranium-233 metal and ZPR III 48 (§5.4d).

For the experimental determination of the reactivity effects, the assembly is brought to (delayed) critical with a void at the position where the sample is to be placed. The sample is then inserted and the resulting reactivity change, Δk, is determined from the motion of a calibrated control rod required to maintain criticality. The rod is calibrated in terms of reactivity as a function of position, with the sample absent, in the usual manner from measurement of the asymptotic reactor period.[12]

The change in reactivity caused by insertion of a sample of material in the assembly is commonly reported in cents per gram-atom. A dollar (100 cents) is the reactivity change which will take a system from prompt to delayed critical, i.e., Δk is then equal to β, the effective delayed-neutron fraction for the given system (§9.2b); hence, the reactivity change in general is equal to $\Delta k/\beta$ in dollars or $100\,\Delta k/\beta$ in cents. The reactivity effect in cents per gram-atom is then given by $100\,A\Delta k/\beta m$, where m is the mass of the sample in grams and A is the atomic weight of the element (or nuclide) present.

In order to obtain easily measurable reactivity changes by the method described above, it is sometimes necessary to use samples which are large enough to produce significant local perturbations of the neutron flux. Under these

conditions, a correction should be made, by using second-order perturbation theory[13] to reduce the reactivities to values applicable to very small samples which would not perturb the flux.

For computing the reactivity effects of the small samples, the fluxes and adjoints are determined according to the 24-group, S_8 approximation using the DTF IV code, as described in §5.4d. The value of $\Delta k/k$, which is essentially equal to Δk, is then obtained from the perturbation theory equation (6.71). The results are then expressed in cents per gram-atom of the sample element (or nuclide).

It was seen in §§6.3b, 6.3c that, in one-speed theory, the effect on k of a sample at the center of a sphere was due mainly to neutron absorption (or fission) in the sample and was essentially independent of the scattering; for a sample on the surface, however, the changes resulted from scattering (and fission), but were independent of the absorption cross section. These one-speed results are also largely true for energy-dependent situations, except that the neutron energy changes accompanying scattering (and fission) must be taken into account. This means that central reactivity values are now sensitive to elastic scattering, particularly from the nuclei of low mass number, and to inelastic scattering. Such scatterings transfer neutrons to lower energies where they have a different importance. Nevertheless, for strongly absorbing (or fissile) nuclides, the central reactivity values are dominated by absorption (or fission).

From equation (6.71), it is apparent that a change in k resulting from a change in the neutron absorption cross section at energy E is proportional to the product of the flux and adjoint at that energy. Hence, from a knowledge of $\Phi\Phi^\dagger$ as a function of energy, it is possible to determine how errors in the absorption cross sections would affect the computed reactivity. It has been found in this manner[14] that for the Godiva and Jezebel assemblies the energy range of about 0.1 to 5 MeV is important for determining reactivity effects, although higher energies are emphasized more in Jezebel (plutonium-239) than Godiva (uranium-235). For ZPR-III 48, which contains elements of low mass number, the important energy range is from about 0.01 to 1 MeV.

Some experimental values of central reactivity effects, in cents per gram-atom, together with the results computed from equation (6.71), are given in Table 6.1.[15] The fissile species is indicated for each assembly. The generally good agreement between calculated and experimental results, especially for the fissile nuclides, uranium-233, uranium-235, and plutonium-239, implies that, on the whole, the nuclear data are satisfactory in the important energy ranges indicated by the $\Phi\Phi^\dagger$ values.

Correction of Cross Sections

Although the observed reactivity changes agree reasonably well with the values calculated from the cross-section library, there are some discrepancies. For

TABLE 6.1. CENTRAL REACTIVITY CHANGES IN CRITICAL ASSEMBLIES[15] (CENTS/GRAM-ATOM)

Assembly	^{233}U	*Godiva* (^{235}U)	*Topsy* (^{235}U)	*Jezebel* (^{239}Pu)	*ZPR-III 48* (^{239}Pu)
β	0.0029	0.0065	0.0062	0.00191	0.00338

Sample	*Calc.*	*Exp.*	*Calc.*	*Exp.*	*Calc.*	*Exp.*	*Calc.*	*Exp.*	*Calc.*	*Exp.*
H	155	-	50.5	47.8	72.5	67.6	45.4	62.8	−0.9	—
D	67.2	70.0	23.0	17.8	31.6	24.0	−5.9	−5.3	−0.2	—
Be	31.6	-	6.23	7.3	8.91	9.2	17.3	15.5	0	—
^{10}B	−143	—	−40.9	−55.3	−67.1	—	−191	−251	−16.7	−30.8
C	5.75	3.0	1.70	2.4	2.60	2.4	−7.28	−6.9	−0.2	—
^{23}Na	2.6	—	0.12	—	0.14	—	−12.9	—	−0.07	−0.01
Fe	−2.54	—	−1.68	−0.2	−2.71	−2.2	−22.2	−21.5	−0.2	−2.1
^{232}Th	−9.14	—	−10.0	−1.4	−17.5	−7.6	−85.3	−64.7	−3.6	—
^{233}U	978	955	255	—	364	359	1358	1359	39.7	—
^{235}U	594	-	146	149	207	208	798	804	23.9	24.2
^{238}U	146	135	23.7	24.3	28.7	26.7	98.0	114	−1.6	−2.1
^{239}Pu	1136	—	286	285	403	403	1591	1592	35.0	34.9
^{240}Pu	724	—	158	170	210	286	983	1038	2.9	5.0
^{241}Pu	1077	—	276	—	398	—	1495	—	52.5	—

example, the calculated central reactivity change caused by uranium-238 is substantially less than the experimental value in Jezebel, but is somewhat larger in Topsy. The disagreement between measured and computed reactivity effects is brought out in Fig. 6.2 and 6.3; they show the effects associated with uranium-238 in the two assemblies as a function of the distance of the sample from the center of the core. The calculated reactivity changes, especially near the center, are seen to be too high in Topsy and too low in Jezebel.

The differences between calculated and observed reactivities may be due either to errors in the neutron group fluxes used in the computations or to errors in the cross-section data for uranium-238. The first possibility could be assessed by examining all the central reactivity data, as given in Table 6.1, for a particular assembly. If the group fluxes were incorrect, then there would be consistent differences between all the measured and computed reactivity effects. The excellent agreement for the fissile nuclides suggests that this is not the case. It must be concluded, therefore, that in this instance the errors are probably in the uranium-238 cross sections. As mentioned in §5.4c, direct measurements of neutron flux can also be used to check the accuracy of the group fluxes.

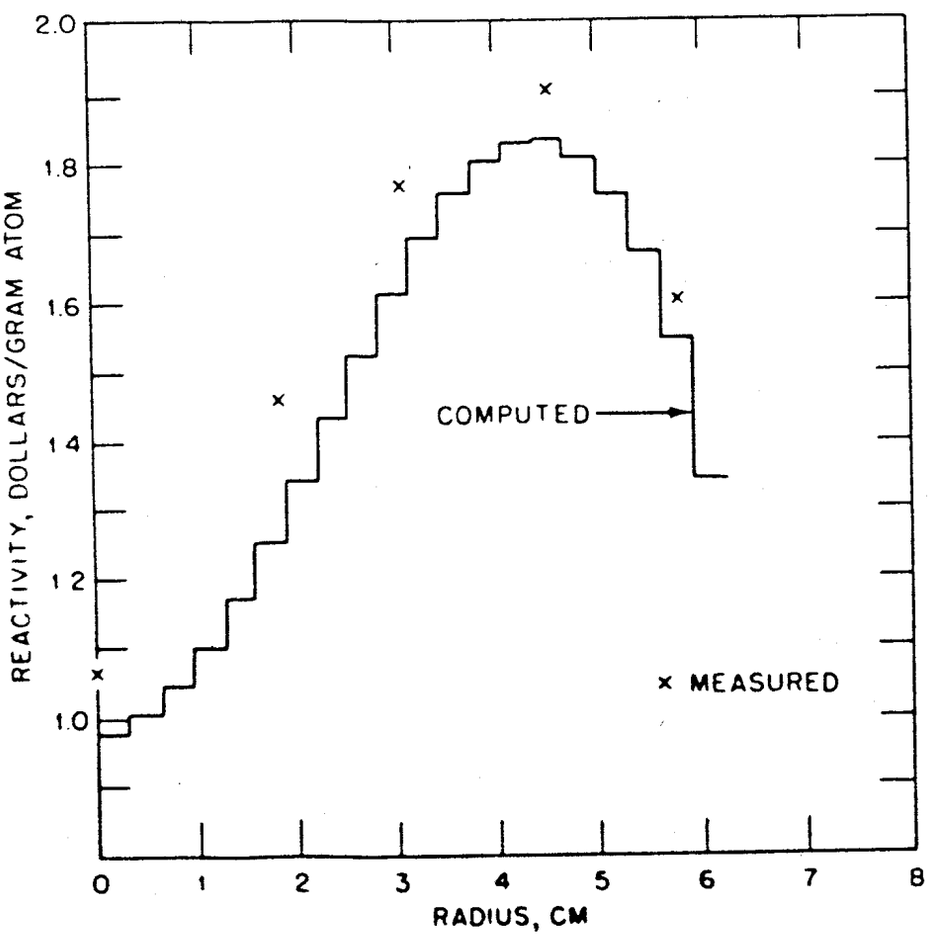

FIG. 6.2 MEASURED AND COMPUTED REACTIVITY EFFECTS OF URANIUM-238 ON THE JEZEBEL ASSEMBLY (AFTER C. B. MILLS, UNPUBLISHED).

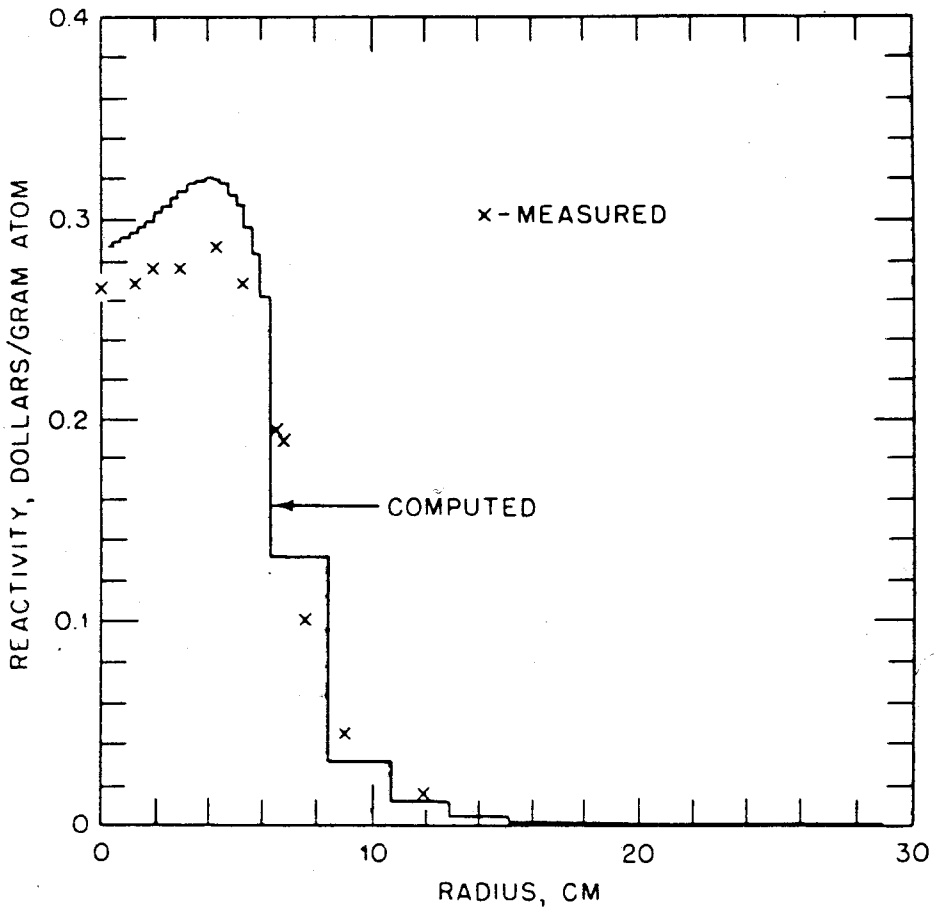

FIG. 6.3 MEASURED AND COMPUTED REACTIVITY EFFECTS OF URANIUM-238 ON THE TOPSY ASSEMBLY (AFTER C. B. MILLS, REF. 14).

The central reactivity effect of uranium-238 is the result of a positive effect from fissions caused by neutrons of high energy, greater than about 1.4 MeV, and a negative contribution from (n, γ) reactions, mostly due to neutrons of low energy. There is also a contribution of variable sign from inelastic scattering. (Elastic scattering from uranium-238 results in such small changes in neutron energy that the corresponding central reactivity effect can be neglected.) As will be shown later, the data in Table 6.1 indicate that the effect of elastic scattering is positive in Topsy (uranium-235 fuel) and negative in Jezebel (plutonium-239 fuel). By analogy, it is to be expected that the effects of inelastic scattering would have the same respective signs. Consequently, one way to improve the agreement between the observed and calculated reactivity effects for uranium-238 would be to decrease the inelastic scattering cross sections of this nuclide.

Another possibility arises from the faster neutron spectrum in Jezebel than in Topsy. If the cross sections of uranium-238 for fission at high neutron energies and for the (n, γ) reaction at low energies were both increased, the difference between the experimental and computed reactivity effects could be largely eliminated. The desirability of making such changes could be assessed by varying

the relevant uranium-238 cross sections within experimental limits and determining the effects on the central reactivity of small samples of uranium-238 in Jezebel, Topsy, and other systems. The modified cross sections could also be tested by using them to evaluate the effective multiplication factors for systems which contain appreciable amounts of uranium-238.

The general conclusions to be drawn from the material presented above is that the particular nuclear data library used in the computations is fairly good for neutrons of high energy, e.g., $E_n \gtrsim 0.1$ MeV, but the reactivity results suggest possible errors in some cross sections. Thus, the data used for design studies, particularly of fast reactors, must be continuously reevaluated in the light of new measurements on microscopic cross sections or of the results of integral experiments with critical assemblies. In this connection "benchmark" experiments, i.e., highly accurate measurements with critical assemblies, provide essential integral tests of both the nuclear data and the computing methods. It is particularly important that a variety of critical assemblies be used in these studies and, furthermore, that different types of measurements be made. Reactivity effects have been emphasized here, but there are other possibilities; some of these were mentioned in §5.4d and they are discussed in the references given there.

Other Reactivity Effects

In addition to providing a means for evaluating nuclear data, the results in Table 6.1 lead to some other conclusions of general interest. It will be observed, for example, that when fission or absorption (or both) of the sample has the dominant effect on the central reactivity, e.g., boron-10 and the fertile and fissile nuclides, the reactivity changes are much larger in the assemblies containing uranium-233 and plutonium-239 than in those having uranium-235 as the fissile material. The main reason is that a dollar (or cent) of reactivity is worth more in uranium-235 because β is larger than for the other fissile nuclides (see Table 6.1). When allowance is made for the differences in β, it is found that the absolute reactivity changes for a given sample are not greatly different in the several assemblies. For a specific fissile material in the assembly core, a particular central sample has a greater absolute reactivity effect in a small system, such as Jezebel, than in a larger one, such as ZPR-III 48.

An absorbing material, e.g., boron-10, has a negative effect on the central reactivity, whereas fissile materials produce a positive change. The effect of a fertile nuclide, e.g., thorium-232 or uranium-238, will include a positive contribution due to fissions caused by high-energy neutrons and a negative contribution from the absorption of neutrons of lower energy. For thorium-232, the net effect is negative for all the assemblies under consideration, whereas for the more readily fissionable uranium-238 the net effect is positive in all the metal (very fast neutron) systems, but is negative in the somewhat slower neutron spectrum of ZPR-III 48.

For the weakly absorbing lighter nuclides, such as hydrogen, deuterium, beryllium, carbon, and sodium, the central reactivity effects are largely due to moderation, by elastic scattering, whereby the energies of the neutrons are reduced. The positive or negative character of the net effect depends on whether the importance (adjoint) of the neutrons decreases or increases, respectively, with energy. From Table 6.1 it is evident that in assemblies with uranium-233 or -235 as the fuel, the central reactivity change caused by an elastic scatterer is positive, i.e., the importance of the scattered neutron (of lower energy) is generally greater than for the incident neutron (of higher energy).

For Jezebel and ZPR-III 48, which are fueled with plutonium-239, the central reactivity effects of deuterium, carbon, and sodium are negative, indicating a greater importance for the neutrons of higher energy. The chief reason for this behavior is that, in comparison with other fissile nuclides, there is a marked decrease in the capture-to-fission ratio, α, for plutonium-239 with increasing neutron energy (Fig. 6.4). In addition, there is a slight increase in the fission cross section at an energy of about 1 MeV.

The reactivity effects of beryllium and hydrogen in Jezebel are seen to be

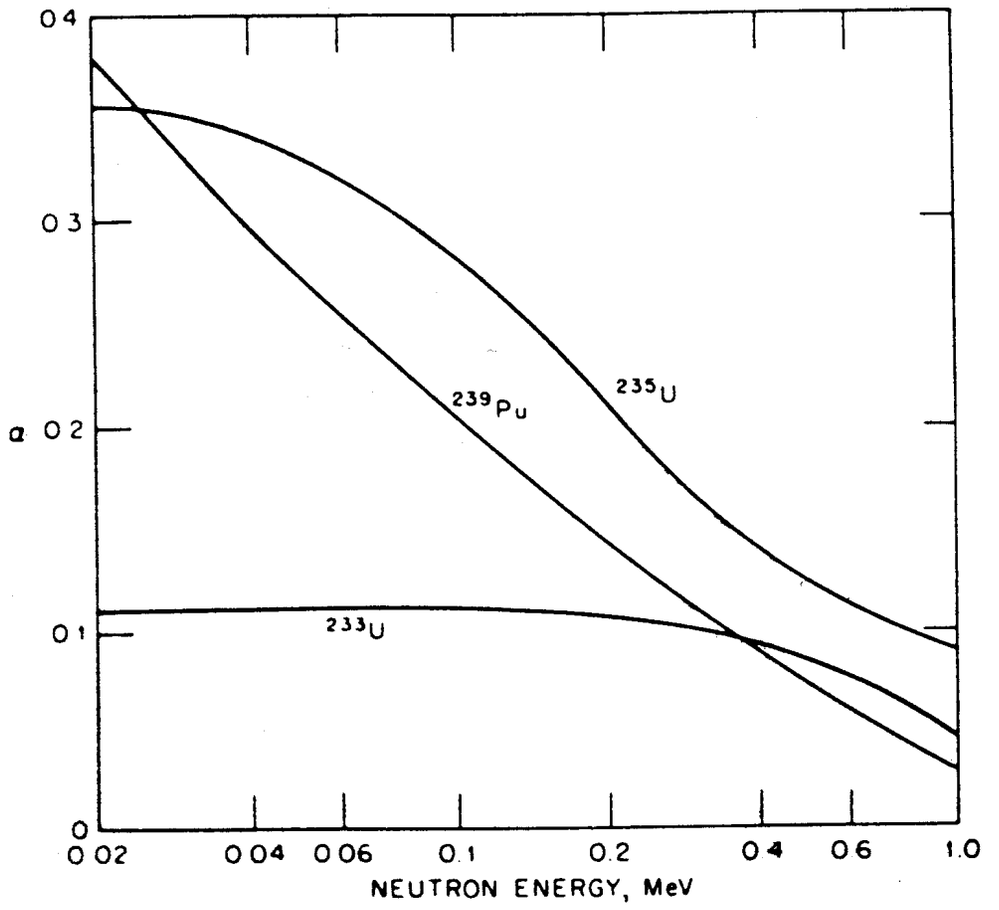

FIG. 6.4 VARIATION OF α (CAPTURE-TO-FISSION CROSS SECTION RATIO) WITH NEUTRON ENERGY (AFTER BNL-325, SUPPL. 2, 2ND ED., VOL. III, 1965).

positive, in contrast to those of the other light elements. For beryllium the main cause is the $(n, 2n)$ reaction which takes place to a significant extent in a fast-neutron spectrum such as that of the Jezebel assembly. The reactivity change produced by hydrogen is a special case; the positive effect in Jezebel is the result of the large neutron energy loss in a collision with a hydrogen nucleus. In ZPR-III 48, however, a small negative effect is to be expected.

The negative reactivity effect of sodium is of considerable significance in the design of fast reactors having plutonium-239 as fuel. If some of the sodium coolant is removed from near the center of the core of such a reactor, the consequent shift of the neutron spectrum to higher energies may result in an increase in the reactivity. Hence, if a fast-reactor excursion, i.e., a significant increase in reactivity, causes a loss of central sodium coolant, the excursion will be aggravated. This situation would not be expected to arise if uranium-235 or, especially, uranium-233 is the fuel, since the reactivity would decrease.

The foregoing discussion has referred to the effects of samples at the center of the reactor core. If the sample is not at the center, however, there will be positive reactivity contributions from the transport (or reflecting) properties of the material. This problem was considered for the one-speed model in §6.3b, and the only difference in the energy-dependent situation is, as before, that allowance must be made for the neutron energy changes in scattering.

Any nuclide, even the strong neutron absorber boron-10, may thus be expected to have a positive reactivity effect near the edge of a bare core. The weakly absorbing (moderating) elements of low mass number will have positive effects over much of the core, away from the center. In a plutonium-239 fast reactor, for example, the reactivity effect of sodium would tend to be negative in the central part of the core, as seen above, but it would be positive near the outside of the core (and in the surrounding blanket). Whether the net reactivity effect would be positive or negative will depend on the core size, composition, etc. A small core with considerable neutron leakage, for example, would favor a positive reactivity effect of sodium. This would represent a safety feature of small fast-reactor cores against accidents resulting in loss of coolant.

6.4 VARIATIONAL METHODS

6.4a Applications of Variational Methods

Variational methods have been found to be useful in neutron transport theory in at least two different ways. In the first, relatively accurate values of certain quantities are obtained by evaluating integrals involving relatively inaccurate values of the flux and adjoint. For example, in a subcritical system with a source, described by the time-independent inhomogeneous transport equation, a flux-

weighted integral is obtained from relatively inaccurate values of the flux and adjoint. By a flux-weighted integral is meant a quantity such as

$$\iiint \sigma_x(\mathbf{r}, E)\Phi(\mathbf{r}, \boldsymbol{\Omega}, E)\, dV\, d\boldsymbol{\Omega}\, dE,$$

which represents an interaction rate specified by the cross section σ_x. This use of variational methods is somewhat analogous to perturbation theory where, for example, a perturbed value of α, good to the first order, is obtained from equation (6.64) by using an unperturbed flux that is good only to zero order. Similarly, in applying a variational method to an inhomogeneous problem, i.e., a problem with a source, an accurate flux-weighted integral, e.g., absorptions in a fuel rod caused by a source in the moderator, is to be obtained from approximate values of the flux and adjoint. Perturbation theory may be regarded as an application of such variational methods.

Another, somewhat similar, application of variational methods, which will be described later, is to determine the eigenvalue for a homogeneous, i.e., source free, problem. Furthermore, in treating the transport of thermal neutrons, it is often required to evaluate the ratio of absorptions in the fuel to absorptions in the moderator. Variational expressions have been developed for such relations.[16] Variational methods have also been used to analyze the flux near a free surface, e.g., in deriving the extrapolation distance.[17]

A somewhat different use of the variational approach is to construct approximations systematically to exact solutions. An example of this type of application, which is considered in §6.4i, is the self-consistent derivation of the group constants that can be used for the multigroup calculations discussed in Chapters 4 and 5.

6.4b Evaluation of Flux-Weighted Integrals

Consider a time-independent inhomogeneous problem, namely, a subcritical system with a source. Suppose the exact angular flux, Φ_0, satisfies the equation

$$-\mathbf{L}\Phi_0 = Q, \tag{6.84}$$

where $\mathbf{L}$ is the transport operator. Alternatively, $\mathbf{L}$ may be an integral operator (§1.2a *et seq.*) or an approximation, such as a P_1 operator; in the latter case Φ_0 would be a two-component vector having the total flux and the current as the components. An adjoint equation to (6.84) will be

$$-\mathbf{L}^\dagger\Phi_0^\dagger = Q^\dagger, \tag{6.85}$$

where $Q^\dagger$ is the adjoint source.

It will now be shown how variational theory can be applied so as to use approximate values of the neutron flux and adjoint to obtain an accurate value of the inner product $(Q^\dagger, \Phi_0)$, that is, of the flux-weighted integral $\int Q^\dagger\Phi_0\, d\xi$,

where ξ represents the variables. The adjoint source is then specified in accordance with the problem under consideration. Suppose, for example, it is required to determine an accurate value of the fission rate, $\int \sigma_f \Phi_0 \, d\xi$, due to the given source Q for a situation in which only an inaccurate estimate of Φ_0 is available. In this case, the appropriate choice of the source in the adjoint equation (6.85) would be $Q^\dagger = \sigma_f(\mathbf{r}, E)$, the fission cross section, as will be seen in due course. Alternatively, an improved estimate of the flux itself could be obtained by letting $Q^\dagger$ be a delta function.

For the present, it will be assumed that Φ_0 and $\Phi_0^\dagger$ satisfy the usual free-surface flux and adjoint boundary conditions, and that they are both continuous functions of space. If $\mathbf{L}$ is the transport operator then, as seen earlier, $(\Phi_0^\dagger, \mathbf{L}\Phi_0) = (\Phi_0, \mathbf{L}^\dagger\Phi_0^\dagger)$. (It will be shown later that if the boundary and continuity conditions are not satisfied by Φ_0 and $\Phi_0^\dagger$, this result will not hold.) In order to obtain an accurate value of $(Q^\dagger, \Phi_0)$ from an inaccurate value of the flux, Φ, use will be made of the functional J,[18] defined by

$$\mathrm{J} = (Q^\dagger, \Phi) + (\Phi^\dagger, Q) + (\Phi^\dagger, \mathbf{L}\Phi), \tag{6.86}$$

where Φ and $\Phi^\dagger$ are estimates, often called *trial functions*, of the exact angular flux Φ_0 and the exact adjoint $\Phi_0^\dagger$, respectively, so that

$$\Phi = \Phi_0 + \delta\Phi \quad \text{and} \quad \Phi^\dagger = \Phi_0^\dagger + \delta\Phi^\dagger. \tag{6.87}$$

In addition, it is postulated, for the present, that the trial functions Φ and $\Phi^\dagger$ satisfy the boundary and continuity conditions. The modifications in the treatment required for discontinuous trial functions are described in a later section (§6.4f).

By substituting equations (6.87) into equation (6.86), it is found that

$$\begin{aligned}\mathrm{J} = {} & (Q^\dagger, \Phi_0) + (\Phi_0^\dagger, Q) + (\Phi_0^\dagger, \mathbf{L}\Phi_0) \\ & + (\delta\Phi^\dagger, Q) + (\delta\Phi^\dagger, \mathbf{L}\Phi_0) \\ & + (Q^\dagger, \delta\Phi) + (\Phi_0^\dagger, \mathbf{L}\,\delta\Phi) \\ & + (\delta\Phi^\dagger, \mathbf{L}\,\delta\Phi).\end{aligned} \tag{6.88}$$

In this equation, the three terms on the right of the first line are equal to the exact value of the functional, to be denoted by J_0. Moreover, these terms are all equal in magnitude since, in view of equations (6.84) and (6.85) and the definition of $\mathbf{L}^\dagger$,

$$(Q^\dagger, \Phi_0) = -(\Phi_0, \mathbf{L}^\dagger\Phi_0^\dagger) = -(\Phi_0^\dagger, \mathbf{L}\Phi_0) = (\Phi_0^\dagger, Q) = \mathrm{J}_0. \tag{6.89}$$

The two terms on the second line of equation (6.88) cancel, by equation (6.84), and so also do the two terms on the third line, as may be seen by using equation (6.85) and the identity

$$(\Phi_0^\dagger, \mathbf{L}\,\delta\Phi) = (\delta\Phi, \mathbf{L}^\dagger\Phi_0^\dagger).$$

which holds because $\delta\Phi$ satisfies the required boundary and continuity conditions. Hence, equation (6.88) reduces to

$$J = J_0 + (\delta\Phi^\dagger, \mathbf{L}\,\delta\Phi). \tag{6.90}$$

From this result, it is seen that the estimate, J, of the functional, based on the inaccurate flux, is equal to the desired exact value, J_0, with a correction proportional to the product of $\delta\Phi^\dagger$ and $\mathbf{L}\,\delta\Phi$. If these quantities are small, the correction would be second order in small quantities, and then J would be a very good estimate of J_0, i.e., of $(Q^\dagger, \Phi_0)$. In particular, J would be expected to be a better estimate than could be obtained, for example, from the inner product $(Q^\dagger, \Phi)$, since this would have an error $(Q^\dagger, \delta\Phi)$, which is first order in small quantities. If the fission rate (σ_f, Φ_0) is desired, then from equation (6.89) it is evident that $Q^\dagger$ should be chosen equal to σ_f.

For the special case of one-speed theory with isotropic scattering, the foregoing expectations can be confirmed rigorously, but for more general transport problems there are some difficulties, as will be seen below. The reason why variational methods are so powerful in one-speed theory is that, as already shown, the transport operator is then almost self-adjoint. Indeed, for one-speed problems with isotropic scattering, it is fruitful to use the integral form of the transport equation (§1.2c), which involves the total flux and a self-adjoint or symmetric integral operator.

An example of this approach is given in §6.4d, where it is seen that, because a self-adjoint operator is involved, the correction term must be positive. Hence, the exact value, J_0, of the functional is a minimum value, and a systematic approach to improving J is indicated. A trial function is used for Φ_0, which is here identical with $\Phi^\dagger$, with several free parameters; these are varied until a minimum value for J is found. At the minimum, the derivative of J with respect to each of the free parameters is zero. This minimum is the best value and a clear procedure is available for determining whether one trial function is better than another.

For general, energy-dependent problems, the situation is less satisfactory. In the first place, the sign of the correction term is not generally known, so that, although J may give an accurate estimate of J_0, there is no clear way of deciding which is the best of the trial functions. Nevertheless, trial functions with free parameters are often used in energy-dependent problems[19] and the parameters are varied until a stationary value of J is found, i.e., a value of J for which the derivative of J with respect to each of the free parameters is zero. In other words, if ξ_i represents each of the i free parameters, a stationary value of J is one for which $\partial J/\partial \xi_i = 0$ for all i. There is no assurance, however, that the stationary value, if it exists at all, is a good one. An exception arises in connection with thermalization problems, where the transport operator can be made almost self-adjoint (§7.2c); the situation is then similar to that in one-speed theory.

It should be noted, too, that the correction term in equation (6.90) contains $\mathbf{L}\,\delta\Phi$ rather than just $\delta\Phi$. Smallness of $\delta\Phi$ does not necessarily guarantee that $\mathbf{L}\,\delta\Phi$ will also be small. The reason is that the neutron transport operator, e.g., in equation (6.5), is not a bounded operator, since it contains derivatives[20]; thus, if $\delta\Phi$ is small but $\nabla\,\delta\Phi$ is large, then $\mathbf{L}\,\delta\Phi$ will be large. Nevertheless, it is usually found that if the estimates of Φ and $\Phi^\dagger$ are good, the functional J is quite accurate.

There is a simple manner in which the functional J can sometimes be improved upon. It can be seen from equation (6.90) that J will depend on the normalization of Φ and $\Phi^\dagger$. If, for example,

$$\Phi = (1 + a)\Phi_0 \quad \text{and} \quad \Phi^\dagger = (1 + b)\Phi_0^\dagger,$$

so that Φ and $\Phi^\dagger$ are in error only by being incorrectly normalized, it follows from equation (6.90) that

$$\mathrm{J} = \mathrm{J}_0(1 - ab).$$

By using an alternative functional, this dependence on the normalization of Φ and $\Phi^\dagger$ may be removed.

One such functional is obtained by letting

$$\Phi = C\Phi_1 \quad \text{and} \quad \Phi^\dagger = C^\dagger\Phi_1^\dagger,$$

and determining the normalizing factors C and $C^\dagger$ by making J stationary with respect to these factors. Thus, if $\partial \mathrm{J}/\partial C = 0$, it follows that

$$C^\dagger = -\frac{(Q^\dagger, \Phi_1)}{(\Phi_1^\dagger, \mathbf{L}\Phi_1)}$$

and if $\partial \mathrm{J}^\dagger/\partial C^\dagger = 0$,

$$C = -\frac{(Q, \Phi_1^\dagger)}{(\Phi_1^\dagger, \mathbf{L}\Phi_1)}.$$

If the results obtained above are substituted in equation (6.86) for J to obtain the modified functional, J_S, it is found that the three terms on the right all have the same value; since two appear with minus signs and one with a plus sign, the final result is

$$\mathrm{J}_S = -\frac{(Q^\dagger, \Phi_1)(Q, \Phi_1^\dagger)}{(\Phi_1^\dagger, \mathbf{L}\Phi_1)}. \tag{6.91}$$

This is sometimes called the Schwinger variational expression and is represented by the symbol H; the symbol J_S is used here, however, to emphasize that it is equivalent to J. As it is for J, the error is formally of the order of $\delta\Phi^\dagger\,\delta\Phi$. By the use of trial functions for Φ_1 and $\Phi_1^\dagger$ a stationary value for J_S can be found; this is a good estimate of J_0 and hence of $(Q^\dagger, \Phi_0)$, as before. The functional in equation (6.91) and several others have been treated in the literature.[21] In some one-speed problems it is possible to obtain both upper and lower bounds to J_S.[22]

In summary, it may be stated that the functionals J and J_S in equations (6.86) and (6.91) may be used to obtain estimates of a desired quantity, J_0, by inserting trial functions in these equations. Frequently, free parameters are included in the trial functions and they are varied to make J or J_S stationary. However, except for one-speed and thermalization problems, there is no guarantee that the stationary value is the best value.

6.4c Determination of Eigenvalues

So far, the functionals have been considered for estimating weighted integrals of the flux in inhomogeneous problems. The procedure for the homogeneous (source-free) eigenvalue problem is similar. For example, if the fundamental eigenvalue α is being sought, Q may be replaced formally by $-(\alpha/v)\Phi$ and $Q^\dagger$ by $-(\alpha/v)\Phi^\dagger$. With these substitutions, equations (6.84) and (6.85) would become the equations for the eigenvalue α. Let the same replacements be made in the functional J_S of equation (6.91). Consider, first, the result that would be obtained if Φ_1 and $\Phi_1^\dagger$ were exact, i.e., Φ_0 and $\Phi_0^\dagger$, respectively; the exact functional, denoted by J_0, would then be

$$J_0 = -\frac{\alpha^2[(1/v)\Phi_0^\dagger, \Phi_0]^2}{(\Phi_0^\dagger, \mathbf{L}\Phi_0)}.$$

By making use of the eigenvalue equation

$$\mathbf{L}\Phi_0 = \frac{\alpha}{v}\Phi_0,$$

it follows that

$$J_0 = -\alpha\left(\frac{1}{v}\Phi_0^\dagger, \Phi_0\right).$$

Upon equating the two expressions for J_0, the exact value of α is found to be

$$\alpha = \frac{(\Phi_0^\dagger, \mathbf{L}\Phi_0)}{[(1/v)\Phi_0^\dagger, \Phi_0]},$$

and the required functional for estimating α is

$$\alpha \simeq \frac{(\Phi^\dagger, \mathbf{L}\Phi)}{[(1/v)\Phi^\dagger, \Phi]}. \tag{6.92}$$

This expression for α is reminiscent of perturbation theory; for example, in equation (6.63), both α and α^* can be regarded as having been derived from the variational equation (6.92).

6.4d Applications of Variational Methods to One-Speed Problems

It was mentioned earlier that variational methods are especially useful in one-speed problems because the operators for the angular flux are almost self-adjoint; in the integral transport equation for the total flux with isotropic

scattering they are truly self-adjoint (§6.1h). Historically, variational calculations proved of great value in providing the most accurate critical dimensions for simple systems; these served as standards of comparison with other procedures for many years.[23] Two examples are given below of criticality calculations and one of an inhomogeneous problem with a source.

Critical Thickness of a Slab (Isotropic Scattering)

Consider a uniform slab, infinite in two dimensions. Let the units of distance be chosen so that $\sigma = 1$, and let the thickness of the slab be $2a$. The average number of neutrons emerging (isotropically) from a collision with a nucleus is c, as in §2.1b. It is desired to find the critical thickness of the slab for fixed c or, alternatively, the critical value of c for a fixed thickness. The method of solving the latter problem will be described here.

By combining equation (1.38), with the energy variable removed, and the considerations in §2.1c, the required one-speed integral equation is obtained, namely,

$$\phi(x) = \frac{1}{2}\int_{-a}^{a} E_1(|x - x'|)[c\phi(x') + Q(x')]\,dx'. \tag{6.93}$$

Since there is no independent source in the criticality problem, $Q(x') = 0$; hence, the integral equation is

$$\phi(x) = \frac{c}{2}\int_{-a}^{a} E_1(|x - x'|)\phi(x')\,dx'. \tag{6.94}$$

It is desired to find the eigenvalue c, actually the smallest eigenvalue c, for fixed a.

There are at least two reasons for using integral transport theory in this problem. First, because the integral equation involves the total neutron flux and the operator is truly self-adjoint. And second, the total flux is a function of only one variable, and so is simpler to work with than the angular flux.

In order to apply the theory developed in the preceding section, equation (6.94) may be written as

$$\frac{1}{c}\phi = \mathbf{L}\phi, \tag{6.95}$$

where the linear operator, $\mathbf{L}$, is now the integral operator defined by

$$\mathbf{L}\phi = \frac{1}{2}\int_{-a}^{a} E_1(|x - x'|)\phi(x')\,dx'. \tag{6.96}$$

The equation (6.95) resembles an α eigenvalue equation with $1/c$ replacing α/v.

Hence, by analogy with the variational equation (6.92) for α, it may be expected that $1/c$ could be found from the corresponding equation

$$\frac{1}{c} \simeq \frac{(\phi^\dagger, \mathbf{L}\phi)}{(\phi^\dagger, \phi)}$$

$$= \frac{(\phi, \mathbf{L}\phi)}{(\phi, \phi)}$$

since the total flux and its adjoint are now equal (§6.1h). Upon introducing the explicit form of $\mathbf{L}$ from equation (6.96), and the values of the inner products, which in this case are integrals over x from $-a$ to a, it is found that

$$\frac{1}{c} \simeq \frac{\frac{1}{2}\int_{-a}^{a}\int_{-a}^{a} E_1(|x - x'|)\phi(x)\phi(x')\,dx'\,dx}{\int_{-a}^{a} \phi^2(x)\,dx}. \tag{6.97}$$

Equation (6.97) is the required variational expression for $1/c$; it will now be shown that the value of $1/c$ derived from this equation is less than or equal to the exact value for all trial functions, ϕ. Consider equation (6.94) as an eigenvalue equation for the eigenvalue c_i and the eigenfunction ϕ_i, i.e.,

$$\phi_i(x) = \frac{c_i}{2}\int_{-a}^{a} E_1(|x - x'|)\phi_i(x')\,dx'. \tag{6.98}$$

This is a linear integral equation with a symmetric (and nondegenerate) kernel, i.e.,

$$E_1(|x - x'|) = E_1(|x' - x|),$$

which is simply another way of saying that the integral operator is self-adjoint. From the general theory of such equations,[21] it is known that there exist an infinite number of real positive eigenvalues $\{c_i\}$ with orthogonal eigenfunctions $\{\phi_i\}$.

Let the eigenvalues be ordered so that $c_0 < c_1 < c_2, \ldots$, etc.; then c_0 is the fundamental eigenvalue which is being sought. In addition, any well-behaved trial function may be expanded as a series of eigenfunctions; thus,

$$\phi(x) = \sum_{i=0}^{\infty} b_i\phi_i(x). \tag{6.99}$$

It will be assumed for convenience that the eigenfunctions are normalized so that

$$\int_{-a}^{a} \phi_i(x)\phi_j(x)\,dx = \delta_{ij}, \tag{6.100}$$

where δ_{ij} is the Kronecker delta. If the expansion of equation (6.99) is inserted into equation (6.97) and use is made of equation (6.100), it is found that

$$\frac{1}{c} = \sum_{i=0}^{\infty} \frac{1}{c_i} b_i^2 \Big/ \sum_{i=0}^{\infty} b_i^2 \leqslant \frac{1}{c_0}. \tag{6.101}$$

The inequality on the right arises from the fact that c_0 is the smallest eigenvalue.

It follows, therefore, that the value of $1/c$ obtained from equation (6.97) is always less than the desired value, $1/c_0$. Hence, a trial function with some free parameters may be introduced into equation (6.97) and the parameters varied so as to maximize $1/c$. For example, with a simple trial function

$$\phi(x) = 1 - \beta x^2,$$

having β as a variable parameter, it is possible to obtain values of c accurate to three or four significant figures.[25] The procedure is to insert this trial function into equation (6.97) and find the value of β for which the derivative with respect to β is zero. In addition, it should be verified that the stationary value is a maximum and not a minimum.

Critical Radius of a Sphere

For a sphere of radius a, the integral equation corresponding to equation (6.94) is derived from equation (1.41) as

$$r\phi(r) = \frac{c}{2}\int_{-a}^{a} E_1(|r - r'|)r'\phi(r')\,dr',$$

where $\phi(r) = \phi(-r)$. The variational expression for $1/c$, analogous to equation (6.97) for the slab, is then

$$\frac{1}{c} \simeq \frac{\frac{1}{2}\int_{-a}^{a}\int_{-a}^{a} E_1(|r - r'|)r'\phi(r')r\phi(r)\,dr'\,dr}{\int_{-a}^{a}[r\phi(r)]^2\,dr}. \tag{6.102}$$

As before, $1/c_0$ will be the upper limit of values of $1/c$ calculated from equation (6.102). By using a fourth-order trial function of the form

$$\phi(r) = 1 - \beta r^2 - \beta' r^4,$$

with β and β' as adjustable parameters, very accurate values of $1/c$ have been found. These formed the basis of the "exact" entries in Table 5.3 except for $c - 1 \ll 1$. The accuracy could be judged by the very small effect on $1/c$ of variations in β'.[26]

6.4e An Absorption Probability Problem

Another example of the application of variational methods is to a classical problem in one-speed theory. Suppose there are two uniform regions with an isotropic and uniform source in one region, e.g., a moderator; it is required to determine the absorptions in an adjacent region, e.g., a fuel element. This is the situation in computing the disadvantage factor[27] in a one-speed treatment of thermal neutrons. On the basis of the results in §2.7b, however, the source can

be taken in either of the two regions, since the reciprocity relationship of equation (2.101) shows how $P_{F\to M}$ can be determined if $P_{M\to F}$ is known, and vice versa. The calculation given below will, therefore, be concerned with the evaluation of $P_{F\to M}$, the probability that a neutron born in the fuel region will be absorbed in the surrounding moderator.

In §§2.8b, 2.8c, the foregoing considerations were used to describe collision (or absorption) probabilities in purely absorbing media. In the present treatment, this restriction is not necessary. The main objective here is to show that even when the original one-speed problem is not obviously self-adjoint, some elementary manipulations may serve to make it so.

Suppose, for simplicity, that the fuel region is a slab located within an infinite moderator region (Fig. 6.5). The total flux then satisfies the relation [cf. equation (6.93)]

$$\phi = \frac{1}{2}\int_{-\infty}^{\infty} E_1(|x - x'|)[c(x')\phi(x') + Q(x')]\,dx', \tag{6.103}$$

where $Q(x')$ is constant in the fuel and zero in the moderator; the values of c are c_F and c_M in fuel and moderator, respectively. Distances are measured in units of the mean free paths which are not necessarily the same in the two regions. Since all the neutrons must be absorbed either in the fuel or in the moderator, it follows that

$$P_{F\to M} = 1 - (1 - c_F)\frac{\bar{\phi}_F}{Q}, \tag{6.104}$$

where $\bar{\phi}_F$ is the average value of the flux in the fuel region, so that $(1 - c_F)\bar{\phi}_F/Q$ is the probability of neutron absorption in the fuel region. Hence, the problem will be solved if $\bar{\phi}_F$ can be determined.

There are two unfavorable aspects of equation (6.103): first, the integral kernel is not symmetric, since it contains $c(x')$, and second, Q appears in a

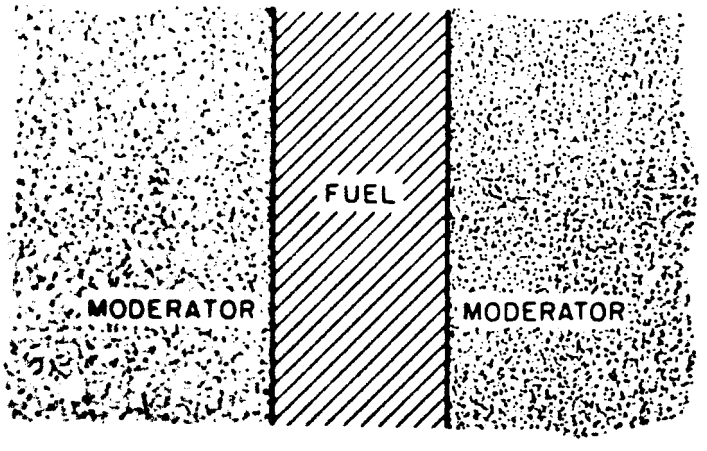

FIG. 6.5 FUEL SLAB IN INFINITE MODERATOR.

complicated manner. These difficulties can be avoided by introducing a symmetric function. Let

$$\psi(x) \equiv \frac{1}{\sqrt{c(x)}} [c(x)\phi(x) + Q(x)] \tag{6.105}$$

and

$$S(x) \equiv \frac{1}{\sqrt{c(x)}} Q(x), \tag{6.106}$$

and the symmetric function $K(x, x')$ is then defined by

$$K(x, x') = \delta(x - x') - \sqrt{c(x)}\,[\tfrac{1}{2}E_1(|x - x'|)\sqrt{c(x')}]. \tag{6.107}$$

If equations (6.105), (6.106), and (6.107) are introduced into equation (6.103), the result may be written as

$$\int_{-\infty}^{\infty} K(x, x')\psi(x')\,dx' = S(x). \tag{6.108}$$

This equation is of the general form $-\mathbf{L}\psi(x) = S(x)$, as in equation (6.84), where $S(x)$ is constant in the fuel and zero in the moderator. From equation (6.104), together with the average of equation (6.105) over the fuel region, it follows that

$$P_{\mathrm{F}\to\mathrm{M}} = \frac{1}{c_{\mathrm{F}}}\left[1 - (1 - c_{\mathrm{F}})\frac{\bar{\psi}_{\mathrm{F}}}{S}\right]. \tag{6.109}$$

Consider the variational functional, J_S, of equation (6.91), in the form

$$\mathrm{J}_S = \frac{\left[\int_{-\infty}^{\infty} \psi(x)S(x)\,dx\right]^2}{\int_{-\infty}^{\infty}\int_{-\infty}^{\infty} \psi(x')K(x, x')\psi(x)\,dx'\,dx}.$$

From equation (6.108), the exact value of J_S, i.e., J_0, is

$$\mathrm{J}_0 = \int_{-\infty}^{\infty} \psi(x)S(x)\,dx = S\int_{\mathrm{Fuel}} \psi(x)\,dx = S\bar{\psi}_{\mathrm{F}}x_{\mathrm{F}},$$

where x_{F} is the thickness of the fuel region, i.e.,

$$\int_{\mathrm{Fuel}} dx = x_{\mathrm{F}}.$$

It can be shown[28] that J_S will always be less than J_0; hence, a trial function may be chosen and variations made so as to maximize J_S, and thus yield the best estimate of $\bar{\psi}_{\mathrm{F}}$. By using fairly simple but realistic trial functions, e.g., a constant in the fuel region and a diffusion theory solution in the moderator, and varying their relative magnitudes it is possible to obtain an accurate value for $P_{\mathrm{F}\to\mathrm{M}}$ from equation (6.109).[29]

It should be mentioned that a problem like the one treated above can be solved very easily by using a computer code based on the discrete ordinates approximation. It is of interest, however, to see how the variational method can provide an alternative and accurate solution.

6.4f Discontinuous Trial Functions

In the foregoing, the admissible trial functions Φ and $\Phi^\dagger$ have been restricted to those satisfying the boundary and continuity conditions, for only then will $(\Phi^\dagger, \mathbf{L}\Phi) = (\Phi, \mathbf{L}^\dagger\Phi^\dagger)$; otherwise boundary and discontinuity terms will remain as will now be seen. Since it is frequently convenient to permit trial functions which do not satisfy the boundary and continuity conditions, although the exact functions do, the consequences must be considered.[30] Such a situation might arise if a P_1 flux estimate were to be used with the exact transport operator $\mathbf{L}$, or if a piecewise flux estimate were made that could not satisfy the continuity condition.

The time-independent transport operator, $\mathbf{L}$, and its adjoint $\mathbf{L}^\dagger$ are defined by equations (6.5) and (6.7), respectively, as

$$-\mathbf{L}\Phi(\mathbf{r}, \Omega, E) = \Omega\cdot\nabla\Phi + \sigma\Phi - \iint \sigma f(\mathbf{r}; \Omega', E' \to \Omega, E) \times \Phi(\mathbf{r}, \Omega', E')\, d\Omega'\, dE' \quad (6.110)$$

and

$$-\mathbf{L}^\dagger\Phi^\dagger(\mathbf{r}, \Omega, E) = -\Omega\cdot\nabla\Phi^\dagger + \sigma\Phi^\dagger - \iint \sigma f(\mathbf{r}; \Omega, E \to \Omega', E') \times \Phi^\dagger(\mathbf{r}, \Omega', E')\, d\Omega'\, dE'. \quad (6.111)$$

If trial functions, with discontinuities assumed to exist at some interior surfaces A_i, are inserted into equations (6.110) and (6.111), the derivative terms become infinite at these surfaces. When $\mathbf{L}\Phi$ is integrated in an inner product, the integral of the derivative then contributes a jump (or discontinuity) condition on A_i.

In order to see this, multiply equation (6.110) by $\Phi^\dagger$ and equation (6.111) by Φ, subtract and integrate over the range of variables; all terms on the right, with the exception of the gradient terms, will cancel, as shown in §6.1c. Because the boundary and continuity conditions used before are not applicable, the gradient terms will remain and the result is

$$(\Phi^\dagger, -\mathbf{L}\Phi) = (\Phi, -\mathbf{L}^\dagger\Phi^\dagger) + (\Phi^\dagger, \Omega\cdot\nabla\Phi) + (\Phi, \Omega\cdot\nabla\Phi^\dagger). \quad (6.112)$$

To convert the last two terms to a surface integral, the volume integral in the inner product may be interpreted as a sum of integrals over each of the volumes, V_i, within which Φ and $\Phi^\dagger$ are continuous. For each such volume

$$\int_{V_i} dV \iint (\Phi^\dagger\Omega\cdot\nabla\Phi + \Phi\Omega\cdot\nabla\Phi^\dagger)\, d\Omega\, dE$$

$$= \int_{V_i} dV \iint (\nabla\cdot\Omega\Phi\Phi^\dagger)\, d\Omega\, dE = \int_{A_i} dA \iint \hat{\mathbf{n}}\cdot\Omega\Phi\Phi^\dagger\, d\Omega\, dE. \quad (6.113)$$

By adding the contributions for each volume, a contribution is obtained from each surface A_i equal to $\hat{\mathbf{n}}\cdot\boldsymbol{\Omega}$ multiplied by the discontinuity (or jump) in $\Phi\Phi^\dagger$, which may be denoted by

$$\text{Discontinuity} = [\Phi\Phi^\dagger(+) - \Phi\Phi^\dagger(-)],$$

where the plus $(+)$ side has $\hat{\mathbf{n}}$ as an outward normal and the minus $(-)$ side as an inward normal. Use of equation (6.113) for each individual volume in connection with equation (6.112) then gives for the whole volume with a bounding surface A_B,

$$(\Phi^\dagger, -\mathbf{L}\Phi) = (\Phi, -\mathbf{L}^\dagger\Phi^\dagger) + \int_{A_B} dA \iint \hat{\mathbf{n}}\cdot\boldsymbol{\Omega}\Phi\Phi^\dagger\, d\boldsymbol{\Omega}\, dE + \sum_i \int_{A_i} dA \iint \hat{\mathbf{n}}\cdot\boldsymbol{\Omega}[\Phi\Phi^\dagger(+) - \Phi\Phi^\dagger(-)]\, d\boldsymbol{\Omega}\, dE. \quad (6.114)$$

Equation (6.114) is a generalization of equation (6.6) for trial functions Φ and $\Phi^\dagger$ which do not satisfy the boundary or continuity conditions. It should be recalled, however, that in evaluating the volume integrals in the inner products, the integration is carried over each of the volumes in which Φ and $\Phi^\dagger$ are continuous and the results are then summed. The A_i surfaces of discontinuity then appear only as surface terms. Alternatively, the surface terms could be included in the prescription for evaluating $(\Phi^\dagger, -\mathbf{L}\Phi)$.

To allow for trial functions of the type under consideration, it would appear that the surface terms could be subtracted from the functional in equation (6.86). Although this would give an error in $(Q^\dagger, \Phi)$ equal to $(\delta\Phi^\dagger, \mathbf{L}\,\delta\Phi)$ plus surface terms proportional to $\delta\Phi^\dagger\,\delta\Phi$, it would not yield $(Q^\dagger, \Phi) = (\Phi^\dagger, Q)$ to this order of accuracy. A more symmetrical functional can be found by using the identity

$$\Phi^\dagger(+)\Phi(+) - \Phi^\dagger(-)\Phi(-) \equiv \bar{\Phi}^\dagger[\Phi(+) - \Phi(-)] + \bar{\Phi}[\Phi^\dagger(+) - \Phi^\dagger(-)], \quad (6.115)$$

where $\bar{\Phi}$ and $\bar{\Phi}^\dagger$ are the average flux and adjoint, respectively, at a surface of discontinuity, i.e.,

$$\bar{\Phi} = \tfrac{1}{2}[\Phi(+) + \Phi(-)] \quad \text{and} \quad \bar{\Phi}^\dagger = \tfrac{1}{2}[\Phi^\dagger(+) + \Phi^\dagger(-)].$$

If equation (6.115) is substituted into equation (6.114), it is found that

$$(\Phi^\dagger, -\mathbf{L}\Phi) - \int_{A_B} dA \iint_{\hat{\mathbf{n}}\cdot\boldsymbol{\Omega}<0} d\boldsymbol{\Omega}\, dE(\hat{\mathbf{n}}\cdot\boldsymbol{\Omega})\Phi\Phi^\dagger - \sum_i \int_{A_i} dA \iint d\boldsymbol{\Omega}\, dE(\hat{\mathbf{n}}\cdot\boldsymbol{\Omega})\bar{\Phi}^\dagger[\Phi(+) - \Phi(-)]$$

$$= (\Phi, -\mathbf{L}^\dagger\Phi^\dagger) + \int_{A_B} dA \iint_{\hat{\mathbf{n}}\cdot\boldsymbol{\Omega}>0} d\boldsymbol{\Omega}\, dE(\hat{\mathbf{n}}\cdot\boldsymbol{\Omega})\Phi\Phi^\dagger + \sum_i \int_{A_i} dA \iint d\boldsymbol{\Omega}\, dE(\hat{\mathbf{n}}\cdot\boldsymbol{\Omega})\bar{\Phi}[\Phi^\dagger(+) - \Phi^\dagger(-)]. \quad (6.116)$$

By using this result, the functional

$$J' = (Q^\dagger, \Phi) + (\Phi^\dagger, Q) + (\Phi^\dagger, \mathbf{L}\Phi) + \int_{A_B} dA \iint\limits_{\hat{\mathbf{n}}\cdot\Omega<0} d\Omega\, dE(\hat{\mathbf{n}}\cdot\Omega)\Phi\Phi^\dagger$$

$$+ \sum_i \int_{A_i} dA \iint d\Omega\, dE(\hat{\mathbf{n}}\cdot\Omega)\bar{\Phi}^\dagger[\Phi(+) - \Phi(-)] \quad (6.117)$$

is derived, which gives

$$J' = J_0 + (\delta\Phi^\dagger, \mathbf{L}\,\delta\Phi) + \text{surface terms proportional to } \delta\Phi^\dagger\,\delta\Phi, \quad (6.118)$$

even for trial functions which are discontinuous and do not satisfy the boundary conditions. In obtaining equation (6.118), it has been taken into consideration that the exact solutions Φ_0 and $\Phi_0^\dagger$ do satisfy the boundary and continuity conditions. From equation (6.116), it can be shown that the functional J' is identical with

$$J' = (Q^\dagger, \Phi) + (\Phi^\dagger, Q) + (\Phi, \mathbf{L}^\dagger\Phi^\dagger) - \int_{A_B} dA \iint\limits_{\hat{\mathbf{n}}\cdot\Omega>0} d\Omega\, dE(\hat{\mathbf{n}}\cdot\Omega)\Phi\Phi^\dagger$$

$$- \sum_i \int_{A_i} dA \iint d\Omega\, dE(\hat{\mathbf{n}}\cdot\Omega)\bar{\Phi}[\Phi^\dagger(+) - \Phi^\dagger(-)]. \quad (6.119)$$

For applications of the functionals under consideration, the literature should be consulted.[31]

6.4g The J Functional as a Lagrangian

An entirely different use of variational functionals is based on the fact that the J functional can be considered as a Lagrangian function for the system, in the sense that if it is required that the functional be stationary for small but arbitrary variations of Φ and $\Phi^\dagger$, then equations can be found which are satisfied by Φ and $\Phi^\dagger$. It will be seen that this procedure leads to a systematic way of deriving approximations to the neutron transport equation.[32]

According to Hamilton's principle in mechanics, the time integral of the Lagrangian function, between fixed end points, should be stationary when the trajectory of the system is varied about the actual trajectory by small but arbitrary amounts. From this principle, equations can be derived that must be satisfied by the system along the actual trajectory. These are called the Euler equations which, for a simple mechanical system, are simply Newton's laws of motion.[33]

Consider the J functional, given by equation (6.86), for the inhomogeneous problem, i.e.,

$$J = (Q^\dagger, \Phi) + (\Phi^\dagger, Q) + (\Phi^\dagger, \mathbf{L}\Phi), \quad (6.120)$$

where the trial functions Φ and $\Phi^\dagger$ are well behaved in the sense that they satisfy the boundary and continuity conditions. If small but arbitrary variations are

made in Φ and $\Phi^\dagger$, with the varied functions still being well behaved, then, to the first order in small quantities, δJ, the variation in J, is given by

$$\delta J = (Q^\dagger, \delta\Phi) + (\delta\Phi^\dagger, Q) + (\delta\Phi, \mathbf{L}^\dagger\Phi^\dagger) + (\delta\Phi^\dagger, \mathbf{L}\Phi). \tag{6.121}$$

Since $\delta\Phi$ and $\delta\Phi^\dagger$ are arbitrary, it is apparent that δJ can be zero, i.e., J made stationary or independent of the variations $\delta\Phi$ and $\delta\Phi^\dagger$, only if

$$-\mathbf{L}\Phi = Q \quad \text{and} \quad -\mathbf{L}^\dagger\Phi^\dagger = Q^\dagger, \tag{6.122}$$

which are the transport and adjoint equations satisfied by the exact values of Φ and $\Phi^\dagger$. These are, in the calculus of variations, the Euler equations. Thus, the requirement that J be stationary can be satisfied only if Φ and $\Phi^\dagger$ are solutions of the transport and adjoint equations, respectively.

It is possible to relax the requirement that Φ and $\Phi^\dagger$ are well behaved and thereby allow discontinuous trial functions which do not satisfy the boundary conditions. The functionals given by equations (6.117) and (6.119) are used and in order to make $\delta J = 0$, the trial functions should not only satisfy equations (6.122) wherever they are continuous, but they should also satisfy the boundary conditions and be continuous on every surface A_i. To show that this is so, $\delta J'$ is obtained from equation (6.117) and then the expression for the term $(\Phi^\dagger, \mathbf{L}\,\delta\Phi)$ is derived from equation (6.116). By setting all the coefficients of $\delta\Phi$ and $\delta\Phi^\dagger$ equal to zero, equations (6.122) are obtained plus the boundary and continuity conditions on Φ and $\Phi^\dagger$.

The conclusion to be drawn, therefore, is that the requirement that the functional be stationary for small but arbitrary variations in Φ and $\Phi^\dagger$ is equivalent to the transport and adjoint equations (6.122), together with the boundary and continuity conditions. Of course, only the exact flux Φ_0 and adjoint $\Phi_0^\dagger$ can satisfy all these requirements. Nevertheless, the result is useful because it is possible to insert approximate functions for Φ and $\Phi^\dagger$, and then to employ the Euler equations to deduce, in a systematic manner, approximate equations which should be satisfied by the flux and adjoint. When approximate values of the flux and adjoint are used, however, the possible variations are no longer completely arbitrary but are restricted to those allowed by the particular functional forms assumed for Φ and $\Phi^\dagger$.

The general philosophy underlying the foregoing approach, which will be illustrated below, is as follows. If the functional J is made stationary with respect to all small variations of flux and adjoint, then the corresponding values of Φ and $\Phi^\dagger$ must be the exact solutions to the transport problem. On the other hand, if J is made stationary with respect to a limited class of variations, then Φ and $\Phi^\dagger$ may be the "best" with respect to that class of variations. In one-speed theory, this concept of a "best" solution can be made precise since, as seen earlier, the exact value of J is an upper or lower limit to the estimated value; hence, the most accurate estimate of J is always a stationary (maximum or minimum) value. For more general (energy-dependent) problems the mathe-

matical qualification is less clear. Nevertheless, the variational method is intuitively attractive, and it has been found to be useful in practice.

Finally, it is of interest to note that the equation containing the approximate $\Phi^\dagger$ will indeed be adjoint to that for the approximate Φ, a result which is frequently not true for the equations derived in a more straightforward way.

6.4h Variational Derivation of Multigroup Equations

To illustrate the procedure outlined above, the variational principle will be used to derive the P_1 multigroup equations. It will be seen that the equations satisfied by the group fluxes and adjoints have the expected form, but that the group cross sections are defined in terms of a bilinear weighting by both flux and adjoint, instead of by the flux alone as in Chapter 4. Moreover, once the multigroup equations have been solved for the group fluxes and adjoints, the same variational expression can be used to find the flux and adjoints as functions of energy within a group. The group constants can then be recomputed, so that the within-group spectra, group cross sections, and group fluxes can be found by iteration in a self-consistent manner.

For plane geometry, consider the trial functions

$$\Phi(x, \mu, E) \simeq \phi_{0,g}(x)\psi_{0,g}(E) + 3\mu\phi_{1,g}(x)\psi_{1,g}(E) \tag{6.123}$$

and

$$\Phi^\dagger(x, \mu, E) \simeq \phi^\dagger_{0,g}(x)\psi^\dagger_{0,g}(E) + 3\mu\phi^\dagger_{1,g}(x)\psi^\dagger_{1,g}(E), \tag{6.124}$$

where

$$E_g \leqslant E \leqslant E_{g-1},$$

so that g is a group index which changes as the energy changes across a group boundary. The trial functions are seen to be of P_1 form in their dependence on μ [cf. equation (3.42)], whereas those parts of the trial function that represent the total flux ($4\pi\phi_{0g}\psi_{0g}$) and current ($4\pi\phi_{1g}\psi_{1g}$) are taken to be separable functions of position and energy within a group. It is assumed, for the present, that ψ and $\psi^\dagger$ are known functions of the energy; they may be obtained, for example, from infinite medium or B_1 calculations (§4.5c). These within-group spectra will often be functions of space in a multiregion system, but for simplicity such explicit dependence on the region will not be included. The normalization of these spectra is somewhat arbitrary and a convenient system is the following:

$$\int_g \psi_{0,g}(E)\, dE = 1 \tag{6.125}$$

$$\int_g \psi_{0,g}(E)\psi^\dagger_{0,g}(E)\, dE = 1 \tag{6.126}$$

$$\int_g \psi_{0,g}(E)\psi^\dagger_{1,g}(E)\, dE = 1 \tag{6.127}$$

$$\int_g \psi^\dagger_{0,g}(E)\psi_{1,g}(E)\, dE = 1 \tag{6.128}$$

From equation (6.125), it is seen that by this normalization $\phi_{0,g}(x)$ is simply $1/4\pi$ times the total flux of neutrons in group g. If the ψ and $\psi^\dagger$ functions do not vary greatly with energy within a group, it follows that

$$\psi_{0,g} \simeq \psi_{1,g} \simeq \frac{1}{\Delta E_g}$$

and

$$\psi^\dagger_{0,g} \simeq \psi^\dagger_{1,g} \simeq 1.$$

If the within-group spectra, ψ and $\psi^\dagger$, are assumed to be known, the equations satisfied by the group fluxes and adjoints can be determined from the variational principle, i.e., by inserting equations (6.123) and (6.124) into equation (6.120) for J and requiring that J be stationary for small but arbitrary variations in $\phi_{0,g}$, $\phi_{1,g}$, $\phi^\dagger_{0,g}$, and $\phi^\dagger_{1,g}$, as will now be shown.

For plane geometry, the transport operator is

$$-\mathbf{L} = \mu \frac{\partial}{\partial x} + \sigma(x, E) - 2\pi \iint \sigma f(x; \mu', E' \to \mu, E)\, d\mu'\, dE',$$

so that by equation (6.123),

$$\begin{aligned} -\mathbf{L}\Phi = \left[\mu \frac{\partial}{\partial x} + \sigma(x, E)\right][\phi_{0g}(x)\psi_{0,g}(E) + 3\mu\phi_{1,g}(x)\psi_{1,g}(E)] \\ - \sum_{g'} \int_{g'} [\sigma_0(x; E' \to E)\phi_{0,g'}(x)\psi_{0,g'}(E) \\ + 3\mu\sigma_1(x; E' \to E)\phi_{1,g'}(x)\psi_{1,g'}(E)]\, dE', \end{aligned} \tag{6.129}$$

where σ_0 and σ_1 are the usual Legendre components of the scattering cross section [cf. equation (4.4)]. If equations (6.123) and (6.129) are substituted into the definition of the inner product $(\Phi^\dagger, \mathbf{L}\Phi)$, i.e.,

$$(\Phi^\dagger, \mathbf{L}\Phi) = \int dx \int dE \int_{-1}^{1} \Phi^\dagger\, \mathbf{L}\Phi\, d\mu,$$

the integrations over μ can be performed immediately to give

$$\begin{aligned} \tfrac{1}{2}(\Phi^\dagger, \mathbf{L}\Phi) = -\int dx \int dE \Big\{ \phi^\dagger_{0,g}(x)\psi^\dagger_{0,g}(E)\Big[\sigma(x, E)\phi_{0,g}(x)\psi_{0,g}(E) \\ + \frac{d}{dx}\{\phi_{1,g}(x)\psi_{1,g}(E)\} - \sum_{g'} \int_{g'} \sigma_0(x; E' \to E)\phi_{0,g'}(x)\psi_{0,g'}(E')\, dE'\Big] \\ + \phi^\dagger_{1,g}(x)\psi^\dagger_{1,g}(E)\Big[3\sigma(x, E)\phi_{1,g}(x)\psi_{1,g}(E) + \frac{d}{dx}\{\phi_{0,g}(x)\psi_{0,g}(E)\} \\ - 3\sum_{g'} \int_{g'} \sigma_1(x; E' \to E)\phi_{1,g'}(x)\psi_{1,g'}(E')\, dE'\Big]\Big\}. \end{aligned} \tag{6.130}$$

In addition, the integration can be performed over each energy group since $\psi_{0,g}(E)$, $\psi_{1,g}(E)$, $\psi^\dagger_{0,g}(E)$, and $\psi^\dagger_{1,g}(E)$ are assumed to be known functions of the energy.

If this result is inserted into the functional J, as defined by equation (6.120), the functions $\phi^\dagger_{0,g}(x)$ and $\phi^\dagger_{1,g}(x)$ may be varied arbitrarily and the Euler equations obtained by setting the coefficients of $\delta\phi^\dagger_{0,g}$ and $\delta\phi^\dagger_{1,g}$ equal to zero. By using the normalizations in equations (6.125)–(6.128), the results may be written in typical multigroup form [compare, for example, equations (4.30) and (4.31)]; thus, by setting the coefficient of $\delta\phi^\dagger_{0,g}$ equal to zero it is found that

$$\frac{d}{dx}[\phi_{1,g}(x)] + \sigma_{0,g}\phi_{0,g}(x) = \sum_{g'} \sigma_{0,g'\to g}(x)\phi_{0,g'}(x) + Q_{0,g}(x) \tag{6.131}$$

and by setting the coefficient of $\delta\phi^\dagger_{1,g}$ equal to zero,

$$\frac{d}{dx}[\phi_{0,g}(x)] + 3\sigma_{1,g}\phi_{1,g}(x) = 3\sum_{g'} \sigma_{1,g'\to g}(x)\phi_{1,g'}(x) + 3Q_{1,g}(x), \tag{6.132}$$

where

$$Q_{0,g}(x) \equiv \frac{1}{2}\int_g \psi^\dagger_{0,g}(E)\,dE \int_{-1}^{1} Q(x, \mu, E)\,d\mu \tag{6.133}$$

$$Q_{1,g}(x) \equiv \frac{1}{2}\int_g \psi^\dagger_{1,g}(E)\,dE \int_{-1}^{1} \mu Q(x, \mu, E)\,d\mu \tag{6.134}$$

and the group constants are defined by

$$\sigma_{i,g}(x) \equiv \int_g \sigma(x, E)\psi^\dagger_{i,g}(E)\psi_{i,g}(E)\,dE \qquad (i = 0, 1) \tag{6.135}$$

$$\sigma_{i,g'\to g}(x) \equiv \int_g dE \int_{g'} \sigma_i(x; E' \to E)\psi_{i,g'}(E')\psi^\dagger_{i,g}(E)\,dE' \qquad (i = 0, 1). \tag{6.136}$$

Comparison with the results in Chapter 4 shows that equations (6.131) and (6.132) are identical in form with the multigroup P_1 equations, but the group constants are now defined with both flux and adjoint (importance) weighting.

By returning to the functional J and varying $\phi_{0,g}$ and $\phi_{1,g}$, the adjoint equations

$$-\frac{d}{dx}[\phi^\dagger_{1,g}(x)] + \sigma_{0,g}\phi^\dagger_{0,g}(x) = \sum_{g'} \sigma_{0,g\to g'}\phi^\dagger_{0,g'}(x) + Q^\dagger_{0,g}(x) \tag{6.137}$$

and

$$-\frac{d}{dx}[\phi^\dagger_{0,g}(x)] + 3\sigma_{1,g}\phi^\dagger_{1,g}(x) = 3\sum_{g'} \sigma_{1,g\to g'}\phi^\dagger_{1,g'}(x) + 3Q^\dagger_{1,g}(x) \tag{6.138}$$

may be obtained; $Q^\dagger_{0,g}$ and $Q^\dagger_{1,g}$ are defined as in equations (6.133) and (6.134), with each Q being replaced by its adjoint $Q^\dagger$ and each $\psi^\dagger$ by the corresponding ψ. The group constants are the same as in equations (6.135) and (6.136). Thus,

equations (6.137) and (6.138) are clearly adjoint to equations (6.131) and (6.132), respectively (cf. §6.2c). For a generalization to time-dependent problems (with delayed neutrons), see Ref. 34.

Some comment should be made concerning the boundary conditions in connection with the use of equation (6.130) for $(\Phi^\dagger, \mathbf{L}\Phi)$ in the derivation of equations (6.137) and (6.138). A partial integration over x was required in order to transfer the d/dx operation from the flux in equation (6.130) to the adjoint. Although this leaves an integral, which may be reduced by the normalization conditions in equations (6.127) and (6.128), i.e.,

$$\int_g [\phi^\dagger_{0,g}(x)\psi^\dagger_{0,g}(E)\phi_{1,g}(x)\psi_{1,g}(E) + \phi^\dagger_{1,g}(x)\psi^\dagger_{1,g}(E)\phi_{0,g}(x)\psi_{0,g}(E)]\,dE = \phi^\dagger_{0,g}(x)\,\phi_{1,g}(x) + \phi^\dagger_{1,g}(x)\,\phi_{0,g}(x), \quad (6.139)$$

to be evaluated at the boundaries, it has been omitted in obtaining equations (6.137) and (6.138). This omission could be justified, however, if the boundary condition $\phi_{0,g} = \phi^\dagger_{0,g} = 0$ were used; such a boundary condition for the flux is familiar from Chapter 4. Further reference to this matter is made below.

Relatively little use has yet been made of bilinearly (flux and adjoint) averaged group constants, primarily because the group adjoints must be estimated in addition to the group fluxes. When the bilinear averaging has been used, however, it seems to be superior to simple flux averaging, at least for problems involving only a few groups.[35] When a large number of groups can be employed, the adjoint weighting is less important, because the adjoint function will not vary significantly across a group.

The trial functions in equations (6.123) and (6.124) do not satisfy transport theory boundary conditions. If they are used in the functional J′ of equation (6.117), it is found that more requirements are placed on the functions than can be satisfied. For example, the boundary condition requires that

$$\int_0^1 \mu\Phi\,d\mu = \int_0^1 \mu^2\Phi\,d\mu = 0.$$

For the one-speed problem, this redundancy in boundary conditions can be removed and an excellent value for the extrapolation distance can be obtained by restricting the trial functions to those for which

$$\frac{\phi_0(x)}{\phi_1(x)} = -\frac{\phi^\dagger_0(x)}{\phi^\dagger_1(x)} \quad (6.139a)$$

at the boundary.[36] For the energy-dependent case, use of equation (6.139a) for each group would make the boundary terms in equation (6.139) equal to zero and is therefore a natural choice.

6.4i Self-Consistent Determination of Group Constants

As just seen, multigroup equations have been obtained from equation (6.130) by considering the $\psi(E)$ functions to be known, integrating over a group, and then

deriving the Euler equations satisfied by the $\phi(x)$ functions. Once the multigroup equations have been solved, however, so that the functions $\phi_{0,g}(x)$, $\phi_{1,g}(x)$, $\phi^{\dagger}_{0,g}(x)$, and $\phi^{\dagger}_{1,g}(x)$ are known, the procedure can be reversed. Starting with equation (6.130) again, the $\phi(x)$ functions can be treated as known and integration carried over a space region, which need not coincide with the original choice. The Euler equations satisfied by the $\psi(E)$ functions can then be determined; from these, the within-group spectra, i.e., the $\psi(E)$ functions, can be obtained. This process could be iterated to obtain within-group spectra, group constants, and group fluxes in a self-consistent manner. Moreover, during the iteration the dependence of the results on the number of energy groups and space regions, within which the $\psi(E)$ functions are defined, could be explored.

For example, suppose that $\psi^{\dagger}_{0,g}(E)$ and $\psi^{\dagger}_{1,g}(E)$ in the functional J are varied and, using equation (6.130), the coefficients of the variation are set equal to zero. Upon integration over some space region R it is found that

$$Q_{0,g}(E) - \tilde{\sigma}_0(E)\psi_{0,g}(E) - \gamma_{1,g}\psi_{1,g}(E) + \sum_{g'} \int_{g'} \tilde{\sigma}_{0,g'}(E' \to E)\psi_{0,g'}(E')\, dE' = 0 \quad (6.140)$$

and

$$3Q_{1,g}(E) - 3\tilde{\sigma}_1(E)\psi_{1,g}(E) - \gamma_{0,g}\psi_{0,g}(E) + 3\sum_{g'} \int_{g'} \tilde{\sigma}_{1,g'}(E' \to E)\psi_{1,g'}(E')\, dE' = 0, \quad (6.141)$$

where

$$Q_{i,g}(E) \equiv \int_R \phi^{\dagger}_{i,g}(x) \int_{-1}^{1} \tfrac{1}{2} P_i(\mu) Q(x, \mu, E)\, d\mu\, dx \qquad (i = 0, 1)$$

$$\tilde{\sigma}_i(E) \equiv \int_R \phi^{\dagger}_{i,g}(x)\sigma(x, E)\phi_{i,g}(x)\, dx \qquad (i = 0, 1)$$

$$\tilde{\sigma}_{i,g'}(E' \to E) \equiv \int_R \phi^{\dagger}_{i,g}(x)\sigma_i(x; E' \to E)\phi_{i,g'}(x)\, dx \qquad (i = 0, 1)$$

$$\gamma_{1,g} \equiv \int_R \phi^{\dagger}_{0,g}(x) \frac{d}{dx} [\phi_{1,g}(x)]\, dx$$

$$\gamma_{0,g} \equiv \int_R \phi^{\dagger}_{1,g}(x) \frac{d}{dx} [\phi_{0,g}(x)]\, dx.$$

From equations (6.140) and (6.141), it is seen that $\psi_{0,g}(E)$ and $\psi_{1,g}(E)$ are the solutions of two coupled integral equations. Except for the coupling term containing $\gamma_{1,g}$, equation (6.140) is similar to an expression for the neutron energy spectrum in an infinite medium. In fact, since the cross sections will, as a rule, be independent of x, throughout any one region R, the cross sections $\tilde{\sigma}_0$ and $\tilde{\sigma}_{0,g}$.

will have their infinite medium values, except for normalization constants which are related to the choice of normalization in equations (6.125)–(6.128). The integral equations (6.140) and (6.141) can be solved numerically to yield the within-group spectra $\psi(E)$ to any desired accuracy, and so a self-consistent method is available for determining them from the group fluxes.

To appreciate the significance of the $\gamma_{1,g}$ term in equation (6.140), the conservation relation of equation (1.17) may be written, for the time-independent situation, as

$$Q(\mathbf{r}, E) - \sigma\phi(\mathbf{r}, E) - \nabla\cdot\mathbf{J}(\mathbf{r}, E) + \int \sigma' f\phi'\, dE' = 0. \tag{6.142}$$

If this is integrated over the space region R, there is then a precise correspondence between the first, second, and fourth terms of the resulting expression with the corresponding terms of equation (6.140). The third term in equation (6.142) becomes

$$\int_R \nabla\cdot\mathbf{J}(\mathbf{r}, E)\, dV = \int_{\substack{\text{Surface}\\ \text{of } R}} \hat{\mathbf{n}}\cdot\mathbf{J}(\mathbf{r}, E)\, dA = \text{net leakage out of } R.$$

Hence, the term $\gamma_{1,g}\psi_{1,g}(E)$ in equation (6.140) is an approximation to the energy-dependent leakage of neutrons out of the region R. An analogous, but more complicated, interpretation may be given to the coupling term $\gamma_{0,g}\psi_{0,g}(E)$ in equation (6.141). Applications have been made of these considerations.[37]

6.4j Other Applications of Variational Methods

It has been seen that variational methods provide a means for obtaining approximations to the neutron transport equation in a systematic manner. The same general approach can be used to study a number of physically plausible approximations to the neutron flux that would otherwise be difficult to formulate. Four situations of interest are outlined below.

First, it may be possible to express the flux in a three-dimensional system as a product of solutions for one- and two-dimensional systems.[38] Second, an attempt could be made to expand the angular flux near boundaries by means of specially tailored functions or by unusual combinations of expansions.[39] Third, near a temperature discontinuity, the thermal flux might be expanded as the sum of two infinite medium distributions appropriate to the hotter and colder regions, respectively, and then the spatial dependence of the coefficients of the two spectra may be determined.[40] Finally, solutions to time-dependent problems could be synthesized, using different space-dependent functions in different time intervals.[41] These and other applications of variational methods are reviewed in Ref. 42.

The solution of geometrically complicated two- or three-dimensional problems, such as often occur in reactors, by direct multigroup methods is hardly

possible at present. The synthesis of such solutions as products or other superpositions of more elementary solutions is, therefore, of great practical interest. The procedure will be illustrated by considering the simplest case.[43]

Suppose it is required to solve a one-speed, diffusion theory, criticality problem in two-dimensional rectangular geometry by combining one-dimensional solutions. If the coordinates are taken as x, y, the diffusion equation may be written as

$$\mathbf{L}\phi = -\nabla \cdot D(x, y)\nabla\phi(x, y) + \sigma(x, y)\phi(x, y) = 0, \tag{6.143}$$

with the flux and *all trial functions* assumed to be zero on some rectangular boundary. It can be shown from equation (6.143) that, as expected for a one-speed problem, $\mathbf{L}$ is self-adjoint, and that

$$(\phi, \mathbf{L}\phi) = \int dx \int dy[D(x, y)(\nabla\phi)^2 + \sigma(x, y)\phi^2(x, y)]. \tag{6.144}$$

It is required to express $\phi(x, y)$ as a product of two trial functions, namely,

$$\phi(x, y) = \phi_1(x)\phi_2(y),$$

so that equation (6.144) becomes

$$(\phi, \mathbf{L}\phi) = \int dx \int dy \left[D\left\{\phi_1^2\left(\frac{d\phi_2(y)}{dy}\right)^2 + \phi_2^2\left(\frac{d\phi_1(x)}{dx}\right)^2\right\} + \sigma\phi_1^2\phi_2^2\right].$$

Suppose $\phi_1(x)$ is varied and the coefficients of $\delta\phi_1(x)$ are set equal to zero; an Euler equation to be satisfied by $\phi_1(x)$ is obtained. In a similar manner an Euler equation can be derived for $\phi_2(x)$. These equations are

$$\left.\begin{aligned} &-\frac{d}{dx}\left[D_1(x)\frac{d\phi_1(x)}{dx}\right] + [\sigma_1(x) + D_1(x)B_1^2(x)]\phi_1(x) = 0 \\ &\text{and} \\ &-\frac{d}{dy}\left[D_2(y)\frac{d\phi_2(y)}{dy}\right] + [\sigma_2(y) + D_2(y)B_2^2(y)]\phi_2(y) = 0 \end{aligned}\right\} \tag{6.145}$$

where

$$\left.\begin{aligned} &D_1(x) = \int \phi_2^2(y)D(x, y)\,dy \quad \text{and} \quad D_2(y) = \int \phi_1^2(x)D(x, y)\,dx \\ &\sigma_1(x) = \int \phi_2^2(y)\sigma(x, y)\,dy \quad \text{and} \quad \sigma_2(y) = \int \phi_1^2(x)\sigma(x, y)\,dx \\ &D_1(x)B_1^2(x) = \int D(x, y)\left[\frac{d\phi_2(y)}{dy}\right]^2 dy \\ &\text{and} \\ &D_2(y)B_2^2(y) = \int D(x, y)\left[\frac{d\phi_1(x)}{dx}\right]^2 dx. \end{aligned}\right\} \tag{6.146}$$

The equations (6.145) are seen to have the simple form of one-dimensional diffusion equations with the added terms DB^2 which may be interpreted as representing neutron leakages in the suppressed direction. In simple cases, B_1^2 may be related to the buckling associated with the y dependence of the flux. Suppose, for example, that all the cross sections are constant and

$$\phi_2(y) = \sqrt{\frac{2}{y_0}} \cos \frac{\pi y}{y_0},$$

so that the flux vanishes at $y = \pm y_0/2$, and the normalization is such that

$$\int_{-y_0/2}^{y_0/2} \phi_2^2(y)\, dy = 1.$$

It is then found that $\sigma_1 = \sigma$ and $D_1 = D$; furthermore,

$$D_1 B_1^2 = D \left(\frac{\pi}{y_0}\right)^2,$$

indicating that B_1^2 is the buckling associated with the y direction. Similarly, B_2^2 is the buckling associated with the x direction.

The equations (6.145) and (6.146) have been solved in a recursive manner. A value of $\phi_2(y)$ is postulated or, more simply, σ_1, D_1, and B_1^2 are postulated, and a solution is obtained for $\phi_1(x)$; this is then used in the equations (6.146) to derive σ_2, D_2, and $D_2 B_2^2$. By utilizing these quantities, $\phi_2(y)$ can be found, and the procedure is repeated until convergence is attained, usually in only one or two iterations. It is of interest to mention that expressions similar to equations (6.145) have been used for some years to derive approximate solutions to two-dimensional problems, but the values of σ, D, and B^2 were usually obtained in an ad hoc manner, rather than in the systematic way described above.

Generalizations to multigroup problems with various trial functions are to be found in the literature.[44] The physical principles involved have been described in preceding sections, but it is often quite complicated to keep track of them in a detailed multigroup calculation. Derivations of discrete ordinates equations from variational principles have also been suggested.[45]

EXERCISES

1. For a constant source in a subcritical system, assume an expansion as in equation (6.42) and derive the expansion coefficients $a_i(t)$.
2. Verify that if the inner product $(\Phi^\dagger, \mathbf{L}\Phi)$ is formed with $\Phi^\dagger$ and Φ in one-speed P_1 form (§6.2b), the result is the same, except for a constant (4π) of normalization, as is obtained upon multiplying the left side of equation (6.49) by $\phi^\dagger$ and of equation (6.50) by $\mathbf{J}^\dagger \cdot$ and integrating over volume.
3. Verify that the one-speed diffusion theory operator is self-adjoint.
4. Verify that the multigroup P_1 equations (6.56) and (6.57) are adjoint to equations (6.54) and (6.55).

5. Suppose that a small, purely absorbing spherical lump is introduced into a cavity in a system. It is desired to use perturbation theory to estimate the change in k, but the neutron flux is depressed appreciably within the lump as a result of absorption. Use collision probability methods to estimate the flux depression and thus obtain an expression for Δk taking into account the flux depression in the absorber.[46]
6. It is desired to find the change in α due to the addition of a small amount of material to the surface of a spherical system. Instead of considering perturbed and unperturbed systems with different boundaries, boundary conditions can be imposed at a radius large enough to enclose either system and then apply the theory of §6.3b. Find expressions for $\Delta\alpha$ resulting from the perturbation referred to above in energy-dependent transport theory and in multigroup diffusion theory.
7. Verify that equation (6.92) gives a value of α for which the error is proportional to the product of $\delta\Phi$ and $\delta\Phi^\dagger$.
8. Show that equation (6.118) is valid.
9. For a one-speed problem in a spherical system, compare the effects on α of a perturbation as given by transport theory (§6.3b) and by diffusion theory. Make the comparison for purely absorbing and purely scattering perturbing samples, as a function of the radius of the sphere.
10. Derive equation (6.93) from equation (1.38) and the considerations in §2.1b.
11. Derive equation (6.36), noting that for the final condition on $G^\dagger$ a delta function, rather than unit importance, must be used.
12. Derive equations (6.140) and (6.141).

REFERENCES

1. Case, K. M., and P. F. Zweifel, "Linear Transport Theory," Addison-Wesley Publishing Co., Inc., 1967, Section 2.7.
2. Courant, R., and D. Hilbert, "Methods of Mathematical Physics," Interscience Publishers, Inc., 1953, Vol. I, Chap. 3.
3. Ussachoff (or Usachev), L. N., *Proc. First U.N. Conf. on Peaceful Uses of At. Energy*, 5, 503 (1955); see also J. Lewins, "Importance: The Adjoint Function," Pergamon Press, 1965.
4. Jörgens, K., *Comm. Pure Appl. Math.*, XI, 219 (1958); G. M. Wing, "Introduction to Transport Theory," Wiley and Sons, Inc., 1962, Chap. 8.
5. Case, K. M., and P. F. Zweifel, Ref. 1, Appendix D.
6. Habetler, G. J., and M. A. Martino, *Proc. Symp. Appl. Math.*, XI, Am. Math. Soc., 1961, p. 127; R. S. Varga, *ibid.*, p. 164.
7. Such adjoint operators were introduced by E. P. Wigner, "Effect of Small Perturbations on Pile Period," Manhattan Project Report CP-G-3048 (1945); see also, H. Brooks, "Perturbation Methods in Multigroup Calculations," General Electric Co. Report KAPL-71 (1948); R. Ehrlich, and H. Hurwitz, Jr., *Nucleonics*, 12, No. 2, 23 (1954).
8. Gantmacher, F. R., "The Theory of Matrices," English Translation, Chelsea Publishing Co., Vol. I, 1959, p. 82.
9. Carlson, B. G., and K. D. Lathrop in "Computing Methods in Reactor Physics," H. Greenspan, C. N. Kelber, and D. Okrent, eds., Gordon and Breach, 1968, Section 3.10.2.
10. Hansen, G. E., and C. Maier, *Nucl. Sci. Eng.*, 8, 532 (1960).
11. Glasstone, S., and M. C. Edlund, "Elements of Nuclear Reactor Theory," D. Van Nostrand Co., Inc., 1952, §§13.11 *et seq.*; J. R. Lamarsh, "Introduction to Nuclear Reactor Theory," Addison-Wesley Publishing Co., Inc., 1966, Section 15-3.

12. Glasstone, S., and A. Sesonske, "Nuclear Reactor Engineering," D. Van Nostrand Co., Inc., 1962, p. 287.
13. Hansen, G. E., and C. Maier, Ref. 10.
14. Mills, C. B., *Nucl. Applic.*, **5**, 211 (1968).
15. Mills, C. B., Ref. 14.
16. Usachev, L. N., *Atomn. Energiia* (transl.), **15**, 1255 (1963); G. C. Pomraning, *J. Nucl. Energy*, **21**, 285 (1967); A. Gandini, *ibid.*, **21**, 755 (1967); *Nucl. Sci. Eng.*, **35**, 141 (1969).
17. Davison, B., "Neutron Transport Theory," Oxford University Press, 1957, Section 15.5.
18. Roussopoulos, P., *Compt. rend.*, **236**, 1858 (1953); applied by J. Devooght, *Phys. Rev.*, **111**, 665 (1958).
19. Francis, N. C., *et al.*, *Proc. Second U.N. Conf. on Peaceful Uses of At. Energy*, **16**, 517 (1958); R. Goldstein and E. Cohen, *Nucl. Sci. Eng.*, **13**, 132 (1962).
20. Pomraning, G. C., *Nucl. Sci. Eng.*, **28**, 150 (1967).
21. Davison, B., Ref. 17, Chap. XV, N. C. Francis, *et al.*, Ref. 19; S. Kaplan and J. Davis, *Nucl. Sci. Eng.*, **28**, 166 (1967); G. C. Pomraning, *ibid.*, **29**, 220 (1967).
22. Kaplan, S., and J. Davis, Ref. 21; A. J. Buslik, *Nucl. Sci. Eng.*, **35**, 303 (1969).
23. Carlson, B. G., and G. I. Bell, *Proc. Second U.N. Conf. on Peaceful Uses of At. Energy*, **16**, 535 (1958); B. Davison, Ref. 17, Chap. XV.
24. Courant, R., and D. Hilbert, Ref. 2.
25. Davison, B., Ref. 17, Section 15.2.
26. Davison, B., Ref. 17, Section 15.2; B. G. Carlson and G. I. Bell, Ref. 23.
27. Lamarsh, J. R., Ref. 11, p. 373.
28. Francis, N. C., *et al.*, Ref. 19.
29. Francis, N. C., *et al.*, Ref. 19.
30. Selengut, D. S., *Trans. Am. Nucl. Soc.*, **5**, 40 (1962); G. C. Pomraning and M. Clark, Jr., *Nucl. Sci. Eng.*, **16**, 147 (1963); E. L. Wachspress and M. Becker, Proc. Conf. on Applic. Computing Methods to Reactor Problems, Argonne National Laboratory Report ANL-7050 (1965), p. 791.
31. Wachspress, E. L., and M. Becker, Ref. 30; M. L. Lancefield, *Nucl. Sci. Eng.*, **37**, 423 (1969).
32. Selengut, D. S., Hanford Works Quarterly Physics Report HW-59126 (1959).
33. For discussion of the calculus of variations, including approaches useful in transport theory, see E. Courant and D. Hilbert, Ref. 2, Vol. I, Chap. IV; for applications, see S. Kaplan and J. Davis, Ref. 21.
34. Henry, A. F., *Nucl. Sci. Eng.*, **27**, 493 (1967).
35. Pitterle, T. A., and C. W. Maynard, *Trans. Am. Nucl. Soc.*, **8**, 1, 205 (1965); W. W. Little, Jr., and R. W. Hardie, *Nucl. Sci. Eng.*, **29**, 402 (1967); A. J. Buslik, *ibid.*, **32**, 233 (1968); see, however, J. B. Yasinsky and S. Kaplan, *ibid.*, **31**, 354 (1968).
36. Pomraning, G. C., and M. Clark, Jr., Ref. 30.
37. Toivanen, T., *J. Nucl. Energy*, **22**, 283 (1968); M. J. Lancefield, Ref. 31; A. J. Buslik, *Trans. Am. Nucl. Soc.*, **12**, 152 (1969); R. B. Nicholson, *ibid.*, **12**, 731 (1969); R. J. Neuhold and K. O. Ott, *Nucl. Sci. Eng.*, **39**, 14 (1970).
38. Kaplan, S., *Nucl. Sci. Eng.*, **13**, 22 (1962); E. L. Wachspress and M. Becker, Ref. 30.
39. Kaplan, S., J. A. Davis, and M. Natelson, *Nucl. Sci. Eng.*, **28**, 364 (1967).
40. Calame, G. P. and F. D. Federighi, *Nucl. Sci. Eng.*, **10**, 190 (1961).
41. Yasinsky, J. B., *Nucl. Sci. Eng.*, **29**, 381 (1967).
42. Kaplan, S., "Synthesis Methods in Reactor Analysis," in *Adv. Nucl. Sci. Tech.*, **3**, 233 (1966); alternative approaches of B. G. Galerkin are also mentioned in this reference.
43. Selengut, D. S., Ref. 32.
44. Kaplan, S., Ref. 42; E. L. Wachspress and M. Becker, Ref. 30; S. Kaplan, O. J. Marlowe, and R. Caldwell, "Equations and Programs for Solutions of the Neutron Group Diffusion Equations by Synthesis Approximations," Westinghouse Report WAPM-TM-377 (1963).
45. Kaplan, S., *Nucl. Sci. Eng.*, **34**, 76 (1968); M. Natelson and E. M. Gelbard, *Trans. Am. Nucl. Soc.*, **11**, 530 (1968).
46. Hansen, G. E., and C. Maier, Ref. 10.

2.3.5

7. NEUTRON THERMALIZATION

7.1 GENERAL CONSIDERATIONS

7.1a Introduction

The slowing down of the fission neutrons in a thermal reactor is conveniently treated in two parts. If the neutron energy is in excess of a value of the order of 1 eV, the thermal motion of the scattering nucleus may be neglected and the nucleus can be assumed to be at rest in the laboratory system. Furthermore, the nucleus (or atom) may be treated as being free, i.e., unbound, because the binding energy in a molecule is not significant in comparison with the energy involved in the neutron-nucleus interaction. Hence, for neutrons with energies greater than about 1 eV, i.e., in the *slowing-down region*, it is possible to use simple slowing-down theory, involving elastic scattering with known cross sections.[1] The elastic scattering formulas used in Chapter 4 are based on this consideration. Except for fine structure in the resonance region, the neutron flux at any energy is then, to first approximation, inversely proportional to the energy.

The slowing down of neutrons with energies below 1 eV, i.e., in the thermal region, is called *thermalization*, because the neutron energies are comparable with the thermal energy of the scattering nuclei and the latter can no longer be regarded as being at rest. If the scattering nucleus is in motion, neutrons may gain energy, by up-scattering, as well as lose energy in collisions. Hence, up-scattering, which can be ignored in the slowing-down region, must now be taken into consideration. In addition, allowance must be made for the binding of the nuclei in molecules or in a crystal lattice. If the nucleus is in a bound

state, it cannot recoil freely in a collision; instead there is an interaction between the scattering nucleus and its neighbors in the molecule or solid. Finally, the possibility of interference effects in the thermal region must not be overlooked. Since the de Broglie wavelength (§1.1b) of a neutron of very low energy becomes comparable with the separation of the nuclei in a molecule or a crystal, interference can occur between the neutrons scattered from different nuclei.

As a consequence of the three effects just outlined, the scattering cross sections required for use in the transport equation in the thermal energy region are complicated functions of the energy. The cross sections depend on the physical and chemical forms and temperature of the scattering material and, in some cases, also on the orientation of the material relative to the direction of the neutron motion. Because of the complexity of the scattering cross sections in the thermal region, most of the data are not yet available from experimental measurements, although considerable progress is being made in this connection (§7.4g). Consequently, for a satisfactory treatment of the thermalization problem, it is generally necessary to use scattering cross sections computed according to various models of the scattering process.

Absorption cross sections, on the other hand, can be taken to be the same as for the free nuclei, since the binding and interference lead to negligible changes in absorption.[1a]

Since these models are not exact, it is important to have some physical understanding of the approximations involved and of their range of validity. Unfortunately, to explain the situation completely would require the use of quantum mechanics and solid-state theory. In order to avoid this, some of the important results are introduced without derivation. Nevertheless, it is hoped that the reader will be able to acquire some comprehension of the main ideas, if not of all the details involved.

Before proceeding with a discussion of the problems of thermalization, some indication may be given of the situations for which the methods described in this chapter are or are not important. In some reactors, notably fast reactors, for example, thermalization is of no concern. Furthermore, in a large, homogeneous (uniform temperature), well-moderated reactor, it is probably a good approximation to treat all the thermal neutrons as having a Maxwellian energy spectrum at a temperature close to or somewhat above that of the moderator (§7.6f), without being concerned with the precise method of thermalization.

In a heterogeneous reactor with large temperature gradients, however, or in any system with only partial thermalization, i.e., where many of the neutrons are absorbed before they are completely thermalized, a detailed treatment is essential. In such cases, the energy spectrum of thermal neutrons is not simple and calculations based on appropriate scattering models are required. Realistic calculations of this type are particularly important for predicting temperature coefficients, i.e., the effect on criticality of temperature changes in various components of the reactor, such as fuel, moderator, reflector, or coolant.

7.1b Thermal Motion of Scattering Nuclei

It is apparent that any motion of the scattering nuclei will affect the kinematics of a collision with a neutron. In any material at temperature T, a free atom (or molecule) has an average kinetic (thermal) energy of $\frac{3}{2}kT$, where k is the Boltzmann constant, 8.617×10^{-5} eV/°K. Thus, whenever a neutron has energy comparable with kT, i.e., about 0.025 eV at normal room temperature, the kinematics of its collision with a nucleus will be strongly affected by the thermal energy of the nucleus.

The actual energy distribution of the scattering nuclei will depend on their chemical binding, if any, because of the interactions between the atoms in the scattering material. Consequently, a realistic treatment of the kinematics of scattering for actual materials requires a consideration of the chemical binding problem. The simplest model for thermalization is, therefore, one in which there is no chemical binding in the moderator, i.e., a monatomic gas. In this case, the energy distribution among the atoms is simple, namely, the Maxwell-Boltzmann distribution, and it is possible to derive an accurate expression for the interchange of energy of a neutron with the gas atoms. The procedure will be described in §7.3c in order to gain some physical insight into the thermalization process and also because the ideal monatomic-gas model resembles the actual behavior of liquid and solid materials at high temperatures.

7.1c Chemical Binding

To examine the effects of chemical binding, it is useful to distinguish between elastic and inelastic scattering. According to convention, a scattering is said to be inelastic if any of the internal quantum states of the scatterer are changed as a result of the collision with a neutron, and to be elastic if there is no such change. In considering the scattering of neutrons having energies of the order of 1 MeV, for example, the scattering is inelastic if the nucleus itself is in an excited (higher energy) state after the collision, and elastic if the nucleus remains in its ground state.

For neutrons of low energy, e.g., of the order of 1 eV or so, excitation of the nucleus as a whole is, of course, impossible in a scattering collision. A nucleus (or atom) bound in a molecule is, however, in a system which has discrete quantum energy states associated with the vibration of the atoms in the molecule and with the rotation of the molecule as a whole. In the collision of a neutron, even one of low energy, with a nucleus bound in a molecule or with the molecule as a whole, there can then be a change in the vibrational or rotational (or both) quantum states due to a loss or gain of energy. Such a collision would thus be described as inelastic scattering. In elastic scattering of a low-energy neutron, the vibrational and rotational energies of the molecule are unaffected, but the molecule as a whole will recoil so as to conserve energy and momentum. Because

the molecule has kinetic (thermal) energy, however, it is possible for the neutron to gain energy in an elastic scattering.

In a nuclear reactor, molecular gases, e.g., carbon dioxide coolant, may be present; the considerations indicated above will then be directly applicable. Of greater practical interest, however, are liquid moderators, such as light and heavy water, which are composed of molecules. These substances cannot be treated accurately as collections of independent molecules since there is continuous interaction between them. Nevertheless, it has been found useful to start out by considering the scattering from individual molecules and then to impose modifications based on some model of the molecular interactions in the liquid state.

At a higher level of complication is the scattering of a neutron by a nucleus (or nuclei) bound in a crystal lattice, such as beryllium or graphite. In inelastic scattering, the vibrational excitation of the crystal will be changed as a result of the collision with a thermal neutron. A quantum of vibrational energy in a crystal is called a *phonon*, and inelastic scattering of the type under consideration is said to be accompanied by the emission or absorption of phonons. In elastic scattering from a crystal, the crystal as a whole recoils so as to conserve momentum with the neutron, but the resulting change in the neutron energy is negligible. It is of interest to note that a theory of the recoil of the whole crystal, which is an essential feature of the Mössbauer effect in the emission and absorption of gamma rays, was first developed for neutron scattering.[2]

In order to compute energy transfer between a neutron and the nuclei in a crystal lattice it is the practice to employ a more-or-less detailed model of the crystal. Such models, however, are quite approximate and the results of the calculations must be tested by comparison with experiment when possible.

In conclusion, there is a general feature of chemical binding that should be noted, namely, that the scattering cross section of a tightly bound nucleus is larger than that of the same nucleus in the free state.* The reason for this will be evident from the following considerations. For a free atom, the neutrons are scattered isotropically in the center-of-mass coordinate system where this system consists only of the neutron and the single scattering atom. If the atom is bound in a molecule, so that the molecule as a whole recoils in elastic scattering, and there is no inelastic scattering, the neutron scattering will again be isotropic in the center-of-mass system. But the latter system now consists of the neutron and the whole molecule containing the scattering atom. If the mass of the molecule is relatively large compared with that of the neutron, the center-of-mass system is then essentially identical with the laboratory system. Thus, scattering by a tightly bound atom may be regarded as being isotropic in the laboratory system, whereas for a free atom it is isotropic in the neutron-atom center-of-mass system.

* In some situations, the scattering cross section may be smaller for the bound nucleus as the result of interference effects (cf., §7.1d).

In general, therefore, the differential cross sections for the free and bound atoms will not be the same. The relationship between them may be derived in the following manner. Let $\sigma_{free}(\mu')$ be the differential cross section for scattering from a free atom through a scattering angle having the cosine μ' in the center-of-mass system. Similarly, let $\sigma_b(\mu)$ be the differential cross section for scattering from a bound atom with μ the cosine of the scattering angle in the laboratory system. Since, as stated above, both kinds of scattering will be isotropic, it follows that

$$\sigma_{free}(\mu') = \text{constant} = \frac{\sigma_{free}}{4\pi}$$

$$\sigma_b(\mu) = \text{constant} = \frac{\sigma_b}{4\pi},$$

where σ_{free} and σ_b are the respective total scattering cross sections. Furthermore, in general,

$$\sigma_{free}(\mu')\, d\mu' = \sigma_{free}(\mu)\, d\mu$$

$$\sigma_b(\mu')\, d\mu' = \sigma_b(\mu)\, d\mu.$$

If the neutron is scattered in the forward direction, i.e., $\mu = \mu' = 1$, so that the nucleus does not recoil, the mass of the nucleus is immaterial and the differential cross sections in the laboratory system will be the same for bound and free atoms, i.e.,

$$\sigma_{free}(\mu = 1) = \sigma_b(\mu = 1).$$

Upon combining the foregoing relations, it is found that

$$\sigma_b = 4\pi\sigma_b(\mu = 1) = 4\pi\sigma_{free}(\mu = 1)$$

$$= 4\pi\sigma_{free}(\mu')\left.\frac{d\mu'}{d\mu}\right|_{\mu=\mu'=1} = \sigma_{free}\left.\frac{d\mu'}{d\mu}\right|_{\mu=\mu'=1}.$$

By using the familiar expression[3] relating the cosines of the scattering angles in the laboratory (μ) and center-of-mass (μ') systems, i.e.,

$$\mu = \frac{1 + A\mu'}{\sqrt{1 + 2A\mu' + A^2}},$$

it is found that

$$\sigma_b = \left(1 + \frac{1}{A}\right)^2 \sigma_{free}, \tag{7.1}$$

where A is the mass of the scattering atom relative to that of the neutron. Since equation (7.1) gives the ratio of σ_b to σ_{free}, the cross sections may both be either macroscopic or microscopic values.

It is evident that σ_b, the scattering cross section for a tightly bound atom, must be larger than the value σ_{free} for the free atom. The ratio σ_b/σ_{free} is seen to

be greater the smaller the mass of the scattering atom; thus for hydrogen, $A \approx 1$ and σ_b should be approximately $4\sigma_{free}$. This is in agreement with experiment; for neutrons of low energy, the microscopic cross section $\sigma_b \approx 80$ barns whereas $\sigma_{free} \approx 20$ barns. When the neutron energy approaches the binding energy of the atom in the molecule, however, σ_b decreases and tends to become equal to σ_{free}.

7.1d Interference Effects: Coherent and Incoherent Scattering

When particles (or waves) are scattered elastically or inelastically from a regular system of scattering centers, the possibility must be considered that the scattering contributions from the various centers will interfere with one another. This interference may become important when the (de Broglie) wavelength of the particles is of the order of the distance between the scattering centers. The actual (not reduced) wavelength of neutrons of energy E eV is given by the de Broglie equation as

$$\lambda = \frac{2.86 \times 10^{-9}}{\sqrt{E}} \text{ cm.} \tag{7.2}$$

Hence, for neutrons of 0.01-eV energy, the wavelength of 2.86×10^{-8} cm is comparable to the spacing between atoms in a molecule or a crystal. Interference effects will therefore often be important in the scattering of thermal neutrons.

In computing neutron interference effects, it is not sufficient merely to add the scattered intensities from the various scattering centers; it is necessary to add the amplitudes with due regard for the phase differences between the scattered waves. The general procedure is identical with that used in connection with the scattering of light. For slow neutrons the interference phenomena form the basis of neutron diffraction which, like x-ray diffraction, is used for the study of crystal structure.[4]

Interference effects are manifestations of *coherent scattering*, i.e., scattering in which the amplitudes of the scattered waves are to be added in a coherent fashion with definite phase relations. In the elastic scattering of slow neutrons from crystals, this addition gives rise to the Bragg scattering peaks, i.e., scattering occurs preferentially in certain directions.

For a crystal with a spacing d between lattice (scattering) planes, there will be strong reflections whenever

$$n\lambda = 2d \sin \theta, \qquad n = 1, 2, \ldots \tag{7.3}$$

where θ is the angle between the neutron direction and the lattice planes (Fig. 7.1). Upon inserting equation (7.2) into (7.3), it is seen that the condition for strong reflection is

$$\sqrt{E} = \frac{n}{d} \frac{0.143}{\sin \theta}, \tag{7.4}$$

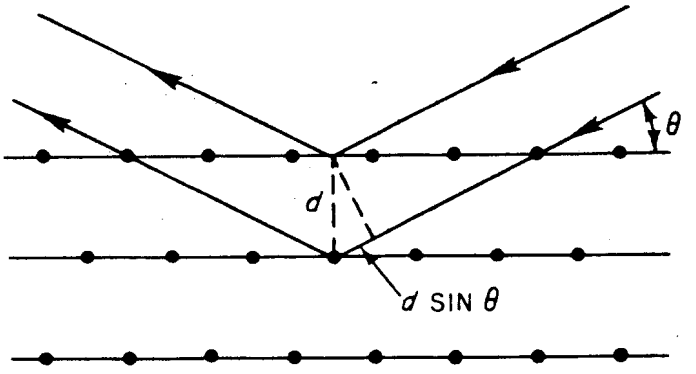

FIG. 7.1 DERIVATION OF THE BRAGG EQUATION FOR COHERENT SCATTERING.

where E is in eV and the spacing d between lattice planes is in angstroms.

If neutrons with a continuous energy spectrum are incident on a *single crystal* at a fixed angle, θ, then only those neutrons satisfying equation (7.4) will be reflected strongly. In this manner monochromatic (or monoenergetic) neutrons can be obtained. Suppose, on the other hand, the neutrons are incident on a *polycrystalline material*, such as ordinary beryllium or graphite, in which large numbers of microcrystals, with dimensions small in comparison with a mean free path, are oriented at random. Then for any sufficiently high neutron energy there will always be some crystals for which equation (7.4) is satisfied. The elastic scattering cross section, as a function of energy, then shows pronounced structure, as seen in Fig. 7.2 for beryllium.[5]

If the neutron wavelength λ is greater than $2d_{\max}$, where $d_{\max}$ is the largest distance between lattice planes in the microcrystals, then equation (7.3) can no longer be satisfied, and there can be no Bragg scattering. The maximum neutron wavelength, equal to $2d_{\max}$, at which such scattering can occur is called the *Bragg cutoff*. The corresponding neutron energy, below which there can be no Bragg scattering, is then given by equation (7.2) as $0.0204/(d_{\max})^2$ eV, where $d_{\max}$ is in angstroms. In Fig. 7.2, the cutoff is seen to occur at a neutron energy of about 0.005 eV; hence, for beryllium the spacing $d_{\max}$ is $\simeq$ 2Å. Incidentally, the break seen in the cross section curve just above 0.005 eV, indicates that there are important scattering planes in beryllium with a spacing somewhat less than $d_{\max}$.

A complication arises in the coherent scattering of slow neutrons because not all nuclei in a given material scatter in the same manner. Clearly, nuclei of different elements will scatter differently and so also will the various isotopes of a given element. In addition, if the nucleus has a spin, the scattering will depend upon whether the neutron (spin $\frac{1}{2}$) and the nucleus (spin I) combine to scatter in a state of spin $I + \frac{1}{2}$ or $I - \frac{1}{2}$.

To a good approximation, the elastic scattering of a low-energy neutron by a tightly bound nucleus, in a definite spin state, can be described by a real *scattering amplitude* (or *scattering length*), a, having the units of length, which may be

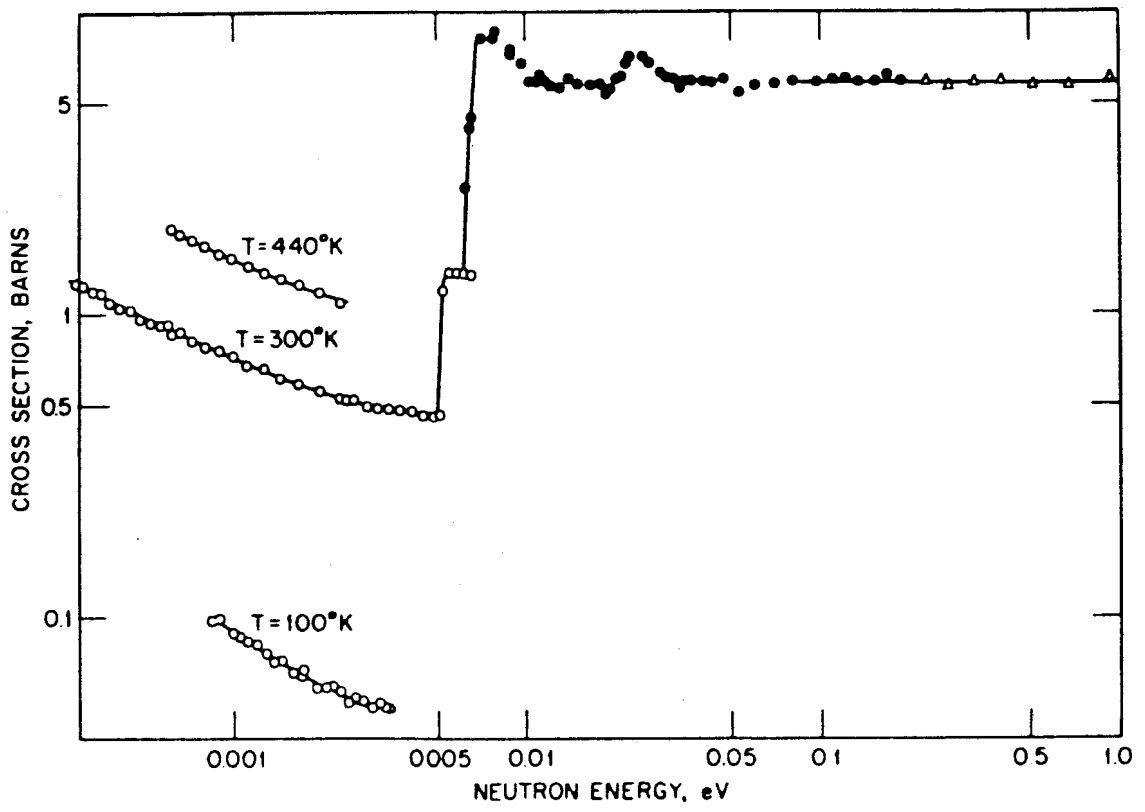

FIG. 7.2 ELASTIC SCATTERING CROSS SECTIONS OF BERYLLIUM (AFTER BNL-325).

positive or negative.[6] The corresponding *microscopic* bound scattering cross section, σ_b, is then

$$\sigma_b = 4\pi a^2.$$

In order to describe the coherent scattering from the nuclei of a nuclide with spin, the average scattering amplitude must be used. If a_+ is the amplitude for scattering in the $I + \frac{1}{2}$ spin state of the neutron-nucleus system, which occurs with probability $(I + 1)/(2I + 1)$, and a_- is the amplitude for scattering in the $I - \frac{1}{2}$ spin state, which occurs with probability $I/(2I + 1)$, then the average scattering amplitude, called the coherent scattering amplitude, a_{coh}, is

$$a_{coh} = \frac{I + 1}{2I + 1} a_+ + \frac{I}{2I + 1} a_-.$$

The coherent (microscopic) scattering cross section is then defined by

$$\sigma_{coh} = 4\pi a_{coh}^2.$$

There is also an average scattering cross section, given by

$$\bar{\sigma}_b = 4\pi\left(\frac{I + 1}{2I + 1} a_+^2 + \frac{I}{2I + 1} a_-^2\right).$$

The difference between $\bar{\sigma}_b$ and σ_{coh} is called the incoherent scattering cross section, σ_{inc}; hence,

$$\sigma_{inc} = \bar{\sigma}_b - \sigma_{coh} = 4\pi \frac{I(I+1)}{(2I+1)^2}(a_+ - a_-)^2.$$

For a combination of isotopes, the foregoing results may be written in the general forms

$$\sigma_{coh} = 4\pi(\bar{a})^2$$
$$\bar{\sigma}_b = 4\pi\overline{a^2}$$
$$\sigma_{inc} = \bar{\sigma}_b - \sigma_{coh} = 4\pi[\overline{a^2} - (\bar{a})^2],$$

where the bars over the a terms denote averages with respect both to the spin and the relative abundance of the isotopes.

It will be seen in §7.3d that the coherent and incoherent cross sections enter into the general cross sections for elastic and inelastic scattering from bound nuclei in crystals (and other materials). For materials with nuclei having randomly oriented spins, it has been shown that the proper value of the coherent cross section to be used in calculations is σ_{coh}, as defined above. If the spins of adjacent (or nearby) nuclei are correlated or if there are other correlations between such nuclei, the situation is more complex.[7]

An examination of the cross sections of the most important moderating materials shows that, within experimental error, scattering is entirely coherent for beryllium, carbon, and oxygen. For the latter two elements this is to be expected as the predominant isotopes, carbon-12 and oxygen-16, have zero nuclear spin. Scattering is largely coherent ($\sigma_{coh} = 5.4$ barns and $\bar{\sigma}_b = 7.6$ barns) for deuterium, and almost entirely incoherent for hydrogen ($\sigma_{coh} = 1.8$ barns and $\bar{\sigma}_b = 81.5$ barns). The foregoing values are for nuclei with randomly oriented spins. The incoherence of the scattering in hydrogen is a consequence of the strong spin dependence of the neutron-proton forces. It is of interest to mention that this dependence has been partly determined by observing the difference in the coherent scattering of neutrons from molecules of orthohydrogen, i.e., H_2 with parallel nuclear spins, and parahydrogen, with antiparallel nuclear spins.[8]

It will be seen in due course that the coherent and incoherent contributions enter into the general cross sections for elastic and inelastic scattering from various materials. The variations of cross sections with energy in the thermal region are, however, quite complex, as may be seen from an examination of Fig. 7.2 (see also Fig. 7.12). The reason for the complexity, as will become apparent later in this chapter, is that the elastic and inelastic scattering cross sections depend not only on the constants $\bar{\sigma}_b$, σ_{inc}, and σ_{coh}, but also on the dynamics of the scattering system.

7.2 GENERAL FEATURES OF NEUTRON THERMALIZATION

7.2a The Maxwell Distribution

When neutrons are moderated in a large medium with little (or no) absorption, they may attain approximate thermal equilibrium with the moderator at the

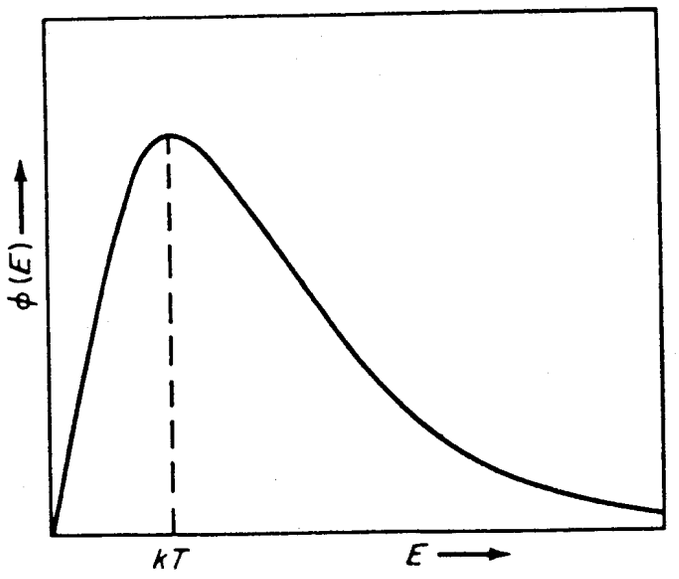

FIG. 7.3 MAXWELLIAN DISTRIBUTION OF THERMAL NEUTRON ENERGIES.

existing (uniform) temperature. In thermal equilibrium the neutrons will have a Maxwellian spectrum[9]; in terms of neutron density, this requires that at temperature T,

$$n(E)\,dE = \frac{2n_{th}}{\sqrt{\pi}kT}\sqrt{\frac{E}{kT}}\,e^{-E/kT}\,dE, \tag{7.5}$$

where $n(E)\,dE$ is the number of neutrons per unit volume having energy in the range between E and $E + dE$, and n_{th} is the total density of thermalized neutrons. In practice, as is well known, the actual spectrum of so-called thermal neutrons generally departs from a Maxwellian distribution, and the extent of such departure is of considerable importance.

The energy dependence of the neutron flux, $\phi(E)$, for a Maxwellian spectrum can be obtained by multiplying equation (7.5) by $v = \sqrt{2E/m}$; the result may then be expressed as

$$\phi(E)\,dE = \phi_{th}M(E, T)\,dE, \tag{7.6}$$

where

$$M(E, T) \equiv \frac{E}{(kT)^2}\,e^{-E/kT}, \tag{7.7}$$

so that

$$\int_0^\infty M(E, T)\,dE = 1,$$

and

$$\phi_{th} = \sqrt{\frac{8kT}{\pi m}}\,n_{th}.$$

It is of interest to note that $\sqrt{8kT/\pi m}$ is the average speed in a Maxwellian distribution. If equation (7.7) is differentiated with respect to E and the result set equal to zero, it is found that a maximum in the flux occurs when the neutron energy is kT (Fig. 7.3). Thus, kT is referred to as the most probable energy for the thermal neutron flux.

7.2b The Transport Equation for Thermal Neutrons

It was mentioned in Chapter 1 that for some neutron transport problems, e.g., in rapidly flowing fluids or single crystals where the direction of flow or crystal axes define preferred directions in space, the total cross sections for slow neutrons depend significantly on the direction of neutron motion. These special situations will not be considered in this text, because they are not usually significant in nuclear reactors. In most polycrystalline materials, for example, the neutron mean free path is usually large in comparison with the crystallite dimensions; hence, with a random orientation of the crystallites, there is no preferred direction on a macroscopic scale.* Consequently, the ordinary transport equation will be used in the treatment of neutron thermalization. It is convenient, however, to adopt a somewhat different notation for the cross sections.

As long as attention is confined to thermal neutrons, with energy $\leqslant 1$ eV, for example, collisions may be divided into two categories: those from which *thermal neutrons* emerge and those from which such neutrons do not emerge. The former category involves only scatterings, both elastic and inelastic, in the general sense described in §7.1c; the corresponding macroscopic cross section is denoted by $\sigma_s(\mathbf{r}, E)$. The collisions in the category from which thermal neutrons do not emerge include all absorption reactions, such as (n, γ) and (n, α) reactions, and also fission, because essentially all the neutrons produced have high energies. In the present context, all such reactions, including fission, will be called absorptions, and the corresponding macroscopic cross section will be denoted by $\sigma_a(\mathbf{r}, E)$.

For neutrons in the thermal energy range, the quantities σ, and $\sigma' f$ which appear in the neutron transport equation (1.14) are then given by

$$\sigma \equiv \sigma(\mathbf{r}, E) = \sigma_s(\mathbf{r}, E) + \sigma_a(\mathbf{r}, E),$$

and

$$\begin{aligned}\sigma' f &\equiv \sigma(\mathbf{r}, E') f(\mathbf{r}; \Omega', E' \to \Omega, E) \\ &= \sigma_s(\mathbf{r}, E') f_s(\mathbf{r}; \Omega', E' \to \Omega, E).\end{aligned}$$

Since the function f_s now describes scattering only, it is normalized to unity (§1.1b), so that

$$\iint f_s(\mathbf{r}; \Omega', E' \to \Omega, E)\, d\Omega\, dE = 1. \tag{7.8}$$

* For certain kinds of graphite, such as extruded graphite and pyrographite, the crystallites may be partially aligned and then the preferred direction should be taken into account.

For neutrons in the thermal energy region, the transport equation (1.14) then takes the form

$$\frac{1}{v}\frac{\partial \Phi}{\partial t} + \boldsymbol{\Omega}\cdot\nabla\Phi + [\sigma_s(\mathbf{r}, E) + \sigma_a(\mathbf{r}, E)]\Phi$$

$$= \iint \sigma_s(\mathbf{r}, E')f_s(\mathbf{r}; \boldsymbol{\Omega}', E' \to \boldsymbol{\Omega}, E)\Phi(\mathbf{r}, \boldsymbol{\Omega}', E', t)\, d\boldsymbol{\Omega}'\, dE' + Q(\mathbf{r}, \boldsymbol{\Omega}, E, t). \quad (7.9)$$

As stated earlier, for a large moderating system at uniform temperature with little or no absorption, the energy distribution of the thermal neutron flux will be approximately Maxwellian. In fact, for the limit of an infinite, source-free medium at constant temperature and zero absorption it is possible to have a neutron population which is strictly Maxwellian, independent of time and space. This means that $M(E, T)$ must satisfy the thermal neutron transport equation with no time dependence, i.e., $\partial\Phi/\partial t = 0$, no space dependence, i.e., $\nabla\Phi = 0$, no absorption, i.e., $\sigma_a = 0$, and no source, i.e., $Q = 0$. Hence, in these circumstances, the transport equation (7.9) for thermal neutrons may be written as

$$\sigma_s(\mathbf{r}, E)M(E, T) = \iint \sigma_s(\mathbf{r}, E')f_s(\mathbf{r}; \boldsymbol{\Omega}', E' \to \boldsymbol{\Omega}, E)M(E', T)\, d\boldsymbol{\Omega}'\, dE'. \quad (7.10)$$

The constraint represented by equation (7.10) must be satisfied by any scattering cross section. It is actually an aspect of the general *principle of detailed balance* which is applicable to a system at thermal equilibrium.[10] In the present case of scattering of neutrons by nuclei in thermal equilibrium at temperature T, the detailed balance requirement is that

$$M(E, T)\sigma_s(\mathbf{r}, E)f_s(\mathbf{r}; -\boldsymbol{\Omega}, E \to -\boldsymbol{\Omega}', E') = M(E', T)\sigma_s(\mathbf{r}, E')f_s(\mathbf{r}; \boldsymbol{\Omega}', E' \to \boldsymbol{\Omega}, E). \quad (7.11)$$

This equation states that, in a system in thermal (Maxwellian) equilibrium, the rate of scattering collisions with nuclei by neutrons of energy E from which neutrons emerge with energy E' is equal to the rate of such collisions by neutrons of energy E' from which neutrons emerge with energy E. Upon integration of equation (7.11) over $-\boldsymbol{\Omega}'$ and E', and using the normalization relation of equation (7.8). the result is equation (7.10).

The detailed balance equation (7.11), which is more restrictive than equation (7.10), is useful in thermalization problems. In the first place, most scattering cross sections used in thermalization calculations are computed from some theoretical model and contain many approximations. It is important, however, that they at least admit the Maxwell distribution as a solution in the limit of large volume and weak absorption. This can be assured by requiring that the cross sections satisfy the detailed balance condition of equation (7.11). It will be seen in §7.3d how this condition may be imposed systematically by using certain symmetry properties of scattering functions.

7.2c Reciprocity Relation for Thermal Neutrons

Even more important is that the condition of detailed balance, applied to a medium at a uniform temperature, implies a reciprocity relation. It will be recalled that in Chapter 2 such a relation, known as the optical reciprocity theorem, was derived for one-speed theory, and was represented succinctly in terms of the Green's functions by equation (2.99), i.e.,

$$G(\mathbf{r}_2, \boldsymbol{\Omega}_2 \to \mathbf{r}_1, -\boldsymbol{\Omega}_1) = G(\mathbf{r}_1, \boldsymbol{\Omega}_1 \to \mathbf{r}_2, -\boldsymbol{\Omega}_2), \tag{7.12}$$

which relates the neutron flux at $\mathbf{r}_1$ due to a source at $\mathbf{r}_2$ with the flux at $\mathbf{r}_2$ due to a source at $\mathbf{r}_1$.

For general energy-dependent problems, however, this simple relation does not hold, but there is a reciprocity relation between the flux and the adjoint Green's function [equation (6.13)]. The reason for the difference in behavior is that the energy-dependent transport operator is not self-adjoint, but the transport operator for the one-speed problem is almost self-adjoint, where "almost" means that it is necessary only to change the sign of the direction of neutron travel, i.e., the sign of $\boldsymbol{\Omega}$ and of t (§6.1f).

It will now be shown that the thermalization transport operator can be made almost self-adjoint by an elementary transformation and that this is the reason for the existence of a simple reciprocity relation. Consider an inhomogeneous, time-independent transport problem [cf. equations (6.4) and (6.5)], represented by

$$\begin{aligned} -\mathbf{L}\Phi &= \boldsymbol{\Omega}\cdot\nabla\Phi + (\sigma_a + \sigma_s)\Phi \\ &\quad - \iint \sigma_s(\mathbf{r}, E') f_s(\mathbf{r}; \boldsymbol{\Omega}'E' \to \boldsymbol{\Omega}, E)\Phi(\mathbf{r}, \boldsymbol{\Omega}', E')\, d\boldsymbol{\Omega}'\, dE' \\ &= Q(\mathbf{r}, \boldsymbol{\Omega}, E). \end{aligned} \tag{7.13}$$

The corresponding adjoint equation [cf. equation (6.7)] is

$$\begin{aligned} -\mathbf{L}^\dagger\Phi^\dagger &= -\boldsymbol{\Omega}\cdot\nabla\Phi^\dagger + (\sigma_a + \sigma_s)\Phi^\dagger \\ &\quad - \iint \sigma_s(\mathbf{r}, E) f_s(\mathbf{r}; \boldsymbol{\Omega}, E \to \boldsymbol{\Omega}', E')\Phi^\dagger(\mathbf{r}, \boldsymbol{\Omega}', E')\, d\boldsymbol{\Omega}'\, dE' \\ &= Q^\dagger(\mathbf{r}, \boldsymbol{\Omega}, E), \end{aligned} \tag{7.14}$$

where the symbols have the same significance as in Chapter 6. The usual free-surface conditions are implied for the angular flux, Φ, and its adjoint, $\Phi^\dagger$.

The functions ψ and $\psi^\dagger$ are now defined by

$$\psi(\mathbf{r}, \boldsymbol{\Omega}, E) \equiv \frac{1}{\sqrt{M(E, T)}}\, \Phi(\mathbf{r}, \boldsymbol{\Omega}, E)$$

$$\psi^\dagger(\mathbf{r}, \boldsymbol{\Omega}, E) \equiv \sqrt{M(E, T)}\, \Phi^\dagger(\mathbf{r}, \boldsymbol{\Omega}, E),$$

where T is the temperature of the medium which must be uniform.

If these expressions are substituted into equations (7.13) and (7.14), respectively, it is found that

$$\boldsymbol{\Omega}\cdot\nabla\psi + (\sigma_a + \sigma_s)\psi - \iint \sigma_s' f(\mathbf{r}; \boldsymbol{\Omega}', E' \to \boldsymbol{\Omega}, E) \times \sqrt{\frac{M(E', T)}{M(E, T)}}\,\psi(\mathbf{r}, \boldsymbol{\Omega}', E')\, d\boldsymbol{\Omega}'\, dE' = \frac{Q}{\sqrt{M}} \quad (7.15)$$

and

$$-\boldsymbol{\Omega}\cdot\nabla\psi^\dagger + (\sigma_a + \sigma_s)\psi^\dagger - \iint \sigma_s f(\mathbf{r}; \boldsymbol{\Omega}, E \to \boldsymbol{\Omega}', E') \times \sqrt{\frac{M(E, T)}{M(E', T)}}\,\psi^\dagger(\mathbf{r}, \boldsymbol{\Omega}', E')\, d\boldsymbol{\Omega}'\, dE' = \sqrt{M}\, Q^\dagger, \quad (7.16)$$

where σ_s' is $\sigma_s(\mathbf{r}, E')$ and σ_s is $\sigma_s(\mathbf{r}, E)$.

If the variables in equation (7.16) are changed from $\boldsymbol{\Omega}$ and $\boldsymbol{\Omega}'$ to $-\boldsymbol{\Omega}$ and $-\boldsymbol{\Omega}'$, respectively, the result is

$$\boldsymbol{\Omega}\cdot\nabla\psi^\dagger(\mathbf{r}, -\boldsymbol{\Omega}, E) + (\sigma_a + \sigma_s)\psi^\dagger - \iint \sigma_s f(\mathbf{r}; -\boldsymbol{\Omega}, E \to -\boldsymbol{\Omega}', E') \times \sqrt{\frac{M(E, T)}{M(E', T)}}\,\psi^\dagger(\mathbf{r}, -\boldsymbol{\Omega}', E')\, d\boldsymbol{\Omega}'\, dE' = \sqrt{M}\, Q^\dagger(\mathbf{r}, -\boldsymbol{\Omega}, E). \quad (7.17)$$

According to the condition of detailed balance, i.e., equation (7.11), the factor multiplying $\psi^\dagger$ in the integrand of equation (7.17) is identical with that multiplying ψ in the integrand of equation (7.15). Thus, the left side of equation (7.17) is the same as that of equation (7.15), with $\psi^\dagger(\mathbf{r}, -\boldsymbol{\Omega}, E)$ substituted for $\psi(\mathbf{r}, \boldsymbol{\Omega}, E)$. It follows, therefore, that the operator which acts on ψ is almost self-adjoint, i.e., it is self-adjoint except for the sign of $\boldsymbol{\Omega}$.

Suppose that

$$Q = Q^\dagger = \delta(\mathbf{r} - \mathbf{r}_1)\,\delta(\boldsymbol{\Omega} - \boldsymbol{\Omega}_1)\,\delta(E - E_1),$$

so that $\Phi(\mathbf{r}, \boldsymbol{\Omega}, E)$ and $\Phi^\dagger(\mathbf{r}, \boldsymbol{\Omega}, E)$ are Green's functions, i.e.,

$$\Phi = G(\mathbf{r}_1, \boldsymbol{\Omega}_1, E_1 \to \mathbf{r}, \boldsymbol{\Omega}, E)$$

and

$$\Phi^\dagger = G^\dagger(\mathbf{r}_1, \boldsymbol{\Omega}_1, E_1 \to \mathbf{r}, \boldsymbol{\Omega}, E),$$

and the equivalent functions corresponding to ψ and $\psi^\dagger$ are

$$\psi = \psi(\mathbf{r}_1, \boldsymbol{\Omega}_1, E_1 \to \mathbf{r}, \boldsymbol{\Omega}, E)$$

and

$$\psi^\dagger = \psi^\dagger(\mathbf{r}_1, \boldsymbol{\Omega}_1, E_1 \to \mathbf{r}, \boldsymbol{\Omega}, E).$$

By considering equations (7.15) and (7.17), it is seen that the sources for ψ and $\psi^\dagger$ now differ by the factor $M(E_1, T)$. It follows, therefore that

$$M(E_1, T)\psi(\mathbf{r}_1, \boldsymbol{\Omega}_1, E_1 \to \mathbf{r}, \boldsymbol{\Omega}, E) = \psi^\dagger(\mathbf{r}_1, -\boldsymbol{\Omega}_1, E_1 \to \mathbf{r}, -\boldsymbol{\Omega}, E), \quad (7.18)$$

where the change from Ω_1 to $-\Omega_1$ on the right results from the difference in the source directions in equations (7.15) and (7.17), and the change from Ω to $-\Omega$ from the correspondence between $\psi(\mathbf{r}, \Omega, E)$ and $\psi^\dagger(\mathbf{r}, -\Omega, E)$. Upon introducing the definitions of ψ and $\psi^\dagger$ on page 327, equation (7.18) becomes

$$M(E_1, T)G(\mathbf{r}_1, \Omega_1, E_1 \to \mathbf{r}, \Omega, E) = M(E, T)G^\dagger(\mathbf{r}_1, -\Omega_1, E_1 \to \mathbf{r}, -\Omega, E), \tag{7.19}$$

which is the desired reciprocity relation between the Green's functions for the flux and its adjoint for thermalization problems.

If the general relationship, equation (6.13), between the Green's functions is combined with equation (7.19), the result is

$$M(E_1, T)G(\mathbf{r}_1, \Omega_1, E_1 \to \mathbf{r}, \Omega, E) = M(E, T)G(\mathbf{r}, -\Omega, E \to \mathbf{r}_1, -\Omega_1, E_1). \tag{7.20}$$

This is similar to equation (7.12) of one-speed theory, except that each side is weighted by the Maxwellian of the source. Thus, as in one-speed theory (§2.7b) the solutions of various simple thermalization problems may be related to each other.

The basis of the reciprocity relation of equation (7.20) is that, by using the detailed balance condition, the thermal transport operator can be made almost self-adjoint by an elementary transformation. It is important from the theoretical standpoint that the transport operator can thus be made almost self-adjoint because self-adjoint operators are understood much better than are operators which are not self-adjoint. Thus, for thermalization problems, conclusions can be drawn concerning the existence of eigenvalues and other properties of the solutions that are not possible for more general energy-dependent problems.[11]

The foregoing results indicate a similarity between thermalization problems in a medium of uniform temperature, but otherwise of arbitrary complexity, and one-speed problems. If, however, the temperature of the medium is not uniform, the reciprocity relations do not hold. The reason is, formally, that in the transformation to the ψ equations when T is a function of $\mathbf{r}$, the factor $M(E, T(\mathbf{r}))$ will not commute with the gradient operator, i.e.,

$$M(E, T(\mathbf{r}))\nabla \neq \nabla M(E, T(\mathbf{r})),$$

and the derivation of the relation between ψ and $\psi^\dagger$ breaks down.

7.3 NEUTRON SCATTERING LAWS

7.3a Scattering from a Monatomic Gas

In this section, consideration will be given to some neutron scattering laws, that is, specifications of the quantities σ_s and f_s to be used in the transport equation in the treatment of thermalization problems. The discussion will begin with the

simplest of scattering models, in which the scatterer is a monatomic gas. It will then be extended to more realistic moderator systems, including molecules and crystals. As in nearly all portions of this book, the symbol σ is used to represent macroscopic cross sections.

The problem of the thermalization of neutrons in a monatomic gas is simple enough for the scattering laws to be derived explicitly.[12] Although there are no important moderators that are monatomic gases, it seems worth while, nevertheless, to develop the scattering laws for the simple case because (*a*) they exhibit qualitative features which are of general applicability and (*b*) they form a useful standard for comparison with more realistic but more complex laws for scattering in other media. In addition, these laws are all based on approximate models, and so it is reasonable to start from the simple (exact) model of the monatomic gas since it is, at least, qualitatively useful.

Consider a collision between a monatomic gas atom, having velocity $\mathbf{V}$, and a neutron with velocity $\mathbf{v}$. The relative velocity, $\mathbf{v}_r$, between the two particles is then

$$\mathbf{v}_r = \mathbf{v} - \mathbf{V},$$

and if μ is the cosine between the velocity vectors, i.e., $\mu = \mathbf{v}\cdot\mathbf{V}/vV$, the relative speed, v_r, is

$$v_r = \sqrt{v^2 + V^2 - 2vV\mu}.$$

If $P(\mathbf{V})\,d\mathbf{V}$ is the probability that a nucleus (or atom) has velocity $\mathbf{V}$ within $d\mathbf{V}$ about $\mathbf{V}$, the probability that a neutron will collide with such a nucleus is

$$\text{Probability of collision per sec} = v_r\sigma_{s0}P(\mathbf{V})\,d\mathbf{V}, \tag{7.21}$$

where σ_{s0} is the (energy-independent) macroscopic cross section for a free (or isolated) atom at rest, i.e., the microscopic cross section of the atom multiplied by the number of atoms per unit volume of gas.* The total collision (scattering) rate for a neutron of velocity $\mathbf{v}$ is then found by integrating equation (7.21) over all atom velocities $\mathbf{V}$. The corresponding macroscopic scattering cross section, $\sigma_s(v)$, is obtained upon dividing this rate by v; hence,

$$\sigma_s(v) = \frac{\sigma_{s0}}{v}\int v_r P(\mathbf{V})\,d\mathbf{V}. \tag{7.22}$$

If A is the mass of the nucleus relative to that of the neutron, i.e., $M = Am$, where M is the actual mass of the nucleus and m is the mass of the neutron, then for an isotropic Maxwellian distribution of nuclear velocities

$$P(\mathbf{V})\,d\mathbf{V} = \left(\frac{M}{2\pi kT}\right)^{3/2} e^{-MV^2/2kT}V^2\,d\varphi\,d\mu\,dV, \tag{7.23}$$

* If σ_{free} of §7.1c is taken to be the macroscopic cross section, it is identical with σ_{s0}.

where the v direction has been chosen as the polar axis of a spherical coordinate system. If this expression is inserted into equation (7.22), integration over the azimuthal angle, φ, yields 2π, and hence

$$\sigma_s(v) = \frac{\sigma_{s0}}{v}\int_{-1}^{1}\int_{0}^{\infty} v_r\left(\frac{M}{2\pi kT}\right)^{3/2} e^{-MV^2/2kT} 2\pi V^2\, dV\, d\mu.$$

Upon evaluating the integrals, the result is

$$\sigma_s(E) = \frac{\sigma_{s0}}{\beta^2}\left[(\beta^2 + \tfrac{1}{2})\operatorname{erf}\beta + \frac{1}{\sqrt{\pi}}\beta e^{-\beta^2}\right], \tag{7.24}$$

where $E = \frac{1}{2}mv^2$ is the kinetic energy of the neutrons, $\beta^2 = AE/kT$, and erf stands for the error function (see Appendix).

The limiting behavior of $\sigma_s(E)$ for small and large values of the neutron energy is of some interest. When E is small, erf β is proportional to β; equation (7.24) then reduces to

$$\sigma_s(E) \propto \frac{\sigma_{s0}}{\beta} \propto \frac{\sigma_{s0}}{v} \quad \text{for } E \text{ small.} \tag{7.25}$$

Consequently, when the neutron energy, E (and hence its speed, v), is small, the scattering cross section is proportional to $1/v$.

The physical significance of this result may be seen by noting that when v is very small, v_r is almost equal to V; the collision rate (or probability), as given by equation (7.21) is then independent of the neutron speed and depends only on V, the speed of the atoms. This collision rate is then simply the rate at which the moving atoms collide with (or bump into) the neutron. Since the scattering cross section is the collision probability per unit distance of neutron motion, it is $1/v$ times the constant scattering collision rate. Hence, the scattering cross section for very slow neutrons is proportional to $1/v$.

At high energies, erf $\beta \to 1$, and since β^2 is large, equation (7.24) leads to $\sigma_s(E) = \sigma_{s0}$, the single atom scattering cross section. As expected, at high neutron energies, the scattering cross section is independent of the thermal motion of the gas atoms. The same limiting behavior of $\sigma_s(E)$ at low and high energies also follows from the scattering laws for more realistic systems.

7.3b The Scattering Function for a Monatomic Gas

In order to calculate the *scattering function* (or *scattering kernel*)

$$\sigma_s(E')f_s(E' \to E, \mu_0),$$

where μ_0 is the cosine of the neutron scattering angle, it is necessary first to determine the probability $p(v' \to v, \mu_0)$ that a neutron of speed v' will emerge with speed v from a collision with an atom of velocity V in a monatomic gas.*

* The term "free gas" is commonly used in the literature in connection with scattering by a monatomic gas; the latter terminology is preferred here, however, as it is more specific.

Once this has been done, the result is multiplied by $v_r P(\mathbf{V})\sigma_{s0}/v'$ and integrated over all atom velocities, i.e., all V and μ, to obtain $\sigma_s f_s$. The derivation is lengthy and so only the result will be given here.[13]

The quantities ϵ and κ are defined by

$$\epsilon = E' - E = \text{energy change (or energy transfer) of a neutron*}$$

and

$$\hbar\kappa = m|v' - v| = \text{momentum change (or momentum transfer) of a neutron}$$

$$= m\sqrt{v'^2 + v^2 - 2\mu_0 vv'},$$

or

$$\hbar^2\kappa^2 = 2m(E' + E - 2\mu_0\sqrt{EE'}),$$

where $\hbar$ is the reduced Planck constant (§1.1b).

The result of the derivation referred to above can then be written as

$$\sigma_s(E')f_s(E' \to E; \mu_0)$$

$$= \frac{\sigma_{s0}[1 + (1/A)]^2}{4\pi}\sqrt{\frac{E}{E'}}\sqrt{\frac{Am}{2\pi kT\hbar^2\kappa^2}}\exp - \left[\frac{Am}{2kT\hbar^2\kappa^2}\left(\epsilon - \frac{\hbar^2\kappa^2}{2Am}\right)^2\right]. \quad (7.26)$$

It is apparent that $\sqrt{E'/E}\sigma_s f_s$, for scattering by a monatomic gas with atoms of mass Am, is a function only of ϵ and κ, i.e., the change in energy and momentum of the neutron. It will be seen later that this is true, in general, for other scattering laws, although the vector $\boldsymbol{\kappa}$ may be involved rather than its magnitude, κ.

In the limit as $T \to 0$, i.e., when E/kT and E'/kT are large, equation (7.26) reduces to the familiar slowing down relationship for energies above the thermal region, given in Chapter 4. Thus, when T is small, the exponential in equation (7.26) will be very small unless

$$\epsilon \approx \frac{\hbar^2\kappa^2}{2mA}.$$

If the expressions for ϵ and κ given above are inserted, this condition implies the well known result (§1.1b)

$$\mu_0 = \frac{1}{2}\left[(A + 1)\sqrt{\frac{E}{E'}} - (A - 1)\sqrt{\frac{E'}{E}}\right].$$

Moreover, if the exponential in equation (7.26) is integrated over a small

* Some writers represent the energy change, ϵ, by $\hbar\omega$, but this leads to confusion with another common use of the symbol ω (§7.4d).

angular range, which includes this value of μ_0, it is found that, for T small, the normalization leads to

$$\sqrt{\frac{Am}{2\pi kT\hbar^2\kappa^2}}\exp-\left[\frac{Am}{2kT\hbar^2\kappa^2}\left(\epsilon-\frac{\hbar^2\kappa^2}{2Am}\right)^2\right]$$
$$=\frac{A}{2\sqrt{EE'}}\,\delta\left\{\mu_0-\frac{1}{2}\left[(A+1)\sqrt{\frac{E}{E'}}+(A-1)\sqrt{\frac{E'}{E}}\right]\right\}.$$

If this substitution is made in equation (7.26), it is seen directly that, at low temperature (or E large relative to kT),

$$\sigma_s(E')f_s(E'\to E;\mu_0)=\frac{\sigma_{s0}}{2\pi(1-\alpha)E'}\,\delta\left\{\mu_0-\frac{1}{2}\left[(A+1)\sqrt{\frac{E}{E'}}-(A-1)\sqrt{\frac{E'}{E}}\right]\right\},$$

as in equation (4.5).

7.3c The Energy Transfer Function for a Monatomic Gas

Since the scattering function (or kernel) just considered involves both the energy and momentum changes of the neutron, it is not easy to display its dependence on temperature. The situation is easier to understand if the scattering function is integrated over all scattering angles, μ_0, to obtain the *energy transfer function* $\sigma_s(E')f_s(E'\to E)$, i.e.,

$$\sigma_s(E')f_s(E'\to E)=2\pi\int_{-1}^{1}\sigma_s(E')f(E'\to E;\mu_0)\,d\mu_0.$$

The energy transfer function can be derived by integrating equation (7.26) over μ_0, but an alternative approach is of interest.

Consider, once again, the collisions between neutrons of speed v' and gas atoms of speed V and direction cosine μ relative to v', for which the collision rate is given by equation (7.21). It is required, first, to determine the probability $g(v'\to v)\,dv$ that the neutron will have a final speed between v and $v+dv$ without regard to the scattering angle, μ_0. For this purpose, it is convenient to transform to the center-of-mass coordinate system; the velocity, $\mathbf{V}_c$, of the center of mass in the laboratory system is then given by

$$\mathbf{V}_c=\frac{\mathbf{v}'+A\mathbf{V}}{A+1},$$

where $\mathbf{v}'$ and $\mathbf{V}$ refer to the laboratory system.

The scattering in the center-of-mass system is isotropic, and the initial and final speeds of the neutron in this system are

$$v_c'=v_c=\frac{A}{A+1}v_r.$$

Let θ denote the angle between $\mathbf{V}_c$ and $\mathbf{v}_c$, the final neutron velocity in the center-of-mass system (Fig. 7.4), then the final neutron speed, v, in the laboratory system is

$$v = \sqrt{V_c^2 + \left(\frac{A}{A+1} v_r\right)^2 + 2V_c\left(\frac{A}{A+1} v_r\right) \cos\theta}. \tag{7.27}$$

For a collision with an atom having fixed values of V and μ, V_c and v_r are fixed. Furthermore, since the scattering is isotropic in the center-of-mass system, the probability of a neutron emerging from the collision with direction $\cos\theta$ is proportional to $d\cos\theta$. But, from equation (7.27),

$$v\,dv = V_c\left(\frac{A}{A+1} v_r\right) d\cos\theta.$$

Hence, the probability for v to lie in the interval dv is proportional to $v\,dv$, and

$$g(v' \to v) \propto v.$$

The value of v may range from a minimum, $v_{\min}$, when $\cos\theta = -1$, to a maximum, $v_{\max}$, when $\cos\theta = 1$; then, from equation (7.27),

$$v_{\min} = \left|V_c - \frac{A}{A+1} v_r\right|$$

and

$$v_{\max} = V_c + \frac{A}{A+1} v_r.$$

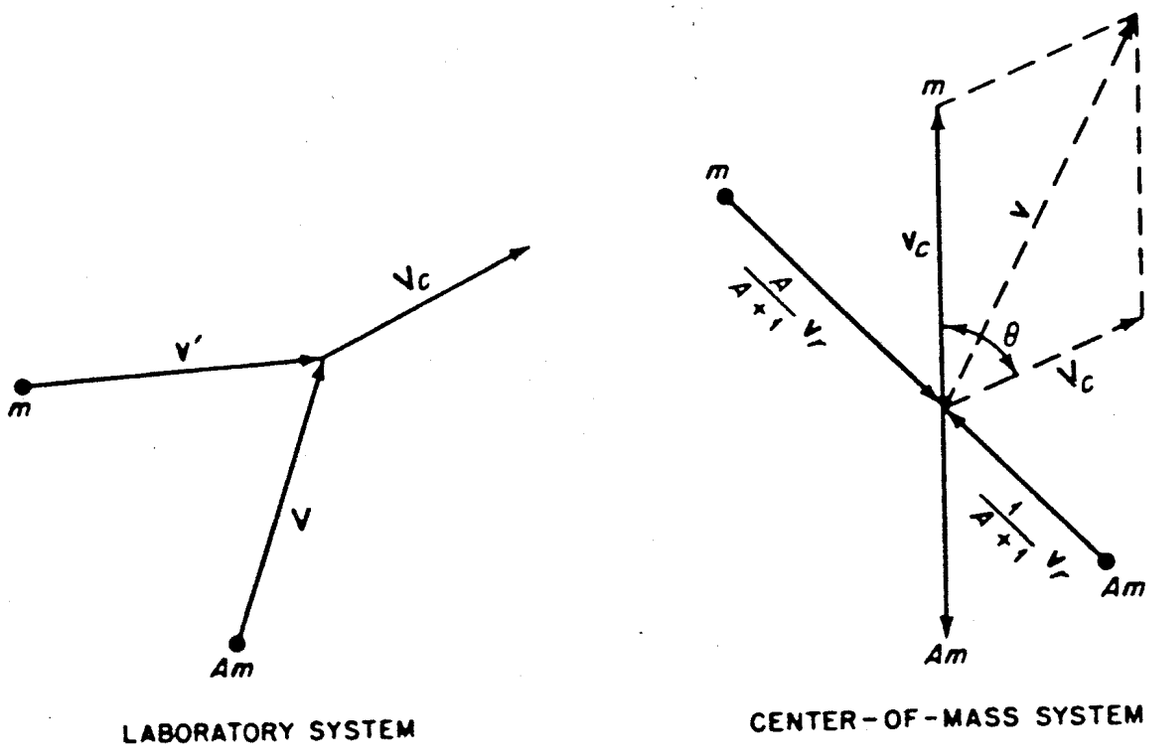

FIG. 7.4 SCATTERING IN LABORATORY AND CENTER-OF-MASS SYSTEMS.

It follows, therefore, that

$$\begin{aligned} g(v' \to v) &= 0 && \text{for } v < v_{\min} \\ &= \frac{2v}{v_{\max}^2 - v_{\min}^2} && \text{for } v_{\min} \leqslant v \leqslant v_{\max} \\ &= 0 && \text{for } v > v_{\max}. \end{aligned} \tag{7.28}$$

Upon multiplying the collision rate between an atom of speed V and a neutron of speed v', as given by equations (7.21) and (7.23), by the probability $g(v' \to v)$ that the neutron will have final speed v, dividing by v', and integrating over all atom velocities, it is found that the velocity transfer cross section is

$$\sigma_s(v')f_s(v' \to v) = \frac{\sigma_{s0}}{v'} \int_0^\infty \int_{-1}^1 v_r g(v' \to v) 2\pi P(V)\, d\mu\, dV. \tag{7.29}$$

This is the probability, per unit distance of neutron motion, that the neutron is scattered from v' to v.

Since

$$\sigma_s(E')f_s(E' \to E)\, dE = \sigma_s(v')f_s(v' \to v)\, dv$$

and

$$\frac{dE}{dv} = mv,$$

it follows that

$$\sigma_s(E')f_s(E' \to E) = \frac{1}{mv}\, \sigma_s(v')f_s(v' \to v).$$

When this result is set into equation (7.29) and the integrals are evaluated, as in deriving equation (7.24), it is found that

$$\begin{aligned} \sigma_s(E')f_s(E' \to E) = \frac{\sigma_{s0}}{E'} \frac{\eta^2}{2} \Bigg\{ & \exp\left(\frac{E'}{kT} - \frac{E}{kT}\right) \Bigg[\operatorname{erf}\left(\eta\sqrt{\frac{E'}{kT}} - \rho\sqrt{\frac{E}{kT}}\right) \\ & \pm \operatorname{erf}\left(\eta\sqrt{\frac{E'}{kT}} + \rho\sqrt{\frac{E}{kT}}\right) \Bigg] + \operatorname{erf}\left(\eta\sqrt{\frac{E}{kT}} - \rho\sqrt{\frac{E'}{kT}}\right) \\ & \mp \operatorname{erf}\left(\eta\sqrt{\frac{E}{kT}} + \rho\sqrt{\frac{E'}{kT}}\right) \Bigg\}, \end{aligned} \tag{7.30}$$

where η and ρ are defined by

$$\eta \equiv \frac{A+1}{2\sqrt{A}} \quad \text{and} \quad \rho \equiv \frac{A-1}{2\sqrt{A}}.$$

The upper signs in equation (7.30) are to be used if $E' < E$ and the lower signs if $E' > E$.

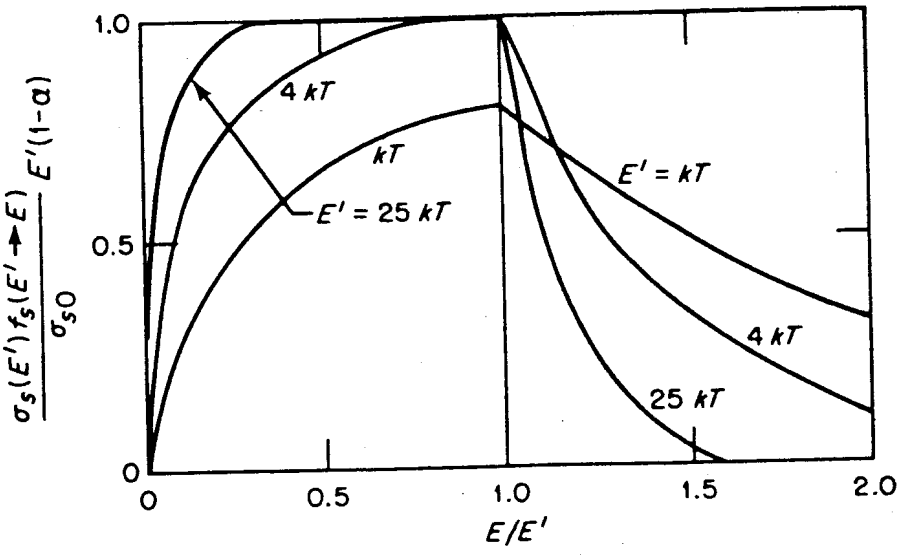

FIG. 7.5 ENERGY TRANSFER FUNCTION IN A MONATOMIC GAS WITH $A = 1$ (AFTER K. H. BECKURTS AND K. WIRTZ, REF. 14).

The dependence of the energy transfer function on the gas temperature is shown in Figs. 7.5 and 7.6,[14] as a function of E/E'; the ordinates are given relative to the atom at rest. Figure 7.5 is for a gas of free protons ($A = 1$) and Fig. 7.6 for a gas of oxygen atoms ($A = 16$). It is seen that at high neutron energies, i.e., $E' \gg kT$, the scattering is very much like that from nuclei (or atoms) at rest; in these circumstances, down-scattering in energy, i.e., $E/E' < 1$, is more important than up-scattering. As the energy approaches kT, however, up-scattering becomes important and a neutron is likely to gain energy in a collision with a gas atom. The up-scattering effect is evidently more important for light nuclei (protons) than it is for the heavier nuclei.

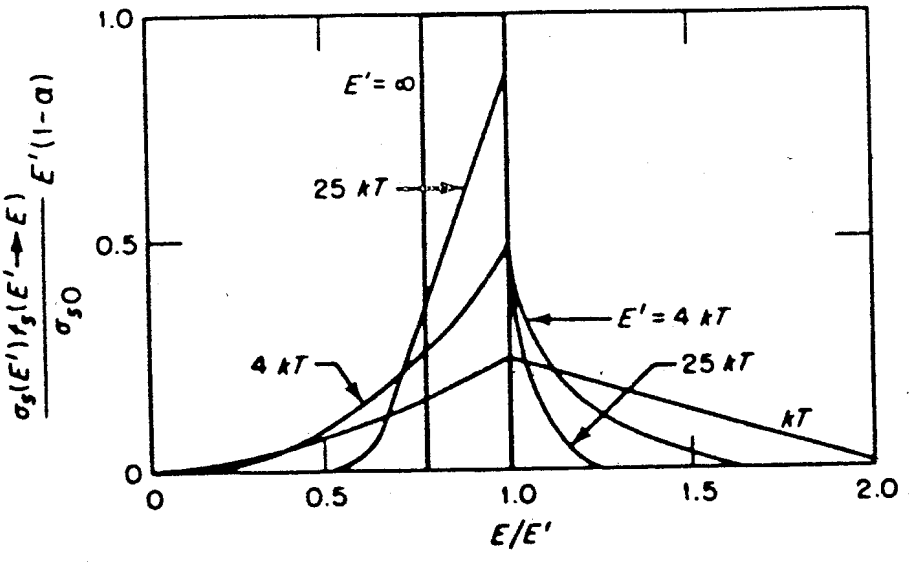

FIG. 7.6 ENERGY TRANSFER FUNCTION IN A MONATOMIC GAS WITH $A = 16$ (AFTER K. H. BECKURTS AND K. WIRTZ, REF. 14).

It may be noted that for a proton gas, $\eta = 1$ and $\rho = 0$; then equation (7.30) takes the particularly simple form

$$\sigma_s(E')f_s(E' \to E) = \frac{\sigma_{s0}}{E'} \exp\frac{E' - E}{kT} \operatorname{erf}\sqrt{\frac{E'}{kT}} \quad \text{for } E' < E \tag{7.31}$$

$$= \frac{\sigma_{s0}}{E'} \operatorname{erf}\sqrt{\frac{E}{kT}} \quad \text{for } E' > E. \tag{7.32}$$

The foregoing expressions for $\sigma_s f_s$ can be used to treat the monatomic gas model in general transport problems. Such calculations are frequently employed, as indicated earlier, for comparison with more complicated scattering models. These models are found to be equivalent to the monatomic gas model at high temperatures.[15] Furthermore, this gas model has often been used with the mass of the scattering atom not equal to its actual mass but to some higher (semi-empirical) mass chosen to simulate binding effects in the realistic system.[16]

7.3d The General Scattering Law

A quantum-mechanical theory of neutron scattering from a system of bound nuclei, first proposed by E. Fermi,[17] using the Born approximation and what is now called the Fermi "pseudo-potential," has been refined by others.[18] A number of essentially equivalent theoretical expressions have been derived[19] and some of the more useful formulations will be discussed here.

Suppose neutrons are undergoing scattering in a medium containing bound atoms of a single element; the scattering may be dependent on the nuclear spin and different isotopes, as in §7.1d, but the difference in mass of the isotopes is neglected. It has been shown[20] that the scattering function may then be written as the sum of double differential coherent and incoherent macroscopic cross sections, i.e.,

$$\sigma_s(E')f_s(\Omega', E' \to \Omega, E) = \sigma_{\text{coh}}(\Omega', E' \to \Omega, E) + \sigma_{\text{inc}}(\Omega', E' \to \Omega, E) \tag{7.33}$$

where the terms on the right of equation (7.33) are given by

$$\sigma_{\text{coh}}(\Omega', E' \to \Omega, E) = \frac{\sigma_{\text{coh}}}{4\pi\hbar}\sqrt{\frac{E}{E'}}\frac{1}{2\pi}\int_{-\infty}^{\infty}\int e^{i(\varkappa\cdot\mathbf{r} - \epsilon t/\hbar)}G(\mathbf{r}, t)\,\mathbf{dr}\,dt \tag{7.34}$$

and

$$\sigma_{\text{inc}}(\Omega, E' \to \Omega, E) = \frac{\sigma_{\text{inc}}}{4\pi\hbar}\sqrt{\frac{E}{E'}}\frac{1}{2\pi}\int_{-\infty}^{\infty}\int e^{i(\varkappa\cdot\mathbf{r} - \epsilon t/\hbar)}G_s(\mathbf{r}, t)\,\mathbf{dr}\,dt, \tag{7.35}$$

and the integration over $\mathbf{r}$ extends over all space.*

* The symbol $\mathbf{dr}$ is used when the integration is over all space, instead of over a finite volume when dV is employed (see §1.1b).

In these equations, σ_{coh} and σ_{inc} are the bound coherent and incoherent cross sections defined in §7.1d, except that here (and in what follows) they are *macroscopic* cross sections; $\hbar$ is the reduced Planck constant. As before, $\epsilon = E' - E$ is the energy change of the neutron or the energy transfer to (or from) the scattering nucleus. The quantity $\hbar\boldsymbol{\varkappa}$ is now the neutron momentum change vector, defined by

$$\hbar\boldsymbol{\varkappa} = m(\mathbf{v}' - \mathbf{v}).$$

The functions G and G_s, which are *not* Green's functions, will be considered presently.

Before proceeding, attention may be called to a number of features of equation (7.34) and (7.35). First, it is seen that the nuclear aspects of the scattering are entirely contained in the quantities σ_{coh} and σ_{inc}; that is to say, these cross sections are sufficient to characterize the nuclear interaction between a neutron and a nucleus (or atom). The dynamics of the scattering system and, in particular, the interactions between the scattering atoms on the other hand, are contained in the G functions. This separation of the scattering function into two factors, one containing the neutron-nucleus interaction information and the other the binding information, is a consequence of the use of the Born approximation and the Fermi pseudo-potential.[21] In addition, it should be noted that the integrals involve only *changes* in the neutron momentum and energy.

The functions G and G_s are known as *pair distribution functions*,[22] and in the absence of quantum effects they may be interpreted in the following manner. If a scattering atom is at the origin at time zero, then $G(\mathbf{r}, t)$ is defined as the probability that a second atom will be present within a unit volume at position $\mathbf{r}$ at time t. The function $G(\mathbf{r}, t)$ may be written as the sum of two parts: one, $G_s(\mathbf{r}, t)$, where s stands for "self," applies when the second atom is the same (identically) as the first, and $G_d(\mathbf{r}, t)$, where d is for "distinct," refers to different (or distinct) atoms. Hence,

$$G(\mathbf{r}, t) = G_s(\mathbf{r}, t) + G_d(\mathbf{r}, t),$$

where G_s is the probability that an atom which is at the origin at the time zero will be at $\mathbf{r}$ at time t, whereas G_d is the probability that another atom will be at $\mathbf{r}, t$. These interpretations of the G functions are useful in suggesting approximations, as will be seen in due course.

The scattering laws expressed by equations (7.34) and (7.35) are often written in slightly different forms. Thus, using the definition

$$S(\boldsymbol{\varkappa}, \epsilon) \equiv \frac{1}{2\pi}\int_{-\infty}^{\infty}\int e^{i(\boldsymbol{\varkappa}\cdot\mathbf{r} - \epsilon t/\hbar)}G(\mathbf{r}, t)\,d\mathbf{r}\,dt, \tag{7.36}$$

equation (7.34) may be written as

$$\sigma_{coh}(\Omega', E' \to \Omega, E) = \frac{\sigma_{coh}}{4\pi\hbar}\sqrt{\frac{E}{E'}}\,S(\boldsymbol{\varkappa}, \epsilon), \tag{7.37}$$

and if $S_s(\boldsymbol{\varkappa}, \epsilon)$, which is also sometimes represented by $S_{inc}(\boldsymbol{\varkappa}, \epsilon)$, is defined in an analogous manner with $G_s(\mathbf{r}, t)$, there is an expression similar to equation (7.37) for $\sigma_{inc}(\boldsymbol{\Omega}', E' \to \boldsymbol{\Omega}, E)$, namely

$$\sigma_{inc}(\boldsymbol{\Omega}', E' \to \boldsymbol{\Omega}, E) = \frac{\sigma_{inc}}{4\pi\hbar}\sqrt{\frac{E}{E'}}\, S_s(\boldsymbol{\varkappa}, \epsilon). \tag{7.38}$$

The detailed balance condition, expressed by equation (7.11), can be written in terms of the functions $S(\boldsymbol{\varkappa}, \epsilon)$. This condition would relate a collision having momentum and energy changes $\hbar\boldsymbol{\varkappa}$ and ϵ with the inverse collision having changes $-\hbar\boldsymbol{\varkappa}$ and $-\epsilon$. If equations (7.33), (7.37), and (7.38) are substituted into equation (7.11), the result is

$$M(E, T)\sqrt{\frac{E'}{E}}\,[\sigma_{coh}S(-\boldsymbol{\varkappa}, -\epsilon) + \sigma_{inc}S_s(-\boldsymbol{\varkappa}, -\epsilon)]$$

$$= M(E', T)\sqrt{\frac{E}{E'}}\,[\sigma_{coh}S(\boldsymbol{\varkappa}, \epsilon) + \sigma_{inc}S_s(\boldsymbol{\varkappa}, \epsilon)]$$

This equation must be satisfied by both the coherent and incoherent parts separately; upon making this separation and introducing equation (7.7) for the Maxwell distribution, $M(E, T)$ it is found that

$$S(\boldsymbol{\varkappa}, \epsilon) = e^{\epsilon/kT}S(-\boldsymbol{\varkappa}, -\epsilon) \tag{7.39}$$

and

$$S_s(\boldsymbol{\varkappa}, \epsilon) = e^{\epsilon/kT}S_s(-\boldsymbol{\varkappa}, -\epsilon). \tag{7.40}$$

In view of the importance of the detailed balance condition, calculations of the scattering functions are often set up so that the equations (7.39) and (7.40) are satisfied automatically. In particular, equation (7.39) may be written

$$e^{-\epsilon/2kT}S(\boldsymbol{\varkappa}, \epsilon) = e^{\epsilon/2kT}S(-\boldsymbol{\varkappa}, -\epsilon), \tag{7.41}$$

so that $e^{-\epsilon/2kT}S(\boldsymbol{\varkappa}, \epsilon)$ must be an even function of ϵ.

It will be seen that in many scattering models, including those for polycrystalline solids and molecular liquids, $S(\boldsymbol{\varkappa}, \epsilon)$ is a function of $\boldsymbol{\varkappa}^2$ and ϵ, and not of the vector $\boldsymbol{\varkappa}$ directly. When this is the case, it is convenient to define new dimensionless variables[23]

$$\alpha \equiv \frac{\hbar^2\kappa^2}{2AmkT} = \frac{E' + E - 2\mu_0\sqrt{EE'}}{AkT} \tag{7.42}$$

$$\beta \equiv \frac{-\epsilon}{kT} = \frac{E - E'}{kT}. \tag{7.43}$$

If $S(\alpha, \beta)$ is now defined by

$$S(\alpha, \beta) \equiv kTe^{\beta/2}S(\boldsymbol{\varkappa}, \epsilon), \tag{7.44}$$

it is seen that the detailed balance condition [equation (7.41)] requires that $S(\alpha, \beta)$ be an even function of β.

Experimental scattering cross sections are frequently interpreted in terms of the function $S(\alpha, \beta)$, as will be seen in §7.4g. If this function can be determined experimentally for negative values of β, i.e., for down-scattering, it can be extended to positive values, i.e., to up-scattering, by imposing the detailed balance condition. From the equations in this section, the scattering cross section is given by

$$\sigma_s(E')f_s(\Omega', E' \to \Omega, E) = \frac{1}{4\pi\hbar kT}\sqrt{\frac{E}{E'}}\, e^{-\beta/2}[\sigma_{coh}S(\alpha, \beta) + \sigma_{inc}S_s(\alpha, \beta)],$$

where $S_s(\alpha, \beta)$ is defined in a manner similar to equation (7.44).

Reference may be made to another form of the scattering law that is frequently employed. It includes a function $\chi(\varkappa, t)$ that is intermediate between G and S, and is therefore called the *intermediate scattering function*. The coherent and incoherent forms are defined by

$$\chi_{coh}(\varkappa, t) = \int e^{i(\varkappa\cdot\mathbf{r})}G(\mathbf{r}, t)\, d\mathbf{r} \tag{7.45}$$

and similarly

$$\chi_{inc}(\varkappa, t) = \int e^{i(\varkappa\cdot\mathbf{r})}G_s(\mathbf{r}, t)\, d\mathbf{r}, \tag{7.46}$$

so that the scattering functions in equations (7.34) and (7.35) can be written as

$$\sigma_{coh}(\Omega', E' \to \Omega, E) = \frac{\sigma_{coh}}{4\pi\hbar}\sqrt{\frac{E}{E'}}\frac{1}{2\pi}\int_{-\infty}^{\infty} e^{-i\epsilon t/\hbar}\chi_{coh}(\varkappa, t)\, dt \tag{7.47}$$

and

$$\sigma_{inc}(\Omega', E' \to \Omega, E) = \frac{\sigma_{inc}}{4\pi\hbar}\sqrt{\frac{E}{E'}}\frac{1}{2\pi}\int_{-\infty}^{\infty} e^{-i\epsilon t/\hbar}\chi_{inc}(\varkappa, t)\, dt. \tag{7.48}$$

7.3e The Incoherent Approximation

In view of the interpretation given above of the pair distribution functions, the "distinct" part of G, i.e., $G_d(\mathbf{r}, t)$, contains all the interference effects of the scattering. The reason is that interference is the result of the addition of the scattering amplitudes from different, i.e., distinct, atoms, and the correlations between such atoms are entirely contained in G_d. It was seen in §7.1d that these interference effects are important in elastic scattering, giving rise, for example, to Bragg peaks at particular angles with single crystals and to scattering cross-section peaks in polycrystalline materials, as in Fig. 7.2.

For *inelastic scattering*, however, especially in polycrystalline solids and in liquids, the interference effects are much less important.[24] Consequently, in

considering inelastic scattering, it is a good approximation to set $G_d = 0$; then equations (7.34) and (7.35) can be combined to give

$$\sigma_s(E')f_s(\Omega', E' \to \Omega, E)$$

$$= \frac{\sigma_{coh} + \sigma_{inc}}{4\pi\hbar}\sqrt{\frac{E}{E'}}\frac{1}{2\pi}\int_{-\infty}^{\infty}\int e^{i(\varkappa\cdot\mathbf{r} - \epsilon t/\hbar)}G_s(\mathbf{r}, t)\,\mathbf{dr}\,dt, \quad (7.49)$$

in accordance with equation (7.33). This result is known as the *incoherent approximation*, but it is important to recognize that both σ_{coh} and σ_{inc} are included. All that has really been done is to neglect the "distinct" part of the pair distribution function that gives rise to interference effects. Since G_d is complicated, the incoherent approximation represents a substantial simplification over the original form of the scattering function.

Because interference effects are usually significant for elastic scattering, particularly from crystals, it is evident that the incoherent approximation will not generally be satisfactory for treating elastic scattering. There are some situations, however, when elastic scattering is unimportant. For example, in a large homogeneous thermal reactor, the spectrum of thermal neutrons will be determined mainly by the competition between neutron thermalization and absorption. The thermalization or, more correctly, the energy transfer is determined to a great extent by the inelastic scattering. Thus, although the elastic scattering will affect the neutron transport properties, it will have little influence on the energy transfer in a large system. The incoherent approximation is then permissible.

Another situation of interest in which the incoherent approximation can be used is for scattering by hydrogen. It was seen in §7.1d that for randomly oriented proton spins, neutron scattering by hydrogen is almost entirely incoherent. In these circumstances, the neglect of G_d in equation (7.34) for the coherent scattering will cause very little error.

7.4 SCATTERING IN BOUND-ATOM SYSTEMS

7.4a Results of Quantum Mechanical Calculations

Detailed calculations of the neutron scattering law in bound-atom systems usually begin with the intermediate scattering functions, $\chi(\varkappa, t)$ and $\chi_{inc}(\varkappa, t)$ defined by equations (7.45) and (7.46). These functions can be calculated from a quantum-mechanical description of the dynamics of the scattering system. In particular, it has been shown[25] that for scattering for a system of N nuclei of one kind that

$$\chi_{coh}(\varkappa, t) = \frac{1}{N}\sum_{l,l'=1}^{N}\sum_{i} P_i(T)\langle\psi_i|e^{-i\varkappa\cdot\mathbf{r}_l(0)}e^{i\varkappa\cdot\mathbf{r}_{l'}(t)}|\psi_i\rangle \quad (7.50)$$

and

$$\chi_{\text{inc}}(\varkappa, t) = \frac{1}{N}\sum_{l=1}^{N}\sum_{i} P_i(T)\langle\psi_i|e^{-i\varkappa\cdot\mathbf{r}_l(0)}e^{i\varkappa\cdot\mathbf{r}_{l'}(t)}|\psi_i\rangle, \tag{7.51}$$

where the symbols $\langle|\ |\rangle$ indicate that a quantum mechanical expectation value is to be computed by integration over the variables of the wave function ψ_i. In these equations the indices l and l' refer to the various scattering atoms present, whereas i labels the quantum mechanical state of the system. The quantity $P_i(T)$ is the probability that the system is initially in the quantum state represented by ψ_i with energy E_i, so that, according to statistical mechanics,

$$P_i(T) = e^{-E_i/kT}\Big/\sum_{i} e^{-E_i/kT}.$$

From equations (7.50) and (7.51) it is possible to derive the intermediate scattering function for any system in which the quantum states are known. For example,[26] in considering a molecular gas in its electronic ground state it is often a good approximation to write the wave function, ψ_i, as the product of the known translational, rotational, and vibrational wave functions, i.e.,

$$\psi_i \simeq \psi_{i(T)}\psi_{i(R)}\psi_{i(V)}.$$

For realistic scattering systems, such as crystalline solids and molecular liquids, the quantum states are not known in detail, and it is then the practice to apply an approximate model for calculating the scattering function. In order to understand the features such a model should have, it will be useful to consider a few relatively simple scattering systems.

7.4b Intermediate Scattering Function for Monatomic Gas

For scattering from a monatomic gas with atoms of mass Am, the intermediate scattering function is found[27] to be

$$\chi_{\text{inc}}(\varkappa, t) = \chi_{\text{coh}}(\varkappa, t) = \exp -\left[\frac{\kappa^2}{2Am}(kTt^2 - i\hbar t)\right]. \tag{7.52}$$

In this case, $\chi_{\text{inc}} = \chi_{\text{coh}}$ since there is no interference between the various scattering atoms; that is to say, there is no contribution from the $l \neq l'$ terms in equation (7.50). By substituting the results of equation (7.52) into equation (7.47) or (7.48), and using equation (7.33), it is possible to derive equation (7.26) for the scattering function.

It is worth noting that for small times, equation (7.52) reduces to

$$\chi_{\text{inc}} \simeq \exp\left(\frac{\hbar\kappa^2}{2Am}it\right) \quad \text{for } t \text{ small.} \tag{7.53}$$

This result applies more generally than for a monatomic gas; it is usually the correct limiting form for small values of t in other systems.

7.4c Isotropic Harmonic Oscillator

In the isotropic harmonic model, the scattering atom of mass Am is considered to be bound to other atoms by an isotropic harmonic force; the atoms oscillate, as though they were connected by springs, and the restoring force at any instant is proportional to the displacement of the atom from its equilibrium (or reference) position. This model was used in the first attempt to represent neutron scattering from bound nuclei.[28] It is sometimes referred to as the Einstein crystal model, because it is similar to one used by A. Einstein for computing specific heats of solids.[29] If the energy quantum of oscillation is $\hbar\omega_0$, where ω_0 is the angular oscillation frequency, then for incoherent scattering the isotropic harmonic model leads to[30]

$$\chi_{\text{inc}}(\boldsymbol{\kappa}, t) = \exp\left\{\frac{\hbar\kappa^2}{2Am\omega_0}[(\bar{n}+1)(e^{i\omega_0 t}-1)+\bar{n}(e^{-i\omega_0 t}-1)]\right\}, \quad (7.54)$$

where $\bar{n}$ is the average number of oscillator quanta excited at the existing temperature, T, i.e.,

$$\bar{n} = \frac{1}{e^{\hbar\omega_0/kT}-1}.$$

If the atom were weakly bound in the crystal, the vibrational energy quantum $\hbar\omega_0$ would be small in comparison with the thermal energy kT; then since $\hbar\omega_0/kT \ll 1$, the expression for $\bar{n}$ reduces to $\bar{n} = kT/\hbar\omega_0$. If this value for $\bar{n}$ is inserted into equation (7.54) and the exponentials are expanded and the limit is taken for $\omega_0 \to 0$, the result is the same as equation (7.52) for a monatomic gas. Thus the scattering atom behaves as if it were free in a gas, since the weak binding has essentially no effect on neutron scattering. Although this result has been derived for a particular model, it is true in general when the vibrational energy is small in comparison with kT [31]; thus, the monatomic gas model represents the high-temperature limit for scattering from bound systems. In practice, vibrational energies are often in the vicinity of 0.1 eV; hence the temperatures would have to be very high, e.g., $\gg 1000°$K, for the limit to be realized.

The limit of strong binding or low temperature, i.e. when $\hbar\omega_0/kT \gg 1$, is somewhat more interesting; then $\bar{n} \approx 0$, and equation (7.54) becomes

$$\chi_{\text{inc}}(\boldsymbol{\kappa}, t) = \exp\left\{\frac{\hbar\kappa^2}{2Am\omega_0}(e^{i\omega_0 t}-1)\right\}. \quad (7.55)$$

This zero-temperature form of χ_{inc} would apply to a situation in which the neutron could only *lose* energy in a scattering collision, since the oscillating atom is initially in its lowest energy state.

If the bound (macroscopic) scattering cross section, σ_b, is represented by

$$\sigma_b = \sigma_{\text{coh}} + \sigma_{\text{inc}},$$

then in the incoherent approximation, i.e., using equations (7.47) and (7.49), the

zero-temperature isotropic harmonic oscillator equation (7.55) gives the scattering function as

$$\sigma_s(E')f_s(\Omega', E' \to \Omega, E)$$
$$= \frac{\sigma_b}{4\pi}\sqrt{\frac{E}{E'}}\frac{1}{2\pi\hbar}\int_{-\infty}^{\infty} e^{-i\epsilon t/\hbar}\exp\left\{\frac{\hbar\kappa^2}{2Am\omega_0}(e^{i\omega_0 t}-1)\right\}dt. \quad (7.56)$$

Upon expanding the exponential as

$$\exp\left\{\frac{\hbar\kappa^2}{2Am\omega_0}(e^{i\omega_0 t}-1)\right\} = \exp\left(-\frac{\hbar\kappa^2}{2Am\omega_0}\right)\sum_{n=0}^{\infty}\frac{1}{n!}\left(\frac{\hbar\kappa^2}{2Am\omega_0}\right)^n e^{in\omega_0 t},$$

and using the representation of the Dirac delta function (see Appendix)

$$\frac{1}{2\pi}\int_{-\infty}^{\infty} e^{itx}\,dt = \delta(x), \quad (7.57)$$

it is found that

$$\sigma_s(E')f_s(\Omega', E' \to \Omega, E)$$
$$= \frac{\sigma_b}{4\pi}\sqrt{\frac{E}{E'}}\exp\left(-\frac{\hbar\kappa^2}{2Am\omega_0}\right)\sum_{n=0}^{\infty}\frac{1}{n!}\left(\frac{\hbar\kappa^2}{2Am\omega_0}\right)^n \delta(\epsilon - n\hbar\omega_0), \quad (7.58)$$

which is the form derived by E. Fermi.[32]

It will be noted that the nth term in the expansion contains $\delta(\epsilon - n\hbar\omega_0)$ and thus corresponds to the excitation of n vibrational quanta of the oscillating atom, with an energy loss of $n\hbar\omega_0$ by the neutron. The expression of equation (7.58) is consequently known as the *phonon expansion* since the nth term represents the creation of n phonons in the crystal (§7.1c).

The energy transfer cross section may be found by integrating equation (7.58) over all scattering angles, μ_0; the total scattering cross section is obtained by integrating over all final energies, E. If the total scattering cross section is denoted by $\sigma_s(E')$, i.e.,

$$\sigma_s(E') = \sum_{n=0}^{\infty}\sigma_n(E'),$$

then, from equation (7.58),

$$\sigma_n(E') = \frac{\sigma_b}{4\pi}\int_0^{E'}\sqrt{\frac{E}{E'}}\int\exp\left(-\frac{\hbar\kappa^2}{2Am\omega_0}\right)\frac{1}{n!}\left(\frac{\hbar\kappa^2}{2Am\omega_0}\right)^n \delta(\epsilon - n\hbar\omega_0)\,d\Omega\,dE. \quad (7.59)$$

In this equation, ϵ and κ^2 are functions of E, E', and of the scattering angle, μ_0, given by

$$\epsilon = E' - E$$

and

$$\hbar^2\kappa^2 = 2m(E' + E - 2\mu_0\sqrt{EE'})$$

as in §7.3b. The $d\Omega$ in equation (7.59) is replaced by $2\pi\, d\mu_0$, and the variable changed from μ_0 to x, where

$$x \equiv \frac{\hbar\kappa^2}{2Am\omega_0},$$

then

$$|d\mu_0| = \frac{A\hbar\omega_0}{2\sqrt{EE'}}\,|dx|.$$

Upon integrating equation (7.59) first over E, the delta function requires that

$$E = E' - n\hbar\omega_0,$$

and introduction of the variable x leads to

$$\begin{aligned} \sigma_n(E') &= \frac{\sigma_b}{4}\frac{A\hbar\omega_0}{E'}\frac{1}{n!}\int_{x_-}^{x_+} x^n e^{-x}\,dx \quad \text{if} \quad E'/\hbar\omega_0 \geqslant n \\ &= 0 \qquad\qquad\qquad\qquad\qquad\quad \text{if} \quad E'/\hbar\omega_0 < n, \end{aligned} \tag{7.60}$$

where the limits of integration are defined by

$$x_\pm = \frac{(\sqrt{E'} \pm \sqrt{E' - n\hbar\omega_0})^2}{A\hbar\omega_0}.$$

In particular, the cross section for no phonon excitation, i.e., $n = 0$, is given by

$$\sigma_0(E') = \frac{\sigma_b}{4}\frac{A\hbar\omega_0}{E'}\left[1 - \exp\left(-\frac{4E'}{A\hbar\omega_0}\right)\right]. \tag{7.61}$$

At low neutron energies, there is not sufficient energy available to excite phonons, so that the total scattering cross section is

$$\sigma_s(E') = \sigma_0(E') \quad \text{for} \quad E' \text{ small.}$$

It follows from equation (7.61), therefore, that

$$\sigma_s(E') \to \sigma_b \quad \text{as} \quad E' \to 0, \tag{7.62}$$

as expected. At higher energies, however, it is seen that $\sigma_0(E')$ decreases as $1/E'$.

The phonon expansion developed above, in equations (7.56) through (7.62), is for a zero-temperature oscillator. A similar phonon expansion can be made for finite temperatures, but the results are more complicated.[33] For oscillators at finite temperature, the scattered neutron may gain energy by absorbing phonons from the solid as well as lose energy by the creation of phonons, i.e., absorption of energy by the solid.

To return to the zero-temperature phonon approximation, it is of interest to examine the results for the scattering of neutrons by bound protons, i.e., hydrogen atoms, for which $A = 1$. The curve in Fig. 7.7[34] shows the calculated ratio of $\sigma_s(E')/\sigma_{s0}$, where σ_{s0}, defined in §7.3a, is the scattering cross section of

free gaseous hydrogen atoms, as a function of the neutron energy relative to the phonon (vibrational quantum) energy, i.e., $E'/\hbar\omega_0$. The value of σ_{s0} for hydrogen is taken to be $\sigma_b/4$, in accordance with the arguments in §7.1c. Hence, from equation (7.62) for $E' = 0$, it follows that $\sigma_s(E')/\sigma_{s0} = 4$. As E' increases, it is seen that the scattering cross section ratio decreases approximately as $1/E'$, provided $E' < \hbar\omega_0$ and no phonons are excited. When $E'/\hbar\omega_0$ is 1, one phonon can be excited, and there is a sudden increase in the scattering cross section due to the contribution of $\sigma_1(E')$; there are subsequent jumps at $E'/\hbar\omega_0 = 2$ when two phonons can be excited and contribute to the total scattering, and so on.

It is seen from Fig. 7.7 that at the higher neutron energies the scattering cross section approaches the monatomic gas value, i.e., $\sigma_s(E')/\sigma_{s0} = 1$. It can be shown[35] that, at such neutron energies, the energy transfers are about the same in scattering from monatomic hydrogen gas, i.e., free protons, as from oscillator (bound) protons with the same average kinetic energy. Thus, at high neutron energies, e.g., $E' > 10\hbar\omega_0$, the scattering is not significantly affected by the chemical binding of the scattering atoms. On the other hand, it is clear that, in the phonon model, there will be no energy transfer at all from the neutron to the bound atom when $E' < \hbar\omega_0$, and the transfer will be small for $E' \approx \hbar\omega_0$.

The theory described above, of neutron scattering by protons bound by an isotropic harmonic potential, is of interest for several reasons. In the first place, the model exhibits the effects of chemical binding in an especially simple and clear manner. Second, it furnishes an introduction to methods for treating more

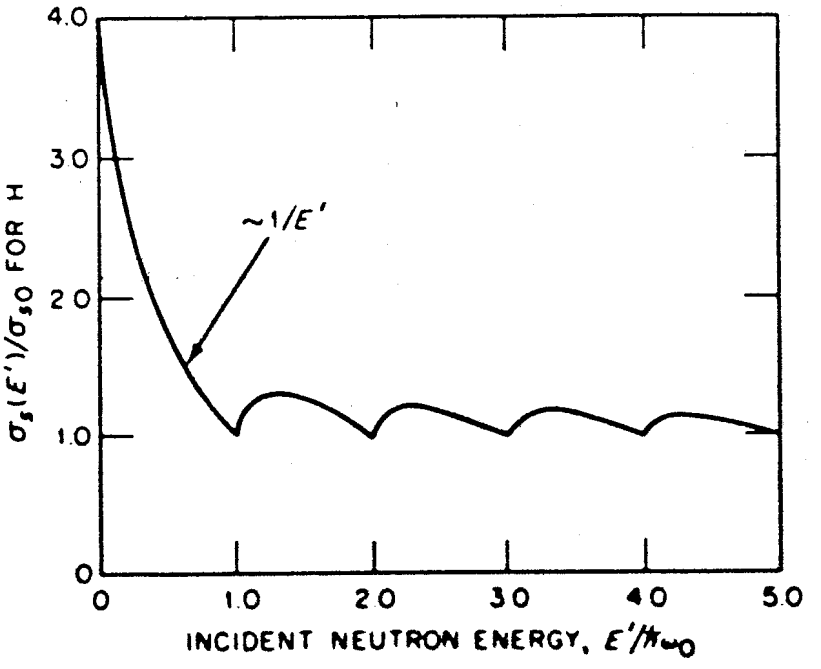

FIG. 7.7 CALCULATED RATIO OF SCATTERING CROSS SECTIONS OF BOUND AND FREE HYDROGEN ATOMS VS INCIDENT NEUTRON ENERGY (AFTER E. FERMI, REF. 34).

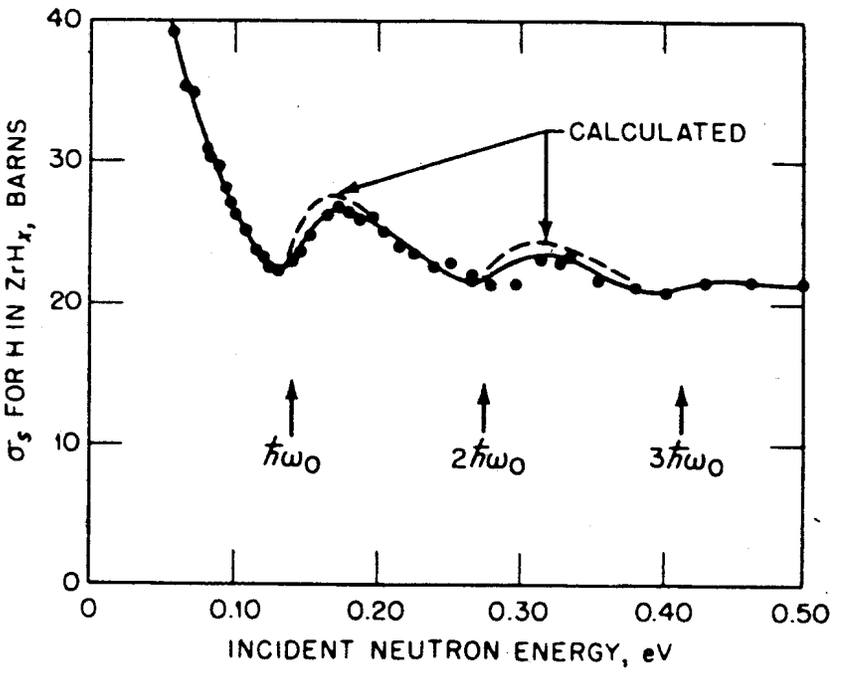

FIG. 7.8 OBSERVED AND CALCULATED (HARMONIC OSCILLATOR) SCATTERING CROSS SECTIONS OF HYDROGEN IN ZrH_x (AFTER A. W. MCREYNOLDS, *ET AL.*, REF. 37).

realistic scattering solids. Furthermore, it turns out to be a good first approximation to the scattering in some actual moderators, particularly zirconium hydride.[36]

In the crystal lattice of zirconium hydride, each hydrogen atom is at the center of a tetrahedron formed by four zirconium atoms. Because of the large mass ratio, $A_{Zr}/A_H \approx 91$, and the symmetrical environment of the protons, the binding is quite well approximated by considering the protons to be harmonically bound, as in an Einstein solid, with $\hbar\omega_0 = 0.137$ eV. The (microscopic) scattering cross sections of hydrogen in zirconium hydride, obtained by subtracting the cross section for zirconium from the experimental values for the hydride, are shown in Fig. 7.8 as a function of neutron energy.[37] The resemblance to Fig. 7.7 is striking; the rounding off of the curve in Fig. 7.8 at neutron energies of $\hbar\omega_0$, $2\hbar\omega_0$, etc., is due to thermal motion of the bound atoms.

A discrepancy between the isotropic harmonic model and an actual crystal arises from the possibility that a neutron having energy less than $\hbar\omega_0$ may lose energy even at low temperatures. The reason is that, in the crystal, the neutron can excite other vibrational modes, namely, the so-called acoustical modes, with energies less than $\hbar\omega_0$, the energy of the Einstein oscillator.[38]

7.4d Scattering by Real Crystalline Solids: Cubic Crystals

In the theory of the solid state[39] it is well known that the Einstein crystal represents only a crude approximation to the phonon spectrum, i.e., the spectrum

of vibrational frequencies, of a real monatomic crystal. For the Einstein solid, the vibrational frequencies are required to be multiples of ω_0, but in actual situations they do not have this simple relationship. For scattering from a *simple cubic crystal* it is possible, however, to devise a scattering law, not much more complicated than that for an Einstein crystal, which has been widely used for treating inelastic scattering from crystalline moderators.

In making this derivation, the following approximations and assumptions are involved: (1) The incoherent approximation is used; that is, as in §7.3e, interference effects are neglected. (2) It is assumed that atoms of only one kind are present in the solid; they are bound by harmonic interatomic forces in a crystal with cubic symmetry having one atom per unit cell in the crystal lattice. (3) The possible vibrational modes (or quanta) are described by a continuous spectrum, $f(\omega)$, normalized so that

$$\int_0^\infty f(\omega)\, d\omega = 1,$$

where $f(\omega)\, d\omega$ is the probability that the lattice will have normal modes of vibration between ω and $\omega + d\omega$. In practice, there will be an upper limit, ω_{max}, to the frequency spectrum, and this is allowed for by setting $f(\omega) = 0$ for $\omega > \omega_{max}$.

Under these conditions, the intermediate scattering function may be written as[40]

$$\chi_{inc}(\varkappa, t) = \exp\left\{\frac{\hbar\kappa^2}{2Am}\,[\gamma(t) - \gamma(0)]\right\} \tag{7.63}$$

where

$$\gamma(t) = \int_0^\infty \left\{\coth\left(\frac{\hbar\omega}{2kT}\right)\cos\omega t + i\sin\omega t\right\}\frac{f(\omega)}{\omega}\, d\omega. \tag{7.64}$$

The function $\gamma(0)$ is obtained from equation (7.64) by setting $t = 0$; thus,

$$\gamma(0) = \int_0^\infty \coth\left(\frac{\hbar\omega}{2kT}\right)\frac{f(\omega)}{\omega}\, d\omega.$$

By extending $f(\omega)$ to negative frequencies by defining $f(-\omega) = f(\omega)$, it can be shown that

$$\gamma(t) - \gamma(0) = \int_{-\infty}^{\infty} \frac{f(\omega)e^{-\hbar\omega/2kT}}{2\omega\sinh(\hbar\omega/2kT)}\,(e^{-i\omega t} - 1)\, d\omega. \tag{7.65}$$

Upon combining equations (7.47), (7.48), and (7.49) with (7.63) and (7.65), the double differential scattering cross section is given by

$$\sigma_s(E')f_s(\Omega', E' \to \Omega, E) = \frac{\sigma_b}{4\pi\hbar}\sqrt{\frac{E}{E'}}\,\frac{1}{2\pi}\int_{-\infty}^{\infty} e^{-i\kappa\iota/\hbar}$$

$$\times \exp\left[\frac{\hbar\kappa^2}{2Am}\int_{-\infty}^{\infty}\frac{f(\omega)e^{-\hbar\omega/2kT}}{2\omega\sinh(\hbar\omega/2kT)}\,(e^{-i\omega t} - 1)\, d\omega\right] dt. \tag{7.66}$$

This expression has been used extensively for obtaining inelastic scattering cross sections in thermalization studies, and appropriate computer programs have been developed.[41] In these codes, the function $f(\omega)$, as well as the temperature and the mass number, A, of the scattering material specify the problem.

Some comments may be made concerning equation (7.66). First, if only one mode of vibration is allowed, then this expression reduces to equation (7.54) for a harmonic oscillator (or Einstein crystal). In verifying this, allowance must be made for the inclusion of both positive and negative frequencies in equation (7.66); $f(\omega)$ for a single mode of vibration must then be represented by

$$f(\omega) = \delta(\omega - \omega_0) + \delta(\omega + \omega_0),$$

thus permitting frequencies of ω_0 and $-\omega_0$.

A phonon expansion may be made for the scattering, just as in §7.4c, by expanding the exponential as a power series, i.e.,

$$\exp\left[\frac{\hbar\kappa^2}{2Am}\gamma(t)\right] = \sum_{n=0}^{\infty}\frac{1}{n!}\left[\frac{\hbar\kappa^2}{2Am}\gamma(t)\right]^n.$$

The nth term in this expression can then be shown to correspond to the excitation or absorption of n phonons. In practice, if $f(\omega)$ is known, then the first few terms in the expansion may be evaluated numerically, but the higher terms are so complicated that they are usually approximated.

It has been found that equation (7.66) gives reasonably accurate values for inelastic scattering cross sections even when the conditions assumed in its derivation are not satisfied. Thus, it has been applied to solids in which the crystals do not have cubic symmetry, the interatomic forces are not harmonic, and there is more than one atom per unit cell. In performing the computations for such materials, the function $f(\omega)$ is usually taken from some model of the crystal dynamics from which the normal modes of vibration can be evaluated. As an example, scattering by graphite will be discussed in §7.4h. It is also possible to derive approximate values of $f(\omega)$ from measured scattering cross sections, as will be seen in §7.4g.

Typically, values of the double differential cross section calculated from equation (7.66) agree with those obtained experimentally. There may be marked discrepancies at some values of energy and momentum transfer, but the over-all trends are reasonable. Moreover, for reactor calculations, the main concern is the effect of the scattering cross sections on the neutron spectrum in the system. Errors in detailed aspects of the cross sections can often be tolerated because they have little effect on the neutron spectrum. It is important to note, however, that if the model used for computing $\sigma_s f_s$ is not firmly based on the physics of the scattering medium, then experimental checks must be made on the validity of the calculated spectrum.

Efforts are continually being made[42] to assess or remove the approximations involved in the derivation of equation (7.66). Nevertheless, it appears that the

inelastic cross sections derived from this equation are adequate for a variety of neutron transport problems.

Since equation (7.66) makes use of the incoherent approximation, in which interference effects are neglected, it is evident that it cannot be applied to elastic scattering, for which interference effects are important. For systems in which transport of thermal neutrons is significant, the coherent elastic scattering should be taken into account. This involves the evaluation of χ_{coh}, given by equation (7.50), using the techniques of solid-state theory; the details are, however, beyond the scope of this book.[43]

7.4e Liquids: Model of the Diffusing Atom

A simple and suggestive classical model has been proposed for treating the scattering of neutrons by monatomic liquids.[44] An atom is considered to be diffusing in the liquid, and the pair distribution function, $G_s(\mathbf{r}, t)$, can then be found by using its classical interpretation as the probability that an atom present at the origin at time zero will be at $\mathbf{r}$ at time t. If the position probability of the atom is governed by the diffusion equation

$$\frac{\partial G_s}{\partial t} = Dv\nabla^2 G_s, \tag{7.67}$$

with D a diffusion coefficient, together with the condition

$$G_s(\mathbf{r}, 0) = \delta(\mathbf{r}),$$

then the solution is

$$G_s(\mathbf{r}, t) = \frac{\exp(-r^2/4Dvt)}{(4\pi Dvt)^{3/2}}. \tag{7.68}$$

It will be observed that equation (7.68) is similar to the expression derived from Fermi age theory for the slowing down of neutrons from a point source.[45] More generally, the result is familiar in heat conduction.[46]

By using equation (7.68), the incoherent intermediate scattering function may be obtained from equation (7.46). Upon performing the Fourier transformation,[47] the result is

$$\chi_{inc}(\boldsymbol{\kappa}, t) = \exp(-\kappa^2 Dvt), \tag{7.69}$$

In more accurate theories of scattering by liquids, the coefficient of κ^2, i.e., Dvt, is replaced by more general functions of the time.[48]

7.4f The Gaussian Approximation

In all the scattering models considered above, the intermediate scattering function in the incoherent approximation can be written in the form

$$\chi_{inc}(\boldsymbol{\kappa}, t) = \exp\left\{\frac{\hbar\kappa^2}{2Am}[\gamma(t) - \gamma(0)]\right\}. \tag{7.70}$$

For the simple cubic crystal, this actual expression was used in equation (7.63); it is also applicable to the Einstein crystal and the free monatomic gas, which have been seen to be special cases of the cubic crystal (§§7.4c, 7.4d). Moreover, the classical model of an atom diffusing in a liquid, i.e., equation (7.69), is of the same form with

$$\gamma(t) = -\frac{2DvAm}{\hbar} t.$$

According to equation (7.65), the function $\gamma(t) - \gamma(0)$ is negative for $t > 0$ for the cubic crystal, and it is also negative for the diffusing atom. It follows, therefore, that equation (7.70) is a Gaussian function of κ for any $t > 0$. Thus, insofar as the dependence of χ_{inc} on κ, the momentum transfer, is concerned, equation (7.70) is Gaussian for all the cases considered.

Because of its considerable generality, equation (7.70) has been used extensively for determining scattering from systems, such as liquids, for which accurate theoretical treatments are not available. Under these circumstances, it is known as the *Gaussian approximation*. In applying this approximation, $\gamma(t)$ must be known and it is often derived from equation (7.65) with $f(\omega)$ estimated from physical considerations. An application of this procedure in connection with the scattering of neutrons by water is described in §7.4h.

The function $\gamma(t) - \gamma(0)$ may be given a simple classical interpretation by more or less reversing the derivation for the diffusing atom. It can be shown that the Fourier transform of $\chi_{\text{inc}}(\boldsymbol{\varkappa}, t)$ gives the pair distribution function, $G_s(\mathbf{r}, t)$. Thus, the Fourier inversion theorem[49] applied to equation (7.46) yields

$$G_s(\mathbf{r}, t) = \frac{1}{8\pi^3} \int e^{-i(\boldsymbol{\varkappa}\cdot\mathbf{r})} \chi_{\text{inc}}(\boldsymbol{\varkappa}, t)\, d\boldsymbol{\varkappa}. \tag{7.71}$$

If this is combined with equation (7.70), using the definition

$$-a^2 \equiv \frac{\gamma(t) - \gamma(0)}{2Am} \hbar, \tag{7.72}$$

it is found that

$$G_s(\mathbf{r}, t) = \frac{\exp(-r^2/4a^2)}{(4\pi a^2)^{3/2}}. \tag{7.73}$$

It should be observed that G_s is properly normalized as a probability, i.e.,

$$\int G_s(\mathbf{r}, t)\, \mathbf{dr} = 1,$$

and that the mean of r^2 is given by

$$\overline{r^2} = \int r^2 G_s(\mathbf{r}, t)\, \mathbf{dr} = 6a^2.$$

Thus, the expected mean square displacement of the atom during the time t, i.e., $\overline{r^2}$, is proportional to a^2 and hence to $\gamma(t) - \gamma(0)$. This is the required physical significance of the latter function.

Since the foregoing is based on a *classical* interpretation of $G_s(\mathbf{r}, t)$, it should be employed only with classical forms of $\gamma(t)$. These may be found from expressions derived earlier by considering the classical limit of $\hbar \to 0$. For example, in the case of a monatomic gas, equation (7.52), together with equations (7.70) and (7.72), gives, in the limit $\hbar \to 0$,

$$a^2 = \frac{kT}{2Am} t^2 \quad \text{(monatomic gas)}.$$

Similarly, for the other models:

$$a^2 = \frac{kT}{Am} \int_0^\infty \frac{f(\omega)}{\omega^2} (1 - \cos \omega t)\, d\omega \quad \text{(simple cubic crystal)}$$

$$a^2 = \frac{kT}{Am} \frac{1 - \cos \omega_0 t}{\omega_0^2} \quad \text{(harmonic oscillator or Einstein crystal)}$$

and

$$a^2 = Dvt \quad \text{(diffusing atom)}.$$

The values of a^2, i.e., one-sixth the mean square displacements, for these models are plotted in Fig. 7.9 as functions of time, with arbitrary scales.[50] The vibrational frequency spectrum of the crystal was assumed to be of the Debye form

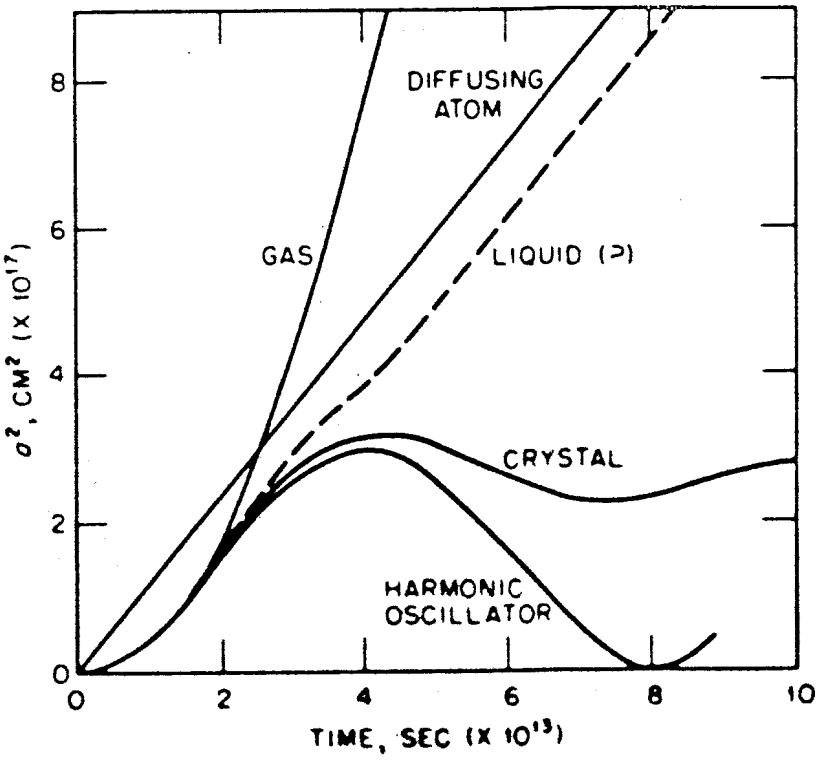

FIG. 7.9 VALUES OF THE QUANTITY a^2 AS FUNCTION OF TIME FOR VARIOUS MODELS (AFTER G. H. VINEYARD, REF. 44).

$f(\omega) = 3\omega^2/\omega_{\max}^2$.[51] A conjectured behavior for an atom in a liquid is indicated by the broken curve; at short times this is like the one for a monatomic gas (or simple crystal) and at long times it parallels that of a diffusing atom.

7.4g Experimental Determination of Scattering Laws

As noted in §7.1a, scattering cross sections in the thermal region are complicated functions of the neutron energy; it is thus not practical to measure these cross sections over the full range of neutron energies and scattering angles. Such scattering cross sections as have been determined experimentally are useful, however, in at least two respects. First, they may be compared with the predictions of theoretical models, thereby confirming or indicating deficiencies in the theory, as in §7.4c. Second, the experimental cross sections may be used to determine some parameters or a function in a semiempirical expression for the scattering cross sections. Once this determination has been made, the cross sections for other neutron energies and scattering angles may be computed from the given expression.

To illustrate the latter application, suppose that an inelastic scattering cross section has been measured and that it is desired to fit it to the form of equation (7.66), which applies to a simple cubic crystal. Thus, the function $f(\omega)$ is to be determined. First, the function $S_s(\varkappa, \epsilon)$ is derived from the experimental cross sections by means of equation (7.38) using the incoherent approximation.

Furthermore, according to equations (7.38) and (7.66),

$$S_s(\varkappa, \epsilon) = \frac{1}{2\pi}\int_{-\infty}^{\infty} e^{-i\epsilon t/\hbar} \exp\left[\frac{\hbar\kappa^2}{2Am}\int_{-\infty}^{\infty} \frac{f(\omega)e^{-\hbar\omega/2kT}}{2\omega \sinh(\hbar\omega/2kT)}(e^{-i\omega t} - 1)\,d\omega\right] dt. \tag{7.74}$$

For small values of κ^2, i.e., small momentum transfer, the exponent in the square brackets in equation (7.74) may be expanded. By using the representation of the delta function in equation (7.57), it is thus found that if $\epsilon = -\hbar\omega$, then

$$\lim_{\varkappa \to 0}\left[\frac{S_s(\varkappa, \epsilon)}{\kappa^2}\right] = \frac{\hbar}{2Am}\frac{e^{-\hbar\omega/2kT}}{2\omega \sinh(\hbar\omega/2kT)} f(\omega), \tag{7.75}$$

which can be solved for $f(\omega)$ if $S_s(\varkappa, \epsilon)$ is known for small $\varkappa$. Thus, by extrapolating results derived from the measured scattering cross sections to low momentum transfers, it is possible to derive an empirical frequency function, $f(\omega)$, for use in the scattering law. Once $f(\omega)$ is available, $\sigma_s f_s$ can be computed for all neutron energies from equation (7.66). In practice, the function $S_s(\alpha, \beta)$, defined by equation (7.44), is generally used rather than $S_s(\varkappa, \epsilon)$ for extrapolation purposes.[52] In this case, it is found that the frequency function is given as a function of β $(= \hbar\omega/kT)$ by

$$f(\beta) = 2\beta \sinh(\tfrac{1}{2}\beta) \lim_{\alpha \to 0}\left[\frac{S_s(\alpha, \beta)}{\alpha}\right].$$

It should be mentioned that there are a number of difficulties in determining the semiempirical scattering laws in the manner indicated above. In the first place, substantial corrections may have to be made to the experimental data to correct for multiple scattering[53] and for elastic and coherent scattering. In addition, it is necessary that the scattering law should be both reasonable physically and simple enough to be determined from the experimental data. In the next section, mention will be made of some semiempirical scattering calculations.

7.4h Applications to Actual Moderators

The considerations of the preceding sections will now be applied to actual moderators, graphite and water, in particular. Some reference will also be made to the results for other moderators.

Graphite as Moderator

The crystal structure of graphite is somewhat unusual. The carbon atoms are arranged in a hexagonal pattern in planar sheets; adjacent atoms in each sheet

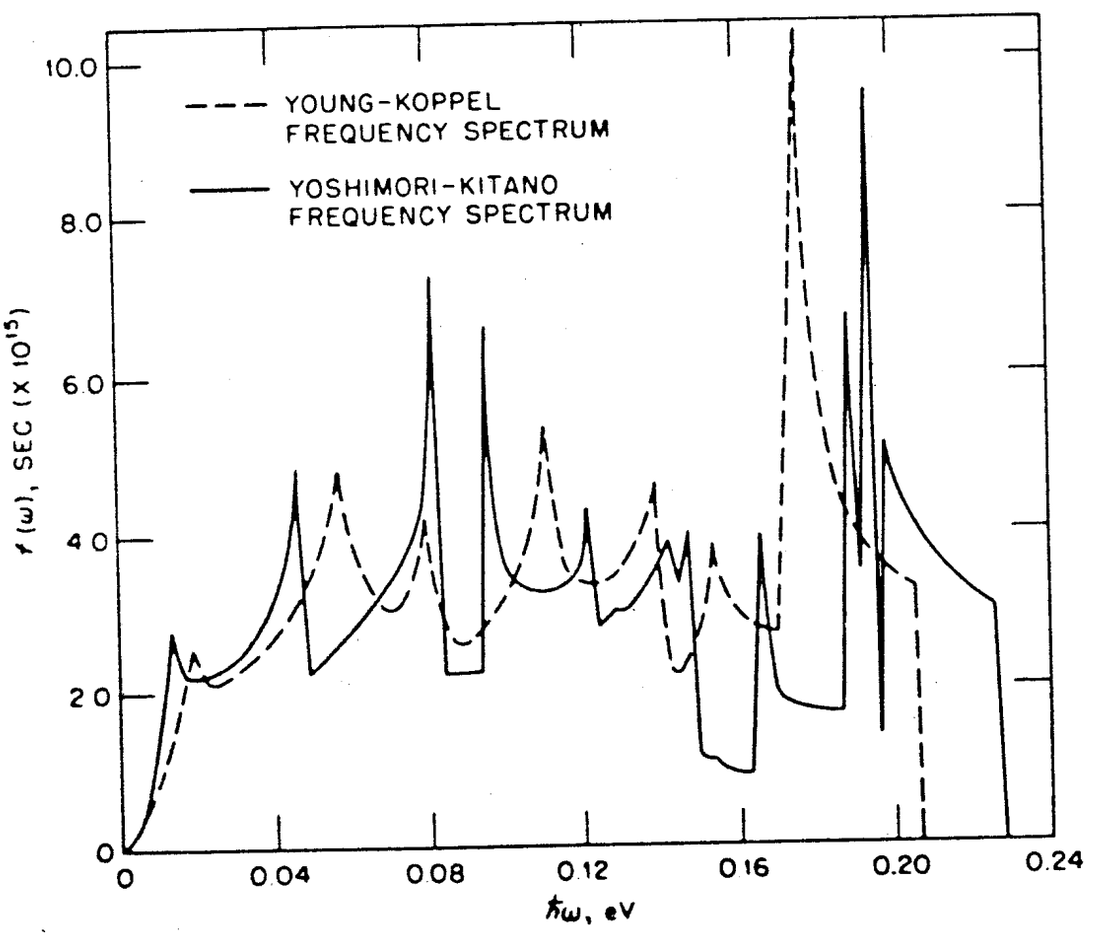

FIG. 7.10 PHONON SPECTRA FOR GRAPHITE DERIVED FROM TWO DIFFERENT MODELS (AFTER J. A. YOUNG AND J. U. KOPPEL, REF. 55).

are bound strongly, but the atoms in different sheets interact only weakly. Thus graphite is highly anisotropic; the thermal conductivity, for example, is quite different in the directions parallel and perpendicular, respectively, to the sheets of atoms. Nevertheless, values in good agreement with the measured double differential inelastic scattering cross sections of polycrystalline graphite have been obtained by using equation (7.66) for a cubic crystal in the incoherent approximation.[54] For these calculations, the phonon spectra, $f(\omega)$, in Fig. 7.10, were derived from models of the interatomic forces in graphite; the values for two slightly different models are shown.[55] The details of either spectrum are not to be taken too seriously because they result from specific features of the calculational model used. The general characteristics of the phonon spectra in Fig. 7.10 are believed to be reasonable; thus, they give fairly good agreement with the observed specific heat of graphite.

Simpler frequency spectra have been derived by the semiempirical method described in §7.4g.[56] As an example, the spectrum, $f(\beta)$, extrapolated from scattering measurements on graphite is given in Fig. 7.11,[57] together with one of the calculated spectra from Fig. 7.10, also expressed as $f(\beta)$. It is apparent that the frequency distributions are similar although they differ considerably in detail.

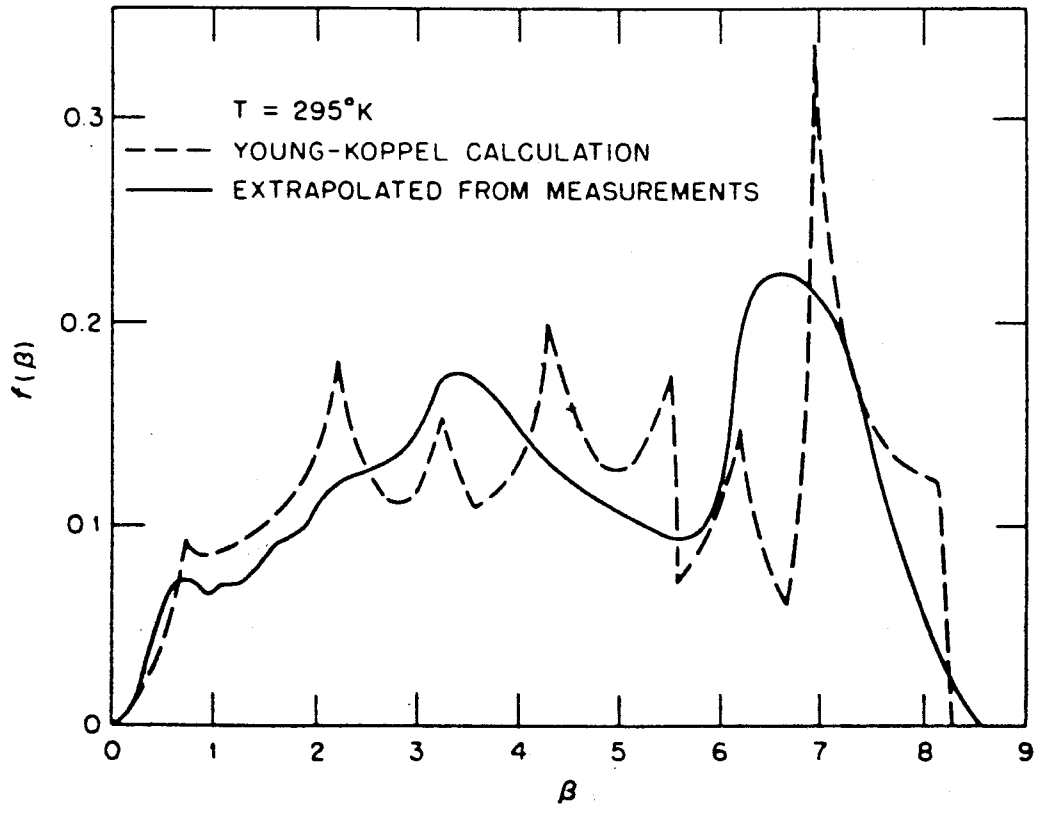

FIG. 7.11 COMPARISON OF PHONON SPECTRA FOR GRAPHITE CALCULATED AND EXTRAPOLATED FROM SCATTERING MEASUREMENTS (AFTER F. CARVALHO, REF. 56).

For most practical purposes, any one of the phonon spectra in Figs. 7.10 and 7.11 could be used; the resulting neutron spectra would be very similar.

In addition to the inelastic cross sections for graphite obtained from equation (7.66) and the Young-Koppel frequency spectrum in Fig. 7.10, the elastic scattering cross section has been computed without using the incoherent approximation.[58] The total scattering cross sections obtained in this way are in good agreement with observation, as can be seen from Fig. 7.12; this shows the

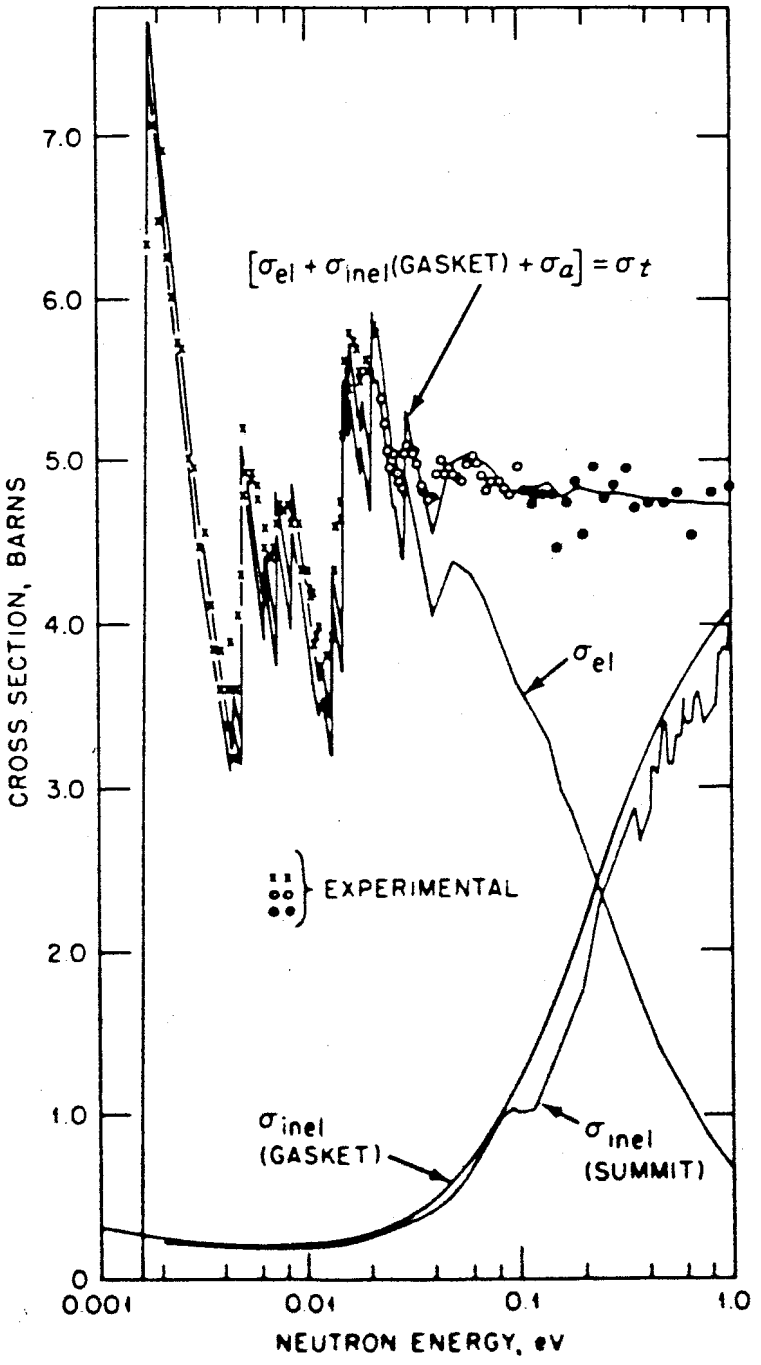

FIG. 7.12 EXPERIMENTAL AND CALCULATED CROSS SECTION OF GRAPHITE; GASKET AND SUMMIT REFER TO CODES USED IN THE CALCULATIONS (AFTER J. A. YOUNG, REF. 58).

calculated inelastic, elastic, and total scattering cross sections for graphite as functions of the neutron energy, compared with the experimental points. The almost vertical line at the left represents the Bragg cutoff in the coherent (elastic) scattering, followed by fine structure due to interference effects (§7.1d).

For comparison with experimental data, the thermal neutron energy spectrum has been calculated for graphite using scattering cross sections determined from (*a*) the crystal model and (*b*) the monatomic gas ($A = 12$) model. The sources from slowing down from higher energies were obtained by the procedure described in §7.7a, and allowance for leakage was made on the basis of diffusion theory by writing

$$\nabla \cdot \mathbf{J} = -D\nabla^2\phi = DB^2\phi$$

for the leakage term in the conservation equation (1.17). Since the experimental medium was large, a simple diffusion theory approximation to the leakage was justified.

The results of the calculations are given in Figs. 7.13 and 7.14, for temperatures of 323°K and 810°K, respectively.[59] The experimental points were obtained with a large block of graphite poisoned with boron so that the microscopic absorption cross section for a neutron of 0.025 eV energy is 0.4 barn per carbon atom. A pulse of fast neutrons was generated in the block and the spectrum of thermal neutrons was measured by the time-of-flight method.[60] The extent of the boron poisoning was chosen so as to maximize the sensitivity of the spectrum to

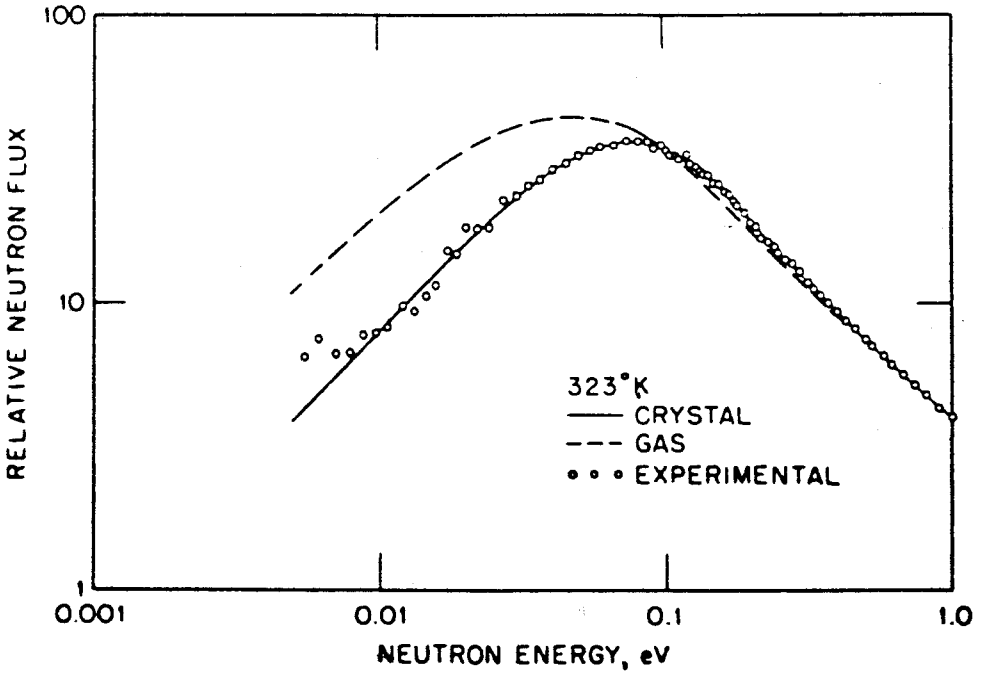

FIG. 7.13 EXPERIMENTAL AND CALCULATED NEUTRON ENERGY SPECTRUM IN GRAPHITE AT 323°K (AFTER D. E. PARKS, *ET AL.*, REF. 59).

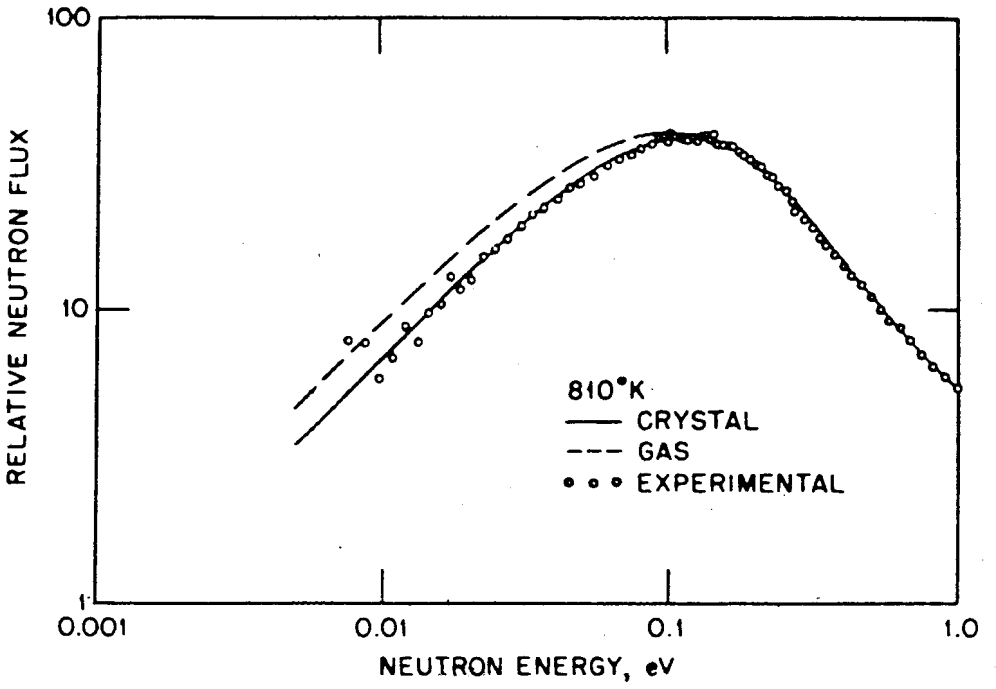

FIG. 7.14 EXPERIMENTAL AND CALCULATED NEUTRON ENERGY SPECTRUM IN GRAPHITE AT 810°K (AFTER D. E. PARKS, *ET AL.*, REF. 59).

binding effects. For much less boron, the spectrum would be close to Maxwellian no matter what the mechanism of thermalization, whereas for much more, relatively few neutrons would reach thermal energies.

From the figures, it is apparent that the effects of atomic binding in the graphite are substantial at (or near) normal room temperature, whereas they are much less at high temperature. Moreover, the effect of binding becomes less significant for higher neutron energies; as noted in §7.4c, the monatomic gas model is then a good approximation. At both ordinary and high temperatures the experimental data are seen to be well reproduced by the crystal model.

It is evident, therefore, that the scattering cross sections derived from a relatively simple binding model are sufficiently accurate for computing the thermal neutron spectrum in a reactor. There still remains, of course, interest in improving the theoretical approach and in understanding more clearly the importance of the various approximations made.[61]

Water as Moderator

The scattering of neutrons by individual water molecules, as in water vapor, could be calculated from first principles. The energy of the molecule can be described in terms of three degrees of freedom of translation, three of rotation, and three of vibration. A quantum mechanical formulation of each type of motion has been made.[62] By using available data from molecular spectra to

derive the $P_i(T)$ values, the intermediate scattering function could then be computed from equations (7.50) and (7.51). Water vapor is, however, of no great interest as a moderator.

For liquid water, the situation is much more complicated and no complete theory is available. It is believed that the atomic vibrations are much the same in the liquid as in water vapor, but the rotational motion is strongly hindered and the translation is completely changed. In an early model, called the Nelkin model,[63] to be considered below, the hindered rotational motion was approximated by a torsional oscillation. Although later models have a somewhat better physical content and give better agreement with measured double differential scattering cross sections, the over-all results are essentially equivalent.[64]

For the calculation of scattering in liquid water by the Nelkin model, the incoherent approximation is used to treat the scattering by the hydrogen; as seen in §7.3e, this should be a good approximation for uncorrelated proton spins. In addition, the Gaussian approximation is employed, with a spectrum, $f(\omega)$, representing a set of discrete oscillator frequencies; this is equivalent to the use of equation (7.66) with

$$f(\omega) = \sum_{i=1}^{4} \frac{1}{A_i} \delta(\omega - \omega_i),$$

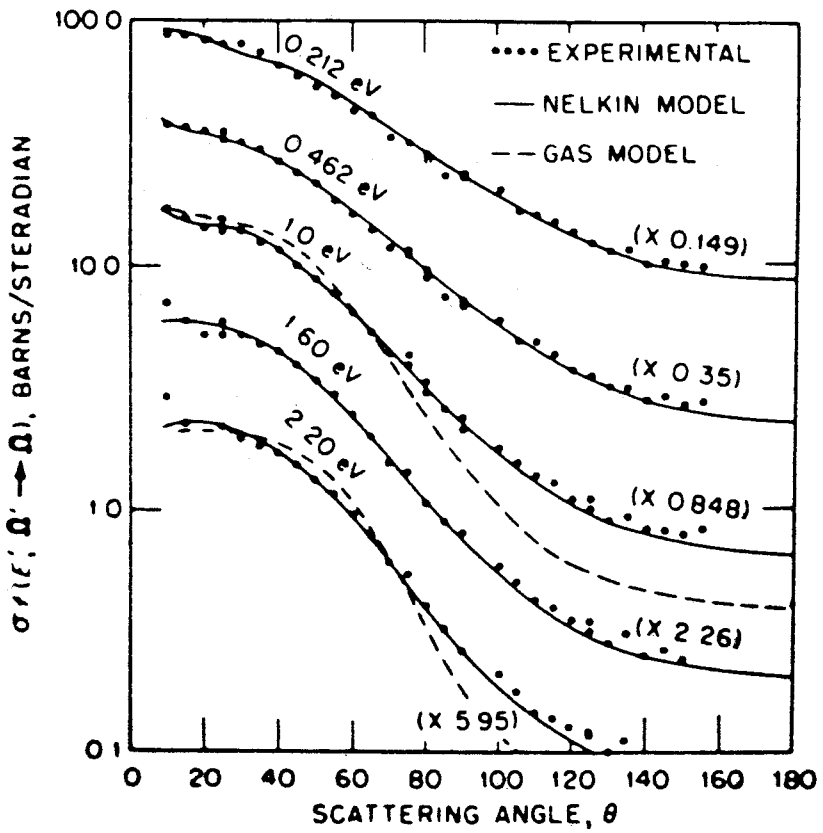

FIG. 7.15 EXPERIMENTAL AND CALCULATED DIFFERENTIAL SCATTERING CROSS SECTIONS IN LIQUID WATER AT VARIOUS INCIDENT NEUTRON ENERGIES (AFTER J. R. BEYSTER, REF. 64).

where $A_i m$ is a somewhat arbitrary effective mass of the ith quantum state. The first term in this summation is chosen to represent the translational motion of the free gas molecules, i.e., with $A_1 = 18$ and $\omega_1 = 0$ (§7.4c). The second term was taken to represent the hindered rotation (torsional oscillation) with $\hbar\omega_2 = 0.06$ eV, whereas the remaining two terms were for vibrational modes with $\hbar\omega_3 = 0.205$ eV and $\hbar\omega_4 = 0.481$ eV. The masses associated with these motions were taken to be $A_2 = 2.32$, $A_3 = 5.84$, and $A_4 = 2.92$.

The single differential scattering cross section, $\sigma f(E'; \mathbf{\Omega}' \rightarrow \mathbf{\Omega})$, which is the integral of $\sigma f(E', \mathbf{\Omega}' \rightarrow E, \mathbf{\Omega})$ over E, computed in the manner indicated above, is compared in Fig. 7.15 with experimental data and the results of free (monatomic) gas model calculations.[65] Agreement of the Nelkin model with experi-

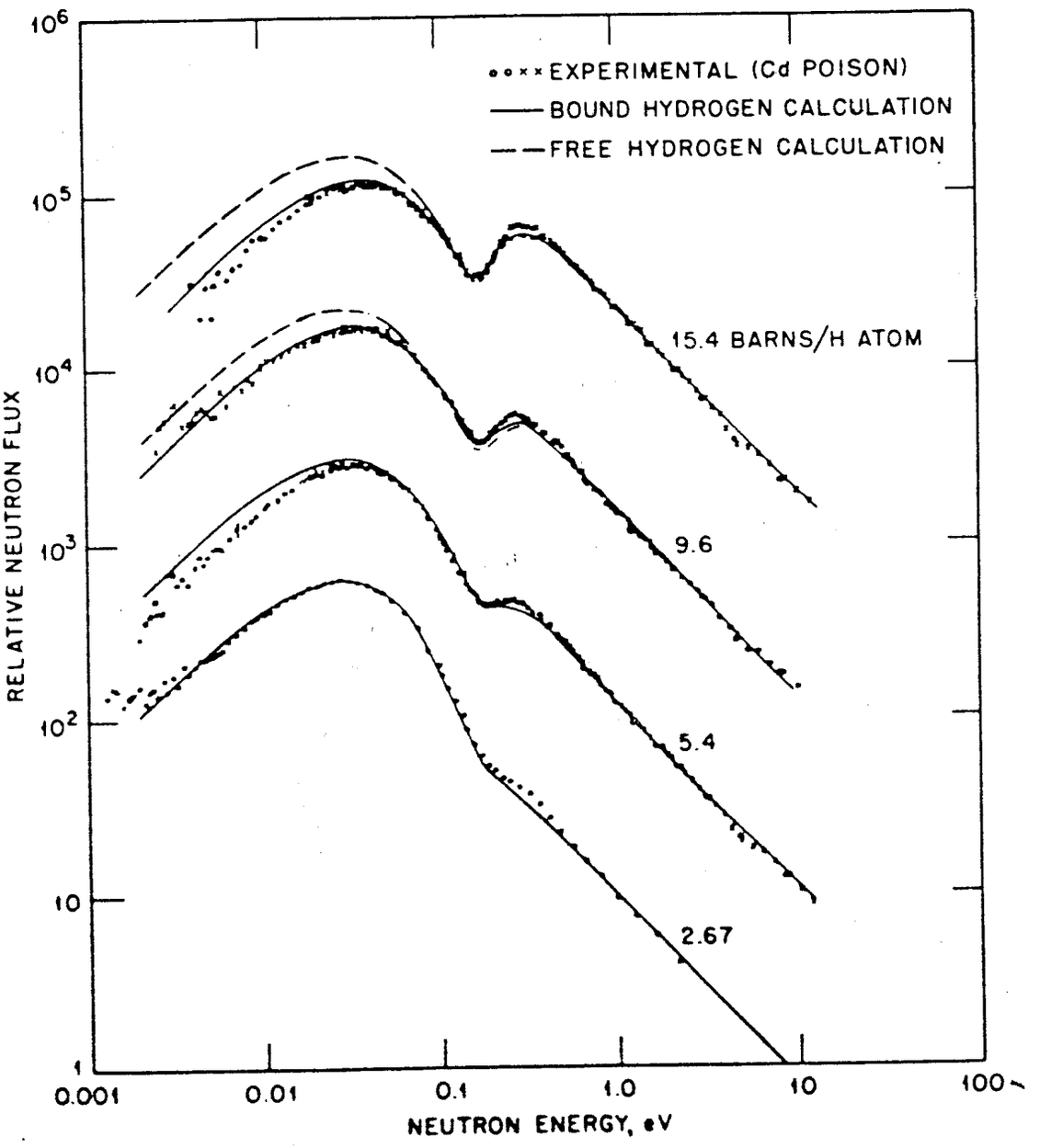

FIG. 7.16 EXPERIMENTAL AND CALCULATED NEUTRON ENERGY SPECTRUM IN WATER WITH ADDED CADMIUM POISON (AFTER J. R. BEYSTER, *ET AL.*, REF. 67).

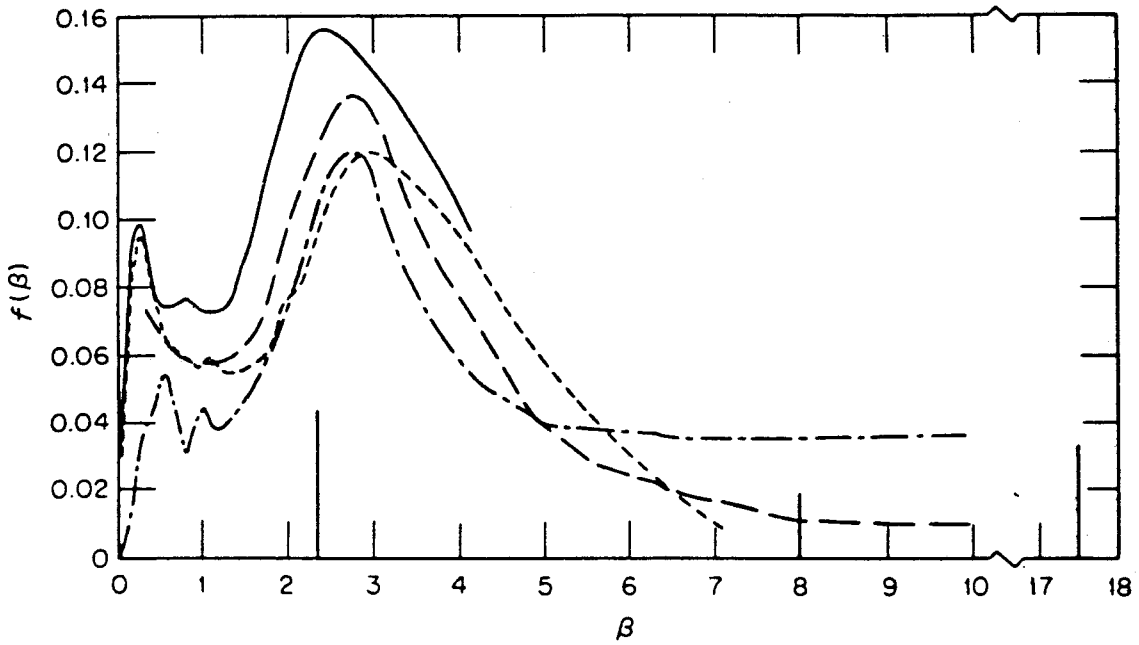

FIG. 7.17 VARIOUS SEMIEMPIRICAL PHONON SPECTRA IN WATER AND FREQUENCIES OF NELKIN MODEL (AFTER W. GLÄSER, REF. 70).

ment is seen to be good. Somewhat less satisfactory agreement has been obtained between calculated and observed values of the double differential cross section.[66]

Many comparisons have also been made of computed and experimental thermal neutron energy spectra in light water with various added poisons. The calculational procedure was the same as described above for graphite. An example of the results obtained, in which the observations were made with a pulsed neutron source in conjunction with time-of-flight measurements, is shown in Fig. 7.16.[67] The bound (Nelkin) scattering model is seen to represent the actual spectrum quite accurately, whereas the gas model is less satisfactory. It may be mentioned, however, that various semiempirical treatments of water as a free gas with a particle mass depending on the neutron energy have been appreciably more successful than indicated in Fig. 7.16.[68]

A number of improvements of the Nelkin scattering model for liquid water have been proposed and compared with experimental data.[69] In addition, the semiempirical method has been used to develop better treatments of hindered translation and rotation. The results of some determinations of the phonon spectrum, $f(\beta)$, for water are shown in Fig. 7.17, where the vertical lines indicate the discrete frequencies of the simple Nelkin model.[70]

Other Moderators

Models have also been developed for treating the scattering of thermal neutrons by other moderators, including heavy water (deuterium oxide), beryllium, and

zirconium hydride.[71] These will not be discussed in detail, but some comments are of interest.

The dynamics of a D_2O molecule in liquid heavy water is similar to that of the H_2O molecule in ordinary (light) water. Thus, three vibrational modes together with hindered rotation and translation characterize the behavior of the atoms in the D_2O molecule. By using the incoherent approximation, a model has been developed for scattering in heavy water, similar to that described above for ordinary water, except that the quantities ω_i and A_i differ in the two cases.[72]

There is, however, a further problem in connection with neutron scattering by heavy water. It was pointed out in §7.1d that the scattering from protons, i.e., light hydrogen nuclei, with randomly oriented spins was almost entirely incoherent. But this is not so for scattering from deuterons with random spins, for which the microscopic $\sigma_{coh} = 5.4$ barns and $\sigma_{inc} = 2.2$ barns. Consequently, the effects of interference in the scattering from the two deuterons in the D_2O molecule must be considered. In addition, the oxygen atom contributes relatively more to the scattering term in D_2O, and this contribution may interfere with that from the deuterons. These interference effects have been taken into account in a refinement of the model referred to above.[73]

Scattering models for beryllium are similar in principle to that already described for graphite. The main difference, as far as inelastic scattering is concerned, is that a different phonon spectrum must be used in the incoherent approximation.[74] The coherent effects, which are important for elastic scattering, depend upon the crystal structure (§7.1d), and so they will, of course, not be the same for beryllium as for graphite.

It has been already noted (cf. Fig. 7.8) that neutron scattering by the hydrogen atoms in zirconium hydride is remarkably well represented at high energies by the isotropic harmonic oscillator model. For further refinements in treating this and other moderators, the literature should be consulted.[75]

From the examples considered above, it is evident that the simplified models of bound scattering systems, with appropriate modifications, can be used to furnish the thermal neutron scattering cross sections required for reactor calculations. In particular, the incoherent Gaussian approximation has been found to have a wide range of applicability.

7.5 THERMALIZATION AND NEUTRON TRANSPORT

7.5a Introduction

In the preceding sections, various methods have been described for calculating the scattering of thermal neutrons by bound nuclei. Such calculations are an essential aspect of nuclear reactor physics because the cross sections have not been measured, at least not for the full range of parameters required to specify the scattering. The calculational models may thus be regarded as techniques for

interpolation and extrapolation from the measured cross section data. In addition, however, the models have much intrinsic physical content.

Once a model is available for computing the double differential scattering cross section, $\sigma_s f_s(\mathbf{r}; \mathbf{\Omega}', E' \to \mathbf{\Omega}, E)$, as a function of neutron energy, it may be used to generate multigroup constants by the methods described in Chapters 4 and 5. In practice, this is usually done by setting up a fine energy mesh, containing a hundred or so energies to span the range $0 < E \lesssim 1.0\,\text{eV}$. The cross sections at these mesh points are then used to generate the group cross sections.

In all the scattering models discussed in the preceding section, $\sigma_s f_s$ turned out to be a function of κ^2 and ϵ only, and not of the vector $\boldsymbol{\kappa}$. Such was the case for all the inelastic cross sections, based on the incoherent approximation, and for the elastic cross sections for polycrystalline solids and molecular liquids, although it is not so for single crystals. This means that the double differential cross sections are usually functions of the initial and final neutron energies and of $\mu_0 = \mathbf{\Omega}' \cdot \mathbf{\Omega}$, but not of $\mathbf{\Omega}'$ and $\mathbf{\Omega}$ separately. Consequently, the required Legendre components of the scattering between any two energies, E' and E, of the mesh may be computed, e.g.,

$$\int P_l(\mu_0)\sigma_s f_s(\mathbf{r}; E' \to E, \mu_0)\, d\mu_0,$$

from the scattering model. These values are then used in the numerical integration over group energies to determine the group constants for the thermal neutrons.

As in any problem of the evaluation of group constants, the number of groups required depends on the available knowledge of the neutron energy spectrum within each group. If the energy dependence of the neutron flux in the thermal range is known accurately, then all the thermal neutrons might be treated as a single group. This could be done, for example, in a large homogeneous reactor where the thermal energy spectrum could be computed by the B_N method (§4.5c). The group constants could then be calculated for a single group, using cross sections obtained from an appropriate scattering model. Of course, if the spectrum is known to be very nearly Maxwellian throughout the system, then detailed calculations of the scattering cross sections would be unnecessary.

For more complicated cases, such as heterogeneous systems with marked temperature gradients, the neutron spectrum will not be known. A substantial number of thermal groups, e.g., ten or so, will then be required and the results will not be very sensitive to the flux weighting within the individual groups.

Any of the methods developed in Chapters 4 and 5 may be used for treating the transport of thermal neutrons by the multigroup method. A particularly important thermalization problem is that for a lattice with temperature gradients; the S_N method can then be employed for cell geometry with reflecting (or white) boundary conditions. If the lattice geometry is sufficiently complex, it may be necessary to use the Monte Carlo approach. Another procedure, based on

collision probabilities, will be described here; it has been used extensively for treating neutron thermalization problems in heterogeneous systems.

7.5b The Method of Collision Probabilities

The method of collision probabilities is derived from the integral transport equation (1.29) with isotropic scattering; the time-independent form of this equation is

$$\phi(\mathbf{r}, E) = \int K(\mathbf{r}, \mathbf{r}', E)\left[\int \sigma f(\mathbf{r}'; E' \to E)\phi(\mathbf{r}', E')\, dE' + Q(\mathbf{r}', E)\right] dV', \quad (7.76)$$

where the kernel K is defined by

$$K(\mathbf{r}, \mathbf{r}', E) \equiv \frac{\exp\left[-\tau(E; \mathbf{r}' \to \mathbf{r})\right]}{4\pi|\mathbf{r} - \mathbf{r}'|^2} \quad (7.77)$$

and τ is the optical path length (§1.2b), i.e., the number of mean free paths between the points $\mathbf{r}'$ and $\mathbf{r}$. It should be noted that it has been assumed that the source, as well as the scattering, is isotropic.

The energy variable in equation (7.76) may be converted into multigroup form by integrating over an energy interval in the usual manner; the result may be written in the form

$$\phi_g(\mathbf{r}) = \int K_g(\mathbf{r}, \mathbf{r}')\left[\sum_{g'} \sigma_{g' \to g}(\mathbf{r}')\phi_{g'}(\mathbf{r}') + Q_g(\mathbf{r}')\right] dV', \qquad g = 1, 2, \ldots, G \quad (7.78)$$

where the group-averaged quantities are defined in much the same way as in Chapters 4 and 5.

Suppose it is desired to solve the equations (7.78) for the thermal neutrons in a lattice cell represented in cross section in Fig. 7.18. In treating the thermal groups alone, Q_g can represent the neutrons which are slowed down into thermal groups from higher energies; an estimate of Q_g can then usually be made easily

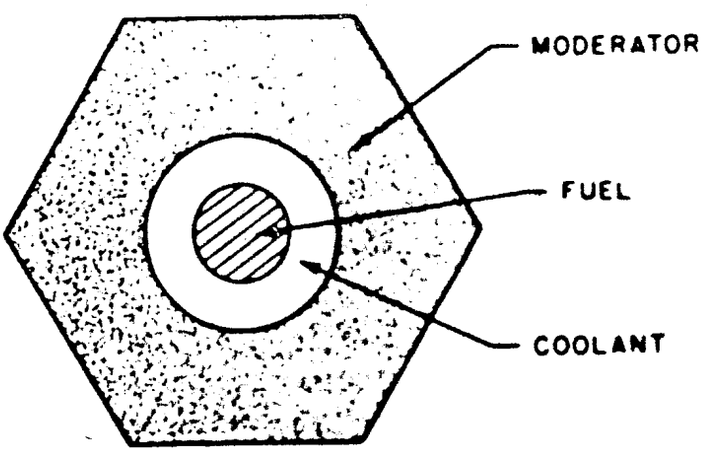

FIG. 7.18 LATTICE CELL

(§7.7a). The lattice cell is now divided into a large number, I, of subregions, such that within each of these regions the flux and source in any group may be taken to be constant. Within the ith subregion ($i = 1, 2, \ldots, I$), let

$$\sigma_{g'\to g}(\mathbf{r}') = \sigma_{g'\to g,i}$$

and let the flux be $\bar{\phi}_{g',i}$ and the source $\bar{Q}_{g,i}$.

The equations (7.78) may now be rewritten, with the volume integral expressed as the sum of I volume integrals over each of the I subregions; thus,

$$\phi_g(\mathbf{r}) = \sum_{i=1}^{I} \left[\sum_{g'} \sigma_{g'\to g,i}\bar{\phi}_{g',i} + \bar{Q}_{g,i}\right] \int_{V_i} K_g(\mathbf{r}, \mathbf{r}')\, dV', \tag{7.79}$$

where V_i is the volume of the ith subregion. If this expression is integrated over the jth subregion, the left-hand side of equation (7.79) becomes $V_j\bar{\phi}_{g,j}$, and if $K_{g,i\to j}$ is defined by

$$K_{g,i\to j} \equiv \frac{1}{V_j}\int_{V_j}\int_{V_i} K_g(\mathbf{r}, \mathbf{r}')\, dV'\, dV, \tag{7.80}$$

the result is

$$\bar{\phi}_{g,j} = \sum_{i}^{I} \left[\sum_{g'=1}^{G} \sigma_{g'\to g,i}\bar{\phi}_{g',i} + \bar{Q}_{g,i}\right] K_{g,i\to j}. \qquad j = 1, 2, \ldots, I. \tag{7.81}$$

Once the transport coefficients, $K_{g,i\to j}$, have been determined, this set of algebraic equations can be solved for the values of $\bar{\phi}_{g,j}$.

The transport coefficients are closely related to the collision probabilities which were treated in §2.8, as can be seen in the following manner. If the cross sections in group g are assumed to be constant, it follows, from the definition in equation (7.77), that

$$K_g(\mathbf{r}, \mathbf{r}') = K(\mathbf{r}, \mathbf{r}', E_g) = \frac{\exp\left[-\tau(E_g; \mathbf{r}' \to \mathbf{r})\right]}{4\pi|\mathbf{r} - \mathbf{r}'|^2}. \tag{7.82}$$

Then, from equation (7.80),

$$K_{g,i\to j} = \frac{1}{V_j}\int_{V_j}\int_{V_i} \frac{\exp\left[-\tau(E_g; \mathbf{r}' \to \mathbf{r})\right]}{4\pi|\mathbf{r} - \mathbf{r}'|^2}\, dV'\, dV. \tag{7.83}$$

From the considerations in §1.2c, however, it is known that the quantity

$$\sigma_g(\mathbf{r}) \frac{\exp\left[-\tau(E_g; \mathbf{r}' \to \mathbf{r})\right]}{4\pi|\mathbf{r} - \mathbf{r}'|^2}\, dV \tag{7.84}$$

is the probability that a neutron born at $\mathbf{r}'$, with energy E_g, will have its next collision within the small volume element dV about $\mathbf{r}$; $\sigma_g(\mathbf{r})$ is the total cross section for a neutron of energy E_g at $\mathbf{r}$. It follows, therefore, that the average probability for a neutron born in V_i to have its next collision in V_j can be found

by averaging the expression (7.84) over $\mathbf{r}'$ in V_i and integrating over $\mathbf{r}$ in V_j. If the result is denoted by $P_{g,i\to j}$, in the notation of §2.8b, then

$$P_{g,i\to j} = \frac{\sigma_g(j)}{V_i}\int_{V_j}\int_{V_i}\frac{\exp\left[-\tau(E_g;\mathbf{r}'\to\mathbf{r})\right]}{4\pi|\mathbf{r}-\mathbf{r}'|^2}\,dV'\,dV. \tag{7.85}$$

Upon comparing equations (7.83) and (7.85), it is seen that

$$K_{g,i\to j} = \frac{V_i}{V_j\sigma_g(j)}P_{g,i\to j}, \tag{7.86}$$

which is the required relation between the transport coefficient and the collision probability in the gth group.

The coefficients $K_{g,i\to j}$ can be determined in several different ways including, in appropriate cases, (*a*) analytic or numerical evaluation of the integrals in equation (7.83), (*b*) by high-order S_N methods, or (*c*) by Monte Carlo techniques. If the second or third of these procedures is used, then it is probably easiest to compute the collision probabilities and then to obtain the transport coefficients from equation (7.86).

The system of equations (7.81) can be solved by iterative methods, starting with a guess of the flux distribution, similar to those described in Chapter 4. A computer code, known as THERMOS, based on this technique has been employed to a considerable extent.[76] The method is most useful for small lattice cells where the number of subregions, I, is not very large. The reason is that in integral transport theory each subregion communicates directly with all other such regions; that is to say, $K_{g,i\to j}$ is finite for all values of i and j, and so the number of coefficients will be I^2 for each group. In the P_N or S_N method, however, based on the ordinary (differential) form of the neutron transport equation, each space point communicates only with adjacent space points with a simple coefficient. Hence, when I must be large, the P_N or S_N approach is preferable to that involving collision probabilities.

It should be recalled, in conclusion, that in the foregoing treatment the scattering has been assumed to be isotropic. This restriction is not easily removed, although in principle it would be possible to work with the integral equation (1.31) for anisotropic scattering and such scattering has been incorporated into collision probability codes.[77] In practice, however, good results can often be obtained by using the transport approximation described in §5.4b, or in other ways.[78]

7.6 EIGENVALUES AND THERMALIZATION PROBLEMS

7.6a Introduction

In preceding chapters, the eigenvalues α and k were treated with special emphasis on their relation to criticality. In these problems, the presence of fissile material

was essential, since fission was responsible for neutron multiplication and for the possibility of criticality. Moreover, only in fission could the neutrons gain significantly in energy; hence, fission was required in order that the energy spectrum could be self-regulating in the range up to around 10 MeV.

In thermalization problems some eigenvalues are also of interest; this is not because they are associated with criticality but because they can be measured and related to energy transfer and neutron transport properties of the thermalizing medium. The eigenvalue problems in thermalization arise from considering a medium which contains no fissile material but in which there is a neutron source. The character of the source will be seen to define the eigenvalue problem.

After the neutrons from the source are slowed down into the thermal energy range, they can either gain or lose energy in scattering collisions with the nuclei in the thermalizing medium. Such scatterings will tend to bring the neutrons into thermal equilibrium with the nuclei, i.e., into a Maxwellian energy spectrum (§7.2a). On the other hand, absorption and leakage will, in general, tend to prevent the neutrons from attaining complete equilibrium. As a result, the actual spectrum will deviate from the Maxwellian distribution. By studying these deviations, especially as they appear in certain eigenvalues, information can be gained concerning those properties of the medium which were mentioned above. For example, scattering models may be confirmed or modifications may be indicated.[79]

7.6b Types of Eigenvalue Problems

Among the more interesting neutron sources are those with a simple time dependence, namely, a short pulse or a sinusoidal time variation, or a simple space dependence, e.g., a plane source. After a short neutron pulse, the neutron population decays with time and it is of interest to consider the asymptotic time behavior of the angular flux. This inquiry leads, as in §1.5a, to an α eigenvalue problem in which solutions are sought of the time-dependent transport problem represented by

$$\frac{\partial \Phi_i}{\partial t} = \alpha_i \Phi_i,$$

where α_i is the appropriate time decay eigenvalue. For a system of thermal neutrons, as is under consideration in this chapter, the transport equation (7.9) for the eigenvalue α_i can then be written as

$$\frac{\alpha_i}{v}\Phi_i + \boldsymbol{\Omega}\cdot\nabla\Phi_i + (\sigma_a + \sigma_s)\Phi_i = \iint \sigma_s f_s \Phi_i' \, d\Omega' \, dE'. \tag{7.87}$$

Since no fissile material is present, there is no possibility that α_i can be positive.

Solutions to equation (7.87) may be expected, however, for various negative values of α_i and the least negative of these, i.e., α_0, is of greatest interest. As

before (§1.5c), the associated eigenfunction, Φ_0, will be nonnegative. It was mentioned in §1.5c that for sufficiently small systems there may exist no solution to equation (7.87) for α_0. In thermalization studies, the dependence of α_0 on the size of the system can be measured and related to theoretical results using various scattering models, as will be seen in due course.

Another simple source is a steady (time-independent) plane source in an infinite medium. Such a source may, for example, be approximated by the neutrons leaking from the face of a reactor into an exponential column. The rate at which the neutron flux falls off with distance from the source gives the thermal-neutron relaxation length (§2.2b). If the plane source is at $x = 0$, then for large positive values of x, asymptotic solutions of the form $e^{-\kappa x}$ may be sought. Hence, by writing

$$\Phi(x, \mu, E) = e^{-\kappa x}\Phi(\mu, E), \tag{7.88}$$

the time-independent transport equation for $x > 0$ is

$$-\mu\kappa\Phi(\mu, E) + [\sigma_a(E) + \sigma_s(E)]\Phi(\mu, E) = \iint \sigma_s f_s \Phi(\mu', E')\, d\Omega'\, dE', \tag{7.89}$$

with κ as the eigenvalue.*

It will be recalled that in one-speed theory with isotropic scattering (§2.2b), one such value of κ was found, namely, $\kappa = 1/\nu_0$, and it was associated with the asymptotic solution of the transport equation. In thermalization problems, if the cross sections were independent of energy and the scattering isotropic, $1/\nu_0$ would also be the desired eigenvalue. But for realistic cross sections, which are energy dependent, the situation is more complicated. In one-speed theory there was a singular solution for any $\kappa > \sigma$, i.e., for $\nu < 1$ (§2.2c); for energy-dependent problems singular solutions also exist when κ is sufficiently large, but they are not of primary interest here.

A further possibility is a sinusoidal (or *neutron wave*) source, located at $x = 0$, varying as $e^{i\omega t}$. In this case, solutions of the wave form

$$\Phi(x, \mu, E, t) = \Phi(\mu, E)e^{-\kappa x + i\omega t}$$

appear reasonable.† The eigenvalues κ could then be sought for a fixed ω, and they would satisfy the transport equation

$$\left(\frac{i\omega}{v} - \mu\kappa + \sigma_a + \sigma_s\right)\Phi(\mu, E) = \iint \sigma_s f_s \Phi(\mu', E')\, d\Omega'\, dE'. \tag{7.90}$$

From neutron-wave experiments with modulated sources, an attempt can be made to determine the dependence of κ on ω.[80]

* The eigenvalue κ is frequently represented by κ, but the latter is used earlier in this chapter to indicate change in momentum.

† Note that ω refers to the imposed frequency of the (sinusoidal) source; it is not related in any way to the phonon frequencies in §7.4d.

TABLE 7.1. PARAMETERS AND RELATED EIGENVALUES

Experiment	a	b	*Parameter*	*Eigenvalue*
Pulsed source in infinite medium	$\alpha + \sigma_{a0}v_0$	0	$\sigma_{a0}v_0$	α
Pulsed source in large (finite) medium	$\alpha + \sigma_{a0}v_0$	iB	$\sigma_{a0}v_0, B$	α
Diffusion length measurement	$\sigma_{a0}v_0$	$-\mathrm{K}$	$\sigma_{a0}v_0$	K
Neutron wave experiment	$i\omega + \sigma_{a0}v_0$	$-\mathrm{K}$	$\sigma_{a0}v_0, \omega$	K

Greater generality can be achieved by taking two other matters into consideration. First, in a large but finite medium the spatial dependence of the neutron angular flux may be well approximated by a sinusoidal function, e.g., $\Phi \propto e^{iBx}$. For a pulsed source in such a medium, the asymptotic solutions might be expected to be of the form $e^{\alpha t + iBx}$; the equation for the eigenvalue α is then

$$\left(\frac{\alpha}{v} + iB\mu + \sigma_a + \sigma_s\right)\Phi(\mu, E) = \iint \sigma_s f_s \Phi(\mu', E')\, d\Omega'\, dE', \qquad (7.91)$$

which is the same as equation (7.90) with α substituted for $i\omega$ and iB for $-\mathrm{K}$.

Second, if the absorption cross section varies as $1/v$, then σ_a in equation (7.91) may be replaced by $\sigma_{a0}v_0/v$, where σ_{a0} is the cross section at an arbitrary reference neutron velocity, v_0. It is then seen that α/v and σ_a may be combined to give $(\alpha + \sigma_{a0}v_0)/v$ and the quantity $\alpha + \sigma_{a0}v_0$ may be regarded as an eigenvalue. By considering various media which differ only in σ_{a0}, e.g., in their boron-10 content, it would be predicted from equation (7.91) that $\alpha + \sigma_{a0}v_0$ should remain constant.

All the equations presented above may be included in the general form

$$\left(\frac{a}{v} + b\mu + \sigma_s(E)\right)\Phi(\mu, E) = \iint \sigma_s f_s \Phi(\mu', E')\, d\Omega'\, dE', \qquad (7.92)$$

where a and b may be regarded as complex numbers; one of these may be fixed as a parameter and the other sought as an eigenvalue, as indicated in Table 7.1. It is thus apparent that the results of various kinds of experiments can be related to each other; an example of such a relationship, based on diffusion theory, is given in §7.6e.

7.6c Existence of the Eigenvalues

In the foregoing discussion, the eigenvalues being sought correspond to well-behaved, i.e., positive and reasonably continuous, eigenfunctions. Thus singular eigenfunctions, such as occur in one-speed theory, are not being considered. It is possible, however, that under some conditions there will be no eigenvalues with well-behaved eigenfunctions.

If, in equation (7.92), $a = b = 0$, then it is apparent from equation (7.10) that the Maxwell distribution $\Phi = M(E, T)$ is a solution. This means that if $a = 0$

and b is the eigenvalue or if $b = 0$ and a is the eigenvalue, then in either case there exists a zero eigenvalue with a Maxwellian eigenfunction. Moreover, it is generally found[81] that if either a or b is fixed and small, then the eigenvalue exists and may be determined by perturbation methods. If, however, a or b is fixed but large, then it may be that no well-behaved eigenfunctions exist. It will be seen later that this statement needs some qualification, but, in a rough way, it is a useful summary of the situation.

Another point to bear in mind is that there are some limits which the various eigenvalues may not exceed. Eigenvalues exceeding the limit belong to a continuous spectrum and are associated with singular eigenfunctions, much as in §2.2c.* For the complete solution of a pulsed neutron source or a neutron wave (sinusoidal source) problem, these singular eigenfunctions would have to be taken into consideration, but for asymptotic solutions, in time or space, the discrete eigenvalues are sufficient, provided they exist.

The κ *Eigenvalue*

The conditions for the existence of discrete eigenvalues may be derived in connection with the neutron diffusion length experiment by rewriting equation (7.89) in the form

$$[-\mu\kappa + \sigma(E)]\Phi(\mu, E) = \iint \sigma_s f_s \Phi(\mu', E')\, d\Omega'\, dE'. \tag{7.93}$$

Since positive values of Φ are being sought, the right-hand side is positive; hence, κ cannot exceed $\sigma(E)$, for, if it did, $-\mu\kappa + \sigma(E)$ would be negative for $\mu = 1$. If $[\sigma(E)]_{\min}$ denotes the smallest values of the total cross section as a function of neutron energy, then for discrete values of κ to exist, the condition is

$$\kappa \leqslant [\sigma(E)]_{\min}. \tag{7.94}$$

It has been shown[83] that real values of κ larger than $[\sigma(E)]_{\min}$ belong to the continuous spectrum and are associated with singular eigenfunctions.

The experimental conditions under which a discrete eigenvalue, i.e., a relaxation length, may or may not exist are of interest. According to equation (7.88), a discrete eigenvalue implies that, at distances far from the source, the neutron population will decay approximately as $e^{-\kappa x}$, with the same exponent for all neutron energies represented in the spectrum. This asymptotic (or equilibrium) spectrum is independent of the neutron source. Since neutrons of energy E cannot decay faster than $e^{-\sigma(E)x}$, the spectrum as a whole cannot decay faster than $\exp\{-[\sigma(E)_{\min}]x\}$ and this imposes the limit in equation (7.94).

Intuitively, the asymptotic spectrum, independent of the source, implies an efficient transfer of energy between the neutrons and the scattering nuclei, so that an equilibrium spectrum can be established. If some strong effect opposes

* It is also possible that a point eigenvalue might be "embedded" in the continuous spectrum, but this does not generally seem to occur in thermalization problems.[82]

the attainment of equilibrium, then it is reasonable to expect that there will be no equilibrium spectrum and hence no discrete eigenvalue. Three such effects are noted below: (*a*) a direct contribution from the source at an energy for which $\sigma(E)$ is small; (*b*) strong absorption, and (*c*) leakage in a finite medium.

For liquid and gaseous media, the minimum value of the total cross section, i.e., $[\sigma(E)]_{\min}$, will occur at the highest neutron energy in the problem, as in §7.3a. If this minimum value is too small, then well-behaved eigenfunctions may not exist. Consider, for example, a plane source of fission neutrons in a moderator.[84] For this problem, the energy range will be $0 \leqslant E \lesssim 10$ MeV, but it is possible that, far from the source, there will be an asymptotic spectrum of thermal neutrons and negligible numbers of fast neutrons. Such will be the case for moderators of graphite, beryllium, and heavy water. In ordinary water, however, the distribution of neutrons far from the source is governed by those neutrons of highest energy which have streamed from the source without making any collision with nuclei. These high-energy neutrons represent a singular population and no discrete eigenvalue κ exists. For source neutrons of lower energy $[\sigma(E)]_{\min}$ is larger and κ may then exist.[85]

For crystalline moderators, the minimum value of $\sigma(E)$ will occur for energies just below the Bragg cutoff (see Figs. 7.2 and 7.12). At such energies, the elastic scattering cross section is zero and the inelastic scattering will be very small, especially at low temperatures. With such small values of $[\sigma(E)]_{\min}$, there may again be doubts about the existence of the κ eigenvalues.

Next, consider the effect of an absorber mixed with the moderator. Suppose that, for the pure moderator, a discrete relaxation length exists. As absorber is added, κ will increase, i.e., the asymptotic neutron spectrum will decay more rapidly with distance. It is of interest to know if, for a finite concentration of absorber, κ will reach the limit given by equation (7.94), so that, for higher concentrations, there will be no asymptotic spectrum.

For the particular case of an absorber for which $\sigma(E)$ varies as $1/v$ (or $1/\sqrt{E}$), it has been proved that such a critical concentration does exist[86]; for higher concentrations, the absorption is so strong that asymptotic spectra cannot be established. It might appear, therefore, that for a sufficiently high concentration of a $1/v$-absorber, there would not be an exponential relaxation of the neutron flux far from the source. Nevertheless, it has been found, both theoretically[87] and experimentally,[88] that the decay is very nearly exponential with a relaxation length greater than $[\sigma(E)]_{\min}$.

A somewhat similar vanishing of the discrete relaxation length is found in the diffusion of neutrons in a finite medium, such as a prism, finite in the x and y directions but infinite in the z direction and with a source at $z = 0$. Asymptotic solutions, with approximately exponential decay with distance in the z direction, are sought; as before, they must satisfy equation (7.94). It has been found that, for a sufficiently thin prism, there is no discrete eigenvalue, κ, i.e., no solution with exponential decay.[89]

Finally, in experiments with a modulated neutron source, there may be no waves if the modulation frequency is sufficiently high. That is to say, when ω is too large, there will be no discrete eigenvalue κ for equation (7.90). However, when the response of a detector is examined, wavelike solutions may be found. The study of modulated sources is attracting considerable interest and the literature on this and related topics is expanding rapidly.[90]

The α Eigenvalue

The foregoing has concerned the κ eigenvalue (or relaxation length); consideration will now be given to the α eigenvalue (or time-decay constant). As seen in Chapter 1, these eigenvalues may not exist if the system is very small, i.e., with dimensions of the order of a mean free path or less. Broadly speaking, a small system corresponds to a large value of the buckling, i.e., large B in equation (7.91). For small systems, however, the approximation of e^{iBx} for the spatial distribution of the flux is a poor one; the transport equation should then be solved with free-surface boundary conditions. When this is done it is found that there is a lower limit for α_0,[91] and if the system is small there may be no values of α above this limit.

The occurrence of this limit may be understood from a heuristic argument. Consider the integral transport equation for the eigenvalue α with isotropic scattering, in a homogeneous medium, i.e.,

$$\phi(\mathbf{r}, E) = \int\int \frac{\exp\{-[\sigma(E) + (\alpha/v)]|\mathbf{r} - \mathbf{r}'|\}}{4\pi|\mathbf{r} - \mathbf{r}'|^2} \sigma f(\mathbf{r}'; E' \to E)\phi(\mathbf{r}', E')\, dV'dE'. \tag{7.95}$$

This is the same as equation (7.76) except that $\tau(E; \mathbf{r}' \to \mathbf{r})$ in the exponential term has been replaced by $[\sigma(E) + \alpha/v]|\mathbf{r} - \mathbf{r}'|$. Since a homogeneous medium is under consideration, the optical path length, τ, would normally be replaced by $\sigma(E)|\mathbf{r} - \mathbf{r}'|$ because both quantities represent the number of mean free paths between $\mathbf{r}$ and $\mathbf{r}'$ (§1.2b). For the eigenvalue problem, however, it is necessary to add α/v to the total cross section, i.e., α/v appears as an absorption cross section (§1.5f). For the present problem, $Q = 0$, and solutions are being sought of the form

$$\phi(\mathbf{r}, E, t) = \phi(\mathbf{r}, E)e^{\alpha t}.$$

Upon substituting this expression into equation (7.76), together with the value of τ given above, equation (7.95) is obtained.

It is reasonable to suppose that α must be such that the exponential in equation (7.95) never becomes both positive and infinite, for if such an exponential were allowed, it would appear that $\phi(\mathbf{r}, E)$ would be unbounded and, therefore, singular and not well-behaved. If this view is accepted, then there are two cases to be examined: (*a*) unbounded media and (*b*) bounded media.

For an unbounded medium, such as a slab (finite in thickness but infinite in the two other dimensions), $|\mathbf{r} - \mathbf{r}'|$ can become infinite and hence it is required that $\sigma(E) + \alpha/v \geqslant 0$ or, in other words,

$$\alpha_0 \geqslant -[v\sigma(E)]_{\min} \quad \text{for unbounded medium,} \tag{7.96}$$

where $[v\sigma(E)]_{\min}$ implies the minimum value of $v\sigma$ over the energy range under consideration. All values of $\alpha < -[v\sigma(E)]_{\min}$ belong to the continuous spectrum, i.e., they are associated with singular eigenfunctions.[92] It should be noted that for one-speed theory (§1.5c), all discrete eigenvalues were constrained to have $\alpha > -v\sigma$, and a continuum of eigenvalues with singular eigenfunctions was found for more negative values of α. Hence, the present argument is consistent with rigorous one-speed results. It is known that α_0 always exists in one-speed problems, but for the energy-dependent situation, α_0 may not exist for sufficiently thin slabs, as will be seen below.[93]

For bounded media, $|\mathbf{r} - \mathbf{r}'|$ will be finite, but $\sigma(E) + \alpha/v$ will diverge as $v \to 0$. In particular, all absorption cross sections vary as $1/v$ at low energies, and, in most models, the inelastic cross sections, e.g., as in equation (7.25), also show the same $(1/\sqrt{E})$ dependence. In any event, to keep the exponent in equation (7.95) negative as $v \to 0$, it is required that

$$\alpha_0 \geqslant -\lim_{v \to 0} [v\sigma(E)] \quad \text{for bounded medium.} \tag{7.97}$$

In practice the conditions given by equations (7.96) and (7.97) usually coincide because the minimum value of $v\sigma$ is generally also the limiting value as the neutron energy (or speed) approaches zero.

For a finite medium α_0 must then be not smaller than the limit in equation (7.97) for the eigenvalue to be discrete. But, as smaller and smaller systems are considered, it is to be expected on physical grounds that α_0 will decrease monotonically. Hence, there might be a size for which

$$\alpha_0 = -\lim_{v \to 0} [v\sigma(E)]$$

and for smaller sizes α_0 would not exist. These expectations have been confirmed by rigorous analysis for the monatomic gas scattering model[94] and for idealized models of scattering by solids.[95] It has been shown that there is a limiting value of α_0, equal to that given above, i.e., $-\lim [v\sigma(E)]$ as $v \to 0$, and that this eigenvalue does not exist for small systems. It should be pointed out, however, that proof of the existence of this limit for finite systems depends on use of the transport equation in the limit of zero energy, where it is not strictly valid (§1.5c). If the range of neutron speeds is artificially bounded away from zero, then no such limit is found for finite systems.[96]

7.6d Calculation of Eigenvalues and Eigenfunctions

In obtaining the general features of eigenvalues and eigenfunctions, considerable use has been made of approximate degenerate scattering functions.[97] But when

fairly realistic models are used to describe neutron scattering from liquids or crystals, such as the incoherent Gaussian approximation, the resulting σ_s and $\sigma_s f_s$ are so complicated that the eigenvalues (and associated eigenfunctions) can be obtained only by numerical methods.[98] An alternative approach is then to apply multigroup procedures to the energy variable.

Consider, for example, the problem of computing the set of time-decay eigenvalues $\{\alpha_l\}$ for a system in which the spatial dependence of the neutron flux can be approximated by e^{iBx}. Equation (7.91) is then applicable and the scattering function can be expanded as a sum of Legendre polynomials, in the usual way; thus,

$$\left[\frac{\alpha}{v} + iB\mu + \sigma(E)\right]\Phi(\mu, E) = \sum_{l=0}^{\infty} \frac{2l+1}{4\pi} P_l(\mu)\sigma_{sl}(E' \to E)\phi_l(E'), \quad (7.98)$$

as in equation (4.2). In this expression, B is regarded as known and α is the desired eigenvalue (Table 7.1); alternatively, α could be known with B to be determined. In either case, a solution could be found by expanding $\Phi(\mu, E)$ in Legendre polynomials, as in Chapter 4, and introducing a multigroup representation of the energy. Many groups could be used in the usual manner in order to minimize uncertainties in the group constants.

If a P_N expansion is used for $\Phi(\mu, E)$, there would be obtained a set of $(N+1)G$ homogeneous linear equations for the $N+1$ Legendre components of the flux in G groups. A solution would be possible only if the determinant of the coefficients were zero and this condition would lead to $(N+1)G$ possible values of α and thus $(N+1)G$ eigenvalues. It is expected, and confirmed by experience,[99] that the eigenvalue with the largest real part is real and is associated with a positive eigenfunction; this is α_0 and it may be compared with experimental values. Once an eigenvalue has been determined, the associated eigenfunction can be found by solving a system of $(N+1)G$ linear homogeneous algebraic equations for the $(N+1)G$ components of the eigenfunction.

Since the $(N+1)G$ values of α referred to above are found as roots of a polynomial, they are all discrete. It is natural to consider, therefore, what has become of the continuous range of eigenvalues, for which $\alpha < -[v\sigma(E)]_{\min}$, associated with the singular eigenfunctions. In practice, they show up as easily recognizable discrete eigenvalues because the corresponding eigenfunctions have a rapid and irregular dependence on energy.[100] In the multigroup problem these discrete eigenvalues have α less than the minimum of $v\sigma$ as it occurs in the multigroup representation of v (or E) and σ.

In the multigroup treatment, α_0 exists even for arbitrarily small systems; that is to say, the eigenfunction associated with the largest (least negative) real α is possible for all values of B.[101] Indeed, this is true not only when the spatial dependence of the flux is approximated by e^{iBx}, but also for the multigroup thermalization problem for a slab with free-surface boundary conditions.[102] When the theoretical treatment predicts that α_0 should not exist for a continuous,

i.e., nongroup, distribution of the energy, but a value is found by multigroup methods or by experiment (or both), it is sometimes referred to as a "pseudo-fundamental" eigenvalue. It is believed that although this α_0 is not the largest time-decay constant for the neutrons in the system, it may approximate the rate at which most of the neutrons decay.[103]

The experimental evidence concerning the existence of decay rates exceeding the limit given by equation (7.97) is controversial. Experiments on such small systems, typically with dimensions of the order of a neutron mean free path, are difficult to perform and interpret. Although decay rates exceeding the limit have been reported, it is not certain that they truly represent exponential decay.[104]

In the approach described above, B and α could be represented as complex numbers, so that the whole variety of eigenvalue problems considered in §7.6b could be treated in the same way. Alternatively, an attempt could be made to solve equation (7.98) by the B_N method (§4.5c). This would have the advantage of rapid convergence, but the disadvantage that the eigenvalues appear in a much more complicated form. The procedure has been used to find fundamental eigenvalues, such as α_0,[105] but it is probably less suitable than the P_N method for treating higher eigenvalues.

Instead of using a multigroup representation of the energy, the energy dependence could be expressed as a complete set of energy functions, such as the Laguerre polynomials. Considerable work has been done along these lines, generally with quite approximate scattering functions.[106]

7.6e Eigenvalues in Diffusion Theory

In diffusion theory, the relationship between some of the eigenvalues noted in §7.6b is especially clear. The source-free, time-dependent diffusion equation for a plane homogeneous medium [cf. equation (4.18)] is

$$\frac{1}{v}\frac{\partial\phi(x, E, t)}{\partial t} - D\frac{\partial^2\phi}{\partial x^2} + \left(\frac{\sigma_{a0}v_0}{v} + \sigma_s\right)\phi = \int \sigma_{s0}(E' \to E)\phi(x, E', t)\,dE', \quad (7.99)$$

where the absorption cross section has been explicitly taken to vary as $1/v$, i.e., $\sigma_a = \sigma_{a0}v_0/v$. Consider, first, a problem involving a pulsed source of neutrons with a spatial dependence of the flux approximated by e^{iBx} and the eigenvalue α_0 to be determined. The equation for α_0 is then of the form

$$\left[\frac{\alpha_0 + \sigma_{a0}v_0}{v} + DB^2 + \sigma_s(E)\right]\phi(E) = \int \sigma_{s0}(E' \to E)\phi(E')\,dE'. \quad (7.100)$$

Next suppose a diffusion length, i.e., the decay of the thermal flux with distance from a steady source, is being measured in a medium with varying amounts of a $1/v$-absorber. Let

$$\sigma_a(E) = \frac{\sigma_{a0} + \delta\sigma_{a0}}{v}v_0,$$

where σ_{a0} has the same significance as before and $\delta\sigma_{a0}$ represents the effect of the absorber. Since the source is a steady one, the flux will not depend on time and it will depend on space as $e^{-\kappa x}$. Hence the equation for κ, is

$$\left[\frac{\sigma_{a0} + \delta\sigma_{a0}}{v} v_0 - D\kappa^2 + \sigma_s(E)\right]\phi(E) = \int \sigma_{s0}(E' \to E)\phi(E')\,dE'. \quad (7.101)$$

Equations (7.100) and (7.101) are seen to be of the same form, with $-\kappa^2$ in equation (7.101) replacing B^2 in equation (7.100) and $\delta\sigma_{a0}$ replacing α_0. Since α_0 must be negative, it follows that $\delta\sigma_{a0}$ and α_0 must be opposite in sign, assuming that absorber is added, rather than removed, i.e., $\delta\sigma_{a0} > 0$. The similarity between the two equations indicates that the pulsed neutron results may be continued to negative B^2 so as to connect with the diffusion-length results, as shown in Fig. 7.19.[107] In the pulsed neutron region, α_0 is the eigenvalue with B as the variable parameter, whereas in the diffusion-length (or static) region κ is the eigenvalue and $\delta\sigma_{a0}$ is the parameter.

The following features of Fig. 7.19 are of interest: (1) The value of $|\alpha_0|$ cannot exceed $(\sigma v)_{\min}$, as noted in §7.6c. (2) When $B^2 = 0$, i.e., for an infinite medium, $\alpha_0 = -\sigma_{a0}v_0$; this situation is discussed further below. (3) When $\delta\sigma_{a0}v_0$ is zero, κ is denoted by κ_0; the quantity $1/\kappa_0 = L_0$ is then the diffusion length for thermal neutrons in the unpoisoned medium, i.e., the flux will vary as e^{-x/L_0}. (4) The maximum value of κ cannot exceed the minimum value of $\sigma(E)$, as shown by equation (7.94).

The expected correspondence between pulsed source and diffusion-length experiments has been observed in practice. The results of measurements made

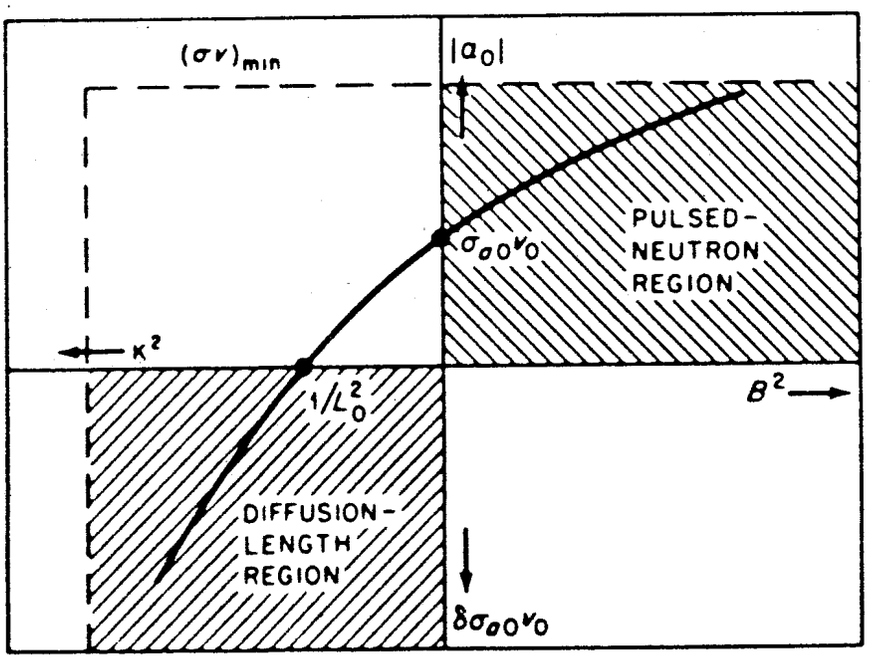

FIG. 7.19 CONTINUITY OF DIFFUSION-LENGTH AND PULSED-NEUTRON REGIONS (AFTER H. C. HONECK, REF. 105).

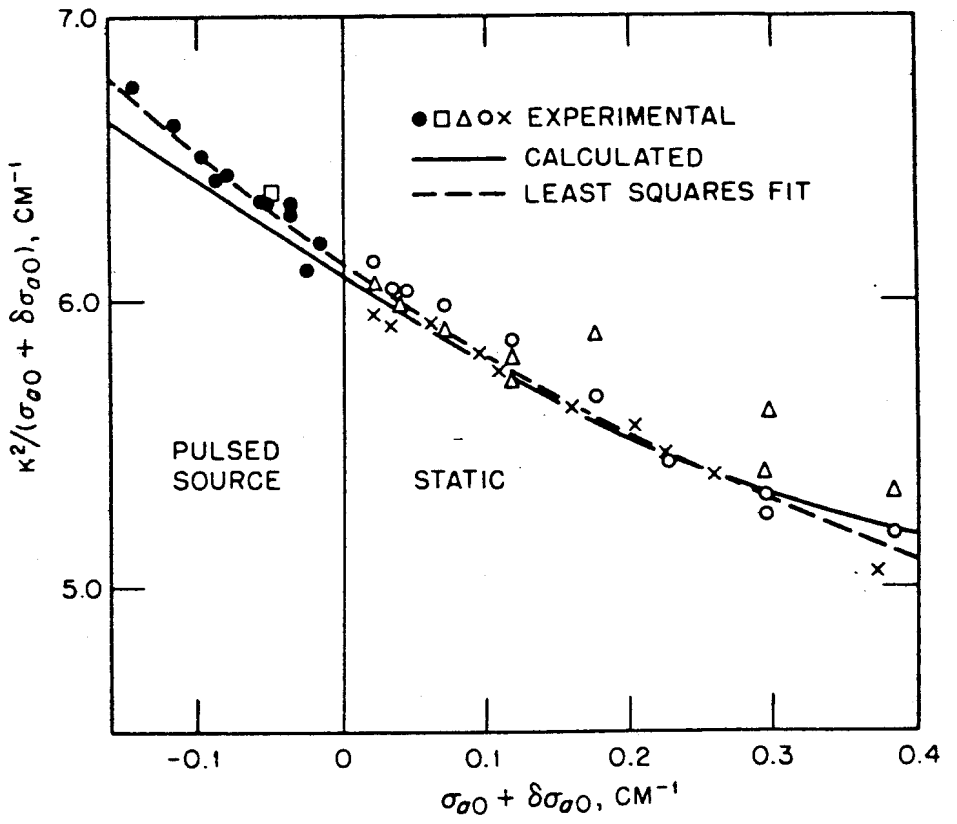

FIG. 7.20 DIFFUSION-LENGTH (STATIC) AND PULSED-SOURCE MEASUREMENTS IN WATER (AFTER P. B. PARKS, *ET AL.*, REF. 108).

in water, for example, are given in Fig. 7.20[108]; the ordinates are $\kappa^2/(\sigma_{a0} + \delta\sigma_{a0})$ and the abscissae are $\sigma_{a0} + \delta\sigma_{a0}$, with the cross sections corresponding to $E_0 = kT$ ($T = 293°K$). For the pulsed-source region, $\sigma_{a0} + \delta\sigma_{a0}$ becomes $\sigma_{a0} + \alpha_0$ and κ^2 becomes $-B^2$. The curve shown in the figure was calculated[109] for the pulsed region by using the Nelkin model (§7.4h) and extrapolated into the static region.[110]

In the discussion of Fig. 7.19, it was noted that when $B^2 = 0$, i.e., for an infinite medium, $\alpha_0 = -\sigma_{a0}v_0$ for a system containing a $1/v$-absorber; it has not been established, however, that $-\sigma_{a0}v_0$ is a fundamental eigenvalue. If the foregoing values of B^2 and α_0 are inserted in equation (7.100), the latter becomes

$$\sigma_s(E)\phi(E) = \int \sigma_{s0}(E' \to E)\phi(E')\,dE', \tag{7.102}$$

which is equivalent to equation (7.10) for the flux in an infinite, source-free, nonabsorbing medium. As noted in §7.2b, the Maxwell distribution

$$\phi(E) = M(E, T)$$

is a solution of this equation. Hence, $M(E, T)$ is an eigenfunction of equation (7.100) and $-\sigma_{a0}v_0$ is the corresponding eigenvalue. Furthermore, it can be

shown[111] that $-\sigma_{a0}v_0$ is indeed the fundamental eigenvalue α_0, i.e., the one with the largest real part. It follows, therefore, that for an infinite medium with a $1/v$-absorber, $\alpha_0 = -\sigma_{a0}v_0$ and the fundamental eigenfunction is $M(E, T)$, so that the neutron flux has a Maxwellian distribution. Although this result was derived from the diffusion theory equation (7.100), it is quite general, since for a space-independent solution in an infinite medium there is no diffusion and no net current.

7.6f Deviations from the Maxwell Distribution

In this final section, the manner in which the flux eigenfunctions associated with the various eigenvalues deviate from a Maxwellian distribution will be examined. For the pulsed-source experiment in an infinite medium, i.e., $B = 0$ in equation (7.91) or (7.100), $\alpha_0 = -\sigma_{a0}v_0$, and the eigenfunction is Maxwellian, as just seen. For a large but finite system, the diffusion equation (7.100) may be used with a finite but small value of B in order to obtain the dependence of the eigenvalue, α, and the eigenfunction, $\phi(E)$, on the size of the system, i.e., on B. For this purpose, it is convenient to rewrite equation (7.100) for a $1/v$-absorber in the form

$$\left[\frac{\alpha + \sigma_{a0}v_0}{v} + D(E)B^2\right]\phi(E) = q\phi(E), \tag{7.103}$$

where q is defined by

$$q\phi(E) \equiv \int \sigma_{s0}(E' \to E)\phi(E')\,dE' - \sigma_s(E)\phi(E). \tag{7.104}$$

By integrating equation (7.104) over all energies and noting that

$$\int \sigma_{s0}(E' \to E)\,dE = \sigma_s(E'),$$

it is seen that

$$\int q\phi(E)\,dE = 0 \tag{7.105}$$

for any function $\phi(E)$.

For small values of B, a perturbation method may be used in which α and ϕ are expressed as power series in B^2; thus,

$$\alpha = \alpha_0 + \alpha_1 B^2 + \alpha_2 B^4 + \cdots \tag{7.106}$$

$$\phi(E) = \phi_0(E) + B^2\phi_1(E) + B^4\phi_2(E) + \cdots. \tag{7.107}$$

Upon inserting these series in equation (7.103) and equating coefficients of equal powers of B, it is found that

$$\frac{\alpha_0 + \sigma_{a0}v_0}{v}\phi_0(E) = q\phi_0(E) \tag{7.108}$$

$$\frac{\alpha_0 + \sigma_{a0}v_0}{v}\phi_1(E) + \left[\frac{\alpha_1}{v} + D(E)\right]\phi_0(E) = q\phi_1(E) \tag{7.109}$$

$$\frac{\alpha_0 + \sigma_{a0}v_0}{v}\phi_2(E) + \left[\frac{\alpha_1}{v} + D(E)\right]\phi_1(E) + \frac{\alpha_2}{v}\phi_0(E) = q\phi_2(E). \tag{7.110}$$

Equations (7.108), (7.109), and (7.110) are now integrated over all energies and it then follows, from equation (7.104), that the right-hand side is zero in each case. Equation (7.108) then gives, as expected,

$$\alpha_0 = -\sigma_{a0}v_0, \tag{7.111}$$

and, moreover, from the arguments near the end of §7.6e,

$$\phi_0(E) = M(E, T).$$

Consequently, from the integrations of equations (7.109) and (7.110), it is found that

$$-\alpha_1 = \frac{\int D(E)M(E, T)\,dE}{\int (1/v)M(E, T)\,dE} \equiv \bar{D} \tag{7.112}$$

$$-\alpha_2 = \frac{\int [D(E) - (\bar{D}/v)]\phi_1(E)\,dE}{\int (1/v)M(E, T)\,dE} \equiv -C_d, \tag{7.113}$$

where $\bar{D}$, the *diffusion coefficient*, and C_d, called the *diffusion cooling coefficient*, are defined by equations (7.112) and (7.113), respectively.

By making use of equations (7.111), (7.112), and (7.113), equation (7.106) may be written as

$$\alpha = -\sigma_{a0}v_0 - \bar{D}B^2 + C_dB^4 + \cdots. \tag{7.114}$$

It will be noted that $\bar{D}$ is determined, according to equation (7.112), by the diffusion constant $D(E)$ and the Maxwell distribution $M(E, T)$. Hence, the first term in equation (7.114) that involves deviations of the neutron flux from the Maxwellian distribution is the "diffusion cooling" term, C_dB^4. The origin and naming of this term can be understood from the following discussion.

A $1/v$-absorber does not perturb the Maxwellian distribution in an infinite medium because the lifetime of a neutron against absorption by such an absorber, namely $[\sigma_a(E)v]^{-1}$, is independent of the neutron energy. Hence, all neutrons are absorbed at the same rate and the Maxwell spectrum is not perturbed by $1/v$-absorption. This explains why the first two terms on the right of equation (7.114) do not represent any departure from a Maxwellian distribution.

The lifetime of a neutron of energy E against leakage from a system, however, is approximately $[vD(E)B^2]^{-1}$. For gaseous and liquid moderators, the quantity $vD(E)$ increases with neutron energy in the thermal region, so that neutrons of higher energy leak (or diffuse) out faster than those of lower energy. The net effect of this preferential leakage of the more energetic neutrons is to shift the neutron spectrum to lower energies relative to a Maxwellian distribution at the temperature of the moderator. If the shifted spectrum were to be characterized by a "neutron temperature,"[112] the latter would then be lower than the moderator temperature. This accounts for the use of the term diffusion cooling. According to equations (7.113) and (7.114), the diffusion cooling coefficient, C_d, represents, in the term C_dB^4, the first-order effect of the shift in the spectrum on the time decay constant, α, of the neutron population.

In crystalline moderators there is an additional effect arising from the very large value of $D(E)$ for neutrons with energies below the Bragg cutoff energy. Thus, the leakage of these neutrons of very low energies is also favored.

The computation of the diffusion cooling coefficient, from equation (7.113), requires a knowledge of the deviation, ϕ_1, of the neutron spectrum from the Maxwellian distribution. This can be obtained either by numerical methods for realistic thermalization models or analytically for simplified models.[113] The coefficient, C_d, is found to be positive and to be larger for moderators with rela-

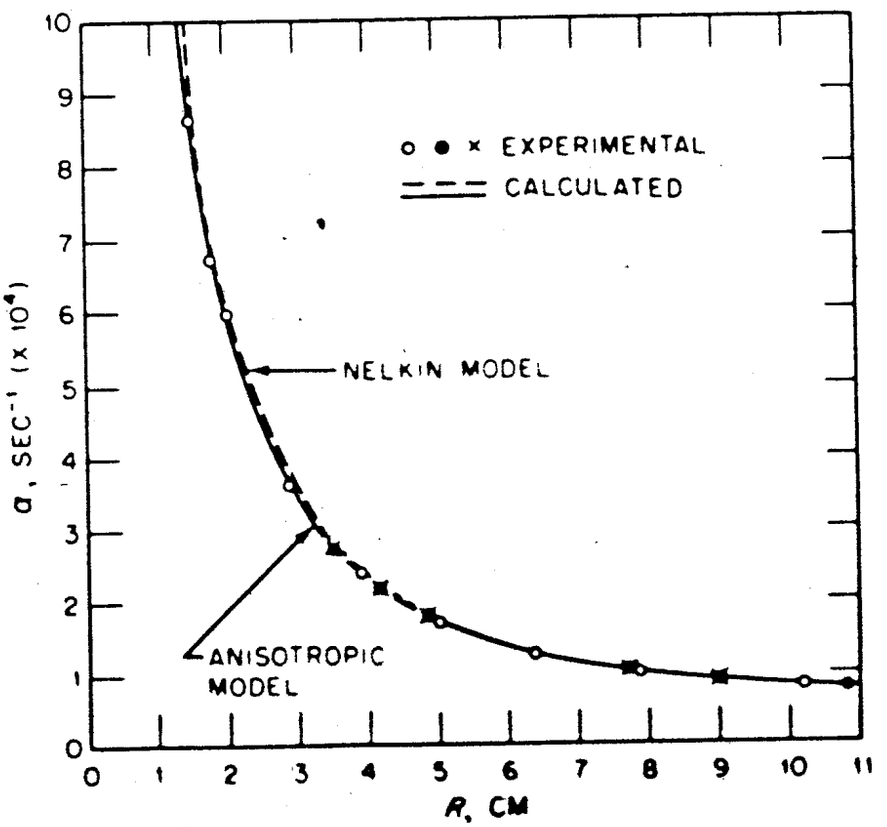

FIG. 7.21 EXPERIMENTAL AND CALCULATED VALUES OF α IN SPHERES OF WATER (AFTER J. J. DORNING, REF. 115).

tively poor energy transfer, e.g., graphite, than for those with good energy transfer, such as ordinary (light) water.

The parameters $\bar{D}$ and C_d can be determined from experimental measurements of time decay (or die-away) with a pulsed neutron source, by fitting the dependence of α on B^2 to an expression of the form of equation (7.114) or by other means.[114] The results are generally in good agreement with calculations based on realistic scattering models. For small systems, where the diffusion cooling effect is most significant, representation of neutron leakage by diffusion theory, i.e., with a DB^2 term as in equation (7.100), is, of course, not adequate. A more accurate treatment of the neutron transport problem is then required to yield reliable results. An example of such a calculation is given in Fig. 7.21.[115] The experimental values of α, for small spherical light-water systems of various radii, are indicated by the points; these may be compared with the curves computed using the S_4 approximation with 30 energy groups, based on either the Nelkin scattering model or an improved (anisotropic) model.[116] The agreement is seen to be very good, especially in the latter case.

Perturbation expressions, such as those embodied in equations (7.106) and (7.107), can be used in the treatment of other eigenvalue problems.[117] For example, it is found in diffusion-length measurements that there is a "diffusion heating" effect analogous to the effect of diffusion cooling just considered, as observed in pulsed, die-away experiments. In the diffusion theory of the diffusion-length experiment, the neutron flux would be assumed to be time independent and to vary as $e^{-\kappa x}$ with distance x from the source. The equation for the eigenvalue would then be, according to equation (7.103),

$$\left[\frac{\sigma_{a0}v_0}{v} - \kappa^2 D(E)\right]\phi(E) = q\phi(E). \tag{7.115}$$

This differs from equation (7.103) in the respect that there is no α/v term and B^2 has been replaced by $-\kappa^2$. For $\sigma_{a0} = 0$, equation (7.115) has a solution for $\kappa^2 = 0$; then $q\phi(E) = 0$ and the flux has a Maxwellian distribution, according to equations (7.102) and (7.104). When σ_{a0} is finite, the neutron flux deviates from Maxwellian behavior and it is found experimentally that the distribution is shifted to higher energies; this is the effect referred to as *diffusion heating* and the neutron spectrum is said to be "hardened." The cause of diffusion heating is that neutrons of higher energies diffuse into a given volume element more readily than do those of lower energies. In diffusion cooling there is a net diffusion of neutrons *out* of any volume element, whereas in diffusion heating the net diffusion is *into* the volume element. The neutron energy spectrum is determined by a balance between absorption occurring at a rate independent of energy in the presence of a $1/v$ absorber, and diffusion, which is energy dependent. Hence, when the neutrons of higher energy diffuse preferentially *into* a given volume element, the spectrum is shifted to higher energies.

In addition to diffusion heating, there is a form of spectrum hardening due to neutron absorption. It has been seen that, in an infinite medium, the Maxwell distribution remains a valid eigenfunction for the eigenvalue α_0, even when a $1/v$-absorber is present. This means that long after a source pulse, the neutron spectrum in a large (infinite) medium will be Maxwellian. The situation is quite different in connection with the neutron energy distribution resulting from a steady source of fast neutrons, constant in time and space. A slowing-down spectrum will then join into the thermal distribution of neutrons, and the latter will be shifted to higher energies than for a Maxwellian distribution. Figure 7.22, for example, shows the spectrum for neutrons of low energy in water at 296°K containing a $1/v$-absorber, with σ_a equal to 5.2 barns per hydrogen atom.[118] Similar results are obtained for any finite concentration of an absorber with a cross section that is related inversely (or approximately so) to the neutron velocity. If, however, the absorber has resonances in the thermal region, the energy variation of the flux is different (§8.1f).[119]

In nuclear reactors, diffusion cooling, due to the leakage of fast neutrons, is relatively insignificant except in very small systems, but hardening of the spectrum as a result of the absorption of thermal neutrons is generally important in thermal reactors. In early treatments, the energy spectrum of thermal neutrons was often fitted, somewhat arbitrarily, to a Maxwellian distribution, with an empirical neutron temperature, T_N, which was higher than the actual moderator

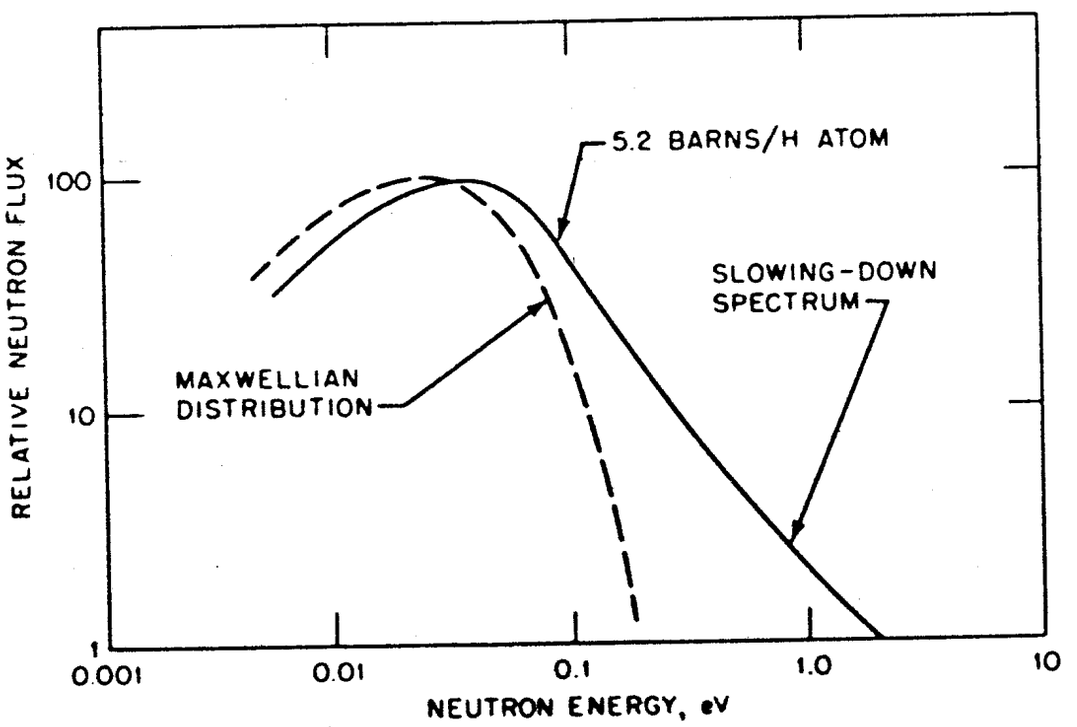

FIG. 7.22 NEUTRON ENERGY SPECTRUM IN WATER CONTAINING A $1/v$-ABSORBER (AFTER J. A. YOUNG AND D. HUFFMAN, REF. 118).

temperature, T_m. Studies have been made of the variation of $(T_N - T_m)/T_m$ with the concentration of absorber, and correlations of the form

$$T_N = T_m\left(1 + C\frac{\sigma_{a0}}{\xi\sigma_{s0}}\right)$$

have been proposed,[120] where C is a constant and ξ is the average (free atom) logarithmic energy loss per collision (§4.7d). If σ_{a0} is taken as the absorption cross section $\sigma_a(E)$ at $E = kT_m$, then C is approximately 1.6 for all moderators of interest, i.e., with small mass numbers.

The representation of the thermal neutron spectrum by a Maxwell distribution shifted to a higher temperature than actually exists in the reactor is fairly satisfactory provided there is little absorption, e.g., for $\sigma_{a0}/\xi\sigma_{s0} \lesssim 0.2$. More generally, however, it is not accurate. Nevertheless, the treatment does point up the tendency for the thermal neutron spectrum to be hardened relative to the Maxwellian distribution at the temperature of the moderator, T_m, and indicates the extent of the hardening in a qualitative manner.

7.7 APPENDIX TO CHAPTER 7

7.7a Source of Thermal Neutrons from Slowing Down

The source, $Q(E)$, of neutrons which are slowed down into the thermal energy range can usually be derived from the following simple considerations. A neutron energy, E_0, of the order of 1 eV, is selected and it is assumed that for higher energies a purely slowing-down spectrum is applicable (§7.1a); that is,

$$\phi(E) = \frac{\phi_0}{E} \quad \text{for} \quad E > E_0.$$

The rate at which neutrons are scattered to energies below E_0 can then be obtained by using the appropriate scattering kernel as derived in the main part of this chapter. If E_0 is sufficiently large, it is satisfactory, however, to employ the free-atom scattering kernel (§4.2b)

$$\begin{aligned} \sigma_s f_s(E' \to E) &= \frac{\sigma_s}{(1-\alpha)E'} \quad \text{if} \quad \alpha E' \leqslant E \leqslant E' \\ &= 0 \qquad\qquad\quad \text{if} \quad E > E' \text{ or } E < \alpha E', \end{aligned}$$

where α is $(A-1)^2/(A+1)^2$.

The source, $Q(E)$, of neutrons scattered from energies E' above E_0 to energies $E < E_0$ is then

$$\begin{aligned} Q(E) &= \int_{E_0}^{\infty} \phi(E')\sigma_s f_s(E' \to E)\, dE' \\ &= \frac{\sigma_s\phi_0}{1-\alpha}\int_{E_0}^{E/\alpha} \frac{dE'}{(E')^2}. \end{aligned}$$

Hence

$$Q(E) = \frac{\sigma_s \phi_0}{1-\alpha}\left(\frac{1}{E_0} - \frac{\alpha}{E}\right) \quad \text{if} \quad E \geqslant \alpha E_0$$

$$= 0 \qquad\qquad\qquad\qquad \text{if} \quad E < \alpha E_0.$$

The expressions derived above are for slowing down in a medium consisting of a single atomic species; the results can be readily generalized to a moderator containing two or more types of atoms.

When absorption or leakage is important during slowing down, as in heavily poisoned or small systems, the neutron flux above the energy E_0 does not vary as $1/E$. Improved estimates can be made, however, by the use of age theory or slowing-down theory.[121] If the spatial dependence of the source is required, it can usually be taken in some normal mode, e.g., e^{iBx} (cf. §7.6d) for a reactor that is not too small.

EXERCISES

1. Derive equation (7.20) by considering the two transport equations satisfied by the two Green's functions, multiplying each equation by the appropriate $M \times G$ and integrating over all variables.
2. Show that equation (7.26) satisfies the detailed balance equation (7.11).
3. Use equation (7.52) to derive the monatomic gas scattering cross section in equation (7.26).
4. Determine the scattering function $S(\alpha, \beta)$ for the monatomic gas, i.e., from equation (7.26).
5. Verify that for high temperatures, i.e., for $kT \gg \hbar\omega_0$, the harmonic oscillator scattering cross section, σ_s, reduces to that for a monatomic gas. Try to do the same for $\sigma_s f_s$.[122]
6. Show that equation (7.66) reduces to the equation for an Einstein oscillator if $f(\omega)$ is a delta function.
7. Simplify equation (7.30) for a "heavy gas" moderator, i.e., for $A \gg 1$ and $E' \gg kT/A$, and show that in these circumstances

$$\int_0^\infty (E' - E)\sigma_s(E')f_s(E' \to E)\,dE = \frac{2\sigma_{s0}}{A}(E' - 2kT)$$

$$\int_0^\infty (E' - E)^2\sigma_s(E')f_s(E' \to E)\,dE = \frac{4\sigma_{s0}}{A}E'kT.$$

8. Consider neutrons being moderated in an infinite medium consisting of a heavy gas. Show that the neutron flux, $\phi(E)$, satisfies the differential equation

$$\sigma_a(E)\phi(E) = \frac{2\sigma_{s0}}{A}\frac{d}{dE}\left[(E - kT)\phi(E) + EkT\frac{d\phi(E)}{dE}\right].$$

(Introduce $\psi(E) = \phi(E)/M(E, T)$ into the transport equation and in the integrand expand $\psi(E')$ in a Taylor series about E; then use the results of Exercise 7.[123])

9. Show that in a finite medium the presence of a $1/v$-absorber will not affect the eigenfunction associated with the fundamental α eigenvalue. Find the effect of the absorber on α. If the absorption cross section departs to a small extent from the $1/v$ dependence, i.e., $\sigma_a = (\sigma_{a0}v_0/v) + \delta\sigma(E)$, find a first-order expression for the change in α due to $\delta\sigma$.

REFERENCES

1. Glasstone, S., and M. C. Edlund, "The Elements of Nuclear Reactor Theory," D. Van Nostrand Co., Inc., 1952, Chap. VI; J. R. Lamarsh, "Introduction to Nuclear Reactor Theory," Addison-Wesley Publishing Co., Inc., 1966, Chaps. 6 and 7; A. M. Weinberg and E. P. Wigner, "The Physical Theory of Neutron Chain Reactors," University of Chicago Press, 1958, Chap. X.

1a. Lamb, W. E., *Phys. Rev.*, **51**, 187 (1937); H. Rietschel, *Nucl. Phys.*, **A139**, 100 (1969); H. Rietschel, W. Schott, and J. Fink, *Nucl. Sci. Eng.*, **38**, 180 (1969).

2. Lamb, W. E., *Phys. Rev.*, **55**, 190 (1939).

3. Weinberg, A. M., and E. P. Wigner, Ref. 1, p. 281.

4. See, for example, D. J. Hughes, "Neutron Optics," Interscience Publishers, Inc., 1954.

5. "Neutron Cross Sections," Brookhaven National Laboratory Report BNL-325 (1958).

6. Fermi, E., *Ricerca Sci.*, **7**, 13 (1936), reprinted in E. Fermi, "Collected Papers," E. Segrè, Chairman of editorial board, University of Chicago Press, 1952, Vol. I, p. 980; J. M. Blatt and V. F. Weisskopf, "Theoretical Nuclear Physics," John Wiley and Sons, Inc., 1952, pp. 44-80; G. C. Summerfield, *Ann. Phys.*, **26**, 72 (1964).

7. Lomer, W. M., and G. G. Low in "Thermal Neutron Scattering," P. A. Egelstaff, ed., Academic Press, 1965, Chap. 1; D. E. Parks, M. S. Nelkin, N. F. Wikner, and J. R. Beyster, "Slow Neutron Scattering and Thermalization, with Reactor Applications," W. A. Benjamin, Inc., 1970, Section 2.1.

8. Blatt, J. M., and V. F. Weisskopf, Ref. 6, pp. 80 *et seq.*

9. Beckurts, K. H., and K. Wirtz, "Neutron Physics," English transl. Springer-Verlag, 1964, pp. 98-100.

10. Williams, M. M. R., "Slowing Down and Thermalization of Neutrons," John Wiley and Sons, Inc., 1966, p. 20; D. E. Parks, *et al.*, Ref. 7, Section 2.3.

11. Kuščer, I., in "Developments in Transport Theory," E. Inönü and P. F. Zweifel, eds., Academic Press, 1967, pp. 243 *et seq*; I. Kuščer and N. J. McCormick, *Nucl. Sci. Eng.*, **26**, 522 (1966); N. Corngold, *Proc. Symp. Appl. Math.*, "Transport Theory," Am. Math. Soc., 1969, Vol. I, p. 79.

12. Wigner, E. P., and J. E. Wilkins, Jr., "Effect of the Temperature of the Moderator on the Velocity Distribution of Neutrons with Numerical Calculations for Hydrogen as Moderator," U.S. AEC Report AECD-2275 (1944).

13. Osborne, R. K., *Nucl. Sci. Eng.*, **3**, 29 (1958); C. L. Blackshaw and R. L. Murray, *ibid.*, **27**, 520 (1967); M. M. R. Williams, Ref. 10, p. 26.

14. Beckurts, K. H., and K. Wirtz, Ref. 9, p. 182.

15. Parks, D. E., *et al.*, Ref. 7, Section 2.5.

16. Sachs, R. G., and E. Teller, *Phys. Rev.*, **60**, 18 (1941); T. L. Krieger and M. S. Nelkin, *ibid.*, **106**, 290 (1956); M. M. R. Williams, Ref. 10, p. 28.

17. Fermi, E., Ref. 6.

18. Placzek, G., and L. Van Hove, *Phys. Rev.*, **93**, 107 (1954); G. C. Wick, *ibid.*, **94**, 1228 (1954); L. Van Hove, *ibid.*, **95**, 249 (1954); A. C. Zemach and R. L. Glauber, *ibid.*, **101**, 118 (1956).

19. Williams, M. M. R., Ref. 10, Appendix IV; D. E. Parks, *et al.*, Ref. 7, Chap. 2.

20. Van Hove, L., Ref. 18.

21. Blatt, J. M., and V. F. Weisskopf, Ref. 6, pp. 71 *et seq.*; D. E. Parks, *et al.*, Ref. 7, Section 2.1.

22. Van Hove, L., Ref. 18.
23. Egelstaff, P. A., *Nucl. Sci. Eng.*, **12**, 250 (1962).
24. Placzek, G., and L. Van Hove, *Nuovo Cimento*, **1**, 233 (1955); W. Marshall and R. Stuart, in "Inelastic Scattering of Neutrons in Solids and Liquids," IAEA, 1961, p. 75; D. E. Parks, *et al.*, Ref. 7, Section 3.1; H. Takahashi, *Nucl. Sci. Eng.*, **37**, 198 (1969); R. Conn, *ibid.*, **40**, 17 (1970).
25. See citations in Ref. 18; also, D. E. Parks, *et al.*, Ref. 7, Section 2.4.
26. Zemach, A. C., and R. L. Glauber, *Phys. Rev.*, **101**, 129 (1956); see also citations in Ref. 18.
27. Williams, M. M. R., Ref. 10, p. 543.
28. Fermi, E., Ref. 6.
29. Einstein, A., *Ann. Physik*, **22**, 180, 860 (1906); **34**, 170 (1911).
30. Williams, M. M. R., Ref. 10, Appendix IV; D. E. Parks, *et al.*, Ref. 7, Section 2.5.
31. Parks, D. E., *et al.*, Ref. 7, Sections 2.5, 3.2.
32. Fermi, E., Ref. 6.
33. Beckurts, K. H., and K. Wirtz, Ref. 9, pp. 188 *et seq.*
34. Fermi, E., Ref. 6.
35. Beckurts, K. H., and K. Wirtz, Ref. 9, p. 189; D. E. Parks, *et al.*, Ref. 7, Section 2.5.
36. Koppel, J. U. in "Reactor Physics in the Resonance and the Thermal Regions," A. J. Goodjohn and G. C. Pomraning, eds., The M.I.T. Press, 1967, Vol. I, p. 27.
37. McReynolds, A. W., *et al.*, *Second U.N. Conf. on Peaceful Uses of At. Energy*, **16**, 297 (1958).
38. Reichard, W., in "Neutron Thermalization and Reactor Spectra," IAEA, 1968, Vol. II, p. 411.
39. See, for example, F. Seitz, "Modern Theory of Solids," McGraw-Hill Book Co., 1940, Chap. III.
40. Sjölander, A., *Arkiv Fysik*, **14**, 315 (1958); M. M. R. Williams, Ref. 10, p. 31 and Appendix IV.
41. Koppel, J. U., J. R. Triplett, and Y. D. Naliboff, "GASKET, A Unified Code for Thermal Neutron Scattering," General Atomic Report GA-7417 (1966); W. W. Clendenin, "Calculation of Thermal Neutron Scattering Cross Sections for Crystalline Materials: The TOR Program," Los Alamos Scientific Laboratory Report LA-3823 (1967).
42. Sjölander, A., Ref. 40; J. A. Young, in Ref. 36, Vol. I, p. 3; J. U. Koppel and J. A. Young, in Ref. 36, Vol. I, p. 333; H. Takahashi, Ref. 24.
43. Parks, D. E., *et al.*, Ref. 7, Section 2.6.
44. Vineyard, G. H., *Phys. Rev.*, **110**, 999 (1958); see also A. K. Agrawal and S. Yip, *Nucl. Sci. Eng.*, **37**, 368 (1969).
45. Glasstone, S., and M. C. Edlund, Ref. 1, Chap. VI; J. R. Lamarsh, Ref. 1, Chap. 6; A. M. Weinberg and E. P. Wigner, Ref. 1, pp. 321 *et seq.*
46. See, for example, H. S. Carslaw and J. C. Jaeger, "Conduction of Heat in Solids," Oxford University Press, 1947.
47. Sneddon, J. M., "Fourier Transforms," McGraw-Hill Book Co., 1951, Chap. 1.
48. Williams, M. M. R., Ref. 10, pp. 47 *et seq.*; D. E. Parks, *et al.*, Ref. 7, Section 2-9.3.
49. Sneddon, J. M., Ref. 47.
50. Vineyard, G. H., Ref. 44.
51. Seitz, F., Ref. 39, Section 19.
52. Parks, D. E., *et al.*, Ref. 7, Section 3.3; P. A. Egelstaff and P. Schofield, *Nucl. Sci. Eng.*, **12**, 260 (1962).
53. Slaggie, E. L., in Ref. 38, Vol. I, p. 311.
54. Wikner, N. F., G. D. Joanou, and D. E. Parks, *Nucl. Sci. Eng.*, **19**, 108 (1964); D. E. Parks, *et al.*, Ref. 7, Section 3-4.2.
55. Young, J. A., and J. U. Koppel, *J. Chem. Phys.*, **42**, 357 (1965).
56. Carvalho, F., *Nucl. Sci. Eng.*, **34**, 224 (1968); W. L. Whittemore, *ibid.*, **33**, 31 (1968).
57. Carvalho, F., Ref. 56.
58. Young, J. A., in Ref. 36, Vol. I, p. 3.

59. Parks D. E., J. R. Beyster, and N. F. Wikner, *Nucl. Sci. Eng.*, **13**, 306 (1962).
60. Parks, D. E., *et al.*, Ref. 59.
61. Young, J. A., in Ref. 36, Vol. I, p. 3; H. Takahashi, Ref. 24; R. Conn, Ref. 24.
62. Zemach, A. C., and R. L. Glauber, Ref. 26.
63. Nelkin, M. S., *Phys. Rev.*, **119**, 741 (1960); D. E. Parks, *et al.*, Ref. 7, Section 3-4.1.
64. Koppel, J. U., and J. A. Young, *Nucl. Sci. Eng.*, **19**, 412 (1964); J. U. Koppel, Ref. 36; H. L. McMurray, G. J. Russell, and R. M. Brugger, *Nucl. Sci. Eng.*, **25**, 248, (1966); J. R. Beyster, *ibid*, **31**, 254 (1968); D. E. Parks, *et al.*, Ref. 7, Section 3-4.1.
65. Beyster, J. R., Ref. 64.
66. Brugger, R. M., *Nucl. Sci. Eng.*, **33**, 187 (1968).
67. Beyster, J. R., *et al.*, *Nucl. Sci. Eng.*, **9**, 168 (1961).
68. E. M. Gelbard, J. A. Davis, and E. Schmidt, in Proc. Brookhaven Conf. on Neutron Thermalization, Brookhaven National Laboratory Report BNL-719 (1962), Vol. IV, p. 1175.
69. Brugger, R. M., Ref. 66; J. J. Dorning, *Nucl. Sci. Eng.*, **33**, 81 (1968).
70. Gläser, W., in Ref. 38, Vol. I, p. 235.
71. Parks, D. E., *et al.*, Ref. 7, Section 3.4.
72. Honeck, H. C., *Trans. Am. Nucl. Soc.*, **5**, 47 (1962).
73. Butler, D., *Proc. Phys. Soc.* (Lond.), **81**, 276, 294 (1963); O. K. Hurling, *Nucl. Sci. Eng.*, **33**, 41 (1968); W. L. Whittemore, *ibid.*, **33**, 195 (1968).
74. Parks, D. E., *et al.*, Ref. 7, Section 3-4.4; J. A. Young, Ref. 36, Vol. I, p. 3.
75. Beyster, J. R., and J. A. Young, *Ann. Rev. Nucl. Sci.*, **17**, 97 (1967); Parks, D. E., *et al.*, Ref. 7, Section 3-4.3.
76. Honeck, H. C., "THERMOS, A Thermalization Transport Code for Reactor Lattice Calculations," Brookhaven National Laboratory Report BNL-5826 (1961); see also *Nucl. Sci. Eng.*, **8**, 193 (1960).
77. Harper, R. G., *J. Nucl. Energy*, **21**, 767 (1967).
78. Pomraning, G. C., in Ref. 36, Vol. I, p. 207.
79. Parks, D. E., *et al.*, Ref. 7, Chap. 8, especially Section 8-9; see also the publication cited in Ref. 38.
80. Perez, R. B., and R. S. Booth in Symp. on Pulsed Neutron Research, IAEA, 1965, Vol. II, p. 701; M. N. Moore, *Nucl. Sci. Eng.*, **26**, 354 (1966); J. J. Duderstadt, *ibid.*, **29**, 156 (1967); *J. Math. Phys.*, **10**, 266 (1969); M. M. R. Williams, *J. Nucl. Energy*, **22**, 153 (1968).
81. Williams, M. M. R., Ref. 10, pp. 133, 177; D. E. Parks, *et al.*, Ref. 7, Chap. 8.
82. Kuščer, I., in Ref. 38, Vol. I, p. 3; see, however, R. Conn and N. Corngold, *Nucl. Sci. Eng.*, **37**, 85 (1969).
83. Corngold, N., *Nucl. Sci. Eng.*, **19**, 80 (1964).
84. Parks, D. E., *et al.*, Ref. 7, Section 8-1.5.
85. Parks, D. E., *et al.*, Ref. 7, Section 8-1.5.
86. Corngold, N., Ref. 83; *Nucl. Sci. Eng.*, **24**, 410 (1966).
87. Dorning, J. J., and J. K. Thurber, *Trans. Am. Nucl. Soc.*, **11**, 379 (1968).
88. Baumann, N. P., P. B. Parks, and D. J. Pellarin, in Ref. 38, Vol. II, p. 177.
89. Williams, M. M. R., in Ref. 38, Vol. I, p. 27.
90. Perez, R. B., *Nucl. Sci. Eng.*, **30**, 95 (1967); F. Ahmed, P. S. Grover, and L. S. Kothari, *ibid.*, **31**, 484 (1968); J. J. Duderstadt, *ibid.*, **33**, 119 (1968); J. J. Dorning and J. K. Thurber, *Trans. Am. Soc.*, **11**, 580 (1968); H. G. Kaper, J. H. Ferziger, and S. U. Loyalka in Ref. 38, Vol. I, p. 95; J. J. Dorning, B. Nicolaenko, and J. K. Thurber in Neutron Transport Theory Conf., AEC Report ORO 3858-1 (1969), p. 2.
91. Nelkin, M. S., *Physica*, **79**, 261 (1963); S. Albertoni and B. Montagnini, *J. Math. Anal. Applic.*, **13**, 19 (1966); R. Bednarz, in Symp. on Pulsed Neutron Research, IAEA, 1965, Vol. I, p. 259; M. Borysiewicz and J. R. Mika, in Ref. 38, Vol. I, p. 45; R. Conn and N. Corngold, Ref. 82.
92. Kuščer, I., in Ref. 38, Vol. I, p. 3.
93. Mockel, A., *Nucl. Sci. Eng.*, **26**, 279 (1966); S. Ukai, *J. Nucl. Sci. Technol.* (Tokyo), **3**, 430 (1966).
94. Albertoni, S., and B. Montagnini, Ref. 91.

95. Albertoni, S., and B. Montagnini, Ref. 91; R. Bednarz, Ref. 91; M. Borysiewicz and J. R. Mika, Ref. 91.
96. Ghatak, A. K., *J. Nucl. Energy*, **21**, 509 (1967); F. Ahmed and A. K. Ghatak, *Nucl. Sci. Eng.*, **33**, 106 (1968).
97. Williams, M. M. R., Ref. 10, p. 119; N. Corngold and K. Durgan, *Nucl. Sci. Eng.*, **29**, 354 (1967).
98. Shapiro, C. S., "Time Eigenvalues and Degenerate Kernels in Neutron Thermalization," Brookhaven National Laboratory Report BNL-8433 (1964); C. S. Shapiro and N. Corngold, *Phys. Rev.*, **137**, A1686 (1965).
99. Ohanian, M. J., and P. B. Daitch, *Nucl. Sci. Eng.*, **19**, 343 (1964); W. W. Clendenin, *ibid.*, **36**, 1 (1969).
100. Ohanian, M. J., and P. B. Daitch, Ref. 99.
101. Ohanian, M. J., and P. B. Daitch, Ref. 99.
102. Pimbley, G. H., *J. Math. Mech.*, **8**, 837 (1959).
103. Jenkins, J. D., and P. B. Daitch, *Nucl. Sci. Eng.*, **31**, 222 (1968); R. Conn and N. Corngold, *ibid.*, **37**, 94 (1969).
104. A. Ritchie and M. Rainbow, *Nucl. Sci. Eng.*, **28**, 306 (1967).
105. Honeck, H. C., in Proc. Brookhaven Conf. on Neutron Thermalization, Brookhaven National Laboratory Report BNL-719 (1962), Vol. IV, p. 1186.
106. See, for example, C. S. Shapiro and N. Corngold, Ref. 98; J. H. Warner, Jr., and R. C. Erdmann, *Nucl. Sci. Eng.*, **35**, 332 (1969).
107. Honeck, H. C., Ref. 105.
108. Parks, P. B., *et al.*, *Nucl. Sci. Eng.*, **33**, 209 (1968).
109. Dorning, J. J., *Nucl. Sci. Eng.*, **33**, 65, 81 (1968).
110. Honeck, H. C., Ref. 105.
111. Nelkin, M. S., *Nucl. Sci. Eng.*, **7**, 710 (1960).
112. Beckurts, K. H., and K. Wirtz, Ref. 9, p. 215.
113. Beckurts, K. H., and K. Wirtz, Ref. 9, p. 215; M. M. R. Williams, Ref. 10, pp. 135 *et seq.*
114. Beckurts, K. H., and K. Wirtz, Ref. 9, p. 387; P. B. Parks, *et al.*, Ref. 108.
115. Dorning, J. J., *Nucl. Sci. Eng.*, **33**, 81 (1968).
116. Koppel, J. U., and J. A. Young, Ref. 64.
117. Williams, M. M. R., Ref. 10, p. 176.
118. Young, J. A., and D. Huffman, "Experimental and Theoretical Neutron Spectra," General Atomic Report GA-5319 (1964).
119. Beyster, J. R., *et al.*, Ref. 67.
120. Beckurts, K. H., and K. Wirtz, Ref. 9, p. 205.
121. Glasstone, S., and M. C. Edlund, Ref. 1, Chap. VI; J. R. Lamarsh, Ref. 1, Chaps. 6, 7; A. M. Weinberg and E. P. Wigner, Ref. 1, Chap. XI.
122. Parks, D. E., *et al.*, Ref. 7, Section 2-5.
123. Beckurts, K. H., and K. Wirtz, Ref. 9, p. 201; H. Hurwitz, M. S. Nelkin, and E. J. Habetler, *Nucl. Sci. Eng.*, **1**, 280 (1956).

8. RESONANCE ABSORPTION

8.1 RESONANCE CROSS SECTIONS

8.1a Introduction

In the "resonance energy" region, from roughly 1 eV to 100 keV, the main absorption of neutrons by heavy nuclei takes place at relatively sharply defined resonance energies.* A typical example of the cross-section variation in the resonance region is provided by uranium-238; the widths of the resonance peaks for the (n, γ) reaction are of the order of 0.1 eV and their energy separation is about 20 eV (Fig. 8.1).

In all reactors, some of the neutrons will be absorbed in the resonance energy region and in the design of certain reactors, notably those using natural (or slightly enriched) uranium as the fuel, an accurate treatment of the resonance absorption is essential.[2] Moreover, the resonance absorption changes with the temperature of the fuel, due to Doppler broadening of the resonances. The resultant temperature dependence of the reactivity is then often an important feature in the reactor control. For these reasons, consideration will be given in this chapter to the physical bases of the effects of resonance absorption on criticality and how these effects may be taken into account in reactor design studies.

The pronounced resonance structure in the dependence of cross section on neutron energy leads to a corresponding fine structure in the neutron flux. In

* There is some direct, nonresonance absorption, not involving the formation of a compound nucleus, in the resonance region. It appears to have no practical significance, although it is of theoretical interest.[1]

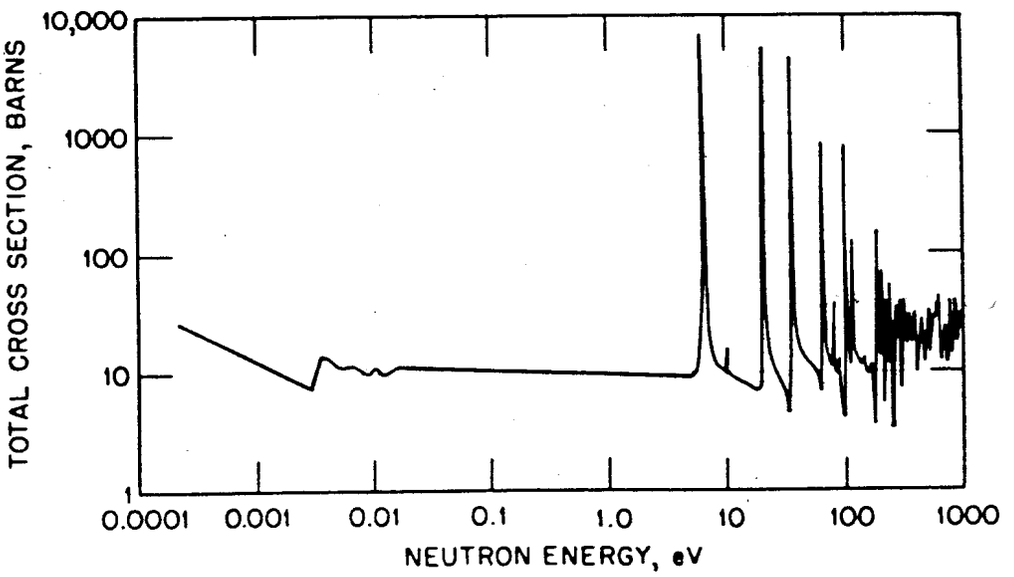

FIG. 8.1 TOTAL CROSS SECTION OF URANIUM-238 VS NEUTRON ENERGY SHOWING RESONANCES (ADAPTED FROM BNL-325).

general, there will be dips in the neutron flux at those energies (and locations) where there is strong resonance absorption or scattering. This fine structure must, of course, be taken into account in determining group cross sections for use in multigroup calculations as described in Chapter 4.

The detailed energy-dependent cross sections which are required for computing the energy-dependent flux and the group cross sections are not simply taken from experimental determinations. One reason is that when neutron cross sections are measured in the laboratory, the experimental energy resolution is not adequate to yield the required detailed variation of the cross sections with neutron energy except toward the lower-energy end of the resonance region.

Even at sufficiently low energies, however, in what is known as the *region of resolved resonances*, the experimental results are usually expressed better in terms of a few resonance parameters, such as the energy of the resonance, its amplitude, and width, than as energy-dependent cross sections. Theory is then used to reconstruct the latter from the resonance parameters. In some cases, such as neutron absorption by uranium-238, this approach has a special advantage; the resonance parameters can be derived from experimental values of the *total* cross section and then theoretical methods can be used to obtain the (n, γ) cross sections which are difficult to measure directly.

In practice, the region of resolved resonances will depend on the nature of nuclide under consideration. When the resonances are widely separated they can be resolved up to higher neutron energies than is possible for closely-spaced resonances. At present, the region of resolved resonances extends up to a few kilo-electron volts for the fertile nuclei and to about 50 eV (or so) for the important fissile species.

At higher neutron energies, it is not possible to achieve adequate resolution of

the individual resonances; the experimental cross sections then represent averages over several (or many) resonances. In this *region of unresolved resonances*, theory must be used to deduce the probable details of the resonance structure. When neutron absorption in this region is important, as it is for fast reactors, the necessity for relying on theoretical considerations in deriving the cross sections has significant consequences (§8.2a *et seq.*).

Another factor which makes it undesirable to use measured energy-dependent cross sections in the resonance region arises from the Doppler effect. The resonances are broadened as a result of the thermal motion of the nuclei; this motion depends on the temperature of the neutron-absorbing medium and on the binding of the nuclei. The considerations of Chapter 7 may be generalized to describe the thermal motion but, as will be seen in §8.1d, it is usually adequate to assume that the velocity distribution of the nuclei is Maxwellian.

The Doppler broadening of resonances has an important influence on the reactivity of a system and, in particular, on its temperature coefficient. Although it can be shown (§8.1d) that the area under a resonance peak is essentially independent of temperature, the broadening decreases the corresponding dip in the neutron flux. As a result, there is an increase in the product of the flux and the cross section, which determines the absorption probability and is involved in the group cross sections. This matter will be considered later in some detail (§8.3a), but for the present it may be noted that an increase in the temperature of the material containing neutron-absorbing nuclei always results in Doppler broadening of resonances and an increase in resonance absorption.

In order to take into account the effect of Doppler broadening on reactivity or other reactor properties, the basic cross sections in the resonance region must be adjusted appropriately for the broadening before they are used in computing group constants. It is not feasible to measure the temperature dependence of cross sections, i.e., the actual Doppler broadening, but it is a relatively simple matter to take the broadening into account in cross sections which are derived from experimental or theoretical resonance parameters.

In this chapter, the nature of the resonance cross sections will first be examined; in particular, consideration will be given to the expected energy dependence of cross sections in the vicinity of a resonance. Next, the dependence of the neutron flux on the energy will be studied in a homogeneous medium with a resonance absorber. The objective is to derive the absorption and group constants for such a medium. Subsequently, resonance absorption in a heterogeneous medium will be treated. Finally, some applications to thermal and fast reactors will be considered and comparisons will be made with experimental results.

8.1b The Single-Level Breit-Wigner Formula

The resonances occurring in the neutron cross sections of heavy nuclei arise from the combination of a neutron and the target nucleus to yield a compound nucleus which may subsequently decay (§8.2b) in various ways, e.g., neutron

emission, gamma-ray emission, and sometimes fission. At the peak of a resonance, the neutron energy is such as to favor the formation of the compound nucleus in a definite quantum state, i.e., with a definite angular momentum (or spin) and parity. For the case of a single resonance which is well separated from other resonances corresponding to states of the same spin and parity, the variation of the cross section with energy can be expressed in a particularly simple form, namely, by the Breit-Wigner single-level formula.[3]

Suppose that a neutron, having a spin of $\frac{1}{2}$, i.e., an intrinsic angular momentum of $\frac{1}{2}\hbar$, and an orbital angular momentum of $l\hbar$ combines with a target nucleus of spin I, where I is either an integer (or zero) or half integral, to form a compound state of spin J. According to the vector addition of angular momenta,[4] the spin J must satisfy the requirement that

$$|I - l \pm \tfrac{1}{2}| \leqslant J \leqslant I + l + \tfrac{1}{2}$$

unless $l > I + 1$, in which case the lower limit is 0 or $\frac{1}{2}$.

Reaction Cross Sections

In the vicinity of a resonance at energy E_0, the macroscopic cross section for a neutron of energy E undergoing a reaction of type x, for target nuclei at rest, i.e., no thermal motion, is then given by

$$\sigma_x(E) = N\pi\lambda^2 g \frac{\Gamma_n \Gamma_x}{(E - E_0)^2 + \frac{1}{4}\Gamma^2}, \tag{8.1}$$

where N is the number of target nuclei per unit volume, required to make σ_x a macroscopic cross section, λ is the reduced de Broglie wavelength of the neutron, about which more will be said shortly, Γ_n,Γ_x, and Γ are, respectively, the width for neutron emission, the width for the reaction x, and the total width of the resonance,* i.e.,

$$\Gamma = \Gamma_n + \sum_x \Gamma_x,$$

and g, a statistical factor which gives the probability that the particular compound state is realized, is expressed by

$$g = \frac{2J + 1}{2(2I + 1)}.$$

In many situations of interest, only s-wave, i.e., $l = 0$, neutrons need to be considered; then g reduces to

$$g = \frac{1}{2}\left(1 \pm \frac{1}{2I + 1}\right)$$

* The "width" is a measure of the probability that the compound nucleus will decay in a specific manner; it is equal to $\hbar$ times the decay constant for the particular process. The latter is, in general, dependent on the energy (§8.2b); hence, the widths Γ_n, Γ_x, and Γ, may vary to some extent with energy within a given resonance.

unless $I = 0$ when $g = 1$. In practice, the Breit-Wigner equation (8.1) is of greatest interest for radiative capture, i.e., $x = \gamma$, and fission, i.e., $x = f$, reactions.

It should be noted that the Breit-Wigner formula is derived for the center-of-mass system; hence for a neutron of velocity v, the value of λ is given by

$$\lambda = \frac{\hbar}{\mu v},$$

with μ the reduced mass of the neutron-nucleus system, i.e.,

$$\mu = \frac{Am}{A + 1},$$

where, as in preceding chapters, m is the mass of the neutron and Am is the mass of the target nucleus. The resonance parameters, such as the neutron energy and various widths, are then defined in the center-of-mass system. The cross sections can, of course, be transformed to the laboratory system, and λ will have the same meaning as above. Usually, however, equation (8.1) is applied (incorrectly), with $\lambda = \hbar/mv$, to interpret experimental data in the laboratory system and to derive the tabulated resonance parameters.[5] Consequently, when the latter are used in conjunction with equation (8.1), it is necessary that λ be taken to be equal to $\hbar/mv$. For neutron reactions with heavy nuclei, i.e., for $A \gg m$, the center-of-mass and laboratory systems are nearly the same, i.e., $\mu \approx m$, so that these considerations are of little import. But they must not be overlooked when the Breit-Wigner formula is applied to reactions involving light nuclei.[6]

Scattering Cross Sections

The elastic scattering cross sections in the vicinity of a resonance are given by a formula similar to, but somewhat more complicated than, equation (8.1). For the lth partial wave (§1.6c), it is

$$\sigma_{s,l}(E) = N\pi\lambda^2 g\left|\frac{i\Gamma_n}{E - E_0 + \frac{1}{2}i\Gamma} + e^{2i\delta_l} - 1\right|^2 + N\pi\lambda^2(2l + 1 - g)|e^{2i\delta_l} - 1|^2, \quad (8.2)$$

where δ_l is the phase shift associated with the potential (or nonresonant) scattering.[7] Of the two terms in equation (8.2), the first represents the elastic scattering for a compound nucleus with total spin J (and fixed parity); in addition to the resonant part of this scattering, which is proportional to Γ_n, there is interference between the resonant and potential scattering. This point will be seen more clearly below. The second term in equation (8.2) gives the potential scattering where the total spin is not equal to J, and this does not intefere with the resonance scattering.

Upon working out the squares in equation (8.2) and utilizing the identity

$$\cos 2\delta_l = 1 - 2\sin^2 \delta_l,$$

it is found that

$$\sigma_{s,l}(E) = \frac{N\pi\lambda^2 g}{(E - E_0)^2 + \frac{1}{4}\Gamma^2}\left[\Gamma_n^2 - 2\Gamma_n\Gamma \sin^2 \delta_l + 2\Gamma_n(E - E_0)\sin 2\delta_l\right] + 4N\pi\lambda^2(2l + 1)\sin^2 \delta_l. \quad (8.3)$$

In this expression, the first of the four terms on the right is the resonance scattering, i.e., equation (8.1) with $\Gamma_x = \Gamma_n$, and the last is the potential scattering; the two middle terms give the interference between the two types of scattering.

Total Cross Sections

By adding equation (8.3) for the scattering cross section to equation (8.1) for the reaction cross section, the total cross section for neutrons of angular momentum $l\hbar$, in the vicinity of a resonance, is then given by

$$\sigma_{t,l}(E) = \frac{N\pi\lambda^2 g\Gamma_n}{(E - E_0)^2 + \frac{1}{4}\Gamma^2}\left[\Gamma - 2\Gamma \sin^2 \delta_l + 2(E - E_0)\sin 2\delta_l\right] + 4N\pi\lambda^2(2l + 1)\sin^2 \delta_l. \quad (8.4)$$

To a good approximation, δ_l may be computed from a hard-sphere nuclear model[8]; the result is

$$\tan \delta_l = \frac{j_l(R/\lambda)}{n_l(R/\lambda)}, \quad (8.5)$$

where j_l and n_l are the spherical Bessel and Neumann functions,[9] respectively, and R is the nuclear radius, approximately equal to $1.25A^{1/3} \times 10^{-13}$ cm. For $l = 0$ (s-wave) neutrons, equation (8.5) becomes

$$\delta_0 = \frac{R}{\lambda} \quad (8.6)$$

and for $l = 1$ (p-wave) neutrons,

$$\delta_1 = \frac{R}{\lambda} - \tan^{-1}\frac{R}{\lambda}. \quad (8.7)$$

The most important neutron absorption resonances, except possibly for fast reactors, where neutrons of high energy play a significant role (§8.2d), are those for which $l = 0$, so that $\delta_l = \delta_0$ is equal to R/λ. Furthermore, it may be assumed that R/λ is small. For example, for uranium-238, $R = 7.7 \times 10^{-13}$ cm, and

$$\frac{R}{\lambda} = \frac{7.7 \times 10^{-13}}{4.55 \times 10^{-10}}\sqrt{E(\text{eV})}$$

$$= 1.7 \times 10^{-3}\sqrt{E(\text{eV})}.$$

Consequently, R/λ is small for neutron energies less than 10 keV or so. In this event, it is possible to write

$$\sin \delta_0 \approx \delta_0 = \frac{R}{\lambda}.$$

If this value is used in equation (8.3) for the scattering cross section (for s-wave neutrons), it is found that

$$\sigma_{s,0}(E) = \frac{N\pi\lambda^2 g}{(E - E_0) + \frac{1}{4}\Gamma^2}\left[\Gamma_n^2 + 4\Gamma_n(E - E_0)\frac{R}{\lambda}\right] + \sigma_{\text{pot}}, \tag{8.8}$$

where a small interference term has been dropped and the potential scattering cross section for $l = 0$ neutrons, represented by σ_{pot} and given by

$$\sigma_{\text{pot}} = 4N\pi R^2, \tag{8.9}$$

has been introduced.

Attention will now be directed to the quantities in equations (8.1) and (8.8), namely, λ, Γ_n, and Γ, that depend on the neutron energy. Since λ is inversely proportional to the neutron velocity, it follows that the dependence on energy can be written as

$$\lambda = \lambda_0\sqrt{\frac{E_0}{E}},$$

where λ_0 is the value of the reduced wavelength of the neutron at the resonance peak.

According to the theory of nuclear reactions,[10] the resonance width, Γ_x, for a particular type of decay (or the corresponding decay constant) may be represented as the product of a "reduced width" (§8.2b), which is essentially independent of energy within a given resonance, and a "penetration factor," which is a function of the neutron energy. If, in a particular decay process, a neutron of angular momentum $l\hbar$ is emitted, the penetration factor is proportional to $E^{l+(1/2)}$ for the energy range of interest.[11] For the emission of an s-wave ($l = 0$) neutron, for example, the width Γ_n will vary as $\sqrt{E}$. Consequently, the dependence of Γ_n on energy may be represented by

$$\Gamma_n = \Gamma_n(E_0)\sqrt{\frac{E}{E_0}},$$

where $\Gamma_n(E_0)$ is the width of the resonance corresponding to the energy of the peak.

For γ-ray emission or fission, on the other hand, the "penetration factor" does not vary significantly with the neutron energy across the range spanned by the resonance. The reason is that the energy of the compound nucleus which is available for these reactions is always very large in comparison with the variation

of energy across a resonance. Hence, Γ_x may be taken to be independent of the neutron energy, so that

$$\Gamma = \Gamma_n(E_0)\sqrt{\frac{E}{E_0}} + \sum_x \Gamma_x.$$

In most cases, the resonance energy E_0 is large in comparison with the width Γ, and it has been shown[12] that it is then a good approximation to ignore the energy dependence of Γ and to write

$$\Gamma = \Gamma_n(E_0) + \sum_x \Gamma_x,$$

where $\Gamma_n(E_0)$ is as defined above; this approximation will be used in the subsequent treatment, although allowance for the variation of Γ_n with energy will be made when this quantity appears alone.

The peak value of the total resonance cross section, σ_0, i.e., the sum of the resonance absorption and scattering cross sections at E_0, is obtained by setting $E = E_0$ in equations (8.1) and (8.8) and adding; thus,

$$\sigma_0 = 4N\pi\lambda\!\!\!^{-2}_0 g\frac{\Gamma_n(E_0)}{\Gamma}. \tag{8.10}$$

Upon making this substitution, equations (8.1) and (8.8) become

$$\sigma_x(E) = \sigma_0\frac{\Gamma_x}{\Gamma}\sqrt{\frac{E_0}{E}}\frac{\Gamma^2}{4(E-E_0)^2+\Gamma^2} \tag{8.11}$$

and

$$\sigma_{s,0}(E) = \sigma_0\sqrt{\frac{E_0}{E}}\frac{\Gamma^2}{4(E-E_0)^2+\Gamma^2}\left[\frac{\Gamma_n}{\Gamma} + \frac{4(E-E_0)}{\Gamma}\frac{R}{\lambda\!\!\!^{-}}\right] + \sigma_{\text{pot}}. \tag{8.12}$$

The total cross section for $l = 0$ neutrons, i.e.,

$$\sigma_{t,0}(E) = \sigma_{s,0} + \sum_x \sigma_x,$$

is then given by

$$\sigma_{t,0}(E) = \sigma_0\sqrt{\frac{E_0}{E}}\frac{\Gamma^2}{4(E-E_0)^2+\Gamma^2}\left[1 + \frac{4(E-E_0)}{\Gamma}\frac{R}{\lambda\!\!\!^{-}}\right] + \sigma_{\text{pot}}. \tag{8.13}$$

The general nature of the variation of $\sigma_x(E)$ and $\sigma_{s,0}(E)$ in the vicinity of a resonance, in accordance with equations (8.11) and (8.12), is shown in Fig. 8.2. The dip in the scattering cross-section curve at energies just below that of the resonance peak and the general asymmetry of the curve are due to the interference term in the square brackets in equation (8.12). It is seen that this term is negative when $E < E_0$ and positive when $E > E_0$. Consequently, there is a decrease in $\sigma_{s,0}$ to the left of the resonance peak and an increase to the right which together lead to the asymmetry in the curve.

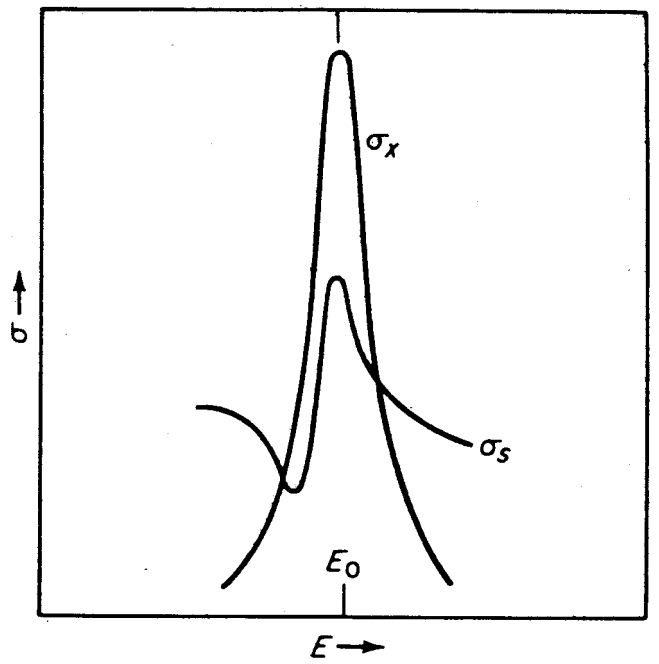

FIG. 8.2 REACTION AND SCATTERING CROSS SECTIONS VS NEUTRON ENERGY IN VICINITY OF A RESONANCE.

Results analogous to the foregoing may be obtained for p-wave ($l = 1$) scattering by using δ_1, given by equation (8.7), in place of δ_0. If $R/\lambda\!\!\!^{-} < 1$, as it is usually, $\tan^{-1} R/\lambda\!\!\!^{-}$ may be expanded in the form

$$\tan^{-1}\frac{R}{\lambda\!\!\!^{-}} = \frac{R}{\lambda\!\!\!^{-}} - \frac{1}{3}\left(\frac{R}{\lambda\!\!\!^{-}}\right)^3 - \frac{1}{5}\left(\frac{R}{\lambda\!\!\!^{-}}\right)^5 - \cdots$$

so that

$$\delta_1 \approx \frac{1}{3}\left(\frac{R}{\lambda\!\!\!^{-}}\right)^3 - \frac{1}{5}\left(\frac{R}{\lambda\!\!\!^{-}}\right)^5 + \cdots.$$

For fast reactors, p-wave resonances are often important, particularly in determining the temperature coefficient of reactivity due to the Doppler effect (§8.5b). The neutron energies making the major contribution to the p-waves in the evaluation of this Doppler coefficient are usually less than (or of the order of) 10 keV.[13] For such energies, for heavy target nuclei, $\delta_0 = R/\lambda\!\!\!^{-} \lesssim 0.17$, as seen above for uranium-238, and $\delta_1 \lesssim 2 \times 10^{-3}$; hence δ_1 is very small compared to δ_0. It follows, therefore, that in the energy region of about 10 keV or less, the effects of interference, which involve δ_1, etc., and of p-wave potential scattering are very small relative to s-wave effects. Consequently, they are frequently neglected. It should be understood that the total cross section for any nuclide will represent the sum of contributions over all l values, but for resonance absorption the contributions only for $l = 0$ and $l = 1$ are important.

So far it has been assumed that the single-level Breit-Wigner formula is

applicable. Situations in which corrections must be made will be considered in due course.

8.1c Experimental Determination of Resonance Parameters

Some brief comments may be made here concerning the experimental determination of the resonance parameters. It can be seen from equation (8.1) that if $E = E_0 \pm \frac{1}{2}\Gamma$, the cross section at this energy would be half the cross section at the peak of the resonance ($E = E_0$). It would appear, therefore, that in the plot of cross section versus neutron energy, the energy span (or width) of the curve at half the height of the peak is equal to the resonance width.

Although use of the term "width" arose in this manner, it is not practical to determine the resonance width by simply plotting the measured cross sections as a function of neutron energy in the resonance region. In the first place, the resonance is broadened by the Doppler effect (§8.1d), whereas the required width, which applies to nuclei at rest, must not include the Doppler broadening. In addition, and perhaps more important, the neutrons used in cross-section determinations are not precisely monoenergetic nor can their energy always be measured exactly. Consequently, except at low energies, e.g., $\lesssim 10$ eV, the detailed shape of a resonance cannot be obtained experimentally. On the other hand, the total area under the resonance, which is independent of the Doppler broadening (§8.1d), is relatively insensitive to the observational errors, and this forms the basis for most determinations of the resonance parameters.

A theoretical expression for the area under a resonance is obtained by integration of equation (8.13) after making two simple approximations. First, $\sqrt{E_0/E}$ is taken to be unity throughout the resonance; this is permissible since, for the nuclides of interest, E_0 is generally greater than 10 eV, whereas the range of E across the resonance is usually of the order of 0.1 eV. For the same reason, $E_0/\Gamma \gg 1$, and setting $-E_0/\Gamma = -\infty$ in the limit of the integral below constitutes the second approximation. It is then found that the interference term integrates to zero, and if x is defined as $2(E - E_0)/\Gamma$,

$$\int_0^\infty [\sigma_{t,0}(E) - \sigma_{pot}]\, dE = \tfrac{1}{2}\sigma_0\Gamma \int_{-\infty}^{\infty} \frac{dx}{1 + x^2} = \tfrac{1}{2}\pi\sigma_0\Gamma.$$

This result, which gives the area under a resonance, for the total minus the potential scattering cross section, is the same regardless of whether there is or is not any Doppler broadening [cf. equation (8.27)].

The area can be determined experimentally, using total cross sections obtained by the transmission method, with the given material for various neutron energies and the potential scattering cross section from equation (8.9) or, better, from the more-or-less constant measured cross sections between resonances. If the result is set equal to $\frac{1}{2}\pi\sigma_0\Gamma$, the quantity $\sigma_0\Gamma$ can be evaluated. According to equation (8.10), this can be simply related to $g\Gamma_n(E_0)$ for s-wave

($l = 0$) neutrons, provided λ_0 is known. The latter requires a knowledge of E_0, the energy of the resonance peak, and this is readily obtained from the energy at which neutron transmission through the material is a minimum. For the fertile nuclides, uranium-238 and thorium-232, g is known to be 1 for s-wave neutrons, since $I = 0$; hence $\Gamma_n(E_0)$ can be derived from the neutron transmission measurements. Thus, the two resonance parameters E_0 and Γ_n can be evaluated.

For the experimental determination by the transmission method of the area under a resonance, it is the usual practice to employ thin samples of material. The ratio of transmitted to incident neutron intensity (or flux), for a sample of thickness d, is ideally equal to $\exp(-\sigma_{t,0}d)$. For a thin sample, $\sigma_{t,0}d \ll 1$, and hence the fraction of incident neutrons transmitted is essentially $1 - \sigma_{t,0}d$. The cross section $\sigma_{t,0}$ can thus be readily determined for neutrons of known energy E.

If a thick sample is employed in a transmission experiment, so that essentially all the incident neutrons with energies near the resonance peak are removed, it is possible to calculate $\sigma_0\Gamma^2$ from the results. To see this, suppose that equation (8.13) for the total cross section in the vicinity of a resonance is simplified by neglecting the interference and potential scattering, i.e.,

$$\sigma_{t,0}(E) = \frac{\sigma_0}{1 + \dfrac{4(E - E_0)^2}{\Gamma^2}},$$

(Essentially the same conclusion is reached by a more involved treatment including the small neglected quantities.) The fraction of neutrons of energy E transmitted through a thick sample, which will be represented by $T(E)$, is then equal to $\exp[-\sigma_{t,0}(E)d]$, where $\sigma_{t,0}(E)$ may be replaced by the expression given above.

If $T(E)$ for a thick sample is measured for monoenergetic neutrons of various energies in the vicinities of a resonance, the results fall on a curve like that in Fig. 8.3. The area, A, of the marked dip, due to almost zero transmission of neutrons with energies near E_0 is then

$$A = \int_0^\infty [1 - T(E)]\,dE = \int_0^\infty \left\{1 - \exp\left[-\frac{\sigma_0 d}{1 + 4(E - E_0)^2/\Gamma^2}\right]\right\} dE.$$

Since $\sigma_0 d \gg 1$ for a thick sample, the exponential becomes significant only when $4(E - E_0)^2/\Gamma^2 \gg 1$; it is then possible to write

$$1 + \frac{4(E - E_0)^2}{\Gamma^2} \approx \frac{4(E - E_0)^2}{\Gamma^2},$$

so that

$$A \approx \int_0^\infty \left\{1 - \exp\left[-\frac{\Gamma^2\sigma_0 d}{4(E - E_0)^2}\right]\right\} dE.$$

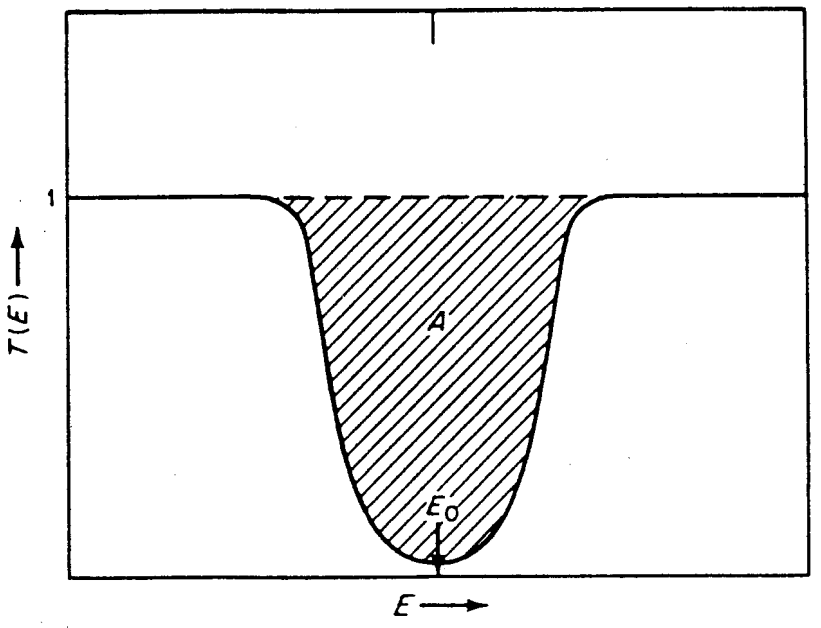

FIG. 8.3 NEUTRON TRANSMISSION OF THICK ABSORBER IN VICINITY OF A RESONANCE.

Upon introducing the variable

$$x \equiv \frac{2(E - E_0)}{\sqrt{\sigma_0 d}\,\Gamma},$$

it is found that

$$A = C\sqrt{\sigma_0 d}\,\Gamma = \sqrt{\pi\sigma_0 d}\,\Gamma,$$

where

$$C = \tfrac{1}{2}\int_{-\infty}^{\infty} (1 - e^{-1/x^2})\,dx = \sqrt{\pi}.$$

The physical reason for this value of A is that the width of the dip in Fig. 8.3 is proportional to $\sqrt{\sigma_0}\,\Gamma$.

The area A can be determined experimentally for a thick absorber of known thickness d, and from this $\sqrt{\sigma_0}\,\Gamma$ (or $\sigma_0\Gamma^2$) can be obtained. Since $\sigma_0\Gamma$ has been derived from transmission measurements with a thin sample, the resonance parameters σ_0 and Γ can be evaluated. Hence, E_0, σ_0, $g\Gamma_n$, and Γ are available from the experiments. For the fertile nuclides, $\Gamma = \Gamma_n + \Gamma_\gamma$, at energies less than 1 MeV, and so Γ_γ can be obtained. Consequently, as indicated earlier, the $\sigma_\gamma(E)$ cross sections in the vicinity of a resonance, as given by equation (8.11) with $x = \gamma$, can be derived from transmission measurements based on the total cross section.

For the fissile nuclei, the total width of the resonance includes the fission width Γ_f and, moreover, g may not be known with certainty. Hence, Γ_f and Γ_γ must generally be determined by separate experiments. The fission and radiative capture cross sections are measured on thin samples by detection of the fission fragments and gamma rays, respectively. The area under a resonance, in the

plot of the appropriate cross section versus neutron energy, is then equal to $\frac{1}{2}\pi\sigma_0\Gamma_f$ for fission and $\frac{1}{2}\pi\sigma_0\Gamma_\gamma$ for radiative capture. Since σ_0 (and Γ) can be derived from transmission measurements with thin and thick samples, as described above, Γ_f and Γ_γ can be evaluated; Γ_n can now be obtained without necessarily knowing g.

The measurement of Γ_γ can often be avoided because it is known to be approximately the same for all resonances of a given nuclide (§8.2b). Hence, if it has been measured for one or a few resonances the same value may be assumed for other resonances. Moreover, in some instances Γ_γ for a given nuclide has been estimated from the values of adjacent nuclides.

8.1d Doppler Broadening

It will be recalled that the expressions for the cross sections derived earlier refer to nuclei at rest in the laboratory system, i.e., with no thermal motion. When the nuclei are in thermal motion, the resonances will be broadened as a result of the Doppler effect. This motion can be taken into account by an extension of the considerations of the preceding chapter. For example, it has been shown[14] that the Doppler broadened cross section for a neutron reaction of type x can be written as

$$\sigma_x(E) = \tfrac{1}{4}\sigma_0\Gamma\Gamma_x \int_{-\infty}^{\infty} \frac{S(\mathbf{p}, \epsilon)\, d\epsilon}{[(E - E_0) - \epsilon]^2 + \frac{1}{4}\Gamma^2}, \tag{8.14}$$

where σ_0, Γ, and Γ_x have the same significance as in the preceding section, $\mathbf{p}$ is the neutron momentum vector, i.e., $p = \sqrt{2mE}$, and $S(\mathbf{p}, \epsilon)$ is the function defined in equation (7.36) with the neutron momentum, $\mathbf{p}$, rather than the momentum change, $\hbar\boldsymbol{\varkappa}$. Thus, any of the models developed in Chapter 7 could be used to compute $S(\mathbf{p}, \epsilon)$, and hence $\sigma_x(E)$, as a function of temperature.

A simpler approach is based on the finding that,[15] provided the temperature of the medium containing the absorbing nuclei is not "too low," it is a good approximation to assume a Maxwell distribution of the nuclear velocities at (or slightly above) the temperature of the medium. In particular, if the temperature exceeds the Debye temperature, θ_D,* the approximation is a good one. At such temperatures, all the vibrational modes of a solid are excited with appreciable probability; the velocity distribution of the atoms (or nuclei) is then insensitive to the details of the binding. Hence, a Maxwellian distribution may be assumed.

For metallic uranium and thorium, the Debye temperatures are less than 200°K,[16] and so the approximation referred to above may be used at room (and higher) temperatures. For materials with higher Debye temperatures, such as U_3O_8 with $\theta_D = 500$°K, however, a better procedure at room temperature is to

* The Debye temperature is equal to $h\nu_{max}/k$, where ν_{max} is the maximum vibration frequency of the atoms in a solid and h and k are the Planck and Boltzmann constants, respectively.

take the temperature of the Maxwellian distribution to be such that the average kinetic energy is the same as for the actual solid.[17]

The shape of the Doppler broadened resonance will now be derived based on the assumption that the nuclear velocity distribution can be approximated by a Maxwellian spectrum.[18] In equations (8.11), (8.12), and (8.13), which are valid for nuclei at rest, E represents the neutron energy in the laboratory system. It is convenient to write

$$E = \tfrac{1}{2}mv_r^2,$$

where v_r, the relative neutron-nucleus speed, is equal to v, the actual neutron speed, for nuclei at rest. Consider a neutron having a definite velocity $\mathbf{v}$ in the laboratory system but suppose the nuclei are moving with velocity $\mathbf{V}$ in the same system; the relative velocity is then

$$\mathbf{v}_r = \mathbf{v} - \mathbf{V},$$

and the neutron-nucleus interactions will take place with a cross section $\sigma(E_r)$, where

$$E_r = \tfrac{1}{2}mv_r^2.$$

If $P(\mathbf{V})\,d\mathbf{V}$ is the probability that a nucleus has a velocity within $d\mathbf{V}$ about $\mathbf{V}$, the probability of reactions of type x with such nuclei is

$$\text{Probability of reaction } x \text{ per sec} = v_r\sigma_x(E_r)P(\mathbf{V})\,d\mathbf{V}. \tag{8.15}$$

Hence, the total probability of a reaction per second is found by integrating over all nuclear velocities, and the macroscopic cross section is obtained upon dividing by v; the result is

$$\sigma_x(E) = \frac{1}{v}\int v_r\sigma_x(E_r)P(\mathbf{V})\,d\mathbf{V}. \tag{8.16}$$

This derivation is the same as that used in obtaining equation (7.22), except that it has been generalized in order to allow for the energy dependence of the cross sections in the integrand.

In the present situation, the evaluation of the integral in equation (8.16) may be simplified by taking advantage of the fact that the neutron velocity is large compared with the nuclear velocities. The procedure is as follows. A coordinate system is chosen such that the z axis is in the direction of the neutron velocity; then

$$E_r = \tfrac{1}{2}m(\mathbf{v} - \mathbf{V})^2 = \tfrac{1}{2}m[(v - V_z)^2 + V_x^2 + V_y^2], \tag{8.17}$$

where V_x, V_y, and V_z are the components of $\mathbf{V}$. The neutron speed is given by

$$v = \sqrt{\frac{2E}{m}}$$

and the most probable nuclear speed in a Maxwell distribution is

$$V_{m.p.} = \sqrt{\frac{2kT}{M}},$$

where M is the nuclear mass; hence,

$$\frac{v}{V_{\text{m.p.}}} = \sqrt{\frac{EM}{kTm}}.$$

This ratio is generally large for neutrons with energies in the resonance region. For example, consider a 10-eV neutron, i.e., $E = 10$ eV, and a temperature, T, of 1200°K, so that $kT = 0.1$ eV; for a nucleus of $M = 238$, $v/V_{\text{m.p.}}$ is $> 10^2$. Hence, the terms V_x^2, V_y^2, and V_z^2 in equation (8.17) may be neglected,[19] with the result that

$$E_r \approx \tfrac{1}{2}m(v^2 - 2vV_z). \tag{8.18}$$

Furthermore

$$v_r = \sqrt{\frac{2E_r}{m}}. \tag{8.19}$$

In accordance with equation (7.23), the Maxwellian velocity distribution may be written as

$$P(\mathbf{V})\,d\mathbf{V} = \left(\frac{M}{2\pi kT}\right)^{3/2} e^{-MV^2/2kT}\,dV_x\,dV_y\,dV_z, \tag{8.20}$$

where the normalization

$$\int P(\mathbf{V})\,d\mathbf{V} = 1$$

is appropriate for a probability distribution. It is then found that

$$\int_{-\infty}^{\infty}\int_{-\infty}^{\infty} P(\mathbf{V})\,dV_x\,dV_y = \left(\frac{M}{2\pi kT}\right)^{1/2} e^{-MV_z^2/2kT}, \tag{8.21}$$

which is just the distribution for one velocity component. By using equations (8.11), (8.18), (8.19), and (8.21) in connection with equation (8.16), the latter gives $\sigma_x(E)$ as a function of temperature; thus,

$$\sigma_x(E) = \sigma_0 \frac{\Gamma_x}{\Gamma}\sqrt{\frac{E_0}{E}\left(\frac{M}{2\pi kT}\right)}\int_{-\infty}^{\infty} e^{-MV_z^2/2kT}\,\frac{\Gamma^2}{4(E_r - E_0)^2 + \Gamma^2}\,dV_z. \tag{8.22}$$

The form of the integral in equation (8.22) may be simplified by defining the following quantities:

$$X \equiv \frac{2}{\Gamma}(E_r - E_0)$$

$$Y \equiv \frac{2}{\Gamma}(E - E_0)$$

$$\Delta \equiv \sqrt{\frac{4kTE}{A}} \approx \sqrt{\frac{4kTE_0}{A}}$$

and

$$\zeta \equiv \frac{\Gamma}{\Delta},$$

where A is the ratio of the masses of the nucleus and a neutron. By making the substitutions in equation (8.22), the latter takes the form

$$\sigma_x(E) = \sigma_0 \frac{\Gamma_x}{\Gamma} \sqrt{\frac{E_0}{E}}\, \Psi(\zeta, Y), \tag{8.23}$$

where $\Psi(\zeta, Y)$ is a function defined by

$$\Psi(\zeta, Y) \equiv \frac{\zeta}{2\sqrt{\pi}} \int_{-\infty}^{\infty} \frac{\exp\left[-\frac{1}{4}\zeta^2(X - Y)^2\right]}{1 + X^2}\, dX. \tag{8.24}$$

This Doppler function has been studied extensively and tabulated values have been published[20]; several computer programs are also available for rapid determination of $\Psi(\zeta, Y)$.[21] The quantity Δ, called the *Doppler width*, is a measure of the width of the resonance due to thermal motion; it should be noted that Δ, and hence ζ, contains the effect of temperature on the shape of the resonance. Although a number of approximations have been made in deriving equation (8.23), it is sufficiently accurate for most practical applications.[22]

The behavior of $\Psi(\zeta, Y)$ and $\sigma_x(E)$ in the limiting situations of ζ large and ζ small is of interest. At very low temperatures, the Doppler broadening is small so that ζ is large; in these circumstances, the integral in equation (8.24) is very small except when $X \simeq Y$. Upon setting $X = Y$ in the denominator, it is found that

$$\Psi(\zeta, Y) \simeq \frac{1}{1 + Y^2} \quad \text{for large } \zeta. \tag{8.25}$$

If this is inserted into equation (8.23), the result obtained is identical with equation (8.11) for the unbroadened resonance.

For very high temperatures, i.e., extreme Doppler broadening, ζ is very small; the integral in equation (8.24) may then be approximated by the product of the integral of $dX/(1 + X^2)$ and the value of the exponential for $X = 0$. It is thus found that

$$\Psi(\zeta, Y) \simeq \frac{\sqrt{\pi}}{2}\, \zeta \exp\left(-\tfrac{1}{4}\zeta^2 Y^2\right) \quad \text{for small } \zeta,$$

and equation (8.23) becomes

$$\sigma_x(E) = \sigma_0 \frac{\Gamma_x}{\Delta} \sqrt{\frac{E_0}{E}} \frac{\sqrt{\pi}}{2} \exp\left[-\left(\frac{E - E_0}{\Delta}\right)^2\right]. \tag{8.26}$$

This expression, which is valid near the resonance peak for sufficiently high temperature, i.e., ζ small and $Y \ll \zeta^{-2}$, represents a Gaussian distribution curve with a maximum at $E = E_0$ and a width ($\sqrt{2}$ × the standard deviation) of Δ; this

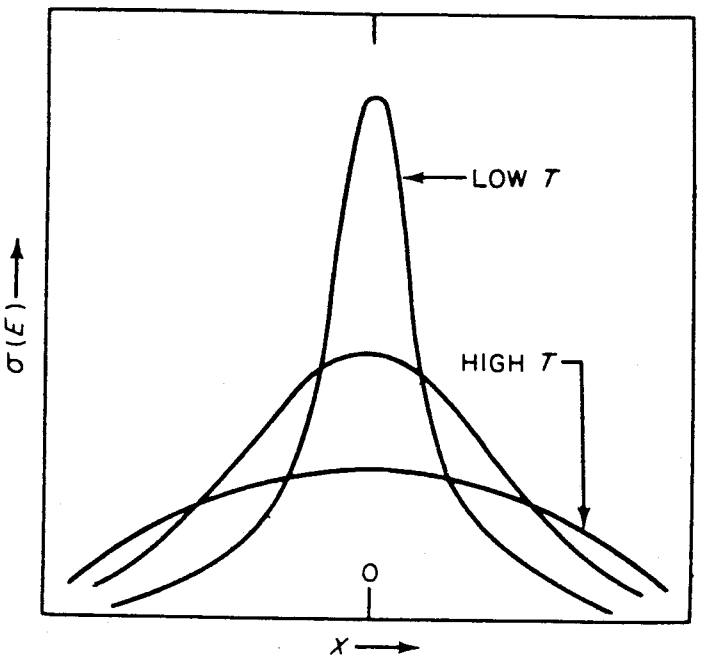

FIG. 8.4 DOPPLER BROADENING OF A RESONANCE WITH INCREASING TEMPERATURE.

is why Δ has been called the Doppler width. Furthermore, for large values of Y, when $Y \gg \zeta^{-2}$, i.e., far out in the wings of the resonance, there exists an asymptotic expansion[23]

$$\Psi \approx \frac{1}{1 + Y^2}\left[1 + \frac{2}{\zeta^2}\frac{3Y^2 - 1}{(1 + Y^2)^2} + \cdots\right]$$

so that the cross-section curve recovers its natural shape far away from the resonance peak.

Although the shape of a resonance is changed markedly by Doppler broadening, as may be seen from the typical curves in Fig. 8.4 derived from equation (8.23), it is found that the area under the curve does not change significantly. That is to say, it can be shown that the integral of $\sigma_x(E)\,dE$ over all energies is approximately constant. For the reason given in §8.1c, $\sqrt{E_0/E}$ can be set equal to unity within a resonance, and so equation (8.23) can be written as

$$\int \sigma_x(E)\,dE = \sigma_0 \frac{\Gamma_x}{\Gamma}\int_0^\infty \Psi(\zeta, Y)\,dE$$

$$= \tfrac{1}{2}\sigma_0\Gamma_x\int_{-\infty}^{\infty}\Psi(\zeta, Y)\,dY.$$

By using the definition of $\Psi(\zeta, Y)$ in equation (8.24), and integrating over Y and X, in that order, it is found that

$$\int_{-\infty}^{\infty}\Psi(\zeta, Y)\,dY = \pi,$$

and consequently, the area under the resonance, i.e.,

$$\int \sigma_x(E)\, dE = \tfrac{1}{2}\pi\sigma_0\Gamma_x, \tag{8.27}$$

is independent of temperature. By using more accurate expressions for the Doppler broadening (see Exercises 1 and 2), it can be shown that the relative change in the area is proportional to kT/AE_0, when the latter is small. In stars and nuclear explosions these changes may be significant,[24] but in reactors they are usually negligible.

Hence, in spite of Doppler broadening of the resonance by an increase in temperature, the area remains essentially unchanged. Nevertheless, the broadening has an effect on reactivity because neutron reaction rates (and group cross sections) involve the products of cross sections and neutron flux. As a result of the less marked dips in the flux in a resonance, Doppler broadening increases neutron absorption (§8.3e).

Expressions for the Doppler broadened scattering cross sections may be derived in a manner analogous to that given above for reaction cross sections. In equation (8.16) the expression for $\sigma_{s,0}$ from equation (8.12) is substituted, instead of σ_x, and the same manipulations are performed as before. If $\sqrt{E_0/E}$ is set equal to unity as in the foregoing treatment, the result is

$$\sigma_{s,0}(E) = \sigma_0 \frac{\Gamma_n}{\Gamma} \Psi(\zeta, Y) + \sigma_0 \frac{R}{\lambda} \chi(\zeta, Y) + \sigma_{pot}, \tag{8.28}$$

where the Doppler function $\chi(\zeta, Y)$ is defined by

$$\chi(\zeta, Y) \equiv \frac{\zeta}{\sqrt{\pi}} \int_{-\infty}^{\infty} \frac{X \exp\left[-\tfrac{1}{4}\zeta^2(X - Y)^2\right]}{1 + X^2}\, dX. \tag{8.29}$$

Tabulations and computer programs for obtaining $\chi(\zeta, Y)$ are also available.[25] In tracing back the second term on the right of equation (8.28), it will be seen that it arises from interference between resonance and potential scattering. The function $\chi(\zeta, Y)$ may thus be regarded as representing the extent of this interference.

8.1e Overlap and Interference of Resonances

The Doppler broadened cross sections have been derived above for an isolated (single-level) Breit-Wigner resonance. In computing the neutron absorption in the resonance region, it is sometimes possible to sum the absorptions in a series of levels, each being treated as more or less independent of the others. There are certain circumstances, however, in which it is not adequate to take the resonances one at a time.

The absorption in one resonance will obviously perturb the neutron flux in resonances of lower energy; this matter, which is not of great practical importance, is best treated numerically and it will be discussed briefly in §8.3h.

For the present, three situations will be considered; they are (*a*) accidental overlap of adjacent resonances due to their proximity, (*b*) overlap due to Doppler broadening, and (*c*) level interference, i.e., failure of the Breit-Wigner single-level formula. These effects will be examined in turn.

In computing resonance absorption, account should, of course, be taken of all the materials present in the system. It may then happen that a few of the resonances of different nuclides, e.g., uranium-235 and uranium-238, occur at energies that are very close to one another. In addition, it is possible for adjacent resonances for a single nuclide to differ so little in energy that there is significant overlap. This can arise because the sequences of resonances with different quantum numbers (J and parity) are independent; consequently, resonances in different sequences may overlap.*

In studying the energy dependence of the neutron flux in the resonances, the absorption in the combination of overlapping resonances should then be considered, rather than in one resonance at a time. In practice, however, the effects of accidental overlap on reactivity and its temperature coefficient are generally small[26]; there are nevertheless a few cases, e.g., the energy region around 20 eV for tungsten, where they are significant.[27]

The effect of overlap due to Doppler broadening is more important than the one just considered. According to the definition given above, the Doppler width, Δ, increases with the temperature, T, and the neutron energy, E_0, at the resonance peak. For sufficiently high temperature and resonance energy, the Doppler width will become comparable with the spacing between resonances having the same quantum members (§8.3i). Adjacent resonances in the same sequence will then overlap at high temperatures or high neutron energies (or both).

In uranium-235, for example, the average spacing of s-wave resonances is about 1 eV. At a temperature of about 700° K, i.e., $kT = 0.06$ eV, and $E_0 =$ 1 keV, the value of Δ is approximately 1 eV; for $E_0 = 10$ keV, at the same temperature, Δ is roughly 3 eV. Consequently, at a neutron energy in the vicinity of 1 keV (or more) the s-wave resonances of uranium-235 will exhibit strong overlap as a result of Doppler broadening.

For uranium-238 the average spacing of s-wave resonances is about 20 eV (see Table 8.1), but the Doppler widths are similar to those for uranium-235. Hence, for uranium-238, overlap of s-wave resonances will not be significant until the neutron energy is more than 100 keV. It should be noted, however, that p-wave resonances are important for uranium-238. The spacing between successive resonances of this type is about a third that of s-wave resonances[28]; thus, overlap between adjacent p-wave resonances becomes effective at lower energies. At around 40 keV the spacing is about equal to the Doppler width.

A theory of strongly overlapping resonances is given in §8.3i. For fast reactors, overlap of an intermediate character is also important and special treatment is required.[29]

* The spacing of resonances in one sequence is discussed in §8.2c.

Finally, there is the difficult problem arising from the failure of the single-level Breit-Wigner formula.[30] This occurs when the normal spacing between resonances in the same sequence is not large compared with the level widths, Γ. In these circumstances, the adjacent resonances do not contribute independently but interfere with one another. Unfortunately, such interference effects occur in the fission cross sections of the fissile nuclides, uranium-233 and -235 and plutonium-239 and -241.[31] Interference effects of this kind are much less important, however, for the (n, γ) cross sections of the fissile nuclides and for the fertile nuclides, thorium-232 and uranium-238.[32] When there is interference of adjacent resonances, even at moderate temperatures and low neutron energies, a number of difficulties are encountered. In particular, it is presently not possible to derive from the measured cross sections of the fissile nuclides a unique set of physically significant resonance parameters which could be extrapolated to the region of unresolved resonances (§8.2b).[33]

For the energy region where the resonances in the fissile nuclei have been resolved experimentally, namely, for neutron energies below about 50 eV, there are various practical ways of solving this problem. Thus, it is possible to fit the cross sections, to a reasonable extent, by a sum of single-level Breit-Wigner resonances; regardless of whether these resonances represent states of the compound nucleus or not, they can be used as a basis for Doppler broadening calculations.

A more satisfactory approach, however, is based on the observation that, even when interference effects are important, the cross sections can be expressed as a sum of asymmetric quasiresonances.[34] Thus, the (unbroadened) reaction and total cross sections for *nuclei at rest* can be represented by

$$\sigma_x(E) = \frac{C}{\sqrt{E}} \sum_i \frac{\frac{1}{2}\Gamma_i G_{ix} + (E_i - E)H_{ix}}{(E - E_i)^2 + \frac{1}{4}\Gamma_i^2} \tag{8.30}$$

$$\sigma_t(E) = \frac{C}{\sqrt{E}} \sum_i \frac{\frac{1}{2}\Gamma_i G_{it} + (E_i - E)H_{it}}{(E - E_i)^2 + \frac{1}{4}\Gamma_i^2} + \sigma_{pot} \tag{8.31}$$

and the scattering cross sections are given by the difference

$$\sigma_s(E) = \sigma_t - \sum_x \sigma_x.$$

In these expressions, C is a constant, E_i is the energy of the ith quasiresonance and Γ_i is its width; G_{ix}, G_{it}, H_{ix}, and H_{it} are energy-independent parameters chosen to fit the experimental data.

Other methods have been proposed for fitting the experimental cross sections,[35] but the procedure described above has the advantage that the Doppler broadening can be obtained by using the functions $\Psi(\zeta, Y)$ and $\chi(\zeta, Y)$ of the

preceding section. With a Doppler broadening due to a Maxwellian distribution of velocities, for example, it is found that

$$\sigma_x(E) = \frac{C}{\sqrt{E}} \sum_i \frac{1}{\Gamma_i} [2G_{ix}\Psi(\zeta_i, Y_i) - H_{ix}\chi(\zeta_i, Y_i)]. \tag{8.32}$$

Some effects of these interference phenomena and the associated uncertainties will be considered in §8.3i.

8.1f Resonance Absorption at Low Energies

Several nuclides which are important in the operation of a reactor have prominent resonances at relatively low energies, i.e., below about 1 eV. Examples are the fissile species plutonium-239 and -241,* the fertile nuclide plutonium-240, and the fission products rhodium-103, xenon-135, and samarium-149. The variation of the cross sections of some of these nuclides with energy at low neutron

* Uranium-235 has a resonance at an energy of 0.28 eV, but it is a weak one.

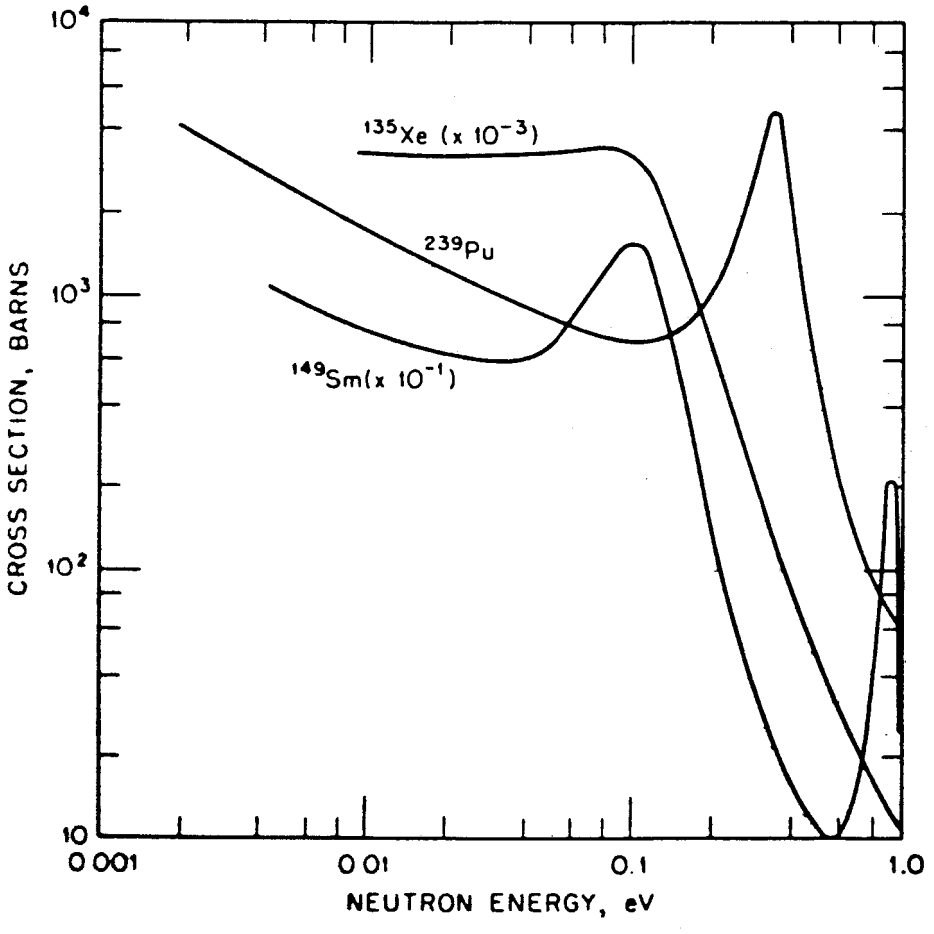

FIG. 8.5 EXAMPLES OF RESONANCES AT NEUTRON ENERGIES BELOW 1 eV (ADAPTED FROM BNL-325).

energies are shown in Fig. 8.5. For such well-resolved, low-energy resonances, the resonance parameters are known.

In thermal reactors containing appreciable amounts of the aforementioned species, i.e., in amounts sufficient to perturb the thermal flux, the low-energy resonances should be taken into account explicitly. In particular, when calculating the thermal neutron spectrum using a thermalization model and a multigroup representation of this spectrum, as described in Chapter 7, the detailed resonance absorption cross sections should be included. As a result of the low-energy resonances, the relative reaction rates for fission and absorption will depend on the reactor (moderator) temperature. Hence these resonances will influence the temperature dependence of the reactivity.

8.2 THE UNRESOLVED RESONANCE PARAMETERS

8.2a Introduction

It has been seen that experimentally derived resonance parameters, i.e., E_0, Γ_n, and Γ_x, are available for characterizing measured cross sections for sufficiently low energies, e.g., less than about 4 keV for fertile nuclides and less than some 50 eV for fissile species. At higher energies, i.e., in the region of unresolved resonances, experimental resonance parameters are not available. It is then necessary to use theoretical considerations to infer the probable resonance structure underlying the measured cross sections as a function of neutron energy. This is particularly important for fast reactors since many of the neutrons have energies in the region of unresolved resonances.

To some extent the procedure used amounts to extrapolating to higher energies the parameters of the resolved resonances measured at the lower energies. Moreover, the theory is sometimes useful for determining resonance parameters, especially Γ_γ, which are difficult to measure at low energies. The treatment is based on a study of the systematic variations of resonance parameters, especially their dependence on the neutron energy. This involves two aspects: first, the expected distribution about their average values of the resonance parameters, in particular the widths Γ_n and Γ_x and the energy separation between adjacent resonances, and second, the dependence of the average values on neutron energy and properties of the reacting nucleus, such as spin and parity.

With the foregoing information available, it is possible to construct a hypothetical sequence of resonances having the required properties. This sequence may then be used to represent a region of unresolved resonances in calculations of the Doppler effect on reactivity, and so on.[36] In many cases, as will be seen in §8.2d, such an explicit sequence is not required and a knowledge of the average resonance parameters and their distribution with energy is sufficient.

It should be noted at the outset that there is no quantitative theory which can be relied upon to predict the variations in the resonance parameters. Neverthe-

less, the combination of qualitative theoretical considerations with measurements at low neutron energies permits useful estimates to be made. In the next section, attention will be directed to the distributions of resonance widths about their average values.

8.2b Decay Channels and Level Width Distribution

It was mentioned earlier that the resonances under consideration correspond to especially favorable energies (and spin and parity) for the neutron and target nucleus to form a particular quantum state of a compound nucleus. This state is formed with several million electron volts of excitation energy, made up of the binding energy of the neutron in the compound nucleus and of the kinetic energy in the center-of-mass system. The state may decay, i.e., lose its excitation energy, in various ways, including always neutron reemission and gamma-ray emission and sometimes fission. An energy level diagram depicting these possibilities is shown in Fig. 8.6, where the zero of energy is taken to be that of the target nucleus plus the unbound neutron at rest.

Each particular mode of deexcitation is called a *decay channel.* Thus, in Fig. 8.6, neutron reemission is one channel, the emission of a gamma ray γ_1 (of a particular energy) is a second channel, of γ_2 (of another energy) is a third channel, and so on. The point that is being brought out is that there is only one

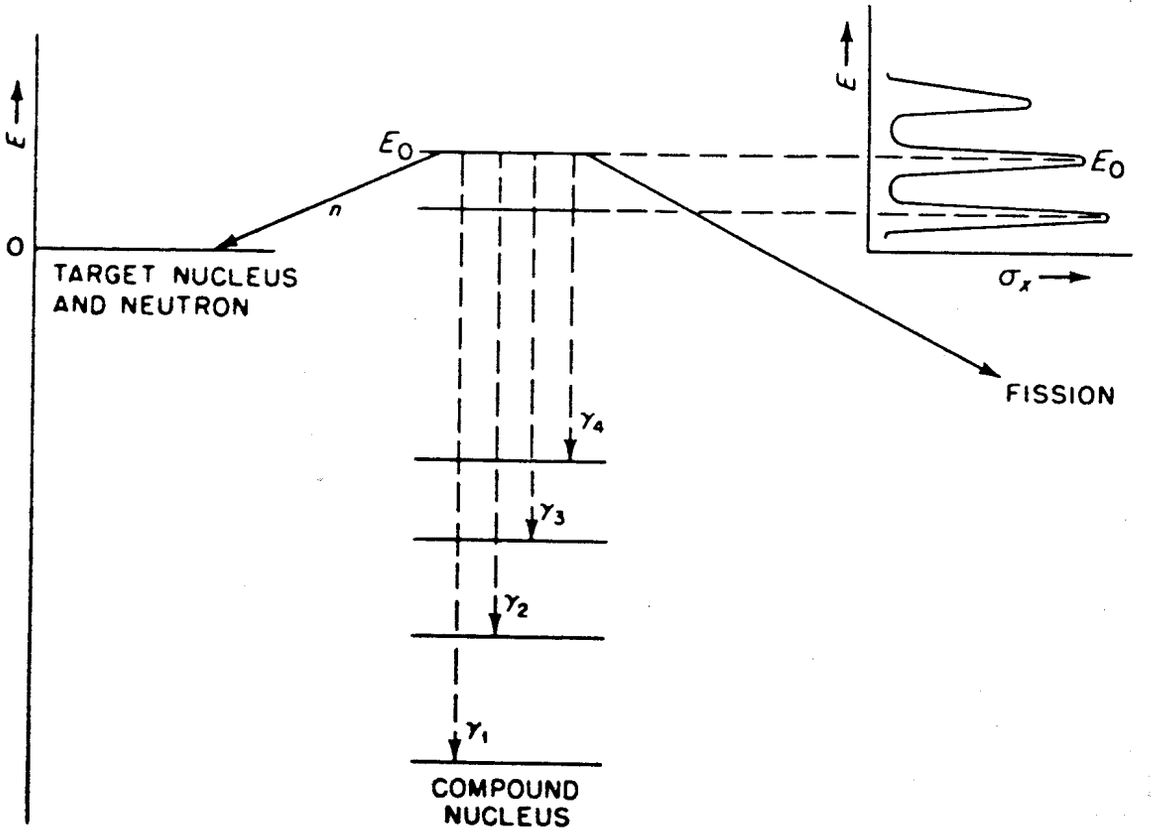

FIG. 8.6 ENERGY-LEVEL DIAGRAM INDICATING DECAY CHANNELS FOR A COMPOUND NUCLEUS OF ENERGY E_0 AND OCCURRENCE OF RESONANCES.

channel for neutron reemission but several channels for gamma-ray emission. According to current views, there are a few (typically two or three) channels available (or open) for fission.[37]

If the number of open channels for a given kind of decay is known, it is possible to estimate how the corresponding resonance width Γ_x varies for a set of equivalent resonances. By using the arguments of the theory of nuclear reactions, it has been shown[38] that if n equally probable channels are available for a given type, x, of decay of the compound nucleus, e.g., gamma-ray emission, then the corresponding reduced partial width,* represented by Γ_x^0, will have a "chi-square" probability distribution with n degrees of freedom.

This means that if x is defined by

$$x \equiv \frac{\Gamma_x^0}{\bar{\Gamma}_x^0},$$

where $\bar{\Gamma}_x^0$ is the average value of Γ_x^0 over all the resonances for states with the same spin and parity, the probability $P_n(x)\,dx$ that x will lie between x and $x + dx$ is given by

$$P_n(x)\,dx = \frac{n}{2\Gamma(\frac{1}{2}n)}\left(\frac{nx}{2}\right)^{(1/2)n-1}\exp\left(-\frac{nx}{2}\right)dx, \tag{8.33}$$

where $\Gamma(\frac{1}{2}n)$ in the denominator of the first factor on the right side represents a gamma function. It can be shown that

$$\int_0^\infty P_n(x)\,dx = \int_0^\infty xP_n(x)\,dx = 1$$

and that

$$\int_0^\infty (x - \bar{x})^2 P_n(x)\,dx = \int_0^\infty (x - 1)^2 P_n(x)\,dx = \frac{2}{n}. \tag{8.34}$$

It follows from equation (8.34) that the deviation from the mean of a chi-square distribution decreases with increasing n. Some of these distributions are indicated in Fig. 8.7.[39]

The applicability of the foregoing conclusions to experimental resonance widths has been amply confirmed.[40] Consider, first, neutron reemission at energies low enough for inelastic scattering and $l > 0$ channels to be ignored. Then only one channel, reemission of a neutron with $l = 0$, is open. It was noted in §8.1b that, for this case, the neutron width is equal to the product of a reduced width and a penetration factor proportional to $\sqrt{E}$. This led to the conclusion that Γ_n varies as $\sqrt{E}$ over a single resonance. The same penetration factor applies to all the $l = 0$ neutron widths; hence, the reduced neutron width, Γ_n^0, the distribution of which is under consideration, is obtained by dividing the

* The relationship of the reduced width, which was referred to in §8.1b, to the actual (or measured) resonance width is discussed in subsequent paragraphs.

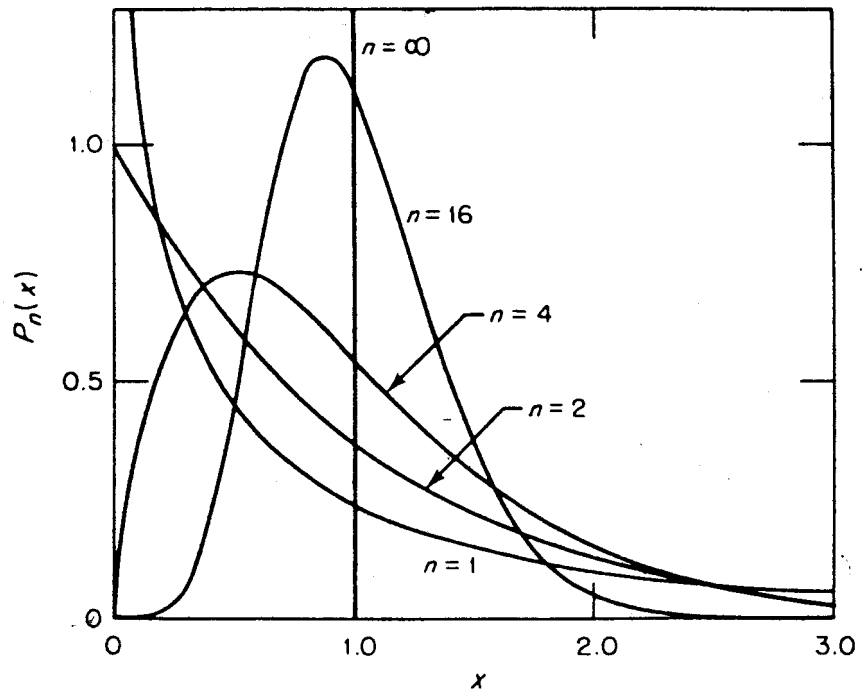

FIG. 8.7 CHI-SQUARE DISTRIBUTIONS (AFTER C. E. PORTER AND R. G. THOMAS, REF. 38).

experimental width Γ_n by $\sqrt{E}$. In general, for the ith resonance, $\Gamma^0_{ni} = \Gamma_n/\sqrt{E_i}$, where Γ_n and E_i are usually expressed in electron volts.

The data on reduced neutron widths are quite consistent with $\Gamma^0_{ni}/\bar{\Gamma}^0_n$ satisfying the chi-square distribution for one degree of freedom, i.e., equation (8.33) with $n = 1$; thus,

$$P_1(x)\,dx = \frac{1}{2\sqrt{\pi}}\sqrt{\frac{2}{x}}\,e^{-x/2}\,dx. \tag{8.35}$$

This is often called the Porter-Thomas distribution.[41] In a region of unresolved resonances, neutron widths are generally assumed to have the same probability distribution. To determine this distribution, all that need be known is the average width, Γ_n, for the resonances in the unresolved region. When values of l higher than $l = 0$ are present, however, there are some instances where the use of $n = 2$ in equation (8.33) is appropriate.[42]

For radiative capture reactions, i.e., deexcitation of the compound nucleus by gamma-ray emission, many channels are open and a large number are more or less equally probable, as may be judged from the complexity of the spectra of the gamma rays accompanying radiative capture of neutrons by heavy nuclei. Moreover, the penetration factors for radiative capture (and also for fission), unlike those for neutron reemission, vary only slowly with neutron energy; they may, therefore, be taken to be constant over the energy range of a few kilo-electron volts. The reason is that the quantity analogous to a penetration factor is given by the total gamma-ray energy raised to some integral power; since this

energy is in the vicinity of one or more million electron volts, a variation of a few kilo-electron volts in the neutron energy has no significant effect.[43] The experimental widths for radiative capture, Γ_γ, may thus be used in place of the reduced widths for the present purpose.

In view of the existence of many channels which are more or less equally probable, it is to be expected, therefore, that the Γ_γ distribution will lie within a narrow range; that is to say, the value of n in equation (8.33) will be very large. Since it is difficult to detect experimentally any significant variations of Γ_γ among resonances for a given nuclide, it is generally assumed that Γ_γ is constant, i.e., it is the same for all resonances of the nuclide. This (see Fig. 8.7) corresponds to setting n equal to infinity in equation (8.33). From measurements of Γ_γ for 62 resonances of uranium-238, the distribution was found to be consistent with $n = 44 \pm 8$.[44]

Fission of the common fissile nuclides by neutrons of low energy is believed to involve only a few decay channels. In the curve in Fig. 8.8 representing the potential energy of the compound nucleus versus the deformation in the fission process, the few (three) channels corresponding to definite states of the compound nucleus are shown at the potential energy maximum. These are states of the compound nucleus with definite quantum numbers through which fission can take place.[45] It is to be expected, therefore, that $\Gamma_f/\bar{\Gamma}_f$ would be distributed in accordance with equation (8.33) with $n \simeq 2$ or 3. For comparison with experiment, actual widths, rather than reduced widths, may be used because the

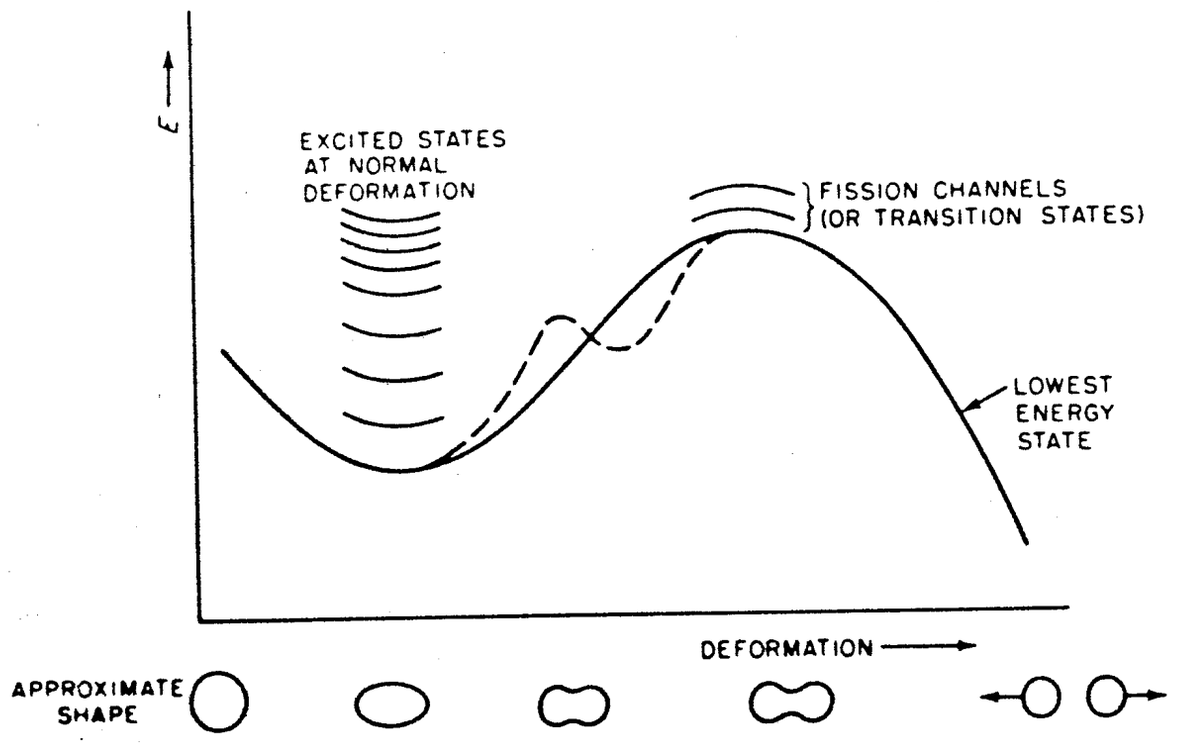

FIG. 8.8 SCHEMATIC POTENTIAL ENERGY DIAGRAM (AND NUCLEAR SHAPES) FOR FISSION.

penetration factors do not vary much in the relatively narrow energy range in which the resolved resonances occur.

To some extent, this expectation has been confirmed experimentally,[46] but there are some reservations. First, the various fission channels are not equally likely, i.e., they are not open to the same extent, and second, it is difficult to be sure that the values of Γ_f derived from the experiments are meaningful because of the overlap effects of adjacent resonances mentioned earlier. Consequently, although the fission widths are qualitatively in agreement with the treatment based on the chi-square distribution, it is difficult to draw precise conclusions from the results. Various procedures have, therefore, been tried for predicting fission widths in the unresolved region. Generally, a chi-square distribution with $n \simeq 2$ is employed, but it is also possible to generate hypothetical fission cross sections which include a reasonable allowance for overlap effects.[47]

It is of interest to mention that a double-humped fission barrier, such as that shown by the dashed curve in Fig. 8.8, has been indicated both by experiment[48] and theory.[49] This may be responsible for a periodic modulation of average fission cross sections, with periods of the order of a few kilo-electron volts.[50] It is not yet known, however, if such effects are of any significance for reactor physics.

8.2c Resonance Peak (or Level) Spacings

It has been found that adjacent resonances for states with the same spin and parity tend to be fairly well separated in energy. The suggestion was made[51] that the spacing D between adjacent resonance peaks (or energy levels in the compound nucleus) could be represented by

$$P(z)\,dz = \frac{\pi}{2}\exp\left(-\tfrac{1}{4}\pi z^2\right)z\,dz \tag{8.36}$$

with

$$z \equiv \frac{D}{\bar{D}},$$

where $\bar{D}$ is the average spacing in the sequence. It is evident that

$$\int_0^\infty P(z)\,dz = \int_0^\infty zP(z)\,dz = 1.$$

Further theoretical analysis has confirmed the reasonable nature of this distribution and it has been found to be in agreement with experiment.[52] It will be noted that equation (8.36) predicts only a few levels with very small spacings, because for small z the distribution varies as $z\,dz$.

For making calculations, the distributions given by equation (8.33) are somewhat easier to work with than those from equation (8.36). Consequently, $D/\bar{D}$ is sometimes assumed to be distributed in accordance with equation (8.33) with $n = 8$ or 10, and the results are quite similar to those given by equation (8.36).

As already mentioned, the spacings under consideration apply to adjacent levels in a given sequence. Levels of the compound nucleus with different quantum numbers or levels of different nuclei are independent of one another. Hence there is no correlation between the energy values of such resonances.

The probability $P(z)$ in equation (8.36) is defined in terms of the spacing between adjacent but distinct levels (or resonance peaks). For situations involving overlapping resonances, the probability is also of interest that there is a level within the distance (in energy) $z\bar{D}$ of a given level without regard to the number of intervening levels. Let $\Omega(z)\,dz$ be the probability that a level lies in the energy range between $z\bar{D}$ and $(z + dz)\bar{D}$ of the given level in the same sequence. This function is probably very complicated, but if it is assumed that the correlation between level positions in general is due only to the correlation of adjacent levels,[53] then $\Omega(z)$ may be derived in terms of $P(z)$.

The probability, $\Omega(z)$ satisfies the integral equation

$$\Omega(z) = P(z) + \int_0^z P(z - z')\Omega(z')\,dz', \tag{8.37}$$

as may be seen in the following manner. Either the level in dz is adjacent to the given level (at $z = 0$) or there is another level at z' ($0 \leqslant z' \leqslant z$) which is adjacent to the level at z. The probability of adjacent levels separated by z is $P(z)$, the first term in equation (8.37). The probability of another level at z' is $\Omega(z')$, so that the second term in the equation is the sum of probabilities that there is a level at z' with an adjacent level at z. Thus, the sum of the two terms gives the probability of there being a level between $z\bar{D}$ and $(z + dz)\bar{D}$.

Equation (8.37) may be solved for $\Omega(z)$ either approximately or exactly for some choices of $P(z)$.[54] For example, if $P(z)$ is obtained from equation (8.33) with $n = 8$, it is found that

$$\Omega(z) = 1 - 2(\sin 4z)e^{-4z} - e^{-8z}. \tag{8.38}$$

It follows from equation (8.38) that $\Omega(z)$ approaches unity for large z. This is, in fact, a general property of $\Omega(z)$, as may be deduced from equation (8.37). When z is large, $P(z)$ approaches zero and hence, if $\Omega(z)$ is unity for large z, equation (8.37) would require that

$$1 = \int_0^z P(z - z')\,dz',$$

which is the normalization condition satisfied by $P(z)$.

The significance of the conclusion that $\Omega(z)$ approaches unity for large z is that at a large distance (in energy) from the reference resonance, which is at $z = 0$, it is equally probable that a resonance will be found anywhere. Thus, the expected number of resonances is unity for a unit interval in z, which corresponds to the interval $\bar{D}$ in energy.

8.2d Average Resonance Parameters

The average (or mean) values of the resonance parameters are required in order to apply the results of the preceding section in making predictions of the resonance structure of the energy region of unresolved resonances. The quantities of interest are $\bar{\Gamma}_\gamma$, $\bar{\Gamma}_n$ (or $\bar{\Gamma}_n^0$), $\bar{\Gamma}_f$, and $\bar{D}$. Of these, $\bar{\Gamma}_\gamma$ is obtained from the known (resolved) resonances at low energies and, as already implied, it may be assumed to be the same at all energies. In addition, it is a fairly good approximation to take Γ_γ to be constant for all resonances of a given nuclide. It has also been seen that, for $l = 0$ resonances, $\bar{\Gamma}_n$ (or rather Γ_n) is proportional to $\sqrt{E}$. Furthermore, it has been found that over a limited energy range, e.g., up to about 1 keV, $\bar{\Gamma}_f$ and $\bar{D}$ do not vary very much for resonances with the same J value. Some average resonance parameters based on the foregoing considerations are given in Table 8.1.[55] (The quantities S_0 and S_1 are described below.) For higher energies, the energy dependence of $\bar{\Gamma}_f$ has been estimated from channel theories of fission,[56] but experimental results on "subthreshold" fission may lead to some revision of these theories.[57]

It is thus apparent that as long as $l = 0$ resonances predominate, it is possible to predict the average values of the resonance parameters fairly well up to moderately high neutron energies. At higher energies, where $l = 1$ resonances are important, a more general approach, which is also useful at low energies, may be employed. This is based on the requirement that the average resonance parameters should yield average cross sections which are in agreement with experiment. Thus, in the energy region of unresolved resonances, there are usually available measurements of cross sections for which the individual resonances are not resolved but have been averaged over. These average resonance parameters must be consistent with the measured cross sections.

Consider a sequence of resonances having the same values of J and of l. According to equation (8.27), the area under a given resonance is

$$\int \sigma_x(E)\, dE = \tfrac{1}{2}\pi\sigma_0\Gamma_x = \tfrac{1}{2}\pi\sigma_{00}\frac{\Gamma_x}{\Gamma}\Gamma_n(E_0), \tag{8.39}$$

TABLE 8.1. AVERAGE PARAMETERS FOR RESOLVED RESONANCES[55]

	Uranium-238	*Uranium*-235	*Plutonium*-239
$\bar{\Gamma}_\gamma$, meV	19	45	39
$\bar{\Gamma}_f$ (*s*-waves), meV	—	53	41 ($J = 1^+$) 1500 ($J = 0^+$)
$\bar{\Gamma}_n^0$ (*s*-wave), meV	1.9	0.1	0.3 ($J = 1^+$) 0.9 ($J = 0^+$)
$\bar{D}$, eV	21	1.0	3.1 ($J = 1^+$) 8.8 ($J = 0^+$)
S_0	0.9×10^{-4}	0.91×10^{-4}	1.07×10^{-4}
S_1	2.5×10^{-4}	2.0×10^{-4}	2.5×10^{-4}

where σ_0 is given by equation (8.10) and σ_{00} is defined by

$$\sigma_{00} = 4N\pi\lambda_0^2 g,$$

so that

$$\sigma_0 = \sigma_{00}\frac{\Gamma_n(E_0)}{\Gamma}.$$

Suppose the average cross section is being sought over an energy interval ΔE which contains many resonances and is, therefore, large in comparison with the average resonance spacing, $\bar{D}$. The interval must not be so large, however, that the average resonance parameters will change much within ΔE. The expected number of resonances within the interval ΔE will then be $\Delta E/\bar{D}$.

The average cross section may now be found by taking the average contribution of a single resonance, averaged over the distribution of resonance widths, divided by $\bar{D}$; thus, using equation (8.39),

$$\langle\sigma_x\rangle_{J,l} = \left[\frac{\pi}{2\bar{D}}\langle\sigma_0\Gamma_x\rangle\right]_{J,l} = \left[\frac{\pi\sigma_{00}}{2\bar{D}}\left\langle\frac{\Gamma_n\Gamma_x}{\Gamma}\right\rangle\right]_{J,l}, \tag{8.40}$$

where the subscripts J, l indicate that a particular sequence of resonances is under consideration. Such quantities as $\bar{D}$ and $\bar{\Gamma}_n$ will depend on J and l. The brackets $\langle\ \rangle$ imply that an average is being taken over all the resonance partial widths.

For example, for uranium-238, $\Gamma = \Gamma_n + \Gamma_\gamma$; it will be assumed that Γ_γ is constant, whereas $x = \Gamma_n^0/\bar{\Gamma}_n^0$ is distributed in accordance with equation (8.35). It is then found that

$$\left\langle\frac{\Gamma_n\Gamma_\gamma}{\Gamma}\right\rangle = \left\langle\frac{\Gamma_n\Gamma_\gamma}{\Gamma_n + \Gamma_\gamma}\right\rangle = \int_0^\infty \frac{x\bar{\Gamma}_n\Gamma_\gamma}{x\bar{\Gamma}_n + \Gamma_\gamma}P_1(x)\,dx.$$

Such quantities have been computed and are available in graphical form.[58]

For a fissile nuclide, for which $y = \Gamma_f/\bar{\Gamma}_f$ has a distribution given by equation (8.33) with $n \simeq 2$,

$$\langle\sigma_\gamma\rangle \propto \left\langle\frac{\Gamma_n\Gamma_\gamma}{\Gamma_n + \Gamma_f + \Gamma_\gamma}\right\rangle = \int_0^\infty\int_0^\infty \frac{x\bar{\Gamma}_n\Gamma_\gamma}{x\bar{\Gamma}_n + y\bar{\Gamma}_f + \Gamma_\gamma}P_1(x)P_n(y)\,dx\,dy$$

whereas

$$\langle\sigma_f\rangle \propto \left\langle\frac{\Gamma_n\Gamma_f}{\Gamma_n + \Gamma_f + \Gamma_\gamma}\right\rangle = \int_0^\infty\int_0^\infty \frac{(x\bar{\Gamma}_n)(y\bar{\Gamma}_f)}{x\bar{\Gamma}_n + y\bar{\Gamma}_f + \Gamma_\gamma}P_1(x)P_n(y)\,dx\,dy.$$

The important ratio of the average of neutron captures to fissions would then be the ratio of the two integrals given above. Although the resulting quantity is quite complicated, it can be computed readily.

The average value of the scattering cross section may be expressed in a form similar to equation (8.40), using equation (8.28) for σ_s; for a sequence of resonance it is found that

$$\langle \sigma_s \rangle_{J,l} = \left[\frac{\pi \sigma_{00}}{2\bar{D}} \left\langle \frac{\Gamma_n \Gamma_n}{\Gamma} \right\rangle \right]_{J,l} + g\sigma_{\text{pot}}, \tag{8.41}$$

where use has been made of the fact that the integral of the resonance interference function is zero.

To compute the average cross section for comparison with experiment, the foregoing expressions must be summed over all contributing sequences of resonances, i.e., over all J and l values which are important; thus,

$$\langle \sigma_x \rangle = \sum_{J,l} \langle \sigma_x \rangle_{J,l}$$

$$\langle \sigma_s \rangle = \sum_{J,l} \langle \sigma_s \rangle_{J,l}$$

and

$$\langle \sigma_t \rangle = \langle \sigma_s \rangle + \sum_{x} \langle \sigma_x \rangle.$$

When experimental values of the average cross sections are available and the number of contributing J and l values is small, the results derived above are useful for determining the average resonance parameters. For example, at low neutron energies, i.e., up to about (or less than) 1 to 10 keV, depending on the particular nuclide, only $l = 0$ resonances need be considered. If $I = 0$ for the target nucleus, then $J = \frac{1}{2}$ and there is only a single sequence of resonances. If $I \neq 0$, then $J = I \pm \frac{1}{2}$, so that two sequences are involved.

At higher energies $l = 1$ resonances become significant and further sequences must be included. In these circumstances, nuclear models may be used to suggest the relative values of some of the parameters. Thus, the dependence of $\bar{D}$ on spin can be obtained from models of the nuclear level densities,[59] and for values of J which are not too large it can be assumed that

$$\bar{D}_J \propto (2J + 1)^{-1}.$$

Moreover, values of $\bar{\Gamma}_n/\bar{D}$ may be estimated from calculations of neutron *strength functions*.[60]

In particular, the s-wave ($l = 0$) strength function is usually defined by

$$S_0 = \frac{\bar{\Gamma}_n}{\bar{D}\sqrt{E}} \tag{8.42}$$

and the p-wave ($l = 1$) strength function is given by

$$S_1 = \frac{\bar{\Gamma}_n}{\bar{D}\sqrt{E}} \frac{1 + (R/\lambda)^2}{(R/\lambda)^2}, \tag{8.43}$$

where R and λ have the same significance as before. In equations (8.42) and

(8.43) the values of $\bar{\Gamma}_n$ and $\bar{D}$ are appropriate to the sequence of $l = 0$ and $l = 1$ resonances, respectively, under consideration.

Strength functions, which are of the order of 10^{-4} (see Table 8.1), can be calculated within a factor of about two for most nuclei from optical models of the nucleus. They can often be estimated more accurately, however, from the known values for adjacent nuclei.[61] From the strength functions, $\bar{\Gamma}_n/\bar{D}$ can be derived by means of equations (8.42) and (8.43) and then used for determining average cross sections. For example, suppose that Γ_x in equation (8.40) is large compared to Γ_n; then $\Gamma_n\Gamma_x/\Gamma$ is approximately equal to Γ_n. Under these conditions, it follows that

$$\langle \sigma_x \rangle \approx \frac{\pi \sigma_{00}}{2} \frac{\bar{\Gamma}_n}{\bar{D}}.$$

Hence, for s-wave neutrons, $\langle \sigma_x \rangle$ is proportional to the strength function, S_0, times $\sqrt{E}$.

A possible method for making use of the foregoing procedures is to fix most of the average resonance parameters and leave a few adjustable to fit the measured average cross sections. It is not proposed to consider further details here. Suffice it to say that, by using these and similar combinations of theory and experiment, it is possible to deduce many properties of the average resonance parameters. However, especially at higher neutron energies, there will remain a degree of uncertainty in the unresolved resonances for which allowance must be made. This uncertainty is not important for thermal reactors, for which the unresolved resonances play a minor role, but it is significant for fast reactors.[62]

It has now been seen how cross sections are to be represented in the resonance regions, i.e., by Doppler broadened shape functions, as in equations (8.23) and (8.28), with resonance parameters determined from experiment or from combinations of experiment and theory. Given such cross sections, it would be possible to use them in a general (numerical) scheme for generating multigroup constants, such as that given in §4.5a. Certain approximations have been found to be useful, both for avoiding some of the effort which would be involved in such a general approach and for providing physical insight into the results. More important, special treatments must be developed for obtaining multigroup constants in lattice geometry. A method based on collision probabilities will be described in §8.4a *et seq*.

Some insight into the problems and terminology of resonance absorption may be obtained by considering first the simplest situation, namely, a homogeneous system. This will be done in the following section.

8.3 RESONANCE ABSORPTION IN HOMOGENEOUS SYSTEMS

8.3a Effective Resonance Integral

In every nuclear reactor, some neutrons are slowed down into the energy region where resonances occur and they are absorbed. Consideration will now be given

to resonance absorption in an idealized case which will serve to illustrate the essential physical features. The system to be treated consists of a homogeneous mixture of a moderator and a material with cross-section resonances in which neutrons are absorbed. It is assumed that a source, independent of space and time, is supplying neutrons, e.g., by fission, which are being slowed down into the resonance region.

For evaluating the resonance absorption in such a homogeneous medium with known (measured or assumed) resonances, the only problem is to determine the energy dependence of the neutron flux; the product of the absorption cross section and the flux then gives the absorption. In principle (and in practice) the flux can be computed to any desired degree of accuracy by numerical solution of the slowing down integral equations. But a number of fairly accurate approximations reduce the effort involved and also clarify the physical situation.

Before attempting to determine the neutron flux, it is convenient to consider what use will be made of the results and to introduce a way of summarizing them. Suppose, for the moment, that the flux $\phi(E)$ is sought in the vicinity of a single resonance with a peak at $E = E_t$ and let the flux be normalized so that the asymptotic value, i.e., the flux unperturbed by resonances, at energies just above E_t is given by

$$\phi_{as}(E) = \frac{1}{E}.$$

The reaction rate within a resonance for the flux based on this normalization is then

$$\text{Reaction rate per cm}^3 \text{ per sec} = \int \sigma_{xt}(E)\phi(E)\,dE, \tag{8.44}$$

where σ_{xt} denotes the cross section for reactions of type x in the vicinity of the resonance at E_t. The quantity in equation (8.44) is called the *effective resonance integral* and is represented by I_{xt}, i.e.,

$$I_{xt} = \int \sigma_{xt}\phi\,dE, \tag{8.45}$$

where $\phi = 1/E$ above the resonance.

The contribution of the resonance to a flux-weighted multigroup cross section, as in equation (4.26), is conventionally stated in terms of an effective group cross section, δ, where, for example,

$$\delta_{xt} = \frac{\int_g \sigma_{xt}\phi\,dE}{\int_g \phi\,dE} \approx \frac{I_{xt}}{\ln \dfrac{E_{g-1}}{E_g}}. \tag{8.46}$$

In obtaining the last form of equation (8.46) it is assumed that $\phi = 1/E$ over nearly all the energy range of the group g (§4.5b).

It is also useful to determine the probability that the neutrons are absorbed in the resonance, rather than being moderated to lower energies. For this purpose the competition between absorptions and slowing down must be assessed. When the asymptotic flux is $1/E$, the corresponding slowing down density, i.e., the number of neutrons per cm^3 per sec which are moderated to energies below E, may be written[63] as

$$q = \sum \xi \sigma_s,$$

where ξ is, as usual, the average logarithmic energy decrement per collision; the sum is taken over all scattering nuclei. If the scattering cross section of the moderator is σ_m and the off-resonance (or potential) scattering cross section of the absorbing nucleus is σ_{pot}, then

$$q = \xi_m \sigma_m + \xi_a \sigma_{pot},$$

where ξ_m and ξ_a refer to the moderator and absorber, respectively.

The probability of absorption in the resonance i is now given by

$$P_{abs,i} = \frac{\int \sigma_{ai} \phi \, dE}{q} = \frac{I_{ai}}{\xi_m \sigma_m + \xi_a \sigma_{pot}}. \tag{8.47}$$

The corresponding escape (or noncapture) probability is then

$$P_{esc,i} = 1 - P_{abs,i}.$$

For a group of resonances, assuming the flux to be proportional to $1/E$ in the absence of the resonances,

$$P_{esc} = \prod_i (1 - P_{abs,i}). \tag{8.48}$$

If all the individual absorption probabilities are small, as is usually the case, equation (8.48) may be approximated by

$$P_{esc} \approx \exp\left(-\sum_i P_{abs,i}\right) = \exp\left[-\sum_i \frac{I_{ai}}{\xi_m \sigma_m + \xi_a \sigma_{pot}}\right]. \tag{8.49}$$

The quantity $\sum_i I_{ai}$ is then frequently called the total effective resonance integral.

8.3b Evaluation of Neutron Flux

Suppose the neutron energies are low enough for s-wave scattering by the moderator and s-wave scattering plus absorption by the absorber nuclei to be the only important kinds of collisions. If the neutron flux is independent of space and time and the scattering is s-wave only, so that σf is given by equation (4.5), the transport equation takes the form of a slowing down equation

$$\sigma(E)\phi(E) = \int_E^{E/\alpha_m} \frac{\sigma_m}{(1 - \alpha_m)E'} \phi(E') \, dE' + \int_E^{E/\alpha_a} \frac{\sigma_s(E')}{(1 - \alpha_a)E'} \phi(E') \, dE', \tag{8.50}$$

where α is the quantity defined in §4.2b; the scattering cross section, σ_m, of the moderator is assumed to be independent of energy, but that of the absorber, σ_s, is not. The total cross section on the left of equation (8.50) is given by

$$\sigma(E) = \sigma_m + \sigma_s(E) + \sigma_a(E)$$

$$= \sigma_m + \sigma_s(E) + \sum_x \sigma_x(E).$$

Equation (8.50) could be solved numerically to any desired degree of accuracy. Thus, $\phi(E)$ can be assumed to be known at high energies, e.g., $\phi = 1/E$ for $E > E_{max}$, where E_{max} represents some energy beyond the resonance. Then the integrals in equation (8.50) can be evaluated and the equation can be solved for the flux at $E_{max} - \epsilon$, with ϵ small. The procedure could then be repeated using this flux to obtain the solution $\phi(E)$ for $E \leqslant E_{max}$. In practice, equation (8.50) would normally be expressed with the neutron lethargy rather than energy as the independent variable (cf. §8.4c).

There would be no difficulty in including the scattering of neutrons with higher angular momenta ($l \geqslant 1$), e.g., p-wave scattering, in such a numerical approach. The scattering kernels would be different, but they are known (§4.2b). As noted in §8.1b, however, the effects of p-wave scattering are less important than for s-waves; most of the effect can be taken into account by including p-wave scattering in $\sigma(E)$ on the left side of equation (8.50).

Multigroup cross sections could be determined by means of the fluxes derived in this manner using purely numerical methods; the required cross sections are taken as detailed functions of the neutron energy. In many cases, however, the required group cross sections can be derived from the resonance parameters (and temperature) by making some approximations in order to evaluate the integrals in equation (8.50). These approximate procedures, described below, are nearly always adequate for preliminary calculations and they provide useful insight into the physical situation. Attention will first be paid to resonances which are not Doppler broadened and for which simple results can be obtained. The complications due to Doppler broadening will then be examined. In practical problems of resonance absorption by heavy nuclei, Doppler broadening must always be taken into account.

8.3c The Narrow Resonance Approximation

Suppose that a solution is being sought for the flux $\phi(E)$ in the vicinity of a narrow resonance at E_i. A better condition for narrowness will be given below, but for the present it may be supposed that a narrow resonance is defined by the width being less than the neutron energy loss per collision. Since the energy loss

per collision with a heavy absorber nucleus is less than with a moderator nucleus, the condition for a narrow resonance* may be written

$$\Gamma \ll (1 - \alpha_a)E_i.$$

For $E \simeq E_i$, such a resonance will have very little effect on the integrals in equation (8.50). In other words, the integrals will be dominated by contributions which are far enough from the resonance in question so that the flux is not significantly perturbed by it. Neglect of the effect of a resonance on the flux in the integrals of equation (8.50) is known as the *narrow resonance* (NR) approximation. In this approximation, $\sigma_s(E')$ is set equal to σ_{pot} so that the contribution of the resonance is not included in the scattering integral, i.e., the second integral in equation (8.50).

Since $1 - \alpha_m$ is much larger than $1 - \alpha_a$, the NR approximation is nearly always a good one for the moderator and so it is generally used in evaluating the first integral in equation (8.50). In some cases, however, it is not applicable to the absorber; this situation will be discussed later. For the present it is assumed that the NR approximation is good for the absorber, as well as for the moderator, and so it will be utilized here for both integrals in equation (8.50).

If the resonances are well separated, it is reasonable to assume that other resonances do not affect the integral very much. Neglect of the effect of these other resonances is referred to as the *flux recovery* approximation, because it implies that the flux "recovers" to an asymptotic value between resonances. Under certain conditions of resonance spacing this approximation may be poor,[64] but on the whole it has been found to be quite satisfactory.[65]

With the two approximations just described, the flux in the integrals may be expressed by an asymptotic form. The integrals can then be evaluated and equation (8.50) can be solved for $\phi(E)$. Thus, if *in the integrals*

$$\phi(E') = \phi_{as} = 1/E'$$

and $\sigma_s(E')$ is set equal to σ_{pot}, as mentioned above, equation (8.50) becomes

$$\sigma(E)\phi(E) = \frac{\sigma_m + \sigma_{pot}}{E}$$

or, solving for $\phi(E)$,

$$\phi(E) = \frac{\sigma_m + \sigma_{pot}}{\sigma(E)} \frac{1}{E}. \tag{8.51}$$

It is evident, therefore, that since the numerator is constant, the flux will have a pronounced dip at the energy corresponding to a resonance (Fig. 8.9).

Equation (8.51) expresses the NR approximation to the neutron flux. It is valid for all sufficiently high energies and for the narrow resonances associated

* For a Doppler broadened resonance, a comparable criterion would be

$$\sqrt{\Gamma^2 + \Delta^2} \ll (1 - \alpha_a)E_i.$$

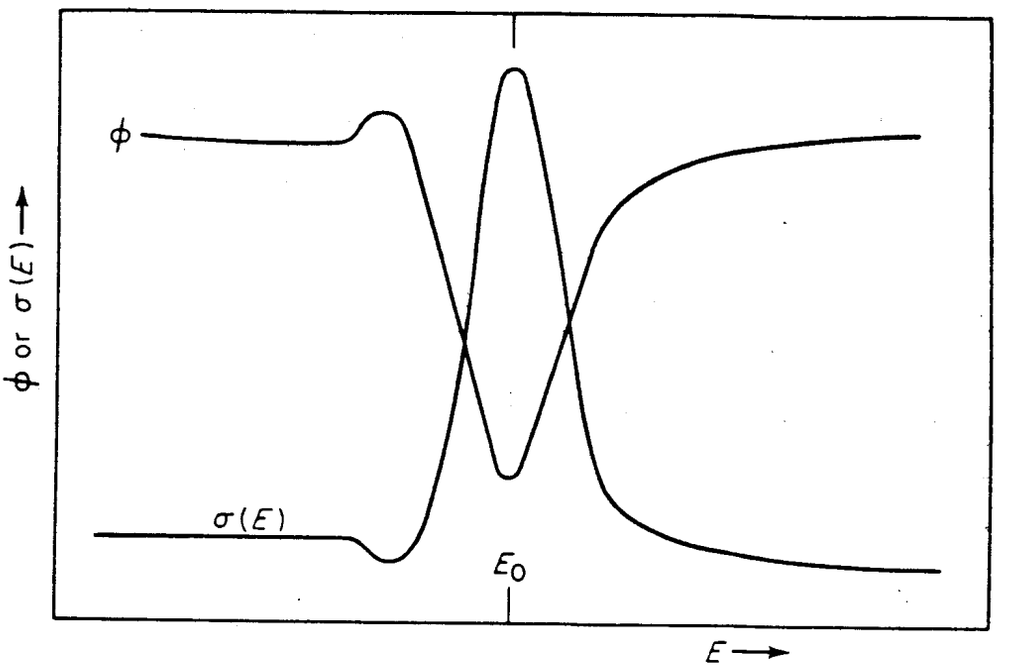

FIG. 8.9 CROSS SECTIONS AND NEUTRON FLUX IN VICINITY OF A NARROW RESONANCE.

with absorption by heavy (fissile and fertile) elements. For example, consider a resonance at $E_i = 1$ keV; the maximum energy loss accompanying the collision of a neutron of this energy with a uranium-238 nucleus is given by

$$(1 - \alpha_a)E_i = \frac{4A_aE_i}{(1 + A_a)^2} = 17 \text{ eV}.$$

For collision with an oxygen nucleus, on the other hand, it is 220 eV. Both of these energy losses are large compared to resonance widths and so the narrow resonance approximation can be justified at energies above 1 keV (or even less).

An alternative (and better) condition for the self-consistency and validity of the NR approximation can be derived in the following manner. According to equation (8.51), the flux $\phi(E)$ will depart from its asymptotic value in the neighborhood of the resonance. But, the flux was assumed to be asymptotic in the integrals. Consequently, for the approximation to be consistent, the contribution to the integrals must be small from regions where $\phi(E)$ departs from its asymptotic value.

Consider, in particular, the energies at which $\phi = 1/2E$ (or $E\phi = \frac{1}{2}$), so that the NR flux is half the asymptotic value. This usually turns out to be far out on the wing of a resonance where the natural shape of the cross-section curve is valid. If, for simplicity, the interference between potential and resonance scattering is ignored and, furthermore, $\sqrt{E_0/E}$ is taken as unity, equation (8.13) reduces to

$$\sigma_s + \sum_x \sigma_x(E) = \frac{\sigma_0\Gamma^2}{4(E - E_i)^2 + \Gamma^2} + \sigma_{pot}.$$

Then, if $E\phi = \frac{1}{2}$, with ϕ given by equation (8.51) and noting that $\sigma(E) = \sigma_m + \sigma_s + \sum_x \sigma_x(E)$, it follows that $\sigma_m + \sigma_{pot}$ is one-half of the total cross section,i.e.,

$$\sigma_m + \sigma_{pot} = \tfrac{1}{2}\left(\sigma_m + \sigma_{pot} + \frac{\sigma_0\Gamma^2}{4(E - E_i)^2 + \Gamma^2}\right)$$

or

$$|E - E_i| = \tfrac{1}{2}\Gamma\sqrt{\frac{\sigma_0}{\sigma_m + \sigma_{pot}} - 1}.$$

The energy interval $2|E - E_i|$, over which the flux is so perturbed as to be half the asymptotic value (or less), is called the *practical width* of the resonance, and is represented by Γ_P. For cases of interest, $\sigma_0 \gg \sigma_m + \sigma_{pot}$ and hence the practical width may be defined by

$$\Gamma_P = \Gamma\sqrt{\frac{\sigma_0}{\sigma_m + \sigma_{pot}}}. \tag{8.52}$$

A better condition for the NR approximation than the one given earlier would then be

$$\Gamma_P \ll (1 - \alpha_a)E_i.$$

Approximations which can be used when this condition is not well satisfied are discussed later (§8.3g).

For Doppler broadened resonances, Γ_P is, in principle, a function of temperature. As noted earlier, however, in most cases of importance the practical width is determined by the wings of the resonance where Doppler broadening does not affect the shape. Hence, Γ_P is essentially independent of temperature and is equal to the value in equation (8.52).

If the flux is represented by equation (8.51), then the number of reactions per cm^3 per sec, i.e., the effective resonance integral, is obtained from equation (8.45) as

$$\text{Reaction rate per cm}^3 \text{ per sec} = I_{xi} = \int_{E_1}^{E_2} \sigma_{xi}(E)\phi(E)\,dE$$

$$= (\sigma_m + \sigma_{pot})\int_{E_1}^{E_2} \frac{\sigma_x(E)}{\sigma(E)}\frac{dE}{E}, \tag{8.53}$$

where E_1 and E_2 are energy limits chosen to include the resonance of interest at E_i. In the NR approximation, the effective cross section, defined by equation (8.46), is then

$$\bar{\sigma}_{xi} = \frac{I_{xi}}{\int_{E_1}^{E_2}\phi(E)\,dE} = \frac{\int_{E_1}^{E_2}\frac{\sigma_x(E)}{\sigma(E)}\frac{dE}{E}}{\int_{E_1}^{E_2}\frac{1}{\sigma(E)}\frac{dE}{E}}, \tag{8.54}$$

in which the constant factor $(\sigma_m + \sigma_{pot})$ has been cancelled in numerator and denominator.

Further simplifications, which are often quite accurate, can be made to equation (8.54). In the numerator of this equation, the main contribution to the integral is from $E \simeq E'$, and so $1/E$ can be set equal to $1/E_i$. Then, in the denominator, $1/\sigma(E) \simeq 1/(\sigma_m + \sigma_{pot})$ over most of the energy range, whereas near the resonance the former is smaller; hence $1/\sigma(E)$ may be replaced by the constant $1/(\sigma_m + \sigma_{pot})$. Then equation (8.54) becomes

$$\tilde{\sigma}_{xi} \simeq \frac{\sigma_m + \sigma_{pot}}{E_i \ln (E_2/E_1)} \int_{E_1}^{E_2} \frac{\sigma_x(E)}{\sigma(E)}\, dE. \tag{8.55}$$

If E_1 and E_2 represent the energy boundaries of a group in multigroup theory, then $\tilde{\sigma}_{xi}$, given by equation (8.55), would represent the contribution of the resonance at E_i to the group cross section for reactions of type x.

8.3d Absorption Probability in the NR Approximation

As in equation (8.47), the probability of absorption, $P_{abs,i}$, is equal to the given resonance integral, i.e., I_{xi} as represented by equation (8.53), divided by the slowing down density; thus,

$$P_{abs,i} = \frac{1}{\bar{\xi}} \int_{E_1}^{E_2} \frac{\sigma_a(E)}{\sigma(E)} \frac{dE}{E} \simeq \frac{1}{\bar{\xi} E_i} \int_{E_1}^{E_2} \frac{\sigma_a(E)}{\sigma(E)}\, dE, \tag{8.56}$$

where, as before, $\sigma_a(E)$, is the sum of all the reaction cross sections of the absorber, and $\bar{\xi}$ is defined by

$$\bar{\xi} = \frac{\xi_m \sigma_m + \xi_a \sigma_{pot}}{\sigma_m + \sigma_{pot}}.$$

The resonance escape probability for a group of resonances is now obtained from equation (8.48) as

$$P_{esc} = \prod_i \left(1 - \frac{1}{\bar{\xi}} \int_{E_i^-}^{E_i^+} \frac{\sigma_a(E)}{\sigma(E)} \frac{dE}{E}\right),$$

where E_i^- is an energy between E_{i-1} and E_i, and E_i^+ is between E_i and E_{i+1}. The product may be represented to a good approximation by an exponential, so that

$$P_{esc} \approx \exp\left[-\frac{1}{\bar{\xi}} \int_{E_{min}}^{E_{max}} \frac{\sigma_a(E)}{\sigma(E)} \frac{dE}{E}\right], \tag{8.57}$$

where E_{min} is typically chosen as around the cadmium cutoff energy, approximately 0.4 eV, whereas E_{max} is some large energy beyond the resonances, e.g., around 100 keV. Equation (8.57) is the expression for the resonance escape probability in a homogeneous system as given by the NR approximation.

If the absorber is very dilute, then σ_{pot} and σ_s in equation (8.53) can be neglected in comparison with σ_m, and the total resonance integral at infinite dilution, I_∞, may be written as

$$I_\infty = \sigma_m \int \frac{\sigma_a(E)}{\sigma(E)} \frac{dE}{E} = \int \sigma_a(E) \frac{dE}{E},$$

where σ_a, for all reactions, has replaced σ_x and σ has been set equal to σ_m in obtaining the final result. The corresponding integral at finite dilutions is

$$I_a = (\sigma_m + \sigma_{pot}) \int \frac{\sigma_a(E)}{\sigma(E)} \frac{dE}{E} \tag{8.58}$$

and hence equation (8.57) becomes

$$P_{esc} \approx \exp\left[-\frac{I_a}{\xi(\sigma_m + \sigma_{pot})}\right]. \tag{8.59}$$

The resonance escape probability can be measured[66] and then the total effective resonance integral may be derived from equation (8.59). Thus, the effective resonance integral provides a convenient device for summarizing experimental data.[67]

For fertile nuclides, the experimental resonance integrals do not agree well with the values derived from equation (8.58) using experimental resonance parameters, primarily because the NR approximation is not valid for the largest low-energy resonances.[68] Comparisons of experimental and calculated resonance integrals are given in §8.5a.

The integrals involved in the resonance absorption will now be examined and in the process an assessment can be made of the accuracy of the NR approximation. Suppose it is required to evaluate an integral such as the one in equation (8.53), with $1/E$ replaced by $1/E_t$, or the one in equation (8.58), i.e.,

$$I_{xt} = \frac{\sigma_m + \sigma_{pot}}{E_t} \int \frac{\sigma_x(E)}{\sigma(E)} dE. \tag{8.60}$$

In the absence of Doppler broadening and assuming the single-level Breit-Wigner formula to be applicable, $\sigma_x(E)$ can be taken from equation (8.11) and $\sigma(E)$, the total cross section, from equation (8.13) with σ_{pot} replaced by $\sigma_m + \sigma_{pot}$ to take into account potential scattering by both moderator and absorber. In addition, E_t is substituted for E_0. Since it is usually adequate to set $\sqrt{E_t/E} = 1$, the expression for I_{xt} becomes

$$I_{xt} = \frac{\sigma_m + \sigma_{pot}}{E_t} \int_{E_1}^{E_2} \frac{\sigma_0 \Gamma_x/\Gamma}{\sigma_0\left[1 + \frac{4(E - E_t)}{\Gamma} \frac{R}{\lambda}\right] + (\sigma_m + \sigma_{pot})\left[1 + \frac{4(E - E_t)^2}{\Gamma^2}\right]} dE. \tag{8.61}$$

As in §8.1d, Y is defined by

$$Y \equiv \frac{2}{\Gamma}(E - E_i),$$

and E_1 and E_2 are taken such that $|E_1 - E_i|$ and $|E_2 - E_i|$ are both much greater than the total resonance width Γ; equation (8.61) may then be written as

$$I_{xi} = \frac{\sigma_m + \sigma_{pot}}{E_i} \int_{-\infty}^{\infty} \frac{dY}{aY^2 + bY + c} = \frac{\pi(\sigma_m + \sigma_{pot})}{E_i\sqrt{ac - \frac{1}{4}b^2}}, \tag{8.62}$$

where

$$a \equiv \frac{2(\sigma_m + \sigma_{pot})}{\sigma_0\Gamma_x}$$

$$b \equiv \frac{4R}{\lambda\Gamma_x}$$

$$c \equiv a + \frac{2}{\Gamma_x}.$$

Thus, the resonance integral, and hence the effective cross section $\tilde{\sigma}_{xi}$, can be expressed in terms of the resonance parameters.

The absorption probability for a single reaction, as given by equation (8.56) with σ_x replacing σ_a, now becomes

$$P_{abs,xi} = \frac{\pi}{\bar{\xi}aE_i} \frac{1}{\sqrt{\frac{c}{a} - \frac{b^2}{4a^2}}}. \tag{8.63}$$

Upon substituting the expressions given above for a, b, and c, and using equations (8.9) and (8.10) for the potential scattering and peak resonance cross sections, respectively, to evaluate $b^2/4a^2$, equation (8.63) takes the form

$$P_{abs,xi} = \frac{\frac{1}{2}\pi\sigma_0\Gamma_x}{\bar{\xi}(\sigma_m + \sigma_{pot})E_i} \frac{1}{\sqrt{1 + \frac{\sigma_0}{\sigma_m + \sigma_{pot}}\left(1 - \frac{g\Gamma_n}{\Gamma}\frac{\sigma_{pot}}{\sigma_m + \sigma_{pot}}\right)}}. \tag{8.64}$$

The physical significance of the terms of this expression can be understood by writing it as

$$P_{abs,xi} = A\frac{1}{\sqrt{1 + BC}}, \tag{8.65}$$

where

$$A \equiv \frac{\frac{1}{2}\pi\sigma_0\Gamma_x}{\bar{\xi}(\sigma_m + \sigma_{pot})E_i}$$

$$B \equiv \frac{\sigma_0}{\sigma_m + \sigma_{pot}}$$

$$C \equiv 1 - \frac{g\Gamma_n}{\Gamma}\frac{\sigma_{pot}}{\sigma_m + \sigma_{pot}}.$$

If the absorber is infinitely dilute, then $\sigma(E)$ in equation (8.60) is equal to $\sigma_m + \sigma_{pot} \approx \sigma_m$ and hence, writing $I_{\infty,xi}$ for the effective resonance integral at infinite dilution,

$$I_{\infty,xi} = \frac{1}{E_i}\int \sigma_x(E)\,dE$$

$$= \frac{\frac{1}{2}\pi\sigma_0\Gamma_x}{E_i},$$

where equation (8.27) has been used for the integral. If $I_{\infty,xi}$ is divided by the slowing down density, $\xi(\sigma_m + \sigma_{pot})$, the result, which is identical with the term A, is the resonance absorption probability at infinite dilution. This result is obtained in the absence of flux depression by the resonance.

If interference between resonance and potential scattering were neglected, the quantity b in equation (8.62) would be zero, and equation (8.65) would become

$$P_{abs,xi} = A\frac{1}{\sqrt{1+B}} \quad \text{(no interference)}.$$

Thus, the infinitely dilute resonance absorption is decreased by the factor $1/\sqrt{(1+B)}$ because of the flux depression at the resonance. The quantity, B, i.e., $\sigma_0/(\sigma_m + \sigma_{pot})$, is the ratio of the peak value of the resonance cross section to the cross section away from the peak (Fig. 8.10).

Finally, the term C in equation (8.60) represents the increase in the resonance absorption due to interference between resonance and potential scattering.

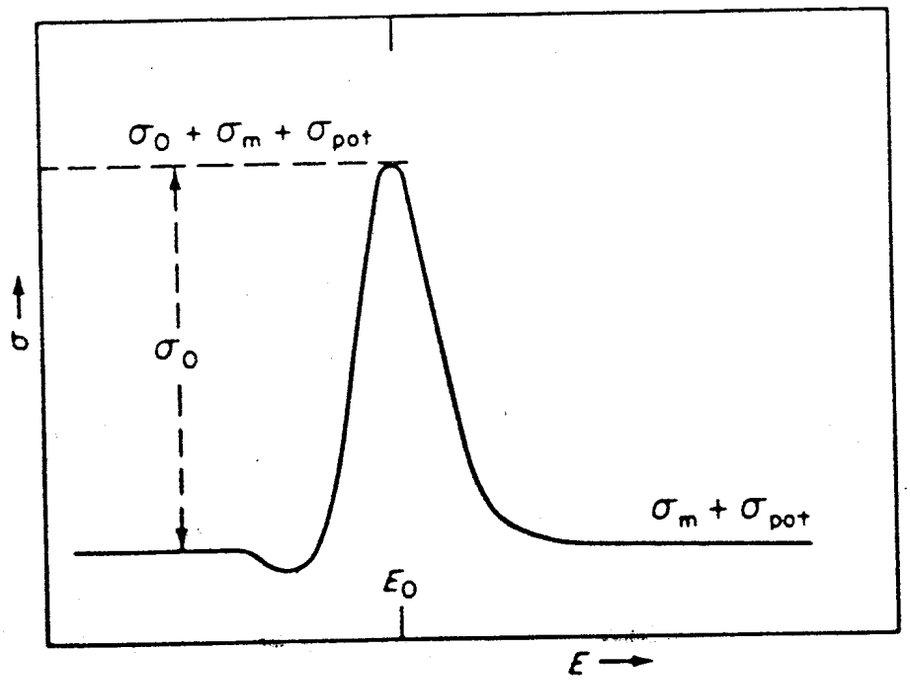

FIG. 8.10 CROSS SECTIONS IN THE VICINITY OF A RESONANCE.

For most resonances, the effect is small although there are some significant exceptions.[69]

8.3e Doppler Broadening in the NR Approximation

When Doppler broadening of the resonances is taken into account, the equations for the NR approximation become somewhat more complicated. Thus, the cross sections for single levels may be taken from equations (8.23) and (8.28). When interference between resonance and potential scattering is negligible, the results may be expressed in terms of the tabulated function[70] $J(\zeta, \beta)$, defined by

$$J(\zeta, \beta) \equiv \frac{1}{2}\int_{-\infty}^{\infty} \frac{\Psi(\zeta, Y)}{\Psi(\zeta, Y) + \beta}\, dY, \tag{8.66}$$

where β is a function of cross sections (and sometimes also resonance widths) to be derived below, and $\zeta = \Gamma/\Delta$ as before.

In particular, if $\sqrt{E/E_0}$ is set equal to unity, it is found that

$$\int \frac{\sigma_x(E)}{\sigma(E)}\, dE = \int_{E_1}^{E_2} \frac{(\sigma_0\Gamma_x/\Gamma)\Psi(\zeta, Y)}{\sigma_0\Psi(\zeta, Y) + \sigma_m + \sigma_{pot}}\, dE$$

$$= \Gamma_x J\left(\zeta, \frac{\sigma_m + \sigma_{pot}}{\sigma_0}\right). \tag{8.67}$$

Thus, for a single resonance, the effective cross section from equation (8.55) becomes

$$\tilde{\sigma}_{xi} = \frac{\sigma_m + \sigma_{pot}}{\ln(E_2/E_1)} \frac{\Gamma_{xi}}{E_i} J\left(\zeta, \frac{\sigma_m + \sigma_{pot}}{\sigma_0}\right)$$

and from equation (8.56),

$$P_{abs,i} = \frac{\Gamma_{xi}}{\bar{\xi}E_i} J\left(\zeta, \frac{\sigma_m + \sigma_{pot}}{\sigma_0}\right).$$

For a series of resonances, the total effective resonance integral for reaction x is obtained from equation (8.58) as

$$I_x = (\sigma_m + \sigma_{pot}) \sum_i \frac{\Gamma_{xi}}{E_i} J\left(\zeta_i, \frac{\sigma_m + \sigma_{pot}}{\sigma_{0i}}\right).$$

The general behavior of $J(\zeta, \beta)$ as β varies is shown in Fig. 8.11.[71] It is seen that when β is large, J is independent of ζ and, hence, of the temperature. The reason is that for large β, i.e., when $(\sigma_m + \sigma_p)/\sigma_0$ is large, the flux depression by the resonance is small. Hence, the denominator of equation (8.67) is close to $\sigma_m + \sigma_{pot}$ and the numerator $\int \sigma_x(E)\, dE$, which is the area under the resonance,

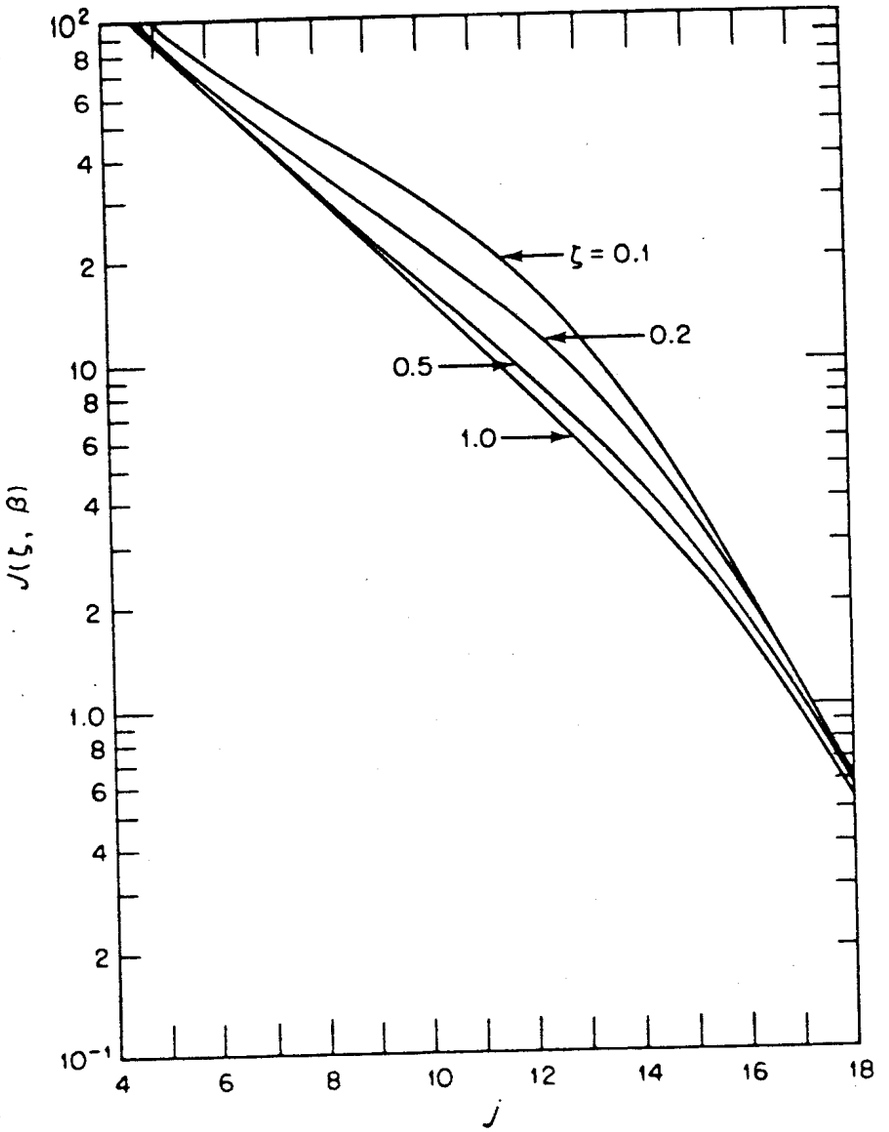

FIG. 8.11 THE FUNCTION $J(\zeta, \beta)$ VS j, WHERE $\beta = 2^j \times 10^{-5}$ (AFTER L. DRESNER, REF. 71).

is essentially independent of temperature and, therefore, of ζ; hence, when β is large, J is also independent of ζ (and of temperature).

For small values of β, Fig. 8.11 shows that J is again independent of ζ, at least unless ζ is very small, i.e., T is very large. This arises because when β is small, $\sigma_0 \Psi(\zeta, Y) \gg \sigma_m + \sigma_{pot}$ until Y becomes large, i.e., at energies some distance from (on the wings of) the resonance. On the wings, the cross-section curve has its natural shape (§8.1d) unless T is very large, so that J is independent of ζ.

At low temperatures, i.e., for $\zeta \gg 1$, J is independent of ζ and thus of temperature. The reason is that when ζ is large, the resonance has its natural, unbroadened shape.

It is also seen from Fig. 8.11 that, for any value of β, the function J increases or remains constant as ζ is decreased, i.e., with increasing temperature. In other

words, the resonance absorption must increase (or be unchanged) when the temperature is increased. This result is found to be quite general and not limited to the NR approximation. The physical basis is that when a resonance is broadened by the Doppler effect, the neutron flux depression is decreased (Fig. 8.12) whereas the area under the cross section curve is essentially constant. Hence, the absorption, i.e., the product of the flux and the cross section, increases with increasing temperature.

The effect of Doppler broadening in increasing absorption is most marked when $J(\zeta, \beta)$ varies significantly with ζ, at a given β. This is seen from Fig. 8.11 to occur particularly in the range $10^{-3} \lesssim \beta \lesssim 1$.* Consequently, such resonances are likely to be the ones which contribute to the temperature coefficient of reactivity (§8.4e). In the NR approximation, this coefficient would include a term proportional to $\partial J/\partial T$, and in view of the definition of ζ (and of Δ), it follows that

$$\frac{\partial J}{\partial T} = -\frac{1}{2}\frac{\zeta}{T}\frac{\partial J}{\partial \zeta}.$$

Hence, resonances with values of β and ζ such that $\partial J/\partial \zeta$ is large will make important contributions to the temperature coefficient of reactivity.

When the interference between resonance and potential scattering cannot be ignored in the Doppler broadened cross sections or when the resonance cross sections cannot be represented by a single-level Breit-Wigner formula, the results cannot be summarized in terms of J functions. Nevertheless, the qualitative effects of Doppler broadening are the same as those derived above.

* This corresponds approximately to $7 \lesssim j \lesssim 16$ in Fig. 8.11.

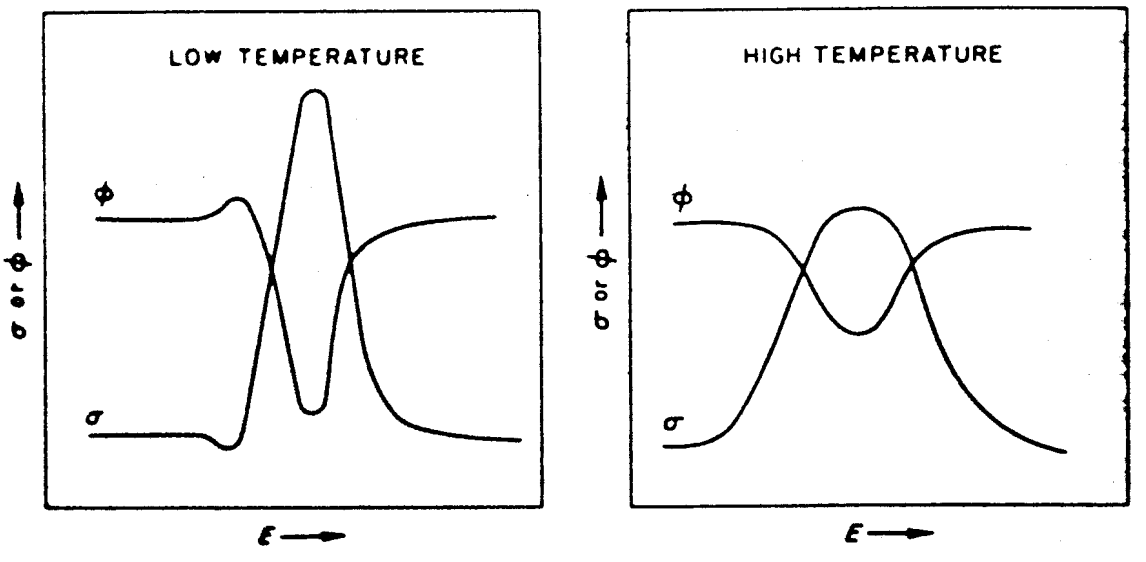

FIG. 8.12 INCREASE OF RESONANCE ABSORPTION WITH INCREASING TEMPERATURE.

8.3f The NRIM Approximation

It will be recalled that the condition for the NR approximation is that the (maximum) energy loss in an elastic scattering collision with an absorber nucleus, i.e., $(1 - \alpha_a)E_i$, in the vicinity of a resonance should be much greater than the practical width, Γ_P, of the resonance. There are instances, especially for some of the strong, low-energy resonances of uranium-238, for which σ_0 is large and E_i small, where this NR condition does not hold. For example, for the 6.67-eV resonance of uranium-238 in a 1:1 mixture with hydrogen as moderator, Γ_P is approximately 1 eV, whereas $(1 - \alpha_a)E_i$ is around 0.1 eV.

Under such conditions, when $(1 - \alpha_a)E_i \ll \Gamma_P$, the NR approximation fails for the second integral in equation (8.50), although it is usually satisfactory for the first (moderator) integral. A better and equally simple approach is then to assume that the resonance is narrow (NR) for collisions with the moderator, but it is so wide for the heavy absorber nuclei that the latter may be assumed to have infinite mass (IM). Thus, energy loss in collisions with absorber nuclei are neglected. This leads to what is called the NRIM (or sometimes NRIA, where A refers to the mass of the absorber atom) approximation. The NRIM approximation is applicable only to a few of the low-energy resonances of the fertile nuclei, but these few resonances may account for a large fraction of the resonance absorption in a thermal reactor.[72]

In the NRIM approximation, the second integral in equation (8.50) becomes

$$\lim_{\alpha_a \to 1} \int_E^{E/\alpha_a} \frac{\sigma_s(E')\phi(E')}{(1 - \alpha_a)E}\, dE' = \sigma_s(E)\phi(E). \tag{8.68}$$

The first integral is the same as before, since the NR approximation is retained for moderator collisions, i.e., σ_m/E, and hence it is found from equation (8.50) that

$$\phi(E) = \frac{\sigma_m}{\sigma_m + \sigma_a(E)} \frac{1}{E} \tag{8.69}$$

since $\sigma(E) = \sigma_m + \sigma_s(E) + \sigma_a(E)$. By comparison with equation (8.51), it is seen that scattering by the absorber nuclei now has no effect on the flux. This is, of course, to be expected since scattering from an infinitely heavy nucleus, i.e., without energy loss, would have no influence on the competition between moderation and absorption.

If equation (8.69) is used for the flux in deriving expressions for reaction rates, absorption probabilities, etc., the only difference from the NR results will be the elimination of σ_{pot}, the replacement of $\sigma(E)$ by $\sigma_m + \sigma_a(E)$, and of $\bar{\xi}$ by ξ_m. For example, instead of equation (8.56), the NRIM approximation would give

$$P_{abs,x1} = \frac{1}{\xi_m E_i} \int_{E_1}^{E_2} \frac{\sigma_x(E)}{\sigma_m + \sigma_a(E)} \frac{dE}{E}.$$

For an unbroadened single-level resonance, the resonance integral would be, in terms of resonance parameters,

$$I_{xi} = \frac{\sigma_m}{E_i}\int \frac{\sigma_x(E)}{\sigma_m + \sigma_a(E)}\frac{dE}{E}$$

$$\approx \frac{\sigma_m}{E_i}\int \frac{\sigma_0\Gamma_x/\Gamma}{\sigma_0\dfrac{(\Gamma-\Gamma_n)}{\Gamma} + \sigma_m\left[1+\dfrac{4(E-E_i)^2}{\Gamma^2}\right]}\,dE$$

$$= \frac{\frac{1}{2}\pi\sigma_0\Gamma_x}{E_i\sqrt{1+\dfrac{\Gamma-\Gamma_n}{\Gamma}\dfrac{\sigma_0}{\sigma_m}}}.$$

The absorption probability is then

$$P_{\text{abs},xi} = \frac{\frac{1}{2}\pi\sigma_0\Gamma_x}{\xi_m\sigma_m E_i}\cdot\frac{1}{\sqrt{1+\dfrac{\Gamma-\Gamma_n}{\Gamma}\dfrac{\sigma_0}{\sigma_m}}}, \tag{8.70}$$

which may be compared with equation (8.64) for the NR approximation.

Expressions analogous to those given in the preceding section may be obtained for Doppler broadened resonances. The quantity β in $J(\zeta, \beta)$ is now expressed by

$$\beta = \frac{\sigma_m\Gamma}{\sigma_0(\Gamma-\Gamma_n)}.$$

In the third and fourth columns of Table 8.2, the values of P_{abs} are given for individual unbroadened resonances of uranium-238, in a 1:1 atomic mixture with hydrogen, for both NR and NRIM approximations.[73] (The values in the last two columns will be discussed in the next section.) It is seen from the results

TABLE 8.2. CALCULATED RESONANCE ABSORPTION PROBABILITIES.[73]

				Iterated Values	
E_i, *eV*	Γ, *eV*	*NR*	*NRIM*	*NR*	*NRIM*
66.3	0.050	0.0224	0.0260	0.0261	0.0253
81.3	0.0271	0.00652	0.00556	0.00630	0.00627
90	0.0251	0.00114	0.00097	0.00113	0.00113
103.5	0.092*	0.0139	0.0217	0.0214	0.0202
117.5	0.040	0.00826	0.00856	0.00836	0.00840
146	0.0259	0.00178	0.00150	0.00176	0.00177
166	0.029	0.00298	0.00263	0.00294	0.00294
192	0.165*	0.00596	0.01245	0.00914	0.01043

* Strong resonances.

in the table that the NRIM approximations often gives more absorption in a resonance, especially a strong one, than does the NR approximation.

8.3g Improved and Intermediate Approximations

For resonances which are neither narrow nor wide, it is possible to improve upon the NR and NRIM approximations without the necessity for an excessive amount of numerical work. Two such improvements are the iterative method[74] and the quite successful intermediate resonance absorption treatment.[75] Since the NR approximation is usually a good one for neutron collisions with the moderator, although not necessarily with heavy absorber nuclei, it will be assumed to apply to the moderator only. This is, however, by no means the most general situation for which iterative and intermediate methods have been devised.[76]

With the NR approximation for the moderator, equation (8.50) becomes

$$\sigma(E)\phi(E) = \frac{\sigma_m}{E} + \int_E^{E/\alpha_a} \frac{\sigma_s(E')\phi(E')}{(1-\alpha_a)E'}\,dE', \tag{8.71}$$

which can be written in the form

$$\sigma(E)\phi(E) = \frac{\sigma_m}{E} + \mathbf{K}\phi, \tag{8.72}$$

where $\mathbf{K}$ is the integral operator in equation (8.71).

Consider the iterative sequence defined by

$$\sigma(E)\phi^{(n)}(E) = \frac{\sigma_m}{E} + \mathbf{K}\phi^{(n-1)}. \tag{8.73}$$

The first guess, $\phi^{(1)}$, for the flux may be taken as the NR approximation, i.e., equation (8.51), which is

$$\phi^{(1)}(E) = \frac{\sigma_m + \sigma_{pot}}{\sigma_m + \sigma_s + \sigma_a}\frac{1}{E} \quad \text{(NR approximation)}$$

or from the NRIM approximation of equation (8.69),

$$\phi^{(1)}(E) = \frac{\sigma_m}{\sigma_m + \sigma_a}\frac{1}{E} \quad \text{(NRIM approximation)}$$

or in the intermediate form

$$\phi^{(1)}(E) = \frac{\sigma_m + \lambda\sigma_{pot}}{\sigma_m + \lambda\sigma_s + \sigma_a}\frac{1}{E} \quad \text{(intermediate)} \tag{8.74}$$

where λ, which lies in the range $0 < \lambda < 1$, is to be determined.

It will now be shown in a heuristic manner that the sequence defined by equation (8.73) converges to the true flux, i.e.,

$$\phi^{(n)} \xrightarrow{n\to\infty} \phi.$$

Let

$$\phi^{(n)} = \phi + \epsilon^{(n)},$$

then from equations (8.72) and (8.73),

$$\sigma(E)\epsilon^{(n)} = \mathbf{K}\epsilon^{(n-1)}.$$

According to the definition of the operator **K**, it contains only scatterings from heavy (absorber) nuclei; consequently, $\epsilon^{(n)}$ may be interpreted as the flux of neutrons arising from scattering collisions of neutrons in the flux $\epsilon^{(n-1)}$ with heavy nuclei. All other collisions of $\epsilon^{(n-1)}$ neutrons will not contribute to $\epsilon^{(n)}$; that is to say, they will result in absorption. Hence, the neutrons in $\epsilon^{(n)}$ will have $n-1$ scattering collisions with the heavy nuclei, and no other collisions, starting from $\epsilon^{(1)}$. For a large n, this is a very unlikely situation, the probability of which approaches zero as n approaches infinity; hence,

$$\epsilon^{(n)} \xrightarrow{n\to\infty} 0,$$

and $\phi^{(n)}$ converges to the true flux.

The performance of the iterations in equation (8.73) rapidly becomes complicated as n increases. For the NR and NRIM approximations, starting with the $\phi^{(1)}$ values given above, it is not difficult to obtain $\phi^{(2)}$ for unbroadened resonances. The corresponding absorption probabilities in some of the uranium-238 resonances are given in the last two columns of Table 8.2. It is of interest to note that the iterated NR and NRIM results are in much closer agreement than are those for the uniterated approximations. Iterations beyond $\phi^{(2)}$ become impractical.

In the intermediate resonance (IR) absorption method,[77] the value of $\phi^{(1)}$ is obtained from equation (8.74) with an arbitrary value of λ, and $\phi^{(2)}$ is computed from equation (8.73). The resonance absorption is then calculated using both $\phi^{(1)}$ and $\phi^{(2)}$ and λ is adjusted so that the two absorptions are equal. The justification for this procedure is as follows. If $\phi^{(1)}$ were exact, i.e., $\phi^{(1)} = \phi$, then comparison of equations (8.72) and (8.73) shows that $\phi^{(2)} = \phi$ also. Thus, the resonance absorption would not vary with iteration if $\phi^{(1)} = \phi$. Hence, $\phi^{(1)}$ is chosen so that the absorption is not affected by iteration until $\phi^{(3)}$. In practice, the value of λ obtained in this way turns out to be reasonable; for example, $\lambda \to 1$ for narrow resonances and $\lambda \to 0$ for wide resonances, and the results are in good agreement with those obtained by Monte Carlo methods[78] or by numerical integration of equation (8.50).

For unbroadened single resonances, with interference between resonance and potential scattering being neglected, λ can be derived in closed form. But for a broadened single resonance, the problem becomes much more difficult. It has been found, however, that use of the value for λ computed for the unbroadened resonance together with the shape of the broadened resonance gives good results.[79]

The variational method (Chapter 6) has also been used to determine λ. The values are much the same as those obtained by the procedures described above. Since the variational method is more complicated the iterative techniques are to be preferred.[80]

If the cross sections cannot be expressed in a simple manner, e.g., if the single-level Breit-Wigner formula fails to represent σ_a or σ due to overlap or interference effects, or if the NR approximation is not applicable to the moderator, some progress can be made by using analytic methods. For practical purposes, however, it would appear that direct numerical solution of equation (8.50), using the experimental cross sections, is the most efficient procedure. Codes have been written for obtaining the required solutions.[81] As a general rule, the NR approximation is made for the moderator, so that equation (8.71) is the one that is solved. With a fast digital computer, these numerical solutions can be obtained so rapidly that such procedures have largely replaced analytical methods for detailed reactor design studies. The numerical computation of resonance integrals is described in §8.4c.

8.3h Resonances and Multigroup Constants

The main effect of resonances on the effective multiplication factor (or reactivity) or other eigenvalues arises from neutron absorption, both radiative capture and fission. Apart from the energy regions near resonance peaks, such absorption has relatively little effect on neutron transport. Hence, in estimating multigroup cross sections in equations (4.26) and (4.27), for example, it is vital that proper account be taken of resonance absorption in $\sigma_{0,g}$. In the $\sigma_{n,g}$ values for $n > 1$, which are involved in the transport equation, however, less care is required with the resonances, and in the transfer cross sections, $\sigma_{n,g'\to g}$, they may be ignored except for $g' = g$.

It has been seen that the experimental data on resonances can be conveniently (and reliably) expressed in terms of resonance parameters. Furthermore, methods have been developed for determining analytically the fine structure of the flux, i.e., $\phi_0(E)$, in the neighborhood of a single resonance. The reaction rate for a given resonance was thus evaluated, e.g., by equation (8.53). The effective cross section due to a series of well-separated (or isolated) resonances can then be found as the sum of contributions from each resonance in a given energy group, e.g., from equation (8.55). These procedures have been found to be fairly accurate in treating resonance absorption in thorium-232 and uranium-238, at least in the region of unresolved resonances.[82]

Although no allowance would have been made for attenuation of the asymptotic (between resonance) flux within the group due to leakage and (nonresonance) absorption, such effects could be included in a straightforward manner. For example, the actual rapidly varying cross section, $\sigma_x(E)$, which includes the resonances, could be replaced by a slowly varying effective cross section $\bar{\sigma}_x(E)$,

as in §8.3a, which is then used in a standard B_N calculation (§4.5c). The replacement of σ_x by $\tilde{\sigma}_x$ takes into account the resonance structure of the energy dependence of the flux, whereas the B_N approximation then follows the gross depletion of the flux with energy due to leakage and absorption.

When resolved resonances overlap, as a result of the Doppler effect (or because of the near coincidence of the resonance energies), it is possible to obtain Doppler broadened cross sections and to determine the required reaction rates using values of the flux computed by numerical solution[83] of the integral equations (8.50) or (8.71) or by Monte Carlo methods.[84] The contribution of the (n, γ) and (n, f) reactions to $\sigma_{0,g}$ would then be equal to the corresponding reaction rates, for neutrons in the group g, divided by the flux in that group. The contribution of resonance scattering to $\sigma_{0,g}$ and also to $\sigma_{0,g\to g}$ can be obtained in the same way and a small allowance could be put into $\sigma_{0,g\to g+1}$. When the resonance parameters are not known, e.g., in the unresolved resonances, they must be generated using mean values and the probability distribution in the manner discussed earlier. Once an acceptable sequence has been generated, it may be used with various temperatures to determine the dependence of resonance absorption on temperature.[85]

8.3i Strongly Overlapping Resonances

At high neutron energies, the resonances for a given nuclide generally overlap strongly. This is largely due to Doppler broadening because, in accordance with its definition, the Doppler width varies as the square root of the resonance energy. Thus, the resonances are bound to be broad at high energies, so that overlapping is favored. Furthermore, the resonances are more closely spaced at

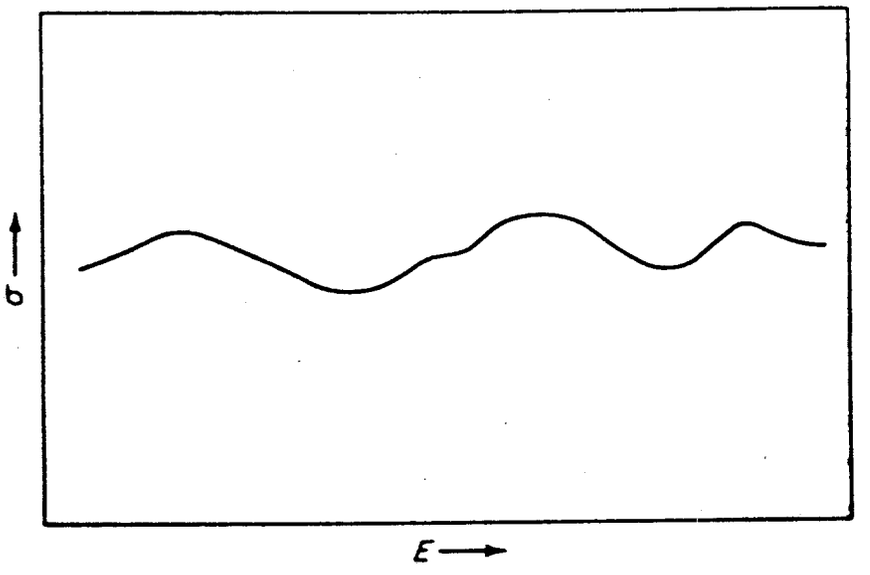

FIG. 8.13 OVERLAPPING RESONANCES AT HIGH NEUTRON ENERGIES.

high than at low energies, mainly because more J and l values are represented. At high energies, therefore, it is expected that the resonance peaks will protrude only slightly above a more-or-less constant cross-section background,[86] as in Fig. 8.13. These peaks cannot be resolved in measured cross sections but must be inferred from the systematics of the resonance parameters as described in §8.2c. Such energy regions are important for fast reactors and they may be treated in a particularly simple manner.

At high neutron energies, the NR approximation must be valid because E_t is so large. It is then useful to define an effective cross section, $\bar{\sigma}_x$, as the ratio of reaction rate to flux averaged over an energy interval ΔE, so that there are many resonances in this interval, but the variation in the average resonance parameters is assumed to be small. By using the NR approximation for the flux, as in equation (8.51), neglecting the variations in E over the interval ΔE, and writing

$$\sigma(E) = \sigma_m + \sigma_r(E),$$

where σ_r includes all the resonances and the potential scattering,

$$\bar{\sigma}_x = \frac{\int_{\Delta E} \dfrac{\sigma_x(E)}{\sigma_m + \sigma_r(E)}\, dE}{\int_{\Delta E} \dfrac{1}{\sigma_m + \sigma_r(E)}\, dE}. \tag{8.75}$$

Let

$$\sigma_x(E) = \bar{\sigma}_x + \delta\sigma_x(E)$$

and

$$\sigma_r(E) = \bar{\sigma}_r + \delta\sigma_r(E),$$

where $\bar{\sigma}_x$ and $\bar{\sigma}_r$ are the local (over ΔE) energy averages of σ_x and σ_r, i.e.,

$$\bar{\sigma}_x = \frac{1}{\Delta E}\int_{\Delta E} \sigma_x(E)\, dE$$

and

$$\bar{\sigma}_r = \frac{1}{\Delta E}\int_{\Delta E} \sigma_r(E)\, dE.$$

Hence, the integrals of $\delta\sigma_x$ and $\delta\sigma_r$ over ΔE vanish; thus,

$$\int_{\Delta E} \delta\sigma_x(E)\, dE = \int_{\Delta E} \delta\sigma_r(E)\, dE = 0.$$

The essential assumption of strong overlap is now made, namely, that $\delta\sigma_x$ and $\delta\sigma_r$ are small compared to $\bar{\sigma}_x$ and $\bar{\sigma}_r$. With this assumption,

$$\frac{1}{\sigma_m + \sigma_r(E)} = \frac{1}{\bar{\sigma}\left[1 + \dfrac{\delta\sigma_r(E)}{\bar{\sigma}}\right]} \approx \frac{1}{\bar{\sigma}}\left[1 - \frac{\delta\sigma_r(E)}{\bar{\sigma}}\right],$$

where $\bar{\sigma} \equiv \sigma_m + \bar{\sigma}_r$, and then equation (8.75) becomes

$$\bar{\sigma}_x = \frac{\int_{\Delta E} (\bar{\sigma}_x + \delta\sigma_x)\left(1 - \frac{\delta\sigma_r}{\bar{\sigma}}\right) dE}{\int_{\Delta E} \left(1 - \frac{\delta\sigma_r}{\bar{\sigma}}\right) dE}.$$

Since the integrals of $\delta\sigma_x$ and $\delta\sigma_r$ are zero, it follows that

$$\tilde{\sigma}_x = \bar{\sigma}_x - \frac{1}{\bar{\sigma}}(\overline{\delta\sigma_x\, \delta\sigma_r}), \tag{8.76}$$

where

$$\overline{\delta\sigma_x\, \delta\sigma_r} = \frac{1}{\Delta E}\int_{\Delta E} \delta\sigma_x(E)\, \delta\sigma_r(E)\, dE.$$

By using the definitions of $\sigma_x(E)$ and $\sigma_r(E)$ given above, equation (8.76) may be written as

$$\tilde{\sigma}_x = \bar{\sigma}_x - \frac{1}{\bar{\sigma}}(\overline{\sigma_x\sigma_r} - \bar{\sigma}_x\bar{\sigma}_r), \tag{8.77}$$

where

$$\overline{\sigma_x\sigma_r} = \frac{1}{\Delta E}\int_{\Delta E} \sigma_x(E)\sigma_r(E)\, dE.$$

In computing the energy averaged quantities in equation (8.77), account must be taken of all the sequences of resonances, i.e., all the l and J values. Since the overlap of resonances is strong only at sufficiently high neutron energies, e.g., $E \gtrsim 100$ keV for the fertile nuclides and more than a few kilo-electron volts for fissile nuclides, p-wave resonances will be important; hence $l = 0$ and $l = 1$ and $J \leqslant I + \frac{3}{2}$ values must be included. Within each sequence of resonances the averages must be taken over the distributions of resonance parameters. In the evaluation of $\bar{\sigma}_x$ and $\bar{\sigma}_r$, each sequence contributes an average cross section as in equations (8.40) and (8.41). Alternatively, $\bar{\sigma}_x$ and $\bar{\sigma}_r$ can be derived from experimental cross sections if they are available.It may be noted that $\bar{\sigma}_x$ and $\bar{\sigma}_r$ are independent of temperature; the temperature dependence is included in $\overline{\sigma_x\sigma_r}$ (or $\overline{\delta\sigma_x\, \delta\sigma_r}$).

The quantity $\overline{\delta\sigma_x\, \delta\sigma_r}$, which is required to derive $\tilde{\sigma}_x$ from $\bar{\sigma}_x$ by equation (8.76), can be readily computed for a particular sequence of resonances,[87] but when several sequences are involved, including p-wave resonances, the situation is more complicated.[88] Moreover, in either case there will be some uncertainties in the resonance parameters in the unresolved resonance region. This difficulty is particularly acute for the fissile nuclides (§8.2b).[89] Qualitatively, however, the results can be understood in a simple way. First, it is to be expected that $\delta\sigma_x(E)$ and $\delta\sigma_r(E)$ will exhibit similar behavior as functions of E. For example, both will tend to be positive if there are an unusually large number of resonances or a

few unusually strong resonances near energy E. Hence, $\overline{\delta\sigma_x\,\delta\sigma_r}$ will be a positive quantity and, from equation (8.76), $\bar{\sigma}_x < \bar{\sigma}_x$.

An estimate of $\overline{\delta\sigma_x\,\delta\sigma_r}$ can be made in the following manner. At an energy E where there is a strong overlap of resonances, the Doppler width, Δ, must be large compared with the average spacing, $\tilde{D}$, between resonances of all kinds, i.e., $\Delta/\tilde{D} \gg 1$; it should be noted that $\tilde{D}$ refers to all the important resonances and not merely to those of one sequence as in §8.2c. In addition, for such resonances $\Delta \gg \Gamma$, so that the effective width of the resonance may be taken as the Doppler width.

The number, n_r, of resonances which make important contributions to the cross section at energy E will be roughly those lying within the energy interval 2Δ about E, i.e., $n_r \approx 2\Delta/\tilde{D}$. As E is varied through a range ΔE, this number may be expected to vary by amounts of the order of $\pm\sqrt{n_r}$; hence, the fractional variation is given by

$$\frac{1}{\sqrt{n_r}} = \sqrt{\frac{\tilde{D}}{2\Delta}}.$$

Because of the change in the number of contributing resonances, there will be corresponding variations in σ_x of the same order of magnitude, so that

$$\frac{|\delta\sigma_x(E)|}{\bar{\sigma}_x} \approx \sqrt{\frac{\tilde{D}}{2\Delta}}.$$

It is to be expected, therefore, that

$$\overline{\delta\sigma_x\,\delta\sigma_r} \approx \bar{\sigma}_x\bar{\sigma}_r\frac{\tilde{D}}{2\Delta}$$

or

$$\overline{\delta\sigma_x\,\delta\sigma_r} = C\bar{\sigma}_x\bar{\sigma}_r\frac{\tilde{D}}{2\Delta}, \tag{8.78}$$

where C is a number of the order of magnitude of unity.

Equation (8.78) has been confirmed by more detailed analysis for a single sequence of levels, in which case $\tilde{D} = \bar{D}^{[90]}$; in addition, it is found that C is quite insensitive to the temperature. Hence, the temperature dependence of $\bar{\sigma}_x$ is primarily due to the Doppler width in equation (8.78). Upon combining this equation with equation (8.76), it is found that

$$\frac{\partial\bar{\sigma}_x}{\partial T} = \frac{C\bar{\sigma}_x\bar{\sigma}_r}{\bar{\sigma}}\frac{\tilde{D}}{4T\Delta} \propto T^{-3/2}.$$

Such expressions would be used in determining the temperature coefficient of reactivity of a reactor.

Once the effective reaction cross section $\bar{\sigma}_x$ has been obtained, it may be used, for most purposes, in place of σ_x in generating multigroup constants. It is

evident that $\bar{\sigma}_x$ will be a slowly varying function of neutron energy whereas σ_x contains all the resonance structure. The replacement of σ_x by $\bar{\sigma}_x$ could, however, lead to some errors in determining transport effects, but such errors are generally small, especially as at high energies $\bar{\sigma}_x$ and $\tilde{\sigma}_x$ do not differ greatly. Although the absolute differences between these quantities are not important, their variations with temperature are significant in determining the safety of fast reactors (§8.4e).

The procedures described above are applicable at high neutron energies where the resonance Doppler width, Δ, is large compared to the mean spacing, $\tilde{D}$. At lower energies, e.g., in the vicinity of 10 keV for the fertile nuclides, where Δ and $\tilde{D}$ are comparable, the overlap of resonances is significant, but there does not appear to be any simple way to determine it. The best approach in this region is a purely numerical one. Thus, a sequence of resonances may be constructed by sampling from the expected distribution of resonance parameters.[91] A Doppler broadened cross section is thus obtained and it may be used to evaluate the effective cross sections and their variation with temperature. This must be done for a number of independent sequences, to make sure that the results are not sensitive to the precise sequence selected.

8.4 RESONANCE ABSORPTION IN HETEROGENEOUS SYSTEMS

8.4a Method of Collision Probabilities

In most reactors and in many critical experiments, the absorbing material, e.g., fuel rods or foils, is arranged heterogeneously within the bulk of the moderator. Such heterogeneous systems have been of interest since the earliest reactor studies indicated that, in order to achieve criticality with natural uranium fuel and a graphite moderator, it was necessary to have the uranium in lumps or rods. As a result of such a heterogeneous arrangement, the resonance absorption in uranium-238, which caused a loss of neutrons, was significantly less than in a homogeneous system of the same over-all composition.

In the first theories to be developed for resonance absorption in heterogeneous systems,[92] the absorption was divided into separate contributions from the surface of the fuel rod and from its volume. Good resonance parameters were not available for quantitative comparison with experimental data, but the qualitative features of the theory seemed to agree with the early experiments. Some years later, a different theoretical treatment of resonance absorption was reported from the U.S.S.R.[93] and efforts were made to understand and reconcile the two alternative approaches. In the course of these studies, the collision probability method for determining resonance absorption in heterogeneous systems was developed.[94] It is this method which will be described here. It will

be seen that, as for a homogeneous medium, the problem is to find the fine structure of the neutron flux, but now it must be known as a function of space as well as of energy.

Consider a two-region system having the absorbing material plus some admixed moderator in region F with volume V_F, and the main external moderator in region M, volume V_M (Fig. 8.14). The moderator in region F may be different from that in region M. The respective regions may be complex geometrically, e.g., region F might be a periodic array of cruciform fuel rods, but within each region the densities and compositions are assumed to be uniform. The macroscopic scattering cross sections of the moderator, σ_{mF} in region F and σ_{mM} in region M, are taken to be constant or slowly varying with energy, whereas the cross sections of the absorber (heavy) nuclei in region F, i.e., $\sigma_{aF}(E)$ and $\sigma_{sF}(E)$, have resonances. A time-independent neutron flux is assumed to exist in both regions, supplied by moderation from a fission source at higher energies.

The collision probabilities P_F and P_M that will be used are defined in the following manner. Let $P_i(E)$ be the probability that a neutron originating in region i with an energy E will make its next collision in the other region; for example, if region F is an isolated rod, then P_F will be an escape probability (§2.7b). In addition, let $\phi_F(E)$ and $\phi_M(E)$ be the volume-averaged neutron fluxes in the two regions.

Consider the total collision rate of neutrons of energy E in region F. If the total cross section in this region is denoted by σ_{tF}, where

$$\sigma_{tF} = \sigma_{aF} + \sigma_{sF} + \sigma_{mF}, \tag{8.79}$$

then the total collision rate will be

$$\text{Collision rate in region F} = V_F \sigma_{tF}(E)\phi_F(E). \tag{8.80}$$

Some of the neutrons of energy E will have had their last collisions in region M;

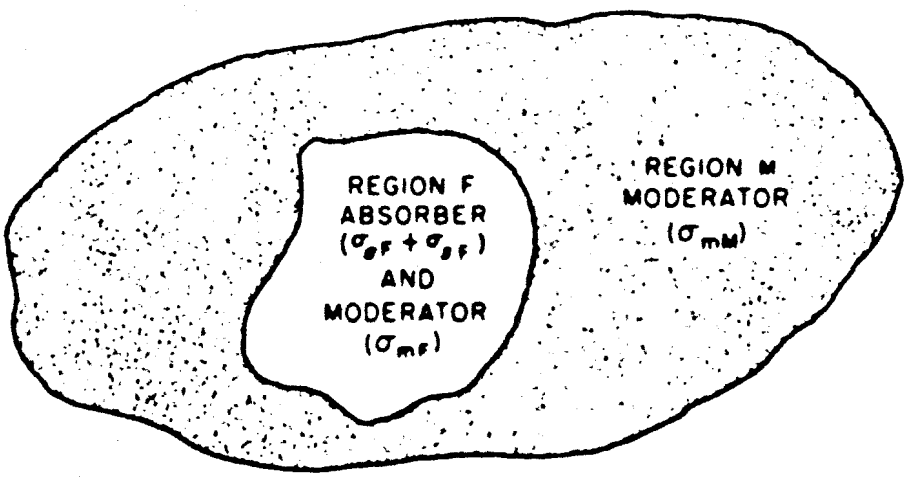

FIG. 8.14 ABSORBER (F) AND MODERATOR (M) REGIONS.

that is to say, they will have arrived at energy E by making a collision in region M and will make their next collision in region F. Hence,

$$\text{Collision rate in region F due to neutrons from region M} = P_M(E)V_M \int_E^{E/\alpha_{mM}} \frac{\sigma_{mM}\phi_M(E')}{(1-\alpha_{mM})E'}\,dE', \quad (8.81)$$

where the integral multiplied by V_M is the rate at which neutrons reach E in region M and P_M is the probability that they will make their next collision in region F.

Similarly, the collision rate in region F due to neutrons which have arrived at energy E by making a collision in the same region is

$$\text{Collision rate in region F due to neutrons from region F} = [1-P_F(E)]V_F\left\{\int_E^{E/\alpha_{mF}} \frac{\sigma_{mF}\phi_F(E')}{(1-\alpha_{mF})E'}\,dE' + \int_E^{E/\alpha_a} \frac{\sigma_{aF}\phi_M(E')}{(1-\alpha_a)E'}\,dE'\right\}, \quad (8.82)$$

where the first integral represents the scatterings from the admixed moderator in region F and the second those from the absorber nuclei. The sum of equations (8.81) and (8.82) must equal equation (8.80); hence,

$$V_F\sigma_{tF}(E)\phi_F = (1-P_F)V_F\left\{\int_E^{E/\alpha_{mF}} \frac{\sigma_{mF}\phi_F}{(1-\alpha_{mF})E'}\,dE' + \int_E^{E/\alpha_a} \frac{\sigma_{aF}\phi_F}{(1-\alpha_a)E'}\,dE'\right\} + P_M V_M \int_E^{E/\alpha_{mM}} \frac{\sigma_{mM}\phi_M}{(1-\alpha_{mM})E'}\,dE'. \quad (8.83)$$

This is the fundamental balance equation for computing resonance absorption in heterogeneous assemblies. It will be observed that if there is only one region, namely, region F, so that $P_F = 0$ and $V_M = 0$, then equation (8.83) reduces to equation (8.50) for a homogeneous system.

Although equation (8.83) is exact, some approximations must be made in deriving the collision probabilities. In most heterogeneous systems, the spatial distribution of neutrons, at least for those with energies not near a resonance peak, is largely independent of position in each region. Consequently, the reasonable postulate, called the *flat source* (or *flat flux*) approximation, is made for deriving P_F and P_M. In this approximation, $P_F(E)$ and $P_M(E)$ are obtained for uniform, i.e., spatially constant, sources of neutrons in regions F and M. It is evident, therefore, that $P_F(E)$ and $P_M(E)$ are the quantities discussed in §§2.8b,c. In the present case, every collision removes a neutron from energy E, because it is either absorbed or its energy is changed by scattering. Thus, in treating the neutrons at energy E as a one-speed problem, both media appear to be purely absorbing. Hence, P_F in the present treatment is equivalent to $P_{F\to M}$ of §2.8c, and P_M is equivalent to $P_{M\to F}$.

The general reciprocity relation, i.e., equation (2.101), may now be written as

$$\sigma_{\mathrm{mM}} V_{\mathrm{M}} P_{\mathrm{M}} = \sigma_{t\mathrm{F}} V_{\mathrm{F}} P_{\mathrm{F}},$$

and if this is used to eliminate P_{M} from equation (8.83), the result is

$$\sigma_{t\mathrm{F}}\phi_{\mathrm{F}} = (1 - P_{\mathrm{F}})\left\{\int_E^{E/\alpha_{\mathrm{mF}}} \frac{\sigma_{\mathrm{mF}}\phi_{\mathrm{F}}}{(1 - \alpha_{\mathrm{mF}})E'}\, dE' + \int_E^{E/\alpha_{\mathrm{a}}} \frac{\sigma_{s\mathrm{F}}\phi_{\mathrm{F}}}{(1 - \alpha_{\mathrm{a}})E'}\, dE'\right\}$$

$$+ P_{\mathrm{F}}\sigma_{t\mathrm{F}} \int_E^{E/\alpha_{\mathrm{mM}}} \frac{\phi_{\mathrm{M}}}{(1 - \alpha_{\mathrm{mM}})E'}\, dE'. \tag{8.84}$$

In order to proceed further, the narrow resonance approximation may be made for both the moderator integrals in equation (8.84). Thus, in the first and third integrals, the flux may be replaced by an asymptotic value normalized so that

$$\phi_{\mathrm{F}} = \phi_{\mathrm{M}} = \frac{1}{E}.$$

The integrals can then be evaluated to give

$$\sigma_{t\mathrm{F}}\phi_{\mathrm{F}} = (1 - P_{\mathrm{F}}) \int_E^{E/\alpha_{\mathrm{a}}} \frac{\sigma_{s\mathrm{F}}\phi_{\mathrm{F}}}{(1 - \alpha_{\mathrm{a}})E'}\, dE' + [\sigma_{\mathrm{mF}} + P_{\mathrm{F}}(\sigma_{a\mathrm{F}} + \sigma_{s\mathrm{F}})]\frac{1}{E}. \tag{8.85}$$

As before, for a homogeneous system P_{F} would be zero, and this equation would reduce to equation (8.71).

Values of P_{F} may be derived from the considerations of §2.8c, and equation (8.85) can be solved numerically (§8.4c) to yield the flux, $\phi_{\mathrm{F}}(E)$. From the flux, the reaction rates $\int \sigma_x\phi_{\mathrm{F}}\, dE$ and the effective cross sections can be computed.[95] It will now be shown, however, that if a rational approximation is used for P_{F} (§2.8b), the solution to equation (8.85) is equivalent to that for a particular homogeneous system. For many practical calculations, the rational (and equivalence) relations are sufficiently accurate.

8.4b Equivalence Relations

On the basis of the various rational approximations considered in §2.8b *et seq.*, the escape probability, P_{F} (or $P_{\mathrm{F}\to\mathrm{M}}$), can be written in the general form

$$P_{\mathrm{F}}(E) = \frac{\sigma_e}{\sigma_{t\mathrm{F}}(E) + \sigma_e}$$

where the quantity σ_e is a reciprocal length and therefore has the dimensions of a macroscopic cross section. As will soon be seen, σ_e may be regarded as an effective moderator scattering cross section representing the effects of heterogeneity on the resonance absorption. For the particular case of an isolated fuel

rod, $P_F = P_{esc}$ in the terminology of §2.8b, and equation (2.114) gives the rational approximation for which

$$\sigma_e = \frac{1}{\bar{R}_F},$$

where $\bar{R}_F$ is the average chord length in region F, as defined in §2.8b. According to equation (2.112), $\bar{R}_F$ is related to the volume V_F and to A, the area of the surface common to the two regions, by

$$\bar{R}_F = \frac{4V_F}{A}.$$

When the absorbing region is more complicated, e.g., a periodic array, then P_F is not just the escape probability, but $P_{F\to M}$ for which the rational approximation is given by equation (2.122). In this case,

$$\sigma_e = \frac{1 - C}{\bar{R}_F},$$

where C is the Dancoff correction (§2.8c). When C is computed for a "black" absorber, i.e., one which absorbs all neutrons entering region F, it is found to be independent of energy. Consequently, σ_e then has the feature of being energy independent, which is desirable if it is to be equivalent to a moderator scattering cross section.

If the fully rational approximation of equation (2.123) is used for P_F, then

$$\sigma_e = \frac{1}{\tilde{R}_F},$$

where $\tilde{R}_F$, the effective chord length in region F, defined by equation (2.124), in the present notation is

$$\tilde{R}_F = \bar{R}_F \frac{1 + \sigma_{mM}\bar{R}_M}{\sigma_{mM}\bar{R}_M}, \tag{8.86}$$

where $\bar{R}_M$ is the mean chord length in region M. For well-separated fuel regions, $\sigma_{mM}\bar{R}_M \gg 1$ and then $\tilde{R}_F = \bar{R}_F$ and $\sigma_e = 1/\bar{R}_F$, as obtained above for an isolated fuel rod.

Upon inserting the rational approximation for P_r into equation (8.85) and multiplying by $(\sigma_{sr} + \sigma_e)/\sigma_{tr}$, it follows that

$$(\sigma_{tr} + \sigma_e)\phi_r(E) = \int_E^{E/\alpha_a} \frac{\sigma_{sF}\phi_F}{(1 - \alpha_a)E'}\,dE' + (\sigma_{mr} + \sigma_e)\frac{1}{E}. \tag{8.87}$$

Since $\sigma_{tr} = \sigma_{ar} + \sigma_{sr} + \sigma_{mr}$, it is seen that in equation (8.87) the admixed moderator cross section σ_{mr} always appears added to σ_e. Moreover, by comparison with equation (8.71), it is evident that, for heterogeneous assemblies, $\sigma_{mr} + \sigma_e$ plays the same role as σ_m does for a homogeneous system. Hence, as

stated above, σ_e represents the contribution of heterogeneity to the moderator (scattering) cross section.

Furthermore, it is to be expected that for very closely-spaced fuel regions, the admixed moderator in region F would have the same effectiveness as the outside moderator in region M. This can be shown by considering the fully rational approximation. For closely-spaced fuel regions, $\sigma_{mM}\bar{R}_M \ll 1$; then equation (8.86) gives

$$\tilde{R}_F = \frac{\bar{R}_F}{\sigma_{mM}\bar{R}_M} \quad \text{and} \quad \sigma_e = \frac{\sigma_{mM}\bar{R}_M}{\bar{R}_F}.$$

But since $\bar{R}_i = 4V_i/A$, where A is the common boundary between the fuel region F and the moderator region M,

$$\sigma_e = \sigma_{mM}\frac{V_M}{V_F},$$

and hence,

$$\sigma_{mF} + \sigma_e = \sigma_{mF} + \frac{V_M}{V_F}\sigma_{mM}.$$

Since, according to equation (8.87), $\sigma_{mF} + \sigma_e$ determines the effect of the moderator on the flux, the result just derived shows that, for closely-spaced fuel elements, a moderator nucleus has the same effect regardless of whether it is in the fuel region or in the bulk moderator.

From the fact that $\sigma_{mF} + \sigma_e$ in a heterogeneous system is equivalent to σ_m in a homogeneous system, it appears that the ratio of $\sigma_{mF} + \sigma_e$ to the absorber cross sections $\sigma_{aF} + \sigma_{sF}$ will determine the energy-dependence of the neutron flux. This conclusion can be cast in the form of a useful equivalence relation. Suppose there are a number of systems, possibly with different moderators, which have the same ratios of various kinds of heavy absorbing nuclei, e.g., the same ratio of uranium-235 to uranium-238, and are at the same temperature. Then, for all these systems σ_{aF} and σ_{sF} will be the same, except for a constant factor equal to N_a, the total number of heavy nuclei per unit volume. If equation (8.87) is divided by N_a, the result can be written as

$$\left(\frac{\sigma_{aF} + \sigma_{sF}}{N_a} + \frac{\sigma_{mF} + \sigma_e}{N_a}\right)\phi_F(E) = \int_E^{E/\alpha_a} \frac{\sigma_{sF}\phi_F}{N_a(1-\alpha_a)E'}\,dE' + \frac{\sigma_{mF} + \sigma_e}{N_a}\frac{1}{E}. \quad (8.88)$$

The value of $(\sigma_{aF} + \sigma_{sF})/N_a$ is the same for all the systems under consideration and so all systems having the same values of $(\sigma_{mF} + \sigma_e)/N_a$ will have the same flux (relative to the asymptotic flux) and the same reaction rates and resonance integrals (per heavy nucleus).

The result derived above may be stated as an *equivalence principle*: heterogeneous systems having the same values of $(\sigma_{mF} + \sigma_e)/N_a$, regardless of the nature of the moderator, will have the same resonance integrals, and a heterogeneous system will have the same resonance integral as a homogeneous system

with σ_m/N_a equal to $(\sigma_{mF} + \sigma_e)/N_a$. The equivalence applies also to reaction rates but not to the *probabilities* of reaction, since the latter depend on the competition between reaction and slowing down. The slowing down is determined by ξ_{mM} and σ_{mM}, and these quantities will depend on the particular moderator in each assembly.

The expected equivalence has been confirmed experimentally in the comparison of heterogeneous systems with either uranium metal or uranium dioxide (UO_2) as the fuel.[96] In general, the equivalence principle is accurate enough to be very useful, particularly in comparing similar systems, although where high precision is desirable the rational approximation to P_F should not be used. Other possibilities are then to solve equation (8.85) numerically (§8.4c) or to utilize some adjusted rational approximations for P_F.[97]

When the rational approximation to P_F is employed, so that equation (8.87) is to be solved for the flux, there is no fundamental difference between the treatment for homogeneous and heterogeneous systems. Any of the methods already described for homogeneous systems may be used. For example, the integral in equation (8.87) may be evaluated by the NR or NRIM approximation or by means of an intermediate theory. All the results obtained previously for reaction rates and group cross sections hold when $(\sigma_{mF} + \sigma_e)/N_a$ for the heterogeneous assembly is equal to σ_m/N_a for the homogeneous system. The situation is most easily stated in terms of microscopic cross sections. The quantity $(\sigma_{mF} + \sigma_e)/N_a$ is similar to a microscopic cross section per absorber nucleus, and this must remain unchanged in the equivalent homogeneous system if the group microscopic cross sections are to be preserved. The quantity $(\sigma_{mF} + \sigma_e)/N_a$ is frequently denoted by σ_p, an effective microscopic cross section.

In the foregoing theoretical development using collision probabilities, three important approximations were made. In reverse order, they were (*a*) a rational approximation for P_r, (*b*) the NR approximation for moderator collisions, and (*c*) the flat source approximation. These will be considered in turn.

The main reason for using the rational approximation to P_F is that it leads to the equivalence relations. Methods developed for homogeneous systems can then be applied directly to heterogeneous systems and experimental results may be compared for a variety of configurations. As seen in §2.8b, however, the rational approximation is of limited accuracy. Moreover, if equation (8.85) is solved numerically, accurate values of P_r may be used instead of a rational approximation.

As far as the NR approximation is concerned, it is not required, in principle, since numerical solution of equation (8.84) is possible just as it is for equation (8.85). But the NR approximation for moderator collisions does permit a substantial simplification which is usually accurate enough for practical purposes.

The crucial feature of the method of collision probabilities is the use of the flat source approximation to determine P_r and P_M. If this approximation is not used, then it becomes necessary to determine the spatial dependence of the flux

by Monte Carlo methods,[98] by multigroup calculations with a fine energy structure,[99] or in other ways.[100] The problem is most troublesome for large fuel lumps and for resonances with much scattering, as is the case for some of the stronger, low-energy resonances in tungsten for which Γ_n/Γ is the order of ten[101] and for the principal resonances in manganese and cobalt[102] which are often used as neutron-flux detectors.

8.4c Numerical Computation of Resonance Integrals

A number of instances have been mentioned in preceding sections in which numerical methods must be used to evaluate resonance absorption, e.g., when resonances overlap either as a result of Doppler broadening (with $\Delta \approx \tilde{D}$) or because of accidental near coincidence of resonance energies (§8.1e) or when accurate collision probabilities are used for a heterogeneous system. The same general procedure may be used in all these situations provided the collision probabilities may be regarded as known; in practice this means that they are computed using the flat-source approximation. Such a general approach is described below[103]; with the available computer codes, it can be used conveniently even when simpler approximations would be adequate.

Suppose, for example, that it is desired to solve equation (8.85) for the neutron flux; the cross sections and collision probability, P_r, are to be regarded as known (calculated or given) functions of neutron energy. Once the flux is known, resonance integrals and effective cross sections may be evaluated by using the equations in §8.3a.

For numerical work, it is convenient to transform from the flux to the collision density as the fundamental unknown, because the latter is a much smoother function of the energy. For example, in the NR approximation the collision density shows no fine structure in the vicinity of a resonance. Furthermore, it is convenient to use the lethargy, u, in place of the neutron energy as the independent variable (§4.7a); thus,

$$u = \ln \frac{E_{max}}{E},$$

where E_{max} is some energy above which the flux has its asymptotic form, i.e., it is proportional to $1/E$.

Let the volume averaged collision density in the fuel region F at lethargy u be denoted by $F(u)$, so that

$$F(u) = \sigma_{tF}\phi_r(E), \tag{8.89}$$

where σ_{tF} is the total fuel cross section, as given by equation (8.79). It should be noted that although $F(u)$ is expressed as a function of lethargy, it is actually the

collision density per unit energy.[104] By using equation (8.89) and converting the variable from energy to lethargy, equation (8.85) becomes

$$F(u) = [1 - P_F(u)] \int_{u-\Delta_\alpha}^{u} F(u') \frac{\sigma_{sF}(u')}{(1 - \alpha_a)\sigma_{tF}(u')}\, du' + [\sigma_{mF} + P_F(\sigma_{aF} + \sigma_{sF})] \frac{e^u}{E_{max}}, \tag{8.90}$$

where

$$\Delta_\alpha \equiv \ln \frac{1}{\alpha_a}.$$

Equation (8.90) may be solved by approximating the integral by a sum, using a numerical quadrature formula, such as Simpson's rule. The solution is first sought for $u = n\,\Delta u$, where $n = 1, 2, 3, \ldots$, until the desired range in u has been covered. A number of computer codes have been written to carry out this program or its equivalent.[105] They include the computation of $\sigma_{aF}(E)$ and $\sigma_{sF}(E)$ from input resonance parameters and temperature; they contain collision probabilities for various geometries, and as output they give the resonance integrals or effective cross sections, as desired. For example, the resonance integral for absorption is given by

$$I = E_{max} \int F(u) \frac{\sigma_{aF}(u)}{\sigma_{tF}(u)}\, e^{-u}\, du. \tag{8.91}$$

The codes are employed extensively for generating resonance absorption cross sections for use in multigroup calculations. The results obtained in this manner may be expected to be reliable provided that the input resonance parameters are accurate and the flat-source approximation is adequate for the P_F computation.

In a numerical procedure such as the one just outlined, there is evidently no need to use a NR approximation for the moderator integral, since it too could be evaluated numerically. Furthermore, homogeneous and various heterogeneous geometries can be treated in the same program.

8.4d Approximate Dependence on Geometry

The approximate dependence of resonance integrals on the geometry of a heterogeneous system may be derived in the following manner. The rational approximation for P_r is made, so that the equivalence relation can be employed and the NR approximation is used for all collisions. Incidentally, the results obtained also hold for the NRIM approximation.

For a homogeneous system with a single unbroadened resonance, the resonance integral may be derived from equation (8.64) for the resonance absorption; if the interference term is neglected, the result is

$$I_{x1} = \frac{\frac{1}{2}\pi\sigma_0\Gamma_x}{E_1} \frac{1}{\sqrt{1 + \dfrac{\sigma_0}{\sigma_m + \sigma_{pot}}}} = I_{\infty,x1} \frac{1}{\sqrt{1 + \dfrac{\sigma_0}{\sigma_m + \sigma_{pot}}}}, \tag{8.92}$$

where $I_{\infty,xi}$ is the resonance integral for infinite dilution, i.e., with $\phi = 1/E_i$ throughout the resonance. For the equivalent heterogeneous system, σ_m must be replaced by $\sigma_{mF} + \sigma_e$. In addition, for the most important resonances,

$$\sigma_0 \gg \sigma_{mF} + \sigma_e + \sigma_{pot};$$

hence, equation (8.92) can be written as

$$I_{xi} \approx I_{\infty,xi}\sqrt{\frac{\sigma_{mF} + \sigma_{pot}}{\sigma_0} + \frac{\sigma_e}{\sigma_0}}. \tag{8.93}$$

For a single resonance, $(\sigma_{mF} + \sigma_{pot})/\sigma_0$ is a constant and all the geometrical dependence is contained in σ_e. For an isolated fuel region, it was seen earlier that $\sigma_e = 1/\bar{R}_F = A/4V_F$; hence,

$$\sigma_e \propto \frac{A}{V_F} \propto \frac{A}{M},$$

where M, the mass of the fuel region, is equal to $V_F\rho_F$, with ρ_F the density.* Hence, from equation (8.93) it appears that expressions of the form

$$I_{xi} \approx \sqrt{a + b\frac{A}{M}} \approx a' + b'\sqrt{\frac{A}{M}} \tag{8.94}$$

may be approximately valid. This approximate dependence of the resonance integral on the geometry, i.e., area and mass, of the fuel region was first suggested by Russian physicists[106] and it has been confirmed by experiment, as will be seen in the next section. However, in view of the many approximations made in deriving equation (8.94) it would not be expected to be a very precise relationship.

In some reactors, the geometrical complexity of the fuel elements in a heterogeneous array may be quite considerable, e.g., fuel rods may be grouped in clusters so that different rods have different P_F values. For survey calculations, the rational approximation may be generalized, but for greater accuracy it is necessary to resort to Monte Carlo methods.[107] Once Monte Carlo or experimental experience has been gained with a particular configuration, it may be possible to use adjusted collision probabilities to give reliable results.

In the foregoing treatment Doppler broadening has been ignored. It is of interest, of course, to know how the resonance integrals in a heterogeneous system will change with temperature. From the discussion of the $J(\zeta, \beta)$ function in §8.3e, it would appear that the effect of temperature will be quite complicated. Both detailed calculations and experiment, however, have indicated that the approximate relationship

$$I = I_0(1 + \beta\sqrt{T}), \tag{8.95}$$

where T is the absolute temperature and β is roughly constant, is obeyed.[108]

* Conventionally, the surface area of the fuel region is represented by S; the symbol A is used here, however, for consistency with other parts of the book.

A special problem may arise when the temperature in a fuel rod is markedly nonuniform. In such cases, an "effective temperature" is used in determining the Doppler broadening of the resonances.[109]

8.4e The Doppler Effect in Fast Reactors

The Doppler effect and its influence on the temperature coefficient of reactivity are of considerable importance in connection with fast-reactor safety. Consequently, this aspect of the resonance problem has received much attention. Nevertheless, because of the uncertainties and complexities involved, the theoretical treatment is not in a very satisfactory state. The following discussion will therefore be restricted to some qualitative comments and references to the literature.[110]

In a fast (breeder) reactor, the fissile material would be largely plutonium-239 with some plutonium-241; the fertile material, uranium-238 (and some plutonium-240) acts as a neutron absorber. The low-energy part of the neutron spectrum, below about 10 keV, will be markedly affected by the presence of elements of relatively low mass number, such as carbon, oxygen, and sodium.

As already seen, resonances at sufficiently high neutron energies overlap strongly, and hence Doppler broadening produces little change. On the other hand, at sufficiently low energies there are very few neutrons since most have been absorbed during the moderation process. Consequently, in practice there will be an intermediate energy region from which the contribution of Doppler broadening to reactivity is most important (Fig. 8.15). This energy range is frequently in the neighborhood of 1 keV, although for a very fast system it could be above 10 keV.

For uranium-238, it is clear that Doppler broadening will increase the resonance absorption (§8.3e) and decrease the reactivity. This effect can be

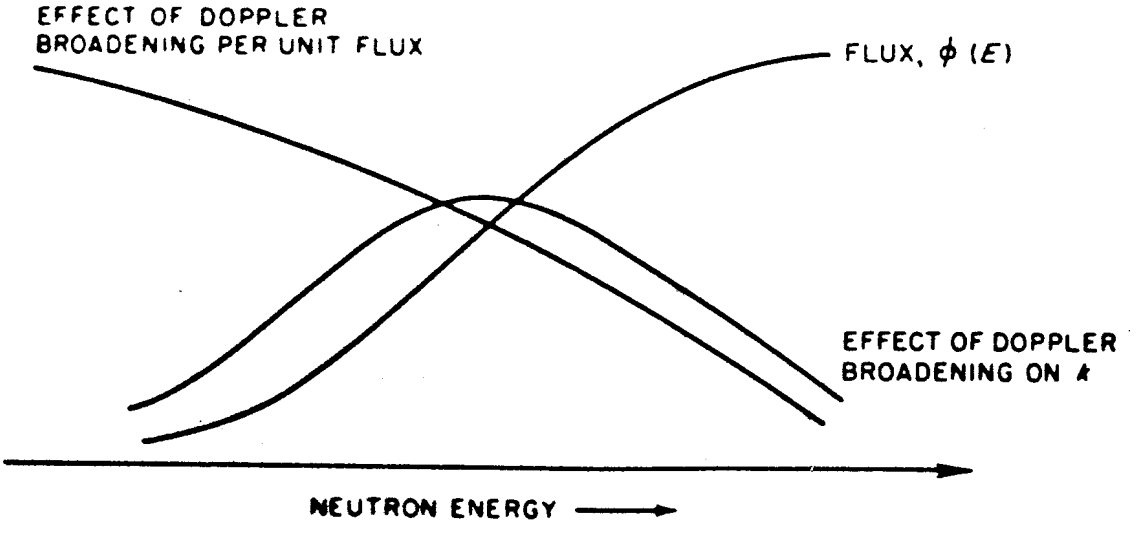

FIG. 8.15 DOPPLER EFFECT ON REACTIVITY AS FUNCTION OF ENERGY.

calculated with a considerable degree of confidence. For fissile materials, such as plutonium-239, Doppler broadening increases the effective cross sections for both fission and radiative capture, and since the resonances are resolved only up to neutron energies of about 50 eV, substantially all of the reactivity effects in a fast system arise from the broadening of unresolved resonances. Here doubts concerning the resonance parameters, including mean values, distributions, and correct forms, make the calculations highly uncertain.

Moreover, there is some cancellation of the effects due to increases in both the (n, γ) and (n,f) cross sections. It is likely that the effective capture cross section increases more rapidly with temperature than does the effective fission cross section because the resonances which are important for fission tend to have larger widths than those which are important for neutron capture. Hence, it is not clear, in principle, whether the Doppler broadening of the resonances in the fissile material will increase or decrease the reactivity of a fast-neutron system.

Experimental efforts to study the Doppler effects for capture and fission in fissile materials have not clarified the situation, except in showing that the net effect is small.[111] Consequently, if there is sufficient uranium-238 present, e.g., about three times as much as the fissile species, the over-all result of the Doppler broadening is to produce a negative temperature coefficient of reactivity. The calculations indicate that $\partial k/\partial T$ (or $(\Delta k/k)/\Delta T$) ranges from about -10^{-6} per °K up to perhaps -10^{-5} per °K; although these values are quite small, they nevertheless appear to be important for fast reactor safety.

8.5 COMPARISON OF THEORY AND EXPERIMENT

8.5a Thermal Reactors

In most thermal reactors, the neutron flux in the resonance region varies very nearly as $1/E$, with the fine structure due to individual resonances superimposed. Hence, the quantity of interest for resonance absorption is the resonance integral over all the resonances. Moreover, the situation of greatest practical importance is one in which fuel rods of natural uranium or uranium of low enrichment in uranium-235 are arranged as a lattice, i.e., a periodic array of rods, in a moderator. The resonance absorption under these conditions has been studied extensively, both experimentally and theoretically. In general, good agreement has been obtained between theory and observation.

In a series of experiments, resonance absorption was measured in lattices of rods of uranium metal and of uranium oxide with heavy water as moderator.[112*] The values of the resonance integrals have been expressed by fitting the results to relationships of the form of equation (8.94). In terms of the microscopic

* Methods used for determining resonance integrals experimentally are described in Ref. 113.

resonance integral, with dimensions of barns, the data, with A/M in cm²/g, are well represented by

$$I \text{ (barns)} = 2.95 + 25.8\sqrt{\frac{A}{M}} \quad \text{for uranium metal}$$

and

$$I \text{ (barns)} = 4.45 + 26.6\sqrt{\frac{A}{M}} \quad \text{for uranium dioxide.}$$

In Table 8.3, the values of the resonance integrals of uranium-238 in rods of natural uranium metal and uranium dioxide of different radii, as derived from these expressions, are compared with the results obtained by calculation.[114] In this calculation, equation (8.85) was solved numerically using exact values for P_r.[115] The line labeled "unresolved" refers to unresolved *s*-wave resonances for which the average resonance parameters can be derived with a fair degree of confidence from the experimental values at lower energies. The *p*-wave resonances are included only to the extent of adding a constant estimated value of 1.6 barns. The "oxygen correction" for uranium dioxide, in the lower part of the table, represents the difference between the NR approximation for the admixed oxygen in the fuel, as in equation (8.85), and the results obtained

TABLE 8.3 COMPARISON OF CALCULATED AND EXPERIMENTAL RESONANCE INTEGRALS OF URANIUM-238 AT 300°K.[114]

Uranium Metal, Density 18.7 *g/cm³*					
Rod Radius (cm)	0.1055	0.211	0.422	0.844	1.69
A/M (cm²/g)	1.013	0.507	0.254	0.127	0.0634
Resolved (barns)	25.29	18.04	12.91	9.31	6.75
Unresolved (barns)	1.96	1.67	1.40	1.18	1.03
Total + 1.6 barns	28.85	21.31	15.91	12.09	9.38
$2.95 + 25.8\sqrt{A/M}$	28.91	21.28	15.95	12.18	9.45

Uranium Dioxide, Density 10.2 *g/cm³*					
Rod Radius (cm)	0.125	0.25	0.50	1.0	2.0
A/M (cm²/g)	1.570	0.785	0.393	0.196	0.098
Resolved (barns)	34.40	24.62	18.01	13.59	10.74
Unresolved (barns)	2.21	1.94	1.68	1.46	1.30
Oxygen Correction	−0.08	−0.14	−0.25	−0.43	−0.68
Total + 1.6 barns	38.13	28.02	21.04	16.22	12.96
$4.45 + 26.6\sqrt{A/M}$	37.76	27.95	21.10	16.23	12.76

by numerical solution of the slowing down integral for the oxygen, i.e., using equation (8.84). This correction is significant only for the few resonances of lowest energy.

The agreement between the theoretical and observed resonance integrals in Table 8.3 is perhaps better than would be expected. In fact, in other experiments, values differing by up to 5 percent from those recorded here, with corresponding differences in the quantities a' and b' in equation (8.94), have been reported.[116] Nevertheless, it appears that an equation of this form does represent the experimental resonance integrals in heterogeneous systems and that the calculated values are in general agreement with those observed. Furthermore, the infinitely dilute resonance integral of 270 barns for uranium-238, derived from the resonance parameters (§8.3d), agrees with the experimental value of about 280 barns determined directly.[117]

Measurements have also been made of the temperature dependence of the resonance integrals.[118] Both theoretical and experimental results have been expressed in the form of a relationship similar to equation (8.95), namely,

$$I(T) = I(300°\text{K})[1 + \beta(\sqrt{T} - \sqrt{300})].$$

Some of the experimental values of β are compared with those derived from theory[119] in Table 8.4. Again, the agreement between observed and calculated results is good.

A detailed examination of the calculations[120] shows that the most important resonances for determining the resonance integrals and their temperature

TABLE 8.4. COMPARISON OF CALCULATED AND EXPERIMENTAL TEMPERATURE COEFFICIENTS OF RESONANCE INTEGRALS OF URANIUM-238.[119]

Uranium Metal		
Rod Radius (cm)	0.4	1.4
$\beta \times 10^2$: Calculated	0.62	0.55
Observed	0.64	0.55

Uranium Dioxide			
Rod Radius (cm)	0.4	0.85	1.4
$\beta \times 10^2$: Calculated	0.81	0.67	0.61
Observed	0.84	0.69	0.63

coefficients are those of lowest energy. Nevertheless, it can be seen from Table 8.3 that the unresolved resonances, with which the *p*-wave resonances must be included, may contribute as much as 20% (or more) to the total resonance integral.

Resonance absorption has also been determined experimentally for thorium-232 in heterogeneous assemblies, and again satisfactory agreement has been found between theory and experiment.[121] It is to be concluded, therefore, that there is a good theoretical basis for calculating resonance absorption in thermal reactor lattices.

8.5b Fast Reactors

For fast reactors, comparison of theoretical and experimental results is difficult for various reasons. The NR approximation is valid for all scatterings and heterogeneity may be largely ignored because of the small spacing between the fuel elements. But there are complications which are less significant in calculations for thermal systems. First, the fast-reactor fuel contains a substantial proportion of a fissile nuclide and both capture and fission in the resonances of this material must be computed. Then, unresolved and *p*-wave resonances are important because of the high neutron energies; also, under these conditions, strong overlap will occur. At sufficiently high energies the treatment in §8.3i can be used for the latter, and at low energies the resonances are well separated. In between, however, there is the difficult region of intermediate overlap.

Finally, since the over-all spectrum of a fast reactor is highly dependent on the detailed composition, there is no simple way of reporting and comparing resonance absorption except for specific systems. In making calculations, a common procedure is to replace rapidly-varying actual cross sections by slowly-varying effective cross sections which are computed by taking the fine structure of the flux into account. These effective cross sections are used in multigroup calculations in the usual manner for the given system.

On the experimental side, there is no clear way to measure the resonance absorption and attention has been focused on trying to determine the variation of the absorption with temperature. To this end, measurements are made of the variation of reactivity with temperature; contributions from thermal expansion and from other less obvious effects are subtracted to obtain the temperature coefficient due to the Doppler broadening of the resonances.

An example of this type of comparison between experimental and theoretical results is provided by a study of the fertile nuclides in a fast-reactor neutron spectrum. In an experiment with the zero-power fast reactor assembly ZPR-III 45, the temperature of a uranium-238 rod 1-inch in diameter was raised from 500 to 1100 K and the resulting decrease in reactivity was measured; in this particular case, $\Delta k/k$ was found to be -26.8×10^{-6}.[122] For the calculations, the effective (multigroup) cross sections, the reactor flux, and the adjoint were

computed and $\Delta k/k$ evaluated by means of equation (6.71). The best value determined in this manner was -26.4×10^{-6}.

In this case, the agreement between the observed reactivity change with temperature and that computed on the basis of the expected Doppler effect is excellent. Although the agreement is not always so impressive, it is generally found to be good for the fertile nuclides.[123] For the fissile species, on the other hand, there is considerable uncertainty in both experimental and calculated effects of Doppler broadening. The agreement between observed and computed reactivity changes with temperature obtained so far is not good.[124] In the design of fast reactors, the uncertainty in the temperature coefficient is taken into consideration, so that such reactors can operate just as safely as thermal reactors.

EXERCISES

1. By starting from equations (8.16) and (8.20), show that the Doppler broadened cross section is given without approximation by

$$v\sigma_x(E) = \frac{\int_0^\infty v_r\sigma(E_r)(e^{-X} - e^{-Y})\,dE_r}{\int_0^\infty (e^{-X} - e^{-Y})\,dE_r}.$$

where

$$X \equiv \frac{A}{kT}(\sqrt{E} - \sqrt{E_r})^2 \quad \text{and} \quad Y \equiv \frac{A}{kT}(\sqrt{E} + \sqrt{E_r})^2.$$

(Hint: First choose $V_\perp$ $(= \sqrt{V_x^2 + V_y^2})$, V_z, and the azimuthal angle, φ, as variables of integration, and integrate over φ. Then change to the variables V_z and E_r and integrate over V_z.) Show that the expression given above reduces to equation (8.22) when E/kT is large.[125]

2. By using the expression in the preceding exercise, show that the relative variation with temperature of the area under a resonance is proportional to kT/AE_0 for small values of kT/AE_0.[126]
3. Verify the properties of the chi-square distribution in §8.2b, especially equation (8.34).
4. Compute the average s-wave neutron capture cross section for uranium-238 as a function of neutron energy in the range from 1 to 100 keV. Assume that the strength function $S_0 = 10^{-4}$, that $\bar{D} = 20$ eV, and $\Gamma_\gamma = 0.020$ eV, independent of energy. The neutron widths may be assumed to have a Porter-Thomas distribution. Values of the function

$$\frac{\left\langle \dfrac{\Gamma_n\Gamma_\gamma}{\Gamma_n + \Gamma_\gamma} \right\rangle}{\dfrac{\bar{\Gamma}_n\bar{\Gamma}_\gamma}{\bar{\Gamma}_n + \bar{\Gamma}_\gamma}}$$

may be taken from Fig. 4 in Ref. 127. Compare the results with the experimental values[128] and suggest a reason for the discrepancy.

5. Consider a sequence of resonances in which both capture and fission are possible. Derive the ratio of average capture to average fission cross section as a function of $\Gamma_\gamma/\overline{\Gamma}_f$, for values of the latter between 0.01 and 1. The following assumptions are to be made: Γ_γ is the same for all the resonances, Γ_f has a chi-square distribution with two degrees of freedom, and $\overline{\Gamma}_n \ll \Gamma$. Show what the result would be for $\overline{\Gamma}_n \gg \Gamma_\gamma + \overline{\Gamma}_f$.[129]
6. Derive the limiting form for low temperatures of the function $J(\zeta, \beta)$, defined by equation (8.66).
7. Compute the resonance integrals for $T = 300°$, 600°, and 1200°K for a uranium-238 resonance, with $E_0 = 66.3$ eV, $\Gamma_\gamma = 0.020$ eV, and $\Gamma = 0.050$ eV, assuming $\sigma_{pot} + \sigma_m = 10, 10^2, 10^3$, and infinity barns per uranium atom. Use the NR approximation and ignore interference between resonance and potential scattering. Discuss the results obtained. (For the validity of the NR approximation and neglect of interference effects, see Ref. 130.)
8. Show that under such conditions that the NR approximation is valid, the difference between $\phi^{(1)}$ and $\phi^{(2)}$, given by equation (8.73), is small when the NR form of $\phi^{(1)}$ is used.

REFERENCES

1. Price, D. L., *et al.*, *Nucl. Phys.*, **A121**, 630 (1968); J. E. Lynn, "The Theory of Neutron Resonance Reactions," Oxford University Press, 1968, pp. 333 *et seq.*
2. See, for example, A. M. Weinberg and E. P. Wigner, "The Physical Theory of Neutron Chain Reactors," University of Chicago Press, 1958, Chap. XIX; J. R. Lamarsh, "Introduction to Nuclear Reactor Theory," Addison-Wesley Publishing Co., Inc., 1966, Section 11-3.
3. Breit, G., and E. P. Wigner, *Phys. Rev.*, **49**, 519 (1936); see also, J. E. Lynn, Ref. 1, pp. 56 *et seq.*
4. Blatt, J. M., and V. F. Weisskopf, "Theoretical Nuclear Physics," John Wiley and Sons, Inc., 1952, pp. 423 *et seq.*, and Appendix A-5.
5. "Neutron Cross Sections," Brookhaven National Laboratory Report BNL-325 and supplements.
6. Devaney, J. J., L. O. Bardwell, and R. E. Anderson, "Thorium Cross Sections and their Temperature Dependence," Los Alamos Scientific Laboratory Report LA-2525 (1961); also G. W. Hinman and J. B. Sampson, "A Rigorous Determination of Doppler Broadening of Nuclear Resonances for a Maxwellian Gas Absorber," General Atomic Report GA-3603 (1962).
7. Blatt, J. M., and V. F. Weisskopf, Ref. 4, pp. 328 *et seq.*, and p. 393.
8. Blatt, J. M., and V. F. Weisskopf, Ref. 4, pp. 329 *et seq.*; J. E. Lynn, Ref. 1, p. 44.
9. Abramowitz, M., and I. Stegun, eds., "Handbook of Mathematical Functions," Dover Publications, Inc., 1965.
10. Blatt, J. M., and V. F. Weisskopf, Ref. 4, pp. 383 *et seq.*, and p. 557; also A. M. Lane and R. G. Thomas, *Rev. Mod. Phys.*, **30**, 257 (1958); J. E. Lynn, Ref. 1, p. 58.
11. Blatt, J. M., and V. F. Weisskopf, Ref. 4, p. 361; J. E. Lynn, Ref. 1, p. 43.
12. Hinman, G. W., *et al.*, *Nucl. Sci. Eng.*, **16**, 202 (1963); J. J. Devaney, "The Approximate Doppler Broadening of Isolated Nuclear Resonances," Los Alamos Scientific Laboratory Report LA-3315 (1965).
13. Nordheim, L. W., "The Doppler Coefficient," Chap. 4 in "The Technology of Nuclear Reactor Safety," T. J. Thompson and J. G. Beckerley, eds., The M.I.T. Press, Vol. I, 1964; R. B. Nicholson and E. A. Fischer, "The Doppler Effect in Fast Reactors," in *Adv. Nucl. Sci. Tech.*, **4**, 109 (1968).
14. Nelkin, M. S., and D. E. Parks, *Phys. Rev.*, **119**, 1060 (1960).
15. Nelkin, M. S., and D. E. Parks, Ref. 14; also W. E. Lamb, *Phys. Rev.*, **55**, 190 (1939).

16. American Institute of Physics Handbook, 2nd ed., 1963, p. 4–61.
17. Nelkin, M. S., and D. E. Parks, Ref. 14. For an example of peculiar resonance shapes when $T \ll \theta_D$, see C. Lajeunesse, *et al.*, *Trans. Am. Nucl. Soc.*, **11**, 183 (1968).
18. See, for example, H. Margenau and G. M. Murphy, "Mathematics of Physics and Chemistry," D. Van Nostrand Co., Inc., 1943, Section 12.7.
19. Bethe, H. A., and G. Placzek, *Phys. Rev.*, **51**, 462 (1937).
20. A short tabulation is given by T. D. Beynon and I. S. Grant, *Nucl. Sci. Eng.*, **17**, 547 (1963); for more complete tabulations, see K. K. Seth and R. H. Tabony, "A Tabulation of the Doppler Integrals $\psi(x, t)$ and $\phi(x, t)$," U.S. AEC Report TID-21304 (1964); and especially Y. Dandeu, *et al.*, Centre d'Etudes Nucleaires, CEA, Saclay (France) Report CEA-R-2824 (1965).
21. O'Shea, D. M., and H. C. Thacher, *Trans. Am. Nucl. Soc.*, **6**, 36 (1963); E. M. Gelbard, *ibid.*, **6**, 257 (1963).
22. Hinman, G. W., *et al.*, Ref. 12; Y. Ishiguro, *Nucl. Sci. Eng.*, **24**, 375 (1966).
23. See, for example, M. Born, "Optik," Springer Verlag, 1933, p. 486.
24. Canfield, E., *Trans. Am. Nucl. Soc.*, **11**, 185 (1968).
25. See citations in Refs. 20 and 21.
26. Nicholson, R. B., and E. A. Fischer, Ref. 13.
27. Shook, D. F., and D. Bogart, *Nucl. Sci. Eng.*, **31**, 415 (1968).
28. Gilbert, A., and A. G. W. Cameron, *Canad. J. Phys.*, **43**, 1446 (1965).
29. Nicholson, R. B., and E. A. Fischer, Ref. 13.
30. Lane, A. M., and R. G. Thomas, Ref. 10; R. E. Lynn, Ref. 1, Chap. 2.
31. Lynn, R. E., Ref. 1, pp. 365 *et seq.*
32. Lynn, R. E., Ref. 1, pp. 342 *et seq.*
33. Lynn, R. E., Ref. 1, pp. 399 *et seq.*
34. Adler, F. T., and D. B. Adler, in "Reactor Physics in the Resonance and Thermal Regions," A. J. Goodjohn and G. C. Pomraning, eds., The M.I.T. Press, 1966, Vol. II, p. 47.
35. Lynn, R. E., Ref. 1, pp. 366 *et seq.*
36. Dyos, M. W., *Nucl. Sci. Eng.*, **34**, 181 (1968); C. R. Adkins, T. E. Murley, and M. W. Dyos, *ibid.*, **36**, 336 (1969); Y. Ishiguro, *et al.*, *ibid.*, **40**, 25 (1970).
37. Bohr, A., *Proc. Second U.N. Conf. on Peaceful Uses of At. Energy*, **2**, 151 (1958); J. A. Wheeler, in "Fast Neutron Physics," J. B. Marion and J. L. Fowler, eds., Interscience Publishers, Inc., 1963, Vol. II, p. 2051; A. Michaudon, in Proc. Conf. on Neutron Cross Sections and Technology, National Bureau of Standards Special Publication, No. 299 (1968), Vol. I, p. 427.
38. Porter, C. E., and R. G. Thomas, *Phys. Rev.*, **104**, 483 (1956).
39. Porter, C. E., and R. G. Thomas, Ref. 38.
40. Garrison, J. D., *Ann. Phys.*, **30**, 269 (1964); J. E. Lynn, Ref. 1, pp. 219 *et seq.*, and pp. 301 *et seq.*
41. Porter, C. E., and R. G. Thomas, Ref. 38.
42. Nicholson, R. B., and E. A. Fischer, Ref. 13.
43. Lynn, J. E., Ref. 1, pp. 321 *et seq.*
44. Glass, N., *et al.*, in Proc. Conf. on Neutron Cross Sections and Technology, Ref. 37, Vol. I, p. 573.
45. Bohr, A., Ref. 37; J. A. Wheeler, Ref. 37.
46. Michaudon, A., Ref. 37; J. E. Lynn, Ref. 1, pp. 391 *et seq.*
47. Lynn, J. E., Ref. 1, pp. 388 *et seq.*; M. S. Moore and D. D. Simpson, "Measurement and Analysis of Cross Sections of Fissile Nuclides," in Proc. Conf. on Neutron Cross Section Technology, CONF-660303 (1966), Vol. II, p. 840.
48. Lynn, J. E., Ref. 1, p. 459; G. D. James, *Nucl. Phys.*, **A123**, 24 (1969).
49. Strutinsky, V. M., *Nucl. Phys.*, **A95**, 420 (1967); S. Bjørnholm and V. M. Strutinsky, *ibid.*, **A136**, 1 (1969).
50. Schmidt, J. J., in Ref. 34, Vol. II, p. 223.
51. Wigner, E. P. in Proc. Gatlinburg Conference, Oak Ridge National Laboratory Publication ORNL-2309 (1956), p. 59; J. E. Lynn, Ref. 1, p. 177.
52. Lynn, J. E., Ref. 1, Chap. V.

53. Lynn, J. E., Ref. 1, pp. 197 *et seq*, especially p. 202.
54. Hwang, R. N., *Nucl. Sci. Eng.*, **21**, 523 (1965).
55. Schmidt, J. J., Ref. 50; A. Michaudon, Ref. 37; N. Glass, *et al.*, Ref. 44; J. E. Lynn, Ref. 1, pp. 391 *et seq.*
56. Wheeler, J. A., Ref. 37.
57. James, G. D., Ref. 48.
58. Lane, A. M., and J. E. Lynn, *Proc. Phys. Soc.* (Lond.), **A70**, 557 (1957).
59. Gilbert, A., and A. G. W. Cameron, Ref. 28.
60. Thomas, R. G., *Phys. Rev.*, **97**, 224 (1955); A. M. Lane and R. G. Thomas, Ref. 10.
61. Lynn, R. E., Ref. 1, pp. 236, 286.
62. Nordheim, L. W., Ref. 13; R. B. Nicholson and E. A. Fischer, Ref. 13.
63. See, for example, S. Glasstone and M. C. Edlund, "The Elements of Nuclear Reactor Theory," D. Van Nostrand Co., Inc., 1952, §§6.69 *et seq.*
64. Weinberg, A. M., and E. P. Wigner, Ref. 2, p. 304; L. Dresner, "Resonance Absorption in Nuclear Reactors," Pergamon Press, 1960, p. 100.
65. Nordheim, L. W., Ref. 13.
66. Weinberg, A. M., and E. P. Wigner, Ref. 2, p. 675; L. Dresner, Ref. 64, Chap. 8.
67. Dresner, L., Ref. 64, Chap. 8; "Reactor Physics Constants," Argonne National Laboratory Report ANL-5800 (1963), pp. 163 *et seq.*
68. Chernick, J., and A. R. Vernon, *Nucl. Sci. Eng.*, **4**, 649 (1958).
69. Rothenstein, W., and J. Chernick, *Nucl. Sci. Eng.*, **7**, 454 (1960); G. I. Bell, *ibid.*, **9**, 409 (1961).
70. "Reactor Physics Constants," Ref. 67, Section 3.6.4; L. Dresner, Ref. 64, p. 42; V. W. Nather and L. W. Nordheim, "Extended Tables for Computation of the Volume Term of the Resonance Integral," General Atomic Report GA-2460 (1961). The function may also be computed rapidly if desired, cf., J. Helholtz, A. Z. Livolsi, and D. H. Roy, *Trans. Am. Nucl. Soc.*, **11**, 312 (1968) and N. M. Steen, *Nucl. Sci. Eng.*, **38**, 244 (1969).
71. Dresner, L., Ref. 64, p. 43.
72. Chernick, J., and A. R. Vernon, Ref. 68.
73. Chernick, J., and A. R. Vernon, Ref. 68.
74. Dresner, L., Ref. 64, p. 50; J. Chernick and A. R. Vernon, Ref. 68; M. W. Dyos and A. Keane, *Nucl. Sci. Eng.*, **26**, 530 (1966).
75. Goldstein, R., and E. R. Cohen, *Nucl. Sci. Eng.*, **13**, 132 (1962); R. Goldstein, *ibid.*, **22**, 387 (1965).
76. See, for example, Y. Ishiguro and H. Takano, *Nucl. Sci. Eng.*, **31**, 388 (1968) or J. Mikkelson, *ibid.*, **39**, 403 (1970).
77. Goldstein, R., and E. R. Cohen, Ref. 75.
78. Goldstein, R., in Ref. 34, Vol. II, p. 37.
79. Goldstein, R., Ref. 78.
80. Goldstein, R., and E. R. Cohen, Ref. 75.
81. Kuncir, G. F., "A Program for the Calculation of Resonance Integrals," General Atomic Report GA-2525 (1961); C. A. Stevens and C. V. Smith, "GAROL, A Computer Program for Evaluating Resonance Absorption Including Resonance Overlap." General Atomic Report GA-6637 (1965).
82. Chernick, J., and A. R. Vernon, Ref. 68; L. Dresner, Ref. 64; Chap. 8; F. T. Adler, G. W. Hinman, and L. W. Nordheim, *Proc. Second U.N. Conf. on Peaceful Uses of At. Energy*, **16**, 155 (1958); L. W. Nordheim, Ref. 13.
83. Nordheim, L. W., and G. F. Kuncir, "A Program of Research and Calculations of Resonance Absorption," General Atomic Report GA-2527 (1961).
84. Levine, M. M., in Ref. 34, Vol. II, p. 85.
85. Citations in Ref. 36.
86. Feshbach, H., G. Goertzel, and H. Yamauchi, *Nucl. Sci. Eng.*, **1**, 4 (1956).
87. Feshbach, H., *et al.*, Ref. 86.
88. Nordheim, L. W., Ref. 13; R. B. Nicholson and E. A. Fischer, Ref. 13.
89. Hwang, R. N., *Nucl. Sci. Eng.*, **36**, 67, 82 (1969); **39**, 32 (1970).
90. Nordheim, L. W., Ref. 13.

91. Citations in Ref. 36; see also R. N. Hwang, Ref. 89.
92. Dancoff, S. M., and M. Ginsburg, "Surface Resonance Absorption in a Close-Packed Lattice," Manhattan Project Report CP-2157 (1944); E. Cruetz, *et al.*, *J. Appl. Phys.*, **26**, 257 *et seq.* (1955).
93. Gurevich, I. I., and I. Y. Pomeranchuk, *Proc. First U.N. Conf. on Peaceful Uses of At. Energy*, **5**, 466 (1955).
94. Chernick, J., *Proc. First U.N. Conf. on Peaceful Uses of At. Energy*, **5**, 215 (1955).
95. Kuncir, G. F., Ref. 81; C. A. Stevens and C. V. Smith, Ref. 81.
96. Dresner, L., Ref. 64, Chap. 8.
97. Bell, G. I., "Theory of Effective Cross Sections," Los Alamos Scientific Laboratory Report LA-2322 (1959); Y. Ishiguro and H. Takano, Ref. 76 and citations therein; J. P. Plummer and R. G. Palmer, *Trans. Am. Nucl. Soc.*, **12**, 625 (1969); E. M. Gelbard and N. M. Steen, *ibid.*, **12**, 626 (1969).
98. Levine, M. M., Ref. 84.
99. Roach, W. H., *Nucl. Sci. Eng.*, **34**, 331 (1968).
100. Van Binnebeek, J. J., *Nucl. Sci. Eng.*, **36**, 47 (1968).
101. Shook, D. F., and D. Bogart, *Nucl. Sci. Eng.*, **31**, 415 (1968); C. P. Pierce and D. F. Shook, *ibid.*, **31**, 431 (1968).
102. Roach, W. H., Ref. 99.
103. Nordheim, L. W., and G. F. Kuncir, Ref. 83.
104. Glasstone, S., and M. C. Edlund, Ref. 63, §§6.30 *et seq.*
105. Kuncir, G. F., Ref. 81; C. A. Stevens and C. V. Smith, Ref. 81.
106. Gurevich, I. I., and I. Y. Pomeranchuk, Ref. 93; see also A. M. Weinberg and E. P. Wigner, Ref. 2, p. 683.
107. Levine, M. M., Ref. 84.
108. Nordheim, L. W., Ref. 13.
109. Dresner, L., *Nucl. Sci. Eng.*, **11**, 39 (1961); see also J. J. Van Binnebeek, Ref. 100.
110. Nordheim, L. W., Ref. 13; R. B. Nicholson and E. A. Fischer, Ref. 13; R. N. Hwang, Ref. 89.
111. Greebler, P., and G. R. Pflasterer, in Ref. 34, Vol. II, p. 343; F. C. Schoenig, F. A. White, and F. Feiner, *Nucl. Sci. Eng.*, **37**, 66 (1969).
112. Hellstrand, E., and C. Lundgren, *Nucl. Sci. Eng.*, **12**, 435 (1962).
113. Weinberg, A. M., and E. P. Wigner, Ref. 2, p. 675; E. Hellstrand, in Ref. 34, Vol. II, p. 151.
114. Nordheim, L. W., Ref. 13.
115. Case, K. M., F. de Hoffmann, and G. Placzek, "Introduction to the Theory of Neutron Diffusion," Vol. I, U.S. AEC Report 1953, Table 4.
116. Hellstrand, E., Ref. 113.
117. Drake, M. K., *Nucleonics*, **24**, No. 8, 108 (1966).
118. Hellstrand, E., P. Blomberg, and S. Hörner, *Nucl. Sci. Eng.*, **8**, 497 (1960).
119. Nordheim, L. W., Ref. 13.
120. Nordheim, L. W., Ref. 13.
121. Nordheim, L. W., J. Hardy, Jr., and B. L. Palowitch, *Nucl. Sci. Eng.*, **29**, 111 (1967).
122. Fischer, G. J., *et al.*, *Nucl. Sci. Eng.*, **25**, 37 (1966).
123. Greebler, P., and G. R. Pflasterer, Ref. 111.
124. Fischer, G. J., *et al.*, Ref. 122; P. Greebler and G. R. Pflasterer, Ref. 111.
125. Hinman, G. W., *et al.*, *Nucl. Sci. Eng.*, **16**, 202 (1963); **18**, 531 (1964).
126. Canfield, E., Ref. 24.
127. Lane, A. M., and J. E. Lynn, Ref. 58.
128. Stehn, J. R., *et al.*, "Neutron Cross Sections," Vol. III, $Z = 88$ to 98, Brookhaven National Laboratory Report BNL-325, 2nd ed., Suppl. 2.
129. Oleksa, S., *J. Nucl. Energy*, **A5**, 16 (1957); G. I. Bell, *Phys. Rev.*, **158**, 1127 (1967).
130. Chernick, J., and A. R. Vernon, *Nucl. Sci. Eng.*, **4**, 656 (1958); G. I. Bell, *ibid.*, **9**, 409 (1961).

9. REACTOR DYNAMICS: THE POINT REACTOR AND RELATED MODELS

9.1 INTRODUCTION

9.1a Time-Dependent Problems

Attention thus far has been largely confined to time-independent problems in the physics of nuclear reactors. In particular, in the earlier chapters of the book various methods were described for solving the transport equation for steady-state systems. By using these methods, it was possible to predict critical configurations, the spatial distribution of the neutron flux (or reactor power), nuclear reaction rates, and so on.

Consideration will now be given to situations in which the neutron flux varies with time. Such time-dependent problems always arise, for example, in the startup and shutdown of a reactor. They are also of fundamental practical importance in investigating the stability and controllability of a reactor, both under normal operating conditions and as the result of an accidental increase (or excursion) in reactivity, the failure of a coolant pump, or other abnormal situation. Furthermore, several time-dependent experiments have been used to determine quantities of interest, such as the reactivity of a chain-reacting system and also its diffusion and thermalization properties. There are many time-dependent problems that may be included under the heading of reactor dynamics,* but only a limited selection, which appear to be of special interest, will be discussed here.

* The term reactor dynamics, as used here, includes the time dependence of the neutron population and related quantities in a reactor (kinetics) and the factors which are responsible for this dependence.

The present chapter is primarily concerned with approaches in which the space and energy dependences of the neutron flux are treated in a very approximate manner. In particular, emphasis will be placed on the so-called "point reactor" model (§9.2c) and to relatively straightforward generalizations of this model. In Chapter 10, attention will be given to methods for solving various space-dependent problems.

It will be seen in due course that problems in reactor dynamics are relatively straightforward provided they are restricted to linearized point models. When space dependence or a full treatment of a nonlinear system of equations (or both) must be taken into account, the situations become much more complicated. In many such cases it is not yet possible to carry out a quantitative treatment, although qualitative conclusions can be drawn.

The first step in the solution of time-dependent problems is to have a method for determining the manner in which a neutron population varies with time, for example, in a subcritical or supercritical system or in a critical system in which a neutron source or cross sections change with time. In the treatment of these problems, it is frequently necessary to include the delayed neutrons, since their decay constants will often determine the time behavior of the neutron population. Consequently, the time-dependent neutron transport equation, derived in Chapter 1, will be supplemented with an appropriate allowance for the delayed neutrons.

It is important to recognize, however, that the times involved in the appearance of the delayed neutrons, namely, of the order of seconds, are very long compared to any times associated with the diffusion or reaction of neutrons. For this reason, the time scales in reactor kinetics problems usually fall into one of two categories: (*a*) very short times in which the neutron populations can change significantly but the delayed-neutron sources can not, and (*b*) longer times in which the sources of delayed neutron can change to a significant extent. Use will be made in the present chapter of this natural separation of time scales.

9.1b The Transport Equation with Delayed Neutrons

It is well known that the emission of some of the neutrons accompanying fission is delayed by times ranging from less than a second to a minute or so. These delayed neutrons result when the beta decay of a fission product leads to such a highly excited state in the daughter nucleus that neutron emission is energetically possible. Several fission products are precursors of the delayed-neutron emitters, but for practical purposes it has been found possible to divide them into six groups. In each group, the precursors decay exponentially with a characteristic half-life, which determines the rate of emission of the delayed fission neutrons. The relative and absolute abundances of the delayed-neutron precursors are functions of the kind of fission, i.e., nature of the nuclide and energy of the

neutron inducing fission, in which they are produced, and so also are the decay constants to a slight extent.[1]

The expected density of precursors in the jth group is represented by $C_j(\mathbf{r}, t)$ and the corresponding decay constant is λ_j, where $j = 1, 2, \ldots, 6$. The expected rate of emission of delayed neutrons is then $\lambda_j C_j$, and these neutrons will have a normalized energy spectrum represented by $\chi_j(E)$. For simplicity, and because it is essentially true under the conditions in a reactor, it will be assumed here that λ_j and χ_j are independent of the kind of fission in which the delayed neutrons are produced. Moreover, to simplify the notation, the normalized spectrum of prompt neutrons will be indicated by $\chi_p(E)$.

Let $\nu(\mathbf{r}, E)$ be the expected total number of neutrons emitted per fission at $\mathbf{r}$ caused by a neutron of energy E, and $\beta_j(\mathbf{r}, E)$ the fraction of this total that comes from the jth group of precursors. Then $\beta_j(\mathbf{r}, E)\nu(\mathbf{r}, E)$ is the expected number of precursors created by a fission at $\mathbf{r}$ due to a neutron of energy E. If $\beta(\mathbf{r}, E)$ is defined by

$$\beta(\mathbf{r}, E) = \sum_j \beta_j(\mathbf{r}, E),$$

then $[1 - \beta(\mathbf{r}, E)]\nu(\mathbf{r}, E)$ is the expected number of prompt neutrons resulting from a fission at $\mathbf{r}$ by a neutron of energy E.

Consequently, if a fission at $\mathbf{r}$ at time zero is caused by a neutron of energy E', the probable emission of neutrons per unit time as a function of time, t, and emerging energy E, will be

$$\chi_p(E)[1 - \beta(\mathbf{r}, E')]\nu(\mathbf{r}, E')\,\delta(t) + \sum_j \chi_j(E)\beta_j\lambda_j\nu(\mathbf{r}, E')e^{-\lambda_j t},$$

where $\delta(t)$ is a Dirac function. For reactors with stationary fuel,* this expression, with $t - t'$ substituted for t, may be inserted in the time-dependent transport equation (1.14); the result is

$$\begin{aligned}\frac{1}{v}\frac{\partial\Phi(\mathbf{r}, \boldsymbol{\Omega}, E, t)}{\partial t} + \boldsymbol{\Omega}\cdot\nabla\Phi + \sigma\Phi \\ = \iint \sum_{x \neq f} \sigma_x f_x(\mathbf{r}; \boldsymbol{\Omega}', E' \to \boldsymbol{\Omega}, E; t)\Phi(\mathbf{r}, \boldsymbol{\Omega}', E', t)\,d\boldsymbol{\Omega}'\,dE' \\ + Q(\mathbf{r}, \boldsymbol{\Omega}, E, t) + \int_{-\infty}^{t}\iint \sigma_f(\mathbf{r}, E', t')\Phi(\mathbf{r}, \boldsymbol{\Omega}', E', t') \\ \times \left[\tilde{\chi}_p(1 - \beta)\nu\,\delta(t - t') + \sum_j \tilde{\chi}_j\beta_j\lambda_j\nu e^{-\lambda_j(t-t')}\right] d\boldsymbol{\Omega}'\,dE'\,dt', \quad (9.1)\end{aligned}$$

* In a reactor with moving (fluid) fuel, a fission at one point will lead to the emission of delayed neutrons at other points. Even when the fuel is stationary, some of the precursors which are volatile, e.g., isotopes of bromine and iodine, are not stationary. Such effects cannot be formulated accurately in a conventional neutron transport equation and they will be ignored here; they have, however, been treated approximately in some cases.[2]

where $\chi/4\pi$, the neutron emission per unit solid angle, has been replaced by $\tilde{\chi}$. The time-dependent transport equation (9.1) with delayed neutrons is given here because it is sometimes used in theoretical studies of reactor dynamics. For the present purposes, it is more convenient, and often useful for understanding the physical situation, to introduce the precursor densities directly into the transport equation; thus,

$$\frac{1}{v}\frac{\partial \Phi}{\partial t} + \mathbf{\Omega}\cdot\nabla\Phi + \sigma\Phi = \iint \sum_{x \neq f} \sigma_x f_x \Phi' \, d\mathbf{\Omega}' \, dE' + \iint \tilde{\chi}_p(1-\beta)\nu\sigma_f\Phi' \, d\mathbf{\Omega}' \, dE' + \sum_j \lambda_j C_j(\mathbf{r}, t)\tilde{\chi}_j + Q \quad (9.2)$$

and

$$\frac{\partial C_j(\mathbf{r}, t)}{\partial t} + \lambda_j C_j = \iint \beta_j \nu \sigma_f \Phi' \, d\mathbf{\Omega}' \, dE', \quad (9.3)$$

where

$$\begin{aligned} \sigma &\equiv \sigma(\mathbf{r}, E, t) \\ \sigma_x &\equiv \sigma_x(\mathbf{r}, E', t) \quad \text{for } x \neq f \\ \sigma_f &\equiv \sigma_f(\mathbf{r}, E', t) \\ f_x &\equiv f_x(\mathbf{r}; \mathbf{\Omega}', E' \to \mathbf{\Omega}, E; t) \\ \Phi' &\equiv \Phi(\mathbf{r}, \mathbf{\Omega}', E', t) \\ \nu &\equiv \nu(\mathbf{r}, E') \\ Q &\equiv Q(\mathbf{r}, \mathbf{\Omega}, E, t), \end{aligned}$$

and β and β_j refer to energy E' and $\tilde{\chi}_p$ and $\tilde{\chi}_j$ to energy E. If equation (9.3) were solved for C_j in terms of Φ' and the result inserted in equation (9.2), the transport equation (9.1) would be obtained.

For equations (9.1), (9.2), and (9.3), the various cross sections, σ, $\sigma_x f_x$, and σ_f, have been indicated above as explicit functions of time; the purpose is to take into account such changes as may arise from the motion of control rods and from various feedback effects (§9.1c) and from fuel burnup (§10.2b). The quantities connected with fission, e.g., ν, χ_p, and χ_j, could also be regarded as functions of time, but for simplicity such time dependence has not been written out.

Equation (9.1) or equations (9.2) and (9.3) provide an exact formulation of the variation of the neutron angular flux with time taking into account the delayed neutrons. In principle, these equations can be solved by straightforward numerical methods, i.e., by replacing derivatives by differences, and in practice solutions have been obtained in this way for a number of problems involving simple geometries and diffusion theory.[3] Even in these cases, however, the numerical calculations are quite lengthy and are, therefore, expensive in computer time. For problems with more complicated geometry and feedback effects, the direct numerical methods are so difficult that gross simplifications are usually made before solutions are attempted.

In many problems, for example, a separation can be made of the space and energy dependence of the flux, on the one hand, from its time dependence in the point reactor, on the other hand. This method and some generalizations will be developed in §9.2a, *et seq.* Alternative methods are based on the expansion of the neutron flux in modes whereby the spatial dependence may be retained in approximate form in the time-dependent equations. Such approaches to solving the transport equation with delayed neutrons will be described in Chapter 10.

Delayed fission neutrons play a role in all reactors, but in some there may be another source (or sources) of delayed neutrons. If the reactor contains deuterium, e.g., as heavy water, or beryllium, gamma rays of relatively low energy, emitted by the fission products, can cause neutrons to be released by the (γ, n) reaction. The thresholds for these photoneutron reactions are 1.67 and 2.23 MeV for beryllium and deuterium, respectively. In thermal reactors with large amounts of heavy water or beryllium as moderator, these photoneutrons may be comparable in importance with the delayed neutrons from fission. Although the photoneutrons may be less abundant by an order of magnitude, they have much longer decay times than the delayed fission neutrons and may thus completely dominate the time behavior of a reactor very near critical. For reactors with moderators of heavy water or beryllium, the photoneutrons can be approximated in the point-reactor model as one or more additional groups of delayed neutrons.[4]

Even in reactors in which ordinary water is the moderator (and coolant), there is always some deuterium present in the water. The delayed photoneutrons from this deuterium may act as a strong neutron source after the reactor has been shut down. Such a source may, indeed, frequently be stronger than an imposed neutron source.[5] However, it does not affect the reactor dynamics significantly under operating conditions.

9.1c Feedback Effects

The equations given above allow for the influence of delayed neutrons on the time behavior of a reactor, but they do not take into consideration certain other effects which may be important in reactor dynamics. For a reactor operating at any substantial power, for example, account must be taken of the effect of the neutron population and the power level on the criticality (or reactivity) of the system. In particular, the power level will affect the temperature and changes in temperature will alter the criticality by causing changes in geometry, density, neutron spectrum, and microscopic cross sections. Allowance must be made for these *feedback mechanisms*, i.e., mechanisms whereby the reactor operating conditions affect the criticality, in treating time-dependent problems of a reactor operating at power.

Several of the feedback effects are included in the equations of reactor dynamics in a relatively crude manner by the use of "lumped" parameters,

such as "fuel temperature," "moderator temperature," etc. (§9.4a). Detailed calculations of heat transfer, fluid flow, and so on, are nevertheless required for the determination of these parameters. In spite of this simplification, the resulting equations are nonlinear and a full analysis of any but the more tractable models is difficult even for a point reactor. For small departures from critical, however, the equations can be linearized by making some approximations, and then they can be solved readily, as will be seen in due course.

9.2 THE POINT REACTOR

9.2a The Amplitude and Shape Factors

The space and energy dependence could be eliminated from equations (9.2) and (9.3) by integrating over $\mathbf{r}$, Ω, and E. But the time derivatives would then appear as small differences between large numbers, so that this approach is not practical. It has been found better to consider *differences* between the actual system and some just critical (time-independent) reference system. Moreover, by introducing an adjoint function for the critical system, expressions for the reactivity can be obtained which are insensitive to errors in the flux, as in §6.3c. The time-independent adjoint equation [cf. equation (6.69)] for such a system may be written as

$$-\Omega\cdot\nabla\Phi_0^\dagger + \sigma_0\Phi_0^\dagger = \iint\left[\sum_{x\neq f}\{\sigma_{x0}f_{x0}(\mathbf{r};\Omega,E\to\Omega',E')\} + \tilde{\chi}(E')\nu(\mathbf{r},E)\sigma_{f0}(\mathbf{r},E)\right] \times \Phi_0^\dagger(\mathbf{r},\Omega',E')\,d\Omega'\,dE', \quad (9.4)$$

where the zero subscript indicates values of the various quantities in the (critical) reference state. In practice $\Phi_0^\dagger$ could be found by the methods described in Chapters 4 and 5 for the calculation of the k eigenfunction; the number of neutrons per fission is varied until the condition for criticality is found. As usual, $\Phi_0^\dagger$ is assumed to satisfy the boundary condition of zero outgoing importance, whereas for Φ it is assumed there are no incoming neutrons. For later use, $\Phi_0^\dagger$ is normalized in some definite but arbitrary way.

For the point-reactor treatment[6] of a time-dependent problem, $\Phi(\mathbf{r},\Omega,E,t)$ is first written as the product of an *amplitude factor* $P(t)$, which is dependent on time only, and a *shape factor* (or *shape function*) $\psi(\mathbf{r},\Omega,E,t)$; thus,

$$\Phi(\mathbf{r},\Omega,E,t) = P(t)\psi(\mathbf{r},\Omega,E,t). \quad (9.5)$$

It will be seen in §9.2c that the point-reactor model is obtained when the time dependence of the shape function is ignored, i.e., when ψ is taken to be independent of time. For the present, however, the time dependence will be retained in the shape function so that various improvements on the point-reactor treatment can be developed. In writing the angular neutron flux as the product of the two factors in equation (9.5), the intent is that the amplitude factor, $P(t)$, should

describe most of the time dependence whereas the shape factor, ψ, will change very little with time.

The shape factor is normalized so that

$$\frac{\partial}{\partial t}\left[\iiint \frac{1}{v}\,\Phi_0^\dagger(\mathbf{r}, \Omega, E)\psi(\mathbf{r}, \Omega, E, t)\,dV\,d\Omega\,dE\right] = 0, \tag{9.6}$$

where v is the neutron velocity. The volume integral is taken over the interior of the convex surface on which the boundary conditions are imposed. The purpose of the normalization in equation (9.6) is to satisfy the requirement that

$$\iiint \frac{1}{v}\,\Phi_0^\dagger\,\frac{\partial \Phi}{\partial t}\,dV\,d\Omega\,dE = \frac{\partial P(t)}{\partial t}\iiint \frac{1}{v}\,\Phi_0^\dagger\psi\,dV\,d\Omega\,dE. \tag{9.7}$$

Such a normalization can always be made in principle and other normalizations are possible.[7]

The determination of the appropriate shape function, ψ, may sometimes, e.g., for severe space-dependent reactivity transients, be so difficult as to render the approach of doubtful value. But when the system is disturbed only slightly from its initial state, a time-independent value of ψ can be found to a good approximation. In these circumstances, the point-reactor treatment has been found to be useful for solving the problems involved. The shape function will be discussed in more detail in §9.2c.

Although $\Phi_0^\dagger$ has been normalized above, equation (9.6) does not determine any normalization on ψ and P. Hence, $P(t)$ may be normalized independently in any convenient manner. In particular, $P(t_0)$ may be set equal to the reactor power at some time t_0. This will then fix the normalization of the shape function ψ at $t = t_0$, and from equation (9.6) the normalization will be determined at all other times. However, $P(t)$ will still be nearly equal to the reactor power at all times t for which the shape function does not differ greatly from that at $t = t_0$, as can be seen from the following considerations.

The reactor power may be represented by

$$\text{Power} = \epsilon_f \iiint \sigma_f(\mathbf{r}, E)\Phi(\mathbf{r}, \Omega, E, t)\,dV\,d\Omega\,dE$$

$$= P(t)\epsilon_f \iiint \sigma_f(\mathbf{r}, E)\psi(\mathbf{r}, \Omega, E, t)\,dV\,d\Omega\,dE,$$

where ϵ_f is the average energy release per fission and the fission cross section is, for simplicity, taken to be independent of time. If, then, at $t = t_0$, the power is set equal to $P(t_0)$, it follows that

$$\epsilon_f \iiint \sigma_f(\mathbf{r}, E)\psi(\mathbf{r}, \Omega, E, t_0)\,dV\,d\Omega\,dE = 1.$$

If at other times t, the shape factor ψ is not very different, this relationship will remain essentially correct, and the power will be approximately equal to $P(t)$

at such times. When the flux shape changes significantly, however, it may not be possible to identify $P(t)$ with the reactor power even approximately.

Alternatively, the amplitude factor $P(t)$ may be normalized so that $P(t_0)$ is equal to the neutron population, i.e., the total number of neutrons present, at time t_0. Again, $P(t)$ will then represent the neutron population at any other time, t, provided the shape factor does not change very much. In most instances, however, normalization to the power is more convenient; this is especially true when feedback effects are considered, since they are affected by the power level of the reactor.

9.2b The Reactor Kinetics Equations

In deriving the equations for the time-dependent behavior (or kinetics) of a point reactor, the procedure is somewhat similar to that used in several instances in Chapter 6. First, equation (9.2) is multiplied by $\Phi_0^\dagger$ and equation (9.4) by Φ; the results are then subtracted and integrated over volume, angle, and energy, with equation (9.7) being used in the term containing $\partial\Phi/\partial t$. The gradient terms are eliminated by utilizing the divergence theorem and boundary conditions, as in §6.1c. The final result consists of the source and precursor terms and some terms involving differences, e.g., between σ and σ_0, of bilinear weighted cross sections (§6.4h); it may be written as

$$\frac{dP(t)}{dt} = \frac{\rho(t) - \bar{\beta}(t)}{\Lambda(t)} P(t) + \sum_j \lambda_j c_j(t) + Q(t), \tag{9.8}$$

where the quantities $\rho(t)$, $\bar{\beta}_j(t)$, $\bar{\beta}(t)$, $\Lambda(t)$, $c_j(t)$, and $Q(t)$ are defined below. Furthermore, if equation (9.3) is multiplied by $\chi_j(E)\Phi_0^\dagger$ and integrated over all variables, it is found that

$$\frac{dc_j(t)}{dt} = \frac{\bar{\beta}_j(t)}{\Lambda(t)} P(t) - \lambda_j c_j(t) \qquad j = 1, 2, \ldots, 6. \tag{9.9}$$

Equations (9.8) and (9.9) describe the kinetic behavior of a reactor. The parameter $\rho(t)$ is given by

$$\rho(t) \equiv \frac{1}{F}\left\{\int\cdots\int \Delta\left[\sum_{x \neq f} \sigma_x f_x(\mathbf{r}; \boldsymbol{\Omega}', E' \to \boldsymbol{\Omega}, E; t) + \bar{\chi}(E)\nu\sigma_f(\mathbf{r}, E', t)\right]\right.$$
$$\times \psi(\mathbf{r}, \boldsymbol{\Omega}', E', t)\Phi_0^\dagger(\mathbf{r}, \boldsymbol{\Omega}, E)\, dV\, d\boldsymbol{\Omega}\, dE\, d\boldsymbol{\Omega}'\, dE'$$
$$\left. - \iiint \Delta\sigma(\mathbf{r}, E, t)\psi(\mathbf{r}, \boldsymbol{\Omega}, E, t)\Phi_0^\dagger(\mathbf{r}, \boldsymbol{\Omega}, E)\, dV\, d\boldsymbol{\Omega}\, dE\right\}, \tag{9.10}$$

where the Δ's represent the differences between the respective quantities, σf and σ, in the time-varying state and in the time-independent (critical) reference

state, e.g., $\Delta\sigma = \sigma - \sigma_0$. The other parameters in equations (9.8) and (9.9) are given by

$$\bar{\beta}_j(t) \equiv \frac{1}{F}\int\cdots\int \tilde{\chi}_j(E)\beta_j\nu\sigma_f(\mathbf{r}, E')\psi(\mathbf{r}, \boldsymbol{\Omega}', E', t) \times \Phi_0^\dagger(\mathbf{r}, \boldsymbol{\Omega}, E)\, dV\, d\boldsymbol{\Omega}\, dE\, d\boldsymbol{\Omega}'\, dE' \tag{9.11}$$

$$\bar{\beta}(t) \equiv \sum_j \bar{\beta}_j(t) \tag{9.12}$$

$$\Lambda(t) \equiv \frac{1}{F}\int\int\int \frac{1}{v}\psi(\mathbf{r}, \boldsymbol{\Omega}, E, t)\Phi_0^\dagger(\mathbf{r}, \boldsymbol{\Omega}, E)\, dV\, d\boldsymbol{\Omega}\, dE \tag{9.13}$$

$$c_j(t) \equiv \frac{1}{\Lambda F}\int\int\int \tilde{\chi}_j(E)C_j(\mathbf{r}, t)\Phi_0^\dagger(\mathbf{r}, \boldsymbol{\Omega}, E)\, dV\, d\boldsymbol{\Omega}\, dE \tag{9.14}$$

and

$$Q(t) \equiv \frac{1}{\Lambda F}\int\int\int Q(\mathbf{r}, \boldsymbol{\Omega}, E, t)\Phi_0^\dagger(\mathbf{r}, \boldsymbol{\Omega}, E)\, dV\, d\boldsymbol{\Omega}\, dE. \tag{9.15}$$

The factor $1/F$ in the foregoing definitions is more or less arbitrary. It has no effect on the solutions to equations (9.8) and (9.9) since it always cancels in the numerator and denominator of each term. In practice, however, F is chosen so that the various parameters have a physical interpretation for simple situations. A reasonable choice for F in this respect is

$$F(t) \equiv \int\cdots\int \tilde{\chi}(E)\nu\sigma_f(\mathbf{r}, E')\psi(\mathbf{r}, \boldsymbol{\Omega}', E', t)\Phi_0^\dagger(\mathbf{r}, \boldsymbol{\Omega}, E)\, dV\, d\boldsymbol{\Omega}\, dE\, d\boldsymbol{\Omega}'\, dE'. \tag{9.16}$$

With this value for F, it will be seen below that the quantities in equation (9.8) can be given a physical interpretation.

It is important to realize that the individual parameters defined above are to some extent arbitrary; first, because $\Phi_0^\dagger$ is not completely determined, i.e., the reference critical system is somewhat arbitrary, and, second, because of the choice in the value of F. Nevertheless, the various parameters are related, so that care must be taken to define them consistently. Once a consistent choice has been made, however, such as that given above, the parameters are quite definite.

Consider, for example, equation (9.10) for $\rho(t)$. With F given by equation (9.16), the expression for ρ is very similar to that for the relative change in the effective multiplication factor, k, i.e., $\Delta k/k^*$, in equation (6.71) produced by changes in the cross section. In fact, if the shape function, ψ, has the same dependence on $\mathbf{r}$, $\boldsymbol{\Omega}$, and E as the fundamental angular flux eigenfunction $\Phi(\mathbf{r}, \boldsymbol{\Omega}, E)$ for the reference critical system, equation (9.10) would be identical with equation (6.71), and then

$$\rho = \frac{k-1}{k}. \tag{9.17}$$

This is the relation used to define the reactivity in elementary treatments of reactor kinetics[8]; hence, the quantity represented by equations (9.10) and (9.16) is here called the reactivity.

In general, the shape function will not vary with $\mathbf{r}$, Ω, and E in the same way as does the eigenfunction of k in the critical state. Under these conditions, ρ is not simply related to the static multiplication constant, k. Instead, equation (9.10) represents a generalization to dynamics problems, and it may be used to define a dynamic multiplication factor, k_d, by writing

$$\rho = \frac{k_d - 1}{k_d},$$

but k_d would be related only indirectly to k for a static problem. Nevertheless, in many instances, as will be seen below, ψ may be closely approximated by the eigenfunction of k, so that $k_d \simeq k$ and the elementary interpretation of ρ as the reactivity is quite accurate.

If, as in §1.5e, fission is regarded as the event separating successive generations of neutrons, Λ, as given by equation (9.13), is the mean neutron generation time. For neutrons of one speed in an infinite medium, equation (9.13) reduces to $\Lambda = 1/\nu\sigma_f v$; for a system at (or close to) critical, this is equivalent to $1/\sigma_a v$, which is the conventional elementary definition of the lifetime of a prompt neutron in an infinite system.[9] More generally from equations (9.13) and (9.16), Λ is the (adjoint-weighted) neutron population divided by the (adjoint-weighted) rate of emission of fission neutrons.

The quantity β_j, defined by equation (9.11), is the effective delayed-neutron fraction from the jth group of precursors, and β is the total effective delayed-neutron fraction. Even for a uniform reactor core, the effective fractions differ from the actual fractions because allowance is made in the former for the fact that the delayed neutrons have lower energies than the prompt fission neutrons. Thus, the delayed neutrons usually have a greater importance in thermal reactors than do the prompt neutrons, and in some cases β_j may be greater than β_j by 20% or so.[10]

If $P(t)$ in equations (9.8) and (9.9) is taken to represent the neutron population, i.e., the total number of neutrons, then c_j is the effective number of delayed-neutron precursors of the jth group present. On the other hand if, as is commonly done, $P(t)$ represents the reactor power, c_j is the number of precursors multiplied by a rate at which energy is produced per neutron. Some writers use a different symbol for c_j in these circumstances, but this is not necessary provided its significance is borne in mind.

9.2c The Shape Factor

No approximations have been made so far in deriving the reactor kinetics equations from equations (9.2) and (9.3); however, the development is purely formal unless the flux shape factor $\psi(\mathbf{r}, \Omega, E, t)$ can be found for evaluating the

parameters defined by equations (9.10) through (9.16). Fortunately, there are a number of situations for which this can be done fairly easily and they will be outlined below.

Before discussing these situations, reference will be made to a matter of nomenclature. In some cases, as already indicated, a time-independent shape function is employed to determine the parameters referred to above, for use in equations (9.8) and (9.9); the resulting expressions for the reactor kinetics are then said to describe a *point-reactor model.* It is in this sense that the term "point reactor" will be used in making comparisons, mostly in Chapter 10, with other, more accurate treatments of the spatial (and energy) variation of the neutron flux in time-dependent problems.

It should be noted, however, that the reactor kinetics equations (9.8) and (9.9) are often used in a quite different way; the parameters are not computed for a detailed shape factor but are postulated, perhaps on the basis of experimental considerations. The equations (9.8) and (9.9) are then often referred to as the *point-reactor kinetics equations*, simply to indicate that no account is being taken of the spatial dependence of the neutron flux. This is the approach that will be taken in most of the subsequent sections in the present chapter.

Consider, first, the exact equation which is satisfied by the shape factor. By inserting equation (9.5) into equation (9.1) and dividing through by $P(t)$, it is found that

$$\frac{1}{v}\left[\frac{\partial\psi}{\partial t} + \frac{1}{P(t)}\frac{dP}{dt}\psi\right] + \boldsymbol{\Omega}\cdot\nabla\psi + \sigma\psi$$

$$= \iint \sum_{x\neq f} \sigma_x f_x \psi'\, d\boldsymbol{\Omega}'\, dE' + \frac{Q}{P(t)}$$

$$+ \iint \tilde{\chi}_p(1-\beta)\nu\sigma_f\psi'\, d\boldsymbol{\Omega}'\, dE' + \frac{Q_d(\mathbf{r}, \boldsymbol{\Omega}, E, t)}{P(t)}, \quad (9.18)$$

where Q_d represents the delayed-neutron precursor decay rate at time t, i.e.,

$$Q_d = \int_{-\infty}^{t}\iint \nu\sigma_f(\mathbf{r}, E', t')P(t')\psi(\mathbf{r}, \boldsymbol{\Omega}', E', t')\sum_j \beta_j\tilde{\chi}_j\lambda_j e^{-\lambda_j(t-t')}\, d\boldsymbol{\Omega}'\, dE'\, dt'. \quad (9.19)$$

Equation (9.18), with Q_d as just defined, is thus an exact relationship which should be satisfied by $\psi(\mathbf{r}, \boldsymbol{\Omega}, E, t)$.

Equations (9.18) and (9.19), together with the reactor kinetics equations, constitute a system of equations equivalent to equations (9.2) and (9.3). The new equations are, however, much more cumbersome than the original ones and progress will have been made only insofar as approximate solutions of equation (9.18) can be found. Some simple situations in which this is possible will first be noted and then more general approximation procedures will be described.

If a reactor is on an asymptotic period, i.e., the reactor geometry is unchanged and the transients have died out (§§1.5b, 9.2e, 10.1d), the flux is truly separable into a product of a function of space and a function $e^{\alpha t}$ of time. The space dependence, for any α, can then be found by setting $P(t)$ proportional to $e^{\alpha t}$ in equations (9.18) and (9.19), and $Q = 0$, and solving for ψ, which will not be a function of time.

Furthermore, provided the reactor is not near or above prompt critical, α will be small, and so the second term on the left of equation (9.18), which is equal to $\alpha\psi/v$, can be neglected. Only the delayed-neutron source term $Q_d/P(t)$ will then depend on α. A change in the delayed-neutron source will, however, be equivalent to a small change in the fission-neutron source, and for this case the shape factor can usually be determined by a k eigenvalue calculation, i.e., an adjustment of the magnitude of the fission spectrum required to achieve exact criticality (§1.5e). When the reactor is above prompt critical, the term $\alpha\psi/v$ is no longer negligible; but now the delayed-neutron term $Q_d/P(t)$ becomes small and hence ψ can be found from an α eigenvalue calculation, as described in Chapters 4 and 5. These topics will be considered further in §10.1d.

A second situation of interest is that in which the departure from criticality is so small that the shape of $\Phi(\mathbf{r}, \Omega, E, t)$ is well approximated by that in the critical condition. As in perturbation theory, it is required that the shape must not change much locally, as well as grossly. The shape function may then again be derived from a k calculation. In considering the stability of an operating reactor, small perturbations from criticality are generally assumed; the shape function for this analysis can then be approximated quite simply and with sufficient accuracy.

The cases just discussed are somewhat special in the respect that the shape factor is not a function of time; hence, for these cases the point reactor defined above is accurate. There are, however, many important situations in which ψ does change with time, yet where simple approximations are possible. In particular, in large, high-power reactors, such as are now becoming of commercial interest, spatial transients must be considered in several contexts. When a large reactor is perturbed nonuniformly, e.g., by motion of control rods, by the accumulation of xenon-135, or by the burnup of fuel, the spatial dependence of the flux may be affected in important ways.

When the power changes are sufficiently slow, as in xenon or burnup problems, the time derivatives in equation (9.18) can be neglected, and so also can the time variations of P and ψ in computing Q_d. Once more, the delayed-neutron source can be combined with the source of prompt neutrons and a k eigenvalue calculation can be made to determine the shape factor at any particular time. Since the reactor conditions change gradually with time, the shape factor will also change but, for any given time, ψ can be computed from the conditions at that time. This procedure, which is called the *adiabatic approximation*,[11] is certainly applicable for sufficiently slow time variations of the reactor power (or

neutron flux). But it has been shown that it can describe the major part of the spatial effects in reactor kinetics even for fairly rapid power transients, such as may accompany the movement of a group of control rods.[12]

For a more accurate treatment of spatial effects in rapid reactor kinetics, an improvement on the adiabatic approximation can be achieved by considering the solution $\psi(\mathbf{r}, \mathbf{\Omega}, E, t)$ of equations (9.18) and (9.19) in more detail. When a reactor is suddenly perturbed, it is to be expected that the prompt-neutron population will adjust to the new conditions in a short time, of the order of a few prompt-neutron lifetimes. The delayed-neutron precursors, however, will reflect the conditions, especially the spatial dependence of ψ, before the perturbation until several precursor lifetimes have passed. Moreover, as seen from equation (9.18), the decay of the delayed-neutron precursors furnishes a neutron source, Q_d, which is involved in the determination of the shape factor, ψ.

It is evident, therefore, that the main deficiency of the adiabatic approximation is a failure to account for the sluggishness of the delayed-neutron precursors in changing the shape factor, ψ. An improved treatment, called the *quasistatic approximation*,[13] is possible, however, by computing Q_d from equation (9.19) and using this in equation (9.18) with $(\partial\psi/\partial t)/v$ set equal to zero. The quantity $[\partial P(t)/\partial t]/P(t)$ can then be taken from the solution of equation (9.8) for the last of a series of time intervals (see below). Accurate shape factors have been obtained by this approximation even for severe space-dependent transients.[14] It is also possible to include the term $\partial\psi/\partial t$ by approximating it as

$$\frac{\partial\psi}{\partial t} \approx \frac{\psi(\mathbf{r}, \mathbf{\Omega}, E, t) - \psi(\mathbf{r}, \mathbf{\Omega}, E, t - \Delta t)}{\Delta t}$$

and then solving equation (9.18) for $\psi(\mathbf{r}, \mathbf{\Omega}, E, t)$. This amounts to a full numerical solution of the time-dependent problem which may be quite efficient if the time steps for computing ψ can be much larger than those for computing $P(t)$.[15]

The advantage of the three types of approximation described above, i.e., the shape function independent of time and the adiabatic and quasistatic approximations, as compared to a direct numerical solution of the time-dependent transport equation, i.e., the combination of equations (9.2) and (9.3), is that the shape factor is determined infrequently. In a problem in which the amplitude, $P(t)$, changes by several orders of magnitude, the calculation of ψ is made, typically, one or only a few times. On the other hand, because of the large variations, $P(t)$ may have to be determined, using the point-reactor form of the kinetics equations (9.8) and (9.9), for many small time steps. Since computations of the shape factor are much more time consuming than solution of the point-reactor kinetics equations, it is a great advantage to be able to limit the number of the former that need to be made.

In §10.1c, the results of some of these approximations will be compared for certain situations involving extreme changes of the shape factor during a

transient. Other methods of treating such space-dependent problems will also be described in Chapter 10.

There is a special but important case in which a careful interpretation of the approximations is required. It will be seen in §9.3b that it is often useful to examine the response of a reactor to a small sinusoidal perturbation caused, for example, by the oscillation of a control rod. Suppose that this perturbation does not change the neutron flux significantly either in amplitude or shape; then, the unperturbed shape function can be used for obtaining the various parameters in equations (9.10) through (9.16). But when the response of the reactor is sensed with a localized neutron detector, as is usually the case, the small changes in the shape may be just as significant in determining the detector response as the small perturbations in the amplitude.

For a large reactor, these spatial effects in the observed response are often important. They can be calculated by using either an approximation, as described above, or from the exact equations (9.2) and (9.3) by introducing a localized sinusoidal variation proportional to $e^{i\omega t}$, where ω is the perturbation frequency, in the cross sections and solving for the corresponding sinusoidal variation in the neutron flux.[16] This approach will be considered in more detail in §9.3c.

Once a shape function has been determined and $\Phi_0^\dagger$ and F have been fixed, the parameters appearing in the point-reactor equations can be computed. Of greatest interest is the reactivity, ρ, which, as seen from equation (9.10), is proportional to the changes in the macroscopic cross sections that occur in going from the critical reference state to the actual state of the system. Some of these changes may be controlled by external circumstances, e.g., the motion of a control rod. In other cases, however, the changes may result from normal operation of the reactor at power, as mentioned earlier in the reference to feedback mechanisms; these will be discussed in some detail in later sections.

9.2d The Zero-Power Point Reactor

For a reactor which is operating at an appreciable power level, the reactivity will generally be a function of the reactor temperature and, therefore, it will be affected by $P(t)$ and also by its previous history, i.e., by $P(t')$ where $t' < t$. Since $\rho(t)$ is then a functional of $P(t)$, equation (9.8) is nonlinear in P and, in general, difficult to analyze. When the power level is so low that the reactor temperatures are unaffected by $P(t)$, the problem is linear and simple to solve. Such a situation is important for understanding experiments on critical assemblies and for reactor startup and other conditions. When $\rho(t)$ is independent of $P(t)$, the result is called the *zero-power (point) reactor model.*

Since there is no feedback mechanism in the zero-power reactor, equations (9.8) and (9.9) are complete, assuming that the parameters ρ, Λ, Q, and β_j are known. These equations are then the zero-power, point-reactor equations. The

two equations can, however, be combined to yield a single expression which is sometimes useful. For this purpose, equation (9.9) is solved for $c_j(t)$; thus,

$$c_j(t) = c_j(0)e^{-\lambda_j t} + \int_0^t \frac{\bar{\beta}_j}{\Lambda} P(t')e^{-\lambda_j(t-t')}\,dt'.$$

Then this result is substituted into equation (9.8) to give

$$\frac{dP(t)}{dt} = \frac{\rho(t) - \bar{\beta}(t)}{\Lambda} P(t) + \sum_j \lambda_j \left[c_j(0)e^{-\lambda_j t} + \int_0^t \frac{\bar{\beta}_j}{\Lambda} P(t')e^{-\lambda_j(t-t')}\,dt' \right] + Q(t). \tag{9.20}$$

9.2e Asymptotic Period-Reactivity Relation

Solutions of equations (9.8) and (9.9) or of equation (9.20) have been obtained for special cases.[17] A familiar one is that in which a subcritical reactor is made slightly supercritical by a sudden (step) increase in the reactivity. As is well known, the neutron population will start to increase and, after an initial transient, it will do so at an asymptotic rate which is related to the stable (or steady-state) reactor period.

Suppose that before time zero the reactor is subcritical and the neutron population and precursors are maintained constant by a constant source Q. If the reactivity at (and prior to) $t = 0$ is represented by ρ_-, where $\rho_- < 0$, equations (9.8) and (9.9) at $t = 0$ are

$$\frac{\rho_- - \bar{\beta}}{\Lambda} P_0 + \sum_j \lambda_j c_{j0} + Q = 0 \tag{9.21}$$

and

$$\lambda_j c_{j0} = \frac{\bar{\beta}_j}{\Lambda} P_0. \tag{9.22}$$

At $t = 0$, the reactivity is suddenly increased to ρ_+, where $\rho_+ > 0$, i.e., the reactor is slightly supercritical, with the source still present. Upon taking the Laplace transforms[18] of equations (9.8) and (9.9), with

$$P(s) \equiv \mathscr{L}P(t) = \int_0^\infty e^{-st}P(t)\,dt$$

and

$$c_j(s) \equiv \mathscr{L}c_j(t) = \int_0^\infty e^{-st}c_j(t)\,dt,$$

the results are

$$sP(s) - P_0 = \frac{\rho_+ - \bar{\beta}}{\Lambda} P(s) + \sum_j \lambda_j c_j(s) + \frac{Q}{s} \tag{9.23}$$

and

$$sc_j(s) - c_{j0} = \frac{\bar{\beta}_j}{\Lambda} P(s) - \lambda_j c_j(s). \tag{9.24}$$

(It should be noted that a function of the argument s, here and elsewhere, denotes a Laplace transform.) By using equation (9.22) for c_{j0}, equation (9.24) can be used to eliminate $c_j(s)$ from equation (9.23), with the result

$$P(s) = \frac{P_0\left(\Lambda + \sum_j \frac{\beta_j}{s + \lambda_j}\right) + \frac{\Lambda Q}{s}}{s\Lambda + \sum_j \frac{s\beta_j}{s + \lambda_j} - \rho_+}. \tag{9.25}$$

The inverse transform of $P(s)$ will now give the time-dependent solution $P(t)$ for $t > 0$. The general features of this solution are determined by the roots of the denominator of equation (9.25); these are the values of ω_k for which

$$\rho_+ = \Lambda\omega_k + \sum_j \frac{\omega_k\beta_j}{\omega_k + \lambda_j}. \tag{9.26}$$

By using the methods of residues[19] to evaluate the inverse transform of equation (9.25), it is found that

$$P(t) = \sum_k P_k e^{\omega_k t} - \frac{\Lambda Q}{\rho_+}, \tag{9.27}$$

with the coefficients P_k being given by

$$P_k = \frac{P_0\left(\Lambda + \sum_j \frac{\beta_j}{\omega_k + \lambda_j}\right) + \frac{\Lambda Q}{\omega_k}}{\Lambda + \sum_j \frac{\lambda_j\beta_j}{(\omega_k + \lambda_j)^2}}. \tag{9.28}$$

There are seven possible values of k, corresponding to the six groups of delayed neutrons (or precursors), and at late times the solution to equation (9.27) is dominated by the term with the most positive ω_k. This is usually represented by ω_0 and $1/\omega_0$ is the asymptotic (or stable) reactor period. The other six (negative) values of ω_k correspond to transient terms which die away in a short time.

The relation between reactivity and reactor period, as given by equation (9.26), commonly known as the *inhour equation*, has been frequently applied in studies of reactor kinetics. It is desirable, therefore, to examine its physical implications. In the derivation of equation (9.26) it was assumed that the reactivity is suddenly changed from ρ_- to a constant value ρ_+. A change of this nature might be accomplished, approximately, by the sudden motion of a control rod, and such an experiment will now be considered. Ignoring, for simplicity, the time required for the actual motion, suppose that the rod is moved instantaneously at time $t = 0$ from some initial position to a final position. If the shape factors, $\psi(\mathbf{r}, \Omega, E, t)$, corresponding to the initial and final positions of the control rod are much the same, either function could be used to compute the reactivity change as well as the parameters β_j and Λ. These could then be employed to calculate the asymptotic period by means of equation (9.26). Alternatively, if

β_j and Λ have been found in this (or some other) way, the reactivity (or worth) of control rod motion could be determined.

Suppose, however, that the shape function does change substantially as a result of the rod motion, so that it reaches a time-independent value only after the transients, which are associated with the decay of the delayed-neutron precursors, have died away. During the time the shape factor is changing, so also is the reactivity, according to equation (9.10), even though the control rod does not move. Under these conditions, the reactivity would approach its final value, ρ_+, after a delay of perhaps several seconds; only then would the asymptotic period be attained. The situation is as indicated in Fig. 9.1.

These considerations are important for large reactors, in which the different spatial regions are loosely coupled, i.e., the dimensions of the regions are large compared with the neutron diffusion length, especially when the reactivity changes are large and are caused by localized perturbations. The gross shape of the neutron flux and the shape function can be changed significantly by rod motion and it may take several seconds for the new shape to be established.[20] For small, tightly coupled systems, on the other hand, particularly if the reactivity perturbations are small, the situation is different. Although the shape function may change locally, i.e., in the immediate vicinity of the control rod, such changes are rapid and do not depend on the decay of the delayed-neutron precursors.

The inhour equation (9.26) has been widely employed for deriving reactivity values from observed asymptotic periods as, for instance, in the calibration of control rods. The values of β_j and Λ for the reactor are generally available, to a

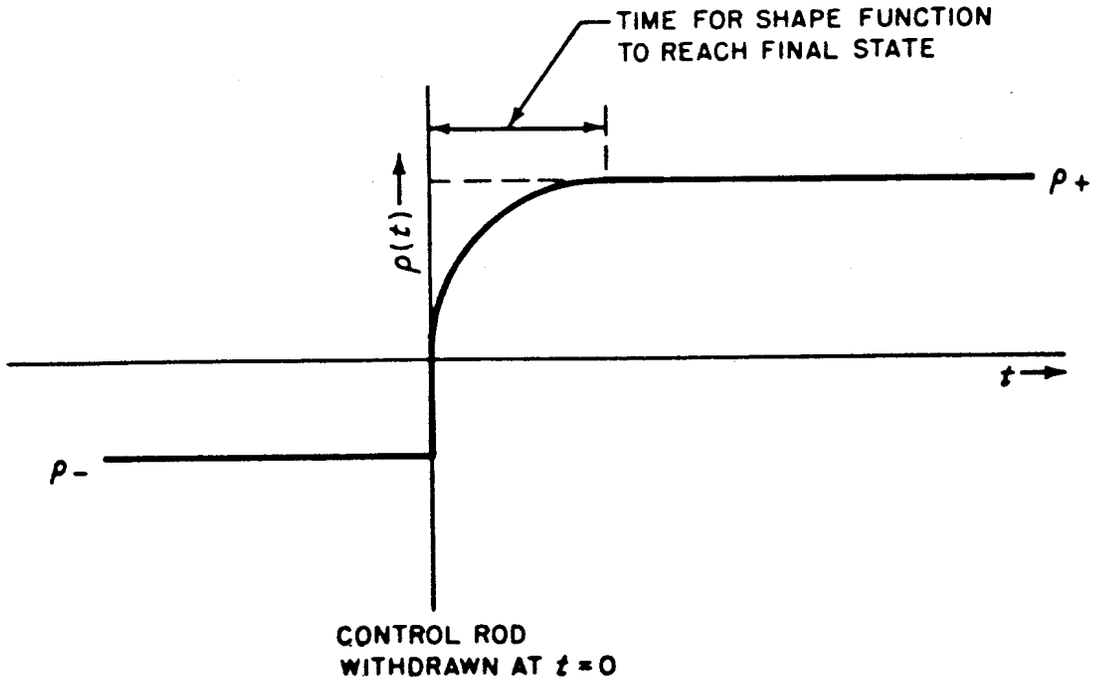

FIG. 9.1 CHANGE OF SHAPE FUNCTION AS A RESULT OF CONTROL ROD MOTION.

good approximation, either from equations (9.11) and (9.13) with an estimated shape factor or from other considerations. For example,[21] the quantity $\bar{\beta}$ can be obtained from measurements of the difference in mass between prompt and delayed critical, together with an interpretation of this mass difference in terms of k as given by perturbation theory (§6.3c). When using point-reactor relations, however, such as the inhour equation, it should be borne in mind that the parameters ρ, $\bar{\beta}_j$, and Λ are properly and consistently defined in terms of the shape factor, $\psi(\mathbf{r}, \mathbf{\Omega}, E, t)$, which, in turn, reflects the over-all neutronic state of the reactor at a specified time.

9.2f Numerical Solutions of the Point-Reactor Equations and the Zero Prompt Lifetime Approximation

In many cases of interest, the reactor kinetics equations (9.8) and (9.9) cannot be solved in closed form and numerical methods of solution must be used. In practice, solutions are usually sought to these equations supplemented by feedback relations (§9.4a), but an important difficulty in their solution can be appreciated even without considering feedback effects.

Except for cases of very fast transients, it may be required to follow the solutions over many seconds or even minutes. A difficulty then arises for the following reason. Equations (9.8) and (9.9) represent a set of $J + 1$ first-order coupled differential equations, where J is the total number of delayed-neutron groups. The solution of these equations by standard difference techniques, e.g., by the Runge-Kutta method, is not efficient, however, because for accuracy it is necessary to use small time steps which are determined by the prompt neutron lifetime, Λ.[22] Consequently, a number of fairly specialized integration procedures have been developed and digital codes are available for obtaining reliable solutions.[23]

There is also a simpler general approach based on the assumption, in physical terms, that the prompt-neutron lifetime is so short that it can be set equal to zero, provided the system is not at or above prompt critical. This is called the *zero prompt-neutron lifetime* (or in brief, the *zero prompt lifetime*) *approximation*. For the reason to be given later, it is also sometimes referred to as the *prompt-jump approximation*.

Equation (9.20), which is equivalent to equations (9.8) and (9.9), may be written in the form

$$\Lambda \frac{dP(t)}{dt} = [\rho(t) - \bar{\beta}(t)]P(t) + \sum_j \lambda_j \left[\Lambda c_{j0} e^{-\lambda_j t} + \int_0^t \beta_j(t') P(t') e^{-\lambda_j (t - t')} \, dt' \right] + \Lambda Q(t), \quad (9.29)$$

where, for simplicity, Λ is taken to be independent of time, and $c_{j0} \equiv c_j(0)$. If

the prompt lifetime, Λ, is small, the two terms on the right side of this equation that are multiplied by Λ cannot be set equal to zero because they are source terms for the problem, and multiplication by Λ simply converts them into sources per neutron lifetime. As Λ gets smaller, both $P(t)$ and the sources thus decrease proportionately (see end of §9.2b). For small Λ, however, the left side of equation (9.29) goes to zero more rapidly than the right side, except perhaps for fast transients. Thus, the assumption of a prompt-neutron lifetime of zero consists in setting the left side of equation (9.29) equal to zero.

The situation may be expressed mathematically by expanding $P(t)$ in the form

$$P(t) = P_0(t) + \Lambda P_1(t) + \cdots,$$

substituting into equation (9.29), and equating the coefficients of each power of Λ to zero. From the coefficient of Λ^0, it is found that

$$[\rho(t) - \bar{\beta}(t)]P_0(t) + \sum_j \lambda_j \int_0^t \bar{\beta}_j(t')P_0(t')e^{-\lambda_j(t-t')}\,dt' = 0,$$

and the solution of this equation is $P_0(t) = 0$. By setting the coefficient of Λ equal to zero, it is found that $P_1(t)$ satisfies the equation

$$[\rho(t) - \bar{\beta}(t)]P_1(t) + \sum_j \lambda_j \left[c_{j0}e^{-\lambda_j t} + \int_0^t \bar{\beta}_j(t')P_1(t')e^{-\lambda_j(t-t')}\,dt'\right] + Q(t) = 0. \tag{9.30}$$

The zero prompt lifetime approximation then consists in terminating the series at P_1, i.e., since $P_0(t) = 0$,

$$P(t) = \Lambda P_1(t).$$

In other words, it is seen that in this approximation $\Lambda P_1(t)$ satisfies equation (9.29) with $dP(t)/dt = 0$. (Systematic improvements on the zero prompt lifetime approximation can be obtained by the use of singular perturbation theory.[24])

Equation (9.30) can be solved numerically by using time steps, which are independent of Λ, to evaluate the integral. If $\rho - \bar{\beta} > 1$, i.e., for a system above prompt critical, however, this approach fails; all terms on the left side of equation (9.30) are then positive and their sum cannot possibly be equal to zero.

For analytical work, it is convenient to make use of a further simplification of the zero prompt lifetime approximation. First, it is assumed that there is only one (average) group of delayed-neutron precursors, characterized by β and λ; furthermore, β is assumed to be constant, independent of time, and Q is taken as zero. Then, upon differentiating equation (9.30) and using equation (9.30) in the result, it is found that

$$[\rho(t) - \beta]\frac{dP(t)}{dt} + \left[\frac{d\rho(t)}{dt} + \lambda\rho(t)\right]P(t) = 0. \tag{9.31}$$

This simple form of the zero prompt lifetime approximation is sometimes used in analytical studies.

Since in the zero prompt lifetime approximation the kinetic equation (9.29) is solved with the time derivative set equal to zero, the power, $P(t)$, can respond instantaneously to any change in reactivity. Thus, if $dP/dt = 0$ in equation (9.29), the result can be written as

$$[\bar{\beta}(t) - \rho(t)]P(t) = \Lambda[Q_d(t) + Q(t)], \tag{9.32}$$

where $Q_d(t)$ represents the delayed-neutron precursor decay rate, i.e.,

$$\Lambda Q_d(t) = \sum_j \lambda_j \left[\Lambda c_{j0} e^{-\lambda_j t} + \int_0^t \bar{\beta}_j(t')P(t')e^{-\lambda_j(t-t')}\,dt'\right].$$

Hence, if $\rho(t)$ were to undergo a sudden jump, the right side of equation (9.32) would not change for a while; but $P(t)$ would also show a prompt jump in order to satisfy this equation. Thus, the zero prompt lifetime approximation is also referred to as the prompt-jump approximation. In this book, the former terminology is preferred since it indicates more clearly the physical content of the approximation.

9.2g The Linearized Kinetics Equations

It was mentioned earlier that, in a reactor operating at power, the reactivity is a function of the power. Hence, the kinetics equation (9.8) will be a nonlinear equation in the reactor power. If a reactor operating at power undergoes a *small perturbation* in reactivity, however, it is possible to linearize the equations for the point reactor. The resulting simple expressions, which are derived here, will find application in several subsequent sections.

Consider a system operating in a steady state at power P_0 in the absence of any source. Such a system is critical and hence $\rho = 0$. The kinetics equations (9.8) and (9.9) for the point-reactor model will then have time-independent solutions P_0 and c_{j0}, obtained by setting dc_j/dt in equation (9.9) equal to zero, i.e.,

$$\lambda_j c_{j0} = \frac{\bar{\beta}_j}{\Lambda} P_0. \tag{9.33}$$

This result also satisfies equation (9.8), with $dP/dt = 0$, $\rho = 0$, and $Q = 0$, as may be seen by summing equation (9.33) over j, and recalling that $\sum \bar{\beta}_j = \bar{\beta}$.

Suppose that the reactivity is perturbed from zero by a small amount $\delta\rho(t)$ and that this causes the power and delayed-neutron precursors to be perturbed by small quantities; thus,

$$P(t) = P_0 + \delta P(t) \tag{9.34}$$

and

$$c_j(t) = c_{j0} + \delta c_j(t). \tag{9.35}$$

If these expressions are inserted into equations (9.8) and (9.9), with $Q = 0$, and the steady-state condition (9.33) is satisfied, it is found that

$$\frac{d[\delta P(t)]}{dt} = \frac{\delta\rho(t)}{\Lambda}[P_0 + \delta P(t)] - \frac{\bar{\beta}}{\Lambda}\delta P(t) + \sum_j \lambda_j \delta c_j(t) \tag{9.36}$$

and

$$\frac{d[\delta c_j(t)]}{dt} = \frac{\bar{\beta}_j}{\Lambda}\delta P(t) - \lambda_j \delta c_j(t). \tag{9.37}$$

In equation (9.36), the term $\delta\rho(t)\,\delta P(t)/\Lambda$ is second order in small quantities and hence it may be neglected if the perturbations are small, as postulated above. Then equations (9.36) and (9.37) can be written as

$$\frac{d(\delta P)}{dt} = \frac{P_0}{\Lambda}\delta\rho - \frac{\bar{\beta}}{\Lambda}\delta P + \sum_j \lambda_j \delta c_j \tag{9.38}$$

and

$$\frac{d(\delta c_j)}{dt} = \frac{\bar{\beta}_j}{\Lambda}\delta P - \lambda_j \delta c_j. \tag{9.39}$$

These are the linearized kinetics equations for a point reactor.

It is important to bear in mind that equation (9.38) can be used only when $\delta\rho\,\delta P/\Lambda$ is small. Whenever the solution of the linearized equations predicts a large power perturbation, the nonlinear equation (9.36) must be considered since the neglected term may greatly alter the character of the solution. As long as $\delta\rho$ and δP are sufficiently small, however, as is the case in some of the situations considered below, the linearized equations may be used.

9.3 TRANSFER FUNCTIONS

9.3a The Zero-Power Transfer Function

Useful information about a reactor can be obtained by studying its response to small perturbations of the reactivity. In particular, conclusions concerning the stability of a reactor when it is operating at power can be drawn from the response to small sinusoidal perturbations. The response characteristics are then summarized in terms of a transfer function, which is defined below. The study of reactor transfer functions, both experimentally and theoretically, is of great importance in connection with the control of nuclear reactors. As the first stage in the treatment of this aspect of reactor dynamics, consideration will be given to the power response of a system operating at very low (or zero) power to a small reactivity oscillation. The determination and use of transfer functions are described in §9.5a *et seq.*

Suppose that the system under consideration is critical, with no source, and that the reactivity is changed by a small amount; if the power also changes to a

small extent only, the conditions are then such that the linearized equations (9.38) and (9.39) are applicable. Upon taking Laplace transforms of these equations, with $\delta P(0) = \delta c_j(0) = 0$, so that

$$\mathscr{L}\frac{d(\delta P)}{dt} = s\mathscr{L}(\delta P) = s\,\delta P(s)$$

and

$$\mathscr{L}\frac{d(\delta c_j)}{dt} = s\mathscr{L}(\delta c_j) = s\,\delta c_j(s),$$

equations (9.38) and (9.39) become

$$s\,\delta P(s) = \frac{P_0}{\Lambda}\,\delta\rho(s) - \frac{\bar{\beta}}{\Lambda}\,\delta P(s) + \sum_j \lambda_j\,\delta c_j(s) \tag{9.40}$$

and

$$s\,\delta c_j(s) = \frac{\bar{\beta}_j}{\Lambda}\,\delta P(s) - \lambda_j\,\delta c_j(s). \tag{9.41}$$

Upon solving for $\delta P(s)$ in terms of $\delta\rho(s)$, it is found that

$$\delta P(s) = \delta\rho(s) P_0 R(s)$$

or

$$\frac{\delta P(s)}{\delta\rho(s)} = P_0 R(s), \tag{9.42}$$

where

$$R(s) = \frac{1}{s\Lambda + \sum_j \dfrac{s\bar{\beta}_j}{s + \lambda_j}}. \tag{9.43}$$

The response (or output) of any physical system to an information (or input) signal applied to it is expressed by the *transfer function* of the system. It may be defined for the present purpose by

$$\text{Transfer function} = \frac{\text{Laplace transform of response}}{\text{Laplace transform of perturbation}}.$$

It follows, therefore, that if δP is the change in power of a reactor operating in the steady (or critical) state, in response to a small change $\delta\rho$ in the reactivity, $\delta P(s)/\delta\rho(s)$ is the appropriate transfer function. Hence, in the case under consideration, equation (9.42) gives for the linearized system

$$\text{Transfer function} = P_0 R(s). \tag{9.44}$$

There are alternative, but equivalent, expressions for this particular transfer function. For example, if the response is stated as the change in power relative

to the initial (steady-state) value, i.e., $\delta P/P_0$, the transfer function would be just $R(s)$, as given by equation (9.43).*

The transfer function for the linearized system defined by equation (9.43) or equation (9.44) is called the zero-power (or open-loop) transfer function. The reason is that the power level is not allowed to affect the reactivity in any way. In other words, feedback effects are not considered; if there is a feedback loop (see Fig. 9.5), it is regarded as being open. This would be true in practice only if the reactor is operating at such a low, essentially zero, power that the temperature, and related reactor conditions, remain unchanged during operation. The more general problem of a point reactor with feedback is taken up in §9.4a *et seq.*

9.3b Sinusoidal Reactivity Perturbations

For the special case in which a reactor is perturbed by small sinusoidal oscillations about the steady ($\rho = 0$) state,

$$\delta\rho(t) = \delta\rho \cos \omega t$$

and then

$$\delta\rho(s) = \frac{s\,\delta\rho}{s^2 + \omega^2} = \frac{s\,\delta\rho}{(s - i\omega)(s + i\omega)},$$

where ω is the oscillation frequency. Upon inverting the Laplace transform[25] of the power change, $\delta P(s)$, given by equation (9.42), the poles of $\delta\rho(s)$ at $s = \pm i\omega$ would give the long-term power variation; the other poles of $\delta\rho(s)$ at negative real values of s would lead only to transients (§9.2e).

Thus, for the specified sinusoidal reactivity variation, the inverse transform of equation (9.42) leads to

$$\delta P(t) = \frac{P_0\,\delta\rho}{2\pi i}\int_{b-i\infty}^{b+i\infty} R(s)\,\frac{s}{(s - i\omega)(s + i\omega)}\,e^{st}\,ds.$$

By using contour integration to evaluate the integral, it is found when t is large, so that the poles at $s = \pm i\omega$ give the only contribution, that

$$\delta P(t) \xrightarrow[t\ \text{large}]{} \tfrac{1}{2}P_0\,\delta\rho[R(i\omega)e^{i\omega t} + R(-i\omega)e^{-i\omega t}]. \tag{9.45}$$

If $R(i\omega)$ is written as the product of its absolute value and a phase factor, i.e.,

$$R(i\omega) = |R(i\omega)|e^{i\theta}, \tag{9.46}$$

then

$$\delta P(t) \xrightarrow[t\ \text{large}]{} P_0\,\delta\rho|R(i\omega)|\cos(\omega t + \theta). \tag{9.47}$$

It is evident from this result that if a reactor operating at low power in the steady state is subjected to a sinusoidal perturbation in reactivity, the power will

* The reactivity is often expressed in dollar units, as defined in §6.3f. When reactivity is measured in dollars, the transfer function would be $\beta P_0 R(s)$.

oscillate with the same frequency but with the phase shifted by the angle θ radians; the amplitude of the power oscillations is proportional to $|R(i\omega)|$. In practice, θ is either negative or close to zero (see Fig. 9.3); consequently, as expected, the power response lags behind the reactivity change.

The amplitude $|R(i\omega)|$ and the phase angle θ, as functions of ω, are the essential components of $R(i\omega)$, which is equal (or proportional) to the reactivity-to-power transfer function for a reactor operating at low power. Equation (9.47) provides a basis for the experimental measurement of both amplitude and the phase angle. Other methods for determining these quantities will be mentioned later.

Alternatively, $|R(i\omega)|$ and θ for a given system can be calculated from equation (9.43) with s replaced by $i\omega$; thus,

$$R(i\omega) = \frac{1}{i\omega\Lambda + \sum_j \dfrac{i\omega\beta_j}{i\omega + \lambda_j}},$$

and $R(i\omega)$ can be computed for specified values of Λ and β_j. To obtain the amplitude and phase angle, the result may be expressed in the form of equation (9.46) or, alternatively, as

$$R(i\omega) = \text{Re}\,[R(i\omega)] + i\,\text{Im}\,[R(i\omega)].$$

If the values of Re $[R(i\omega)]$ are plotted as abscissae and Im $[R(i\omega)]$ as ordinates, as in Fig. 9.2, the amplitude $|R(i\omega)|$ is the magnitude of the vector, and θ gives its direction, where

$$\tan\theta = \frac{\text{Im}\,[R(i\omega)]}{\text{Re}\,[R(i\omega)]}.$$

A comparison of observed and calculated zero-power transfer functions for some reactors and critical assemblies is given in Fig. 9.3; the points are the

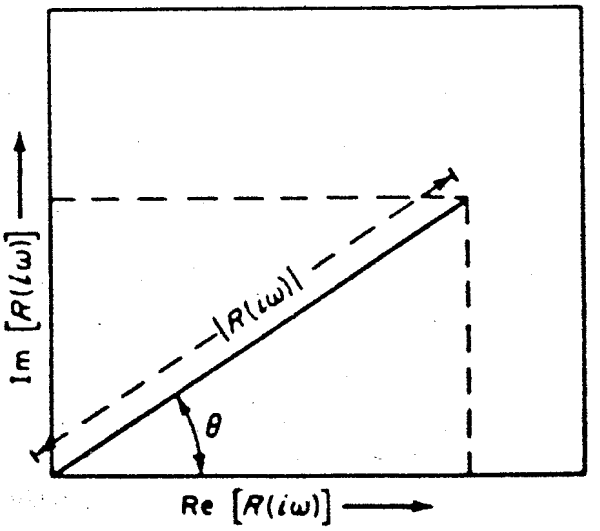

FIG. 9.2 REPRESENTATION OF AMPLITUDE AND PHASE ANGLE.

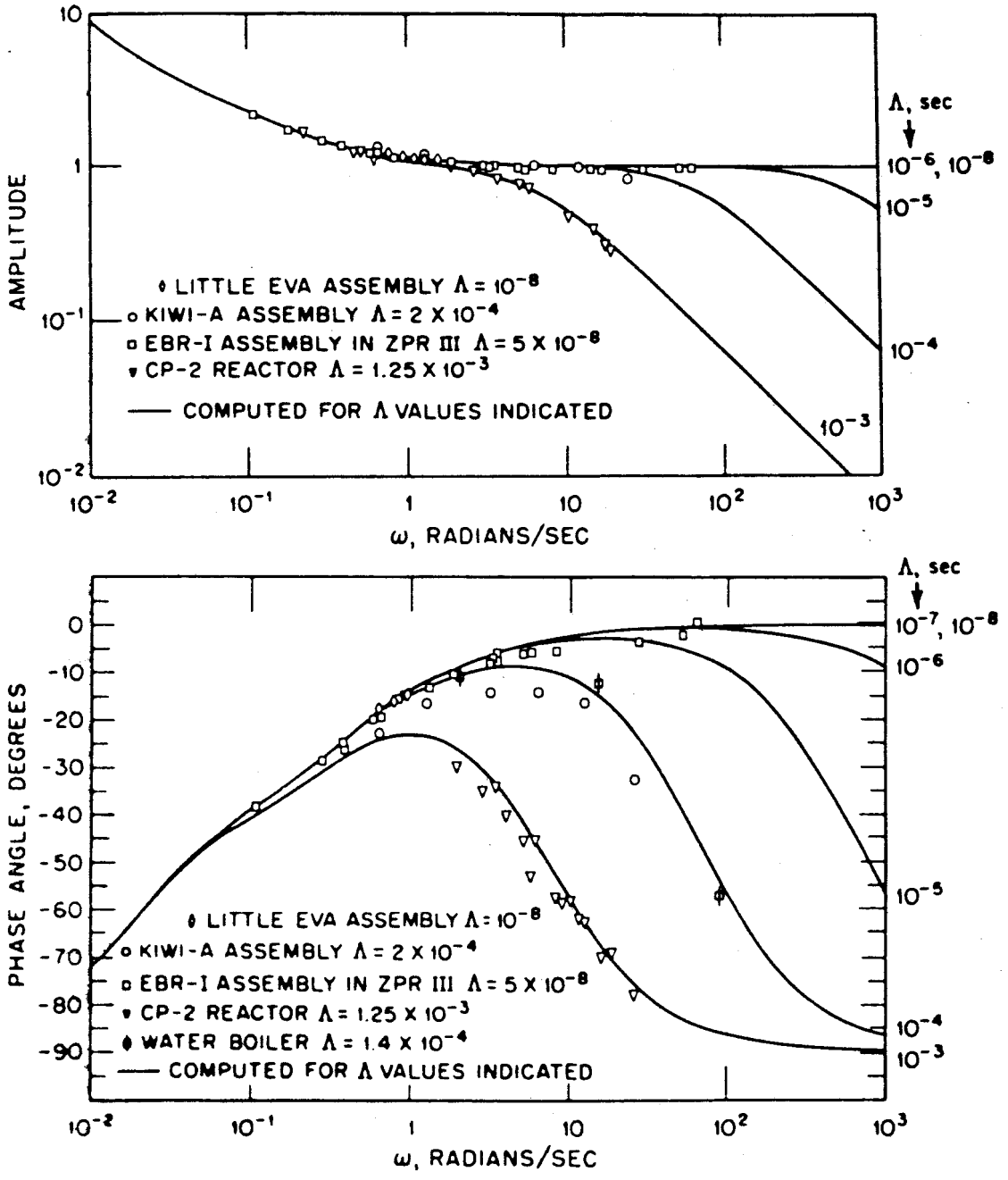

FIG. 9.3 EXPERIMENTAL AND CALCULATED ZERO-POWER TRANSFER FUNCTIONS FOR REPRESENTATIVE FAST, INTERMEDIATE, AND THERMAL URANIUM-235 SYSTEMS (AFTER G. R. KEEPIN, REF. 26).

experimental data for the indicated systems.[26] The full lines show the amplitude and phase angle (in degrees) as a function of the oscillation frequency in radians per second calculated for values of Λ ranging from 10^{-8} to 10^{-3} sec. The effective delayed neutron fractions, β_j, used are for uranium-235, which is the common fissile material; the β_j's were assumed to be the same in all the systems. The zero-power transfer functions have been tabulated for the common fissile nuclides.[27]

9.3c Space Dependence of Transfer Functions

In considering the transfer functions of large, loosely coupled systems, it is necessary to take spatial effects into account. As noted in §9.2c, the reason is that, for such systems, the variations of the shape function, $\psi(\mathbf{r}, \mathbf{\Omega}, E, t)$, with time may be as important as the variations of $P(t)$. Thus, when the transfer function is measured, by taking the output to be that indicated by a localized neutron detector, it will be sensitive to oscillations in ψ as well as in the power, $P(t)$. It is possible, however, to define a space-dependent transfer function by considering a ratio of detector output to sinusoidal reactivity input and to compute such a transfer function without solving the complete time-dependent problem.[28]

In order to understand the procedure, the time-dependent transport equation (9.2) is written as

$$\frac{1}{v}\frac{\partial \Phi}{\partial t} = \mathbf{L}_p\Phi + \sum_j \lambda_j C_j(\mathbf{r}, t)\tilde{\chi}_j + Q, \tag{9.48}$$

where $\mathbf{L}_p$ represents a prompt-neutron transport operator; this is similar to $\mathbf{L}$ in §6.1b except that the prompt neutrons are here explicitly the only ones considered as emerging from fission. A solution to this equation, together with equation (9.3), which is reproduced for convenience, i.e.,

$$\frac{\partial C_j(\mathbf{r}, t)}{\partial t} + \lambda_j C_j = \iint \beta_j \nu\sigma_f \Phi' \, d\mathbf{\Omega}' \, dE', \tag{9.49}$$

is now sought for a small localized disturbance in some cross section, denoted as $\delta\mathbf{L}e^{i\omega t}$.

Suppose that in the absence of any disturbance, there are time-independent solutions, Φ_0 and C_{j0}, due to a steady source, Q. During the course of the disturbance, the solutions may then be assumed to be of the form

$$\Phi = \Phi_0 + \delta\Phi e^{i\omega t}$$

and

$$C_j = C_{j0} + \delta C_j e^{i\omega t},$$

where $\delta\Phi$ and δC_j may be complex functions of $\mathbf{r}$, $\mathbf{\Omega}$, and E. If these expressions for Φ and C_j are inserted in equation (9.48) and the steady-state conditions are taken into account, the result, after linearization by dropping terms in $\delta\mathbf{L}\,\delta\Phi$, is found to be

$$\frac{i\omega}{v}\delta\Phi = \mathbf{L}_p\,\delta\Phi + \delta\mathbf{L}\Phi_0 + \sum_j \lambda_j\,\delta C_j\tilde{\chi}_j. \tag{9.50}$$

In a similar way, equation (9.49) gives

$$\delta C_j = \frac{1}{i\omega + \lambda_j}\iint \beta_j\nu\sigma\,\delta\Phi' \, d\mathbf{\Omega}' \, dE'. \tag{9.51}$$

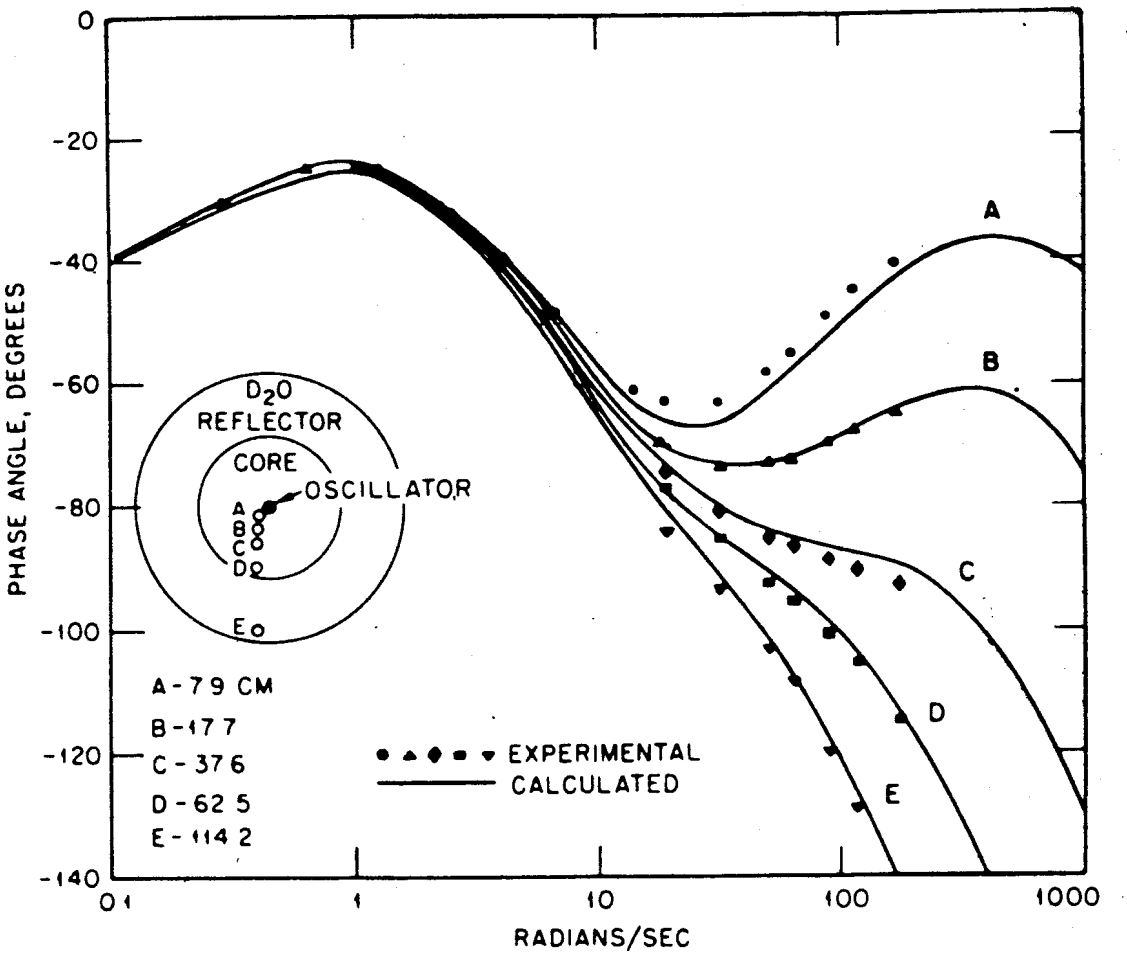

FIG. 9.4 EXPERIMENTAL AND OBSERVED PHASE ANGLES AS FUNCTION OF POSITION (AFTER C. E. COHN, *ET AL.*, REF. 29).

Equation (9.51) may now be substituted into equation (9.50) and the result separated into real and imaginary parts. Solutions can then be sought for the real and imaginary parts of $\delta\Phi$ from which the amplitude and phase angle of a suitably defined space-dependent transfer function can be found.

A calculation of this type has been made by using a two-group diffusion theory form of L_p. The results were then compared with the experimental values for the NORA reactor, an enriched-uranium critical assembly moderated by heavy water.[29] The measurements are made by observing the response of the reactor at a given point to a sinusoidal disturbance introduced elsewhere (see inset in Fig. 9.4). The observed values of the phase angle and the computed curves, for various distances from an oscillating control rod, are shown in Fig. 9.4. There is clearly a strong spatial dependence of the transfer function in this case.

The foregoing remarks concerning the space dependence of transfer functions do not imply that it is incorrect to consider space-independent transfer functions even for large systems. In principle, such transfer functions can always be defined by considering $P(t)$ as the output. The problem is simply that the variations in $P(t)$ do not represent the situation completely; moreover, such variations are

difficult to measure precisely. There are other experimental problems involved in the determination of transfer functions, e.g., approximating a sinusoidal reactivity input; more will be said about this in §9.5b.

9.4 THE POINT REACTOR WITH FEEDBACK

9.4a Introduction

In the zero-power point reactor, the power level is assumed to be so low that it does not affect the reactivity; hence, there are no feedback effects. It is necessary now to examine the consequences of feedback mechanisms especially insofar as they influence the stability of a reactor operating at power. For the present purpose a feedback mechanism is regarded as a physical effect whereby the neutron population or reactor power, $P(t)$, alters the reactivity, $\rho(t)$.

It is evident from equation (9.10) that changes in reactivity arise from changes in the macroscopic cross sections and by such changes alone. There is a slight complication since, for a given $\Delta\sigma$, the reactivity may change due to changes in the shape function, ψ, which can be caused by changes in the source. In general, however, it is basically changes in the macroscopic cross sections that influence the reactivity. Such changes will occur either when the nuclear densities change or when there is a change in the microscopic cross sections. This distinction provides a convenient way of separating feedback effects.

Feedback reactivity can arise from changes in temperature in a reactor operating at power. First, the densities of the reactor materials will be affected by temperature due to thermal expansion. Density changes can also be the result of phase changes, e.g., conversion of water into steam. In addition, temperature changes may lead to mechanical motion, e.g., bending, of fuel elements or other reactor components. Furthermore, temperature can alter the microscopic cross sections; this may arise from changes in the thermal neutron scattering laws and from the Doppler broadening of resonances. Changes in microscopic cross sections also result from the accumulation of fission products; in this connection xenon-135 is especially important.

Changes in reactivity with temperature are described by temperature coefficients of reactivity which can be expressed in various ways. For stable operation of a reactor, negative temperature coefficients are, of course, desirable. If the temperature of a reactor always remained uniform during operation, an isothermal temperature coefficient of reactivity could be obtained. In practice, however, when a reactor is at a power level high enough for feedback mechanisms to be significant, the temperature will not be uniform and the isothermal temperature coefficient will not be applicable. In situations of this kind appropriate average temperatures are used.

In order to determine the temperature distribution throughout an operating reactor, detailed engineering calculations are required of heat transfer and

coolant flow. The results are then incorporated in the equations of reactor dynamics for determining feedback effects by introducing them in terms of "lumped" parameters of the system. These are, for example, "fuel temperature," "moderator temperature," and "coolant temperature" and their associated temperature coefficients of reactivity. In principle, these temperatures should be averages, based on the actual temperature distribution, weighted to give the correct reactivities. The effective temperatures of the various regions are coupled by parameters derived from engineering calculations.

Because of these and other approximations, including the neglect or simplification of spatial effects in point-reactor kinetics, there is always some degree of uncertainty in the calculation of reactivity changes arising from feedback mechanisms. It would be desirable for the performance of the reactor to be insensitive to the approximations, but, in any event, the expected feedback effects should be verified by means of an experimental program, at least during reactor startup and early operation.

Of the situations in which feedback effects are important, three will be treated here. The first involves small oscillations of the power (and reactivity) about some equilibrium value. This represents, indeed, a common practice for studying the stability of a reactor by observing its response to small, more-or-less sinusoidal, oscillations in reactivity. In analyzing this stability, the kinetics equations can be linearized, thereby greatly simplifying the problem. The stability investigated in this manner, i.e., against small oscillations, is referred to as "stability in the small."

The second situation of interest is that in which larger variations or oscillations of power or reactivity are permitted; in this case, nonlinear effects of feedback must be taken into account. These nonlinearities make the analysis much more difficult so that it has been possible to obtain partial results only in some special cases. For large oscillations, at least two kinds of stability are distinguished; they are asymptotic stability when the oscillations damp out with time, and Lagrange stability when the oscillations remain finite but bounded.[30]

Finally, consideration will be given to very large excursions which bring the reactivity above prompt critical. In extreme cases such excursions are terminated only by fairly violent disruption of the core, e.g., by melting or by ejection of the (liquid) moderator. The matter of interest here is to determine the consequences of a single transient or pulse. Such problems arise in the analysis of pulsed reactors,[31] in fast-transient safety tests on various water-moderated systems,[32] and in considering the damage which may follow the accidental achievement of a highly supercritical state.

9.4b The Transfer Function with Feedback

There are several possible ways of introducing feedback into the reactor kinetics equations, but the simplest, from a physical viewpoint, is to use the temperature,

as indicated above, to characterize the state of various regions. The simple case will be considered in which the feedback is determined by the average (lumped) temperature of the fuel, T_F, and of the moderator (or coolant), T_M.*

It should be noted that reactivity effects associated with temperature changes in the fuel are relatively prompt, since the fuel temperature responds, usually with little delay, to changes in the reactor power. Moreover, there is no appreciable lag between a change in fuel temperature and the corresponding changes in the cross sections of the fuel which affect the reactivity. On the other hand, reactivity effects due to changes of temperature of the moderator (or coolant) are delayed because heat must flow from the fuel before these temperatures can be established.

Suppose that under steady operating conditions, the power (or neutron population) is P_0 and the fuel and moderator (or coolant) temperatures are T_{F0} and T_{M0}, respectively. It will be assumed that small perturbations about these conditions can be represented by

$$\frac{d(\delta T_F)}{dt} = a\,\delta P - \omega_F\,\delta T_F \tag{9.52}$$

and

$$\frac{d(\delta T_M)}{dt} = b\,\delta T_F - \omega_M\,\delta T_M, \tag{9.53}$$

where δT_F, δT_M, and δP are the deviations of the actual temperatures and power from their steady-state values, and ω_F and ω_M are the decay constants of the fuel and moderator temperatures. Equation (9.52) expresses the fact that the fuel temperature responds directly to the changes in the power, whereas equation (9.53) implies that the moderator responds to the change in the fuel temperature. The thermal responses to a sharp power pulse $\delta P = p_0\,\delta(t)$, where $\delta(t)$ is a Dirac function, are then

$$\delta T_F = ap_0 e^{-\omega_F t} \tag{9.54}$$

and

$$\delta T_M = \frac{abp_0}{\omega_M - \omega_F}(e^{-\omega_F t} - e^{-\omega_M t}). \tag{9.55}$$

These equations show that the fuel temperature responds promptly to the power change, but the response of the moderator is delayed. If $\omega_F \gg \omega_M$, as is generally true, this time delay is of the order of $1/\omega_F$.

If the reactivity temperature coefficients of fuel and moderator are r_F and r_M, respectively, and if $\delta\rho_{ex}$ is some externally imposed reactivity change on a steady-state reactor, the actual reactivity is

$$\delta\rho = \delta\rho_{ex} + r_F\,\delta T_F + r_M\,\delta T_M. \tag{9.56}$$

* The symbol T_M, as used here and in later sections, refers to the temperature of any component of the reactor that affects the reactivity in a delayed manner in response to a change in the power.

Models such as the one described by equations (9.52) and (9.53) give the reactivity as a *linear function* of the power at earlier times; the most general relation of this kind is

$$\delta\rho(t) = \delta\rho_{ex}(t) + \int_0^t f(t - \tau)\, \delta P(\tau)\, d\tau, \tag{9.57}$$

where it is assumed that $\delta P(t) = 0$ for $t < 0$. Equation (9.57) describes how the reactivity at time t is affected by the power at preceding times; the function f, which appears in this equation, is determined by the feedback mechanisms of the system. The equation must be combined with the reactor kinetics equations in order to determine the system response, δP, which results from some imposed reactivity, $\delta\rho_{ex}$. Since small variations are involved in all quantities, it is appropriate to use the linearized forms of the kinetics equations, i.e., equations (9.38) and (9.39). These two equations together with equation (9.57) now describe the system.

From equations (9.54), (9.55), and (9.56), it is seen that, for the simple model under consideration, $f(t)$, which here represents the effect of fuel and moderator feedback, is given by

$$f(t) = a\left[r_F e^{-\omega_F t} + \frac{r_M b(e^{-\omega_F t} - e^{-\omega_M t})}{\omega_M - \omega_F}\right]. \tag{9.58}$$

The next step in the development is to take the Laplace transforms of the kinetics equations and of the feedback equation (9.57). For the kinetics equations, these are given by equations (9.40) and (9.41). Upon taking the Laplace transform of equation (9.57) and utilizing the convolution form of the integral[33] to write

$$\delta\rho(s) = \delta\rho_{ex}(s) + F(s)\, \delta P(s),$$

where $F(s)$ is the Laplace transform of $f(t)$, it is found from equations (9.40) and (9.41) that the transfer function, represented by $H(s)$, is

$$\frac{\delta P(s)}{\delta\rho_{ex}(s)} = \frac{P_0 R(s)}{1 - P_0 R(s) F(s)} \equiv H(s), \tag{9.59}$$

where $R(s)$ is exactly as defined by equation (9.43). In fact, when the feedback term $F(s)$ is zero (or P_0 is very small), equation (9.59) reduces to the zero-power transfer function of equation (9.42).

Equation (9.59) is often represented in the form of a block diagram, such as that shown in Fig. 9.5. In an actual reactor system, the feedback block marked $F(s)$ would be broken down into a number of components to allow for other factors in addition to that of temperature. These would include the effect of coolant velocity derived from studies of heat transfer and fluid mechanics,[34] with appropriate time delays. There would also be a feedback loop to allow for automatic movement of control rods based on sensing the changes in power. For complex systems of this kind, the transfer functions cannot be determined by

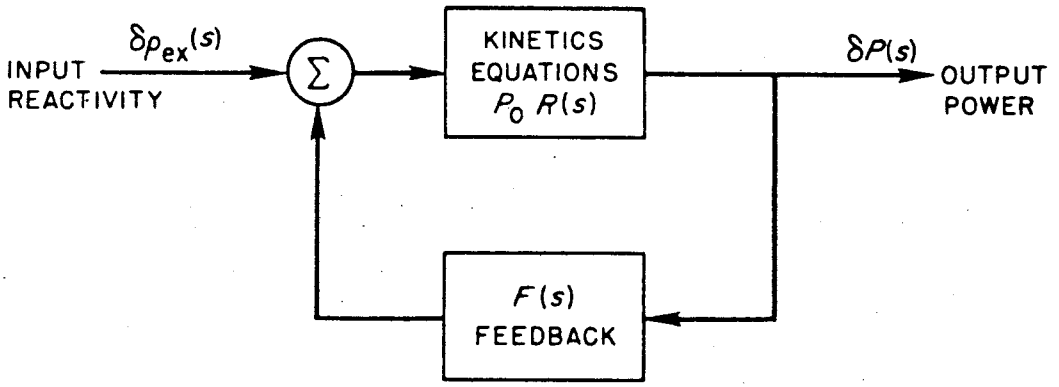

FIG. 9.5 SCHEMATIC REPRESENTATION OF FEEDBACK IN A REACTOR.

analytical procedures, but they can be readily obtained by simulating the reactor and the various feedback mechanisms on an analog computer.[35]

To return to the case under discussion of a simple linear feedback, the time response of the system to an imposed reactivity $\delta\rho_{ex}(t)$ can be found by inverting the Laplace transforms in equation (9.59). Thus, if $h(t)$ is the inverse transform of the transfer function $H(s)$, then

$$\delta P(t) = \int_0^t \delta\rho_{ex}(\tau)h(t - \tau)\, d\tau, \tag{9.60}$$

so that $h(t)$ is the impulse response function (or Green's function) of the system.

9.4c Stability Conditions

The stability of the system with feedback can be investigated by examining the poles of the Laplace transform, $H(s)$. These poles are solutions of the characteristic equation

$$1 - P_0R(s)F(s) = 0, \tag{9.61}$$

which includes the power; it is obtained by setting the denominator of equation (9.59) equal to zero. The poles of $R(s)$ in the numerator determine the response for the zero-power reactor (cf. §§9.2e, 9.3a) but these are not applicable here (for finite power) since $R(s)$ also appears in the denominator.

Suppose equation (9.61) has a simple root, so that $H(s)$ has a pole, at $s = \mathscr{S}$. Then, when the Laplace transform $\delta P(s)$ is inverted to obtain $\delta P(t)$, a term will be obtained proportional to $e^{\mathscr{S}t}$. If the real part of $\mathscr{S}$ is positive, i.e., $\mathscr{S}$ is a root in the right-half plane of the plot of Im (s) versus Re (s), as indicated by one of the circled crosses in Fig. 9.6, then the $\delta P(t)$ will grow exponentially with time, thus indicating an unstable (or unbounded) response to the applied reactivity perturbation. It should be mentioned that the exponential growth of $\delta P(t)$ is to be expected only from the linearized kinetics equations, i.e., for small perturbations of reactivity and power. For a large power excursion, nonlinear

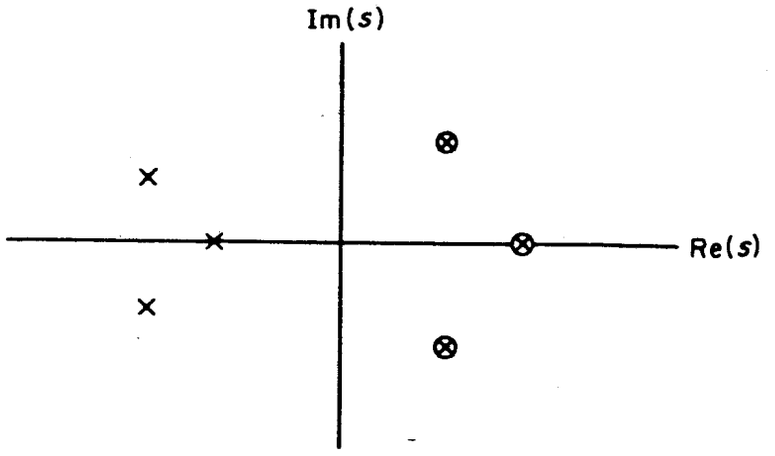

FIG. 9.6 DEVELOPMENT OF STABILITY CONDITIONS.

kinetics equations or a more general treatment would have to be used to determine the behavior.

If, on the other hand, the real part of $\mathscr{S}$ is negative, i.e., it lies in the left half-plane of Fig. 9.6, as shown by the uncircled crosses, the root will produce a contribution to $\delta P(t)$ that decays with time. Since what is true for one pole will be true for the others, it follows that if all roots are in the left half-plane, the system would be stable to a small perturbation in the reactivity. Hence, from the standpoint of reactor safety, it is important to determine if any of the poles of $H(s)$, i.e., roots of equation (9.61), lie in the right half-plane.

Another way of deriving conditions for stability is as follows. If a system is stable to a small increase, $\delta\rho_{ex}$, in the reactivity, it is to be expected that, at late times after the reactivity increase, $\delta P(t)$ will approach some constant positive value such that $\delta\rho(t) = 0$. Hence, at late times, it follows from equation (9.57) that for a stable response

$$0 = \delta\rho_{ex} + \delta P \int_0^\infty f(t)\,dt = \delta\rho_{ex} + F(0)\,\delta P,$$

where $f(t)$ is a feedback function. The quantity $F(0)$ is a Laplace transform representing the value of $F(s)$ when $s = 0$, i.e., in the steady state of the reactor; it is consequently called the *steady-state power coefficient*. A necessary, but not sufficient, condition for stability is then

$$F(0) = \int_0^\infty f(t)\,dt < 0. \tag{9.62}$$

Thus, the steady-state power coefficient of a reactor must be negative for stability; this conclusion has also been extended to nonlinear feedback problems.[36]

9.4d Power Limits for Stability

Another general feature of interest is that the linear feedback model may exhibit power thresholds at which instabilities develop. Suppose that somewhere in the right half-plane, the real part of $R(s)F(s)$ is positive whereas the imaginary part is zero. There will then be some power at which the product of P_0 and the real part is equal to unity; this will represent a root of the characteristic equation (9.61) and hence corresponds to an instability. The reactor will evidently be stable for lower powers, as far as this root is concerned, but it will become unstable at a critical power level at which the feedback becomes strong enough to drive the instability.

Actually, the situation is not quite as simple as this because the feedback function, $f(t)$, will itself depend on the power P_0 to some extent. Nevertheless, the principle that each mode of instability will tend to have a definite power threshold is correct. The physical reason is that at low powers not enough energy is being fed into the mode to drive it, and damping keeps the mode amplitude limited. At higher powers, the driving power exceeds the damping, at least in the simple linear theory.

Some insight into the onset of instability in linear theory can be obtained by, first, considering the situation at low power. Provided $R(s) \neq 0$, the characteristic equation (9.61) may be divided by $R(s)$; the result, together with equation (9.43) for $R(s)$, can be written as

$$G(s) = \frac{1}{R(s)} - P_0F(s) = \Lambda s + \sum_j \frac{\bar{\beta}_j s}{s + \lambda_j} - P_0F(s) = 0. \qquad (9.63)$$

If P_0 is small, the roots of $G(s)$ are then very nearly the roots of $1/R(s)$; these

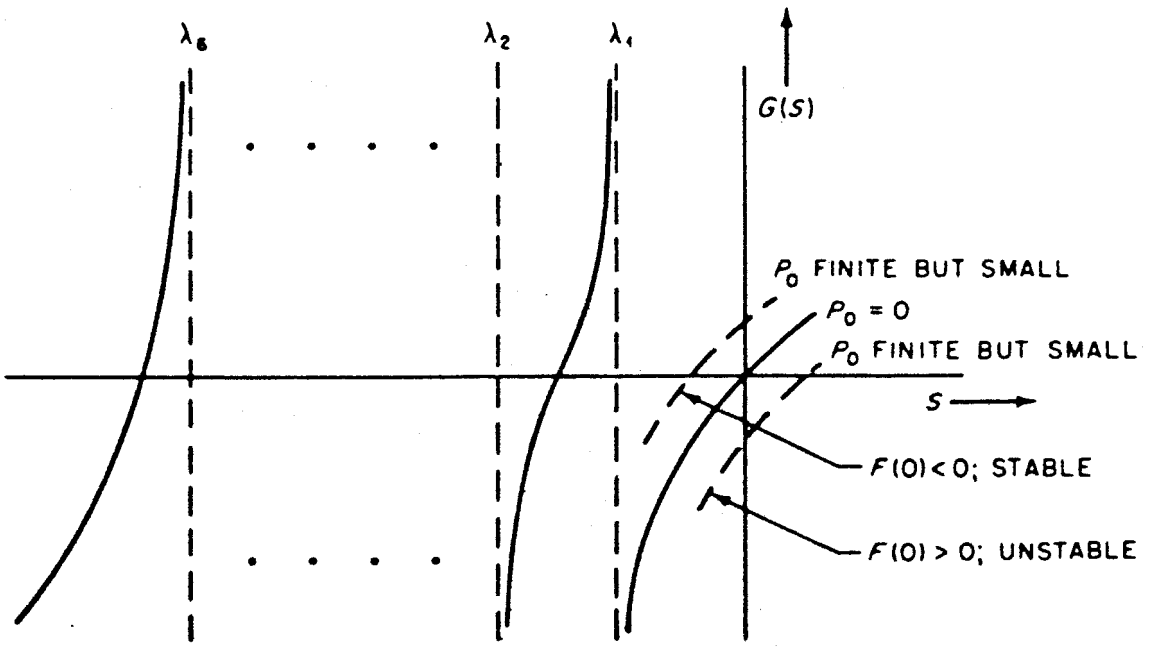

FIG. 9.7 ROOTS OF $G(s)$ AND ONSET OF INSTABILITY IN LINEAR THEORY.

will occur for $s = 0$ and for six ($j = 1, 2, \ldots, 6$) negative values of s. This can be seen by plotting $G(s)$ for $P_0 = 0$, actually $1/R(s)$, versus s for real values of s, as in Fig. 9.7.

For small but significant P_0, the root at $s = 0$ will move to the left or to the right according to whether the steady-state power coefficient, $F(0)$, is less than or greater than zero. In the former case the system will be stable, according to equation (9.62), and in the latter case it will be unstable.

The situation at higher values of P_0 can be understood by considering the behavior of the roots of the characteristic equation (9.63), i.e., $G(s) = 0$; these roots are the poles of $H(s)$. The particular case illustrated is one in which the system is stable when P_0 is small, but instability occurs at some higher power. Some simple examples are given in §9.4f. At zero power, the roots are just those of $1/R_s = 0$, and are indicated by $\mathscr{S}_1$, $\mathscr{S}_2$, $\mathscr{S}_3$, etc., in Fig. 9.8. If the steady-state power coefficient, $F(0)$, is negative, then at higher powers the root $\mathscr{S}_1$ will have a more negative real value and will move to the left, whereas some of the other roots may move to the right. At the same time, because of the $F(s)$ factor in equation (9.63), some of the higher solutions will have formed conjugate pairs, provided $G(s)$ is real for real s. The roots of equation (9.63) for moderate powers are indicated by the crosses in Fig. 9.9.

As the power is increased further, $\mathscr{S}_1$ and $\mathscr{S}_2$ approach each other in this example and then form a conjugate pair; with increasing P_0 the points move to the right, i.e., Re ($\mathscr{S}_1$) and Re ($\mathscr{S}_1^*$) become less negative, and farther apart, i.e., |Im ($\mathscr{S}_1$)| increases. The situation is depicted in Fig. 9.10. At a sufficiently high power, the roots will cross the imaginary axis and enter the right half-plane; as seen earlier, the system then becomes unstable. In this manner, therefore, a reactor with a negative steady-state power coefficient that is stable at low power could become unstable at a sufficiently high power. A specific example of the effect of increasing power on stability will be given later (§9.5e).

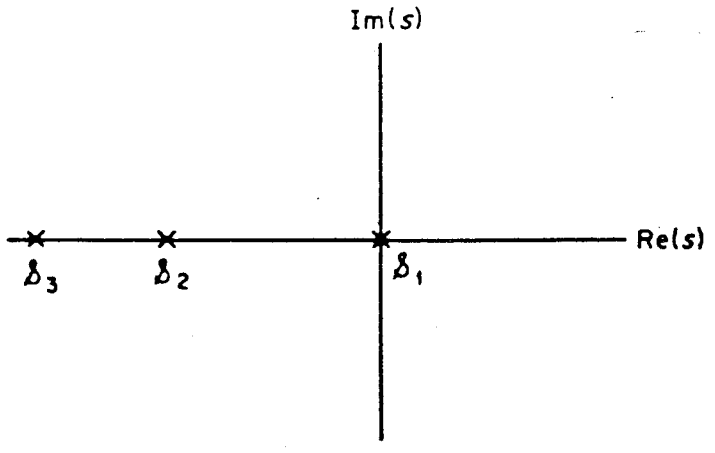

FIG. 9.8 ROOTS OF THE CHARACTERISTIC EQUATION (9.63) AT ZERO POWER.

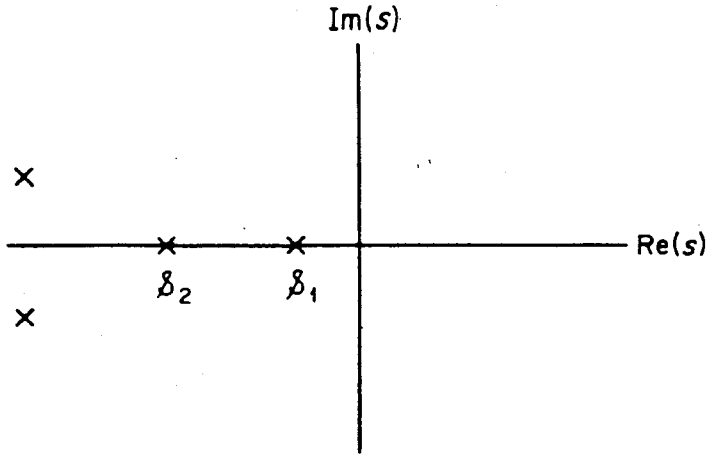

FIG. 9.9 BEHAVIOR OF ROOTS OF THE CHARACTERISTIC EQUATION (9.63) AT HIGHER POWER.

When the roots $\mathcal{S}_1$ and $\mathcal{S}_1^*$ of the characteristic equation, for significant values of P_0, are close to the imaginary axis, i.e., when Re $(\mathcal{S}_1)$ is small and negative, the reactor will have a tendency to exhibit spontaneous power oscillations at a frequency of Im $(\mathcal{S}_1)$. The reason is that oscillations at this frequency are barely damped and hence are readily excited. In addition, as will be shown below, the power would exhibit a large response to imposed reactivity oscillations at frequencies near Im $(\mathcal{S}_1)$. Mathematically, this arises because the transfer function for imaginary values of $\mathcal{S}$ will have a peak or *resonance* at a frequency ω_0, approximately equal to $|\text{Im}\,(\mathcal{S}_1)|$ when Re $(\mathcal{S}_1) \approx 0$. The occurrence of resonances in transfer functions for actual reactors is described in §9.5e.

Suppose that at some power the characteristic equation has a pair of roots, $\mathcal{S}_1$ and its complex conjugate $\mathcal{S}_1^*$, which are near the imaginary axis, i.e.,

$$\mathcal{S}_1 = -\epsilon + i\omega_0,$$

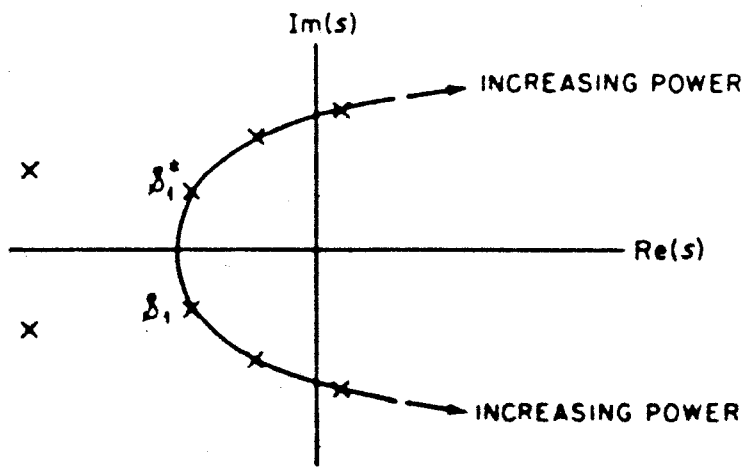

FIG. 9.10 EFFECT OF INCREASING POWER ON THE ROOTS OF EQUATION (9.63).

where ϵ is small. Then, for values of s close to $\mathscr{S}_1$ or $\mathscr{S}_1^*$, the expression for $H(s)$ can be given (approximately) by

$$H(s) \simeq \frac{H_0}{(s-\mathscr{S}_1)(s-\mathscr{S}_1^*)} = \frac{H_0}{(s+\epsilon)^2+\omega_0^2},$$

where H_0 is a constant. To determine the response of the system to the sinusoidal reactivity perturbation $\delta\rho \cos \omega_0 t$ of frequency ω_0, the value for resonance, the procedure is the same as in §9.3b, except that $P_0\, R(s)$ is now replaced by $H(s)$, i.e., compare equations (9.59) and (9.42). The result is

$$\delta P(t) \xrightarrow[t \text{ large}]{} \tfrac{1}{2}\,\delta\rho[H(i\omega_0)e^{i\omega_0 t} + H(-i\omega_0)e^{-i\omega_0 t}].$$

For $\epsilon/\omega_0 \ll 1$, however, $H(\pm i\omega_0) = \pm H_0/2i\omega_0\epsilon$, and hence

$$\delta P(t) \xrightarrow[t \text{ large}]{} \frac{\delta\rho}{2}\frac{H_0}{\omega_0\epsilon}\sin \omega_0 t.$$

This expression shows that the power response to a perturbation at the resonant frequency is proportional to $1/\epsilon$; thus, for small ϵ the response would be large. Moreover, at the resonance frequency the power change lags 90° behind the imposed reactivity perturbation.

9.4e Stability and Reactivity Perturbation Frequency

The problems of stability and instability can be considered from still another point of view. Since a system becomes unstable when the characteristic equation (9.63) has a root for purely imaginary s, it is convenient to set s equal to $i\omega$; the equation for instability is then

$$G(i\omega) = \frac{1}{R(i\omega)} - P_0F(i\omega) = i\omega\Lambda + \sum_j \frac{\beta_j i\omega}{i\omega+\lambda_j} - P_0F(i\omega) = 0, \quad (9.64)$$

where $1/R(i\omega)$ and $F(i\omega)$ are both complex functions of a reactivity perturbation frequency ω.

If for some value of ω, represented by ω_0, these functions i.e., $1/R(i\omega)$ and $F(i\omega)$, have the same phase, i.e., the same ratio of real and imaginary parts, there will be a value of P_0 for which $G(i\omega_0) = 0$; this will then represent an instability.

Figure 9.11, for example, shows the variation of the phase angle θ with frequency for $1/R(i\omega)$ and for a hypothetical feedback function $F(i\omega)$. For a sufficiently large power, P_0, instability occurs at the frequency ω_0, where the two curves cross; this represents the resonant frequency of the system. Since $G(i\omega)$ is then zero, the transfer function $H(i\omega)$ is very large; as stated above, a reactivity perturbation of frequency ω_0 will produce a large response at the given power. At still higher power, the power oscillations would be predicted to diverge according to the linear theory.

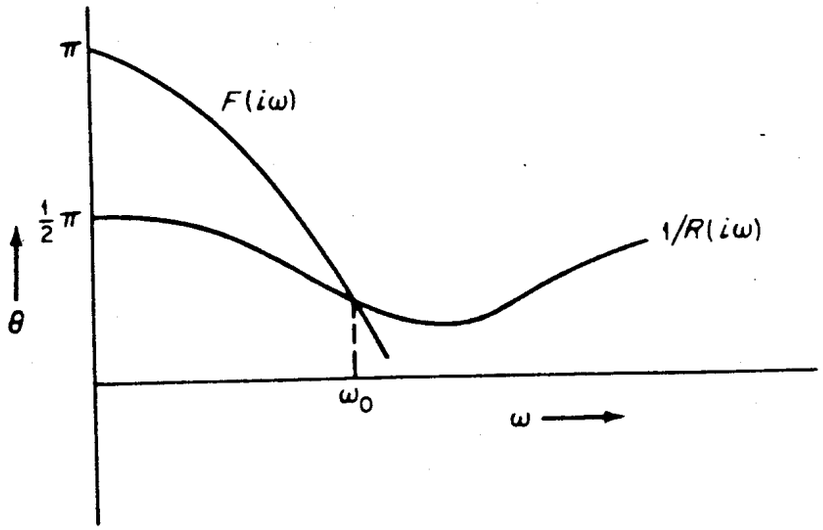

FIG. 9.11 OCCURRENCE OF AN INSTABILITY.

Since $1/R(i\omega)$ is a general function which, according to equation (9.43), depends only on the prompt-neutron lifetime, Λ, and the delayed-neutron constants, β_j, λ_j, the behavior of its phase as ω is varied can be readily determined. From equation (9.64), it can be seen that

$$\mathrm{Re}\left[\frac{1}{R(i\omega)}\right] = \sum_j \frac{\omega^2 \beta_j}{\omega^2 + \lambda_j^2}$$

and

$$\mathrm{Im}\left[\frac{1}{R(i\omega)}\right] = \omega\Lambda + \sum_j \frac{\omega\beta_j\lambda_j}{\omega^2 + \lambda_j^2}.$$

These functions are plotted in Fig. 9.12, with ω as a variable parameter, for $\Lambda = 10^{-3}$, 10^{-4}, and 10^{-5} sec. The values of β_j and λ_j used are those for uranium-235, but the results are qualitatively the same for other fissile nuclides.

It will be observed that the curves can be separated conveniently into two parts. The part at the left, for the small values of ω, is independent of the prompt-neutron lifetime and is determined by the characteristics of the delayed neutrons; on the other hand, the part on the right, for larger values of ω, is dependent on Λ and hence is governed by the prompt neutrons. The frequencies ω_s, which separate the two parts of each curve, are very approximately at the minima in Fig. 9.12, where $(\partial\,\mathrm{Im}/\partial\omega)_{\omega_s} = 0$; it is found that, for uranium-235 as the fissile material,

$$\omega_s \approx \sqrt{\frac{\sum_j \beta_j\lambda_j}{\Lambda}} \approx \frac{0.05}{\sqrt{\Lambda}}.$$

It is seen from Fig. 9.12 that $1/R(i\omega)$ lies in the upper right quadrant of the complex plane, i.e., both real and imaginary parts are positive, for all values of $\omega > 0$. It follows, therefore, from equation (9.64) that for instability to be

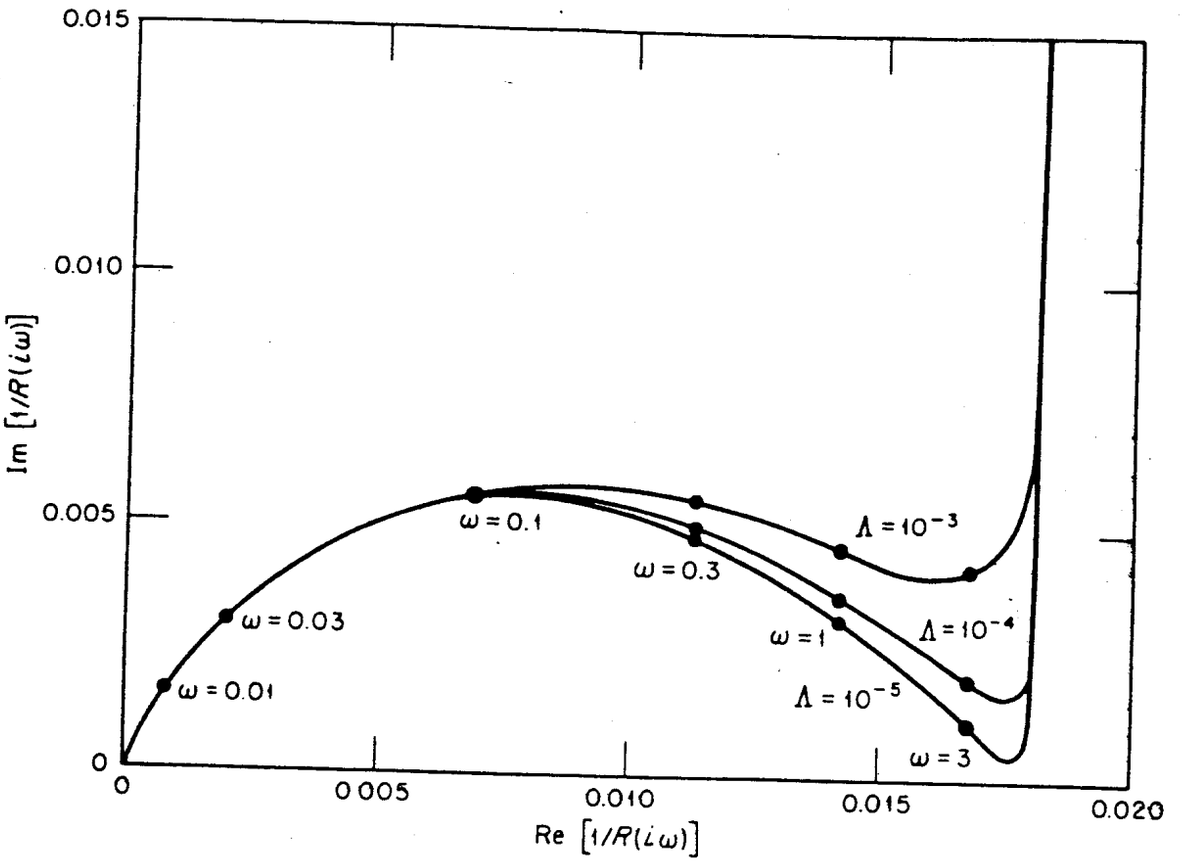

FIG. 9.12 REAL AND IMAGINARY PARTS OF $1/R(i\omega)$ FOR A URANIUM-235 SYSTEM.

possible, the feedback function $F(i\omega)$ must lie in the same quadrant. Hence, necessary conditions for instability are

$$\text{Re}\,[F(i\omega)] > 0 \quad \text{and} \quad \text{Im}\,[F(i\omega)] > 0.$$

It must be remembered that these conditions have been derived for linearized theory and they also involve the assumption that the roots of $G(s)$ start in the left half-plane and move to the right at sufficiently large values of P_0, as indicated earlier. It will be shown that the latter assumption is satisfied for many simple feedback mechanisms but it may not necessarily be true for all kinds of feedback.

According to linearized theory, therefore, a *sufficient* criterion for stability of the system is that for no value of ω shall both Re $[F(i\omega)] > 0$ and Im $[F(i\omega)] > 0$, i.e., the real and imaginary parts of $F(i\omega)$ be positive. In §9.4i, analogous stability criteria will be described for situations in which the reactor kinetics equations are not linearized.

It may be noted, incidentally, that for simple feedback models the roots of the characteristic equation, with $G(s) = 0$, can be examined explicitly.[37] In many models they are found to be roots of a polynomial and hence depend on P_0 in a continuous manner. Consequently, for these models, the criterion of instability derived above, based on an examination of $G(i\omega)$, can be justified rigorously. One such model will be considered in §9.4f.

It has been seen that the resonance frequency (or frequencies) of a system depends on the phase of the feedback function, $F(i\omega)$. The phase will, in turn, be affected by the time constants that are important in the physical feedback mechanisms, e.g., time for heat to flow from the fuel to the coolant, time for coolant to pass through the reactor core, etc. It follows that the resonance frequencies will be of the order of magnitude of the inverse of the important time constants. Some examples are given in the next section.

9.4f Simple Models of Feedback

Consider the simple model, represented by equations (9.52) and (9.53), in which the fuel temperature increases promptly and the moderator (or other reactor component) is then heated by the fuel. By taking the Laplace transform of equation (9.58) it is found that

$$F(s) = \frac{F_F(0)}{1 + \dfrac{s}{\omega_F}} + \frac{F_M(0)}{\left(1 + \dfrac{s}{\omega_F}\right)\left(1 + \dfrac{s}{\omega_M}\right)}, \tag{9.65}$$

where $F_F(0)$ and $F_M(0)$, the steady-state ($s = 0$) responses of the fuel and moderator, respectively, are given by

$$F_F(0) = \frac{ar_F}{\omega_F} \quad \text{and} \quad F_M(0) = \frac{abr_M}{\omega_F\omega_M},$$

and

$$F_M(0) + F_F(0) = F(0).$$

For stable behavior of a reactor when operating at steady power, it is required that $F(0) < 0$. But if this is achieved primarily by having a large negative value of $F_M(0)$, i.e., large delayed feedback, there is the possibility that an instability may occur. The reason is that, during the time required for the delayed feedback to become effective, the imposed reactivity perturbation may change sign. Hence it is possible for the feedback reactivity to be in phase with the imposed reactivity, thus enhancing the perturbation.

Suppose, for simplicity, that $F_F(0) = 0$, so that there is no feedback from the fuel; then from equation (9.65)

$$F(i\omega) = \frac{F_M(0)\left[1 - \dfrac{\omega^2}{\omega_F\omega_M} - i\left(\dfrac{\omega}{\omega_F} + \dfrac{\omega}{\omega_M}\right)\right]}{\left(1 + \dfrac{\omega^2}{\omega_F^2}\right)\left(1 + \dfrac{\omega^2}{\omega_M^2}\right)}. \tag{9.66}$$

Since it is being postulated that $F_M(0) < 0$, the imaginary part of $F(i\omega)$ will be positive for all values of $\omega > 0$. The real part, however, will start out negative for small values of ω, it will go through zero at $\omega = \sqrt{\omega_F\omega_M}$, and will then become positive for higher frequencies. Consequently, since both Re $[F(i\omega)]$

and Im $[F(i\omega)]$ can be positive, instability can occur for negative values of $F_M(0)$. For practical cases, it is of course possible that the power level at which such instability is predicted is so high as to be of no practical interest.

The general character of the plot of Im $[F(i\omega)]$ versus Re $[F(i\omega)]$ with increasing values of ω is shown in Fig. 9.13; curve *a* refers to the case under consideration in which there is no reactivity feedback from the fuel. The real part of $F(i\omega)$ starts at the left, i.e., it is negative, and becomes positive when $\omega > \sqrt{\omega_F \omega_M}$. Since the imaginary part of $F(i\omega)$ is always positive, it is seen that instability can occur under these conditions.

On the other hand, for a sufficiently large negative fuel feedback, the plot of the real and imaginary parts of $F(i\omega)$, with increasing ω, is indicated by curve *b*; the system is then always stable to small perturbations of reactivity.

Suppose $F(0)$ is negative, so that the reactor is stable at low power, but the fuel feedback coefficient, $F_F(0)$, is positive, i.e., $F_M(0)$ is negative and $|F_M(0)| > F_F(0)$. The reactor can become unstable at higher powers, as in Fig. 9.13*c*. This will now be shown explicitly by using equation (9.63) with $F(s)$ replaced by equation (9.65). For simplicity, only one group of delayed neutrons is considered; thus,

$$G(s) = \Lambda s + \frac{\beta s}{s + \lambda} - P_0 \left[\frac{F_F(0)}{1 + \dfrac{s}{\omega_F}} - \frac{|F_M(0)|}{\left(1 + \dfrac{s}{\omega_F}\right)\left(1 + \dfrac{s}{\omega_M}\right)} \right] = 0. \quad (9.67)$$

It will be assumed that Λ is small enough so that, for values of s of interest, the term Λs may be neglected, i.e., the zero prompt-lifetime approximation is

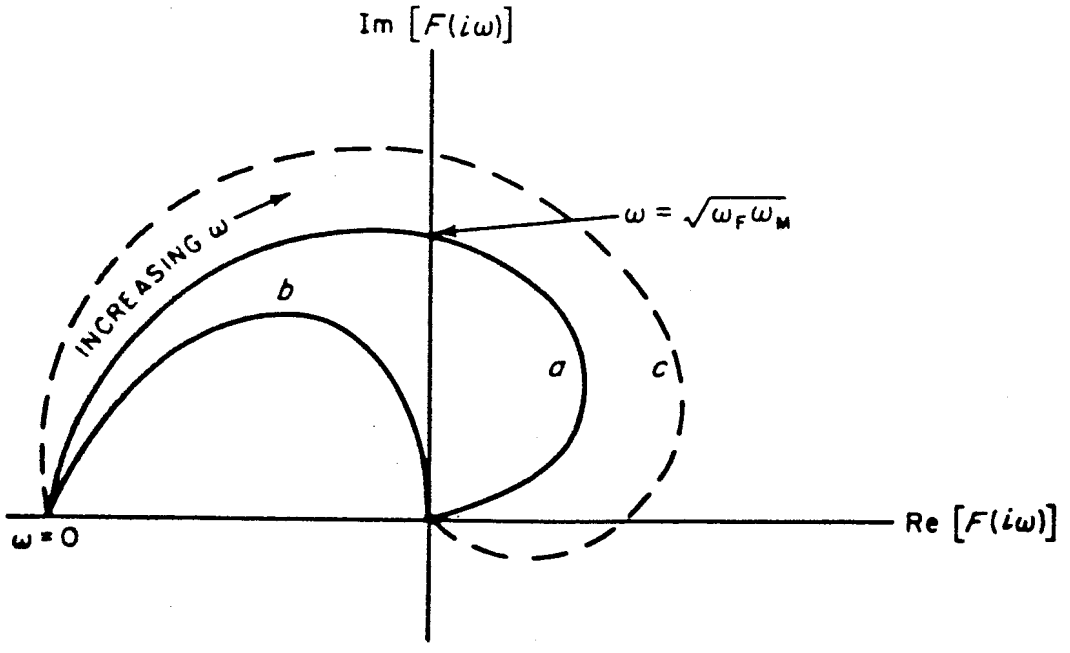

FIG. 9.13 EFFECTS OF FUEL FEEDBACK ON STABILITY.

made, and that ω_F is so large that $1 + s/\omega_F$ may be set equal to unity; then equation (9.67) becomes

$$G(s) \approx \frac{\beta s}{s + \lambda} - P_0\left[F_F(0) - \frac{|F_M(0)|}{1 + \frac{s}{\omega_M}}\right] = 0.$$

If the unit of time is chosen such that $\lambda = 1$ and the unit of power is taken as $\beta/|F_M(0)|$, it is found that

$$\frac{s}{s + 1} - P_0\left(\epsilon - \frac{\omega_M}{s + \omega_M}\right) = 0$$

where

$$\epsilon = \frac{F_F(0)}{|F_M(0)|} < 1.$$

Upon multiplying by $(s + 1)(s + \omega_M)$, the result is

$$s^2(1 - P_0\epsilon) + s\{\omega_M[1 + P_0(1 - \epsilon)] - P_0\epsilon\} + \omega_M P_0(1 - \epsilon) = 0. \quad (9.68)$$

Equation (9.68) has two roots, represented by $\mathscr{S}_{1,2}$, given by

$$\mathscr{S}_{1,2} = \frac{1}{2(1 - P_0\epsilon)} \times [-\omega_M(1 + aP_0) \pm \sqrt{\omega_M^2(1 + aP_0)^2 - 4\omega_M P_0(1 - P_0\epsilon)(1 - \epsilon)}] \quad (9.69)$$

where

$$a = 1 - \epsilon - \frac{\epsilon}{\omega_M}.$$

Let $\epsilon = \frac{1}{2}$ and $\omega_M = \frac{1}{4}$, so that $a = -\frac{3}{2}$; then equation (9.69) becomes

$$\mathscr{S}_{1,2} = \frac{1}{8(1 - \frac{1}{2}P_0)}[-(1 - \tfrac{3}{2}P_0) \pm \sqrt{(1 - \tfrac{3}{2}P_0)^2 - 8P_0(1 - \tfrac{1}{2}P_0)}]$$

$$= \frac{1}{8(1 - \frac{1}{2}P_0)}[(\tfrac{3}{2}P_0 - 1) \pm \sqrt{1 - 11P_0 + \tfrac{25}{4}P_0^2}].$$

As the value of P_0 is increased from zero, the roots $\mathscr{S}_1$ and $\mathscr{S}_2$ remain real and negative until $P_0 = 0.0962$ when the square root term is zero; the two roots then coalesce. At somewhat higher reactor powers, the square root is imaginary and then $\mathscr{S}_1$ and $\mathscr{S}_2$ are complex conjugates. When the value of P_0 is $\frac{2}{3}$, the roots are pure imaginary, and then the system becomes unstable (Fig. 9.14). For $P_0 = 1.664$, in the present case, the square root vanishes again so that the two roots become identical. At still higher power $\mathscr{S}_1$ and $\mathscr{S}_2$ are once more different and real.

When the roots cross the imaginary axis, the value of $|\mathrm{Im}\,(s)|$ is about 0.35; this is of the same order of magnitude as ω_M assumed for the calculations.

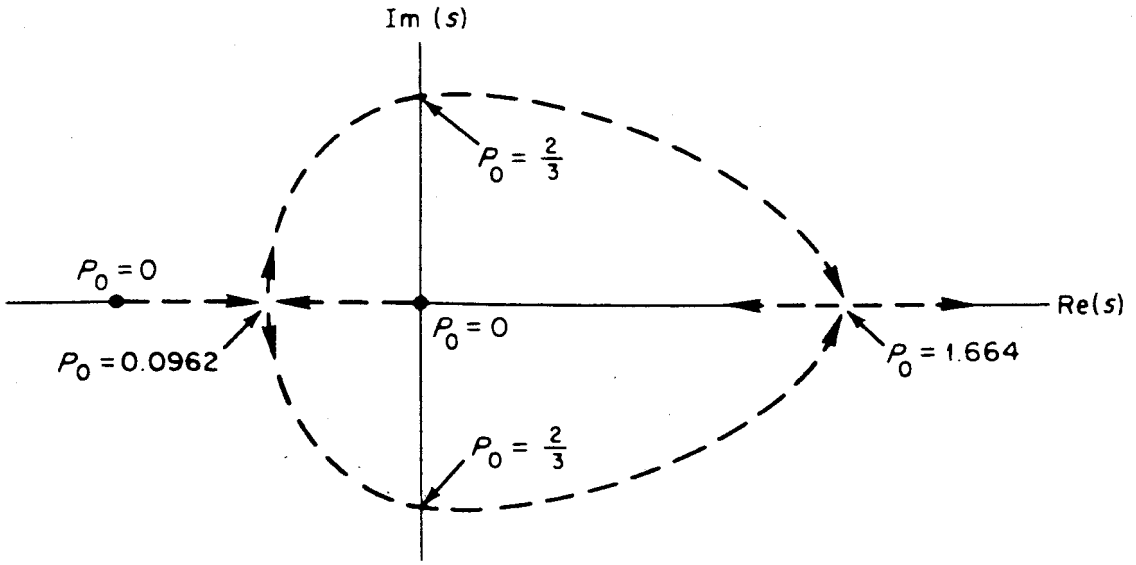

FIG. 9.14 ILLUSTRATIVE CALCULATION SHOWING CHARACTERISTIC ROOTS AND ONSET OF INSTABILITY DUE TO POSITIVE FUEL FEEDBACK.

Hence, in this example, the typical frequency for resonance, when P_0 is slightly less than $\frac{2}{3}$, is comparable with the reciprocal of the decay time ($\approx 1/\omega_M$).

Simple models of feedback, similar to the ones treated above, have proved useful for understanding the important physical effects in the safety of fast reactors[38] and boiling water reactors. Further reference to this matter will be made later in connection with a discussion of the measured transfer functions for such reactors.

For the realistic interpretation of the behavior of an actual power reactor, much more detailed models of feedback must, of course, be used. The transfer functions are then determined by means of an analogue or digital computer for comparison with experiment. Nevertheless, simple models, such as those described here, are useful for providing physical insight into some of the important feedback mechanisms. For example, they suggest a danger of instability when the primary feedback mechanism is a delayed negative temperature coefficient and indicate the desirability of a comparable negative prompt coefficient.

9.4g Other Sources of Instability

When there is a time lag for fluid flow associated with delayed feedback, then equation (9.53) may be replaced, at least approximately, by

$$\frac{d[\delta T_M(t)]}{dt} = b\,\delta T_F(t - \Delta t) - \omega_M\,\delta T_M(t),$$

where Δt is the time delay; $\delta T_M(t)$ refers to time t and $\delta T_F(t - \Delta t)$ to time

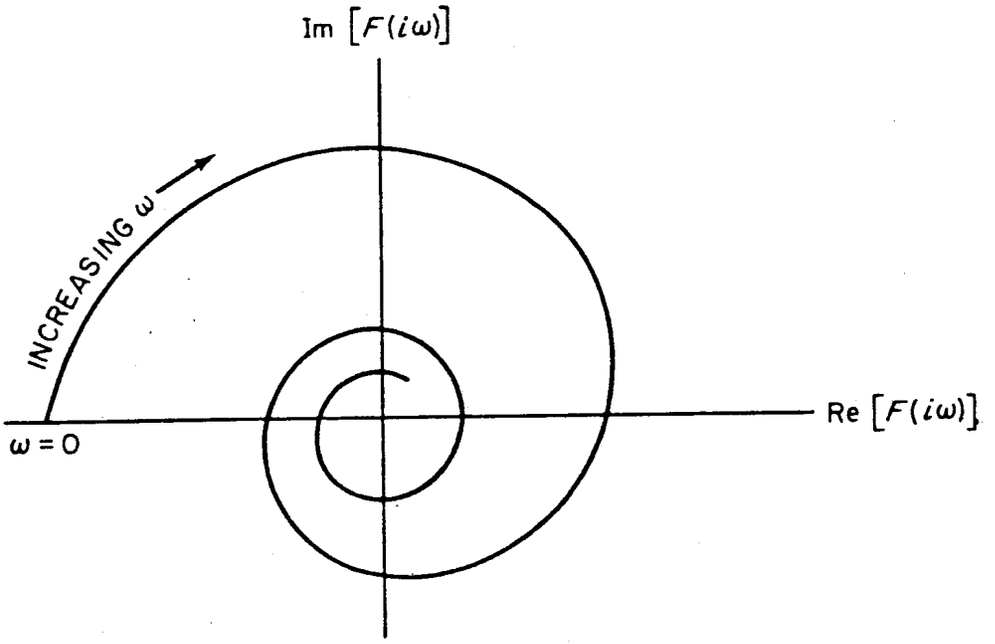

FIG. 9.15 RESONANCES AT SEVERAL HARMONIC FREQUENCIES DUE TO TIME LAG IN FEEDBACK.

$t - \Delta t$. Instead of the second term in equation (9.65), with s replaced by $i\omega$, it would be found that

$$F_M(i\omega) = \frac{F_M(0)e^{-i\omega\Delta t}}{\left(1 + \frac{i\omega}{\omega_F}\right)\left(1 + \frac{i\omega}{\omega_M}\right)} \tag{9.70}$$

and this can lead to instabilities similar to those described above.

If $F_F(0)$ is positive, then combination with equation (9.70) can lead to a variation of Re $[F(i\omega)]$ and Im $[F(i\omega)]$ with frequency in the manner shown in Fig. 9.15. There will then be several frequencies (or harmonics) at which enhanced responses (or resonances) to reactivity disturbances will occur. The fundamental resonant frequency for instability is then of the order of $1/\Delta t$.

Another example of an instability mechanism is that in which acoustical modes or mechanical oscillations may sometimes be amplified to cause an instability. In homogeneous reactors, there can be a gross oscillation of the fluid fuel in and out of the core as the density of the liquid changes.[39]

9.4h Relative Importance of Delayed and Prompt Neutrons

In studies of reactor stability, two quite different approximations have sometimes been made. The first is the zero prompt lifetime approximation which, as seen in §9.2f, is useful in some numerical schemes for solving the reactor kinetics equations. From Fig. 9.12, it is clear that this approximation will change $1/R(i\omega)$ only at high frequencies and it is expected, therefore, that it would be good for the study of low-frequency stability, i.e., with $\omega < \omega_s$ defined in §9.4e.

Another approximation is to neglect the delayed neutrons entirely. Then $1/R(i\omega)$ becomes equal simply to $i\omega\Lambda$ and is purely imaginary for all values of ω; this is certainly not a good approximation for low frequencies, and so it is not useful except possibly for disturbances of high frequency. The significance of the approximation is that it often makes the system appear to be less stable; hence, if stability can be demonstrated in the absence of delayed neutrons, the system is usually even more stable with delayed neutrons.

This may be seen by considering the behavior of $F(i\omega)$ with increasing ω. The reactor is assumed to have a steady-state stability, so that $F(0) < 0$. For potential instabilities, as explained in §9.4c, $F(i\omega)$ has to get into the upper right quadrant of the plot of Im $[F(i\omega)]$ against Re $[F(i\omega)]$, i.e., both real and imaginary parts of $F(i\omega)$ are positive. In particular, with increasing ω, the point representing $F(i\omega)$ must cross the Im axis. If it does so by crossing this axis with Im $[F(i\omega)] > 0$, as in Fig. 9.15, then if $1/R(i\omega)$ is simply $i\omega\Lambda$ there is an immediate instability at some power. It is reasonable to believe that this will occur at a lower power than will any possible instability when delayed neutrons are included. Hence, when crossing of the Im axis occurs in this manner, delayed neutrons will improve the stability; this situation is represented by curve *a* in Fig. 9.16.

If, with increasing ω, however, $F(i\omega)$ crosses the Im axis when Im $[F(i\omega)] < 0$, as in curve *b*, the situation is quite different. The system could be stable in the absence of delayed neutrons, but it might be unstable with delayed neutrons.[40]

From the practical point of view of reactor stability it would appear, therefore, that the delayed neutrons should not be neglected. An exceptional situation arises in the treatment of very fast transients for then the delayed neutrons play essentially no part (§9.6a).

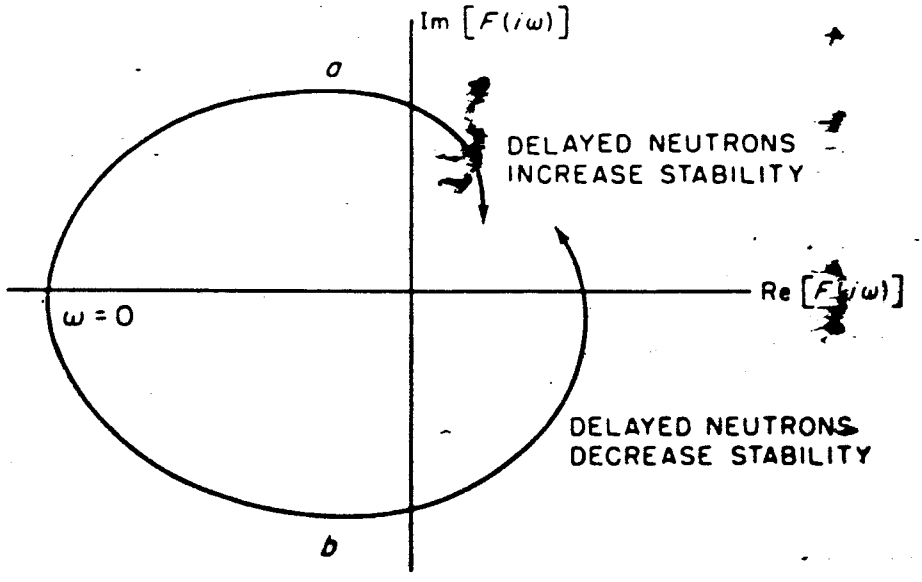

FIG. 9.16 EFFECT OF DELAYED NEUTRONS ON STABILITY.

9.4i Feedback in a Nonlinear Point Reactor

The results obtained above refer to stability in the small, i.e., when there are arbitrarily small oscillations about some initial steady-state conditions. In these circumstances the term $\delta\rho(t)\,\delta P(t)$ could be neglected and the kinetics equations were linearized (§9.2g). When variations of larger amplitude are considered, however, the equations governing the stability are nonlinear; first, the whole term $\delta\rho(t)[P_0 + \delta P(t)]$ must be retained, rather than just setting it equal to $\delta\rho(t)P_0$, and second, the feedback reactivity will no longer be related in a linear manner to the change in the power, as in equation (9.57).

When nonlinear effects are taken into account, the results of the stability analysis may be quite different from those for a linearized model. A system which was stable for small oscillations about P_0 might be unstable for power variations of large amplitude. A simple situation of this kind would occur if the oscillations carried the reactor to a higher power P_1 at which it is unstable for small oscillations. On the other hand, a system exhibiting instability in the small may have its oscillations bounded by nonlinear effects and the bounds may be such as not to endanger the reactor operation.

As mentioned earlier, nonlinear feedback can lead to various types of stability, including asymptotic stability and Lagrange stability (§9.4a). These two kinds of stability may exist only for perturbations within some limited range of parameters; such stability is then said to exist within a particular domain.

Several approaches have been made to the solution of the problem of stability based on nonlinear kinetics equations, but none is really satisfactory. In the first place, attention has generally been limited to linear feedback, as expressed by equation (9.57), and so the only nonlinearity has been in the term

$$\delta\rho(t)[P_0 + \delta P(t)].$$

Second, the various conditions which have been derived with regard to the feedback function $F(i\omega)$ are sufficient to insure stability but they are not *necessary* conditions. This means that the stability conditions found can be too restrictive. Finally, it has been seen that a typical mode of stability in the linear model will have a power threshold below which the reactor is stable. Some of the conditions on $F(i\omega)$ for nonlinear kinetics have been derived for all powers and do not take this threshold behavior into account.

In an attempt to derive stability conditions for all powers, it has been shown,[41] neglecting delayed neutrons, that a system would be asymptotically stable provided

$$\text{Re}\,[F(i\omega)] < 0 \quad \text{for all } \omega.$$

Furthermore, it has been demonstrated[42] that delayed neutrons do not alter this criterion. This stability condition is seen to be consistent with the results of linear theory which indicated (§9.4e) that there would be stability if $\text{Re}\,[F(i\omega)] < 0$ or if $\text{Re}\,[F(i\omega)] > 0$ and $\text{Im}\,[F(i\omega)] < 0$. As derived, the condition that

Re $[F(i\omega)] < 0$ for all ω is sufficient but not necessary for stability; from linear theory it may be suspected that this is overly restrictive.

A method has been described for predicting instability bounds for systems which are stable according to the linearized theory.[43] Information of this type should be useful in indicating the limits of validity of the results obtained by the use of linear models.

A possible procedure for assessing the stability of a system governed by nonlinear differential equations is to use the second (or direct) method of A. M. Liapunov.[44] In this approach, a Liapunov function is sought which is a generalization of the energy for a mechanical system in the sense that it must be a positive definite function of the variables, i.e., power, temperature, etc., and possess a negative definite time derivative. If such a function can be found, then for the range of variables in which the function exists the system will be asymptotically stable. The Liapunov function has been derived for certain cases[45] and some special treatments have been developed for improving on the results obtained by the Liapunov direct method.[46] There is, however, no general approach to the determination of the Liapunov functions.

From the practical standpoint, nonlinear stability analysis has proved to be much less important than the analysis of linear models. For one thing, nonlinear analysis does not lend itself to general experimental verification. On the whole, studies of nonlinear feedback have indicated that the results obtained from linear theory are not likely to be misleading when applied to problems of reactor stability. In particular, if a reactor is operating in a region of power, temperature, and flow conditions for which stability is well assured according to the linearized equations, it is unlikely that nonlinear effects will lead to instability. It should be realized, however, that when a linearized model predicts instability, an analysis of the nonlinear system must be considered before the physical consequences of the instability can be understood.

9.5 DETERMINATION AND USE OF TRANSFER FUNCTIONS

9.5a Introduction

Several experimental techniques have been used for measuring the transfer function, $H(i\omega)$, and thereby investigating the feedback and stability of operating reactors. By comparing the experimental results with calculations of the amplitude and phase as a function of frequency, it is possible to check whether the reactivity feedback is more or less as expected from the design. Furthermore, incipient instabilities can be detected by the existence of resonance peaks in the amplitude of the transfer function observed at low power.[47] Provided the feedback mechanisms do not change abruptly with the power, conditions which would be hazardous at high power can then be corrected. In addition, it is

possible to detect the malfunction of a reactor component by observing a change in the reactor transfer function.[48]

At the present time it is consequently the common practice to determine the transfer function of a reactor before it is operated at full power. Among the most important methods employed for this purpose are those based on reactor oscillator experiments and on what is known as spectral correlation. These techniques are described below.

9.5b The Reactor Oscillator Method

The simplest method conceptually for measuring the transfer function of a reactor is based on equation (9.47). Although this expression was derived for a system without feedback, it can readily be shown that it is applicable to a reactor with feedback with $H(i\omega)$ replacing $P_0R(i\omega)$. The reactivity is subjected to small sinusoidal oscillations, for example by the in-and-out motion of a control rod; the resulting changes in power, both in amplitude and phase, relative to the imposed reactivity variation, are then measured as a function of the frequency of the variations.[49] The reactivity oscillations must be small so that the linearized kinetics equations are applicable. Spatial effects may also have to be taken into account, as discussed in §9.3c, but they will not be considered further here.

In the employment of the oscillator method (or experiment) some interesting problems arise. First, no matter what kind of instrument is used for measuring the reactor power level, e.g., a neutron detector, it will not give a perfectly steady reading but will exhibit small statistical fluctuations. Consequently, if a clear signal is to be obtained on the detector, the reactivity variations must be substantial; they must not be so large, however, as to invalidate the linear analysis or to perturb the flux sufficiently to make the point-reactor model inapplicable.

Second, the reactivity variations achieved by the movement of a control rod are not perfectly sinusoidal; hence, various harmonics of the fundamental frequency will be excited. To avoid the difficulties arising from the presence of these harmonics, a Fourier analysis can be made of the output in order to determine the fundamental response only.

In fact, the imposed reactivity variation does not even have to be periodic, provided it excites a broad band of frequencies in the output. It can be seen from equation (9.60) that if $\delta\rho_{ex}(t)$ could be made a Dirac delta function, then the impulse response function $h(t)$ could be derived directly from $\delta P(t)$. The transfer function, $H(s)$, would then be simply proportional to the Laplace transform of $\delta P(t)$. The difficulty in applying this method of obtaining the transfer function is that it is impossible physically to realize a delta function change in reactivity. By the use of the cross-correlation method, described in the next section, it is possible, however, to simulate a delta function and thereby determine transfer functions in a relatively simple manner.

9.5c Correlation Methods

The input reactivity and output power of a reactor are related by the convolution integral in equation (9.60). This can be extended to allow for reactivity variations at arbitrarily early times by writing

$$\delta P(t) = \int_{-\infty}^{t} \delta\rho_{ex}(\tau)h(t-\tau)\,d\tau = \int_{0}^{\infty} \delta\rho_{ex}(t-\tau)h(\tau)\,d\tau, \tag{9.71}$$

where, as before, the transfer function, $H(s)$, is the Laplace transform of the impulse response function, $h(t)$.* Equation (9.71) forms the basis of the cross-correlation experiments for measuring $h(t)$ or $H(s)$.[50]

The autocorrelation of a function $x(t)$ is defined by

$$\varphi_{xx}(\tau) = \frac{1}{2T}\int_{-T}^{T} x(t)x(t+\tau)\,dt \tag{9.72}$$

and the cross correlation between two functions $x(t)$ and $y(t)$ is

$$\varphi_{xy}(\tau) = \frac{1}{2T}\int_{-T}^{T} x(t)y(t+\tau)\,dt, \tag{9.73}$$

where, if the functions are periodic, T is the period, and if they are not periodic, then the limit is to be taken as $T \to \infty$. With these definitions, it follows that

$$\varphi_{xx}(\tau) = \varphi_{xx}(-\tau) \quad \text{and} \quad \varphi_{xy}(\tau) = \varphi_{yx}(-\tau).$$

In particular, the cross correlation between reactivity and power is

$$\varphi_{\rho p}(\tau) = \frac{1}{2T}\int_{-T}^{T} \delta\rho_{ex}(t)\,\delta P(t+\tau)\,dt = \frac{1}{2T}\int_{-T}^{T} \delta\rho_{ex}(t-\tau)\,\delta P(t)\,dt. \tag{9.74}$$

Upon using equation (9.71) and rearranging, this becomes

$$\begin{aligned}\varphi_{\rho p}(\tau) &= \frac{1}{2T}\int_{-T}^{T} \delta\rho_{ex}(t-\tau)\left[\int_{0}^{\infty} \delta\rho_{ex}(t-u)h(u)\,du\right] dt \\ &= \int_{0}^{\infty} h(u)\left[\frac{1}{2T}\int_{-T}^{T} \delta\rho_{ex}(t-\tau)\,\delta\rho_{ex}(t-u)\,dt\right] du \\ &= \int_{0}^{\infty} \varphi_{\rho\rho}(\tau-u)h(u)\,du, \end{aligned} \tag{9.75}$$

where u is an integration variable. If this result is compared with equation (9.71), it is seen that the cross correlation between reactivity and power is related to

* In order to obtain the desired relation $\delta P(s) = \delta\rho_{ex}(s)H(s)$, it is here necessary to take the two-sided Laplace transform, i.e., with the integration limits between $-\infty$ and ∞, or the Fourier transform, because reactivity variations at all times prior to the time t are included in equation (9.71). It should be noted that since $h(\tau)$ must be zero for negative τ, the lower limit in the second integral in equation (9.71) may be set to $-\infty$, in which case the integral has the typical convolution (or faltung) form for Fourier transforms.

the reactivity autocorrelation, $\varphi_{\rho\rho}$, in exactly the same way as the power response is to the change in reactivity. Upon taking the Fourier transform (see footnote on p. 511) of equation (9.75), it is found that the transfer function is given by

$$\frac{\mathcal{F}\{\varphi_{\rho p}(\tau)\}}{\mathcal{F}\{\varphi_{\rho\rho}(\tau)\}} = H(-i\omega), \tag{9.76}$$

where the transform

$$\mathcal{F}\{\varphi_{\rho p}(\tau)\} = \int_{-\infty}^{\infty} e^{i\omega\tau}\varphi_{\rho p}(\tau)\, d\tau \tag{9.77}$$

is called the *cross spectral density* and the corresponding expression for $\mathcal{F}\{\varphi_{\rho\rho}(\tau)\}$ is referred to as the *reactivity* (or *input*) *spectral density*.

In the application of equation (9.76) to the experimental determination of the transfer function of an operating reactor,[51] the reactivity is varied over a narrow range in a random manner by the insertion and removal of a small neutron absorber; the corresponding variations in the power are recorded.* The reactivity autocorrelation function, $\varphi_{\rho\rho}$, at time t, is obtained from the values of $\delta\rho_{ex}(t)$ and $\delta\rho_{ex}(t + \tau)$ for a series of delay intervals τ increasing in discrete steps of $\Delta\tau$, about 0.01 sec. The cross correlation function $\varphi_{\rho p}$ is derived in a similar manner from measurements of $\delta\rho_{ex}(t)$ and $\delta P(t + \tau)$. The integrals in equations (9.72) and (9.73) are then evaluated numerically; the integration (or equivalent summation) is carried over the period of observation, usually 5 min or so.

The Fourier transforms of $\varphi_{\rho p}$ and $\varphi_{\rho\rho}$ which appear in equation (9.76) are determined by numerical techniques. Thus, equation (9.77) for the cross spectral density may be written as

$$\mathcal{F}\{\varphi_{\rho p}(\tau)\} \approx \sum_{n} \varphi_{\rho p}(n\,\Delta\tau)(\cos n\omega\,\Delta\tau + i \sin n\omega\,\Delta\tau)\,\Delta\tau,$$

where n is an integer ranging from large negative to large positive values. A similar expression is applicable to $\mathcal{F}\{\varphi_{\rho\rho}(t)\}$. Since both real and imaginary parts of the Fourier transforms can be determined in this manner, it is possible to obtain both the amplitude and phase of the transfer function for a series of values ω.

A simplification of the foregoing procedure can be achieved by making use of reactivity inputs $\delta\rho_{ex}(t)$ which have autocorrelation functions resembling Dirac delta functions. Almost any broadband (noise) input signal will satisfy this requirement; in particular, if $\delta\rho_{ex}$ is made to assume positive and negative values at random times, then

$$\varphi_{\rho\rho}(\tau - u) \simeq A\,\delta(\tau - u),$$

* In practice, the neutron flux, which is proportional to the power, is measured.

where A is a constant and $\delta(\tau - u)$ is a delta function.[52] For this kind of reactivity variation, it follows from equation (9.75) that

$$\varphi_{\rho p}(\tau) \simeq Ah(\tau)$$

and then

$$\mathscr{F}\{\varphi_{\rho p}(\tau)\} \simeq AH(-i\omega).$$

Consequently, both the amplitude and phase of the reactor transfer function can be computed as a function of ω from the cross-correlation data alone.

Experimentally, it is neither possible nor necessary to provide a strictly random reactivity input through the motion of an absorber. In fact, it is convenient to use a periodic input which changes from positive to negative at definite times, so that the reactivity autocorrelation function is nearly a delta function.[53] Such a reactivity input, which is called a pseudorandom binary signal, has been used for the measurement of transfer functions.

9.5d The Reactor Noise Method

A particularly simple method for determining the amplitude, but not the phase angle, of a reactor transfer function depends on the observation of reactor "noise." This refers to the more-or-less random variations in the power that take place continuously during the normal operation of a reactor. All nuclear processes have a statistical basis and the actual neutron population in a reactor will be fluctuating about the average value. Moreover, there are usually minor fluctuations in temperature and in densities, such as those associated with bubble formation in a boiling water reactor. These variations will affect the reactivity and hence generate reactor noise. In the following, it will be convenient to regard the power fluctuations as being induced by unspecified random variations in reactivity.

To relate the noise to the transfer function, consider the autocorrelation function of the power; this may be written as

$$\varphi_{pp}(\tau) = \frac{1}{2T}\int_{-T}^{T} \delta P(t)\, \delta P(t + \tau)\, d\tau$$

and hence, by making use of equation (9.71),

$$\begin{aligned}\varphi_{pp}(\tau) &= \frac{1}{2T}\int_{-T}^{T} dt \int_0^\infty h(u)\, \delta\rho_{ex}(t - u)\, du \int_0^\infty h(v)\, \delta\rho_{ex}(t + \tau - v)\, dv \\ &= \int_0^\infty h(u)\, du \int_0^\infty h(v)\, dv \left[\frac{1}{2T}\int_{-T}^{T} \delta\rho_{ex}(t - u)\, \delta\rho_{ex}(t + \tau - v)\, dt\right] \\ &= \int_0^\infty h(u)\, du \int_0^\infty h(v)\, dv[\varphi_{\rho\rho}(\tau + u - v)].\end{aligned}$$

Fourier transformation then gives

$$\mathcal{F}\{\varphi_{pp}(\tau)\} = H(-i\omega)H(i\omega)\mathcal{F}\{\varphi_{\rho\rho}(\tau)\} \tag{9.78}$$

or

$$|H(i\omega)|^2 = \frac{\mathcal{F}\{\varphi_{pp}(\tau)\}}{\mathcal{F}\{\varphi_{\rho\rho}(\tau)\}}. \tag{9.79}$$

The square of the magnitude of the transfer function is thus equal to the ratio of the power and reactivity spectral densities derived from the respective autocorrelation functions.

The power autocorrelation is in principle obtained quite easily; all that is required is an accurate recording of the reactor power. From this, values of $\delta P(t)$ and $\delta P(t + \tau)$ can be obtained and hence $\varphi_{pp}(\tau)$ can be calculated; the Fourier transform is then derived in the manner already described. The fluctuations in the reactivity, being of internal origin, cannot be measured. If these variations are random, however, $\varphi_{\rho\rho}(\tau)$ is expected to be equivalent to a Dirac delta function in time; hence the Fourier transform is a constant. The amplitude of the transfer function can then be determined directly from the normal fluctuations of the reactor power, i.e., the reactor noise.[54]

The noise method has the great virtue that measurements of the transfer function of a reactor can be made without interfering in any way with normal operation. In this way, the stability can be monitored continuously. The drawbacks are that unless the reactor is noisy, i.e., exhibits substantial inherent power fluctuations, the variations may be so small as to give inaccurate values of $|H(i\omega)|$. The assumption that $\mathcal{F}[\varphi_{\rho\rho}(\tau)]$ is constant may also introduce errors. Moreover, only the amplitude, but not the phase, of $H(i\omega)$ can be evaluated from the reactor noise. Finally, there is the problem that the reactor power must be measured with a detector which itself will introduce some noise into the measurement[55]; corrections must thus be applied for the detector noise. Experiments have been reported in which correlations between the outputs of two detectors were used to monitor continuously the reactivity of a reactor in a subcritical state.[56] This approach appears to have advantages over the single detector correlation method described above.

9.5e Applications of the Transfer Function

The Experimental Breeder Reactor

Two examples of measured transfer functions which indicated possible reactor instabilities at sufficiently high operating powers are of interest. The first example is concerned with one of the early fast reactors, the Experimental Breeder Reactor-I (EBR-I); incidentally, the determination of the transfer function in 1955 was one of the first of such measurements to be made with a reactor. Under certain conditions, an oscillatory behavior of the power was

observed in the Mark II core of the reactor. Consequently, the transfer function was determined under a wide variety of conditions, using the oscillating-rod technique. Some of the results are reproduced in Fig. 9.17; they refer to three operating powers at a constant flow rate (95 gallons/min) of coolant.[57] In agreement with the arguments presented earlier, the reactor is stable at low and moderate powers, but a pronounced resonance, suggesting the approach of instability, appears at a higher power.

Power oscillations that precede the onset of this instability are inconvenient but not necessarily hazardous. In the case of the EBR-I, the frequency at the resonance was about 0.2 radian (0.03 cycle) per sec, as seen from Fig. 9.17. Hence, the period was approximately 30 sec. An oscillation of this frequency can be readily controlled by the normal operation of the control rods, especially if they respond automatically.

The physical causes of the resonance (or instability) in the EBR-I have not been completely elucidated, but it is known that the reactor had a prompt positive fuel feedback coefficient and a larger negative delayed coefficient. As seen in §9.4f, this situation can lead to instability at a sufficiently high operating power. The prompt positive coefficient is believed to have been caused by bowing of the fuel rods toward the center of the reactor, where the fission rate and temperature were above the average values. The delayed negative feedback, on the other hand, was probably due to mechanical motions of the plate supporting the fuel rods.[58] Since the bowing of fuel elements could occur in a reactor of any type, thermal as well as fast, precautions are taken to minimize it.

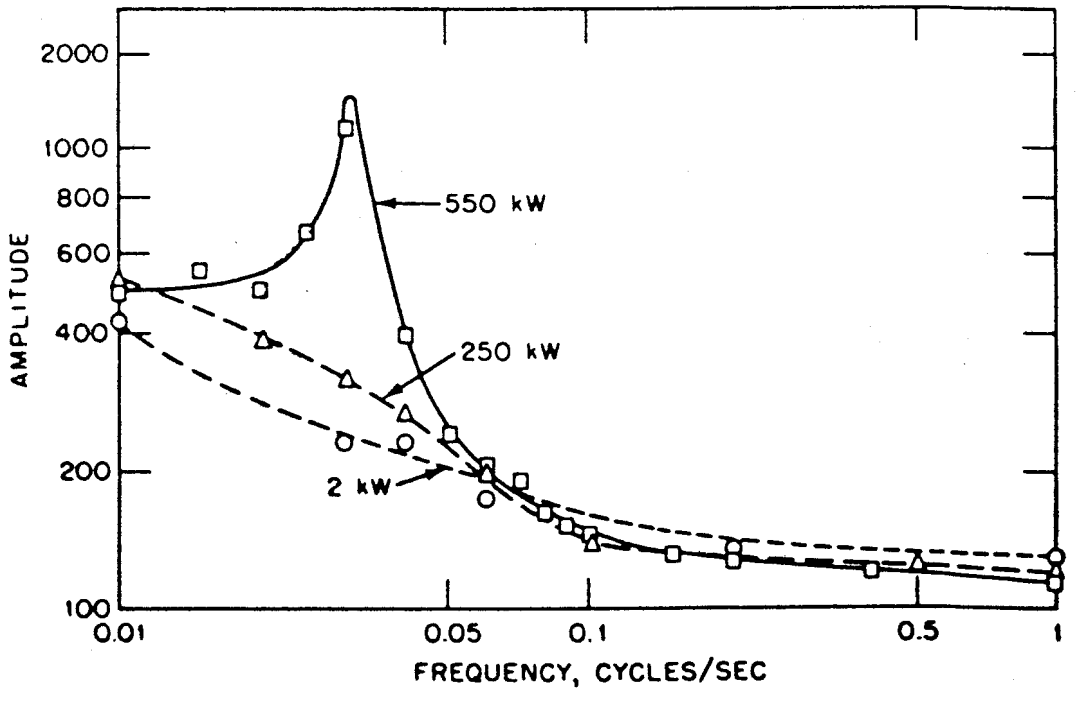

FIG. 9.17 EXPERIMENTAL TRANSFER FUNCTIONS FOR THE EBR-I (AFTER F. W. THALGOTT, *ET AL.*, REF. 57).

It should be mentioned that the partial meltdown of the core of EBR-I, Mark II, which occurred in 1956, was not due to the instability referred to above. The overheating developed during an experimental power excursion and was caused by a combination of circumstances which could have been avoided.[59] However, because of the meltdown, it was not possible to examine the feedback mechanisms in this case.

The Experimental Boiling Water Reactor

In boiling water reactors, the formation of steam voids represents an important feedback mechanism whereby the reactor power affects the reactivity. In the early consideration of such reactors,[60] it was accepted that they should be designed so that formation of steam voids would decrease the reactivity. It was feared, however, that because of the time delays between power generation and bubble formation, the reactor might exhibit instability or oscillatory behavior (§9.4g).

Measurements of the transfer function were made on the Experimental Boiling Water Reactor (EBWR), a heterogeneous reactor moderated and cooled by ordinary water, with natural (convection) circulation. Some of the results obtained, at an operating pressure of 550–600 psig, are shown in Fig. 9.18;

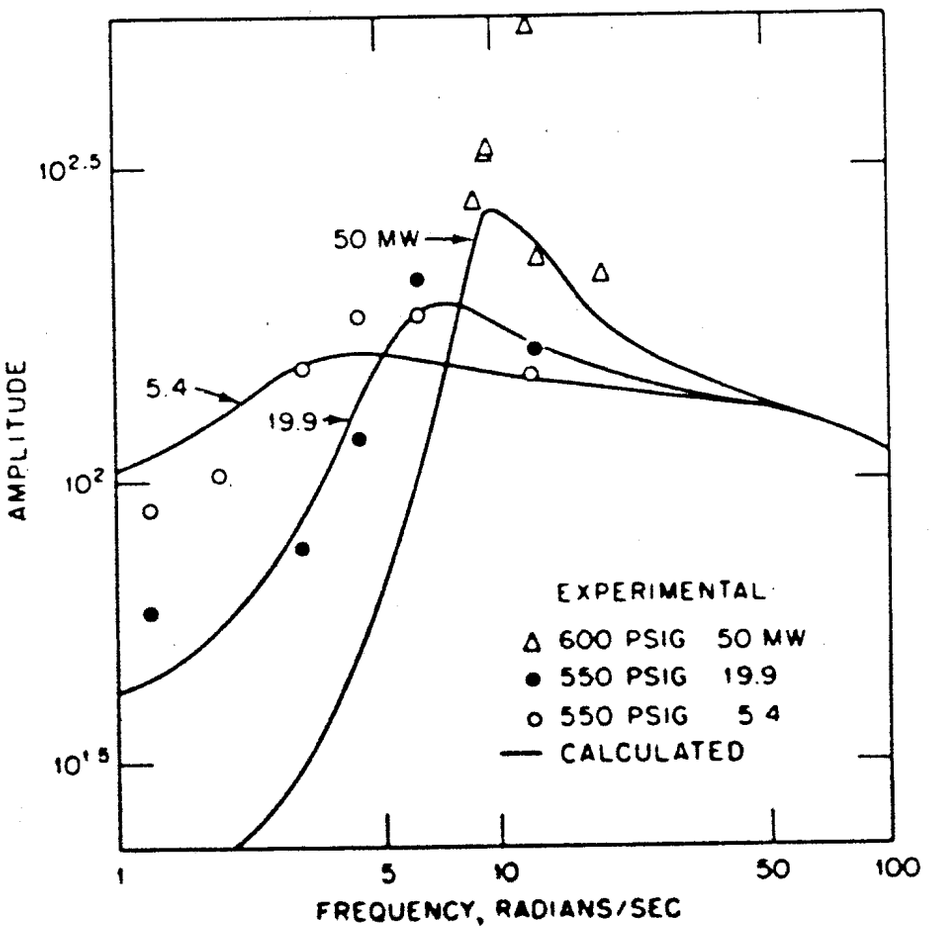

FIG. 9.18 EXPERIMENTAL AND CALCULATED TRANSFER FUNCTIONS FOR THE EBWR (AFTER T. SNYDER AND J. A. THIE, REF. 61).

there are indications of a resonance at a power close to 20 megawatts, and it is quite marked at 50 megawatts. Fairly good agreement with the observed transfer functions was obtained from calculations based on feedback mechanisms arising from various effects, including the formation of steam voids.[61]

The resonances in Fig. 9.18 occur at frequencies in the vicinity of 10 radians (1 or 2 cycles) per sec; the oscillation period is thus 0.5 to 1 sec, which may be too short to be controlled. Hence, the design or operating conditions of a reactor must be adjusted to avoid the instability.[62] Fortunately, it is possible to design boiling water reactors so that these instabilities do not occur even at high power, and currently such reactors are operated at power levels up to 1000 megawatts.

In addition to the oscillations referred to above, as implied by the transfer function, spontaneous power oscillations of small amplitude were observed in the EBWR at about the same frequencies. But they presented no hazard during operation and they are not important in modern boiling water reactors.

9.6 LARGE POWER EXCURSIONS

9.6a The Fuchs-Hansen Model

Large power excursions are of interest in a variety of situations, both real and hypothetical.[63] These include (*a*) pulsed reactors, such as Godiva, TREAT, and TRIGA, (*b*) intentional large increases in reactivity, as in the SPERT, BORAX, and KEWB tests, and (*c*) the analysis of postulated reactor accidents. In all of these cases a system is brought rapidly to a state above prompt critical, so that the neutron population then begins to multiply at a rapid rate. The normal cooling cannot remove the heat being generated and so the temperature rises until some compensation sets in that reduces the reactivity to zero, thereby terminating the excursion. In practice, the manner in which the reactivity is reduced may depend in detail on the reactor design and on the rate at which the neutron population (and power) increases. Hence, for computing the reactivity reduction, a point-reactor model may not be adequate. Nevertheless some useful conclusions can be drawn from such a model of the excursion in which the reactivity reduction is included as a simple feedback parameter. This treatment is sometimes known as the Fuchs-Hansen model,[64] although similar conclusions were reached independently.[65]

Suppose that the reactivity is suddenly increased, i.e., as a step function, thus bringing the value to ρ' above prompt critical, i.e., $\rho' = \rho - \bar{\beta}$, where ρ is the actual reactivity. The assumption is now made that the feedback reactivity is proportional to the energy generated. Since the response to the sudden increase in reactivity is fast, it is justifiable to neglect the delayed neutrons while the transient is under way; hence, equation (9.8) becomes

$$\frac{dP(t)}{dt} = \frac{\rho(t) - \bar{\beta}}{\Lambda} P(t). \tag{9.80}$$

The reactivity at time t is given by

$$\rho(t) - \bar{\beta} = \rho' - \gamma E(t) = \rho' - \gamma \int_0^t P(t')\, dt', \tag{9.81}$$

where γ represents the energy feedback coefficient and $E(t)$ is the total energy generated between time zero and time t. Upon combining equations (9.80) and (9.81), the result is

$$\frac{dP(t)}{dt} = P(t)\left[\alpha_0 - b\int_0^t P(t')\, dt'\right], \tag{9.82}$$

where

$$\alpha_0 = \frac{\rho'}{\Lambda} \quad \text{and} \quad b = \frac{\gamma}{\Lambda}.$$

It will be noted that at $t = 0$, $dP(t)/dt = \alpha_0 P(t)$, and hence α_0 is the initial multiplication rate constant.

Equation (9.82) can be solved in closed form (see §9.7 for the solution); it is found that

$$E(t) = \frac{\alpha_0 + c}{b}\left[\frac{1 - e^{-ct}}{Ae^{-ct} + 1}\right] \tag{9.83}$$

and

$$P(t) = \frac{2c^2 Ae^{-ct}}{b(Ae^{-ct} + 1)^2}, \tag{9.84}$$

where

$$c \equiv \sqrt{\alpha_0^2 + 2bP_0} \tag{9.85}$$

and

$$A \equiv \frac{c + \alpha_0}{c - \alpha_0}. \tag{9.86}$$

A number of interesting results can be derived from these solutions. In a pulsed reactor, it is the general practice to start from a low power in order to obtain a good approximation to a step function increase in reactivity. By starting from a high power, it may not be possible to add reactivity fast enough to do this. If the initial power is low, however, it is easier to increase the reactivity before the feedback term, i.e., $\gamma E(t)$ in equation (9.81), becomes appreciable; there is then effectively a step increase in the reactivity. In fact, it has been found experimentally,[66] in agreement with theory,[67] that a pulsed system, such as the Godiva device of unreflected uranium-235 metal (§5.4c), can be operated with such a weak neutron source that there is a high probability of assembly to a prompt critical state before a divergent chain reaction begins.

If, therefore, the power is assumed to be low before the reactivity is increased, $c \approx \alpha_0$ from equation (9.85), and then from equation (9.86)

$$A \approx \frac{2\alpha_0^2}{bP_0} \gg 1.$$

It is seen, therefore, from equations (9.83) and (9.84) that, at early times, $E(t)$ and $P(t)$ increase exponentially with time in proportion to $e^{\alpha_0 t}$. The power then reaches a maximum at a time which can be found by setting $dP(t)/dt$ equal to zero, i.e.,

$$\frac{dP(t)}{dt} = \frac{2c^3 A}{b} \frac{e^{-ct}[Ae^{-ct} - 1]}{[Ae^{-ct} + 1]^3} = 0.$$

Hence, the power is a maximum when

$$Ae^{-ct} = 1,$$

so that

$$t_{P_{max}} = \frac{\ln A}{c} \approx \frac{\ln A}{\alpha_0}. \tag{9.87}$$

The value of the peak power is thus found from equation (9.84) to be

$$P_{max} \approx \frac{\alpha_0^2}{2b} = \frac{(\rho')^2}{2\Lambda\gamma}. \tag{9.88}$$

At late times, beyond the maximum, the power decreases exponentially as $e^{-\alpha_0 t}$; the power pulse (or burst) is, therefore, approximately symmetrical in time. The power does not drop directly to zero but it tails off because of the fissions due to delayed neutrons, which have been neglected in the foregoing treatment. The contribution of these neutrons can be determined by calculating the number of delayed-neutron precursors produced during the prompt pulse and treating their decay as a neutron source at late times.[68]

The total energy released up to the time the power reaches its peak value, i.e., at the time given by equation (9.87), is obtained from equation (9.83) as

$$E(t_{P_{max}}) \approx \frac{\alpha_0}{b}.$$

The total energy generated is the value at asymptotically large times, namely,

$$E(t) \xrightarrow[t \to \infty]{} \frac{2\alpha_0}{b} = \frac{2\rho'}{\gamma}. \tag{9.89}$$

This again indicates the symmetry of the power pulse, apart from the effect of delayed neutrons.

The results described above have an important bearing on the problem of reactor accidents arising from sudden reactivity excursions. In an excursion starting at a low operating power, the total energy release, as just seen, is $2\rho'/\gamma$,

and is thus independent of Λ, the prompt-neutron lifetime. The essential parameters are then the excess reactivity and the feedback coefficient, and it is immaterial whether the reactor is thermal ($\Lambda \approx 10^{-4}$ to 10^{-3} sec) or fast ($\Lambda \approx 10^{-8}$ to 10^{-7} sec). The peak power, on the other hand, is inversely proportional to the prompt-neutron lifetime. This indicates that the peak pressures and accelerations, caused by material expansion, would be much higher in a reactivity excursion in a fast reactor than in a thermal reactor even though the energy releases may be comparable. In fact, in some models, the peak pressure is found to be proportional to dP/dt and hence, approximately, to $(\rho')^3/\Lambda^2\gamma$; it is thus strongly dependent on the neutron lifetime.

It will be observed that the peak power, peak pressure, and total energy released in the excursion are all inversely proportional to γ, the energy feedback coefficient. From the point of view of reactor safety, it is desirable therefore that the system should have a large (negative) energy coefficient of reactivity. Since the temperature increase will be roughly related to the total energy release, this means a large negative reactivity temperature coefficient will tend to minimize the consequences of a reactivity excursion.

Although the foregoing discussion has referred in particular to a sudden (or step) increase in reactivity, it is also applicable, under certain conditions, to ramp reactivity excursions, i.e., in which the reactivity is increased at a constant rate. If the system exceeds prompt critical before the reactivity feedback becomes appreciable, then the behavior is similar to that for a sudden excursion.[69]

9.6b Pulsed Fast Reactor

The model described above has the advantage of containing only two parameters, namely, $\alpha_0 (= \rho'/\Lambda)$ and $b (= \gamma/\Lambda)$. Because of its simplicity and physical content, it has been used extensively for the interpretation of pulsed reactor experiments.[70] A good example is provided by Godiva II, a critical assembly of bare, highly enriched uranium (about 93.5% uranium-235) metal. By means of adjustable rods of the same material, the reactivity can be increased suddenly by specified amounts, thereby causing a power excursion. This is terminated by the increase in temperature causing the fuel to expand, thus decreasing its density. The resulting decrease in the macroscopic cross sections produces a negative feedback of reactivity which makes the assembly subcritical within a short time. The power production (or fission rate) is determined as a function of time by neutron and gamma-ray detectors; the value of α_0 is calculated from the initial increase in the fission rate.

The results of a series of pulse experiments with Godiva II are shown in Fig. 9.19 for the various indicated values of $1/\alpha_0$, the initial reactor period.[71] The time at which the power maximum is attained is approximately inversely proportional to α_0 and the maximum power is roughly proportional to α_0^2, as required by equations (9.87) and (9.88). There is some deviation from theory

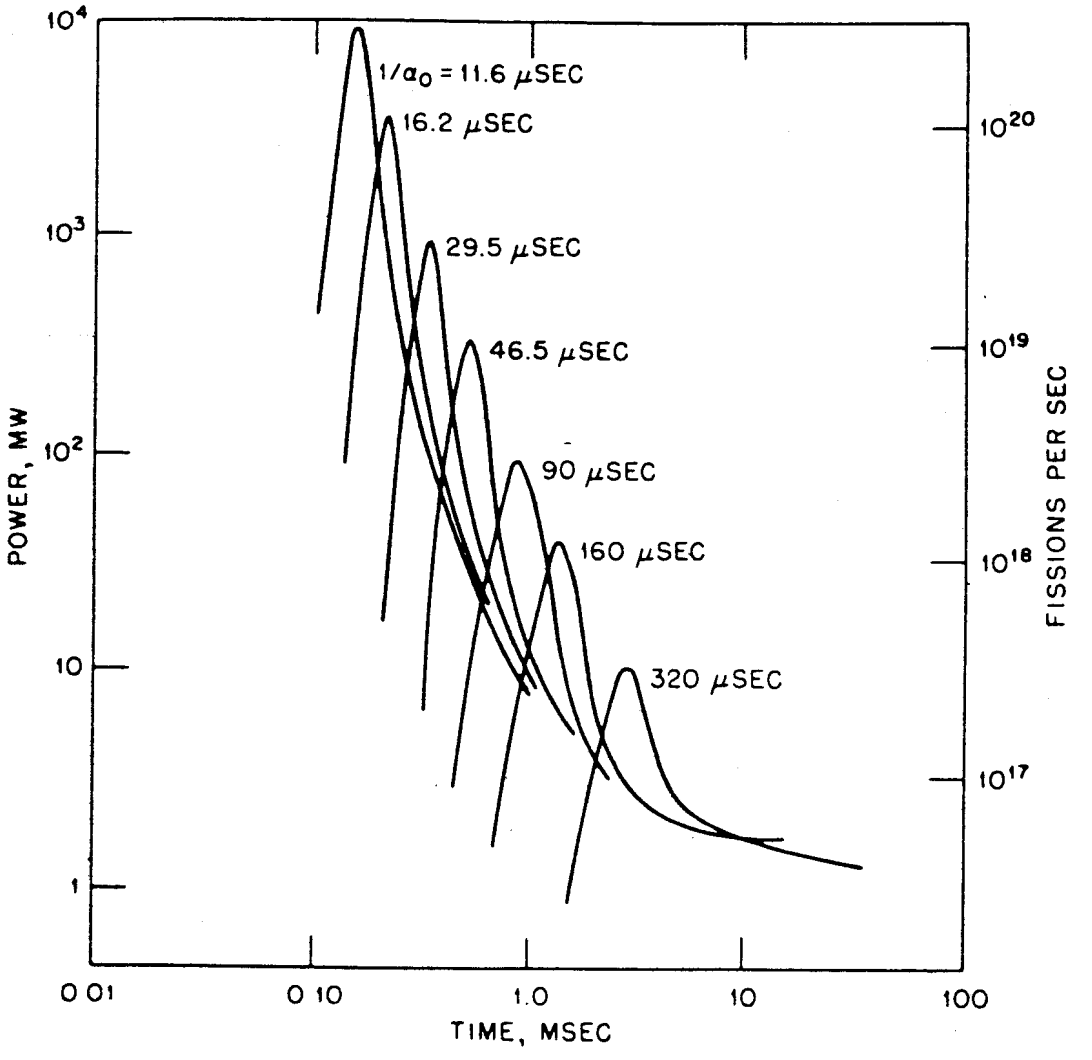

FIG. 9 19 RESULTS OF PULSE EXPERIMENTS IN THE GODIVA-II ASSEMBLY (AFTER T. F. WIMETT AND J. D. ORNDOFF, REF. 71).

for the more violent excursions, with α_0 greater than 5×10^4 sec^{-1} ($1/\alpha_0$ less than 20 μsec), to which reference will be made below. The power pulses are seen to be roughly symmetrical about the maximum except for late times when the delayed neutrons become important.

The total energy generated per pulse was computed both from the increase in temperature and the total activity induced in sulfur by the (n, p) reaction. The results are plotted, on linear scales, in Fig. 9.20[72]; the circles are experimental points and the full line is derived from equations (9.88) and (9.89) as $4P_{max}/\alpha_0$. The agreement between observation and the simple theory is seen to be good up to α_0 values of about 5×10^4 sec^{-1}. The deviations for more violent excursions are due to inertial effects which slow down the expansion; in other words, the expansion, and hence the associated negative reactivity feedback, lags behind the temperature of the fuel. This time delay may be expected to be significant when $1/\alpha_0$ is comparable to (or less than) the time required for a sound wave to

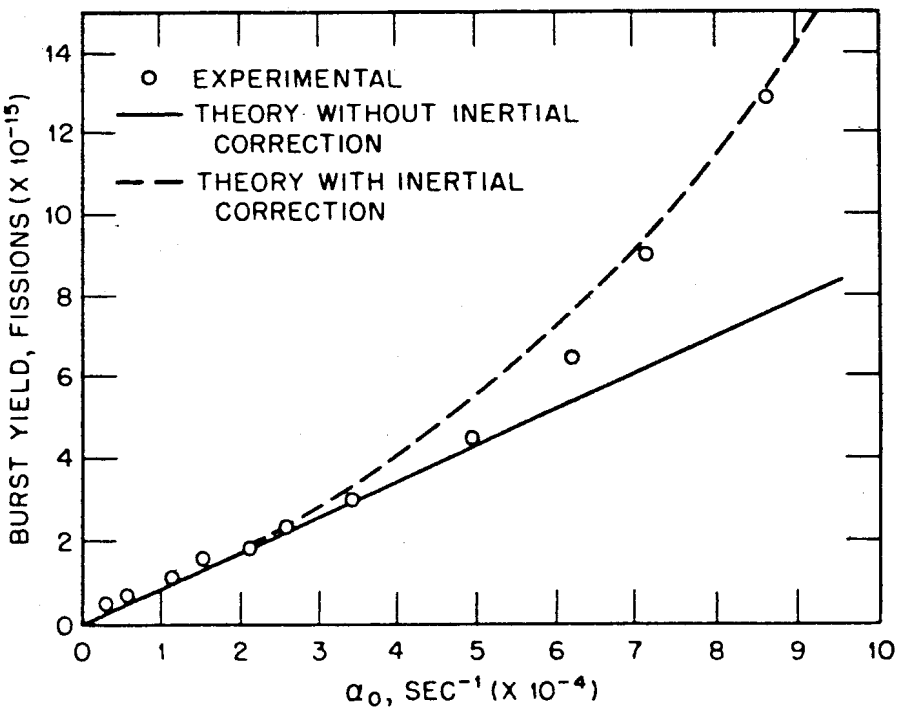

FIG. 9.20 EXPERIMENTAL AND CALCULATED VALUES OF BURST YIELD VS α_0 (AFTER T. F. WIMETT AND J. D. ORNDOFF, REF. 71).

cross the assembly. The effect of inertia is thus not noticeable until the initial reactor period is small, less than 20 μsec for Godiva II.

As a result of the time delay between the energy release (or temperature increase) and the expansion of the assembly, the duration of the pulse is longer than expected in the absence of inertial effects. Consequently, the total energy generated will be appreciably greater than the value indicated by the theory developed in the preceding section. That this is the case is shown by the data in Fig. 9.20. The dashed curve in the figure, which is seen to agree well with the experimental results at the higher values of α_0, was obtained by applying an approximate correction based on the estimated mechanical vibration period of the assembly. This is essentially the time required for a sound wave to traverse it.

9.6c Analysis of Fast-Reactor Accident

From the results given earlier, it is evident that, because of the much shorter neutron lifetime, the peak powers and pressures accompanying a reactivity excursion in a fast reactor can be very much greater than in a thermal reactor. Furthermore, a fast reactor contains so much fissile material that if the coolant could be removed and the core compacted by melting to fill the resulting voids, several critical masses would be present. In some circumstances there might conceivably be an explosion resembling that of an (inefficient) atomic bomb. For these reasons, there has been much interest in estimating the maximum credible explosions that might result from a fast reactor excursion.

In such studies, consideration is given to quite violent accidents. For example, a complete loss of coolant might be postulated; the reactor might then shut down but heating accompanying decay of the fission products could lead to melting of the fuel. This might be followed by collapse of the core into a compact highly supercritical configuration under the influence of gravity. Clearly, the course of such an accident could not be predicted in detail, but in order to discuss the subsequent excursion it is necessary to specify only a few important properties of the collapsing system. In particular, these are the gross geometry, the initial power level, and the rate of reactivity increase during the supercritical phase.

To see how the last two of these factors are involved, consider the collapsing core as it approaches prompt critical, at $t = 0$. At this time, the power level is possibly very low, and it must build up to a much higher level before feedback effects can be felt; during this time the system will become highly supercritical.

In order to determine the extent of the supercriticality, the delayed-neutron precursors can be omitted from the kinetics equations, as in the preceding section, because the times are so short. Hence, equation (9.80) is applicable and it may be written, for simplicity, as

$$\frac{dP}{dt} = \frac{\rho - \bar{\beta}}{\Lambda} P. \tag{9.90}$$

If the reactivity is increasing in a linear manner with time, and since the system is (prompt) critical at $t = 0$, it follows that

$$\rho(t) = \bar{\beta} + \dot{\rho}t,$$

where $\dot{\rho}$ ($= d\rho/dt$), the rate of increase of reactivity, can be estimated from a model of the collapsing core. A solution to equation (9.90) is sought for $t > 0$ in terms of the initial power level, $P(0)$, which is the value at prompt critical. Equation (9.90) can be expressed as

$$\frac{dP}{P} = \frac{\dot{\rho}}{\Lambda} t\, dt$$

and the solution is

$$P(t) = P(0) \exp\left(\frac{\dot{\rho}}{2\Lambda} t^2\right). \tag{9.91}$$

Suppose the feedback is negligible until the total energy generated is E_1. If this energy has been produced by time t_1, the corresponding reactivity is then

$$\rho(t_1) = \bar{\beta} + \dot{\rho}t_1$$

or

$$\rho(t_1) - \bar{\beta} = \dot{\rho}t_1, \tag{9.92}$$

where t_1 is defined by

$$E_1 = \int_0^{t_1} P(t)\,dt = P(0) \int_0^{t_1} \exp\left(\frac{\dot{\rho}}{2\Lambda} t^2\right) dt. \tag{9.93}$$

In order to approximate the integral on the right of this equation, represented by I, let

$$t^2 = u$$

and hence

$$dt = \frac{du}{2\sqrt{u}}.$$

The integral thus becomes

$$I = \frac{1}{2} \int_0^{t_1^2} \exp\left(\frac{\dot{\rho}}{2\Lambda} u\right) \frac{du}{\sqrt{u}}.$$

Repeated integration by parts then gives

$$I = \frac{\Lambda}{\dot{\rho} t_1} \left[\exp\left(\frac{\dot{\rho}}{2\Lambda} t_1^2\right) - 1\right]\left[1 + \frac{\Lambda}{\dot{\rho} t_1^2} + \cdots\right].$$

Since the exponential term is very large, equation (9.93) can be written as

$$E_1 \approx \frac{P(0)\Lambda}{\dot{\rho} t_1} \exp\left(\frac{\dot{\rho}}{2\Lambda} t_1^2\right). \tag{9.94}$$

A rough approximation to t_1 can be found by taking the logarithm of equation (9.94), writing the result as

$$t_1^2 = \frac{2\Lambda}{\dot{\rho}} \left[\ln \frac{E_1 \dot{\rho}}{P(0)\Lambda} + \ln t_1\right],$$

and solving by iteration as follows. The term in t_1 on the right is first ignored and the result is then substituted in $\ln t_1$, and so on. The second approximation, neglecting the ln ln term, is

$$t_1^2 \approx \frac{\Lambda}{\dot{\rho}} \left[\ln \left(\frac{E_1^2 \dot{\rho}}{P(0)^2 \Lambda}\right)\right].$$

If this is inserted into equation (9.92), it is found that

$$\rho(t_1) - \beta = \sqrt{\Lambda \dot{\rho} \ln \left(\frac{E_1^2 \dot{\rho}}{P(0)^2 \Lambda}\right)}. \tag{9.95}$$

This is the excess reactivity, above prompt critical, that is reached when feedback becomes significant. It is seen to vary roughly as the square root of the neutron lifetime and of the rate of reactivity increase, but it is relatively insensitive to E_1 and $P(0)$. For some typical postulated fast reactor accidents, $\rho(t_1) - \beta$ may range up to about a dollar in reactivity, i.e., $\rho(t_1) \approx 2\beta$.

To analyze the excursion further, feedback mechanisms must be postulated. As a rule, the Doppler coefficient of reactivity is about the only temperature (or power) coefficient which can be relied upon in the partially molten and collapsing state of the reactor core. Consequently, if there is a Doppler coefficient (§8.4e), it should be taken into account, since it may have an important effect on the progress of the fast-reactor accident.[73]

In the Bethe-Tait analysis,[74] it is postulated that there is no feedback mechanism, except perhaps for the Doppler effect, for reactivity reduction until the total energy generated in the core reaches a critical value, E^*; then the core material begins to vaporize. As further energy is added, more material is vaporized, thereby building up a pressure which tends to expand the core. With the increase in volume, the reactivity is decreased and the excursion is eventually terminated. The course of the excursion has been estimated by using perturbation theory to predict the reactivity changes due to material motions caused by pressure gradients, and hydrodynamic equations to evaluate these motions. From this treatment approximate results have been obtained in closed form.[75] Subsequently, these results were improved upon by numerical calculations using coupled neutronics and hydrodynamics.[76]

The important parameters for a severe accident, which have also been found to be significant for more moderate accidents, can be derived from relatively simple dimensional arguments. Consider a system which has achieved some degree of excess reactivity, $\Delta\rho$, given approximately by equation (9.95) for $E_1 = E^*$, where feedback commences. For the present treatment, the Doppler effect is assumed to be absent. As the energy approaches E^*, the power and energy release are increasing as $\exp(t\,\Delta\rho/\Lambda)$. During the accompanying expansion, there is insufficient time for any further increase in reactivity; hence, the reactivity may be assumed not to become larger than $\Delta\rho$. When the energy, E, exceeds E^*, its value is given by

$$E - E^* = E^*\left\{\exp\left[\frac{\Delta\rho}{\Lambda}(t - t^*)\right] - 1\right\},$$

where $E = E^*$ when $t = t^*$.

Suppose that the pressure, p, near the center of the core is proportional to $E - E^*$; for a very severe accident, however, $E \gg E^*$, so that at times when the pressures are large

$$p \propto E \propto \exp\left(\frac{\Delta\rho}{\Lambda}t\right).$$

If R is the initial radius of the assembly, i.e., when $t = t^*$, the pressure gradient tending to blow the core apart is roughly proportional to p/R, that is,

$$|\nabla p| \propto \frac{p}{R} \propto \frac{1}{R}\exp\left(\frac{\Delta\rho}{\Lambda}t\right).$$

This pressure gradient produces radial accelerations, such that

$$\ddot{r} \propto |\nabla p| = \frac{c_1}{R} \exp\left(\frac{\Delta\rho}{\Lambda} t\right),$$

where c_1 is approximately constant. Upon integrating this expression twice and neglecting small quantities, it is found that

$$r \approx R\left[1 + \frac{c_1 \Lambda^2}{(\Delta\rho)^2 R^2} \exp\left(\frac{\Delta\rho}{\Lambda} t\right)\right]. \tag{9.96}$$

The expansion eventually decreases the reactivity to zero; hence, the excursion is largely terminated when r has undergone a fractional increase proportional to $\Delta\rho$, i.e., when

$$r = R(1 + c_2 \Delta\rho),$$

where c_2 is a constant. From equation (9.96) it is seen that this happens when

$$\exp\left(\frac{\Delta\rho}{\Lambda} t\right) = \frac{c_2}{c_1} \frac{(\Delta\rho)^3 R^2}{\Lambda^2}.$$

At this time, the energy generated will be

$$E \propto \frac{(\Delta\rho)^3 R^2}{\Lambda^2}. \tag{9.97}$$

It will be noted that, in the present model, the energy generated is proportional to Λ^{-2}, whereas in the Fuchs-Hansen model the energy release, given by equation (9.89), is independent of Λ. The reason is that in the latter case the reactivity was assumed to change as soon as energy is generated without any account being taken of delays due to inertial effects; hence, the excursion was terminated when a certain amount of energy was released, regardless of the value of Λ. In the Bethe-Tait model, however, inertial effects are assumed to be dominant; the reactivity cannot decrease until the pressures have had time to move material and during this time additional energy will have been generated and the amount depends on Λ. The circumstances will, of course, determine which of the two models is to be preferred.

Although the arguments used in deriving the result in (9.97) are not rigorous, detailed numerical calculations[77] have indicated that the proportionality given above is quite good for severe accidents. For mild accidents, the Bethe-Tait model predicts that

$$\left(\frac{E}{E^*} - 1\right) \propto \left[\frac{(\Delta\rho)^3 R^2}{\Lambda^3}\right]^{2/3},$$

and results of numerical computations of the energy have indicated that this is qualitatively correct. The same parameters are thus involved in both mild and severe fast-reactor accidents.

For fast reactors having comparable values of R, the main parameters affecting the severity of an accident are $\Delta\rho$ and Λ, in the combination $(\Delta\rho)^3/\Lambda^2$. According to equation (9.95), $\Delta\rho$ is roughly proportional to $\sqrt{\Lambda\dot{\rho}}$; hence

$$\frac{(\Delta\rho)^3}{\Lambda^2} \propto \frac{(\dot{\rho})^{3/2}}{\sqrt{\Lambda}}.$$

It follows, therefore, that the rate of reactivity increase is the single most important factor in determining how serious a fast-reactor accident might be. It is, however, one of the most uncertain and arbitrary aspects of a postulated accident of this kind.

In designing structures to contain a maximum credible fast-reactor accident, it is important to know how much of the fission energy is released as kinetic energy and how much as internal energy. These quantities must, therefore, be calculated for a detailed hazards analysis. It happens that they appear as a normal part of the numerical calculations[78] and they can also be estimated from the Bethe-Tait analysis.[79]

In connection with the hazards analysis of the Fermi fast reactor, for example, calculations were made of the energy release to be expected for several high rates of reactivity increase.[80] For a uniform collapse of the core under the action of gravity, the Bethe-Tait approach indicated a possible total energy release of about 6×10^8 calories, which is equivalent to 600 kilograms of conventional (chemical) high explosive, for an initial operating power level of 100 megawatts.

9.7 APPENDIX TO CHAPTER 9

In order to solve equation (9.82), let

$$\alpha_0 - b\int_0^t P(t')\,dt' \equiv y(t),$$

so that

$$\frac{dy}{dt} = -bP(t) \quad \text{and} \quad \frac{d^2y}{dt^2} = -b\frac{dP(t)}{dt}.$$

Then equation (9.82) becomes

$$\frac{d^2y}{dt^2} = y\frac{dy}{dt},$$

and upon integrating it is found that

$$\frac{dy}{dt} = \frac{1}{2}(y^2 - c^2). \tag{9.98}$$

The constant c can be found by noting that initially $y(0) = \alpha_0$ and $dy/dt = -bP_0$. It follows, therefore, that

$$c = \sqrt{\alpha_0^2 + 2bP_0}.$$

By making the substitution

$$y \equiv \frac{1}{u(t)} + c,$$

equation (9.98) can be converted into the linear form

$$\frac{du}{dt} + cu = -\frac{1}{2},$$

the solution of which is

$$u(t) = u(0)e^{-ct} - \frac{1}{2c}(1 - e^{-ct})$$

$$= -\frac{1}{2c}\left(1 + \frac{c + \alpha_0}{c - \alpha_0} e^{-ct}\right),$$

where use has been made of the initial condition on u, namely, $u(0) = 1/(\alpha_0 - c)$. Hence, y can be determined and $E(t)$ is found to be given by equation (9.83).

EXERCISES

1. Show that equation (9.1) is obtained when equation (9.3) is solved for C_j and the result is inserted in equation (9.2).
2. Carry out in detail the derivation of equations (9.8) and (9.9).
3. Prove that for six groups of delayed neutrons equation (9.26) has seven roots, ω_k, of which six have negative values.
4. Derive equations (9.27) and (9.28).
5. Verify equation (9.47) by inverting the Laplace transform and retaining the transient terms.
6. Calculate the amplitude and phase angle as a function of frequency, for the zero-power transfer function, assuming one group of delayed neutrons with $\beta = 0.0070$, $\lambda = 0.08\ \text{sec}^{-1}$, and $\Lambda = 10^{-4}$ sec. Compare the results with those in Fig. 9.3.
7. Compute the transfer function $H(i\omega)$ for the model on p. 504 with $P_0 = 0.25$ and 0.5. Plot the results as a function of ω and discuss them.
8. Derive equation (9.78).
9. Derive equation (9.96) and verify that the neglected terms are small; assume that $r = R$ and $dr/dt = 0$ when $t = t^*$.
10. Suppose that just after the prompt-neutron burst described in §9.6a, the reactivity of the system is reduced by $\Delta\rho$, by mechanical means. By neglecting subsequent cooling, estimate (*a*) the total power generated by decay of the delayed-neutron precursors, as compared with the power in the prompt pulse, and (*b*) the initial rate of energy generation due to precursor decay. [Hint: remember to compute the reactivity when the prompt burst terminates.] Note

that in the use of repetitively pulsed reactor sources for time-of-flight measurements, this decay of the precursors would lead to a neutron background.[81]

REFERENCES

1. Keepin, G. R., "Physics of Nuclear Kinetics," Addison-Wesley Publishing Co., Inc., 1965, Chap. 4.
2. Keepin, G. R., Ref. 1, pp. 126, 207, *et seq.*
3. Andrews, J. B., II, and K. F. Hansen, *Nucl. Sci. Eng.*, **31**, 304 (1968); J. B. Yasinsky, M. Natelson, and L. A. Hageman, *ibid.*, **33**, 355 (1968); R. Froelich, *et al.*, *ibid.*, **36**, 257 (1969); W. R. Rhyne and A. C. Lapsley, *ibid.*, **40**, 91 (1970).
4. Keepin, G. R., Ref. 1, Chap. 5; W. W. Graham, III, D. S. Harmer, and C. E. Cohn, *Nucl. Sci. Eng.*, **38**, 33 (1969).
5. Harris, D. R., in "Naval Reactors Physics Handbook," Vol. I, A. Radkowsky, ed. U.S. AEC 1964, pp. 1104 *et seq.*
6. Henry, A. F., *Nucl. Sci. Eng.*, **3**, 52 (1958); see also, E. P. Gyftopoulos, Chap. 3 in "The Technology of Nuclear Reactor Safety," T. J. Thompson and J. G. Beckerley, eds., The M.I.T. Press, Vol. I, 1964; M. Becker, *Nucl. Sci. Eng.*, **31**, 458 (1968); W. M. Stacey, Jr., "Space-Time Nuclear Reactor Kinetics," Academic Press, 1969.
7. Gyftopoulos, E. P., Ref. 6.
8. Glasstone, S., and M. C. Edlund, "The Elements of Nuclear Reactor Theory," D. Van Nostrand Co., Inc., 1952, §10.24; J. R. Lamarsh, "Introduction to Nuclear Reactor Theory," Addison-Wesley Publishing Co., Inc., 1966, p. 424.
9. Glasstone, S., and M. C. Edlund, Ref. 8, §7.34; J. R. Lamarsh, Ref. 8, p. 263.
10. Henry, A. F., Ref. 6; G. R. Keepin, Ref. 1, pp. 104, 178, *et seq.*
11. Scalettar, R., in Proc. Conf. on Neutron Dynamics and Control, D. L. Hetrick and L. E. Weaver, eds., CONF-650413 (1966), p. 342; see also S. Kaplan, *et al.*, *Proc. Third U.N. Conf. on Peaceful Uses of At. Energy*, **4**, 41 (1965).
12. Yasinsky, J. B., and A. F. Henry, *Nucl. Sci. Eng.*, **22**, 171 (1965); K. O. Ott and D. A. Meneley, in Proc. Conf. on Industrial Needs and Academic Research in Reactor Kinetics, Brookhaven National Laboratory Report BNL-50117 (1968), p. 192; *Nucl. Sci. Eng.*, **36**, 402 (1969).
13. Ott, K. O., *Nucl. Sci. Eng.*, **26**, 563 (1966).
14. Ott, K. O., and D. A. Meneley, Ref. 12.
15. Ott, K. O., and D. A. Meneley, Ref. 12.
16. Cohn, C. E., R. J. Johnson, and R. N. Macdonald, *Nucl. Sci. Eng.*, **26**, 198 (1966).
17. See, for example, G. R. Keepin, Ref. 1, Chaps. 7 and 8.
18. Churchill, R. V., "Operational Mathematics," McGraw-Hill Book Co. Inc., 2nd ed., 1958, Chap. 1.
19. Churchill, R. V., Ref. 18, Section 66.
20. Henry, A. F., Ref. 6.
21. Hansen, G. E., and C. Maier, *Nucl. Sci. Eng.*, **8**, 532 (1960).
22. Cohen, E. R., *Proc. Second U. N. Conf. on Peaceful Uses of At. Energy*, **11**, 302 (1958).
23. Keepin, G. R., and C. W. Cox, *Nucl. Sci. Eng.*, **8**, 670 (1960); K. F. Hansen, *et al.*, *ibid.*, **22**, 51 (1965); T. A. Porsching, *ibid.*, **25**, 183 (1966); J. C. Vigil, *ibid.*, **29**, 392 (1967); K. F. Hansen, *et al.*, *Trans. Am. Nucl. Soc.*, **12**, 617 (1969); P. A. Secker, Jr., *ibid.*, **12**, 618 (1969).
24. Canosa, J., *Nukleonik*, **9**, 289 (1967); W. L. Hendry and G. I. Bell, *Nucl. Sci. Eng.*, **35**, 240 (1969); see also G. Birkhoff, "Numerical Solution of the Reactor Kinetics Equation," in "Numerical Solutions of Non-Linear Differential Equations," D. Greenspan, ed., John Wiley and Sons, Inc., 1966.
25. Churchill, R. V., Ref. 18, Chap. 6.
26. Keepin, G. R., Ref. 1, p. 332.
27. Keepin, G. R., Ref. 1, Appendix C.
28. Cohn, C. E., *et al.*, Ref. 16.
29. Cohn, C. E., *et al.*, Ref. 16.
30. Gyftopoulos, E. P., Ref. 6.

31. For review see W. E. Nyer, Chap. 7 in "The Technology of Nuclear Reactor Safety," T. J. Thompson and J. G. Beckerley, eds., The M.I.T. Press, 1964, Vol. 1.
32. Thie, J. A., in Ref. 31, Chap. 8.
33. Churchill, R. V., Ref. 18, Section 13.
34. Gyftopoulos, E. P., and H. B. Smets, *Nucl. Sci. Eng.*, **5**, 405 (1959).
35. Schultz, M. A., "Control of Nuclear Reactors and Power Plants," McGraw-Hill Book Co., 2nd ed., 1961, Chap. 14.
36. Gyftopoulos, E. P., Ref. 6, see p. 188.
37. Schultz, M. A., Ref. 35, Chap. 5. Methods have been developed for assessing stability even when the roots cannot be found explicitly; see M. A. Schultz, Ref. 35, p. 77.
38. Bethe, H. A., "Reactor Safety and Oscillator Tests," Atomic Power Development Associates Report APDA-117 (1956); M. Ash, "Nuclear Reactor Kinetics," McGraw-Hill Book Co., Inc., 1965, Section 3.4.
39. Welton, T. A., *Proc. Symp. Appl. Math.*, XI, Am. Math. Soc., 1961, p. 309.
40. Baran, W., and V. Meyer, *Nucl. Sci. Eng.*, **24**, 356 (1966); H. B. Smets, *ibid.*, **25**, 236 (1966); S. Tan, *ibid.*, **38**, 167 (1969).
41. Welton, T. A., Ref. 39.
42. Akcasu, A. Z., and A. Dalfes, *Nucl. Sci. Eng.*, **8**, 89 (1960); A. Z. Akcasu and P. Akhtar, in Proc. Conf. on Industrial Needs and Academic Research in Reactor Kinetics, Brookhaven National Laboratory Report BNL-50117 (1968), p. 140.
43. Shotkin, L. M., *Nucl. Sci. Eng.*, **35**, 211 (1969).
44. LaSalle, J., and S. Lefschetz, "Stability by Liapunov's Direct Method and Applications," Academic Press, 1961.
45. Popov, V. M., *Proc. Second U.N. Conf. on Peaceful Uses of At. Energy*, **11**, 245 (1958).
46. Gyftopoulos, E. P., *Nucl. Sci. Eng.*, **26**, 26 (1966); J. Devooght, and H. B. Smets, *ibid.*, **28**, 226 (1967); H. B. Smets, *ibid.*, **39**, 289 (1970).
47. Bethe, H. A., Ref. 38.
48. Perry, A. M., in Proc. Conf. on Industrial Needs and Academic Research in Reactor Kinetics, Brookhaven National Laboratory Report BNL-50117 (1968), p. 213.
49. Thalgott, F. W., *et al.*, *Proc. Second U.N. Conf. on Peaceful Uses of At. Energy*, **12**, 242 (1958).
50. Moore, M. N., *Nucl. Sci. Eng.*, **3**, 387 (1958); J. A. Thie, "Reactor Noise," Rowman and Littlefield, Inc., 1963; see also E. P. Gyftopoulos, Ref. 6.
51. Rajagopal, V., *Nucl. Sci. Eng.*, **12**, 218 (1962).
52. Balcomb, J. D., H. B. Demuth, and E. P. Gyftopoulos, *Nucl. Sci. Eng.*, **11**, 159 (1961).
53. Balcomb, J. D., *et al.*, Ref. 52; R. A. Rydin and R. J. Hooper, *Nucl. Sci. Eng.*, **38**, 216 (1969).
54. Thie, J. A., Ref. 50; C. E. Cohn, *Nucl. Sci. Eng.*, **5**, 331 (1959).
55. Pearson, A., and C. G. Lennox, Chap. 6 in Ref. 31, Vol. I.
56. Seifritz, W., and D. Stegemann, *Trans. Am. Nucl. Soc.*, **11**, 565 (1968).
57. Thalgott, F. W., *et al.*, Ref. 49.
58. Smith, R. R., *et al.*, "An Analysis of the Stability of EBR-I, Marks I to III, and Conclusions Pertinent to the Design of Fast Reactors," in "Physics of Fast and Intermediate Reactors," IAEA, 1962, Vol. III, p. 43.
59. Thompson, T. J., Chap. 11 in Ref. 31, Vol. I.
60. Kramer, A. W., "Boiling Water Reactors," Addison-Wesley Publishing Co., Inc., 1958, Chap. 2.
61. Harrer, J. M., *et al.*, *Proc. Second U.N. Conf. on Peaceful Uses of At. Energy*, **9**, 264 (1958); T. Snyder and J. A. Thie, *ibid.*, **11**, 433 (1958); J. A. Thie, *ibid.*, **11**, 440 (1958); A. Iskenderian, *et al.*, in "Operating Experience with Power Reactors," IAEA, 1963, Vol. I, p. 355.
62. Thie, J. A., Chap. 8 in Ref. 31, Vol. I.
63. Nyer, W. E., Chap. 7 in Ref. 31, Vol. I.
64. Fuchs, K., "Efficiency for Very Slow Assembly," Los Alamos Scientific Laboratory Report LA-596 (1946); Hansen, G. E., "Burst Characteristics Associated with the Slow Assembly of Fissionable Materials," Los Alamos Scientific Laboratory Report LA-1441 (1952).

65. Nordheim, L. W., "Physics Section II," Manhattan Project Report CP-2589 (1945), pp. 32–36.
66. Wimett, T. F., *et al.*, *Nucl. Sci. Eng.*, **8**, 691 (1960).
67. Bell, G. I., *Nucl. Sci. Eng.*, **16**, 118 (1963).
68. Wimett, T. F., *et al.*, Ref. 66.
69. Nyer, W. E., Ref. 63; J. Canosa, *Nukleonik*, **10**, 41 (1967); **11**, 131 (1968); R. Froehlich and S. R. Johnson, *ibid.*, **12**, 93 (1969).
70. Nyer, W. E., Ref. 63.
71. Wimett, T. F., and J. D. Orndoff, *Proc. Second U.N. Conf. on Peaceful Uses of At. Energy*, **10**, 449 (1958).
72. Wimett, T. F., and J. D. Orndoff, Ref. 71.
73. Meyer, R. A., and B. Wolfe, "Fast Reactor Meltdown Accidents using Bethe-Tait Analysis," in *Adv. Nucl. Sci. Tech.*, **4**, 197 (1968).
74. Bethe, H. A., and J. H. Tait, "An Estimate of the Order of Magnitude of the Explosion when the Core of a Fast Reactor Collapses," Nuclear Development Associates Report NDA-14-170 (1957); see also, W. J. McCarthy, Jr., and D. Okrent, Chap. 10 in Ref. 31, Vol. I.
75. Bethe, H. A., and J. H. Tait, Ref. 74; W. R. Stratton, T. H. Colvin, and R. B. Lazarus, *Proc. Second U.N. Conf. on Peaceful Uses of At. Energy*, **12**, 196 (1958).
76. Stratton, W. R., *et al.*, Ref. 75; W. J. McCarthy, Jr., and D. Okrent, Ref. 74. For calculations relating to a hypothetical coolant failure accident, see A. K. Agrawal, *et al.*, "SASIA. A Computor Code for the Analysis of Fast Reactor Power and Flow Transients," Argonne National Laboratory Report ANL-7607 (1970).
77. McCarthy, W. J., Jr., and D. Okrent, Ref. 74.
78. Okrent, D., *et al.*, "AX-I, A Computing Program for Coupled Neutronics Hydrodynamics Calculations," Argonne National Laboratory Report ANL-5977 (1959).
79. Meyer, R. A., and B. Wolfe, Ref. 73; H. A. Bethe and J. H. Tait, Ref. 74; W. R. Stratton, *et al.*, Ref. 75.
80. McCarthy, W. J., Jr., and D. Okrent, in Ref. 31, Vol. I, p. 602.
81. "Pulsed Fission Neutron Sources," Session III, Conf. on Intense Neutron Sources, CONF-660925 (1966).

10. SPACE-DEPENDENT REACTOR DYNAMICS AND RELATED TOPICS

10.1 SPACE AND TIME DEPENDENT NEUTRON TRANSPORT PROBLEMS

10.1a Methods of Solution

In this chapter, consideration will be given to time-dependent problems in which the space (and energy) variation of the flux cannot be neglected or approximated as in the point-reactor model emphasized in Chapter 9. It was mentioned in §9.2c that although the reactor kinetics equations (9.8) and (9.9) are exact, they are purely formal unless a good estimate is available of the flux shape factor $\psi(\mathbf{r}, \Omega, E, t)$ at all times, so that the reactivity and other parameters, defined by equations (9.10), etc., can be found. As already seen, the shape factor can be approximated by a time-independent function in certain circumstances, thereby leading to a point-reactor model, or, somewhat more generally, it may be obtained from an adiabatic approximation. Furthermore, in many cases ψ may be found from a quasistatic approximation. A comparison of these three approximations will be made in an example in §10.1c, but first other methods will be considered for solving problems in which the neutron flux is dependent upon both space and time.

It is possible to obtain direct numerical solutions of the time and space dependent neutron transport equation and several computer programs are available for obtaining such solutions.[1] Unfortunately, even for simple approximations to the transport equation, e.g., diffusion theory, the procedures are quite

time consuming. It is probable that progress will be made in accelerating the direct numerical methods; for example, some of the quasistatic approximations[2] or improvements of the zero prompt-neutron lifetime approximation should yield valuable computer programs for obtaining direct numerical solutions.

At present, however, it is perhaps best to regard the direct numerical method for solving the transport equation with dependence on space and time as a "brute force" approach. Its main use is in the solution of important problems of practical interest or for comparison with the results given by approximate procedures. The direct numerical methods will, consequently, not be emphasized in this book.

Another approach to the problem is that of "nodal" analysis in which the reactor is divided into a number of regions or nodes. Each node constitutes a space point in the problem and the parameters that couple the flux at various nodes must be specified.[3] Techniques of this kind have been found to be especially useful for the analysis of coupled cores, such as have been proposed for nuclear propulsion systems and for fast breeder reactors.[4]

Finally, there is a method which is familiar in other branches of mathematical physics, namely, expansion of the neutron flux in the normal modes of the system. This procedure, as applied to space-dependent reactor dynamics, will be examined here. The first point in this connection is to decide on the nature of the modes in which the expansion is to be made. In many aspects of mathematical physics involving inhomogeneous or time-dependent problems, the solutions are expanded as a series of eigenfunctions of a homogeneous time-independent problem. Such an approach may be used for solving the time-dependent neutron transport equation, but a number of difficulties arise both in principle and in practice.

Suppose, for example, that the solution to the time-dependent transport problem is expressed in the form

$$\Phi(\mathbf{r}, \Omega, E, t) = \sum_i T_i(t)\Phi_i(\mathbf{r}, \Omega, E), \tag{10.1}$$

where the functions $\{\Phi_i\}$ are the eigenfunctions of the time-independent problem corresponding to the period eigenvalues $\{\alpha_i\}$ or to the multiplication factor eigenvalues $\{k_i\}$, such as were discussed in earlier chapters and especially in §6.1m. There are uncertainties in connection with such an expansion since, for general transport problems, little is known concerning higher eigenvalues and eigenfunctions and, in particular, it is not known that the discrete eigenvalues form a complete set so that the expansion can be made with confidence (§§1.5b *et seq.*). Indeed, it has been seen that for some simple problems the discrete eigenvalues are not complete but must be supplemented by an integral term, i.e., a contribution from a continuous spectrum.

In the solution of practical reactor problems involving space and time dependence of the neutron flux, simple approximations to the transport equation,

e.g., few-group P_1 or diffusion theory, are generally used. For these approximations, much is known concerning the α and k eigenfunctions (cf. §§4.4c *et seq.*). Moreover, when these approximations are expressed in the form of difference equations, the eigenfunctions have been shown to be complete (§6.1m); hence, in these circumstances, an expansion of the form of equation (10.1) is permissible using either period or multiplication factor eigenfunctions.

There are, however, difficulties in finding the higher eigenfunctions and, in addition, the expansions may not converge rapidly. Furthermore, for determining the expansion coefficients, $T_i(t)$, the adjoint eigenfunctions are also required, as seen in §6.1m, and this increases the amount of effort involved in solving the problem.

10.1b Mode Synthesis and Expansion Methods

For the reasons given above, explicit expansions of the neutron flux in terms of α or k eigenfunctions are not particularly useful for the solution of practical space and time dependent problems. Such eigenfunctions are, nevertheless, conceptually important and in §10.1d it will be shown how they can be generalized to include delayed neutrons. For practical purposes it has been found convenient to choose the modes to be used in equation (10.1) on the basis of physical considerations. The essential requirement is that the actual neutron flux in the calculation should be well represented at all times by the sum of two (or a few) such modes. Symmetry considerations sometimes suggest a simple choice of modes. Examples illustrating mode selection will be given later, but mention may be made here of one special case.

The solution to a diffusion-theory problem in simple geometry might be expanded in terms of the lowest few eigenfunctions of the Helmholtz equation

$$\nabla^2\phi(\mathbf{r}) + B_n^2\phi(\mathbf{r}) = 0,$$

subject to a zero-flux boundary condition on the extrapolated surface of the reactor.[5] These modes would be orthogonal and complete[6] for representing functions of $\mathbf{r}$ but, except in the simplest cases, it might be necessary to use many modes to represent the solution with sufficient accuracy.

Frequently, however, when strictly physical considerations determine the selection of the expansion modes to be used in a transport problem, the modes do not have any simple orthogonality or completeness that can be employed to determine uniquely the expansion coefficients, $T_i(t)$, in equation (10.1). In these circumstances, it is customary to refer to the approach as a *mode synthesis method*,[7] rather than as a mode expansion method. This terminology indicates that an attempt is made to approximate the neutron flux by a sum (or synthesis) of physically reasonable modes, rather than by a mathematically exact expansion in some complete set of modes.

In mode synthesis, there is considerable freedom in determining the expansion coefficients. Variational methods can be used[8] in a manner analogous to that

described in the example in §6.4h. In the latter, the flux was synthesized by assuming P_1 multigroup form and then the expansion coefficients appropriate to that form were sought by means of a variational principle.

A more general procedure for obtaining the expansion coefficients is a method of weighted residuals.[9] Suppose that the expansion (10.1) is inserted into the transport equation, e.g., equation (9.1) or some approximation thereof, using I modes. The result is an integro-differential equation involving I unknown expansion coefficients, $T_i(t)$, multiplied by functions of $\mathbf{r}$, $\mathbf{\Omega}$, and E. If this equation is multiplied by a more-or-less arbitrary weighting function $w_k(\mathbf{r}, \mathbf{\Omega}, E)$ and integrated over the variables $\mathbf{r}$, $\mathbf{\Omega}$, and E, there will be obtained an equation involving the I functions $T_i(t)$ multiplied by constants.

When this is done, using as many independent weight functions as modes, there will be obtained I integro-differential equations for the I expansion coefficients. These equations can be readily solved by numerical methods. In practice, good results have been obtained by using adjoint fluxes corresponding to the synthesis modes as the weighting functions.[10] For some problems, the mode fluxes themselves would serve as reasonable weighting functions.[11]

It is of interest that the kinetics equations for the mode expansion coefficients, $T_i(t)$, are similar to the point-reactor kinetics equations. To show that this is the case, the transport equations (9.2) and (9.3) are written in the form

$$\frac{1}{v}\frac{\partial \Phi(\mathbf{r}, \mathbf{\Omega}, E, t)}{\partial t} + \mathbf{\Omega}\cdot\nabla\Phi + \sigma\Phi = \mathbf{S}\Phi + \tilde{\chi}_p(1-\beta)\mathbf{F}\Phi + \sum_j \lambda_j \tilde{\chi}_j C_j(\mathbf{r}, t) + Q(\mathbf{r}, \mathbf{\Omega}, E, t) \quad (10.2)$$

and

$$\frac{\partial C_j}{\partial t} + \lambda_j C_j = \beta_j \mathbf{F}\Phi, \quad (10.3)$$

where the time-dependent operators indicated by S and F, to suggest scattering and fission, respectively, are defined by

$$\mathbf{S}\Phi \equiv \iint \sum_{x \neq f} \sigma_x f_x(\mathbf{r}; \mathbf{\Omega}', E' \to \mathbf{\Omega}, E; t)\Phi(\mathbf{r}, \mathbf{\Omega}', E', t)\, d\mathbf{\Omega}'\, dE'$$

$$\tilde{\chi}_p(1-\beta)\mathbf{F}\Phi \equiv \iint \tilde{\chi}_p(1-\beta)\nu\sigma_f(\mathbf{r}, E', t)\Phi(\mathbf{r}, \mathbf{\Omega}', E', t)\, d\mathbf{\Omega}'\, dE'$$

and

$$\beta_j \mathbf{F}\Phi \equiv \int \beta_j \nu\sigma_f(\mathbf{r}, E', t)\Phi(\mathbf{r}, \mathbf{\Omega}', E', t)\, d\mathbf{\Omega}'\, dE'.$$

The mode expansion [equation (10.1)] for $\Phi(\mathbf{r}, \mathbf{\Omega}, E, t)$ is now inserted into equations (10.2) and (10.3). Then equation (10.2) is multiplied by $w_k(\mathbf{r}, \mathbf{\Omega}, E)$ and integrated over the variables $\mathbf{r}$, $\mathbf{\Omega}$, E, and equation (10.3) is multiplied by

$w_k\tilde{\chi}_j(E)$ and integrated over the same variables. The results can be expressed in the form

$$\sum_i \Lambda_{ki} \frac{\partial T_i(t)}{\partial t} = \sum_i [\rho(t) - \bar{\beta}(t)]_{ki} T_i(t) + \sum_j \lambda_j c_{jk}(t) + Q_k(t) \tag{10.4}$$

$$\frac{\partial c_{jk}(t)}{\partial t} + \lambda_j c_{jk}(t) = \sum_i [\bar{\beta}_j(t)]_{ki} T_i(t) \tag{10.5}$$

where, using the inner product notation (§6.1a) to indicate integration over $\mathbf{r}$, $\mathbf{\Omega}$, and E,

$$\Lambda_{ki} \equiv \left(w_k, \frac{1}{v}\Phi_i\right)$$

$$[\rho(t) - \bar{\beta}(t)]_{ki} \equiv (w_k, \{-\mathbf{\Omega}\cdot\nabla\Phi_i - \sigma\Phi_i + \mathbf{S}(t)\Phi_i + \tilde{\chi}_p(1-\beta)\mathbf{F}(t)\Phi_i\})$$

$$[\bar{\beta}_j(t)]_{ki} \equiv (w_k, \tilde{\chi}_j\beta_j\mathbf{F}\Phi_i)$$

$$c_{jk}(t) \equiv (w_k, \tilde{\chi}_j C_j(\mathbf{r}, t))$$

$$Q_k(t) \equiv (w_k, Q).$$

If the expansion consists of a single mode, for which $T_i(t) = P(t)$, and if w_k were chosen to be $\Phi^\dagger/F$, in the notation of §9.2b, equations (10.4) and (10.5) would reduce to the point-reactor kinetic equations (9.8) and (9.9), although with different normalizations for the quantities c_j and Q. In the mode synthesis approach, suppose that I modes are used, i.e., $i = 1, 2, \ldots, I$. Then the same number of linearly independent weight functions w_k must also be used, i.e., equations (10.4) and (10.5) hold for $k = 1, 2, \ldots, I$. The resulting system of equations may be written in a compact form by introducing the I-component vectors, $\mathbf{T}$, $\mathbf{Q}$, and $\mathbf{c}_j$; thus,

$$\Lambda \frac{\partial \mathbf{T}(t)}{\partial t} = (\rho - \beta)\mathbf{T}(t) + \sum_j \lambda_j \mathbf{c}_j(t) + \mathbf{Q} \tag{10.6}$$

$$\frac{\partial \mathbf{c}_j(t)}{\partial t} + \lambda_j \mathbf{c}_j(t) = \beta_j \mathbf{T}, \tag{10.7}$$

where Λ, $\rho - \beta$, and β_j are to be regarded as square matrices having the components Λ_{ki}, $[\rho - \beta]_{ki}$, and $[\bar{\beta}_j]_{ki}$ defined above. In equations (10.6) and (10.7), all quantities are known except $\mathbf{T}$ and $\mathbf{c}_j$. By starting from some initial conditions, it would then be possible to solve for these unknowns just as the point-reactor kinetics equations can be solved for $P(t)$ and $c_j(t)$. Thus, equations (10.6) and (10.7) represent a natural generalization of the point-reactor kinetics equations.

10.1c An Example Involving Extreme Flux Tilting

Some of the procedures outlined above for computing the time and space dependent behavior of a neutronic system will be illustrated by means of

postulated situations devised to simulate severe spatial transients in the core of a large thermal, water-moderated reactor.[12] For simplicity, the large core is represented by a homogeneous slab, 240 cm in thickness, together with a transverse (radial) buckling correction for the radial leakage, much as in equations (6.145). The neutron transport is treated by a two-group diffusion theory approximation.

The core is divided into three regions: region I from 0 to 60 cm, region II from 60 to 180 cm, and region III from 180 to 240 cm. The transverse bucklings differ in the three regions, with the value for the middle region being larger than for the other two; hence maximum radial leakage occurs in this region. The initial flux consequently peaks in the outer regions as shown by the bottom curve in Fig. 10.1. Before introducing the perturbation, the reactor is assumed to be at delayed critical.

In the calculations, various spatial transients were induced by changing the

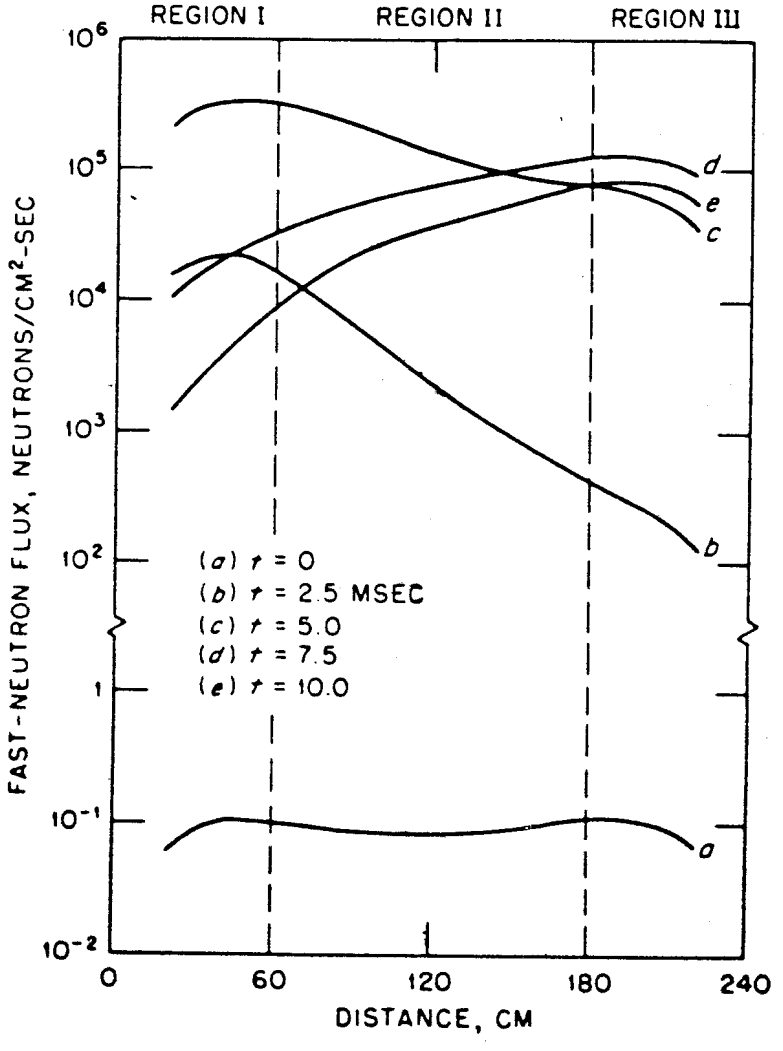

FIG. 10.1 CALCULATED SPATIAL DISTRIBUTION OF FAST-NEUTRON FLUX AS RESULT OF STEP INCREASE IN REACTIVITY (AFTER J. B. YASINSKY AND A.F. HENRY, REF. 12).

number of neutrons per fission in region I. Such a localized perturbation might simulate the gross effect of moving a bank of control rods in this region; some of the postulated changes are, however, considerably more violent than would be reasonable for normal control-rod motion. In all cases, direct numerical solutions to the two-group diffusion equations were obtained; these provide the "exact" results for comparison with those calculated by various approximation methods.

In one example, the reactor was brought above prompt critical by a step increase in ν by about 9.5% at $t = 0$ in region I; this was then followed by a linear (ramp) decrease in ν over a time interval of 0.01 sec to a value about 9.5% below the initial (unperturbed) state. Because the transients are so fast, delayed neutrons may be neglected throughout. As a result of the foregoing changes, there was pronounced "tilting" of the neutron flux; that is to say, the plot of flux versus distance across the slab core had a marked slope. The values of the fast-neutron flux, computed by numerical methods, at several times after $t = 0$ are given in Fig. 10.1.[12] It is evident that soon after the transient is initiated, by increase of ν in region I, the flux is strongly concentrated toward this region (curve *b*); at the end, when the ramp decrease in ν is complete, the tilt, although somewhat smaller, is in the opposite direction (curve *e*).

The numerical results may be used to help in the interpretation of reactor kinetics theory. Consider, first, the equations (9.8) and (9.9); these are exact when the reactivity, ρ, and other parameters are defined by equations (9.10) through (9.16). The shape functions derived from the calculated flux distributions in Fig. 10.1 were used to determine an "exact" reactivity as a function of time

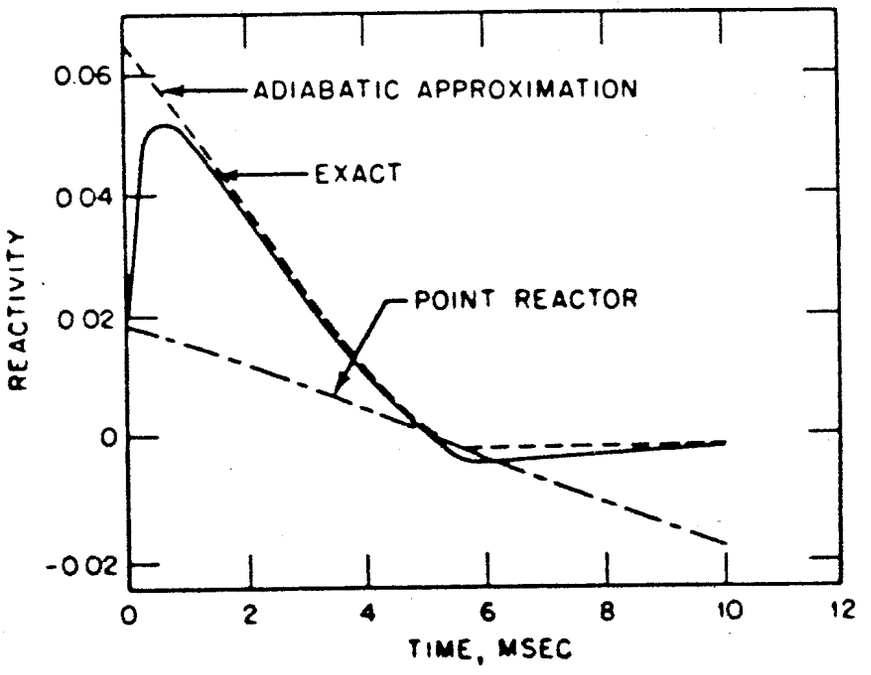

FIG. 10.2 REACTIVITY OBTAINED FROM VARIOUS CALCULATIONS VS TIME (AFTER J. B. YASINSKY AND A. F. HENRY, REF. 13).

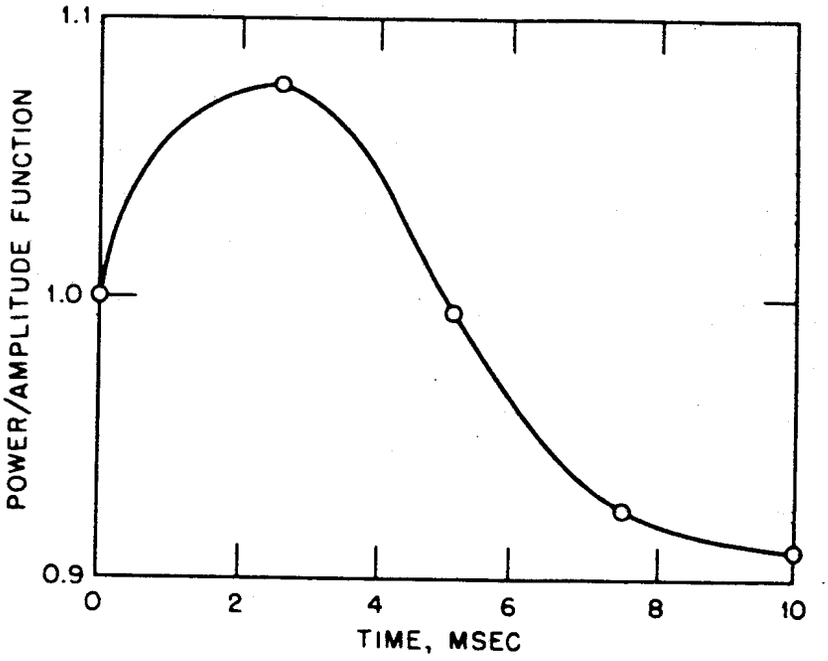

FIG. 10.3 RATIO OF POWER TO AMPLITUDE FUNCTION VS TIME (AFTER J. B. YASINSKY AND A. F. HENRY, REF. 13).

by means of equation (9.10). The result is indicated in Fig. 10.2[13]; it is seen that the reactivity first increases rapidly as the flux tilt toward region I becomes effective, although the value of ν is decreasing over the whole time interval.

Another point which was examined was the extent to which the amplitude function is actually proportional to the power in the transient (§9.2a). In Fig. 10.3, the ratio of the power (or fission rate) to the calculated amplitude function is plotted as a function of time during the transient. The results show that the power and amplitude function do not differ by more than 10 percent, although both change by a factor of about 10^6 during the transit.

The problem considered above has also been treated by several approximation methods. First, a conventional point-reactor treatment was made in which the shape factor used in equations (9.10) through (9.16) was taken to be the unperturbed shape function. In view of the marked tilting of the actual flux, as seen above, it is not surprising that this approximation was very poor, underestimating the peak thermal-neutron flux by a factor of about 10^4 (Fig. 10.4). The corresponding reactivity variation during the transient is also quite different from that given by numerical methods (Fig. 10.2).

In a second calculation, the adiabatic approximation was used in which the shape function at each time was taken to be the k eigenfunction computed from the conditions at that time. As seen in Fig. 10.2, and also in Fig. 10.4 which shows the calculated spatial distribution of the thermal-neutron flux at 7.5×10^{-3} sec after the initial step increase in reactivity, this (adiabatic) approximation is

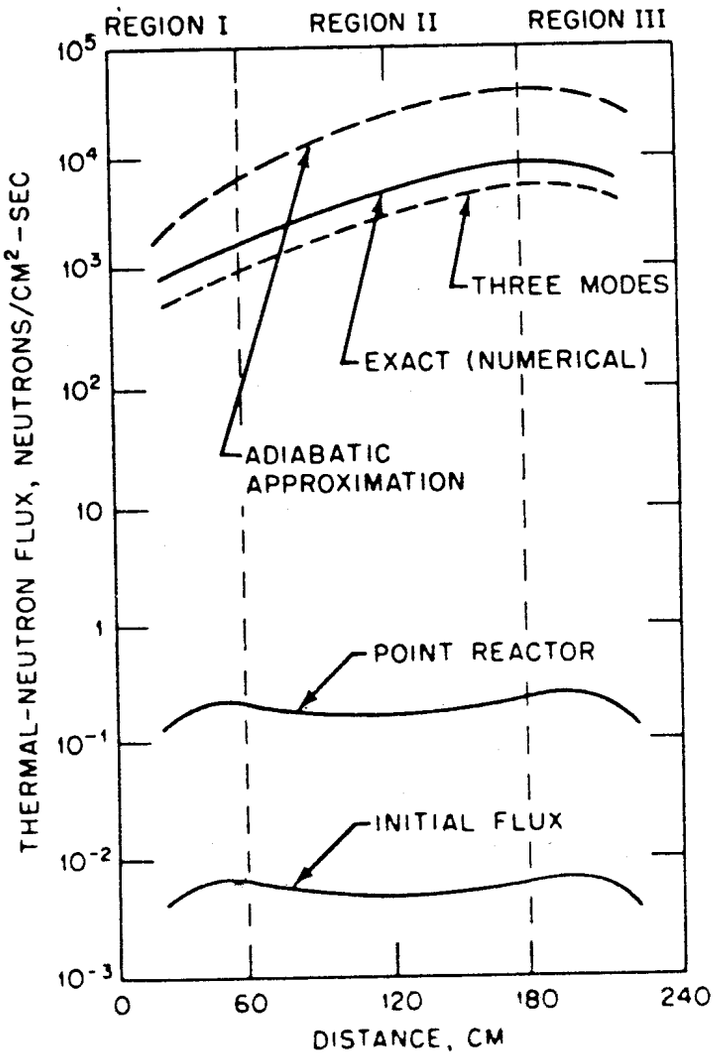

FIG. 10.4 CALCULATED SPATIAL DISTRIBUTION OF THERMAL-NEUTRON FLUX AT 7.5 MSEC AFTER STEP INCREASE IN REACTIVITY (AFTER J. B. YASINSKY AND A. F. HENRY, REF. 13).

much better than the simple point-reactor kinetics, but it is still not very accurate for the violent transient under consideration. Moreover, it should be noted that delayed neutrons play no part in the present problem and so it does not test the effect of lagging due to these neutrons (§9.2c).

Finally, a modal synthesis approximation calculation was made of the thermal-neutron flux distribution. When only two modes were used, representing the unperturbed flux and the flux from an exact calculation at 2.5×10^{-3} sec, the results were poor; a third mode, the flux at 7.5×10^{-3} sec, was required to give fairly good agreement with the "exact" values (Fig. 10.4). The synthesis of three modes is seen to give much better agreement than the adiabatic approximation. If flux modes had not been available from the exact calculations, physical considerations would have guided the choice, the number of modes being increased until the results became insensitive to the number used.

In another series of calculations,[14] the transients were induced by a linear (ramp) increase in ν in region I, i.e., by letting

$$\nu(t) = \nu(0)(1 + At)$$

in this region. For a ramp with $A = 1.508$ and time in seconds, leveling off at $t = 11 \times 10^{-3}$ sec, the numerical results were also compared with those obtained from various approximations except that a quasistatic approximation was used instead of modal synthesis. In the quasistatic approximation, the shape function was computed from equation (9.18) with $\partial\psi/\partial t = 0$. The values of the reactivity as a function of time obtained by the different procedures are shown in Fig. 10.5. It will be noted that the adiabatic reactivity levels off at the end of the ramp, whereas the "exact" and quasistatic values approach the adiabatic result gradually only after the delayed-neutron precursors have adjusted to the new flux shape.

From the foregoing calculations the following conclusions can be drawn. When considering transients involving marked changes in the shape function, the point-reactor kinetics model using a constant shape factor may be grossly misleading. The adiabatic approximation will give better results and will probably overcorrect as compared to the point model. A still further improvement can be obtained by using the modal-synthesis or quasistatic treatments. It

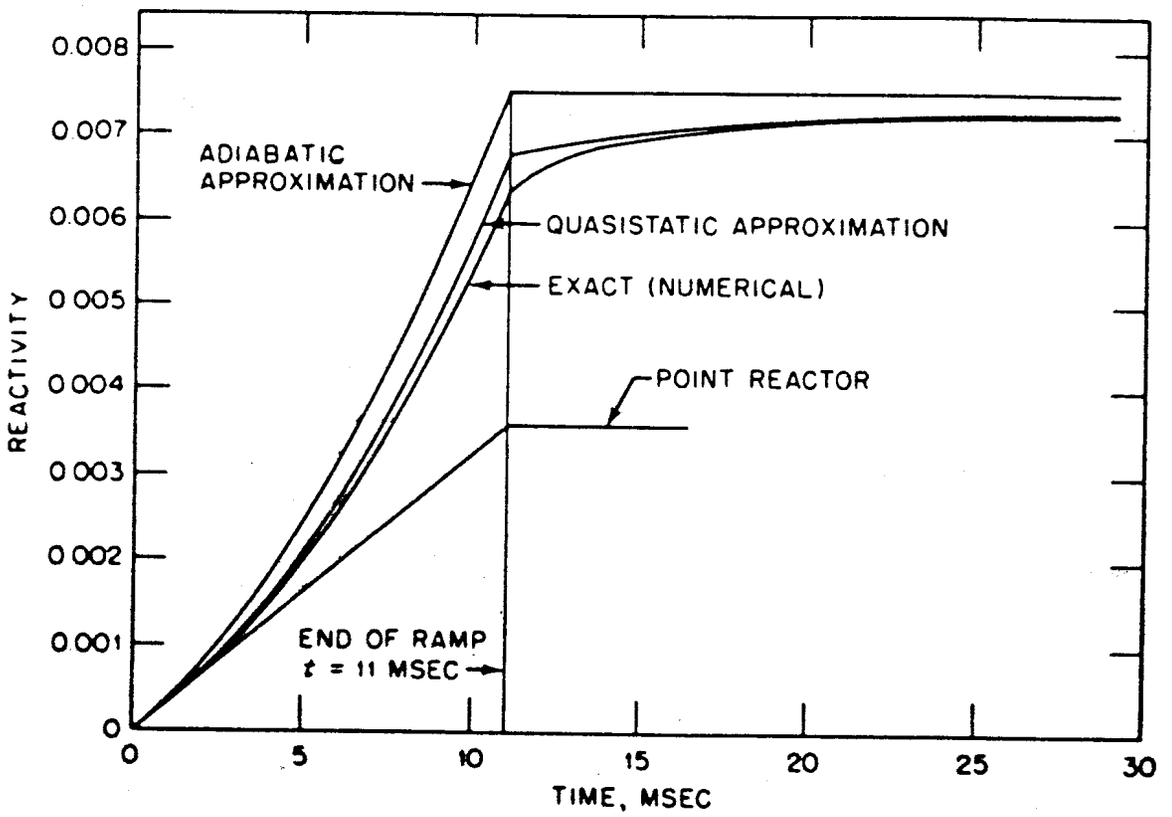

FIG. 10.5 CALCULATIONS OF REACTIVITY AFTER RAMP INSERTION OF LOCAL REACTIVITY IN A THERMAL REACTOR WITH $\Lambda = 1.045 \times 10^{-5}$ SEC AND $\beta = 0.0064$ (AFTER K. O. OTT AND D. A. MENELEY, REF. 14).

should be emphasized that the transient perturbations were not meant to represent any actual cases, but rather to illustrate some general points. Hence, the magnitudes of the deviations among the various approximations must be regarded as being qualitative only.

The problems considered above were designed to simulate situations of extreme flux tilting in a large thermal reactor. For smaller reactors, having a tighter neutronic coupling between regions, the changes in flux are less severe. It would be expected, therefore, that the point-reactor and adiabatic methods might then be applicable. Calculations, performed for a 60-cm slab reactor subjected to a violent transient, similar to the one considered in connection with the 240-cm reactor, indicate improved but still poor accuracy for these approximations.[15]

It appears, therefore, that except for the smallest cores, the point-reactor and adiabatic approximations will often fail to predict the course of violent transients initiated by local changes in reactivity. In this connection, a violent transient is one in which the flux shape changes markedly in a time interval less than (or of the order of) a delayed-neutron lifetime. As mentioned earlier, the point-reactor equations, with constant shape function, will usually be satisfactory for treating very small changes in reactivity. Furthermore, the adiabatic approximation is valid for all sufficiently slow changes of reactivity, such that

$$\frac{1}{\bar{\beta}\lambda}\frac{d\rho}{dt} \ll 1,$$

where λ is an average delayed-neutron decay constant, about 0.1 sec^{-1}. This criterion implies that the change in reactivity during the time $1/\lambda$ should be small compared with $\bar{\beta}$ if the adiabatic approximation is to be used.

10.1d The Period Eigenfunctions and Delayed Neutrons

It was mentioned in §10.1b that, although the period (α) and multiplication factor (k) eigenfunctions are natural modes for use in series solutions of space and time dependent problems, they are not generally useful for that purpose. These eigenfunctions are, however, conceptually important and it will now be shown how the α eigenfunctions are generalized to include delayed neutrons. The ideas which are developed here will be applied to a problem in space-dependent kinetics in §10.1e.

It should be noted, first, that the k eigenfunctions (and their eigenvalues) are not affected by the time lag in the emission of delayed neutrons. The reason is that the k eigenvalue problem is one in which *time-independent* solutions of the transport equation are sought, with the total number of fission neutrons, both prompt and delayed, divided by k. The period eigenvalue problem, on the other hand, is markedly affected by the presence of delayed neutrons. In particular, the long lifetimes of the precursors give rise to slowly decaying α modes (or

eigenfunctions) which are not possible with prompt neutrons alone. In the following development, the transport equations (10.2) and (10.3) will be used with the cross sections being independent of time.

The period (or α) eigenvalue problem is defined by setting

$$\frac{\partial \Phi}{\partial t} = \alpha \Phi \quad \text{and} \quad \frac{\partial C_j}{\partial t} = \alpha C_j, \tag{10.8}$$

and requiring that $Q = 0$, with the flux satisfying the usual boundary condition of zero incoming neutrons. If α_l is an eigenvalue corresponding to the eigenfunctions Φ_l and C_{jl}, it follows from equations (10.2) and (10.3) that

$$\frac{\alpha_l}{v} \Phi_l + \mathbf{\Omega} \cdot \nabla \Phi_l + \sigma \Phi_l = \mathbf{S} \Phi_l + \tilde{\chi}_p (1 - \beta) \mathbf{F} \Phi_l + \sum_j \lambda_j \tilde{\chi}_j C_{jl} \tag{10.9}$$

and

$$\alpha_l C_{jl} + \lambda_j C_{jl} = \beta_j \mathbf{F} \Phi_l. \tag{10.10}$$

In addition, equation (10.10) can be solved for C_{jl} and the result substituted in equation (10.9) to give

$$\frac{\alpha_l}{v} \Phi_l + \mathbf{\Omega} \cdot \nabla \Phi_l + \sigma \Phi_l = \mathbf{S} \Phi_l + \left[\tilde{\chi}_p (1 - \beta) + \sum_j \frac{\lambda_j \tilde{\chi}_j \beta_j}{\alpha_l + \lambda_j} \right] \mathbf{F} \Phi_l. \tag{10.11}$$

Before discussing the possible eigenvalues, α_l, of equation (10.11), it is convenient to write down the equations for the α modes with prompt neutrons only and for the k modes. Both were given in Chapter 1, but the notation did not explicitly take into account the delayed neutrons. Let $\alpha_l^{(p)}$ denote a period eigenvalue with prompt neutrons alone and let $\Phi_l^{(p)}$ represent the corresponding eigenfunction. These will satisfy equation (10.11) with decay of the delayed-neutron precursors being neglected; thus,

$$\frac{\alpha_l^{(p)}}{v} \Phi_l^{(p)} + \mathbf{\Omega} \cdot \nabla \Phi_l^{(p)} + \sigma \Phi_l^{(p)} = \mathbf{S} \Phi_l^{(p)} + \tilde{\chi}_p (1 - \beta) \mathbf{F} \Phi_l^{(p)}. \tag{10.12}$$

On the other hand, the k eigenfunctions are defined by setting the time derivatives in equations (10.2) and (10.3) equal to zero and dividing the number of neutrons per fission by k_m to reach criticality; thus,

$$\mathbf{\Omega} \cdot \nabla \Phi_m + \sigma \Phi_m = \mathbf{S} \Phi_m + \frac{1}{k_m} \tilde{\chi} \mathbf{F} \Phi_m. \tag{10.13}$$

Physical arguments will now be presented in order to deduce some properties of the period eigenvalues, α_l. Although these properties have not been proved rigorously for transport theory, they have been confirmed for approximations, such as few-group diffusion theory in simple geometry. Moreover, they have clear physical content even if they may be lacking in mathematical rigor. The general result will be to divide most (and perhaps all) of the period modes (eigenfunctions) into two classes, namely (*a*) "delayed" modes characterized by

small values of $|\alpha_l|$, i.e., long delay times, and (*b*) rapidly decaying modes, similar to the prompt-neutron modes, i.e., solutions of equation (10.12), characterized by large values of $|\alpha_l|$.

Consider, first, the delayed modes. These are solutions of equation (10.11) with values of α_l of the same order of magnitude as the precursor decay constants, λ_j; that is,

$$|\alpha_l| \lesssim 1 \text{ sec}^{-1}.$$

For such small eigenvalues, the term $\alpha_l \Phi_l / v$ can be neglected, to a first approximation, since α_l / v will be about 10^{-5} times σ even for thermal neutrons. Hence, the terms involving α_l in equation (10.11) serve primarily to change the amplitude of the fission source, $\mathbf{F}\Phi_l$.*

In the k eigenvalue problem, however, the fission source is also multiplied by a factor, namely $1/k_m$ in equation (10.13), so as to achieve criticality. Let Φ_m be a k eigenfunction corresponding to the eigenvalue k_m and suppose that it is possible to choose an eigenfunction Φ_l such that

$$\Phi_l \simeq \Phi_m$$

and

$$\left[\tilde{\chi}_p(1 - \beta) + \sum_j \frac{\lambda_j \tilde{\chi}_j \beta_j}{\alpha_l + \lambda_j}\right] \mathbf{F}\Phi_l \approx \frac{1}{k_m} \tilde{\chi} \mathbf{F}\Phi_m. \tag{10.14}$$

Strict equality would be possible in this last expression only if $\tilde{\chi}_j / \tilde{\chi}_p$ and β_j were true constants, but since they are functions of position and energy the equality is approximate.

If these results are substituted into equation (10.13), there is obtained approximately the α eigenvalue equation (10.11), with α/v set equal to zero. It follows, therefore, that Φ_l, which was selected as a solution of equation (10.14), is approximately an α eigenfunction. Suppose, for simplicity, that $\tilde{\chi}_j / \tilde{\chi}_p$ and β_j are treated as constants; then Φ_l can be equal to Φ_m and equation (10.14) reduces to

$$\tilde{\chi}_p(1 - \beta) + \sum_j \frac{\lambda_j \tilde{\chi}_j \beta_j}{\alpha_l + \lambda_j} = \frac{\tilde{\chi}}{k_m}. \tag{10.15}$$

If there are six groups of delayed-neutron precursors, this equation will be satisfied by six different values of α_l. These six period modes will have the same flux mode, Φ_l, but since the α_l values are different, there will be six different precursor abundances, according to equation (10.10). Each of the six period modes has a small value of $|\alpha_l|$ and is consequently called a delayed mode, to indicate that it arises from the decay of the delayed-neutron precursors.

* If the system contains several types of fissile (and fissionable) nuclides in different regions, the situation is not quite as simple since the quantities β and χ are actually involved in some of the operators in §10.1b. It is to be expected, however, that this will not have a great effect on the general conclusions.

The foregoing argument suggests the following general conclusion. To each k eigenfunction, Φ_m, there correspond six delayed (period) modes, Φ_l, such that $\Phi_l \approx \Phi_m$. The delayed modes differ as to their periods and precursor concentrations, but all the eigenvalues, α_l, are small in absolute value.

It remains, now, to consider the rapidly-decaying period modes; these are similar to the prompt α modes which are defined as solutions of equation (10.12). If the system is below prompt critical, it is known (§1.5a) that the prompt fundamental eigenvalue, $\alpha_0^{(p)}$ (ranging in magnitude, typically, from around 10^6 sec^{-1} for a fast reactor to about 10^3 or 10^2 sec^{-1} for a thermal reactor) will be the least negative eigenvalue.* The higher prompt-modes will have eigenvalues of larger magnitude, i.e., more negative.

Suppose that such a prompt-mode eigenfunction with eigenvalue $\alpha_l^{(p)}$ were inserted into equation (10.11). It would be a proper eigenfunction except for the delayed-neutron terms which would, however, appear divided by the large eigenvalue, $\alpha_l^{(p)}$, and hence would be small. It may be concluded, therefore, that the prompt modes are almost period eigenfunctions even when delayed neutrons are included. It is then reasonable to expect that for each prompt-mode eigenfunction, $\Phi_l^{(p)}$, there will be a similar period mode, Φ_l, i.e.,

$$\Phi_l^{(p)} \approx \Phi_l$$

and hence

$$\alpha_l^{(p)} \approx \alpha_l.$$

Physical arguments have thus been used to suggest that the period eigenfunctions can be divided into the delayed modes and the rapidly-decaying modes, often referred to loosely as the prompt modes. For simple models of neutron transport, these modes have been found explicitly.[16] For more exact treatments, however, it is not known if the modes enumerated above include all of the period modes and the mathematical treatment required for a full analysis will undoubtedly be difficult.

To conclude this section on eigenfunctions and delayed neutrons, the eigenfunctions, $\Phi_l^\dagger$, which are adjoint to the period eigenfunctions, will be considered. By generalizing the methods of Chapter 6 to include delayed neutrons, the adjoint eigenfunctions can be shown to satisfy the relations[17]

$$\frac{\alpha_l^\dagger}{v}\Phi_l^\dagger - \mathbf{\Omega}\cdot\nabla\Phi_l^\dagger + \sigma\Phi_l^\dagger = \mathbf{S}^\dagger\Phi_l^\dagger + [\tilde{\chi}_p(1-\beta)\mathbf{F}]^\dagger\Phi_l^\dagger + \sum_j \beta_j\nu\sigma_f(\mathbf{r}, E)C_{jl}^\dagger(\mathbf{r}) \quad (10.16)$$

and

$$\alpha_l^\dagger C_{jl}^\dagger + \lambda_j C_{jl}^\dagger = \lambda_j \iint \tilde{\chi}_j(E)\Phi_l^\dagger(\mathbf{r}, \Omega, E)\, d\Omega\, dE, \quad (10.17)$$

* For reactors moderated by heavy water or graphite, $\alpha_0^{(p)}$ may be 10 sec^{-1} or even smaller; the distinction between the prompt and delayed period modes is then not clear. For such systems, α_p cannot be neglected in computing the delayed periods and the rapidly-decaying modes will be affected by the delayed neutrons.

where the adjoint operators $\mathbf{S}^\dagger$ and $[\tilde{\chi}_p(1-\beta)\mathbf{F}]^\dagger$ are defined by

$$\mathbf{S}^\dagger\Phi^\dagger \equiv \iint \sum_{x \neq f} \sigma_x f_x(\mathbf{r}; \boldsymbol{\Omega}, E \to \boldsymbol{\Omega}', E')\Phi^\dagger(\mathbf{r}, \boldsymbol{\Omega}', E', t)\, d\boldsymbol{\Omega}'\, dE',$$

and

$$[\tilde{\chi}_p(1-\beta)\mathbf{F}]\Phi^\dagger \equiv \iint \tilde{\chi}_p(E')(1-\beta)\nu\sigma_f(\mathbf{r}, E)\Phi^\dagger(\mathbf{r}, \boldsymbol{\Omega}', E', t)\, d\boldsymbol{\Omega}'\, dE'.$$

In equations (10.16) and (10.17), $\alpha_{l'}^\dagger$ is the eigenvalue, i.e.,

$$\frac{\partial \Phi_{l'}^\dagger}{\partial t} = -\alpha_{l'}^\dagger \Phi_{l'}^\dagger,$$

and the boundary conditions of zero outgoing adjoint are assumed.

The orthogonality relation between flux and adjoint eigenfunctions can be obtained by combining equations (10.9), (10.10), (10.16), and (10.17); by using inner products, the results may be expressed as

$$(\Phi_{l'}^\dagger, (10.9)) + \sum_j \int C_{jl'}^\dagger \times (10.10)\, dV - ((10.16), \Phi_l) - \sum_j \int C_{jl} \times (10.17)\, dV$$

which leads to

$$(\alpha_l - \alpha_{l'}^\dagger)\left[\left(\Phi_{l'}^\dagger, \frac{1}{v}\Phi_l\right) + \sum_j \int (C_{jl'}^\dagger, C_{jl})\, dV\right] = 0. \tag{10.18}$$

In addition, equation (10.10) can be solved for C_{jl} and equation (10.17) for $C_{jl'}^\dagger$, and when the solutions are substituted into (10.18) it is found that

$$(\alpha_l - \alpha_{l'}^\dagger)\left[\left(\Phi_{l'}^\dagger, \frac{1}{v}\Phi_l\right) + \sum_j \frac{\int \lambda_j \beta_j \mathbf{F}\Phi_l \left(\iint \tilde{\chi}_j \Phi_{l'}^\dagger\, d\boldsymbol{\Omega}\, dE\right) dV}{(\lambda_j + \alpha_l)(\lambda_j + \alpha_{l'}^\dagger)}\right] = 0. \tag{10.19}$$

It is possible to derive these orthogonality relations in a more elegant manner by writing equations (10.9) and (10.10) in matrix form.[18] They have been used to suggest generalizations of the inhour equation (9.26) to space-dependent problems.[19] For this treatment, it is argued that, associated with each set of six delayed modes, there will be one prompt mode with a similar flux; furthermore, this set of seven modes is regarded as representing the general form of the inhour equation for the particular flux shape.

10.1e A Pulsed-Source Problem

A problem of practical importance, which can be approached in several different ways, is that of determining the reactivity of a subcritical reactor. For example, the multiplication of neutrons emitted by a steady source can be measured. It is also sometimes possible to obtain information concerning the reactivity from a determination of the power autocorrelation function at short times in a "Rossi-alpha" experiment.[20] One of the simplest methods, however, is to measure the

response of the reactor to a short pulse of neutrons and it is this technique which will be considered here. It has been selected because it will serve to illustrate some of the ideas of the preceding section.

Suppose that an instantaneous pulse of neutrons is injected into a subcritical reactor at time $t = 0$ and the ensuing flux of neutrons is measured by means of a neutron detector. A typical output of such a detector is indicated in Fig. 10.6, in which the important features are emphasized. First there is a peak that dies out very rapidly; this peak is due to prompt neutrons only, i.e., it represents the contribution of the prompt modes to the detector reading. Subsequently, the neutron signal decays more slowly and this represents the effect of delayed-neutron emission.

As shown in Fig. 10.6, there may be a time interval during which the semi-ogarithmic plot is linear; during this time the prompt neutron flux decreases exponentially. The fundamental prompt-neutron mode is then decaying with the time constant $\alpha_0^{(p)}$. At earlier times, the detector signal is affected by the prompt-neutron harmonics, i.e., by prompt modes with more negative values of $\alpha^{(p)}$. Only after these prompt harmonics die out does the neutron population decay with the time constant $\alpha_0^{(p)}$. Some delayed-neutron harmonics also contribute to the signal, as indicated in Fig. 10.6. These are usually less important than the

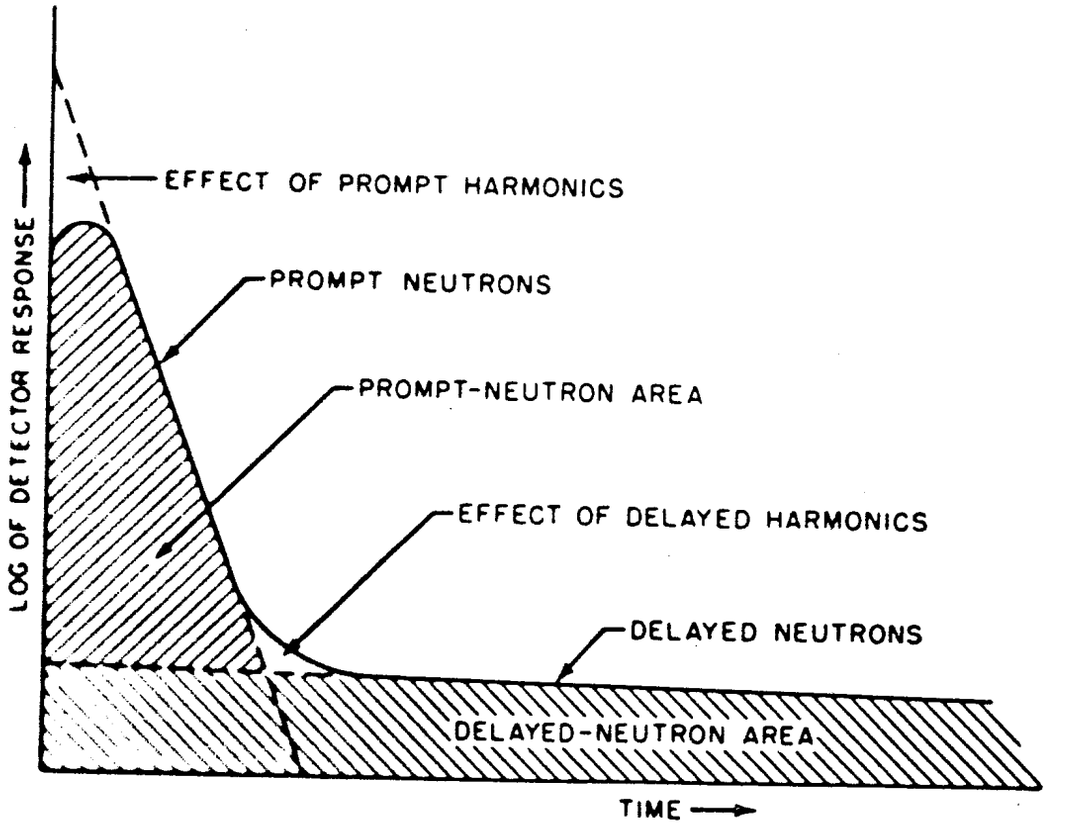

FIG. 10.6 DETECTOR RESPONSE VS TIME AFTER INJECTION OF INSTANTANEOUS NEUTRON PULSE INTO SUBCRITICAL SYSTEM.

prompt harmonics because the sources of delayed neutrons, i.e., the delayed-neutron precursors, are distributed throughout the reactor in something like a fundamental mode whereas the neutron-pulse source is localized.

There are several ways in which the detector output could be used to derive the reactivity of the system. The basic ideas follow from the reactor kinetics equations (9.8) and (9.9), which may be written as

$$\frac{dP}{dt} = \frac{\rho - \beta}{\Lambda} P + \sum_j \lambda_j c_j + Q\,\delta_+(t) \tag{10.20}$$

and

$$\frac{dc_j}{dt} = \frac{\beta_j}{\Lambda} P - \lambda_j c_j, \tag{10.21}$$

together with the assumption that the detector output is proportional to $P(t)$. The source has been represented as a Dirac delta function in time centered at an arbitrarily small positive time, i.e., $\delta_+(t)$, multiplied by Q, the total number of source neutrons. The solution of equations (10.20) and (10.21) is now sought, subject to the initial conditions that $P(0) = 0$ and $c_j(0) = 0$. Although these equations could be solved directly for a point-reactor model, e.g., by Laplace transform methods, it is fruitful to consider some features of the solution that indicate possible experimental approaches when space-dependent effects are important.

During the prompt-neutron pulse, i.e., neglecting decay of the delayed-neutron precursors, the neutron population (and detector signal) will decay as

$$P = Qe^{\alpha t} \quad \text{with } \alpha = \frac{\rho - \beta}{\Lambda}, \tag{10.22}$$

where α is prompt-neutron decay constant and is equivalent to $\alpha_0^{(p)}$. It would thus appear that, from a measurement of the prompt-neutron decay constant, α, it should be possible to obtain ρ if β and Λ were known for the given system. If these two quantities are not known, but the prompt decay constant, α_c, could be measured at delayed critical, i.e., when $\rho = 0$, then

$$\alpha_c = -\frac{\beta}{\Lambda}.$$

Hence, the reactivity in dollar units in the pulsed (subcritical) experiment would be given by

$$\frac{\rho}{\beta} = \frac{\alpha_c - \alpha}{\alpha_c}. \tag{10.23}$$

Although this procedure has been used for determining reactivities,[21] it suffers from the drawback that the parameters β and Λ, particularly Λ, in the subcritical and critical systems are somewhat different.

To overcome this difficulty, another approach can be used. The area under the prompt peak will be proportional to $\int_0^\infty P_p(t)\,dt$, with P_p computed from equation (10.20) without delayed-neutron precursors; thus,

$$\int_0^\infty P_p(t)\,dt = -\frac{Q\Lambda}{\rho - \bar{\beta}} \quad \text{(without delayed-neutron precursors).} \tag{10.24}$$

Upon integrating equations (10.20) and (10.21), however, with delayed neutrons included, the result is

$$\int_0^\infty P(t)\,dt = -\frac{Q\Lambda}{\rho} \quad \text{(with delayed neutrons).} \tag{10.25}$$

The region marked "delayed-neutron area" in Fig. 10.6 is proportional to the area with delayed neutrons, as given by equation (10.25) minus the prompt-neutron area, given by equation (10.24). By combining these equations, it follows that

$$\frac{-\rho}{\bar{\beta}} = \frac{\text{Prompt-neutron area}}{\text{Delayed-neutron area}}. \tag{10.26}$$

By using this relation, the reactivity in dollars can be derived from measurements on the subcritical system only, after injection of a neutron pulse.[22]

The relations developed above have been based on the simplest point-reactor model. In fact, however, the source will be concentrated at some position within the reactor and the neutron population in the reactor will probably be determined by a localized neutron detector. Hence, spatial effects will be present. The source will then excite prompt-neutron harmonics, and so the prompt-neutron area, and to a smaller extent the delayed-neutron area, will depend on the positions of the source and detector. Consequently, when using an expression such as equation (10.26), so also will the measured reactivity.

To avoid the effect of these prompt-neutron harmonics, it has been suggested[23] that attention be paid only to the fundamental prompt-neutron mode in Fig. 10.6. The prompt fundamental mode is extrapolated to zero time, according to its decay constant, α, and this is used to obtain an extrapolated prompt-neutron area for use in equation (10.26); thus,

$$\frac{-\rho}{\bar{\beta}} = \frac{\text{Extrapolated prompt-neutron area}}{\text{Delayed-neutron area}}. \tag{10.27}$$

In still another method,[24] the prompt-neutron harmonics are deemphasized by evaluating a constant a from the relation

$$\int_0^\infty e^{at} P_p(t)\,dt = \int_0^\infty P(t)\,dt.$$

It is then combined with the prompt decay constant, α, to give the reactivity in dollars as

$$\frac{-\rho}{\beta} = -\left(\frac{\alpha}{a} + 1\right). \tag{10.28}$$

In the point-reactor kinetics, a can be evaluated by multiplying equation (10.20), without delayed-neutron precursors, by e^{at} and integrating the result over all times. The term $e^{at}(dP/dt)$ is integrated by parts and it is readily seen that $a = \bar{\beta}/\Lambda$; thus if α is obtained from equation (10.22), the combination leads directly to equation (10.28). The use of the latter for determining reactivities in subcritical systems is generally known as the Garelis-Russell method.

It is thus seen that various procedures have been used to obtain reactivities of subcritical systems from pulsed-source measurements, using either equation (10.23), (10.26), (10.27), or (10.28) to interpret the experiment. Because of spatial effects, the reactivities, except that from equation (10.23), are functions of detector position. In the following discussion it will be shown how these spatial effects can be taken into account.

Suppose that the neutron source is represented by

$$Q(\mathbf{r}, \Omega, E, t) = Q(\mathbf{r}, \Omega, E)\, \delta_+(t)$$

and that the neutron detector is characterized by a cross section $\sigma_d(\mathbf{r}, E)$, such that the expected detector output signal, $D(\mathbf{R}, t)$ can be taken to be

$$D(\mathbf{R}, t) = \iiint \sigma_d(\mathbf{r} - \mathbf{R}, E)\Phi(\mathbf{r}, \Omega, E, t)\, dV\, d\Omega\, dE, \tag{10.29}$$

where $\mathbf{R}$ is a position vector locating the center of the detector. If the time dependence of the detector signal were required, it would be necessary to compute the neutron flux as a function of time. In fact, however, it is necessary to know only the prompt-neutron area or the total area under the detector output in Fig. 10.6, and these areas can be readily computed in the following manner.

Consider the signal due to prompt neutrons alone. This is caused by the prompt flux which is evaluated by ignoring decay of the delayed-neutron precursors. The prompt flux, $\Phi_p(\mathbf{r}, \Omega, E, t)$, then satisfies the transport equation, expressed in the notation of equation (10.2),

$$\frac{1}{v}\frac{\partial \Phi_p}{\partial t} + \Omega \cdot \nabla \Phi_p + \sigma \Phi_p = \mathbf{S}\Phi_p + \tilde{\chi}_p(1 - \beta)\mathbf{F}\Phi_p + Q(\mathbf{r}, \Omega, E)\, \delta_+(t), \tag{10.30}$$

subject to the usual free-surface boundary conditions and the initial condition $\Phi_p(\mathbf{r}, \Omega, E, 0) = 0$. Upon integrating equation (10.30) from $t = 0$ to $t = \infty$ and defining

$$\tilde{\Phi}_p(\mathbf{r}, \Omega, E) \equiv \int_0^\infty \Phi_p(\mathbf{r}, \Omega, E, t)\, dt,$$

the result is

$$\Omega \cdot \nabla \tilde{\Phi}_p + \sigma \tilde{\Phi}_p = S\tilde{\Phi}_p + \tilde{\chi}_p(1 - \beta)F\tilde{\Phi}_p + Q(\mathbf{r}, \Omega, E), \qquad (10.31)$$

where use has been made of the initial condition and the fact that

$$\lim_{t \to \infty} \Phi_p = 0,$$

since the reactor is subcritical.

It is seen, therefore, that the time integrated prompt-neutron flux, $\tilde{\Phi}_p$, satisfies the ordinary time-independent transport equation. Hence, $\tilde{\Phi}_p$ can be determined by any of the standard multigroup methods described in Chapters 4 and 5. The prompt-neutron area in Fig. 10.6, as derived from the detector output, can now be found by integrating equation (10.29) over time; thus

$$\text{Prompt-neutron area} = \int_0^\infty D(\mathbf{R}, t)\, dt = \iiint \sigma_d(\mathbf{r} - \mathbf{R}, E)\tilde{\Phi}_p\, dV\, d\Omega\, dE.$$

The prompt-neutron area is evidently a function of detector position, $\mathbf{R}$, through the spatial dependence of σ_d.

An analogous result can be obtained for the total area under the detector signal. All that is necessary is to integrate equations (10.2) and (10.3) over all time; it is then found that the total time-integrated flux, $\tilde{\Phi}(\mathbf{r}, \Omega, E)$, satisfies equation (10.31) with $\chi_p(1 - \beta)$ replaced by χ. Hence, $\tilde{\Phi}$ can also be computed by standard time-independent methods. The total area can thus be found and the delayed-neutron area is then obtained by subtracting the prompt-neutron area, i.e.,

$$\text{Delayed-neutron area} = \iiint \sigma_d(\tilde{\Phi} - \tilde{\Phi}_p)\, dV\, d\Omega\, dE.$$

The spatial dependence of the reactivity can then be determined by the area-method equation (10.26).

It is also possible to derive the fundamental prompt-mode decay constant, α (or $\alpha_0^{(p)}$), by using the methods of Chapters 4 or 5. Indeed, this is simply the fundamental eigenvalue without delayed neutrons, α_0, which has been discussed in the earlier chapters of this book. Furthermore, the Garelis-Russell constant, a, can be found in the following manner. If equation (10.30) is multiplied by e^{at}, the first term can be written as

$$\frac{e^{at}}{v}\frac{\partial \Phi}{\partial t} = \frac{1}{v}\frac{\partial}{\partial t}(e^{at}\Phi) - \frac{a}{v}e^{at}\Phi.$$

Upon integrating over all times, it is found that the quantity

$$\int_0^\infty e^{at}\Phi_p\, dt,$$

which is what must be used in the Garelis-Russell method, satisfies the same equation as $\tilde{\Phi}_p$, i.e., equation (10.31), except that σ must be replaced by $\sigma - (a/v)$.

Hence a may be interpreted as the negative concentration of a $1/v$-absorber. By using standard time-independent calculational techniques, it is then possible to vary a, by trial and error, until the condition

$$\int_0^\infty e^{at} D_p(\mathbf{R}, t)\, dt = \int_0^\infty D(\mathbf{R}, t)\, dt,$$

where D_p is the detector signal due to prompt neutrons, is satisfied.

In order to obtain the extrapolated prompt-neutron area, for use in equation (10.27), it is necessary to derive the amplitude of the fundamental mode. For this purpose, the prompt-neutron flux is expanded in terms of the prompt α modes, along the lines used in §6.1m. As already stated, this expansion may not be justifiable for transport theory, but it is known to be satisfactory for simple approximations to this theory.

There is, however, one difference between the procedure to be used here and the one in §6.1m. In the latter, the solution to an initial value problem was expressed in normal modes, whereas here the solution to a source problem is sought. The source $Q(\mathbf{r}, \mathbf{\Omega}, E)\, \delta_+(t)$ is, however, equivalent to an initial condition on Φ_p, namely,

$$\Phi_p(\mathbf{r}, \mathbf{\Omega}, E, 0) = vQ(\mathbf{r}, \mathbf{\Omega}, E). \tag{10.32}$$

This can be seen by integrating equation (10.30) over the time interval from $t = 0$ to $t = \epsilon$, where ϵ is very small but large enough to include the delta function. All the integrals are small except for those of the first and last terms, and these give

$$\frac{1}{v}\left[\Phi_p(\mathbf{r}, \mathbf{\Omega}, E, \epsilon) - \Phi_p(\mathbf{r}, \mathbf{\Omega}, E, 0)\right] = Q(\mathbf{r}, \mathbf{\Omega}, E).$$

In this equation, $\Phi_p(t = 0)$ is zero according to the initial condition and consequently $\Phi_p(t = \epsilon) = vQ$. But since ϵ is very small, it may be set equal to zero and hence the result in equation (10.32) follows.

By using the initial condition derived above, together with equation (6.45), it is found that the flux in the fundamental prompt mode is given by

$$\text{Flux in prompt mode} = \frac{(\Phi_0^\dagger, Q)}{((1/v)\Phi_0^\dagger, \Phi_0)}\, \Phi_0(\mathbf{r}, \mathbf{\Omega}, E) \exp(\alpha_0^{(p)} t), \tag{10.33}$$

where Φ_0 and $\Phi_0^\dagger$ are the fundamental prompt-α mode eigenfunction and its adjoint, respectively. The extrapolated prompt-neutron area in the detector signal diagram (Fig. 10.6) is then obtained upon multiplying this expression by σ_d and integrating over all variables including time from zero to infinity. The result is

$$\text{Extrapolated prompt-neutron area} = \frac{1}{|\alpha_0^{(p)}|} \frac{(\Phi_0^\dagger, Q)}{((1/v)\Phi_0^\dagger, \Phi_0)} (\sigma_d, \Phi_0). \tag{10.34}$$

In order to calculate this quantity, the fundamental prompt-α mode and its adjoint must be computed, but here again standard time-independent methods can be used.

In principle, it should now be possible to predict, from time-independent calculations, the reactivity of a subcritical reactor as a function of position, according to the various methods described earlier. The results obtained in this manner may be compared with those derived from the plot of the observed detector output against time, as in Fig. 10.6, with the detector at a number of different locations.

Before making this comparison, it is pertinent to inquire if there is a unique reactivity which these experiments could be designed to yield. In this connection it may be recalled, first, that equation (9.10), which has been used as the definition of reactivity in the reactor kinetic equations, does not define the reactivity uniquely. The reason is that there are no unique cross-section changes which bring the system to critical and a variety of choices can be used for $\Delta\sigma$ and $\Phi_0^\dagger$ in equation (9.10). In practice, however, the resulting reactivities might differ very little. Several other definitions of reactivity, which are appropriate to the situation under consideration here, have been proposed.[25]

One of the most attractive of these definitions is based on the following considerations. It was seen in §9.2b that ρ is analogous to a quantity $(k-1)/k$ which was derived in the treatment of perturbation theory. Hence, a *static reactivity* in dollar units can be defined by the relation

$$\frac{-\rho}{\beta} = \frac{1-k}{k\beta}. \tag{10.35}$$

This definition has the virtue that the eigenvalue k is a unique integral quantity for the system. Moreover, it can be calculated by multigroup (or other) methods. Further arguments have been offered in favor of the static reactivity,[26] which is seen to be closely related to the various experimental quantities discussed earlier in this section. In the treatment which follows, the static reactivity will be compared with experimental values based on the methods already described.

Pulsed-neutron experiments have been performed on a critical assembly moderated and reflected by ordinary water to determine the reactivity according to (*a*) the simple area method by equation (10.26), (*b*) the extrapolated area method by equation (10.27), and (*c*) the Garelis-Russell method. A source of 14-MeV neutrons was introduced on the midplane of the assembly at the core-reflector interface, and boron trifluoride neutron detectors were located at three positions on the midplane. Calculations were also made along the lines described above to predict the space dependence of the various reactivity determinations. The calculations were performed on a one-dimensional model of the assembly using multigroup diffusion theory, and were normalized so as to give the observed prompt decay constant, $\alpha_0^{(p)}$. Some of the results are compared in Fig. 10.7[26]; the points are based on detector readings at the indicated three locations

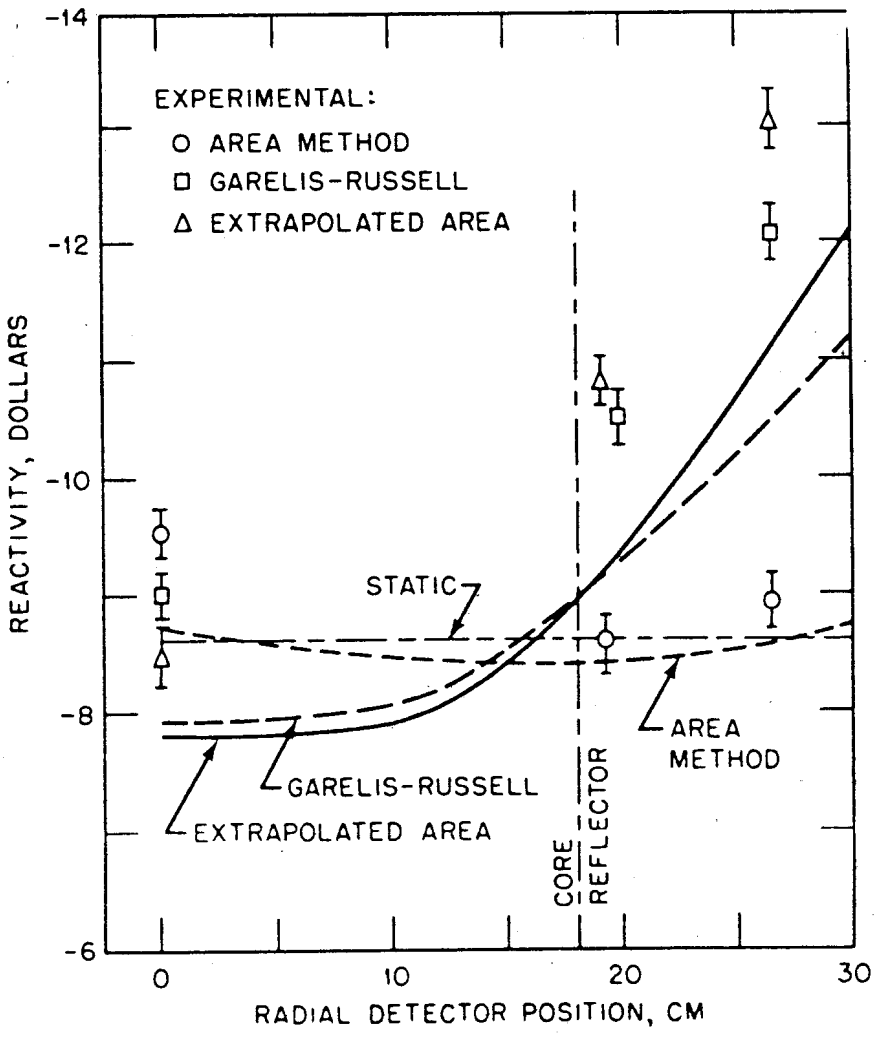

FIG. 10.7 EXPERIMENTAL AND CALCULATED REACTIVITY VS DETECTOR POSITION (AFTER C. F. MASTERS AND K. B. CADY, REF. 26).

whereas the curves are calculated using a prompt decay constant, $\alpha_0^{(p)}$, of 1706 sec^{-1}.

It will be observed that there is a qualitative agreement between the reactivities derived from the detector readings and those calculated from transport theory. Much of the difference between the calculated and observed values is probably due to use of a simple one-dimensional model of the subcritical assembly. Surprisingly, it appears that the simple area method gives results most nearly independent of position; this is probably a fortuitous circumstance arising from the cancellation of harmonic effects in the particular assembly used in the experiments.

10.1f Other Space and Time Dependent Problems

Several other space and time dependent problems have been analyzed. Among these, mention may be made of the pulsed-source[27] and neutron-wave[28] experiments discussed in Chapter 7 as methods for studying the thermalizing properties of various media. In such experiments there is no fissile material present;

hence, there is no fission and no delayed neutrons. The mode-expansion method is used to interpret the measurements, and the characteristics of the fundamental mode are determined.

In the pulsed-neutron experiment, the decay constant, α_0, of the fundamental period mode is of greatest interest. As noted in §7.6f, by studying the variation of α_0 with the size (or buckling) of the system, such parameters as the thermal diffusion length and the diffusion cooling constant of the medium can be derived. In the neutron-wave experiment, the fundamental mode is sought as a function of space for a source varying periodically in time. From the variations of mode properties with source frequency, the thermal diffusion length and other parameters can be determined.[29] In each of these experiments, the effects of higher modes, in particular the spatial harmonics, should be considered, either to establish that they are negligible or to correct for them.

10.1g Xenon-Induced Power Oscillations

It is well known that the fission product xenon-135 (half-life 9.2 hours) has a very large absorption cross section for thermal neutrons, about 3×10^6 barns at 300°K. A small fraction of this nuclear species is formed directly in fission, but the major portion results from the decay of iodine-135 with a half-life of 6.7 hours. Iodine-135 is itself a decay product of tellurium-135, which has a half-life of less than 2 minutes. Consequently, for all practical purposes it may be assumed that the production of xenon-135 is determined solely by the decay of iodine-135, and that the rate of formation of the latter is proportional to the fission rate.

In addition to the familiar poisoning effect due to xenon-135 which occurs in thermal reactors operating at a sufficiently high neutron flux,[30] there is a possibility that it can cause localized oscillations in the power in a large reactor. The flux (or power) may then vary in space and time. For studying the dynamics of such xenon-induced oscillations, the modal expansion method provides a convenient approach.

These oscillations generally arise as a consequence of a localized perturbation leading to an increase in the neutron flux. As a result, the rate of xenon-135 consumption (or burnup) by neutron absorption increases, but since its replacement depends on the decay of iodine-135, there may be a temporary decrease in the local amount of xenon-135. This will permit the neutron flux to increase still further, unless it is compensated by the negative power (or flux) coefficient of reactivity.

Even when there is compensation, so that the power does not diverge continuously, the increased power level will cause an increase in the concentration of iodine-135. Within a short time, decay of the latter will result in an increased local amount of xenon-135, thereby decreasing the power. Thus, oscillations in the reactor power can arise with a period of the order of the iodine-135 lifetime. Whether the oscillations will be damped (stable), undamped, or growing (unstable) will depend on the flux level in the reactor and on other conditions, as

will be seen shortly. Under particularly unfavorable conditions, the power could diverge without oscillation.[31]

Local oscillations in power, caused by xenon-135, have been observed in several large thermal reactors.[32] The reactor must of course be thermal, because in the neutron energy spectrum of a fast or intermediate reactor the absorption cross section of xenon-135 is quite small. Furthermore, it is necessary for the reactor to be large, with dimensions large compared to a neutron migration length, because only in such systems can the spatial harmonics of the flux be excited to an appreciable extent.

In order to simplify the following treatment of xenon-induced oscillations by the modal expansion method, without affecting the basic physics of the problem, a number of approximations will be made. In the first place, it will be assumed, as noted at the beginning of this section, that all the xenon-135 is produced by the decay of iodine-135, the rate of formation of which is determined by the fission rate. Next, since the oscillations are significant only for large, thermal reactors, one-velocity diffusion theory should be adequate for treating neutron transport. Furthermore, since the expected oscillation periods are long, e.g., several hours, it is a good approximation to treat the delayed neutrons as if they appeared promptly.[33] A homogeneous reactor core with plane geometry will be assumed.

In considering the feedback effects of power and xenon-135, the former may be assumed to be instantaneous. For the present purpose, it is convenient to express this in terms of the neutron flux; the reactivity feedback is then represented by $f\phi$, where f is the power coefficient of reactivity in appropriate units. The xenon-135 feedback is proportional to the concentration of this nuclide, but the effect is delayed by its dependence on the decay of iodine-135. In an operating reactor, the control system (automatic or manual) will modify the feedback and this could be included in $f\phi$ if required. The purpose of the present discussion, however, is to understand what would happen in the absence of such adjustment of control rods.

The reactor kinetics equation for one-group diffusion theory in plane geometry, based on the considerations indicated above, is

$$\frac{1}{v}\frac{\partial\phi(x,t)}{\partial t} = D\frac{\partial^2\phi}{\partial x^2} + (k - 1 + f\phi)\sigma_a\phi - \hat{\sigma}_x X\phi, \tag{10.36}$$

where k is the infinite medium multiplication factor, so that $(k - 1)/k$ is the infinite medium reactivity, $\hat{\sigma}_x$ is the *microscopic* absorption cross section of xenon-135, and X is its concentration in nuclei per cm^3; σ_a is the macroscopic absorption cross section of the system without the xenon-135. The value of X at any time is related to the concentration I of iodine-135 by

$$\frac{\partial I(x,t)}{\partial t} = \gamma_I\sigma_f\phi - \lambda_I I \tag{10.37}$$

and

$$\frac{\partial X(x, t)}{\partial t} = \lambda_I I - \lambda_x X - \hat{\sigma}_x X\phi, \tag{10.38}$$

where λ_I and λ_x are the decay constants of iodine-135 and xenon-135, respectively, γ_I is the fractional yield of the former nuclide per fission, and σ_f is the macroscopic fission cross section.

The stability of the system to small perturbations about some stationary solution will now be examined. In order to obtain simple modes in the expansion of ϕ, I, and X, a slab reactor, of thickness a, will be assumed. It is supposed to be well reflected, so that the steady-state flux is spatially uniform; hence, the boundary conditions on the flux are $\partial\phi/\partial x = 0$ at $x = 0$ and $x = a$.

Let ϕ_0, I_0, X_0 be the values of the respective quantities in the steady-state system; then, since $\hat{c}^2\phi_0/\hat{c}x^2$ is zero in the postulated reactor, equations (10.36), (10.37), and (10.38) become

$$(k - 1 + f\phi_0)\sigma_a\phi_0 - \hat{\sigma}_x X_0\phi_0 = 0 \tag{10.39}$$

$$I_0 = \frac{\gamma_I\sigma_f\phi_0}{\lambda_I} \tag{10.40}$$

and

$$X_0 = \frac{\lambda_I I_0}{\lambda_x + \hat{\sigma}_x\phi_0} = \frac{\gamma_I\sigma_f\phi_0}{\lambda_x + \hat{\sigma}_x\phi_0}, \tag{10.41}$$

where k is the multiplication factor the reactor would have in the absence of xenon-135 and power feedback. If equation (10.41) is substituted into (10.39) and solved for ϕ_0, the result is

$$\phi_0 = \frac{k - 1}{\dfrac{\hat{\sigma}_x\gamma_I\sigma_f}{\sigma_a(\lambda_x + \hat{\sigma}_x\phi_0)} - f},$$

which will yield a solution provided that $k > 1$ and the power feedback coefficient of reactivity, f, is negative.

Suppose now that the system is perturbed locally; let ϕ, I, and X represent the small *departures* of the actual magnitudes from their steady-state values. The linearized equations, omitting terms of the second order in small quantities, corresponding to equations (10.36), (10.37), and (10.38) are

$$\frac{1}{v}\frac{\partial\phi}{\partial t} = D\frac{\partial^2\phi}{\partial x^2} + (k - 1 + 2f\phi_0)\sigma_a\phi - \hat{\sigma}_x(X_0\phi + X\phi_0) \tag{10.42}$$

$$\frac{\partial I}{\partial t} = \gamma_I\sigma_f\phi - \lambda_I I \tag{10.43}$$

and

$$\frac{\partial X}{\partial t} = \lambda_I I - \lambda_x X - \hat{\sigma}_x(X_0\phi + X\phi_0). \tag{10.44}$$

The quantities ϕ, I, and X are now expanded in a series of spatial modes. Because of the simple geometry of the slab reactor, these modes can be taken to be the complete set $\{\cos(n\pi x/a)\}$, with $n = 0, 1, \ldots, \infty$. Moreover, because ϕ_0 has been assumed to be space independent, the modes are uncoupled; thus, if the expansions are inserted into equations (10.42), (10.43), and (10.44), and then multiplied by $\cos(m\pi x/a)$ and integrated over $x(0 < x < a)$, only the coefficients of $\cos(m\pi x/a)$ remain.* If the expansions are made in the modes indicated above and the Laplace transforms are taken, using the notation

$$\mathscr{L}[\phi(x, t)] = \sum_{n=0}^{\infty} A_n(s) \cos \frac{n\pi x}{a}$$

$$\mathscr{L}[I(x, t)] = \sum_{n=0}^{\infty} I_n(s) \cos \frac{n\pi x}{a}$$

and

$$\mathscr{L}[X(x, t)] = \sum_{n=0}^{\infty} X_n(s) \cos \frac{n\pi x}{a},$$

it is found, from equations (10.42), (10.43), and (10.44), that

$$\frac{sA_n}{v} = -D\left(\frac{n\pi}{a}\right)^2 A_n + (k - 1 + 2f\phi_0)\sigma_a A_n - \hat{\sigma}_x(X_0 A_n + X_n \phi_0)$$

$$sI_n = \gamma_1 \sigma_f A_n - \lambda_1 I_n$$

$$sX_n = \lambda_1 I_n - \lambda_x X_n - \hat{\sigma}_x(X_0 A_n + X_n \phi_0).$$

These three equations for the nth mode may be combined to yield a single equation for A_n, the Laplace transform of the coefficient of the nth flux mode. In the usual way, those values of s which are the poles of A_n will be the reciprocal periods of the nth mode that determine the stability of the mode. Upon solving the equations for $A_n(s)$ and eliminating k by means of equation (10.39) and X_0 by equation (10.41), it is found that the poles of $A_n(s)$ are the roots of the equation

$$\frac{s}{v} = -D\left(\frac{n\pi}{a}\right)^2 + f\sigma_a\phi_0 - \frac{\hat{\sigma}_x\gamma_1\lambda_1\sigma_f\phi_0}{(s + \lambda_1)(s + \lambda_x + \hat{\sigma}_x\phi_0)}$$

$$+ \frac{\hat{\sigma}_x^2\gamma_1\sigma_f\phi_0^2}{(\lambda_x + \hat{\sigma}_x\phi_0)(s + \lambda_x + \hat{\sigma}_x\phi_0)}.$$

This is a cubic equation in s, the roots of which determine the three reciprocal periods of the nth mode.

The condition for neutral stability is that roots exist for pure imaginary

* For a bare reactor, ϕ_0 is not space independent and the modes are coupled.[34]

$s = i\omega$. For a reactor in which all the variable parameters except f and ϕ_0, i.e., D, a, and v, are fixed, there will be one curve in the f-ϕ_0 plane for which the system has neutral stability for each mode. Such a curve for the fundamental ($n = 0$) mode is shown in Fig. 10.8 for a slab reactor[35]; all points to the right represent stable systems whereas those to the left are unstable. Thus, the ordinates of the curve give the value of the steady-state flux at which the reactor will have neutral stability against xenon-induced oscillations for the given (negative) power feedback coefficient of reactivity (abscissa). Actually, for points on the curve undamped xenon-induced oscillations in neutron flux (and power) will occur in the absence of other factors, e.g., control rod adjustment.

The numerical data in Fig. 10.8 refer to a particular thermal (slab) reactor, but the qualitative conclusions are of general applicability. It is seen that when the steady-state neutron flux in a thermal reactor is sufficiently low, e.g., less

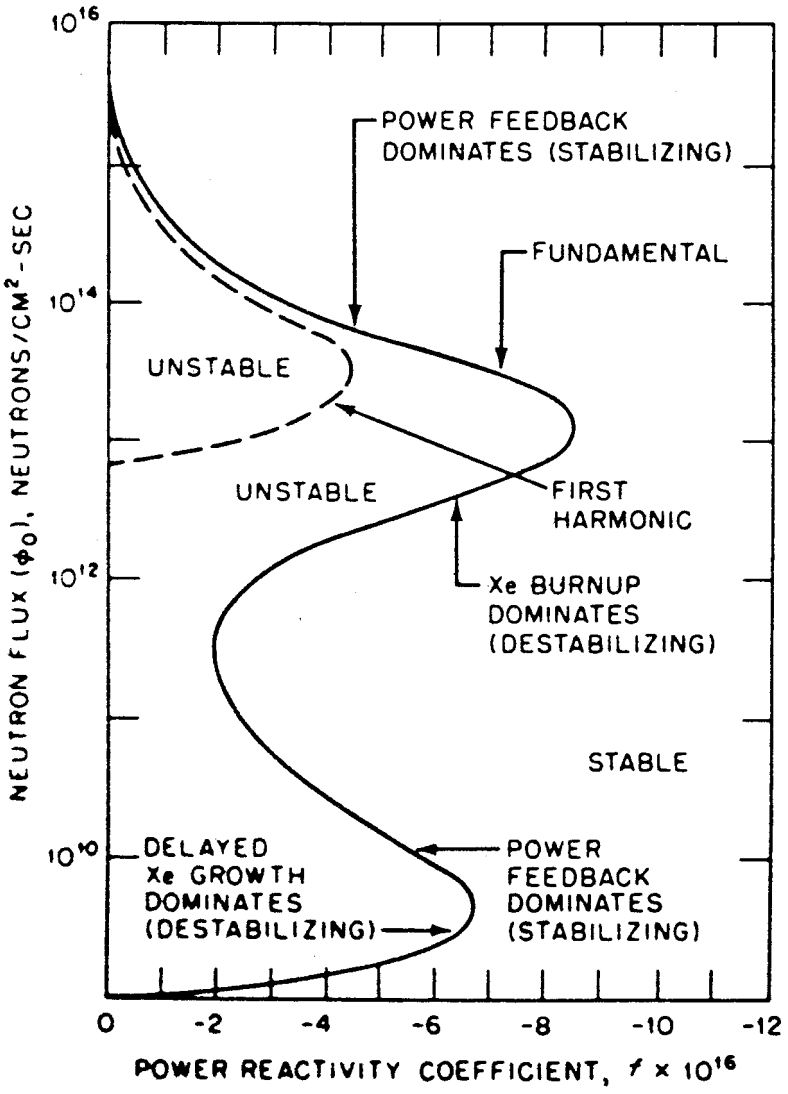

FIG. 10.8 CALCULATED DEPENDENCE OF NEUTRON FLUX VS POWER REACTIVITY COEFFICIENT FOR NEUTRAL STABILITY DUE TO XENON-135 (AFTER J. CANOSA AND H. BROOKS, REF. 35).

than 10^9 neutrons/cm^2-sec, the system is stable against xenon-135, regardless of the (negative) value of the power feedback coefficient. At such low values of the flux, the rate of burnup of xenon-135 by neutron absorption is relatively small and the situation in the reactor is not affected significantly by the delayed formation of this nuclide by the decay of iodine-135. It is instructive to consider how the situation changes as the flux level is increased with a fixed feedback coefficient.

At somewhat higher flux levels than those just considered, the fundamental mode becomes unstable and the critical value of the flux for instability is relatively insensitive to the power feedback, f, over a considerable range. In this region, the destabilizing mechanism is the delayed growth of the xenon-135. At still higher fluxes, i.e., above about 3×10^9 neutrons/cm^2-sec in Fig. 10.8, the power feedback begins to stabilize the system, and in the absence of xenon-135 burnup, the system would be stable at high flux levels. At fluxes greater than about 2×10^{11} neutrons/cm^2-sec for the given system, however, burnup of xenon-135 becomes an important destabilizing influence; it is not overcome by the power feedback until the flux is around 10^{13} neutrons/cm^2-sec. At flux levels above 10^{15} neutrons/cm^2-sec, which do not exist in ordinary thermal reactors, the system would again be stable.

In addition, the possibility of exciting the first harmonic, i.e., $n = 1$, mode should be considered. This mode is readily stabilized by the power coefficient until the flux is fairly high, namely, almost 10^{13} neutrons/cm^2-sec in the case under consideration. Instability can then arise, just as it does for the fundamental mode at lower flux levels, from burnup of xenon-135. The harmonic is always harder to excite than the fundamental; that is to say, for a given value of the power feedback coefficient, a higher neutron flux is required for the harmonic than for the fundamental mode. Thus, the curve of neutral stability for the first harmonic lies to the left of the one for the fundamental; the broken curve in Fig. 10.8, for example, refers to a particular case in which $\sigma_a a^2/D = 1500$. It should be noted that since n appears with $1/a$ in the term $n\pi/a$ in the equations given above, the spatial oscillations for a given n are easier to excite when a is large, i.e., for a large reactor. For a specified reactor, higher harmonics, with $n \geq 2$, are even harder to excite than the first harmonic.

It might appear at first sight that whenever a reactor is stable in the fundamental mode there would be no need to be concerned about exciting the harmonics, but this is not necessarily the case. The first harmonic can be excited in a large, high-flux reactor by a combination of circumstances involving the locations of control rods and neutron (or power) detectors. Suppose that the control rods are at the bottom of the core whereas the detectors are at the top. Insertion of the rods to compensate for an increase in the already high neutron flux will then not prevent the flux from increasing still further where the detectors are located. In this way the conditions for excitation of the first harmonic mode might be realized.

The neutron flux (or power) oscillation period, corresponding to ω of the fundamental mode for neutral stability, is given in Fig. 10.9 as a function of the steady-state flux for a particular reactor.[36] At low fluxes, where delayed growth of xenon-135 is the dominant factor, the periods are long, but they decrease with increasing flux because of the growing importance of the (prompt) power feedback. At a flux level in the vicinity of 2×10^{11} neutrons/cm^2-sec where, as seen above, the effect of xenon-135 burnup becomes important, the periods start to increase again. Then when the flux is greater than some 10^{13} neutrons/cm^2-sec, the power feedback once more becomes dominant and the oscillation periods steadily decrease in length.

Although the model on which the foregoing conclusions are based represents a marked simplification, it embodies the physical effects which are important in determining the conditions under which oscillations due to xenon-135 can occur. Hence, it has proved useful in the analysis and control of the oscillations.

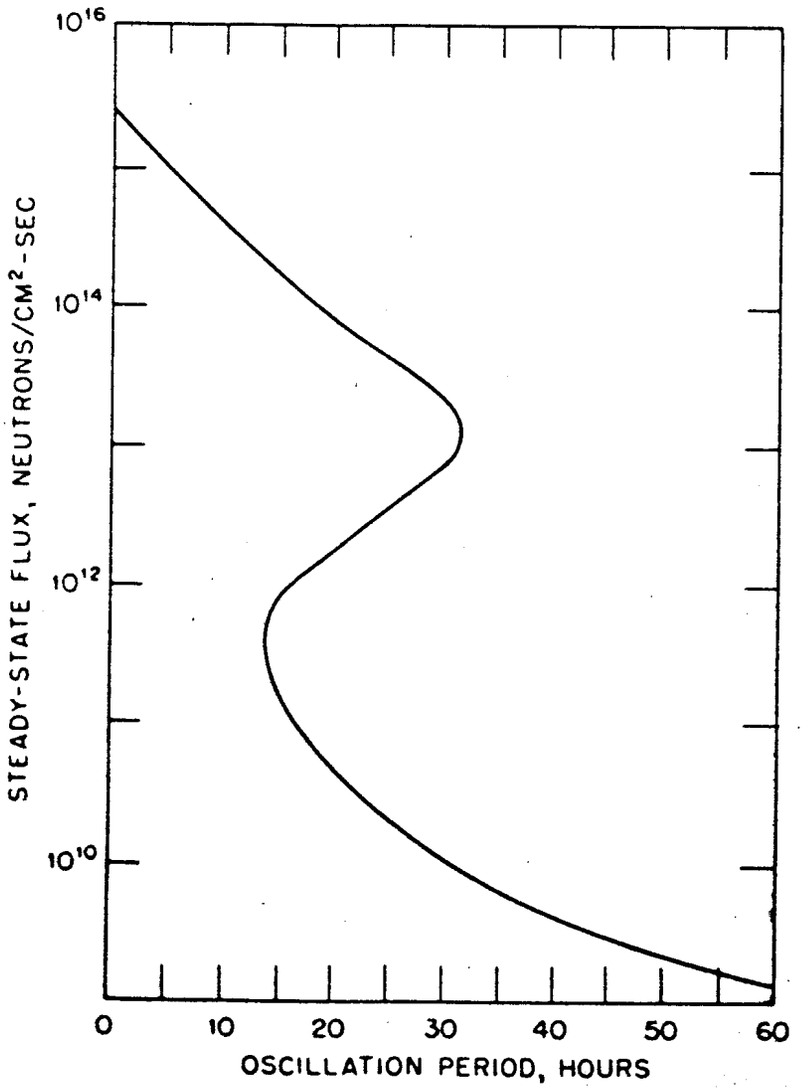

FIG. 10.9 XENON OSCILLATION PERIOD FOR VARIOUS VALUES OF THE STEADY-STATE FLUX (AFTER J. CANOSA AND H. BROOKS, REF. 35).

If the (negative) power coefficient of reactivity is large enough, troublesome oscillations (or instabilities) will not occur for any reasonable values of the operating flux. For safety reasons, however, additional negative feedback is always provided by the control-rod system.

The theory used to derive the results described above is based on the linearized equations (10.42), (10.43), and (10.44); hence, it cannot predict the behavior for oscillations of large amplitude. Such oscillations would, of course, be very undesirable in a reactor and the main purpose of the treatment is to indicate how they may be avoided.

Because the xenon-induced oscillation periods are quite long, they can be readily controlled. Power (or neutron flux) detectors are distributed throughout the reactor in order that local changes may be observed; they can then be quickly compensated for by the motion of appropriate control rods. Thus significant oscillations can be avoided even apart from the effect of the power feedback.

10.2 BURNUP PROBLEMS

10.2a Introduction

Another aspect of reactor dynamics is concerned with the long-term changes in the isotopic composition of the fuel, caused by exposure to the neutron flux under various conditions of reactor operation. These changes, in both time and space, have an important bearing on the operating life of a reactor core and hence, on the reactor economics. In addition, they affect the stability and control of a reactor. Consequently, such changes must be taken into consideration in the design of a reactor system. The term "burnup problems" has been commonly used to describe the theoretical treatment of the changes in the fuel and their effects on the reactor characteristics. Two burnup problems of special interest will be treated in this section, namely, fuel depletion and burnable poisons.

During operation of a reactor, the fissile nuclides are consumed by fission and about two hundred fission products are formed, some directly and others by radioactive decay. A number of these fission products have high or moderately high cross sections for neutron capture; they consequently have a significant influence on the neutron economy (and reactivity) of the system. Furthermore, the conversion of fertile to fissile nuclides has, of course, an important effect on reactor lifetime and control.

In addition, radiative capture of neutrons by both fissile and fertile species leads to the formation of such nuclides as uranium-236, plutonium-240, uranium-239, and so on. These can also capture neutrons or suffer beta decay (or both), so that many new heavy isotopes (or heavy nuclides), i.e., isotopes of thorium, protactinium, uranium, neptunium, plutonium, etc., are present in the fuel after a period of reactor operation.[37]

A complete treatment of fuel burnup would require a knowledge of the cross sections of all the fission products (as well as their yields and radioactive decay constants) and of the heavy isotopes. In principle, the neutron transport equation could then be solved for the conditions existing at various times. In practice, however, this is not possible, partly because of the lack of data and partly because of the excessive time that would be required to make the calculations, even with a fast computer. Consequently, a number of gross simplifications are made; although the results are not highly accurate, they nevertheless provide useful general predictions of reactor behavior, as will be seen.

In order to reduce the number of nuclides that need to be included specifically in a burnup calculation, two general principles are helpful. First, the only fission products treated explicitly are those with particularly large capture cross sections. In practice, this means that, for thermal reactors, the great majority of fission products are lumped into one or a few classes, to each of which is ascribed an average cross section. Xenon-135 and samarium-149 are always considered individually in thermal reactors; a dozen or so others, with fairly large cross sections, may also be included in this manner in an accurate burnup study.[38] In a fast-reactor neutron spectrum there are no exceptionally large cross sections, and so all the fission products can be treated as one or a few classes with average cross sections.

The second principle, which is useful in reducing the number of heavy nuclides that must be included, is that any nuclide with a very short half-life can be omitted from the burnup calculations; formally, in the equations given below, such nuclides may be given a zero half-life. For example, uranium-239, with a half-life of 23.5 minutes does not need to be considered. Consequently, the only heavy nuclides usually treated in burnup problems are the following: uranium-235, -236, and -238, and plutonium-239, -240, -241, and -242 in reactors using natural uranium or uranium slightly enriched in uranium-235 as the fuel; and uranium-233, -234, -235, -236, protactinium-233, and thorium-232 in reactors containing thorium-232 as fertile material.

In some reactors, the introduction of a neutron poison, such as boron-10, which is consumed during the operation, can increase the core life. Since the cross sections of such a burnable poison are usually well known, this substance can be treated explicitly.

The nuclides mentioned above are those which are important in determining the neutron economy of the reactor. In addition, there may be other nuclides that are of interest for other reasons. For example, in a natural uranium reactor, it may be desired to follow the buildup of neptunium-237 and plutonium-238, since the latter is a useful isotopic power source. Another possibility is that the amount of a particular fission product may be required as a radiochemical indicator of the number of fissions that have occurred in a spent fuel element. Hence, the nuclides included specifically in a burnup calculation may frequently exceed those dictated by neutronic considerations alone.

10.2b The Burnup Equations

The fissile and fertile nuclides, fission products, heavy isotopes, and burnable poisons can be treated from a uniform point of view in a burnup calculation. Thus, let $N_i(\mathbf{r}, t)$ be the number of nuclei per unit volume (or concentration) of some nuclide, indicated by i. Then the rate at which N_i changes with time may be written as

$$\frac{dN_i}{dt} = \text{Formation Rate} - \text{Destruction Rate} - \text{Decay Rate}. \quad (10.45)$$

For simplicity, the nuclides may be considered to be formed and lost only as a result of fission, neutron capture, and radioactive (negative beta) decay. The various rates in equation (10.45) can then be expressed in the following manner.

Let N_{i-1} denote the concentration of nuclides which can be converted into type i by neutron capture; that is to say, if i denotes a nuclide with mass and atomic numbers (A, Z), then $i - 1$ implies the nuclide $(A - 1, Z)$. Similarly, let $N_{i'}$ be the concentration of nuclei which yield those of type i by negative beta decay, i.e., with the composition $(A, Z - 1)$; the decay constant for these nuclides is represented by $\lambda_{i'}$. Finally, let N_f be the concentration of fissile and fissionable nuclides, and let $\gamma_{fi}(E)$ be the probability that a type-i nuclide will be formed as a fission product by absorption of a neutron of energy E by a nuclide of type j. If the nuclide of type i is not a fission product then γ_{fi} is zero.

With the foregoing definitions, and others which are self-evident, equation (10.45) may be expressed as

$$\frac{dN_i}{dt} = \sum_j \overline{\gamma_{fi}\sigma_{f,j}} N_j\phi + \bar{\sigma}_{\gamma,i-1}N_{i-1}\phi + \lambda_{i'}N_{i'} - \bar{\sigma}_{f,i}N_i\phi - \bar{\sigma}_{\gamma,i}N_i\phi - \lambda_i N_i, \quad (10.46)$$

where the quantities with bars over them are averages which are defined below.

The first term on the right of equation (10.46) gives the rate of formation of nuclides of type i resulting from fission of nuclides of type j, i.e.,

$$\overline{\gamma_{fi}\sigma_{f,j}} N_j\phi = \int_0^\infty \gamma_{fi}(E)\hat{\sigma}_{f,j}(E)N_j(\mathbf{r}, t)\phi(\mathbf{r}, E, t)\, dE, \quad (10.47)$$

where $\hat{\sigma}_{f,j}(E)$ is the microscopic fission cross section of type j nuclei for neutrons of energy E. If $\phi(\mathbf{r}, t)$ is defined by

$$\phi(\mathbf{r}, t) \equiv \int_0^\infty \phi(\mathbf{r}, E, t)\, dE,$$

then from equation (10.47)

$$\overline{\gamma_{fi}\sigma_{f,j}} = \frac{\int_0^\infty \gamma_{fi}(E)\hat{\sigma}_{f,j}(E)\phi(\mathbf{r}, E, t)\, dE}{\phi(\mathbf{r}, t)}. \quad (10.48)$$

This quantity can be computed as a function of $\mathbf{r}$ and t, provided the neutron flux and the required fission cross sections and fission yield data are available. It will be independent of time if the neutron energy spectrum does not change with time.

The second term in equation (10.46) represents the rate of formation of nuclei of type i by neutron capture in the nuclei of type $i - 1$; thus,

$$\bar{\sigma}_{\gamma,i-1}\phi = \int_0^\infty \hat{\sigma}_{\gamma,i-1}(E)\phi(\mathbf{r}, E, t)\, dE, \tag{10.49}$$

where $\hat{\sigma}_{\gamma,i-1}(E)$ is the microscopic radiative capture cross section for nuclei of type $i - 1$ for neutrons of energy E.

The third term in equation (10.46) is simply the rate of radioactive decay as a result of which nuclides of type i are formed. The fourth term is the rate of destruction of these nuclides by fission, so that

$$\bar{\sigma}_{f,i}\phi = \int \hat{\sigma}_{f,i}(E)\phi(\mathbf{r}, E, t)\, dE,$$

where $\hat{\sigma}_{f,i}(E)$ is again a microscopic cross section. The fifth term is the rate of loss of type-i nuclei as a result of neutron capture and is equivalent to equation (10.49) with i replacing $i - 1$. Finally, the last term is the radioactive decay rate of the nuclei of type i.

In general, at each point in the reactor space mesh there will be an equation (10.46) for every kind of nuclide which is to be followed in a fuel burnup calculation. The resulting differential equations are all coupled together through various formation and destruction processes. In practice, simplifications are made in setting up the equations, as indicated earlier, i.e., by using a small number of fission-product classes and restricting the heavy isotopes that are taken into consideration.

10.2c Solution of the Burnup Equations

The N_i values of all the nuclides included in the calculations will affect the neutron flux, through the neutron transport problem, in a complicated manner. Suppose, however, that the neutron flux is computed at time t, and suppose, furthermore, that the flux can be assumed to remain constant for a substantial time period, Δt, after time t. The coefficients in the differential equations for all the nuclide concentrations could then be calculated and assumed to remain constant from t to $t + \Delta t$. The resulting system of burnup (or depletion) equations can be solved by standard numerical integration techniques, e.g., by the Runge-Kutta method,[39] and thus the values of N_i at $t + \Delta t$ could be found. With the N_i known for all values of i at time $t + \Delta t$, the calculation could be advanced to time $t + \Delta t$ by recomputing the flux at this time, and so on.

Another procedure for solving the burnup equations can be developed by regarding N_i as the ith component of a vector $\mathbf{N}$. Equation (10.46), for $i = 1, 2, \ldots, I$, could then be written as

$$\frac{d\mathbf{N}}{dt} = \mathbf{M}\mathbf{N},$$

where $\mathbf{M}$ is a $I \times I$ square matrix with constant components over the time interval t to $t + \Delta t$. Formally, the solution is

$$\mathbf{N}(t + \Delta t) = e^{\mathbf{M}\,\Delta t}\mathbf{N}(t)$$

and in order to derive $\mathbf{N}(t + \Delta t)$ from $\mathbf{N}(t)$ it is necessary to evaluate the exponential of the matrix $\mathbf{M}\,\Delta t$. One possibility is by way of a power series expansion; thus,

$$e^{\mathbf{M}\,\Delta t} = 1 + \mathbf{M}\,\Delta t + \tfrac{1}{2}(\mathbf{M}\,\Delta t)^2 + \cdots.$$

Some preliminary studies have indicated that refinements of this approach are promising methods of solving the burnup equations.[40]

In some instances, e.g., for systems having only one significant fissile (or fissionable) nuclide, it may be fruitful to rewrite the depletion equations so that each type of nuclide can be formed in only one way. This is always possible, for example, by regarding nuclides of type i formed by neutron capture as completely distinct from the same nuclides resulting from beta decay. Under these conditions, an exact solution can be found at time $t + \Delta t$ in terms of the solution at time t, although, as in the other methods, a computer must be used.[41]

No matter which of the foregoing procedures is employed to solve the burnup equations, the values of N_i are advanced in a series of time intervals Δt during each of which the neutron flux is assumed to remain constant. The procedure is repeated until it has been carried far enough in time. It is reasonable to suppose that accurate solutions can be obtained provided that the Δt are chosen to be sufficiently small for the required purpose; the accuracy can be assessed by noting the variations in the solutions that result from changing, e.g., doubling or halving, the intervals Δt. In long-range burnup calculations, the intervals may be of the order of weeks, or even months, provided it is not desired to follow transients involving nuclides of short life, in particular xenon-135 and iodine-135.

For the solution of the burnup problem it is necessary, as seen above, to compute the flux $\phi(\mathbf{r}, E, t)$ for the operating (critical) reactor at various times. In this calculation, the geometry and composition of the system, as specified by the values of $N_i(\mathbf{r}, t)$, are to be regarded as known. It might be thought, therefore, that the flux could be obtained from a standard k eigenvalue calculation, i.e., using the adiabatic approximation (§9.2c). A difficulty arises, however, because in the operating reactor criticality is maintained by adjusting the control rods. Consequently, in the flux calculation, criticality should, in principle, also be achieved by varying the position or amount of control poison.[42]

Such adjustment of control poison in the calculation suffers from certain drawbacks. In the first place, it is complicated to include control rods explicitly in the flux calculation, and, furthermore, a small error in the prediction of criticality can lead to a large error in the prediction of control rod position. Consequently, the control poison is often treated quite approximately in the flux calculations. For example, the rods may be represented by a uniform distribution of poison in the amount required to give a critical system. As the fuel is depleted, the quantity of control poison is reduced in such a way as to maintain criticality until there is no (or very little) poison remaining at the end of the core life. An alternative procedure is to limit the poison to those general regions of the core where the control rods are located. Then, as the fuel is depleted, the volumes of these regions are decreased, to correspond to withdrawal of the rods, so as to maintain criticality.

In the flux calculation at any time, therefore, the amount of control poison is adjusted in an appropriate manner in order to keep the system in the critical state. Since the flux is spatially dependent, the calculations should be in three-dimensional geometry. If the core can be approximated as a finite cylinder, as is often the case, then a two-dimensional treatment will suffice. For preliminary or general burnup studies, one-dimensional or even point models of the reactor core are often useful; however, for the analysis of an operating reactor a more detailed treatment of the geometry is required.

Because of the difficulty of making such flux calculations and the necessity for repeating them for several (or many) times, it is necessary that the neutron transport calculations be as simple as possible. Hence, a few-group P_1 or diffusion approximation is generally used for determining the gross flux and, in addition, various syntheses or variational methods (§6.4j) can be employed to reduce the dimensionality of the neutron transport equation. Another simplification is to minimize the number of mesh points in the calculation by dividing the reactor core into a relatively small number of zones in each of which the N_i values are assumed to have a uniform spatial distribution.

The burnup calculations described above have referred to the gross behavior of the system without regard to fine structure. Frequently, however, it is required to follow changes with time of such parameters as the concentration of fissile nuclides, heavy-isotope production, specific power, etc., in individual fuel elements and even of their spatial variations within specific elements. If the fuel elements have a simple periodic arrangement in the core then cell calculations will suffice to give the flux, and hence burnup characteristics, within a given fuel element and cell. The nuclear constants for the gross flux calculation are adjusted so that the gross (or over-all) reaction rates for a homogenized system are the same as for the individual cells (§3.6a). If, however, the arrangement of the fuel elements is complex, then a Monte Carlo calculation must be used.

The effect of heterogeneity on fuel burnup has been examined in some detail in connection with studies of the use of recycled, i.e., recovered, plutonium-239

as the fissile species, together with uranium-238 as the fertile material, in water-moderated reactors.[43] It was shown, for example, by using Monte Carlo techniques, that a higher burnup, i.e., a longer core life, can be achieved if the fuel element consists of a thin central "tight pencil" of plutonium (as dioxide) surrounded by the uranium-238 (as dioxide) than if the plutonium is mixed uniformly with the uranium.

Another problem in connection with the fine structure of the neutron flux is that in the vicinity of a control rod. The depression of the flux in such a region reduces the local fuel burnup and the extent of the depression changes during reactor operation as the rod insertion is adjusted. Accurate transport or Monte Carlo calculations may be used to determine the flux (and burnup) in the vicinity of a control rod.

10.2d Results of Burnup Calculations

The best test of burnup calculations is to compare the results for the concentrations of various nuclides with those actually found in spent fuel elements. Such comparisons have been made for the Yankee[44] and Shippingport[45] pressurized-water reactors, and reasonably good agreement was found between computed and observed heavy nuclide concentration ratios. Similar comparisons have been made for a number of other reactors.[46]

Some interesting data will be presented here from a simplified burnup calculation made with the FUELCYC code[47]; this is based on a modified two-group diffusion theory and finite cylindrical (two-dimensional) geometry. Seven mesh points were used in both axial and radial directions. No allowance was made for the heterogeneous structure of the core, and plutonium resonances were treated in an approximate manner. Although the computations were performed for reactors of different types, the results presented here were obtained for a pressurized-water reactor, about 2 meters in length and diameter, using uranium fuel with an initial enrichment of 3.44 atomic percent of uranium-235 and operating at a thermal power of 480 MW.[48]

First, Fig. 10.10 shows the atomic percentages of various heavy nuclides in the fuel as a function of exposure time in the reactor, expressed as the neutron fluence, also referred to as the integrated flux or flux-time, in neutrons/cm^2. These are the kind of data that can be most readily checked by actual analysis of spent (or partially spent) fuel elements, as mentioned above.

The initial spatial distribution of the power density, in one quadrant of the reactor, for a uniform fuel loading, is indicated in Fig. 10.11. Because of the approximately cosine distribution of the neutron flux in both radial and axial directions, the maximum power density is found at the center of the core. After an average burnup of 23,000 MW-days/tonne,* the calculated spatial power

* A tonne (or metric ton) is 1000 kg or 2205 lb.

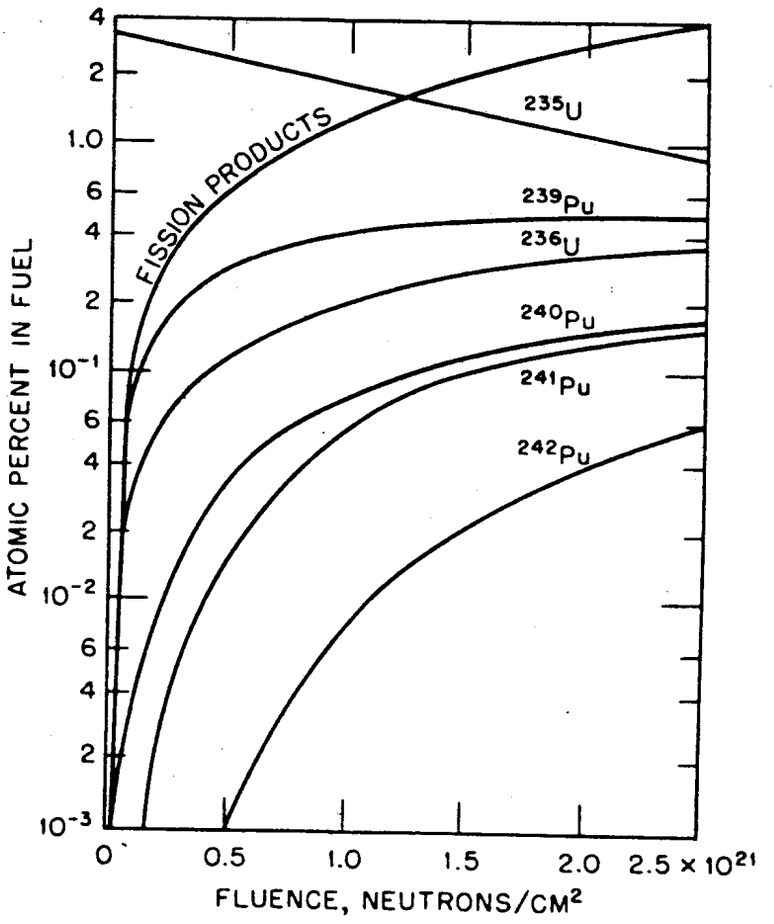

FIG. 10.10 CHANGE IN FUEL COMPOSITION VS NEUTRON FLUENCE (AFTER M. BENEDICT, *ET AL.*, REF. 48).

density distribution is as shown in Fig. 10.12; it is seen that the power density distribution is flatter, i.e., more uniform, than initially and that the maximum has moved well away from the center of the core. The reason for this change is the high burnup of the fuel at the center. This burnup also causes a depression in the central flux; the power density, which depends on the product of the neutron flux and the concentration of fissile species, consequently decreases both because of the burnup itself and the flux depression.

The data in Figs. 10.11 and 10.12 apply to what is called "batch" loading; that is to say, the core is loaded with fuel uniformly at the beginning of operation and no deliberate changes are made during operation. In the calculations criticality is maintained by assuming a uniformly distributed poison which is consumed as the reactor operates.

Another method of core loading (or fuel management) is "out-in" fueling; fresh fuel elements are introduced from the periphery of the core and are moved radially inward with the spent elements being discharged at the axis. In practice, as in the UHTREX reactor,[49] the fuel elements would be moved periodically, but for purposes of calculation the motion is treated as taking place continuously

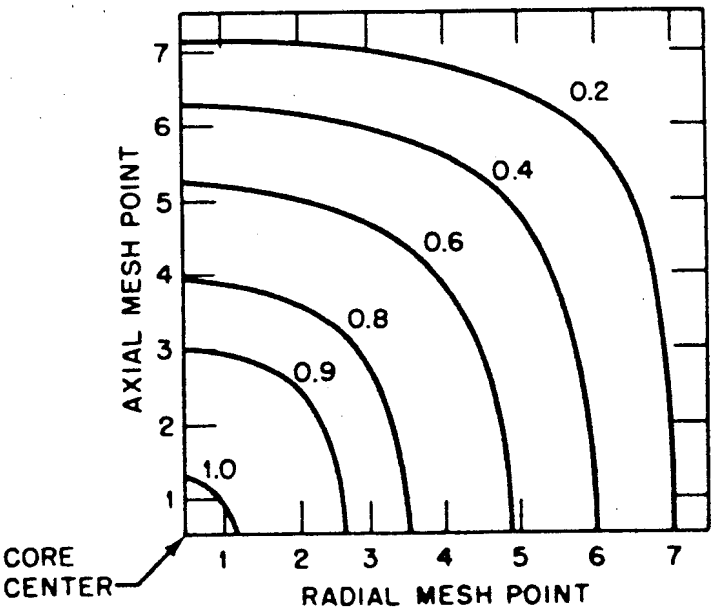

FIG. 10.11 INITIAL CALCULATED SPATIAL POWER DENSITY DISTRIBUTION IN ONE QUADRANT OF REACTOR FOR UNIFORM FUEL LOADING (AFTER M. BENEDICT, *ET AL.*, REF. 48).

at such a rate that the spatial distributions of nuclide concentrations and neutron flux, and hence of power density, remain constant in time, once a steady state has been achieved. The computed (time independent) spatial distribution of the power density in Fig. 10.13 is based on an average burnup of 23,000 MW-days/tonne in the discharge fuel. The "out-in" loading is seen to give a fairly flat radial power distribution at all times, once the steady state has been attained.

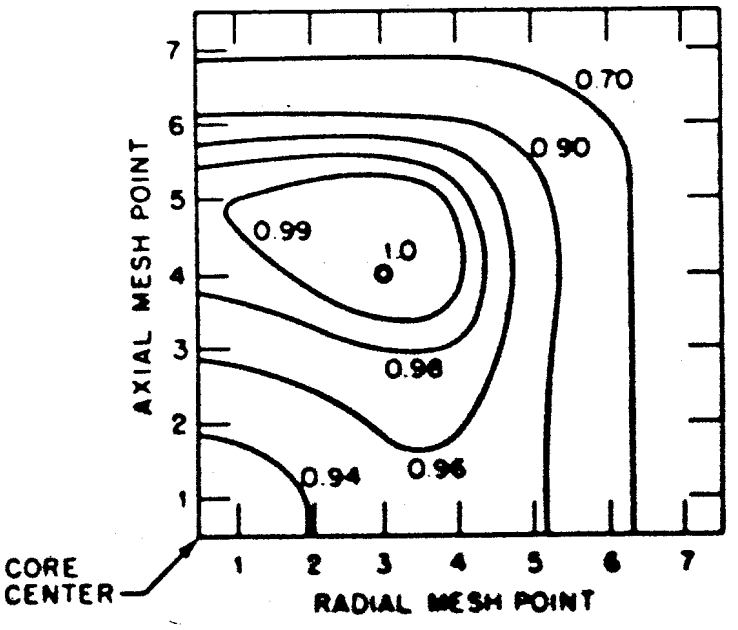

FIG. 10.12 CALCULATED SPATIAL POWER DENSITY DISTRIBUTION AFTER AVERAGE BURNUP OF 23,000 MW-DAYS/TONNE (AFTER M. BENEDICT, *ET AL.*, REF. 48).

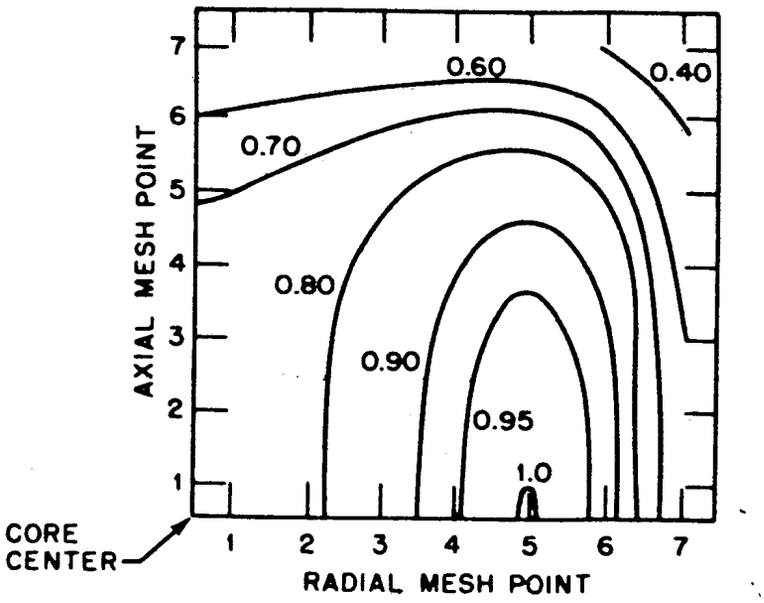

FIG. 10.13 CALCULATED (STEADY-STATE) SPATIAL POWER DENSITY DISTRIBUTION FOR "OUT-IN" FUEL LOADING (AFTER M. BENEDICT, *ET AL.*, REF. 48).

A third fuel-loading strategy is the "bidirectional-axial" method, which is essentially that used in the CANDU (heavy water moderated) reactor.[50] Fresh fuel elements are inserted and spent elements are discharged "continuously" in an axial direction, but the elements in adjacent channels move in opposite directions. The discharge rate in any particular channel varies with its distance from the axis in such a manner that all fuel elements have received the same burnup upon discharge. As in the preceding case, it is assumed that the power density distribution remains unchanged after a steady state has been attained. In bidirectional-axial fueling, the power density distribution is symmetrical about the (radial) midplane.

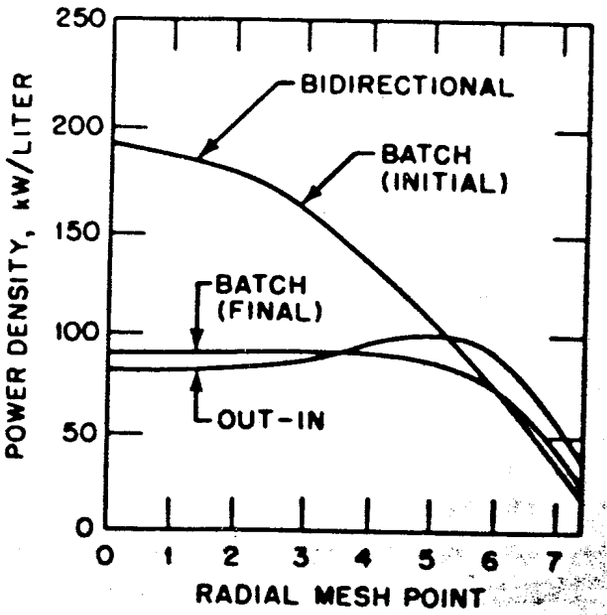

FIG. 10.14 RADIAL POWER DENSITY DISTRIBUTION AT REACTOR MIDPLANE FOR BATCH, BIDIRECTIONAL, AND "OUT-IN" FUEL LOADING; AVERAGE BURNUP 23,000 MW-DAYS/TONNE IN EACH CASE (AFTER M. BENEDICT, *ET AL.*, REF. 48).

The radial power density distributions at the midplane for the three methods of fuel management described here are compared in Fig. 10.14 for a final average burnup of 23,000 MW-days/tonne in each case. For batch loading there are two curves, representing the beginning and end of core life, respectively; thus, the actual power distribution changes during operation of the reactor. For the other two fueling methods, the distribution remains constant. The radial power density distribution for bidirectional-axial fueling is seen to be essentially identical with the initial distribution for batch loading, and much the same is true for the axial distribution. An advantage of the bidirectional procedure, however, is that it gives uniform burnup of the fuel which batch loading does not. If the core life is limited by the maximum burnup in any fuel element, the life of the reactor would thus be significantly shorter for batch loading. Another advantage of bidirectional loading is that it provides better neutron economy since, in principle, no neutrons are wasted by capture in control poisons during steady-state operation.

10.2e The Breeding (or Conversion) Ratio

One of the most important quantities to be obtained from a reactor burnup calculation is the *breeding ratio* or the *conversion ratio* and its variation with time. These ratios are usually defined as the number of fissile nuclides produced in a given time, by capture of neutrons in fertile nuclei, divided by the number of fissile nuclides destroyed in the same time. The ratio is commonly called a conversion ratio if it is less than unity and a breeding ratio if it is greater than unity.

Consider, for example, a fast breeder reactor using a mixture of enriched uranium and recycled plutonium as fuel. In these circumstances, uranium-235, plutonium-239, and plutonium-241 would probably be regarded as the fissile nuclides and uranium-238 and plutonium-240 as the fertile species. The breeding ratio (B.R.) would then be defined by

$$\text{B.R.} = \frac{\text{Formation rate of } {}^{239}\text{Pu} + {}^{241}\text{Pu}}{\text{Destruction rate of } {}^{235}\text{U} + {}^{239}\text{Pu} + {}^{241}\text{Pu}}.$$

Nuclides present in small amounts could be included on the basis of whether they may be regarded as being "fissile" or not. The formation and destruction rates required for deriving the breeding ratio can be readily computed as functions of time in a normal burnup calculation.

The foregoing definition of the breeding ratio (or conversion ratio) is somewhat arbitrary and in a study of fuel cycle economics it is necessary to know the actual expected abundances of all the fissile nuclides in the discharged fuel. Nevertheless, the breeding (or conversion) ratio, as defined above, is a convenient

way of summarizing the manner in which the inventory of fissile species in a reactor is changing.

10.2f Burnable Poisons

Apart from fuel management (and mechanical) considerations, the useful life of a reactor core is often determined by the excess (or built-in) reactivity available at startup. This excess reactivity is then compensated by poison control rods which are adjusted during reactor operation as fissile material is consumed (and generated) and fission product poisons accumulate. The presence of excess reactivity, however, has some drawbacks; for example, accidental loss of control function could lead to a hazardous situation. Furthermore, the neutron flux in the vicinity of control rods is depressed, and hence the power density distribution and fuel burnup are uneven.

The requirement for a significant amount of excess reactivity does not arise in a large converter reactor which can be designed for efficient conversion of fertile into fissile nuclei. Thus, the latter may be replaced almost as fast as they are consumed. In fact, the reactivity of a large natural-uranium, graphite-moderated reactor increases for some time during the early stages of operation (§10.3f). For small reactors, however, the conversion is relatively small, partly because of the loss of neutrons by leakage and partly because it is not possible to include an adequate quantity of fertile material in the core. The drawbacks associated with excess reactivity can then be largely avoided by the use of a burnable poison.[51]

A *burnable poison* is a nuclide with a high (or moderately high) cross section for neutron absorption, with the absorption product having a small neutron cross section. It may be distributed uniformly throughout the core, or it may be in the form of lumps. Ideally, the amount of burnable poison should be such as to compensate for almost the whole excess reactivity at startup. Then, as the reactor operates, the poison should be consumed at such a rate as to maintain exact criticality as the fissile material is depleted and fission product poisons are generated. This ideal may possibly be approached in some cases,[52] but even if not, burnable poisons can be used advantageously. The situation may be explained by means of an elementary example.

Consider a large thermal reactor in which only reactions of thermal neutrons need be taken into account. For simplicity, the distributions of thermal neutrons and of the various nuclides in the core are taken to be uniform. Let σ_f be the macroscopic fission cross section and σ_γ the radiative capture cross section of the fissile species; σ_b is the cross section of the burnable poison, and σ_a is the absorption cross section of other poisons present in the core. These other poisons are assumed to have small microscopic cross sections, so that σ_a remains essentially constant during reactor operation. If the poisoning effects of fission products are neglected and possible conversion of fertile into fissile material is

ignored, the infinite medium multiplication factor for the system may be expressed by

$$k_\infty = \frac{\nu\sigma_f}{\sigma_f + \sigma_\gamma + \sigma_a + \sigma_b}$$

$$= \frac{\nu\sigma_f}{(1 + \alpha)\sigma_f + \sigma_a + \sigma_b}, \tag{10.50}$$

where α is the conventional symbol for σ_γ/σ_f for the fissile nuclide and ν is the average number of neutrons produced per thermal fission.

If the uniform thermal-neutron flux at time t is $\phi(t)$, then the rate of decrease of the concentration, N_f, of fissile nuclei is

$$\frac{dN_f}{dt} = -N_f(t)\hat{\sigma}_f(1 + \alpha)\phi(t),$$

where $\hat{\sigma}_f$ is the microscopic fission cross section. Hence,

$$N_f(t) = N_f(0) \exp\left[-\int_0^t \hat{\sigma}_f(1 + \alpha)\phi(t')\,dt'\right]$$

$$= N_f(0) \exp\left[-\hat{\sigma}_f(1 + \alpha)I(t)\right], \tag{10.51}$$

where $I(t)$ is the integrated neutron flux (or fluence), defined by

$$I(t) \equiv \int_0^t \phi(t')\,dt'.$$

Since $\sigma_f(t)$ is equal to $N_f(t)\hat{\sigma}_f$, it will have the same time dependence as $N_f(t)$.

The variation of the concentration of the burnable poison nuclei, N_b, with time is given by

$$\frac{dN_b}{dt} = -N_b\hat{\sigma}_b\phi(t),$$

so that

$$N_b(t) = N_b(0) \exp\left[-\hat{\sigma}_b I(t)\right].$$

and σ_b will exhibit the same dependence on time. Hence, equation (10.50) may be written as

$$k_\infty(t) = \frac{\nu\sigma_f(0)}{(1 + \alpha)\sigma_f(0) + \sigma_a \exp\left[(1 + \alpha)\hat{\sigma}_f I(t)\right] + \sigma_b(0) \exp\left[\{-\hat{\sigma}_b + (1 + \alpha)\hat{\sigma}_f\}I(t)\right]}. \tag{10.52}$$

From this equation it is seen that without a burnable poison, i.e., with $\sigma_b(0) = 0$, the value of $k_\infty(t)$ will decrease steadily with time. If, on the other

hand, a uniform burnable poison is present with a larger microscopic absorption cross section than that of the fuel, so that

$$\hat{\sigma}_b > (1 + \alpha)\hat{\sigma}_f,$$

then $k_\infty(t)$ can increase with time for a while. The reason is that under the postulated conditions the burnable poison is consumed at a greater rate than is required to compensate for fuel depletion. Eventually, $k_\infty(t)$ will decrease as the poison is used up (or burns out). Even if $\hat{\sigma}_b$ is not greater than $(1 + \alpha)\hat{\sigma}_f$, the decrease of $k_\infty(t)$ with time is less than in the absence of a burnable poison.

The results of some more detailed calculations of the effective multiplication factor in the graphite-moderated, gas-cooled Peach Bottom reactor, which is described in §10.3a, with uniformly distributed boron-10 as burnable poison, are indicated in Fig. 10.15.[53] The thermal-neutron absorption cross section of boron-10 is larger than that of the fissile nuclides in this reactor; hence, the multiplication factor increases at first and then decreases in the course of reactor operation.

For a lifetime of 900 days, the excess reactivity required initially with no burnable poison would be almost 0.14, whereas with the uniformly distributed poison about 0.04 would suffice. In the latter case, however, the control rods would require the capability of compensating for almost 0.08 of reactivity. If the lifetime of the core is governed by the amount of reactivity available in the control rods, then the core life would be larger in the presence of the burnable poison. Thus, a control reactivity of about 0.08 would permit a lifetime of 900 days in the latter case but less than 500 days if a burnable poison is not used.

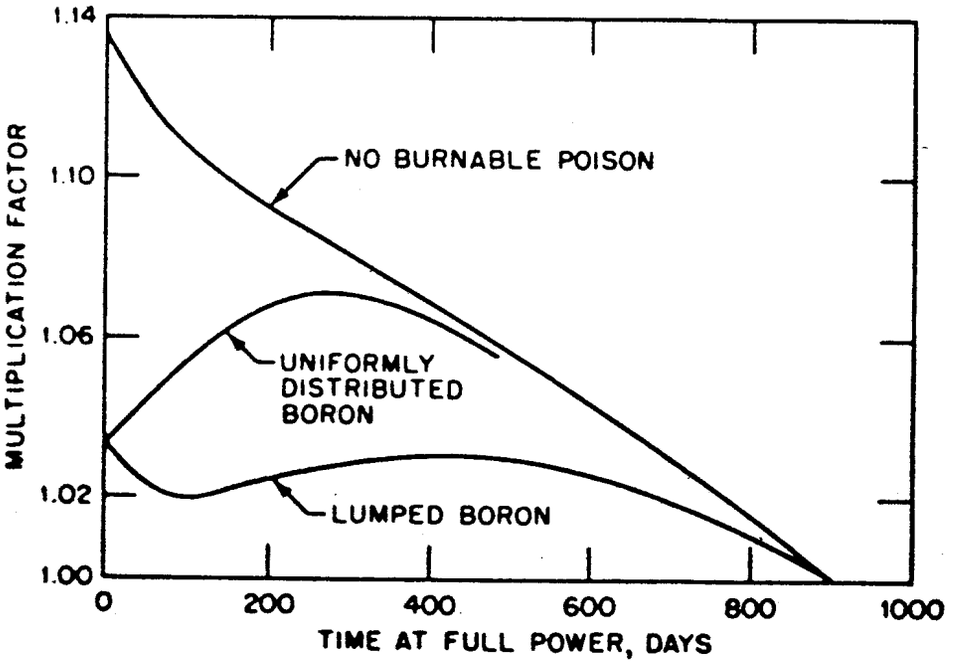

FIG. 10.15 EFFECT OF BURNABLE POISON ON THE EFFECTIVE MULTIPLICATION FACTOR FOR A HIGH-TEMPERATURE GRAPHITE REACTOR (AFTER H. B. STEWART AND M. H. MERRILL, REF. 53).

In the situation just considered, the high absorption cross section of boron-10 for thermal neutrons results in an overcompensation for the normal decrease in reactivity. This disadvantage could be overcome by using a burnable poison with a somewhat smaller cross section. An alternative procedure is to employ the boron in lumped form; the self-shielding of the inner layers of the lump by the boron-10 in the outer layers results in a decreased total absorption of neutrons. The bottom curve in Fig. 10.15 was obtained by treating the boron as lumped with an initial self-shielding factor of 0.5, i.e., the average thermal-neutron flux in the lump is half the average in the surrounding medium. In the early stages of reactor operation the reactivity now decreases. But as the boron-10 burns out and the size of the lumps decreases, the self-shielding factor increases and so also does the neutron absorption. Hence, the reactivity begins to increase and finally decreases as in the case of uniform distribution of the burnable poison. The reactor will now operate for 900 days with an initial excess reactivity of less than 0.04 and the same amount of control capability.

10.2g Flux Flattening with Burnable Poisons

Burnable poisons can also be used to flatten the spatial variation of the neutron flux and thereby to realize a more uniform burnup of the fuel. For example, by simply decreasing the need for control rods in the core, a burnable poison can

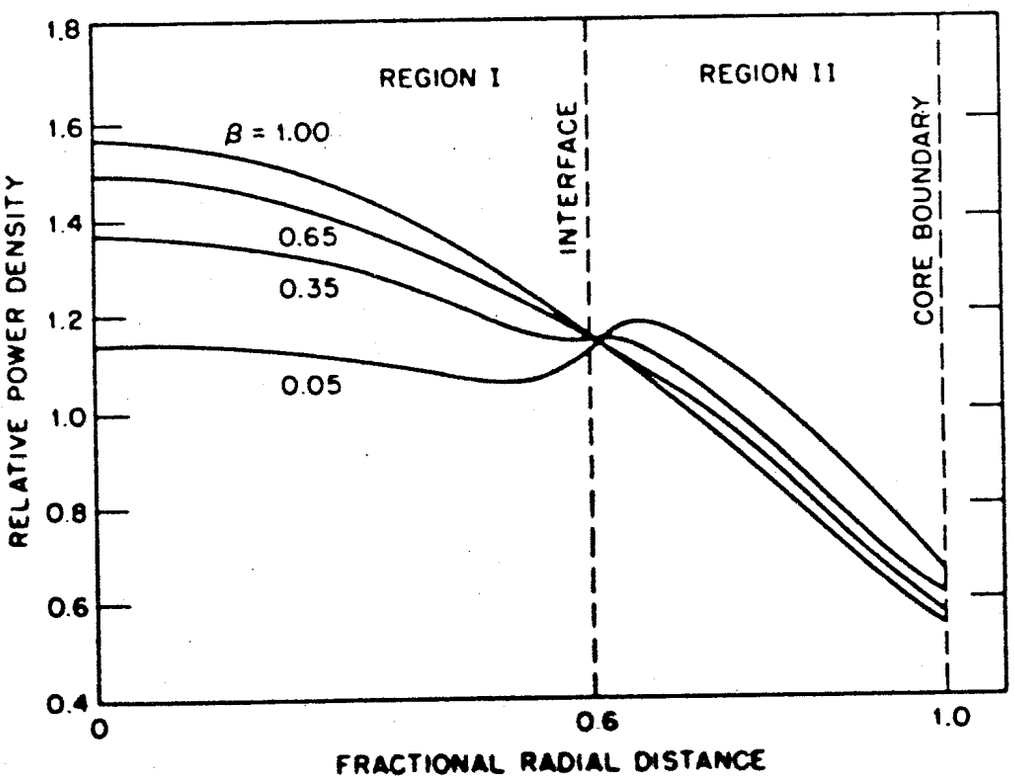

FIG. 10.16 EFFECT OF BURNABLE POISON ON RELATIVE POWER DENSITY IN A TWO-REGION CORE; β IS THE RATIO OF POISON CONCENTRATION IN OUTER (RADIAL) REGION TO THAT IN INNER REGION (AFTER REF. 54).

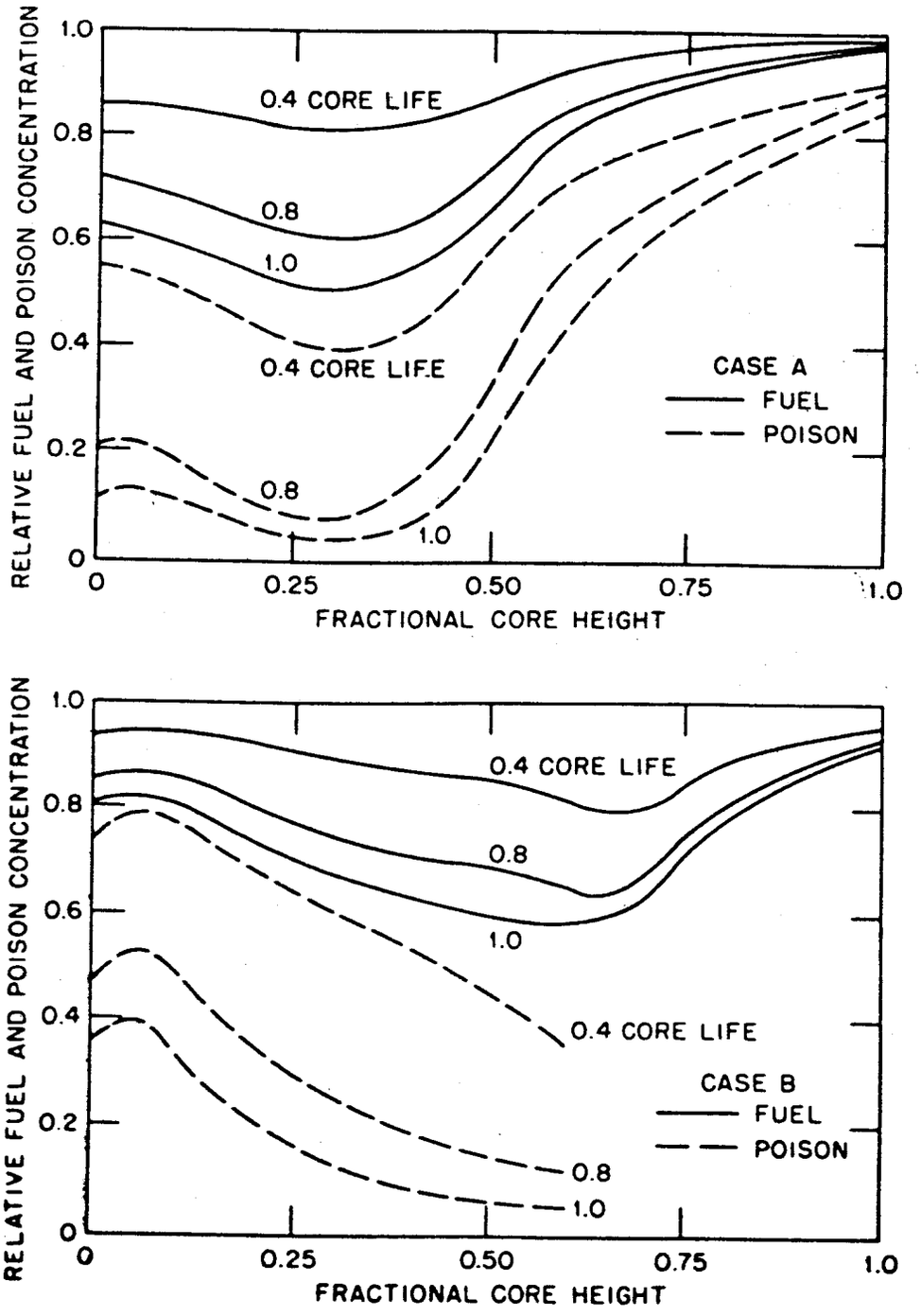

FIG. 10.17 CONSUMPTION OF FUEL AND BURNABLE POISON IN AXIAL DIRECTION AT DIFFERENT FRACTIONS OF CORE LIFE. CASE A: UNIFORM DISTRIBUTION OF POISON; CASE B: POISON EXTENDS THREE-FOURTHS UP CORE (AFTER REF. 55).

minimize the associated flux depressions and nonuniformities in power density. Moreover, it is possible to distribute the poison in such a manner throughout the core as to obtain additional flattening of the power density.

The effect of the distribution of a burnable poison is illustrated for a particular case in Fig. 10.16, which refers to a small water-moderated reactor using highly enriched uranium as the fuel.[54] The cylindrical core is divided into two radial

regions, in each of which the poison is distributed uniformly; the ratio of the poison concentration in the outer region to that in the inner region is represented by β. The curves in Fig. 10.16 show the radial variations of the power density for four values of β; for $\beta = 1$, the poison distribution is uniform throughout the core. It is evident that by having more of the poison in the inner region a substantial flattening of the power density can be achieved.

The situation in Fig. 10.16 refers to radial distributions in a core at the beginning of its life. During operation of the reactor, the power distribution will change, largely as a result of nonuniform burnup of the fuel and to motion of the control rods. It may then prove advantageous to use, in addition, a nonuniform (axial) poison distribution which will compensate for absorptions in the control rods and give both a more uniform flux and fuel burnup.

The curves in Fig. 10.17[55] show how the fuel and the burnable poison are consumed in the axial direction at various times during operation of a cylindrical reactor of the type considered above. The fuel rods are moved as a bank from the top of the reactor, so that they are all inserted to the same depth. The fractional core height in the figure represents the distance from the bottom of the core. In Case A, the burnable poison is distributed uniformly over the length of the reactor; it is seen that the fuel and poison are consumed more rapidly in the lower half of the reactor where the control rods do not penetrate. In Case B, the same amount of poison is used but it extends only three-fourths of the way up the core. The neutron flux, and hence the burnup of the fuel, is more uniform in the axial direction than in Case A.

10.3 CALCULATIONS ON GRAPHITE-MODERATED, GAS-COOLED REACTORS

10.3a Introduction

In concluding this chapter, it is of interest to consider how various static calculations described in earlier chapters may be combined to furnish the input for dynamics calculations and to determine some of the operating characteristics of power reactors. Although spatial dependence is not emphasized in any detail in what follows, the subjects considered have an important relationship to fuel burnup, and so this seems an appropriate place for the discussion given below.

Graphite-moderated, gas-cooled reactors provide an especially clear example because their operating characteristics are determined largely by the behavior of neutrons in the reactor. Consequently, it should be possible to predict such properties as temperature coefficients, based on calculations of Doppler broadening of resonances and shifts in the thermal-neutron energy spectrum. Such calculations will be considered in some detail in this section. The situation is different in water-moderated reactors where, for example, thermal expansion and possible boiling of the moderator-coolant may be the dominant factors in

reactor dynamics. The computation of such effects would require detailed engineering studies of heat transfer, coolant flow, etc., which are not treated in this book.

In discussing some of the calculations made in connection with graphite-moderated reactors, with gaseous coolants, emphasis will be placed on two particular reactors, namely, the Calder Hall (type) reactor in the United Kingdom and the Peach Bottom reactor in Pennsylvania. A brief description will first be given of these two reactors.

The Calder Hall Reactors

There are eight reactors of the Calder Hall type,[56] four at Calder Hall in England and four at Chapelcross in Scotland, designed for the dual purpose of producing both electrical power and plutonium-239. Each reactor operates at a thermal power of approximately 225 MW and generates some 50 MW of electricity. The heterogeneous core, about 9.4 meters in diameter and 6.4 meters in height, contains 1696 vertical (finned) fuel element channels arranged in a square lattice with a pitch of 20.3 cm (Fig. 10.18). The fuel rods are of natural uranium metal, 2.92 cm in diameter, canned in Magnox, a magnesium alloy. The coolant is carbon dioxide gas at a pressure of about 100 psi.

Because they are intended, in part, for the production of plutonium-239, the Calder Hall reactors have a fairly high initial conversion ratio, i.e., number of plutonium-239 nuclei formed to number of uranium-235 nuclei consumed, of around 0.85. The buildup of plutonium-239 has several interesting consequences. In the first place, the reactivity increases for a time after the reactor has been operating. Furthermore, the temperature coefficient changes with burnup, as will be seen in due course, so that the over-all isothermal coefficient becomes positive.

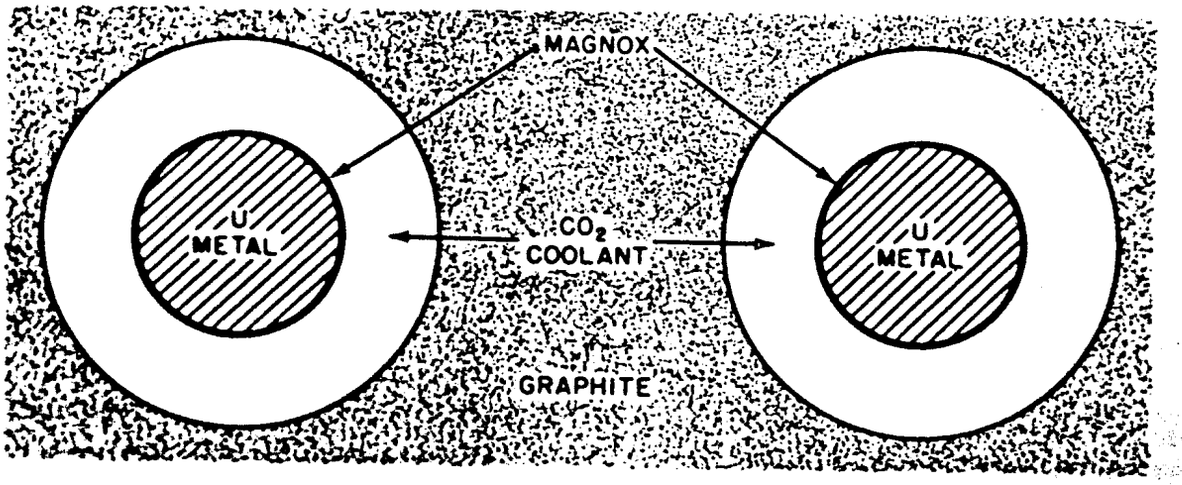

FIG. 10.18 FUEL ELEMENTS OF CALDER HALL REACTORS (LATTICE SPACING NOT TO SCALE).

When the Calder Hall reactors were designed, in the early 1950s, the nuclear data, theoretical methods, particularly computer codes for making neutron transport calculations, and the computers themselves were such that relatively little reliance could be placed on computed reactor parameters. Consequently, much use was made of integral experiments[57] and of the experience gained with the similar plutonium production reactors at Windscale. More recently, modern computational methods have been applied to the Calder Hall reactor design and the results of a unified treatment[58] of the Calder Hall and Peach Bottom reactors will be referred to later.

The Peach Bottom Reactor

The Peach Bottom reactor[59] is a small prototype HTGR (High-Temperature Gas-Cooled Reactor), producing 115 MW of heat and about 40 MW of electrical power. The moderator is graphite, the coolant is helium, and the fuel is a mixture of uranium carbide (UC_2), highly enriched (93 atomic percent) in uranium-235, and thorium carbide (ThC_2) in a graphite matrix. The core is some 2.8 meters in diameter and 2.3 meters high and is composed of a close-packed triangular lattice of fuel elements, 9 cm in diameter. The schematic cross section of a typical fuel element in Fig. 10.19 shows a graphite spine, which provides mechanical strength and also contains a trap for fission-product gases,

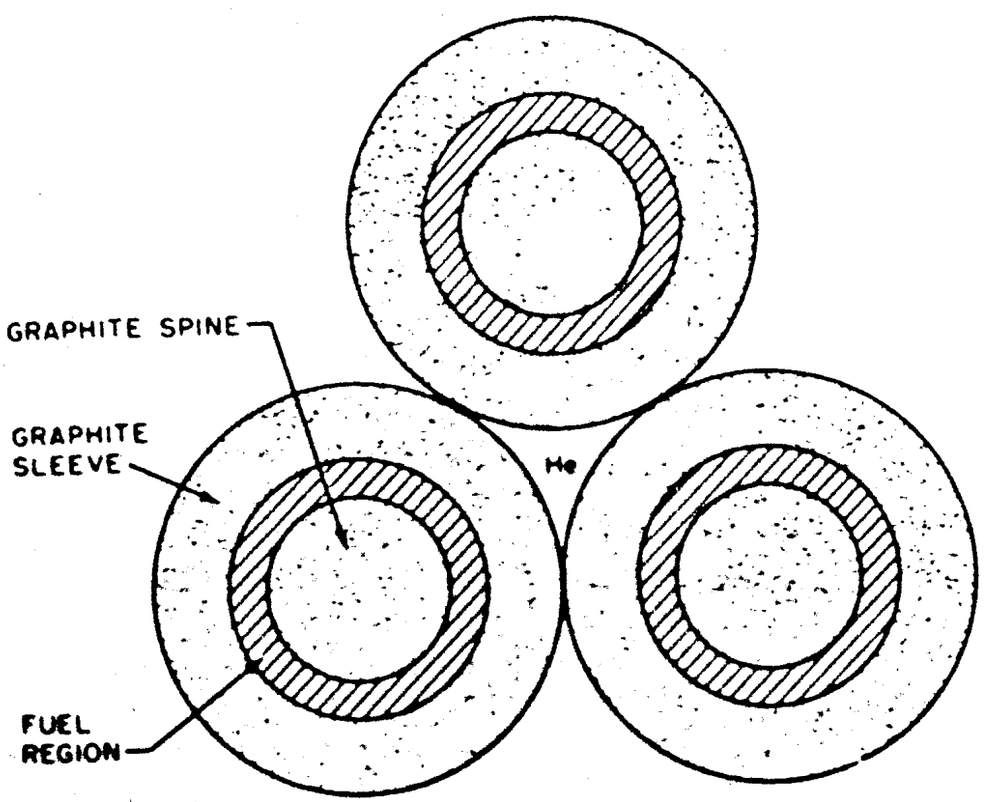

FIG. 10.19 FUEL ELEMENTS OF PEACH BOTTOM REACTOR.

surrounded by an annular fuel region and finally by a sleeve made of impervious graphite.

The reason for using thorium-232 and highly enriched uranium-235, rather than uranium of moderate or low enrichment, as fuel is that the uranium-233 produced from thorium-232 gives a better neutron economy (in a thermal reactor) and a higher conversion ratio than does plutonium-239 derived from uranium-238. For example, at a neutron energy in the vicinity of 0.1 eV, the value of η, the number of fission neutrons produced per neutron absorbed, is approximately 2.30 for uranium-233 and 1.80 for plutonium-239.[60] In the small Peach Bottom reactor, however, the conversion ratio is only about 0.4.[61]

Attention should be called to a special aspect of the Peach Bottom reactor for which allowance must be made in computing resonance capture. Although the fuel is lumped in small discrete particles in a graphite matrix, the fuel region might have been treated as homogeneous were it not for the thorium-232 capture resonances. Because the lump dimensions are not small compared with the mean free paths near the resonance peaks, however, the lumping must be taken into account in computing the resonance absorption. The term "semi-homogeneous" has been used to describe a system of this kind.

10.3b Outline of the Calculational Methods

In the application of multigroup methods to the reactors referred to above, the gross migration of neutrons throughout the core can be treated adequately by a simple approximation, such as P_1 or diffusion theory. This is possible because the cores are large in comparison with neutron mean free paths (and migration lengths). Within the individual lattice cells, however, the detailed variations of the neutron flux with position, energy, and direction must be taken into account, especially in the evaluation of resonance capture and the utilization of thermal neutrons. These two effects are of decisive importance both for the criticality of the reactor and its temperature behavior. In the following discussion emphasis is placed upon calculations which are required to determine criticality and the temperature coefficients of reactivity at various times in the lifetime of the reactor core.

The first step in the calculation is to obtain microscopic cross-section and related data for all the significant nuclides. Such data, especially for uranium-238 (and thorium-232 for the Peach Bottom reactor), must include the resonance parameters, i.e., the measured parameters for the resolved resonances and the theoretical distribution of the parameters for unresolved resonances (Chapter 8).

In principle, similar data should be available for the fissile nuclides present. Because of the uncertainties in the resonance parameters of these nuclides (§8.2b) and their relatively low concentration in the fuel, it is a reasonably good approximation to use cross sections averaged over many resonances for most of the neutron energy range. The resonances at the lowest energies must, however, be included explicitly.

Finally, a model must be specified for the scattering of thermal neutrons in graphite (Chapter 7). For the calculations to be described here, the incoherent approximation was employed with a phonon spectrum, as shown in Fig. 7.10.

The cross-section data in a form suitable for computer processing is used to generate multigroup constants for cell calculations. The computer program GAM-I[62] was used, for example, in the calculations referred to below. This program, based on the P_1 or B_1 approximations (§4.5c) with a guessed value of the buckling, B, can yield group constants for up to 32 groups of nonthermal neutrons; in addition, it includes a treatment of resonance absorption in heterogeneous systems (§8.4c).

Differential cross sections for the scattering of thermal neutrons by graphite were obtained from the SUMMIT program.[63] The results were the numerical values of the scattering cross sections for a fine mesh of initial and final neutron energies. These were then used in the GATHER-I[64] program to yield the thermal-neutron spectrum in an infinite medium and this leads to the thermal group cross sections. The various computations described thus provide multigroup parameters for neutrons of all energies.

The multigroup constants were then employed in a cell calculation to determine the spatial distribution of the neutrons within a lattice cell for each energy group. For the Peach Bottom Reactor, the situation is relatively simple since the lattice cell is a fuel element, which can be assumed to be infinitely long, having the geometric cross section shown in Fig. 10.19.

For the Calder Hall reactor, on the other hand, the lattice cell would include the fuel element, its canning, and coolant passage, and also a proportionate share of the moderator arranged as a cylinder around the fuel element (§3.6a). The spatial distribution of the neutron flux within such a cell, which contains thin regions and media which readily absorb thermal neutrons, cannot be computed adequately by means of P_1 theory. A higher-order P_N approximation or an S_N calculation would be appropriate and an S_N program was used in some of the calculations. If the cell geometry were very complicated, a Monte Carlo treatment might be the best way (perhaps the only way at present) for computing in a reliable manner the flux within the cell.

The cell calculations would give the reaction and scattering rates for all the materials in the cell and for all the neutron energy groups. For use in the gross neutron diffusion calculations, for which the cells are homogenized, effective cross sections are defined in such a way as to preserve the reaction rates when integrated over the whole cell. The procedure for determining these effective cross sections is described in §3.6c.

10.3c Results of Cell Calculations

The results of the calculations[65] have shown that, for the Peach Bottom reactor, which contains fuel elements of small diameter with low concentrations of fissile

material, the spatial variations of the neutron flux within a cell are relatively slight and unimportant. In the Calder Hall reactor lattice, however, there are substantial spatial variations in the flux that depend on the energy, particularly for thermal neutrons. These variations were taken into account by using 26 groups of thermal neutrons. The results are conveniently summarized in Fig. 10.20 in terms of the fuel rod shielding factors for each of these groups. Since the departure of the shielding factor from unity represents a depression of the flux in the fuel relative to that in the moderator, it is evident that the spatial dependence of the flux in a cell varies with the neutron energy. This variation is due to the energy dependence of the neutron absorption cross sections in the fuel.

When the fuel has been burned to the extent of 800 MW-days/tonne (§10.2d), a considerable amount of plutonium-239 is present in the Calder Hall reactor. In calculating the shielding factors, this was assumed to be distributed uniformly throughout the fuel elements. The corresponding shielding factors are indicated by the broken lines in Fig. 10.20. A small shielding factor implies a marked depression of the neutron flux in the fuel and hence a large absorption cross section. Thus, the pronounced dips at 0.3 and 1.0 eV are due to resonances in plutonium-239 and plutonium-240, respectively. The energy (or group) dependence of the shielding factors is important in determining temperature coefficients, as will be seen in §10.3f.

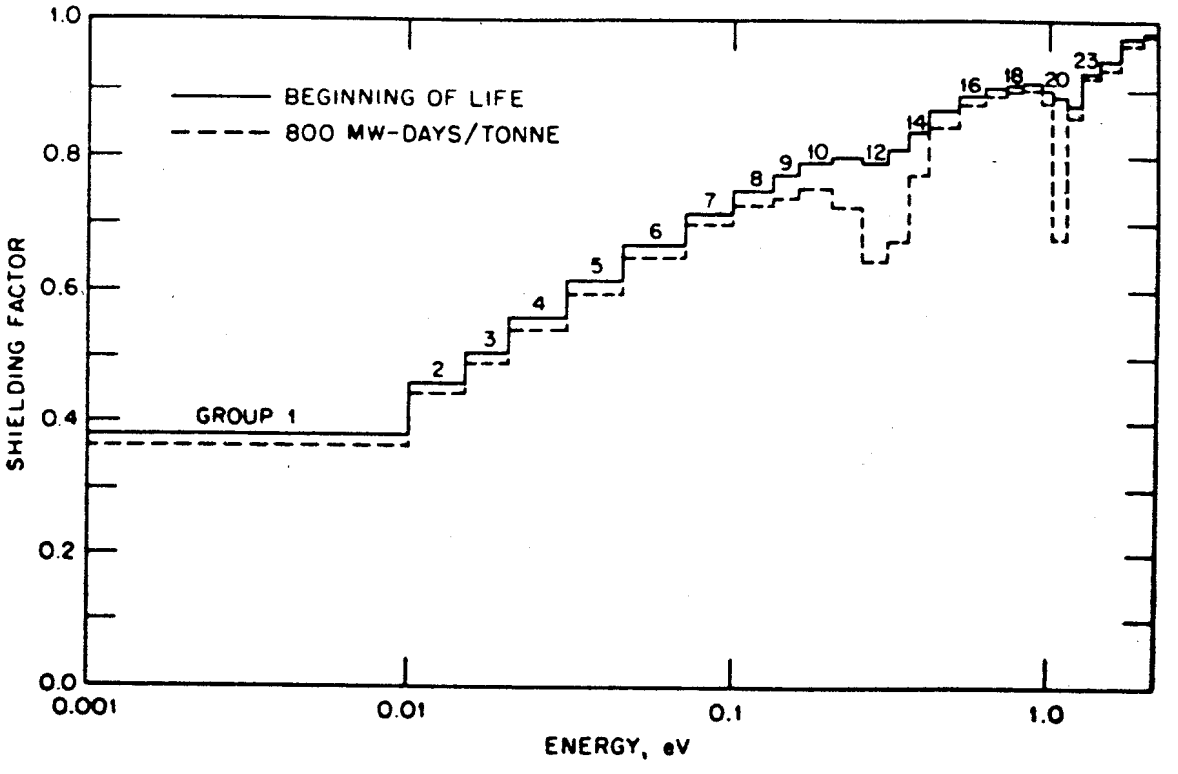

FIG. 10.20 FUEL ROD SHIELDING FACTORS IN 26 THERMAL ENERGY GROUPS CALCULATED FOR CALDER HALL REACTOR (AFTER H. B. STEWART AND M. H. MERRILL, REF. 65).

The foregoing results, which are necessary for predicting reactor behavior, provide an interesting example of the usefulness of multigroup methods and their advantage over simpler treatments of neutron transport, especially for thermal neutrons. It was clear to the earliest designers of heterogeneous graphite reactors that diffusion theory was not adequate for predicting the migration of thermal neutrons in and near fuel rods. Various ingenious methods were devised for combining diffusion theory in the moderator with collision probability or other more accurate theories as applied to the fuel. In this manner, for example, an accurate treatment was developed for the one-speed approximation to thermal-neutron migration in simple geometry.[66] The dependence of the shielding factor on neutron energy within the thermal range, as indicated in Fig. 10.20, can be obtained, however, only by the more detailed multigroup (or equivalent Monte Carlo) calculations.

Effective reaction and scattering cross sections, defined in the manner given earlier, can be derived from the results of the cell calculations. These are then used in a multigroup P_1 or diffusion-theory computation of gross neutron migration. For this purpose it is not necessary to use as many groups as were included in the cell calculation. Typically, a few fast groups together with a few thermal groups suffice and they are obtained by combining a number of the cell groups.

In connection with temperature coefficient calculations, discussed below, two multigroup diffusion-theory codes were used, namely, GAZE-2[67] and GAMBLE,[68] which are one- and two-dimensional, respectively. Both codes allow for up-scattering of neutrons in the thermal-energy range. In applying the one-dimensional code to a reactor with a more-or-less cylindrical core, a DB^2 correction would ordinarily be made to represent leakage in the transverse direction (§6.4j). In the two-dimensional calculation, for finite cylindrical (r, z) geometry, no such correction is required.

Control rods or lumped poisons in the reactor would be treated in an approximate way. A ring of control rods, for instance, would be represented by a cylinder of poison of such amount as to give the expected neutron absorption in the rods, as computed separately by transport or Monte Carlo methods.

The output of the diffusion-theory codes includes the reactivity (or k) and the gross spatial distribution of the neutron flux and various reaction rates; from the fission rates, the over-all (or gross) power distribution can be derived. When these results are combined with the cell calculations, which give the fine structure of the flux, the power density distribution, etc., within the individual fuel elements can be predicted.

The series of computer calculations outlined above are summarized in Table 10.1. The particular codes cited are those applied in the General Atomic (now Gulf General Atomic) organization which was responsible for the design of the Peach Bottom reactor. Other reactor design organizations would usually employ

TABLE 10.1. OUTLINE OF MULTIGROUP CALCULATIONS FOR GAS-COOLED, GRAPHITE-MODERATED REACTOR

Geometry +	Cross-section data, including resonance parameters and thermal scattering model	+ [GAM-1 / SUMMIT / GATHER-1]	
↓			
	Group constants for cell calculation	+ [S_N / cell calc.]	
↓			
	Fluxes within cell and group constants for gross flux calculations	+ [GAZE-2 / GAMBLE]	Control poison calculations
↓			
	k, power distribution, etc.		

their own equivalent computer codes to carry out the same (or similar) set of calculations. Several such code systems are described in Ref. 46.

By varying the temperatures of various regions of the system, either explicitly or by using perturbation theory, it is possible to derive temperature coefficients of reactivity under operating conditions. The changes in reactivity in going from room temperature to the operating temperature can also be computed.

The codes described above can be combined with a burnup program in which the concentrations of important nuclides are varied with time, so that changes in reactor properties with time can be predicted (§10.2c). The FEVER code,[69] for example, has been used in connection with design studies of the Peach Bottom reactor. This code is a one-dimensional, few-group burnup program which generates the required fluxes during the course of the calculation. It follows only gross depletion and not the detailed spatial variations within the lattice cells. Because of the semihomogeneous nature of the Peach Bottom reactor core, the gross depletion is adequate for this system, but it is not appropriate for the Calder Hall reactor in which, as seen above, there are considerable spatial variations of the neutron flux, and hence in the burnup, within the cell.

It may be mentioned that, in spite of the detail which can now be treated in multigroup calculations, an actual design program for a new type of reactor would always include integral experiments to complement and check the computations. Nevertheless, considerable reliance would be placed on the calculations to predict the effects of variations in design parameters on the operating characteristics of the reactor.

10.3d Components of the Effective Multiplication Factor

In order to gain some insight into the physical significance of the results of the multigroup calculations to be described in the subsequent sections, it is helpful to express them in terms of quantities which were employed in the early studies of the theory of thermal reactors. In the simple theory of bare, thermal reactors, for example, the effective multiplication factor, k, is expressed as the product of the infinite medium multiplication factor, k_∞, and the nonleakage probability, P_{nl}; thus,

$$k = k_\infty P_{nl}.$$

Furthermore, k_∞ may be written in the familiar manner as the product of four factors, i.e.,

$$k_\infty = \eta f p \epsilon,$$

where η, in its most general form, is the number of fission neutrons produced per thermal neutron absorbed in fuel, f is called the thermal utilization factor, p is the resonance escape probability, and ϵ is the fast-fission factor.[70]

It should be clearly understood that the four-factor formula will be used here only as a means for expressing the results of detailed multigroup calculations, as described in §10.3c, and of understanding their physical significance. The reactivity (or k), in particular, is derived entirely from multigroup calculations.

Suppose that it is desired to express the results of such a multigroup reactivity calculation in terms of the simple formula

$$k = \eta f p \epsilon P_{nl}. \tag{10.53}$$

There are no unique definitions in multigroup theory for the quantities on the right side of this expression, but a set of consistent definitions can be derived from considerations of neutron economy. It will be recalled (see, for example, §4.4d) that in a multigroup calculation, k will generally be found by iteration of the fission neutrons; furthermore, in §1.5e, k is regarded as the asymptotic ratio of the numbers of neutrons from successive generations of fission, i.e., it is the ratio computed with the flux eigenfunctions corresponding to the eigenvalue k. On this basis, the following consistent definitions[71] could be used for the factors in equation (10.53).

The quantity P_{nl} is first defined as the probability that a source (fission) neutron, with a source spatial distribution given by $\int \phi(\mathbf{r}, E)\nu\sigma_f(\mathbf{r}, E)\, dE$, is absorbed in the reactor core. Thus, P_{nl} is the number of neutrons absorbed in the core divided by the number of fission source neutrons in the k calculation.

The thermal utilization, f, can be defined as the probability that a thermal neutron which is absorbed in the core is absorbed in fissile material. Hence, f could be computed as the thermal-neutron absorptions in fissile nuclides divided by the total thermal absorption in the core. The factor η would then be the number of neutrons produced from thermal fission divided by the number of thermal neutrons absorbed in fissile species.

Along the same lines, the resonance escape probability, p, can be defined as the probability that a neutron which is absorbed in the reactor core is absorbed as a thermal neutron. Finally, the fast-fission factor, ϵ, is defined as the total number of fission neutrons produced divided by the number of neutrons formed as a result of thermal fissions.

In these definitions, it is assumed that all the fissile (and fissionable) material is in the reactor core. To implement the definitions, it is necessary to specify the thermal energy range; this is commonly taken to extend up to about 1 or 2 eV. It will be evident that the four-factor formula for k is useful only when most of the fissions are caused by thermal neutrons, so that p and ϵ are then close to unity.

10.3e The Reactivity Temperature Coefficients

Among the most important properties in determining the operating characteristics and safety of a nuclear reactor are its temperature coefficients of reactivity. In graphite-moderated, gas-cooled reactors, the temperature coefficients arise primarily from neutronic effects, since the effects of coolant density and thermal expansion on reactivity are very slight. In a heterogeneous natural-uranium reactor, such as the Calder Hall type, the over-all temperature coefficient is, to a large extent, determined by two quantities, namely, the fuel and the moderator coefficients.

A negative prompt coefficient associated with the fuel temperature arises from the Doppler broadening of the resonances in uranium-238 (§8.1d); this will always result in an increased absorption with increasing temperature and, hence, a decrease in reactivity. The temperature coefficient associated with the moderator is somewhat delayed (§9.4b) and is due to changes in the thermal-neutron spectrum corresponding to changes in the moderator temperature. This temperature coefficient can be either positive or negative, as will be seen shortly, depending on the amount of plutonium-239 present in the fuel.

A temperature coefficient of reactivity is usually defined as

$$\frac{\partial \rho}{\partial T} = \frac{1}{k}\frac{\partial k}{\partial T},$$

where T is the temperature of interest, e.g., an average (or effective) moderator or fuel temperature. From the discussion in §9.2c, it will be seen that this definition corresponds to use of an adiabatic approximation for defining the reactivity.* Such an approximation is particularly appropriate for the treatment of slow transients. In an actual transient, some problems would arise from the

* Strictly speaking, equation (9.17) would lead to

$$\frac{\partial \rho}{\partial T} = \frac{1}{k^2}\frac{\partial k}{\partial T},$$

but for k close to unity, the temperature coefficient is essentially the same as the one given above.

distribution of temperatures within the fuel and moderator; nevertheless, the temperature coefficients for constant (average or effective) fuel and moderator temperatures are a useful way of summarizing reactor response. In addition to the individual fuel and moderator coefficients, an isothermal temperature coefficient can be defined by considering the whole reactor core to be at a uniform temperature.

The simplest approach to the calculation of the various temperature coefficients referred to above is to evaluate k at two temperatures and then to derive the coefficient from

$$\frac{1}{k}\frac{\partial k}{\partial T} \quad \text{at} \quad \tfrac{1}{2}(T_1 + T_2) \approx \frac{2}{k(T_1) + k(T_2)} \frac{k(T_1) - k(T_2)}{T_1 - T_2}.$$

Alternatively, perturbation theory could be used to obtain the change in k due to a small change in cross sections arising from a change in temperature. Although the latter procedure might be the more accurate, it would involve computation of the detailed adjoint fluxes. Consequently, the first of the two methods was used to obtain the results which are quoted below.

If k is interpreted in terms of equation (10.53), then the temperature coefficient may be expressed as

$$\frac{1}{k}\frac{\partial k}{\partial T} = \frac{1}{\eta}\frac{\partial \eta}{\partial T} + \frac{1}{f}\frac{\partial f}{\partial T} + \frac{1}{p}\frac{\partial p}{\partial T} + \frac{1}{\epsilon}\frac{\partial \epsilon}{\partial T} + \frac{1}{P_{\mathrm{nl}}}\frac{\partial P_{\mathrm{nl}}}{\partial T}. \tag{10.54}$$

Since the fuel temperature coefficient is largely due to the effect of Doppler broadening on the resonance absorption, it may be simply taken to be equal to the third term on the right of equation (10.54); thus,

$$\text{Fuel temperature coefficient} \approx \frac{1}{p}\frac{\partial p}{\partial T}.$$

Hence, to a fair approximation, the remainder may be regarded as the moderator temperature coefficient, i.e.,

$$\text{Moderator temperature coefficient} \approx \frac{1}{k}\frac{\partial k}{\partial T} - \frac{1}{p}\frac{\partial p}{\partial T}.$$

It is evident that the quantity $(1/\eta)(\partial\eta/\partial T)$ is part of the moderator temperature coefficient. The physical reason is that η is determined by the energy spectrum of the thermal neutrons and this is dependent on the temperature of the moderator rather than of the fuel.

For a semihomogeneous reactor, such as one of the Peach Bottom type, the unusual nature of the fuel introduces somewhat different detailed temperature coefficients of reactivity. There would be a very fast coefficient associated with the temperature of the small uranium and thorium carbide particles; this would be negative because of the Doppler broadening enhancement of neutron absorption by thorium-232 with increasing temperature. In referring to the fuel temperature coefficient as very fast, it is assumed that the uranium-235 carbide and

thorium carbide are intimately mixed in the fuel particles. If the carbides were separate, then the temperature response would be delayed because of the necessity for heat to flow from the uranium-235 to the thorium-232 before Doppler increase of the resonance absorption could be effective.

In addition to the fuel coefficient of reactivity, there would be a fairly fast temperature coefficient arising from changes in the neutron spectrum due to temperature changes of the graphite matrix containing the fuel particles. For most purposes, however, this contribution of the moderator could be combined with the one arising from Doppler broadening in thorium-232 to give a prompt temperature coefficient.

Finally, there would be a delayed coefficient, as for the Calder Hall reactor, associated with the temperature of the unloaded graphite. Because of these (and other) complications, only the isothermal temperature coefficient of the Peach Bottom reactor will be considered here in any detail.

10.3f Results for the Calder Hall Reactor

The neutronic properties of a natural-uranium reactor change appreciably during operation as plutonium-239 is produced in the fuel. At the beginning of operation, neutrons are absorbed mainly in the uranium-235 and uranium-238, approximately half in each of these two nuclides. Since the initial conversion ratio is quite high, namely, 0.85 in the Calder Hall reactor, plutonium-239 is generated almost at the same rate as uranium-235 is consumed. But the thermal fission cross section of plutonium-239 is much larger than that for uranium-235; as a consequence, after a short time of operation k increases due to the buildup of plutonium-239 in the reactor.

Effective thermal cross sections, described in §10.3b, are given in Fig. 10.21[72] as a function of temperature, in the energy range up to 2.1 eV, for the Calder Hall lattice. As mentioned previously, the plutonium-239 is assumed to be distributed uniformly in the fuel; actually, however, it will be produced preferentially in the outer parts of the fuel rods where there is less shielding. Hence, the effective plutonium-239 thermal cross sections will be even larger than indicated in the figure. In any event, it is apparent that the cross sections for plutonium-239 are more than double those for uranium-235.

Values of k and of the isothermal temperature coefficients for the Calder Hall reactor were calculated using multigroup methods (§10.3c). The results, interpreted according to the four-factor formula, are recorded in Table 10.2 for the beginning of operation and in Table 10.3 for a composition corresponding to an exposure of about 800 MW-days/tonne, which is about half the fuel life.[73] In making the calculations for Table 10.3, the poisoning effect of fission products, including xenon-135 and samarium-149, was not taken into account. Hence, the reactivity changes are due to consumption of uranium-235 and buildup of plutonium-239 only.

TABLE 10.2. CALCULATED PROPERTIES OF THE CALDER HALL REACTOR AT THE BEGINNING OF OPERATION.[73]

Temp. °K	k	f	η	p	ϵ	P_{nl}
323	1.0355	0.5839	2.0642	0.8193	1.0800	0.9709
530	1.0224	0.5815	2.0568	0.8158	1.0809	0.9694
700	1.0146	0.5816	2.0486	0.8135	1.0814	0.9680
900	1.0078	0.5822	2.0402	0.8112	1.0819	0.9667

Isothermal Temperature Coefficients (in 10^{-5}/°C)

Temp. °K	$\frac{1}{k}\left(\frac{\partial k}{\partial T}\right)$	$\frac{1}{f}\left(\frac{\partial f}{\partial T}\right)$	$\frac{1}{\eta}\left(\frac{\partial \eta}{\partial T}\right)$	$\frac{1}{p}\left(\frac{\partial p}{\partial T}\right)$	$\frac{1}{\epsilon}\left(\frac{\partial \epsilon}{\partial T}\right)$	$\frac{1}{P_{nl}}\left(\frac{\partial P_{nl}}{\partial T}\right)$
426	−6.136	−1.996	−1.723	−2.091	+0.413	−0.736
615	−4.511	+0.0607	−2.355	−1.644	+0.297	−0.871
800	−3.382	+0.563	−2.049	−1.455	+0.218	−0.657

TABLE 10.3. CALCULATED PROPERTIES OF THE CALDER HALL REACTOR AFTER 800 MW-DAYS/TONNE BURNUP.[73]

Temp. °K	k	f	η	p	ϵ	P_{nl}
323	1.0604	0.6052	2.0415	0.8193	1.0779	0.9717
530	1.0578	0.6144	2.0171	0.8157	1.0780	0.9707
700	1.0622	0.6271	1.9925	0.8135	1.0775	0.9698
900	1.0691	0.6415	1.9684	0.8111	1.0768	0.9692

Isothermal Temperature Coefficients (in 10^{-5}/°C)

Temp. °K	$\frac{1}{k}\left(\frac{\partial k}{\partial T}\right)$	$\frac{1}{f}\left(\frac{\partial f}{\partial T}\right)$	$\frac{1}{\eta}\left(\frac{\partial \eta}{\partial T}\right)$	$\frac{1}{p}\left(\frac{\partial p}{\partial T}\right)$	$\frac{1}{\epsilon}\left(\frac{\partial \epsilon}{\partial T}\right)$	$\frac{1}{P_{nl}}\left(\frac{\partial P_{nl}}{\partial T}\right)$
426	−1.168	+7.226	−5.816	−2.089	+0.0111	−0.501
615	+2.453	+12.07	−7.197	−1.647	−0.2602	−0.518
800	+3.219	+11.37	−6.097	−1.454	−0.3058	−0.295

A number of features of Tables 10.2 and 10.3 are of interest. It will be observed, in the first place, that k is larger for the 800 MW-days/tonne core than at the beginning of operation. This is seen to be due to the increase in f, caused by the large cross section of plutonium-239. Moreover, this increase is more than enough to compensate for the decrease in η, which is smaller for plutonium-239 than for uranium-235. The prompt fuel temperature coefficient, expressed by $(1/p)(\partial q/\partial T)$, is negative, as expected, and remains almost unchanged during

800 MW-days/tonne of operation. Evidently, the slight depletion of uranium-238 and the changes in fissile material have little over-all effect in this connection.

The moderator temperature coefficient, taken as the difference between the total coefficient and the contribution from the resonance escape probability, as indicated earlier, is seen to change from negative at the beginning (Table 10.2) to positive after a period of operation (Table 10.3). An examination of the tables shows that the large (positive) increase in $(1/f)(\partial f/\partial T)$ is responsible for the change in sign. Physically, this means that in the middle-of-life core, the proportion of thermal neutrons absorbed by fissile nuclei increases with temperature. From Fig. 10.21, it is evident that this situation arises from the increase in the effective thermal cross section of plutonium-239 with increasing temperature. The basic cause of the increase is the pronounced resonance at a neutron energy of 0.3 eV. The shift in the thermal-neutron spectrum in the moderator with temperature results in more neutrons with energies in the vicinity of the plutonium-239 resonance as the temperature increases in the range of interest.

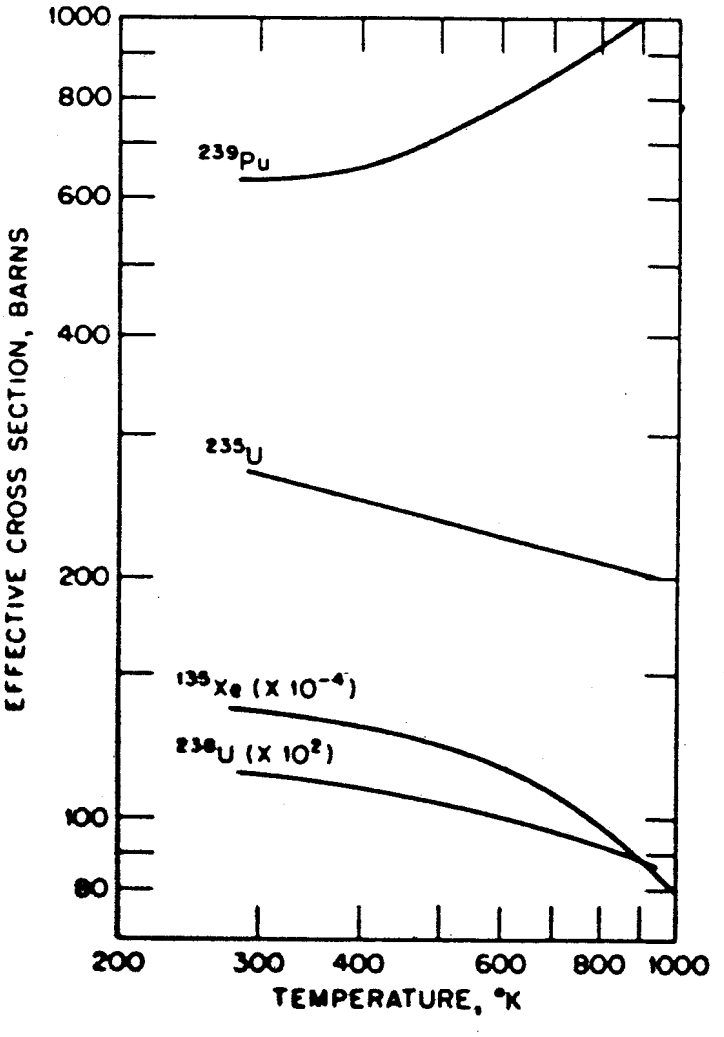

FIG. 10.21 EFFECTIVE THERMAL-NEUTRON CROSS SECTIONS VS TEMPERATURE IN THE CALDER HALL REACTOR AT THE BEGINNING OF CORE LIFE (AFTER H. B. STEWART AND M. H. MERRILL, REF. 72).

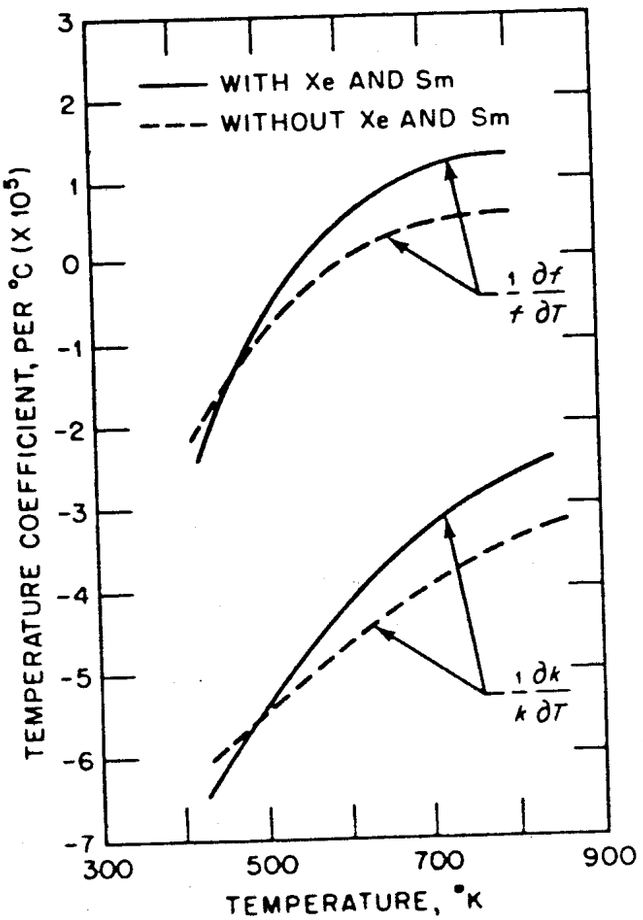

FIG. 10.22 EFFECT OF FISSION-PRODUCT POISONS ON TEMPERATURE COEFFICIENTS (AFTER H. B. STEWART AND M. H. MERRILL, REF. 76).

It follows, therefore, that the positive moderator temperature coefficient in a Calder Hall reactor core which has operated for some time is due to the presence of plutonium-239.

Another matter apparent from Tables 10.2 and 10.3 is that $(1/\eta)(\partial\eta/\partial T)$ has undergone a relatively large negative increase as a result of reactor operation. There are two factors responsible for this change, both being related to the formation of plutonium-239. First, the value of η for plutonium-239 is smaller than for uranium-235 and, second, η for plutonium-239 decreases with temperature or, more specifically, $\partial\eta/\partial E$ is negative for this nuclide for neutron energies $\lesssim 0.3$ eV.

Although several approximations have been made in computing the temperature coefficients under consideration, notably uniform consumption of uranium-235 and buildup of plutonium-239 and neglect of fission-product poisoning, the results are in fairly good agreement with experiment.[74] It might appear, at first sight, that the positive isothermal temperature coefficient of reactivity in the middle of the core life, at temperatures above about 500°K, would lead to a hazardous and unstable situation. However, because of the negative prompt fuel

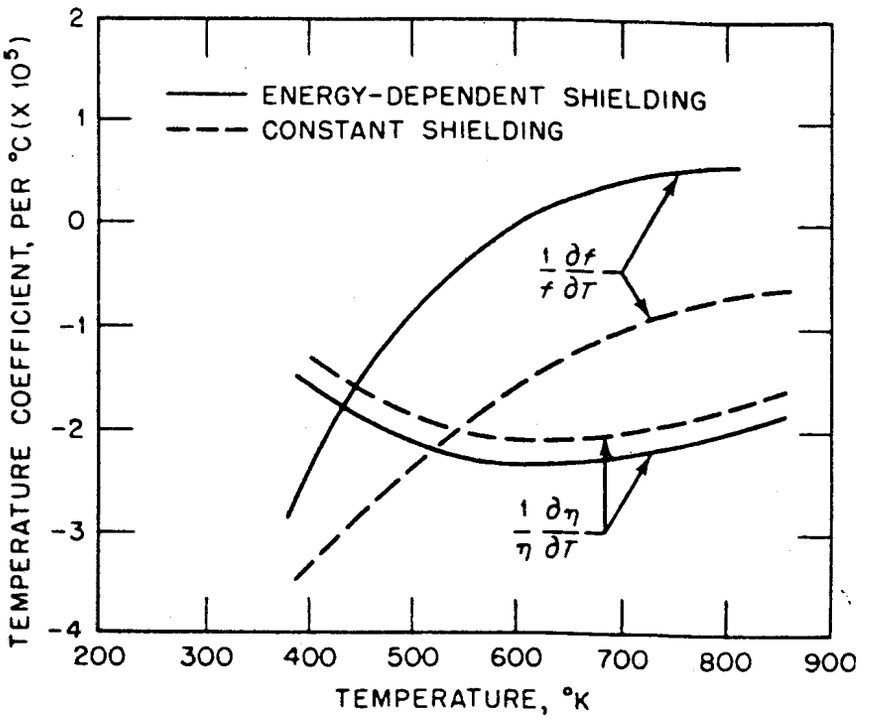

FIG. 10.23 EFFECT OF ENERGY-DEPENDENT SHIELDING FACTOR ON CALCULATED TEMPERATURE COEFFICIENTS (AFTER H. B. STEWART AND M. H. MERRILL, REF. 77).

coefficient, together with the large heat capacity of the moderator and the consequent long delay in the temperature increase, there should be no difficulty in controlling the reactor by rod motion or other means. This has been confirmed by transient experiments on the Calder Hall reactor[75]; the response is either stable or the power may diverge so slowly that it is readily controllable.

Reference may be made to two other aspects of the calculations on the Calder Hall reactor. First, the effect of equilibrium amounts of xenon-135 and samarium-149 on the temperature coefficients has been determined for the beginning of the core life. These fission-product poisons serve primarily to depress the thermal utilization and the influence on the temperature coefficient is indicated in Fig. 10.22.[76]

Finally, it was mentioned earlier that the detailed multigroup treatment of the thermal neutrons in a lattice cell was an important feature of the calculations. This point is illustrated in Fig. 10.23,[77] where it is seen that the temperature coefficient, especially $(1/f)(\partial f/\partial T)$, is substantially affected by the use of energy-dependent shielding factors, as compared with a single (constant) value for thermal neutrons.

10.3g Results for the Peach Bottom Reactor

Since the Peach Bottom reactor is a relatively small prototype HTGR, it has more fissile material per unit volume than would be necessary for a larger reactor of the same type. As a result, the conversion ratio is relatively low, i.e.,

initial expected value 0.4, as stated earlier. Furthermore, ϵ is approximately 1.25 and p about 0.62,[78] both of which differ from unity by more than should be realized in a larger core.

Some effective thermal-neutron (microscopic) cross sections in the energy range up to 2.1 eV, as a function of temperature, are shown in Fig. 10.24; they were computed by multigroup methods for an isothermal core of a small HTGR at the beginning of core life.[79] The dashed curves indicate the variations to be expected for $1/v$-absorbers.

For temperatures up to about 1500°K (or so) the effective absorption cross section of uranium-233 is only slightly larger than for uranium-235. This fact, combined with the low conversion ratio, would imply a relatively rapid decrease in k with burnup of the uranium-235. Consequently, it would be advantageous to use boron-10 as a lumped burnable poison (§10.2f) to reduce the reactivity decrease during operation of the reactor. The sort of gain to be expected in the Peach Bottom reactor was shown in Fig. 10.15, where the lumping of the boron was such as to give an initial self-shielding factor of 0.5. In a larger HTGR, with a high conversion ratio, approaching 0.9, the normal change in reactivity during operation would be less than indicated; in that case there would be no special benefit in the use of a burnable poison.

A prompt negative temperature coefficient of reactivity, caused by Doppler broadening of the thorium-232 resonances, is to be expected in the Peach Bottom reactor. There are, however, some positive coefficients arising from changes in

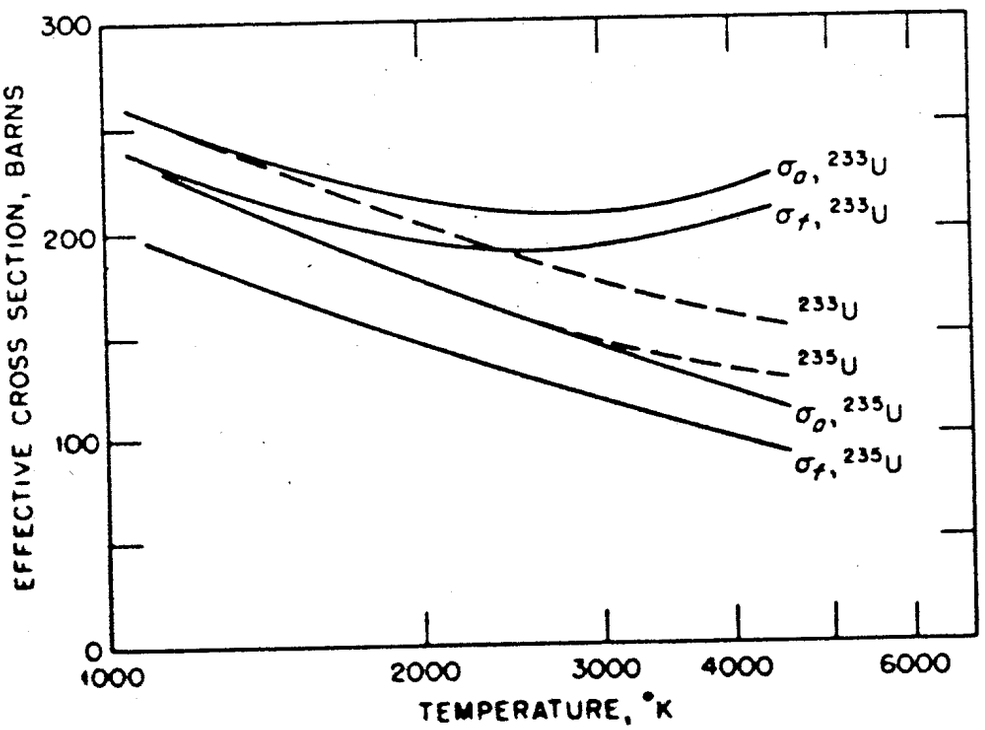

FIG. 10.24 EFFECTIVE THERMAL-NEUTRON CROSS SECTIONS VS TEMPERATURE IN A SMALL HTGR; BROKEN LINES INDICATE EXPECTED RESULTS FOR $1/v$-ABSORBERS (AFTER P. U. FISCHER AND N. F. WICKNER, REF. 79).

the thermal-neutron spectrum. In this energy region, the fissile nuclides, uranium-233 and uranium-235, are competing for neutrons with thorium-232, which is essentially a $1/v$-absorber, with fission-product poisons, and with a burnable poison, if present. Consider, first, the competition of the fissile nuclides with the $1/v$-absorber. The effective thermal absorption cross section of uranium-233 is seen from Fig. 10.24 to decrease less rapidly with temperature than if it exhibited the $1/v$-dependence on energy. Hence, if sufficient uranium-233 is present, it will lead to a positive contribution to $(1/f)(\partial f/\partial T)$ and also to the temperature coefficient. The fission product xenon-135 has a similar effect (see Fig. 10.27), since the effective thermal cross section decreases more rapidly with increasing temperature than does a $1/v$-absorber, as shown in Fig. 10.25.[79]

For a lumped boron-10 burnable poison, on the other hand, the effective cross section falls off with temperature more slowly than a $1/v$-absorber. Hence, it makes a negative contribution to $(1/f)(\partial f/\partial T)$. Under certain conditions, namely, near the end of the core life of the Peach Bottom reactor, when there is a maximum of uranium-233 and a minimum of boron-10 with xenon-135 present, calculations show that the net contribution of the thermal-neutron spectrum to the isothermal temperature coefficient is small and may be positive.[80] Since the prompt coefficients are more negative, however, the over-all (isothermal) temperature coefficient of reactivity is still negative. Thus the situation is not hazardous.

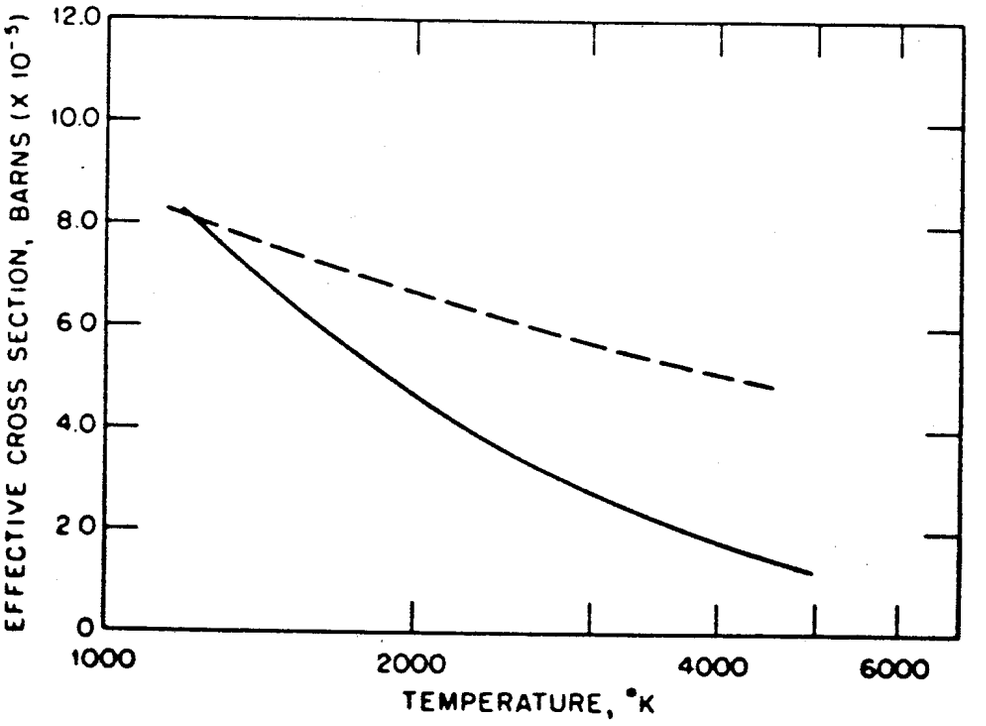

FIG. 10.25 EFFECTIVE THERMAL-NEUTRON CROSS SECTIONS OF XENON-135 VS TEMPERATURE: BROKEN LINE INDICATES $1/v$-BEHAVIOR OF σ_a (AFTER P. U. FISCHER AND N. F. WIKNER, REF. 79).

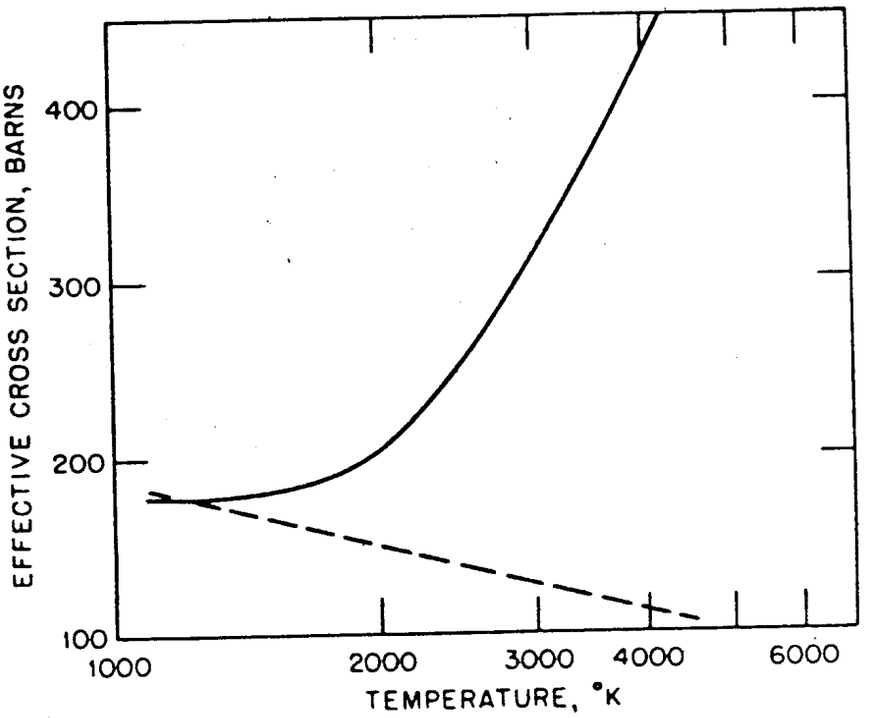

FIG. 10.26 EFFECTIVE THERMAL-NEUTRON CROSS SECTION OF RHODIUM-103 VS TEMPERATURE; BROKEN LINE INDICATES 1/v-BEHAVIOR (AFTER P. U. FISCHER AND N. F. WIKNER, REF. 79).

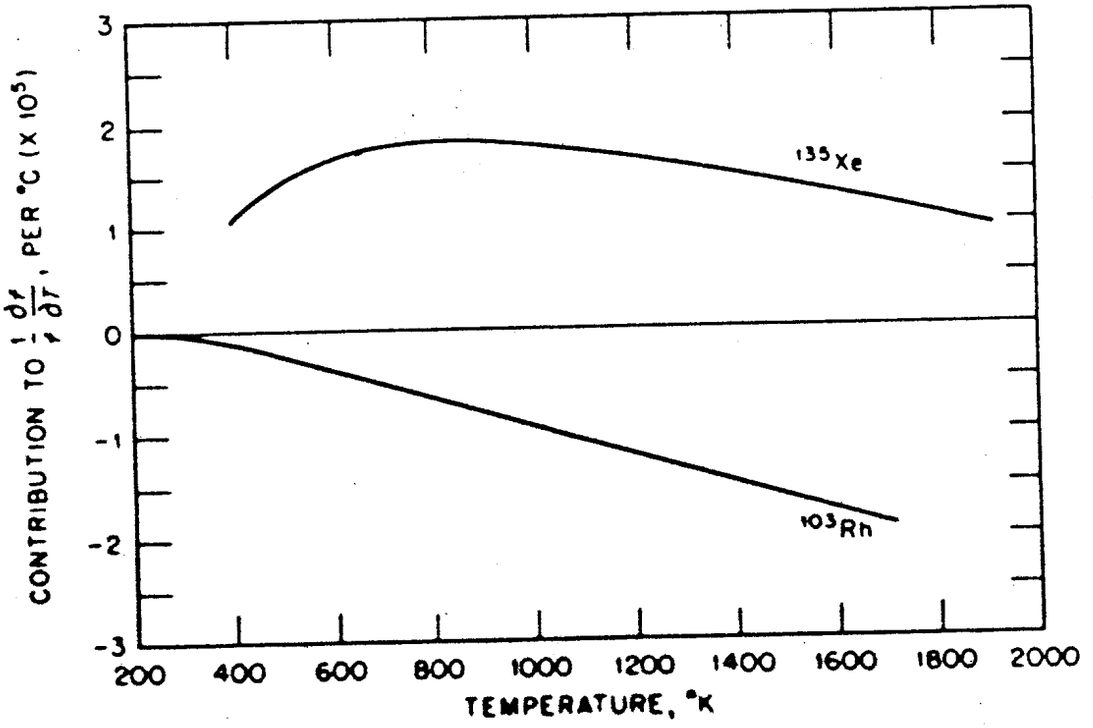

FIG. 10.27 CONTRIBUTIONS OF XENON-135 AND RHODIUM-103 TO TEMPERATURE COEFFICIENT FOR BEGINNING OF LIFE OF PEACH BOTTOM REACTOR (AFTER H. B. STEWART AND M. H. MERRILL, REF. 82).

Even if the over-all temperature coefficient were positive, the reactor could be operated safely because the prompt coefficient is negative. This is the case, as already indicated, for the Calder Hall reactor which has a positive isothermal temperature coefficient around the middle of its core life at the normal operating temperature of about 600°K. In order to increase the temperature stability of the Peach Bottom reactor, rhodium-103 is added to the fuel; the effective thermal-neutron absorption cross section of this nuclide actually increases with temperature[81] above about 1500°K (Fig. 10.26). Hence, it makes a large negative contribution to $(1/f)(\partial f/\partial T)$, as shown by the calculated curve in Fig. 10.27, which corresponds to the addition of 5 kg of rhodium-103 to the almost 2000 kg of fuel mixture.[82] It should be mentioned that rhodium-103 is formed as a fission product and this also contributes to the negative temperature coefficient.

Some calculated values of the isothermal temperature coefficients, and of their components, are given in Tables 10.4 and 10.5, for the beginning and end, respectively, of the core life.[83] The multigroup methods and codes already described were used and allowance was included for the added rhodium-103. The relatively minor contribution of the nonleakage probability to the temperature coefficient is due to variations in the neutron flux in space and energy as the core temperature changes.

TABLE 10.4 ISOTHERMAL TEMPERATURE COEFFICIENTS OF THE PEACH BOTTOM REACTOR AT THE BEGINNING OF CORE LIFE (in 10^{-5}/°C).[83]

Temp. °K	$\frac{1}{k}\left(\frac{\partial k}{\partial T}\right)$	$\frac{1}{\eta}\left(\frac{\partial \eta}{\partial T}\right)$	$\frac{1}{f}\left(\frac{\partial f}{\partial T}\right)$	$\frac{1}{\epsilon}\left(\frac{\partial \epsilon}{\partial T}\right)$	$\frac{1}{p}\left(\frac{\partial p}{\partial T}\right)$	$\frac{1}{P_{nl}}\left(\frac{\partial P_{nl}}{\partial T}\right)$
450	−7.0	−1.0	−1.2	+1.3	−6.1	−0.0
750	−5.5	−1.0	−1.7	+1.2	−3.9	−0.1
1050	−4.7	−0.6	−2.3	+1.2	−2.8	−0.2
1350	−4.3	−0.2	−2.9	+1.0	−2.1	−0.1
1650	−4.4	−0.1	−3.6	+1.3	−1.8	−0.2

TABLE 10.5 ISOTHERMAL TEMPERATURE COEFFICIENTS OF THE PEACH BOTTOM REACTOR AT THE END OF CORE LIFE (in 10^{-5}/°C).[83]

Temp. °K	$\frac{1}{k}\left(\frac{\partial k}{\partial T}\right)$	$\frac{1}{\eta}\left(\frac{\partial \eta}{\partial T}\right)$	$\frac{1}{f}\left(\frac{\partial f}{\partial T}\right)$	$\frac{1}{\epsilon}\left(\frac{\partial \epsilon}{\partial T}\right)$	$\frac{1}{p}\left(\frac{\partial p}{\partial T}\right)$	$\frac{1}{P_{nl}}\left(\frac{\partial P_{nl}}{\partial T}\right)$
750	−3.2	−1.0	+1.6	+0.3	−3.8	−0.3
1350	−2.3	−0.1	−0.1	+0.3	−2.1	−0.3
1900	−3.1	+0.2	−1.8	+0.6	−1.6	−0.4

EXERCISES

1. Consider one-speed *diffusion* theory in a bare slab. The flux may be expanded in spatial modes proportional to $\cos(n\pi x/a)$, where a is the slab thickness, and for each mode there will be seven period eigenvalues. Characterize these eigenvalues for the system. As a further exercise, somewhat more complicated models, such as a two-group bare slab[84] or a reflected reactor,[85] may be considered. The more difficult problem of one-speed *transport* theory for a slab is treated in Ref. 86.
2. When a system is close to (delayed) critical the spatial effects described in §10.1e in connection with the pulsed-source experiments are relatively less important. Explain why by considering the expansion equation (6.45). It may be useful to employ the eigenvalue spectrum found in Exercise 1.
3. Obtain the solutions to the point-reactor equations (10.20) and (10.21) for one group of delayed-neutron precursors, e.g., by Laplace transform methods. Show that when $\Lambda\lambda \ll 1$, the solution has the properties of equations (10.22) and (10.26).
4. In addition to the pulsed-source method, reactivity can be determined by "source-jerk" and "rod-drop" experiments. In the source-jerk method a subcritical system initially contains a source which is withdrawn abruptly. Detector readings are taken before and after withdrawal of the source. In the rod-drop experiment, the system is at delayed critical when control rods are suddenly inserted. The reactivity of the subcritical reactor is then determined.[87]

   By considering the point-reactor kinetics equations, show how these experiments might be interpreted to yield the reactivity in each case. Discuss the problems which arise when spatial effects are taken into account and describe the manner in which these effects may be calculated using time-independent methods. Do these procedures present any advantages over the pulsed-source method?
5. One-speed diffusion theory is to be used to analyze the following pulsed-source problem. Consider slab geometry as in Exercise 1, with a source $Q(x, t) = Q(x)\,\delta(t)$. Expand the time-dependent flux in a complete set of spatial modes and discuss how an experiment might be set up in order to minimize the contribution of the higher modes in a reactivity determination. How will the results change when energy dependence is taken into account? For some actual experimental details, see Ref. 88.
6. By using one-speed diffusion theory, analyze the following neutron-wave experiment. Suppose there is a source $Q(x, t) = \delta(x)e^{i\omega t}$ on the midplane ($x = 0$) of a very long rectangular parallelepiped having thickness d in both the y and z directions. Expand the flux in terms of spatial modes for the y and z dependences and find the x dependence for each solution. Obtain the complete solution and discuss its behavior for large x. For comparison with a realistic experiment Ref. 89 may be consulted.
7. If the half-life of a radioactive nuclide is short enough, the nuclide can be neglected in a burnup calculation (cf. §10.2a). Develop a criterion for the maximum half-life for which such neglect might be permissible.
8. Consider a thermal reactor using uranium enriched to 4 atomic percent in uranium-235 as fuel. Suppose that σ_a in equation (10.50) is such that k_∞ is

initially 1.30, with the reactor in hot operating condition and equilibrium xenon and samarium poisoning and all control rods out. The reactor can operate until k_∞ falls to 1.10; calculate the expected core lifetime in MW-days/tonne of uranium, taking only thermal neutrons into consideration. Fission products, conversion of uranium-238, and all spatial dependences are to be ignored. For simplicity, the cross sections and related quantities may be taken to be the values at 0.06 eV.

Suppose that boron-10 is added homogeneously to the fuel so that k_∞ is initially 1.10. By how much will this decrease the required control capability and the core lifetime? With the same amount of boron-10, suppose the uranium-235 in the fuel is increased so that the initial k_∞ is the same as in the unpoisoned reactor (1.30); calculate the expected core lifetime.

Examine the possibility of using boron-10 as a lumped burnable poison in such a manner as to compensate almost exactly for the changes in reactivity during reactor operation.[90]

9. In a reactor in which thorium-232 is converted into uranium-233, the intermediate protactinium-233 is present for a time long enough for it to capture an appreciable number of neutrons. What fraction of the protactinium-233 will decay and what fraction will capture neutrons in a thermal reactor operating at a temperature of 500°C with an average thermal flux of 10^{14} neutrons cm^2-sec in the fuel? How would this affect the conversion ratio?
10. Suppose that k has been obtained by iteration of a fission source. Use the transport equation, e.g., equation (1.49), to write out the definitions of η, f, p, and ϵ in mathematical form and show that they are self-consistent. Express the results in the notation of multigroup diffusion theory. (Comparison may be made with Table 3-1 of Ref. 53.)
11. By using the effective thermal cross sections in Fig. 10.21 and elementary one-group reactor theory, estimate the reactivity required to compensate for equilibrium xenon-135 poisoning in the Calder Hall reactor. Assume an average operating temperature of 600°K and either estimate the thermal-neutron flux or obtain the value from Ref. 56 and suggest reasons for any discrepancy. Determine the contribution of the equilibrium xenon-135 to $(1/f)(\partial f/\partial T)$ and to the over-all temperature coefficient. Compare the results with those in Fig. 10.27.
12. Calculate the shielding factor for a lump of boron-10 in the form of a sphere with a radius of 1 mean free path for a neutron of 0.025-eV energy. Use collision probability methods and assume that the sphere does not perturb the incident flux from the moderator. Determine the shielding factor as a function of energy and estimate the variation of an effective shielding factor with temperature for a Maxwellian thermal-neutron spectrum. Comment on the results.

REFERENCES

1. Okrent, D., *et al.*, "AX-1, A Computing Program for Coupled Neutronics Hydrodynamics Calculations," Argonne National Laboratory Report ANL-5977 (1959); A. Curtis, *et al.*, "STAB, A Kinetic Three-Dimensional, One Group Digital Computer Code," U.K. AEA Report AEEW-R-77 (1961); J. B. Yasinsky, M. Natelson, and L. A. Hageman, *Nucl. Sci. Eng.*, 33, 355 (1968); R. Froehlich, *et al.*, *Ibid.*, 36, 257 (1969); W. W. Engle and F. R. Mynatt, *Trans. Am. Nucl. Soc.*, 12, 400 (1969).

2. Ott, K. O., and D. A. Meneley, in Proc. Conf. on Industrial Needs and Academic Research in Reactor Kinetics, Brookhaven National Laboratory Report BNL-50117 (1968), p. 192; *Nucl. Sci. Eng.*, **36**, 402 (1969).
3. Kaplan, S., *Proc. Third U.N. Conf. on Peaceful Uses of At. Energy*, **4**, 44 (1965); W. M. Stacey, Jr., "Space-Time Nuclear Reactor Kinetics," Academic Press, 1969, Section 1.4.
4. "Coupled Reactor Kinetics," Proc. Nat. Topical Meeting Am. Nucl. Soc., C. G. Chezem and W. H. Köhler, eds., The Texas A & M Press, 1967.
5. Garabedian, H. L., *Proc. Symp. Appl. Math.*, XI, Am. Math. Soc., 1961, p. 256; H. L. Garabedian and R. E. Lynch, *Nucl. Sci. Eng.*, **21**, 550 (1965).
6. Courant, R., and D. Hilbert, "Methods of Mathematical Physics," Interscience Publishers, Inc., 1953, Vol. I, Chap. 5.
7. Kaplan, S., "Synthesis Methods in Reactor Analysis," in *Adv. Nucl. Sci. Tech.*, **3**, 233 (1966).
8. Kaplan, S., O. J. Marlow, and J. Bewick, *Nucl. Sci. Eng.*, **18**, 163 (1964); J. B. Yasinsky, *ibid.*, **29**, 381 (1969).
9. Kaplan, S., Ref. 7; S. Kaplan, *et al.*, Ref. 8.
10. Kaplan, S., Ref. 7; J. B. Yasinsky, Ref. 8.
11. Kaplan, S., *et al.*, Ref. 8.
12. Yasinsky, J. B., and A. F. Henry, *Nucl. Sci. Eng.*, **22**, 171 (1965).
13. Yasinsky, J. B., and A. F. Henry, Ref. 12.
14. Ott, K. O., and D. A. Meneley, Ref. 2.
15. Yasinsky, J. B., and A. F. Henry, Ref. 12.
16. Henry, A. F., *Nucl. Sci. Eng.*, **20**, 338 (1964); J. R. Mika, *Nukleonik*, **9**, 46 (1967); E. Garelis, *ibid.*, **9**, 187 (1967); H. Kaper, *J. Math. Anal. Appl.*, **19**, 207 (1969); W. M. Stacey, Jr., Ref. 3, Section 1.2.
17. Cohen, E. R., *Proc. Second U.N. Conf. on Peaceful Uses of At. Energy*, **11**, 302 (1958).
18. Henry, A. F., Ref. 16.
19. Henry, A. F., Ref. 16; A. F. Henry, *Trans. Am. Nucl. Soc.*, **9**, 235 (1966).
20. Orndoff, J. D., *Nucl. Sci. Eng.*, **2**, 450 (1957); T. Ijima, *et al.*, *ibid.*, **33**, 344 (1968).
21. Simmons, B. E., and J. S. Ling, *Nucl. Sci. Eng.*, **3**, 595 (1958).
22. Sjöstrand, N. G., *Arkiv Fys.*, **11**, 233 (1956).
23. Gozani, T., *Nukleonik*, **4**, 348 (1962).
24. Garelis, E., and J. L. Russell, *Nucl. Sci. Eng.*, **16**, 263 (1963).
25. Henry, A. F., *Trans. Am. Nucl. Soc.*, **9**, 235 (1966).
26. Masters, C. F., and K. B. Cady, *Nucl. Sci. Eng.*, **29**, 272 (1967).
27. Williams, M. M. R., "Slowing Down and Thermalization of Neutrons," John Wiley and Sons, Inc., 1966, Chaps. 3 and 4.
28. Perez, R. B., and R. E. Uhrig, *Nucl. Sci. Eng.*, **17**, 90 (1963); M. N. Moore, *ibid.*, **21**, 565 (1965); **26**, 354 (1966); M. J. Ohanian, *et al.*, *ibid.*, **30**, 95 (1967).
29. See citations in Ref. 28.
30. Glasstone, S., and M. C. Edlund, "The Elements of Nuclear Reactor Theory," D. Van Nostrand Co., Inc., 1952, §§11.46 *et seq.*; A. M. Weinberg and E. P. Wigner, "The Physical Theory of Neutron Chain Reactors," University of Chicago Press, 1958, pp. 600 *et seq.*; J. R. Lamarsh, "Introduction to Nuclear Reactor Theory," Addison-Wesley Publishing Co., Inc., 1966, Section 13-2.
31. Chernick, J. *et al.*, *Nucl. Sci. Eng.*, **10**, 120 (1960).
32. Kaplan, S., Ref. 3.
33. Chernick, J., *et al.*, Ref. 31.
34. Canosa, J., and H. Brooks, *Nucl. Sci. Eng.*, **26**, 237 (1966).
35. Canosa, J., and H. Brooks, Ref. 34.
36. Canosa, J., and H. Brooks, Ref. 34.
37. Dietrich, J. R., in "The Technology of Nuclear Reactor Safety," T. J. Thompson and J. G. Beckerley, eds., The M.I.T. Press, 1964, Vol. I, Section 8.2.
38. Garrison, J. D., and B. W. Roos, *Nucl. Sci. Eng.*, **12**, 115 (1962); W. H. Walker, Proc. Conf. on Nuclear Data for Reactors, IAEA, 1966, Vol. I, p. 521.
39. See, for example, E. L. Ince, "Ordinary Differential Equations," Dover Publications, Inc., 1944, Appendix B.

40. Lee, C. E., private communication; H. E. Klug, *et. al.*, *Trans. Am. Nucl. Soc.*, **12**, 52 (1969).
41. England, T. R., "CINDER, A One-Point Depletion and Fission Product Program," Westinghouse Report WAPD-TM-34 (1962).
42. R. L. Crowther in "Fuel Burnup Predictions in Thermal Reactors," IAEA, 1968, p. 173.
43. "Some Novel Plutonium Fueling Methods for Thermal Reactors," Battelle-Northwest Laboratory Report BNWL-183 (1965).
44. Jedruch, J., and R. J. Novick, *Nucl. Appl.*, **3**, 507, (1967); R. P. Matsen, *et al.*, *Trans. Am. Nucl. Soc.*, **12**, 31 (1969).
45. Stachew, J. C., *Nucl. Appl.*, **4**, 206 (1968).
46. See "Fuel Burnup Predictions in Thermal Reactors," IAEA, 1968.
47. Shanstrom, R. T., and M. Benedict, *Nucl. Sci. Eng.*, **11**, 377 (1961).
48. Benedict, M., *et al.*, *Nucl. Sci. Eng.*, **11**, 386 (1961).
49. "UHTREX Facility Description and Safety Analysis Report," Los Alamos Scientific Laboratory Report LA-3556 (1967).
50. "Directory of Nuclear Reactors," IAEA, 1962, Vol. IV, p. 169.
51. Radkowsky, A., *Proc. Second U.N. Conf. on Peaceful Uses of At. Energy*, **13**, 426 (1958); "Naval Reactors Physics Handbook," Vol. I, A. Radkowsky, ed. U.S. AEC 1964, Section 4.7.
52. Leonard, J. H., and P. W. Wackman, *Trans. Am. Nucl. Soc.*, **1**, 132 (1958).
53. Stewart, H. B., and M. H. Merrill, in Ref. 37, Vol. I, p. 477 (Fig. 2-2).
54. "Naval Reactors Physics Handbook," Vol. I, A. Radkowsky, ed., U.S. AEC 1964, p. 837 (Fig. 4.85).
55. Ref. 54, p. 833 (Fig. 4.80).
56. *J. Brit. Nucl. Energy Conf.*, **2**, 41 *et seq.* (1957); "Directory of Nuclear Reactors," IAEA, 1962, Vol. IV, p. 183.
57. Cutts, B., *et al.*, *Proc. Second U.N. Conf. on Peaceful Uses of At. Energy*, **12**, 612 (1958).
58. Stewart, H. B., and M. H. Merrill, in Ref. 37, Vol. I, Chap. 9, Section 3; other burnup studies and comparisons with experiment for the Calder Hall reactor are given by J. G. Tyror in Ref. 46, p. 3.
59. de Hoffmann, F., and C. L. Rickard, *Proc. Third U.N. Conf. on Peaceful Uses of At. Energy*, **5**, 101 (1964).
60. "Reactor Physics Constants," Argonne National Laboratory Report ANL-5800 (1963), Section 2.2.1.
61. "The Technology of Nuclear Reactor Safety," T. J. Thompson and J. G. Beckerley, eds. The M.I.T. Press, 1964, Appendix I, Table III; "Directory of Nuclear Reactors," IAEA, 1968, Vol. VII, p. 251.
62. Joanou, G. D., and J. S. Dudek, "GAM-I, A Consistent P_1 Multigroup Code for the Calculation of Fast Neutron Spectra and Multigroup Constants," General Atomic Report GA-1850 (1961).
63. Bell, J., "SUMMIT, An IBM-7090 Program for the Computation of Crystalline Scattering Kernels," General Atomic Report GA-2492 (1962).
64. Stewart, H. B., and M. H. Merrill, in Ref. 37, Vol. I, p. 495.
65. Stewart, H. B., and M. H. Merrill, in Ref. 37, Vol. I, p. 497 (Fig. 3.7).
66. Amouyal, A., B. P. Benoist, and J. Horowitz, *J. Nucl. Energy*, **6**, 79 (1957); see J. R. Lamarsh, Ref. 30, pp. 382 *et seq.*
67. Lenihan, S., "GAZE-2, A One-Dimensional Multigroup Diffusion Code for the IBM-7090," General Atomic Report GA-3152 (1962).
68. Dorsey, J. P., "GAMBLE, A Program for the Solution of the Multigroup Diffusion Equations in Two Dimensions with Arbitrary Group Scattering, etc.," General Atomic Report GA-4246 (1963).
69. Todt, F., "FEVER, A One-Dimensional Few Group Depletion Program for Reactor Analysis," General Atomic Report GA-2749 (1962).
70. Glasstone, S., and M. C. Edlund, Ref. 30, §§4.57 *et seq.*; J. R. Lamarsh, Ref. 30, Section 9-1; A. M. Weinberg and E. P. Wigner, Ref. 30, Chap. VII.
71. Stewart, H. B., and M. H. Merrill, in Ref. 37, Vol. I, p. 490 (Table 3-1).

72. Stewart, H. B., and M. H. Merrill, in Ref. 37, Vol. I, p. 498 (Fig. 3-9).
73. Stewart, H. B., and M. H. Merrill, in Ref. 37, Vol. I, p. 496 (Table 3-6), p. 499 (Table 3-7).
74. Leslie, D. C., "The SPECTROX Method for Thermal Spectra in Lattice Cells," U.K. AEA Report AEEW-M-211 (1961).
75. Brown, G., *et al.*, *Proc. Second U.N. Conf. on Peaceful Uses of At. Energy*, **11**, 202 (1958).
76. Stewart, H. B., and M. H. Merrill, in Ref. 37, Vol. I, p. 498 (Fig. 3-11).
77. Stewart, H. B., and M. H. Merrill, in Ref. 37, Vol. I, p. 497 (Fig. 3-8).
78. Merrill, M. H., "Temperature Coefficient Calculations for Peach Bottom," General Atomic Report GAMD-7357 (1966).
79. Fischer, P. U., and N. F. Wikner, "An Interim Report on the Temperature Coefficient of the 40 MW(e) HTGR," General Atomic Report GA-2307 (1961).
80. D. E. Parks, *et al.*, "Slow Neutron Scattering and Thermalization, with Reactor Applications," W. A. Benjamin, Inc., 1970, Chap. 7.
81. Fischer, P. U. and N. F. Wikner, Ref. 79.
82. Stewart, H. B., and M. H. Merrill, in Ref. 37, Vol. I, p. 500 (Fig. 3-14).
83. Stewart, H. B., and M. H. Merrill, in Ref. 37, Vol. I, p. 500 (Table 3-8), p. 501 (Table 3-9).
84. Henry, A. F., Ref. 16.
85. Garelis, E., Ref. 16.
86. Mika, J., Ref. 16; H. Kaper, Ref. 16.
87. Keepin, G. R., "Physics of Nuclear Kinetics," Addison-Wesley Publishing Co., Inc., 1965, Sections 8.5, 8.6.
88. Preskitt, C. A., *et al.*, *Nucl. Sci. Eng.*, **29**, 283 (1967); an interesting detector configuration is given by T. Ijima, *et al.*, *ibid.*, 33, 344 (1968).
89. Booth, R. S., R. H. Hartley, and R. B. Perez, *Nucl. Sci. Eng.*, **28**, 404 (1967).
90. Leonard, J. H., and P. W. Wackman, Ref. 52.

APPENDIX. SOME MATHEMATICAL FUNCTIONS

THE DELTA FUNCTION

The Dirac delta function, $\delta(x)$, may be defined by the requirements that

$$\delta(x) = 0 \qquad x \neq 0,$$

and

$$\int f(x)\,\delta(x)\,dx = f(0)$$

if the range of integration includes $x = 0$, and is zero otherwise. The second condition must hold for any suitably continuous function, $f(x)$. The delta function may be given a rigorous mathematical interpretation as the limit of a series of increasingly peaked functions; it is in this sense a "generalized function."[1]

Upon change of variable it is seen that

$$\int f(x)\,\delta(x - a)\,dx = f(a)$$

and

$$\int f(x)\,\delta\left(\frac{x}{a}\right)dx = af(0),$$

provided that the range of integration includes $x = a$ or $x = 0$, respectively. More generally, an integral involving $\delta[g(x)]$, where $g(x_0) = 0$ may be interpreted as

$$\int f(x)\,\delta[g(x)]\,dx = \frac{f(x_0)}{\left|\frac{dg}{dx}\right|_{x=x_0}}$$

if the range of integration includes $x = x_0$.

There are many ways to represent the delta function. One, which is used in this book, follows from the Fourier transform formula

$$f(x) = \frac{1}{2\pi}\int_{-\infty}^{\infty}\int_{-\infty}^{\infty} e^{-i\xi(x-y)}f(y)\,dy\,d\xi,$$

which suggests the representation

$$\int_{-\infty}^{\infty} e^{-i\xi x}\,d\xi = 2\pi\,\delta(x).$$

It is consistent with the properties of the delta function to set

$$x\,\delta(x) = 0$$

for all x. From this it follows[2] that the equation

$$A = B$$

does not imply

$$\frac{A}{x} = \frac{B}{x}$$

if the values $x = 0$ is to be included, but rather

$$\frac{A}{x} = \frac{B}{x} + c\,\delta(x),$$

where c is an undetermined constant. Extensive use is made of this observation in developing Case's method in Chapter 2.

THE GAMMA FUNCTION

The gamma function, $\Gamma(x)$, is given by

$$\Gamma(x) = \int_0^{\infty} t^{x-1}e^{-t}\,dt$$

so long as the real part of x is positive. It satisfies the recurrence formula

$$\Gamma(x+1) = x\Gamma(x).$$

Some particular values are

$$\Gamma(1) = 1$$

$$\Gamma(\tfrac{1}{2}) = \sqrt{\pi}$$

and for integral values of x, $x = n + 1$,

$$\Gamma(n+1) = 1\cdot 2\cdots(n) = n!.$$

Tables of the gamma function are available.[3]

THE ERROR FUNCTION

The error function, erf (x), is defined by the integral

$$\operatorname{erf}(x) = \frac{2}{\sqrt{\pi}}\int_0^x e^{-u^2}\,du.$$

As x increases from zero to infinity, erf (x) increases monotonically from zero to one. It may be represented by the series

$$\text{erf}\,(x) = \frac{2}{\sqrt{\pi}}\left(x - \frac{x^3}{3\cdot 1!} + \frac{x^5}{5\cdot 2!} - \frac{x^7}{7\cdot 3!} + \cdots\right)$$

or, for large x, by the asymptotic expansion

$$\text{erf}\,(x) \approx 1 - \frac{e^{-x^2}}{x\sqrt{\pi}}\left(1 - \frac{1}{2x^2} + \frac{1\cdot 3}{(2x^2)^2} - \frac{1\cdot 3\cdot 5}{(2x^2)^3} + \cdots\right).$$

The error function is also available in tabular form.[4]

THE EXPONENTIAL INTEGRALS, $E_n(x)$

The exponential integral, $E_n(x)$, is defined for real positive x and n a positive integer by the integral

$$E_n(x) = \int_1^\infty e^{-xu}u^{-n}\,du.$$

It may be written in the alternative forms

$$E_n(x) = \int_0^1 e^{-x/\mu}\mu^{n-2}\,d\mu = x^{n-1}\int_x^\infty e^{-u}u^{-n}\,du.$$

For $n = 0$, the integration may be carried out with the result

$$E_0(x) = \frac{e^{-x}}{x}.$$

When $n = 1$,

$$E_1(x) = \int_x^\infty \frac{e^{-u}}{u}\,du = -\text{Ei}\,(-x)$$

and the function $-\text{Ei}\,(-x)$ is often called *the* exponential integral.

The exponential integrals satisfy the recurrence relations

$$E_n(x) = \int_x^\infty E_{n-1}(x')\,dx'$$

$$\frac{dE_n(x)}{dx} = -E_{n-1}(x)$$

and

$$E_n(x) = \frac{1}{n-1}\left[e^{-x} - xE_{n-1}(x)\right] \quad \text{for } n > 1. \tag{1}$$

Equation (1) shows that all the exponential integrals can be found from $E_1(x)$. However, it is convenient to have tabulations[5,6] including $n = 2, 3, 4$, for use in neutron transport problems.

For small x, the series expansion is sometimes useful, namely,

$$E_n(x) = \sum_{\substack{m=0 \\ m\neq n-1}}^{\infty} \frac{(-x)^m}{m!(n-1-m)} + (-1)^n\frac{x^{n-1}}{(n-1)!}(\log x - A_n + \gamma) \quad \text{for } n > 0,$$

where γ is Euler's constant ($= 0.577216$), $A_1 = 0$, and $A_n = \sum_{m=1}^{n-1} 1/m$. This shows that as x goes to zero, all the exponential integrals for $n \geq 2$ remain finite, indeed $E_n(0) = 1/(n-1)$. However, $E_1(0)$ diverges logarithmically.

For large x, $E_n(x)$ has the asymptotic expansion

$$E_n(x) \approx \frac{e^{-x}}{x}\left[1 - \frac{n}{x} + \frac{n(n+1)}{x^2} - \frac{n(n+1)(n+2)}{x^3} + \cdots\right].$$

THE LEGENDRE POLYNOMIALS

The Legendre polynomials may be defined by the relations

$$P_0(x) = 1$$

$$P_n(x) = \frac{1}{2^n n!}\frac{d^n}{dx^n}(x^2 - 1)^n \quad \text{for } n = 1, 2, \ldots. \tag{2}$$

They may also be defined as the unique (except for normalization) set of polynomials orthogonal on the interval $-1 \leq x \leq 1$, such that n is the highest power of x in $P_n(x)$. In fact, they satisfy the orthogonality relation

$$\int_{-1}^{1} P_m(x)P_n(x)\,dx = \frac{2\delta_{mn}}{2n+1}$$

where δ_{mn}, the Kronecker delta, is unity if $m = n$ and zero otherwise. The first few polynomials are

$$P_0(x) = 1$$
$$P_1(x) = x$$
$$P_2(x) = \tfrac{1}{2}(3x^2 - 1)$$
$$P_3(x) = \tfrac{1}{2}(5x^3 - 3x).$$

They satisfy the recurrence relations

$$xP_n(x) = \frac{1}{2n+1}[(n+1)P_{n+1}(x) + nP_{n-1}(x)]$$

$$(x^2 - 1)\frac{dP_n}{dx} = n(xP_n - P_{n-1}).$$

The Legendre polynomials form a complete set[7,8] of orthogonal functions for the expansion of a function, $f(x)$, defined on the interval $-1 \leq x \leq 1$. In particular, if $f(x)$ is real and square integrable, i.e., the integral

$$\int_{-1}^{1} |f(x)|^2\,dx$$

exists and is finite, and if the expansion

$$f(x) \simeq \sum_{n=0}^{N} f_n P_n(x)$$

$$f_n = \frac{2n+1}{2}\int_{-1}^{1} f(x)P_n(x)\,dx$$

is considered, then

$$\lim_{N\to\infty}\int_{-1}^{1}\left[f(x) - \sum_{n=0}^{N} f_n P_n(x)\right]^2 dx = 0.$$

This equation is an expression of completeness in that the mean square deviation of the expansion from the function goes to zero as $N \to \infty$. If the function $f(x)$ is piecewise continuous or of bounded variation,[7] then in addition

$$\lim_{N\to\infty} \sum_{n=0}^{N} f_n P_n(x) = f(x), \tag{3}$$

if $f(x)$ is continuous at the point x, whereas the limit approaches

$$\tfrac{1}{2}[f(x + 0) + f(x - 0)]$$

if $f(x)$ is discontinuous at the point x, having the (finite) limits $f(x + 0)$ and $f(x - 0)$ as x is approached from the two sides.

It is of interest to note that equation (3) may be written

$$f(x) = \sum_{n=0}^{\infty} \frac{2n + 1}{2} \int_{-1}^{1} f(x')P_n(x')P_n(x)\, dx'$$

which may be summarized as

$$\delta(x - x') = \sum_{n=0}^{\infty} \frac{2n + 1}{2} P_n(x')P_n(x).$$

Thus, the delta function may also be used in this way to indicate completeness of a set of functions.

When the neutron flux is expanded in Legendre polynomials, $P_n(\mu)$, then except for possible delta functions arising from an anisotropic source, it would be expected that the expansion would converge as in equation (3), with a possible discontinuity in slab geometry at $\mu = 0$ (§3.5a).

THE ASSOCIATED LEGENDRE FUNCTION

The associated Legendre function, $P_l^m(x)$ is defined for integral values of $m = 0, 1, \ldots, l$ by the formula*

$$P_l^m(x) = (-1)^m(1 - x^2)^{m/2} \frac{d^m P_l(x)}{dx^m}.$$

From this it is seen that $P_l^0(x) = P_l(x)$. If equation (2) is used for $P_l(x)$, then it follows that

$$P_l^m(x) = \frac{(-1)^m}{2^l l!} (1 - x^2)^{m/2} \frac{d^{l+m}}{dx^{l+m}} (x^2 - 1)^l$$

and this equation can be used to extend the definition of $P_l^m(x)$ to negative integral values of m such that $|m| \leq l$. It can then be shown that

$$P_l^{-m}(x) = (-1)^m \frac{(l - m)!}{(l + m)!} P_l^m(x).$$

* The choice of phase, $(-1)^m$, for $P_l^m(x)$ is a common one and is used in Ref. 3. It is not employed universally, however, see e.g., Ref. 9, and the reader should check the usage of any particular author.

The associated Legendre functions satisfy the orthogonality relation

$$\int_{-1}^{1} P_l^m P_{l'}^m(x)\,dx = \frac{2}{2l+1}\frac{(l+m)!}{(l-m)!}\,\delta_{ll'}$$

and the recurrence relations

$$xP_l^m(x) = \frac{1}{2l+1}\left[(l-m+1)P_{l+1}^m(x) + (l+m)P_{l-1}^m(x)\right]$$

and

$$(x^2-1)\frac{dP_l^m(x)}{dx} = lxP_l^m(x) - (l+m)P_{l-1}^m(x).$$

The first few associated Legendre functions are

$$P_1^1(x) = -(1-x^2)^{1/2} \qquad P_1^1(\cos\theta) = -\sin\theta$$
$$P_2^1(x) = -3(1-x^2)^{1/2}x \qquad P_2^1(\cos\theta) = -3\sin\theta\cos\theta$$
$$P_2^2(x) = 3(1-x^2) \qquad P_2^2(\cos\theta) = 3\sin^2\theta.$$

THE SPHERICAL HARMONICS

The normalized spherical harmonics, $Y_{lm}(\theta, \varphi)$ are defined by*

$$Y_{lm}(\theta,\varphi) = \sqrt{\frac{2l+1}{4\pi}\frac{(l-m)!}{(l+m)!}}\,P_l^m(\cos\theta)e^{im\varphi}. \tag{4}$$

From equation (4) it can be seen that

$$Y_{l,-m}(\theta,\varphi) = (-1)^m Y_{lm}^*(\theta,\varphi)$$

where Y_{lm}^* is the complex conjugate of Y_{lm}.

The spherical harmonics are orthonormal in that

$$\int_0^{2\pi}\int_{-1}^{1} Y_{lm}(\theta,\varphi)\,Y_{l'm'}^*(\theta,\varphi)\,d\cos\theta\,d\varphi = \delta_{ll'}\,\delta_{mm'}$$

and complete, in that if a function $f(\theta, \varphi)$ is expanded in the series

$$f(\theta,\varphi) = \sum_{l=0}^{L}\sum_{m=-l}^{l} f_{lm}\,Y_{lm}(\theta,\varphi)$$

with

$$f_{lm} = \int_0^{2\pi}\int_{-1}^{1} f(\theta,\varphi)\,Y_{lm}^*(\theta,\varphi)\,d\cos\theta\,d\varphi$$

then

$$\lim_{L\to\infty}\sum_{l=0}^{L}\sum_{m=-l}^{l} f_{lm}\,Y_{lm}(\theta,\varphi) = f(\theta,\varphi).$$

* It may be noted that in some books, the term *spherical harmonic* is used for a solution of Laplace's equation in spherical geometry. This use differs from that given in equation (4) by a power of r, the radial coordinate, and Y_{lm} is then called a *surface harmonic*. Again, the phase convention is not universally used as indicated in the preceding footnote.

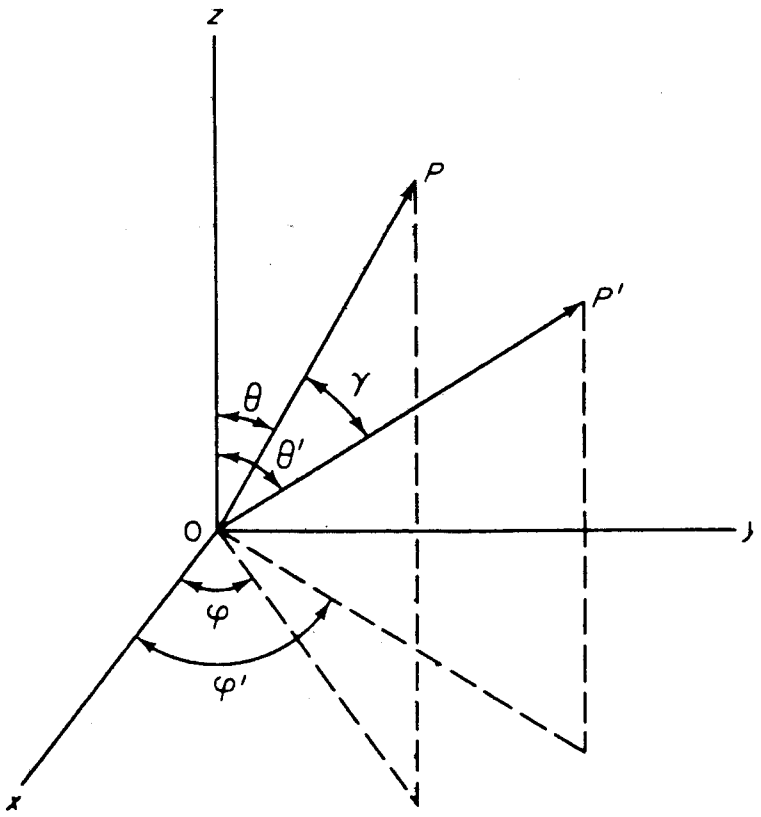

APPENDIX FIG. 1 COORDINATES FOR ADDITION THEOREM OF SPHERICAL HARMONICS.

This limit will be approached for any suitable function $f(\theta, \varphi)$, in particular, if $f(\theta, \varphi)$ is given in the region $-1 \leqslant \cos\theta \leqslant 1$, $0 \leqslant \varphi \leqslant 2\pi$ and is continuous and of bounded variation.[10] If f is piecewise continuous, then at a discontinuity the mean value will be approached. Note that instead of the functions Y_{lm}, the real functions $P_l^m(\cos\theta)\cos m\varphi$ and $P_l^m(\cos\theta)\sin m\varphi$ can equally well be used for the expansions.

The spherical harmonics satisfy the important *addition theorem*. Let two points, P and P', on the unit sphere have the coordinates (θ, φ) and (θ', φ') as shown in Fig. 1 and let γ be the angle between the vectors to P and P'. Then

$$\cos\gamma = \cos\theta\cos\theta' + \sin\theta\sin\theta'\cos(\varphi - \varphi').$$

The addition theorem states

$$P_l(\cos\gamma) = \frac{4\pi}{2l+1}\sum_{m=-l}^{l} Y_{lm}^*(\theta', \varphi')\, Y_{lm}(\theta, \varphi)$$

which, using the definition of Y_{lm} in equation (4), may be readily reduced to the form used in this book

$$P_l(\cos\gamma) = P_l(\cos\theta)P_l(\cos\theta') + 2\sum_{m=1}^{l}\frac{(l-m)!}{(l+m)!}P_l^m(\cos\theta)P_l^m(\cos\theta')\cos[m(\varphi - \varphi')].$$

Derivations of the addition theorem and the other equations involving Legendre functions in this Appendix may be found, for example, in Refs. 7, 10, 11.

REFERENCES

1. Lighthill, M. J., "Introduction to Fourier Analysis and Generalized Functions," Cambridge University Press, 1958.
2. Dirac, P. A. M., "Principles of Quantum Mechanics," Oxford University Press, 4th ed., 1958, p. 58.
3. Abramowitz, M., and I. Stegun, eds., "Handbook of Mathematical Functions," Dover Publications, Inc., 1965, p. 255.
4. Ref. 3, p. 310.
5. Case, K. M., F. de Hoffmann, and G. Placzek, "Introduction to the Theory of Neutron Diffusion," Vol. I, U.S. AEC Report, 1953, Appendix A.
6. Ref. 3, p. 245.
7. Courant, R., and D. Hilbert, "Methods of Mathematical Physics," Interscience Publishers, Inc., Vol. I, 1953, Chap. 2.
8. Dennery, P., and A. Krzywicki, "Mathematics for Physicists," Harper and Row, Publishers, 1967, Chap. III.
9. Jahnke, E., and F. Emde, "Tables of Functions," Dover Publications, Inc., 1945.
10. Hobson, E. W., "Theory of Ellipsoidal and Spherical Harmonics," Chelsea Publishing Co., 1955, p. 344.
11. Whittaker, E. T., and G. N. Watson, "A Course of Modern Analysis," Cambridge University Press, 1946, Chap. XV.

INDEX

Other Van Nostrand Reinhold Books Of Related Interest

SOURCEBOOK ON ATOMIC ENERGY, Third Edition,
By **Samuel Glasstone.** 883 pages, 6" x 9"

This is the standard sourcebook on atomic and nuclear science. The book provides a complete overview of the field, from the earliest theories of the atom and its structure to recent applications of isotopes and radiation in industry, medicine and biology, agriculture, law enforcement, archeology, and cosmology. The book highlights the development of the theory of radioactivity, the concept of isotopes, the design of particle accelerators, and the use of nuclear reactors for power and research. In bringing together the important facts about the current status and possible future of a vital and challenging discipline, the authors demonstrate how nuclear energy is increasingly a part of our daily lives.

NUCLEAR POWER PLANTS
Design, Operating Experience, and Economics
By **Robert L. Loftness,** Atomics International. 546 pages 6" x 9"

This authoritative volume provides significant data on the various types of reactors that have been or are being constructed—their design characteristics, problems, operating experience, and development trends. Written for engineers, executives, and all who follow the development of nuclear plants, the work covers engineering principles, reactor fuels and materials, pressurized water reactors, boiling water reactors, heavy water reactors, liquid metal cooled reactors, fluid fuel reactors, aerospace reactors, and economics.

MANAGEMENT OF RADIOACTIVE WASTES
By **C. A. Mawson,** Environmental Research Branch, Atomic Energy Branch, Atomic Energy of Canada Ltd., Chalk River Nuclear Laboratories. 208 pages, 6" x 9"

Fully summarizing the art of radioactive waste management, this book brings together in one volume material previously available only in technical governmental reports. Covered are sources and nature of radioactive wastes; waste management in the uranium industry; treatment of gaseous effluent; storage and disposal into geological formations, seas, lakes, and rivers; and much more.

Van Nostrand Reinhold Company
450 West 33rd Street, New York, New York 10001

F0684-000-4